

UC Irvine

UC Irvine Electronic Theses and Dissertations

Title

Metal-Hydride Catalysis: Stereoselective Allylation and Hydroacylation

Permalink

<https://escholarship.org/uc/item/0dw39738>

Author

Davison, Ryan

Publication Date

2022

Peer reviewed|Thesis/dissertation

UNIVERSITY OF CALIFORNIA,
IRVINE

Metal-Hydride Catalysis: Stereoselective Allylation and Hydroacylation

DISSERTATION

submitted in partial satisfaction of the requirements
for the degree of

DOCTOR OF PHILOSOPHY

in Chemistry

by

Ryan T. Davison

Dissertation Committee:
Professor Vy M. Dong, Chair
Professor Sergey V. Pronin
Professor Christopher D. Vanderwal

Table of Contents

List of Figures	iv
List of Tables	v
Acknowledgements	vi
Curriculum Vitae	viii
Abstract of the Dissertation	x
Preface	1
Chapter 1 – Catalytic Hydrothiolation: Regio- and Enantioselective Coupling of Thiols and Dienes	9
1.1 Introduction	9
1.2 Results and Discussion	11
1.3 Conclusion and Future Work	15
1.4 Author Contributions	15
1.5 References	17
Chapter 2 – Catalytic Hydrothiolation: Counterion-Controlled Regioselectivity	19
2.1 Introduction	19
2.2 Results and Discussion	21
2.3 Conclusion and Future Work	34
2.4 Author Contributions	34
2.5 References	35
Chapter 3 – Enantioselective Coupling of Dienes and Phosphine Oxides	38
3.1 Introduction	38
3.2 Results and Discussion	39
3.3 Conclusion and Future Work	46
3.4 Author Contributions	46
3.5 References	48
Chapter 4 – Enantioselective Addition of α -Nitroesters to Alkynes	50
4.1 Introduction	50
4.2 Results and Discussion	52
4.3 Conclusion and Future Work	57
4.4 Author Contributions	58
4.5 References	59
Chapter 5 – Cu-Catalyzed Olefin Hydroacylation	62
5.1 Introduction	62
5.2 Results and Discussion	64
5.3 Conclusion and Future Work	65
5.4 Author Contributions	66
5.5 References	67
Conclusion	68

Appendices	69
Appendix 1 Supporting Information for Chapter 1	70
Appendix 2 Supporting Information for Chapter 2	153
Appendix 3 Supporting Information for Chapter 3	215
Appendix 4 Supporting Information for Chapter 4	330
Appendix 5 Supporting Information for Chapter 5	450

List of Figures

Figure P.1	Overview of the dissertation	2
Figure P.2	Allylation chemistry in natural product and drug synthesis	3
Figure P.3	Tsuji-Trost reaction versus transition metal-catalyzed hydrofunctionalization	4
Figure P.4	Additional regioselectivity challenges associated with hydrofunctionalization	5
Figure 1.1	Asymmetric 1,3-diene hydrothiolation	9
Figure 1.2	Proposed Rh-catalyzed hydrothiolation mechanism	10
Figure 1.3	Catalyst-controlled diastereoselective hydrothiolation	15
Figure 2.1	Regiodivergent hydrothiolation of 1,3-dienes	20
Figure 2.2	Empirical guide for 1,2-Markovnikov hydrothiolation	22
Figure 2.3	Proposed mechanism for 1,2-Markovnikov hydrothiolation	23
Figure 2.4	Deuterium-labeling studies for the 1,2-Markovnikov hydrothiolation	24
Figure 2.5	KIE from two parallel reactions using initial rates	25
Figure 2.6	Hammett plot	26
Figure 2.7	Catalyst-controlled diastereoselective 1,2-Markovnikov hydrothiolation	27
Figure 2.8	Enantioselective synthesis of (–)-agelasidine A	28
Figure 2.9	Proposed counterion-controlled regiodivergent hydrothiolations	29
Figure 2.10	Different counterions lead to a switch in regioselectivity	30
Figure 2.11	Proposed 3,4- <i>anti</i> -Markovnikov hydrothiolation mechanism	32
Figure 2.12	Initial mechanistic experiments for 3,4- <i>anti</i> -Markovnikov hydrothiolation	33
Figure 3.1	Asymmetric hydrophosphinylation of 1,3-dienes	38
Figure 3.2	Diastereodivergent hydrophosphinylation	43
Figure 3.3	Proposed 1,3-diene hydrophosphinylation mechanism	44
Figure 3.4	Preliminary mechanistic experiments	45
Figure 4.1	Enantioselective addition of α -nitroesters to alkynes	50
Figure 4.2	Proposed mechanism for Rh-catalyzed allylation	51
Figure 4.3	Mechanistic studies	57
Figure 5.1	Enantioselective 1,3-dicarbonyl synthesis and olefin hydroacylation	62
Figure 5.2	Enantioselective Cu-catalyzed hydrofunctionalization	63

List of Tables

Table 1.1	Ligand effects on asymmetric hydrothiolation	11
Table 1.2	Hydrothiolation with various thiols	12
Table 1.3	Hydrothiolation of various 1,3-dienes	13
Table 2.1	3,4- <i>Anti</i> -Markovnikov hydrothiolation of 1,3-dienes	31
Table 3.1	Ligand and acid effects on asymmetric hydrophosphinylation	40
Table 3.2	Hydrophosphinylation of various 1,3-dienes	41
Table 3.3	Hydrophosphinylation with various phosphine oxides	42
Table 4.1	Investigating various α -nitrocarbonyls	52
Table 4.2	Survey of chiral ligands	53
Table 4.3	α -Nitrocarbonyl scope	54
Table 4.4	Alkyne scope	56
Table 5.1	Surveying chiral ligands	65

Acknowledgements

To Professor Vy Dong — Thank you for giving me the opportunity to join your group, and for all the opportunities that followed. I remember the phone call we had to discuss my admission to UC Irvine. I knew then that the Dong group was the place I wanted to be for my graduate studies. I am grateful for all the big and little things you do for the group. The thing that sticks out to me the most is your unwavering positive attitude towards everything. I have always appreciated that your mentorship extends beyond chemistry – it truly shows that you care about the development and happiness of your students. I would also like to thank your family, Wilmer and Liam Alkhas. Wilmer, I have always appreciated your perspective on chemistry, life, and anything in-between. I fondly remember the time you and Vy dropped everything to help me get back to my family in New York during an emergency – thank you. Liam, it has been such a pleasure to watch you grow up in front of my eyes. I am so excited to see your continued success and developing interests.

To my committee members — Professors Sergey Pronin and Christopher Vanderwal, thank you for serving on my committee and for your time (both in and out of class). I appreciate all the discussions we have had over the past four years. Your unique perspectives will be missed. I would also like to thank my undergraduate advisor, Professor Justin Miller. Justin, thank you for your excitement about chemistry and the opportunity to do undergraduate research. Without either one of those things, I'm not sure if I would have pursued a PhD in chemistry. Thank you for inviting me to Thanksgiving dinners over the years in Los Angeles. I'm thankful we have had the opportunities to stay in touch post-undergraduate.

To Dong group members — Thank you for helping to foster an inclusive and fun place to do research. I cherish all the memories and interactions that I've had with other members of this amazing group. I'd like to thank all the members that I had the privilege to overlap with in the

Dong group. Thank you to the postdoctoral fellows/visiting scholars: Xiaohui Yang, Shaozhen Nie, Jihye Park, Daniel Akwaboah, Aleksandra Holownia, Yusuke Aota, Bubwoong Kang, Patrick Parker, Isaiah Speight, and Hyuk Le for all your advice— you all are my role models. Thank you to the elder graduate students: Daniel Kim, Diane Le, Faben Cruz, Jan Riedel, Zhiwei Chen, and Alexander Lu for all your help. It has been such a pleasure to watch all of you move on to your dream jobs and I'm so excited to see where life takes you next. Thank you to the younger graduate students: Alexander Jiu, Xintong Hou, Erin Kuker, Hannah Slocumb, Brian Daniels, Minghao Wang, Kirsten Ruud, Julie Simon, Antoinette Antonucci, and Camryn Wallace for bringing new energy and shaping the future of the Dong group – I am rooting for you all. Thank you to the undergraduate students that I've had the opportunity to mentor: Nathan Dao and Bryce Gaskins. It's been awesome to see your growth – best of luck. I'd also like to thank the American Chemical Society and Wiley for permission to include portions of Chapters 1–4 in this dissertation.

To my friends and family — Thank you for everything. Your continuous support, strength, and sacrifices have made this possible. I could not have done this without you. I love you.

Curriculum Vitae

Ryan T. Davison

EDUCATION

- 2017 – 2022 **University of California, Irvine** (Irvine, CA)
Ph.D., Organic Chemistry
Advisor: Professor Vy M. Dong
- 2013 – 2017 **Hobart and William Smith Colleges** (Geneva, NY)
B.S., Chemistry (Honors, *summa cum laude*)
Advisor: Professor Justin S. Miller

PROFESSIONAL EXPERIENCE

- 2017 – 2022 **University of California, Irvine** (Irvine, CA)
Graduate Research Student
- Achieved a regio- and enantioselective synthesis of allylic sulfides
 - Accomplished a Pd-catalyzed addition of phosphine oxides to dienes
 - Demonstrated a switch in regioselectivity for catalytic hydrothiolation
 - Achieved an enantioselective addition of α -nitroesters to alkynes
 - Wrote an account that highlights the divergent reactivity of aldehydes
- Advisor: Professor Vy M. Dong
- 2016 – 2017 **Hobart and William Smith Colleges** (Geneva, NY)
Undergraduate Research Student
- Reported a total synthesis of Xyzidepsin, a depsipeptidic analogue of histone deacetylase inhibitor Romidepsin (FK228)
 - Developed a method that unmasks latent thioesters in hydrophobic-compatible conditions
 - Integrated LCMS analysis with depsipeptide synthesis and a semester-long laboratory project for Organic Chemistry II students
- Advisor: Professor Justin S. Miller

HONORS AND AWARDS

- 2022 Allergan Graduate Fellowship in Organic Chemistry (UCI)
- 2021 Colgate-Palmolive Smile with Science Symposium: 1st Place (UCI)
- 2020 Chemistry Department Teaching Program Award (UCI)
- 2019 NSF Graduate Research Fellowship: Honorable Mention (UCI)
- 2017 Phi Beta Kappa (HWS)
- 2017 Achievement Award of the Rochester Section of the ACS (HWS)
- 2017 Rocco L. Fiaschetti '40 Prize (HWS)
- 2017 Carl Aten Physical Chemistry Prize (HWS)
- 2016 Pim Larsson Kovach Achievements Award in Chemistry (HWS)

2016	Undergraduate Award for Achievement in Organic Chemistry (HWS)
2016	Myron J. Dybich Scholarship (HWS)
2013	Hobart Heritage Scholar (HWS)
2013	Faculty Scholarship (HWS)

PUBLICATIONS

- (8) Smith, E. M.; Peraro, L.; Cramer, S. L.; **Davison, R. T.**; Slade, D. J.; Miller, J. S. Semester-Long Solid-Phase Peptide Synthesis Laboratory Targeting Novel, Potential Anticancer Molecules to Complement Second-Semester Organic Coursework. *in preparation*
- (7) Perkins, W. S.; **Davison, R. T.**; Shelkey, G. B.; Lawson, V. E.; Hutton, G. E.; Miller, J. S. Unmasking Latent Thioesters Under Hydrophobic-Compatible Conditions. *J. Pep. Sci.* **2021**, *27*:e3358, 1–5.
- (6) **Davison, R. T.**; Kuker, E. L.; Dong, V. M. Teaching Aldehydes New Tricks Using Rhodium- and Cobalt-Hydride Catalysis. *Acc. Chem. Res.* **2021**, *54*, 1236.
- (5) **Davison, R. T.**; Parker, P. D.; Hou, X.; Chung, C. P.; Augustine, S. A.; Dong, V. M. Enantioselective Addition of α -Nitroesters to Alkynes. *Angew. Chem. Int. Ed.* **2021**, *60*, 4599.
- (4) Zang, X.; Peraro, L.; **Davison, R. T.**; Blum, T. R.; Vallabhaneni, D.; Fennell, C. E.; Cramer, S. L.; Shah, H. K.; Wholly, D. M.; Fink, E. A.; Sivak, J. T.; Ingalls, K. M.; Herr, C. T.; Lawson, V. E.; Burnett, M. R.; Slade, D. J.; Cole, K. E.; Carle, S. A.; Miller, J. S. Synthesis and Biological Evaluation of a Depsipeptidic Histone Deacetylase Inhibitor via a Generalizable Approach Using an Optimized Latent Thioester Solid-Phase Linker. *J. Org. Chem.* **2020**, *85*, 8253.
- (3) Yang, X.-Y.; **Davison, R. T.**; Nie, S.-Z.; Cruz, F. A.; McGinnis, T. M.; Dong, V. M. Catalytic Hydrothiolation: Counterion-Controlled Regioselectivity. *J. Am. Chem. Soc.* **2019**, *141*, 3006.
- (2) Nie, S.-Z.; **Davison, R. T.**; Dong, V. M. Enantioselective Coupling of Dienes and Phosphine Oxides. *J. Am. Chem. Soc.* **2018**, *140*, 16450.
- (1) Yang, X.-Y.; **Davison, R. T.**; Dong, V. M. Catalytic Hydrothiolation: Regio- and Enantioselective Coupling of Thiols and Dienes. *J. Am. Chem. Soc.* **2018**, *140*, 10443.

PRESENTATIONS

- (10) DOC Graduate Research Symposium, Albuquerque, NM, Nov 18–21, **2021** (poster).
- (9) Colgate-Palmolive Smile with Science Symposium, Virtual, Jul 23, **2021** (oral).
- (8) SoCal Merck Virtual Symposium, Virtual, Jul 19, **2021** (poster).
- (7) 2021 #RSCTwitter Poster Conference, Virtual, Mar 3, **2021** (poster).
- (6) 26th International RSC Symposium, Cambridge, UK, Jul 15–18, **2019**. (poster)
- (5) 257th ACS National Meeting, Orlando, FL, Mar 31–Apr 4, **2019**. (oral)
- (4) 255th ACS National Meeting, New Orleans, LA, Mar 18–22, **2018**. (poster)
- (3) HWS Senior Symposium, Geneva, NY, Apr 14, **2017**. (oral)
- (2) HWS Research Symposium, Geneva, NY, Sep 29, **2016**. (poster)
- (1) Summer Organic Research Symposium, Geneva, NY, Jul 6, **2016**. (oral)

Abstract of the Dissertation

Metal-Hydride Catalysis: Stereoselective Allylation and Hydroacylation

by

Ryan T. Davison

Doctor of Philosophy in Chemistry

University of California, Irvine, 2022

Professor Vy M. Dong, Chair

Hydrofunctionalization, which is defined as the addition of a hydrogen atom and another fragment to a degree of unsaturation, is an attractive method for transforming unsaturated hydrocarbons to value-added molecules. We developed Rh-, Pd-, and Cu-H catalysts that are capable of coupling both heteroatom and carbon nucleophiles to unsaturated hydrocarbons. The judicious choice of transition metal source (e.g., transition metal and counterion), bisphosphine ligand, and reaction conditions all play a role in selectively accessing one stereoisomeric product when many other outcomes exist.

In Chapter 1, we develop an enantioselective Rh-catalyzed addition of thiols to 1,3-dienes. The use of $\text{Rh}(\text{cod})_2\text{SbF}_6$ and a bisphosphine ligand allows for the synthesis of allylic sulfides with high regio- and enantiocontrol. The catalyst loading can be lowered to 0.1 mol% and an array of functional groups are compatible. By matching the bisphosphine ligand to the 1,3-diene's substitution pattern, we can transform a wide-range of 1,3-dienes (e.g., cyclic, disubstituted, and butadiene) into chiral sulfide building blocks.

In Chapter 2, we investigate the mechanism of the enantioselective 1,3-diene hydrothiolation (Chapter 1) and determine the fundamental steps that govern regioselectivity.

Guided by these insights, we then develop a complementary hydrothiolation to provide access to homoallylic sulfides. It is now possible for allylic and homoallylic sulfides to be synthesized in a regiodivergent manner by simply switching the Rh source. Mechanistic investigations shed light on the origin of the high regioselectivity observed for both hydrothiolations.

In Chapter 3, we showcase an enantioselective Pd-catalyzed 1,3-diene hydrophosphinylation. This method allows for complementary access to chiral tertiary phosphine oxides. Secondary phosphine oxides and 1,3-dienes can be coupled in high yields, regioselectivities, and enantioselectivities. Mechanistic studies suggest that the reaction proceeds through a reversible 1,3-diene hydrometallation followed by an irreversible C–P reductive elimination.

In Chapter 4, we found that Rh-H catalysis offers an approach to novel α -amino acids (α -AAs). Alkynes and α -nitroesters couple to form allylic α -AA precursors under mild conditions. We apply this method to the synthesis of an α,α -disubstituted α -amino ester. Moreover, initial mechanistic studies suggest that the isomerization of the alkyne starting material to an allene intermediate is reversible and occurs before C–C bond formation.

In Chapter 5, we report preliminary results for an enantioselective Cu-catalyzed olefin hydroacylation. This hydroacylation couples activated acyl electrophiles with α,β -unsaturated carbonyls to afford enantioenriched 1,3-dicarbonyls. The identity of the acyl electrophile has a pronounced effect on enantioselectivity. Future efforts are needed to (1) expand the scope of this transformation and (2) understand the step(s) that control enantioselectivity.

Preface

Over the course of my graduate studies I have had the opportunity to work on projects that center around transition metal-catalyzed hydrofunctionalization (Figure P.1). A common theme in these five research projects is controlling stereoselectivity; the ability to access one stereoisomeric product when other outcomes exist. With this context in mind, I collaborated on the development of three stereoselective 1,3-diene hydrofunctionalizations (Chapters 1–3). The initial leads in these projects were discovered by Drs. Xiao-Hui Yang and Shao-Zhen Nie. We collaborated to investigate the reactions' scopes and mechanisms. I then applied the garnered insights to two ideas that I discovered: an enantioselective addition of α -nitroesters to alkynes (Chapter 4) and a Cu-catalyzed hydroacylation (Chapter 5). I also had the opportunity to highlight our lab's contributions to the area of formyl C–H bond activation (not included in this dissertation). I worked in collaborative teams on all of the research projects and the *Accounts of Chemical Research* article (see the 'Authors Contribution' section within each chapter for further details). The goal of this preface is to provide necessary context for the five chapters of this dissertation (Chapters 1–4 have been published in peer-reviewed journals and are recreated with permission).

Chapters 1–4 of this dissertation detail a global strategy for stereoselective allylation that exploits metal-hydride catalysis. Our lab's interest in transition metal-catalyzed allylation stems from the fact that Nature uses a similar design for the biosynthesis of important carbon frameworks (Figure P.2).¹ A class of enzymes transform dimethylallyl pyrophosphate into a reactive allyl cation intermediate, which can then be captured with various nucleophiles to produce isoprenylated products (e.g., higher-order terpenoids).^{1b} It stands to reason that if allylation chemistry plays an important role in biosynthesis, then it could also be useful in the artificial synthesis of related molecules. While the structures of the six bioactive molecules in Figure P.2

may appear unrelated at first glance, allylation chemistry is a common thread that is involved in these molecules' biosynthesis and/or artificial synthesis.²

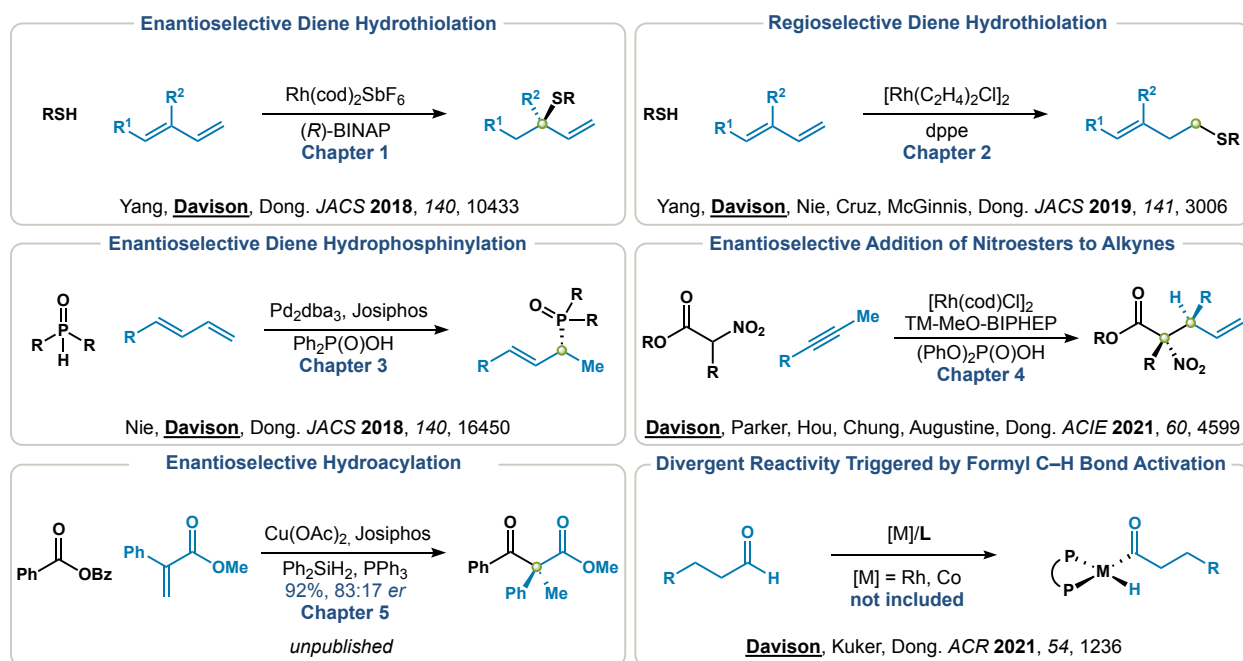
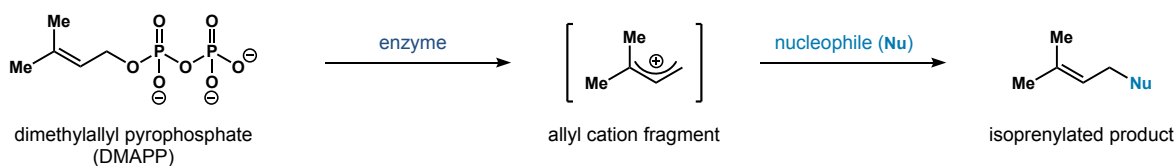


Figure P.1. Overview of the dissertation.

When it comes to artificial synthesis, the Tsuji-Trost reaction³ is arguably the most well-studied and relied upon transformation for installing an allyl fragment in an asymmetric fashion.⁴ As detailed in Figure P.3, the Tsuji-Trost reaction closely resembles Nature's biosynthesis of terpenoids. At its basics, both platforms use: (1) an allylation reagent that contains an allylic leaving group motif, (2) a mode of activating said reagent, and (3) a chiral environment for introducing asymmetry. Said in another way, the Tsuji-Trost reaction uses a transition metal catalyst (typically Pd) to convert allylic leaving group motifs into metal- π -allyl intermediates, which can then be captured with a host of nucleophiles. However, one downfall of this approach is the generation of stoichiometric byproducts related to the leaving group's waste stream. Nonetheless, the mild and straightforward access to synthetically versatile metal- π -allyl complexes has made the Tsuji-Trost reaction a staple in organic synthesis.⁵

Nature's Approach: Enzyme-Controlled Allyl Cation Chemistry



Natural Products and Drugs that Involve Allylation Chemistry

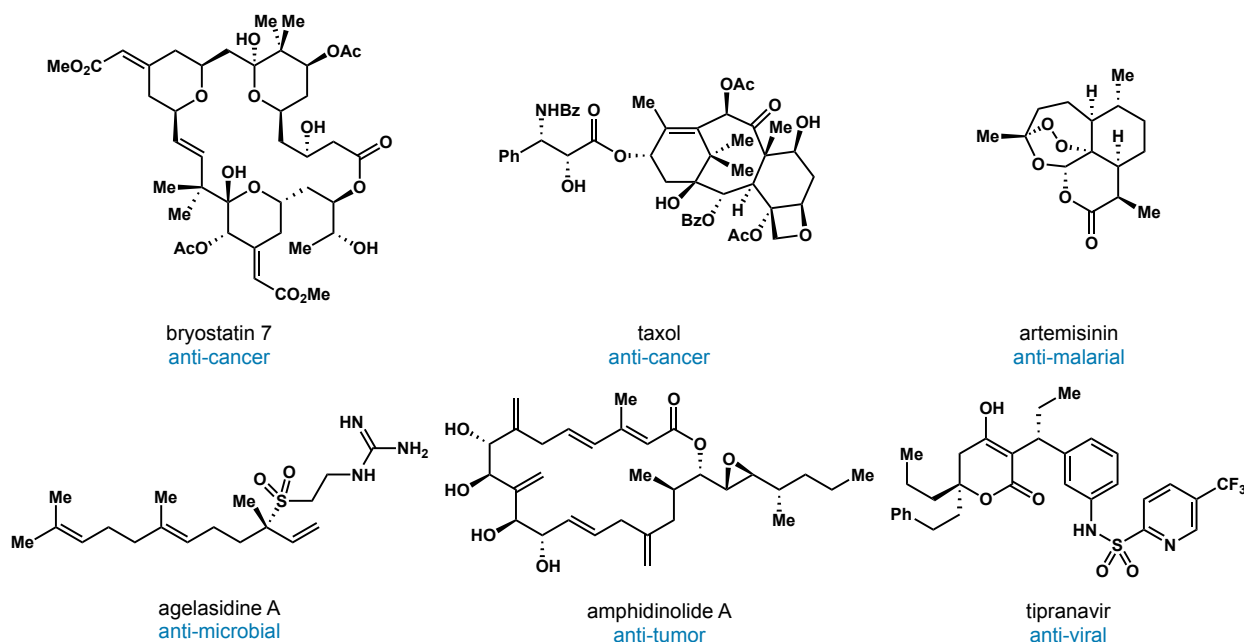


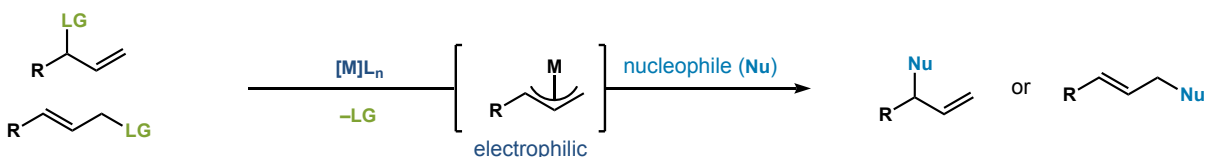
Figure P.2. Allylation chemistry in natural product and drug synthesis.

When thinking about complementary access to Tsuji-Trost type reactivity, our lab turned to transition metal-catalyzed hydrofunctionalization.⁶ Hydrofunctionalization of unsaturated hydrocarbons offers an atom-economical⁷ approach to metal- π -allyl complexes (Figure P.3). Allenes,⁸ 1,3-dienes,⁹ and alkynes¹⁰ have been shown to be suitable precursors for the synthesis of metal- π -allyl complexes. Moreover, by selecting the appropriate conditions, both nucleophilic and electrophilic metal- π -allyl intermediates can be accessed.^{10a,10c} Several research groups have shown that Ru, Ir, and Cu catalysts can furnish nucleophilic metal- π -allyl complexes, whereas Pd and Rh tend to form electrophilic species.⁸⁻¹¹

When I joined Professor Vy Dong's laboratory, we were interested in developing hydrofunctionalizations that proceed through electrophilic metal- π -allyl species due to the

parallels with Nature's approach. We wanted to discover new methods in this area that met both of the following goals: (1) controlling stereoselectivity and (2) finding novel reactivity. Our approach to achieving these two goals was centered around catalyst development. We hypothesized that by studying stereoselective hydrofunctionalizations, we could identify the principles that govern stereoselectivity and reactivity.

Tsuji-Trost Reaction



Transition Metal-Catalyzed Hydrofunctionalization

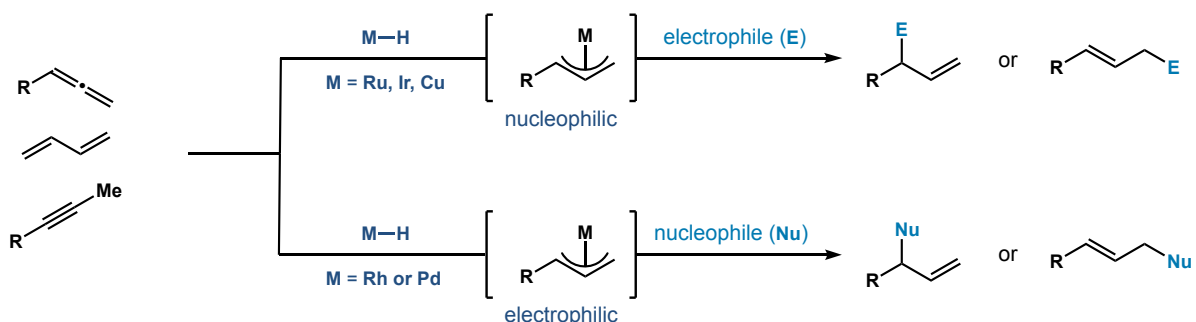
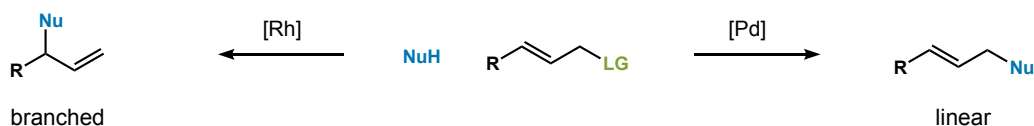


Figure P.3. Tsuji-Trost reaction versus transition metal-catalyzed hydrofunctionalization.

With regards to controlling stereoselectivity, a typical Tsuji-Trost allylation offers the possibility of forming two regioisomers, a branched and linear product (Figure P.4). Seminal reports demonstrated that Pd-catalysis typically favors linear products,³⁻⁵ whereas other transition metal catalysts (e.g., Rh) are capable of forming branched products.¹² While the same trends tend to hold true for transition metal-catalyzed hydrofunctionalization,^{8-10,13} additional regioselectivity challenges arise when using unsaturated hydrocarbons. The first three projects I was part of all focused on functionalizing 1,3-dienes. With this in mind, a simple thought experiment reveals that the hydrofunctionalization of a 2-substituted-1,3-diene can afford a total of 11 possible

stereoisomers, with 6 different regioisomers (Figure P.4). We became interested in discovering catalysts that could selectively access one regioisomer, with the ultimate goal of developing a catalyst library that could access all possible stereoisomers (see Chapters 1–3).¹⁴⁻¹⁶

Tsuji-Trost Reaction: Branched Versus Linear Selectivity



Hydrofunctionalization of a 2-Substituted Diene Affords 11 Possible Stereoisomers

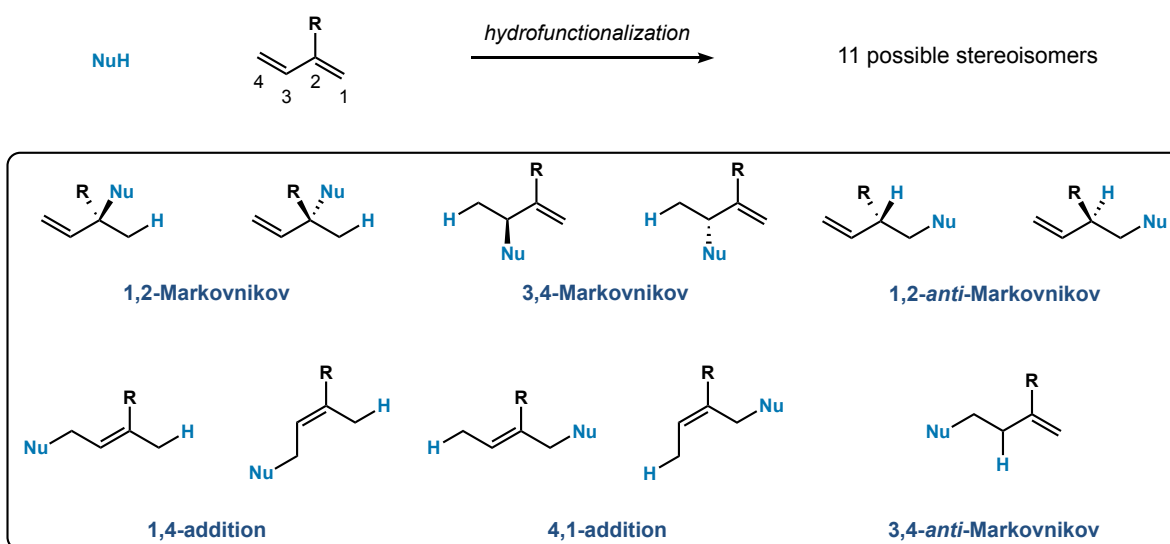


Figure P.4. Additional regioselectivity challenges associated with hydrofunctionalization.

After collaborating on the development of three hydrofunctionalizations that couple heteroatom nucleophiles to 1,3-dienes, I turned my attention to carbon nucleophiles. I discovered two enantioselective methods that form amino acid precursors (Chapter 4)¹⁷ and 1,3-dicarbonyls (Chapter 5). In the former example, I pursued alkyne hydrofunctionalization because only a few reports of asymmetric additions of carbon nucleophiles were known at the time.¹⁸ In the latter example, a novel hydroacylation affords 1,3-dicarbonyls in a complementary fashion to the Claisen reaction. While hydroacylation does not seemingly fit with the theme of this dissertation,

it is a necessary contribution because it represents our lab's future in transition metal-catalyzed hydrofunctionalization: the pursuit of more sustainable first-row transition metal catalysts.

Preface References

- (1) For reviews on terpene biosynthesis, see: (a) Tantillo, D. J. *Nat. Prod. Rep.* **2011**, *28*, 1035–1053. (b) Oldfield, E.; Lin, F.-Y. *Angew. Chem. Int. Ed.* **2012**, *51*, 1124–1137.
- (2) (a) Lu, Y.; Woo, S. K.; Krische, M. J. *J. Am. Chem. Soc.* **2011**, *133*, 13876–13879. (b) Croteau, R.; Ketchum, R. E. B.; Long, R. M.; Kaspera, R.; Wildung, M. R. *Phytochem. Rev.* **2006**, *5*, 75–97. (c) Wen, W.; Yu, R. *Pharmacogn. Rev.* **2011**, *5*, 189–194. (d) Ichikawa, Y.; Kashiwagi, T.; Urano, N. *J. Chem. Soc., Chem. Commun.* **1989**, 987–988. (e) Trost, B. M.; Chisholm, J. D.; Wroblewski, S. T.; Jung, M. *J. Am. Chem. Soc.* **2002**, *124*, 12420–12421. (f) Trost, B. M.; Andersen, N. G. *J. Am. Chem. Soc.* **2002**, *124*, 14320–14321.
- (3) Trost, B. M.; Van Vranken, D. L. *Chem. Rev.* **1996**, *96*, 395–422.
- (4) For the use of the Tsuji-Trost reaction in asymmetric total synthesis, see: (a) Trost, B. M.; Crawley, M. L. *Chem. Rev.* **2003**, *103*, 2921–2944. (b) Lu, Z.; Ma, S. *Angew. Chem. Int. Ed.* **2007**, *47*, 258–297.
- (5) For a recent review on the Tsuji-Trost reaction, see: Noreen, S.; Zahoor, A. F.; Ahmad, S.; Shahzadi, I.; Irfan, A.; Faiz, S. *Curr. Org. Chem.* **2019**, *23*, 1168–1213.
- (6) Hydrofunctionalization. In *Topics in Organometallic Chemistry*; Ananikov, V. P., Tanaka, M., Eds.; Springer: Berlin, **2014**; Vol. 343.
- (7) Trost, B. M. *Science* **1991**, *254*, 1471–1477.
- (8) For reviews, see: (a) Blicek, R.; Taillefer, M.; Monnier, F. *Chem. Rev.* **2020**, *120*, 13545–13598. (b) Koschker, P.; Breit, B. *Acc. Chem. Res.* **2016**, *49*, 1524–1536. For select examples, see: (c) Kim, I. S.; Krische, M. J. *Org. Lett.* **2008**, *10*, 513–515. (d) Koschker, P.; Lumbroso, A.; Breit, B. *J. Am. Chem. Soc.* **2011**, *133*, 20746–20749.
- (9) For reviews, see: ref 6 and (a) McNeill, E.; Ritter, T. *Acc. Chem. Res.* **2015**, *48*, 2330–2343. For select examples, see: (b) Löber, O.; Kawatsura, M.; Hartwig, J. F. *J. Am. Chem. Soc.* **2001**, *123*, 4366–4367. (c) Zbieg, J. R.; Yamaguchi, E.; McInturff, E. L.; Krische, M. J. *Science* **2012**, *336*, 324–327. (d) Adamson, N. J.; Wilbur, K. C. E.; Malcolmson, S. J. *J. Am. Chem. Soc.* **2018**, *140*, 2761–2764. (e) Schmidt, V. A.; Rose Kennedy, C.; Bezdek, M. J.; Chirik, P. J. *J. Am. Chem. Soc.* **2018**, *140*, 3443–3453.
- (10) For reviews, see: ref 8b and (a) Haydl, A. M.; Breit, B.; Liang, T.; Krische, M. J. *Angew. Chem. Int. Ed.* **2017**, *56*, 11312–11325. (b) Thoke, M. B.; Kang, Q. *Synthesis* **2019**, *51*, 2585–2631. (c) Li, G.; Huo, X.; Jiang, X.; Zhang, W. *Chem. Soc. Rev.* **2020**, *49*, 2060–2118. For select examples, see: (d) Kadota, I.; Shibuya, A.; Gyoung, Y. S.; Yamamoto, Y. *J. Am. Chem. Soc.* **1998**, *120*, 10262–10263. (e) Liang, T.; Zhang, W.; Krische, M. J. *J. Am. Chem. Soc.* **2015**, *137*, 16024–16027. (f) Wolf, J.; Werner, H. *Organometallics* **1987**, *6*, 1164–1169.
- (11) For examples of Cu-H mediated allylations, see: (a) Jordan, A. J.; Lalic, G.; Sadighi, J. P. *Chem. Rev.* **2016**, *116*, 8318–8372. (b) Liu, R. Y.; Buchwald, S. L. *Acc. Chem. Res.* **2020**, *53*, 1229–1243.
- (12) (a) Evans, P. A.; Leahy, D. K. *J. Am. Chem. Soc.* **2002**, *124*, 7882–7883. (b) Wright, T. B.; Evans, P. A. *Chem. Rev.* **2021**, *121*, 9196–9242.
- (13) (a) Chen, Q.-A.; Chen, Z.; Dong, V. M. *J. Am. Chem. Soc.* **2015**, *137*, 8392–8395. (b) Yang, X.-H.; Dong, V. M. *J. Am. Chem. Soc.* **2017**, *139*, 1774–1777.
- (14) Yang, X.-Y.; Davison, R. T.; Dong, V. M. *J. Am. Chem. Soc.* **2018**, *140*, 10443–10446.
- (15) Yang, X.-Y.; Davison, R. T.; Nie, S.-Z.; Cruz, F. A.; McGinnis, T. M.; Dong, V. M. *J. Am. Chem. Soc.* **2019**, *141*, 3006–3013.
- (16) Nie, S.-Z.; Davison, R. T.; Dong, V. M. *J. Am. Chem. Soc.* **2018**, *140*, 16450–16454.

(17) Davison, R. T.; Parker, P. D.; Hou, X.; Chung, C. P.; Augustine, S. A.; Dong, V. M. *Angew. Chem. Int. Ed.* **2021**, *60*, 4599–4603.

(18) (a) Cruz, F. A.; Dong, V. M. *J. Am. Chem. Soc.* **2017**, *139*, 1029–1032. (b) Cruz, F. A.; Zhu, Y.; Tercenio, Q. D.; Shen, Z.; Dong, V. M. *J. Am. Chem. Soc.* **2017**, *139*, 10641–10644. (c) Xie, L.; Yang, H.; Ma, M.; Xing, D. *Org. Lett.* **2020**, *22*, 2007–2011. (d) Ji, D.-W.; Yang, F.; Chen, B.-Z.; Min, X.-T.; Kuai, C.-S.; Hu, Y.-C.; Chen, Q.-A. *Chem. Commun.* **2020**, *56*, 8468–8471.

Chapter 1 – Catalytic Hydrothiolation: Regio- and Enantioselective Coupling of Thiols and Dienes¹

1.1 Introduction

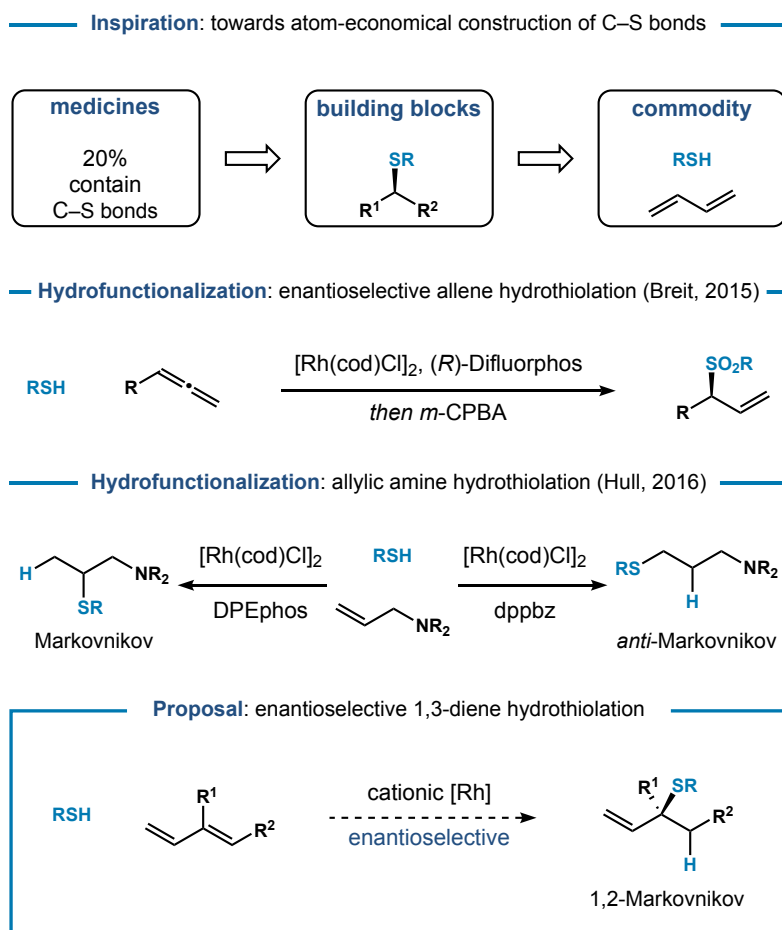


Figure 1.1. Asymmetric 1,3-diene hydrothiolation.

The pursuit of catalysts capable of forging C–S bonds is a valuable goal, as molecules essential to life, from metabolites to macromolecules, contain sulfur atoms.¹ In addition, approximately 20% of all FDA approved drugs are organosulfur compounds.² The direct addition of a thiol to a degree of unsaturation represents an attractive and atom-economical³ approach for generating C–S bonds.⁴ Inspired by this challenge, we chose to focus on the hydrothiolation of

¹ Adapted with permission from Yang, X.-H.; Davison, R. T.; Dong, V. M. *J. Am. Chem. Soc.* **2018**, *140*, 10443–10446. © 2018 American Chemical Society

conjugated dienes, which are readily available and include commodity chemicals, like butadiene and isoprene (Figure 1.1).⁵ One previous hydrothiolation of 1,3-dienes was reported by He, where the application of Au catalysts resulted in racemic mixtures.⁶ By using Rh catalysis, Breit pioneered an enantioselective hydrothiolation of allenes⁷ and Hull achieved a regiodivergent addition to allylic amines.⁸ As a complement to these strategies, we found that Rh catalysts generate allylic sulfides from 1,3-dienes in a regio- and enantioselective fashion, thus allowing petroleum feedstocks to be transformed into enantioenriched building blocks.⁹

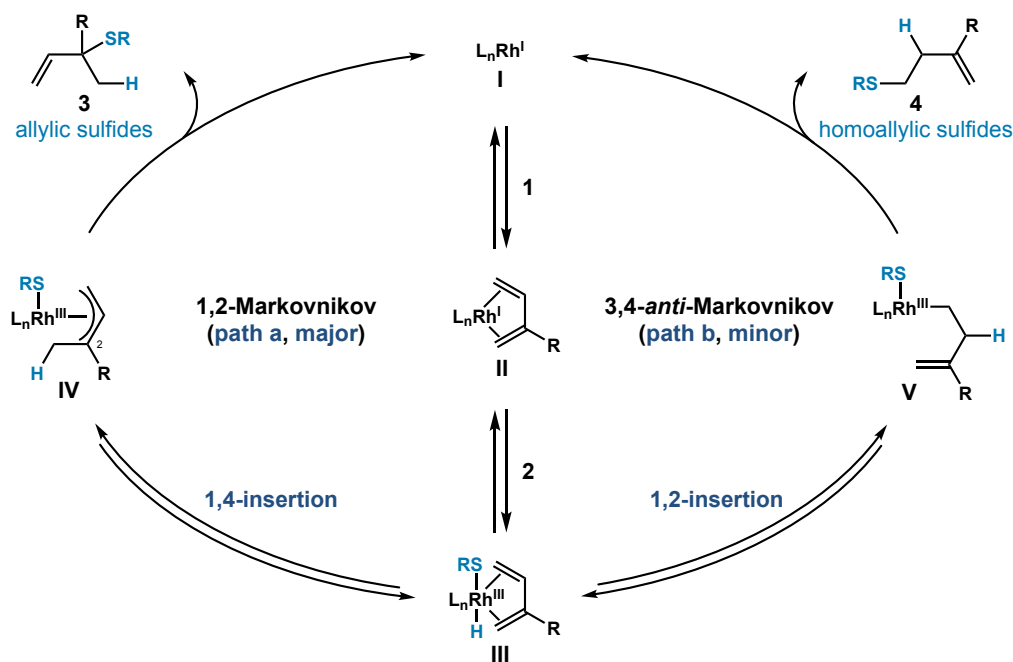


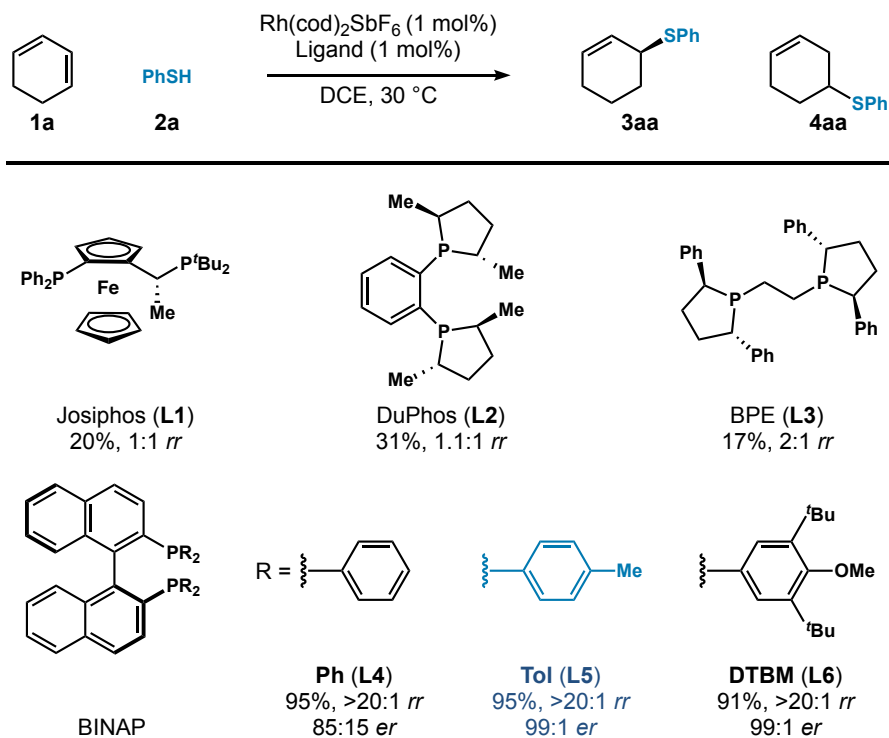
Figure 1.2. Proposed Rh-catalyzed hydrothiolation mechanism.

Though asymmetric hydroamination of dienes has been demonstrated,¹⁰ thiols are more nucleophilic and acidic than amines, thus providing distinct challenges and opportunities for hydrofunctionalization.^{11,12} In this study, we focus on Rh complexes **I**, which we imagined could bind and activate the diene **1** by η^4 -coordination (Figure 1.2). The resulting olefin complex **II** undergoes oxidative addition to a thiol **2** to yield **III**. From **III**, Rh-H insertion can occur via 1,4 or 1,2-insertion, wherein Rh adds to the less hindered position of the diene. In path a, migratory

insertion provides a Rh- π -allyl **IV** after 1,4-insertion. Because reductive elimination tends to favor branched products,¹³ we reasoned **IV** would yield tertiary allylic sulfides **3**.¹⁴ In path b, 1,2-insertion provides **V** and reductive elimination gives homoallylic sulfides **4**.

1.2 Results and Discussion

Table 1.1. Ligand effects on asymmetric hydrothiolation.^[a]



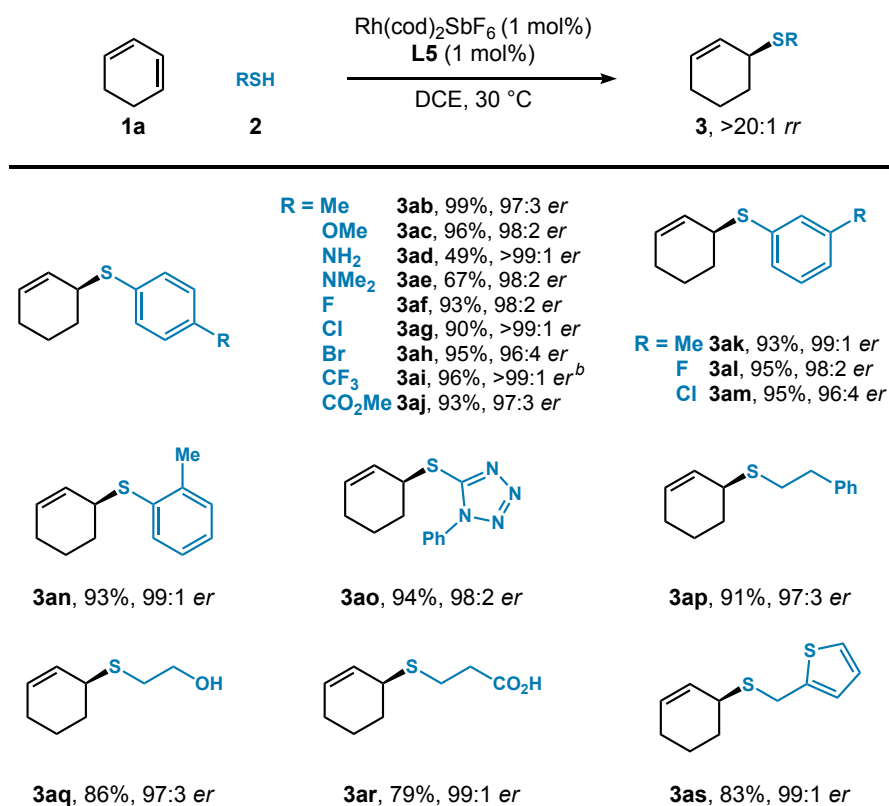
^[a]Reaction conditions: **1a** (0.2 mmol), **2a** (0.1 mmol), $\text{Rh}(\text{cod})_2\text{SbF}_6$ (1 mol%), ligand (1 mol%), DCE (0.2 mL), 30 °C, 3 h. Isolated yields. Regioselectivity ratio (*rr*) is the ratio of **3aa** to **4aa**, which is determined by ¹H NMR analysis of the crude reaction mixture. Enantioselectivity ratio (*er*) is determined by chiral SFC.

With this hypothesis in mind, we chose cyclohexadiene (**1a**) as the model substrate because its symmetric structure minimizes the number of possible isomers. We studied the coupling of **1a** and thiophenol (**2a**) using different bisphosphine ligands in the presence of $\text{Rh}(\text{cod})_2\text{SbF}_6$ (Table 1.1). With the Josiphos (**L1**), DuPhos (**L2**), and BPE (**L3**) ligands, we observe a mixture of the allylic and homoallylic sulfides. In contrast, the BINAP ligand family affords excellent regioselectivity for the allylic sulfide **3aa** (>20:1 *rr*) in high yields ($\geq 91\%$) and enantioselectivity

($\geq 85:15$ *er*). With (*S*)-Tol-BINAP (**L5**), we can lower the catalyst loading to 0.1 mol% and isolate (*S*)-sulfide **3aa**¹⁵ on gram scale (1.2 g, 95% yield, 99:1 *er*).

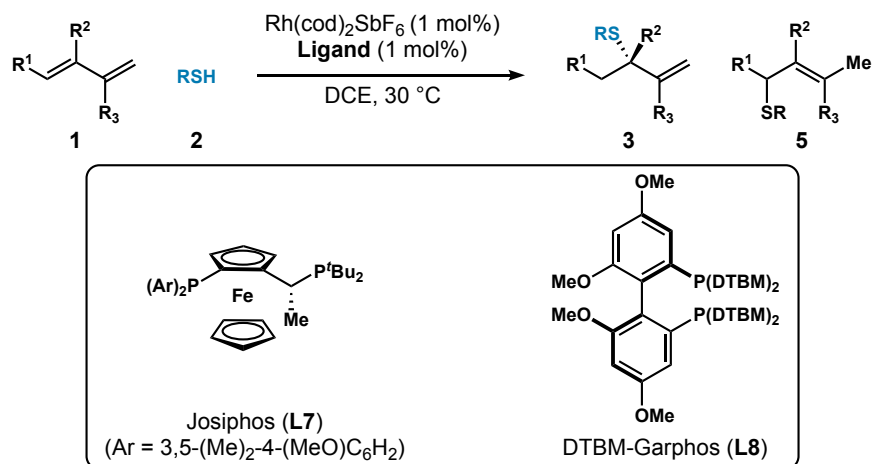
Table 1.2 showcases the scope of this method with 18 different thiols and **1a**, using catalyst Rh(**L5**). High reactivity (**3ab–3as**, 49–99%), enantioselectivity (96:4–>99:1 *er*), and regioselectivity (18:1–>20:1 *rr*) are observed with both aliphatic and aromatic thiol partners. Tertiary thiols (such as *tert*-butylthiol and triphenylmethanethiol) are unreactive thus far, presumably due to steric hindrance. This method is compatible with heteroaryl (**3ao**,¹⁶ **3as**), hydroxyl (**3aq**), carboxyl (**3ar**), amino (**3ad**, **3ae**), and ester groups (**3aj**).

Table 1.2. Hydrothiolation with various thiols.^[a]

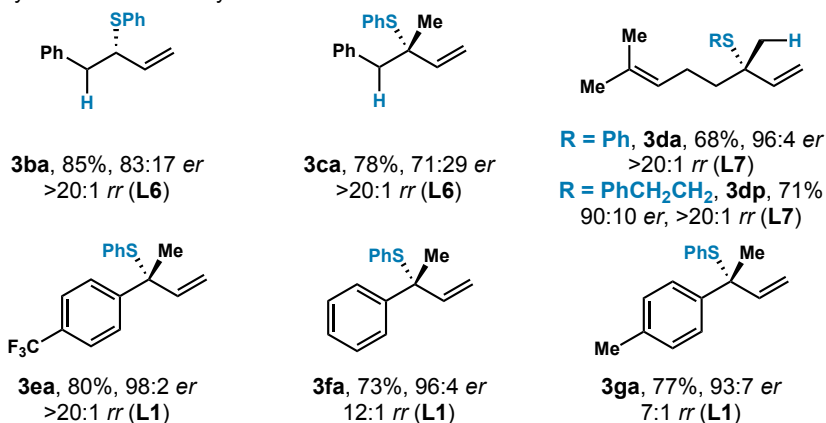


^[a]Reaction conditions: **1a** (0.4 mmol), **2** (0.2 mmol), Rh(cod)₂SbF₆ (1 mol%), **L5** (1 mol%), DCE (0.4 mL), 30 °C, 5 h. Isolated yields. Regioselectivity ratio (*rr*) is the ratio of **3** to **4**, which is determined by ¹H NMR analysis of the crude reaction mixture. Enantioselectivity ratio (*er*) determined by chiral SFC. ^[b]18:1 *rr*.

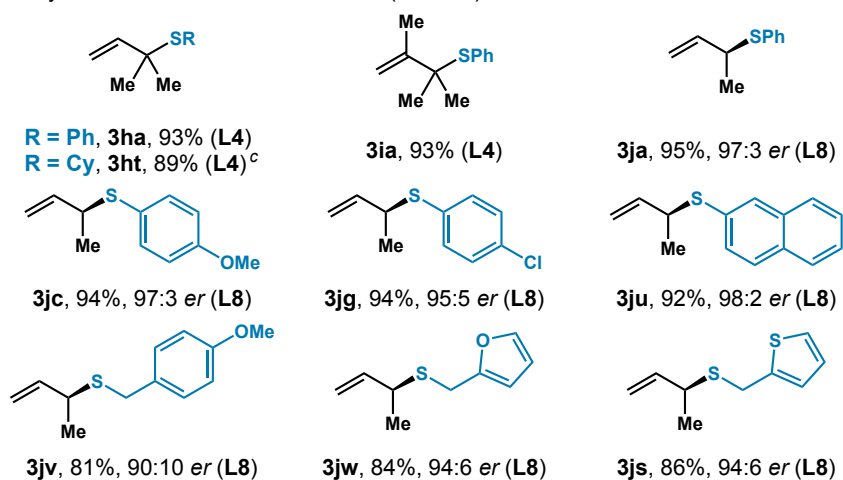
Table 1.3. Hydrothiolation of various 1,3-dienes.^[a]



A. Hydrothiolation of unsymmetric dienes^b



B. Hydrothiolation of feedstock dienes (>20:1 *rr*)



^[a]Reaction conditions: **1** (0.4 mmol), **2** (0.2 mmol), Rh(cod)₂SbF₆ (1 mol%), **L** (1 mol%), DCE (0.4 mL), 30 °C, 5 h. Isolated yields. Ligand used in parentheses. Regioselectivity ratio (*rr*) is the ratio of **3** to **5**, which is determined by ¹H NMR analysis of the crude reaction mixture. Enantioselectivity ratio (*er*) is determined by chiral SFC. ^[b]Using Rh(cod)₂SbF₆ (5 mol%), **L** (5 mol%), 15 h. ^[c]13:1 *rr*.

Next, we investigated hydrothiolation of unsymmetric 1,3-dienes (Table 1.3A). For 1-substituted (**1b**) and 1,2-disubstituted (**1c**) dienes, we found that a bulkier BINAP ligand (**L6**) affords the best results (85%, 83:17 *er* and 78%, 71:29 *er*; respectively). In contrast, the 2-substituted-1,3-dienes reacted poorly in the presence of BINAP ligands. In this case, the Josiphos ligands provide a breakthrough. With **L7**, myrcene (**3d**) can be coupled with an aromatic thiol (**3da**, 68% yield, 96:4 *er*, >20:1 *rr*) and an aliphatic thiol (**3dp**, 71% yield, 90:10 *er*, >20:1 *rr*). 2-Aryl-1,3-dienes undergo hydrothiolation as well (**3ea–3ga**, 73–80%, 93:7–98:2 *er*). The presence of an electron-withdrawing substituent (**3ea**) provides higher regioselectivity (>20:1 *rr*) compared to an electron-donating substituent (**3ga**, 7:1 *rr*).

Isoprene and butadiene are petroleum feedstocks, produced on a million metric ton scale every year and used as monomers to make plastics.¹⁷ Hydrothiolation of isoprene (**1h**) with thiophenol (**2a**) and cyclohexanethiol (**2t**) gives the corresponding tertiary sulfides (**3ha** and **3ht**) in ≥89% yield and ≥13:1 *rr* (Table 1.3B). A commercial diene, 2,3-dimethyl-1,3-butadiene (**1i**), transforms into the tertiary sulfide **3ia** (93%, >20:1 *rr*). The construction of chiral products from butadiene remains a challenge that has inspired hydrohydroxyalkylation,^{5c} cycloadditions¹⁸ and difunctionalizations.¹⁹ To meet this challenge, we simply switched the ligand to DTBM-Garphos (**L8**). With Rh(**L8**), high reactivity (81–95%) and regioselectivity (>20:1 *rr*) are achieved using both aliphatic and aromatic thiols. The products derived from aromatic thiols (**3ja**, **3jc**, **3jg**, **3ju**) are obtained in higher enantioselectivities (95:5–98:2 *er*) than those from aliphatic thiols (**3jv**, **3jw**, **3js**, 90:10–94:6 *er*).

Aside from enantioselective examples, we examined the addition of a L-cysteine ester **2x** to 1,3-cyclohexadiene (Figure 1.3). Either diastereomeric product, **3ax** or **3ax'**, can be generated with high diastereoselectivity (>20:1 *dr*), depending on the enantiomer of **L5** employed.

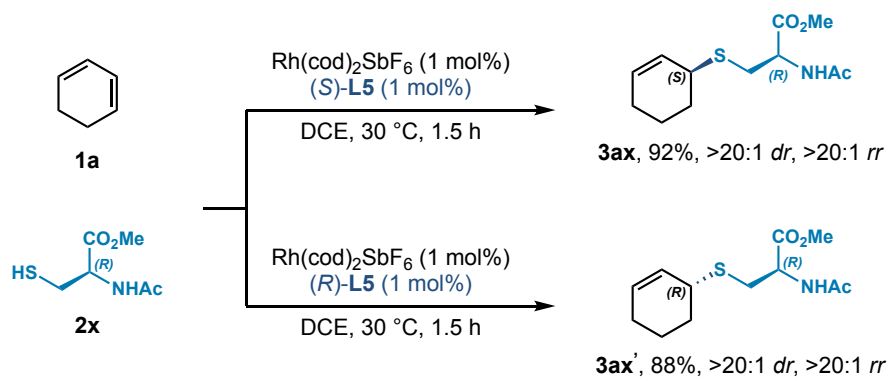


Figure 1.3. Catalyst-controlled diastereoselective hydrothiolation.

1.3 Conclusion and Future Work

In principle, the coupling of a thiol and unsymmetrical diene (e.g., 2-phenyl-1,3-diene, **1f**) can result in up to 11 different isomers.²⁰ In addition to stereoisomers, constitutional isomers may arise due to competing 1,2 versus 1,4-addition, as well as *anti*-Markovnikov versus Markovnikov regioselectivity. By using Rh(cod)₂SbF₆ with a bisphosphine ligand, we obtain allylic sulfides with high chemo-, regio-, and enantiocontrol. The catalyst loading can be lowered to 0.1 mol% and an array of functional groups are compatible, including heteroaryl, hydroxyl, carboxyl, amino, and ester groups. By choosing the appropriate bisphosphine ligand, we can transform a wide range of dienes into chiral sulfides. The observed regiocontrol supports a mechanism distinct from what was previously proposed for related hydroaminations.^{5h,10a} Further studies are warranted to elucidate the mechanism and develop access to other regioisomers.

1.4 Author Contributions

Dr. Xiao-Hui Yang (X.-H.Y.), Ryan T. Davison (R.T.D.), and Prof. Vy M. Dong (V.M.D.) conceived of the project discussed in Chapter 1. X.-H.Y., R.T.D., and V.M.D. co-wrote the text. X.-H.Y. discovered the initial optimized asymmetric conditions for the hydrothiolation. R.T.D. identified the optimal conditions for cyclohexadiene hydrothiolation (Table 1.1) and surveyed 18 thiols as seen in Table 1.2. X.-H.Y. identified the optimal ligands for Table 1.3 and surveyed the

diene scope. R.T.D. demonstrated a catalyst-controlled diastereoselective hydrothiolation (Figure 1.3). All authors analyzed the results and commented on the manuscript.

1.5 References

- (1) For reviews on C–S bond formation, see: (a) Kondo, T.; Mitsudo, T.-A. *Chem. Rev.* **2000**, *100*, 3205–3220. (b) Arisawa, M.; Yamaguchi, M. *Pure Appl. Chem.* **2008**, *80*, 993–1003. (c) Chauhan, P.; Mahajan, S.; Enders, D. *Chem. Rev.* **2014**, *114*, 8807–8864. (d) Shen, C.; Zhang, P.; Sun, Q.; Bai, S.; Andy Hor, T. S.; Liu, X. *Chem. Soc. Rev.* **2015**, *44*, 291–314. (e) Yu, J.-S.; Huang, H.-M.; Ding, P.-G.; Hu, X.-S.; Zhou, F.; Zhou, J. *ACS Catal.* **2016**, *6*, 5319–5344. (f) Qiao, A.; Jiang, X. *Org. Biomol. Chem.* **2017**, *15*, 1942–1946. For review on enzymatic C–S bond formation, see: (g) Dunbar, K. L.; Scharf, D. H.; Litomska, A.; Hertweck, C. *Chem. Rev.* **2017**, *117*, 5521–5577.
- (2) (a) McGrath, N. A.; Brichacek, M.; Njardarson, J. T. *J. Chem. Educ.* **2010**, *87*, 1348–1349. (b) Scott, K. A.; Njardarson, J. T. *Top. Curr. Chem.* **2018**, *376*, 1–34.
- (3) Trost, B. M. *Science* **1991**, *254*, 1471–1477.
- (4) For enantioselective additions to Michael acceptors, see: ref. 1c.
- (5) For select examples of hydrofunctionalizations of dienes, see: (a) Löber, O.; Kawatsura, M.; Hartwig, J. F. *J. Am. Chem. Soc.* **2001**, *123*, 4366–4367. (b) Page, J. P.; RajanBabu, T. V. *J. Am. Chem. Soc.* **2012**, *134*, 6556–6559. (c) Zbieg, J. R.; Yamaguchi, E.; McInturff, E. L.; Krische, M. J. *Science* **2012**, *336*, 324–327. (d) Park, B. Y.; Montgomery, T. P.; Garza, V. J.; Krische, M. J. *J. Am. Chem. Soc.* **2013**, *135*, 16320–16323. (e) Saini, V.; O’Dair, M.; Sigman, M. S. *J. Am. Chem. Soc.* **2015**, *137*, 608–611. (f) Nguyen, K. D.; Herkommer, D.; Krische, M. J. *J. Am. Chem. Soc.* **2016**, *138*, 14210–14213. (g) Marcum, J. S.; Roberts, C. C.; Manan, R. S.; Cervarich, T. N.; Meek, S. J. *J. Am. Chem. Soc.* **2017**, *139*, 15580–15583. (h) Yang, X.-H.; Lu, A.; Dong, V. M. *J. Am. Chem. Soc.* **2017**, *139*, 14049–14052. (i) Gui, Y.-Y.; Hu, N.; Chen, X.-W.; Liao, L.-L.; Ju, T.; Ye, J.-H.; Zhang, Z.; Li, J.; Yu, D.-G. *J. Am. Chem. Soc.* **2017**, *139*, 17011–17014. (j) Adamson, N. J.; Wilbur, K. C. E.; Malcolmson, S. J. *J. Am. Chem. Soc.* **2018**, *140*, 2761–2764. (k) Liu, Y.; Fiorito, D.; Mazet, C. *Chem. Sci.* **2018**, *9*, 5284–5288. (l) Schmidt, V. A.; Rose Kennedy, C.; Bezdek, M. J.; Chirik, P. J. *J. Am. Chem. Soc.* **2018**, *140*, 3443–3453. For reviews, see: (m) Hydrofunctionalization. In *Topics in Organometallic Chemistry*; Ananikov, V. P., Tanaka, M., Eds.; Springer: Berlin, **2014**; Vol. 343. (n) McNeill, E.; Ritter, T. *Acc. Chem. Res.* **2015**, *48*, 2330–2343.
- (6) This Au-catalyzed hydrothiolation provides racemic isomers resulting from 3,4-Markovnikov regioselectivity, see: Brouwer, C.; Rahaman, R.; He, C. *Synlett* **2007**, *11*, 1785–1789.
- (7) (a) Pritzius, A. B.; Breit, B. *Angew. Chem. Int. Ed.* **2015**, *54*, 3121–3125. (b) Pritzius, A. B.; Breit, B. *Angew. Chem. Int. Ed.* **2015**, *54*, 15818–15822.
- (8) Kennemur, J. L.; Kortman, G. D.; Hull, K. L. *J. Am. Chem. Soc.* **2016**, *138*, 11914–11919.
- (9) For the use of sulfides as ligands, see: (a) Mellah, M.; Voituriez, A.; Schulz, E. *Chem. Rev.* **2007**, *107*, 5133–5209. For the use of sulfides in enantioselective rearrangements, see: (b) Schaumann, E. *Top. Curr. Chem.* **2007**, *274*, 1–173. For the use of sulfides in cross-coupling, see: (c) Modha, S. G.; Mehta, V. P.; Van der Eycken, E. K. *Chem. Soc. Rev.* **2013**, *42*, 5042–5055.
- (10) (a) Yang, X.-H.; Dong, V. M. *J. Am. Chem. Soc.* **2017**, *139*, 1774–1777. (b) Adamson, N. J.; Hull, E.; Malcolmson, S. J. *J. Am. Chem. Soc.* **2017**, *139*, 7180–7183.
- (11) For select examples of transition metal-catalyzed hydrothiolation of alkynes, see: (a) Kuniyasu, H.; Ogawa, A.; Sato, K.-I.; Ryu, I.; Kambe, N.; Sonoda, N. *J. Am. Chem. Soc.* **1992**, *114*, 5902–5903. (b) Ogawa, A.; Ikeda, T.; Kimura, K.; Hirao, T. *J. Am. Chem. Soc.* **1999**, *121*, 5108–5114. (c) Cao, C.; Fraser, L. R.; Love, J. A. *J. Am. Chem. Soc.* **2005**, *127*, 17614–17615. (d)

Yang, J.; Sabarre, A.; Fraser, L. A.; Patrick, B. O.; Love, J. A. *J. Org. Chem.* **2009**, *74*, 182–187. (e) Di Giuseppe, A.; Castarlenas, R.; Pérez-Torrente, J. J.; Crucianelli, M.; Polo, V.; Sancho, R.; Lahoz, F. J.; Oro, L. A. *J. Am. Chem. Soc.* **2012**, *134*, 8171–8183.

(12) For select transition metal-catalyzed hydrothiolation of alkenes, see: (a) Tamai, T.; Fujiwara, K.; Higashimae, S.; Nomoto, A.; Ogawa, A. *Org. Lett.* **2016**, *18*, 2114–2117. (b) Cabrero-Antonino, J. R.; Leyva-Pérez, A.; Corma, A. *Adv. Synth. Catal.* **2012**, *354*, 678–687. (c) Tamai, T.; Ogawa, A. *J. Org. Chem.* **2014**, *79*, 5028–5035. (d) Yi, H.; Song, C.; Li, Y.; Pao, C.-W.; Lee, J.-F.; Lei, A. *Chem. Eur. J.* **2016**, *22*, 18331–18334.

(13) (a) Chen, Q.-A.; Chen, Z.; Dong, V. M. *J. Am. Chem. Soc.* **2015**, *137*, 8392–8395. (b) Cruz, F. A.; Dong, V. M. *J. Am. Chem. Soc.* **2017**, *139*, 1029–1032. For reviews, see: (c) Koschker, P.; Breit, B. *Acc. Chem. Res.* **2016**, *49*, 1524–1536. (d) Haydl, A. M.; Breit, B.; Liang, T.; Krische, M. J. *Angew. Chem. Int. Ed.* **2017**, *56*, 11312–11325.

(14) For a review on enantioselective synthesis of tertiary allylic sulfides, see: ref 1e.

(15) The absolute configuration of **3aa** was assigned as *S* in accordance with: Gais, H.-J.; Böhme, A. *J. Org. Chem.* **2002**, *67*, 1153–1161.

(16) The corresponding sulfone has been used in cross-coupling reactions, see: Merchant, R. R.; Edwards, J. T.; Qin, T.; Kruszyk, M. M.; Bi, C.; Che, G.; Bao, D.-H.; Qiao, W.; Sun, L.; Collins, M. R.; Fadeyi, O. O.; Gallego, G. M.; Mousseau, J. J.; Nuhant, P.; Baran, P. S. *Science* **2018**, *360*, 75–80.

(17) For reviews, see: (a) Ezinkwo, G. O.; Tretjakov, V. F.; Talyshinky, R. M.; Ilolov, A. M.; Mutombo, T. A. *Catal. Sustainable Energy* **2013**, *1*, 100–111. (b) Makshina, E. V.; Dusselier, M.; Janssens, W.; Degreève, J.; Jacobs, P. A.; Sels, B. F. *Chem. Soc. Rev.* **2014**, *43*, 7917–7953.

(18) (a) Corey, E. J.; Shibata, T.; Lee, T. W. *J. Am. Chem. Soc.* **2002**, *124*, 3808. (b) Ryu, D. H.; Corey, E. J. *J. Am. Chem. Soc.* **2003**, *125*, 6388–6390. (c) Yeung, Y.-Y.; Hong, S.; Corey, E. J. *J. Am. Chem. Soc.* **2006**, *128*, 6310–6311. (d) Hayashi, Y.; Samanta, S.; Gotah, H.; Ishikawa, H. *Angew. Chem. Int. Ed.* **2008**, *47*, 6634–6637.

(19) (a) Li, X.; Meng, F.; Torker, S.; Shi, Y.; Hoveyda, A. H. *Angew. Chem. Int. Ed.* **2016**, *55*, 9997–10002. (b) Xiong, Y.; Zhang, G. *J. Am. Chem. Soc.* **2018**, *140*, 2735–2738.

(20) See the Supporting Information for details.

Chapter 2 – Catalytic Hydrothiolation: Counterion-Controlled Regioselectivity²

2.1 Introduction

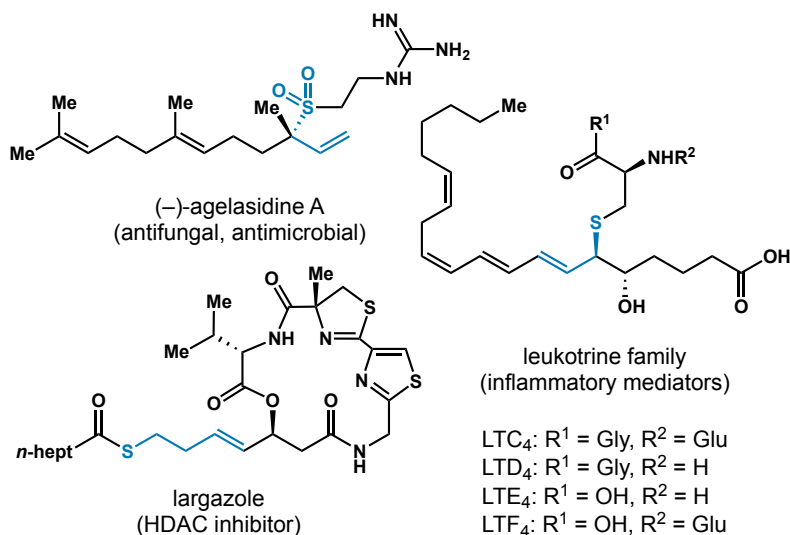
Given the value of organosulfur compounds as metabolites and medicines,¹ synthetic chemists strive to develop versatile methods for accessing these motifs.² Both allylic and homoallylic sulfides, as well as their respective derivatives (e.g., sulfones and thioesters), comprise natural products and analogs with a wide range of bioactivities (Figure 2.1).³ The hydrothiolation of olefins and dienes represents an atom-economical strategy⁴ for constructing C–S bonds.^{5,6} Despite its high atom-economy, hydrothiolation remains an unexploited strategy for the synthesis of complex targets and further development is warranted. Breit demonstrated an enantioselective hydrothiolation of allenes to generate allylic sulfides via Rh catalysis.^{7a,7b} Using Au catalysis, the He group achieved the hydrothiolation of 1,3-dienes to access allylic sulfides, with excellent 3,4-Markovnikov selectivity, albeit as racemic mixtures.^{7c} Our laboratory communicated the first enantioselective 1,2-Markovnikov hydrothiolation of 1,3-dienes to generate allylic sulfides (see Chapter 1).⁸ Although hydrothiolations have been developed to access allylic sulfides from dienes, selective access to the homoallylic isomer has been elusive.

To expand the power of diene hydrothiolation, we focused on elucidating the mechanism for the 1,2-Markovnikov hydrothiolation. In theory, the addition of a thiol to an unsymmetrical diene (e.g., 2-phenyl-1,3-diene), can afford up to 11 isomers.⁹ Yet, the use of cationic Rh and a bisphosphine ligand affords secondary and tertiary sulfide motifs with excellent regioselectivity and enantioselectivity. By studying the mechanism, we determine the fundamental steps that govern regiocontrol. Guided by these insights, we then developed a complementary hydrothiolation to provide access to homoallylic sulfides. While regiodivergent hydrothiolation of

² Adapted with permission from Yang, X.-H.; Davison, R. T.; Nie, S.-Z.; Cruz, F. A.; McGinnis, T. M.; Dong, V. *M. J. Am. Chem. Soc.* **2019**, *141*, 3006–3013. © 2019 American Chemical Society

dienes has not previously been reported, Hull demonstrated a ligand-controlled regiodivergent hydrothiolation of allylic amines.¹⁰ Regiodivergent hydrosilylation of 1,3-dienes has been reported

— **Inspiration:** natural products containing allylic and homoallylic sulfide motifs —



— **Hydrofunctionalization:** enantioselective allene hydrothiolation (Breit, 2015) —

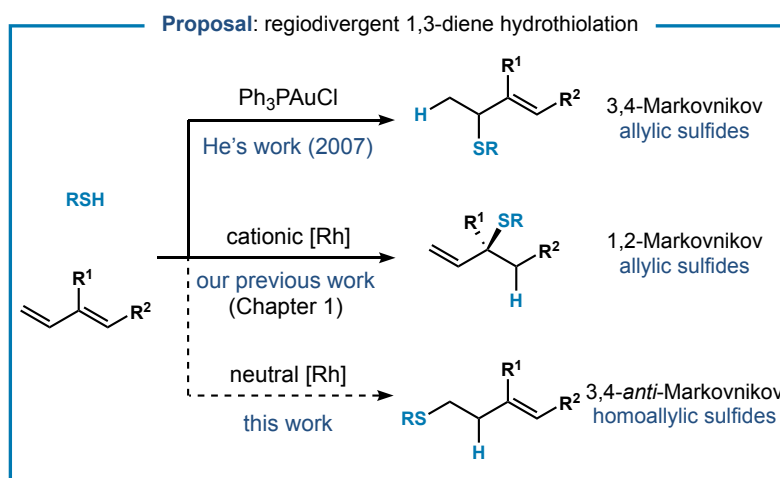
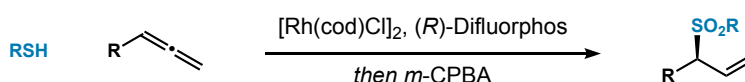


Figure 2.1. Regiodivergent hydrothiolation of 1,3-dienes.

by Ritter through the use of an Fe versus Pt catalyst.¹¹ In this study, we enable access to homoallylic sulfides by simply changing the counterion that coordinates to Rh from SbF_6^- to a more coordinating counterion (Cl^-). The scope and mechanism of this new 1,3-diene

hydrothiolation is presented. We also showcase hydrothiolation in the first enantioselective synthesis of (–)-agelasidine A, a natural product that bears a chiral tertiary sulfide motif.

2.2 Results and Discussion

In our previous studies (see Chapter 1), we observed that different 1,3-diene substitution patterns require the use of different ligand families for optimal results (Figure 2.2).⁸ By using this empirical guide, one can identify either the desired product or the commodity diene of choice to functionalize. For cyclic, 1-substituted, 1,2-disubstituted, and 2,3-disubstituted dienes, we found that the BINAP ligand family is best for furnishing enantioenriched allylic sulfides. Whereas 2-substituted dienes require the use of the Josiphos ligand family. The Garphos ligand scaffold provides good yields and enantioselectivities for 1,3-butadiene. To better understand the catalyst design and its effects on diene hydrofunctionalization, we interrogated the hydrothiolation mechanism to elucidate the factors that affect selectivity.

Based on both literature precedents and the following mechanistic studies, we propose the 1,2-Markovnikov hydrothiolation mechanism depicted in Figure 2.3. Ligand exchange between 1,5-cyclooctadiene (cod) with a bisphosphine ligand, thiol **1**, and diene **2** generates intermediate **I**. In the rate-determining step, oxidative addition results in formation of a η^4 -diene coordinated Rh–H intermediate **II**.¹² Subsequent 1,4-insertion of the diene into the Rh–H bond furnishes Rh- π -allyl intermediate **III**.¹³ Intermediate **III** undergoes reductive elimination to provide **IV**, where product **3** remains coordinated to Rh. Ligand exchange of product **3** with thiol **1** and diene **2** regenerates **I**.

For the model system, we chose to study the mechanism using an achiral ligand, Xantphos, because we previously found that it is an effective ligand for the transformation.⁸ This bisphosphine ligand bears a coordinating oxygen atom that can act as a hemilabile ligand.¹⁴ Our initial mechanistic studies used thiophenol (**1a**) and myrcene (**2a**) to explore the kinetic profile of

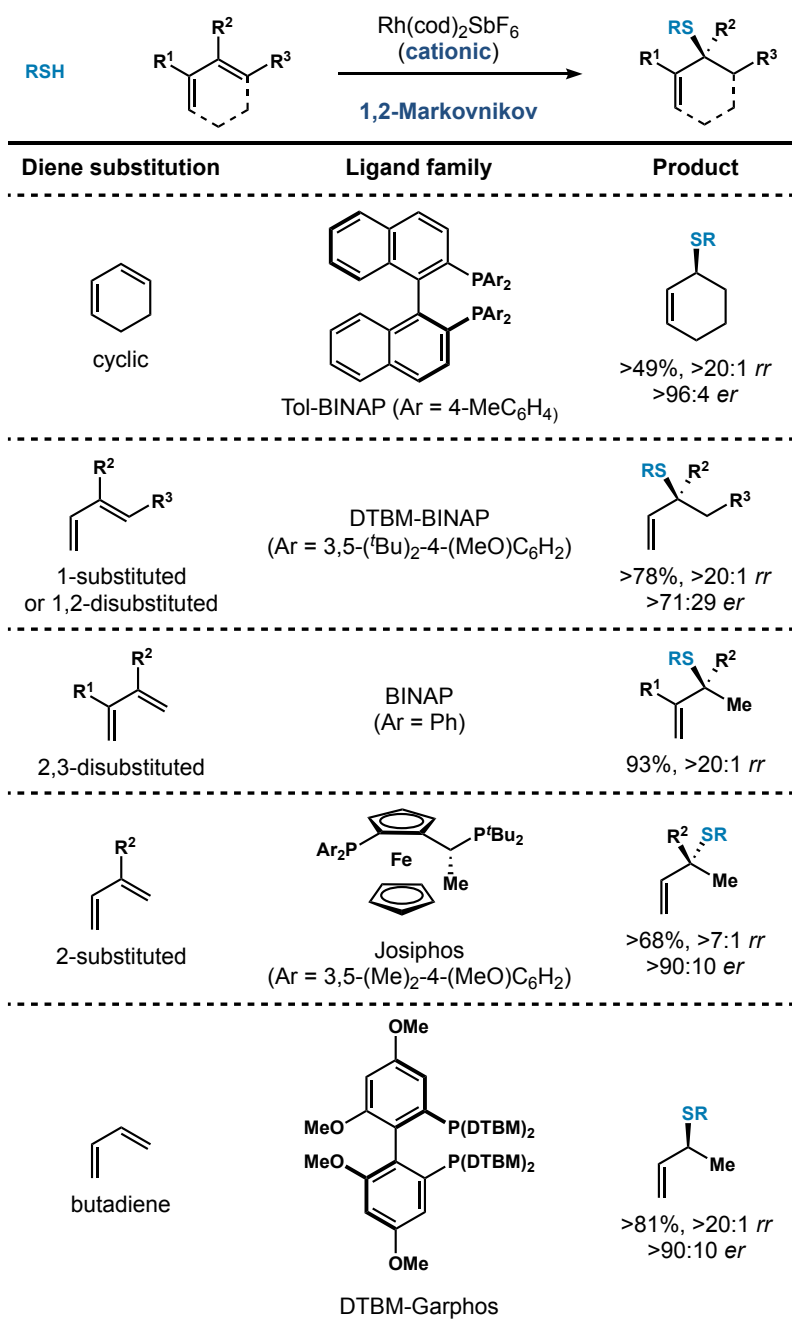


Figure 2.2. Empirical guide for 1,2-Markovnikov hydrothiolation.⁸

the transformation. We found a first-order dependence on the catalyst and a zeroth-order dependence on diene **2a**, which is consistent with a mechanism where the Rh complex **I** is saturated with diene **2** or diene **2** coordination occurs after the rate-determining step (Figure 2.3). We found that thiophenol (**1a**) can participate in two reaction pathways: desired hydrothiolation (path a) or

dimerization (path b).¹⁵ Thiophenol (**1a**) dimerization increases proportionally with its concentration. When adding bis(4-methoxyphenyl) disulfide to a mixture of thiophenol with myrcene under the standard conditions, we observe cross-over products, which suggests that thiol dimerization (path b) is reversible (see Figure S4). In accordance with these competing pathways, we observe a fractional-order dependence (0.4) on thiophenol (**1a**).

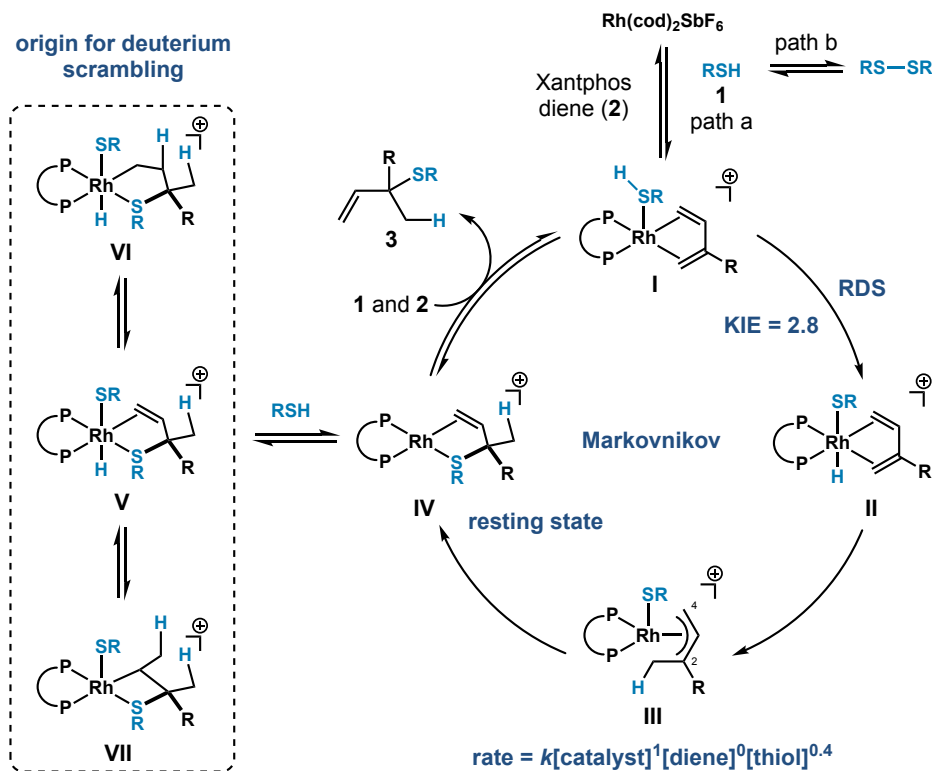


Figure 2.3. Proposed mechanism for 1,2-Markovnikov hydrothiolation.

We also performed deuterium-labeling experiments to further probe the mechanism (Figure 2.4). When subjecting deuterated thiophenol (**d-1a**) and myrcene (**2a**) to the standard conditions, we found that the recovered diene starting material **2a** exhibits no deuterium incorporation (eq 2.1 in Figure 2.4). This lack of scrambling supports our proposal that hydrometallation is an irreversible step in the catalytic cycle. However, we observe deuterium scrambling in the allylic sulfide product **d-3aa**. To examine the origin of this deuterium incorporation, we subjected a non-deuterated product **3aa** to a mixture of deuterated thiophenol

(*d*-**1a**), Rh(cod)₂SbF₆, and Xantphos (eq 2.2 in Figure 2.4). We detected similar deuterium incorporation only in the terminal olefin moiety of *d*-**3aa**'. Collectively, these results suggest that deuterium scrambling in product **3aa** occurs from a pathway external to the catalytic cycle. We hypothesize that intermediate **IV** can undergo oxidative addition to an equivalent of thiol **1** to form complex **V** (Figure 2.3). Subsequent reversible hydrometallation into the terminal olefin results in the deuterium scrambling observed in *d*-**3aa**.

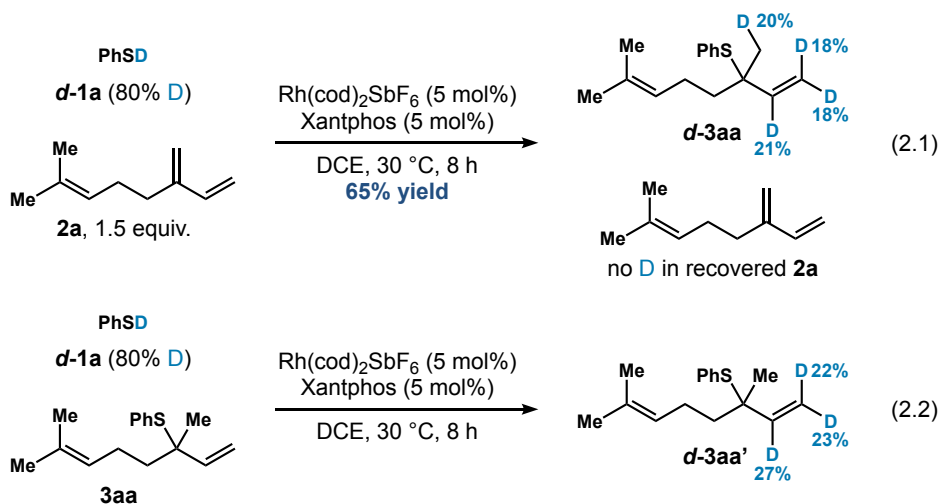


Figure 2.4. Deuterium-labeling studies for the 1,2-Markovnikov hydrothiolation.

Next, we studied key steps of the hydrothiolation by NMR spectroscopy. First, we monitored a mixture of thiophenol (**1a**), Rh(cod)₂SbF₆ (10 mol%), and Xantphos (10 mol%) in DCE-*d*₄ by ¹H NMR analysis. A resonance at −13.5 ppm was observed in less than 10 min at room temperature in the ¹H NMR spectrum, which is consistent with previously reported values for Rh-H complexes.¹⁶ This observation suggests that a Rh-H is rapidly generated from Rh(cod)₂SbF₆ in the presence of Xantphos and thiophenol (**1a**). While observation of a Rh-H does not necessitate its involvement in catalysis, we found that this species is consumed when treated with an equivalent of diene (myrcene, **2a**). In this stoichiometric experiment, we observe formation of a new Rh complex with non-equivalent phosphine resonances in the ³¹P NMR spectrum at −40 °C

[a pair of doublet of doublet signals ($\delta = 26.6$ ppm, $J_{\text{Rh-P}} = 174$ Hz, $J_{\text{P-P}} = 8$ Hz; $\delta = 16.0$ ppm, $J_{\text{Rh-P}} = 115$ Hz, $J_{\text{P-P}} = 8$ Hz)]. When we subject the product **3aa** to a mixture of $\text{Rh}(\text{cod})_2\text{SbF}_6$ and Xantphos in $\text{DCE-}d_4$, we observed the same species by ^{31}P NMR spectroscopy. Based on these results, we propose that intermediate **IV** is the resting state species in the catalytic cycle (Figure 2.3).

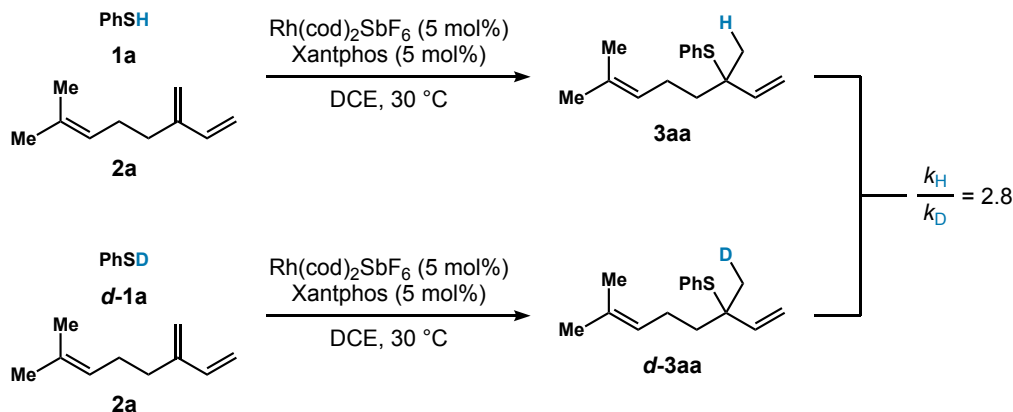


Figure 2.5. KIE from two parallel reactions using initial rates.

To investigate the rate-determining step, we carried out several kinetic experiments. First, a H/D kinetic isotope effect (KIE) experiment with thiophenol (**1a**) and deuterated thiophenol (**d-1a**) was performed. The initial rate constants were determined in parallel, and we observe a primary KIE ($k_{\text{H}}/k_{\text{D}} = 2.8$, Figure 2.5). Second, a Hammett plot was constructed, using various *para*-substituted thiophenols, to determine if there was a rate dependence on the electronic character of the thiol **1** partner (Figure 2.6). A relatively small ρ value (-0.22 ± 0.02) is observed with more electron-rich thiophenols undergoing hydrothiolation slightly faster. We hypothesize that the thiol initially coordinates to Rh to provide a transient species (see **I**, Figure 2.3), which then undergoes oxidative addition of the Rh center into the S–H bond to form Rh–H species **II**. Electron-rich thiols can accelerate this process by stabilizing positive charge build up on the Rh center during the transition state for oxidative addition.

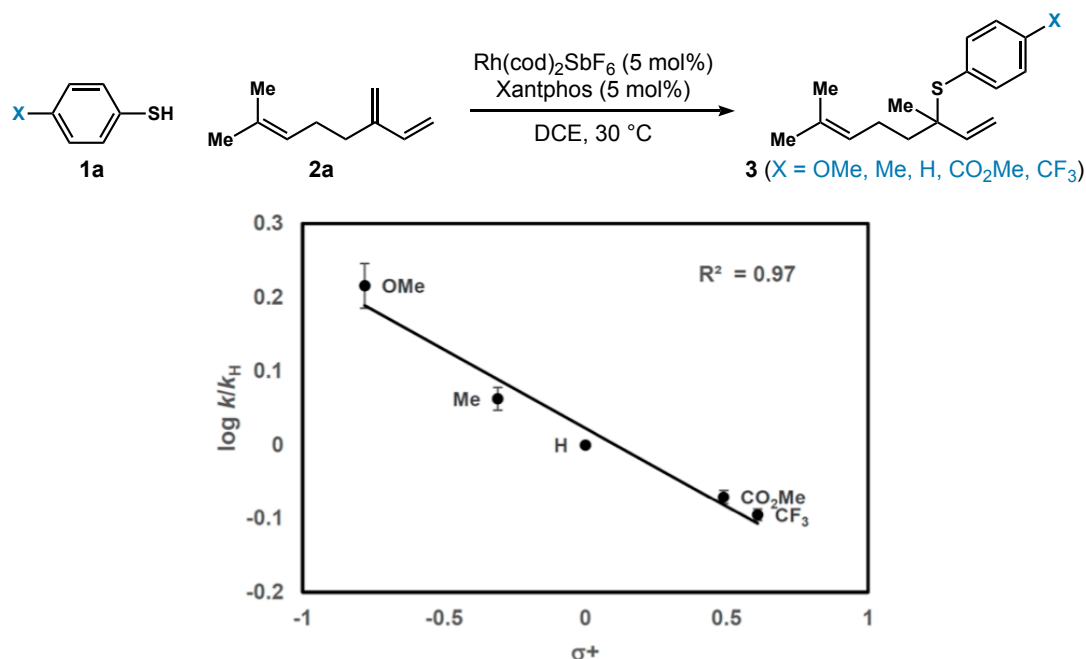


Figure 2.6. Hammett plot [$\log k/k_H = m\sigma^+ + b$ ($m = -0.22 \pm 0.02$; $b = 0.03 \pm 0.01$)].

Based on these mechanistic studies, we reason that the elementary steps from intermediate **II** to **IV** account for the observed regioselectivity (Figure 2.3). Hydrometallation occurs with the bulky Rh center preferentially adding to the less sterically encumbered terminal position (C4). This net 1,4-insertion ultimately yields the Rh- π -allyl intermediate **III**. Reductive elimination of **III** at the more substituted position to form the branched product is preferred, which is consistent with other Rh-catalyzed alkyne, allene, and diene hydrofunctionalizations.¹⁷

When intermediate **II** bears a chiral thiolate ligand, the configuration appears to have little/no influence on the stereochemical outcome. Our initial report included an example of a chiral cysteine-derived thiol undergoing hydrothiolation to selectively give one diastereomer, depending on which enantiomer of the bisphosphine ligand was used (Figure 2.7, entry A).⁸ To elaborate on this observation, we investigated chiral secondary thiols, where the chiral information is closer to the Rh center. Hydrothiolation occurs with high reactivity (**3cb** and **3db**, 83–92% yield, entries B and C), regioselectivity (>20:1 *rr*), and diastereoselectivity (>20:1 *dr*) when using chiral secondary

thiols **1c** and **1d**. These results demonstrate complete catalyst control when forging the C–S bond. Thus, chiral secondary thiols can be transformed to sulfides in a diastereodivergent fashion. With a better understanding of the 1,2-Markovnikov hydrothiolation mechanism, we set out to apply this asymmetric hydrothiolation methodology to the total synthesis of a natural product.

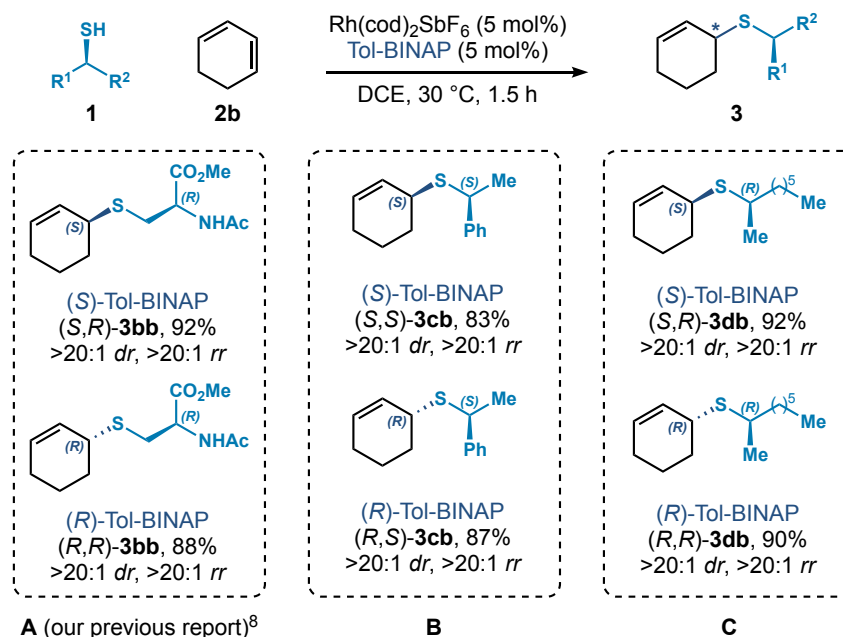


Figure 2.7. Catalyst-controlled diastereoselective 1,2-Markovnikov hydrothiolation.

(–)-Agelasidine A (**4**), an antifungal and antimicrobial agent isolated from marine sponges of the genus *Agelas*,^{3b} has previously been synthesized as a racemate from farnesol. Ichikawa reported two different methods for the installation of the key tertiary sulfide moiety of (±)-agelasidine A; a [2,3]-sigmatropic rearrangement or hetero-Claisen rearrangement have been used to construct the C–S bond and access (±)-**4** in 3 and 8 steps, respectively.¹⁸

We focused on intercepting an enantioenriched variant of sulfone **5**, which was previously elaborated to (±)-**4** in Ichikawa's synthesis (Figure 2.8). To achieve this goal, we focused on coupling β-farnesene (**2c**), which is a renewable feedstock found in many essential oils,¹⁹ and 2-mercaptoethyl acetate (**1e**). Referencing our hydrothiolation guide (Figure 2.2), the Josiphos ligand

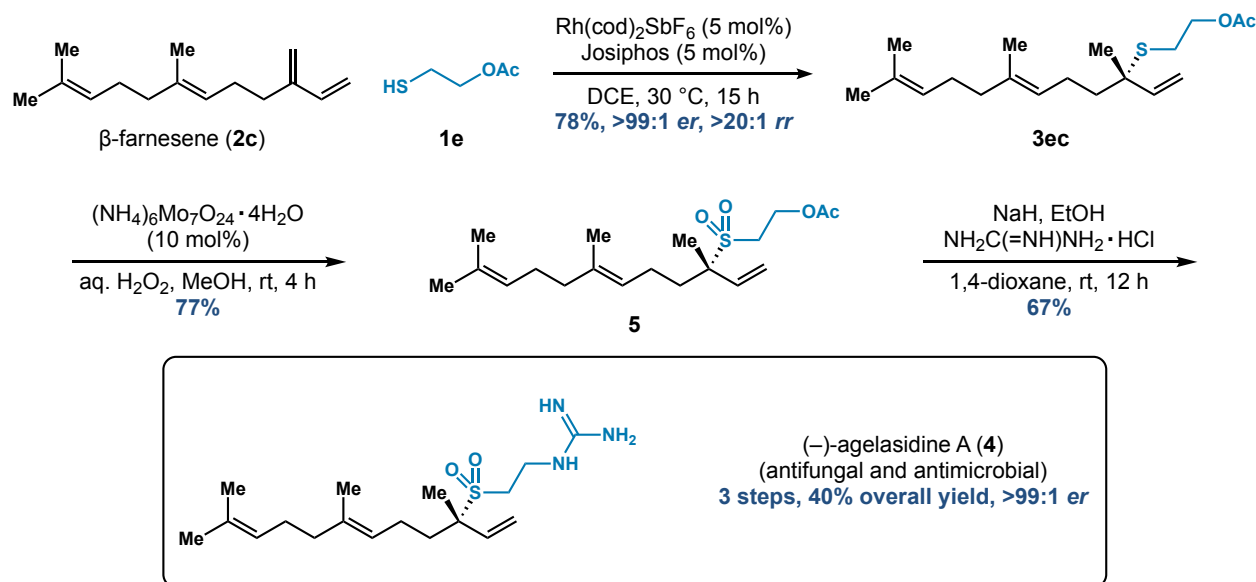


Figure 2.8. Enantioselective synthesis of (-)-agelasidine A.

scaffold is the most promising choice for achieving high reactivity and selectivity because **2c** is a 2-substituted 1,3-diene. In line with this guide, we found that β -farnesene (**2c**) can be coupled with **1e** to give the tertiary sulfide **3ec** in 78% yield with high enantioselectivity ($>99:1$ *er*) when using a Josiphos ligand ($\text{R} = \text{Cy}$, Figure 2.2). Various methods have been developed to chemoselectively oxidize sulfides to the corresponding sulfones.²⁰ We observe high reactivity (77%) when using catalytic $(\text{NH}_4)_6\text{Mo}_7\text{O}_{24} \cdot 4\text{H}_2\text{O}$ and H_2O_2 to oxidize sulfide **3ec** to sulfone **5**.²⁰ⁱ Following Ichikawa's report, we found that enantioenriched sulfone **5** could be transformed to (-)-agelasidine A (**4**, 67% yield) in the presence of excess guanidine.^{18c} Collectively, our approach requires only 3 steps from commercially available β -farnesene (**2c**) to afford (-)-**4** in 40% overall yield. We anticipate that this methodology will be applicable to other natural products and synthetic targets bearing C–S bonds.²¹

Based on the 1,2-Markovnikov mechanism depicted in Figure 2.3, we reasoned that it would be possible to access other hydrothiolation regioisomers by tuning the ligands²² and/or counterions on Rh. Previous reports have demonstrated that coordination modes of 1,3-dienes to a

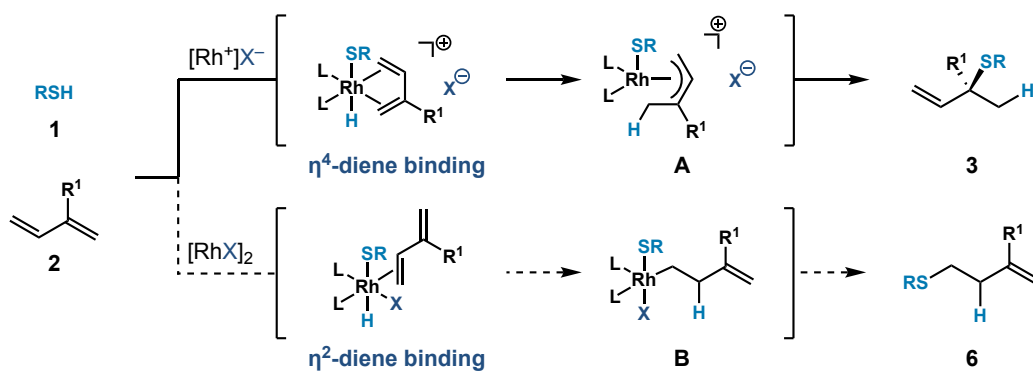


Figure 2.9. Proposed counterion-controlled regiodivergent hydrothiolations.

metal center can switch the observed regioselectivity of transition metal-catalyzed hydrofunctionalizations. For example, Ritter and co-workers found that η^4 -diene coordination provides 1,4-addition products,^{11a} whereas η^2 -diene coordination gives 3,4-*anti*-Markovnikov hydrosilylation products.^{11b} We envisioned using this concept to design a regiodivergent hydrothiolation of 1,3-dienes by switching from η^4 - to η^2 -diene binding. As shown in Figure 2.9, cationic Rh sources prefer η^4 -diene binding due to the presence of two open coordination sites. In contrast, a neutral Rh species would prefer η^2 -diene binding due to the availability of only one coordination site. Subsequent 1,2-insertion would lead to an intermediate **B** in which Rh adds to the less sterically hindered terminal position. Reductive elimination of this Rh-alkyl species **B** would yield homoallylic sulfides **6**.

To begin our study, we chose isoprene (**2d**), a petroleum feedstock, and thiophenol (**1a**) as model substrates (Figure 2.10). Since **6ad** is achiral, we focused on identifying an achiral ligand for the 3,4-*anti*-Markovnikov hydrothiolation. In the early stages of 1,2-Markovnikov hydrothiolation development, we found that Xantphos is a viable choice for the ligand. Indeed, with a combination of $Rh(cod)_2SbF_6$ and Xantphos, the expected tertiary allylic sulfide **3ad** could be synthesized in 83% yield with >20:1 *rr* (entry 1). In stark contrast, when using the neutral $[Rh(cod)Cl]_2$ as a Rh source, the homoallylic sulfide **6ad** is obtained in 74% yield with 1:>20 *rr*

(entry 2). These results suggest that regioselectivity is controlled by the counterion on Rh (SbF_6^- vs Cl^-), which is in line with our proposal (η^4 - vs η^2 -diene coordination).²³ Switching the counterion to I^- or MeO^- lowers the reactivity (18% and 49% yield, respectively, entries 3 and 4) while maintaining high regioselectivity (1:>20 *rr*). With further tuning, we found that $[\text{Rh}(\text{C}_2\text{H}_4)_2\text{Cl}]_2$ and dppe furnishes **6ad** in 94% yield with 1:>20 *rr* in 3 h (entry 5). Furthermore, with this catalyst, we can lower the loading to 0.1 mol% and synthesize **6ad** on gram-scale (1.3 g) in 74% yield with 1:>20 *rr*.

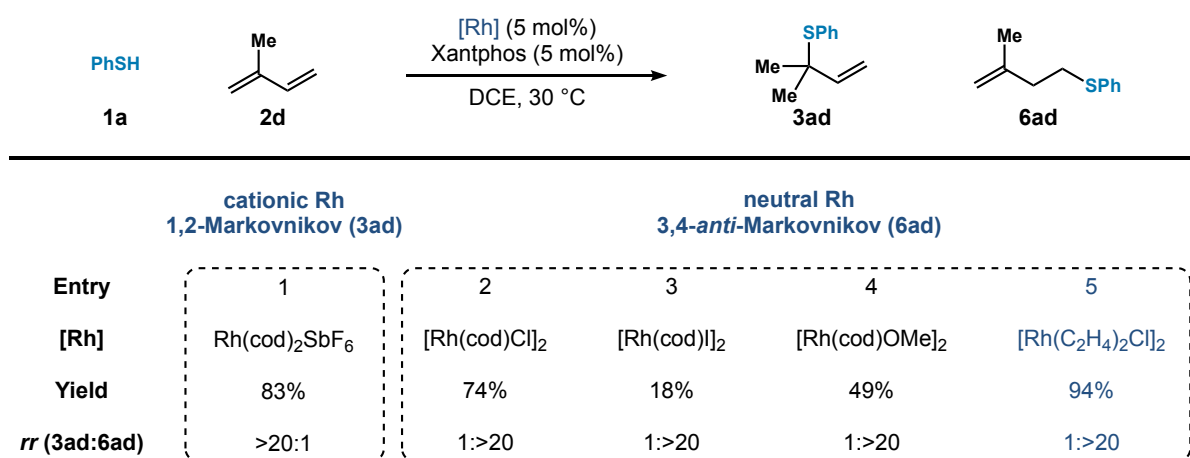
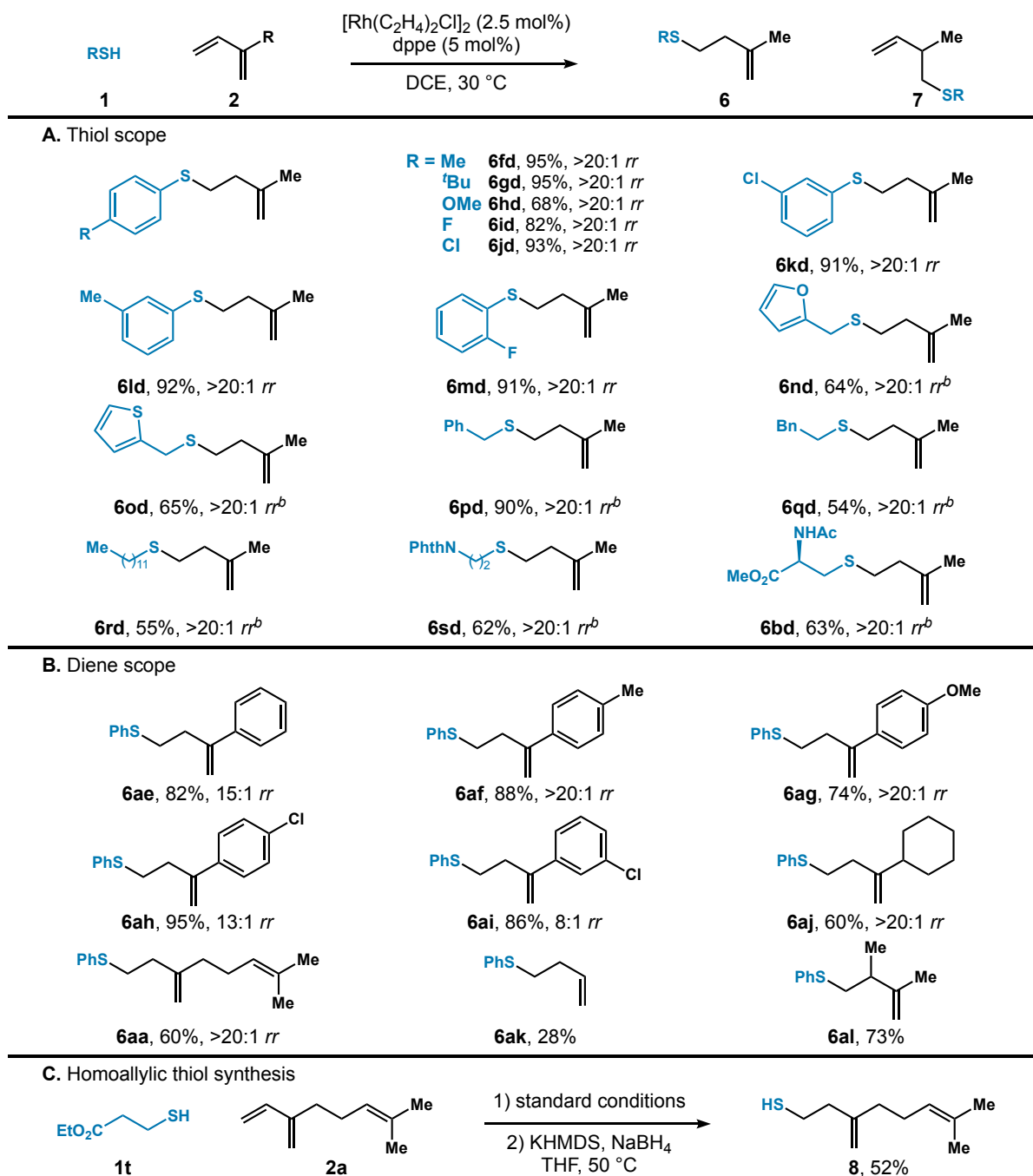


Figure 2.10. Different counterions lead to a switch in regioselectivity.

With these optimal conditions, we examined the coupling of 15 different thiols with isoprene (**2d**) to generate the corresponding homoallylic sulfides (Table 2.1A). High reactivity and regioselectivity are obtained with both aromatic and aliphatic thiol partners ((**6bd**–**6sd**), 54–95%, >20:1 *rr*). Imide (**6sd**), amide (**6bd**), and ester (**6bd**) functionalities are also compatible.

Next, we investigated the scope of the 1,3-diene partner in the 3,4-*anti*-Markovnikov hydrothiolation using thiophenol (**1a**) as a model thiol partner (Table 2.1B). Both aromatic and aliphatic 2-substituted 1,3-dienes are converted to the sulfide products (**6aa**–**6aj**) in high yields (60–95%). The electronics of the 2-aryl ring on the 1,3-diene has a noticeable effect on the regioselectivity of the transformation. Electron-rich 1,3-dienes (**6af**, **6ag**, >20:1 *rr*) yield higher

Table 2.1. 3,4-*Anti*-Markovnikov hydrothiolation of 1,3-dienes.^[a]



^[a]Reaction conditions: **1** (0.2 mmol), **2** (0.4 mmol), [Rh(C₂H₄)₂Cl]₂ (2.5 mol%), dppe (5 mol%), DCE (0.4 mL), 30 °C, 3 h. Isolated yields. Regioselectivity ratio (*rr*) is the ratio of **6** to **7**, which is determined by ¹H NMR analysis of the crude reaction mixture. ^[b]Using [Rh(cod)Cl]₂ (2.5 mol%), Xantphos (5 mol%) and 3,5-dimethylbenzoic acid (50 mol%), 30 °C, 12 h.

regioselectivity than electron-poor 1,3-dienes (**6ah**, **6ai**, 13:1 and 8:1 *rr*, respectively). 3,4-*Anti*-Markovnikov hydrothiolation of butadiene (**2k**) provides the corresponding homoallylic sulfide **6ak** in 28% yield. A 2,3-disubstituted diene **2l** also transforms to the homoallylic sulfide **6al** (73%). Moreover, myrcene (**2a**) could be converted to the corresponding homoallylic thiol **8** via a formal addition of H₂S, which consisted of 3,4-*anti*-Markovnikov hydrothiolation followed by deprotection (Table 2.1C).²⁴

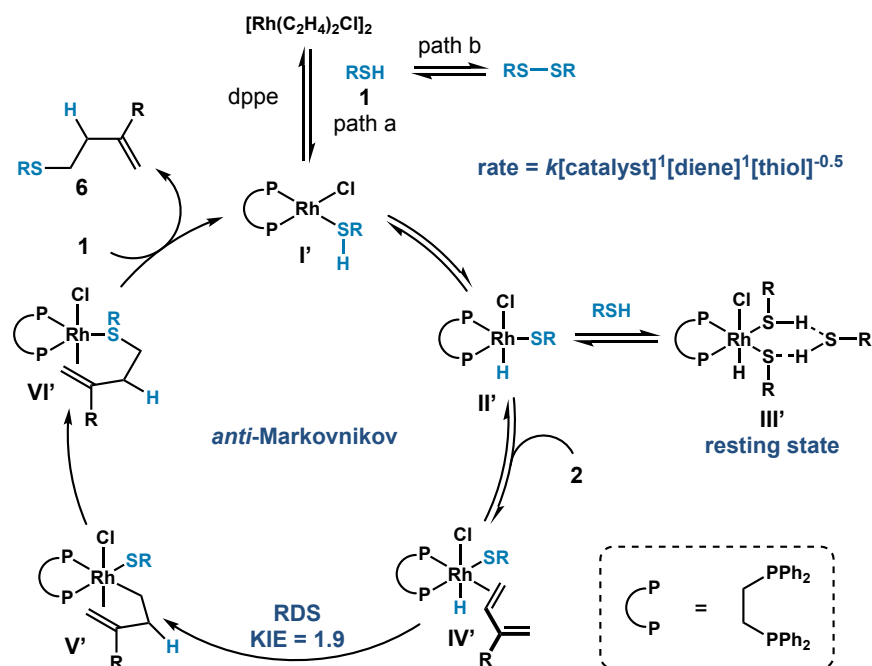


Figure 2.11. Proposed 3,4-*anti*-Markovnikov hydrothiolation mechanism.

Based on kinetic studies and NMR experiments, we propose the mechanism shown in Figure 2.11 for the 3,4-*anti*-Markovnikov hydrothiolation of 1,3-dienes. Oxidative addition of Rh to thiol **1** provides intermediate **II'**. Two equivalents of thiol **1** can then associate to furnish the resting state **III'**. A similar off-cycle resting state with an Ir(III)-H complex bearing a six-membered ring formed from two hydrogen bonds to ethanol has been reported.²⁵ Intermediate **III'** displays a hydride resonance at -15.8 ppm with symmetrical phosphines [doublet ($\delta = 52.2$ ppm,

$J_{\text{Rh-P}} = 94 \text{ Hz}$]. Moreover, a negative half-order dependence on thiol **1** supports the proposed side pathway.

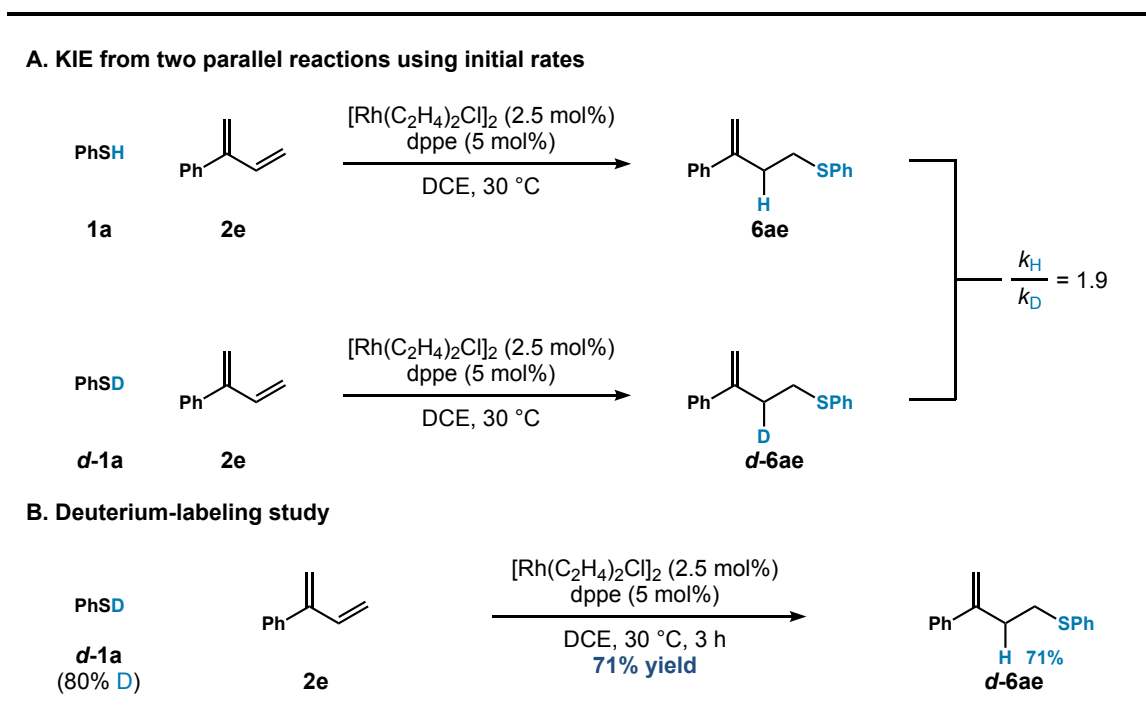


Figure 2.12. Initial mechanistic experiments for 3,4-*anti*-Markovnikov hydrothiolation.

In contrast to the η^4 -diene binding exhibited in **II** (Figure 2.3), we propose that the less substituted olefin coordinates to intermediate **II'** to form η^2 -diene coordinated Rh complex **IV'**. This diene binding mode is due to the presence of one coordination site and could be the foundation for the switch in regioselectivity. Insertion of the 1,3-diene into the Rh–H bond then provides the less sterically encumbered intermediate **V'**. The observed primary KIE ($k_{\text{H}}/k_{\text{D}} = 1.9$, Figure 2.12A) supports that either oxidative addition to the S–H bond or diene insertion into the Rh–H bond is the rate-determining step. Given the first-order rate dependence on diene **2e** and catalyst (Figure 2.11), as well as the results of deuterium incorporation into only the allylic position of **d-6ae** (Figure 2.12B), we propose diene migratory insertion is the rate-determining step. Rh- π -allyl **V'**

then undergoes reductive elimination to yield intermediate **VI'**, which can perform a ligand exchange of product **6** with thiol **1** to regenerate **I'**.

2.3 Conclusion and Future Work

Hydrothiolation of 1,3-dienes provides an efficient and straightforward way to construct primary, secondary, and tertiary sulfides. A concise total synthesis of (–)-agelasidine A (**4**) exemplifies the facile use of this methodology in a synthetic setting. Allylic and homoallylic sulfides can be synthesized in a regiodivergent manner by switching the Rh source. Mechanistic investigations shed light on the origin of the high regioselectivity observed for both hydrothiolations. Future efforts will focus on the development of a unified mechanistic approach for accessing different regioisomers of 1,3-diene hydrofunctionalizations.²⁶

2.4 Author Contributions

Dr. Xiao-Hui Yang (X.-H.Y.), Ryan T. Davison (R.T.D.), and Prof. Vy M. Dong (V.M.D.) conceived of the project discussed in Chapter 2. X.-H.Y., R.T.D., and V.M.D. co-wrote the text. X.-H.Y. was responsible for the mechanistic experiments displayed in Figures 2.3–2.6, 2.11, and 2.12. Tristan M. McGinnis (T.M.M.) expanded the catalyst-controlled diastereoselective hydrothiolation (Figure 2.7). X.-H.Y. and Faben A. Cruz (F.A.C.) reported the first asymmetric total synthesis of (–)-agelasidine A (Figure 2.8). R.T.D. found that the counterion identity can switch the regioselectivity of diene hydrothiolation (Figure 2.10). R.T.D. explored the thiol scope, Dr. Shao-Zhen Nie (S.-Z.N.) examined the diene scope, and T.M.M. executed the homoallylic thiol synthesis (Table 2.1). All authors analyzed the results and commented on the manuscript.

2.5 References

(1) For reviews, see: (a) Iardi, E. A.; Vitaku, E.; Njardarson, J. T. *J. Med. Chem.* **2014**, *57*, 2832–2842. (b) Feng, M.; Tang, B.; Liang, S. H.; Jiang, X. *Curr. Top. Med. Chem.* **2016**, *16*, 1200–1216. (c) Scott, K. A.; Njardarson, J. T. *Top. Curr. Chem.* **2018**, *376*, 1–34.

(2) For reviews on C–S bond formation, see: (a) Kondo, T.; Mitsudo, T.-A. *Chem. Rev.* **2000**, *100*, 3205–3220. (b) Arisawa, M.; Yamaguchi, M. *Pure Appl. Chem.* **2008**, *80*, 993–1003. (c) Chauhan, P.; Mahajan, S.; Enders, D. *Chem. Rev.* **2014**, *114*, 8807–8864. (d) Shen, C.; Zhang, P.; Sun, Q.; Bai, S.; Hor, T. S. A.; Liu, X. *Chem. Soc. Rev.* **2015**, *44*, 291–314. (e) Yu, J.-S.; Huang, H.-M.; Ding, P.-G.; Hu, X.-S.; Zhou, F.; Zhou, J. *ACS Catal.* **2016**, *6*, 5319–5344. (f) Qiao, A.; Jiang, X. *Org. Biomol. Chem.* **2017**, *15*, 1942–1946. For a review on enzymatic C–S bond formation, see: (g) Dunbar, K. L.; Scharf, D. H.; Litomska, A.; Hertweck, C. *Chem. Rev.* **2017**, *117*, 5521–5577.

(3) (a) Bernström, K.; Hammarström, S. *Biochem. Biophys. Res. Commun.* **1982**, *109*, 800–804. (b) Nakamura, H.; Wu, H.; Kobayashi, J.; Ohizumi, Y. *Tetrahedron Lett.* **1983**, *24*, 4105–4108. (c) Sumiyoshi, H.; Wargovich, M. J. *Cancer Res.* **1990**, *50*, 5084–5087. (d) Arora, A.; Siddiqui, I. A.; Shukla, Y. *Mol. Cancer Ther.* **2004**, *3*, 1459–1466. (e) Arunkumar, A.; Vijayababu, M. R.; Venkataraman, P.; Senthikumar, K.; Arunakaran, J. *Biol. Pharm. Bull.* **2006**, *29*, 375–379. (f) Taori, K.; Paul, V. J.; Luesch, H. *J. Am. Chem. Soc.* **2008**, *130*, 1806–1807.

(4) Trost, B. M. *Science* **1991**, *254*, 1471–1477.

(5) For select hydrothiolations of alkenes, see: (a) Cabrero-Antonino, J. R.; LeyvaPerez, A.; Corma, A. *Adv. Synth. Catal.* **2012**, *354*, 678–687. (b) Tamai, T.; Ogawa, A. *J. Org. Chem.* **2014**, *79*, 5028–5035. (c) Tamai, T.; Fujiwara, K.; Higashimae, S.; Nomoto, A.; Ogawa, A. *Org. Lett.* **2016**, *18*, 2114–2117. (d) Yi, H.; Song, C.; Li, Y.; Pao, C.-W.; Lee, J.-F.; Lei, A. *Chem. Eur. J.* **2016**, *22*, 18331–18334. (e) Mosafari, E.; Ripsman, D.; Stephan, D. W. *Chem. Commun.* **2016**, *52*, 8291–8293. (f) Teders, M.; Henkel, C.; Anhäuser, L.; Strieth-Kalthoff, F.; Gómez-Suárez, A.; Kleinmans, R.; Kahnt, A.; Rentmeister, A.; Guldi, D.; Glorius, F. *Nat. Chem.* **2018**, *10*, 981–988. (g) Kristensen, S. K.; Laursen, S. L. R.; Taarning, E.; Skrydstrup, T. *Angew. Chem. Int. Ed.* **2018**, *57*, 13887–13891. For a review, see: (h) Castarlenas, R.; Giuseppe, A. D.; Pérez-Torrente, J. J.; Oro, L. A. *Angew. Chem. Int. Ed.* **2013**, *52*, 211–222.

(6) For select hydrofunctionalizations of 1,3-dienes, see: (a) Zbieg, J. R.; Yamaguchi, E.; McInturff, E. L.; Krische, M. J. *Science* **2012**, *336*, 324–327. (b) Chen, Q.-A.; Kim, D. K.; Dong, V. M. *J. Am. Chem. Soc.* **2014**, *136*, 3772–3775. (c) Saini, V.; O’Dair, M.; Sigman, M. S. *J. Am. Chem. Soc.* **2015**, *137*, 608–611. (d) Marcum, J. S.; Roberts, C. C.; Manan, R. S.; Cervarich, T. N.; Meek, S. J. *J. Am. Chem. Soc.* **2017**, *139*, 15580–15583. (e) Jing, S. M.; Balasanthiran, V.; Pagar, V.; Gallucci, J. C.; RajanBabu, T. V. *J. Am. Chem. Soc.* **2017**, *139*, 18034–18043. (f) Yang, X.-H.; Lu, A.; Dong, V. M. *J. Am. Chem. Soc.* **2017**, *139*, 14049–14052. (g) Gui, Y.-Y.; Hu, N.; Chen, X.-W.; Liao, L.-L.; Ju, T.; Ye, J.-H.; Zhang, Z.; Li, J.; Yu, D.-G. *J. Am. Chem. Soc.* **2017**, *139*, 17011–17014. (h) Thullen, S. M.; Rovis, T. *J. Am. Chem. Soc.* **2017**, *139*, 15504–15508. (i) Adamson, N. J.; Hull, E.; Malcolmson, S. J. *J. Am. Chem. Soc.* **2017**, *139*, 7180–7183. (j) Adamson, N. J.; Wilbur, K. C. E.; Malcolmson, S. J. *J. Am. Chem. Soc.* **2018**, *140*, 2761–2764. (k) Schmidt, V. A.; Kennedy, C. R.; Bezdek, M. J.; Chirik, P. J. *J. Am. Chem. Soc.* **2018**, *140*, 3443–3453. (l) Cheng, L.; Li, M.-M.; Xiao, L.-J.; Xie, J.-H.; Zhou, Q.-L. *J. Am. Chem. Soc.* **2018**, *140*, 11627–11630.

- (7) (a) Pritzius, A. B.; Breit, B. *Angew. Chem. Int. Ed.* **2015**, *54*, 3121–3125. (b) Pritzius, A. B.; Breit, B. *Angew. Chem. Int. Ed.* **2015**, *54*, 15818–15822. (c) Brouwer, C.; Rahaman, R.; He, C. *Synlett* **2007**, *2007*, 1785–1789.
- (8) Yang, X.-H.; Davison, R. T.; Dong, V. M. *J. Am. Chem. Soc.* **2018**, *140*, 10443–10446.
- (9) See Supporting Information for details
- (10) Kennemur, J. L.; Kortman, G. D.; Hull, K. L. *J. Am. Chem. Soc.* **2016**, *138*, 11914–11919.
- (11) (a) Wu, J. Y.; Stanzl, B. N.; Ritter, T. *J. Am. Chem. Soc.* **2010**, *132*, 13214–13216. (b) Parker, S. E.; Börgel, J.; Ritter, T. *J. Am. Chem. Soc.* **2014**, *136*, 4857–4860.
- (12) For examples of oxidative addition of thiols with Rh catalysts, see: (a) Ogawa, A.; Ikeda, T.; Kimura, K.; Hirao, T. *J. Am. Chem. Soc.* **1999**, *121*, 5108–5114. (b) Shoai, S.; Bichler, P.; Kang, B.; Buckley, H.; Love, J. A. *Organometallics* **2007**, *26*, 5778–5781. (c) Han, L.; Li, Y.; Liu, T. *Dalton Trans.* **2018**, *47*, 150–158, and ref. 10
- (13) For the same sterically preferred 1,4-insertion into an Ir–H, see: Nguyen, K. D.; Herkommer, D.; Krische, M. J. *J. Am. Chem. Soc.* **2016**, *138*, 14210–14213.
- (14) Xantphos is a hemilabile ligand that can coordinate through the oxygen atom, see: Ren, P.; Pike, S. D.; Pernik, I.; Weller, A. S.; Willis, M. C. *Organometallics* **2015**, *34*, 711–723.
- (15) For the formation of a disulfide under iron-catalyzed alkene hydrothiolation, see: ref. 5a.
- (16) For the resonance of Rh–H complexes, see: Di Giuseppe, A.; Castarlenas, R.; Pérez-Torrente, J. J.; Crucianelli, M.; Polo, V.; Sancho, R.; Lahoz, F. J.; Oro, L. A. *J. Am. Chem. Soc.* **2012**, *134*, 8171–8183. See also refs. 10 and 12a.
- (17) For reviews, see: (a) Koschker, P.; Breit, B. *Acc. Chem. Res.* **2016**, *49*, 1524–1536. (b) Haydl, A. M.; Breit, B.; Liang, T.; Krische, M. J. *Angew. Chem. Int. Ed.* **2017**, *56*, 11312–11325. For select papers, see: (c) Chen, Q.-A.; Chen, Z.; Dong, V. M. *J. Am. Chem. Soc.* **2015**, *137*, 8392–8395. (d) Yang, X.-H.; Dong, V. M. *J. Am. Chem. Soc.* **2017**, *139*, 1774–1777.
- (18) (a) Ichikawa, Y. *Tetrahedron Lett.* **1988**, *29*, 4957–4958. (b) Ichikawa, Y.; Kashiwagi, T.; Urano, N. *J. Chem. Soc., Chem. Commun.* **1989**, 987–988. (c) Ichikawa, Y.; Kashiwagi, T.; Urano, N. *J. Chem. Soc., Perkin Trans. 1* **1992**, *1*, 1497–1500.
- (19) Simionatto, E.; Porto, C.; Stüker, C. Z.; Dalcol, I. I.; da Silva, U. F. *Quim. Nova* **2007**, *30*, 1923–1925.
- (20) (a) Priebe, W.; Gryniewicz, G. *Tetrahedron Lett.* **1991**, *32*, 7353–7356. (b) Su, W. *Tetrahedron Lett.* **1994**, *35*, 4955–4958. (c) Beckerbauer, R.; Smart, B. E. *J. Org. Chem.* **1995**, *60*, 6186–6187. (d) Barton, D. H. R.; Li, W.; Smith, J. A. *Tetrahedron Lett.* **1998**, *39*, 7055–7058. (e) Choi, S.; Yang, J. D.; Ji, M.; Choi, H.; Kee, M.; Ahn, K. H.; Byeon, S. H.; Baik, W.; Koo, S. *J. Org. Chem.* **2001**, *66*, 8192–8198. (f) Xu, L.; Cheng, J.; Trudell, M. L. *J. Org. Chem.* **2003**, *68*, 5388–5391. (g) Shaabani, A.; Teimouri, F.; Lee, D. G. *Synth. Commun.* **2003**, *33*, 1057–1065. (h) Baciocchi, E.; Gerini, M. F.; Lapi, A. *J. Org. Chem.* **2004**, *69*, 3586–3589. (i) Jeyakumar, K.; Chakravarthy, D. R.; Chand, D. K. *Catal. Commun.* **2009**, *10*, 1948–1951.
- (21) Stout, E. P.; Yu, L. C.; Molinski, T. F. *Eur. J. Org. Chem.* **2012**, *2012*, 5131–5135.
- (22) For a regiodivergent hydrothiolation controlled by ligand choice, see: refs. 10 and 16.
- (23) For coordinating ability of anions to transition metals, see: Díaz-Torres, R.; Alvarez, S. *Dalton Trans.* **2011**, *40*, 10742–10750.
- (24) Jin, L.; Wang, J.; Dong, G. *Angew. Chem. Int. Ed.* **2018**, *57*, 12352–12355.
- (25) Wang, Y.; Huang, Z.; Leng, X.; Zhu, H.; Liu, G.; Huang, Z. *J. Am. Chem. Soc.* **2018**, *140*, 4417–4429.

(26) A recent computational paper (using DFT) was published that explores the regioselectivity switch for Rh-catalyzed diene hydrothiolation, see Wen, X.; Zhou, X.; Li, W.; Du, C.; Ke, Z.; Zhao, C. *ACS Catal.* **2021**, *11*, 7659–7671.

Chapter 3 – Enantioselective Coupling of Dienes and Phosphine Oxides³

3.1 Introduction

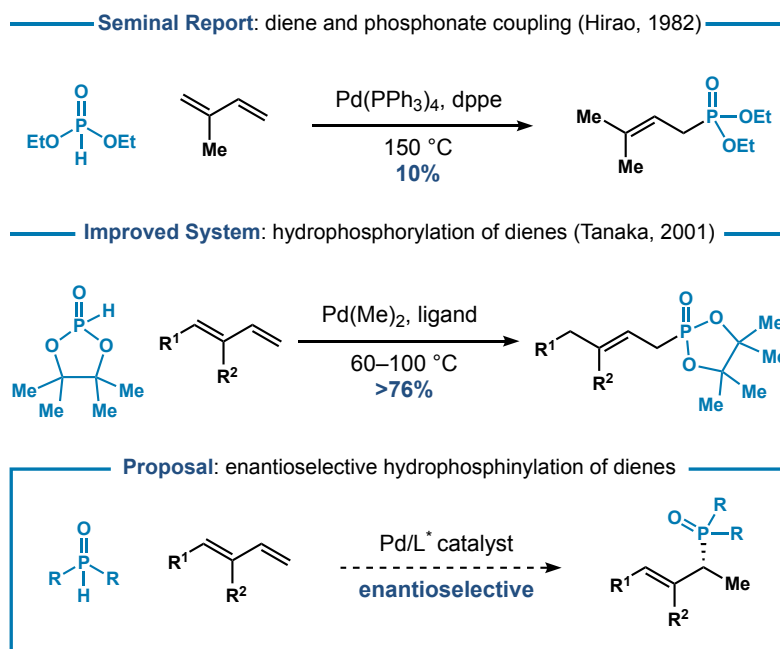


Figure 3.1. Asymmetric hydrophosphinylation of 1,3-dienes.

Conjugated dienes are versatile motifs for constructing molecules that range from natural products to synthetic polymers.^{1,2} In recent years, hydrofunctionalization has emerged as an attractive and atom-economical³ method to transform dienes into valuable building blocks.⁴ In comparison to other hydrofunctionalizations (e.g., hydroboration or hydroformylation), hydrophosphinylation remains in its infancy (Figure 3.1). Hirao first coupled isoprene and diethyl phosphonate to furnish an allylic phosphonate, albeit with low reactivity (10% yield) and at an elevated temperature (150 °C).⁵ Tanaka later improved the hydrophosphorylation of 1,3-dienes by using a more reactive pinacol-based phosphonate to synthesize allylphosphonates.⁶ While promising, this strategy has been restricted to producing achiral regioisomers or racemic mixtures.⁷

³ Adapted with permission from Nie, S.-Z.; Davison, R. T.; Dong, V. M. *J. Am. Chem. Soc.* **2018**, *140*, 16450–16454. © 2018 American Chemical Society

Given the potential for chiral phosphines in catalysis,⁸ as well as the need for novel phosphine motifs in medicine⁹ and agrochemistry,¹⁰ we sought to develop an enantioselective hydrophosphinylation.¹¹ We report the transformation of several petroleum feedstocks and readily available dienes into chiral phosphine oxide building blocks with high regio- and enantioselectivity.

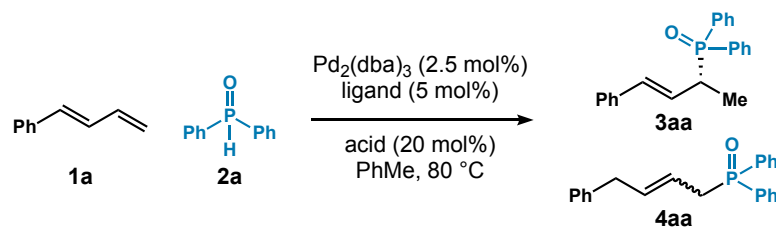
Given previously reported asymmetric hydroamination¹² and hydrothiolation¹³ of 1,3-dienes, we chose to focus on a phosphorus nucleophile that would possess intermediate nucleophilicity compared to amines and thiols. As part of our reaction design, we imagined using phosphine oxides (**2**) as P-nucleophiles because they are air stable, commercially available, and readily reduced to the corresponding phosphine.¹⁴ In addition, the pK_a of **2** (*ca.* 25)¹⁵ is between that of amines and thiols. Although the phosphine oxide reagent and its corresponding product could inhibit catalysis, hydrophosphinylation of alkenes¹⁶ and alkynes¹⁷ using transition metal catalysis and photocatalysis has been reported. Encouraged by these examples, we set out to identify a catalyst that would overcome the established 1,4-addition pathway to furnish the desired chiral regioisomer.

3.2 Results and Discussion

We began our investigations with the coupling of 1-phenylbutadiene (**1a**) and commercially available **2a** (Table 3.1). We examined a range of achiral bisphosphine ligands, with both Rh and Pd sources. While Rh showed no reactivity, Pd was promising for the hydrophosphinylation of **1a**. As highlighted in Table 3.1A, we observe that the ligand bite angle affects hydrophosphinylation.¹⁸ Combining Pd₂(dba)₃ and dppf offers optimal results (90%, >20:1 *rr*). Catalytic amounts of acid provide an increase in the reaction rate; P(V)-based Brønsted acids prove to be the most effective for hydrophosphinylation (Table 3.1B). In the absence of an acid

co-catalyst, we observe 16% of product **3aa** after 3 h and an 87% yield after 24 h. Based on these results, we focused on the Josiphos ligand family with diphenylphosphinic acid as a co-catalyst.¹⁹ As seen in Table 3.1C, with Pd(**L3**) we could lower the catalyst loading to 1 mol% and synthesize **3aa** on gram scale while retaining high reactivity (1.05 g, 91%) and selectivity (>20:1 *rr*, 95:5 *er*).

Table 3.1. Ligand and acid effects on asymmetric hydrophosphinylation.^[a]



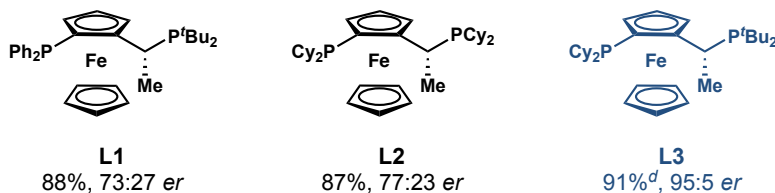
A. Ligand bite angle effects^b

	increasing bite angle →						
Ligand:	dppm	dppe	dppp	dppf	dppb	DPEphos	Xantphos
Yield 3aa :	trace	trace	90%	90%	61%	34%	9%
Time:	16 h	16 h	16 h	3 h	16 h	16 h	16 h

B. Acid effects^c

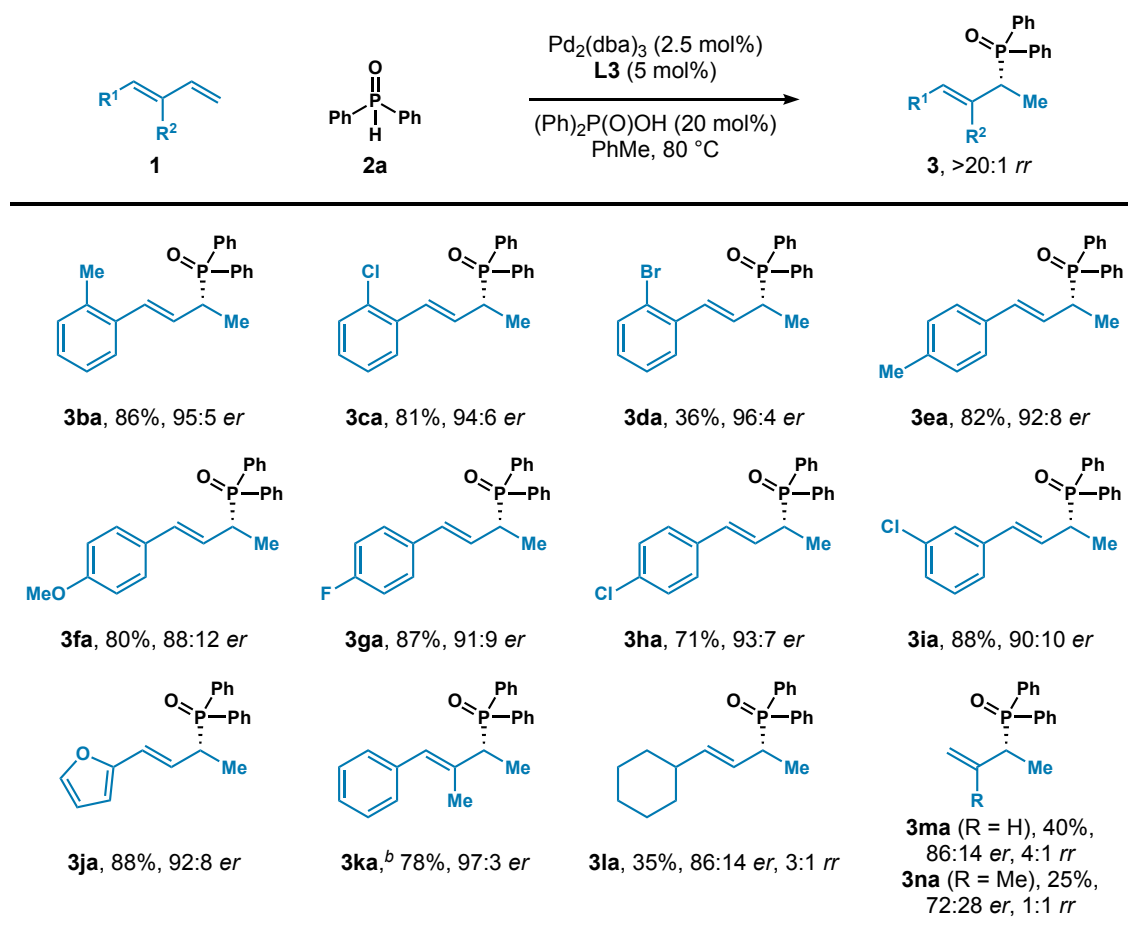
	increasing bite angle →				
Acid:	None	PhCO ₂ H	(Ph) ₂ P(O)OH	(PhO) ₂ P(O)OH	MsOH
Yield 3aa :	16%	51%	90%	87%	72%

C. Chiral ligands



^[a]Reaction conditions: **1a** (0.12 mmol), **2a** (0.10 mmol), Pd₂(dba)₃ (2.5 mol%), ligand (5.0 mol%), acid (20 mol%), toluene (0.40 mL), 3 h (unless otherwise noted). Yield determined by GC-FID analysis of the reaction mixture, which was referenced to 1,3,5-trimethoxybenzene. Regioselectivity ratio (*rr*) is the ratio of **3aa** to **4aa**, which is determined by ³¹P NMR analysis of the crude reaction mixture. Enantioselectivity ratio (*er*) is determined by chiral SFC. See SI for full structure of abbreviations used. Unless otherwise noted, *rr* is >20:1. ^[b]Standard conditions with (Ph)₂P(O)OH as acid. ^[c]Standard conditions with dppf as ligand. ^[d]Isolated yield of **3aa**, 3.47 mmol scale, using Pd₂(dba)₃ (0.50 mol%) and **L3** (1.0 mol%) with standard conditions, 18 h.

Table 3.2. Hydrophosphinylation of various 1,3-dienes.^[a]

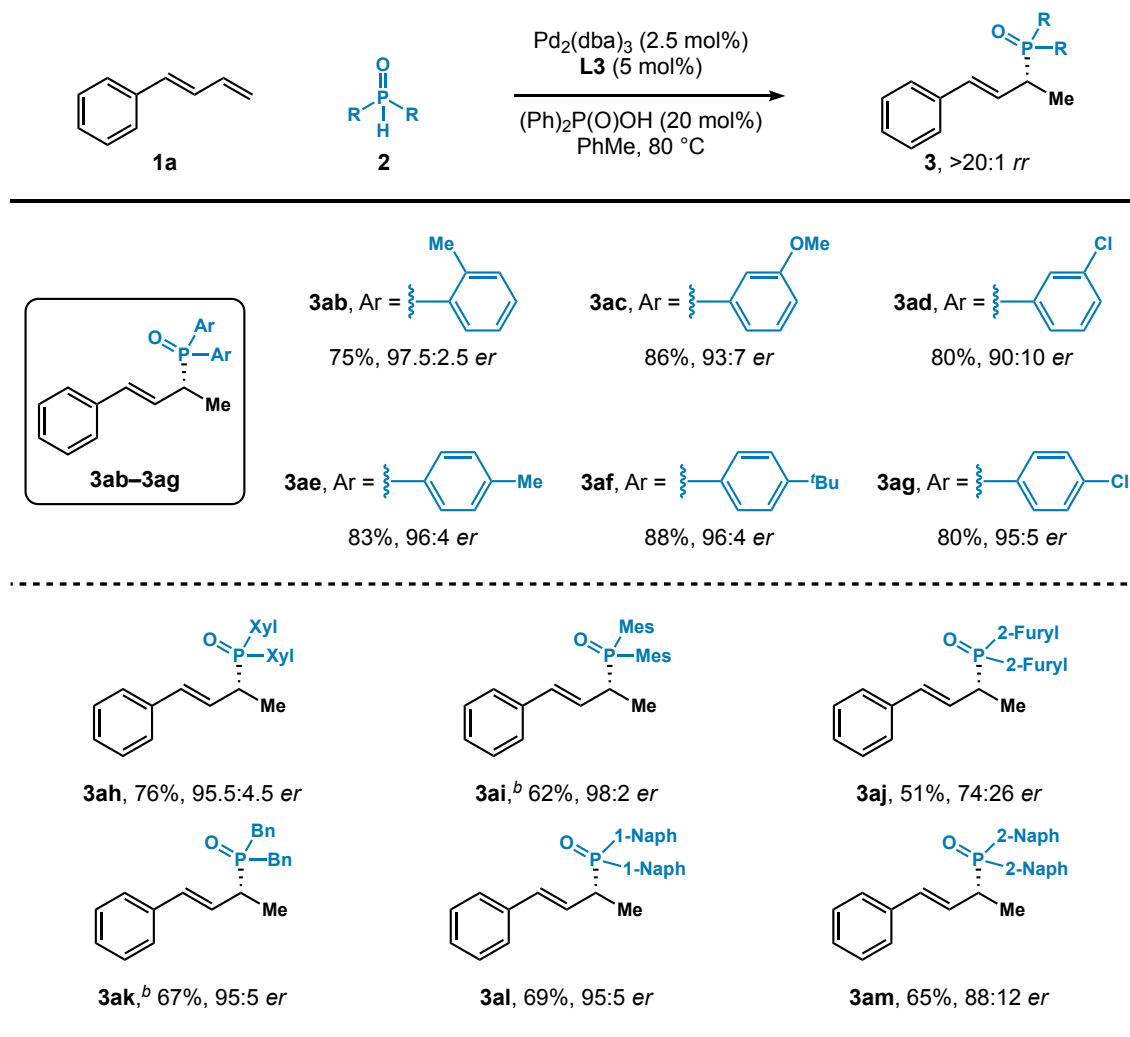


^[a]Reaction conditions: **1** (0.12 mmol), **2a** (0.10 mmol), $\text{Pd}_2(\text{dba})_3$ (2.5 mol%), ligand (5.0 mol%), $(\text{Ph})_2\text{P}(\text{O})\text{OH}$ (20 mol%), toluene (0.40 mL), 6 h. Isolated yield of **3**. Regioselectivity ratio (*rr*) is the ratio of **3** to **4**, which is determined by ^{31}P NMR analysis of the crude reaction mixture. Enantioselectivity ratio (*er*) is determined by chiral SFC. ^[b](*S*)-DTBM-Segphos (5.0 mol%) instead of **L3**, see SI for structure, 24 h.

With these conditions in hand, we investigated the hydrophosphinylation of various 1,3-dienes with phosphine oxide **2a** (Table 3.2). We found that a variety of 1-aryl substituted dienes could be transformed to chiral products **3ba–3ja** with moderate to high reactivity (36–88%) and selectivity ($>20:1$ *rr*, 88:12–96:4 *er*). Dienes containing aryl chlorides (**3ca**, **3ha**, and **3ia**) offer higher reactivity than aryl bromides (**3da**); potentially due to the mitigation of side pathways initiated by oxidative addition into the C–X bond. The petroleum feedstocks butadiene (**1m**) and isoprene (**1n**) can be coupled with **2a** to furnish chiral building blocks **3ma** and **3na**, respectively.

We observe product mixtures of **3ma** and **3na** that equally, or moderately, favor 3,4-addition over the established 1,4-addition previously reported for the hydrophosphorylation of butadiene⁶ (**1m**) and isoprene^{5,6} (**1n**). To examine if the allylic phosphine products (**3ma** and **3na**) could racemize by a sigmatropic rearrangement,²⁰ we resubjected **3ma** to the standard reaction conditions. After

Table 3.3. Hydrophosphinylation with various phosphine oxides.^[a]



^[a]Reaction conditions: **1a** (0.12 mmol), **2** (0.10 mmol), $\text{Pd}_2(\text{dba})_3$ (2.5 mol%), ligand (5.0 mol%), $(\text{Ph})_2\text{P}(\text{O})\text{OH}$ (20 mol%), toluene (0.40 mL), 6 h. Isolated yield of **3**. Regioselectivity ratio (*rr*) is the ratio of **3** to **4**, which is determined by ³¹P NMR analysis of the crude reaction mixture. Enantioselectivity ratio (*er*) is determined by chiral SFC. See SI for full structure of abbreviations used. ^[b]Reaction time is 24 h.

12 h, we observe no change in the enantioselectivity ratio. The 1,2-disubstituted diene (**1k**) and 1-alkyl substituted diene (**1l**) transform to products **3ka** and **3la**, respectively, in the presence of (*S*)-DTBM-Segphos. This result suggests that the diene substitution pattern must be matched with the appropriate ligand family, an observation in agreement with our previous studies on Rh-catalyzed hydrothiolation of 1,3-dienes.¹³

Next, we investigated the hydrophosphinylation of **1a** with structurally and electronically different phosphine oxides (Table 3.3). We observe high reactivity (**3ab–3am**, 51–88%), regioselectivity (>20:1 *rr*), and enantioselectivity (74:26–98:2 *er*). This coupling tolerates aryl (**3ab–3ai**), heterocyclic (**3aj**), and alkyl (**3ak**) phosphine oxides. Mono- (**2a–2g**), di- (**2h**), and trisubstituted (**2i**) aryl groups on the phosphine oxide partner can be coupled with **1a** to afford enantioenriched products (**3aa–3ai**). Fused ring motifs, which are the basis of a large class of ligand scaffolds, can also be incorporated in the phosphine oxide partner to generate products **3al** and **3am**.

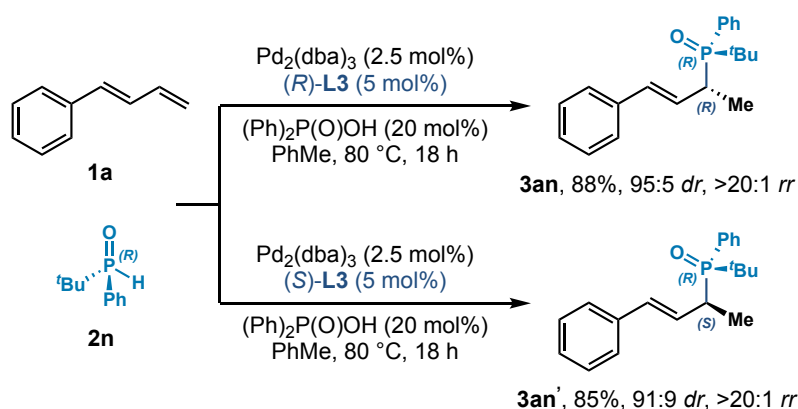


Figure 3.2. Diastereodivergent hydrophosphinylation.

Catalyst-controlled C–P bond formation would enable selective access to diastereomers. To test this idea, we prepared enantiopure phosphine oxide **2n** bearing a *tert*-butyl and phenyl group, a popular motif in chiral ligand design (Figure 3.2).²¹ Depending on the enantiomer of **L3** used, the (*R,R*)-diastereomer **3an**²² or (*R,S*)-diastereomer **3an'** can be obtained with high

diastereocontrol (95:5 and 91:9 *dr*, respectively). This result represents a diastereodivergent strategy for making phosphine oxides.

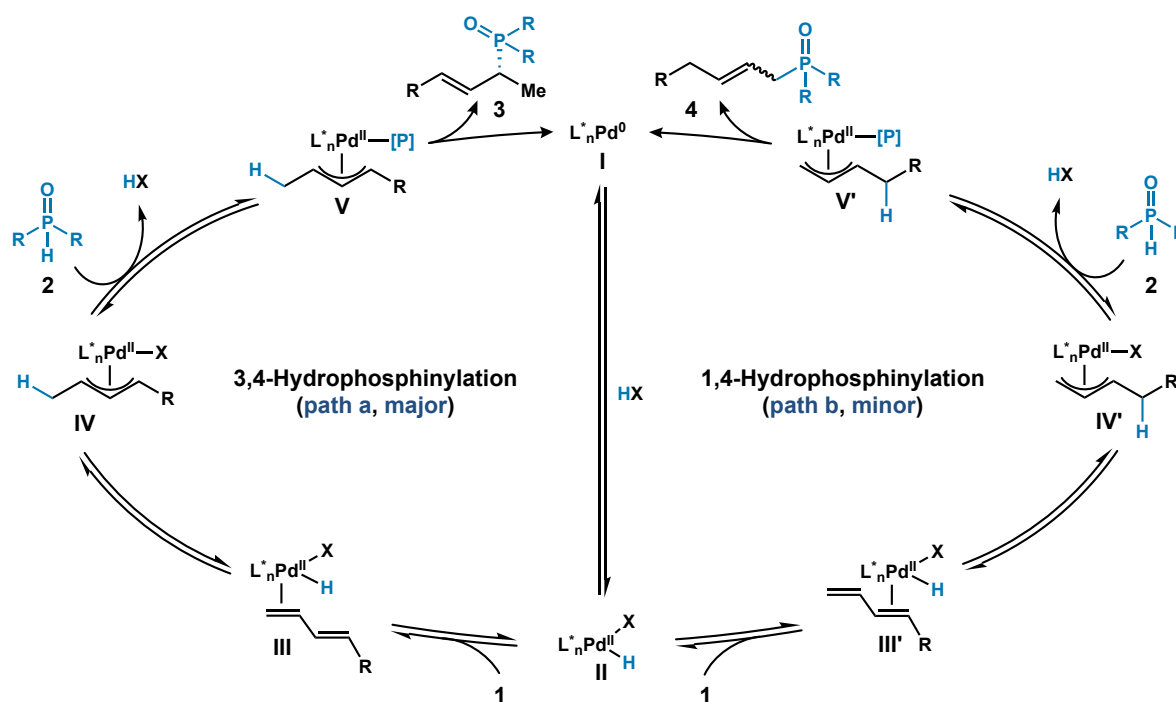


Figure 3.3. Proposed 1,3-diene hydrophosphinylation mechanism.

Based on literature precedents and our own observations, we propose the mechanism depicted in Figure 3.3. The Pd(0) source undergoes ligand substitution with the bisphosphine ligand to form a chiral monomeric species **I**, and subsequent oxidative addition to diphenylphosphinic acid (HX) forms Pd-H species **II**. A related oxidative addition has been implicated as a key step in the hydrophosphinylation of terminal alkynes.^{17e} In the absence of acid additives, we observe a significant induction period.²³ We reason that the addition of an acid cocatalyst (i.e., diphenylphosphinic acid) shortens the induction period and favors the formation of a Pd-H catalyst (e.g., **II**). At this point, two different modes of diene **1** coordination led to the major product **3** (path a) and the minor product **4** (path b). In path a, species **III** undergoes hydrometallation to provide the key Pd- π -allyl intermediate **IV**. Species **IV** then undergoes a

ligand exchange with phosphine oxide **2** to form species **V**. Subsequent reductive elimination of **V** furnishes the allylic phosphine oxide **3** and regenerates **I**.

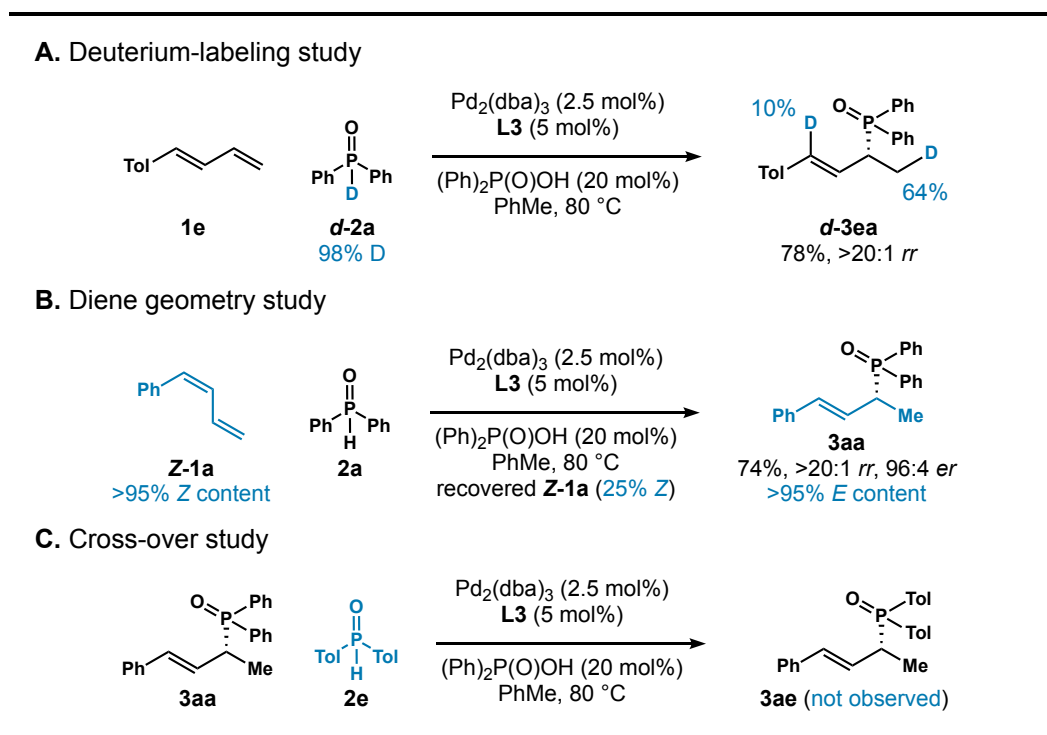


Figure 3.4. Preliminary mechanistic experiments.

To probe the mechanism, we conducted the following experiments (Figure 3.4A–C). First, deuterium-labeled phosphine oxide **d-2a** was subjected to the standard reaction conditions. In this experiment, we see deuterium incorporation at the C1 (10% D) and C4 (64% D) positions of **d-3ea**. If hydrometallation were irreversible, we should observe about a 6:1 mixture of regioisomers for **d-3ea**. In contrast, we observe >20:1 *rr* and thus conclude that hydropalladation is reversible. Second, (*Z*)-1-phenylbutadiene (**Z-1a**) was subjected to the hydrophosphinylation. We observe only the (*E*)-product **3aa** (>95% *E* content) in similar yield (74%) and regioselectivity (>20:1 *rr*) compared to the model substrate (Table 3.1, **3aa**, 90%, >20:1 *rr*). This result suggests that isomerization occurs faster than C–P bond formation. Furthermore, excess diene **Z-1a** is recovered with about 25% *Z* content, which is consistent with a reversible hydropalladation and reversible

diene coordination. By subjecting toluoyl phosphine oxide **2e** and product **3aa** under standard reaction conditions, we confirm that the allylic phosphine oxide **3aa** cannot undergo further substitution to form **3ae**. Our proposal is in line with a study on alkyne hydrophosphinylation where Pd–P bond cleavage requires elevated temperatures and reductive elimination is the rate-determining step.^{17e} We observe that alkyl-substituted dienes (**1l–1n**) form products (**3la–3na**) with lower regioselectivity compared to the aryl-substituted dienes (**3ba–3ka**). Thus, reductive elimination to form the conjugated product is favorable.

3.3 Conclusion and Future Work

The direct construction of chiral phosphines and phosphine oxides has previously been achieved *via* additions to Michael acceptors or transition metal-catalyzed substitutions.^{24,25} We report a complementary way to access chiral phosphine oxides. This study features the first enantioselective 1,3-diene hydrophosphinylation. Phosphine oxides and 1,3-dienes can be coupled to furnish chiral allylic products in high yields, regioselectivities, and enantioselectivities. Mechanistic studies suggest that the coupling proceeds through a reversible hydrometallation of the 1,3-diene partner, followed by irreversible reductive elimination to afford chiral phosphine oxide building blocks.

3.4 Author Contributions

Dr. Shao-Zhen Nie (S.-Z.N.) and Prof. Vy M. Dong (V.M.D.) conceived of the project discussed in Chapter 3. S.-Z.N., Ryan T. Davison (R.T.D.), and V.M.D. co-wrote the text. S.-Z.N. discovered the initial optimized asymmetric conditions for the hydrophosphinylation (Table 3.1). R.T.D. prepared substrates **3ba–3da** and **3ka** in Table 3.2. S.-Z.N. prepared the remaining substrates in Tables 3.2 and 3.3. S.-Z.N. demonstrated a catalyst-controlled diastereodivergent hydrophosphinylation (Figure 3.2). R.T.D. performed all of the mechanistic experiments in Figure

3.4 and the Supporting Information (Appendix 3). All authors analyzed the results and commented on the manuscript.

3.5 References

(1) For selected reviews on 1,3-dienes as building blocks, see: (a) Nicolaou, K. C.; Snyder, S. A.; Montagnon, T.; Vassilikogiannakis, G. *Angew. Chem. Int. Ed.* **2002**, *41*, 1668–1698. (b) Reymond, S.; Cossy, J. *Chem. Rev.* **2008**, *108*, 5359–5406. (c) Chen, J.-R.; Hu, X.-Q.; Lu, L.-Q.; Xiao, W.-J. *Chem. Rev.* **2015**, *115*, 5301–5365. (d) Büschleb, M.; Dorich, S.; Hanessian, S.; Tao, D.; Schenthal, K. B.; Overman, L. E. *Angew. Chem. Int. Ed.* **2016**, *55*, 4156–4186.

(2) For reviews on polymerization of 1,3-dienes, see: (a) Monakov, Y. B.; Mullagaliev, I. R. *Russ. Chem. Bull. Int. Ed.* **2004**, *53*, 1–9. (b) Friebe, L.; Nuyken, O.; Obrecht, W. *Adv. Polym. Sci.* **2006**, *204*, 1–154. (c) Zhang, Z.; Cui, D.; Wang, B.; Liu, B.; Yang, Y. *Struct. Bonding (Berlin, Ger.)* **2010**, *137*, 49–108. (d) Valente, A.; Mortreux, A.; Visseaux, M.; Zinck, P. *Chem. Rev.* **2013**, *113*, 3836–3857. (e) Takeuchi, D. Stereoselective Polymerization of Conjugated Dienes. *Encyclopedia of Polymer Science and Technology*; Wiley: New York, **2013**; pp 1–25.

(3) Trost, B. M. *Science* **1991**, *254*, 1471–1477.

(4) For select hydrofunctionalizations of dienes, see: (a) Löber, O.; Kawatsura, M.; Hartwig, J. F. *J. Am. Chem. Soc.* **2001**, *123*, 4366–4367. (b) Page, J. P.; RajanBabu, T. V. *J. Am. Chem. Soc.* **2012**, *134*, 6556–6559. (c) Zbieg, J. R.; Yamaguchi, E.; McInturff, E. L.; Krische, M. J. *Science* **2012**, *336*, 324–327. (d) Park, B. Y.; Montgomery, T. P.; Garza, V. J.; Krische, M. J. *J. Am. Chem. Soc.* **2013**, *135*, 16320–16323. (e) Chen, Q.-A.; Kim, D. K.; Dong, V. M. *J. Am. Chem. Soc.* **2014**, *136*, 3772–3775. (f) Saini, V.; O'Dair, M.; Sigman, M. S. *J. Am. Chem. Soc.* **2015**, *137*, 608–611. (g) Marcum, J. S.; Roberts, C. C.; Manan, R. S.; Cervarich, T. N.; Meek, S. J. *J. Am. Chem. Soc.* **2017**, *139*, 15580–15583. (h) Yang, X.-H.; Lu, A.; Dong, V. M. *J. Am. Chem. Soc.* **2017**, *139*, 14049–14052. (i) Gui, Y.-Y.; Hu, N.; Chen, X.-W.; Liao, L.-L.; Ju, T.; Ye, J.-H.; Zhang, Z.; Li, J.; Yu, D.-G. *J. Am. Chem. Soc.* **2017**, *139*, 17011–17014. (j) Adamson, N. J.; Hull, E.; Malcolmson, S. J. *J. Am. Chem. Soc.* **2017**, *139*, 7180–7183. (k) Adamson, N. J.; Wilbur, K. C. E.; Malcolmson, S. J. *J. Am. Chem. Soc.* **2018**, *140*, 2761–2764. (l) Schmidt, V. A.; Kennedy, C. R.; Bezdek, M. J.; Chirik, P. J. *J. Am. Chem. Soc.* **2018**, *140*, 3443–3453. For reviews, see: (m) Hydrofunctionalization. *Topics in Organometallic Chemistry*; Ananikov, V. P., Tanaka, M. Eds.; Springer: Berlin, **2014**; Vol. 343. (n) McNeill, E.; Ritter, T. *Acc. Chem. Res.* **2015**, *48*, 2330–2343. (o) Bezzenine-Lafollée, S.; Gil, R.; Prim, D.; Hannedouche, J. *Molecules* **2017**, *22*, 1901–1929.

(5) Hirao, T.; Masunaga, T.; Yamada, N.; Ohshiro, Y.; Agawa, T. *Bull. Chem. Soc. Jpn.* **1982**, *55*, 909–913.

(6) Mirzaei, F.; Han, L.-B.; Tanaka, M. *Tet. Lett.* **2001**, *42*, 297–299.

(7) Two additional examples have been reported for the coupling of hydrophosphorous acid (H₃PO₂) and a 1,3-diene that yield allylic phosphinic acids via Pd-catalyzed 1,4-addition, see: Bravo-Altamirano, K.; Abrunhosa-Thomas, I.; Montchamp, J.-L. *J. Org. Chem.* **2008**, *73*, 2292–2301.

(8) For select reviews of phosphines in catalysis, see: (a) Tolman, C. A. *Chem. Rev.* **1977**, *77*, 313–348. (b) van Leeuwen, P. W. N. M.; Kamer, P. C. J.; Reek, J. N. H.; Dierkes, P. *Chem. Rev.* **2000**, *100*, 2741–2770. (c) Noyori, R.; Ohkuma, T. *Angew. Chem. Int. Ed.* **2001**, *40*, 40–73. (d) Xiao, Y.; Guo, H.; Kwon, O. *Aldrichimica Acta.* **2016**, *49*, 3–13. (e) Ni, H.; Chan, W.-L.; Lu, Y. *Chem. Rev.* **2018**, *118*, 9344–9411.

(9) For reviews of phosphines in medicine, see: (a) Tiekink, E. R. T. *Bioinorg. Chem. Appl.* **2003**, *1*, 53–67. (b) Phillips, A. D.; Gonsalvi, L.; Romerosa, A.; Vizza, F.; Peruzzini, M. *Coord. Chem. Rev.* **2004**, *248*, 955–993. (c) Dominelli, B.; Correia, J. D. G.; Kühn, F. E. *J. Organomet. Chem.* **2018**, *866*, 153–164.

(10) For a select example of phosphines in agrochemicals, see: (a) Schlipalius, D. I.; Valmas, N.; Tuck, A. G.; Jagadeesan, R.; Ma, L.; Kaur, R.; Goldinger, A.; Anderson, C.; Kuang, J.; Zury, S.; Mau, Y. S.; Cheng, Q.; Collins, P. J.; Nayak, M. K.; Schirra, H. J.; Hilliard, M. A.; Ebert, P. R. *Science* **2012**, *338*, 807–810. For a review, see: (b) Nath, N. S.; Bhattacharya, I.; Tuck, A. G.; Schlipalius, D. I.; Ebert, P. R. *J. Toxicol.* **2011**, *2011*, 1–9.

(11) We are using the definition of hydrophosphinylation that refers to the addition of a phosphine oxide P–H bond across a degree of unsaturation, see: Han, L.-B.; Choi, N.; Tanaka, M. *Organometallics* **1996**, *15*, 3259–3261.

(12) Yang, X.-H.; Dong, V. M. *J. Am. Chem. Soc.* **2017**, *139*, 1774–1777.

(13) Yang, X.-H.; Davison, R. T.; Dong, V. M. *J. Am. Chem. Soc.* **2018**, *140*, 10443–10446.

(14) For reviews on reducing phosphine oxides to phosphines, see: (a) Hérault, D.; Nguyen, D. H.; Nuel, D.; Buono, G. *Chem. Soc. Rev.* **2015**, *44*, 2508–2528. (b) Kovács, T.; Keglevich, G. *Curr. Org. Res.* **2017**, *21*, 569–585.

(15) Grayson, M.; Farley, C. E.; Streuli, C. A. *Tetrahedron* **1967**, *23*, 1065–1078.

(16) For select hydrophosphinylations of alkenes, see: (a) Kawaguchi, S.-I.; Nomoto, A.; Sonoda, M.; Ogawa, A. *Tet. Lett.* **2009**, *50*, 624–626. (b) Yoo, W.-J.; Kobayashi, S. *Green. Chem.* **2013**, *15*, 1844–1848. (c) Li, Z.; Fan, F.; Zhang, Z.; Xiao, Y.; Liu, D.; Liu, Z.-Q. *RSC Adv.* **2015**, *5*, 27853–27856.

(17) For select hydrophosphinylations of alkynes, see: (a) Han, L.-B.; Hua, R.; Tanaka, M. *Angew. Chem. Int. Ed.* **1998**, *37*, 94–96. (b) Han, L.-B.; Zhao, C.-Q.; Tanaka, M. *J. Org. Chem.* **2001**, *66*, 5929–5932. (c) Han, L.-B.; Zhang, C.; Yazawa, H.; Shimada, S. *J. Am. Chem. Soc.* **2004**, *126*, 5080–5081. (d) Rooy, S. V.; Cao, C.; Patrick, B. O.; Lam, A.; Love, J. A. *Inorg. Chim. Acta.* **2006**, *359*, 2918–2923. (e) Chen, T.; Zhao, C.-Q.; Han, L.-B. *J. Am. Chem. Soc.* **2018**, *140*, 3139–3155. For a review, see: (f) Xu, Q.; Han, L.-B. *J. Organomet. Chem.* **2011**, *696*, 130–140.

(18) For a review on ligand bite angle effects, see: ref 8b.

(19) We also tried the PHOX ligand scaffold, which has demonstrated high reactivity and enantioselectivity in Pd-catalyzed diene hydroamination (see: ref 4j) and hydroalkylation (see: ref 4k), but observed no reactivity.

(20) Herriott, A. W.; Mislow, K. *Tet. Lett.* **1968**, *9*, 3013–3016.

(21) Lühr, S.; Holz, J.; Börner, A. *ChemCatChem* **2011**, *3*, 1708–1730.

(22) X-ray crystallography data confirmed the absolute configuration of **3an**, CCDC: 1868886. The absolute configuration of compounds **3aa–3am**, **3an'** and **3ba–3na** were assigned by analogy.

(23) See the Supporting Information for more details.

(24) For select enantioselective additions to Michael acceptors, see: (a) Carlone, A.; Bartoli, G.; Bosco, M.; Sambri, L.; Melchiorre, P. *Angew. Chem. Int. Ed.* **2007**, *46*, 4504–4506. (b) Ibrahim, I.; Rios, R.; Vesely, J.; Hammar, P.; Eriksson, L.; Himo, F.; Córdova, A. *Angew. Chem. Int. Ed.* **2007**, *46*, 4507–4510. (c) Feng, J.-J.; Chen, X.-F.; Shi, M.; Duan, W.-L. *J. Am. Chem. Soc.* **2010**, *132*, 5562–5563. (d) Chew, R. J.; Teo, K. Y.; Huang, Y.; Li, B.-B.; Li, Y.; Pullarkat, S. A.; Leung, P.-H. *Chem. Commun.* **2014**, *50*, 8768–8770. For a review, see: (e) Pullarkat, S. A. *Synthesis* **2016**, *48*, 493–503.

(25) For select enantioselective transition metal-catalyzed substitutions, see: (a) Butti, P.; Rochat, R.; Sadow, A. D.; Togni, A. *Angew. Chem. Int. Ed.* **2008**, *47*, 4878–4881. (b) Zhang, L.; Liu, W.; Zhao, X. *Eur. J. Org. Chem.* **2014**, *2014*, 6846–6849. (c) Liu, C.; Wang, Q. *Angew. Chem. Int. Ed.* **2018**, *57*, 4727–4731.

Chapter 4 – Enantioselective Addition of α -Nitroesters to Alkynes⁴

4.1 Introduction

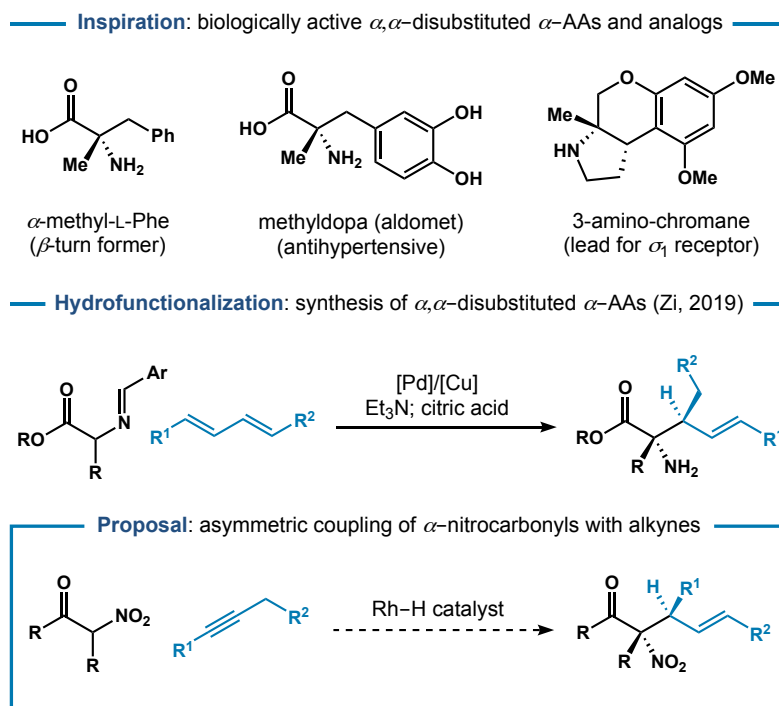


Figure 4.1. Enantioselective addition of α -nitroesters to alkynes.

By designing and synthesizing α -amino acids (α -AAs), chemists have expanded the genetic code, shed light on protein function, and enabled innovative medical applications.¹⁻³ The α,α -disubstituted α -AAs and related analogs attract interest due to their metabolic stability, unique conformations, and potent bioactivity (Figure 4.1).⁴ Enantioenriched α,α -disubstituted α -AAs are targeted by various strategies, including phase-transfer catalysis, organocatalysis, and transition-metal catalysis.⁵ Despite an interest in these motifs, methods for the enantio- and diastereoselective preparation of α,α -disubstituted α -AAs bearing contiguous stereocenters remain sought after;⁶ emerging reports feature pre-functionalized allylic partners. The direct addition of an amino acid surrogate to a π -system represents an attractive approach to α,α -disubstituted α -AAs. Towards this

⁴ Adapted with permission from Davison, R. T.; Parker, P. D.; Hou, X.; Chung, C. P.; Augustine, S. A.; Dong, V. *M. Angew. Chem. Int. Ed.* **2021**, *60*, 4599–4603. © 2021 John Wiley and Sons

end, Zi and coworkers exploited synergistic Pd/Cu catalysis for the stereodivergent coupling of aldimine esters and 1,3-dienes.⁷ In a complementary approach, we propose using a Rh-hydride (Rh-H) catalyst to couple α -nitrocarbonyls and alkynes to generate the corresponding α -AA precursors. This atom-economical⁸ coupling exploits two simple functional groups and provides rapid access to synthons for the building blocks of life.⁹

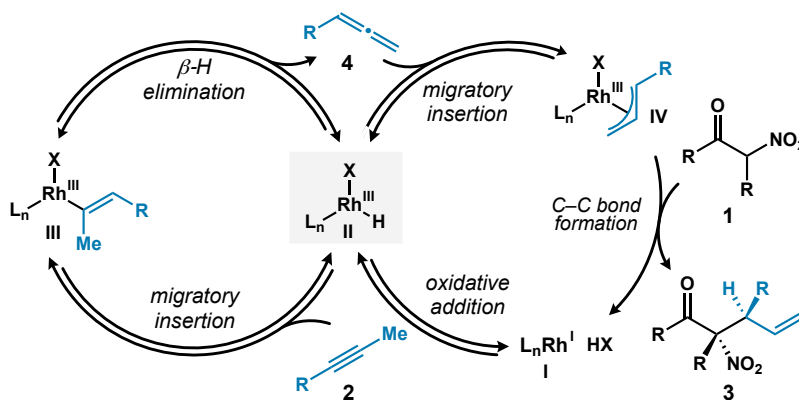


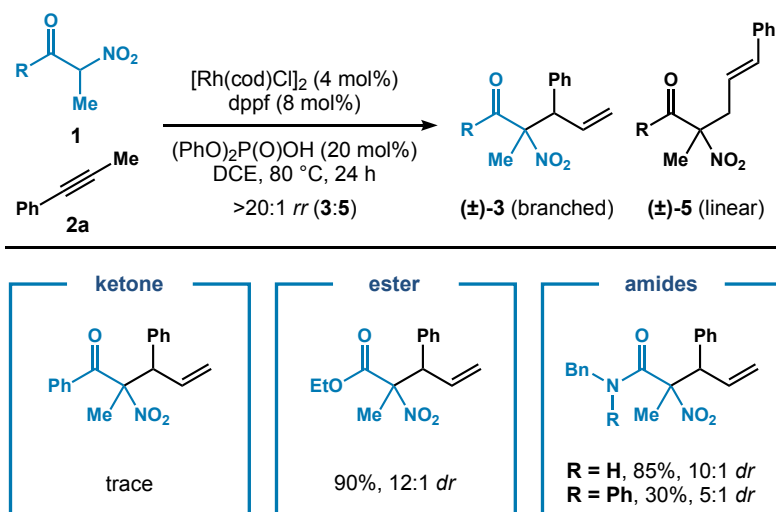
Figure 4.2. Proposed mechanism for Rh-catalyzed allylation.

Based on literature precedent,¹⁰ we envisioned a tandem catalytic cycle for the asymmetric coupling of α -nitrocarbonyls (1) and alkynes (2) to yield α -AA precursors 3 (Figure 4.2). Wolf and Werner discovered that Rh-H complexes isomerize alkynes (2) via an allene intermediate (4) to form Rh- π -allyl species IV.¹¹ By using this isomerization, the Breit laboratory achieved asymmetric and catalytic couplings of alkynes with a wide-range of heteroatom nucleophiles to afford branched allylic products.¹² In comparison, the analogous coupling of alkynes with carbon nucleophiles remains more limited, with only three asymmetric variants.¹³ We previously reported that aldehydes couple to alkynes with high enantio- and diastereoselectivity when using a chiral Rh-H catalyst in synergy with a chiral amine co-catalyst.^{13a} Xing and coworkers expanded this approach for the coupling of ketones with alkynes, however, an achiral amine co-catalyst furnishes the branched products with little to no diastereocontrol.^{13c}

In related studies, we and Breit independently reported that 1,3-dicarbonyls can couple to alkynes to generate branched allylic carbonyl motifs.¹⁴ Promising reactivity and regioselectivity has been achieved. However, obtaining high levels of enantio- and diastereoselectivity has been challenging. It occurred to us that α -nitrocarbonyls display comparable chelation aptitude¹⁵ and acidity ($pK_a = ca. 8$)¹⁶ to 1,3-dicarbonyls. Thus, we imagined α -nitrocarbonyls would be suitable nucleophiles for trapping Rh- π -allyl species **IV**. With this design in mind, we set out to couple α -nitrocarbonyls and alkynes with enantio- and diastereocontrol.

4.2 Results and Discussion

Table 4.1. Investigating various α -nitrocarbonyls.^[a]

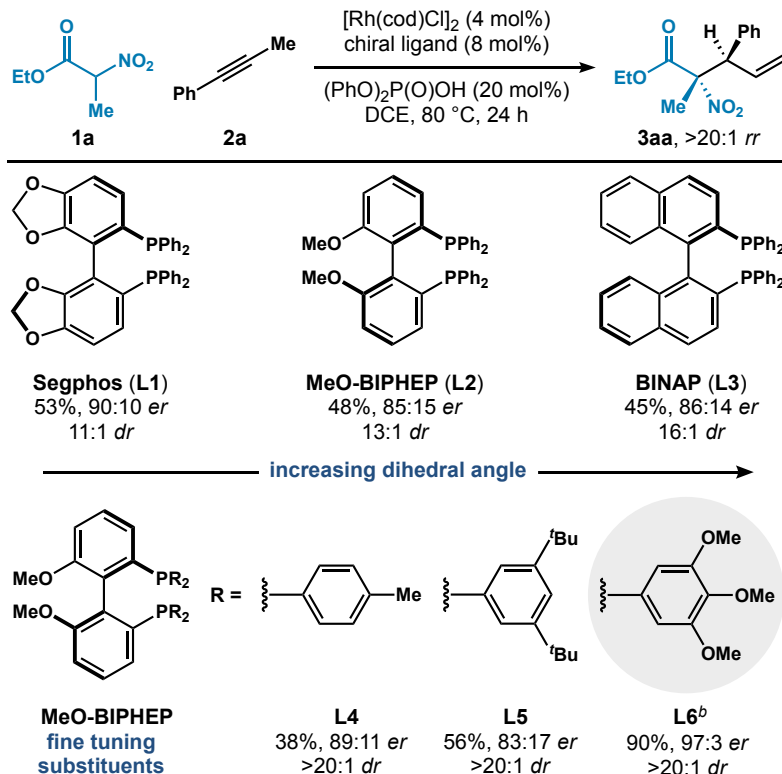


^[a]**1** (0.10 mmol), **2a** (0.15 mmol), [Rh(cod)Cl]₂ (4.0 mol%), dppf (8.0 mol%), (PhO)₂P(O)OH (20 mol%), DCE (0.20 mL), 80 °C, 24 h. Yields determined by ¹H NMR referenced to an internal standard. Cod = 1,5-cyclooctadiene, dppf = 1,1'-bis(diphenylphosphino)ferrocene, DCE = 1,2-dichloroethane.

In preliminary studies, we discovered that various α -nitrocarbonyls (**1**) add to the commercially available alkyne **2a** (Table 4.1). Using a combination of [Rh(cod)Cl]₂, dppf, and diphenyl phosphate, we observe allylic α -nitroketone, α -nitroester, and α -nitroamide products as single regioisomers (>20:1 *rr*) with moderate to high diastereoselectivity (5:1–12:1 *dr*).¹⁷ In accordance with previous reports, there is a preference for the branched regioisomer, which bears two contiguous stereocenters.^{10a-d,12-14} Our findings complement an enantioselective Pd-catalyzed

α -nitroester allylation reported by Ooi and coworkers.¹⁸ In Ooi's study, the use of allylic carbonates affords linear regioisomers with one stereocenter.

Table 4.2. Survey of chiral ligands.^[a]

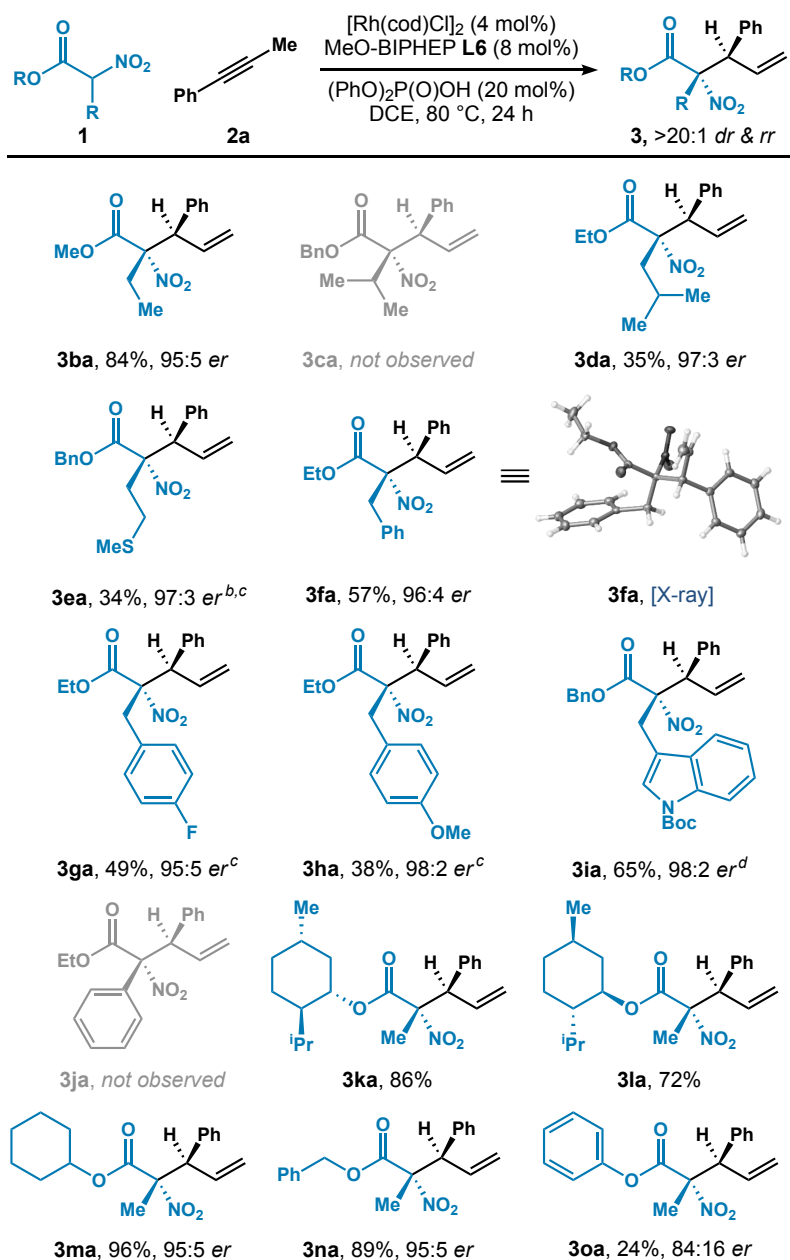


^[a]**1a** (0.10 mmol), **2a** (0.15 mmol), $[\text{Rh}(\text{cod})\text{Cl}]_2$ (4.0 mol%), chiral ligand (8.0 mol%), $(\text{PhO})_2\text{P}(\text{O})\text{OH}$ (20 mol%), DCE (0.20 mL), 80 °C, 24 h. Yields determined by ¹H NMR referenced to an internal standard. ^[b]Isolated yield for a 1 mmol reaction.

Next, we focused on an enantioselective variant for the coupling of α -nitroesters with alkynes because the resulting motifs are readily converted to α -AAs.¹⁹ To identify the appropriate chiral catalyst, we selected α -nitroester **1a** and alkyne **2a** as the model substrates (Table 4.2). Using atropisomeric bisphosphine ligands **L1–L3** with a range of dihedral angles,²⁰ we observe the allylic α -AA precursor **3aa** with moderate yields (45–53%) and enantioselectivities (85:15–90:10 *er*). Ultimately, we found that commercial MeO-BIPHEP **L6** affords **3aa** in 90% yield with 97:3 *er*, $>20:1$ *dr*, and $>20:1$ *rr* on preparative scale (1 mmol).^{21,22} This coupling relies on the use of alkynes as the unsaturated partner instead of activated olefins, imines, propargylic carbonates, and

allylic leaving groups.^{18,19} Therefore, we explored the scope of this transformation to access unique β -aryl- α -nitroester motifs.

Table 4.3. α -Nitrocarbonyl scope.^[a]

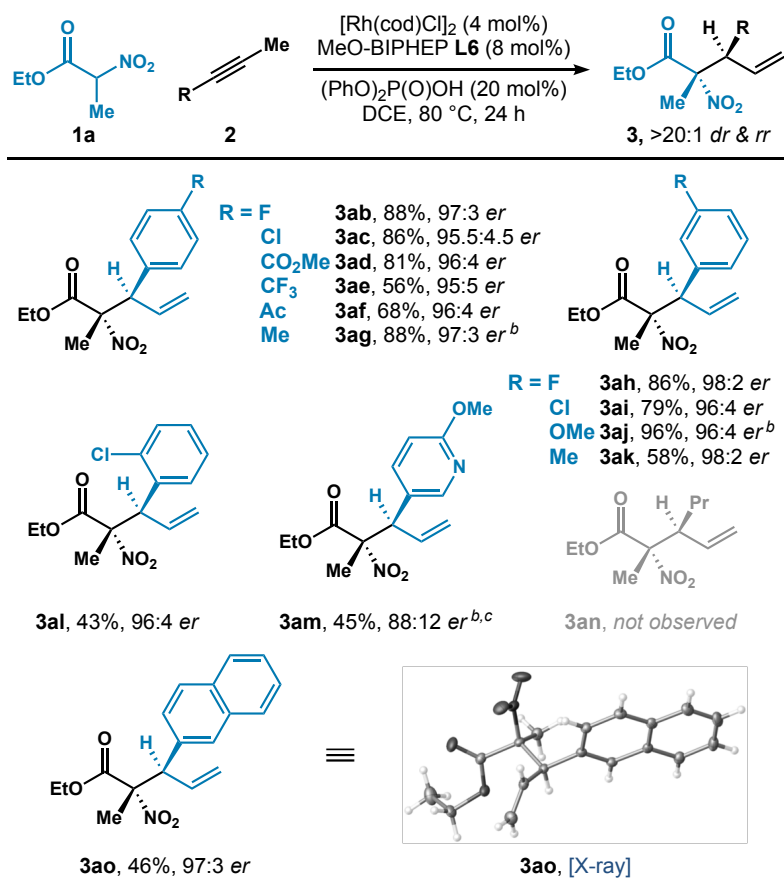


^[a]**1** (0.10 mmol), **2a** (0.15 mmol), $[\text{Rh}(\text{cod})\text{Cl}]_2$ (4.0 mol%), MeO-BIPHEP **L6** (8.0 mol%), $(\text{PhO})_2\text{P}(\text{O})\text{OH}$ (20 mol%), DCE (0.20 mL), 80 °C, 24 h. Isolated yields. ^[b]6:1 *dr*. ^[c]Yields based on recovered starting material (brsm): **3ea** (76%), **3ga** (96%), and **3ha** (65%). ^[d] $[\text{Rh}(\text{cod})\text{Cl}]_2$ (8 mol%) and **L6** (16 mol%) instead of standard conditions.

With this protocol, we explored the asymmetric coupling of various α -nitroesters with **2a** (Table 4.3). Analogs of ethylglycine (**3ba**), leucine (**3da**), methionine (**3ea**), phenylalanine (**3fa**), 4-fluoro-phenylalanine (**3ga**), tyrosine (**3ha**), and tryptophan (**3ia**) are generated with moderate to high yields (34–84%) and excellent levels of enantioselectivity ($\geq 95:5$ *er*). The absolute configuration of **3fa** was confirmed by X-ray crystallographic analysis.^{21,22} In the case of lower yielding substrates, we often recover α -nitroester **1**.²¹ The bulkier β -branched α -nitroesters **1c** and **1j** do not couple to **2a** to form analogs of valine (**3ca**) and phenylglycine (**3ja**), respectively. Alkyl-substituted esters **3ka–3na** provide higher reactivity than aryl ester **3oa**. We observe high levels of diastereocontrol ($>20:1$ *dr*) for forming **3ka** and **3la**, which suggests the C–C bond is forged by catalyst control.

Table 4.4 captures results from our study on the addition of **1a** to various alkynes **2**. Aryl alkynes possessing a variety of electronics and substitution patterns participate in the asymmetric coupling (**3ab–3al** and **3ao**). Alkynes bearing halides (**2b**, **2c**, **2h**, **2i** and **2l**), carbonyls (**2d** and **2f**), and extended π -systems (**2o**) transform to the corresponding allylic α -nitroesters **3**. Aryl alkynes with electron-donating substituents (**1g** and **1j**) display lower conversion under standard conditions. Increasing the catalyst loading results in improved yields of **3ag** and **3aj** (88% and 96%, respectively), while maintaining high stereoselectivity ($\geq 96:4$ *er* and $>20:1$ *dr*). The presence of an ortho-substituent on alkyne **2l** imparts lower reactivity (43%), presumably due to steric hindrance. Pyridyl alkyne **2m** converts to allylic α -nitroester **3am** with a higher catalyst loading. It appears that an aromatic or heteroaromatic substituent on the alkyne is critical for reactivity (see **3an**). The absolute configuration of **3ao** was confirmed by X-ray crystallographic analysis.^{21,22}

Table 4.4. Alkyne scope.^[a]



^[a]**1a** (0.10 mmol), **2** (0.15 mmol), $[\text{Rh}(\text{cod})\text{Cl}]_2$ (4.0 mol%), MeO-BIPHEP **L6** (8.0 mol%), $(\text{PhO})_2\text{P}(\text{O})\text{OH}$ (20 mol%), DCE (0.20 mL), 80 °C, 24 h. Isolated yields. ^[b] $[\text{Rh}(\text{cod})\text{Cl}]_2$ (7.5 mol%) and **L6** (15 mol%) instead of standard conditions. ^[c]15:1 *dr*.

Further experiments provide support for the mechanism depicted in Figure 4.2. First, we monitored a mixture of $[\text{Rh}(\text{cod})\text{Cl}]_2$, MeO-BIPHEP **L6**, and diphenyl phosphate by ¹H NMR spectroscopy.²¹ We observe a resonance in the spectrum at -16.2 ppm. The observed resonance is consistent with reported values for $\text{Rh}^{\text{III}}\text{-H}$ complexes.²³ This resonance disappears in the ¹H NMR spectrum upon the addition of alkyne **2a**. Second, we subjected deuterated alkyne **d-2a** to the standard reaction conditions (Figure 4.3A). We observe deuterium scrambling into the β -, γ -, and δ -positions of allylic α -nitroester **d-3aa**. The incorporation of hydrogen atoms at the δ -position of **d-3aa** supports reversible β -H elimination in the isomerization pathway. Third, to examine the plausibility of an allene intermediate in the catalytic cycle, we subjected 1-phenylallene (**4a**) to the

standard conditions (Figure 4.3B). We observe **3aa** (14% yield) when using an excess of allene **4a**. Moreover, the remaining amount of allene **4a** is consumed. These results agree with previous reports that suggest maintaining a low concentration of allene intermediate **4** slows competitive polymerization.^{10i,12a,24,25}

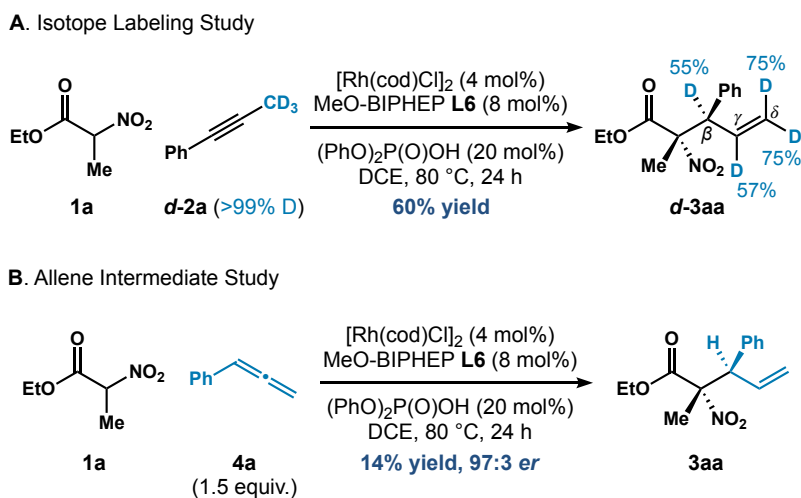
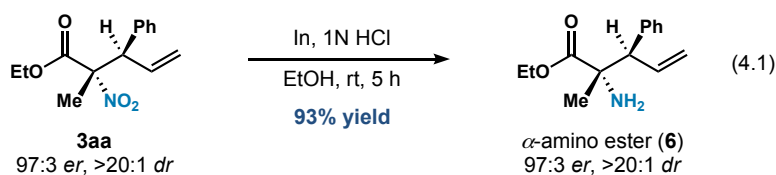


Figure 4.3. Mechanistic studies.

Treating allylic α -nitroester **3aa** with In powder readily yields the corresponding α -amino ester **6** in 93% yield (eq 4.1). This simple reduction allows for rapid access to α,α -disubstituted α -amino esters that contain two contiguous stereocenters, without stereoablation.



4.3 Conclusion and Future Work

The use of Rh-H catalysis offers an approach to novel α -AAs. The allylic α -AA precursors prepared contain an olefin handle that is attractive due to its potential use for protein modifications,²⁶ glycopeptide synthesis,²⁷ and cyclizations.²⁸ Our strategy offers a solution to the challenging preparation of contiguous stereocenters in an acyclic framework with diastereo- and enantiocontrol. Insights from this study will guide the development of related α -nitrocarbonyl

coupling reactions with alkynes. Our laboratory has found initial success in the enantioselective addition of α -nitroamides to alkynes, which could provide a way to couple peptides containing α -nitroamide residues with alkynes.²¹ Future studies will focus on widening scope and understanding the origins of stereocontrol.

4.4 Author Contributions

Ryan T. Davison (R.T.D.) and Prof. Vy M. Dong (V.M.D.) conceived of the project discussed in Chapter 4. R.T.D. and V.M.D. co-wrote the text. R.T.D. identified the optimal conditions for the transformation (Table 4.2) with the aid of Sara A. Augustine (S.A.A.). Dr. Patrick D. Parker (P.D.P.), Xintong Hou (X.H.) and Crystal P. Chung (C.P.C.) explored the α -nitroester scope (Table 4.3). R.T.D. explored the alkyne scope (Table 4.4). X.H. and R.T.D. performed the mechanistic studies in Figure 4.3. R.T.D. demonstrated the chemoselective nitril reduction (eq 4.1). All authors analyzed the results and commented on the manuscript.

4.5 References

- (1) (a) de Graaf, A. J.; Kooijman, M.; Hennink, W. E.; Mastrobattista, E. *Bioconjugate Chem.* **2009**, *20*, 1281–1295. (b) Hodgson, D. R. W.; Sanderson, J. M. *Chem. Soc. Rev.* **2004**, *33*, 422–430. (c) Hoshida, T.; Sisido, M. *Curr. Opin. Chem. Biol.* **2002**, *6*, 809–815. (d) Hendrickson, T. L.; de Crécy-Lagard, V.; Schimmel, P. *Annu. Rev. Biochem.* **2004**, *73*, 147–176. (e) Young, D. D.; Schultz, P. G. *ACS Chem. Biol.* **2018**, *13*, 854–870.
- (2) Liu, C. C.; Schultz, P. G. *Annu. Rev. Biochem.* **2010**, *79*, 413–444.
- (3) (a) Stevenazzi, A.; Marchini, M.; Sandrone, G.; Vergani, B.; Lattanzio, M. *Bioorg. Med. Chem. Lett.* **2014**, *24*, 5349–5356. (b) Blaskovich, M. A. T. *J. Med. Chem.* **2016**, *59*, 10807–10836.
- (4) (a) Tanaka, M. *Chem. Pharm. Bull.* **2007**, *55*, 349–358. (b) Aceña, J. L.; Sorochinsky, A. E.; Soloshonok, V. A. *Synthesis* **2012**, *44*, 1591–1602. (c) Porter, M. R.; Xiao, H.; Wang, J.; Smith, S. B.; Topczewski, J. J. *ACS Med. Chem. Lett.* **2019**, *10*, 1436–1442.
- (5) (a) Cativiela, C.; Díaz-de-Villegas, M. D. *Tetrahedron Asymmetry* **1998**, *9*, 3517–3599. (b) Cativiela, C.; Díaz-de-Villegas, M. D. *Tetrahedron Asymmetry* **2007**, *18*, 569–623. (c) Vogt, H.; Bräse, S. *Org. Biomol. Chem.* **2007**, *5*, 406–430. (d) Nájera, C.; Sansano, J. M. *Chem. Rev.* **2007**, *107*, 4584–4671. (e) Metz, A. E.; Kozłowski, M. C. *J. Org. Chem.* **2015**, *80*, 1–7.
- (6) (a) Trost, B. M.; Ariza, X. *Angew. Chem. Int. Ed.* **1997**, *36*, 2635–2637. (b) Trost, B. M.; Dogra, K. *J. Am. Chem. Soc.* **2002**, *124*, 7256–7257. (c) Chen, W.; Hartwig, J. F. *J. Am. Chem. Soc.* **2013**, *135*, 2068–2071. (d) Wei, X.; Liu, D.; An, Q.; Zhang, W. *Org. Lett.* **2015**, *17*, 5768–5771. (e) Su, Y.-L.; Li, Y.-H.; Chen, Y.-G.; Han, Z.-Y. *Chem. Commun.* **2017**, *53*, 1985–1988. (f) Huo, X.; Zhang, J.; Fu, J.; He, R.; Zhang, W. *J. Am. Chem. Soc.* **2018**, *140*, 2080–2084. (g) Wei, L.; Zhu, Q.; Xu, S.-M.; Chang, X.; Wang, C.-J. *J. Am. Chem. Soc.* **2018**, *140*, 1508–1513. (h) Wu, H.-M.; Zhang, Z.; Xiao, F.; Wei, L.; Dong, X.-Q.; Wang, C.-J. *Org. Lett.* **2020**, *22*, 4852–4857.
- (7) (a) Zhang, Q.; Yu, H.; Shen, L.; Tang, T.; Dong, D.; Chai, W.; Zi, W. *J. Am. Chem. Soc.* **2019**, *141*, 14554–14559. For related studies, see: (b) Goldfogel, M. J.; Meek, S. J. *Chem. Sci.* **2016**, *7*, 4079–4084. (c) Zhang, Z.; Xiao, F.; Wu, H.-M.; Dong, X.-Q.; Wang, C.-J. *Org. Lett.* **2020**, *22*, 569–574.
- (8) Trost, B. M. *Science* **1991**, *254*, 1471–1477.
- (9) Kitadai, N.; Maruyama, S. *Geosci. Front.* **2018**, *9*, 1117–1153.
- (10) For reviews, see: (a) Haydl, A. M.; Breit, B.; Liang, T.; Krische, M. J. *Angew. Chem. Int. Ed.* **2017**, *56*, 11312–11325. (b) Koschker, P.; Breit, B. *Acc. Chem. Res.* **2016**, *49*, 1524–1536. (c) Thoke, M. B.; Kang, Q. *Synthesis* **2019**, *51*, 2585–2631. (d) Li, G.; Huo, X.; Jiang, X.; Zhang, W. *Chem. Soc. Rev.* **2020**, *49*, 2060–2118. For examples, see: (e) Kadota, I.; Shibuya, A.; Gyoung, Y. S.; Yamamoto, Y. *J. Am. Chem. Soc.* **1998**, *120*, 10262–10263. (f) Patil, N. T.; Kadota, I.; Shibuya, A.; Gyoung, Y. S.; Yamamoto, Y. *Adv. Synth. Catal.* **2004**, *346*, 800–804. (g) Yang, C.; Zhang, K.; Wu, Z.; Yao, H.; Lin, A. *Org. Lett.* **2016**, *18*, 5332–5335. (h) Obora, Y.; Hatanaka, S.; Ishii, Y. *Org. Lett.* **2009**, *11*, 3510–3513. (i) Park, B. Y.; Nguyen, K. D.; Chaulagain, M. R.; Komanduri, V.; Krische, M. J. *J. Am. Chem. Soc.* **2014**, *136*, 11902–11905. (j) Liang, T.; Zhang, W.; Krische, M. J. *J. Am. Chem. Soc.* **2015**, *137*, 16024–16027.
- (11) Wolf, J.; Werner, H. *Organometallics* **1987**, *6*, 1164–1169.
- (12) (a) Chen, Q.-A.; Chen, Z.; Dong, V. M. *J. Am. Chem. Soc.* **2015**, *137*, 8392–8395. (b) Haydl, A. M.; Hilpert, L. J.; Breit, B. *Chem. Eur. J.* **2016**, *22*, 6547–6551. (c) Berthold, D.; Breit, B. *Org. Lett.* **2018**, *20*, 598–601. (d) Liu, Z.; Breit, B. *Angew. Chem. Int. Ed.* **2016**, *55*, 8440–8443. (e) Koschker, P.; Kähny, M.; Breit, B. *J. Am. Chem. Soc.* **2015**, *137*, 3131–3137.

(13) (a) Cruz, F. A.; Dong, V. M. *J. Am. Chem. Soc.* **2017**, *139*, 1029–1032. (b) Cruz, F. A.; Zhu, Y.; Tercenio, Q. D.; Shen, Z.; Dong, V. M. *J. Am. Chem. Soc.* **2017**, *139*, 10641–10644. (c) Xie, L.; Yang, H.; Ma, M.; Xing, D. *Org. Lett.* **2020**, *22*, 2007–2011. For a related study, see: (d) Ji, D.-W.; Yang, F.; Chen, B.-Z.; Min, X.-T.; Kuai, C.-S.; Hu, Y.-C.; Chen, Q.-A. *Chem. Commun.* **2020**, *56*, 8468–8471.

(14) (a) Cruz, F. A.; Chen, Z.; Kurtoic, S. I.; Dong, V. M. *Chem. Commun.* **2016**, *52*, 5836–5839. (b) Li, C.; Grugel, C. P.; Breit, B. *Chem. Commun.* **2016**, *52*, 5840–5843. (c) Beck, T. M.; Breit, B. *Eur. J. Org. Chem.* **2016**, *35*, 5839–5844. (d) Beck, T. M.; Breit, B. *Org. Lett.* **2016**, *18*, 124–127. (e) Zheng, W.-F.; Xu, Q.-J.; Kang, Q. *Organometallics* **2017**, *36*, 2323–2330.

(15) (a) Keller, E.; Veldman, N.; Spek, A. L.; Feringa, B. L. *Tetrahedron Asymmetry* **1997**, *8*, 3403–3413. (b) Keller, E.; Feringa, B. L. *Synlett* **1997**, *7*, 842–844.

(16) Kornblum, N.; Blackwood, R. K.; Powers, J. W. *J. Am. Chem. Soc.* **1957**, *10*, 2507–2509.

(17) On the basis of Zi's report (reference 7a), we investigated an aldimine ester and found that it does not couple to alkyne **2a** under the standard conditions.

(18) (a) Ohmatsu, K.; Ito, M.; Kunieda, T.; Ooi, T. *Nat. Chem.* **2012**, *4*, 473–477. For related studies, see: (b) Sawamura, M.; Nakayama, Y.; Tang, W.-M.; Ito, Y. *J. Org. Chem.* **1996**, *61*, 9090–9096. (c) Maki, K.; Kanai, M.; Shibasaki, M. *Tetrahedron* **2007**, *63*, 4250–4257. (d) Trost, B. M.; Surivet, J.-P. *Angew. Chem. Int. Ed.* **2000**, *39*, 3122–3124. (e) Trost, B. M.; Surivet, J.-P. *J. Am. Chem. Soc.* **2000**, *122*, 6291–6262.

(19) For reviews, see: (a) Shipchandler, M. T. *Synthesis* **1979**, *9*, 666–686. (b) N. Ono, *The Nitro Group in Organic Synthesis*, Wiley, New York, **2001**. For examples, see: (c) Li, H.; Wang, Y.; Tang, L.; Wu, F.; Liu, X.; Guo, C.; Foxman, B. M.; Deng, L. *Angew. Chem. Int. Ed.* **2005**, *44*, 105–108. (d) Sing, A.; Johnston, J. N. *J. Am. Chem. Soc.* **2008**, *130*, 5866–5867. (e) Chen, Z.; Morimoto, H.; Matsunaga, S.; Shibasaki, M. *J. Am. Chem. Soc.* **2008**, *130*, 2170–2171. (f) Uraguchi, D.; Koshimoto, K.; Ooi, T. *J. Am. Chem. Soc.* **2008**, *130*, 10878–10879. (g) Cui, H.-F.; Li, P.; Wang, X.-W.; Chai, Z.; Yang, Y.-Q.; Cai, Y.P.; Zhu, S.-Z.; Zhao, G. *Tetrahedron* **2011**, *67*, 312–317. (h) Shirakawa, S.; Terao, S. J.; He, R.; Maruoka, K. *Chem. Commun.* **2011**, *47*, 10557–10559. (i) Li, Y.-Z.; Li, F.; Tian, P.; Lin, G.-Q. *Eur. J. Org. Chem.* **2013**, 1558–1565. (j) Zhu, Q.; Meng, B.; Gu, C.; Xu, Y.; Chen, J.; Lei, C.; Wu, X. *Org. Lett.* **2019**, *21*, 9985–9989.

(20) For an example of enantioselectivity changing as a function of ligand dihedral angle, see: Shimizu, H.; Nagasaki, I.; Matsumura, K.; Sayo, N.; Saito, T. *Acc. Chem. Res.* **2007**, *40*, 1385–1393.

(21) See the Supporting Information for more details.

(22) CCDC 2014416 (**3fa**) and CCDC 2014415 (**3ao**) contain the supplementary crystallographic data for this report. These data can be obtained free of charge from The Cambridge Crystallographic Data Centre. The absolute configurations of the remaining allylic α -AA precursors **3** were assigned by analogy.

(23) (a) Giuseppe, A. D.; Castarlenas, R.; Pérez-Torrente, J. J.; Crucianelli, M.; Polo, V.; Sancho, R.; Lahoz, F. J.; Oro, L. A. *J. Am. Chem. Soc.* **2012**, *134*, 8171–8183. (b) Giuseppe, A. D.; Castarlenas, R.; Pérez-Torrente, J. J.; Lahoz, F. J.; Oro, L. A. *Chem. Eur. J.* **2014**, *20*, 8391–8403. (c) Yang, X.-H.; Davison, R. T.; Nie, S.-Z.; Cruz, F. A.; McGinnis, T. M.; Dong, V. M. *J. Am. Chem. Soc.* **2019**, *141*, 3006–3013.

(24) (a) Osakada, K.; Choi, J.-C.; Koizumi, T.-A.; Yamaguchi, I.; Yamamoto, T. *Organometallics* **1995**, *14*, 4962–4965. (b) Takagi, K.; Tomita, I.; Endo, T. *Macromolecules* **1997**, *30*, 7386–7390.

(25) In agreement with this statement, when we lower the amount of allene used to 0.3 equivalents, we observe **3aa** in 48% yield.

(26) (a) Lin, Y. A.; Chalker, J. M.; Davis, B. G. *ChemBioChem* **2009**, *10*, 959–969. (b) deGruyter, J. N.; Malins, L. R.; Baran, P. S. *Biochemistry* **2017**, *56*, 3863–3873.

(27) Gamblin, D. P.; Scanlan, E. M.; Davis, B. G. *Chem. Rev.* **2009**, *109*, 131–163.

(28) White, C. J.; Yudin, A. K. *Nat. Chem.* **2011**, *3*, 509–524.

Chapter 5 – Cu-Catalyzed Olefin Hydroacylation

5.1 Introduction

The Claisen condensation, discovered in 1887, forges a new C–C bond by reacting an enolizable carbonyl with a suitable acyl electrophile.¹ Nature uses iterative Claisen condensations with acetyl-CoA to synthesize polyketides and fatty acids.² Consequently, the 1,3-dicarbonyl motif is ubiquitous in nature and exhibits a wide range of bioactivities.³ Moreover, 1,3-dicarbonyls are readily derivatized to heterocyclic compounds (e.g., pyrazoles) that have importance to the pharmaceutical industry.⁴⁻⁷ Although the Claisen condensation is a powerful method for 1,3-dicarbonyl synthesis, asymmetric crossed-Claisen condensations are scarce in the literature and often require a chiral auxiliary^{8,9} or acyl transfer reagents.¹⁰⁻¹³ Instead, a common approach to access enantioenriched 1,3-dicarbonyl molecules relies on chemistry (e.g., alkylation) of the parent 1,3-dicarbonyl (Figure 5.1).¹⁴⁻¹⁸

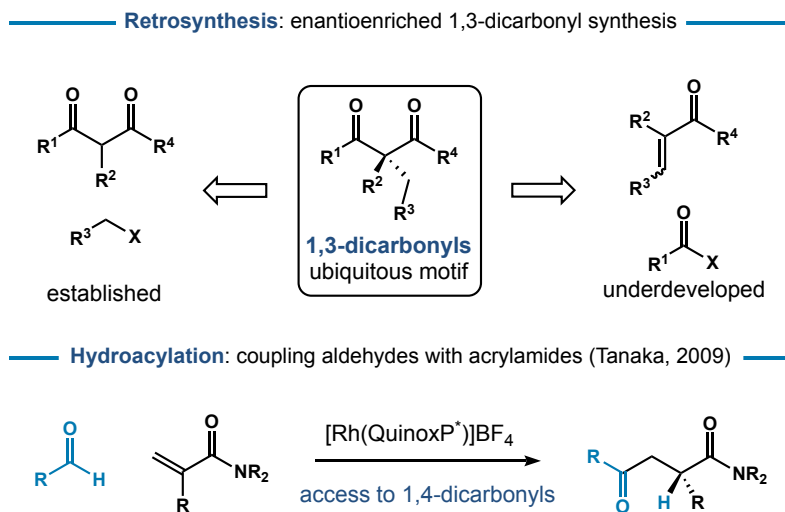


Figure 5.1. Enantioselective 1,3-dicarbonyl synthesis and olefin hydroacylation.

Due to our lab's longstanding interest in stereoselective olefin hydroacylation,¹⁹⁻²¹ we proposed a retrosynthesis of the 1,3-dicarbonyl motif that leads back to an α,β -unsaturated carbonyl and an acyl electrophile (Figure 5.1). By selecting two differentiated reaction partners

(an olefin and an acyl electrophile), we hoped to avoid the chemoselectivity challenges that often plague Claisen condensations.^{9,13} Traditional hydroacylation strategies that leverage formyl C–H bond activation have been explored for α,β -unsaturated carbonyl hydroacylation. Tanaka developed a Rh catalyst that adds aldehydes to acrylamides to afford enantioenriched *1,4-dicarbonyl products* (Figure 5.1).^{22,23} The observed regioselectivity is thought to arise from acrylamide chelation, which directs the hydrometallation event.

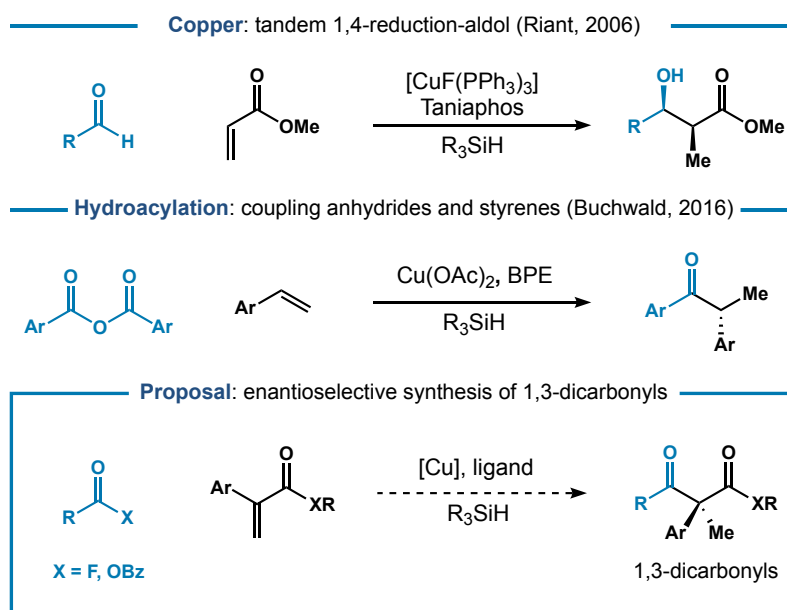


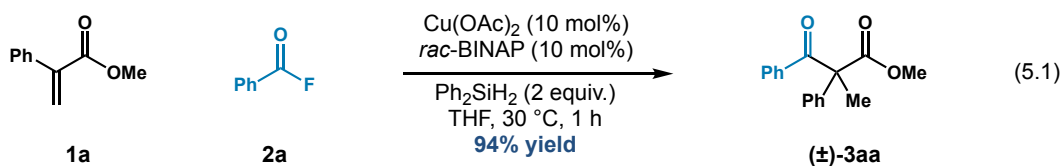
Figure 5.2. Enantioselective Cu-catalyzed hydrofunctionalization.

We hypothesized that a novel catalyst/reaction design could switch the regioselectivity to favor *1,3-dicarbonyl products*. In particular, Cu–H catalysis has emerged as a powerful strategy for α,β -unsaturated carbonyl hydrofunctionalization (Figure 5.2).^{24,25} The use of a Cu–H catalyst allows for the formation of a Cu–enolate *in situ*, which can be trapped with a variety of electrophiles. For example, Riant developed an asymmetric Cu-catalyzed tandem 1,4-reduction-aldol reaction between methyl acrylate and various aldehydes.²⁶ Several years later the Buchwald lab demonstrated that Cu–H catalysis promotes a hydroacylation reaction between carboxylic anhydrides and styrenes.^{27,28} Knowing that Cu–H species can facilitate 1,4-reduction of α,β -

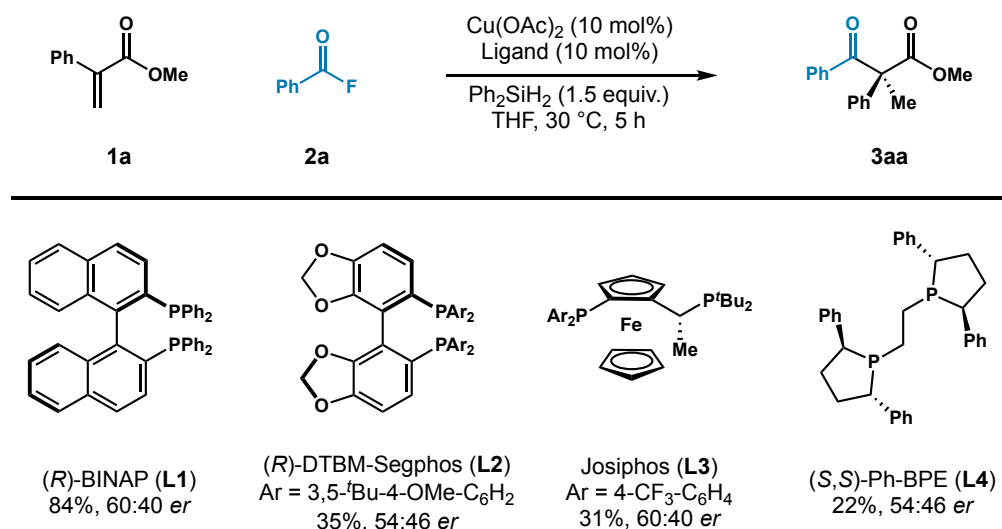
unsaturated carbonyls, we propose an enantioselective olefin hydroacylation that employs activated acyl electrophiles. If achieved, this α,β -unsaturated carbonyl hydroacylation would afford complementary access to enantioenriched 1,3-dicarbonyls.

5.2 Results and Discussion

To begin our studies, we selected acrylates (**1**) and benzoyl fluoride (**2a**) as the model substrates. Benzoyl fluorides (**2**) were identified as an optimal acyl electrophile for a few reasons: (1) they are bench-stable and easy to prepare,²⁹ (2) Cu(I)-allyl species are known to engage with benzoyl fluorides in acylation reactions,³⁰ and (3) the CuF species generated after product formation should readily undergo sigma bond metathesis with a hydrosilane to regenerate the Cu-H catalyst. Gratifyingly, when we subject **1a** and **2a** to a mixture of Cu(OAc)₂, *rac*-BINAP, and diphenylsilane we observe 1,3-dicarbonyl (\pm)-**3aa** in 94% yield (eq 5.1). Other achiral ligands were surveyed but offered inferior reactivity and/or deleterious reduction of benzoyl fluoride (**2a**) to benzyl alcohol.

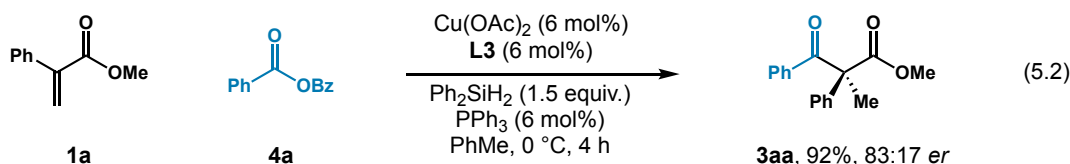


Next, we sought to identify an appropriate chiral ligand that would render the Cu-catalyzed hydroacylation enantioselective. Table 5.1 showcases a survey of ligands that are often employed in asymmetric Cu-H catalysis.^{24,25,31} Changing the ligand's backbone and phosphine substituents has little to no effect on the enantioselectivity of the transformation (54:46–60:40 *er*), but does have an impact on reactivity (22–84%). After extensive reaction optimization, the enantioselectivity remained largely the same with little to no dependence on ligand identity, solvent, and temperature.³²

Table 5.1. Surveying chiral ligands.^[a]

^[a]**1a** (0.050 mmol), **2a** (0.075 mmol), $\text{Cu}(\text{OAc})_2$ (10 mol%), Ligand (10 mol%), Ph_2SiH_2 (1.5 equiv.), THF (0.20 mL), 30 °C, 5 h. Yields determined by ^1H NMR referenced to an internal standard. Enantioselectivity ratio (*er*) is determined by chiral SFC. The absolute configuration of **3aa** is unknown at this time and is depicted for illustrative purposes.

We hypothesized that the low enantioselectivity could be attributed to a kinetically slow capture of the Cu(I)-enolate with the acid fluoride (**2**).^{24,26} To test this hypothesis, we examined carboxylic anhydrides (**4**) as the acyl partner. After resurveying chiral ligands, we found that Josiphos (**L3**) affords **3aa** in 92% yield with 83:17 *er* (eq 5.2). Changing the solvent to toluene (PhMe), lowering the reaction temperature to 0 °C, and adding a secondary ligand (PPh_3)³³ improved the yield and minimized byproduct formation. To date, this is the highest yield and enantioselectivity observed for the asymmetric Cu-catalyzed hydroacylation of α,β -unsaturated carbonyls.



5.3 Conclusion and Future Work

The use of Cu-H catalysis allows for a complementary synthesis of enantioenriched 1,3-dicarbonyls. This enantioselective hydroacylation couples activated acyl electrophiles (acid

fluorides and carboxylic anhydrides) with α,β -unsaturated carbonyls. The use of carboxylic anhydrides instead of acid fluorides allows for higher enantioselectivity. Future efforts will (1) focus on identifying a catalyst and/or reaction conditions that afford higher enantioselectivity, (2) expanding the substrate scope to activated amino acids as well as other classes of α,β -unsaturated carbonyls, and (3) studying the reaction mechanism to provide insights for the development of novel Cu-catalyzed hydrofunctionalizations.

5.4 Author Contributions

Ryan T. Davison (R.T.D.) and Prof. Vy M. Dong (V.M.D.) conceived of the project discussed in Chapter 5. R.T.D. wrote the text. R.T.D. performed all of the experiments in Chapter 5 and the Supporting Information (Appendix 5).

5.5 References

- (1) Claisen, L. *Ber. Dtsch. Chem. Ges.* **1887**, *20*, 655–657.
- (2) Heath, R. J.; Rock, C. O. *Nat. Prod. Rep.* **2002**, *19*, 581–596.
- (3) de Gonzalo, G.; Alcántara, A. R. *Pharmaceuticals* **2021**, *14*, 1043–1067.
- (4) Ke'lin, A. V.; Maioli, A. *Curr. Org. Chem.* **2003**, *7*, 1855–1886.
- (5) Kumar, V.; Kaur, K.; Gupta, G. K.; Sharma, A. K. *Eur. J. Med. Chem.* **2013**, *69*, 735–753.
- (6) Xu, Z.; Gao, C.; Ren, Q.-C.; Song, X.-F.; Feng, L.-S.; Lv, Z.-S. *Eur. J. Med. Chem.* **2017**, *139*, 429–440.
- (7) Mahajan, P.; Nikam, M.; Asrondkar, A.; Bobase, A.; Gill, C. *J. Heterocycl. Chem.* **2017**, *54*, 1415–1422.
- (8) Evans, D. A.; Ennis, M. D.; Le, T. *J. Am. Chem. Soc.* **1984**, *106*, 1154–1156.
- (9) Nagase, R.; Oguni, Y.; Ureshino, S.; Mura, H.; Misaki, T.; Tanabe, Y. *Chem. Commun.* **2013**, *49*, 7001–7003.
- (10) Mermerian, A. H.; Fu, G. C. *J. Am. Chem. Soc.* **2003**, *125*, 4050–4051.
- (11) Mermerian, A. H.; Fu, G. C. *J. Am. Chem. Soc.* **2005**, *127*, 5604–5607.
- (12) Dietz, F. R.; Gröger, H. *Synlett* **2008**, *5*, 663–666.
- (13) Woods, P. A.; Morrill, L. C.; Bragg, R. A.; Smith, A. D. *Chem. Eur. J.* **2011**, *17*, 11060–11067.
- (14) Russo, A.; Fusco, C. D.; Lattanzi, A. *RSC Adv.* **2012**, *2*, 385–397.
- (15) Trost, B. M.; Radinov, R.; Grenzer, E. M. *J. Am. Chem. Soc.* **1997**, *119*, 7879–7880.
- (16) Ooi, T.; Miki, T.; Fukumoto, K.; Maruoka, K. *Adv. Synth. Catal.* **2006**, *348*, 1539–1542.
- (17) Hamashima, Y.; Hotta, D.; Sodeoka, M. *J. Am. Chem. Soc.* **2002**, *124*, 11240–11241.
- (18) Bartoli, G.; Bosco, M.; Carlone, A.; Cavalli, A.; Locatelli, M.; Mazzanti, A.; Ricci, P.; Sambri, L.; Melchiorre, P. *Angew. Chem. Int. Ed.* **2006**, *45*, 4966–4970.
- (19) Murphy, S. K.; Dong, V. M. *Chem. Commun.* **2014**, *50*, 13645–13649.
- (20) Dong, V. M.; Kou, K. G. M.; Le, D. N. Transition-Metal-Catalyzed Hydroacylation. In *Organic Reactions*, Vol. 96; Denmark, S. E., Ed.; Wiley: Hoboken, NJ, 2018; pp 229–592.
- (21) Davison, R. T.; Kuker, E. L.; Dong, V. M. *Acc. Chem. Res.* **2021**, *54*, 1236–1250.
- (22) Tanaka, K.; Shibata, Y.; Suda, T.; Hagiwara, Y.; Hirano, M. *Org. Lett.* **2007**, *9*, 1215–1218.
- (23) Shibata, Y.; Tanaka, K. *J. Am. Chem. Soc.* **2009**, *131*, 12552–12553.
- (24) Deutsch, C.; Krause, N. *Chem. Rev.* **2008**, *108*, 2916–2927.
- (25) Jordan, A. J.; Lalic, G.; Sadighi, J. P. *Chem. Rev.* **2016**, *116*, 8318–8372.
- (26) Chuzel, O.; Deschamp, J.; Chausteur, C.; Riant, O. *Org. Lett.* **2006**, *8*, 5943–5946.
- (27) Bandar, J. S.; Ascic, E.; Buchwald, S. L. *J. Am. Chem. Soc.* **2016**, *138*, 5821–5824.
- (28) Zhou, Y.; Bandar, J. S.; Buchwald, S. L. *J. Am. Chem. Soc.* **2017**, *139*, 8126–8129.
- (29) Ogiwara, Y.; Sakai, N. *Angew. Chem. Int. Ed.* **2020**, *59*, 574–594.
- (30) Boreux, A.; Indukuri, K.; Gagosz, F.; Riant, O. *ACS Catal.* **2017**, *7*, 8200–8204.
- (31) Liu, R. Y.; Buchwald, S. L. *Acc. Chem. Res.* **2020**, *53*, 1229–1243.
- (32) See the Supporting Information for more details.
- (33) Lipshutz, B. H.; Noson, K.; Chrisman, W.; Lower, A. *J. Am. Chem. Soc.* **2003**, *125*, 8779–8789.

Conclusion

Transition metal-hydride catalysis offers a powerful approach for stereoselective allylation and hydroacylation. In particular, 1,3-dienes and alkynes are suitable partners in the atom-economical generation of metal- π -allyl intermediates. These aforementioned organometallic intermediates have been captured with sulfur, phosphorus and carbon nucleophiles to furnish enantioenriched sulfides, phosphine oxides, and amino acid precursors. On the other hand, a Cu-catalyzed α,β -unsaturated carbonyl hydroacylation provides facile access to chiral 1,3-dicarbonyls. In all of these studies the careful selection of the transition metal (Rh, Pd, or Cu), supporting ligand, and hydride source allows for selective access to one stereoisomer when the possibility of others exist. Future efforts will be focused on incorporating the insights gained from these projects to develop related hydrofunctionalizations that employ other first-row transition metal catalysts.

Appendices

Appendix 1	Supporting Information for Chapter 1	70
Appendix 2	Supporting Information for Chapter 2	153
Appendix 3	Supporting Information for Chapter 3	215
Appendix 4	Supporting Information for Chapter 4	330
Appendix 5	Supporting Information for Chapter 5	450

Appendix 1 Supporting Information for Chapter 1

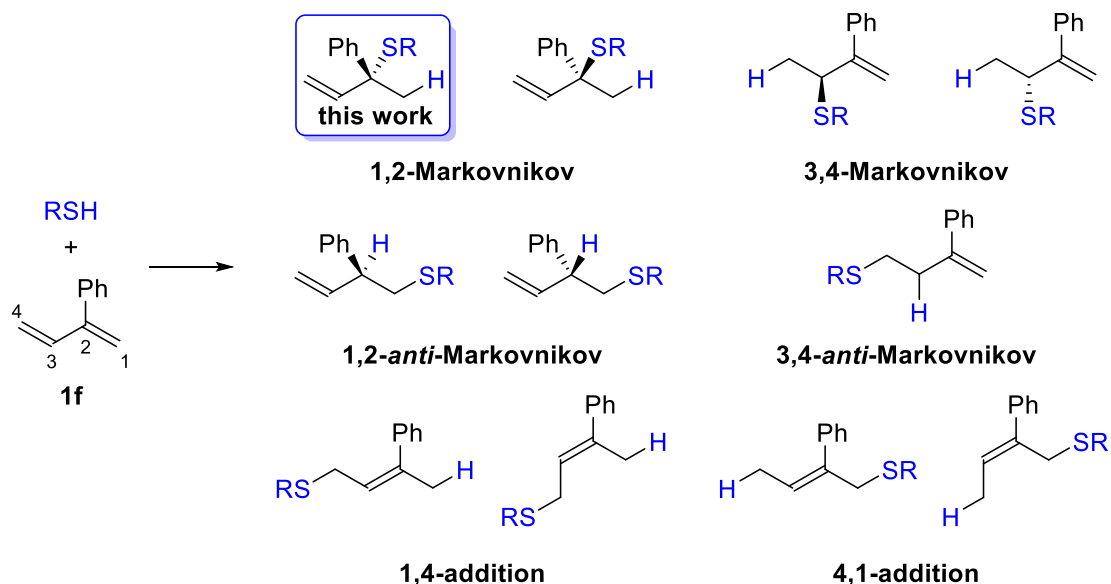
Catalytic Hydrothiolation: Regio- and Enantioselective Coupling of Thiols and Dienes¹

Table of Contents	Page
1. General	71
2. Possible isomers for the hydrothiolation of unsymmetric 1,3-diene 1f	72
3. General procedure for the hydrothiolation of 1,3-dienes	72
4. Derivatization for SFC analysis	72
5. References	83
6. NMR spectra of unknown compounds	84
7. SFC spectra	120

¹ For additional details, see: Yang, X.-H.; Davison, R. T.; Dong, V. M. *J. Am. Chem. Soc.* **2018**, *140*, 10443–10446.

1. General: Commercial reagents were purchased from Sigma Aldrich, Strem, Alfa Aesar, Acros Organics or TCI and used without further purification. 1,2-Dichloroethane, dichloromethane, tetrahydrofuran and methanol were purified using an Innovative Technologies Pure Solv system, degassed by three freeze-pump-thaw cycles, and stored over 3 Å MS within a N₂ filled glove box. All experiments were performed in oven-dried or flame-dried glassware. Reactions were monitored using either thin-layer chromatography (TLC) or gas chromatography using an Agilent Technologies 7890A GC system equipped with an Agilent Technologies 5975C inert XL EI/CI MSD. Visualization of the developed plates was performed under UV light (254 nm) or KMnO₄ stain. Organic solutions were concentrated under reduced pressure on a Büchi rotary evaporator. Purification and isolation of products were performed via silica gel chromatography (both column and preparative thin-layer chromatography). Column chromatography was performed with Silicycle Silia-P Flash Silica Gel using glass columns. Solvents were purchased from Fisher. ¹H and ¹³C NMR spectra were recorded on Bruker CRYO500 or DRX400 spectrometer. ¹H NMR spectra were internally referenced to the residual solvent signal or TMS. ¹³C NMR spectra were internally referenced to the residual solvent signal. Data for ¹H NMR are reported as follows: chemical shift (δ ppm), multiplicity (s = singlet, d = doublet, t = triplet, q = quartet, m = multiplet), coupling constant (Hz), integration. Data for ¹³C NMR are reported in terms of chemical shift (δ ppm). Infrared (IR) spectra were obtained on a Nicolet iS5 FT-IR spectrometer with an iD5 ATR, and are reported in terms of frequency of absorption (cm⁻¹). High resolution mass spectra (HRMS) were obtained on a micromass 70S-250 spectrometer (EI) or an ABI/Sciex QStar Mass Spectrometer (ESI). Enantiomeric excesses for enantioselective reactions were determined by chiral SFC analysis using an Agilent Technologies HPLC (1200 series) system and Aurora A5 Fusion. 1,3-Dienes **3ea-3ga** used here were known compounds and synthesized according to the reported methods.¹

2. Possible isomers for the hydrothiolation of unsymmetric 1,3-diene **1f**



3. General procedure for the hydrothiolation of 1,3-dienes

In a N₂-filled glovebox, ligand (0.002 mmol) and DCE (0.40 mL) were added to a 1 dram vial containing [Rh(cod)₂]SbF₆ (0.002 mmol). The resulting mixture was stirred for 10 min and then, thiol (0.20 mmol), and 1,3-diene (0.40 mmol) were added. The mixture was held at 30 °C until no starting material was observed by TLC. The regioselectivities were determined by ¹H NMR analysis of the unpurified reaction mixture. Isolated yields (obtained by column chromatography on silica gel or preparative thin-layer chromatography) are reported.

4. Derivatization for SFC analysis

The *er* values of the hydrothiolation products were determined by SFC analysis directly when possible. Otherwise, the sulfides were derivatized by one of three methods (A-C) described below.

Method A:

Sulfide product **3** was transformed to the corresponding sulfone for the determination of the *er* value. To a solution of sulfide **3** (0.05 mmol) in DCM (0.25 mL) was added *m*-CPBA (27.1 mg, 0.11 mmol, 70% wt). The resulting mixture was stirred at 0 °C for 20 min, then quenched with NaHCO₃ (1 mL), and extracted with DCM (1 mL × 3). The combined extracts were washed with brine, dried over anhydrous MgSO₄, and concentrated *in vacuo*. After flash chromatography on silica gel (petroleum ether/ethyl acetate = 5:1), the desired sulfone was analyzed by SFC to determine the *er* value.

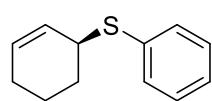
Method B:

Sulfide product **3** was transformed to the corresponding benzoyl ester for the determination of the *er* value. To a solution of sulfide **3** (0.1 mmol) in DCM (1.0 mL) was added benzoyl chloride (35 mg, 0.25 mmol) and pyridine (23 mg, 0.3 mmol). The resulting mixture was stirred at rt for 2 h. The reaction was then quenched with saturated NH₄Cl (1 mL) and extracted with DCM (1 mL × 3). The combined extracts were washed with brine, dried over anhydrous MgSO₄, and concentrated *in vacuo*. After flash chromatography on silica gel (petroleum ether/ethyl acetate = 5:1), the desired benzoyl ester was analyzed by SFC to determine the *er* value.

Method C:

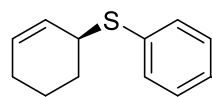
Sulfide product **3** was transformed to the corresponding amide for the determination of the *er* value. Sulfide **3** (0.10 mmol) was treated with aniline (12 μL, 0.12 mmol) in the presence of DMAP (1.2 mg, 0.01 mmol) and DCC (22 mg, 0.11 mmol) in THF (1 mL). The resulting mixture was stirred at rt for 2 h. The reaction was then filtered through celite. The filtrate was diluted with Et₂O (10 mL), washed with 3N HCl (10 mL) and saturated NaHCO₃ (10 mL), dried with MgSO₄, and concentrated *in vacuo*. After flash chromatography on silica gel (petroleum ether/ethyl acetate = 4:1), the desired amide was analyzed by SFC to determine the *er* value.

(*S*)-cyclohex-2-en-1-yl(phenyl)sulfane (**3aa**)²



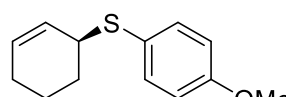
Colorless oil, 95% yield, 99:1 *er*, >20:1 *rr*, $[\alpha]_D^{24} = -132.0$ (*c* 3.2, CHCl₃). ¹H NMR (400 MHz, CDCl₃) δ 7.44 – 7.40 (m, 2H), 7.32 – 7.26 (m, 2H), 7.24 – 7.19 (m, 1H), 5.87 – 5.81 (m, 1H), 5.80 – 5.75 (m, 1H), 3.89 – 3.82 (m, 1H), 2.11 – 2.00 (m, 2H), 1.99 – 1.86 (m, 2H), 1.83 – 1.75 (m, 1H), 1.66 – 1.56 (m, 1H). ¹³C NMR (101 MHz, CDCl₃) δ 135.88, 131.27, 130.38, 128.81, 126.91, 126.56, 43.89, 28.81, 24.94, 19.45. **Chiral SFC**: 250 mm /CHIRALPAK AD, 0.1% *i*PrOH, 1.5 mL/min, 220 nm, 44 °C, nozzle pressure = 200 bar CO₂, *t*_{R1} (minor) = 12.3 min, *t*_{R2} (major) = 12.7 min.

(*S*)-cyclohex-2-en-1-yl(*p*-tolyl)sulfane (**3ab**)



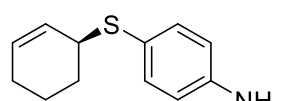
Colorless oil, 99% yield, 97:3 *er*, >20:1 *rr*, $[\alpha]_D^{24} = -117.8$ (*c* 0.5, CHCl₃). ¹H NMR (400 MHz, CDCl₃) δ 7.37 – 7.32 (m, 2H), 7.14 – 7.08 (m, 2H), 5.85 – 5.80 (m, 1H), 5.80 – 5.75 (m, 1H), 3.81 – 3.75 (m, 1H), 2.34 (s, 3H), 2.08 – 1.99 (m, 2H), 1.97 – 1.85 (m, 2H), 1.82 – 1.72 (m, 1H), 1.66 – 1.55 (m, 1H). ¹³C NMR (101 MHz, CDCl₃) δ 136.86, 132.21, 131.99, 130.17, 129.59, 127.15, 44.50, 28.80, 24.95, 21.04, 19.46. **IR** (ATR) 2923, 1491, 1202, 870, 808, 750, 722 cm⁻¹. **HRMS** calculated for C₁₃H₁₆SK [M+K]⁺ 243.0610, found 243.0619. **Chiral SFC**: 100 mm CHIRALCEL OJ-H, 0.1% *i*PrOH, 1.5 mL/min, 220 nm, 44 °C, nozzle pressure = 200 bar CO₂, *t*_{R1} (minor) = 9.2 min, *t*_{R2} (major) = 9.6 min. (**Method A**)

(S)-cyclohex-2-en-1-yl(4-methoxyphenyl)sulfane (3ac)



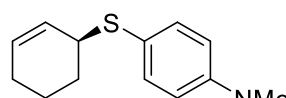
Yellow oil, 96% yield, 98:2 *er*, >20:1 *rr*, $[\alpha]^{24}_D = -109.2$ (*c* 1.9, CHCl₃). ¹H NMR (400 MHz, CDCl₃) δ 7.43 – 7.38 (m, 2H), 6.88 – 6.81 (m, 2H), 5.83 – 5.78 (m, 1H), 5.78 – 5.72 (m, 1H), 3.80 (s, 3H), 3.68 – 3.62 (m, 1H), 2.04 – 1.97 (m, 2H), 1.92 – 1.83 (m, 2H), 1.77 – 1.69 (m, 1H), 1.62 – 1.53 (m, 1H). ¹³C NMR (101 MHz, CDCl₃) δ 159.35, 135.17, 130.07, 127.33, 125.81, 114.38, 55.29, 45.50, 28.75, 24.96, 19.46. IR (ATR) 2935, 1590, 1491, 1283, 1242, 1031, 825 cm⁻¹. HRMS calculated for C₁₃H₁₆OSK [M+K]⁺ 259.0559, found 259.0569. Chiral SFC: 100 mm CHIRALCEL OJ-H, 7.0% *i*PrOH, 2.0 mL/min, 220 nm, 44 °C, nozzle pressure = 200 bar CO₂, *t*_{R1} (minor) = 5.4 min, *t*_{R2} (major) = 5.7 min. (Method A)

(S)-4-(cyclohex-2-en-1-ylthio)aniline (3ad)



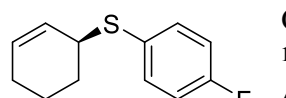
Yellow oil, 49% yield, >99:1 *er*, >20:1 *rr*, $[\alpha]^{24}_D = -120.5$ (*c* 0.4, CHCl₃). ¹H NMR (400 MHz, CDCl₃) δ 7.31 – 7.26 (m, 2H), 6.63 – 6.58 (m, 2H), 5.81 – 5.72 (m, 2H), 3.72 (brs, 2H), 3.62 – 3.56 (m, 1H), 2.04 – 1.96 (m, 2H), 1.92 – 1.82 (m, 2H), 1.76 – 1.68 (m, 1H), 1.62 – 1.51 (m, 1H). ¹³C NMR (101 MHz, CDCl₃) δ 146.25, 135.67, 129.82, 127.54, 122.73, 115.37, 45.76, 28.70, 24.96, 19.47. IR (ATR) 3420, 3355, 2925, 1596, 1493, 822, 723 cm⁻¹. HRMS calculated for C₁₂H₁₆NS [M+H]⁺ 206.1003, found 206.1008. Chiral SFC: 100 mm CHIRALCEL OJ-H, 10.0% *i*PrOH, 2.0 mL/min, 220 nm, 44 °C, nozzle pressure = 200 bar CO₂, *t*_{R1} (minor) = 14.3 min, *t*_{R2} (major) = 15.8 min.

(S)-4-(cyclohex-2-en-1-ylthio)-*N,N*-dimethylaniline (3ae)



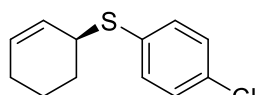
Yellow oil, 67% yield, 98:2 *er*, >20:1 *rr*, $[\alpha]^{24}_D = -95.1$ (*c* 0.6, CHCl₃). ¹H NMR (400 MHz, CDCl₃) δ 7.40 – 7.35 (m, 2H), 6.69 – 6.63 (m, 2H), 5.82 – 5.74 (m, 2H), 3.61 – 3.55 (m, 1H), 2.96 (s, 6H), 2.07 – 1.96 (m, 2H), 1.95 – 1.82 (m, 2H), 1.79 – 1.69 (m, 1H), 1.62 – 1.52 (m, 1H). ¹³C NMR (101 MHz, CDCl₃) δ 150.17, 135.65, 129.68, 127.69, 120.15, 112.57, 45.93, 40.36, 28.75, 25.00, 19.49. IR (ATR) 2926, 1593, 1503, 1350, 1192, 811, 722 cm⁻¹. HRMS calculated for C₁₄H₂₀NS [M+H]⁺ 234.1317, found 234.1320. Chiral SFC: 100 mm CHIRALCEL OJ-H, 10.0% *i*PrOH, 2.0 mL/min, 220 nm, 44 °C, nozzle pressure = 200 bar CO₂, *t*_{R1} (minor) = 6.3 min, *t*_{R2} (major) = 6.9 min.

(S)-cyclohex-2-en-1-yl(4-fluorophenyl)sulfane (3af)



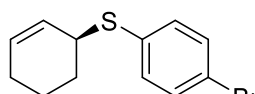
Colorless oil, 93% yield, 98:2 *er*, >20:1 *rr*, $[\alpha]^{24}_D = -120.7$ (*c* 0.9, CHCl₃). ¹H NMR (400 MHz, CDCl₃) δ 7.45 – 7.39 (m, 2H), 7.03 – 6.96 (m, 2H), 5.86 – 5.80 (m, 1H), 5.77 – 5.71 (m, 1H), 3.76 – 3.69 (m, 1H), 2.05 – 1.98 (m, 2H), 1.95 – 1.83 (m, 2H), 1.78 – 1.69 (m, 1H), 1.64 – 1.55 (m, 1H). ¹³C NMR (101 MHz, CDCl₃) δ 162.26 (d, *J* = 248.0 Hz), 134.57 (d, *J* = 8.0 Hz), 130.53, 126.89, 115.88 (d, *J* = 8.0 Hz), 45.06, 28.74, 24.91, 19.42. IR (ATR) 2934, 1438, 870, 756, 736, 722, 690 cm⁻¹. HRMS calculated for C₁₂H₁₃FSK [M+K]⁺ 247.0359, found 247.0355. Chiral SFC: 250 mm CHIRALPAK AD, 2.0% *i*PrOH, 2.0 mL/min, 220 nm, 44 °C, nozzle pressure = 200 bar CO₂, *t*_{R1} (minor) = 22.1 min, *t*_{R2} (major) = 22.8 min. (Method A)

(S)-(4-chlorophenyl)(cyclohex-2-en-1-yl)sulfane (3ag)



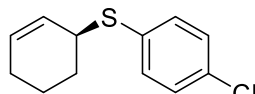
Colorless oil, 90% yield, >99:1 *er*, >20:1 *rr*, $[\alpha]^{24}_D = -143.1$ (*c* 0.5, CHCl₃). ¹H NMR (400 MHz, CDCl₃) δ 7.42 – 7.37 (m, 2H), 7.33 – 7.29 (m, 2H), 5.93 – 5.86 (m, 1H), 5.83 – 5.76 (m, 1H), 3.89 – 3.82 (m, 1H), 2.15 – 2.04 (m, 2H), 2.04 – 1.87 (m, 2H), 1.85 – 1.77 (m, 1H), 1.70 – 1.60 (m, 1H). ¹³C NMR (101 MHz, CDCl₃) δ 134.32, 132.73, 130.76, 128.95, 126.60, 122.74, 44.23, 28.72, 24.89, 19.41. IR (ATR) 2924, 1474, 1094, 1012, 817, 752, 722 cm⁻¹. HRMS calculated for C₁₂H₁₃ClSK [M+K]⁺ 263.0063, found 263.0075. Chiral SFC: 100 mm CHIRALCEL OJ-H, 1.0% *i*PrOH, 1.5 mL/min, 220 nm, 44 °C, nozzle pressure = 200 bar CO₂, *t*_{R1} (minor) = 6.3 min, *t*_{R2} (major) = 6.7 min. (Method A)

(S)-(4-bromophenyl)(cyclohex-2-en-1-yl)sulfane (3ah)



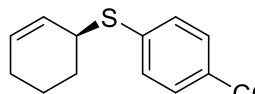
Colorless oil, 95% yield, 96:4 *er*, >20:1 *rr*, $[\alpha]^{24}_D = -87.6$ (*c* 0.8, CHCl₃). ¹H NMR (400 MHz, CDCl₃) δ 7.43 – 7.39 (m, 2H), 7.30 – 7.26 (m, 2H), 5.88 – 5.83 (m, 1H), 5.78 – 5.72 (m, 1H), 3.86 – 3.78 (m, 1H), 2.08 – 2.00 (m, 2H), 1.99 – 1.84 (m, 2H), 1.81 – 1.72 (m, 1H), 1.66 – 1.57 (m, 1H). ¹³C NMR (101 MHz, CDCl₃) δ 135.06, 132.84, 131.89, 130.81, 126.54, 120.61, 44.07, 28.72, 24.89, 19.41. IR (ATR) 2924, 1474, 1094, 1012, 817, 752, 722 cm⁻¹. HRMS calculated for C₁₂H₁₃BrSK [M+K]⁺ 306.9558, found 306.9549. Chiral SFC: 250 mm CHIRALPAK AD, 7.0% *i*PrOH, 2.0 mL/min, 254 nm, 44 °C, nozzle pressure = 200 bar CO₂, *t*_{R1} (minor) = 17.2 min, *t*_{R2} (major) = 19.0 min. (Method A)

(S)-cyclohex-2-en-1-yl(4-(trifluoromethyl)phenyl)sulfane (3ai)



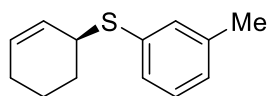
Colorless oil, 96% yield, >99:1 *er*, 18:1 *rr*, $[\alpha]^{24}_D = -93.8$ (*c* 2.4, CHCl₃). ¹H NMR (400 MHz, CDCl₃) δ 7.55 – 7.49 (m, 2H), 7.47 – 7.41 (m, 2H), 5.92 – 5.86 (m, 1H), 5.79 – 5.73 (m, 1H), 4.02 – 3.95 (m, 1H), 2.10 – 1.96 (m, 3H), 1.95 – 1.78 (m, 2H), 1.70 – 1.60 (m, 1H). ¹³C NMR (101 MHz, CDCl₃) δ 141.78 (q, *J* = 1.3 Hz), 131.20, 129.35, 128.10 (q, *J* = 32.8 Hz), 126.25, 126.11 (q, *J* = 213.3 Hz), 125.843 (q, *J* = 3.8 Hz), 42.74, 28.63, 24.82, 19.37. IR (ATR) 2937, 1323, 1119, 1093, 1062, 1013, 822 cm⁻¹. HRMS calculated for C₁₃H₁₃F₃SK [M+K]⁺ 297.0327, found 297.0319. Chiral SFC: 250 mm CHIRALPAK AD, 2.0% *i*PrOH, 2.0 mL/min, 220 nm, 44 °C, nozzle pressure = 200 bar CO₂, *t*_{R1} (major) = 11.0 min, *t*_{R2} (minor) = 12.1 min. (Method A)

methyl (S)-4-(cyclohex-2-en-1-ylthio)benzoate (3aj)



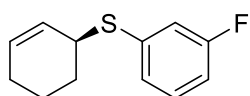
Colorless oil, 93% yield, 97:3 *er*, >20:1 *rr*, $[\alpha]^{24}_D = -92.3$ (*c* 0.98, CHCl₃). ¹H NMR (400 MHz, CDCl₃) δ 7.96 – 7.88 (m, 2H), 7.38 – 7.31 (m, 2H), 5.92 – 5.85 (m, 1H), 5.79 – 5.73 (m, 1H), 4.05 – 3.99 (m, 1H), 3.90 (s, 3H), 2.11 – 1.97 (m, 3H), 1.94 – 1.78 (m, 2H), 1.70 – 1.59 (m, 1H). ¹³C NMR (101 MHz, CDCl₃) δ 166.61, 143.41, 131.08, 129.83, 127.89, 127.07, 125.91, 51.90, 42.16, 28.56, 24.76, 19.33. IR (ATR) 2945, 1716, 1594, 1271, 1181, 1107, 758 cm⁻¹. HRMS calculated for C₁₄H₁₆O₂SK [M+K]⁺ 287.0508, found 287.0507. Chiral SFC: 250 mm CHIRALPAK AD, 7.0% *i*PrOH, 2.0 mL/min, 220 nm, 44 °C, nozzle pressure = 200 bar CO₂, *t*_{R1} (minor) = 17.2 min, *t*_{R2} (major) = 18.2 min. (Method A)

(S)-cyclohex-2-en-1-yl(*m*-tolyl)sulfane (3ak)



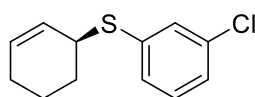
Colorless oil, 93% yield, 99:1 *er*, >20:1 *rr*, $[\alpha]_D^{24} = -130.2$ (*c* 0.5, CHCl₃). ¹H NMR (400 MHz, CDCl₃) δ 7.26 – 7.21 (m, 2H), 7.21 – 7.16 (m, 1H), 7.06 – 7.01 (m, 1H), 5.87 – 5.82 (m, 1H), 5.81 – 5.76 (m, 1H), 3.89 – 3.80 (m, 1H), 2.34 (s, 3H), 2.11 – 2.01 (m, 2H), 2.00 – 1.86 (m, 2H), 1.85 – 1.76 (m, 1H), 1.69 – 1.57 (m, 1H). ¹³C NMR (101 MHz, CDCl₃) δ 138.54, 135.62, 131.83, 130.25, 128.63, 128.17, 127.40, 126.98, 43.81, 28.82, 24.93, 21.28, 19.44. IR (ATR) 2924, 1591, 1474, 870, 774, 750, 722 cm⁻¹. HRMS calculated for C₁₃H₁₆S [M]⁺ 204.0973, found 204.0979. Chiral SFC: 100 mm CHIRALPAK AD-H, 10.0% *i*PrOH, 2.0 mL/min, 220 nm, 44 °C, nozzle pressure = 200 bar CO₂, *t*_{R1} (minor) = 4.2 min, *t*_{R2} (major) = 4.7 min. (Method A)

(S)-cyclohex-2-en-1-yl(3-fluorophenyl)sulfane (3al)



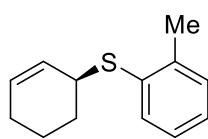
Colorless oil, 95% yield, 98:2 *er*, >20:1 *rr*, $[\alpha]_D^{24} = -125.4$ (*c* 0.5, CHCl₃). ¹H NMR (400 MHz, CDCl₃) δ 7.28 – 7.22 (m, 1H), 7.18 – 7.14 (m, 1H), 7.13 – 7.09 (m, 1H), 6.93 – 6.87 (m, 1H), 5.90 – 5.84 (m, 1H), 5.81 – 5.74 (m, 1H), 3.94 – 3.85 (m, 1H), 2.10 – 1.93 (m, 3H), 1.93 – 1.86 (m, 1H), 1.86 – 1.77 (m, 1H), 1.69 – 1.59 (m, 1H). ¹³C NMR (101 MHz, CDCl₃) δ 162.76 (d, *J* = 249.0 Hz), 138.54 (d, *J* = 7.7 Hz), 130.91, 130.49 (d, *J* = 8.6 Hz), 126.36, 125.99 (d, *J* = 3.0 Hz), 117.06 (d, *J* = 22.5 Hz), 113.25 (d, *J* = 21.2 Hz), 43.52, 28.71, 24.88, 19.39. IR (ATR) 2929, 1598, 1576, 1472, 1215, 879, 773 cm⁻¹. HRMS calculated for C₁₂H₁₃FS [M]⁺ 208.0722, found 208.0715. Chiral SFC: 100 mm CHIRALPAK AD-H, 10.0% *i*PrOH, 2.0 mL/min, 220 nm, 44 °C, nozzle pressure = 200 bar CO₂, *t*_{R1} (minor) = 3.1 min, *t*_{R2} (major) = 3.5 min. (Method A)

(S)-(3-chlorophenyl)(cyclohex-2-en-1-yl)sulfane (3am)



Colorless oil, 95% yield, 96:4 *er*, >20:1 *rr*, $[\alpha]_D^{24} = -104.5$ (*c* 0.6, CHCl₃). ¹H NMR (400 MHz, CDCl₃) δ 7.39 – 7.37 (m, 1H), 7.28 – 7.25 (m, 1H), 7.23 – 7.16 (m, 2H), 5.90 – 5.83 (m, 1H), 5.78 – 5.72 (m, 1H), 3.92 – 3.84 (m, 1H), 2.09 – 1.93 (m, 3H), 1.92 – 1.84 (m, 1H), 1.83 – 1.74 (m, 1H), 1.67 – 1.58 (m, 1H). ¹³C NMR (101 MHz, CDCl₃) δ 138.21, 134.52, 130.94, 130.25, 129.82, 128.73, 126.52, 126.35, 43.72, 28.72, 24.89, 19.37. IR (ATR) 2934, 1576, 1460, 870, 776, 749, 722 cm⁻¹. HRMS calculated for C₁₂H₁₃ClS [M]⁺ 224.0426, found 224.0428. Chiral SFC: 100 mm CHIRALPAK AD-H, 10.0% *i*PrOH, 2.0 mL/min, 220 nm, 44 °C, nozzle pressure = 200 bar CO₂, *t*_{R1} (minor) = 4.6 min, *t*_{R2} (major) = 4.9 min. (Method A)

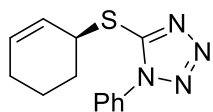
(S)-cyclohex-2-en-1-yl(*o*-tolyl)sulfane (3an)



Colorless oil, 93% yield, 99:1 *er*, >20:1 *rr*, $[\alpha]_D^{24} = -125.6$ (*c* 0.4, CHCl₃). ¹H NMR (400 MHz, CDCl₃) δ 7.41 (dd, *J* = 7.3, 1.7 Hz, 1H), 7.22 – 7.10 (m, 3H), 5.89 – 5.83 (m, 1H), 5.82 – 5.76 (m, 1H), 3.89 – 3.79 (m, 1H), 2.43 (s, 3H), 2.14 – 1.88 (m, 4H), 1.87 – 1.74 (m, 1H), 1.72 – 1.59 (m, 1H). ¹³C NMR (101 MHz, CDCl₃) δ 138.99, 135.28, 130.63, 130.37, 130.22, 126.84, 126.37, 126.28, 43.03, 28.69, 25.00, 20.69, 19.44. IR (ATR) 2926, 1467, 1063, 870, 741, 722, 711 cm⁻¹. HRMS calculated for C₁₃H₁₆S

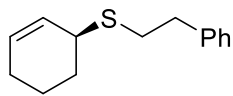
[M]⁺ 204.0973, found 204.0981. **Chiral SFC**: 100 mm CHIRALPAK AD-H, 10.0% *i*PrOH, 2.0 mL/min, 220 nm, 44 °C, nozzle pressure = 200 bar CO₂, t_{R1} (minor) = 4.3 min, t_{R2} (major) = 4.8 min. (**Method A**)

(S)-5-(cyclohex-2-en-1-ylthio)-1-phenyl-1H-tetrazole (3ao)



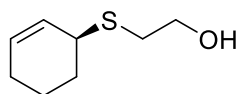
Colorless oil, 94% yield, 98:2 *er*, >20:1 *rr*, [α]²⁴_D = -217.5 (*c* 0.9, CHCl₃). ¹H NMR (400 MHz, CDCl₃) δ 7.60 – 7.48 (m, 5H), 5.98 – 5.91 (m, 1H), 5.86 – 5.80 (m, 1H), 4.77 – 4.70 (m, 1H), 2.22 – 2.03 (m, 4H), 1.86 – 1.65 (m, 2H). ¹³C NMR (101 MHz, CDCl₃) δ 154.07, 133.75, 132.99, 129.96, 129.67, 124.84, 123.84, 44.72, 29.01, 24.81, 19.10. **IR** (ATR) 2925, 1498, 1383, 1014, 868, 758, 724 cm⁻¹. **HRMS** calculated for C₁₃H₁₄N₄SNa [M+Na]⁺ 281.0837, found 281.0843. **Chiral SFC**: 100 mm CHIRALCEL OJ-H, 10.0% *i*PrOH, 2.0 mL/min, 220 nm, 44 °C, nozzle pressure = 200 bar CO₂, t_{R1} (minor) = 4.1 min, t_{R2} (major) = 4.4 min.

(S)-cyclohex-2-en-1-yl(phenethyl)sulfane (3ap)



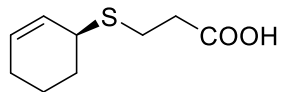
Colorless oil, 91% yield, 97:3 *er*, >20:1 *rr*, [α]²⁴_D = -134.4 (*c* 0.5, CHCl₃). ¹H NMR (400 MHz, CDCl₃) δ 7.33 – 7.28 (m, 2H), 7.25 – 7.20 (m, 3H), 5.82 – 5.77 (m, 1H), 5.74 – 5.68 (m, 1H), 3.42 – 3.35 (m, 1H), 2.94 – 2.87 (m, 2H), 2.85 – 2.78 (m, 2H), 2.06 – 1.93 (m, 3H), 1.92 – 1.81 (m, 1H), 1.81 – 1.72 (m, 1H), 1.66 – 1.53 (m, 1H). ¹³C NMR (101 MHz, CDCl₃) δ 140.73, 129.64, 128.43, 128.41, 127.80, 126.26, 40.86, 36.64, 32.40, 29.49, 24.87, 19.88. **IR** (ATR) 2926, 1496, 1453, 1204, 871, 721, 696 cm⁻¹. **HRMS** calculated for C₁₄H₁₈S [M]⁺ 218.1129, found 218.1136. **Chiral SFC**: 100 mm CHIRALCEL OJ-H, 1.0% *i*PrOH, 1.5 mL/min, 220 nm, 44 °C, nozzle pressure = 200 bar CO₂, t_{R1} (major) = 11.2 min, t_{R2} (minor) = 12.4 min. (**Method A**)

(S)-2-(cyclohex-2-en-1-ylthio)ethan-1-ol (3aq)



Colorless oil, 86% yield, 97:3 *er*, >20:1 *rr*, [α]²⁴_D = -186.5 (*c* 0.6, CHCl₃). ¹H NMR (400 MHz, CDCl₃) δ 5.83 – 5.77 (m, 1H), 5.71 – 5.64 (m, 1H), 3.72 (t, *J* = 6.1 Hz, 2H), 3.43 – 3.33 (m, 1H), 2.83 – 2.70 (m, 2H), 2.27 (brs, 1H), 2.07 – 1.92 (m, 3H), 1.90 – 1.80 (m, 1H), 1.78 – 1.69 (m, 1H), 1.64 – 1.53 (m, 1H). ¹³C NMR (101 MHz, CDCl₃) δ 130.08, 127.49, 60.86, 40.47, 34.09, 29.62, 24.80, 19.71. **IR** (ATR) 3348, 2925, 1039, 1009, 871, 747, 722 cm⁻¹. **HRMS** calculated for C₈H₁₄OSNa [M+Na]⁺ 181.0663, found 181.0661. **Chiral SFC**: 250 mm CHIRALCEL IC, 5.0% *i*PrOH, 2.0 mL/min, 220 nm, 44 °C, nozzle pressure = 200 bar CO₂, t_{R1} (minor) = 7.3 min, t_{R2} (major) = 8.3 min. (**Method B**)

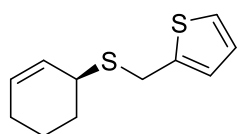
(S)-3-(cyclohex-2-en-1-ylthio)propanoic acid (3ar)



Colorless oil, 79% yield, 99:1 *er*, >20:1 *rr*, [α]²⁴_D = -177.0 (*c* 0.6, CHCl₃). ¹H NMR (400 MHz, CDCl₃) δ 10.70 (brs, 1H), 5.84 – 5.76 (m, 1H), 5.72 – 5.64 (m, 1H), 3.43 – 3.35 (m, 1H), 2.85 – 2.77 (m, 2H), 2.72 – 2.62 (m, 2H), 2.04 – 1.92 (m, 3H), 1.90 – 1.80 (m, 1H), 1.79 – 1.70 (m, 1H), 1.65 – 1.54 (m, 1H). ¹³C NMR (101 MHz, CDCl₃) δ 178.20, 130.09, 127.40, 40.91, 35.00, 29.40, 25.30, 24.81, 19.78. **IR** (ATR)

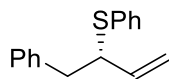
3024, 2928, 1705, 1256, 871, 748, 722 cm^{-1} . **HRMS** calculated for $\text{C}_9\text{H}_{14}\text{O}_2\text{SNa}$ $[\text{M}+\text{Na}]^+$ 209.0612, found 209.0618. **Chiral SFC**: 100 mm CHIRALCEL OJ-H, 6.0% *i*PrOH, 3.0 mL/min, 220 nm, 44 °C, nozzle pressure = 200 bar CO_2 , t_{R1} (minor) = 9.1 min, t_{R2} (major) = 9.6 min. **(Method C)**

(S)-2-((cyclohex-2-en-1-ylthio)methyl)thiophene (3as)



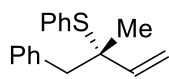
Colorless oil, 83% yield, 99:1 *er*, >20:1 *rr*, $[\alpha]_{\text{D}}^{24} = -96.5$ (*c* 0.5, CHCl_3). **^1H NMR** (400 MHz, CDCl_3) δ 7.19 (dd, $J = 5.0, 1.3$ Hz, 1H), 6.97 – 6.90 (m, 2H), 5.84 – 5.77 (m, 1H), 5.71 – 5.65 (m, 1H), 4.04 – 3.86 (m, 2H), 3.42 – 3.32 (m, 1H), 2.06 – 1.89 (m, 3H), 1.89 – 1.82 (m, 1H), 1.80 – 1.72 (m, 1H), 1.64 – 1.54 (m, 1H). **^{13}C NMR** (101 MHz, CDCl_3) δ 142.45, 130.04, 127.17, 126.62, 125.76, 124.66, 40.32, 29.72, 28.90, 24.89, 19.67. **IR** (ATR) 2927, 1252, 1036, 865, 849, 825, 748 cm^{-1} . **HRMS** calculated for $\text{C}_{11}\text{H}_{15}\text{S}_2$ $[\text{M}+\text{H}]^+$ 211.0615, found 211.0626. **Chiral SFC**: 100 mm CHIRALPAK AD-H, 6.0% *i*PrOH, 2.0 mL/min, 220 nm, 44 °C, nozzle pressure = 200 bar CO_2 , t_{R1} (major) = 19.8 min, t_{R2} (minor) = 21.2 min.

(S)-phenyl(1-phenylbut-3-en-2-yl)sulfane (3ba)



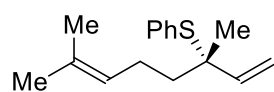
Colorless oil, 85% yield, 83:17 *er*, >20:1 *rr*, $[\alpha]_{\text{D}}^{24} = -2.7$ (*c* 0.5, CHCl_3). **^1H NMR** (500 MHz, CDCl_3) δ 7.48 – 7.43 (m, 2H), 7.38 – 7.32 (m, 4H), 7.31 – 7.23 (m, 4H), 5.79 (ddd, $J = 17.0, 10.1, 8.8$ Hz, 1H), 5.01 – 4.94 (m, 1H), 4.91 – 4.83 (m, 1H), 3.96 – 3.88 (m, 1H), 3.12 (dd, $J = 13.9, 5.9$ Hz, 1H), 2.98 (dd, $J = 13.9, 8.6$ Hz, 1H). **^{13}C NMR** (126 MHz, CDCl_3) δ 138.60, 137.85, 134.56, 132.80, 129.28, 128.68, 128.23, 127.16, 126.46, 116.38, 53.49, 40.85. **IR** (ATR): 3060, 3027, 1480, 1438, 1025, 986, 915, 735 cm^{-1} . **HRMS** calculated for $\text{C}_{16}\text{H}_{17}\text{S}$ $[\text{M}+\text{H}]^+$ 241.1051, found 241.1056. **Chiral SFC**: 100 mm CHIRALCEL OJ-H, 1.0% *i*PrOH, 2.0 mL/min, 220 nm, 44 °C, nozzle pressure = 200 bar CO_2 , t_{R1} (minor) = 5.6 min, t_{R2} (major) = 6.4 min.

(S)-2-methyl-1-phenylbut-3-en-2-yl(phenyl)sulfane (3ca)



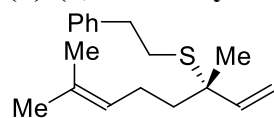
Colorless oil, 78% yield, 71:29 *er*, >20:1 *rr*, $[\alpha]_{\text{D}}^{24} = -9.0$ (*c* 0.5, CHCl_3). **^1H NMR** (500 MHz, CDCl_3) δ 7.51 – 7.47 (m, 2H), 7.37 – 7.21 (m, 6H), 7.19 – 7.16 (m, 2H), 6.01 (dd, $J = 17.4, 10.6$ Hz, 1H), 4.95 (d, $J = 10.6$ Hz, 1H), 4.56 (d, $J = 17.4$ Hz, 1H), 3.05 (d, $J = 13.3$ Hz, 1H), 2.94 (d, $J = 13.3$ Hz, 1H), 1.23 (s, 3H). **^{13}C NMR** (126 MHz, CDCl_3) δ 142.90, 137.44, 136.98, 131.88, 130.73, 128.76, 128.32, 127.72, 126.52, 113.34, 54.18, 47.56, 22.91. **IR** (ATR): 2920, 2851, 1494, 1471, 1438, 1068, 1025, 912, 747 cm^{-1} . **HRMS** calculated for $\text{C}_{17}\text{H}_{19}\text{S}$ $[\text{M}+\text{H}]^+$ 255.1207, found 255.1204. **Chiral SFC**: 100 mm CHIRALCEL OJ-H, 0.2% *i*PrOH, 2.0 mL/min, 220 nm, 44 °C, nozzle pressure = 200 bar CO_2 , t_{R1} (major) = 7.2 min, t_{R2} (minor) = 7.8 min.

(S)-(3,7-dimethylocta-1,6-dien-3-yl)(phenyl)sulfane (3da)



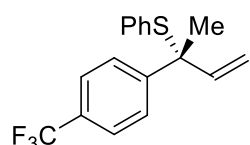
Colorless oil, 68% yield, 96:4 *er*, >20:1 *rr*, $[\alpha]^{24}_D = +24.8$ (*c* 0.5, Et₂O). **¹H NMR** (500 MHz, CDCl₃) δ 7.49 – 7.45 (m, 2H), 7.36 – 7.27 (m, 3H), 5.91 (dd, *J* = 17.4, 10.6 Hz, 1H), 5.08 (t, *J* = 7.5 Hz, 1H), 4.98 (d, *J* = 10.6 Hz, 1H), 4.71 (d, *J* = 17.4 Hz, 1H), 2.19 – 1.99 (m, 2H), 1.69 (s, 3H), 1.66 – 1.59 (m, 5H), 1.31 (s, 3H). **¹³C NMR** (126 MHz, CDCl₃) δ 143.49, 137.29, 132.05, 131.80, 128.60, 128.25, 123.96, 112.64, 53.65, 40.40, 25.66, 23.45, 23.33, 17.65. **IR** (ATR): 2966, 2924, 1438, 1371, 1073, 1025, 995, 910, 748 cm⁻¹. **HRMS** calculated for C₁₆H₂₃S [M+H]⁺ 247.1520, found 247.1522. **Chiral SFC**: 100 mm CHIRALCEL AD-H, 0.5% *i*PrOH, 2.0 mL/min, 220 nm, 44 °C, nozzle pressure = 200 bar CO₂, *t*_{R1} (major) = 1.7 min, *t*_{R2} (minor) = 1.8 min.

(S)-(3,7-dimethylocta-1,6-dien-3-yl)(phenethyl)sulfane (3dp)



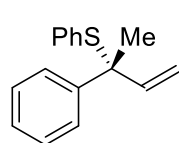
Colorless oil, 71% yield, 90:10 *er*, >20:1 *rr*, $[\alpha]^{24}_D = +10.1$ (*c* 0.5, CHCl₃). **¹H NMR** (400 MHz, CDCl₃) δ 7.31 – 7.25 (m, 2H), 7.22 – 7.16 (m, 3H), 5.82 (dd, *J* = 17.4, 10.6 Hz, 1H), 5.13 – 5.03 (m, 2H), 4.95 (dd, *J* = 17.4, 0.9 Hz, 1H), 2.82 (t, *J* = 8.1 Hz, 2H), 2.68 – 2.54 (m, 2H), 2.15 – 1.94 (m, 2H), 1.68 (s, 3H), 1.63 – 1.57 (m, 5H), 1.36 (s, 3H). **¹³C NMR** (126 MHz, CDCl₃) δ 143.60, 140.98, 131.82, 128.41, 128.40, 126.23, 123.99, 112.18, 50.24, 40.35, 36.18, 30.00, 25.65, 23.49, 23.19, 17.62. **IR** (ATR): 2965, 2923, 1496, 1453, 1373, 1077, 996, 910, 733 cm⁻¹. **HRMS** calculated for C₁₈H₂₇S [M+H]⁺ 275.1833, found 275.1831. **Chiral SFC**: 100 mm CHIRALCEL OJ-H, 0.5% *i*PrOH, 2.0 mL/min, 220 nm, 44 °C, nozzle pressure = 200 bar CO₂, *t*_{R1} (minor) = 2.7 min, *t*_{R2} (major) = 2.9 min.

(R)-phenyl(2-(4-(trifluoromethyl)phenyl)but-3-en-2-yl)sulfane (3ea)



Colorless oil, 80% yield, 98:2 *er*, >20:1 *rr*, $[\alpha]^{24}_D = +68.8$ (*c* 0.5, CHCl₃). **¹H NMR** (400 MHz, CDCl₃) δ 7.67 – 7.54 (m, 4H), 7.35 – 7.21 (m, 5H), 6.28 (dd, *J* = 17.3, 10.6 Hz, 1H), 5.21 (d, *J* = 10.6 Hz, 1H), 5.04 (d, *J* = 17.3 Hz, 1H), 1.71 (s, 3H). **¹³C NMR** (101 MHz, CDCl₃) δ 148.61, 142.10, 136.81, 131.77, 129.11 (q, *J* = 32.2 Hz), 128.98, 128.43, 127.73, 125.02 (q, *J* = 3.8 Hz), 124.14 (q, *J* = 270.7 Hz), 114.26, 56.16, 26.27. **IR** (ATR): 2929, 1616, 1410 1324, 1165, 1115, 1070, 1015, 842 cm⁻¹. **HRMS** calculated for C₁₇H₁₆F₃S [M+H]⁺ 309.0925, found 309.0920. **Chiral SFC**: 100 mm CHIRALCEL OJ-H, 1.0% *i*PrOH, 2.0 mL/min, 220 nm, 44 °C, nozzle pressure = 200 bar CO₂, *t*_{R1} (minor) = 4.3 min, *t*_{R2} (major) = 6.1 min.

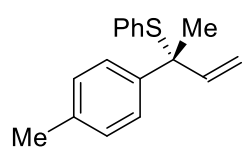
(R)-phenyl(2-phenylbut-3-en-2-yl)sulfane (3fa)



Colorless oil, 73% yield, 96:4 *er*, 12:1 *rr*, $[\alpha]^{24}_D = +56.0$ (*c* 0.5, CHCl₃). **¹H NMR** (500 MHz, CDCl₃) δ 7.56 – 7.49 (m, 2H), 7.34 – 7.27 (m, 5H), 7.22 (dd, *J* = 12.2, 4.9 Hz, 3H), 6.31 (dd, *J* = 17.3, 10.6 Hz, 1H), 5.14 (d, *J* = 10.6 Hz, 1H), 4.98 (d, *J* = 17.3 Hz, 1H), 1.69 (s, 3H). **¹³C NMR** (126 MHz, CDCl₃) δ 144.41, 142.86, 136.75, 132.50, 128.63, 128.25, 128.11, 127.25, 126.95, 113.41, 56.55, 26.22. **IR** (ATR): 2924, 1490, 1438, 1368, 1059, 1025, 915, 747 cm⁻¹. **HRMS** calculated for C₁₆H₁₆SNa [M+Na]⁺ 263.0870, found 263.0875. **Chiral SFC**: 250 mm CHIRALCEL AD-H, 1.0% *i*PrOH, 2.0 mL/min,

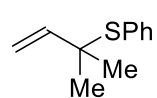
220 nm, 44 °C, nozzle pressure = 200 bar CO₂, t_{R1} (major) = 7.1 min, t_{R2} (minor) = 8.0 min.

(R)-phenyl(2-(p-tolyl)but-3-en-2-yl)sulfane (3ga)



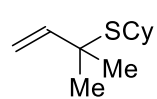
Colorless oil, 77% yield, 93:7 *er*, 7:1 *rr*, $[\alpha]_D^{24} = +54.4$ (*c* 0.5, CHCl₃). ¹H NMR (400 MHz, CDCl₃) δ 7.44 (d, *J* = 8.3 Hz, 2H), 7.36 – 7.21 (m, 5H), 7.15 (d, *J* = 8.5 Hz, 2H), 6.31 (dd, *J* = 17.3, 10.6 Hz, 1H), 5.13 (d, *J* = 10.6 Hz, 1H), 4.96 (d, *J* = 17.3 Hz, 1H), 2.36 (s, 3H), 1.68 (s, 3H). ¹³C NMR (101 MHz, CDCl₃) δ 143.05, 141.43, 136.71, 132.72, 128.83, 128.55, 128.23, 127.08, 126.50, 113.17, 56.38, 26.22, 20.97. IR (ATR): 2923, 1510, 1438, 1060, 1019, 914, 816, 748 cm⁻¹. HRMS calculated for C₁₇H₁₈SNa [M+Na]⁺ 277.1027, found 277.1021. Chiral SFC: 250 mm CHIRALCEL AD-H, 2.0% *i*PrOH, 2.0 mL/min, 220 nm, 44 °C, nozzle pressure = 200 bar CO₂, t_{R1} (major) = 6.6 min, t_{R2} (minor) = 7.8 min.

(2-methylbut-3-en-2-yl)(phenyl)sulfane (3ha)³



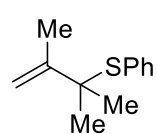
Colorless oil, 93% yield, >20:1 *rr*. ¹H NMR (400 MHz, CDCl₃) δ 7.50 – 7.45 (m, 2H), 7.36 – 7.27 (m, 3H), 5.97 (dd, *J* = 17.4, 10.6 Hz, 1H), 4.92 (d, *J* = 10.6 Hz, 1H), 4.73 (d, *J* = 17.4 Hz, 1H), 1.36 (s, 6H). ¹³C NMR (101 MHz, CDCl₃) δ 144.73, 137.14, 132.48, 128.63, 128.28, 111.57, 49.94, 27.46.

cyclohexyl(2-methylbut-3-en-2-yl)sulfane (3ht)



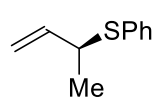
Colorless oil, 89% yield, 13:1 *rr*. ¹H NMR (400 MHz, CDCl₃) δ 5.90 (dd, *J* = 17.8, 10.1 Hz, 1H), 4.98 (s, 1H), 4.94 (dd, *J* = 6.2, 1.0 Hz, 1H), 2.49 – 2.34 (m, 1H), 1.89 (dd, *J* = 9.1, 3.9 Hz, 2H), 1.71 – 1.65 (m, 2H), 1.57 – 1.48 (m, 1H), 1.40 – 1.27 (m, 11H). ¹³C NMR (101 MHz, CDCl₃) δ 145.69, 110.60, 47.24, 42.06, 35.89, 28.09, 26.31, 25.51. IR (ATR): 2925, 2851, 1447, 1125, 998, 907, 733 cm⁻¹. HRMS calculated for C₁₁H₂₀SNa [M+Na]⁺ 207.1183, found 207.1172.

(2,3-dimethylbut-3-en-2-yl)(phenyl)sulfane (3ia)



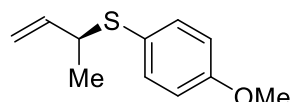
Colorless oil, 93% yield, >20:1 *rr*. ¹H NMR (400 MHz, CDCl₃) δ 7.43 – 7.39 (m, 2H), 7.33 – 7.25 (m, 3H), 4.76 (s, 1H), 4.50 (s, 1H), 2.01 (s, 3H), 1.41 (s, 6H). ¹³C NMR (101 MHz, CDCl₃) δ 148.32, 136.40, 133.30, 128.36, 128.20, 111.77, 53.04, 27.89, 19.76. IR (ATR): 2964, 2923, 1634, 1473, 1438, 1121, 935, 911, 749 cm⁻¹. HRMS calculated for C₁₂H₁₆SNa [M+Na]⁺ 215.0870, found 215.0876.

(S)-but-3-en-2-yl(phenyl)sulfane (3ja)⁴



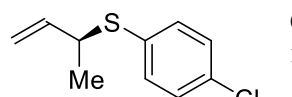
Colorless oil, 95% yield, 97:3 *er*, >20:1 *rr*, $[\alpha]_D^{24} = -13.6$ (*c* 1.0, CHCl₃). ¹H NMR (500 MHz, CDCl₃) δ 7.49 – 7.45 (m, 2H), 7.37 – 7.28 (m, 3H), 5.92 – 5.83 (m, 1H), 5.04 – 4.95 (m, 2H), 3.86 – 3.78 (m, 1H), 1.46 (d, *J* = 6.9 Hz, 3H). Chiral SFC: 250 mm CHIRALCEL OB-H, 2.0% *i*PrOH, 2.0 mL/min, 220 nm, 44 °C, nozzle pressure = 200 bar CO₂, t_{R1} (minor) = 7.0 min, t_{R2} (major) = 7.5 min. (Method A)

(S)-but-3-en-2-yl(4-methoxyphenyl)sulfane (3jc)



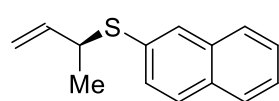
Colorless oil, 94% yield, 97:3 *er*, >20:1 *rr*, $[\alpha]^{24}_D = -3.2$ (*c* 1.0, CHCl₃). ¹H NMR (500 MHz, CDCl₃) δ 7.40 – 7.34 (m, 2H), 6.86 – 6.80 (m, 2H), 5.83 – 5.74 (m, 1H), 4.94 – 4.88 (m, 1H), 4.87 – 4.79 (m, 1H), 3.80 (s, 3H), 3.62 – 3.53 (m, 1H), 1.34 (d, *J* = 6.9 Hz, 3H). ¹³C NMR (126 MHz, CDCl₃) δ 159.52, 140.04, 136.10, 124.74, 114.33, 114.18, 55.24, 47.48, 19.90. IR (ATR): 2962, 1591, 1492, 1462, 1284, 1243, 1172, 1030, 914, 826 cm⁻¹. HRMS calculated for C₁₁H₁₄OSK [M+K]⁺ 233.0402, found 233.0404. Chiral SFC: 250 mm CHIRALCEL OB-H, 2.0% *i*PrOH, 2.0 mL/min, 220 nm, 44 °C, nozzle pressure = 200 bar CO₂, *t*_{R1} (minor) = 6.6 min, *t*_{R2} (major) = 7.0 min. (Method A)

(S)-but-3-en-2-yl(4-chlorophenyl)sulfane (3jg)



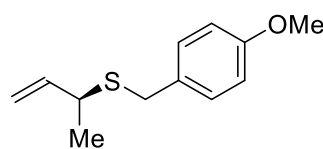
Colorless oil, 94% yield, 95:5 *er*, >20:1 *rr*, $[\alpha]^{24}_D = -14.0$ (*c* 1.0, CHCl₃). ¹H NMR (500 MHz, CDCl₃) δ 7.40 – 7.36 (m, 2H), 7.33 – 7.29 (m, 2H), 5.89 – 5.79 (m, 1H), 5.04 – 4.94 (m, 2H), 3.82 – 3.72 (m, 1H), 1.44 (d, *J* = 6.9 Hz, 3H). ¹³C NMR (126 MHz, CDCl₃) δ 139.57, 134.12, 133.28, 133.21, 128.79, 114.91, 46.66, 20.00. IR (ATR): 2968, 2925, 1475, 1449, 1389, 1094, 1012, 916, 818 cm⁻¹. HRMS calculated for C₁₀H₁₁ClSK [M+K]⁺ 236.9907, found 236.9908. Chiral SFC: 250 mm CHIRALCEL OB-H, 2.0% *i*PrOH, 2.0 mL/min, 220 nm, 44 °C, nozzle pressure = 200 bar CO₂, *t*_{R1} (minor) = 6.9 min, *t*_{R2} (major) = 7.5 min. (Method A)

(S)-but-3-en-2-yl(naphthalen-2-yl)sulfane (3ju)



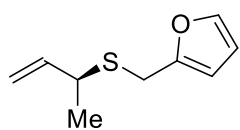
Colorless oil, 92% yield, 98:2 *er*, >20:1 *rr*, $[\alpha]^{24}_D = -20.1$ (*c* 0.5, CHCl₃). ¹H NMR (500 MHz, CDCl₃) δ 8.42 (s, 1H), 8.02 – 7.96 (m, 2H), 7.93 (d, *J* = 8.1 Hz, 1H), 7.82 (dd, *J* = 8.6, 1.8 Hz, 1H), 7.71 – 7.60 (m, 2H), 5.87 (ddd, *J* = 17.2, 10.3, 7.8 Hz, 1H), 5.26 (dd, *J* = 10.3, 0.8 Hz, 1H), 5.10 (dd, *J* = 17.2, 0.8 Hz, 1H), 3.84 – 3.77 (m, 1H), 1.48 (d, *J* = 6.9 Hz, 3H). ¹³C NMR (126 MHz, CDCl₃) δ 135.31, 133.93, 131.97, 131.22, 131.16, 129.46, 129.23, 128.93, 127.95, 127.57, 123.97, 121.88, 64.31, 13.08. IR (ATR): 3053, 2969, 1584, 1500, 1132, 943, 915, 812 cm⁻¹. HRMS calculated for C₁₄H₁₄SNa [M+Na]⁺ 237.0714 found 237.0711. Chiral SFC: 250 mm CHIRALCEL OB-H, 2.0% *i*PrOH, 2.0 mL/min, 220 nm, 44 °C, nozzle pressure = 200 bar CO₂, *t*_{R1} (major) = 20.7 min, *t*_{R2} (minor) = 22.1 min. (Method A)

(S)-but-3-en-2-yl(4-methoxybenzyl)sulfane (3jv)



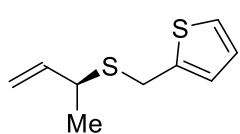
Colorless oil, 81% yield, 90:10 *er*, >20:1 *rr*, $[\alpha]^{24}_D = -60.8$ (*c* 0.5, CHCl₃). ¹H NMR (500 MHz, CDCl₃) δ 7.25 – 7.21 (m, 2H), 6.87 – 6.81 (m, 2H), 5.71 (ddd, *J* = 17.0, 10.0, 8.7 Hz, 1H), 5.09 – 5.04 (m, 1H), 5.03 – 4.97 (m, 1H), 3.80 (s, 3H), 3.63 – 3.59 (m, 2H), 3.25 – 3.15 (m, 1H), 1.30 (d, *J* = 6.9 Hz, 3H). ¹³C NMR (126 MHz, CDCl₃) δ 158.48, 140.51, 130.55, 129.93, 114.30, 113.84, 55.24, 42.34, 34.52, 20.05. IR (ATR): 2925, 1610, 1510, 1300, 1244, 1174, 1033, 915, 829 cm⁻¹. HRMS calculated for C₁₂H₁₆OSK [M+K]⁺ 247.0559, found 247.0561. Chiral SFC: 250 mm CHIRALCEL OB-H, 2.0% *i*PrOH, 2.0 mL/min, 220 nm, 44 °C, nozzle pressure = 200 bar CO₂, *t*_{R1} (major) = 6.8 min, *t*_{R2} (minor) = 7.6 min. (Method A)

(S)-2-((but-3-en-2-ylthio)methyl)furan (3jw)



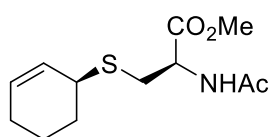
Colorless oil, 84% yield, 94:6 *er*, >20:1 *rr*, $[\alpha]^{24}_D = -164.0$ (*c* 0.5, CHCl₃). **¹H NMR** (500 MHz, CDCl₃) δ 7.36 – 7.33 (m, 1H), 6.31 – 6.27 (m, 1H), 6.16 – 6.11 (m, 1H), 5.67 (ddd, *J* = 17.0, 10.0, 8.9 Hz, 1H), 5.11 – 5.01 (m, 2H), 3.69 – 3.61 (m, 2H), 3.36 – 3.28 (m, 1H), 1.32 (d, *J* = 6.9 Hz, 3H). **¹³C NMR** (126 MHz, CDCl₃) δ 152.16, 141.92, 139.97, 114.79, 110.31, 107.08, 42.66, 27.21, 19.88. **IR** (ATR): 2964, 1633, 1503, 1150, 1009, 933, 916, 804, 733 cm⁻¹. **HRMS** calculated for C₉H₁₂OSK [M+K]⁺ 207.0246, found 207.0243. **Chiral SFC**: 250 mm CHIRALCEL OB-H, 2.0% *i*PrOH, 2.0 mL/min, 220 nm, 44 °C, nozzle pressure = 200 bar CO₂, *t*_{R1} (minor) = 11.9 min, *t*_{R2} (major) = 13.2 min. (Method A)

(S)-2-((but-3-en-2-ylthio)methyl)thiophene (3js)



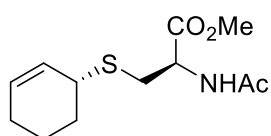
Colorless oil, 86% yield, 94:6 *er*, >20:1 *rr*, $[\alpha]^{24}_D = -117.2$ (*c* 0.5, CHCl₃). **¹H NMR** (500 MHz, CDCl₃) δ 7.21 – 7.15 (m, 1H), 6.94 – 6.87 (m, 2H), 5.69 (ddd, *J* = 17.0, 10.0, 8.9 Hz, 1H), 5.11 – 5.05 (m, 1H), 5.02 (dd, *J* = 17.0, 0.8 Hz, 1H), 3.89 – 3.81 (m, 2H), 3.34 – 3.26 (m, 1H), 1.32 (d, *J* = 6.9 Hz, 3H). **¹³C NMR** (126 MHz, CDCl₃) δ 142.50, 140.01, 126.64, 125.69, 124.58, 114.78, 42.60, 29.48, 19.89. **IR** (ATR): 2963, 2924, 1632, 1450, 1412, 1220, 1028, 990, 915, 850 cm⁻¹. **HRMS** calculated for C₉H₁₂S₂K [M+K]⁺ 223.0017, found 223.0015. **Chiral SFC**: 250 mm CHIRALCEL OB-H, 2.0% *i*PrOH, 2.0 mL/min, 220 nm, 44 °C, nozzle pressure = 200 bar CO₂, *t*_{R1} (minor) = 9.0 min, *t*_{R2} (major) = 10.0 min. (Method A)

methyl *N*-acetyl-*S*-((*S*)-cyclohex-2-en-1-yl)-*L*-cysteinate (3ax)



White solid, 92% yield, >20:1 *dr*, >20:1 *rr*, $[\alpha]^{24}_D = -78.5$ (*c* 0.9, CHCl₃). **¹H NMR** (400 MHz, CDCl₃) δ 6.38 (d, *J* = 7.1 Hz, 1H), 5.82 – 5.74 (m, 1H), 5.66 – 5.56 (m, 1H), 4.82 (dt, *J* = 7.8, 5.0 Hz, 1H), 3.75 (s, 3H), 3.37 – 3.30 (m, 1H), 3.06 – 2.94 (m, 2H), 2.03 (s, 3H), 2.01 – 1.88 (m, 3H), 1.85 – 1.76 (m, 1H), 1.74 – 1.65 (m, 1H), 1.61 – 1.51 (m, 1H). **¹³C NMR** (101 MHz, CDCl₃) δ 171.27, 169.68, 130.38, 126.97, 52.50, 51.88, 41.13, 32.81, 29.27, 24.74, 23.02, 19.48. **IR** (ATR) 3312, 2936, 1736, 1636, 1542, 1247, 1216 cm⁻¹. **HRMS** calculated for C₁₂H₁₉NO₃SNa [M+Na]⁺ 280.0983, found 280.0990.

methyl *N*-acetyl-*S*-((*R*)-cyclohex-2-en-1-yl)-*L*-cysteinate (3ax')

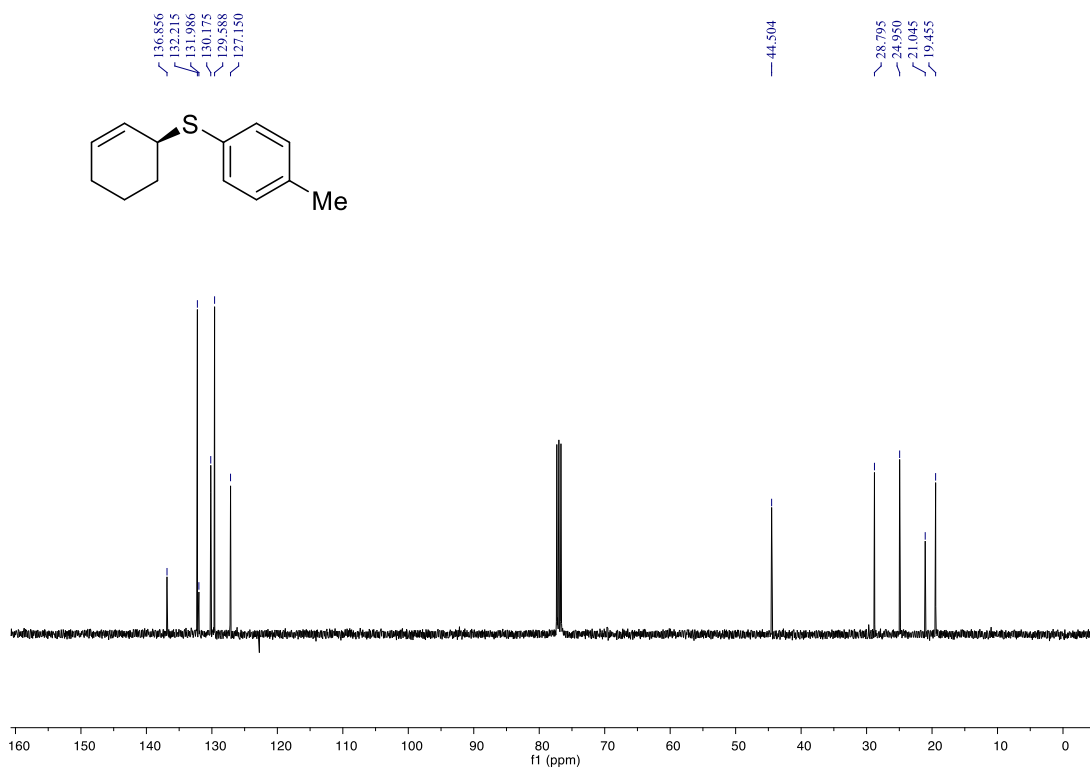
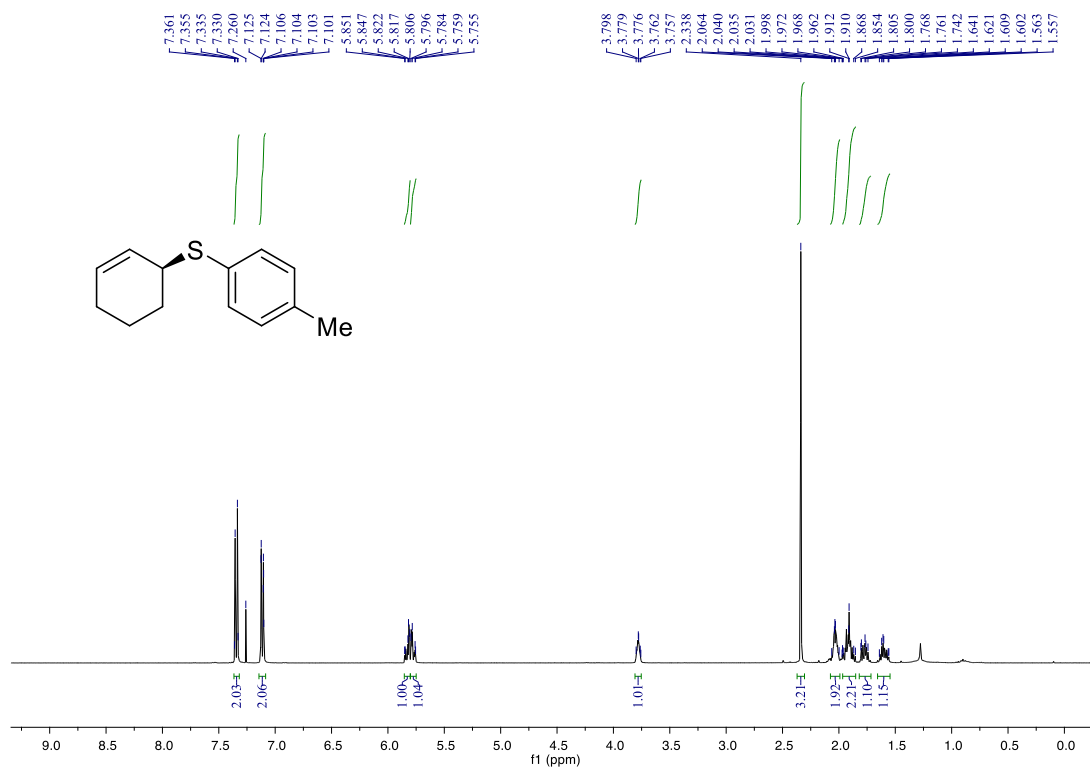


Colorless oil, 88% yield, >20:1 *dr*, >20:1 *rr*, $[\alpha]^{24}_D = +188.1$ (*c* 0.9, CHCl₃). **¹H NMR** (400 MHz, CDCl₃) δ 6.35 (d, *J* = 7.0 Hz, 1H), 5.84 – 5.73 (m, 1H), 5.67 – 5.57 (m, 1H), 4.81 (dt, *J* = 7.6, 5.1 Hz, 1H), 3.74 (s, 3H), 3.37 – 3.31 (m, 1H), 3.04 (dd, *J* = 13.6, 4.9 Hz, 1H), 2.95 (dd, *J* = 13.6, 5.3 Hz, 1H), 2.02 (s, 3H), 2.01 – 1.88 (m, 3H), 1.84 – 1.74 (m, 1H), 1.72 – 1.65 (m, 1H), 1.60 – 1.50 (m, 1H). **¹³C NMR** (101 MHz, CDCl₃) δ 171.26, 169.77, 130.38, 126.95, 52.55, 52.00, 41.13, 32.70, 29.25, 24.76, 23.03, 19.51. **IR** (ATR) 3272, 2931, 1743, 1652, 1538, 1209, 1174 cm⁻¹. **HRMS** calculated for C₁₂H₁₉NO₃SNa [M+Na]⁺ 280.0983, found 280.0986.

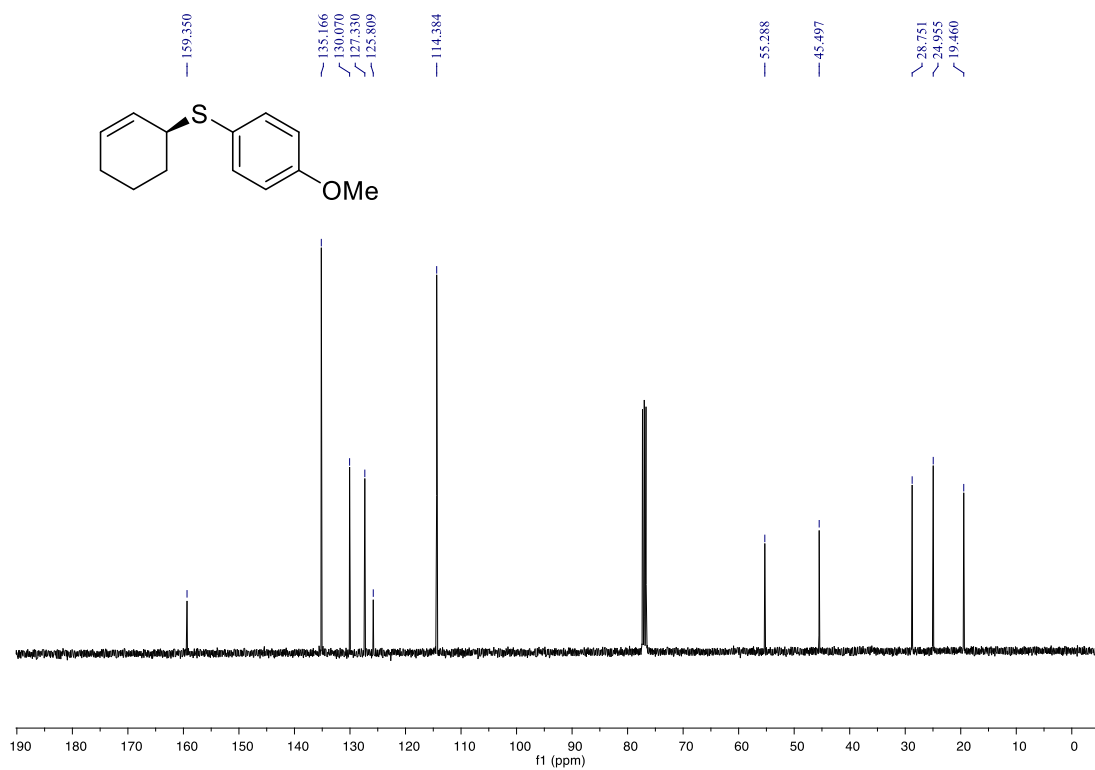
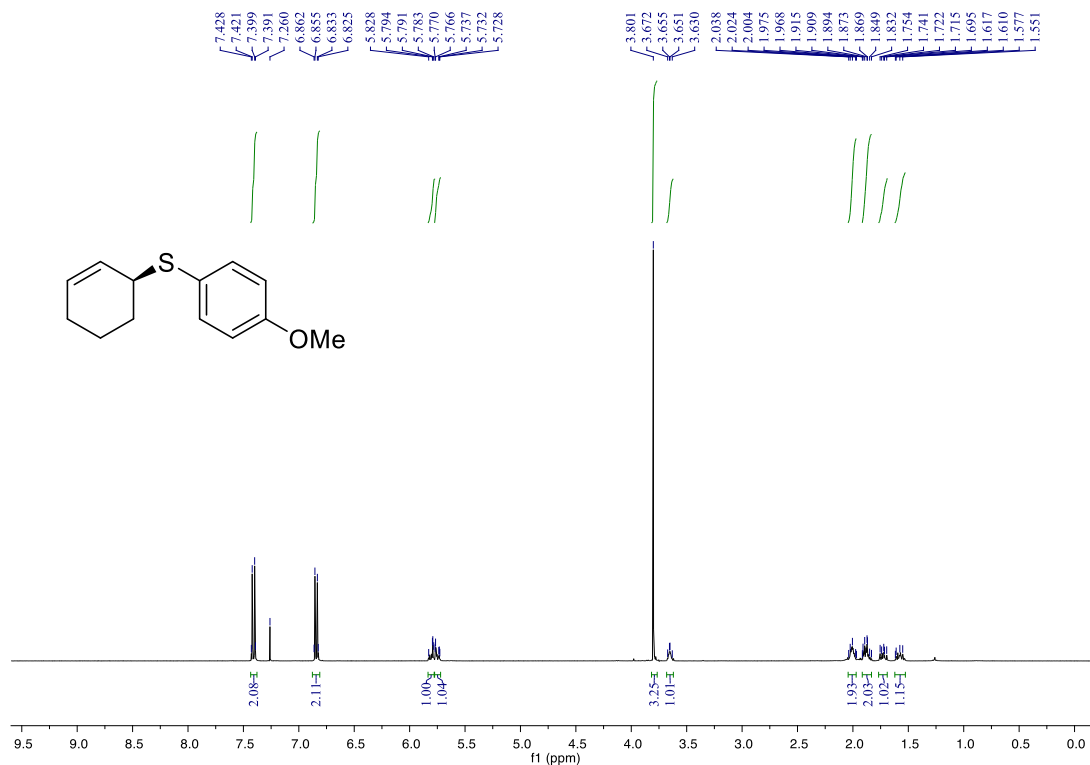
5. References

- (1) Fustero, S.; Bello, P.; Miró, J.; Simón, A.; del Pozo, C. *Chem. Eur. J.* **2012**, *18*, 10991.
- (2) Gais, H.-J.; Böhme, A. *J. Org. Chem.* **2002**, *67*, 1153.
- (3) Holzwarth, M. S.; Frey, W.; Plietker, B. *Chem. Commun.* **2011**, *47*, 11113.
- (4) Zheng, S.; Gao, N.; Liu, W.; Liu, D.; Zhao, X.; Cohen, T. *Org. Lett.* **2010**, *12*, 4454.

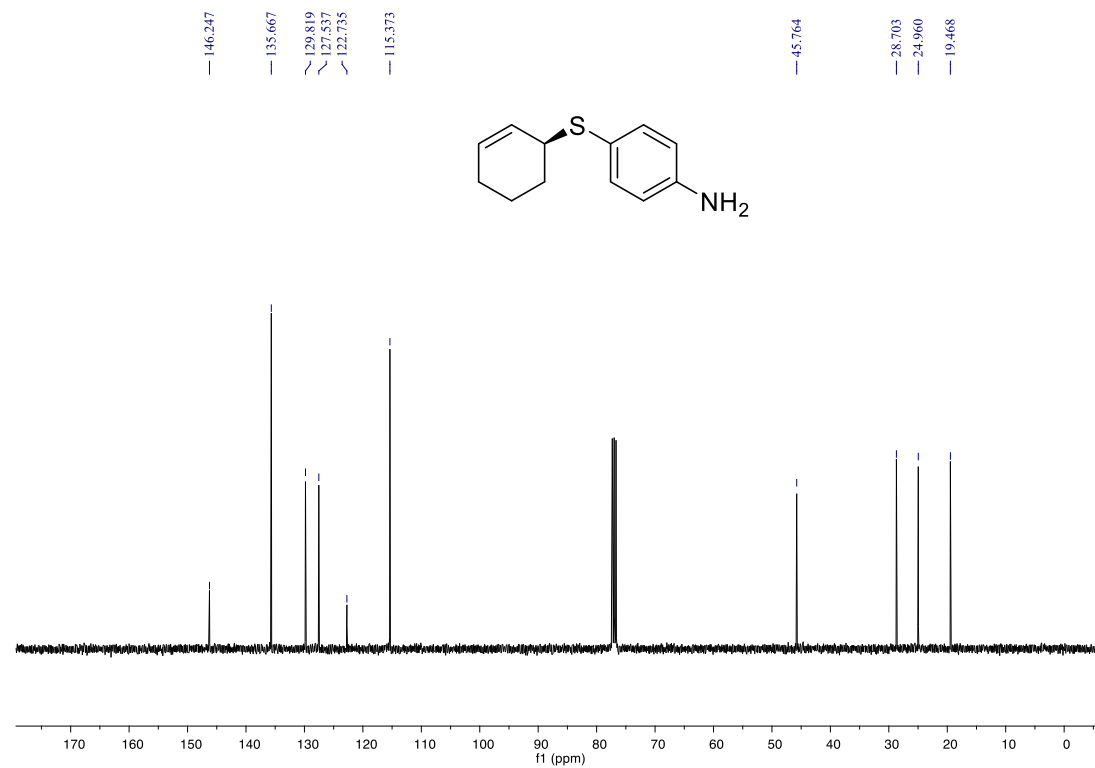
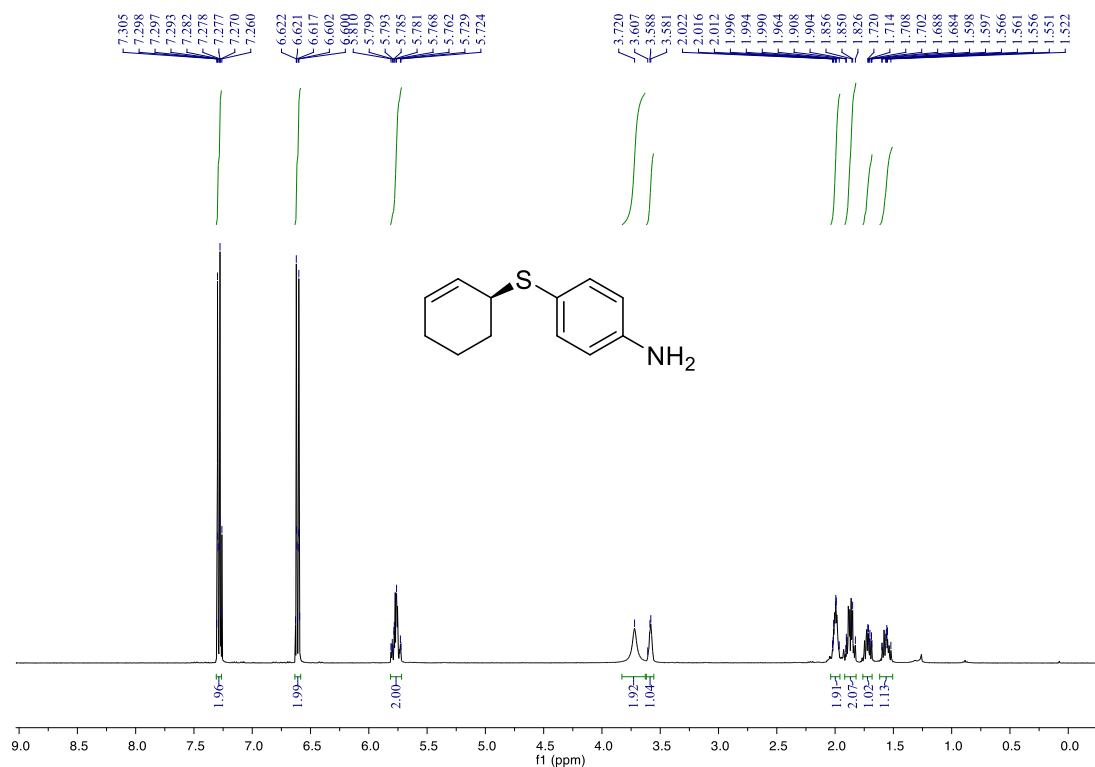
6. NMR spectra of unknown compounds
 (S)-cyclohex-2-en-1-yl(*p*-tolyl)sulfane (3ab)



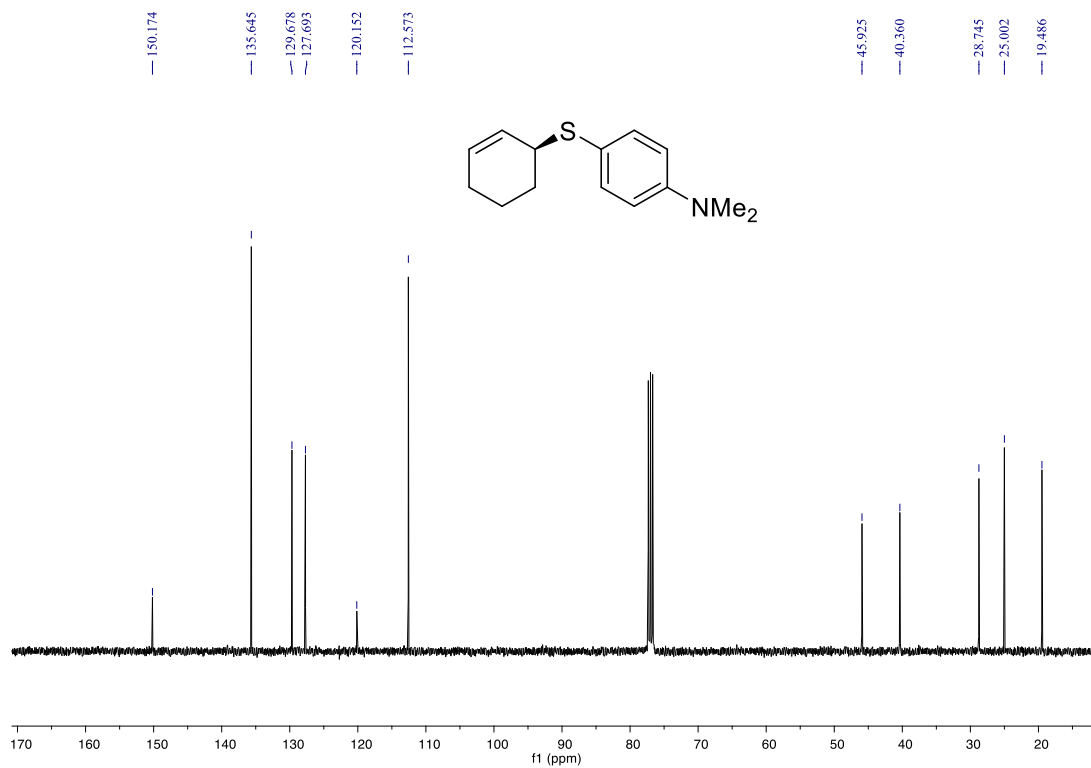
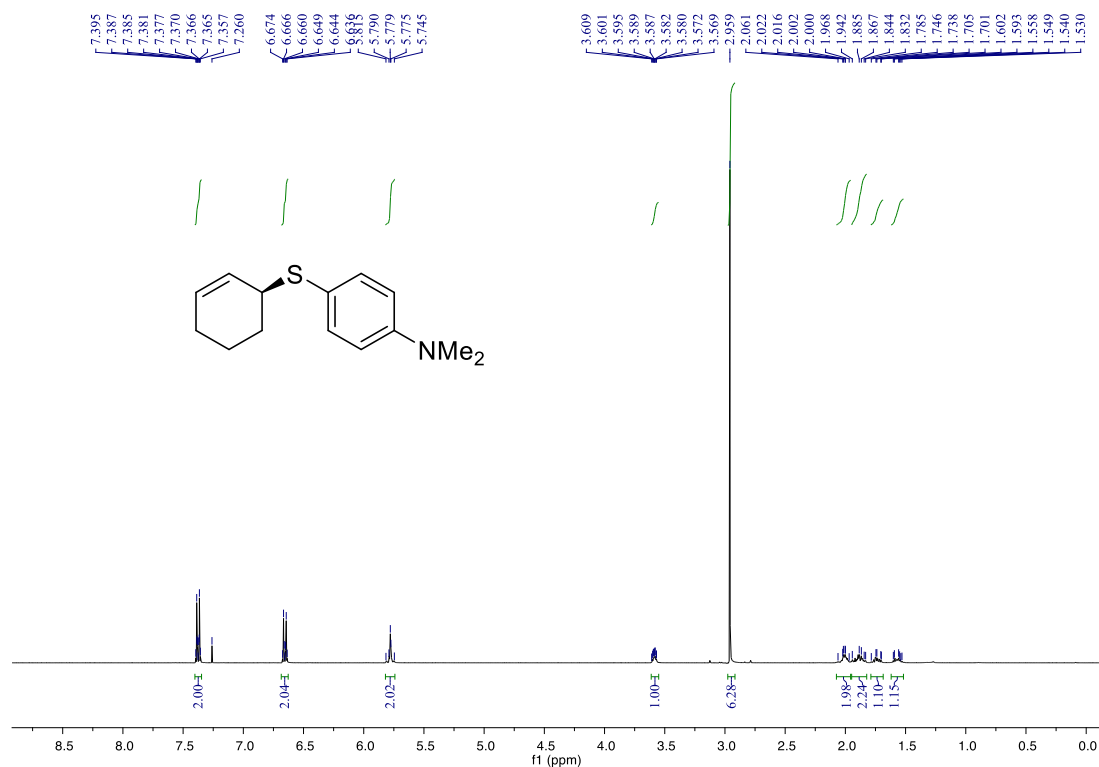
(S)-cyclohex-2-en-1-yl(4-methoxyphenyl)sulfane (3ac)



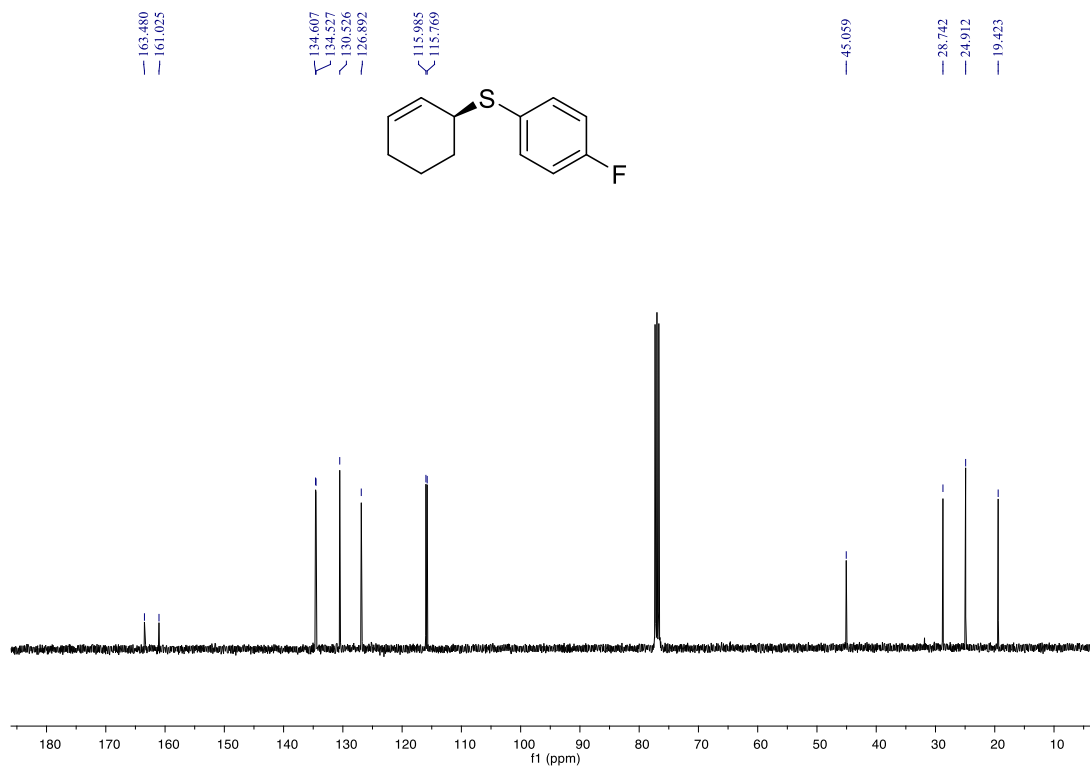
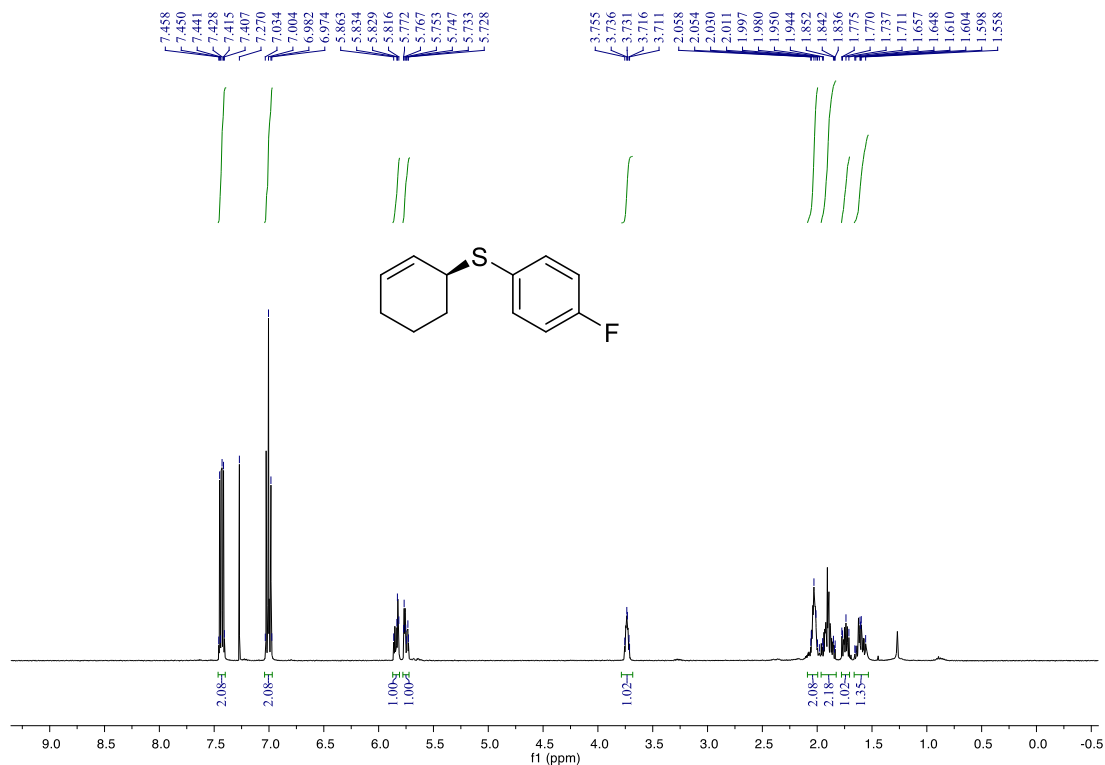
(S)-4-(cyclohex-2-en-1-ylthio)aniline (3ad)



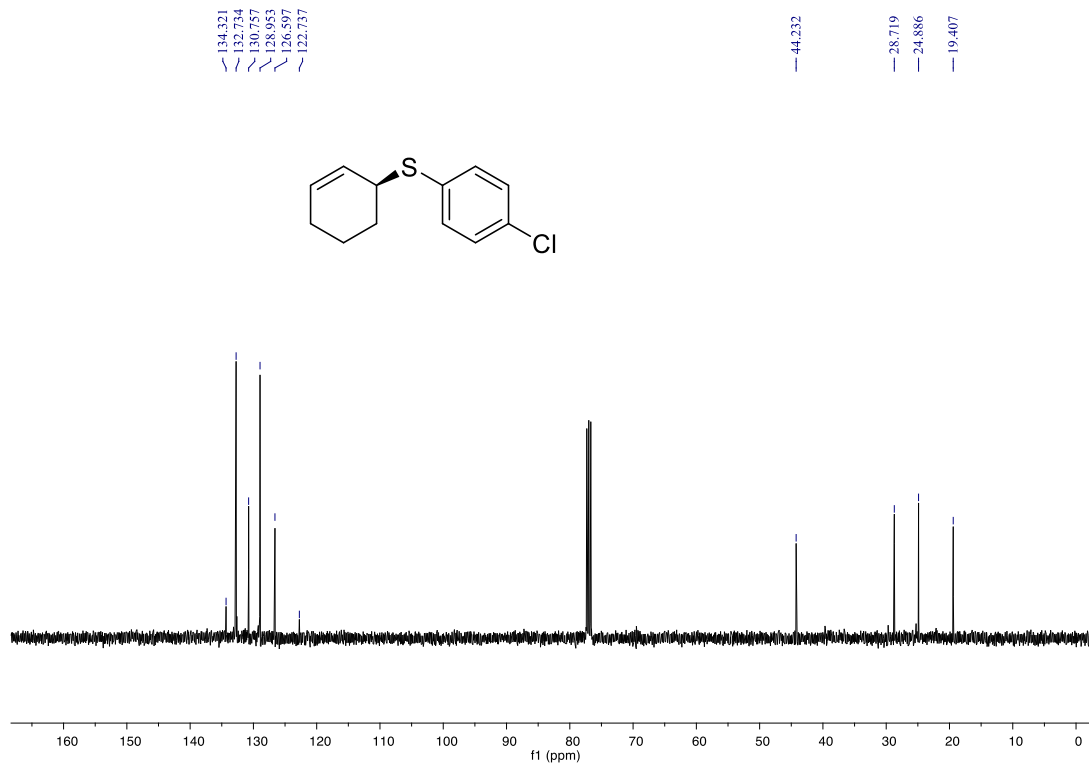
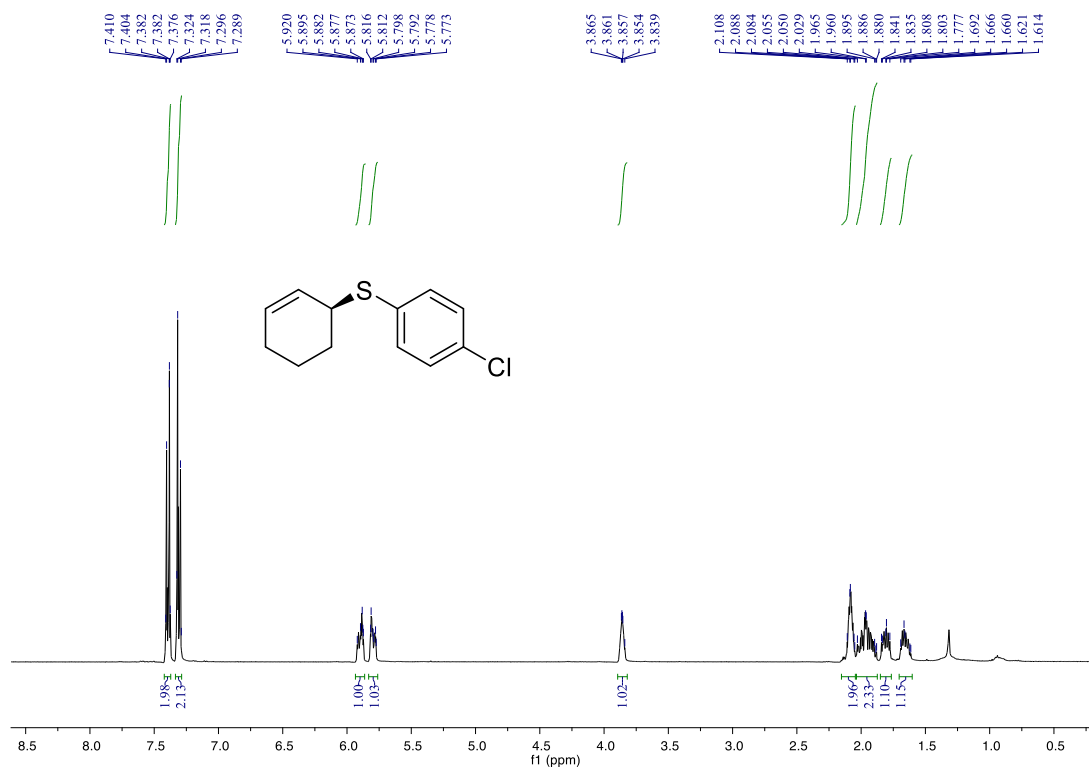
(S)-4-(cyclohex-2-en-1-ylthio)-N,N-dimethylaniline (3ae)



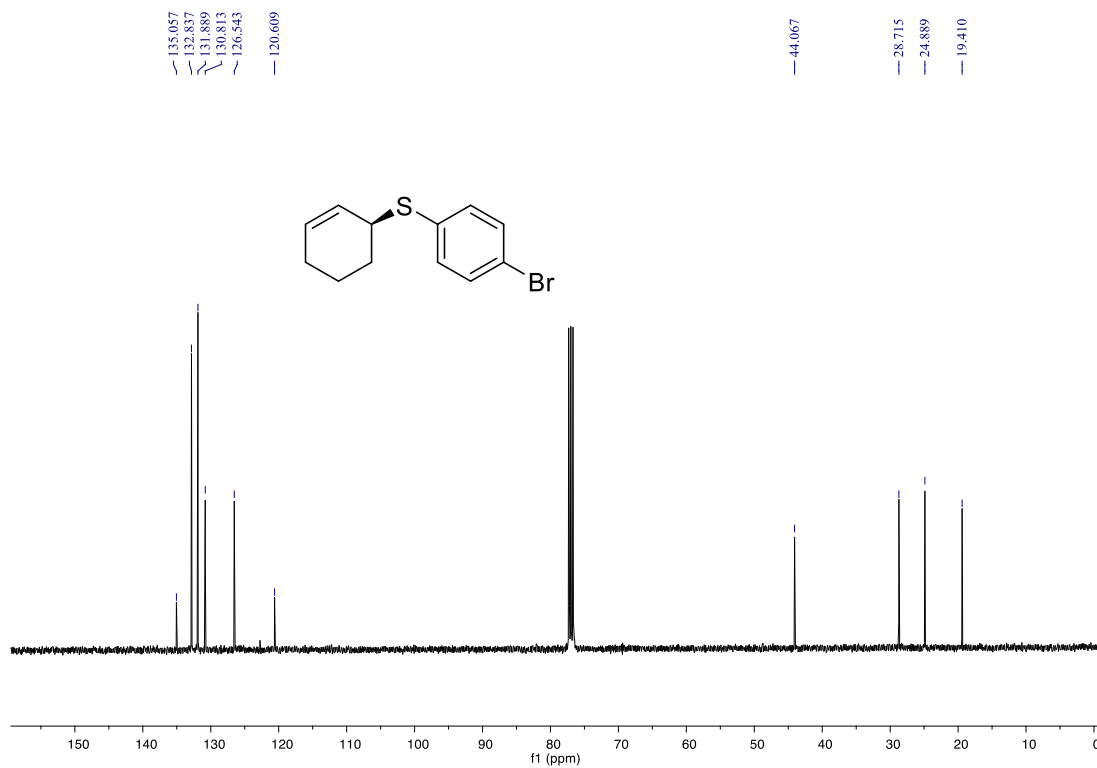
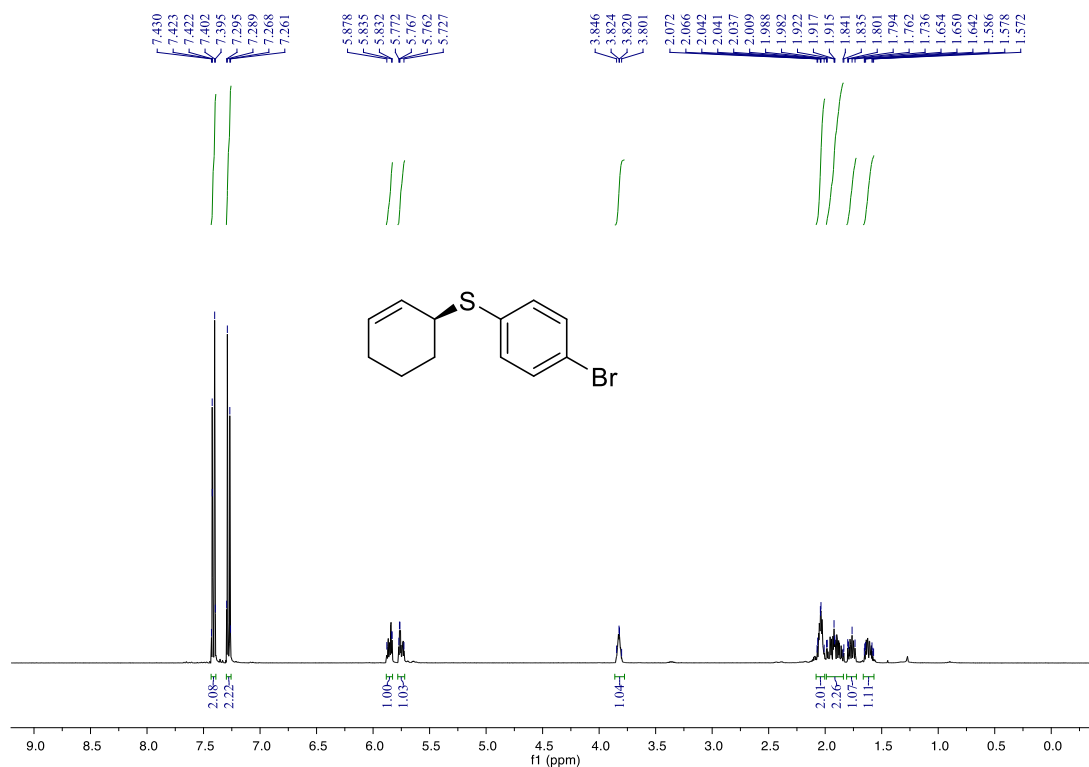
(S)-cyclohex-2-en-1-yl(4-fluorophenyl)sulfane (3af)



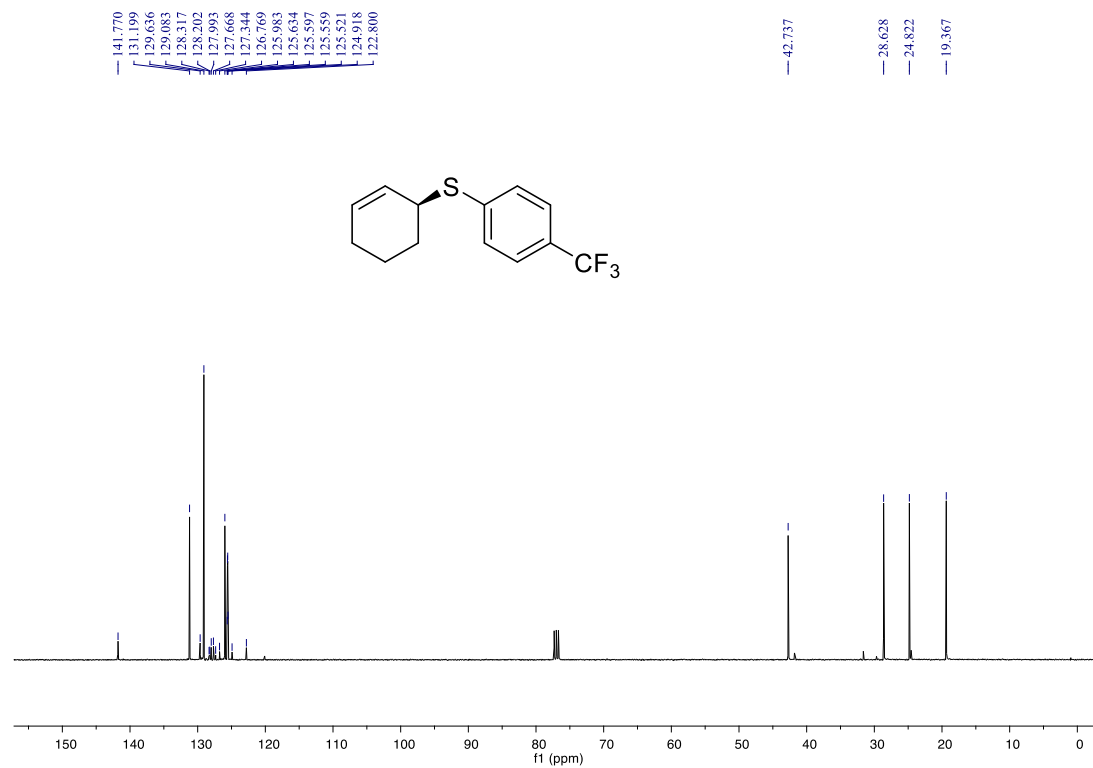
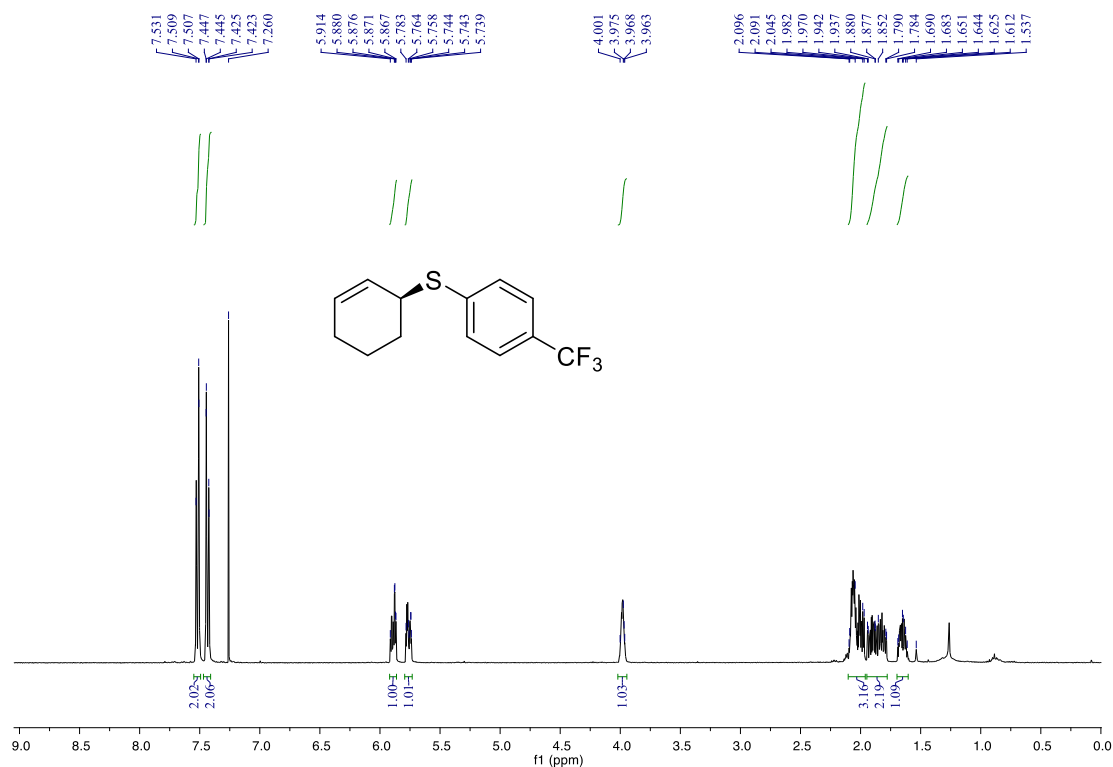
(S)-(4-chlorophenyl)(cyclohex-2-en-1-yl)sulfane (3ag)



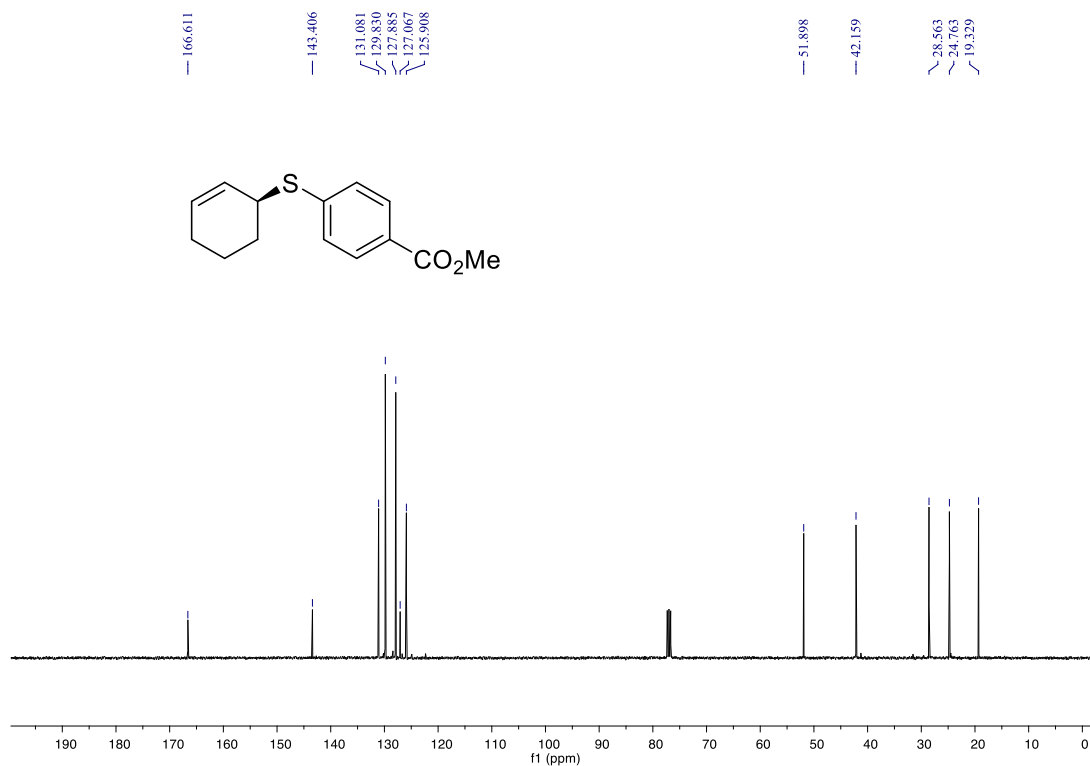
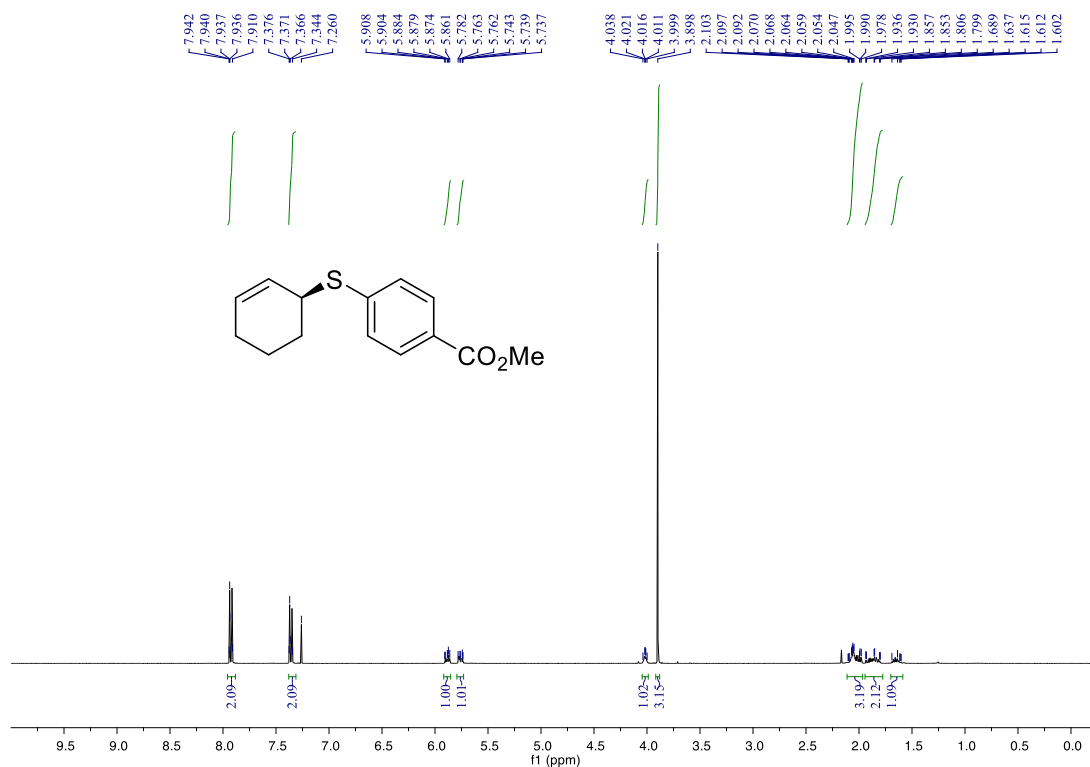
(S)-(4-bromophenyl)(cyclohex-2-en-1-yl)sulfane (3ah)



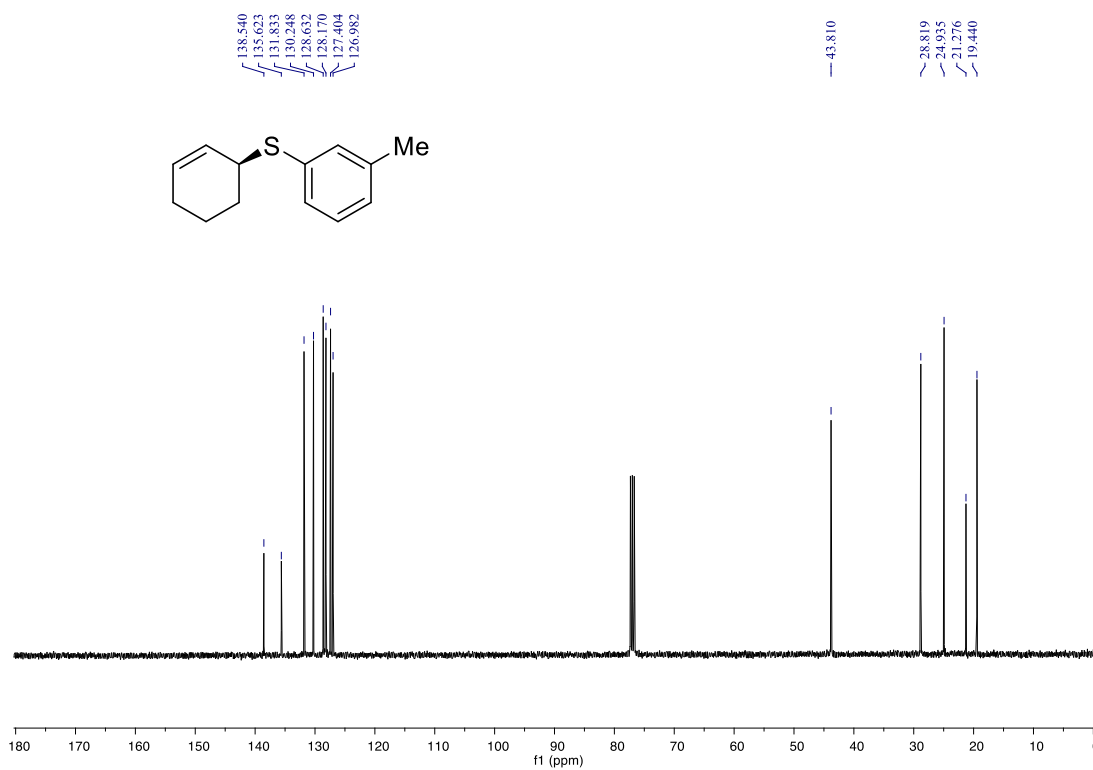
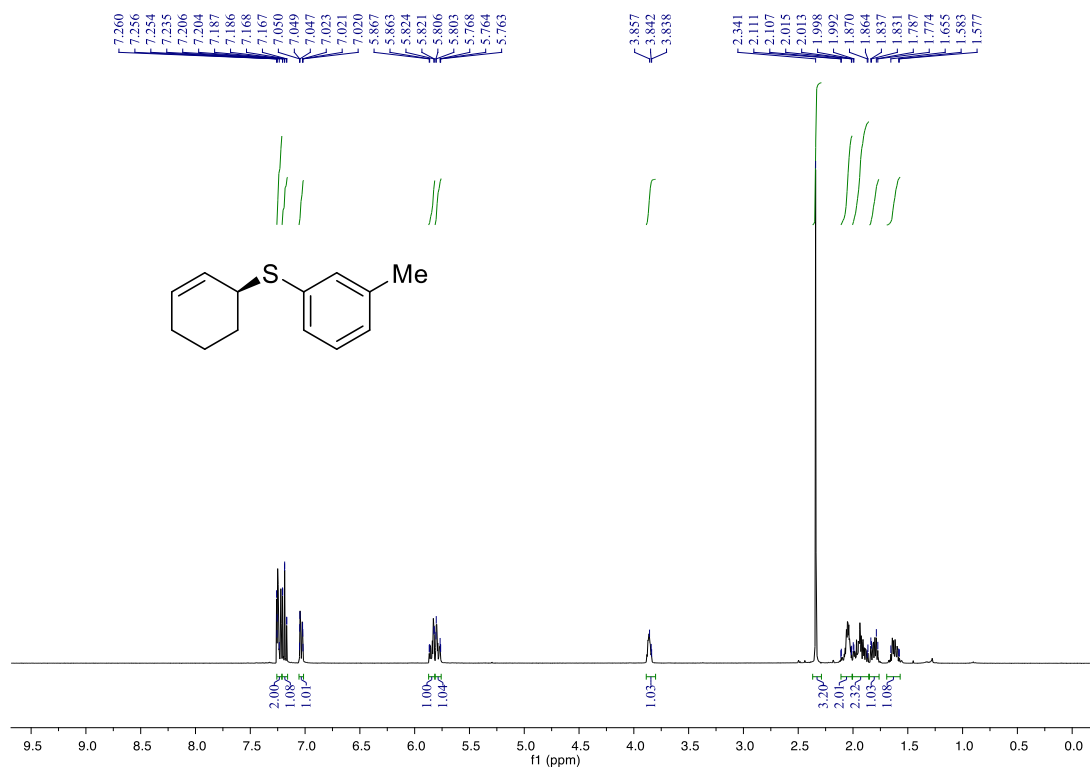
(S)-cyclohex-2-en-1-yl(4-(trifluoromethyl)phenyl)sulfane (3ai)



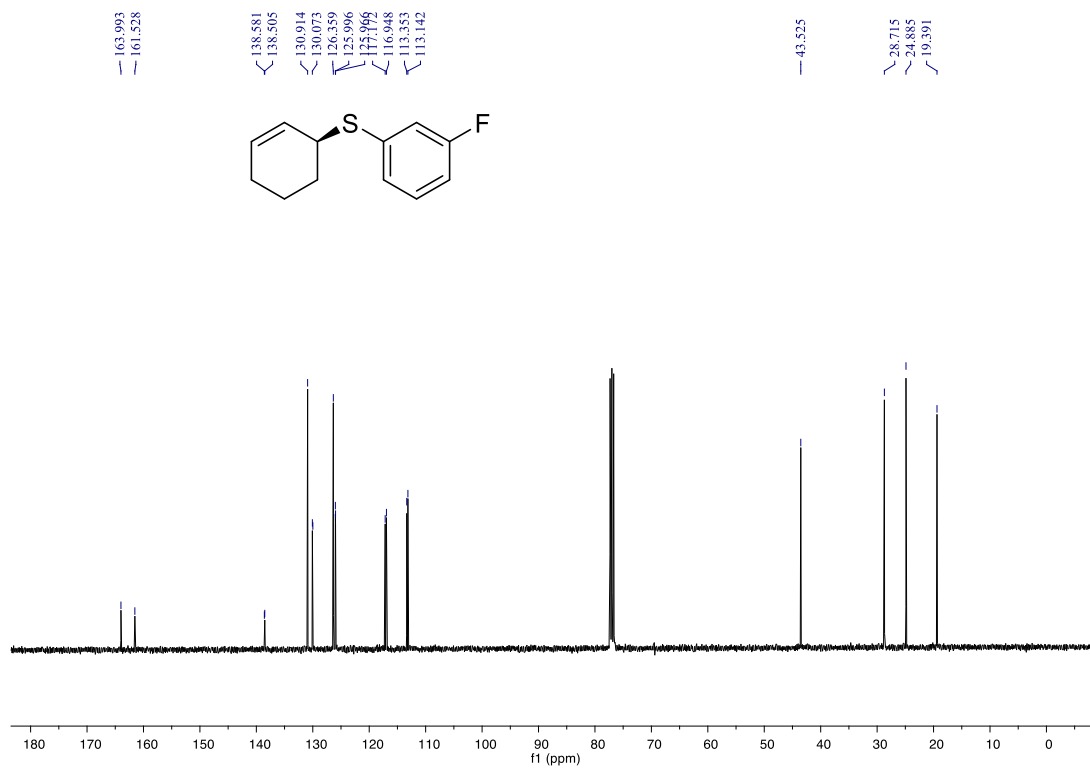
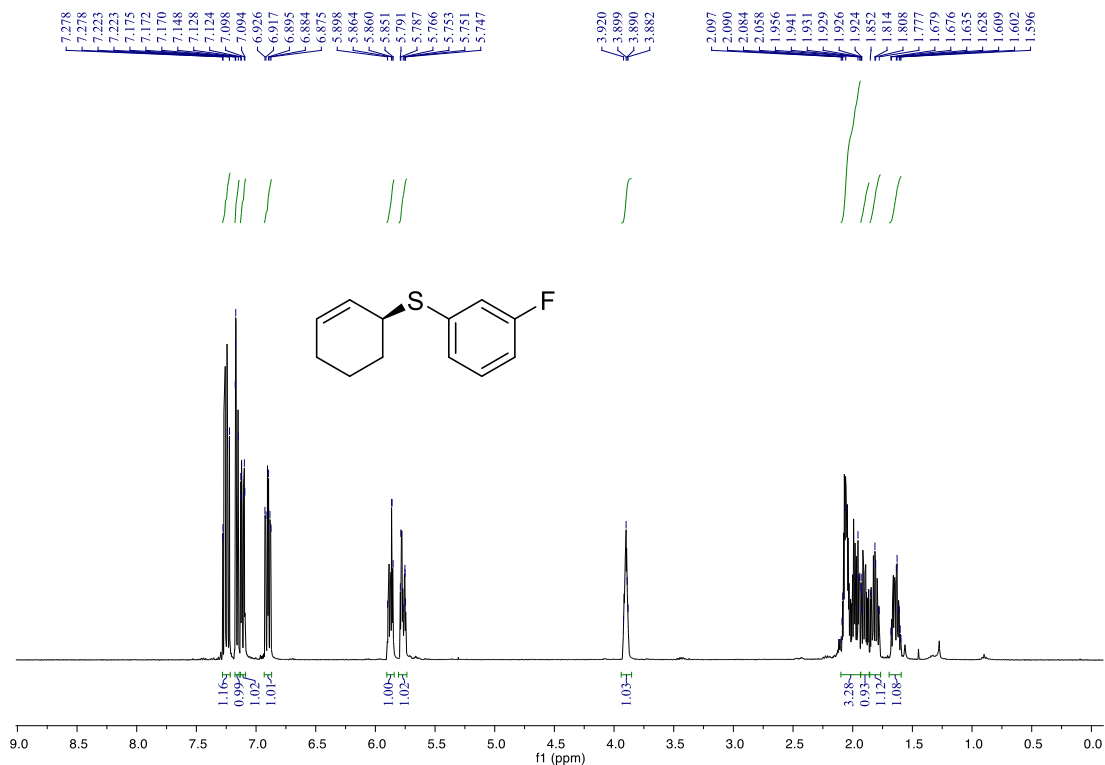
methyl (*S*)-4-(cyclohex-2-en-1-ylthio)benzoate (3aj)



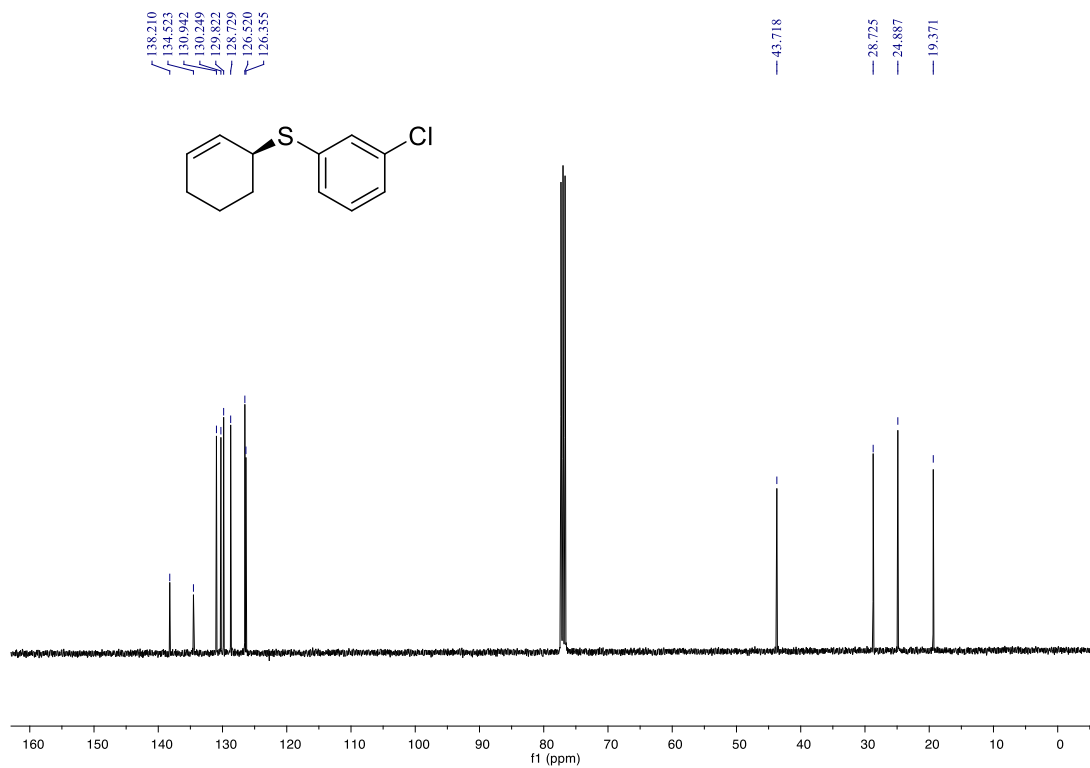
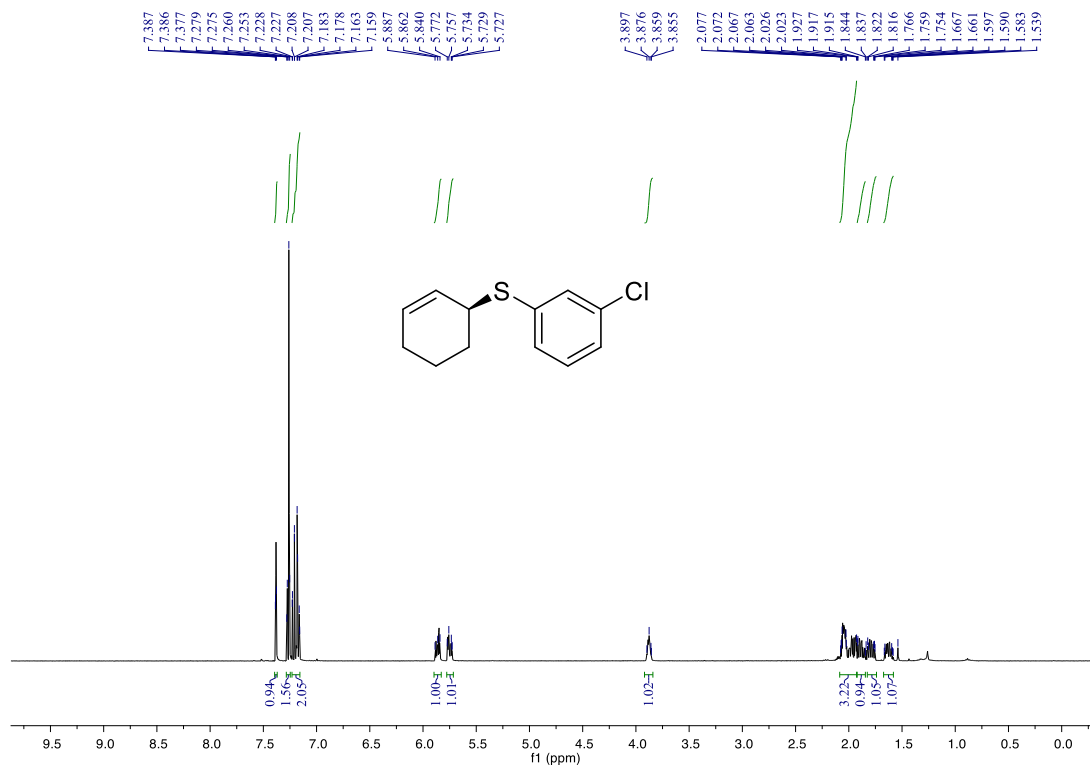
(S)-cyclohex-2-en-1-yl(*m*-tolyl)sulfane (3ak)



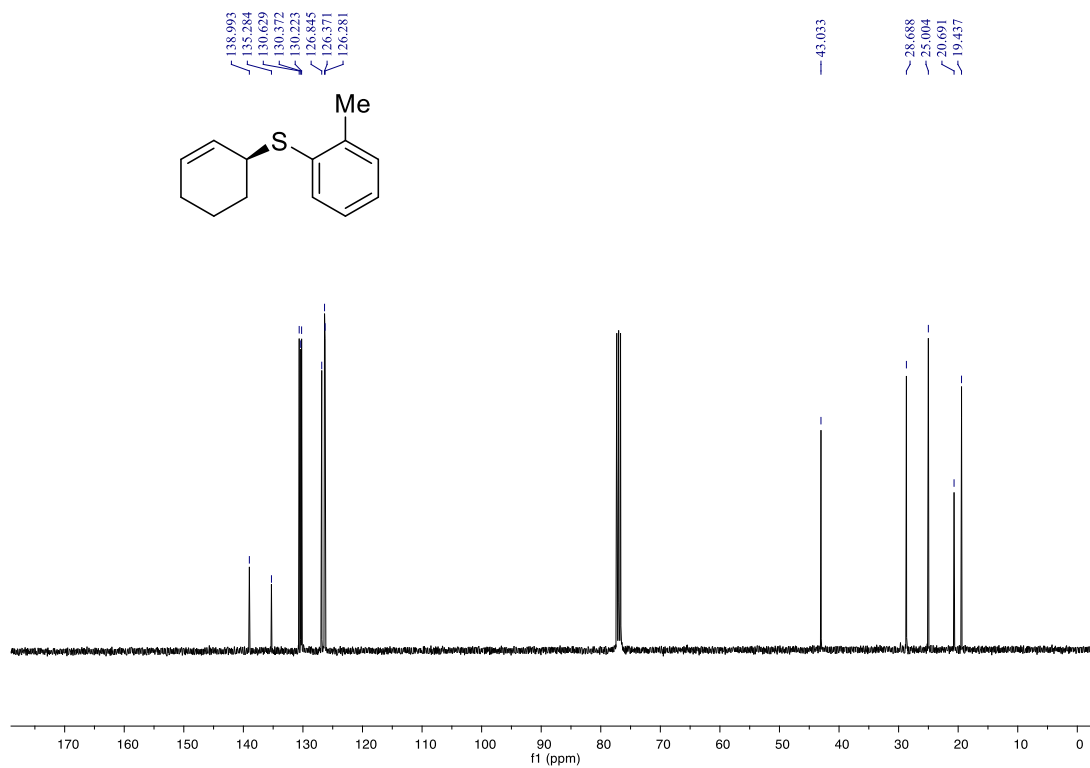
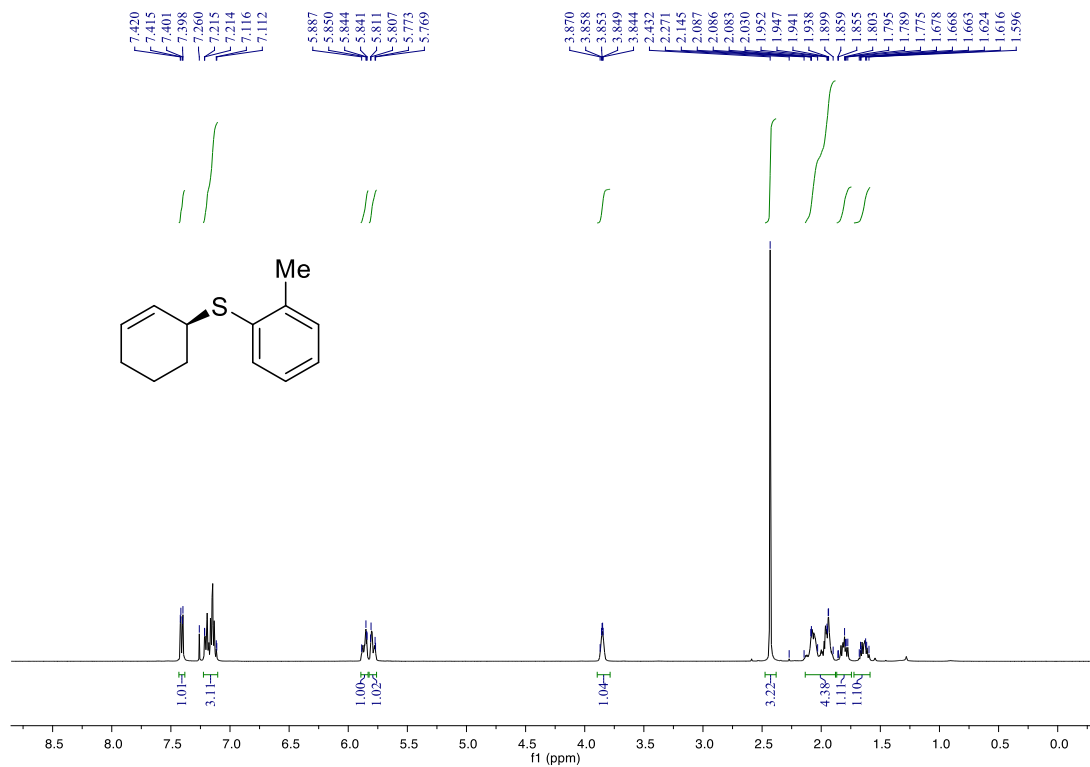
(S)-cyclohex-2-en-1-yl(3-fluorophenyl)sulfane (3al)



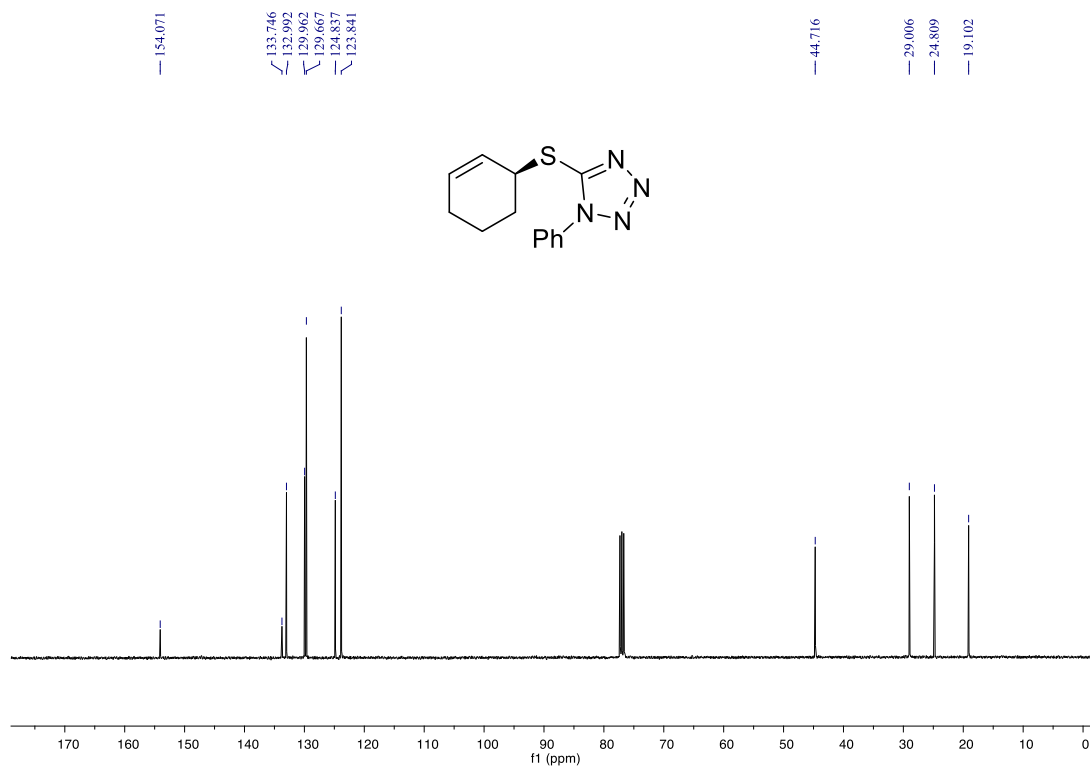
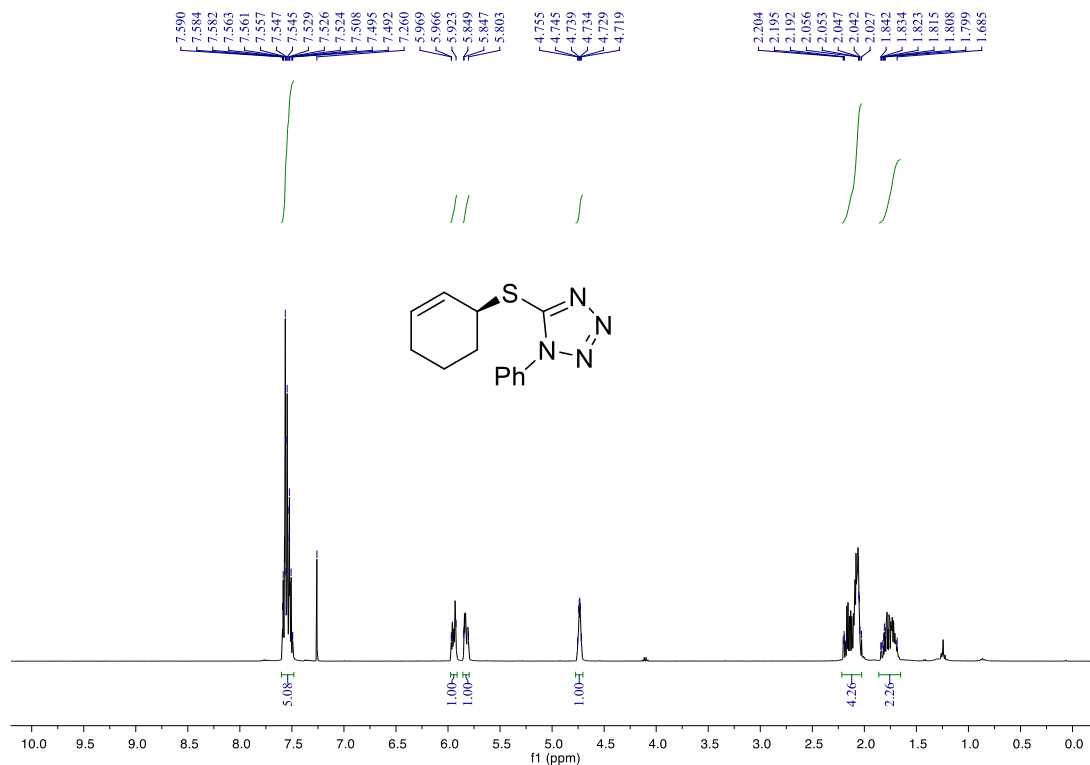
(S)-(3-chlorophenyl)(cyclohex-2-en-1-yl)sulfane (3am)



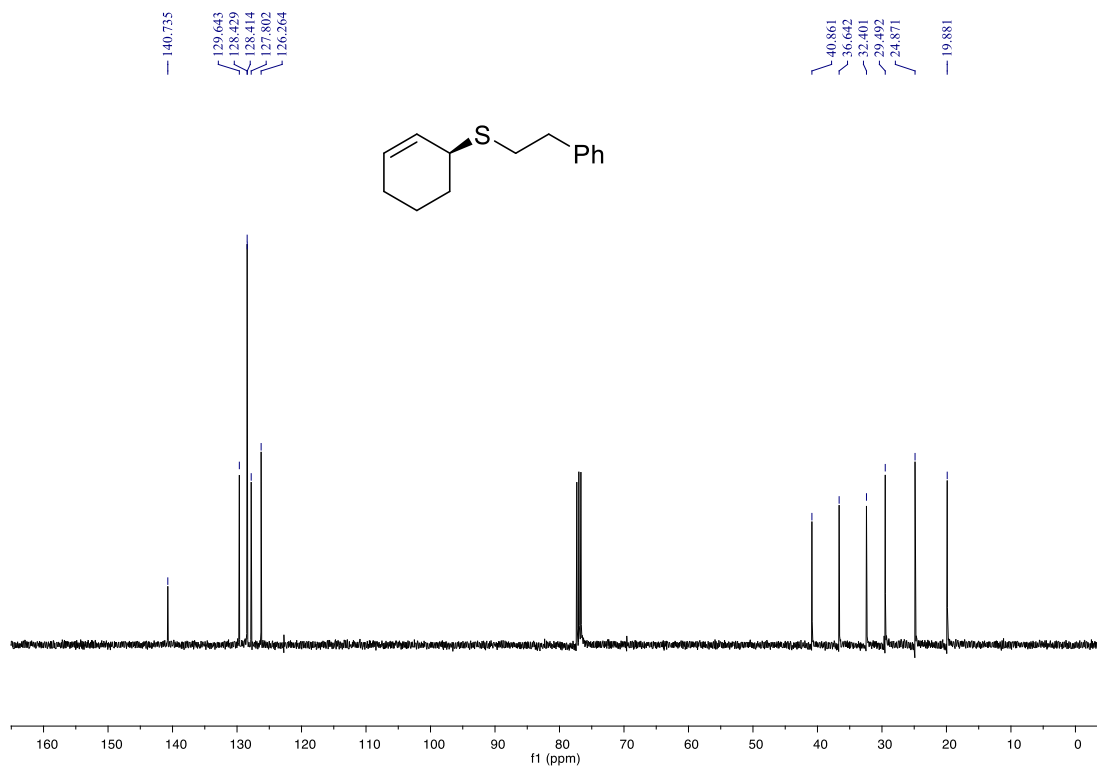
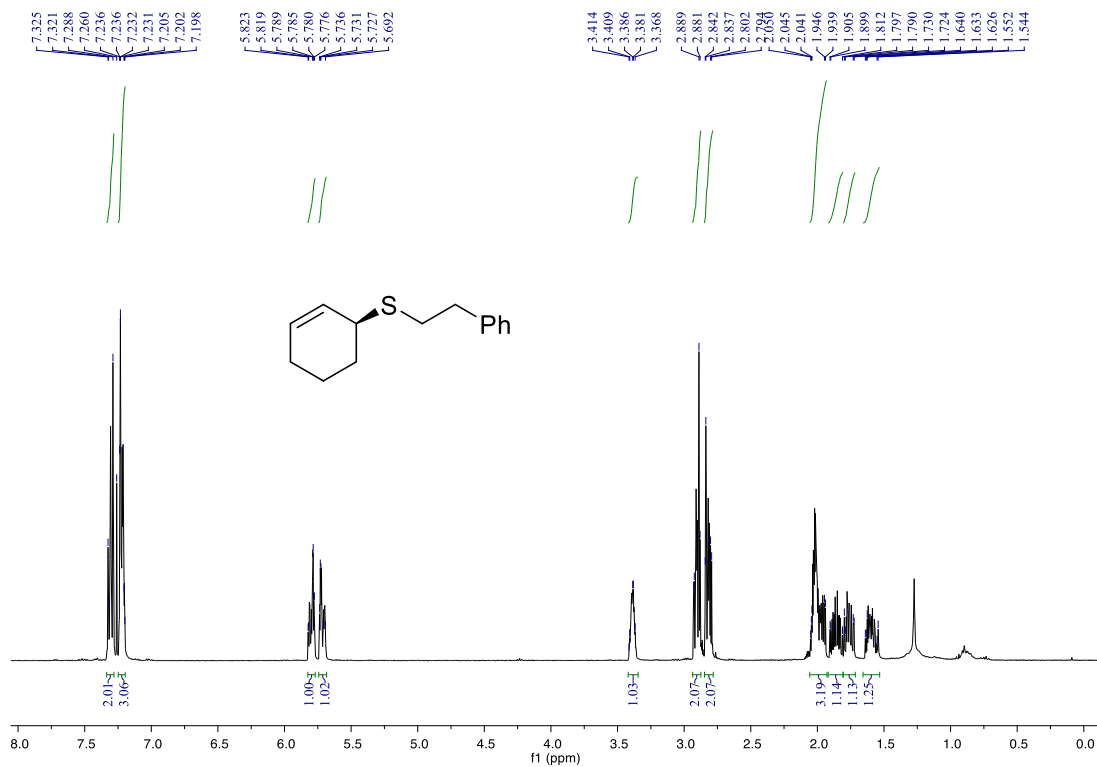
(S)-cyclohex-2-en-1-yl(*o*-tolyl)sulfane (3an)



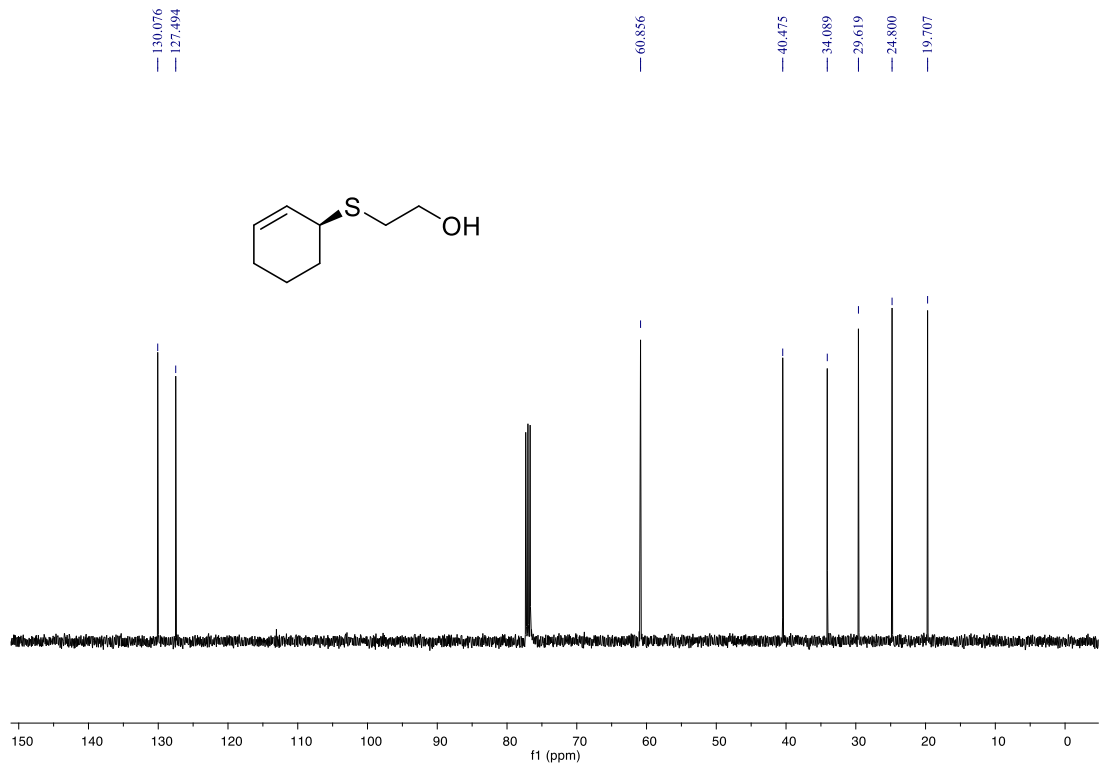
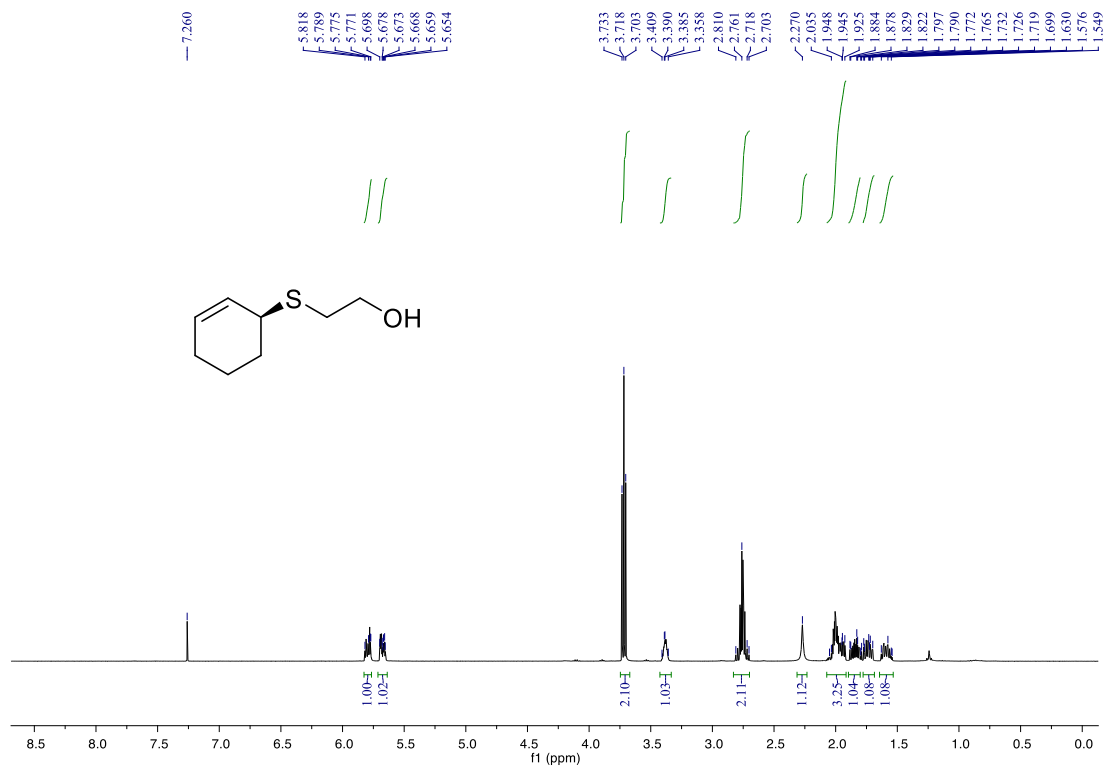
(S)-5-(cyclohex-2-en-1-ylthio)-1-phenyl-1H-tetrazole (3ao)



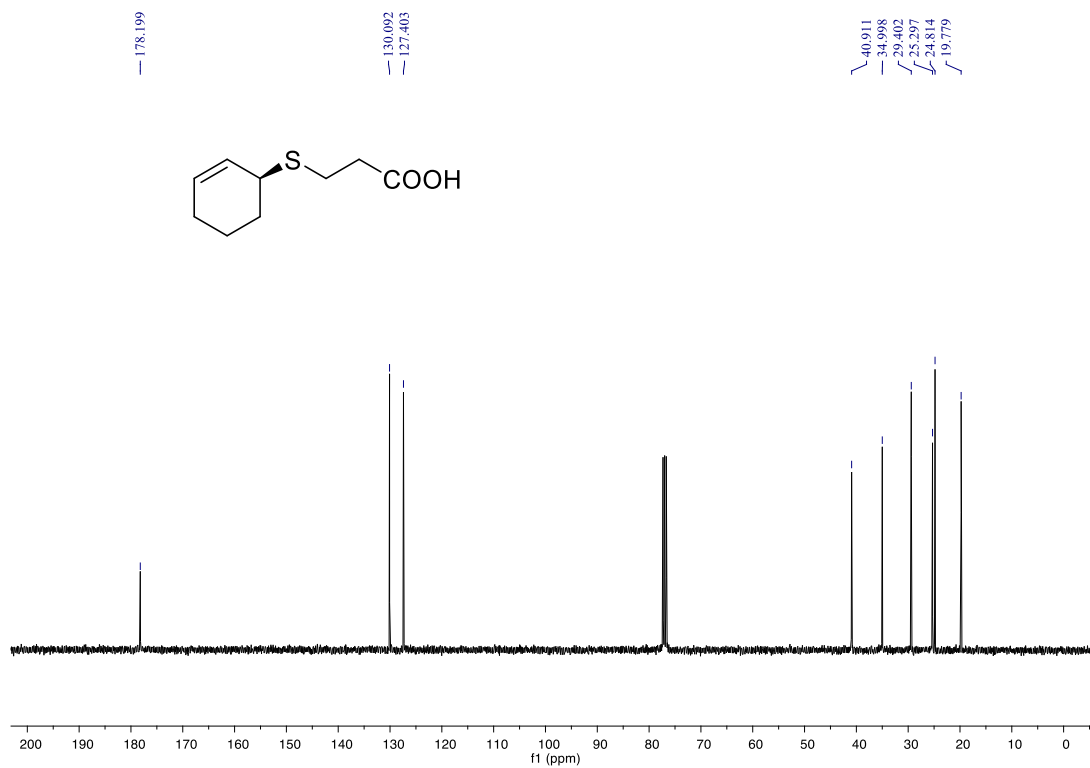
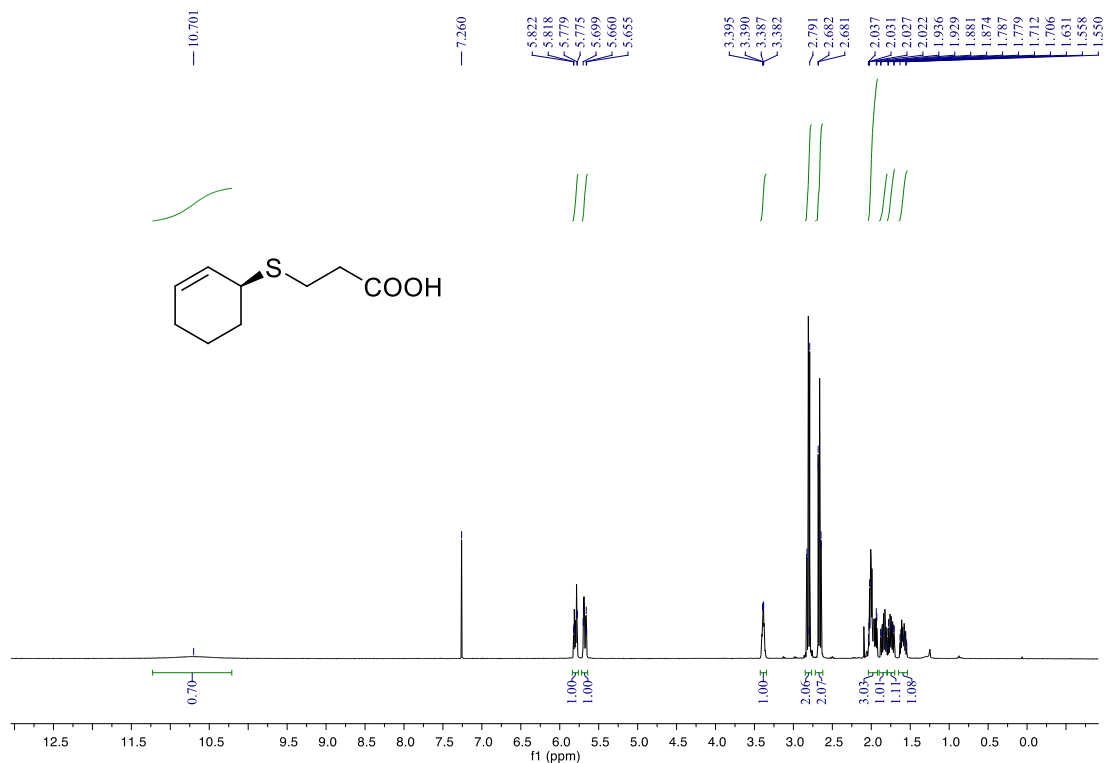
(S)-cyclohex-2-en-1-yl(phenethyl)sulfane (3ap)



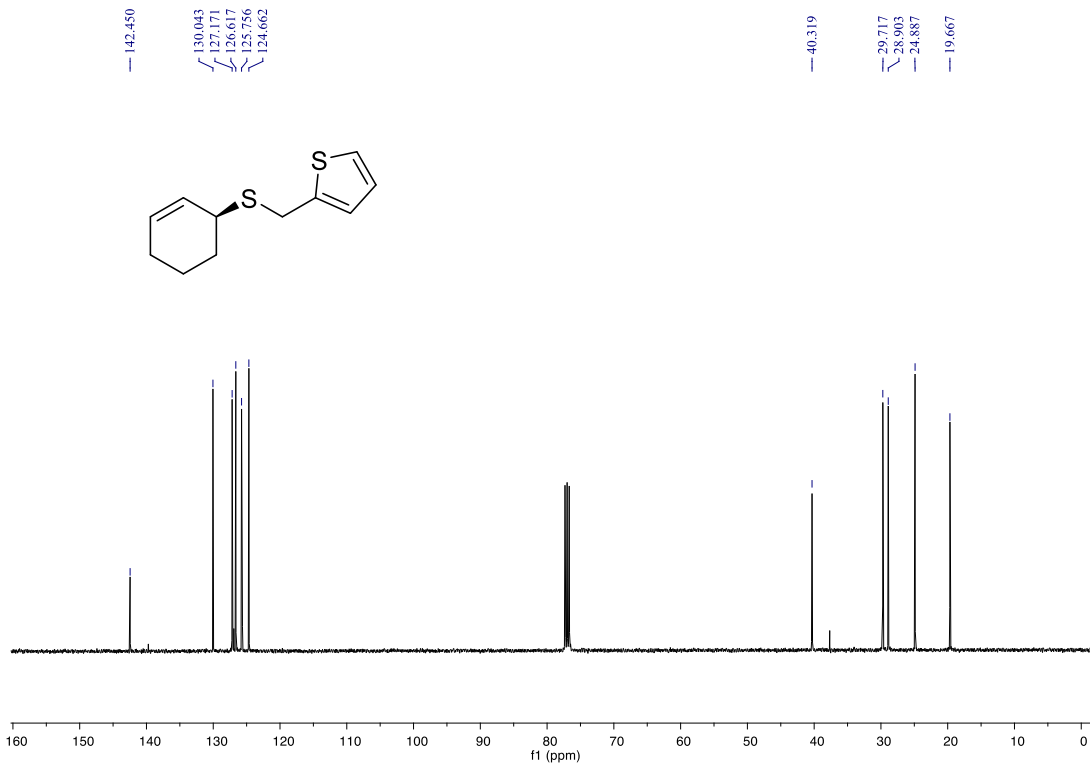
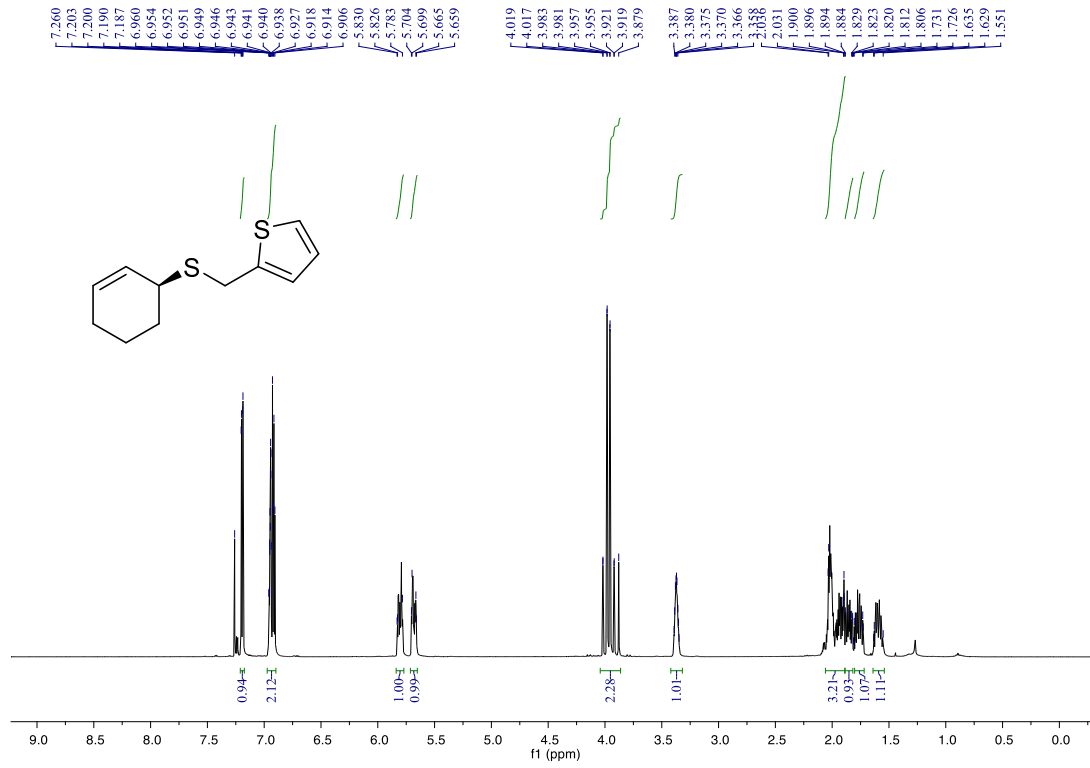
(S)-2-(cyclohex-2-en-1-ylthio)ethan-1-ol (3aq)



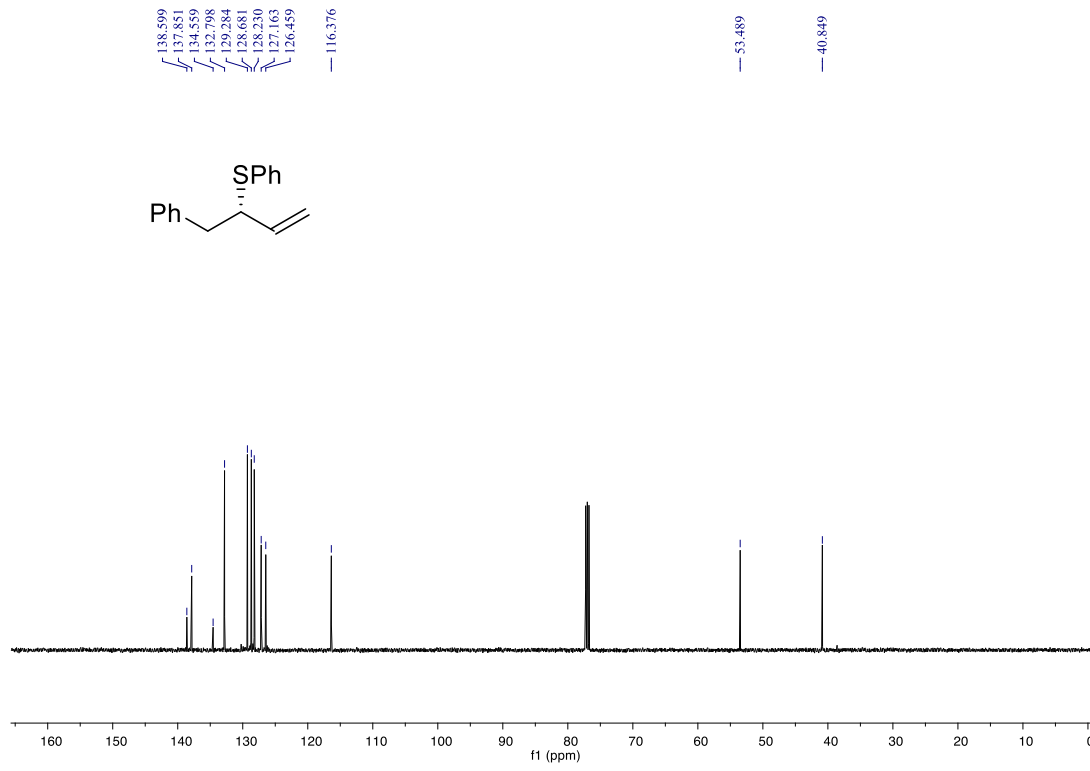
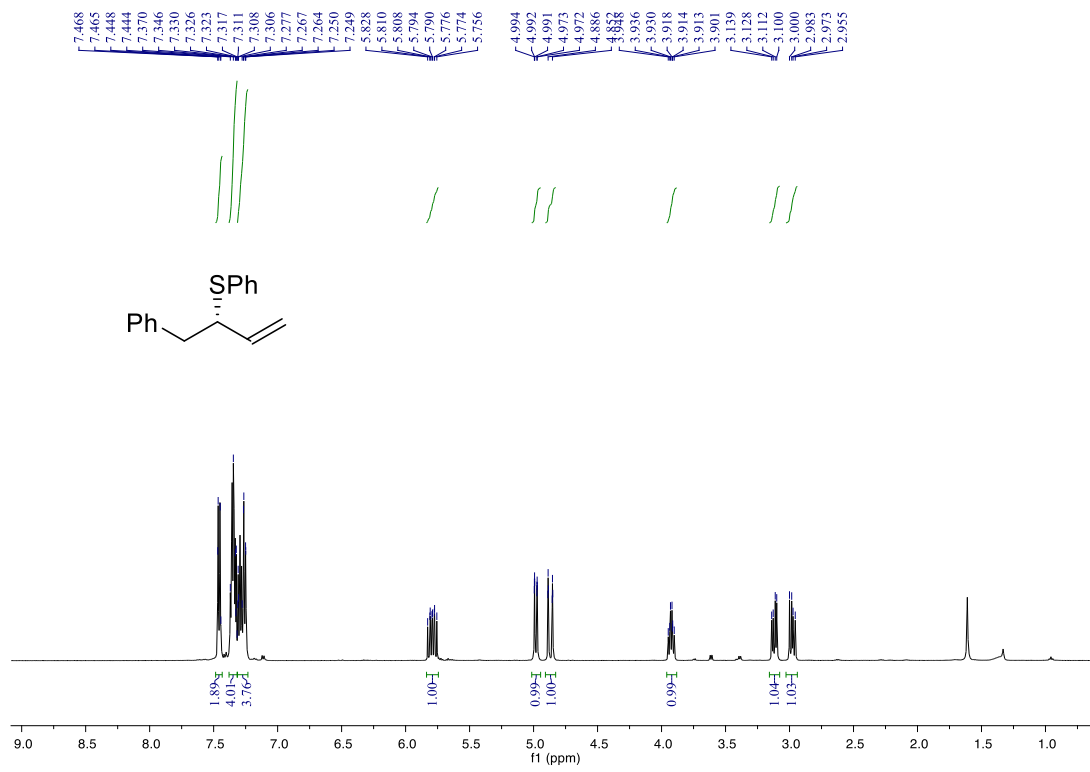
(S)-3-(cyclohex-2-en-1-ylthio)propanoic acid (3ar)



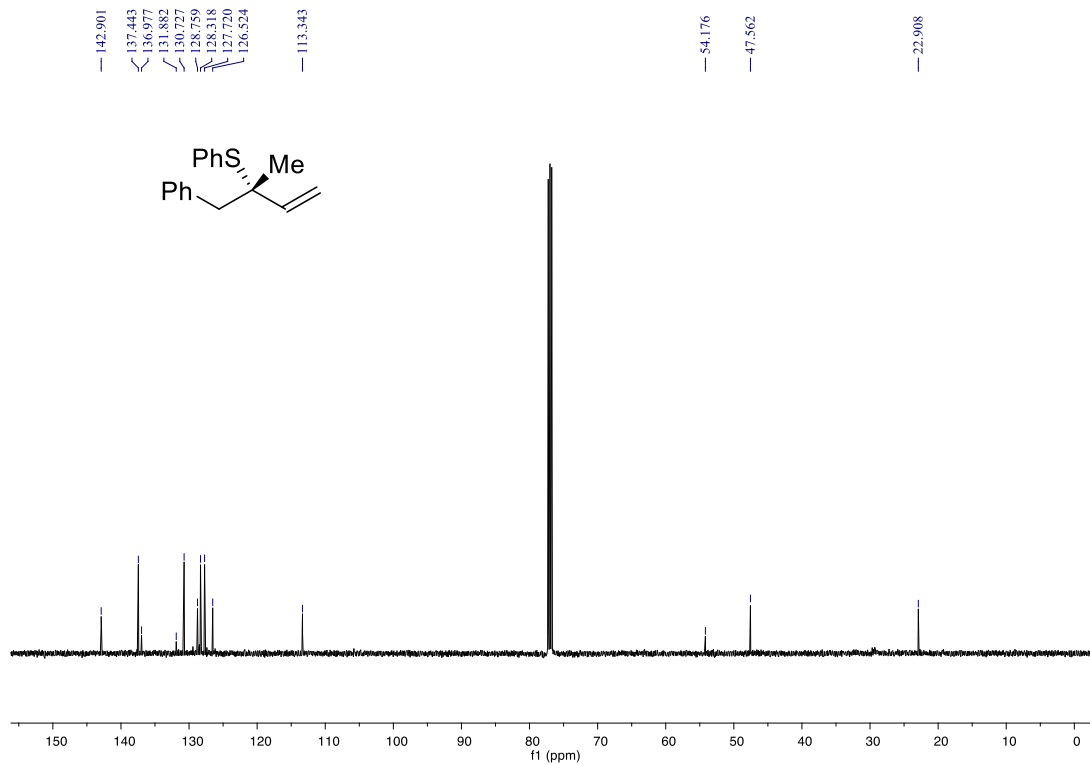
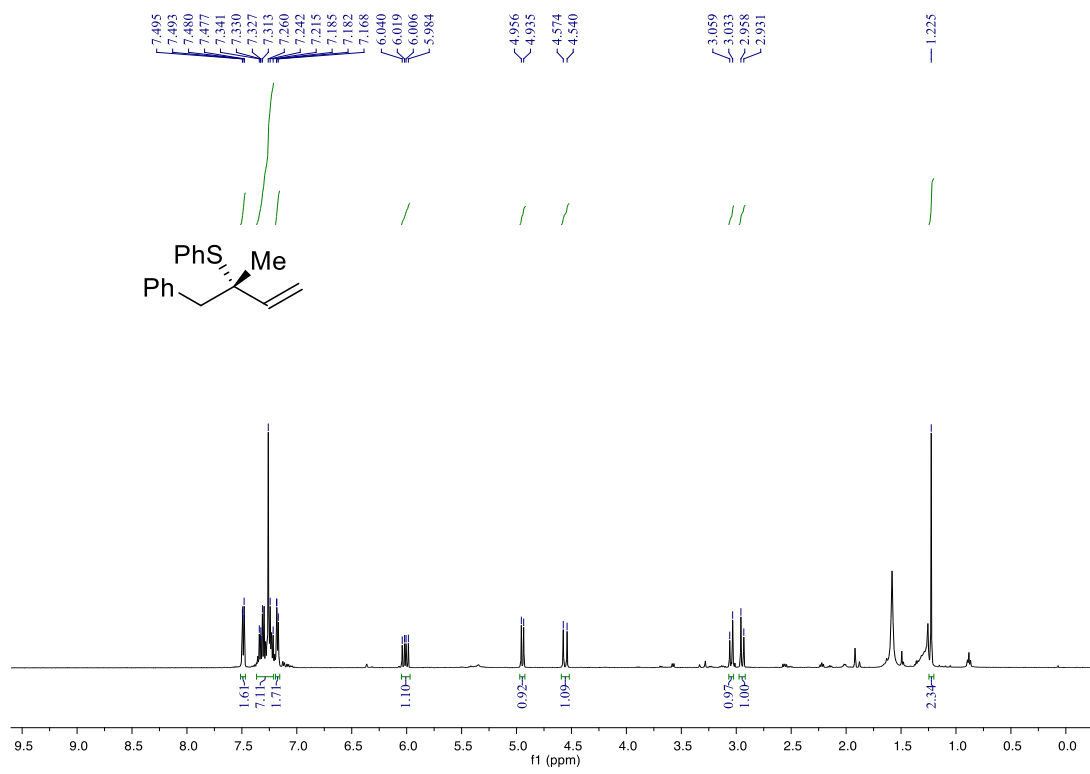
(S)-2-((cyclohex-2-en-1-ylthio)methyl)thiophene (3as)



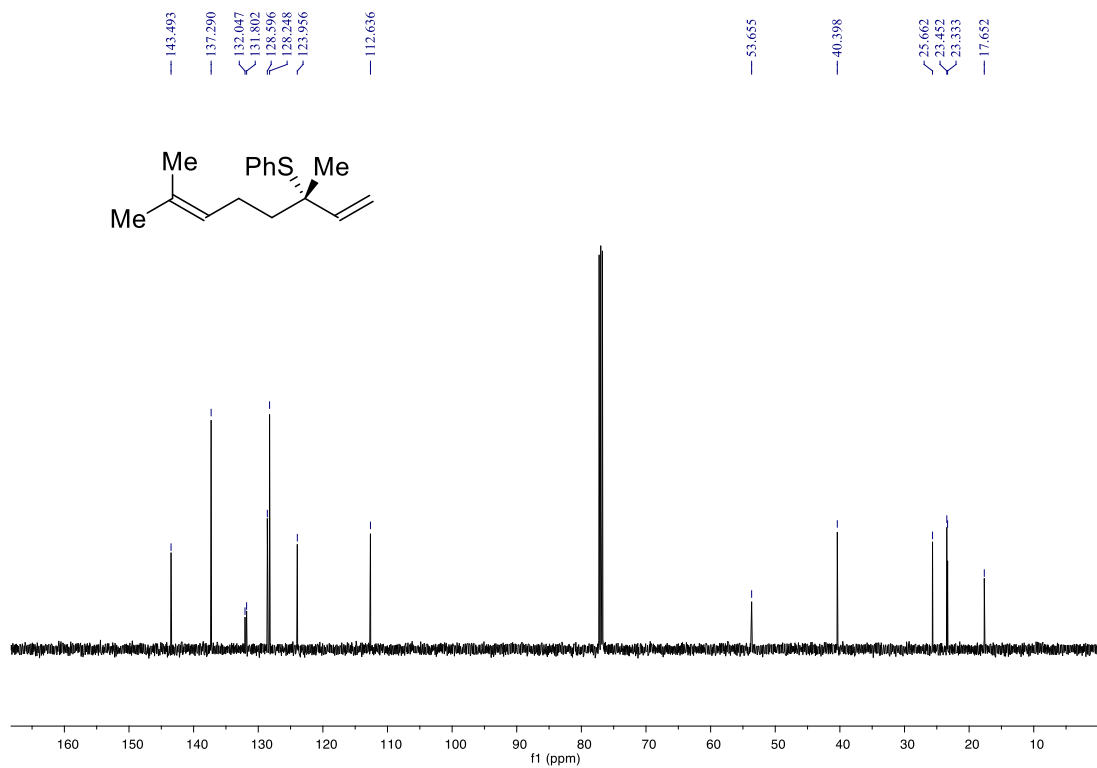
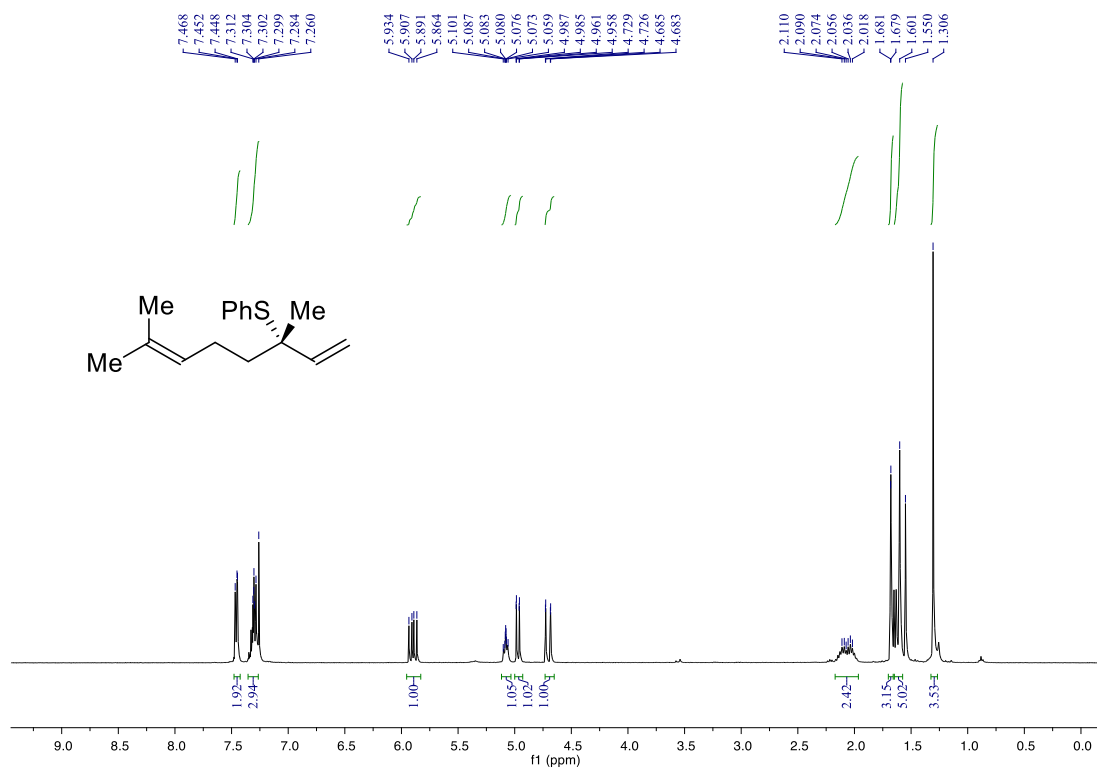
(S)-phenyl(1-phenylbut-3-en-2-yl)sulfane (3ba)



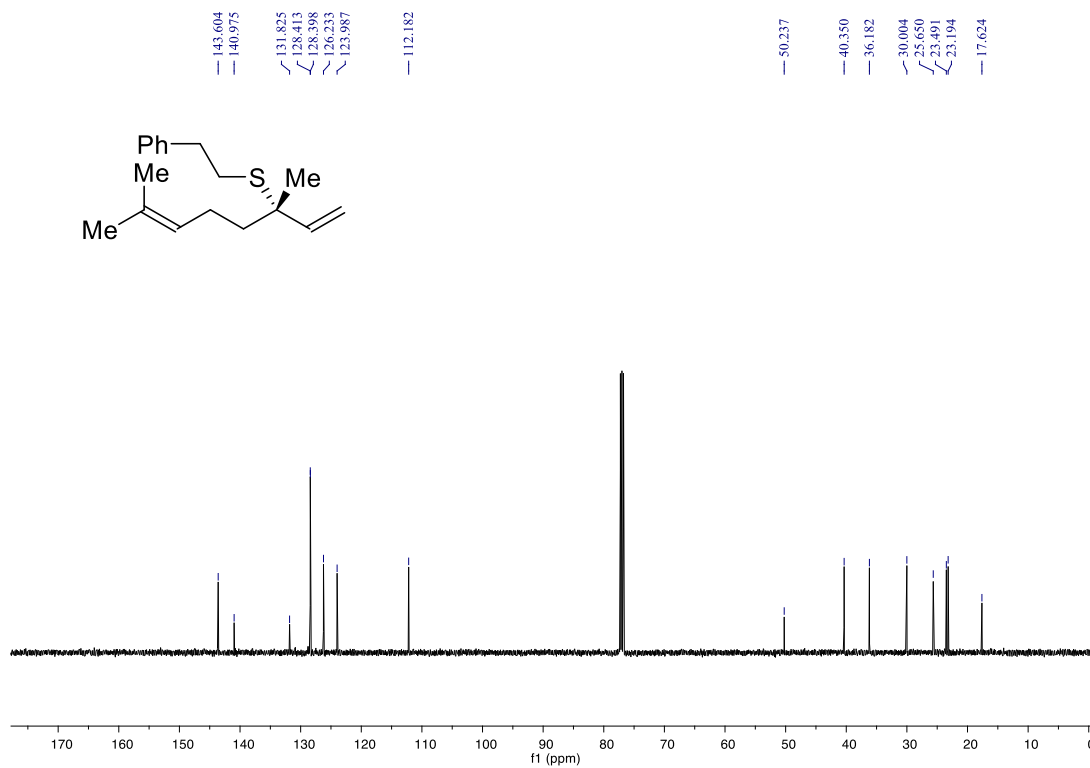
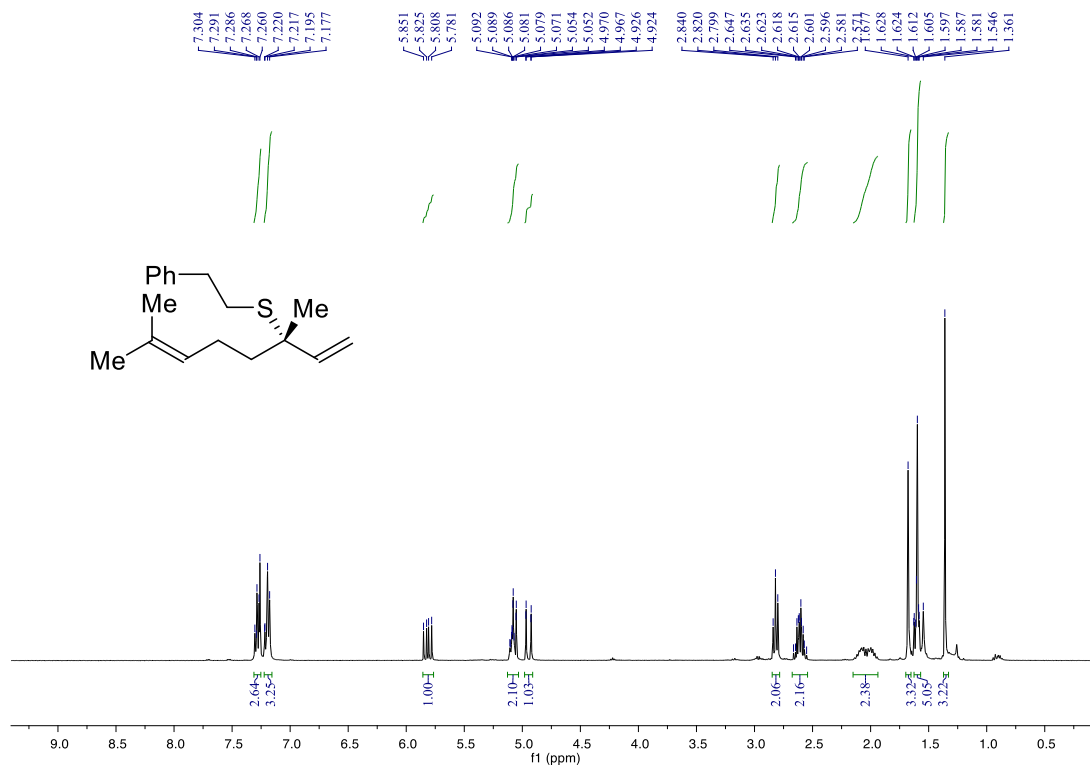
(S)-(2-methyl-1-phenylbut-3-en-2-yl)(phenyl)sulfane (3ca)



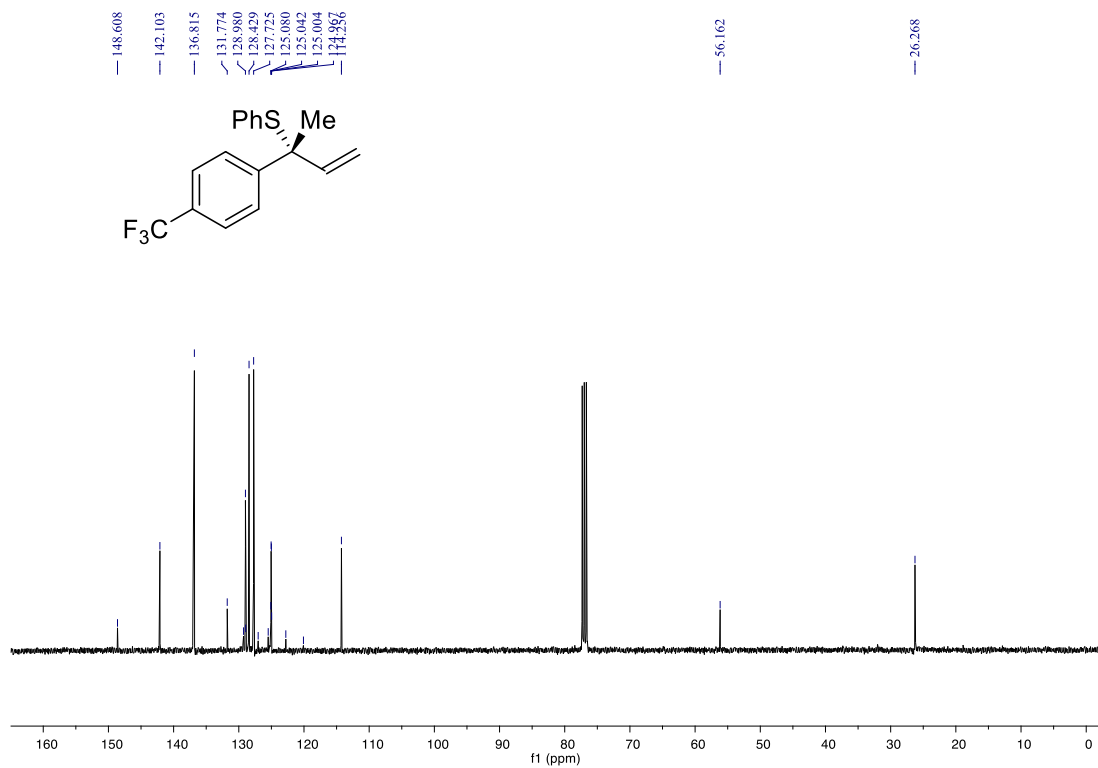
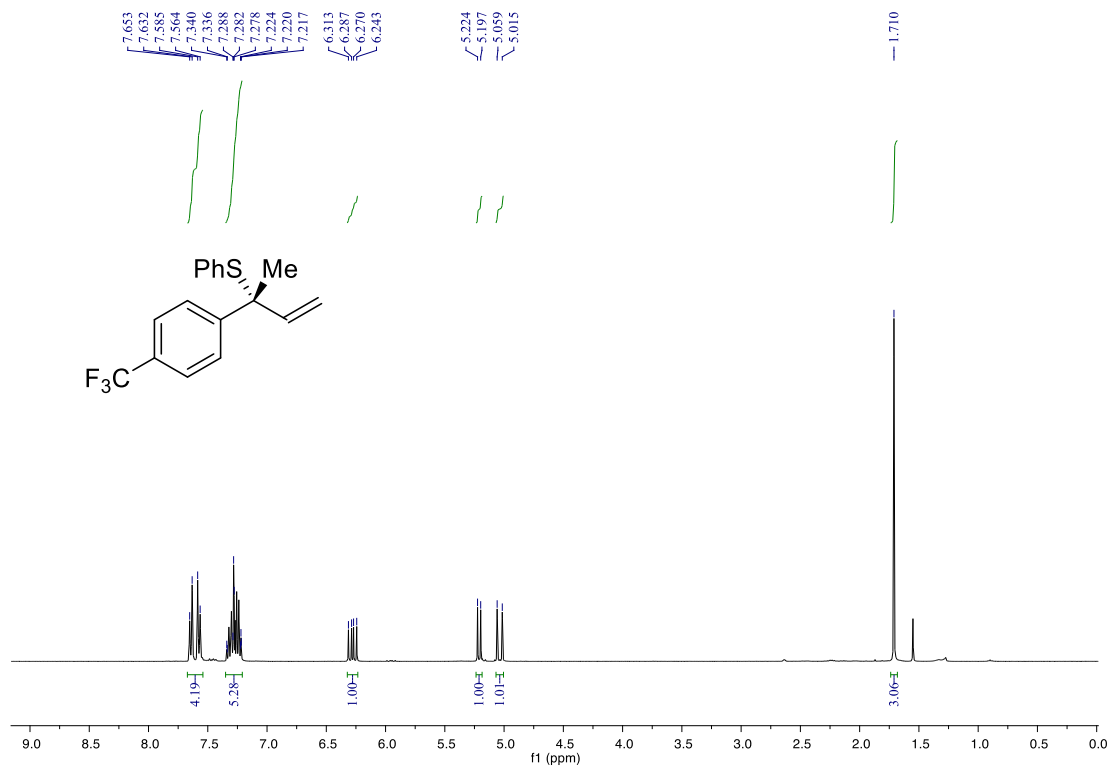
(S)-(3,7-dimethylocta-1,6-dien-3-yl)(phenyl)sulfane (3da)



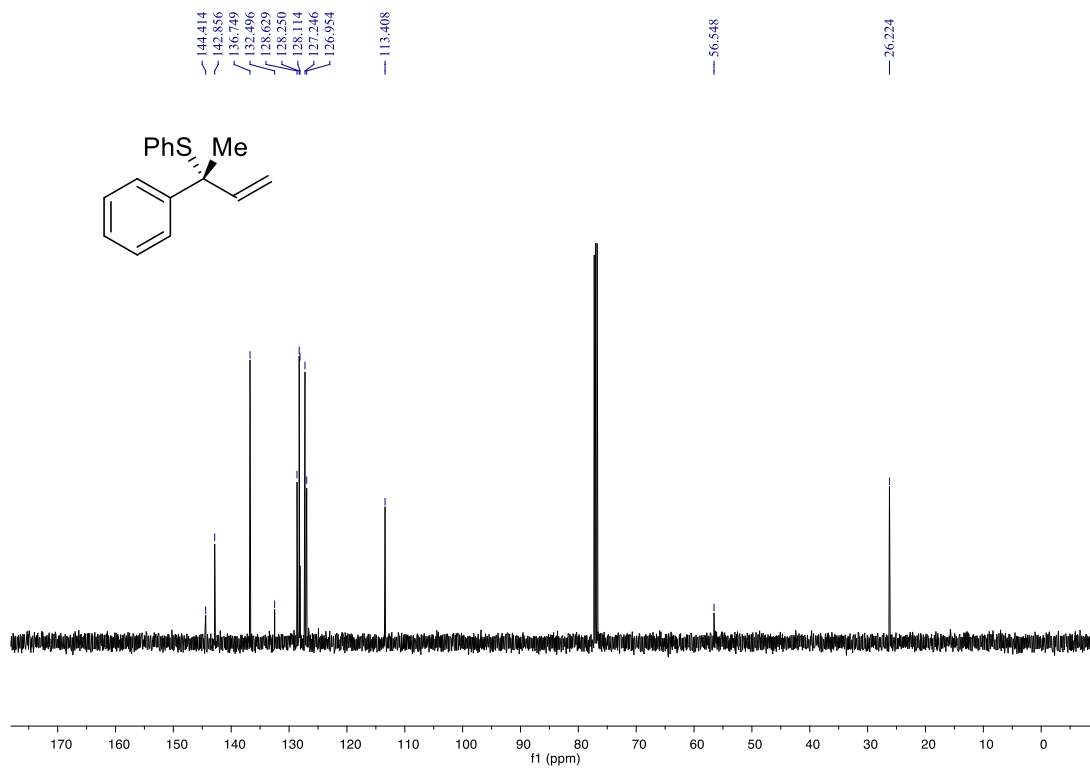
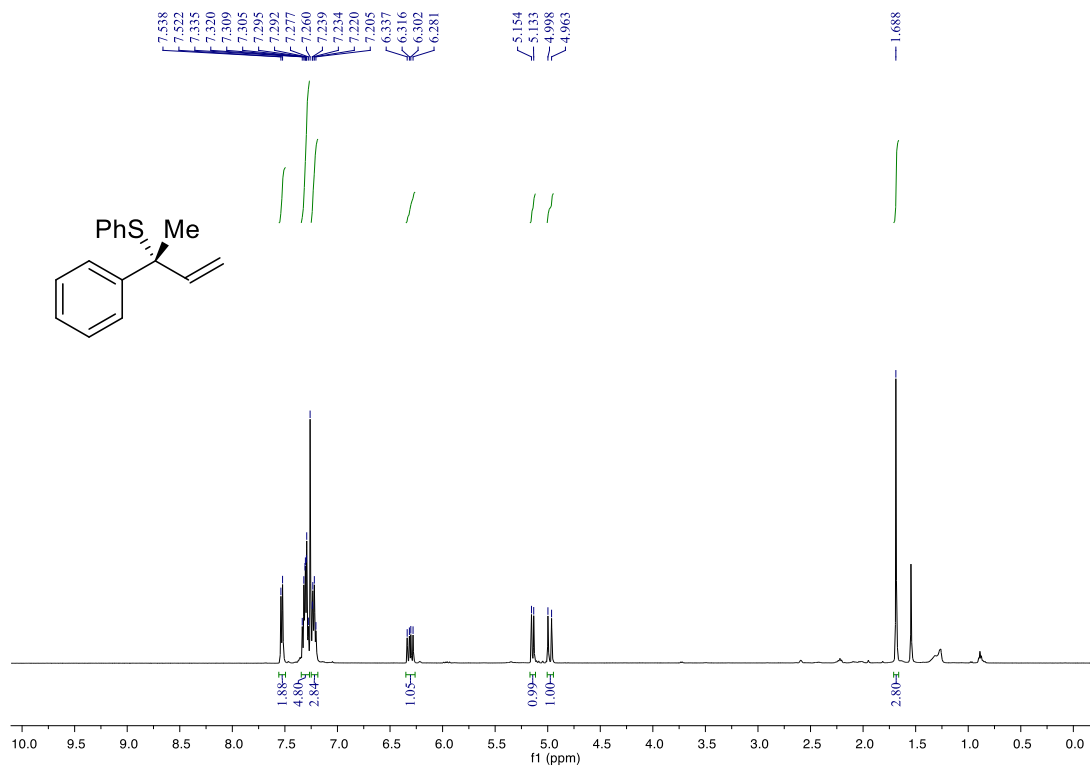
(S)-(3,7-dimethylocta-1,6-dien-3-yl)(phenethyl)sulfane (3dp)



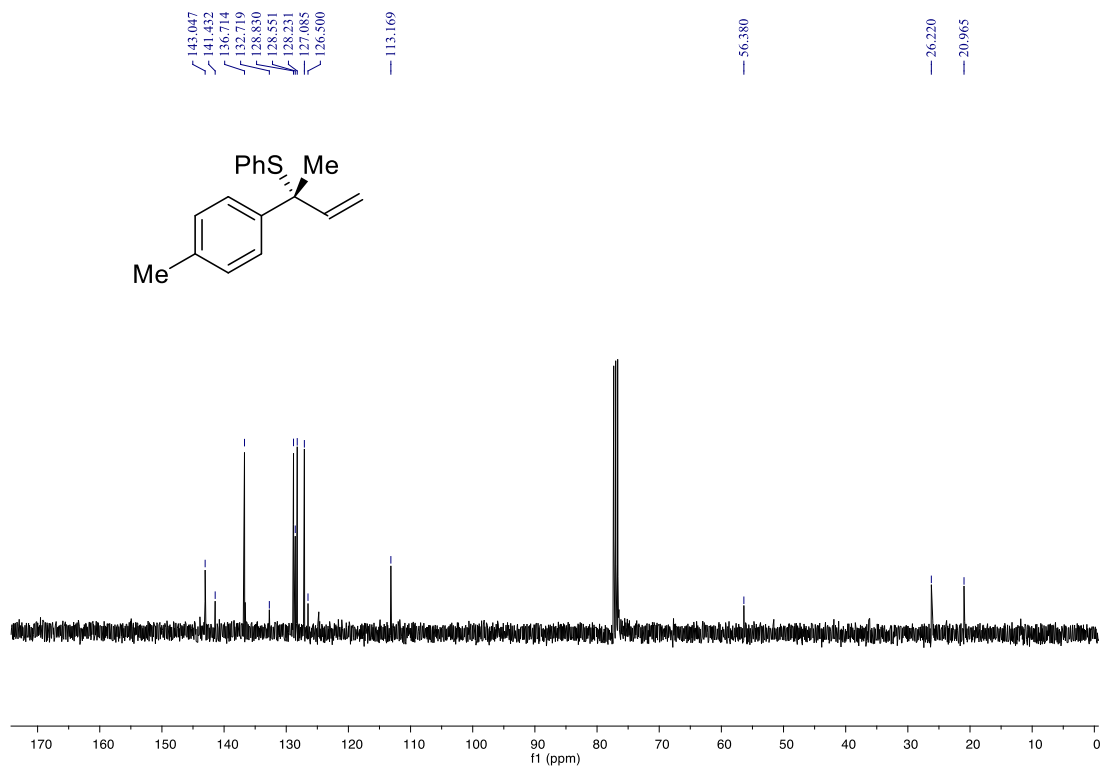
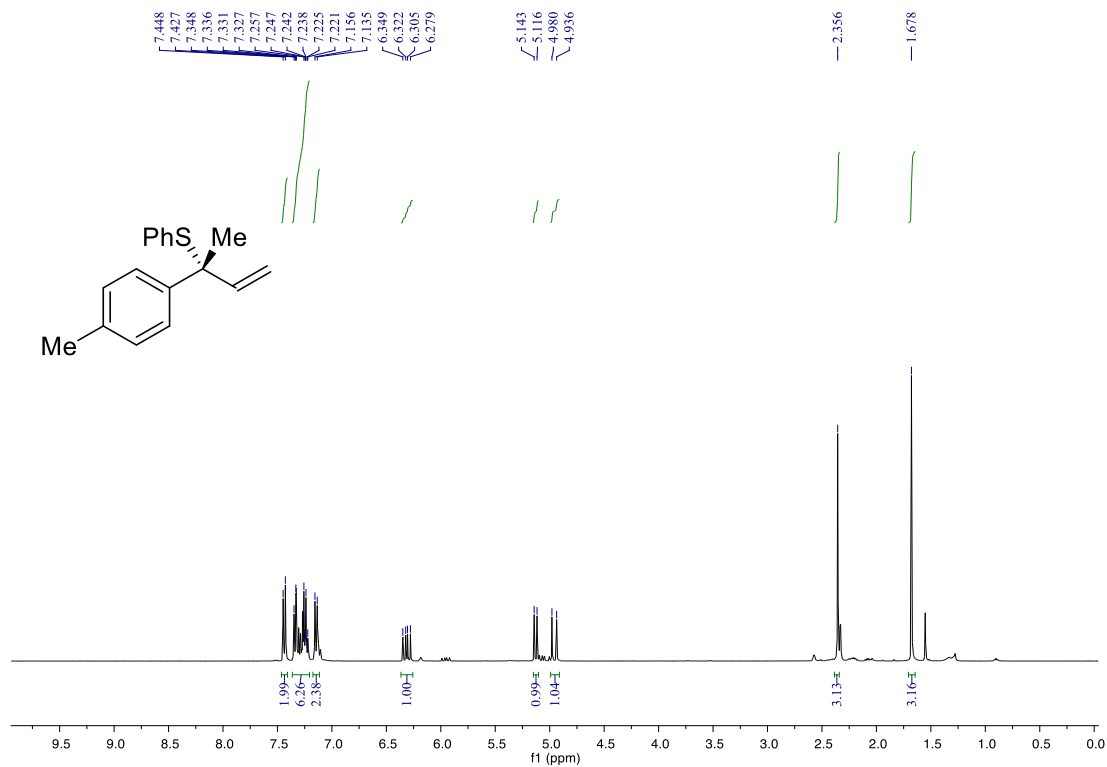
(R)-phenyl(2-(4-(trifluoromethyl)phenyl)but-3-en-2-yl)sulfane (3ea)



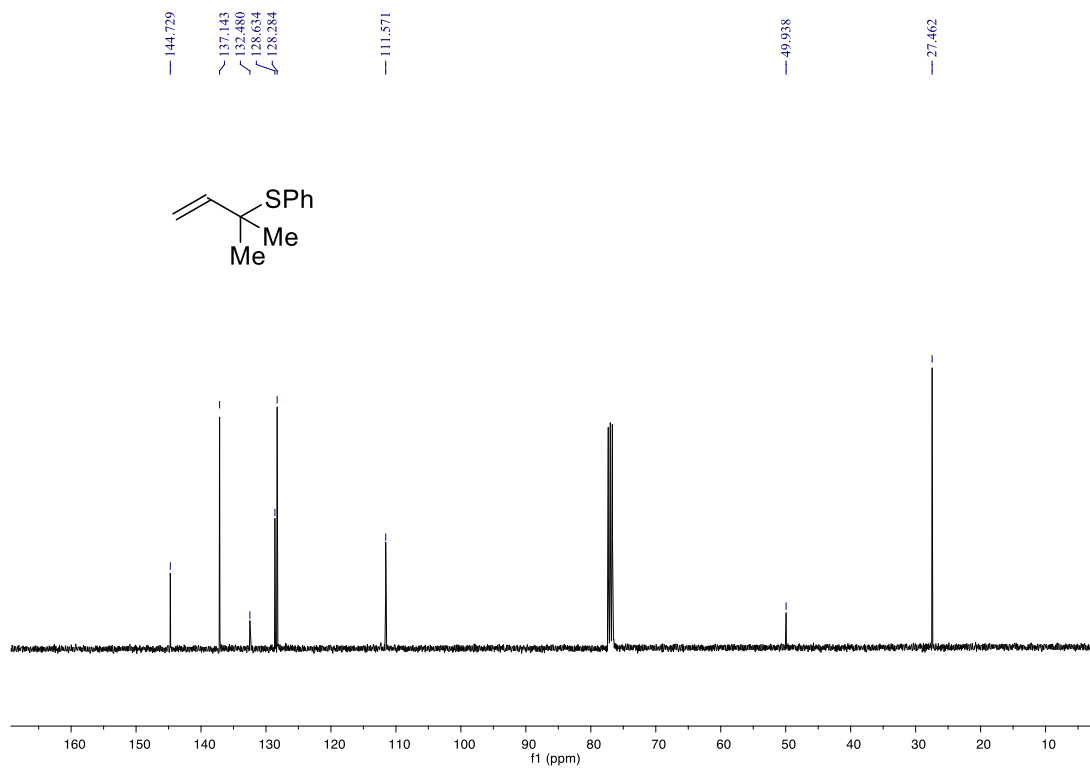
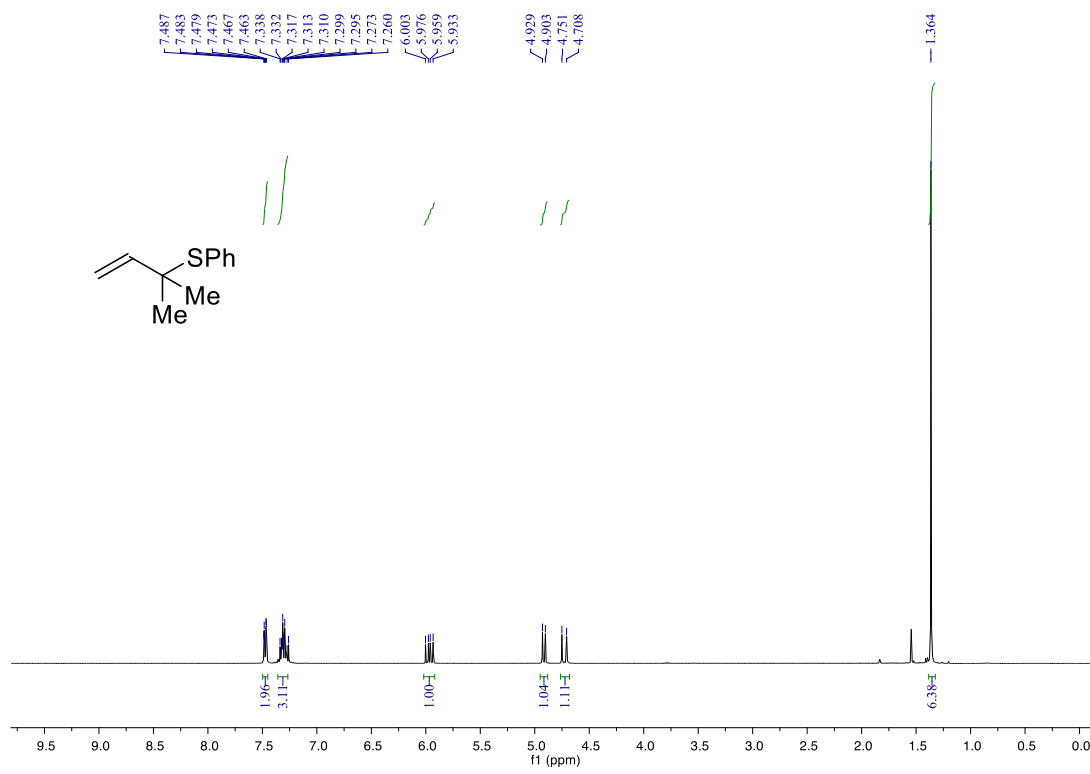
(R)-phenyl(2-phenylbut-3-en-2-yl)sulfane (3fa)



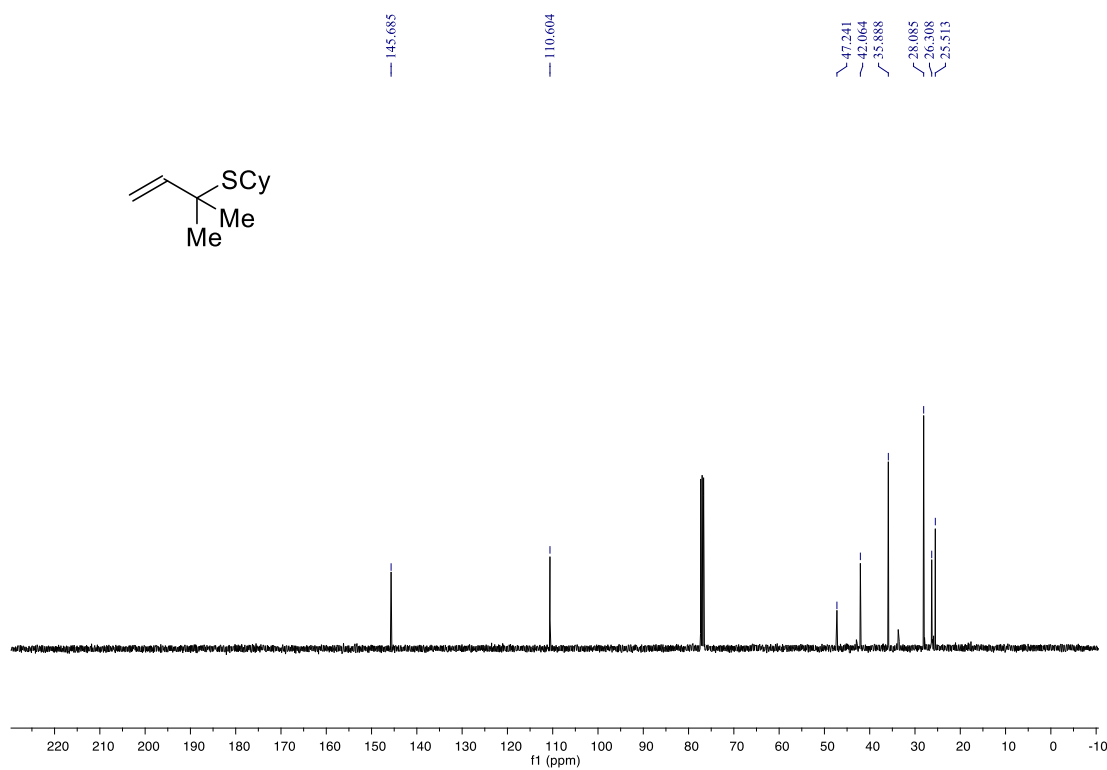
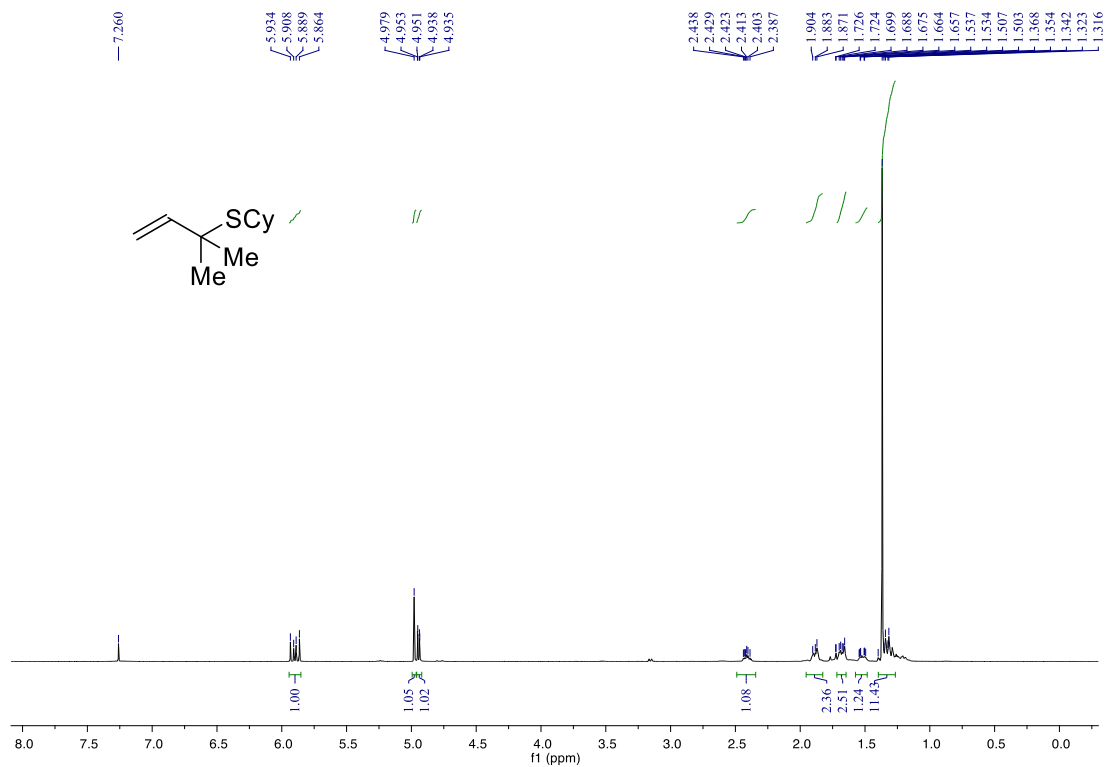
(R)-phenyl(2-(p-tolyl)but-3-en-2-yl)sulfane (3ga)



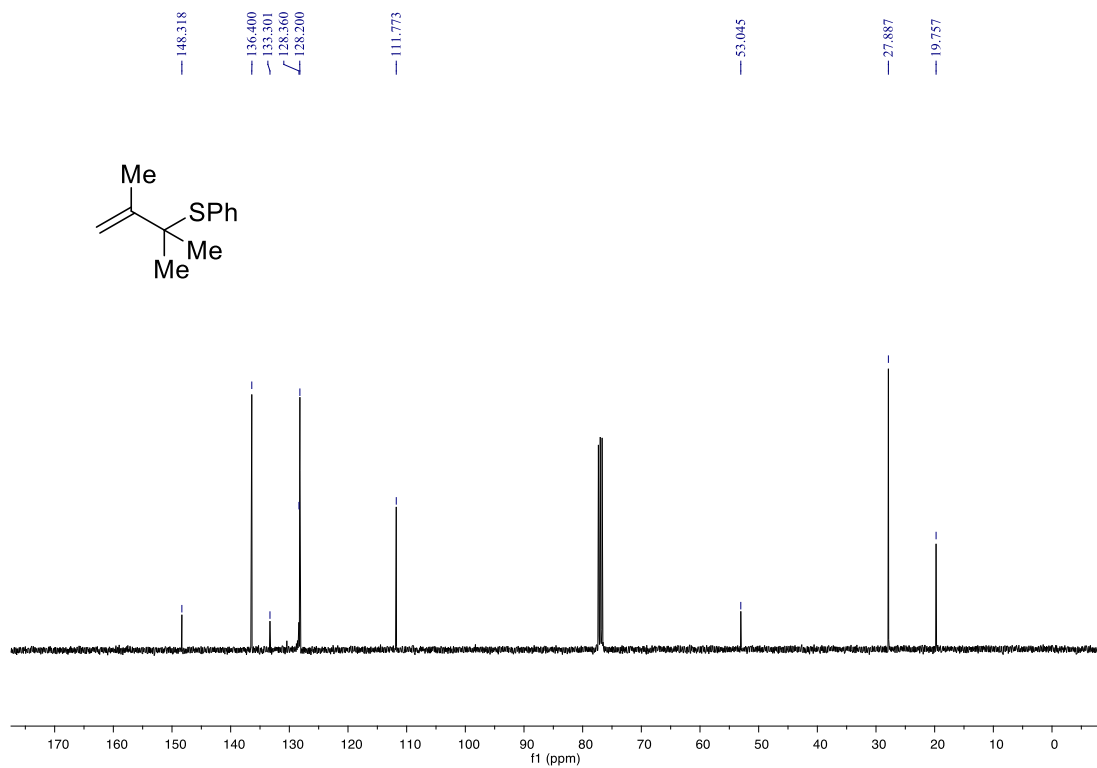
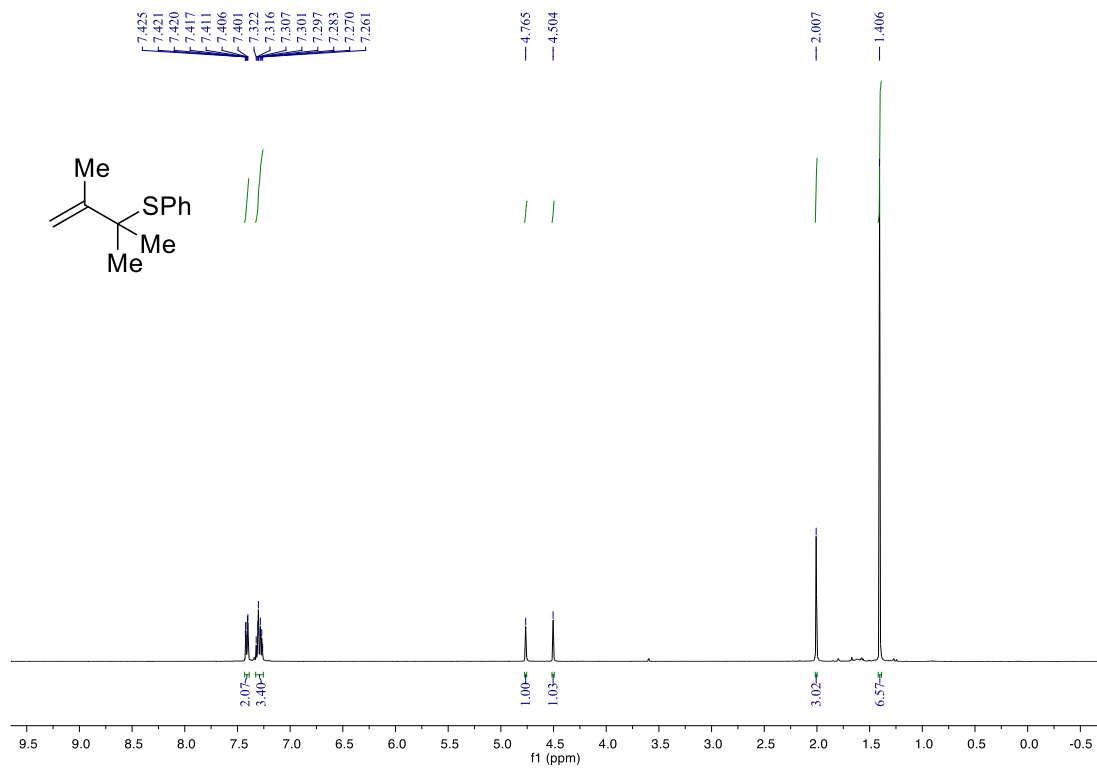
(2-methylbut-3-en-2-yl)(phenyl)sulfane (3ha)



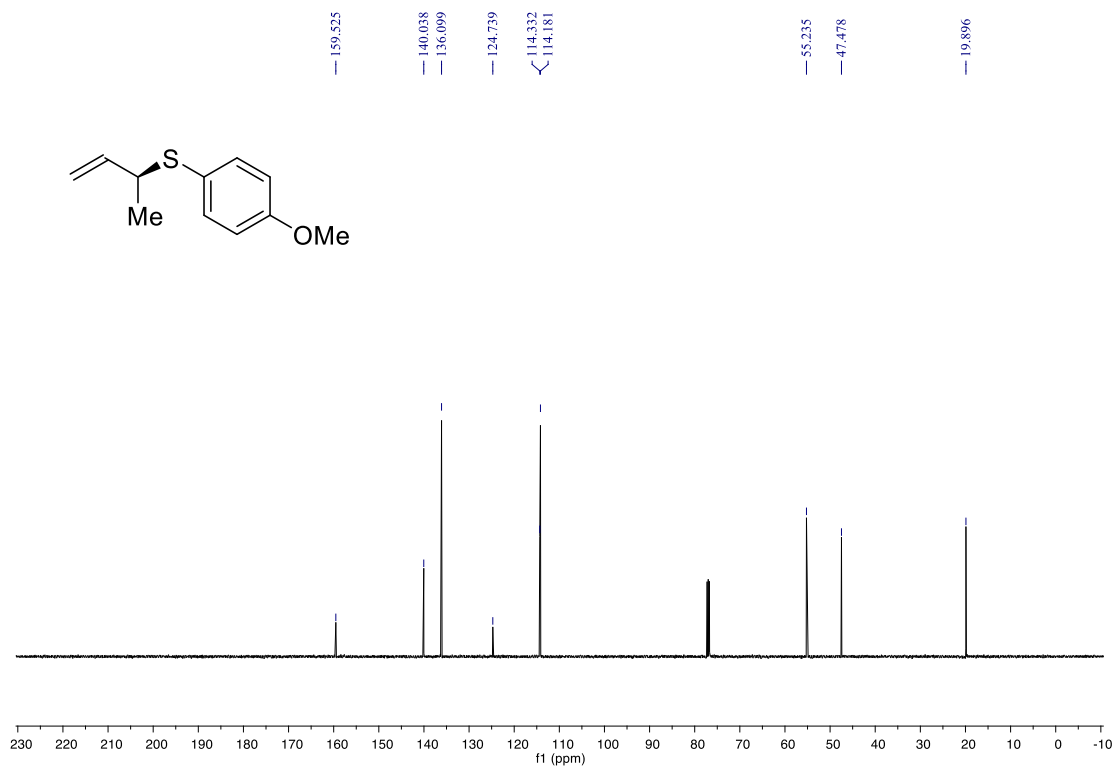
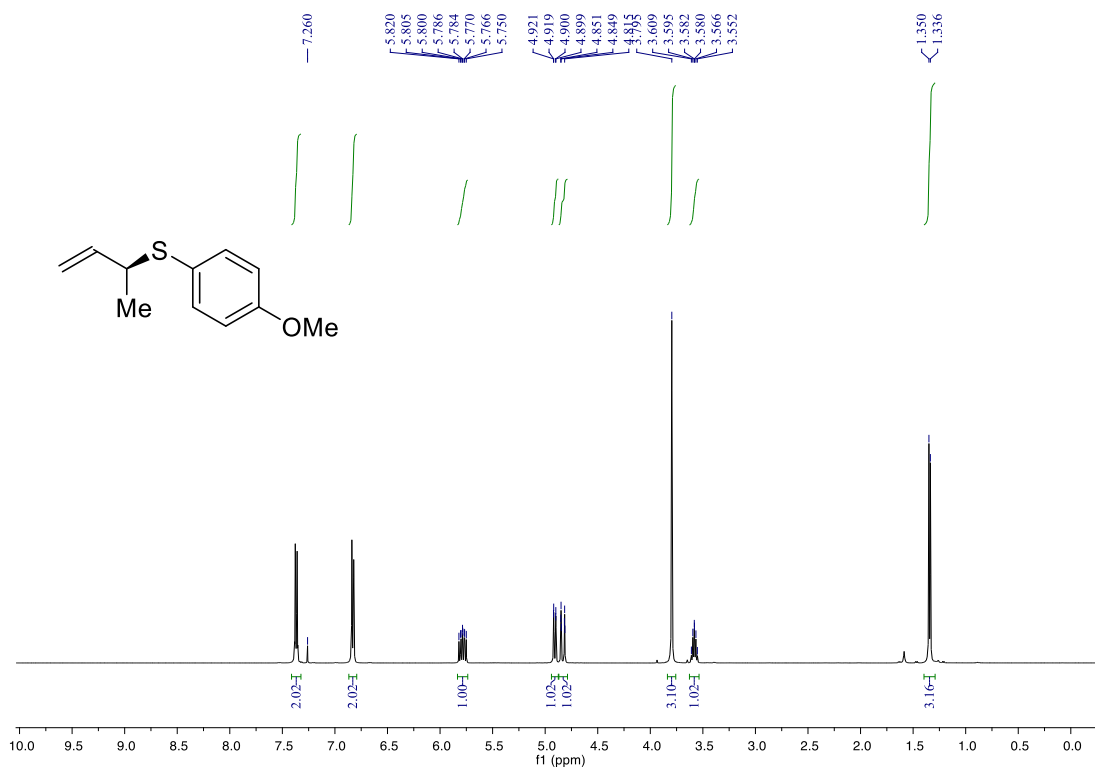
cyclohexyl(2-methylbut-3-en-2-yl)sulfane (3ht)



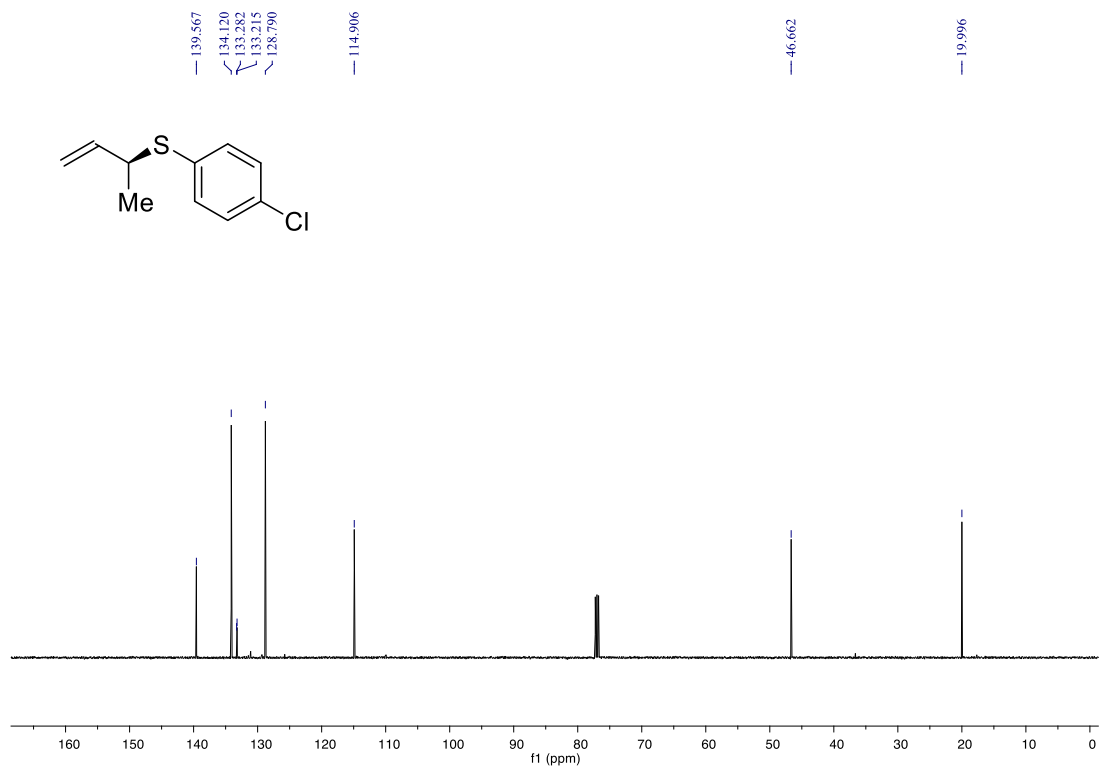
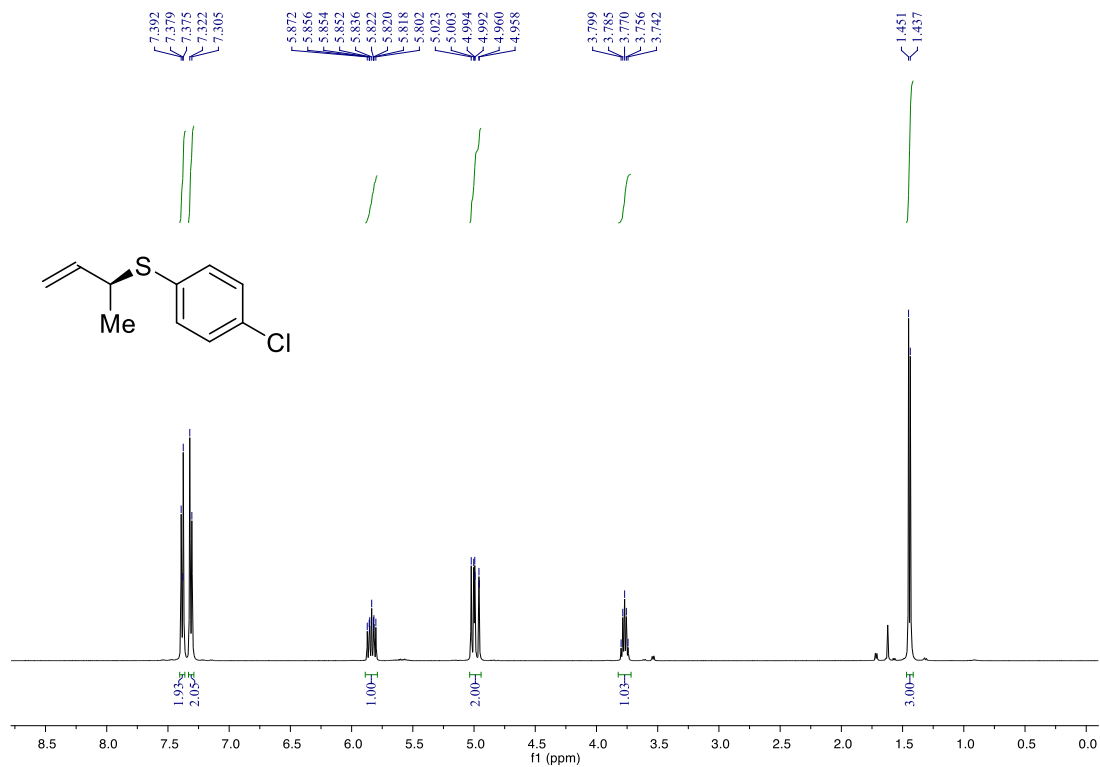
(2,3-dimethylbut-3-en-2-yl)(phenyl)sulfane (3ia)



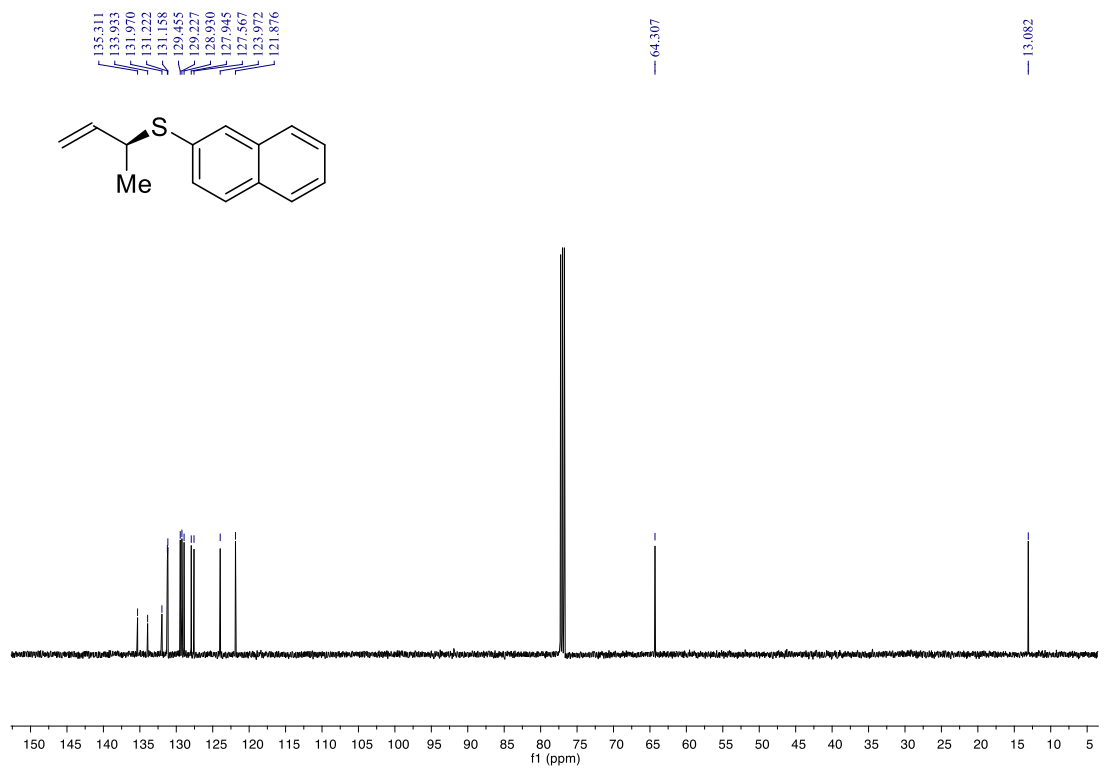
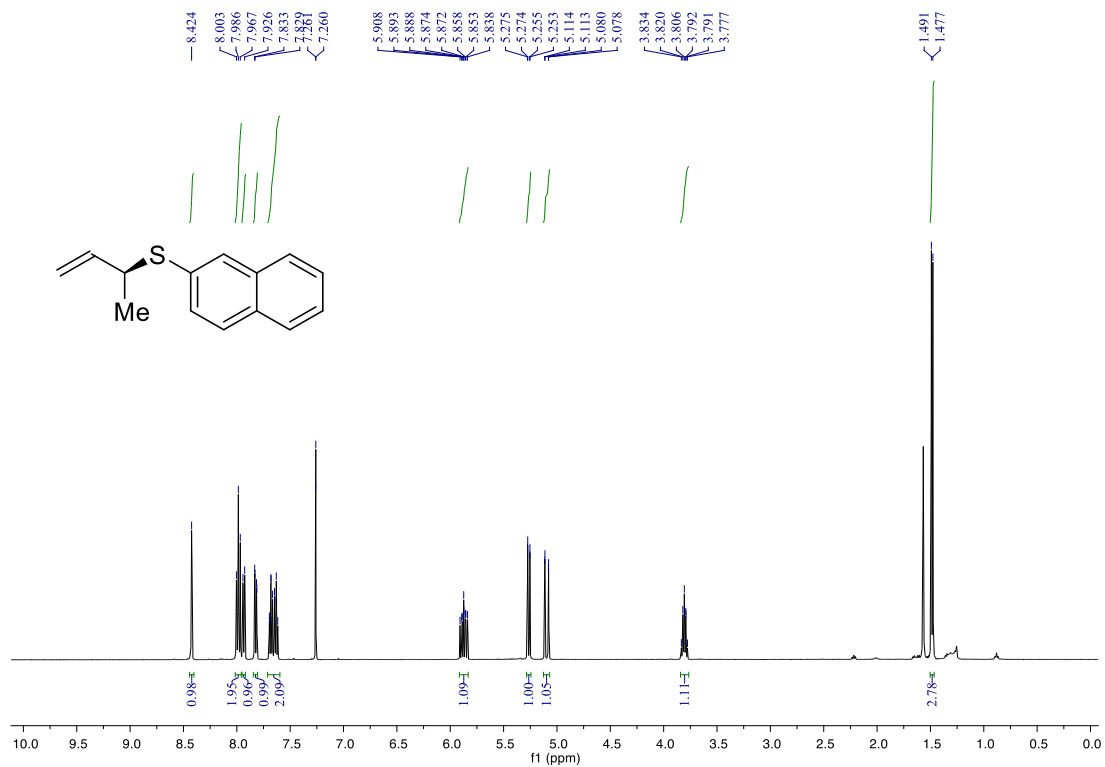
(S)-but-3-en-2-yl(4-methoxyphenyl)sulfane (3jc)



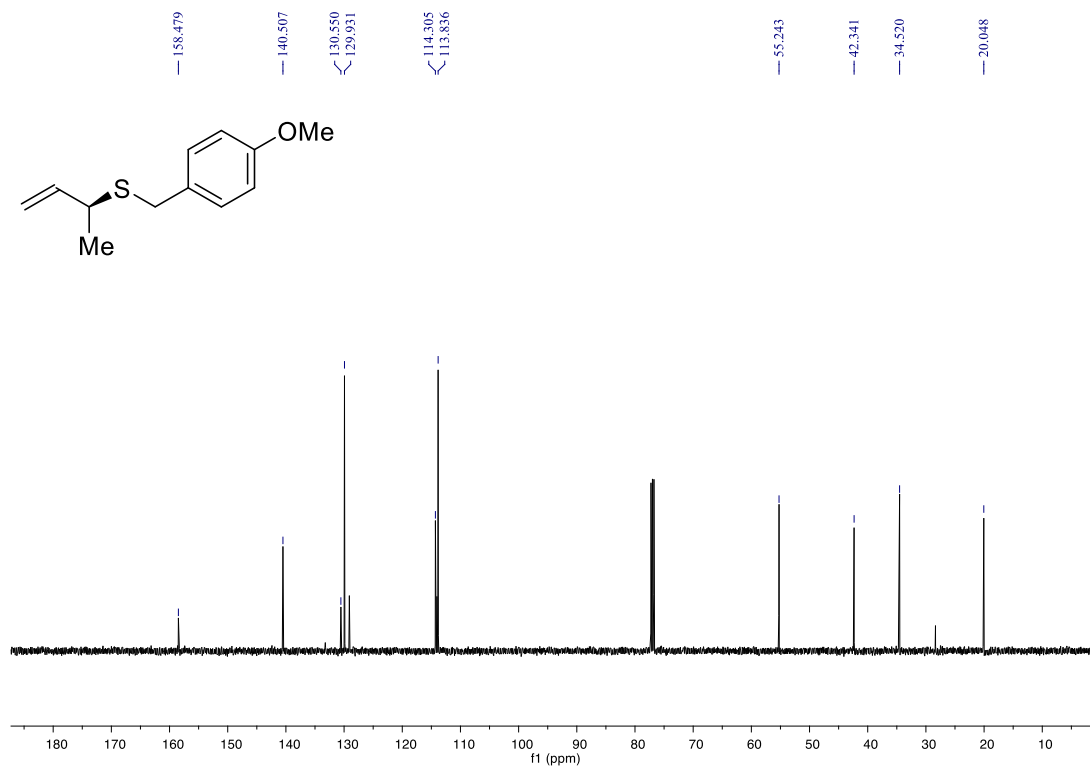
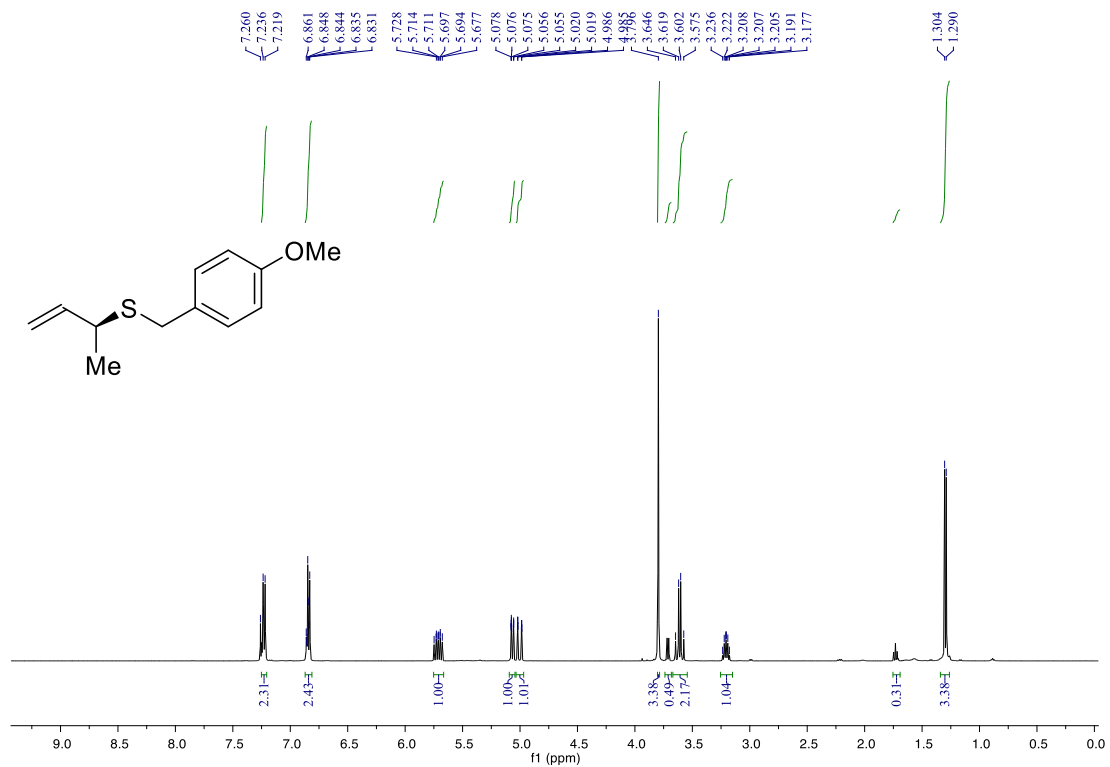
(S)-but-3-en-2-yl(4-chlorophenyl)sulfane (3jg)



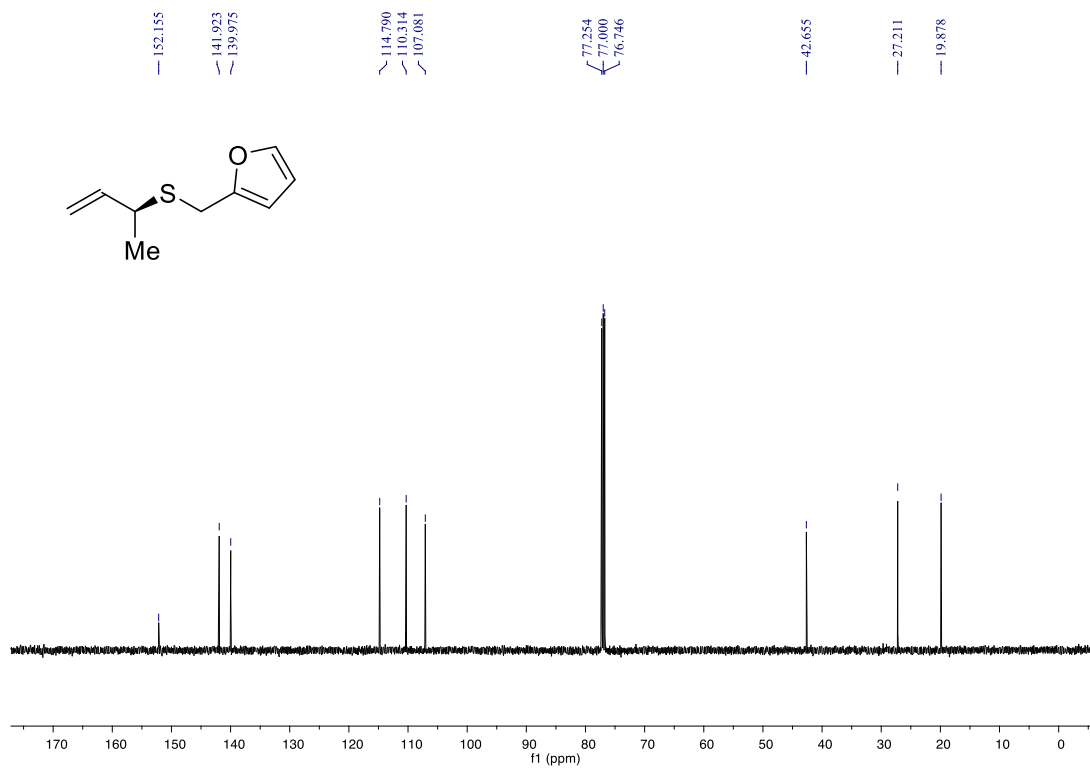
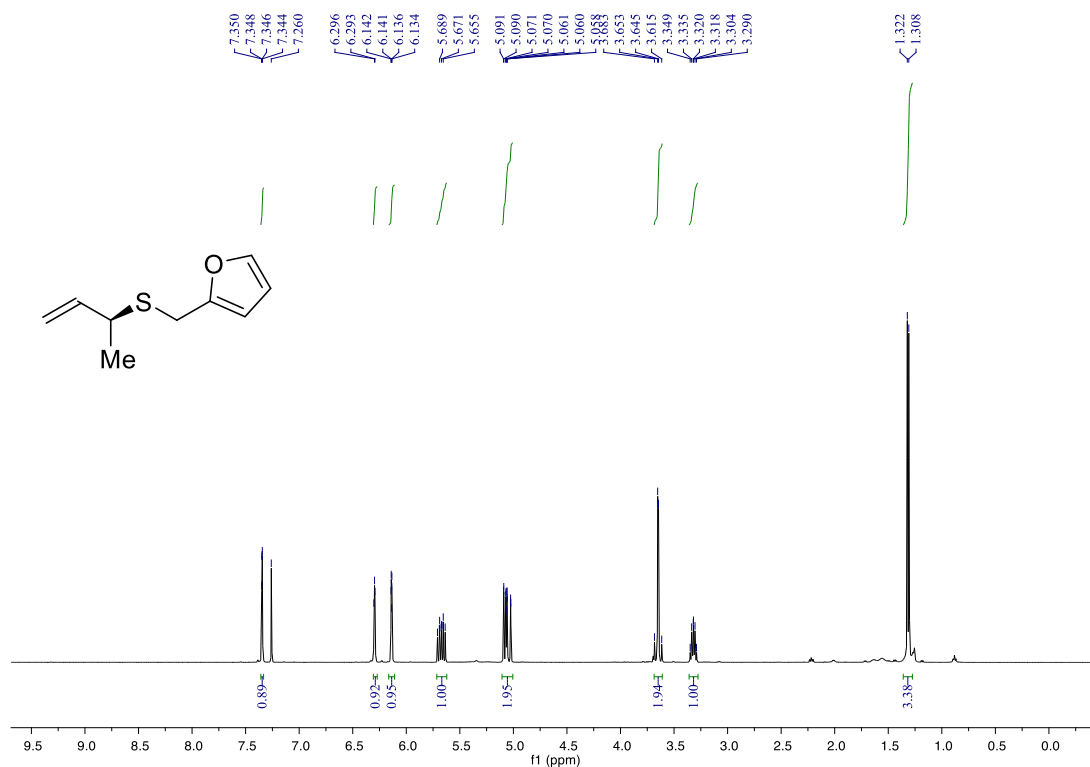
(S)-but-3-en-2-yl(naphthalen-2-yl)sulfane (3ju)



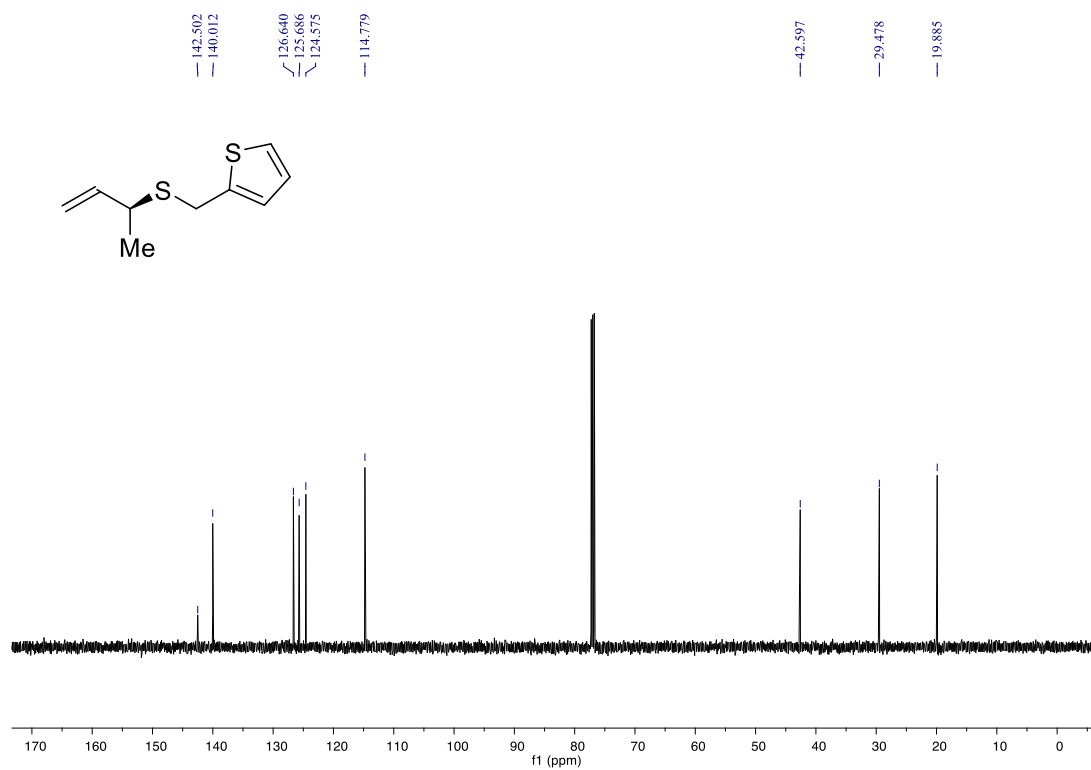
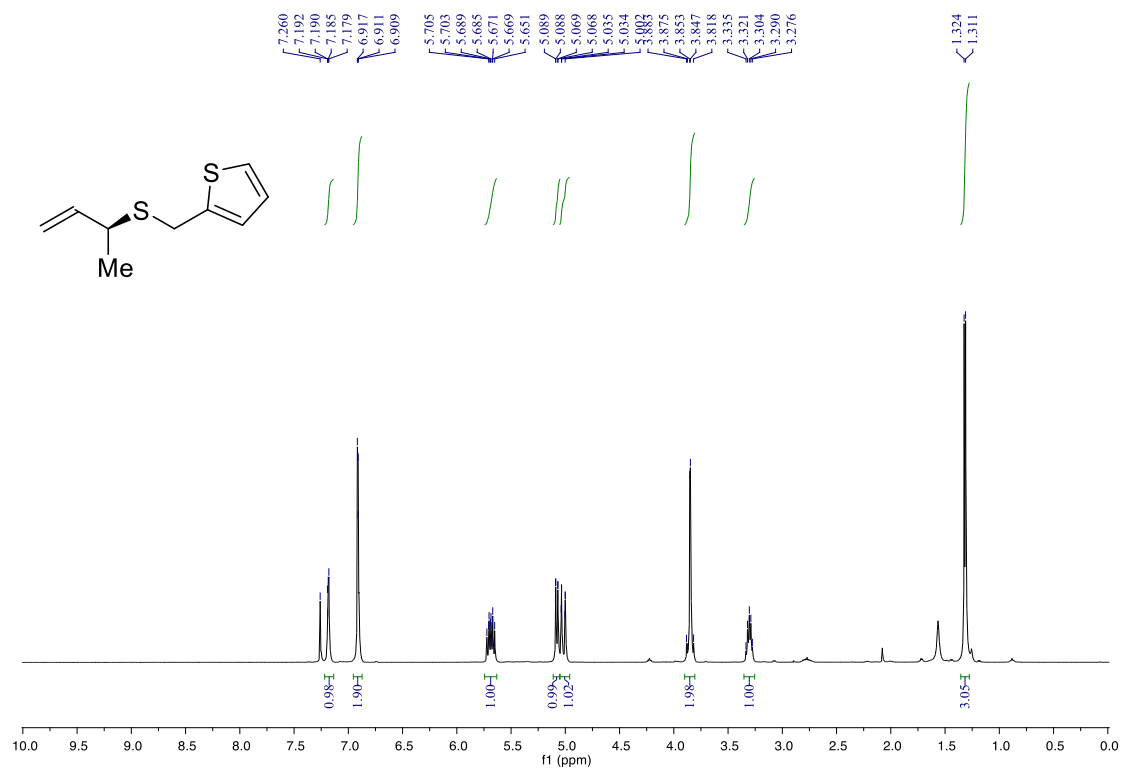
(S)-but-3-en-2-yl(4-methoxybenzyl)sulfane (3jv)



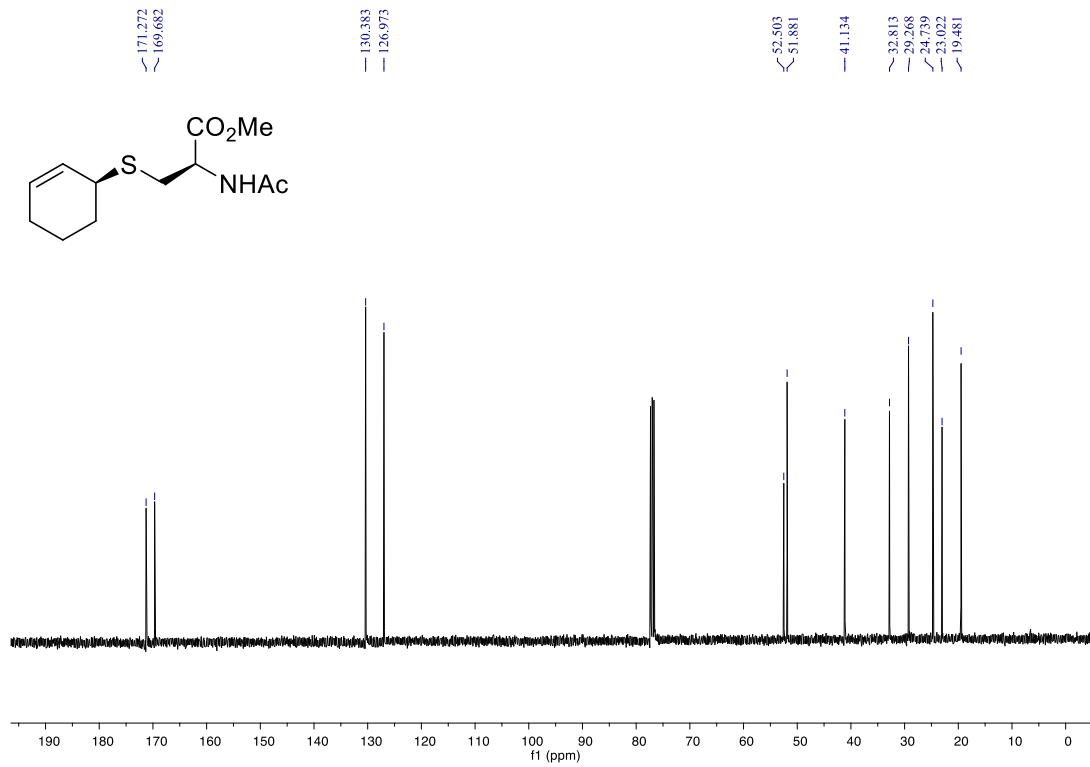
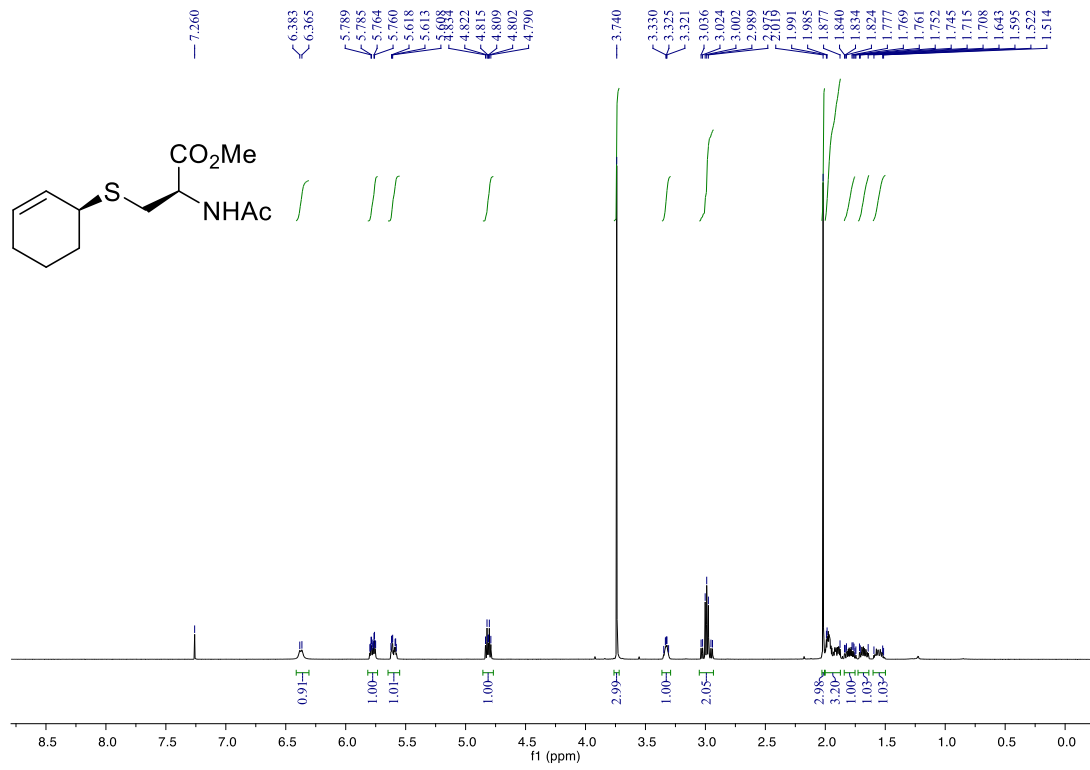
(S)-2-((but-3-en-2-ylthio)methyl)furan (3jw)



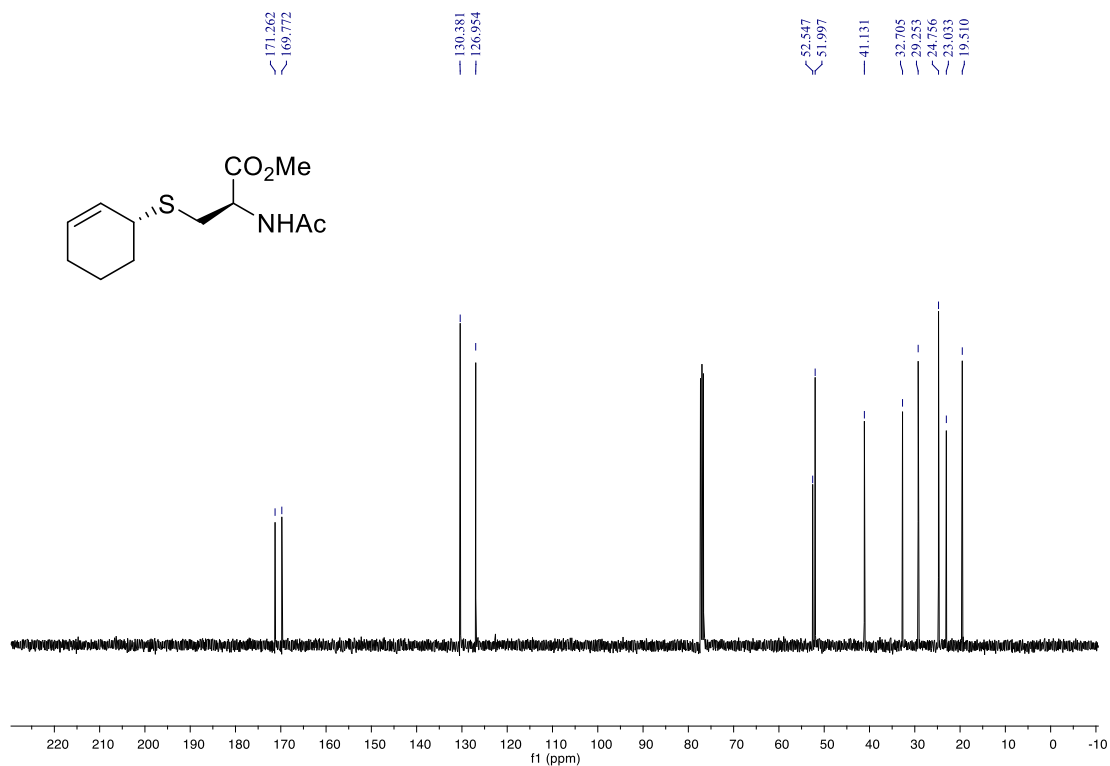
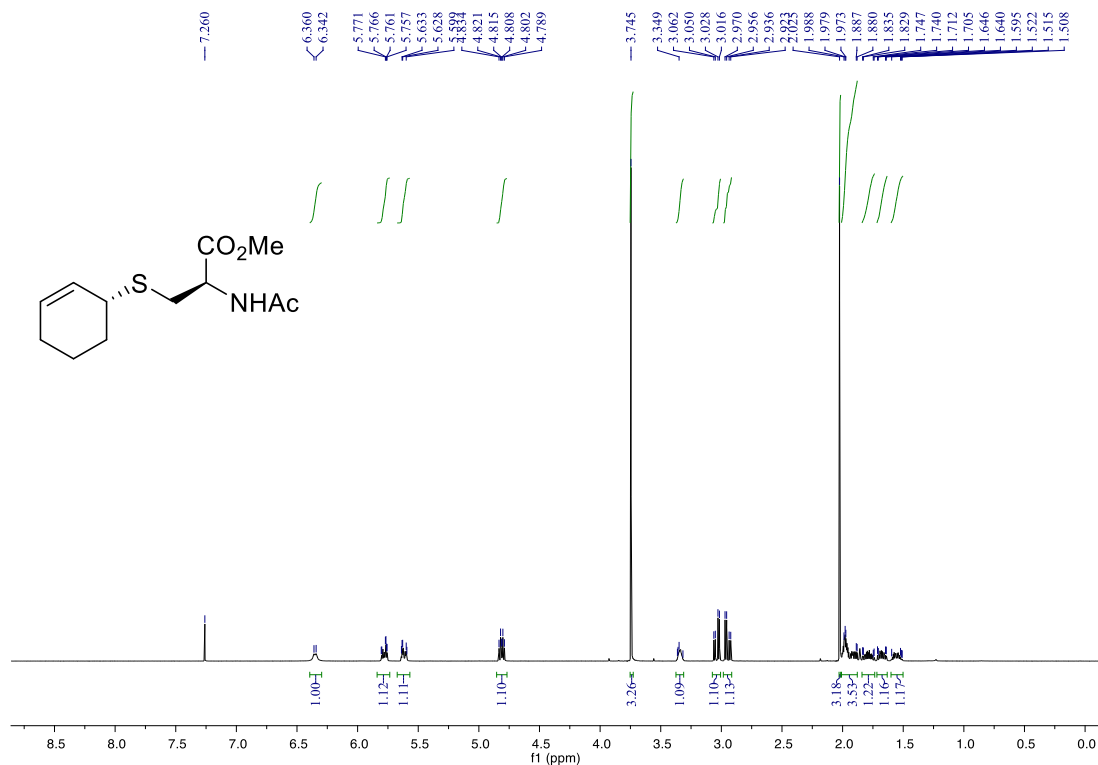
(S)-2-((but-3-en-2-ylthio)methyl)thiophene (3js)



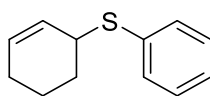
methyl *N*-acetyl-*S*-((*S*)-cyclohex-2-en-1-yl)-L-cysteinate (3ax)



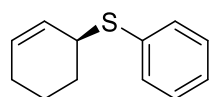
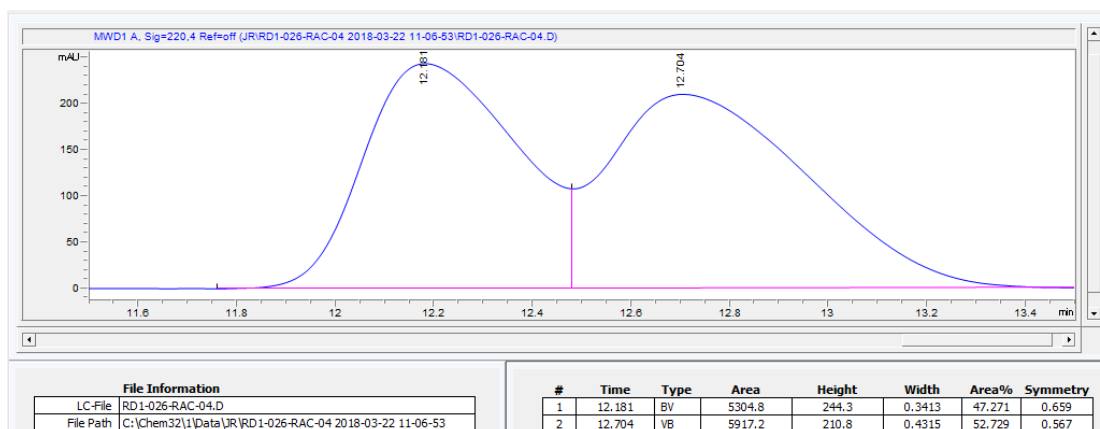
methyl *N*-acetyl-*S*-((*R*)-cyclohex-2-en-1-yl)-L-cysteinate (3ax')



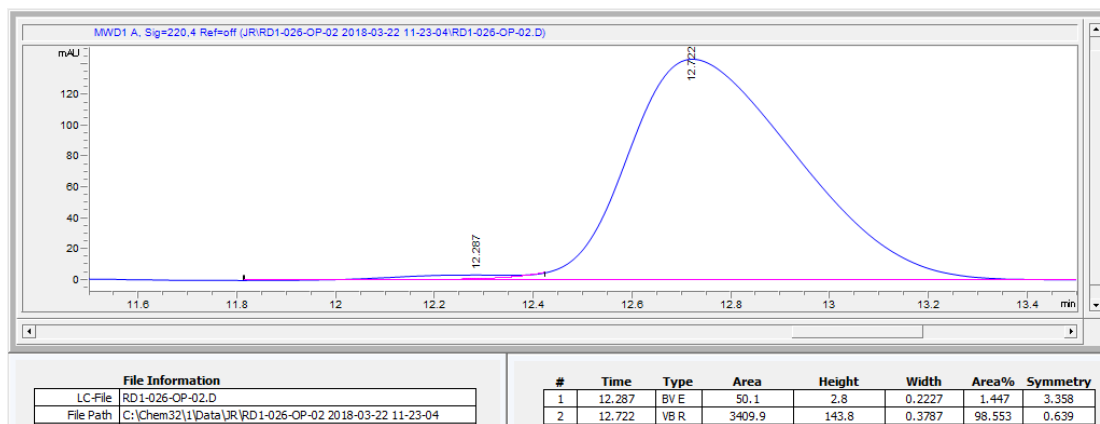
7. SFC spectra

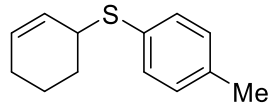


rac-3aa

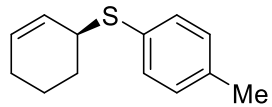
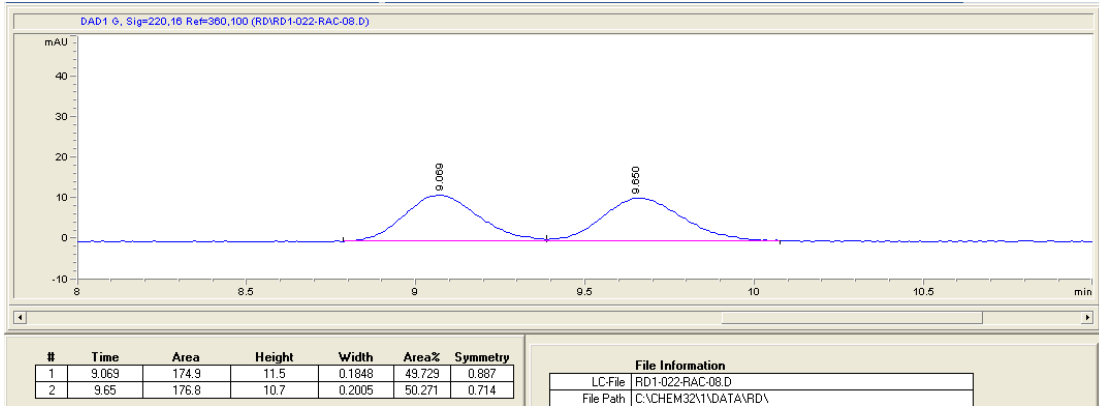


3aa

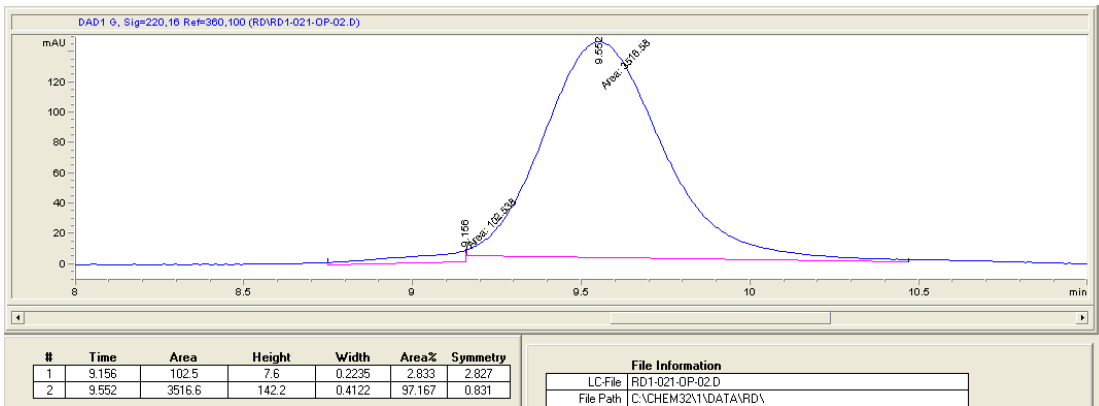


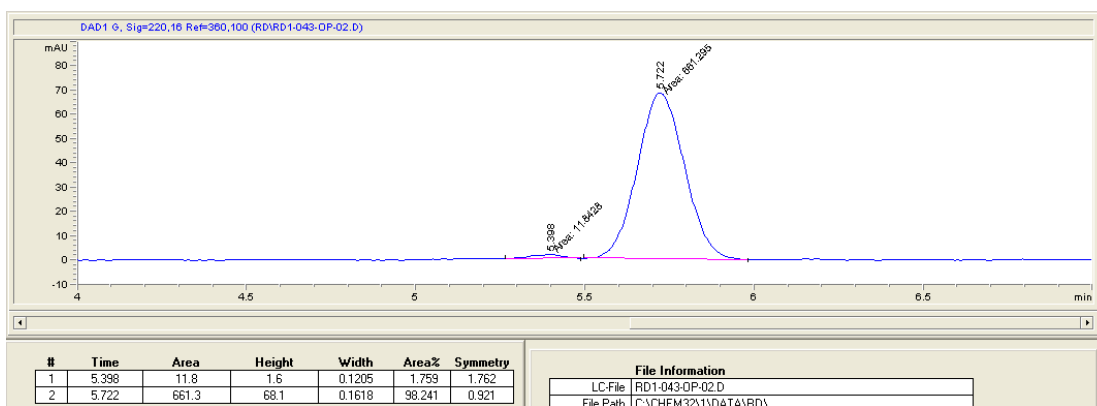
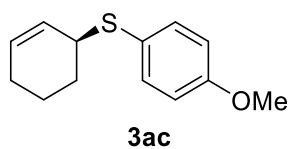
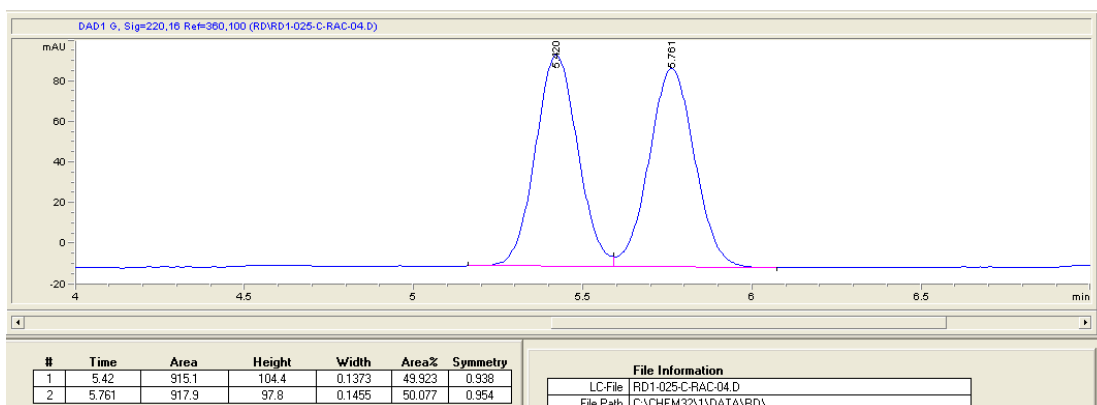
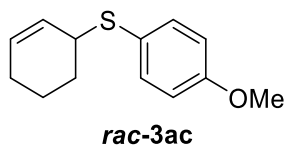


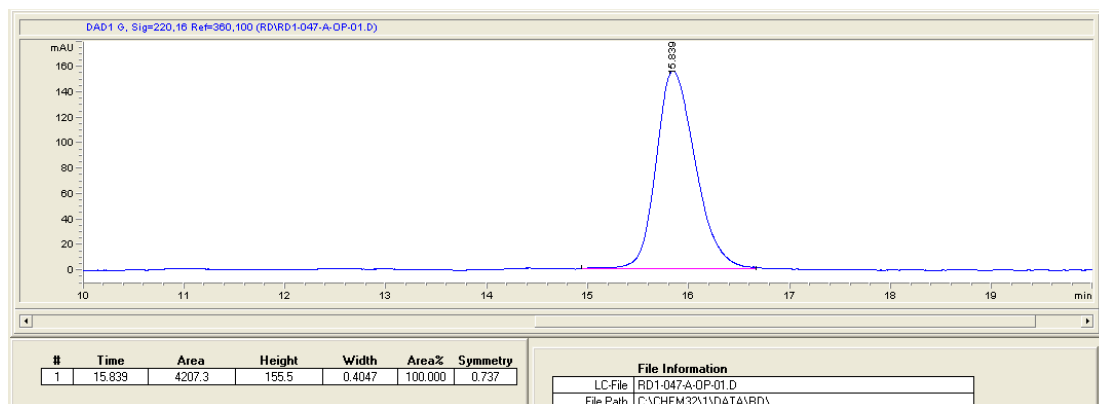
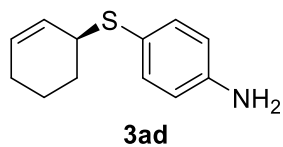
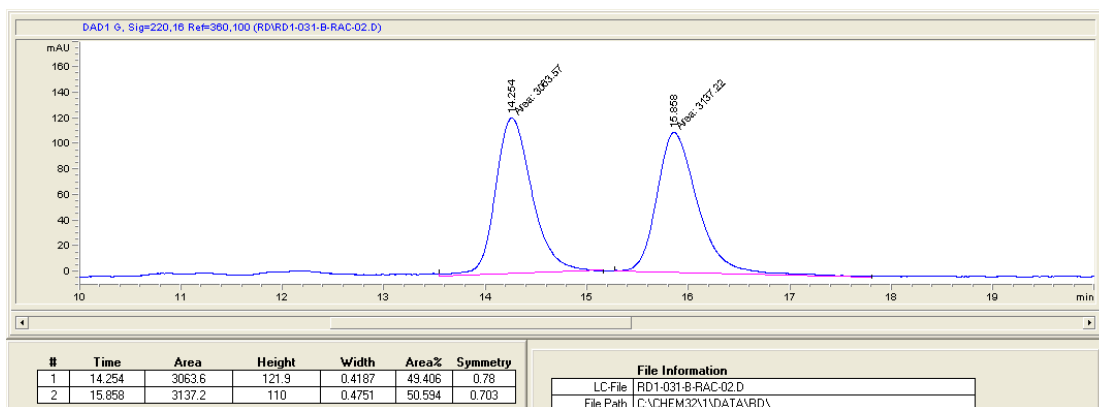
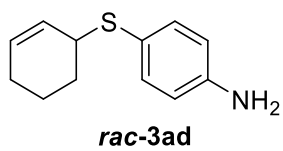
rac-3ab

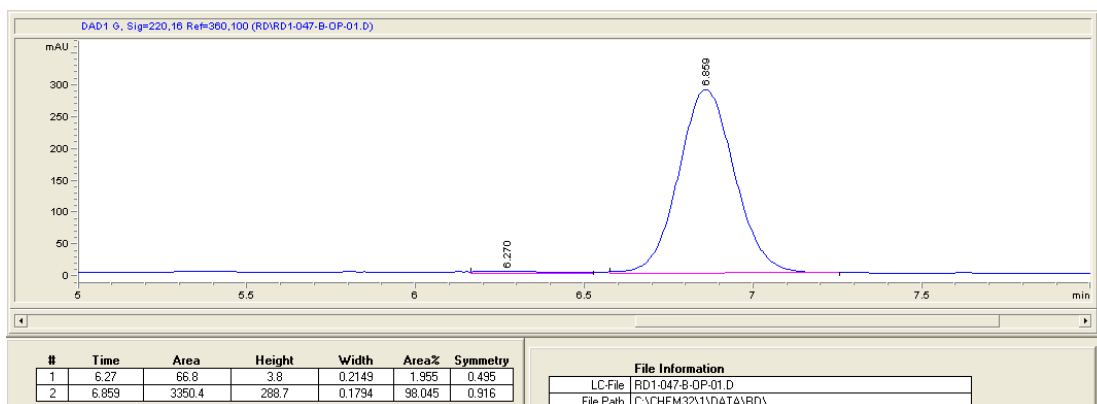
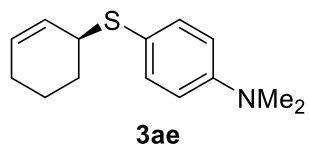
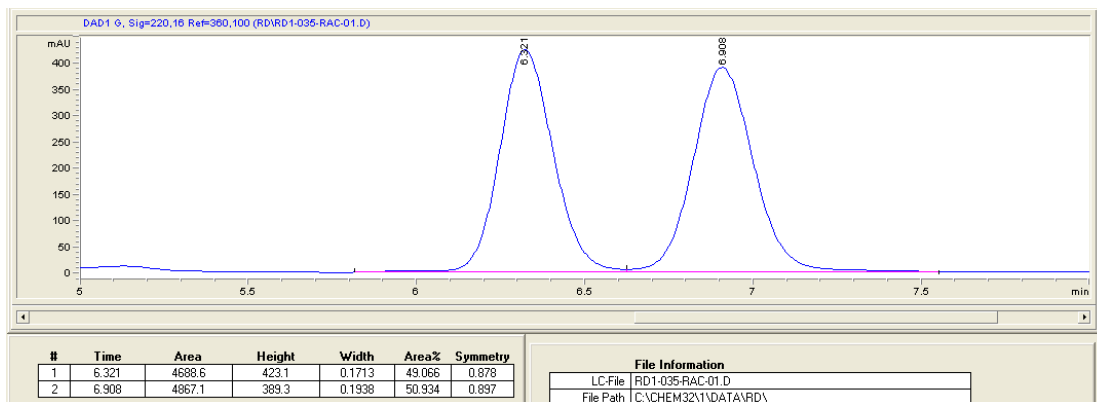
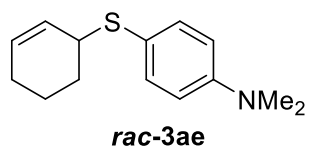


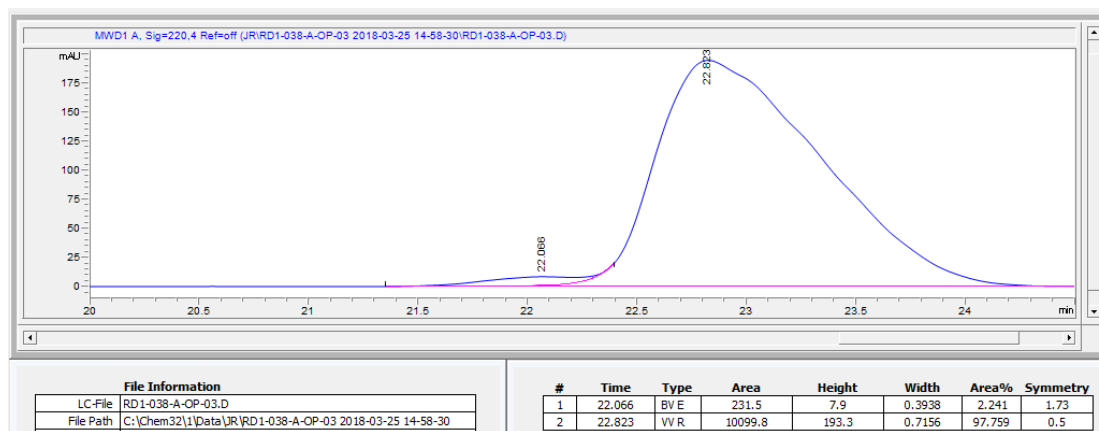
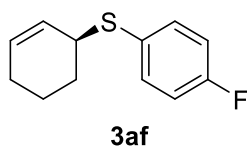
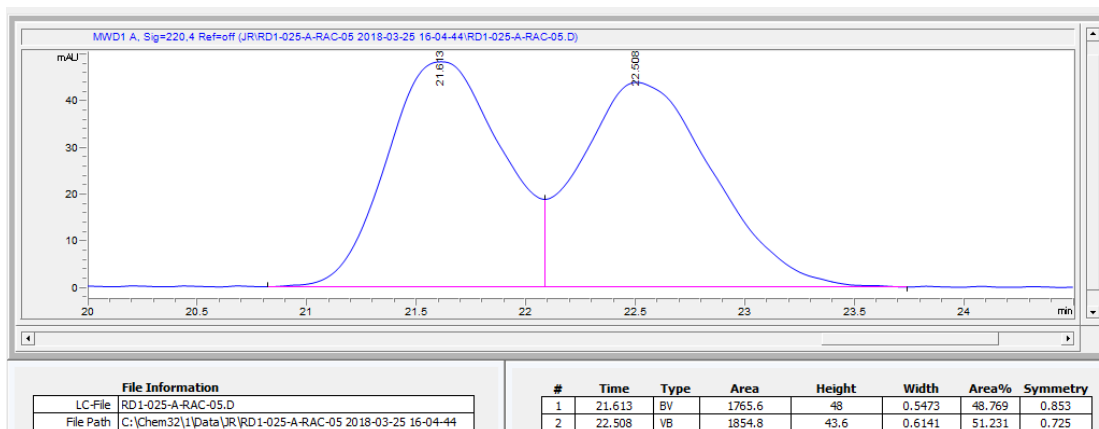
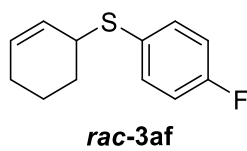
3ab

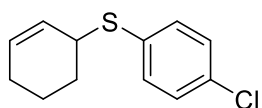




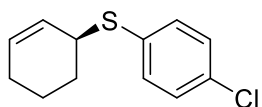
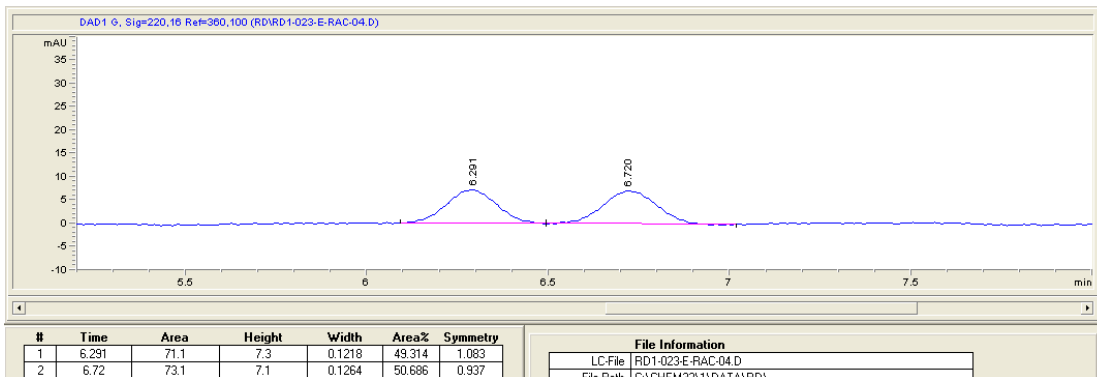




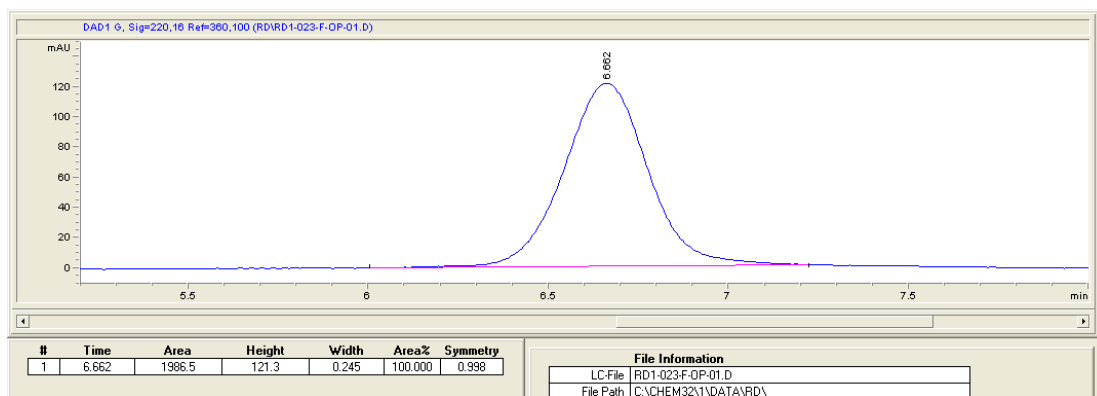


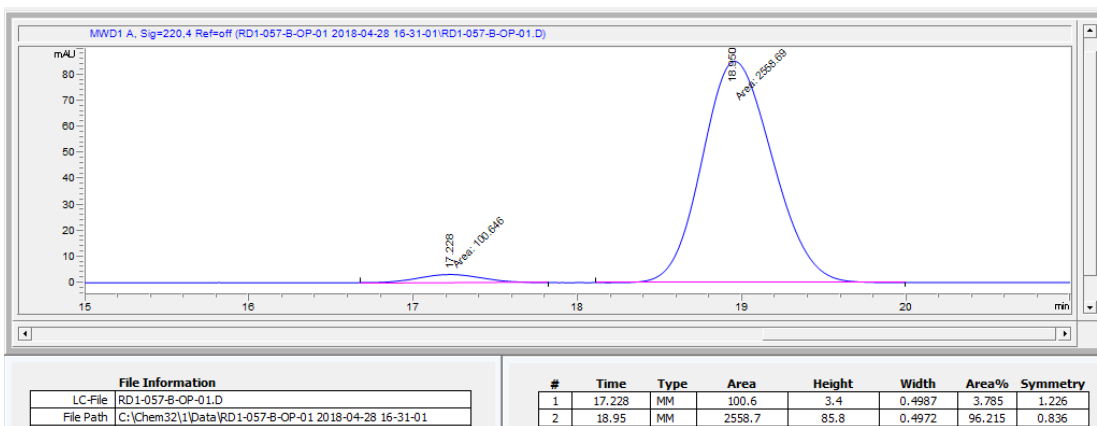
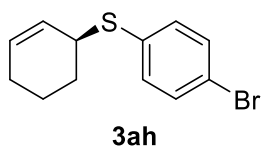
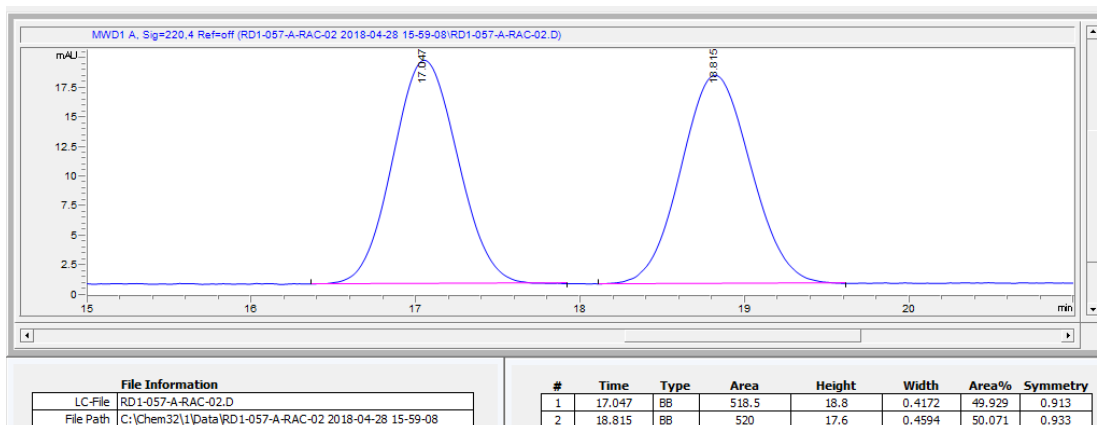
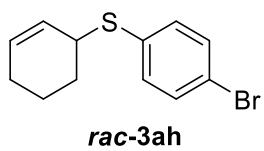


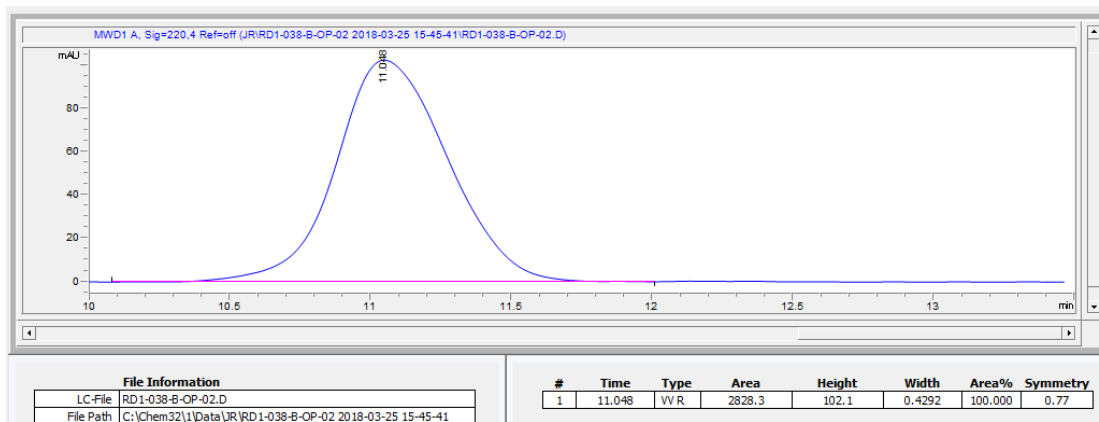
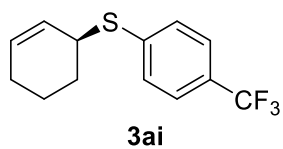
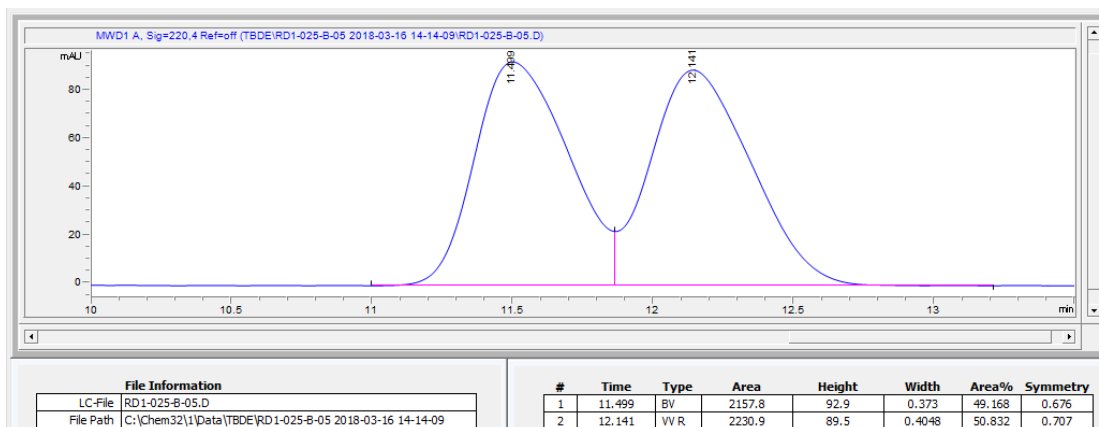
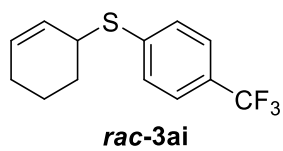
rac-3ag

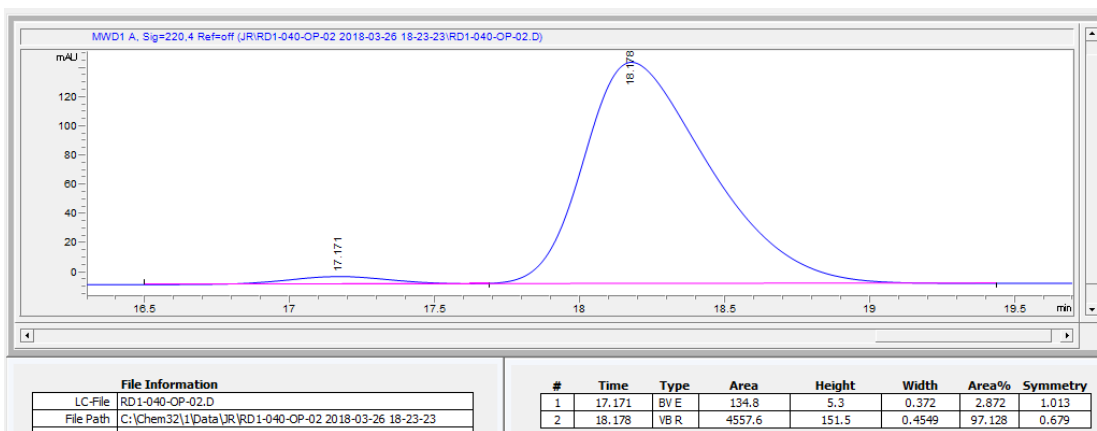
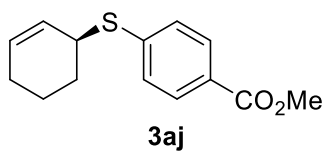
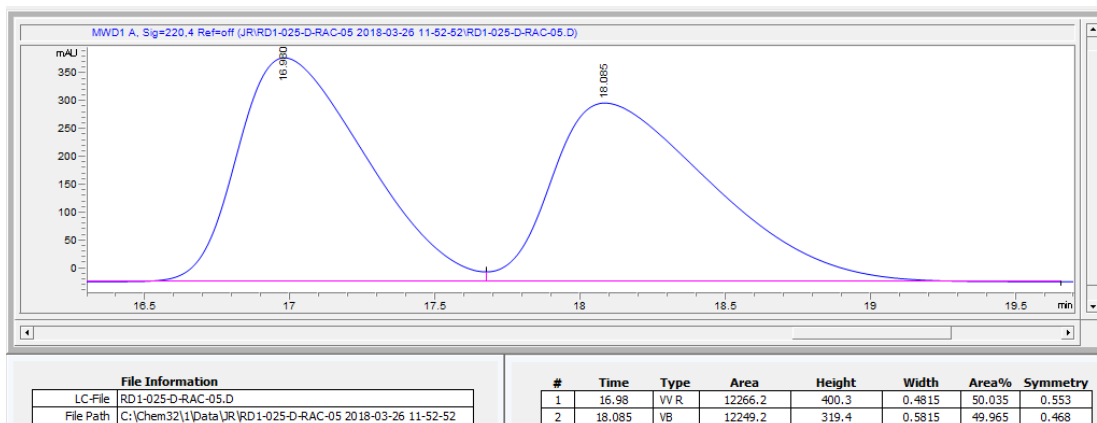
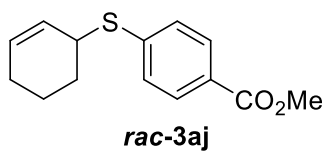


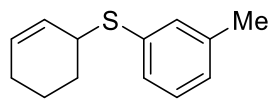
3ag



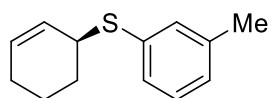
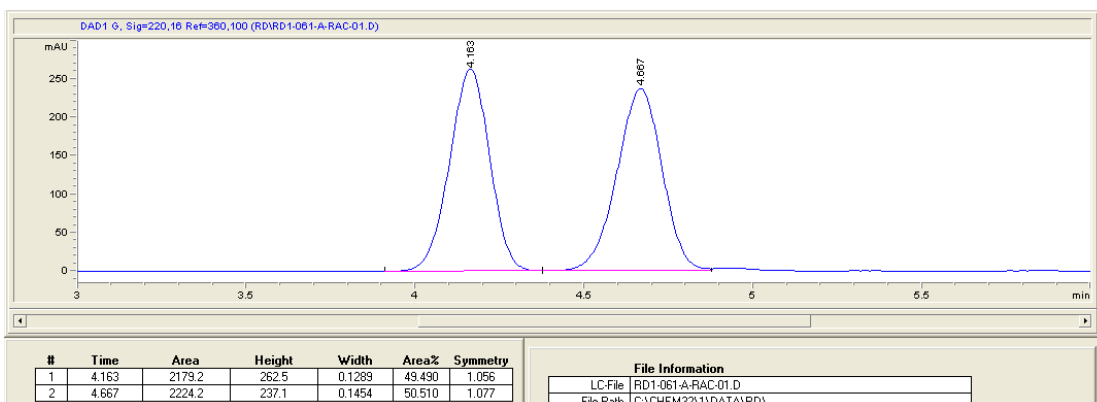




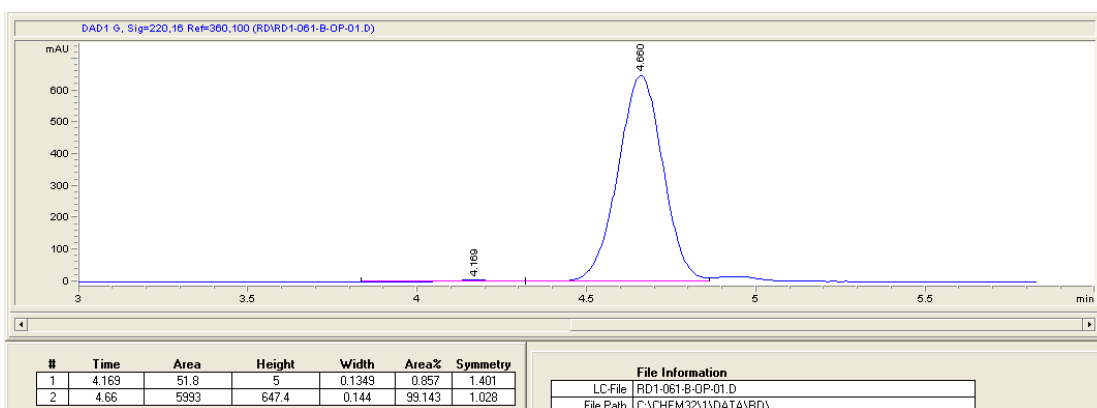


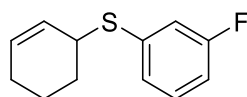


rac-3ak

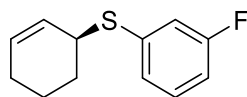
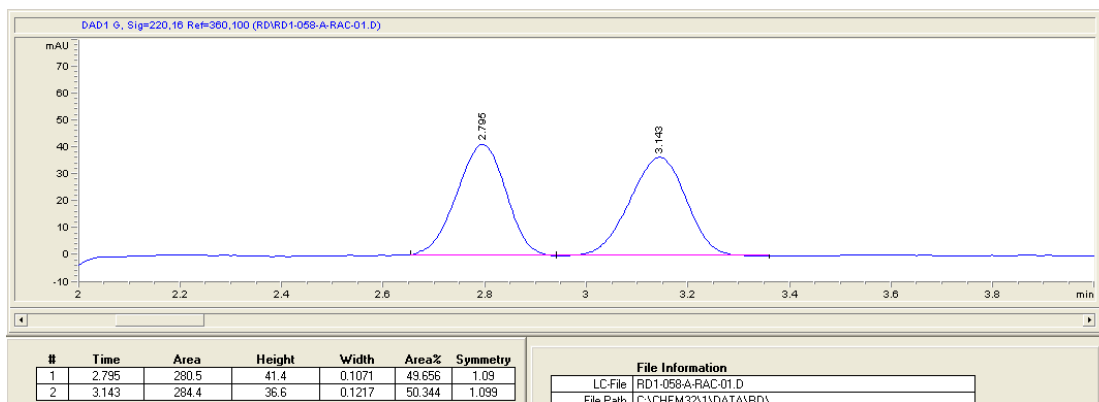


3ak

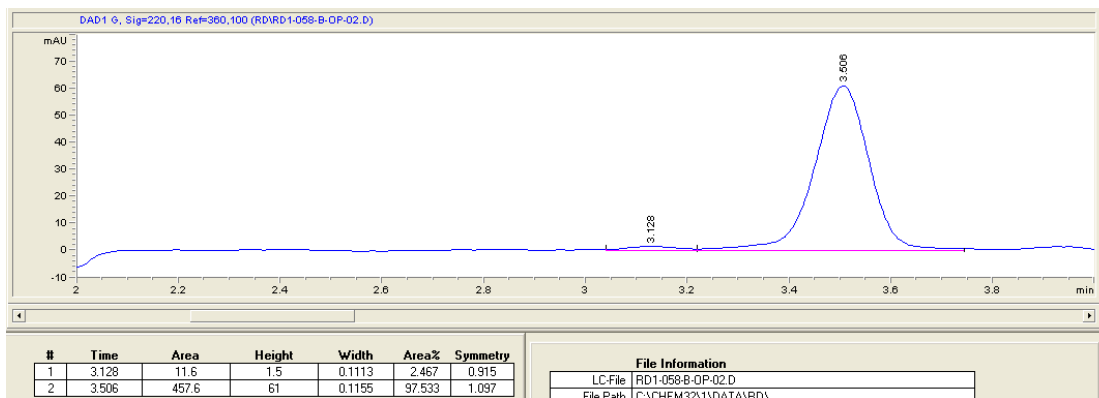


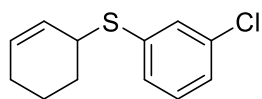


rac-3aI

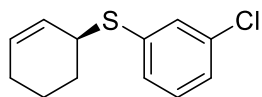
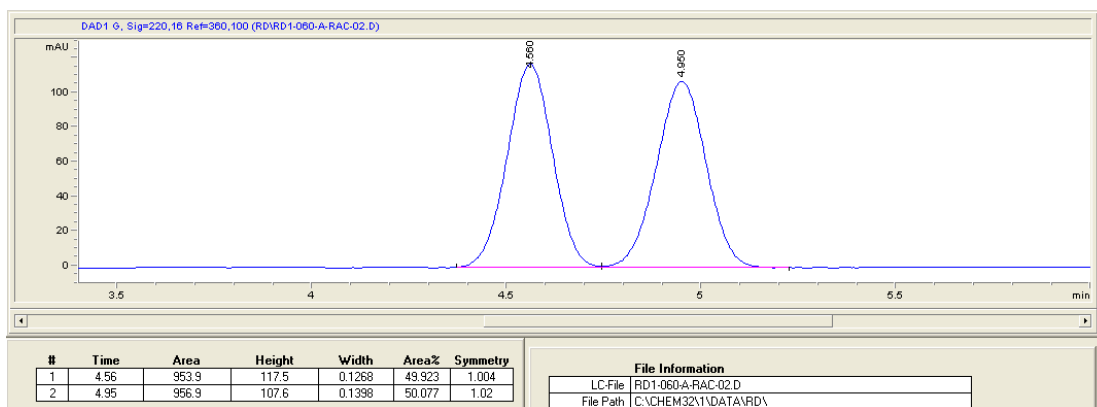


3aI

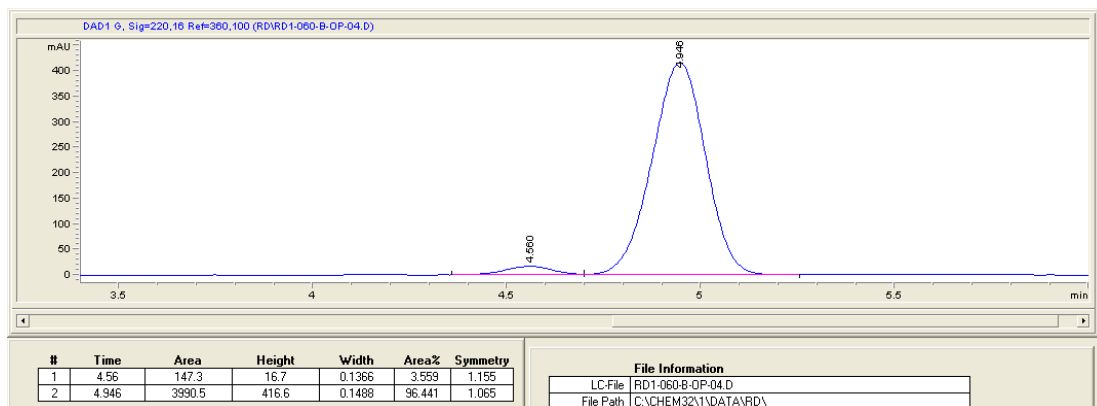


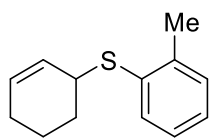


rac-3am

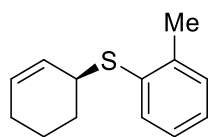
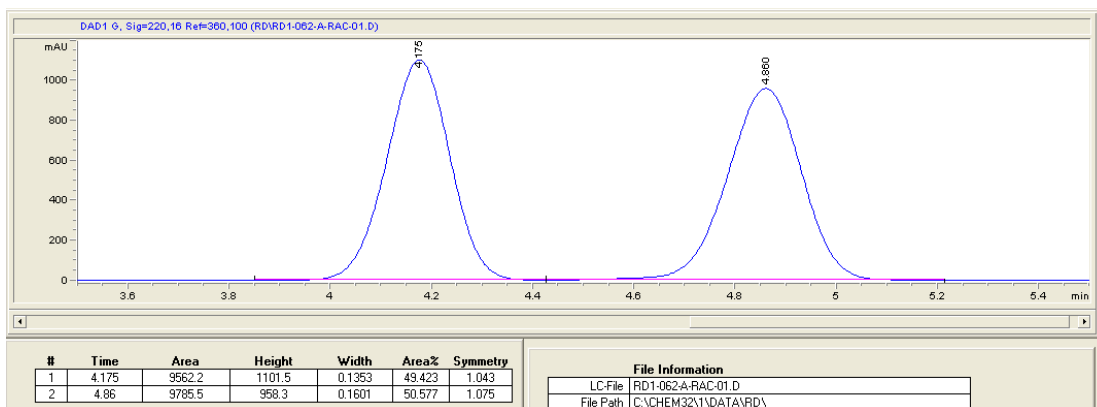


3am

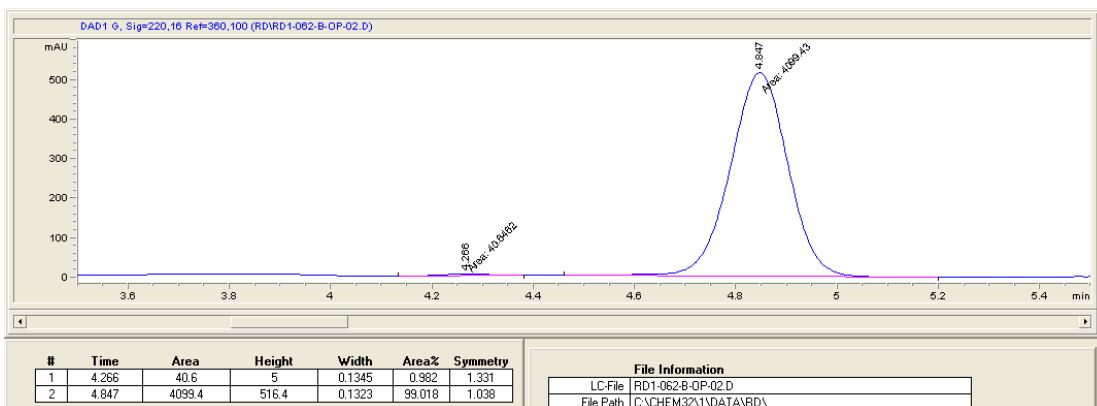


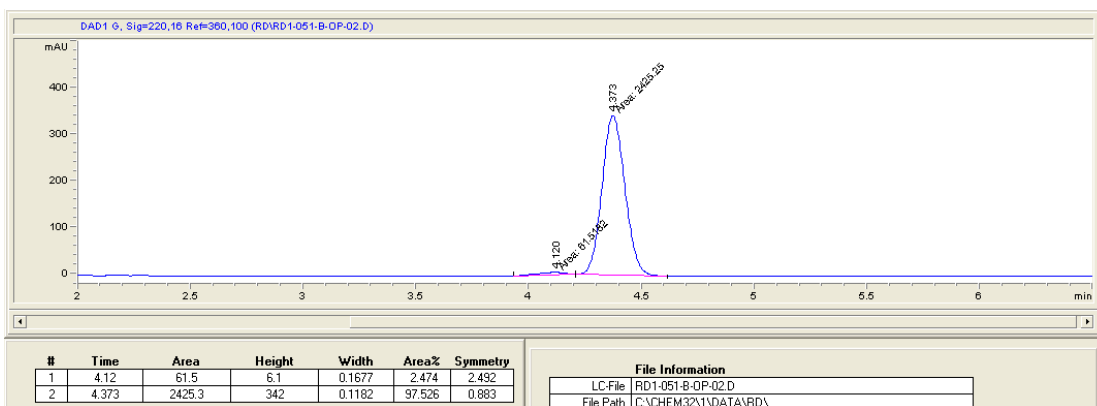
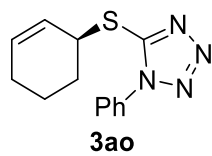
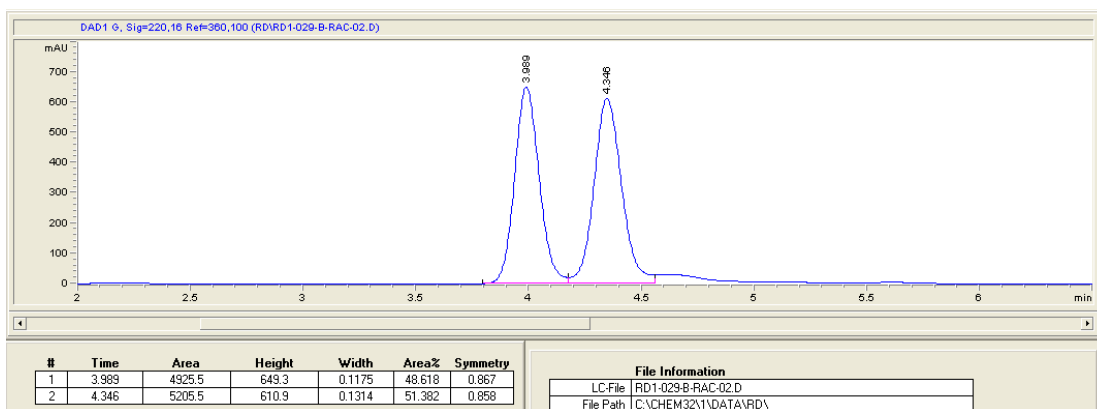
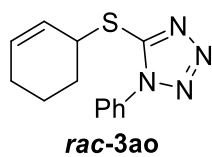


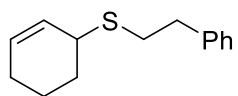
rac-3an



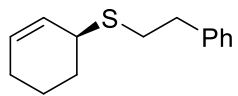
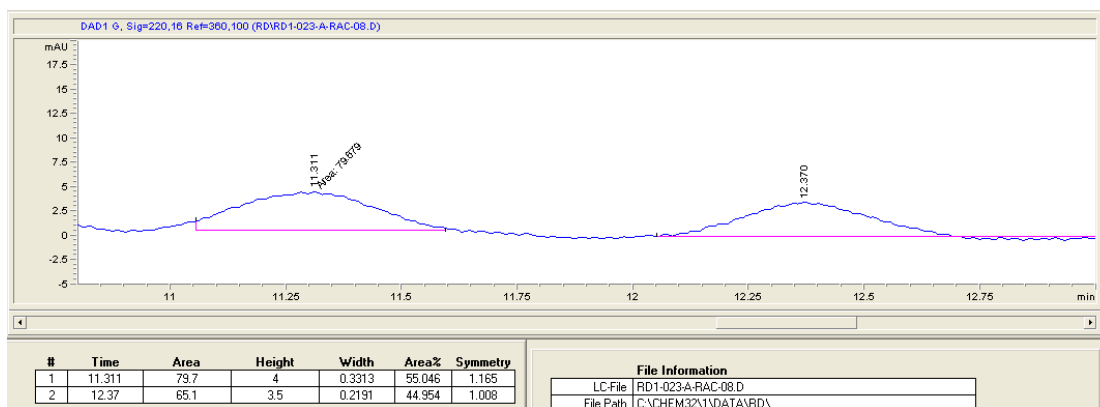
3an



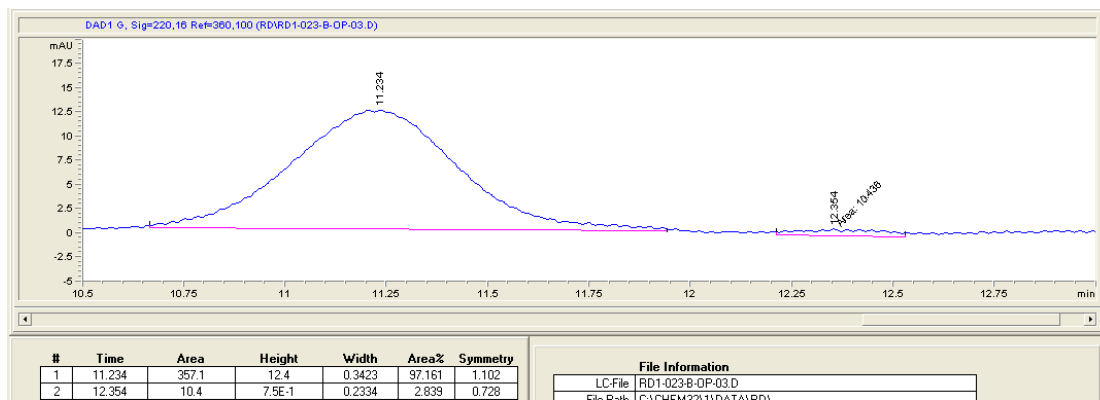


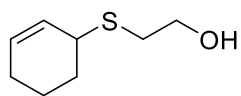


rac-3ap

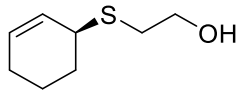
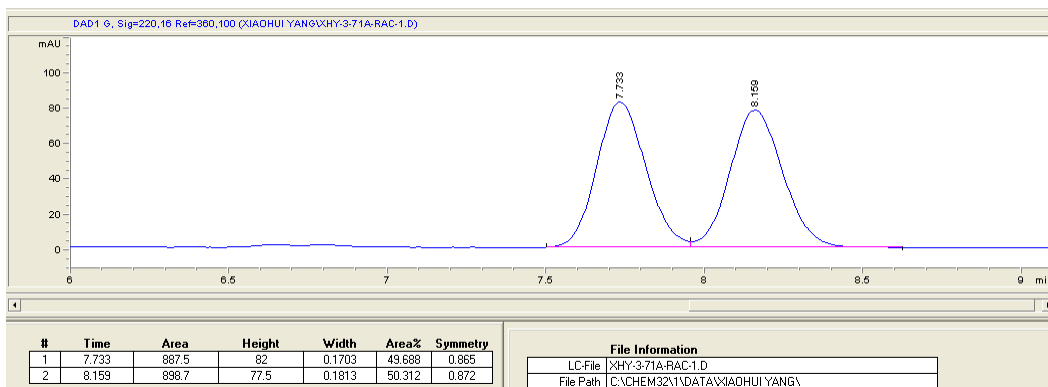


3ap

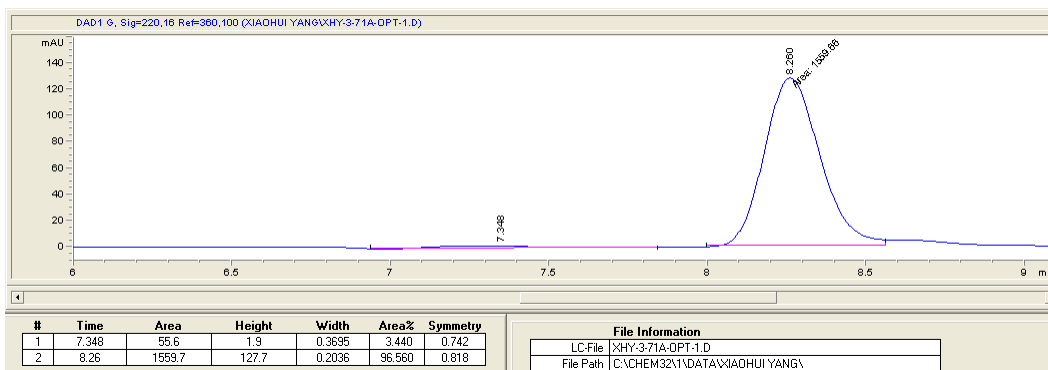


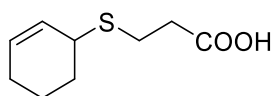


rac-3aq

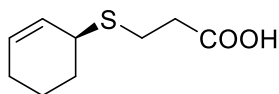
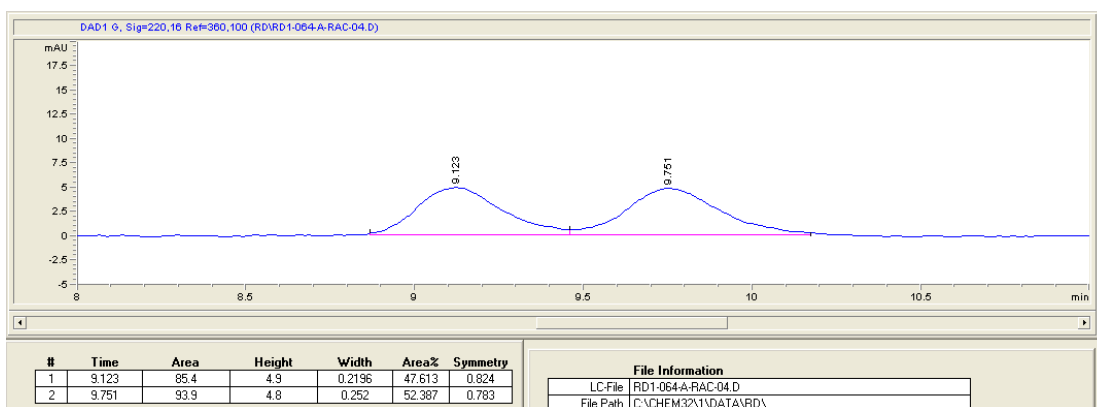


3aq

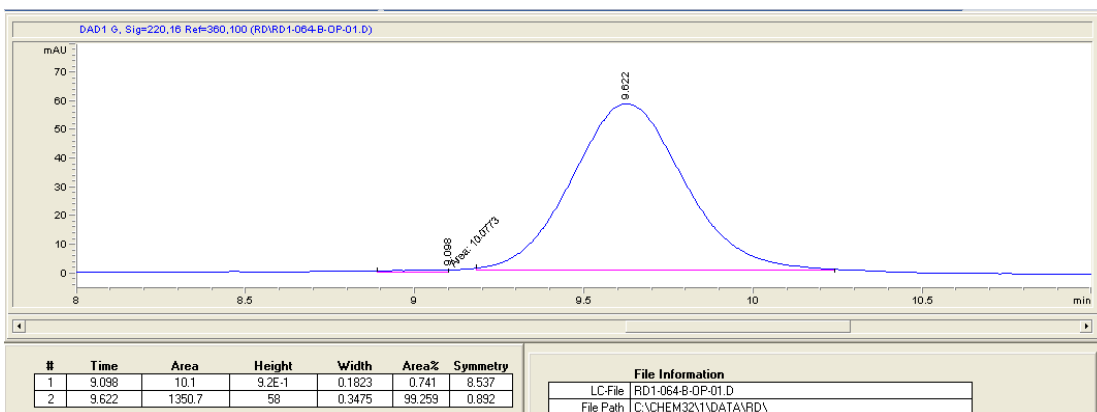


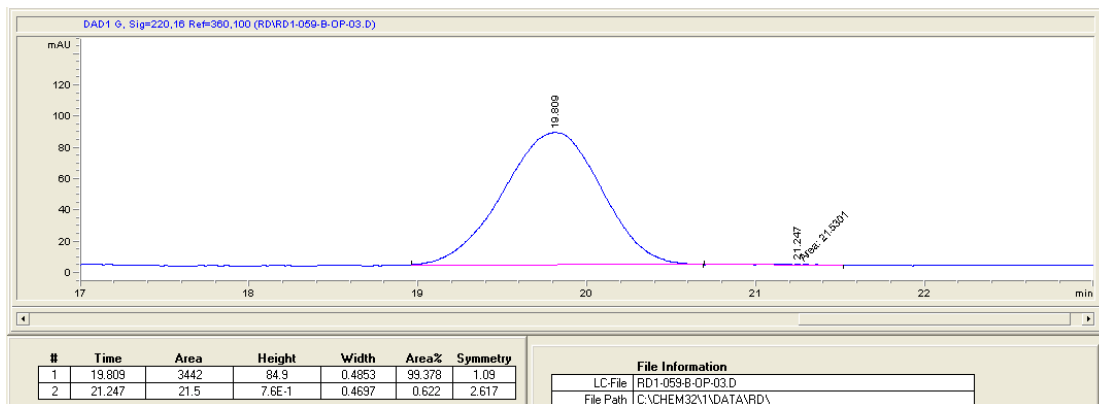
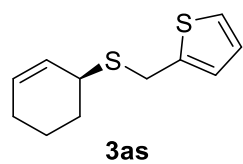
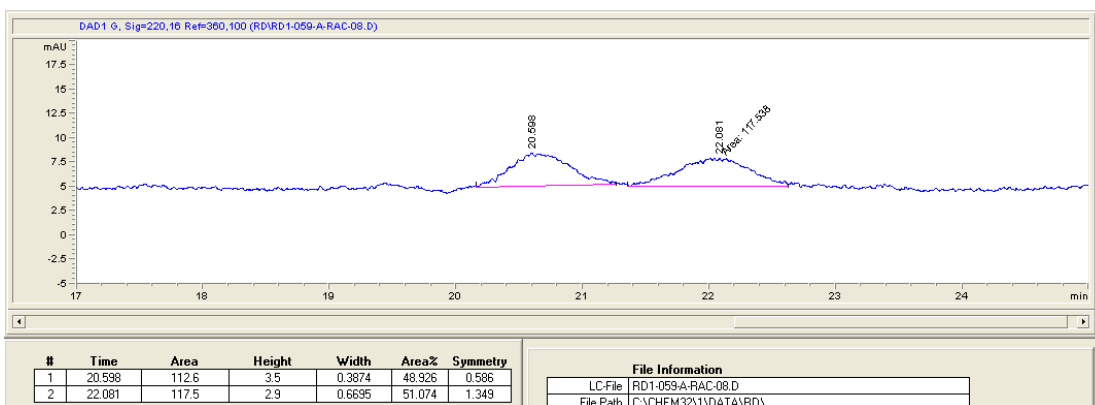
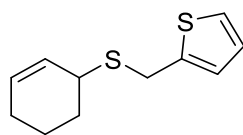


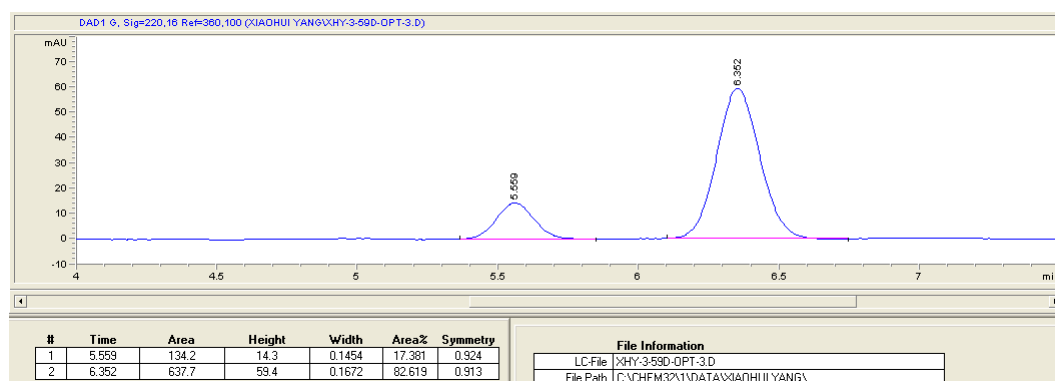
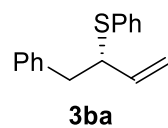
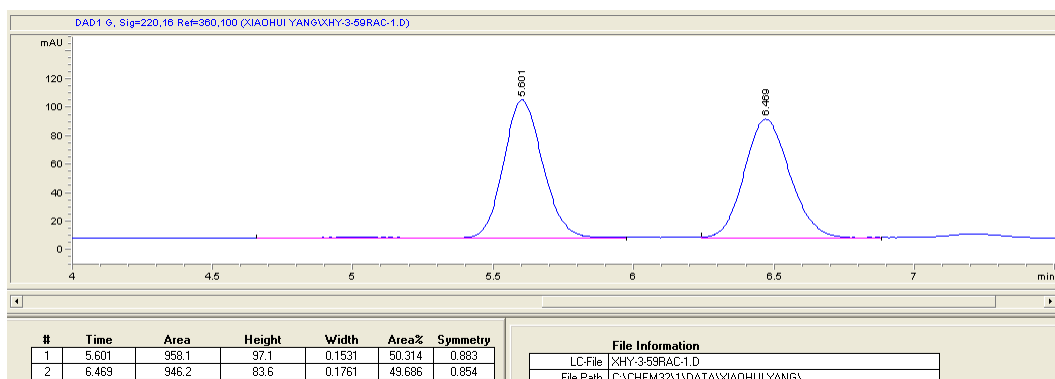
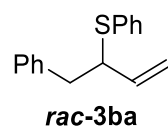
rac-3ar

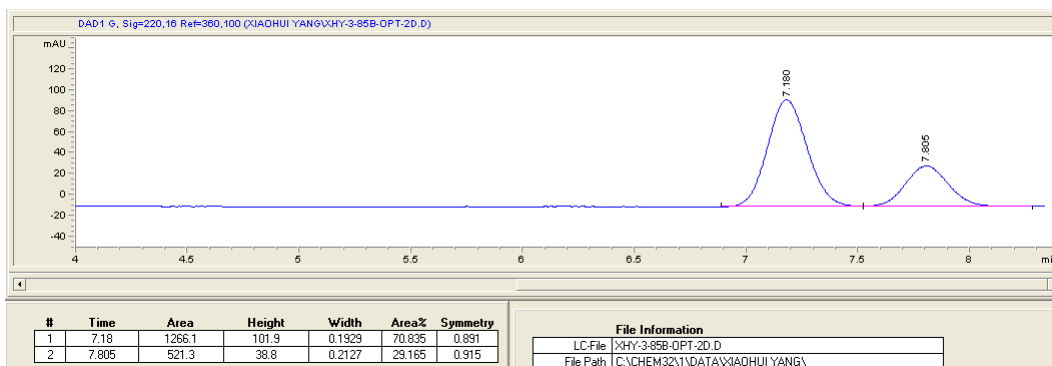
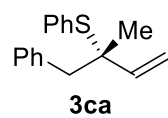
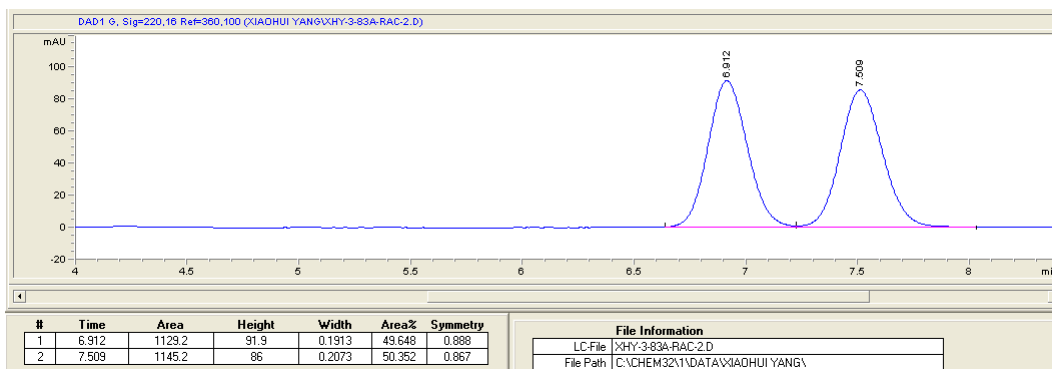
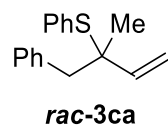


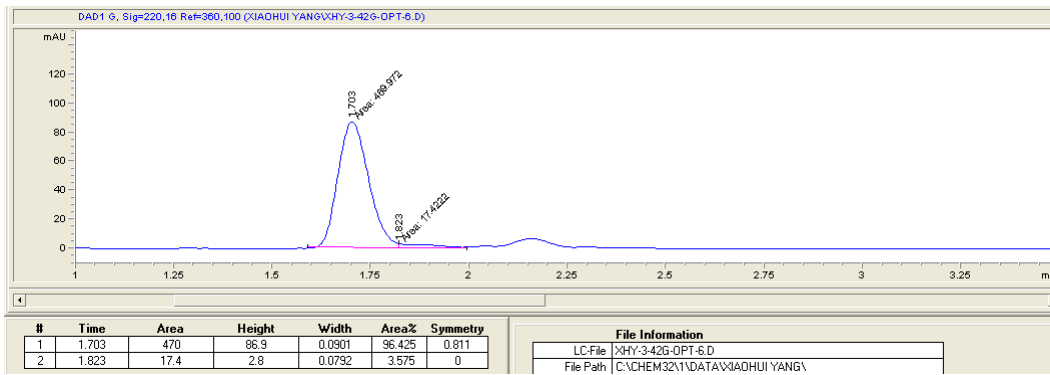
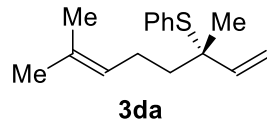
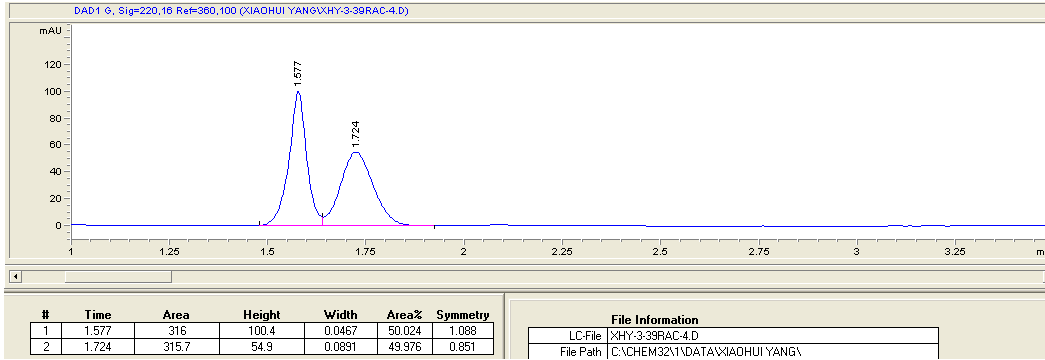
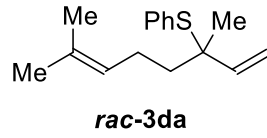
3ar

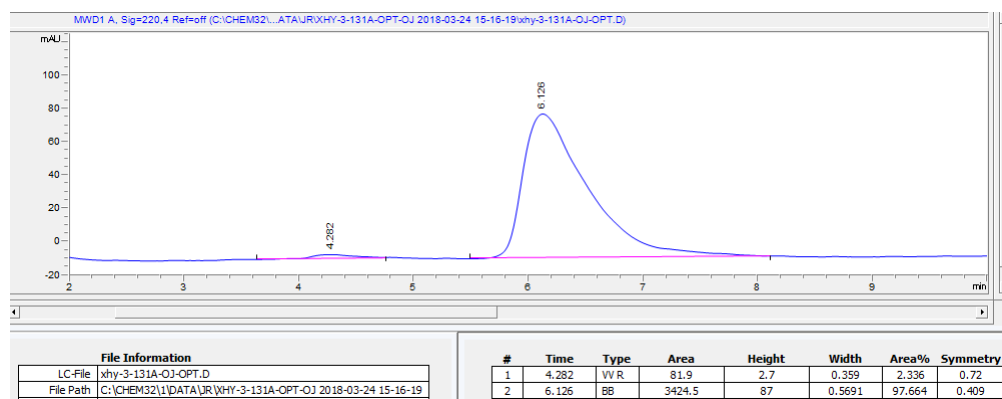
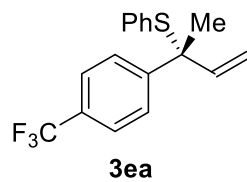
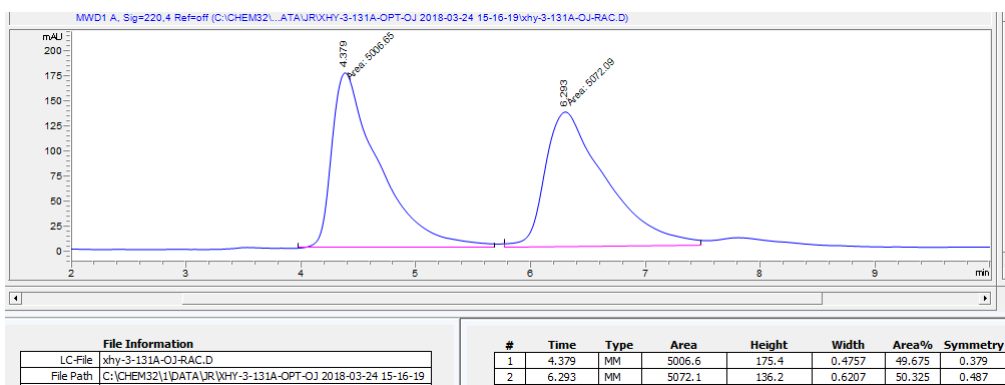
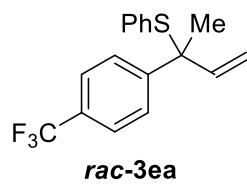


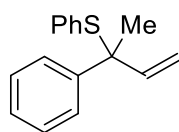




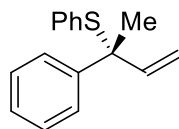
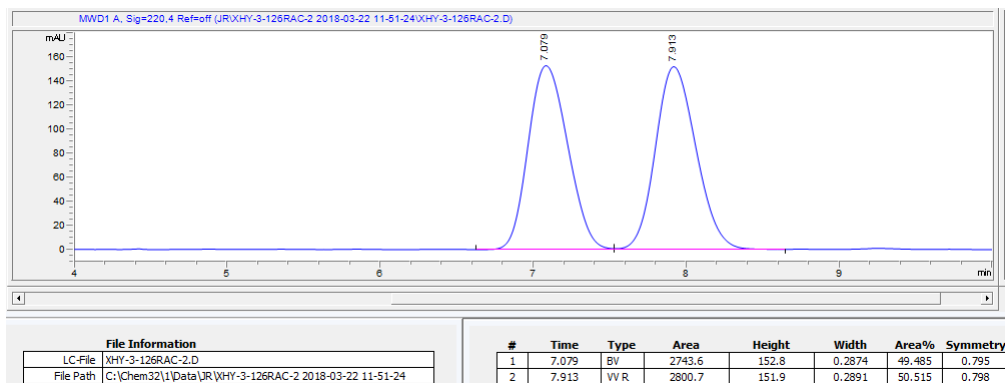




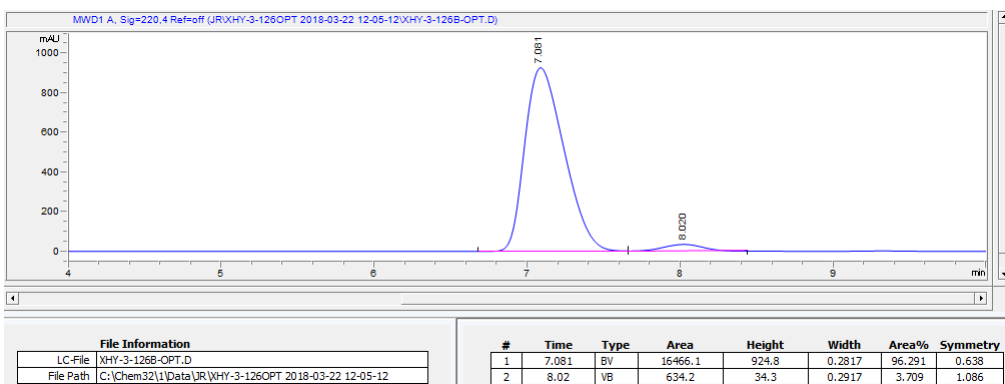


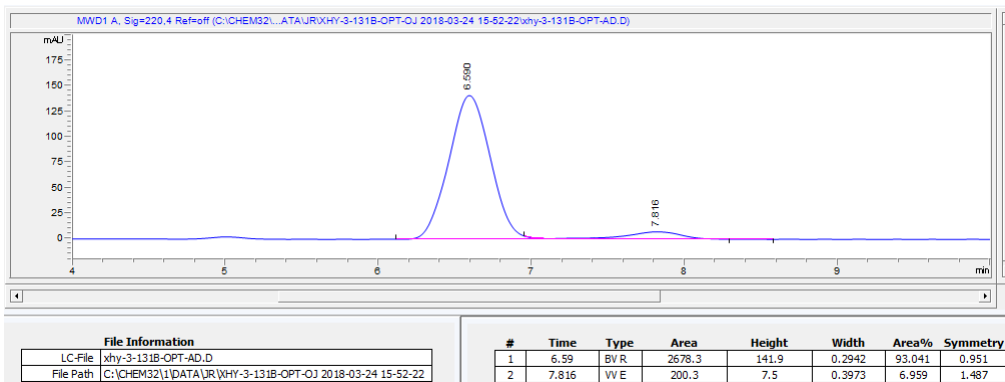
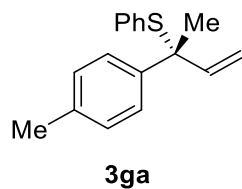
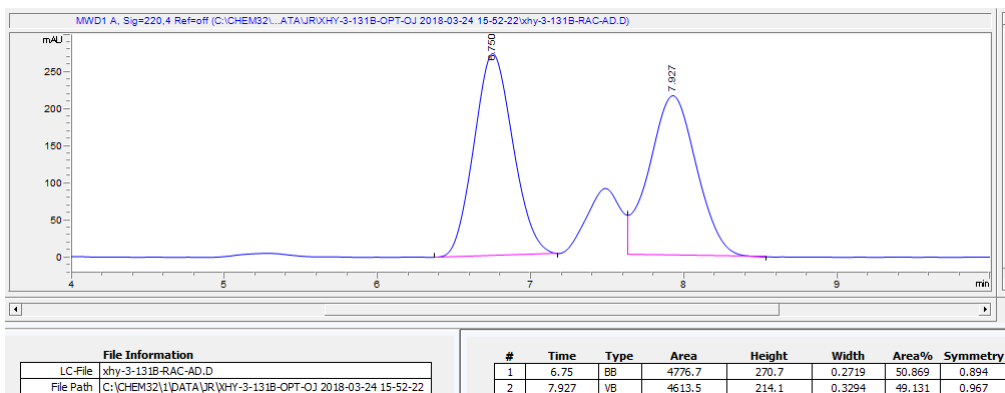
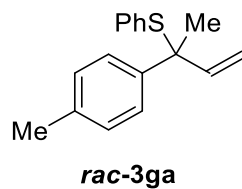


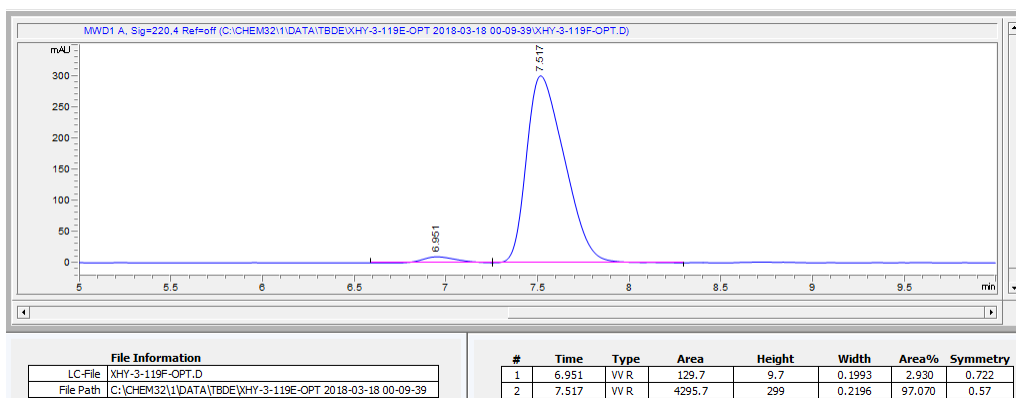
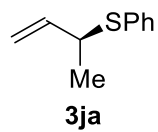
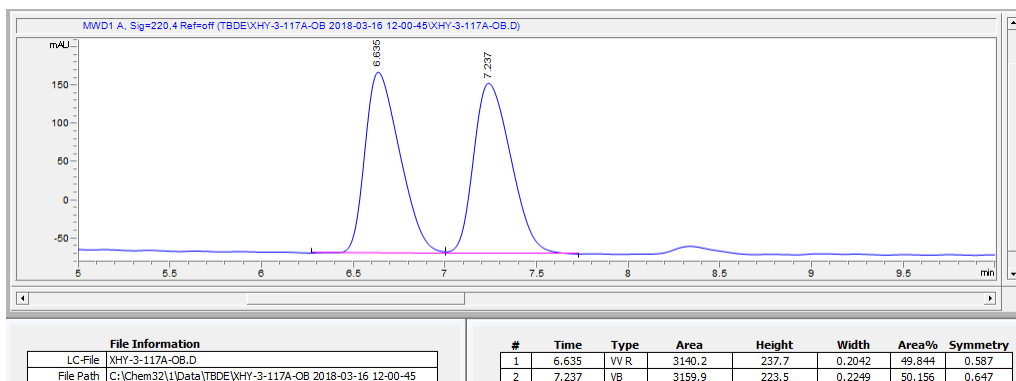
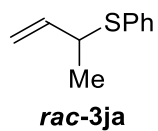
rac-3fa

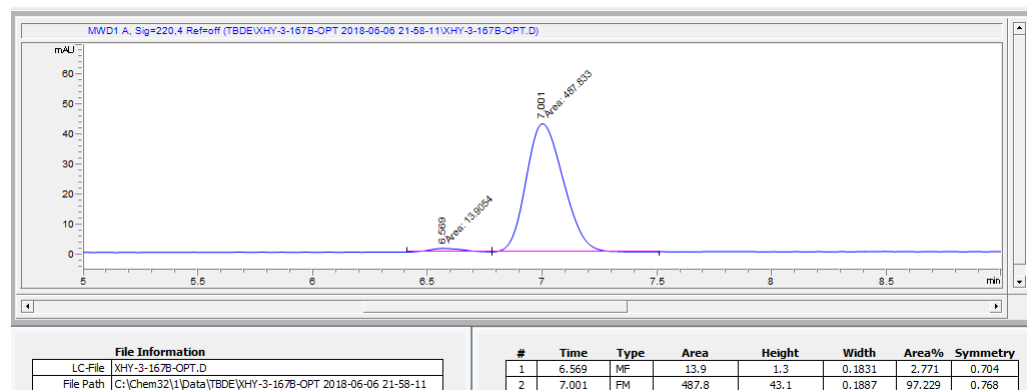
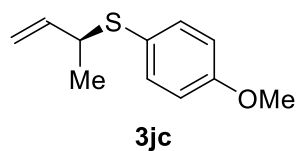
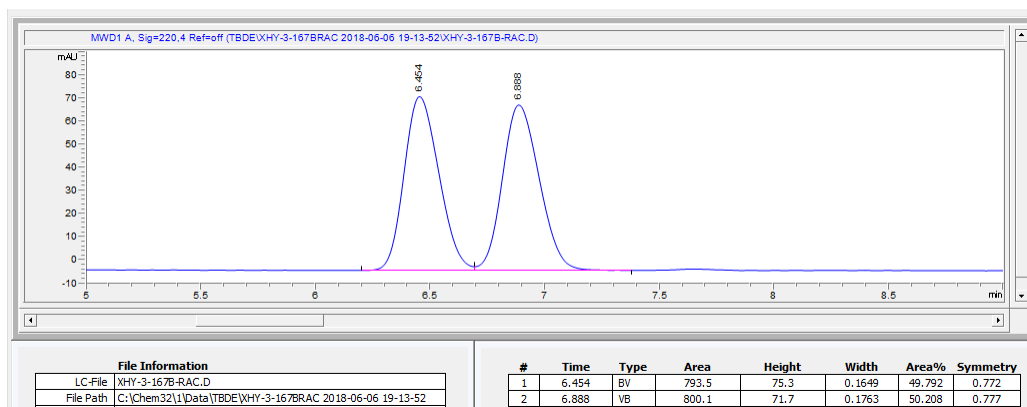
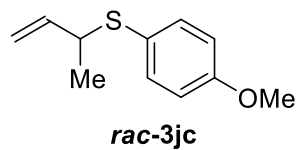


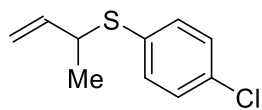
3fa



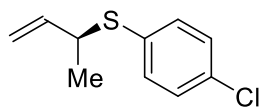
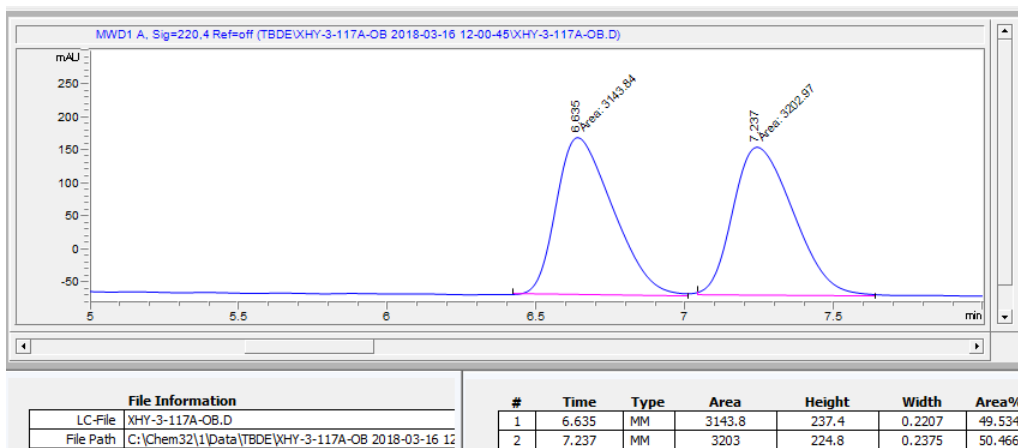




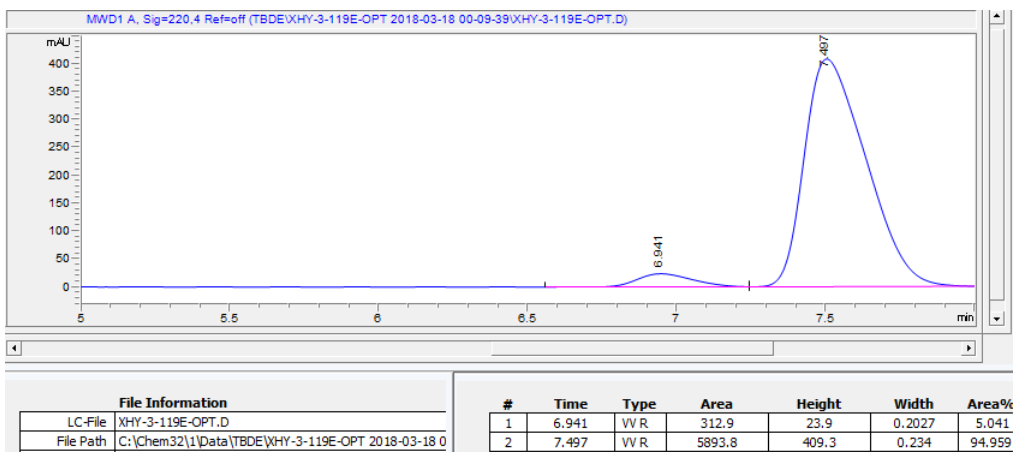


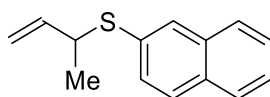


rac-3jg

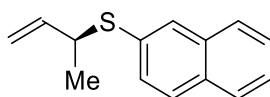
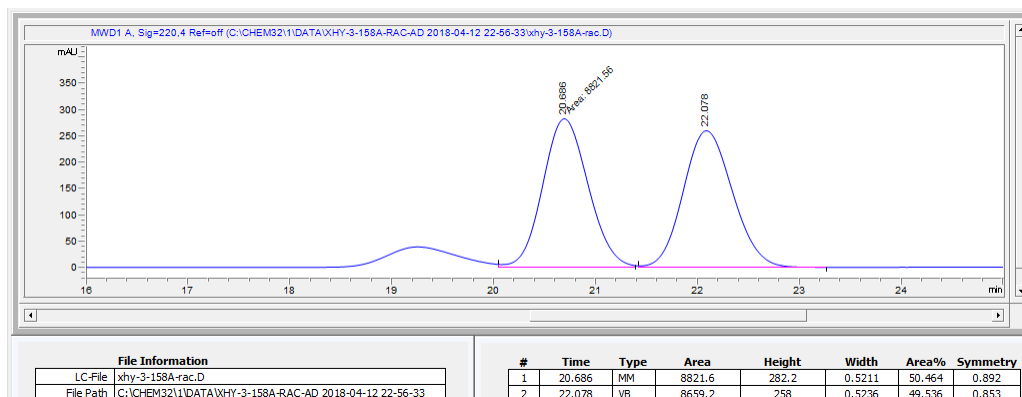


3jg

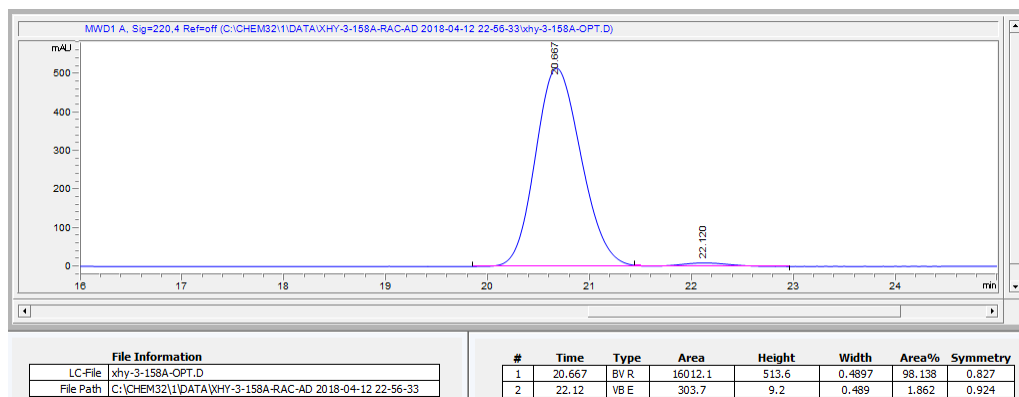


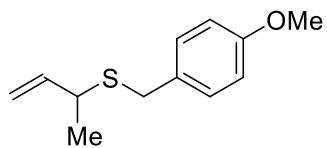


rac-3ju

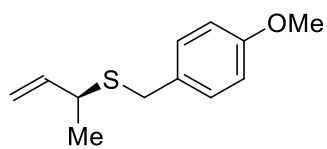
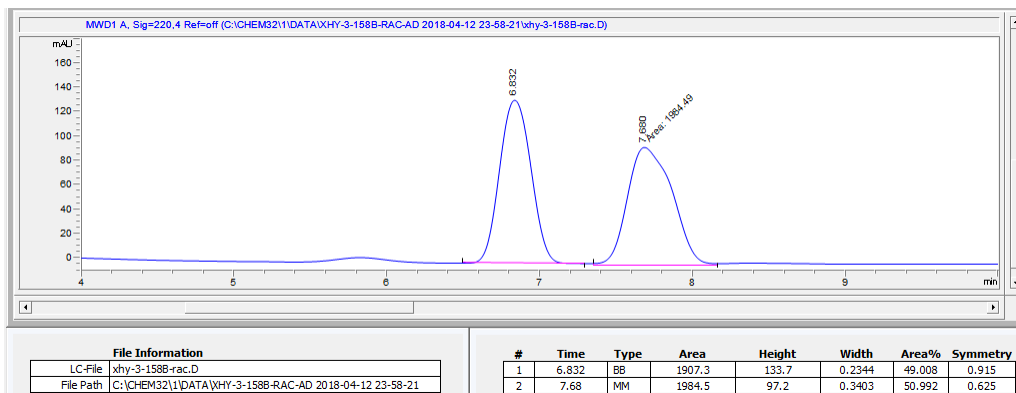


3ju

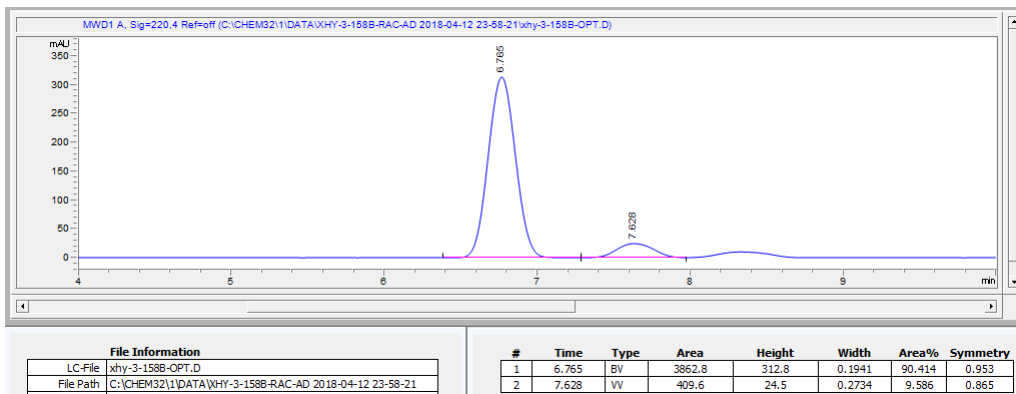


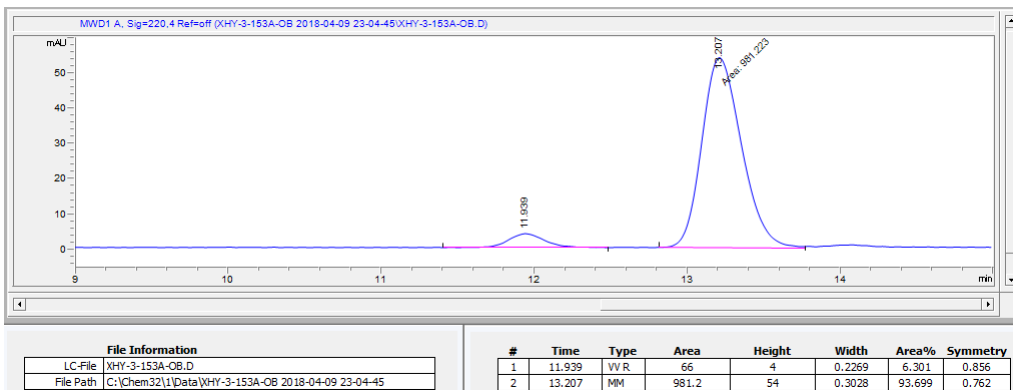
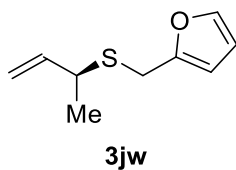
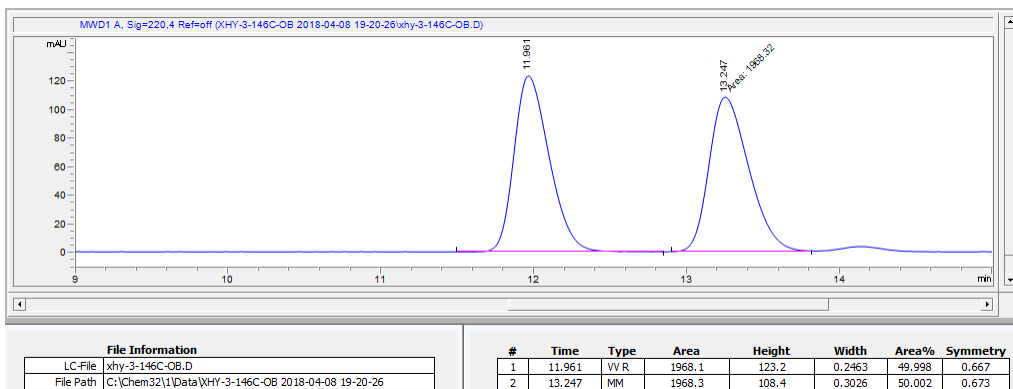
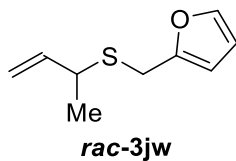


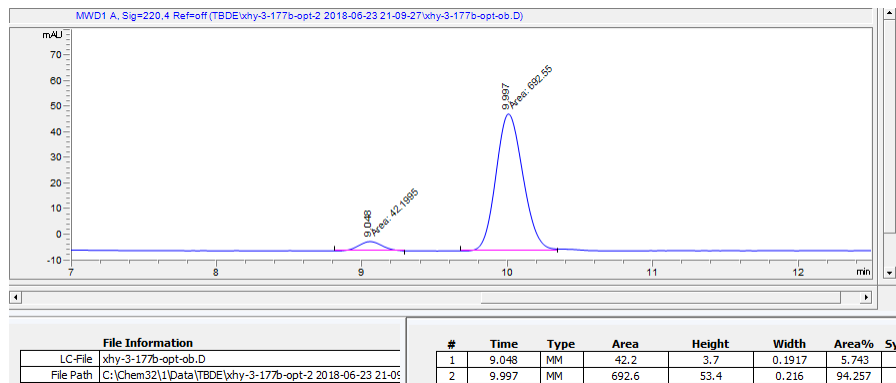
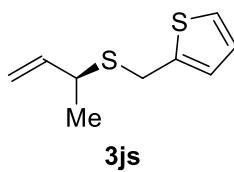
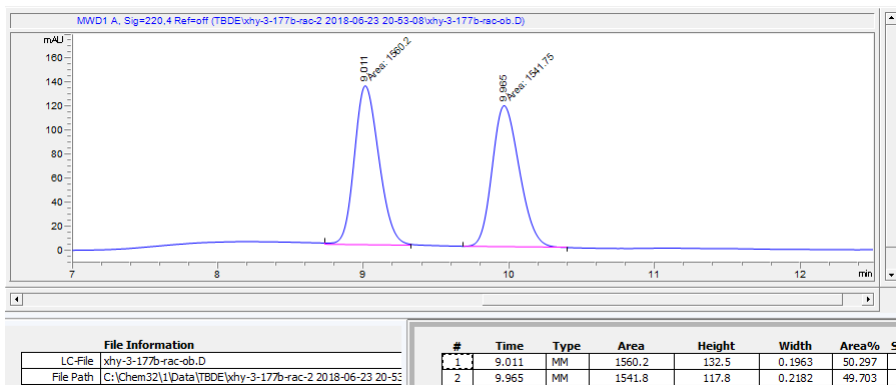
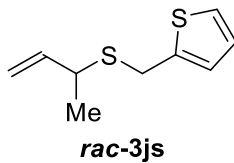
rac-3jv



3jv







Appendix 2 Supporting Information for Chapter 2

Catalytic Hydrothiolation: Counterion-Controlled Regioselectivity¹

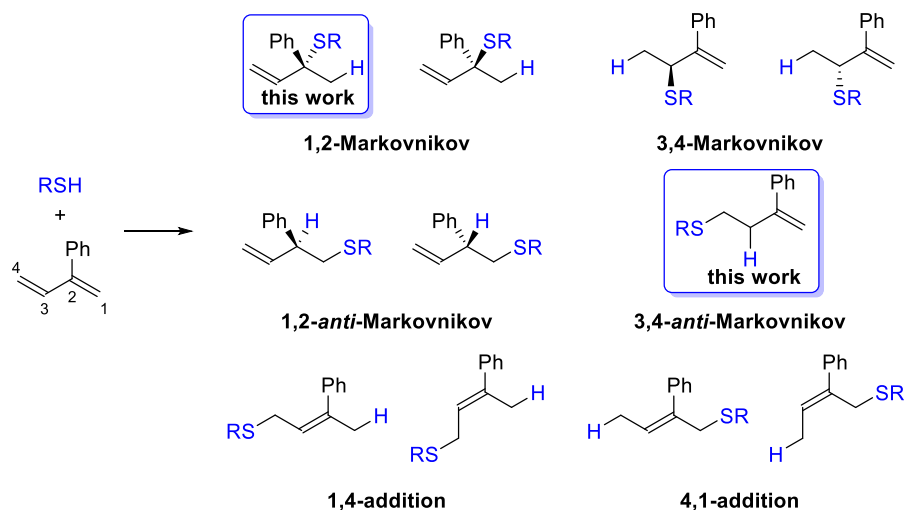
Table of Contents	Page
1. General	154
2. Possible isomers for the hydrothiolation of unsymmetric 1,3-diene	155
3. Mechanism studies for 1,2-Markovnikov hydrothiolation	155
4. Total synthesis of (-)-agelasidine A	167
5. General procedure for 3,4- <i>anti</i> -Markovnikov hydrothiolation	169
6. Mechanism studies for 3,4- <i>anti</i> -Markovnikov hydrothiolation	175
7. References	182
8. NMR spectra of unknown compounds	183
9. SFC spectra	214

¹ For additional details, see: Yang, X.-H.; Davison, R. T.; Nie, S.-Z.; Cruz, F. A.; McGinnis, T. M.; Dong, V. M. *J. Am. Chem. Soc.* **2019**, *141*, 3006–3013.

1. General:

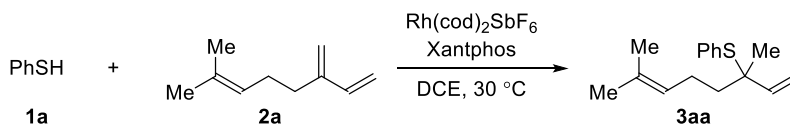
Commercial reagents were purchased from Sigma Aldrich, Strem, Alfa Aesar, Acros Organics or TCI and used without further purification. 1,2-Dichloroethane, 1,4-dioxane, methanol and ethanol were purified using an Innovative Technologies Pure Solv system, degassed by three freeze-pump-thaw cycles, and stored over 3Å MS within a N₂ filled glove box. All experiments were performed in oven-dried or flame-dried glassware. Reactions were monitored using either thin-layer chromatography (TLC) or gas chromatography using an Agilent Technologies 7890A GC system equipped with an Agilent Technologies 5975C inert XL EI/CI MSD. Visualization of the developed plates was performed under UV light (254 nm) or KMnO₄ stain. Organic solutions were concentrated under reduced pressure on a Büchi rotary evaporator. Purification and isolation of products were performed via silica gel chromatography (both column and preparative thin-layer chromatography). Column chromatography was performed with Silicycle Silica-P Flash Silica Gel using glass columns. Solvents were purchased from Fisher. ¹H NMR, ²H NMR, ¹³C NMR, and ³¹P NMR spectra were recorded on Bruker CRYO500 or DRX400 spectrometer. ¹H NMR spectra were internally referenced to the residual solvent signal or TMS. ¹³C NMR spectra were internally referenced to the residual solvent signal. Data for ¹H NMR are reported as follows: chemical shift (δ ppm), multiplicity (s = singlet, d = doublet, t = triplet, q = quartet, m = multiplet), coupling constant (Hz), integration. Data for ²H NMR, ¹³C NMR, and ³¹P NMR are reported in terms of chemical shift (δ ppm). Infrared (IR) spectra were obtained on a Nicolet iS5 FT-IR spectrometer with an iD5 ATR and are reported in terms of frequency of absorption (cm⁻¹). High resolution mass spectra (HRMS) were obtained on a micromass 70S-250 spectrometer (EI) or an ABI/Sciex QStar Mass Spectrometer (ESI). Enantiomeric excesses for enantioselective reactions were determined by chiral SFC analysis using an Agilent Technologies HPLC (1200 series) system and Aurora A5 Fusion. 1,3-Dienes **2e-2g** used here were known compounds and synthesized according to the reported methods.¹

2. Possible isomers for the hydrothiolation of unsymmetric 1,3-diene



3. Mechanism studies for 1,2-Markovnikov hydrothiolation

3.1 Kinetic studies



The kinetic profile of the reaction was studied by obtaining initial rates of the reaction with different concentrations of thiophenol (**1a**), myrcene (**2a**), and Rh-catalyst. No products of decomposition are observed for the system. The rates were monitored by GC-FID analysis using 1,3,5-trimethoxybenzene as an internal standard.

Determination of the reaction order in catalyst

Representative procedure (entry 1):

In a N_2 -filled glove box, a 0.08M catalyst solution was prepared by combining $\text{Rh}(\text{cod})_2\text{SbF}_6$ (44.4 mg, 0.08 mmol), Xantphos (46.3 mg, 0.08 mmol), and DCE (1.0 mL). A solution of reagents was prepared by combining **1a** (55.1 mg, 0.50 mmol), **2a** (102.1 mg, 0.75 mmol), and DCE (1.0 mL). A vial was charged with a stir bar and 1,3,5-trimethoxybenzene (6.0 mg, 0.036 mmol). Next, 0.05 mL of catalyst solution was added to the vial, followed by 0.2 mL of reagent solution. Additional DCE was added to the vial to make the total reaction volume 0.4 mL, and the vial was sealed with a Teflon cap. Aliquots (10 μL) were taken every 5 minutes and quenched with 2 mL of EtOAc. The reaction halts in EtOAc. The amount of **3aa** was monitored by GC-FID analysis.

Table S1. Observed rate versus catalyst concentration for 1,2-Markovnikov hydrothiolation

entry	1	2	3	4
[Rh] (M)	0.01	0.02	0.03	0.04
k_{obs} (M/min)	1.44×10^{-4}	3.09×10^{-4}	3.89×10^{-4}	5.62×10^{-4}

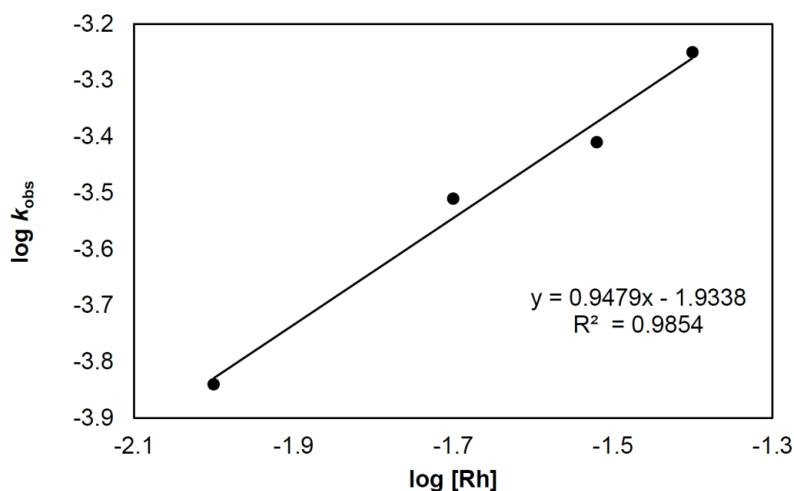


Figure S1. Plot of $\log k_{obs}$ vs $\log[Rh]$ for 1,2-Markovnikov hydrothiolation (first order)

Determination of the reaction order in myrcene (**2a**)

Representative procedure (entry 1):

In a N_2 -filled glove box, a 0.025M catalyst solution was prepared by combining $Rh(cod)_2SbF_6$ (27.8 mg, 0.05 mmol), Xantphos (28.9 mg, 0.05 mmol), and DCE (2.0 mL). A solution of **1a** (110.2 mg, 1.0 mmol) in DCE (2.0 mL) was prepared. A vial was charged with a stir bar, 1,3,5-trimethoxybenzene (6.0 mg, 0.036 mmol), and **2a** (13.6 mg, 0.1 mmol). Catalyst solution (0.2 mL) was added to the vial, followed by 0.2 mL of **1a** solution, and the vial was sealed with a Teflon cap. Aliquots (10 μ L) were taken every 5 minutes and quenched in 2 mL of EtOAc. The reaction halts in EtOAc. The amount of **3aa** was monitored by GC-FID analysis.

Table S2. Observed rate versus myrcene (**2a**) concentration for 1,2-Markovnikov hydrothiolation

entry	1	2	3	4	5
[2a] (Initial) (M)	0.25	0.5	0.75	1.0	1.25
k_{obs} (M/min)	1.01×10^{-4}	1.04×10^{-4}	1.05×10^{-4}	1.03×10^{-4}	1.09×10^{-4}

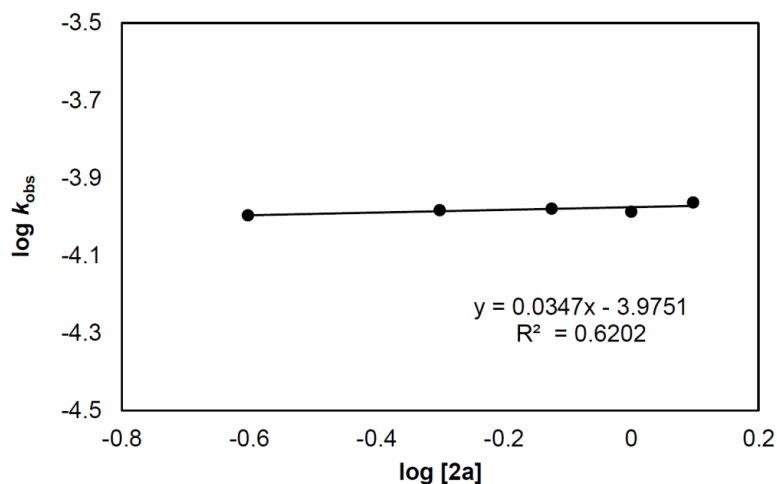


Figure S2. Plot of $\log k_{obs}$ vs $\log[2a]$ for 1,2-Markovnikov hydrothiolation (zero order)

Determination of the reaction order in thiophenol (**1a**)

Representative procedure (entry 1):

In a N_2 -filled glove box, a 0.025M catalyst solution was prepared by combining $Rh(cod)_2SbF_6$ (13.9 mg, 0.025 mmol), Xantphos (14.5 mg, 0.025 mmol), and DCE (1.0 mL). A solution of **2a** (102.2 mg, 0.75 mmol) in DCE (1.0 mL) was prepared. A vial was charged with a stir bar, 1,3,5-trimethoxybenzene (6.0 mg, 0.036 mmol) and **1a** (11.0 mg, 0.1 mmol). Catalyst solution (0.2 mL) was added to the vial, followed by 0.2 mL of **2a** solution, and the vial was sealed with a Teflon cap. Aliquots (10 μ L) were taken every 5 minutes and quenched in 2 mL of EtOAc. The reaction halts in EtOAc. The amount of **3aa** was monitored by GC-FID analysis.

Table S3. Observed rate versus thiophenol (**1a**) concentration for 1,2-Markovnikov hydrothiolation

entry	1	2	3	4
[1a] (Initial) (M)	0.25	0.5	1.0	1.25
k_{obs} (M/min)	1.32×10^{-4}	1.78×10^{-4}	2.18×10^{-4}	2.45×10^{-4}

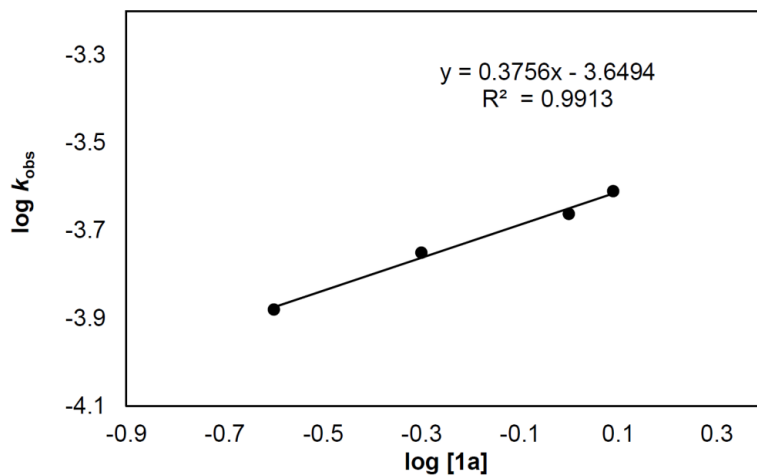


Figure S3. Plot of $\log k_{\text{obs}}$ vs $\log[1\mathbf{a}]$ for 1,2-Markovnikov hydrothiolation (fractional order: 0.4)

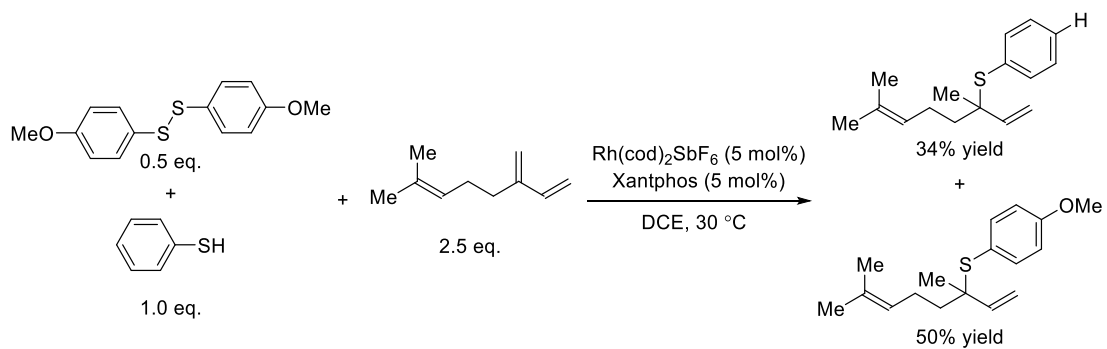


Figure S4. Cross over experiment between disulfide and thiophenol.

3.2 Deuterium-labeling studies

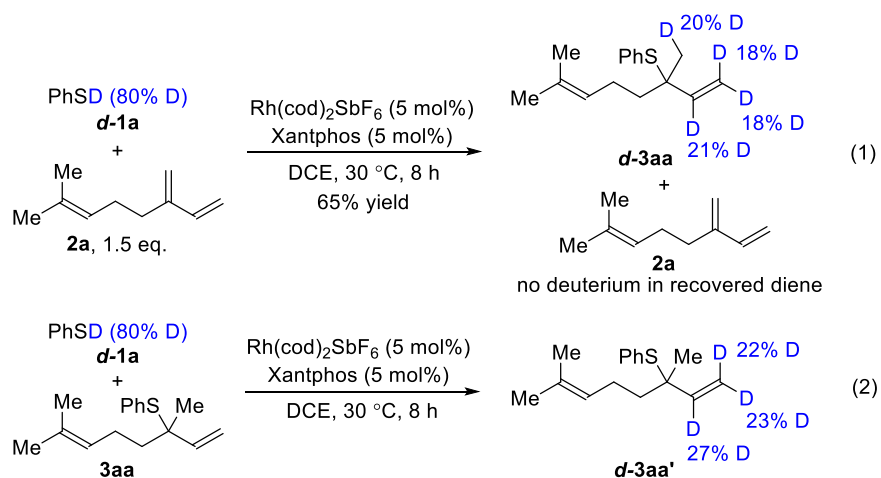


Figure S5. Deuterium-labeling studies for 1,2-Markovnikov hydrothiolation

In a N₂-filled glovebox, Xantphos (2.9 mg, 0.005 mmol) and DCE (0.40 mL) were added to a 1-dram vial containing Rh(cod)₂SbF₆ (2.8 mg, 0.005 mmol). The resulting mixture was stirred for 10 min and then myrcene (**2a**, 20.4 mg, 0.15 mmol, in eq.1) or **3aa** (24.6 mg, 0.1 mmol, in eq.2), and thiol **d-1a** (11.0 mg, 0.10 mmol) were added. The mixture was held at 30 °C until no starting material was observed by TLC. The resulting mixture was then cooled to rt. The regioselectivities were determined by ¹H NMR analysis of the unpurified reaction mixture. The product was purified by preparative thin-layer chromatography (hexanes/EtOAc = 40/1). ¹H NMR for **d-3aa** (400 MHz, CDCl₃) δ 7.49 – 7.43 (m, 2H), 7.34 – 7.26 (m, 3H), 5.94 – 5.85 (m, 0.79H), 5.12 – 5.04 (m, 1H), 5.00 – 4.92 (m, 0.82H), 4.75 – 4.66 (m, 0.82H), 2.18 – 1.96 (m, 2H), 1.68 (s, 3H), 1.65 – 1.59 (m, 5H), 1.31 (s, 2.8H).

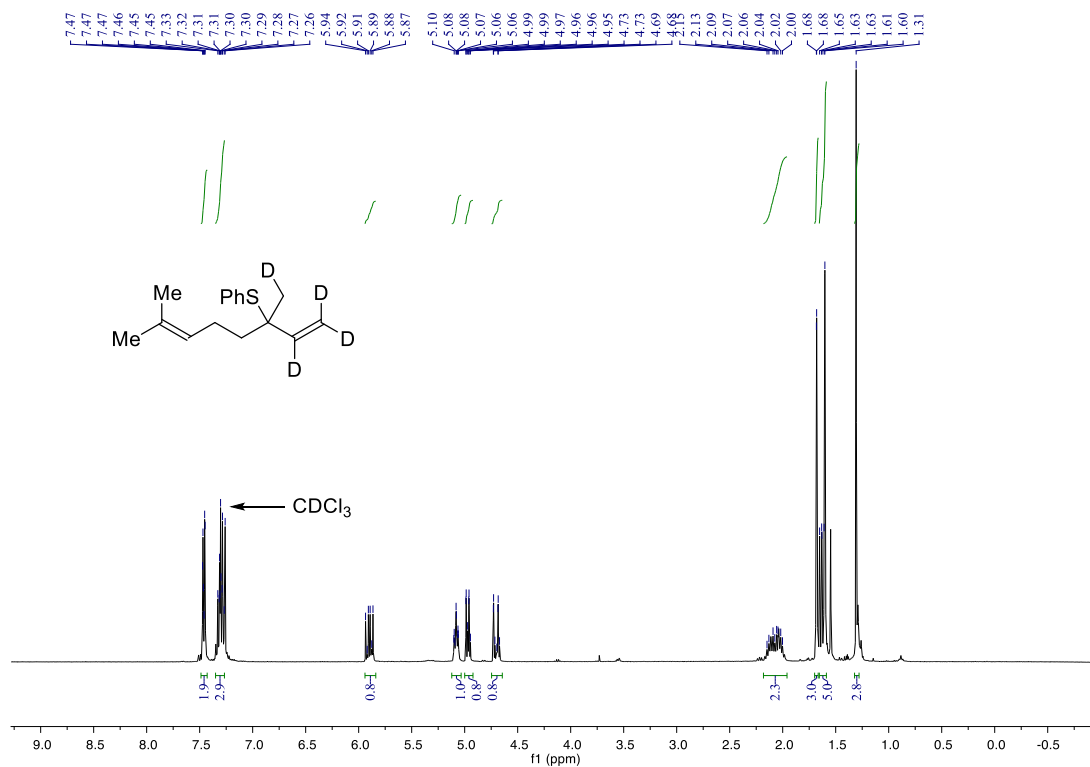


Figure S6. ¹H NMR [400 MHz, CDCl₃ (δ 7.26 ppm)] for *d*-3aa

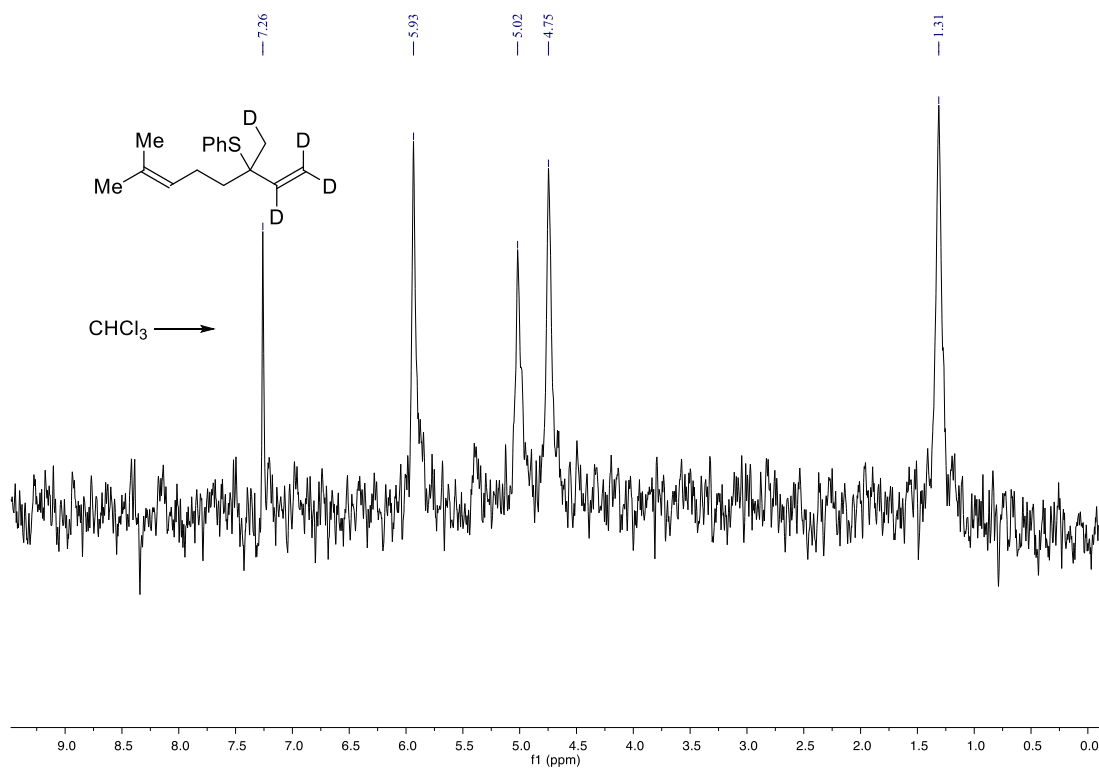


Figure S7. ²H NMR [400 MHz, CHCl₃ (δ 7.26 ppm)] for *d*-3aa

3.3 NMR studies

In a N₂-filled glovebox, Xantphos (5.8 mg, 0.01 mmol) and DCE-*d*₄ (0.50 mL) were added to a 1-dram vial containing Rh(cod)₂SbF₆ (5.6 mg, 0.01 mmol). The resulting mixture was stirred for 10 min and then thiophenol (**1a**, 11.0 mg, 0.10 mmol) was added. The reaction mixture was transferred to a J. Young NMR tube to perform ¹H NMR and ³¹P NMR spectroscopy. A resonance at -13.5 ppm was observed in less than ten minutes at rt in the ¹H NMR spectrum (Figure S8) and an equivalent phosphine resonance in the ³¹P NMR spectrum [doublet (δ = 30.3 ppm, *J*_{Rh-P} = 108 Hz)] was observed (Figure S9). Myrcene (**2a**, 13.6 mg, 0.1 mmol) was then added to this mixture, and the Rh-H resonance disappeared and a new complex with non-equivalent phosphine resonances was formed [a pair of doublet of doublet signals (δ = 26.6 ppm, *J*_{Rh-P} = 174 Hz, *J*_{P-P} = 8 Hz; δ = 16.0 ppm, *J*_{Rh-P} = 115 Hz, *J*_{P-P} = 8 Hz)] (Figure S10). When we subjected the product **3aa** (24.6 mg, 0.10 mmol) to a mixture of Rh(cod)₂SbF₆ (5.6 mg, 0.01 mmol) and Xantphos (5.8 mg, 0.01 mmol) in DCE-*d*₄, we observed the same species by ³¹P NMR spectroscopy (Figure S11). Based on these results and the kinetic studies, we labeled rhodium intermediate **IV** as the resting state in the catalytic cycle (Figure 3).

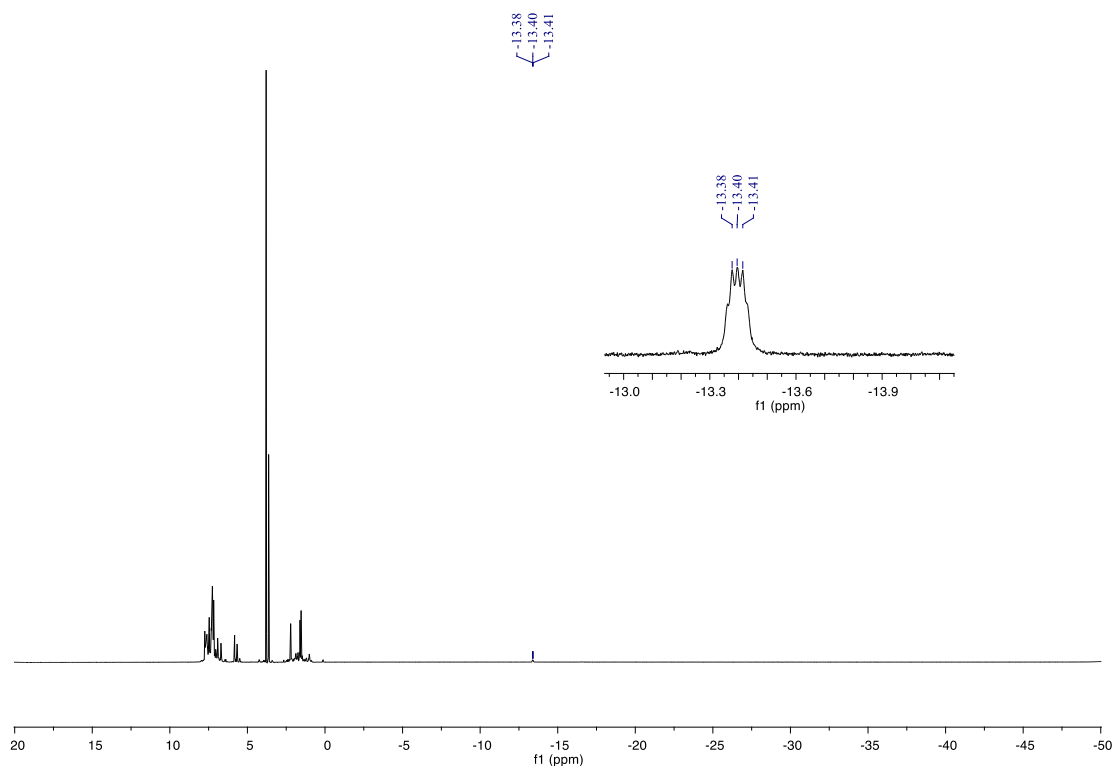


Figure S8. ¹H NMR (500 MHz) for a mixture of Rh(Xantphos)SbF₆ and thiophenol (**1a**) in DCE-*d*₄ (δ 3.79 ppm)

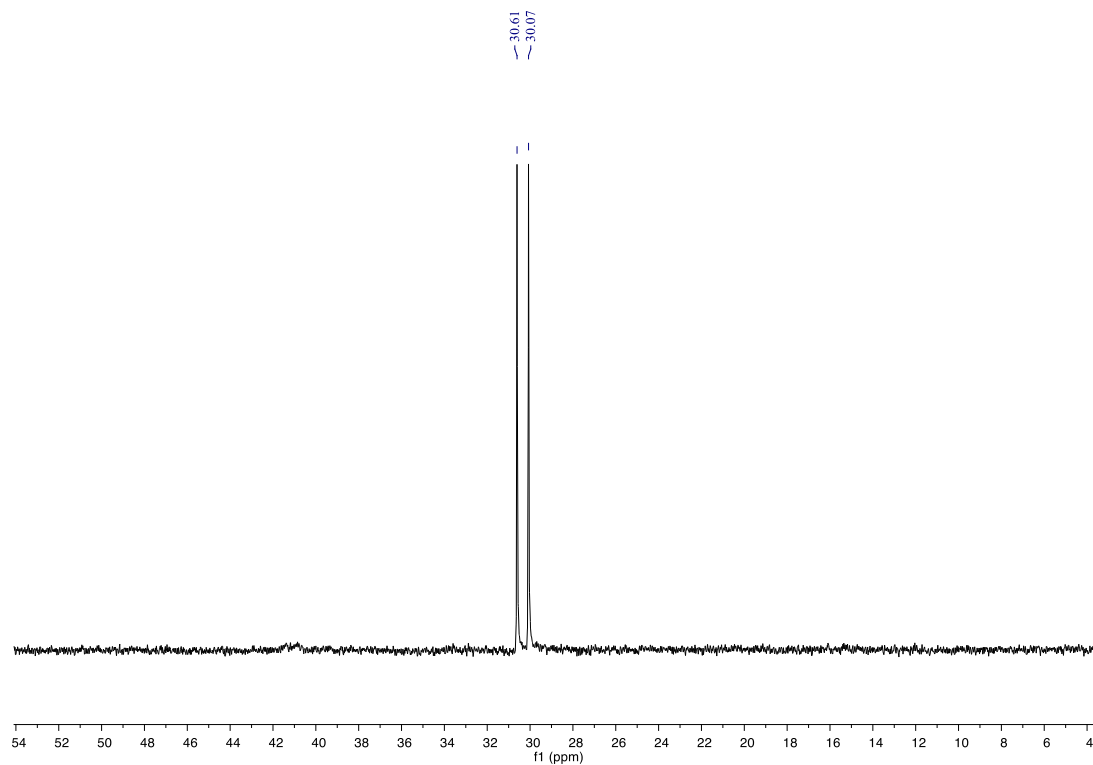


Figure S9. ^{31}P NMR (202 MHz) for a mixture of $\text{Rh}(\text{Xantphos})\text{SbF}_6$ and thiophenol (**1a**) in $\text{DCE-}d_4$

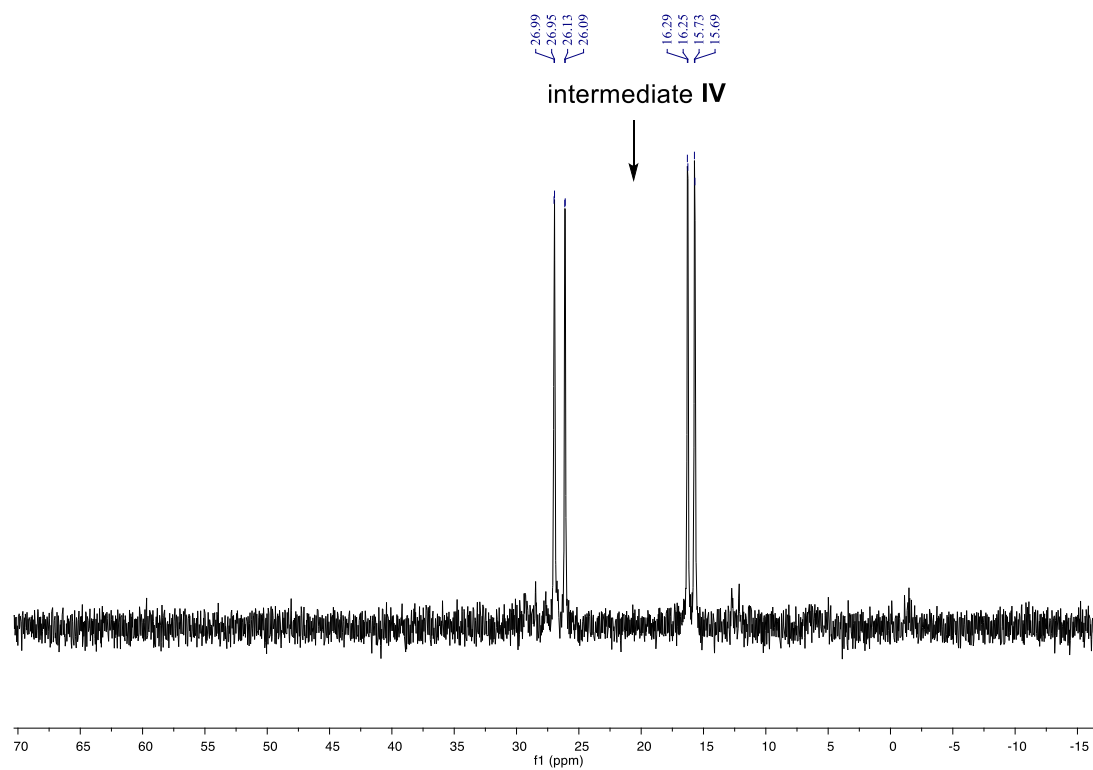


Figure S10. ^{31}P NMR (202 MHz) for a mixture of $\text{Rh}(\text{Xantphos})\text{SbF}_6$, thiophenol (**1a**), and myrcene (**2a**) in $\text{DCE-}d_4$

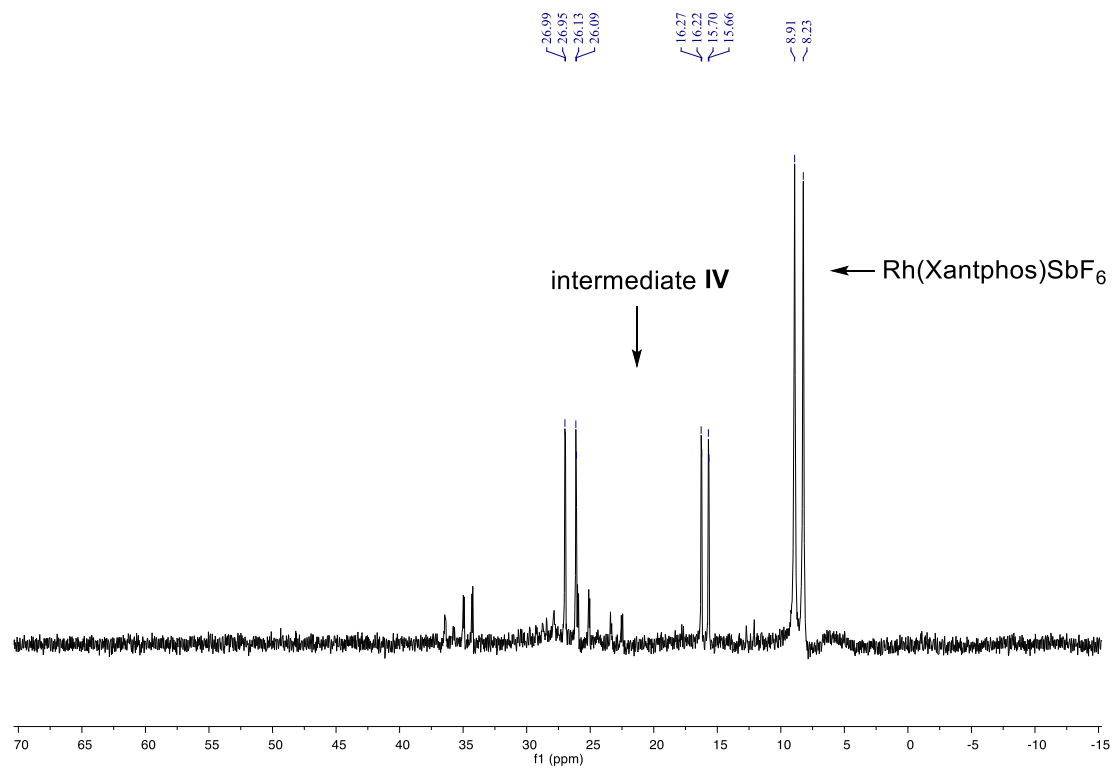
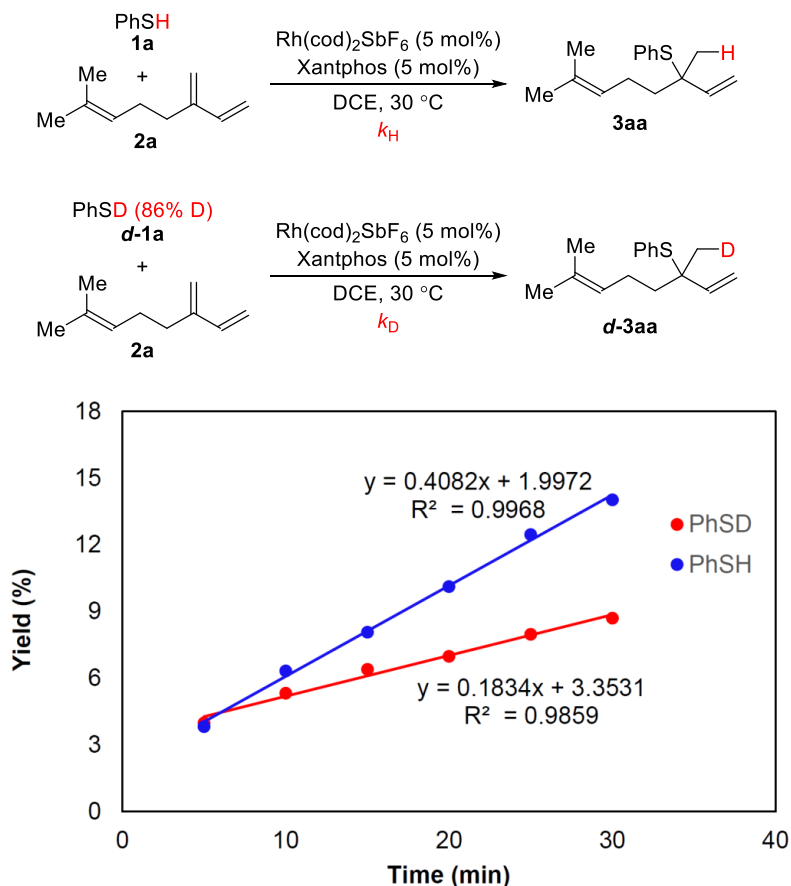


Figure S11. ^{31}P NMR(202 MHz) for a mixture of Rh(Xantphos)SbF_6 and **3aa** in DCE-d_4

3.4 Initial rate *KIE* study

In a N₂-filled glove box, a 0.025M catalyst solution was prepared by combining Rh(cod)₂SbF₆ (13.9 mg, 0.025 mmol), Xantphos (14.5 mg, 0.025 mmol), and DCE (1.0 mL). A solution of **2a** (102.2 mg, 0.75 mmol) in DCE (1.0 mL) was prepared. A vial was charged with a stir bar, 1,3,5-trimethoxybenzene (6.0 mg, 0.036 mmol), and then **1a** (11.0 mg, 0.1 mmol) or **d-1a** (11.1 mg, 0.1 mmol) were added. Catalyst solution (0.2 mL) was added to the vial, followed by 0.2 mL of **2a** solution, and the vial was sealed with a Teflon cap. Aliquots (10 μL) were taken every 5 minutes and quenched in 2 mL of EtOAc. The reaction halts in EtOAc. The amount of **3aa** was monitored by GC-FID analysis.



adjusted initial rate of deuterio species² (considering 14% PhSH):

$$0.183 = 0.86 k_D + 0.14 \times 0.408$$

$$k_D = 0.146$$

$$\text{Calculation of KIE: } k_H/k_D = 0.408/0.146 = 2.8$$

Figure S12. Initial rate *KIE* for 1,2-Markovnikov hydrothiolation

3.5 Hammett plot

In a N₂-filled glove box, a 0.025M catalyst solution was prepared by combining Rh(cod)₂SbF₆ (13.9 mg, 0.025 mmol), Xantphos (14.5 mg, 0.025 mmol), and DCE (1.0 mL). A solution of **2a**

(102.2 mg, 0.75 mmol) in DCE (1.0 mL) was prepared. A vial was charged with a stir bar, 1,3,5-trimethoxybenzene (6.0 mg, 0.036 mmol), and **1a** (5.5 mg, 0.05 mmol) and **1h** (X = OMe, 7.0 mg, 0.05 mmol). Catalyst solution (0.2 mL) was added to the vial, followed by 0.2 mL of **2a** solution, and the vial was sealed with a Teflon cap. After 30 min, the ratio of product **3aa** and **3ha** was detected based on the crude ¹H NMR spectrum. The same procedure was used for the other *para*-substituted thiophenols.

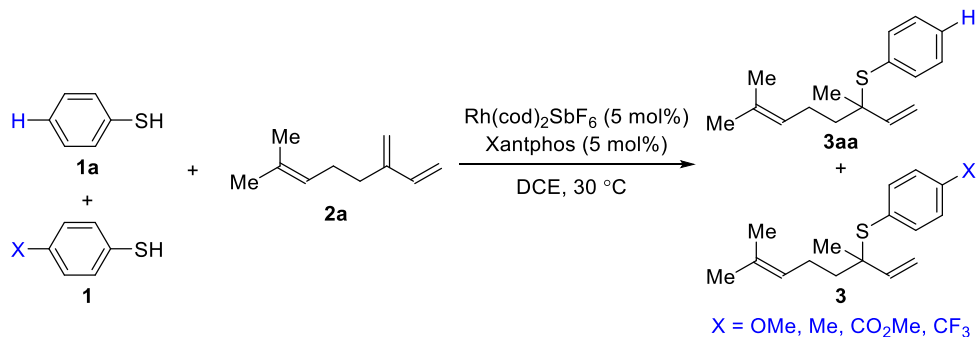


Table S4. Rate ratio versus standard σ^+ for 1,2-Markovnikov hydrothiolation

entry	1	2	3	4	5
X	OMe	Me	H	CO ₂ Me	CF ₃
σ^+	-0.78	-0.31	0	0.49	0.61
k/k_H	1.64	1.16	1	0.85	0.8
$\log k/k_H$	0.216	0.063	0	-0.071	-0.095

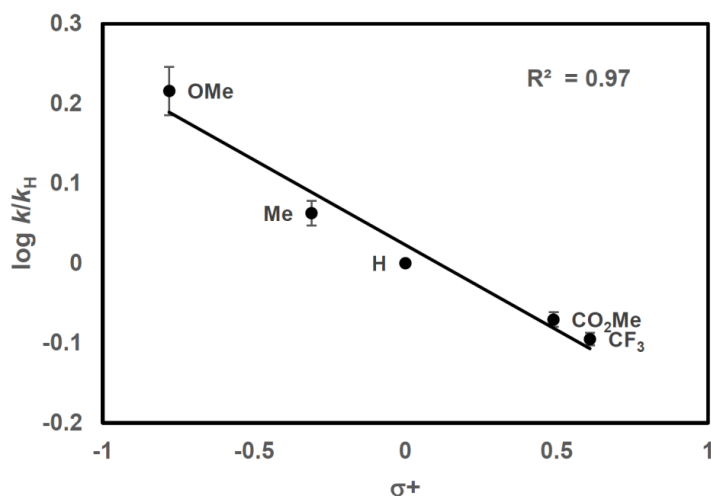


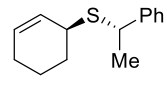
Figure S13. Hammett plot for 1,2-Markovnikov hydrothiolation ($\log k/k_H = m\sigma^+ + b$ ($m = -0.22 \pm 0.02$; $b = 0.03 \pm 0.01$)).

3.6. Catalyst-controlled diastereoselective hydrothiolation (for Figure 2.7)

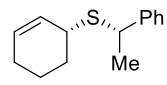
In a N₂-filled glovebox, (*S*)- or (*R*)-Tol-BINAP (1.4 mg, 0.002 mmol) and DCE (0.80 mL) were added to a 1-dram vial containing Rh(cod)₂SbF₆ (1.1 mg, 0.002 mmol). The resulting mixture was

stirred for 10 min and then chiral thiol **1** (0.20 mmol) and 1,3-cyclohexadiene (**2b**, 32.0 mg, 0.40 mmol) were added. The mixture was held at 30 °C until no starting material was observed by TLC. The resulting solution was then cooled to rt. The regioselectivities were determined by ¹H NMR analysis of the unpurified reaction mixture. Isolated yields (obtained by preparative thin-layer chromatography) are reported.

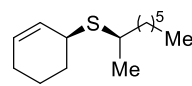
((S)-cyclohex-2-en-1-yl)((S)-1-phenylethyl)sulfane ((S,S)-3cb)

 Colorless oil, 83% yield, >20:1 *dr*, >20:1 *rr*, $[\alpha]_D^{24} = -283.9$ (*c* 1.0, CHCl₃). ¹H NMR (500 MHz, CDCl₃) δ 7.38 – 7.34 (m, 2H), 7.33 – 7.29 (m, 2H), 7.24 – 7.20 (m, 1H), 5.76 – 5.70 (m, 2H), 4.06 (q, *J* = 7.0 Hz, 1H), 3.21 – 3.13 (m, 1H), 2.03 – 1.90 (m, 2H), 1.80 – 1.70 (m, 2H), 1.63 – 1.45 (m, 5H). ¹³C NMR (126 MHz, CDCl₃) δ 144.6, 129.1, 128.6, 128.1, 127.4, 127.1, 44.0, 40.2, 29.5, 25.0, 23.2, 20.1. IR (ATR): 2923, 1490, 1451, 1054, 1026, 871, 751 cm⁻¹. HRMS calculated for C₁₄H₁₈S [M]⁺ 218.1129, found 218.1134.

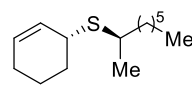
((R)-cyclohex-2-en-1-yl)((S)-1-phenylethyl)sulfane ((R,S)-3cb)

 Colorless oil, 87% yield, >20:1 *dr*, >20:1 *rr*, $[\alpha]_D^{24} = -68.8$ (*c* 0.4, CHCl₃). ¹H NMR (500 MHz, CDCl₃) δ 7.38 – 7.35 (m, 2H), 7.34 – 7.29 (m, 2H), 7.25 – 7.20 (m, 1H), 5.72 – 5.67 (m, 1H), 5.48 – 5.42 (m, 1H), 4.02 (q, *J* = 7.1 Hz, 1H), 3.06 – 2.98 (m, 1H), 2.04 – 1.90 (m, 2H), 1.90 – 1.73 (m, 3H), 1.60 – 1.51 (m, 4H). ¹³C NMR (126 MHz, CDCl₃) δ 144.7, 129.7, 128.7, 127.6, 127.5, 127.2, 43.7, 40.1, 29.3, 25.1, 23.1, 19.6. IR (ATR): 2924, 1490, 1451, 1054, 1026, 871, 751 cm⁻¹. HRMS calculated for C₁₄H₁₈S [M]⁺ 218.1129, found 218.1128.

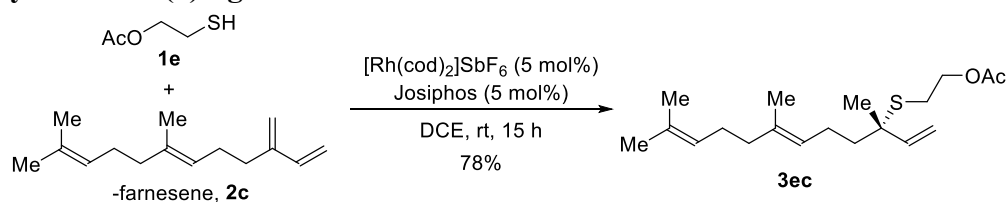
((S)-cyclohex-2-en-1-yl)((R)-octan-2-yl)sulfane ((S,R)-3db)

 Colorless oil, 92% yield, >20:1 *dr*, >20:1 *rr*, $[\alpha]_D^{24} = -160.0$ (*c* 1.0, CHCl₃). ¹H NMR (400 MHz, CDCl₃) δ 5.78 – 5.67 (m, 2H), 3.43 – 3.35 (m, 1H), 2.89 – 2.77 (m, 1H), 2.03 – 1.93 (m, 3H), 1.90 – 1.79 (m, 1H), 1.78 – 1.69 (m, 1H), 1.65 – 1.53 (m, 3H), 1.52 – 1.36 (m, 3H), 1.33 – 1.23 (m, 8H), 0.88 (t, *J* = 6.8 Hz, 3H). ¹³C NMR (101 MHz, CDCl₃) δ 129.0, 128.6, 39.9, 39.6, 37.8, 32.0, 30.4, 29.5, 27.1, 25.1, 22.8, 22.0, 20.2, 14.3. IR (ATR): 2954, 2924, 2855, 1455, 1374, 1202, 1036, 986, 870 cm⁻¹. HRMS calculated for C₁₄H₂₆S [M]⁺ 266.1755, found 266.1751.

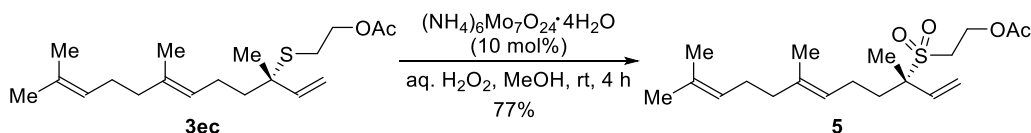
((R)-cyclohex-2-en-1-yl)((R)-octan-2-yl)sulfane ((R,R)-3db)

 Colorless oil, 90% yield, >20:1 *dr*, >20:1 *rr*, $[\alpha]_D^{24} = +145.6$ (*c* 1.0, CHCl₃). ¹H NMR (400 MHz, CDCl₃) δ 5.79 – 5.73 (m, 1H), 5.72 – 5.66 (m, 1H), 3.44 – 3.35 (m, 1H), 2.87 – 2.75 (m, 1H), 2.05 – 1.81 (m, 4H), 1.79 – 1.69 (m, 1H), 1.66 – 1.36 (m, 6H), 1.34 – 1.24 (m, 8H), 0.88 (t, *J* = 6.8 Hz, 3H). ¹³C NMR (101 MHz, CDCl₃) δ 129.3, 128.4, 39.7, 39.4, 37.5, 32.0, 30.2, 29.4, 27.2, 25.1, 22.8, 22.3, 19.8, 14.3. IR (ATR): 2954, 2924, 2855, 1455, 1374, 1203, 995, 870 cm⁻¹. HRMS calculated for C₁₄H₂₆S [M]⁺ 266.1755, found 266.1757.

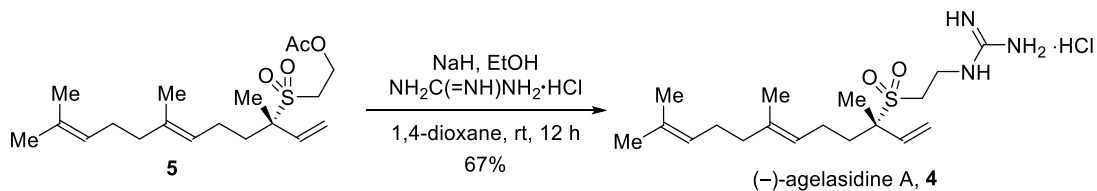
4. Total synthesis of (-)-agelasidine A



In a N_2 -filled glovebox, Josiphos (27.7 mg, 0.05 mmol) and DCE (4.0 mL) were added to a 20 mL vial containing $\text{Rh}(\text{cod})_2\text{SbF}_6$ (27.8 mg, 0.05 mmol). The resulting mixture was stirred for 10 min and then 1,3-diene **2c** (306.6 mg, 1.5 mmol) and thiol **1e** (120.2 mg, 1.0 mmol) were added. The mixture was held at 30 °C for 12 h. DCE was removed under reduced pressure and the pure sulfide **3ec** was obtained after column chromatography (hexanes/ EtOAc = 5/1) as a colorless oil (252.9 mg, 78% yield, >99:1 *er*, >20:1 *rr*). $[\alpha]^{24}_{\text{D}} = +8.2$ (*c* 1.0, CHCl_3). **¹H NMR** (500 MHz, CDCl_3) δ 5.79 (dd, $J = 17.4, 10.6$ Hz, 1H), 5.16 – 5.05 (m, 3H), 4.98 (d, $J = 17.4$ Hz, 1H), 4.14 (t, $J = 7.1$ Hz, 2H), 2.63 – 2.56 (m, 2H), 2.10 – 1.94 (m, 9H), 1.68 (s, 3H), 1.63 – 1.56 (m, 8H), 1.36 (s, 3H). **¹³C NMR** (126 MHz, CDCl_3) δ 171.0, 143.5, 135.8, 131.6, 124.5, 123.9, 113.0, 64.2, 50.7, 40.6, 39.8, 27.5, 26.9, 25.9, 23.7, 23.3, 21.1, 17.9, 16.2. **IR** (ATR): 2966, 2922, 1743, 1449, 1377, 1226, 1026, 997, 913 cm^{-1} . **HRMS** calculated for $\text{C}_{19}\text{H}_{33}\text{O}_2\text{S}$ $[\text{M}+\text{H}]^+$ 325.2201, found 325.2206. **Chiral SFC**: 250 mm CHIRALCEL IC, 2.0% *i*PrOH, 3.0 mL/min, 220 nm, 44 °C, nozzle pressure = 200 bar CO_2 , t_{R1} (minor) = 5.7 min, t_{R2} (major) = 6.1 min.



Based on the literature,³ $(\text{NH}_4)_6\text{Mo}_7\text{O}_{24}\cdot 4\text{H}_2\text{O}$ (90.2 mg, 0.073 mmol) and H_2O_2 (328.7 mg, 2.9 mmol, 30 wt% aqueous solution) were added to a solution of **3ec** (237.0 mg, 0.73 mmol) in MeOH (2 mL). The reaction mixture was stirred for 4 h at rt. MeOH was evaporated and the crude mixture was washed with aq. NaHCO_3 and extracted with Et_2O . The Et_2O was evaporated and followed by column chromatography (hexanes/ EtOAc = 3/1) to obtain the pure sulfone **5** as a colorless oil (200.4 mg, 77% yield). $[\alpha]^{24}_{\text{D}} = +12.4$ (*c* 1.0, CHCl_3). **¹H NMR** (500 MHz, CDCl_3) δ 6.00 (dd, $J = 17.6, 10.8$ Hz, 1H), 5.51 (d, $J = 10.8$ Hz, 1H), 5.39 (d, $J = 17.6$ Hz, 1H), 5.12 – 5.02 (m, 2H), 4.50 (t, $J = 6.6$ Hz, 2H), 3.24 (t, $J = 6.6$ Hz, 2H), 2.10 – 1.88 (m, 11H), 1.67 (s, 3H), 1.59 (s, 3H), 1.57 (s, 3H), 1.50 (s, 3H). **¹³C NMR** (126 MHz, CDCl_3) δ 170.8, 136.7, 135.7, 131.7, 124.3, 122.8, 120.8, 68.3, 57.1, 45.8, 39.8, 31.8, 26.7, 25.8, 22.2, 20.9, 17.8, 16.2, 16.1. **IR** (ATR): 2918, 1743, 1453, 1364, 1292, 1228, 1136, 1044, 933 cm^{-1} . **HRMS** calculated for $\text{C}_{19}\text{H}_{32}\text{O}_4\text{S}$ $[\text{M}]^+$ 356.2021, found 356.2029.



Following the reported procedure,⁴ sodium hydride (268.8 mg, 11.2 mmol) was treated with EtOH (8 ml) at 0 °C under a nitrogen atmosphere. To this solution was added guanidine hydrochloride (1.07 g, 11.2 mmol) at rt. After the mixture was stirred for 1 h, a white precipitate was observed. The solution was filtered and then concentrated under reduced pressure. The resulting guanidine was dissolved in a mixture of 1,4-dioxane (4 mL) and water (4 mL). The solution was cooled to 0 °C and a solution of compound **5** (100 mg, 0.28 mmol) in 1,4-dioxane (4 mL) was added dropwise over the course of 1 h. The cooling bath was removed, and the mixture was stirred for 12 h. 1,4-Dioxane was evaporated off and water was added to the residual oil. The aqueous layer was neutralized with 6 N hydrochloric acid and then extracted with DCM. The combined organic phase was dried with Na₂SO₄ and concentrated under reduced pressure. The residual oil was purified by column chromatography (DCM/MeOH = 3/1) to obtain (-)-agelasidine A hydrogen chloride salt (73.5 mg, 67%) as a white solid. $[\alpha]^{24}_{\text{D}} = +18.6$ (*c* 1.0, MeOH). [lit:⁵ $[\alpha]^{24}_{\text{D}} = +19.1$ (*c* 1.0, MeOH)] **¹H NMR** (500 MHz, CD₃OD) δ 6.01 (dd, *J* = 17.5, 10.8 Hz, 1H), 5.58 (d, *J* = 10.8 Hz, 1H), 5.50 (d, *J* = 17.5 Hz, 1H), 5.14 (t, *J* = 6.4 Hz, 1H), 5.11 – 5.05 (m, 1H), 4.85 (brs, 5H), 3.72 (t, *J* = 6.1 Hz, 2H), 3.34 – 3.28 (m, 3H), 2.13 – 1.81 (m, 8H), 1.67 (s, 3H), 1.60 (s, 6H), 1.53 (s, 3H). **¹³C NMR** (126 MHz, CD₃OD) δ 158.6, 137.4, 136.4, 132.3, 125.3, 124.3, 122.0, 69.2, 46.4, 40.7, 35.8, 33.1, 27.6, 25.9, 23.1, 17.8, 16.3, 16.0. **IR** (ATR): 3337, 2922, 1627, 1449, 1375, 1284, 1130, 1076, 1000, 935, 816 cm⁻¹. **HRMS** calculated for C₁₈H₃₄N₃O₂S [M]⁺ 356.2372, found 356.2387.

5. General procedure for 3,4-*anti*-Markovnikov hydrothiolation (for Table 2.1)

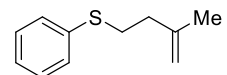
Method A:

In a N₂-filled glovebox, dppe (0.01 mmol) and DCE (0.40 mL) were added to a 1-dram vial containing [Rh(C₂H₄)₂Cl]₂ (0.005 mmol). The resulting mixture was stirred for 10 min, and then 1,3-diene **2** (0.40 mmol) and thiol **1** (0.20 mmol) were added. The mixture was held at 30 °C until no starting material was observed by TLC. The resulting mixture was then cooled to rt. The regioselectivities were determined by ¹H NMR analysis of the unpurified reaction mixture. Isolated yields (obtained by column chromatography on silica gel or preparative thin-layer chromatography) are reported.

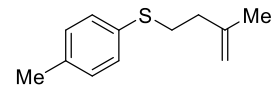
Method B:

In a N₂-filled glovebox, Xantphos (0.01 mmol) and DCE (0.40 mL) were added to a 1-dram vial containing [Rh(cod)Cl]₂ (0.005 mmol). The resulting mixture was stirred for 10 min, and then 3,5-dimethylbenzoic acid (12 mg, 0.08 mmol), 1,3-diene **2** (0.40 mmol) and thiol **1** (0.20 mmol) were added. The mixture was held at 30 °C until no starting material was observed by TLC. The resulting mixture was then cooled to rt. The regioselectivities were determined by ¹H NMR analysis of the unpurified reaction mixture. Isolated yields (obtained by column chromatography on silica gel or preparative thin-layer chromatography) are reported.

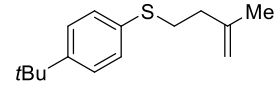
(3-methylbut-3-en-1-yl)(phenyl)sulfane (**6ad**)⁶

 Method A, colorless oil, 94% yield, >20:1 *rr*. ¹H NMR (500 MHz, CDCl₃) δ 7.44 – 7.33 (m, 4H), 7.26 – 7.22 (m, 1H), 4.87 (s, 1H), 4.82 (s, 1H), 3.10 (t, *J* = 8.0 Hz, 2H), 2.41 (t, *J* = 8.0 Hz, 2H), 1.82 (s, 3H). ¹³C NMR (126 MHz, CDCl₃) δ 144.0, 136.7, 129.2, 129.1, 126.0, 111.6, 37.4, 31.9, 22.5. IR (ATR): 2931, 1480, 1438, 889, 736, 689 cm⁻¹. HRMS calculated for C₁₁H₁₅S [M+H]⁺ 179.0894, found 179.0890.

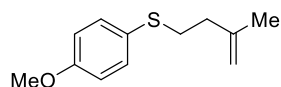
(3-methylbut-3-en-1-yl)(*p*-tolyl)sulfane (**6fd**)

 Method A, colorless oil, 95% yield, >20:1 *rr*. ¹H NMR (400 MHz, CDCl₃) δ 7.29 – 7.25 (m, 2H), 7.13 – 7.07 (m, 2H), 4.79 (s, 1H), 4.74 (s, 1H), 3.02 – 2.96 (m, 2H), 2.35 – 2.30 (m, 5H), 1.76 – 1.72 (m, 3H). ¹³C NMR (101 MHz, CDCl₃) δ 144.1, 136.3, 132.9, 130.2, 129.8, 111.5, 37.6, 32.8, 22.5, 21.2. IR (ATR): 2922, 1492, 1015, 889, 804 cm⁻¹. HRMS calculated for C₁₂H₁₇S [M+H]⁺ 193.1051, found 193.1047.

(4-(*tert*-butyl)phenyl)(3-methylbut-3-en-1-yl)sulfane (**6gd**)

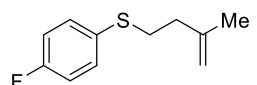
 Method A, colorless oil, 95% yield, >20:1 *rr*. ¹H NMR (400 MHz, CDCl₃) δ 7.34 – 7.27 (m, 4H), 4.82 – 4.78 (m, 1H), 4.78 – 4.72 (m, 1H), 3.05 – 2.98 (m, 2H), 2.35 (t, *J* = 7.8 Hz, 2H), 1.75 (s, 3H), 1.31 (s, 9H). ¹³C NMR (101 MHz, CDCl₃) δ 149.4, 144.1, 133.1, 129.6, 126.1, 111.5, 37.6, 34.6, 32.5, 31.5, 22.5. IR (ATR): 2962, 1120, 1013, 899, 819 cm⁻¹. HRMS calculated for C₁₅H₂₂S [M]⁺ 234.1442, found 234.1440.

(4-methoxyphenyl)(3-methylbut-3-en-1-yl)sulfane (6hd)⁷



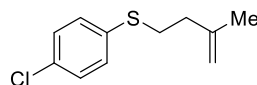
Method A, colorless oil, 68% yield, >20:1 *rr*. **¹H NMR** (400 MHz, CDCl₃) δ 7.38 – 7.33 (m, 2H), 6.88 – 6.81 (m, 2H), 4.78 (s, 1H), 4.71 (s, 1H), 3.80 (s, 3H), 2.97 – 2.88 (m, 2H), 2.34 – 2.25 (m, 2H), 1.72 (s, 3H). **¹³C NMR** (101 MHz, CDCl₃) δ 159.1, 144.1, 133.4, 126.7, 114.7, 111.5, 55.5, 37.7, 34.2, 22.5. **IR** (ATR): 2914, 2360, 1510, 1247, 1174, 1034, 829 cm⁻¹. **HRMS** calculated for C₁₂H₁₆OS [M]⁺ 208.0922, found 208.0927.

(4-fluorophenyl)(3-methylbut-3-en-1-yl)sulfane (6id)



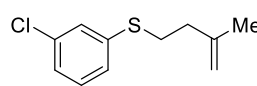
Method A, colorless oil, 82% yield, >20:1 *rr*. **¹H NMR** (400 MHz, CDCl₃) δ 7.38 – 7.31 (m, 2H), 7.03 – 6.97 (m, 2H), 4.79 (s, 1H), 4.72 (s, 1H), 3.02 – 2.93 (m, 2H), 2.30 (t, *J* = 7.7 Hz, 2H), 1.73 (s, 3H). **¹³C NMR** (126 MHz, CDCl₃) δ 161.9 (d, *J* = 245.7 Hz), 143.8, 132.5 (d, *J* = 7.6 Hz), 131.5, 116.2 (d, *J* = 21.4 Hz), 111.7, 37.5, 33.4, 22.4. **¹⁹F NMR** (376 MHz, CDCl₃) δ -116.2. **IR** (ATR): 2933, 1589, 1489, 1225, 1156, 890, 821 cm⁻¹. **HRMS** calculated for C₁₁H₁₃FS [M]⁺ 196.0722, found 196.0713.

(4-chlorophenyl)(3-methylbut-3-en-1-yl)sulfane (6jd)



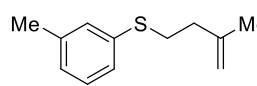
Method A, colorless oil, 93% yield, >20:1 *rr*. **¹H NMR** (400 MHz, CDCl₃) δ 7.32 – 7.24 (m, 4H), 4.82 (s, 1H), 4.75 (s, 1H), 3.05 – 2.99 (m, 2H), 2.34 (t, *J* = 7.7 Hz, 2H), 1.76 (s, 3H). **¹³C NMR** (101 MHz, CDCl₃) δ 143.7, 135.3, 132.1, 130.7, 129.2, 111.8, 37.3, 32.3, 22.4. **IR** (ATR): 2925, 2360, 1476, 1095, 1011, 891, 812 cm⁻¹. **HRMS** calculated for C₁₁H₁₃ClS [M]⁺ 212.0426, found 212.0417.

(3-chlorophenyl)(3-methylbut-3-en-1-yl)sulfane (6kd)



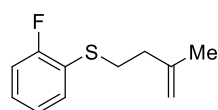
Method A, colorless oil, 91% yield, >20:1 *rr*. **¹H NMR** (400 MHz, CDCl₃) δ 7.31 – 7.28 (m, 1H), 7.21 – 7.17 (m, 2H), 7.16 – 7.12 (m, 1H), 4.82 (s, 1H), 4.76 (s, 1H), 3.07 – 3.00 (m, 2H), 2.35 (t, *J* = 7.7 Hz, 2H), 1.76 (s, 3H). **¹³C NMR** (101 MHz, CDCl₃) δ 143.6, 139.1, 134.8, 130.0, 128.3, 126.8, 126.0, 111.9, 37.1, 31.6, 22.4. **IR** (ATR): 2932, 2360, 1577, 1461, 890, 778, 677 cm⁻¹. **HRMS** calculated for C₁₁H₁₃ClS [M]⁺ 212.0426, found 212.0422.

(3-methylbut-3-en-1-yl)(*m*-tolyl)sulfane (6ld)



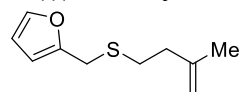
Method A, colorless oil, 92% yield, >20:1 *rr*. **¹H NMR** (400 MHz, CDCl₃) δ 7.22 – 7.11 (m, 3H), 7.03 – 6.96 (m, 1H), 4.81 (s, 1H), 4.76 (s, 1H), 3.08 – 2.98 (m, 2H), 2.39 – 2.30 (m, 5H), 1.76 (s, 3H). **¹³C NMR** (101 MHz, CDCl₃) δ 144.0, 138.8, 136.5, 130.0, 128.9, 126.9, 126.3, 111.6, 37.5, 32.0, 22.5, 21.5. **IR** (ATR): 2916, 1475, 888, 856, 770, 688 cm⁻¹. **HRMS** calculated for C₁₂H₁₆S [M]⁺ 192.0973, found 192.0970.

(2-fluorophenyl)(3-methylbut-3-en-1-yl)sulfane (6md)



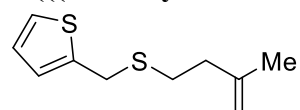
Method A, colorless oil, 91% yield, >20:1 *rr*. $^1\text{H NMR}$ (400 MHz, CDCl_3) δ 7.46 – 7.34 (m, 1H), 7.25 – 7.18 (m, 1H), 7.16 – 7.02 (m, 2H), 4.80 (s, 1H), 4.74 (s, 1H), 3.13 – 2.96 (m, 2H), 2.42 – 2.28 (m, 2H), 1.75 (s, 3H). $^{13}\text{C NMR}$ (126 MHz, CDCl_3) δ 161.7 (d, $J = 245.4$ Hz), 143.7, 132.2 (d, $J = 1.9$ Hz), 128.4 (d, $J = 7.9$ Hz), 124.6 (d, $J = 3.7$ Hz), 123.4 (d, $J = 17.6$ Hz), 115.8 (d, $J = 22.6$ Hz), 111.8, 37.5, 31.7 (d, $J = 2.5$ Hz), 22.4. $^{19}\text{F NMR}$ (376 MHz, CDCl_3) δ -109.9. **IR** (ATR): 2914, 2360, 1510, 1247, 1174, 1034, 829 cm^{-1} . **HRMS** calculated for $\text{C}_{11}\text{H}_{13}\text{FSNa}$ $[\text{M}+\text{Na}]^+$ 219.0620, found 219.0618.

2-(((3-methylbut-3-en-1-yl)thio)methyl)furan (6nd)



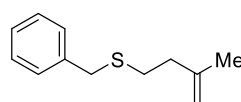
Method B, colorless oil, 64% yield, >20:1 *rr*. $^1\text{H NMR}$ (400 MHz, CDCl_3) δ 7.37 – 7.35 (m, 1H), 6.31 (dd, $J = 3.0, 1.7$ Hz, 1H), 6.19 – 6.17 (m, 1H), 4.77 (d, $J = 0.6$ Hz, 1H), 4.74 – 4.70 (m, 1H), 3.74 (s, 2H), 2.65 – 2.59 (m, 2H), 2.30 – 2.23 (m, 2H), 1.72 (s, 3H). $^{13}\text{C NMR}$ (101 MHz, CDCl_3) δ 152.0, 144.1, 142.2, 111.5, 110.6, 107.5, 37.7, 30.1, 28.5, 22.4. **IR** (ATR): 2919, 1649, 1150, 1010, 886, 735 cm^{-1} . **HRMS** calculated for $\text{C}_{10}\text{H}_{14}\text{OS}$ $[\text{M}]^+$ 182.0765, found 182.0757.

2-(((3-methylbut-3-en-1-yl)thio)methyl)thiophene (6od)



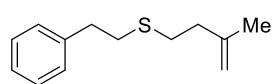
Method B, colorless oil, 65% yield, >20:1 *rr*. $^1\text{H NMR}$ (500 MHz, CDCl_3) δ 7.20 (dd, $J = 4.9, 1.4$ Hz, 1H), 6.95 – 6.88 (m, 2H), 4.77 (s, 1H), 4.71 (s, 1H), 3.94 (s, 2H), 2.61 (dd, $J = 8.4, 7.1$ Hz, 2H), 2.28 (t, $J = 7.7$ Hz, 2H), 1.71 (s, 3H). $^{13}\text{C NMR}$ (126 MHz, CDCl_3) δ 144.1, 142.3, 126.8, 126.2, 125.0, 111.5, 37.6, 30.8, 29.9, 22.4. **IR** (ATR): 2922, 1435, 1035, 889, 850 cm^{-1} . **HRMS** calculated for $\text{C}_{10}\text{H}_{15}\text{S}_2$ $[\text{M}+\text{H}]^+$ 199.0615, found 199.0623.

benzyl(3-methylbut-3-en-1-yl)sulfane (6pd)



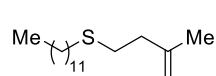
Method B, colorless oil, 90% yield, >20:1 *rr*. $^1\text{H NMR}$ (400 MHz, CDCl_3) δ 7.35 – 7.29 (m, 4H), 7.28 – 7.22 (m, 1H), 4.77 (s, 1H), 4.71 (s, 1H), 3.74 (s, 2H), 2.58 – 2.51 (m, 2H), 2.32 – 2.23 (m, 2H), 1.71 (s, 3H). $^{13}\text{C NMR}$ (101 MHz, CDCl_3) δ 144.2, 138.7, 129.0, 128.7, 127.1, 111.4, 37.7, 36.5, 29.7, 22.3. **IR** (ATR): 2923, 2360, 1057, 970, 794 cm^{-1} . **HRMS** calculated for $\text{C}_{12}\text{H}_{17}\text{S}$ $[\text{M}+\text{H}]^+$ 193.1051, found 193.0942.

(3-methylbut-3-en-1-yl)(phenethyl)sulfane (6qd)



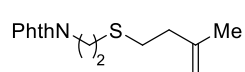
Method B, colorless oil, 54% yield, >20:1 *rr*. $^1\text{H NMR}$ (500 MHz, CDCl_3) δ 7.41 – 7.25 (m, 5H), 4.85 (s, 1H), 4.81 (s, 1H), 3.01 – 2.93 (m, 2H), 2.92 – 2.83 (m, 2H), 2.77 – 2.66 (m, 2H), 2.42 – 2.32 (m, 2H), 1.82 (s, 3H). $^{13}\text{C NMR}$ (126 MHz, CDCl_3) δ 144.3, 140.8, 128.7, 126.5, 111.4, 38.0, 36.6, 33.9, 30.7, 22.4. **IR** (ATR): 2923, 1496, 1453, 1030, 747 cm^{-1} . **HRMS** calculated for $\text{C}_{13}\text{H}_{19}\text{S}$ $[\text{M}+\text{H}]^+$ 207.1207, found 207.1205.

dodecyl(3-methylbut-3-en-1-yl)sulfane (6rd)



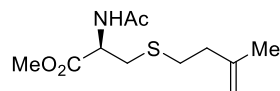
Method B, colorless oil, 55% yield, >20:1 *rr*. $^1\text{H NMR}$ (400 MHz, CDCl_3) δ 4.77 (s, 1H), 4.73 (s, 1H), 2.67 – 2.59 (m, 2H), 2.57 – 2.49 (m, 2H), 2.33 – 2.25 (m, 2H), 1.74 (s, 3H), 1.63 – 1.50 (m, 3H), 1.41 – 1.19 (m, 17H), 0.88 (t, J = 6.8 Hz, 3H). $^{13}\text{C NMR}$ (101 MHz, CDCl_3) δ 144.4, 111.3, 38.1, 32.4, 32.1, 30.5, 29.9, 29.84, 29.82, 29.79, 29.72, 29.5, 29.4, 29.1, 22.9, 22.4, 14.3. **IR** (ATR): 2922, 2852, 2360, 1457, 888, 721 cm^{-1} . **HRMS** calculated for $\text{C}_{17}\text{H}_{35}\text{S}$ $[\text{M}+\text{H}]^+$ 271.2459, found 271.2446.

3-(2-((3-methylbut-3-en-1-yl)thio)ethyl)isoindoline (6sd)



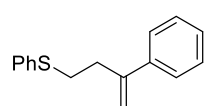
Method B, colorless oil, 62% yield, >20:1 *rr*. $^1\text{H NMR}$ (400 MHz, CDCl_3) δ 7.88 – 7.82 (m, 2H), 7.76 – 7.68 (m, 2H), 4.77 (s, 1H), 4.74 (s, 1H), 3.93 – 3.85 (m, 2H), 2.88 – 2.78 (m, 2H), 2.71 (dd, J = 8.3, 7.1 Hz, 2H), 2.30 (t, J = 7.7 Hz, 2H), 1.74 (s, 3H). $^{13}\text{C NMR}$ (101 MHz, CDCl_3) δ 168.3, 144.0, 134.2, 132.2, 123.5, 111.6, 37.8, 37.3, 30.2, 30.0, 22.3. **IR** (ATR): 2925, 1709, 1392, 1356, 1085, 714 cm^{-1} . **HRMS** calculated for $\text{C}_{15}\text{H}_{18}\text{NS}$ $[\text{M}+\text{H}]^+$ 276.1058, found 276.1067.

methyl *N*-acetyl-*S*-(3-methylbut-3-en-1-yl)-*L*-cysteinate (6bd)



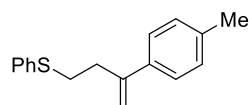
Method B, white solid, 63% yield, >20:1 *rr*. $^1\text{H NMR}$ (400 MHz, CDCl_3) δ 6.30 (d, J = 6.4 Hz, 1H), 4.83 (dt, J = 7.7, 5.0 Hz, 1H), 4.77 (s, 1H), 4.71 (s, 1H), 3.77 (s, 3H), 3.06 – 2.93 (m, 2H), 2.65 – 2.58 (m, 2H), 2.26 (t, J = 7.7 Hz, 2H), 2.04 (s, 3H), 1.72 (s, 3H). $^{13}\text{C NMR}$ (101 MHz, CDCl_3) δ 171.6, 170.0, 143.7, 111.7, 52.8, 52.1, 37.8, 34.4, 31.0, 23.3, 22.3. **IR** (ATR): 3274, 1744, 1538, 1436, 1211, 1175 cm^{-1} . **HRMS** calculated for $\text{C}_{11}\text{H}_{20}\text{NO}_3\text{S}$ $[\text{M}+\text{H}]^+$ 246.1164, found 246.1164.

phenyl(3-phenylbut-3-en-1-yl)sulfane (6ae)

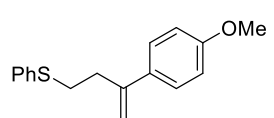


Method A, colorless oil, 82% yield, 15:1 *rr*. $^1\text{H NMR}$ (400 MHz, CDCl_3) δ 7.41 – 7.24 (m, 9H), 7.22 – 7.14 (m, 1H), 5.35 (s, 1H), 5.13 (s, 1H), 3.06 – 2.97 (m, 2H), 2.84 (t, J = 7.5 Hz, 2H). $^{13}\text{C NMR}$ (101 MHz, CDCl_3) δ 146.8, 140.5, 136.5, 129.6, 129.1, 128.6, 127.8, 126.3, 126.2, 113.9, 35.5, 32.7. **IR** (ATR): 2360, 1480, 1438, 898, 777, 737, 690 cm^{-1} . **HRMS** calculated for $\text{C}_{16}\text{H}_{16}\text{S}$ $[\text{M}]^+$ 240.0973, found 240.0979.

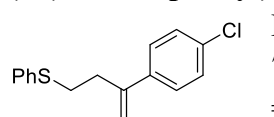
phenyl(3-(*p*-tolyl)but-3-en-1-yl)sulfane (6af)



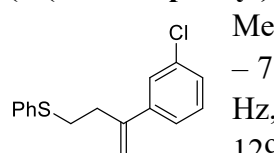
Method A, colorless oil, 88% yield, >20:1 *rr*. $^1\text{H NMR}$ (400 MHz, CDCl_3) δ 7.36 – 7.26 (m, 6H), 7.22 – 7.13 (m, 3H), 5.33 (d, J = 1.0 Hz, 1H), 5.09 (d, J = 1.0 Hz, 1H), 3.06 – 2.99 (m, 2H), 2.87 – 2.79 (m, 2H), 2.37 (s, 3H). $^{13}\text{C NMR}$ (101 MHz, CDCl_3) δ 146.5, 137.6, 137.5, 136.6, 129.5, 129.3, 129.0, 126.2, 126.1, 113.1, 35.5, 32.7, 21.3. **IR** (ATR): 2920, 2360, 1480, 1438, 1025, 823, 736 cm^{-1} . **HRMS** calculated for $\text{C}_{17}\text{H}_{18}\text{S}$ $[\text{M}]^+$ 254.1129, found 254.1136.

(3-(4-methoxyphenyl)but-3-en-1-yl)(phenyl)sulfane (6ag)

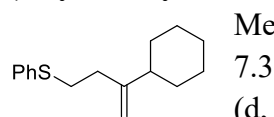
Method A, colorless oil, 74% yield, >20:1 *rr*. **¹H NMR** (500 MHz, CDCl₃) δ 7.41 – 7.31 (m, 6H), 7.27 – 7.23 (m, 1H), 6.95 – 6.90 (m, 2H), 5.34 (d, *J* = 1.2 Hz, 1H), 5.10 (d, *J* = 1.2 Hz, 1H), 3.88 (s, 3H), 3.12 – 3.04 (m, 2H), 2.92 – 2.84 (m, 2H). **¹³C NMR** (126 MHz, CDCl₃) δ 159.4, 146.0, 136.6, 132.8, 129.5, 129.1, 127.4, 126.1, 114.0, 112.3, 55.5, 35.5, 32.7. **IR** (ATR): 2957, 1605, 1512, 1249, 1184, 1028, 889, 730 cm⁻¹. **HRMS** calculated for C₁₇H₁₈OS [M]⁺ 270.1078, found 270.1078.

(3-(4-chlorophenyl)but-3-en-1-yl)(phenyl)sulfane (6ah)

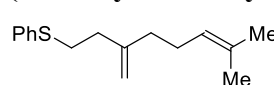
Method A, colorless oil, 95% yield, 13:1 *rr*. **¹H NMR** (400 MHz, CDCl₃) δ 7.36 – 7.16 (m, 9H), 5.33 (s, 1H), 5.14 (s, 1H), 3.03 – 2.96 (m, 2H), 2.81 (t, *J* = 8.0 Hz, 2H). **¹³C NMR** (101 MHz, CDCl₃) δ 145.6, 138.9, 136.3, 133.6, 129.7, 129.1, 128.7, 127.6, 126.3, 114.5, 35.3, 32.6. **IR** (ATR): 2922, 1491, 1438, 1091, 1011, 902, 833, 736 cm⁻¹. **HRMS** calculated for C₁₆H₁₅ClS [M]⁺ 274.0583, found 274.0597.

(3-(3-chlorophenyl)but-3-en-1-yl)(phenyl)sulfane (6ai)

Method A, colorless oil, 86% yield, 8:1 *rr*. **¹H NMR** (400 MHz, CDCl₃) δ 7.38 – 7.12 (m, 9H), 5.36 (s, 1H), 5.17 (s, 1H), 3.10 – 2.91 (m, 2H), 2.80 (t, *J* = 7.6 Hz, 2H). **¹³C NMR** (101 MHz, CDCl₃) δ 145.6, 142.4, 136.2, 134.6, 129.8, 129.7, 129.1, 127.8, 126.5, 126.3, 124.5, 115.1, 35.3, 32.6. **IR** (ATR): 2917, 1560, 1478, 901, 883, 789, 736 cm⁻¹. **HRMS** calculated for C₁₆H₁₅ClS [M]⁺ 274.0583, found 274.0574.

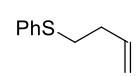
(4-cyclohexylbut-3-en-1-yl)(phenyl)sulfane (6aj)

Method A, colorless oil, 60% yield, >20:1 *rr*. **¹H NMR** (400 MHz, CDCl₃) δ 7.37 – 7.33 (m, 2H), 7.32 – 7.26 (m, 2H), 7.21 – 7.15 (m, 1H), 4.82 (s, 1H), 4.76 (d, *J* = 1.3 Hz, 1H), 3.06 – 2.99 (m, 2H), 2.42 – 2.33 (m, 2H), 1.93 – 1.60 (m, 7H), 1.34 – 1.08 (m, 4H). **¹³C NMR** (101 MHz, CDCl₃) δ 153.6, 137.0, 129.2, 129.1, 126.0, 108.5, 44.4, 34.7, 32.7, 32.6, 26.9, 26.5. **IR** (ATR): 2923, 2850, 1480, 1438, 1025, 887, 735 cm⁻¹. **HRMS** calculated for C₁₆H₂₃S [M+H]⁺ 247.1521, found 247.1529.

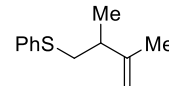
(5-methyl-3-methyleneoct-6-en-1-yl)(phenyl)sulfane (6aa)

Method A, colorless oil, 60% yield, >20:1 *rr*. **¹H NMR** (500 MHz, CDCl₃) δ 7.41 (d, *J* = 7.6 Hz, 2H), 7.38 – 7.32 (m, 2H), 7.24 (t, *J* = 7.3 Hz, 1H), 5.16 (t, *J* = 6.0 Hz, 1H), 4.89 (s, 1H), 4.87 (s, 1H), 3.14 – 3.04 (m, 2H), 2.43 (t, *J* = 7.8 Hz, 2H), 2.21 – 2.05 (m, 4H), 1.75 (s, 3H), 1.66 (s, 3H). **¹³C NMR** (126 MHz, CDCl₃) δ 147.8, 136.8, 132.0, 129.3, 129.1, 126.0, 124.0, 110.6, 36.1, 35.9, 32.3, 26.6, 25.9, 17.9. **IR** (ATR): 2924, 2360, 1438, 1025, 891, 736 cm⁻¹. **HRMS** calculated for C₁₆H₂₃S [M+H]⁺ 247.1521, found 247.1522.

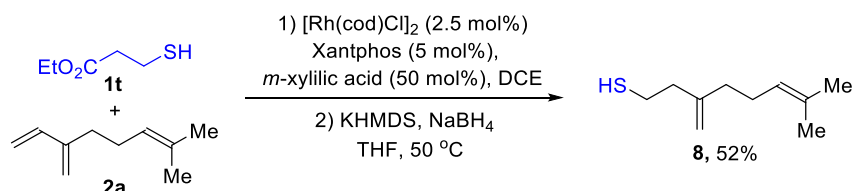
but-3-en-1-yl(phenyl)sulfane (**6ak**)⁸

 Method A, colorless oil, 28% yield. ¹H NMR (400 MHz, CDCl₃) δ 7.43 – 7.29 (m, 4H), 7.23 (d, *J* = 5.9 Hz, 1H), 5.98 – 5.85 (m, 1H), 5.20 – 5.06 (m, 2H), 3.08 – 2.97 (m, 2H), 2.51 – 2.39 (m, 2H). ¹³C NMR (126 MHz, CDCl₃) δ 136.6, 136.6, 129.5, 129.1, 126.1, 116.4, 33.5, 33.2. IR (ATR): 2967, 1584, 1480, 1438, 1091, 1025, 993, 915, 736 cm⁻¹. HRMS calculated for C₁₀H₁₂S [M]⁺ 164.0660, found 164.0664.

(2,3-dimethylbut-3-en-1-yl)(phenyl)sulfane (**6al**)

 Method A, colorless oil, 73% yield. ¹H NMR (500 MHz, CDCl₃) δ 7.43 – 7.38 (m, 2H), 7.37 – 7.31 (m, 2H), 7.26 – 7.20 (m, 1H), 4.91 – 4.81 (m, 2H), 3.11 (dd, *J* = 12.5, 6.7 Hz, 1H), 2.91 (dd, *J* = 12.5, 7.6 Hz, 1H), 2.58 – 2.46 (m, 1H), 1.78 (d, *J* = 0.7 Hz, 3H), 1.23 (d, *J* = 7.6 Hz, 3H). ¹³C NMR (126 MHz, CDCl₃) δ 148.4, 137.3, 129.2, 129.0, 125.9, 111.0, 40.7, 39.4, 19.5, 19.2. IR (ATR): 2965, 1645, 1584, 1480, 1438, 1374, 890, 735, 689 cm⁻¹. HRMS calculated for C₁₂H₁₆S [M]⁺ 192.0973, found 192.0980.

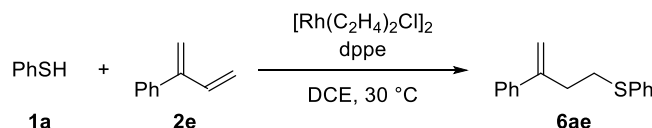
Synthesis of compound **8**



In a N₂-filled glovebox, Xantphos (4.6 mg, 0.008 mmol) and DCE (0.60 mL) were added to a 1-dram vial containing [Rh(cod)Cl]₂ (2.0 mg, 0.004 mmol). The resulting mixture was stirred for 10 min, and then 3,5-dimethylbenzoic acid (12 mg, 0.08 mmol), myrcene (**2a**, 43.6 mg, 0.32 mmol) and thiol **1t** (21.5 mg, 0.16 mmol) were added. The mixture was held at 30 °C until no starting material was observed by TLC. DCE was removed under reduced pressure. The residual oil was dissolved in THF (1.5 mL), followed by adding KHMDS (95.8 mg, 0.48 mmol) and NaBH₄ (1.2 mg, 0.032 mmol) under a nitrogen atmosphere. The reaction mixture was stirred for 12 h at 50 °C. After cooled to 0 °C, 1M HCl was added to quench the reaction. The residue was extracted with EtOAc and the resulting organic layer was washed with saturated brine. The combined organic layer was concentrated and then purified by flash column chromatography on silica gel (hexane) to yield the desired product **8** as a colorless oil (14.2 mg, 52% yield, >20:1 *rr*). ¹H NMR (400 MHz, CDCl₃) δ 5.10 (t, *J* = 6.4 Hz, 1H), 4.84 (s, 1H), 4.79 (s, 1H), 2.69 – 2.58 (m, 2H), 2.34 (t, *J* = 7.3 Hz, 2H), 2.18 – 2.08 (m, 2H), 2.06 – 1.97 (m, 2H), 1.69 (s, 3H), 1.61 (s, 3H), 1.43 (t, *J* = 7.6 Hz, 1H). ¹³C NMR (126 MHz, CDCl₃) δ 147.2, 132.1, 124.0, 111.2, 40.6, 35.9, 26.5, 25.9, 23.0, 17.9. IR (ATR): 2924, 1737, 1446, 1375, 1228, 1007 cm⁻¹. HRMS calculated for C₁₀H₁₈S [M]⁺ 170.1129, found 170.1123.

6. Mechanism studies for 3,4-*anti*-Markovnikov hydrothiolation

6.1 Kinetic studies:



The kinetic profile of the reaction was studied by obtaining initial rates with different concentrations of thiophenol (**1a**), 1,3-diene **2e**, and Rh-catalyst. No products of decomposition are observed for the system. The rates were monitored by GC-FID analysis using 1,3,5-trimethoxybenzene as an internal standard.

Determination of the reaction order in catalyst

Representative procedure (entry 1):

In a N_2 -filled glove box, a 0.0125M catalyst solution was prepared by combining $[\text{Rh}(\text{C}_2\text{H}_4)_2\text{Cl}]_2$ (2.4 mg, 0.00625 mmol), dppe (5.0 mg, 0.0125 mmol), and DCE (1.0 mL). A solution of reagents was prepared by combining **1a** (55.1 mg, 0.50 mmol), **2e** (97.7 mg, 0.750 mmol), and DCE (1.0 mL). A vial was charged with a stir bar and 1,3,5-trimethoxybenzene (6.0 mg, 0.036 mmol). Catalyst solution (80 μL) was added to the vial, followed by 0.2 mL of reagent solution. Additional DCE was added to the vial to make a total reaction volume of 0.4 mL, and the vial was sealed with a Teflon cap. Aliquots (10 μL) were taken every 5 minutes and quenched in 2 mL of EtOAc . The reaction halts in EtOAc . The amount of **6ae** was monitored by GC-FID analysis.

Table S5. Observed rate versus catalyst concentration for 3,4-*anti*-Markovnikov hydrothiolation

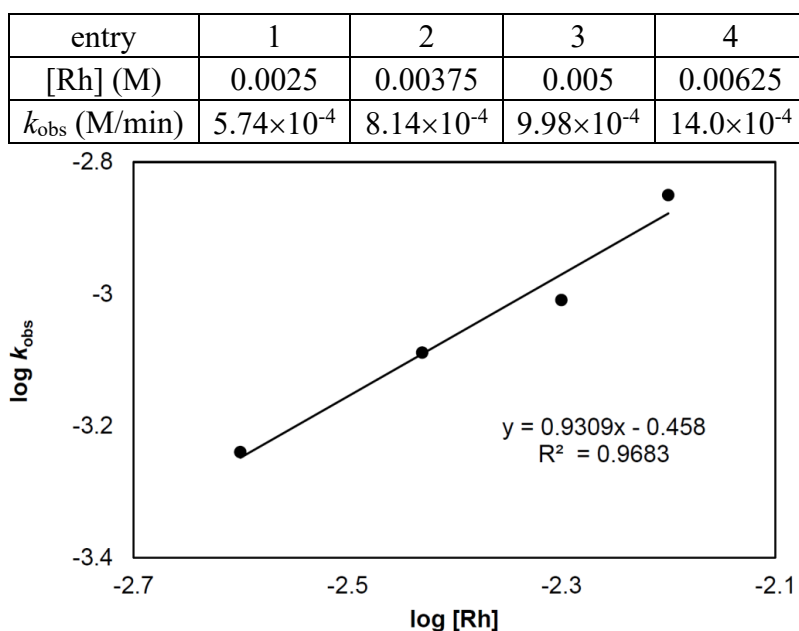


Figure S14. Plot of $\log k_{\text{obs}}$ vs $\log [\text{Rh}]$ for 3,4-*anti*-Markovnikov hydrothiolation (first order)

Determination of the reaction order in diene **2e**

Representative procedure (entry 1):

In a N₂-filled glove box, a 0.005M catalyst solution was prepared by combining [Rh(C₂H₄)₂Cl]₂ (1.9 mg, 0.005 mmol), dppe (4.0 mg, 0.01 mmol), and DCE (2.0 mL). A solution of **1a** (110.2 mg, 1.0 mmol) in DCE (2.0 mL) was prepared. A vial was charged with a stir bar, 1,3,5-trimethoxybenzene (6.0 mg, 0.036 mmol), and **2e** (13.0 mg, 0.1 mmol). Catalyst solution (0.2 mL) was added to the vial, followed by 0.2 mL of **1a** solution, and the vial was sealed with a Teflon cap. Aliquots (10 μL) were taken every 5 minutes and quenched in 2 mL of EtOAc. The reaction halts in EtOAc. The amount of **6ae** was monitored by GC-FID analysis.

Table S6. Observed rate versus 1,3-diene **2e** concentration for 3,4-*anti*-Markovnikov hydrothiolation

entry	1	2	3	4	5
[2e] (Initial) (M)	0.25	0.5	0.75	1.0	1.25
<i>k</i> _{obs} (M/min)	1.82×10 ⁻⁴	3.67×10 ⁻⁴	5.88×10 ⁻⁴	7.58×10 ⁻⁴	8.93×10 ⁻⁴

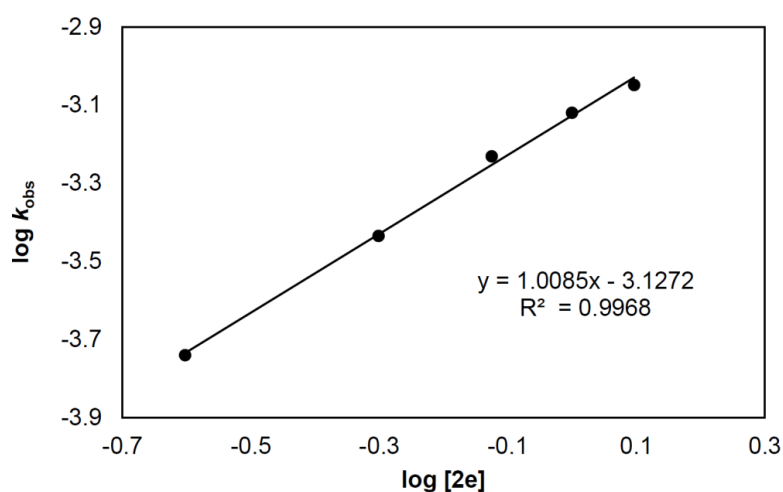


Figure S15. Plot of log*k*_{obs} vs log[**2e**] for 3,4-*anti*-Markovnikov hydrothiolation (first order)

Determination of the reaction order in thiophenol (**1a**)

Representative procedure (entry 1):

In a N₂-filled glove box, a 0.005M catalyst solution was prepared by combining [Rh(C₂H₄)₂Cl]₂ (1.9 mg, 0.005 mmol), dppe (4.0 mg, 0.01 mmol), and DCE (2.0 mL). A solution of **2e** (130.2 mg, 1.0 mmol) in DCE (2.0 mL) was prepared. A vial was charged with a stir bar, 1,3,5-trimethoxybenzene (6.0 mg, 0.036 mmol), and **1a** (6.0 mg, 0.05 mmol). Catalyst solution (0.2 mL) was added to the vial, followed by 0.2 mL of **2e** solution, and the vial was sealed with a Teflon cap. Aliquots (10 μL) were taken every 5 minutes and quenched in 2 mL of EtOAc. The reaction halts in EtOAc. The amount of **6ae** was monitored by GC-FID analysis.

Table S7. Observed rate versus thiophenol **1a** concentration for 3,4-*anti*-Markovnikov hydrothiolation

entry	1	2	3	4	5
[1a] (Initial) (M)	0.125	0.25	0.375	0.5	0.625
k_{obs} (M/min)	5.81×10^{-4}	4.57×10^{-4}	3.47×10^{-4}	2.86×10^{-4}	2.45×10^{-4}

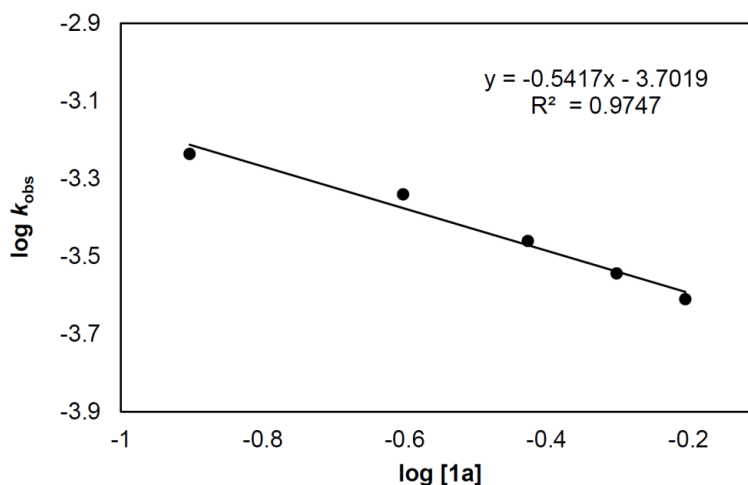
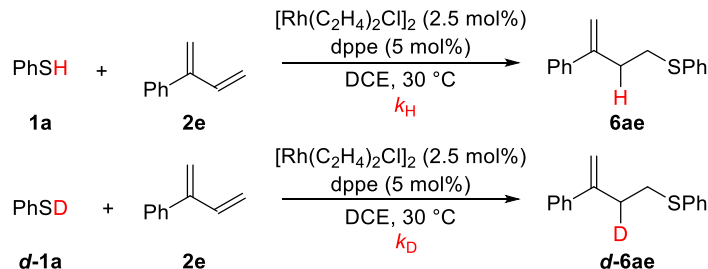
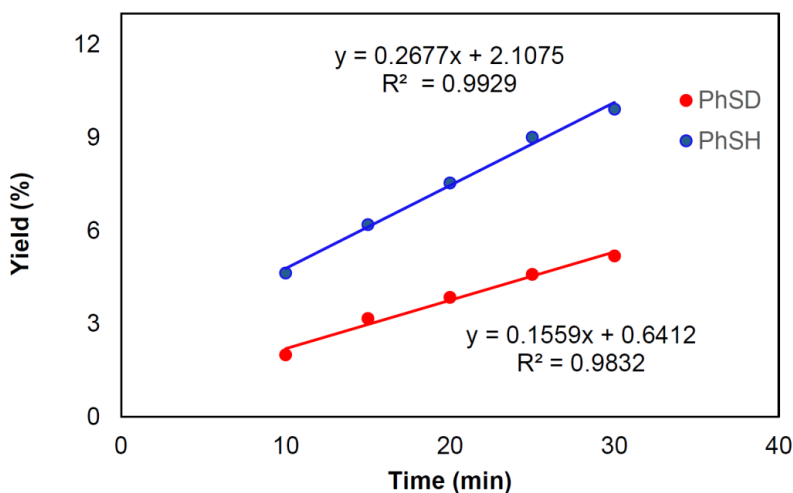


Figure S16. Plot of $\log k_{\text{obs}}$ vs $\log [1a]$ for 3,4-*anti*-Markovnikov hydrothiolation (-0.5 order)

6.2 Initial rate *KIE* study

In a N_2 -filled glove box, a 0.005M catalyst solution was prepared by combining $[\text{Rh}(\text{C}_2\text{H}_4)_2\text{Cl}]_2$ (1.0 mg, 0.0025 mmol), dppe (2.0 mg, 0.005 mmol), and DCE (1.0 mL). A solution of **2e** (65.1 mg, 0.5 mmol) in DCE (1.0 mL) was prepared. A vial was charged with a stir bar, 1,3,5-trimethoxybenzene (6.0 mg, 0.036 mmol), and **1a** (11.0 mg, 0.1 mmol) or *d*-**1a** (11.1 mg, 0.1 mmol). Catalyst solution (0.2 mL) was added to the vial, followed by 0.2 mL of **2e** solution, and the vial was sealed with a Teflon cap. Aliquots (10 μL) were taken every 5 minutes and quenched in 2 mL of EtOAc. The reaction halts in EtOAc. The amount of **6ae** was monitored by GC-FID analysis.





adjusted initial rate of deuterio species (considering 14% PhSH):

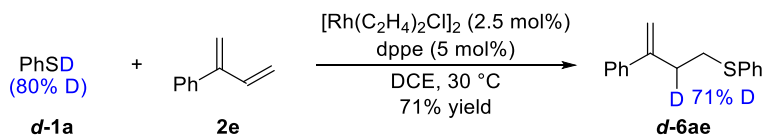
$$0.156 = 0.86 k_D + 0.14 \times 0.268$$

$$k_D = 0.138$$

$$\text{Calculation of KIE: } k_H/k_D = 0.268/0.138 = 1.9$$

Figure S17. Initial rate *KIE* for 3,4-*anti*-Markovnikov hydrothiolation

6.3 Deuterium-labeling study



In a N_2 -filled glovebox, dppe (2.0 mg, 0.005 mmol) and DCE (0.40 mL) were added to a 1-dram vial containing $[\text{Rh}(\text{C}_2\text{H}_4)_2\text{Cl}]_2$ (1.0 mg, 0.0025 mmol). The resulting mixture was stirred for 10 min, and then 1,3-diene **2e** (19.5 mg, 0.15 mmol) and thiol **d-1a** (11.1 mg, 0.10 mmol) were added. The mixture was held at 30 °C until no starting material was observed by TLC. The resulting mixture was then cooled to rt. The product **d-6ae** (17.1 mg, 71% yield) was purified by preparative thin-layer chromatography (hexanes/ EtOAc = 40/1). $^1\text{H NMR}$ (500 MHz, CDCl_3) δ 7.40 – 7.27 (m, 9H), 7.21 – 7.16 (m, 1H), 5.34 (s, 1H), 5.12 (s, 1H), 3.04 – 2.97 (m, 2H), 2.85 – 2.80 (m, 1.29H).

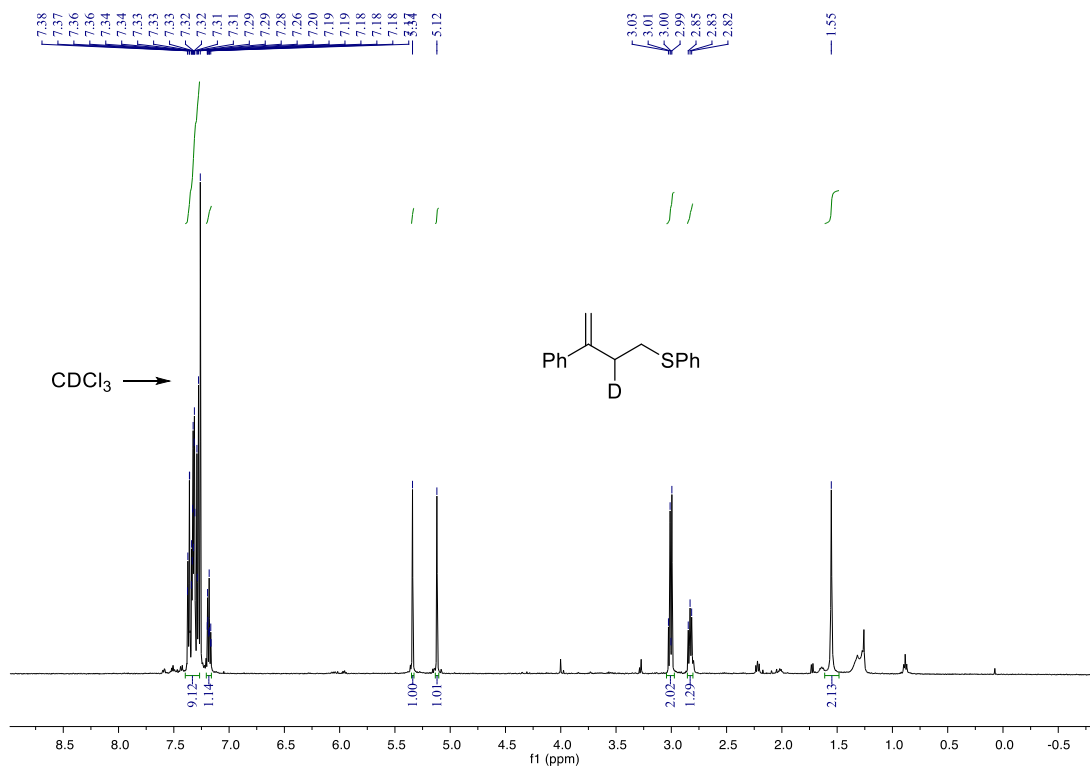


Figure S18. $^1\text{H NMR}$ [500 MHz, CDCl_3 (δ 7.26 ppm)] for *d*-6ae

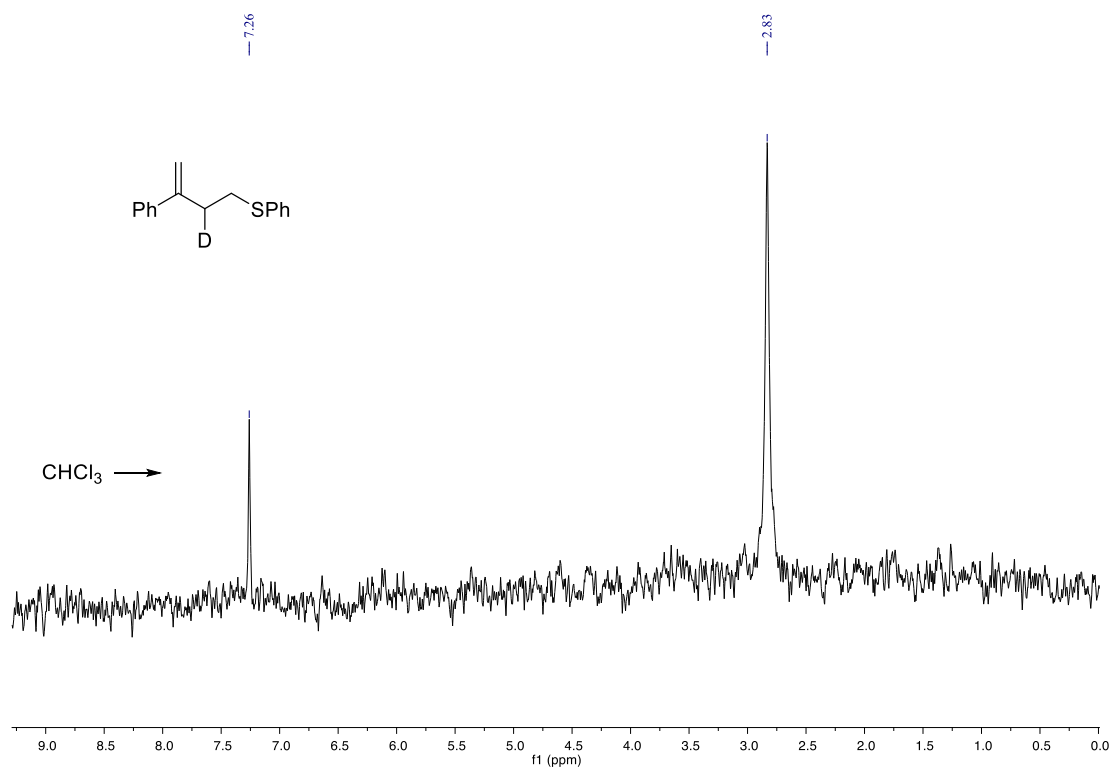


Figure S19. $^2\text{H NMR}$ [500 MHz, CHCl_3 (δ 7.26 ppm)] for *d*-6ae

6.4 NMR studies

In a N₂-filled glovebox, dppe (8.0 mg, 0.02 mmol) and DCE-*d*₄ (0.80 mL) were added to a 1-dram vial containing [Rh(C₂H₄)₂Cl]₂ (3.9 mg, 0.01 mmol). The resulting mixture was stirred for 10 min and then thiophenol (**1a**, 22.0 mg, 0.20 mmol) was added. The reaction mixture was transferred to a J. Young NMR tube to perform ¹H NMR and ³¹P NMR spectroscopy. A resonance at -15.8 ppm was observed in less than ten minutes at rt in the ¹H NMR spectrum (Figure S20) and an equivalent phosphine resonance in the ³¹P NMR spectrum [doublet (δ = 52.2 ppm, *J*_{Rh-P} = 94 Hz)] was observed (Figure S21). The 1,3-diene **2e** (26.0 mg, 0.20 mmol) was then added to this mixture, and we observed the same Rh-H resonance and equivalent resonances in the ³¹P NMR spectrum during the whole reaction progress. Based on these studies and the kinetic study, we labeled the intermediate **III'** as the resting state for 3,4-*anti*-Markovnikov hydrothiolation.

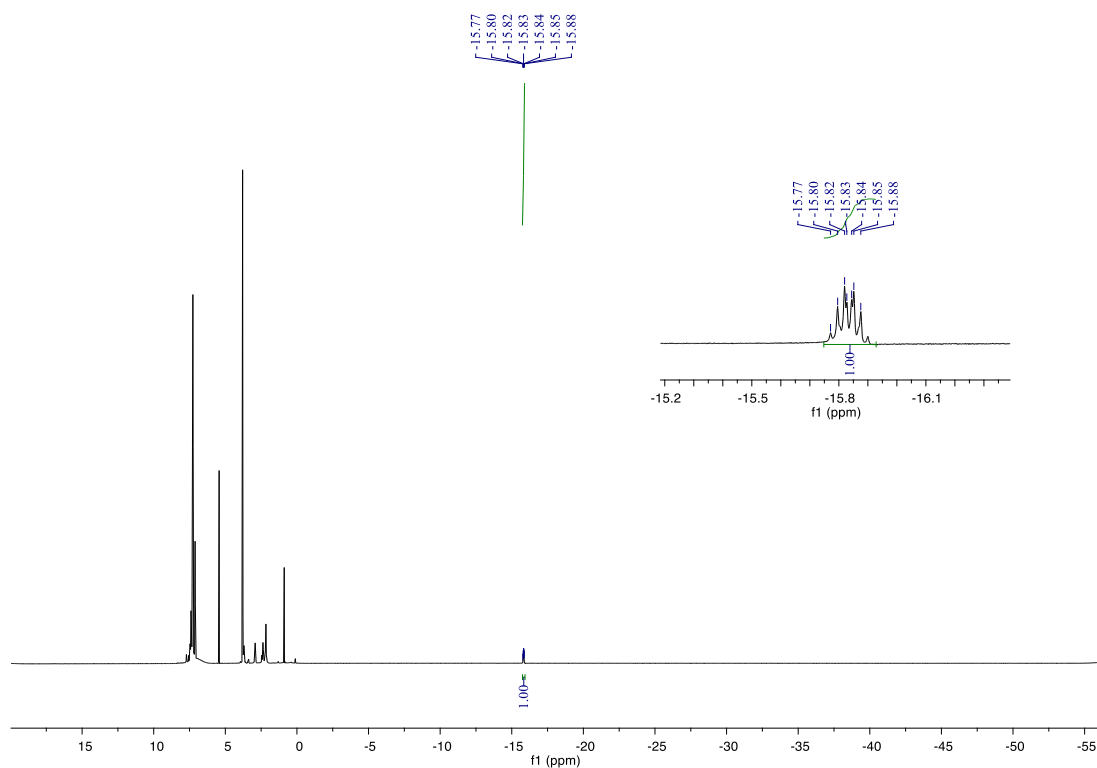


Figure S20. ¹H NMR (500 MHz) spectrum for a mixture of [Rh(dppe)Cl]₂ and thiophenol (**1a**) in DCE-*d*₄ (δ 3.79 ppm)

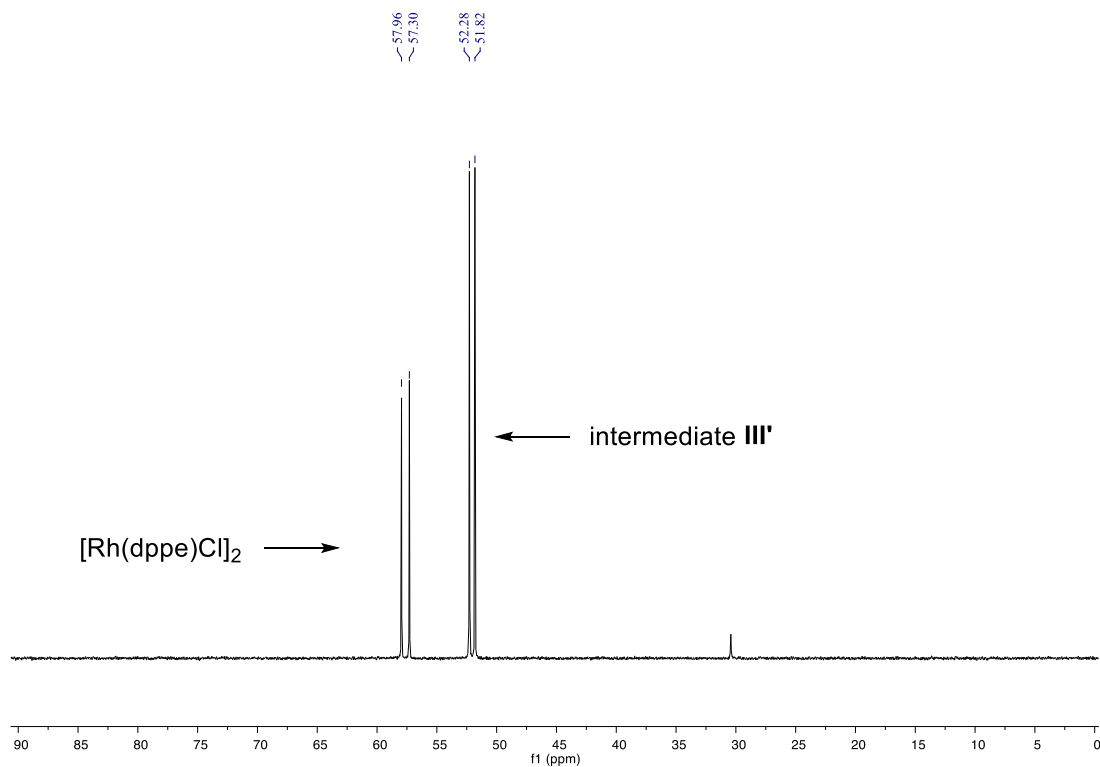
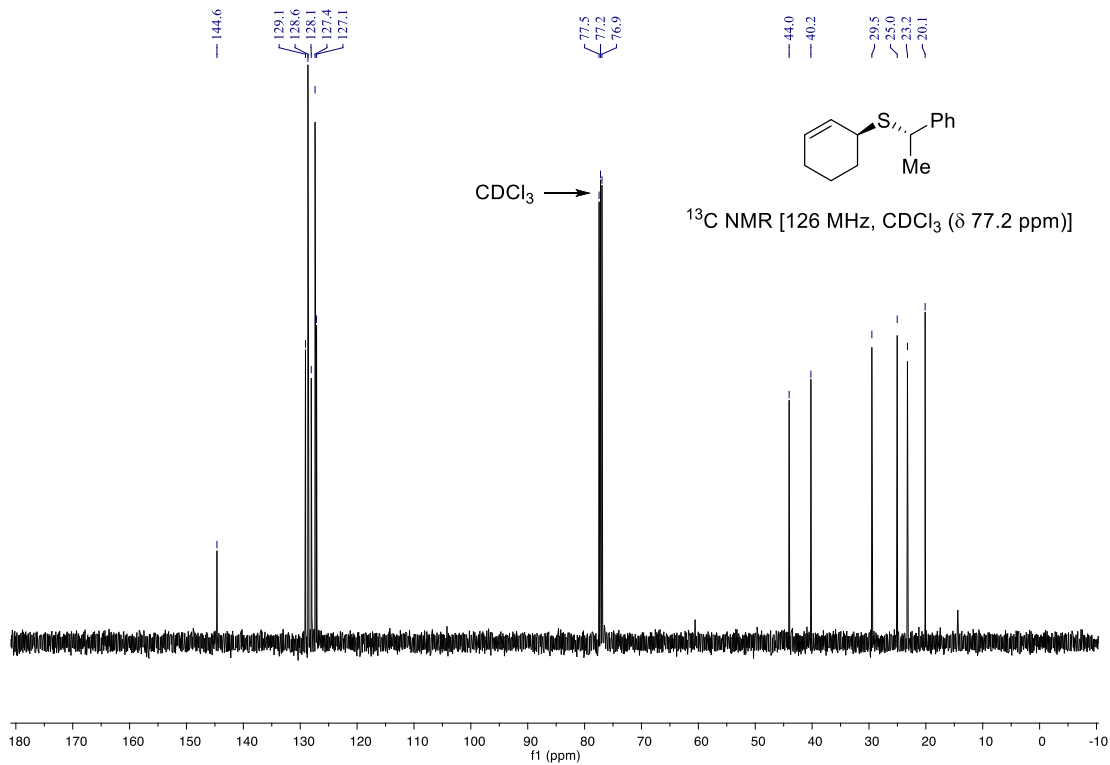
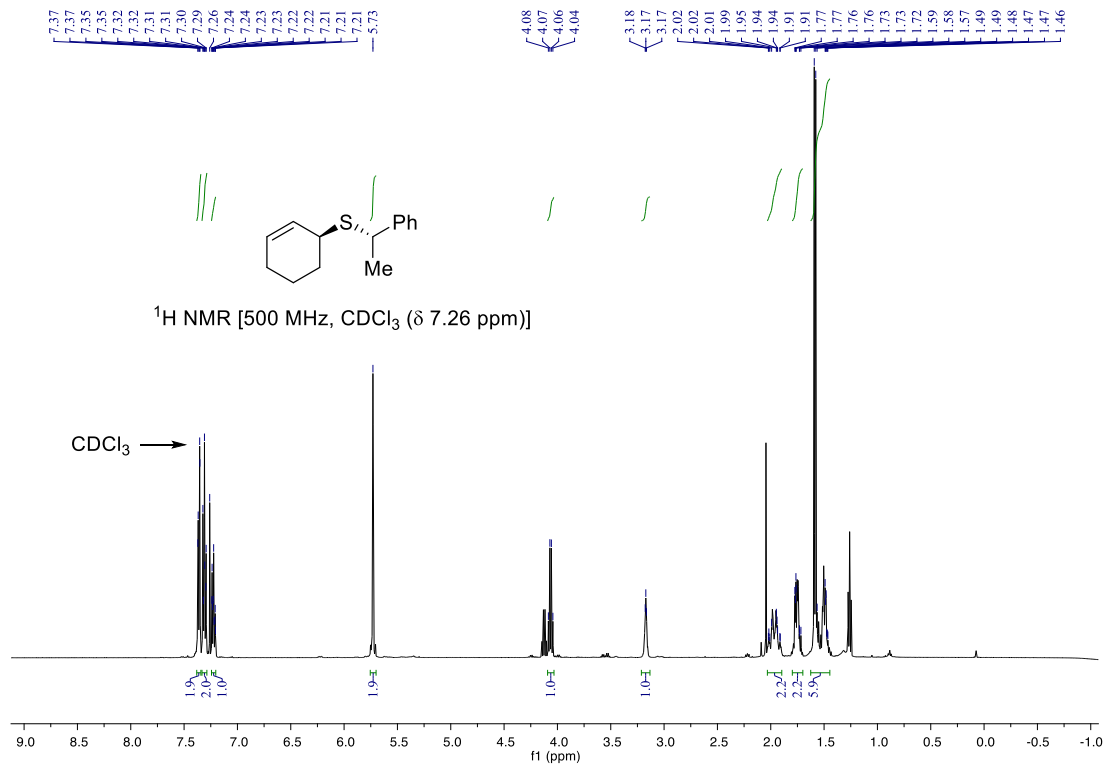


Figure S21. ^{31}P NMR (202 MHz) spectrum for a mixture of $[\text{Rh}(\text{dppe})\text{Cl}]_2$ and thiolphenol (**1a**) in $\text{DCE-}d_4$

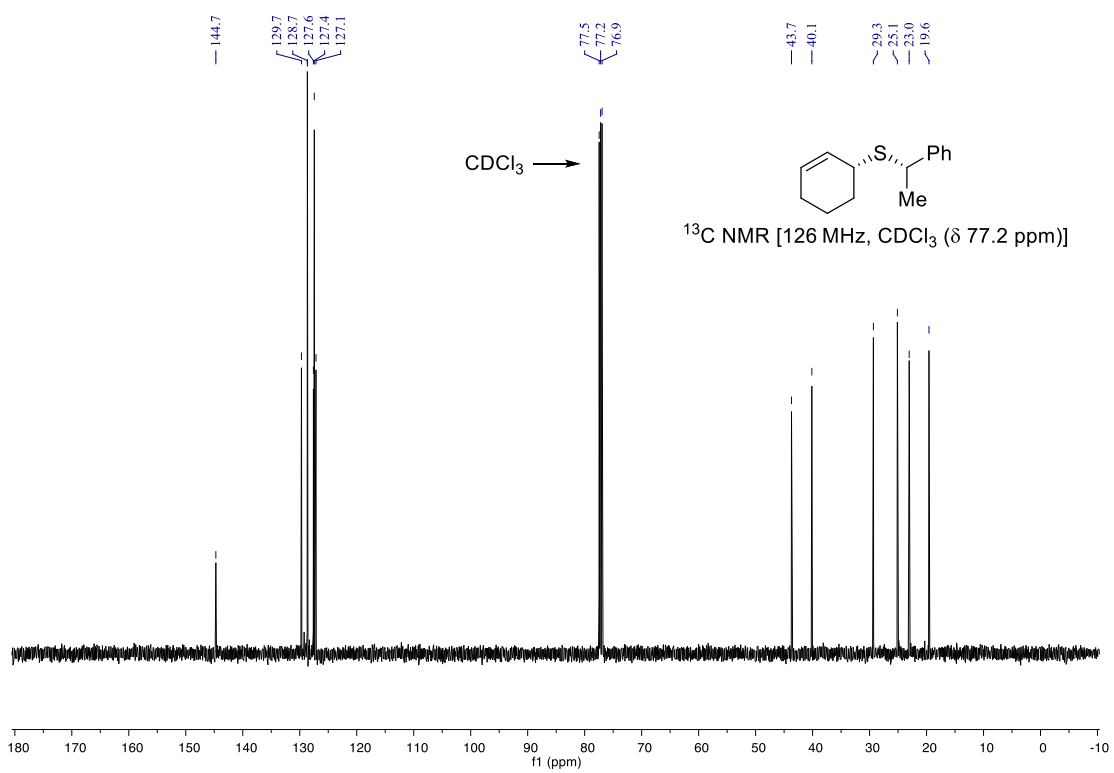
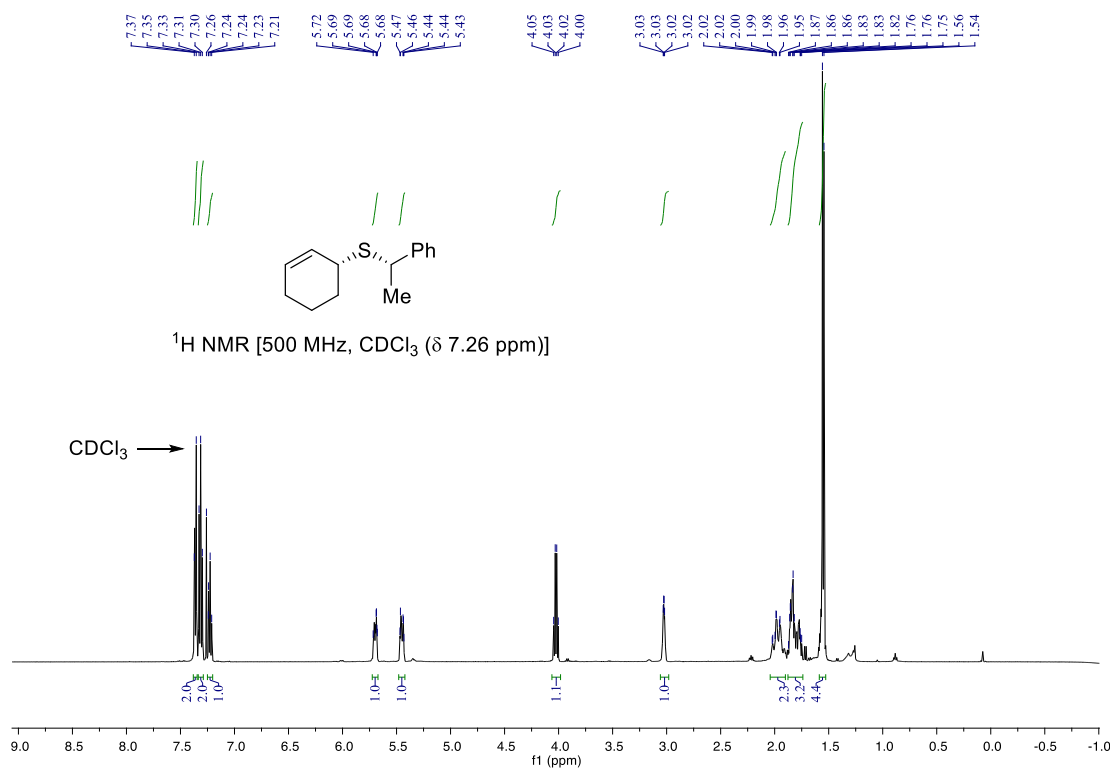
7. References

- (1) Fustero, S.; Bello, P.; Miró, J.; Simón, A.; del Pozo, C. *Chem. Eur. J.* **2012**, *18*, 10991.
- (2) Kennemur, J. L.; Kortman, G. D.; Hull, K. L. *J. Am. Chem. Soc.* **2016**, *138*, 11914.
- (3) Jeyakumar, K.; Chakravarthy, D. R.; Chand, D. K. *Catal. Commun.* **2009**, *10*, 1948.
- (4) Ichikawa, Y.; Kashiwagi, T.; Urano, N. *J. Chem. Soc., Perkin Trans. 1*, **1992**, 1497.
- (5) Nakamura, H.; Wu, H.; Kobayashi, J.; Ohizumi, Y. *Tetrahedron Lett.* **1983**, *24*, 4105.
- (6) Cohen, T.; Kreethadumrongdat, T.; Liu, X.; Kulkarni, V. *J. Am. Chem. Soc.* **2001**, *123*, 3478.
- (7) Shigehisa, H.; Ano, T.; Honma, H.; Ebisawa, K.; Hiroya, K. *Org. Lett.* **2016**, *18*, 3622.
- (8) Coulter, M. M.; Kou, K. G. M.; Galligan, B.; Dong, V. M. *J. Am. Chem. Soc.* **2010**, *132*, 16330.

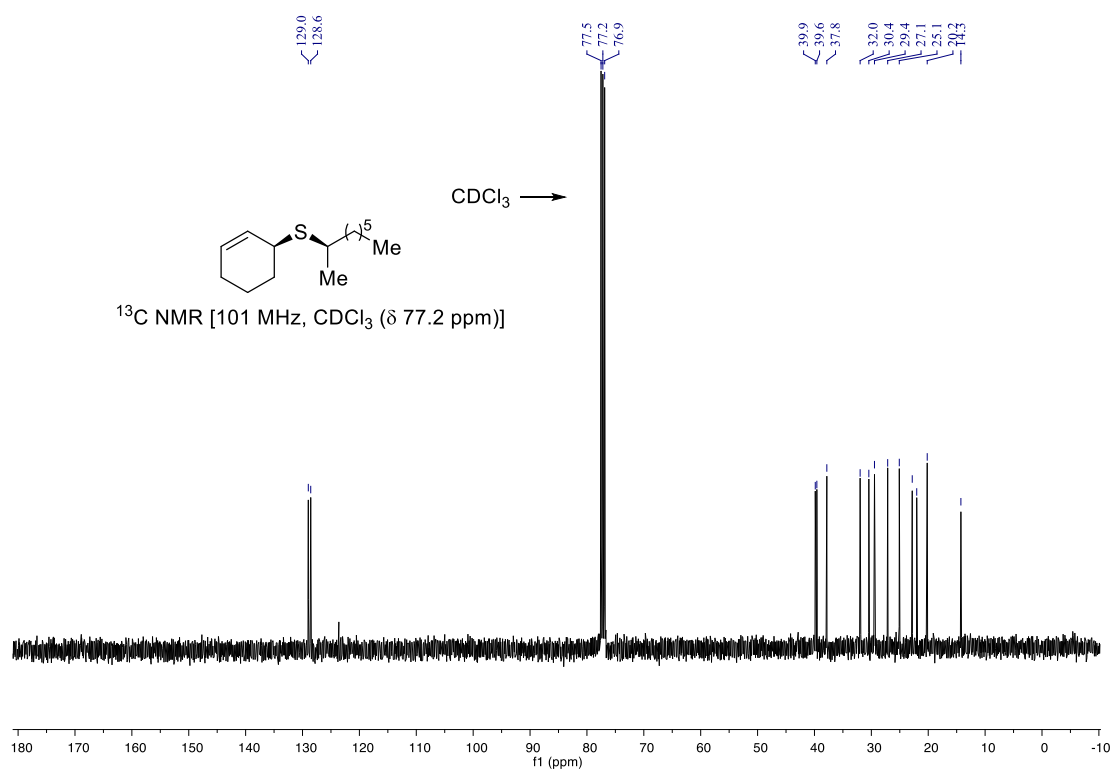
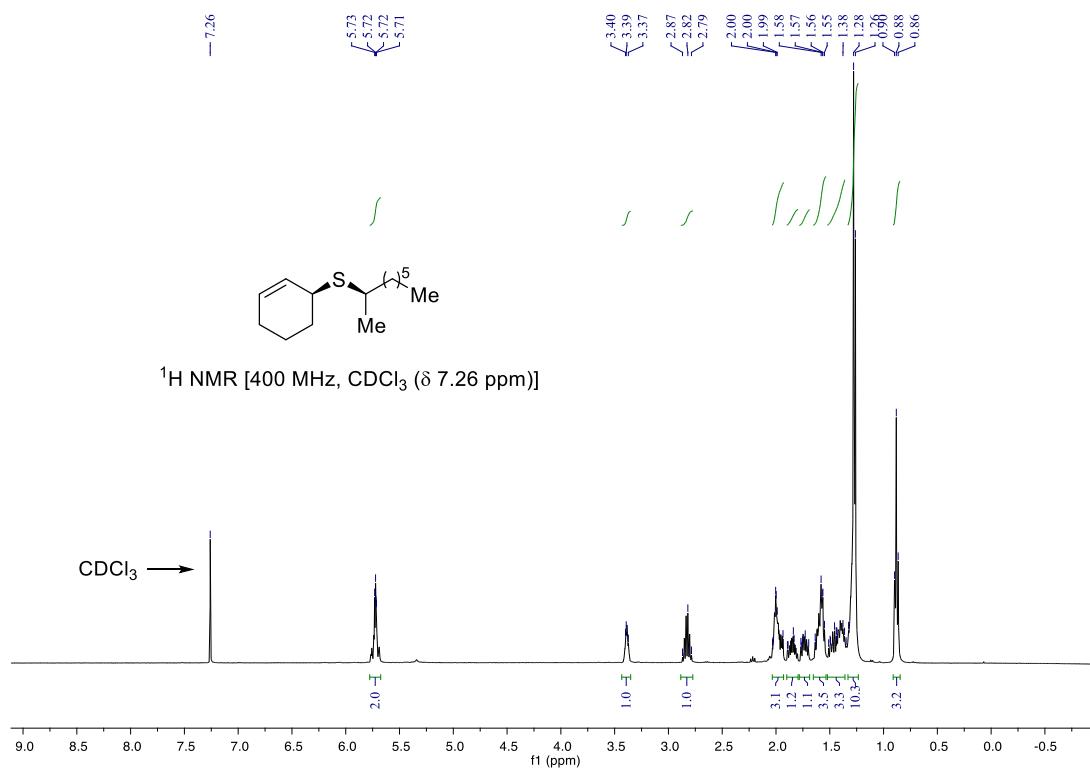
8. NMR spectra of unknown compounds
((S)-cyclohex-2-en-1-yl)((S)-1-phenylethyl)sulfane ((S,S)-3cb)



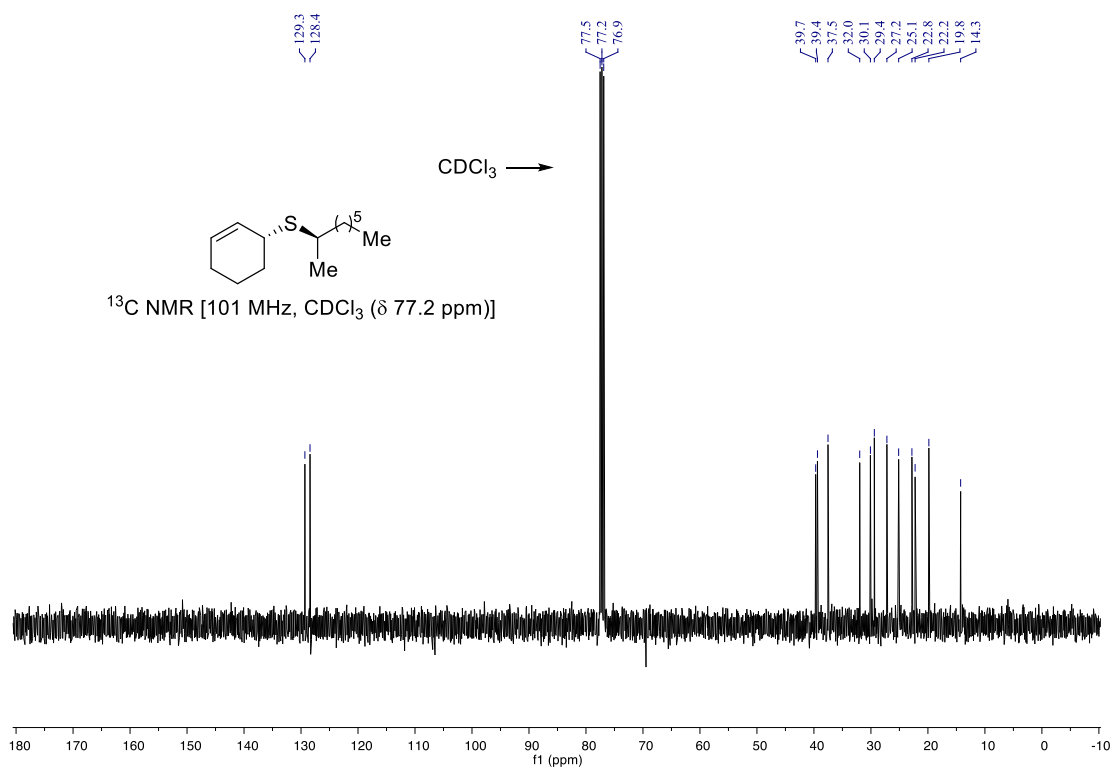
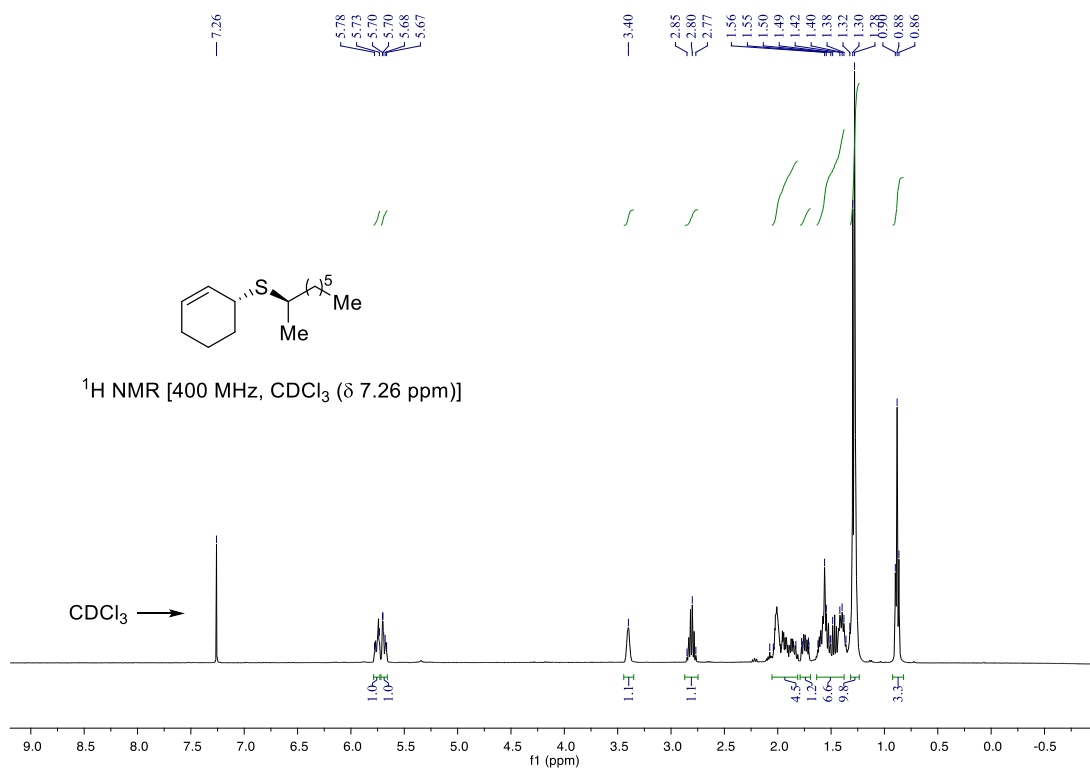
((R)-cyclohex-2-en-1-yl)((S)-1-phenylethyl)sulfane ((R,S)-3b)



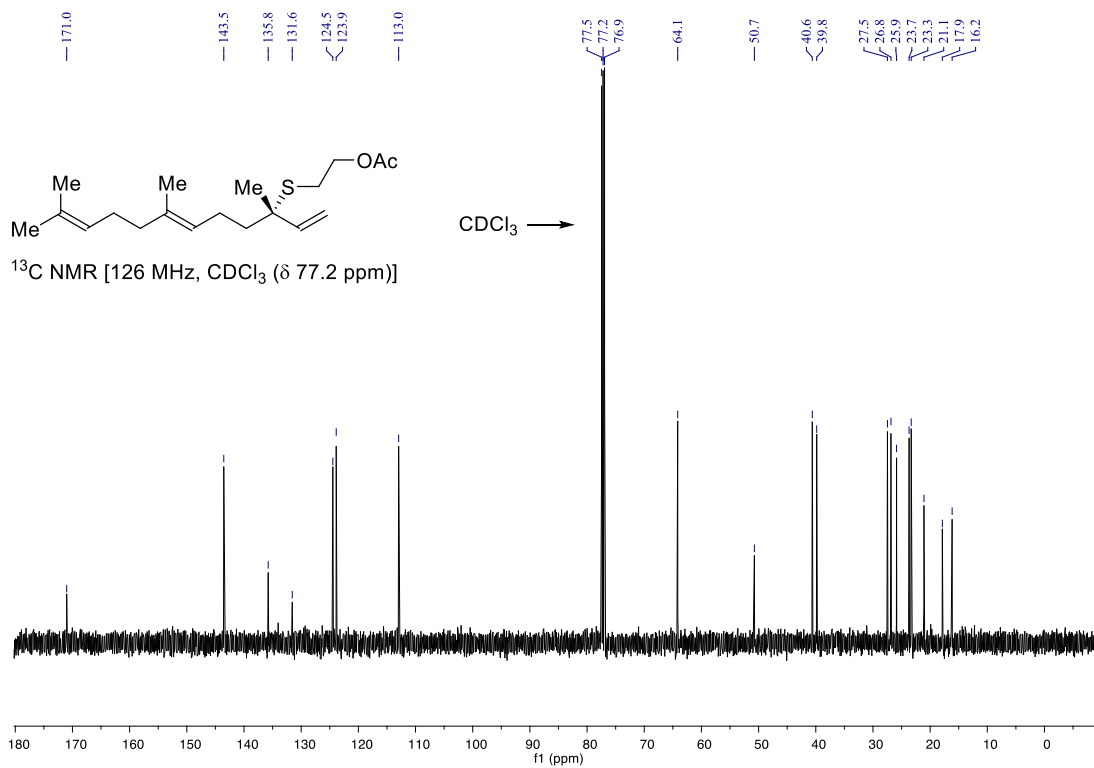
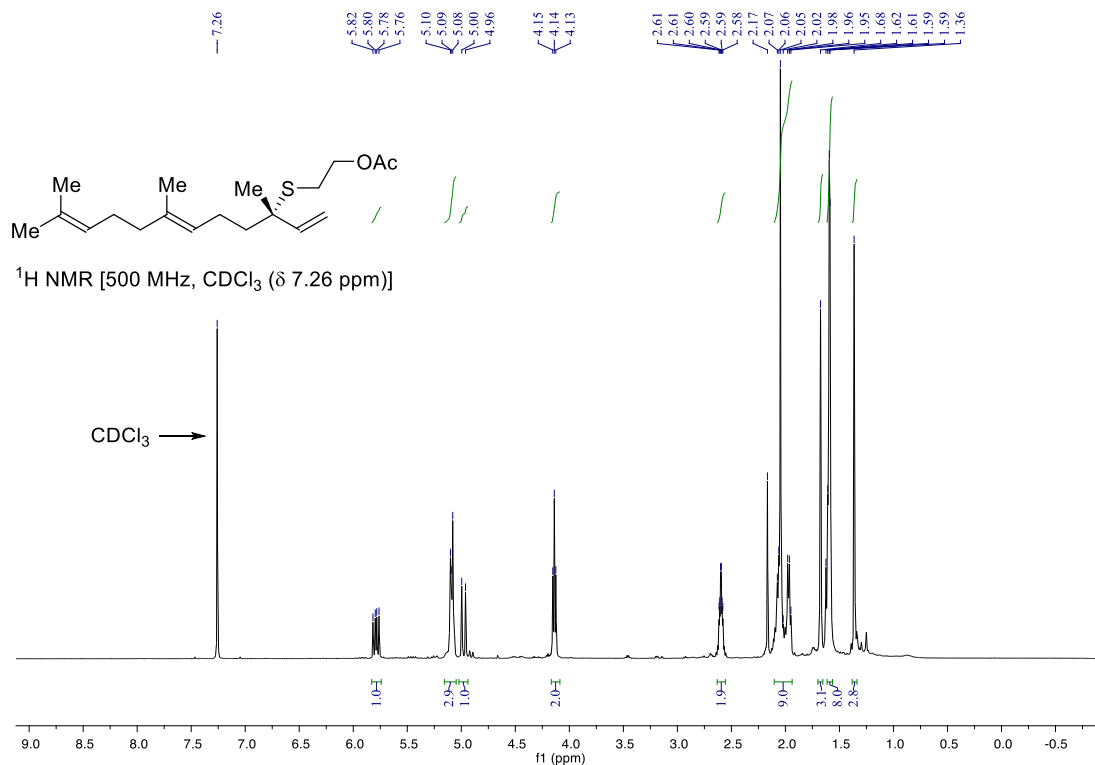
((S)-cyclohex-2-en-1-yl)((R)-octan-2-yl)sulfane ((S,R)-3db)



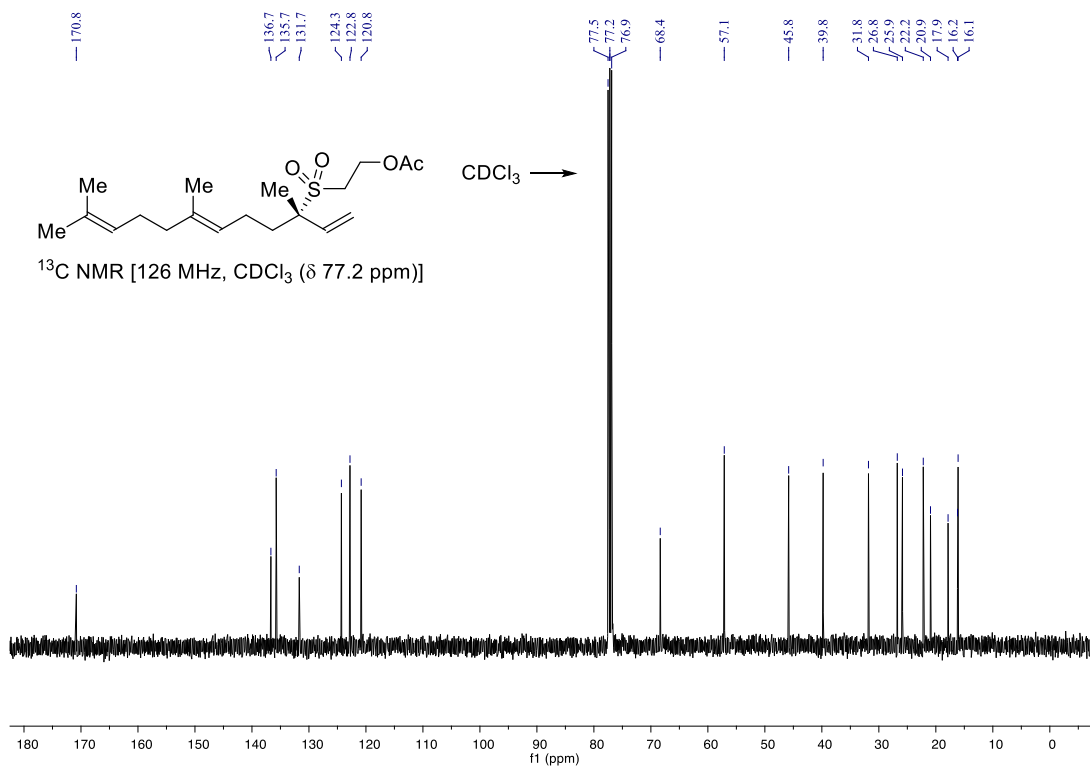
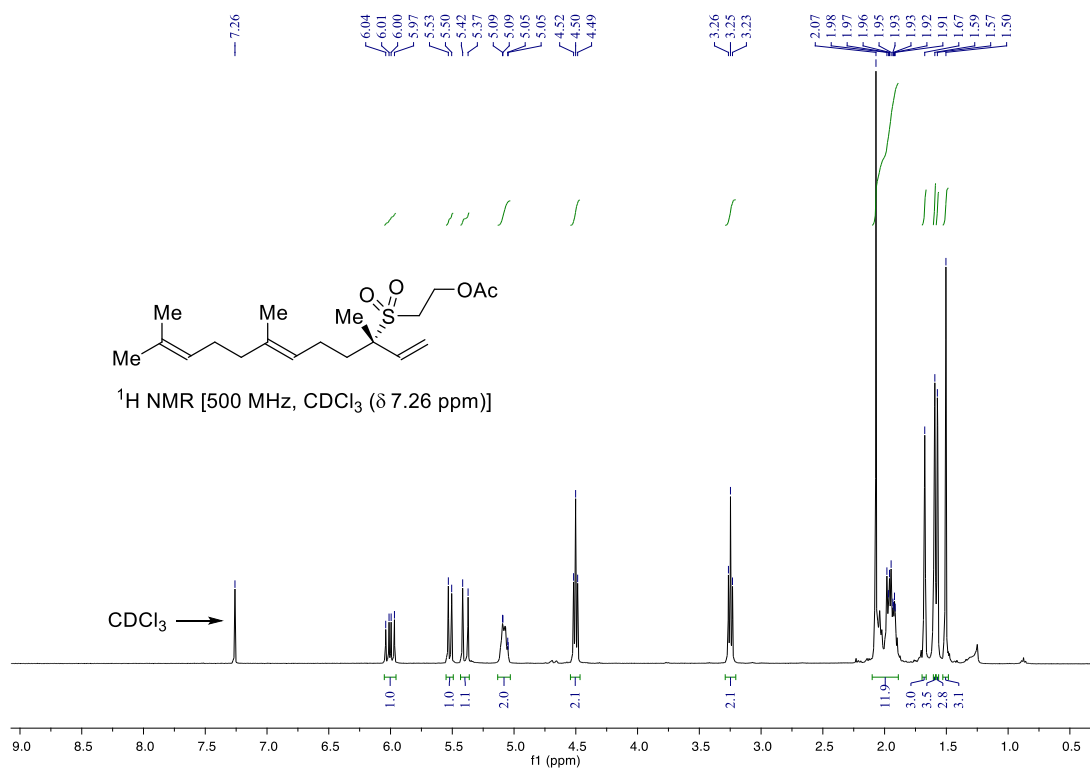
((R)-cyclohex-2-en-1-yl)((R)-octan-2-yl)sulfane ((R,R)-3db)



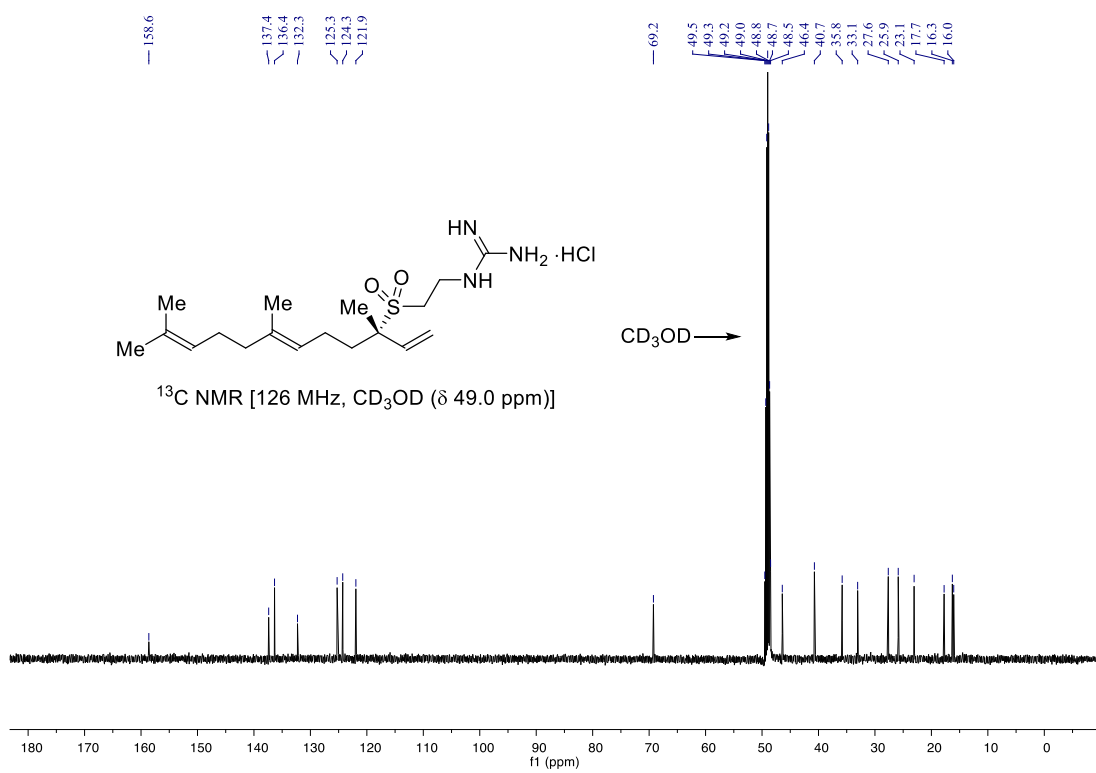
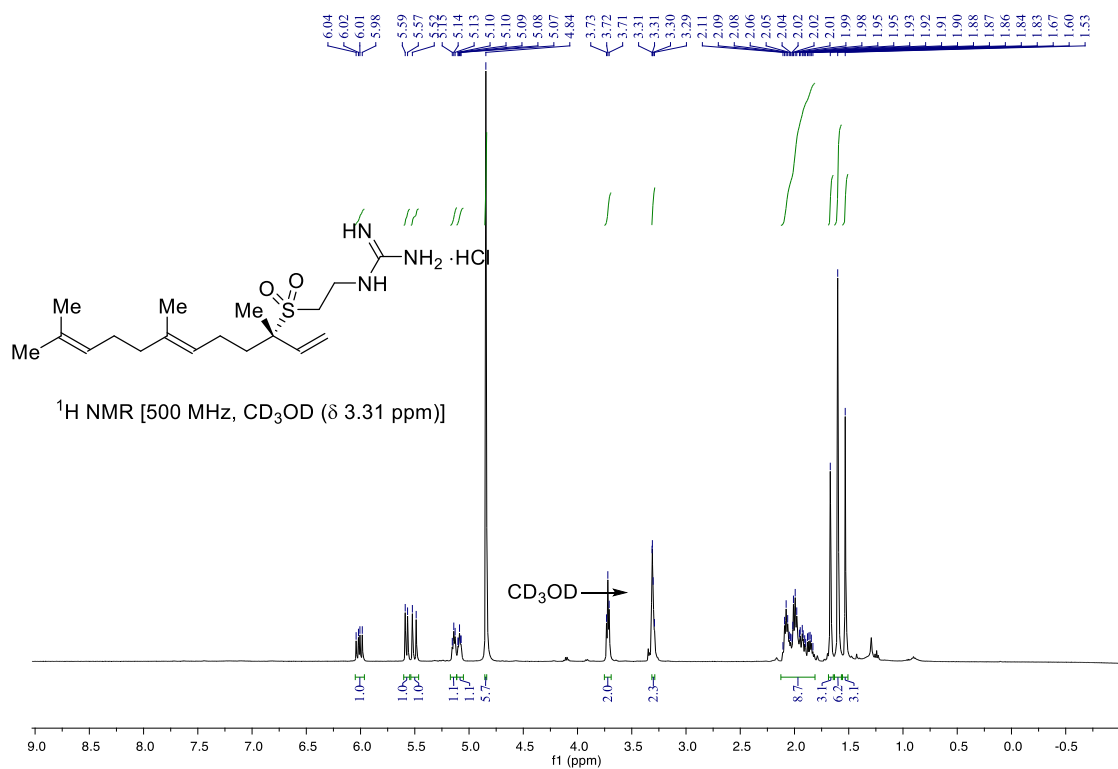
Compound 3ec



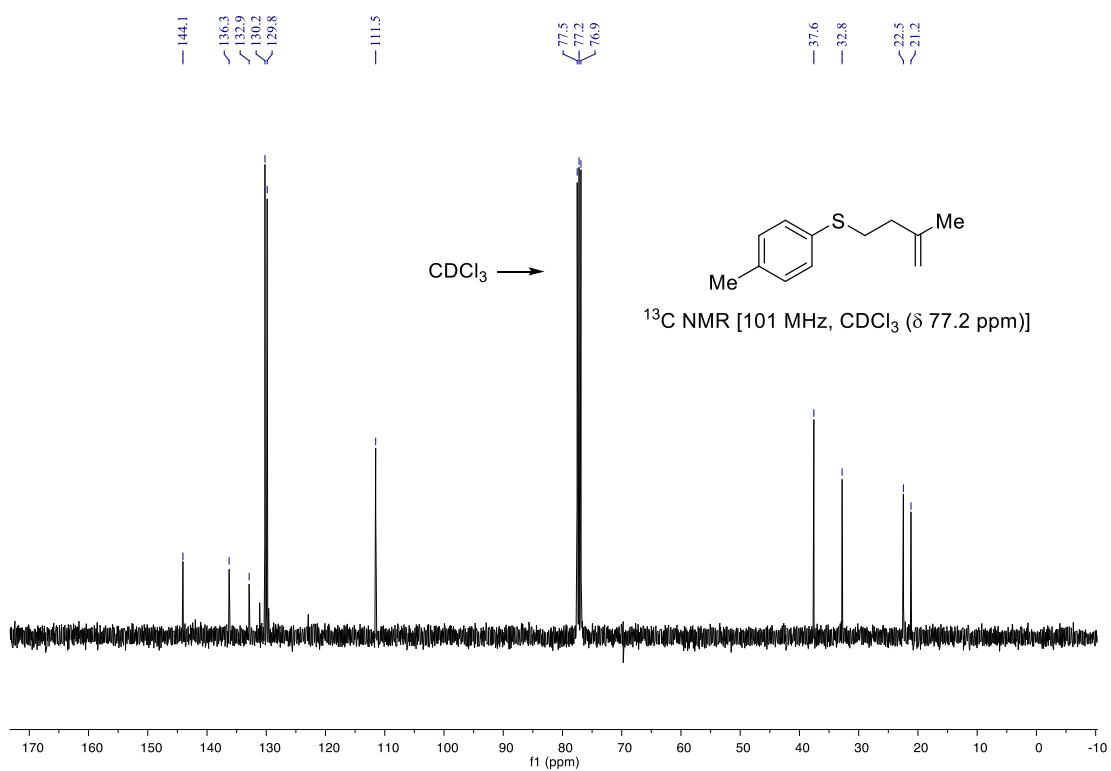
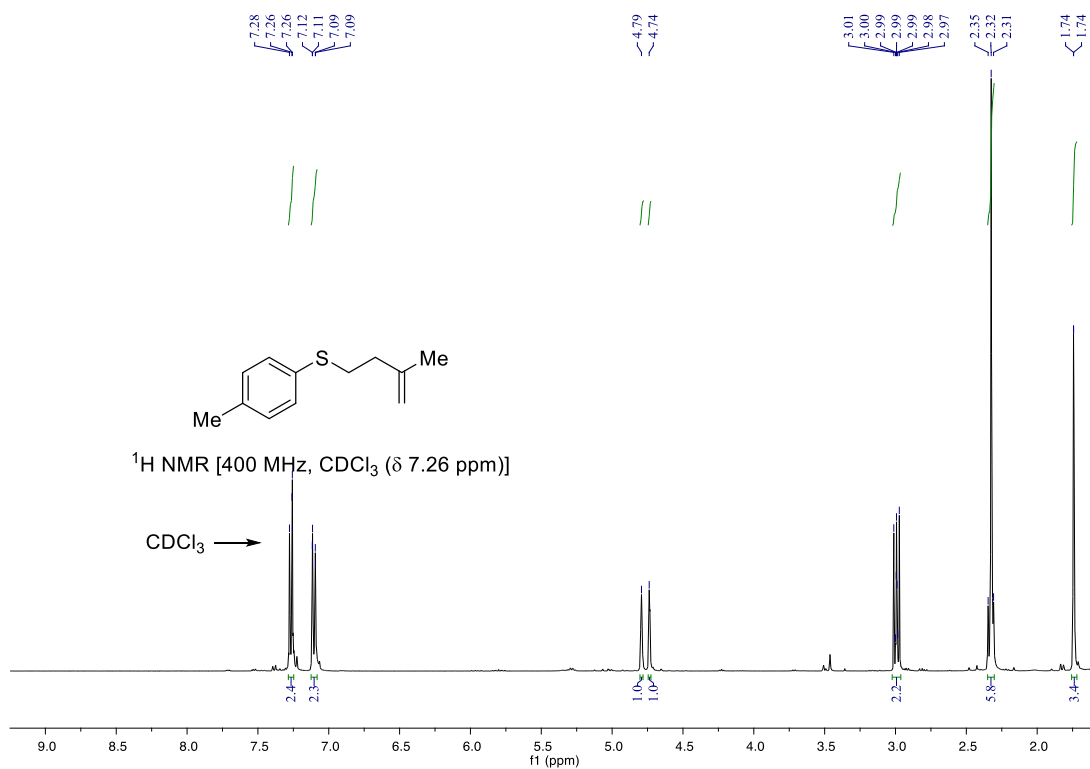
Compound 5



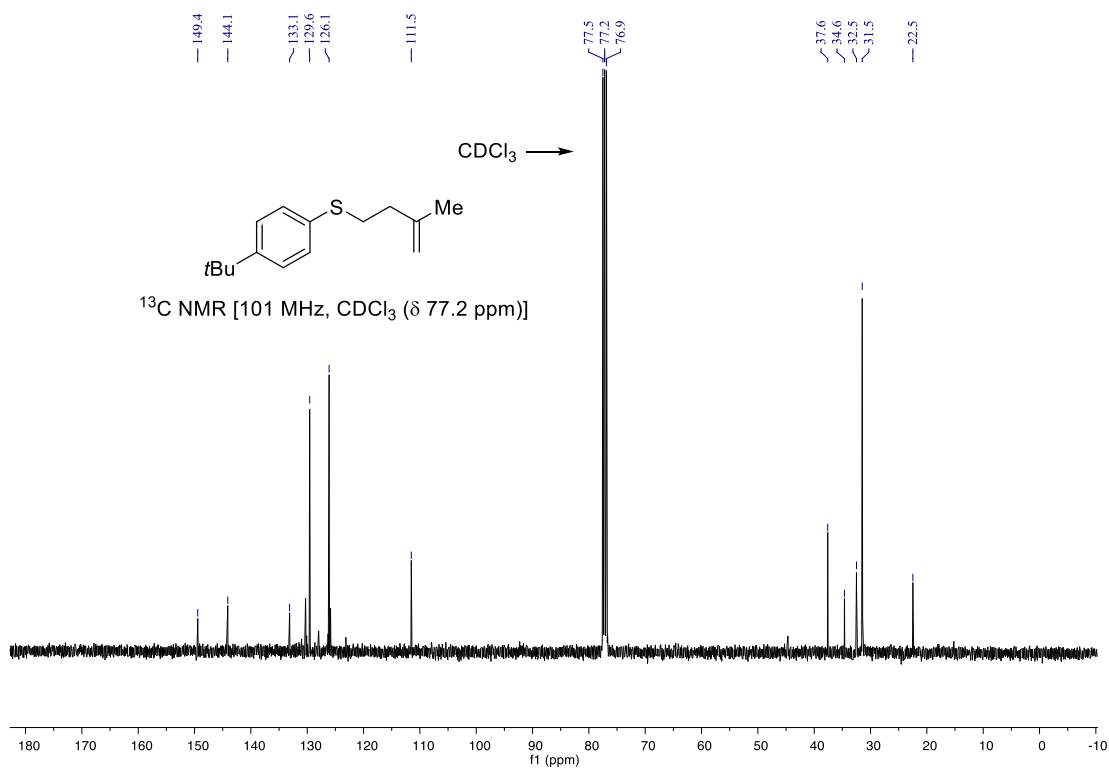
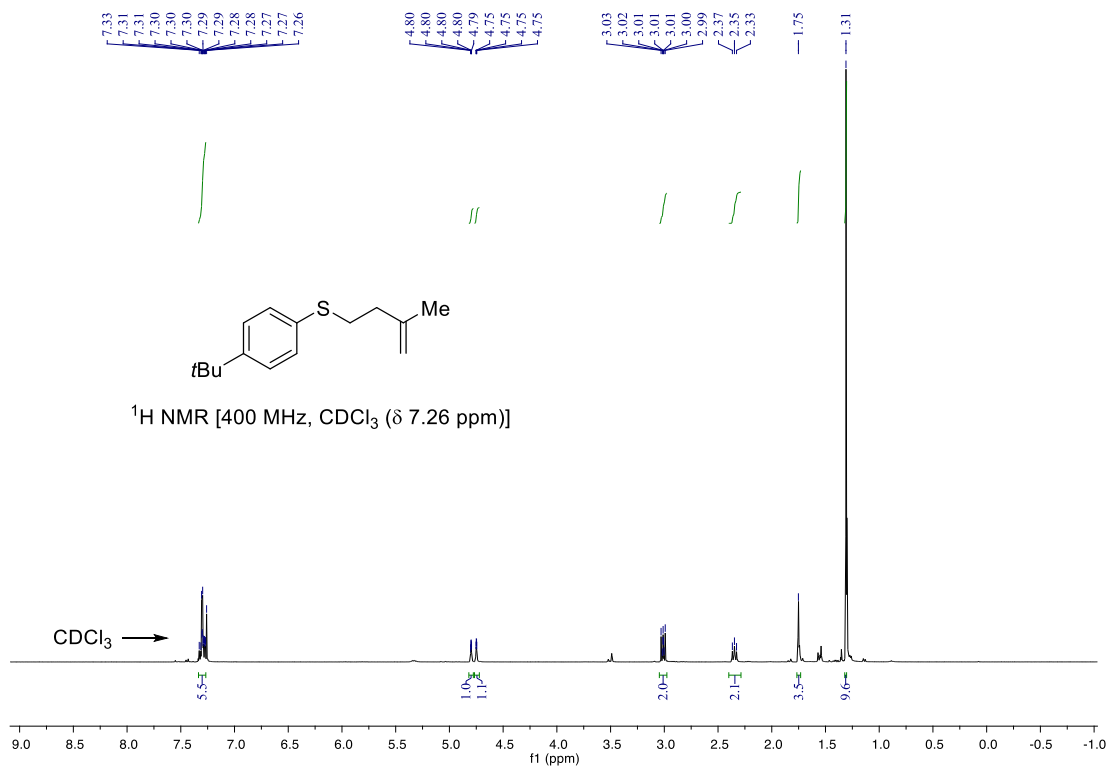
(-)-agelasidine A hydrogen chloride 4



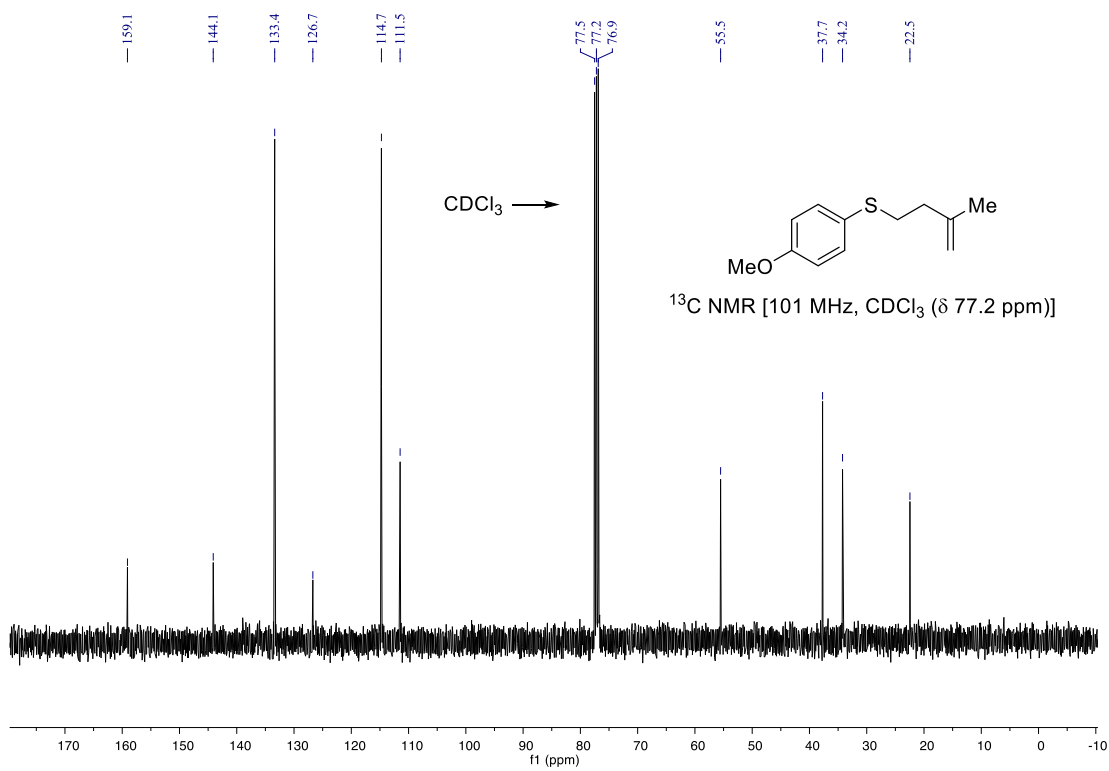
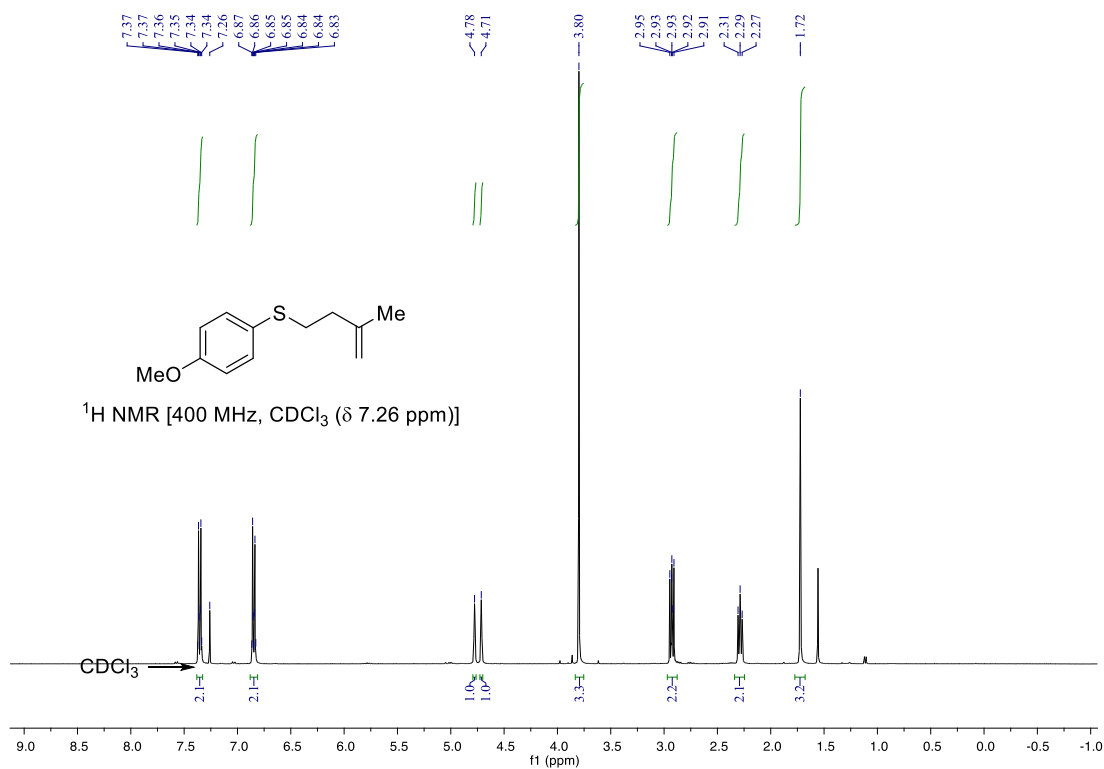
(3-methylbut-3-en-1-yl)(*p*-tolyl)sulfane (6fd)



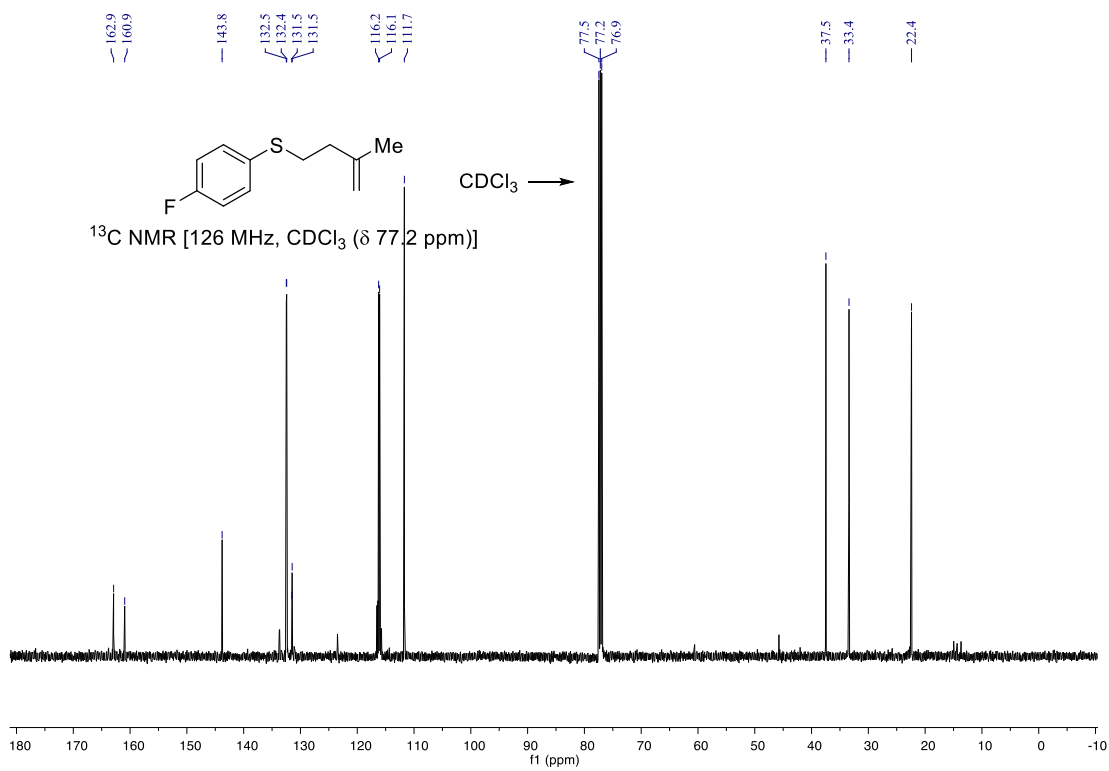
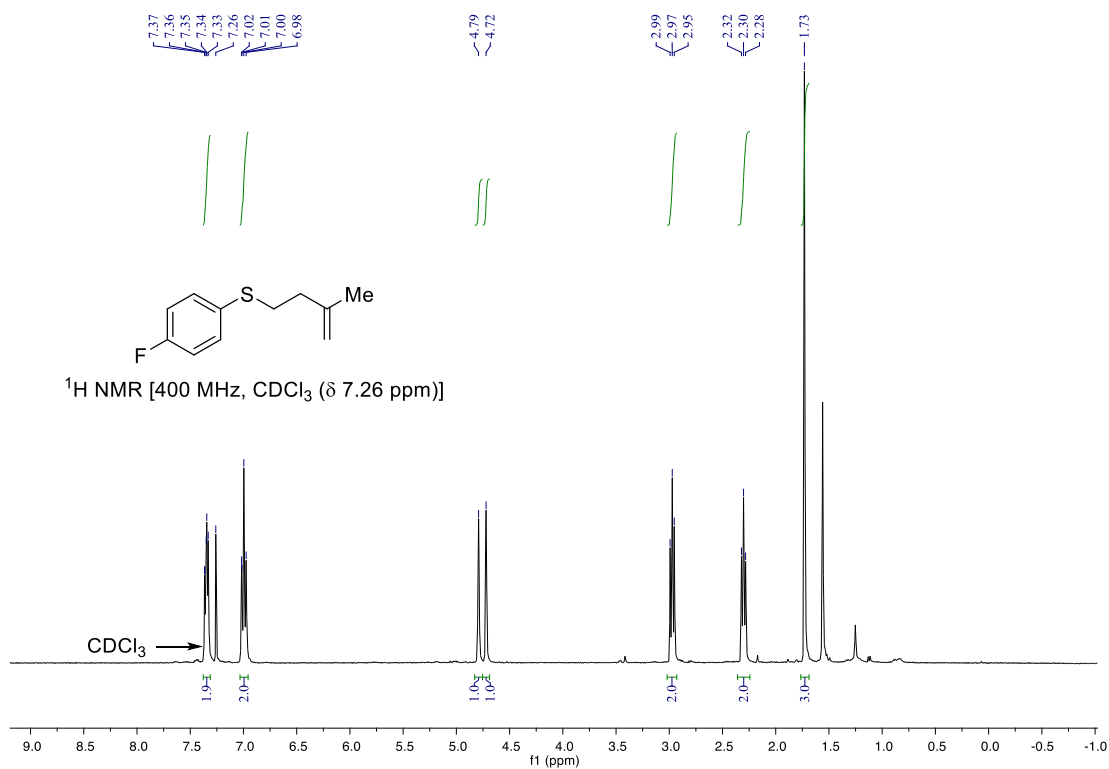
(4-*tert*-butyl)phenyl)(3-methylbut-3-en-1-yl)sulfane (6gd)



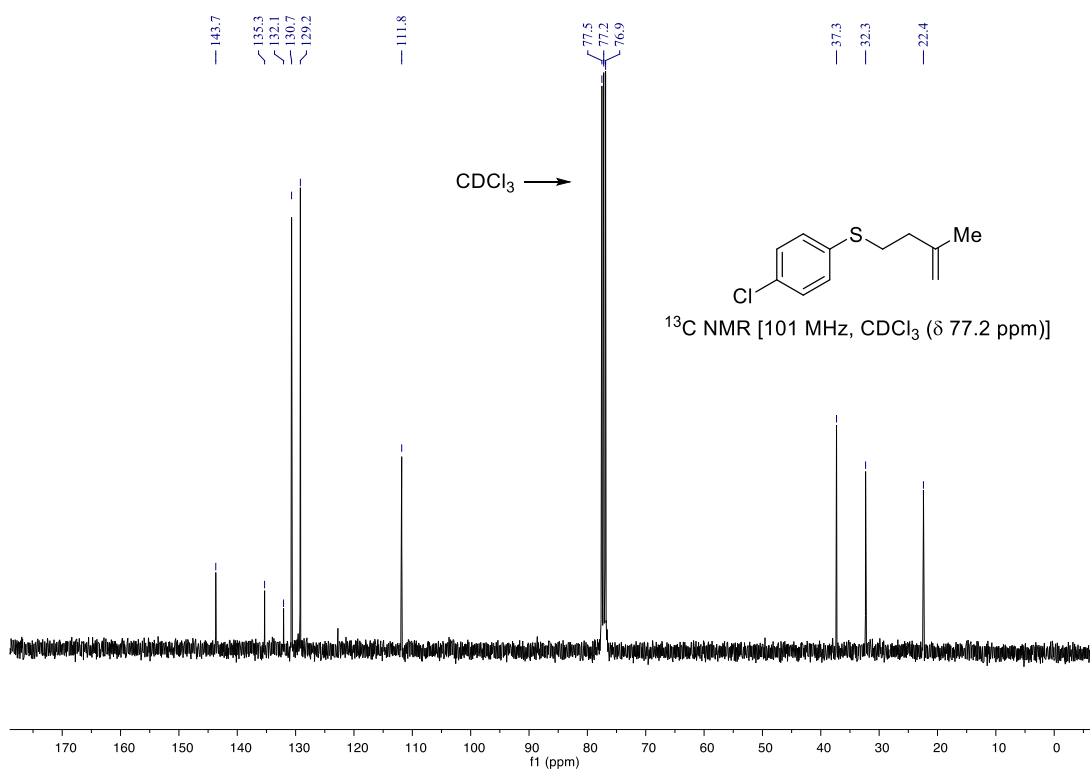
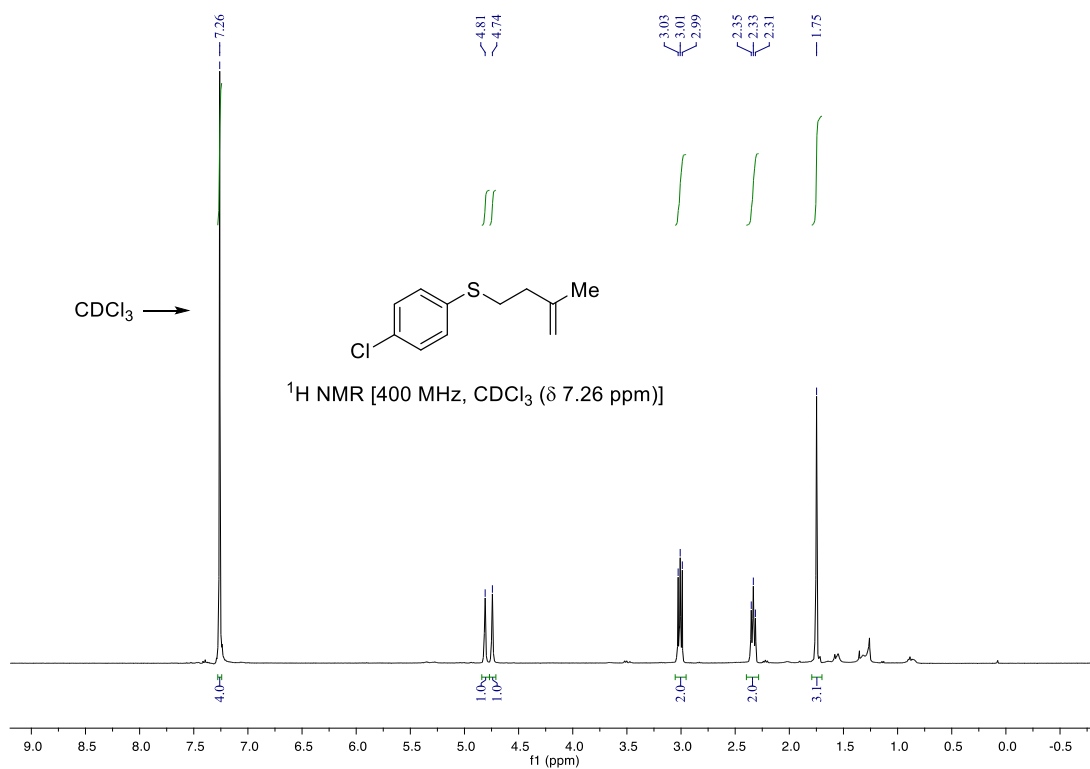
(4-methoxyphenyl)(3-methylbut-3-en-1-yl)sulfane (6hd)



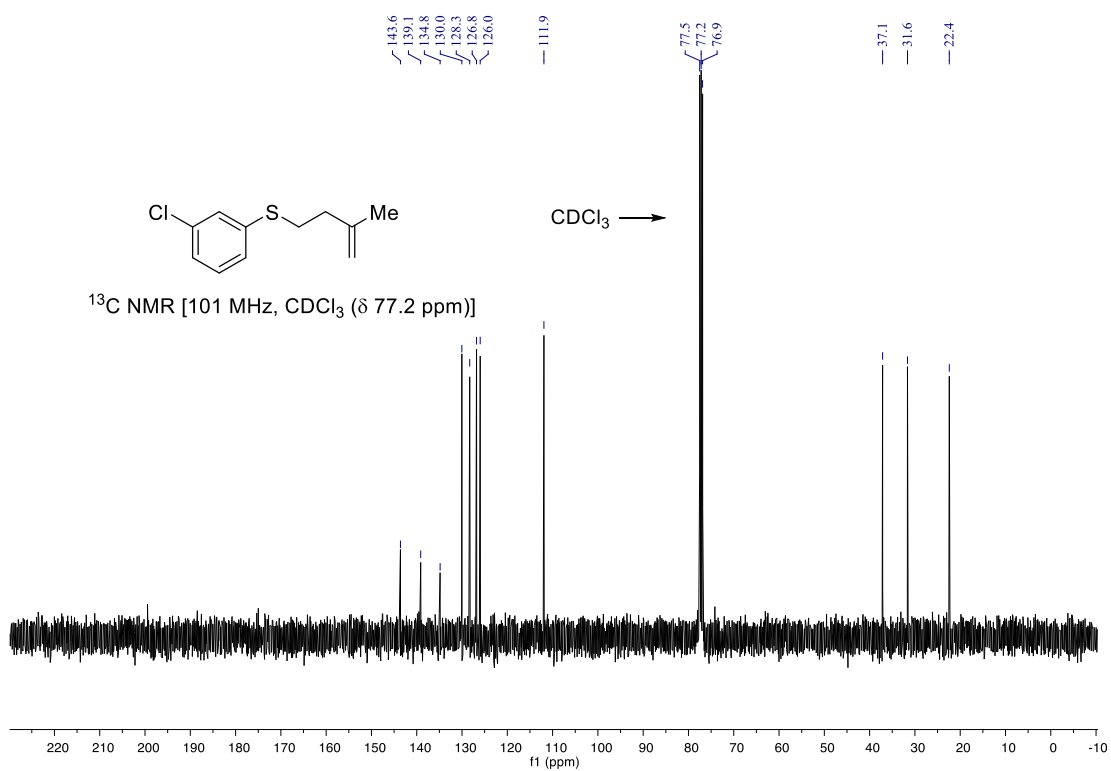
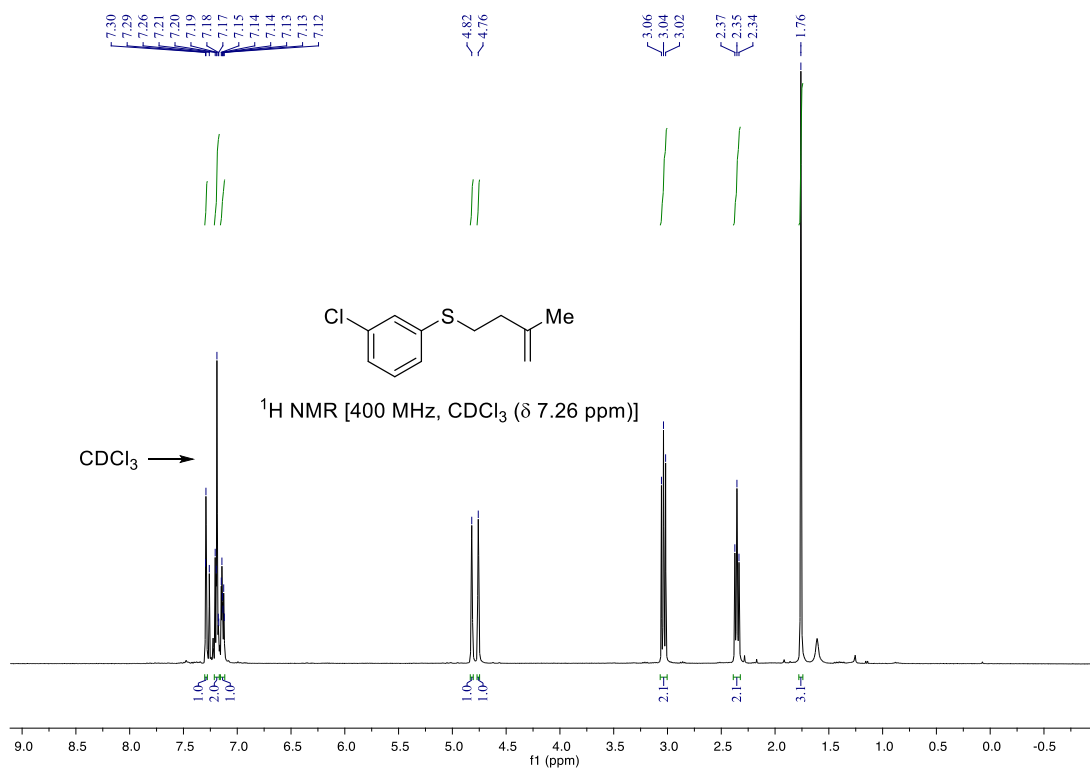
(4-fluorophenyl)(3-methylbut-3-en-1-yl)sulfane (6id)



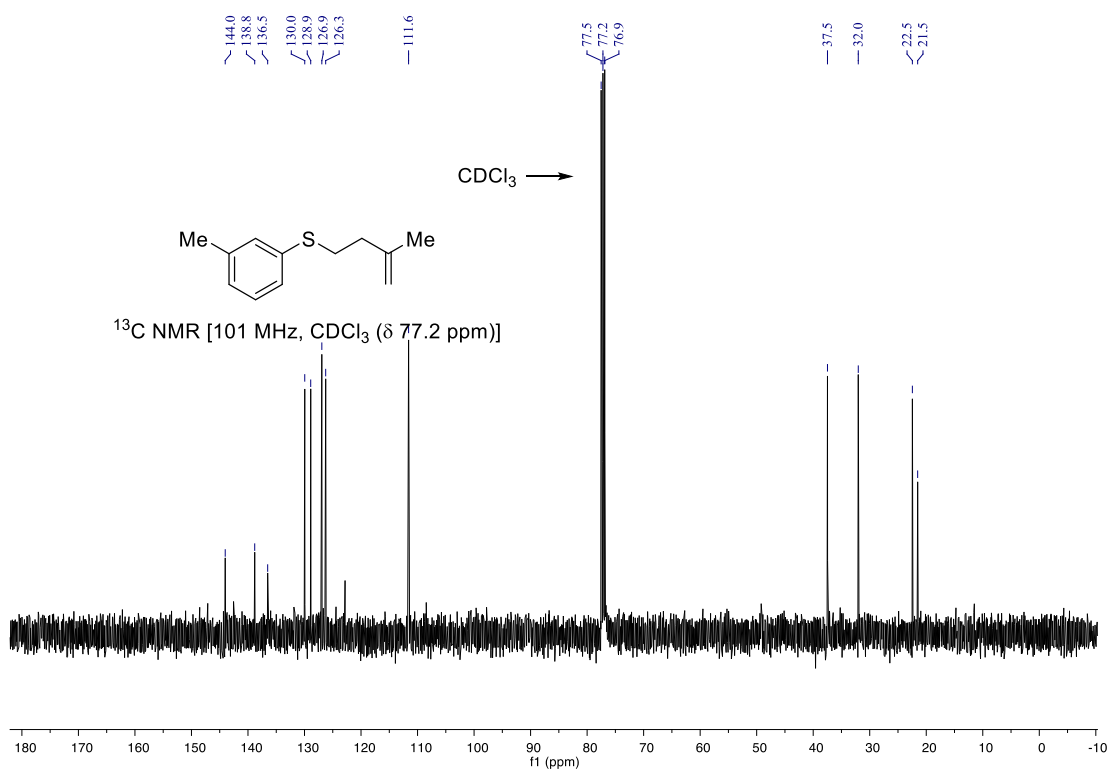
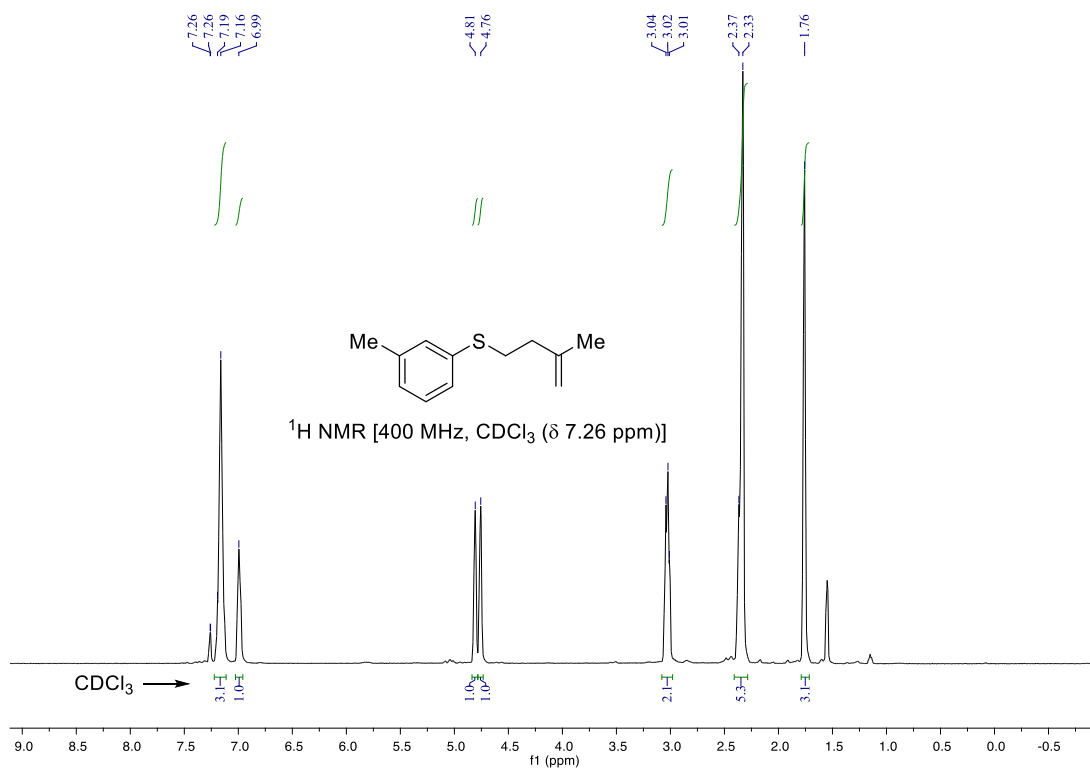
(4-chlorophenyl)(3-methylbut-3-en-1-yl)sulfane (6jd)



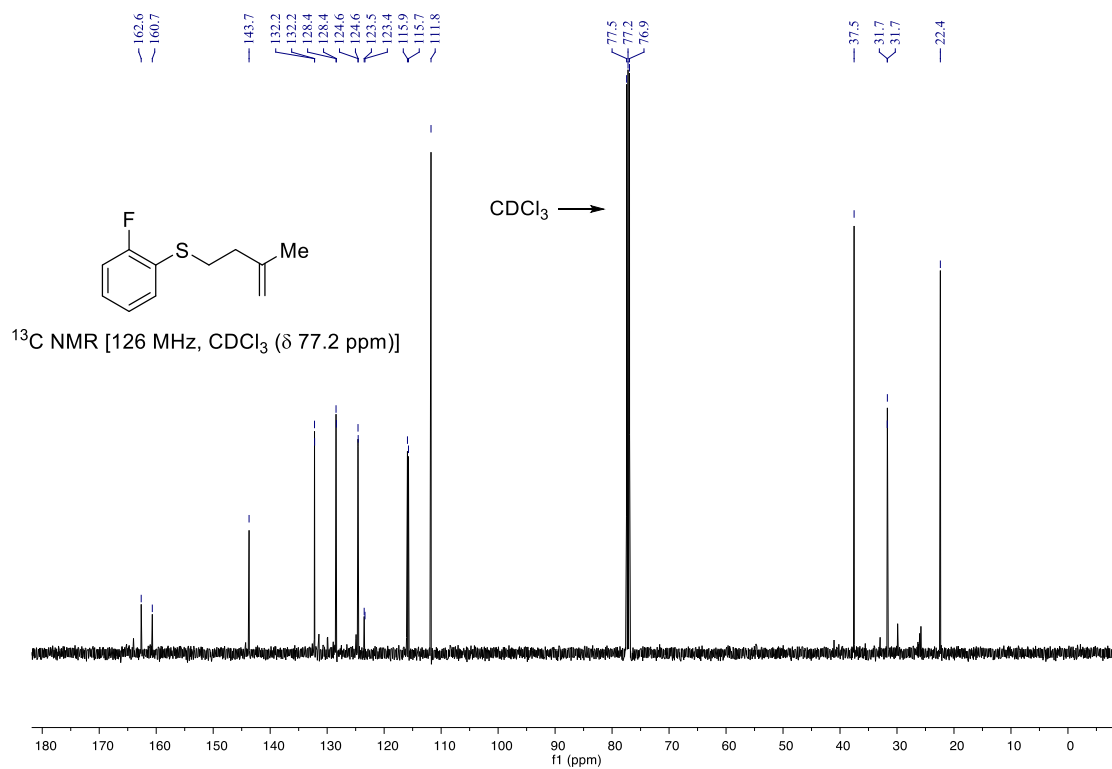
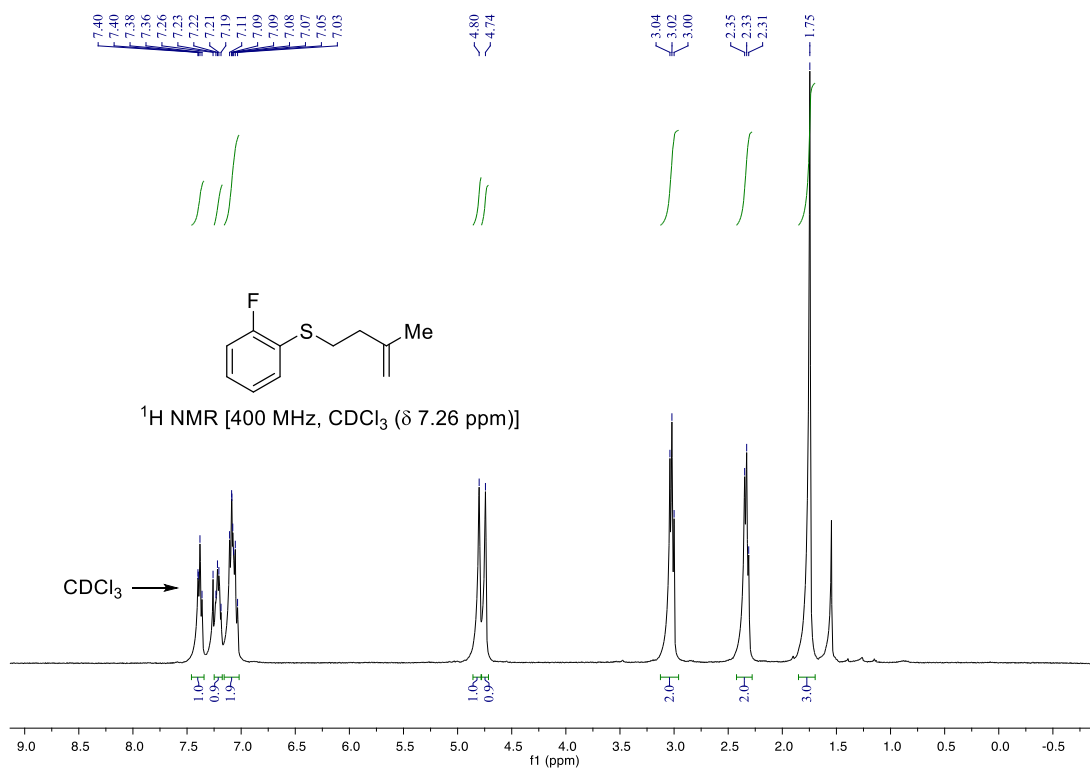
(3-chlorophenyl)(3-methylbut-3-en-1-yl)sulfane (6kd)



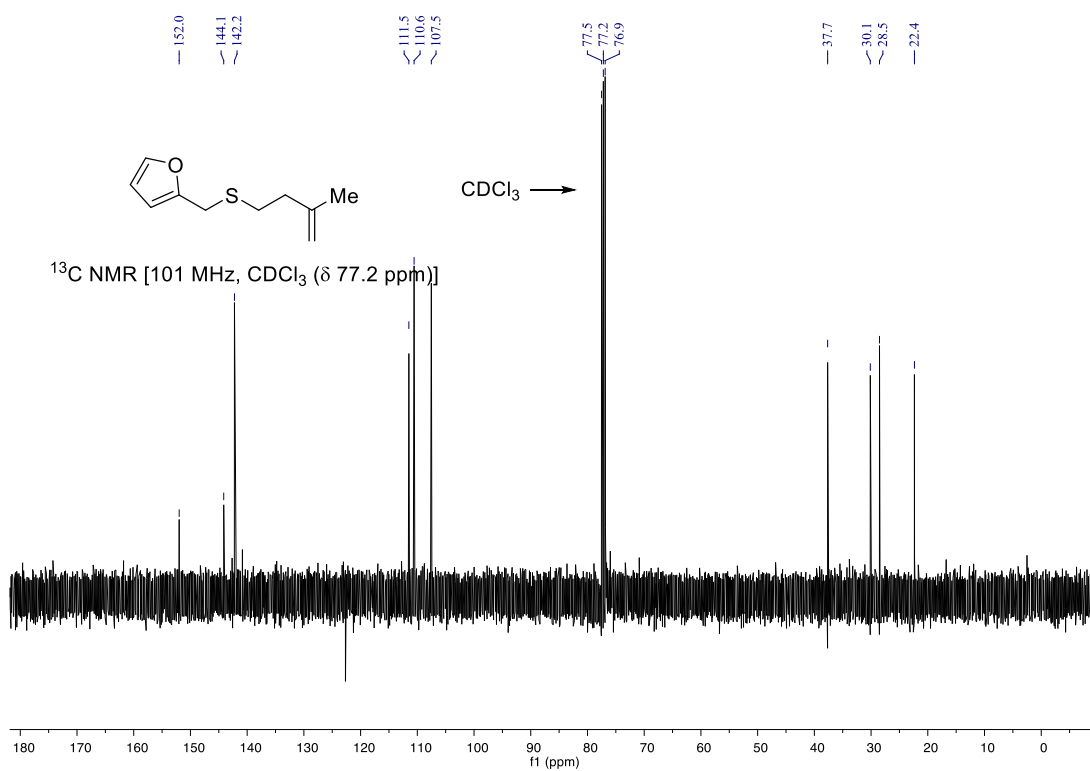
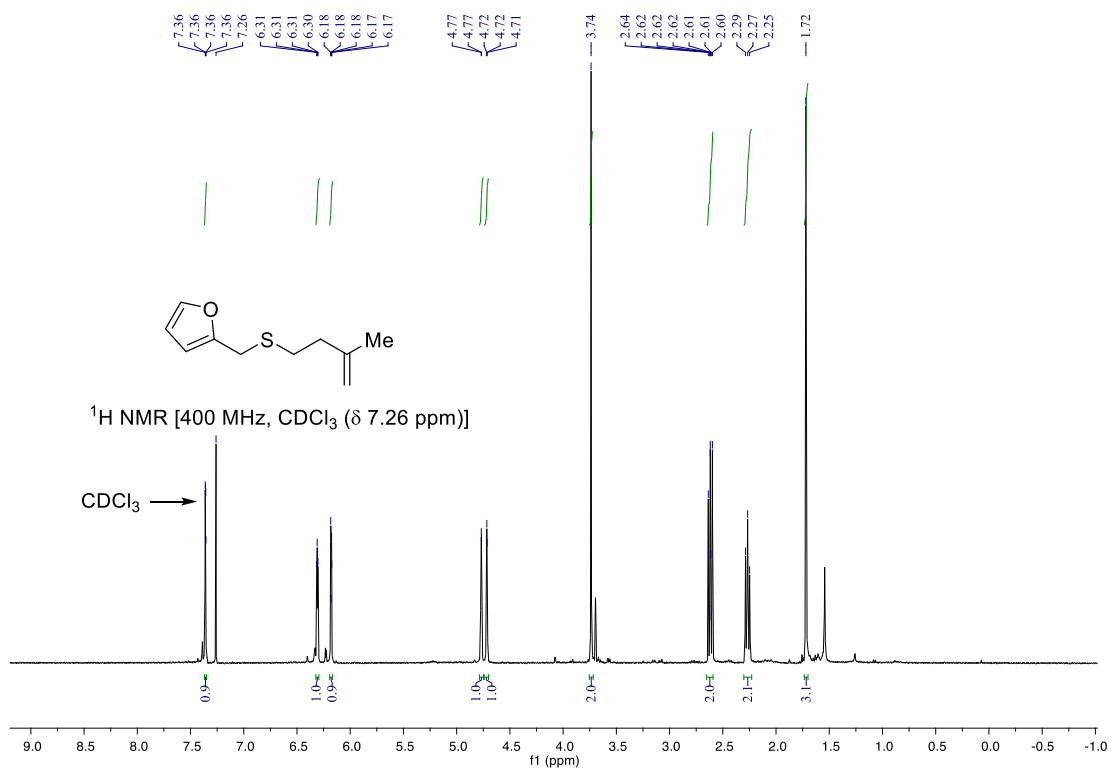
(3-methylbut-3-en-1-yl)(*m*-tolyl)sulfane (6ld)



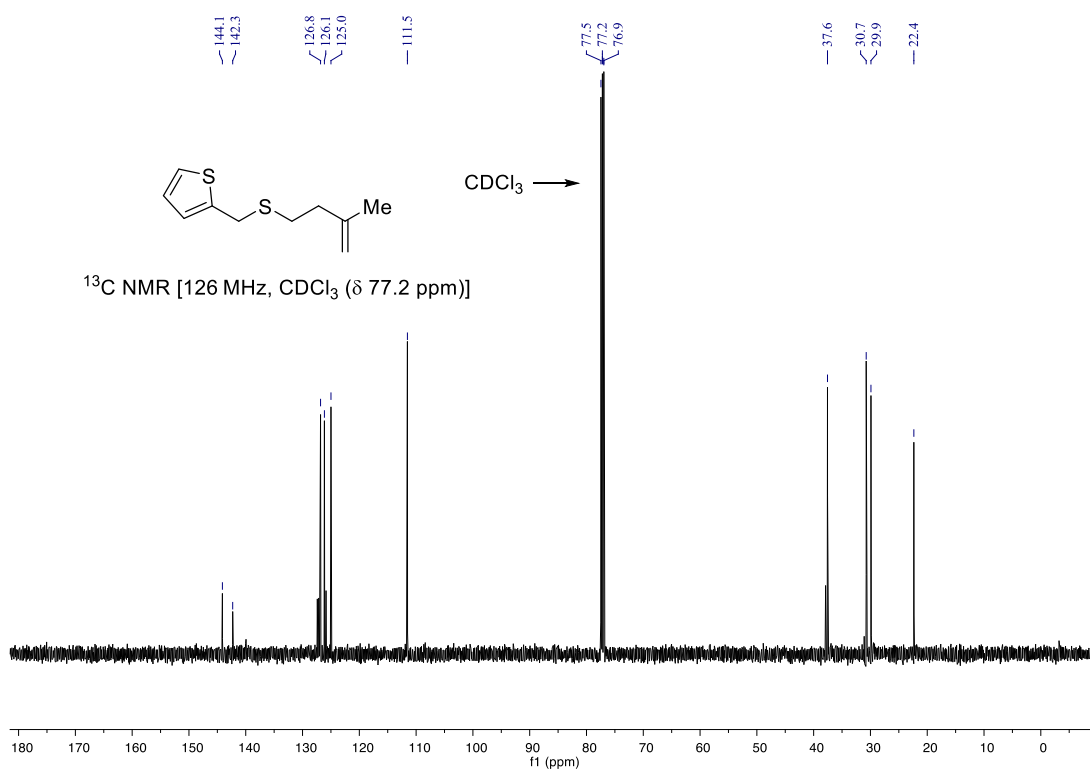
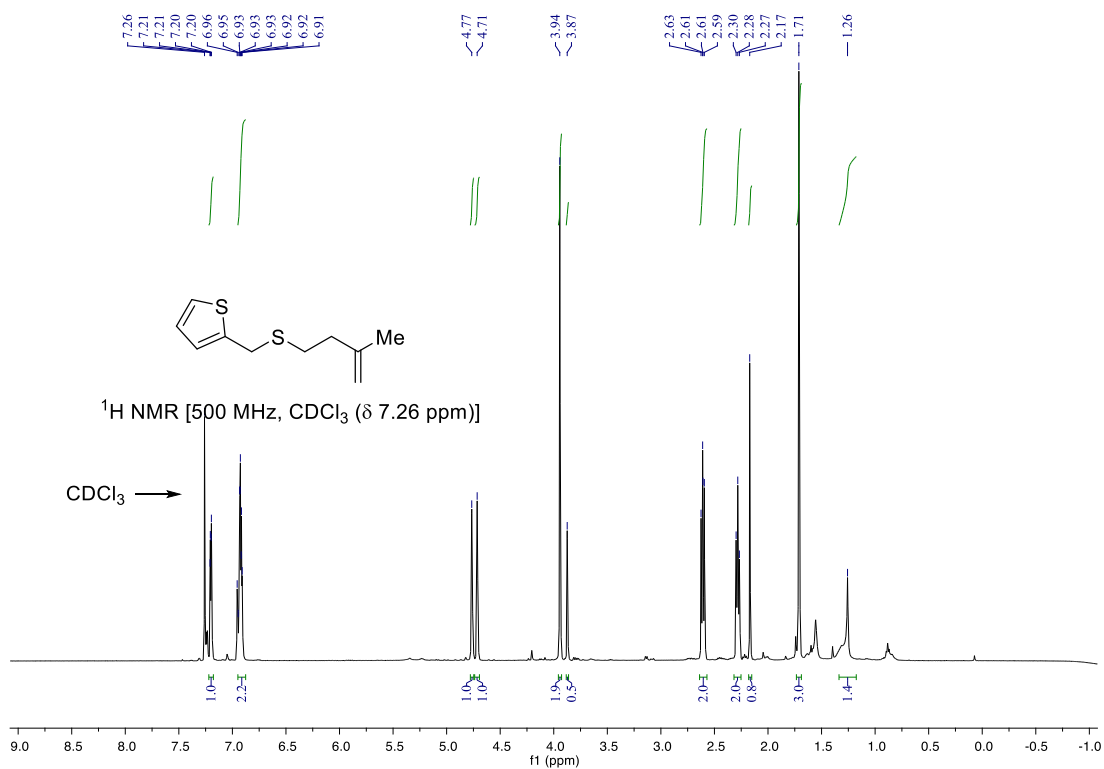
(2-fluorophenyl)(3-methylbut-3-en-1-yl)sulfane (6md)



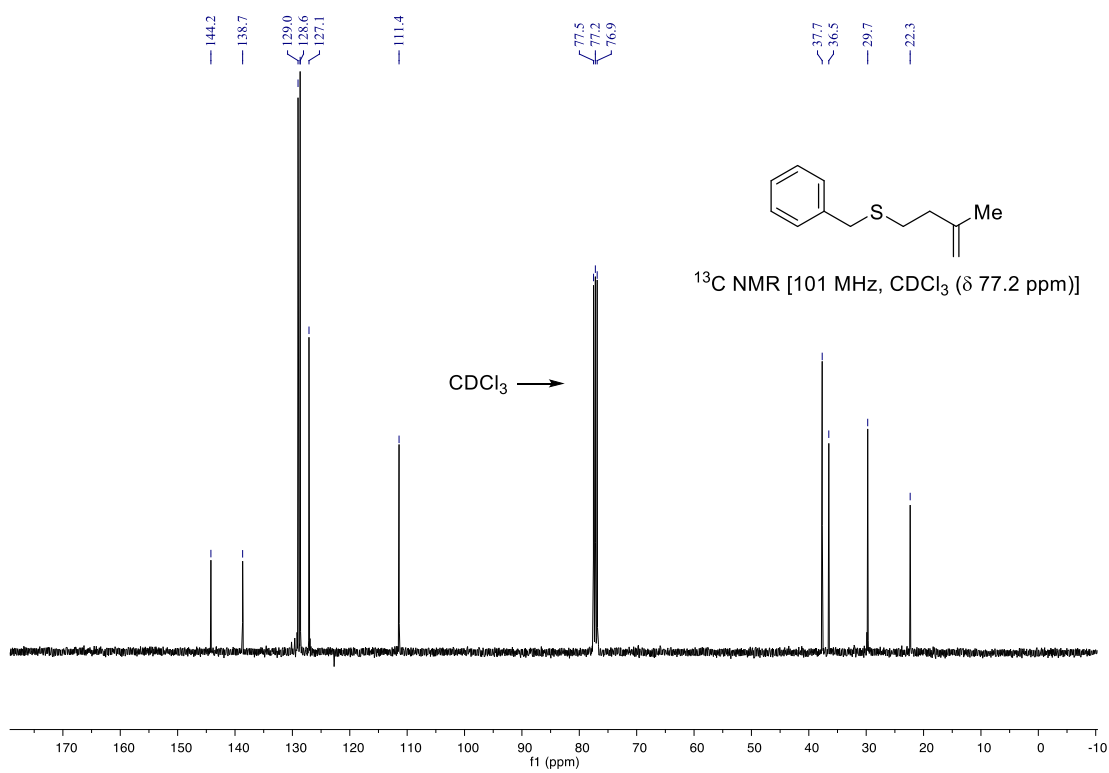
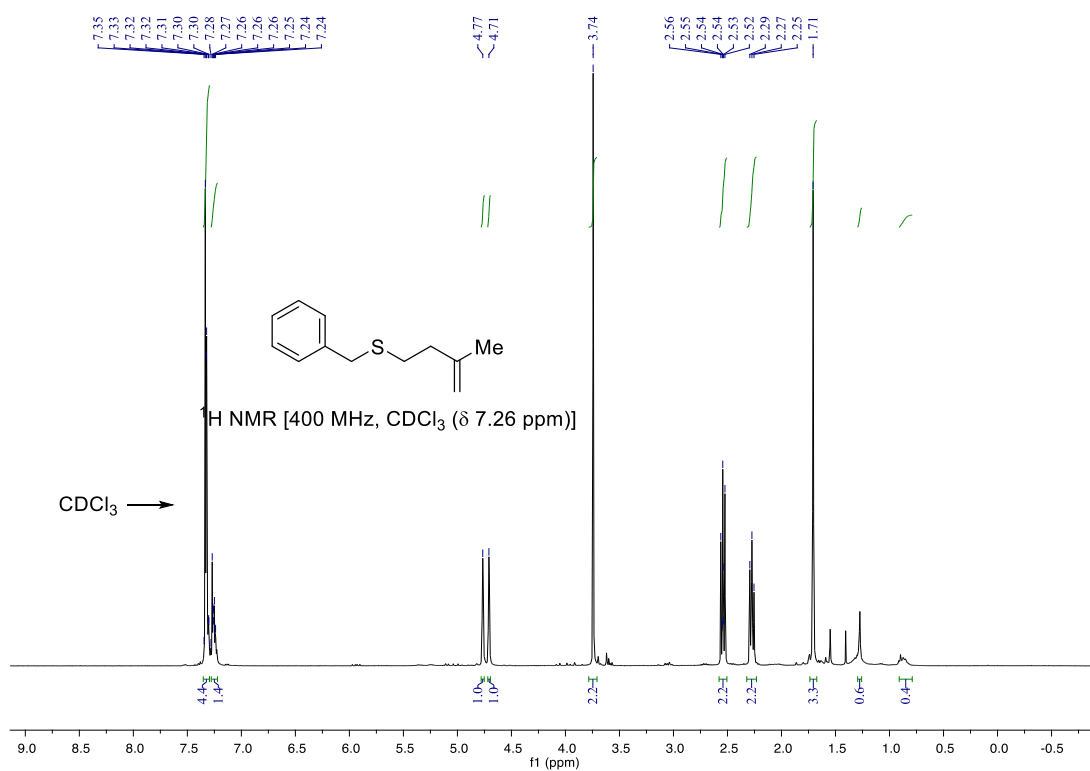
2-(((3-methylbut-3-en-1-yl)thio)methyl)furan (6nd)



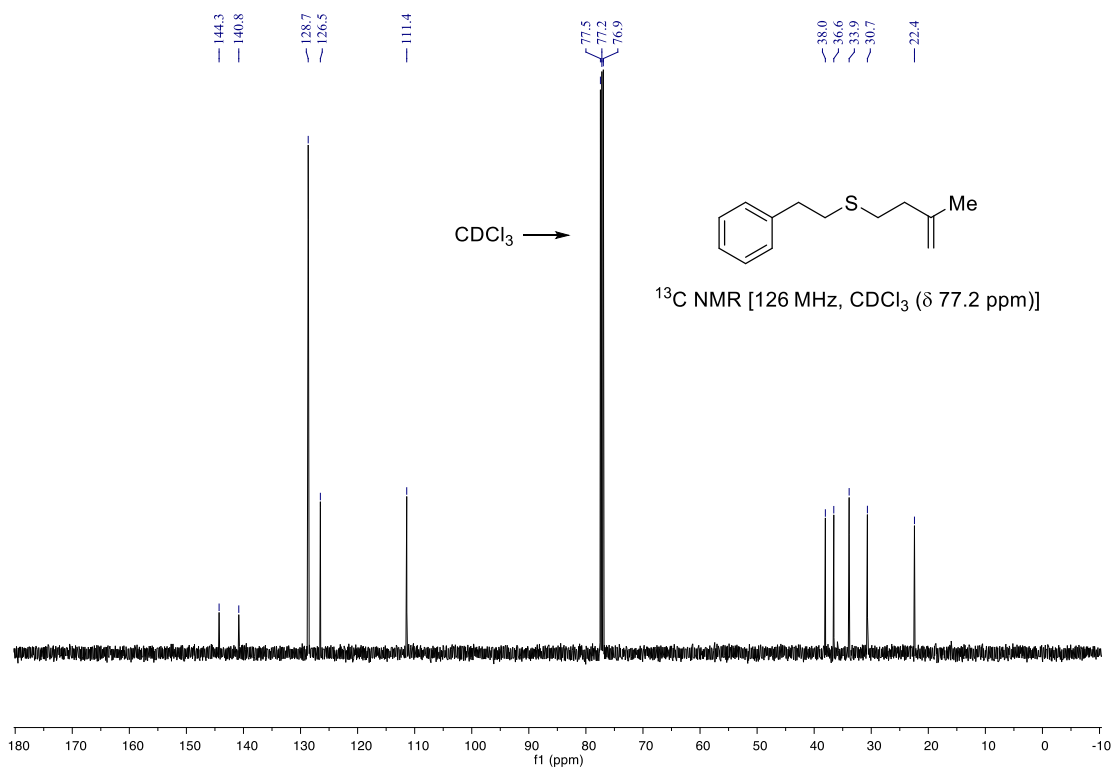
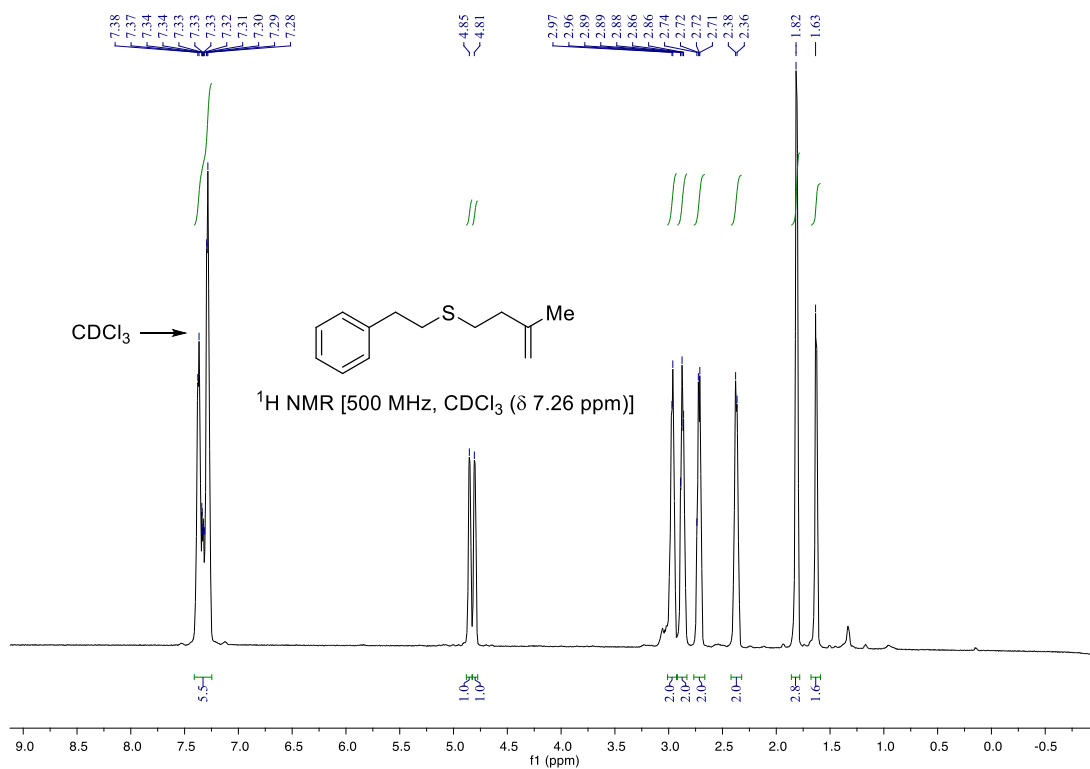
2-(((3-methylbut-3-en-1-yl)thio)methyl)thiophene (60d)



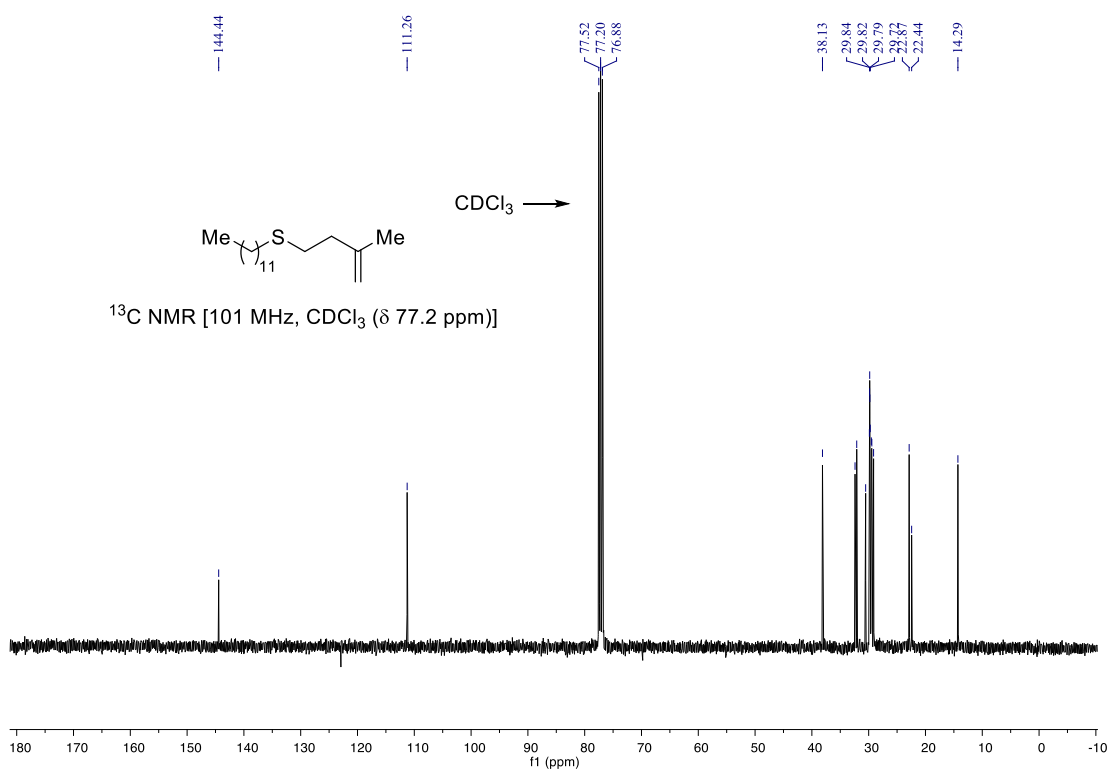
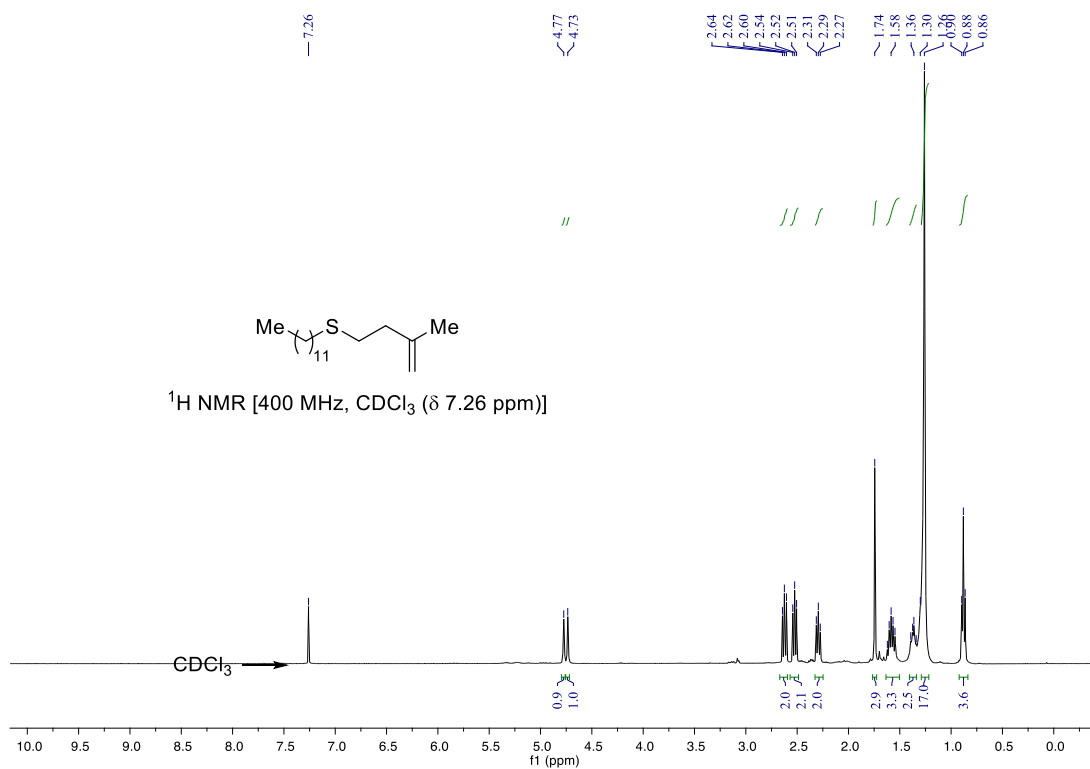
benzyl(3-methylbut-3-en-1-yl)sulfane (6pd)



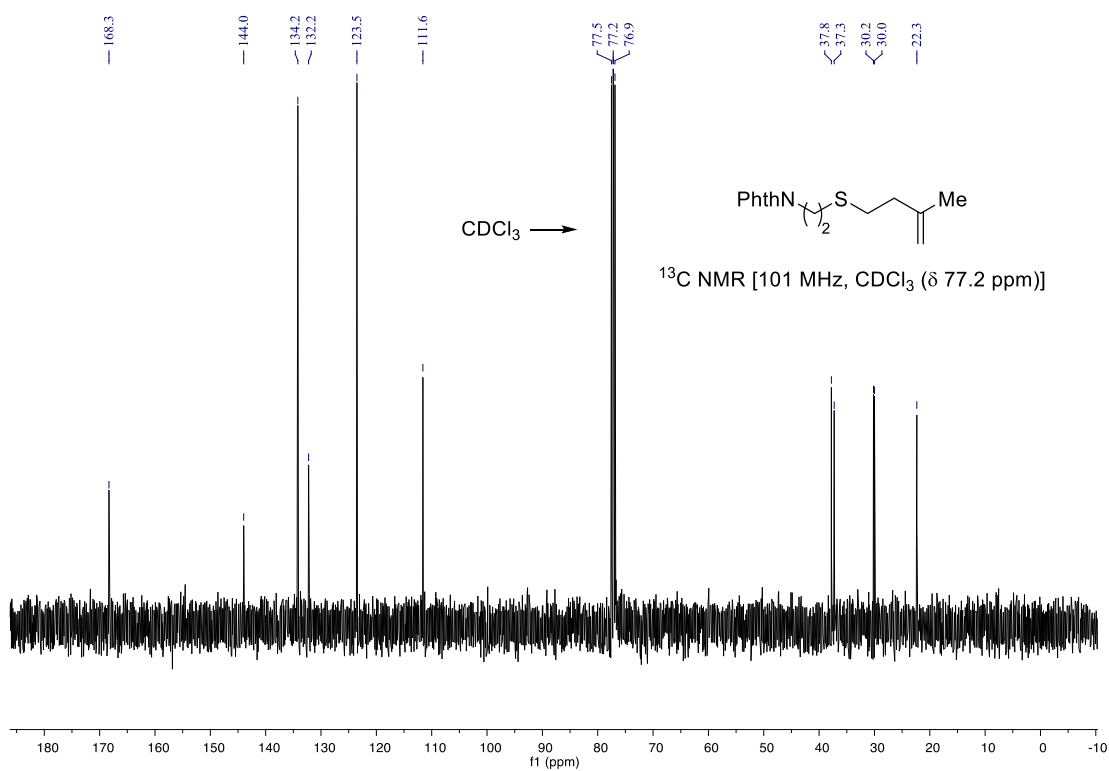
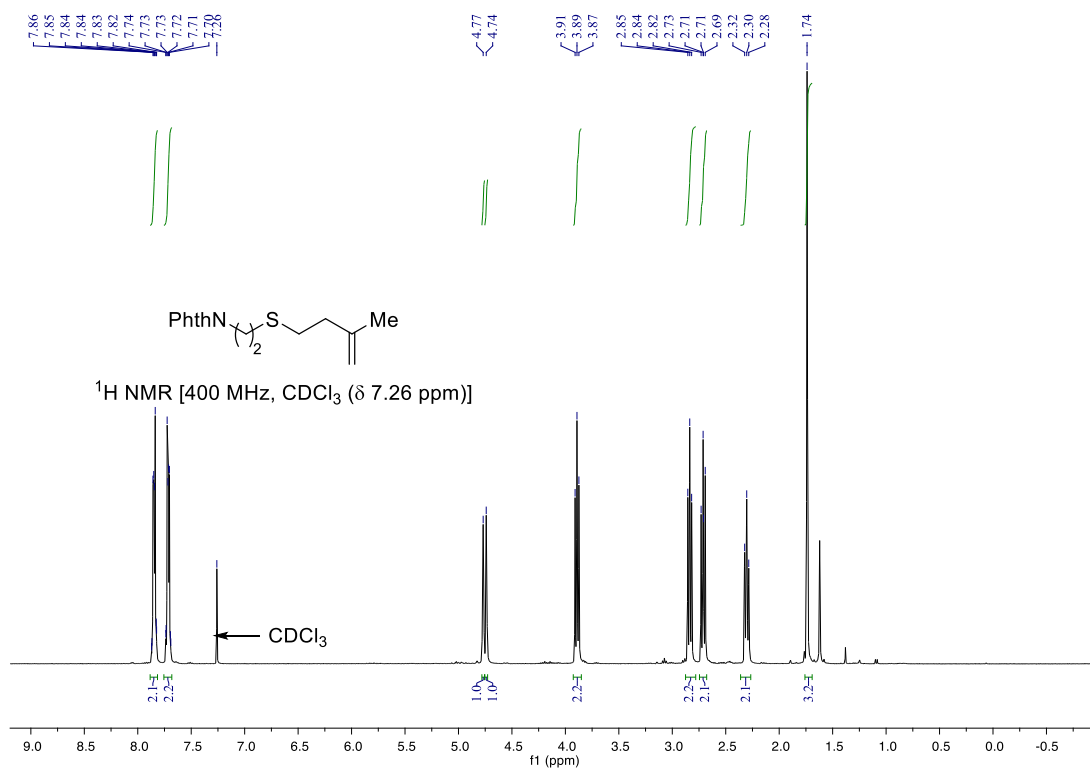
(3-methylbut-3-en-1-yl)(phenethyl)sulfane (6qd)



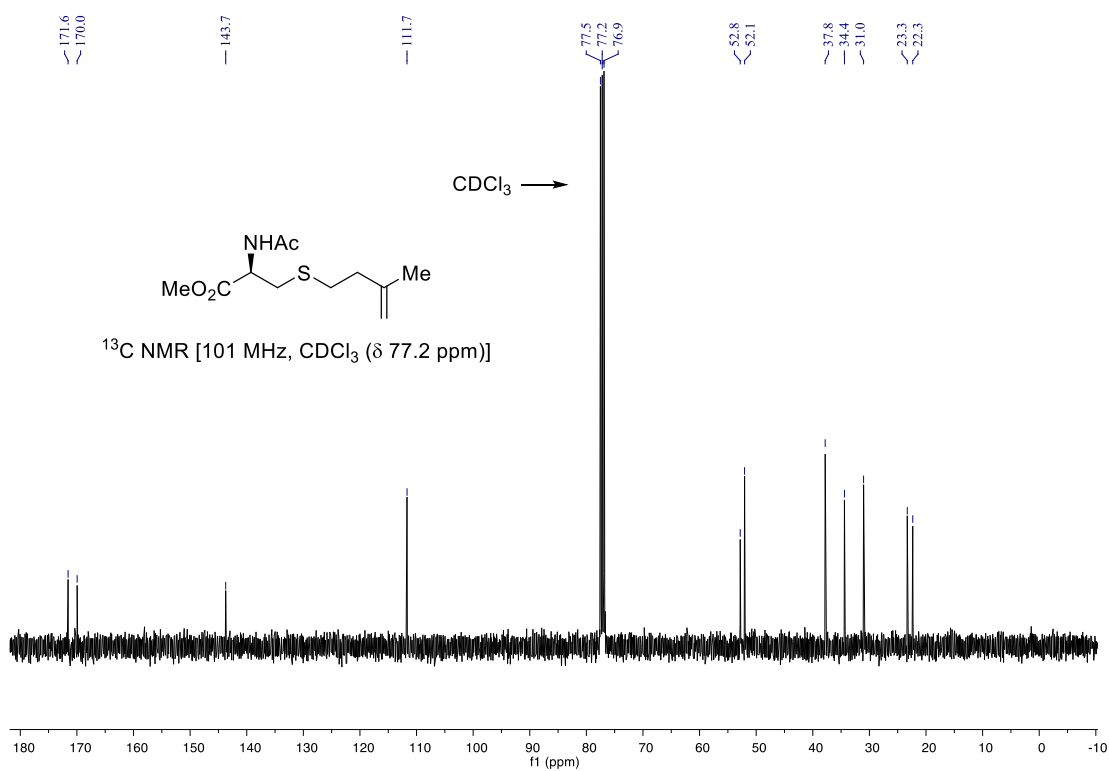
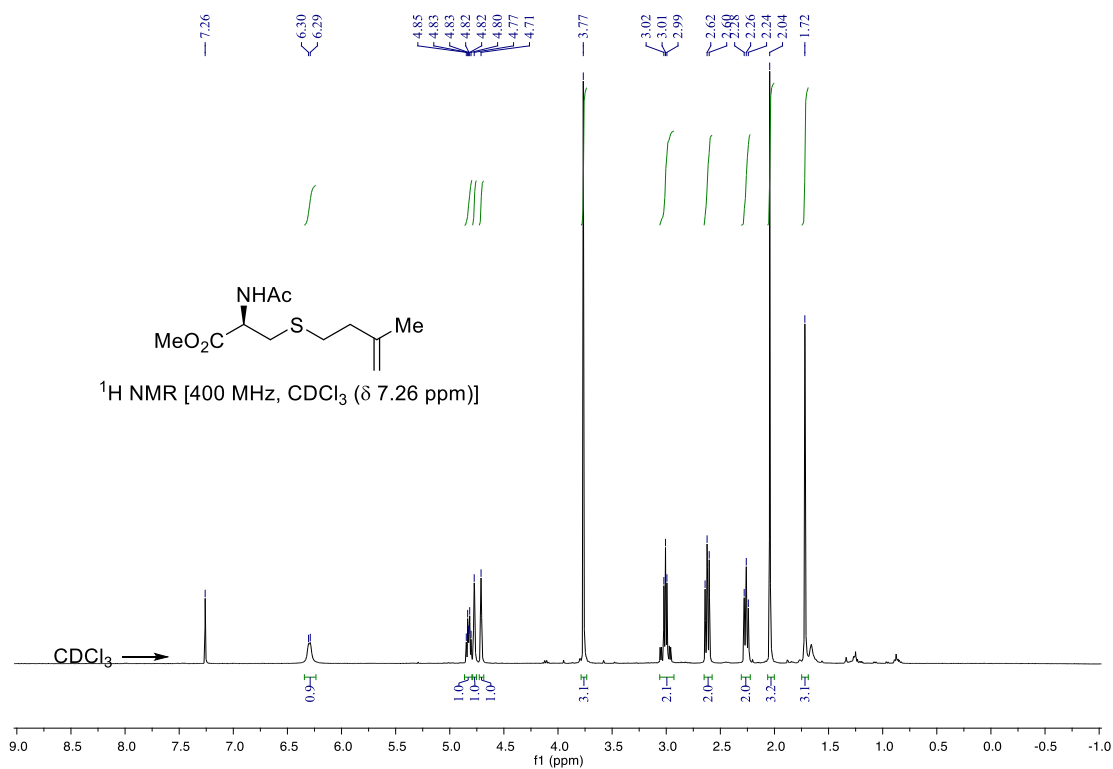
dodecyl(3-methylbut-3-en-1-yl)sulfane (6rd)



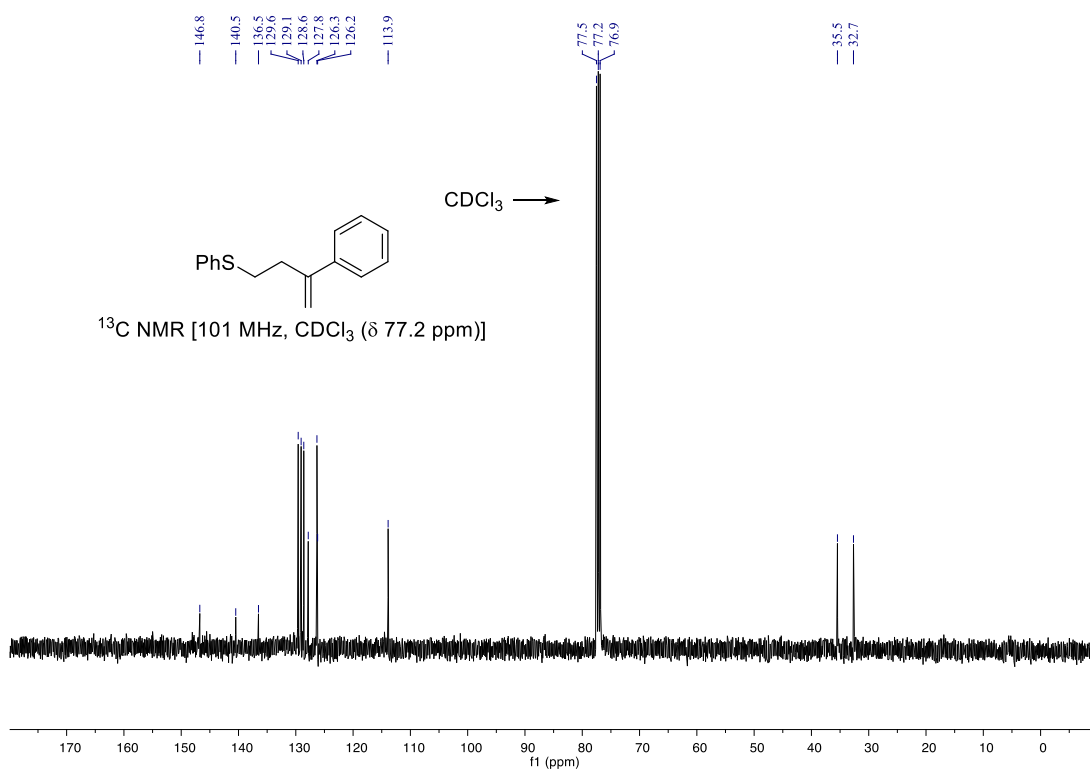
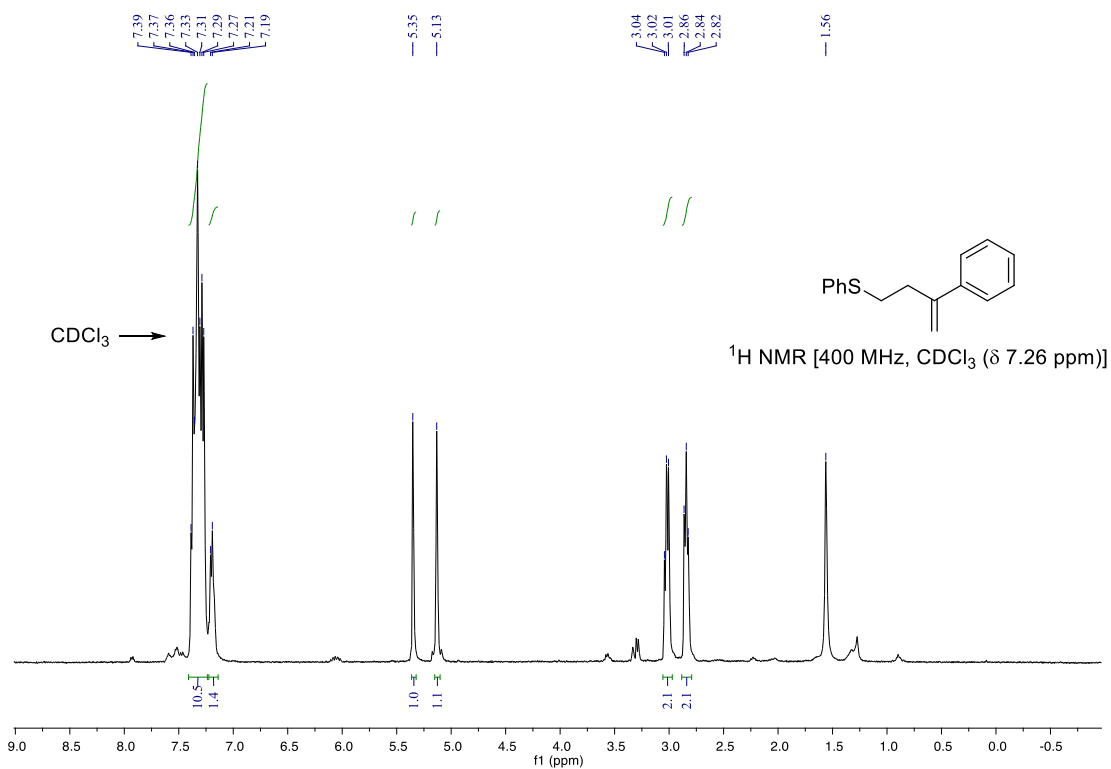
3-(2-((3-methylbut-3-en-1-yl)thio)ethyl)isoindoline (6sd)



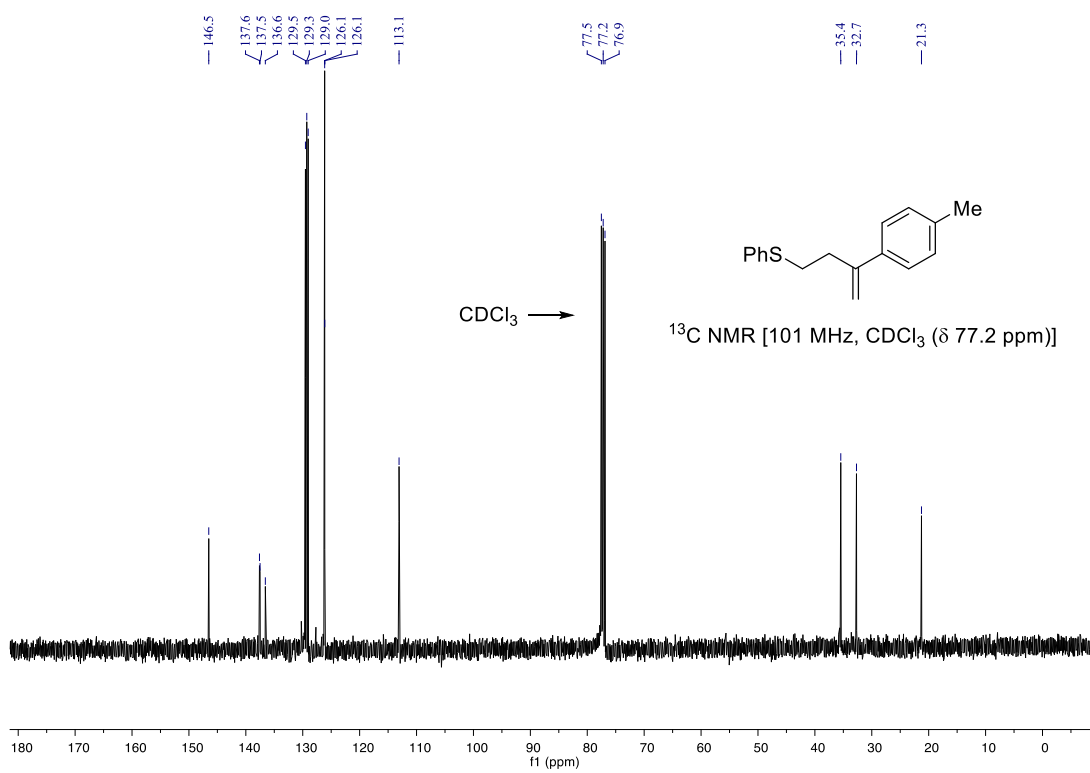
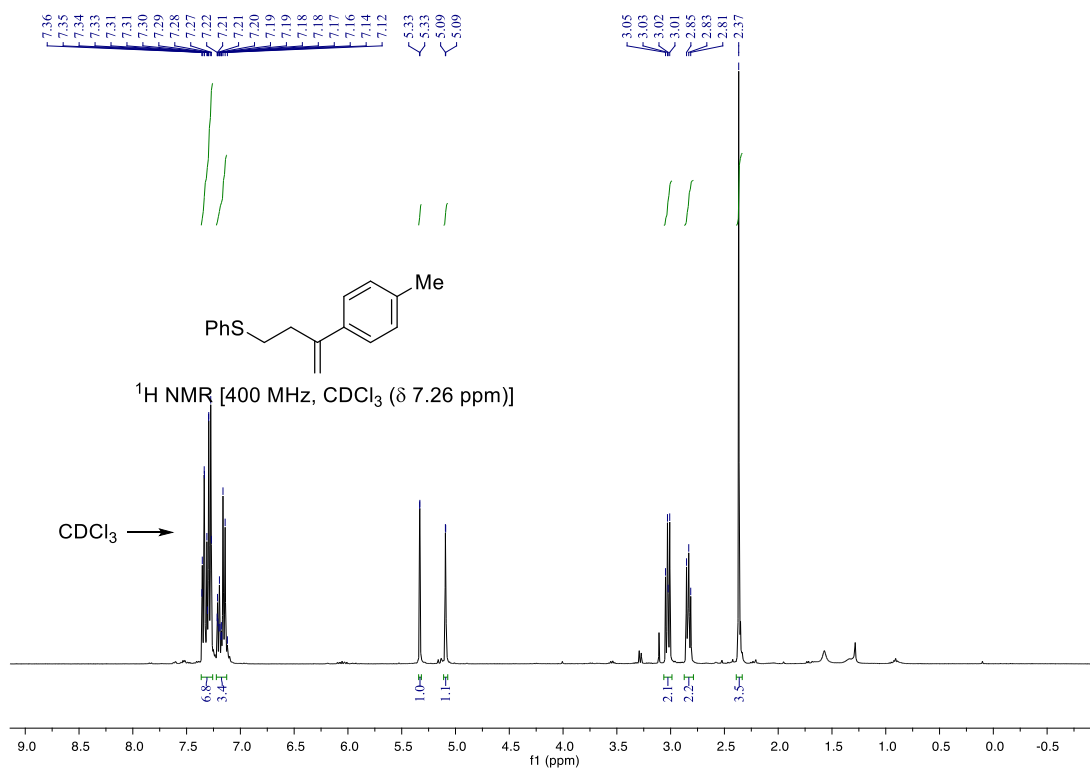
methyl *N*-acetyl-*S*-(3-methylbut-3-en-1-yl)-*L*-cysteinate (6bd)



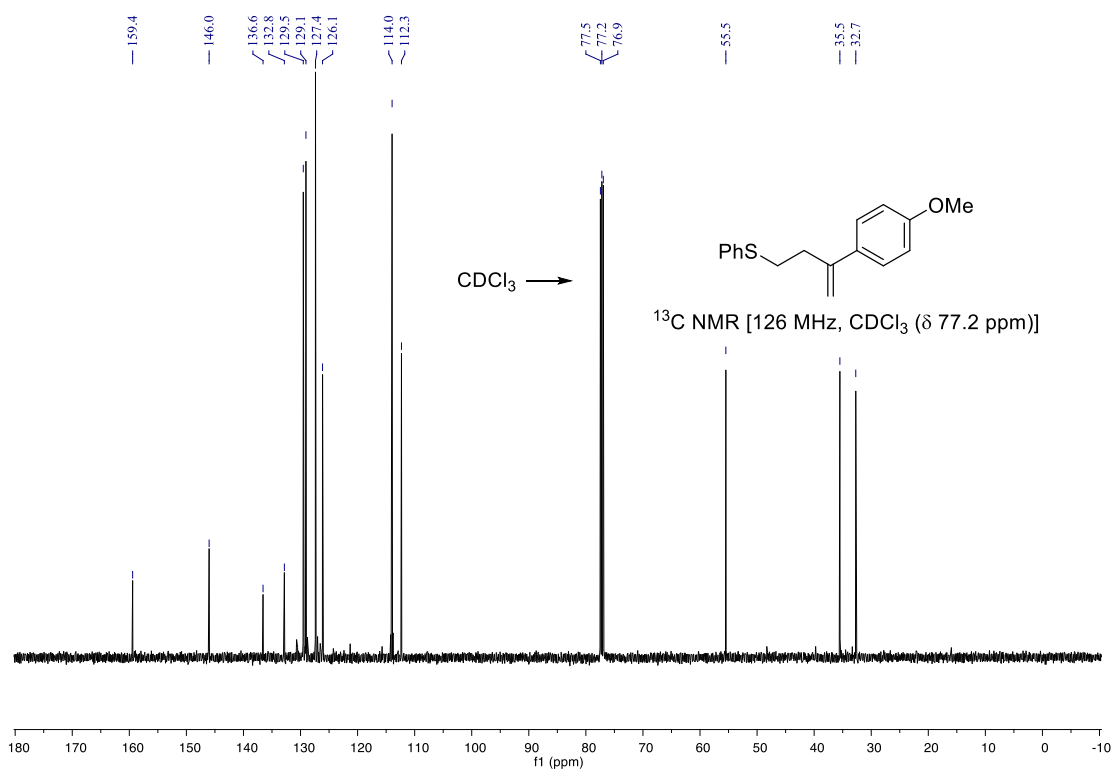
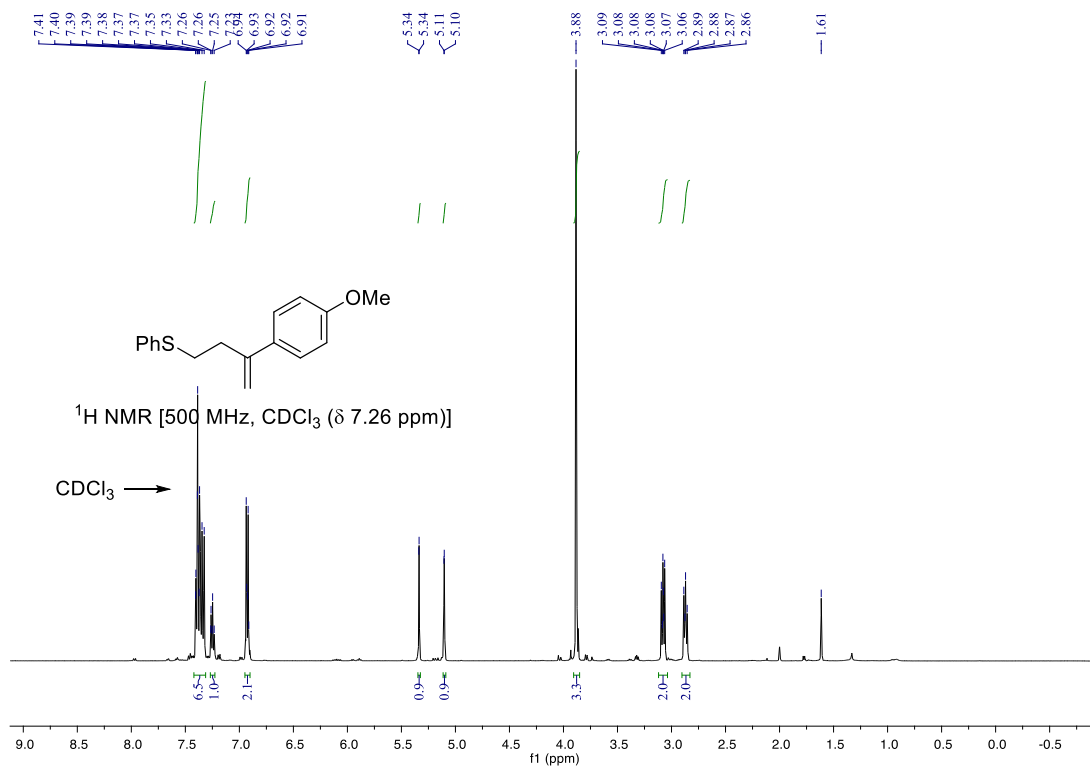
phenyl(3-phenylbut-3-en-1-yl)sulfane (6ae)



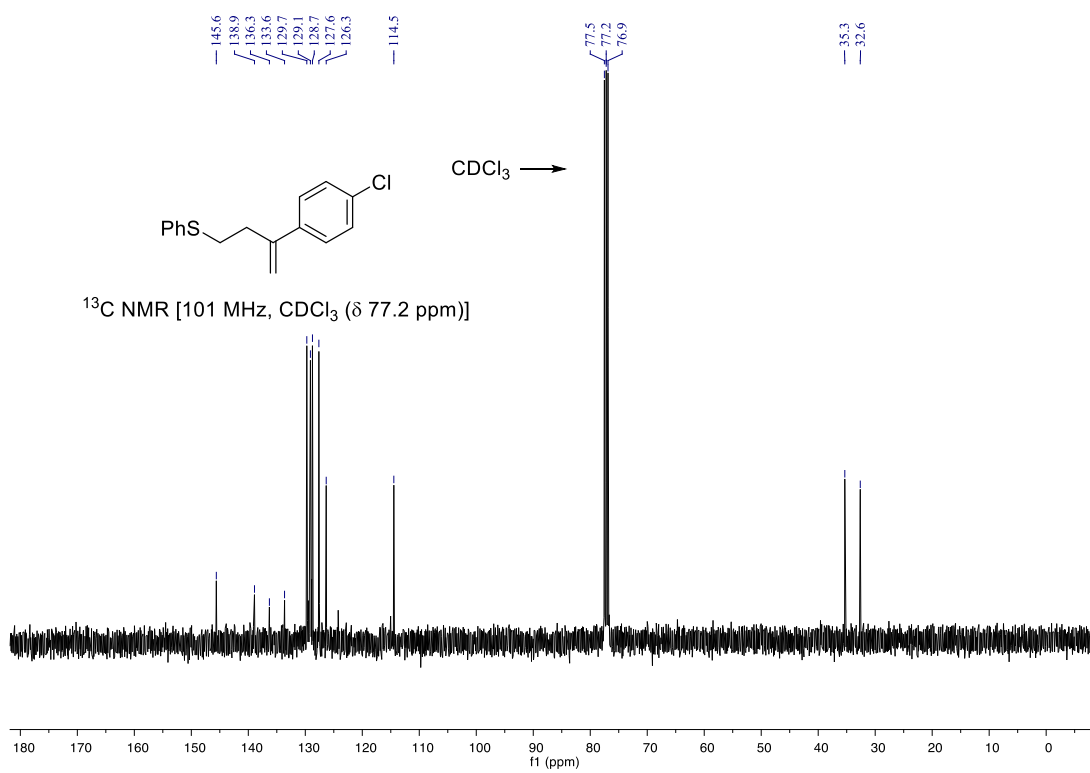
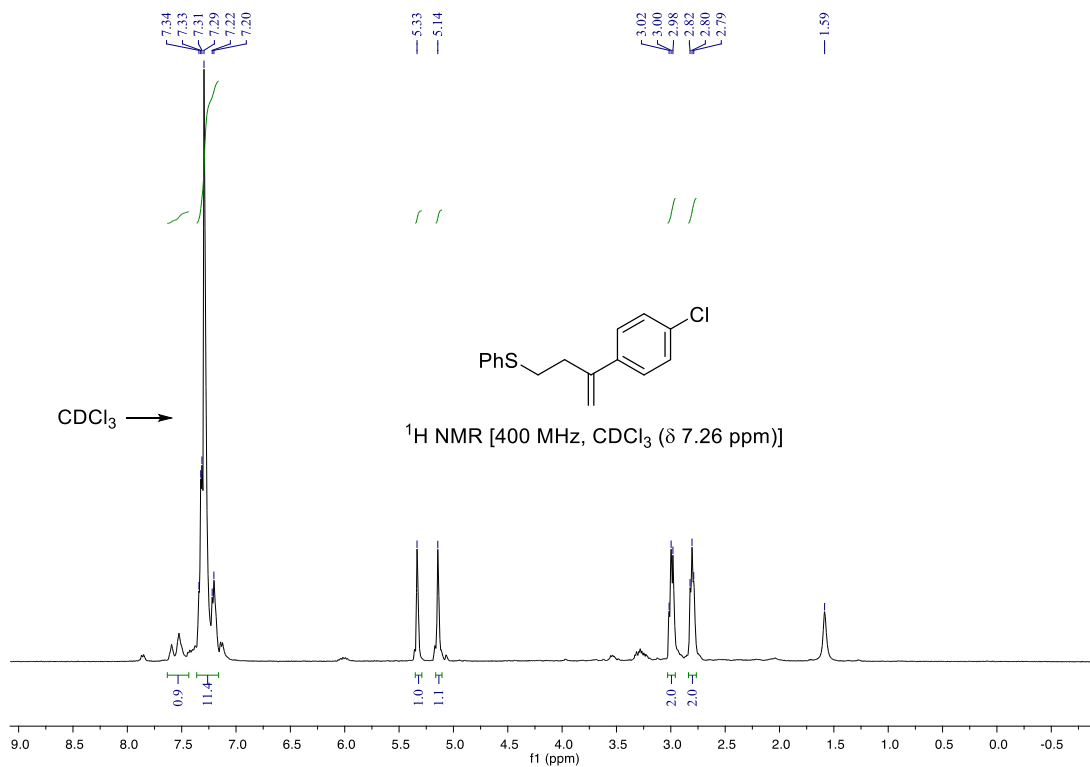
phenyl(3-(*p*-tolyl)but-3-en-1-yl)sulfane (6af)



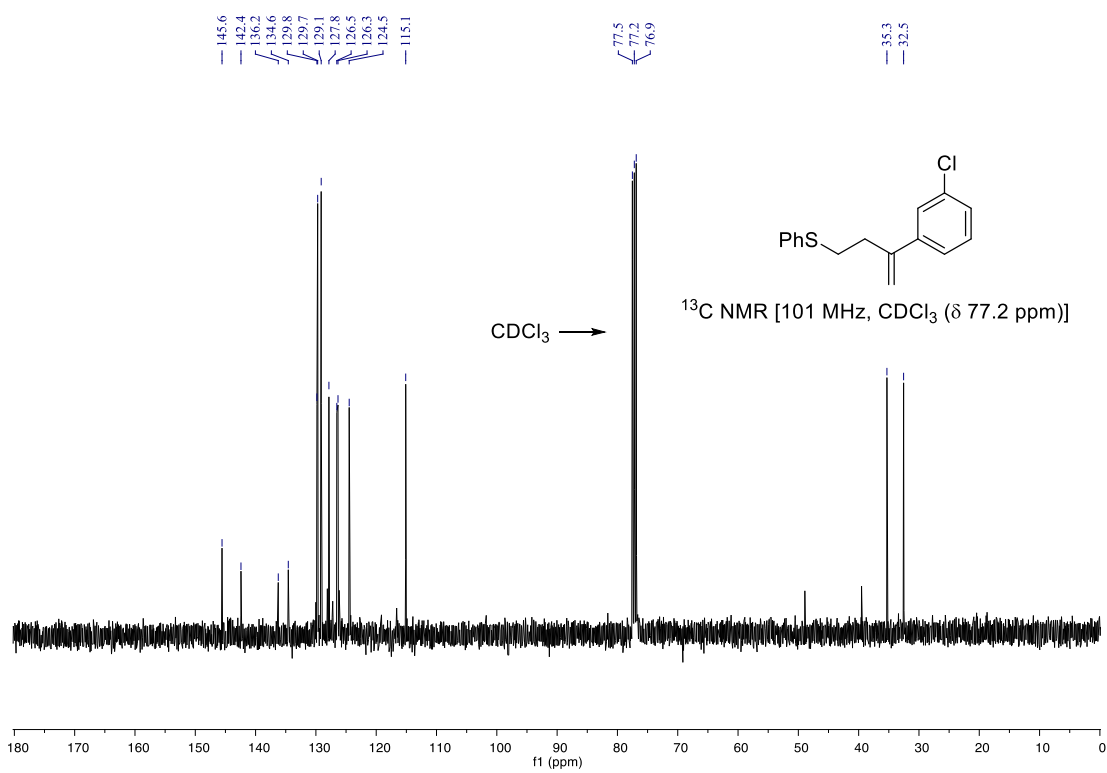
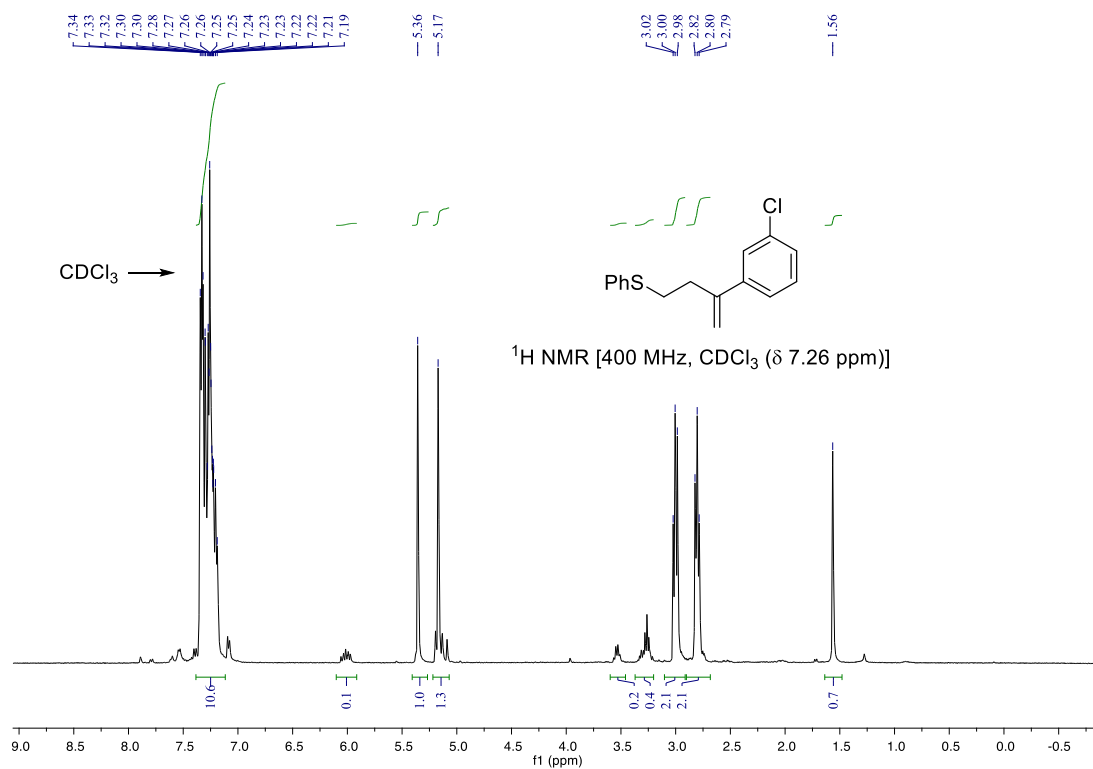
(3-(4-methoxyphenyl)but-3-en-1-yl)(phenyl)sulfane (6ag)



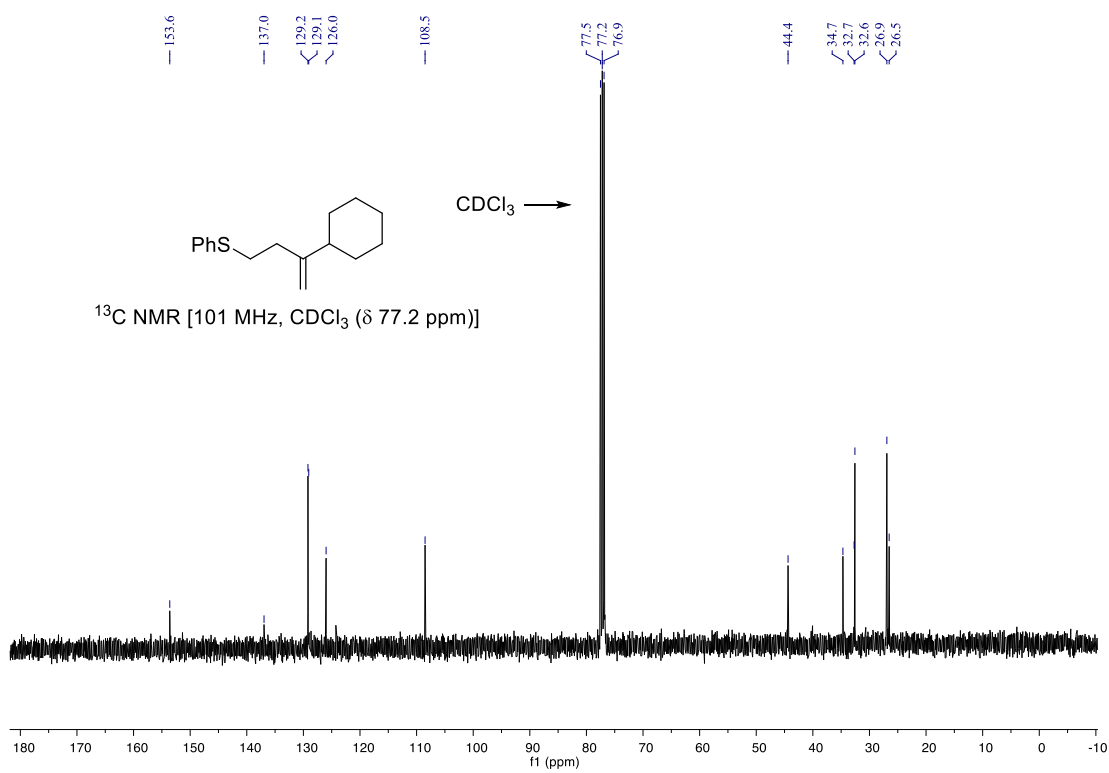
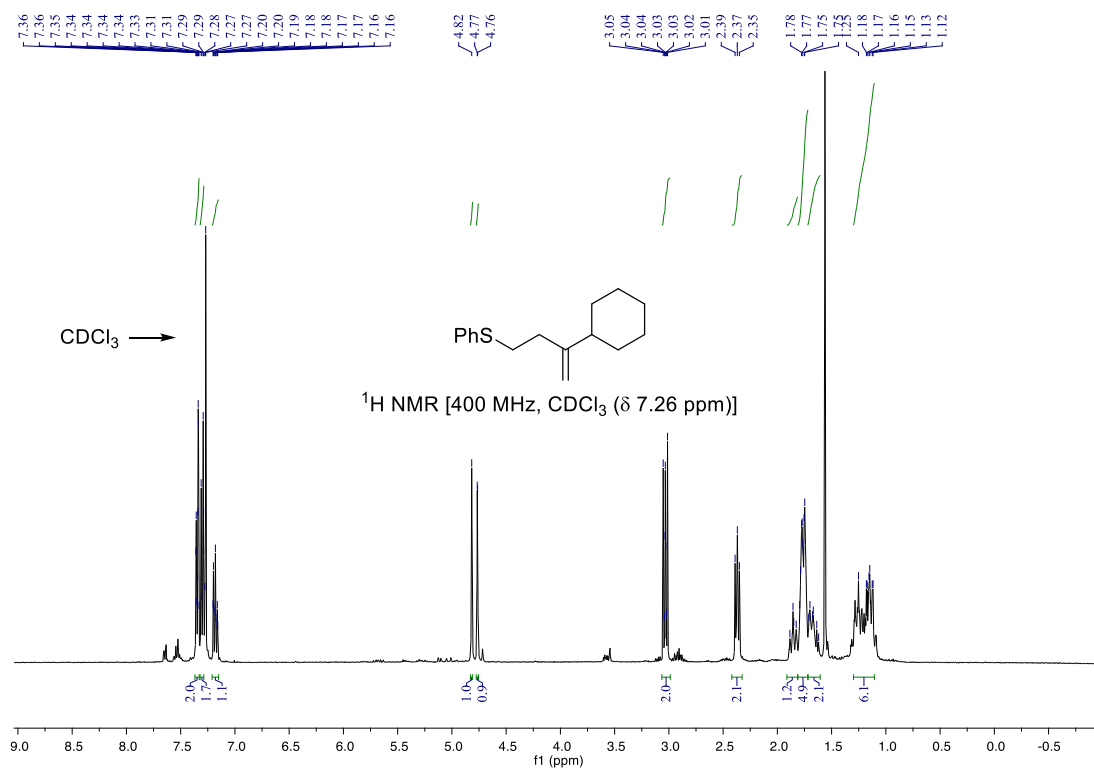
(3-(4-chlorophenyl)but-3-en-1-yl)(phenyl)sulfane (6ah)



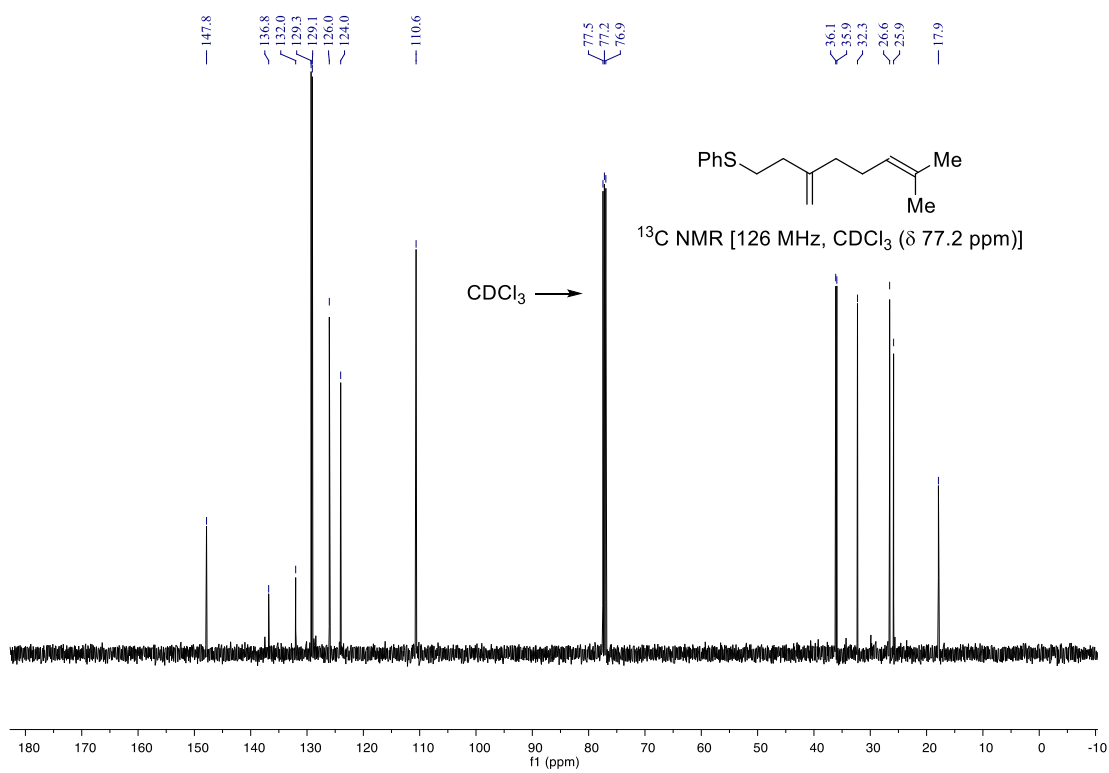
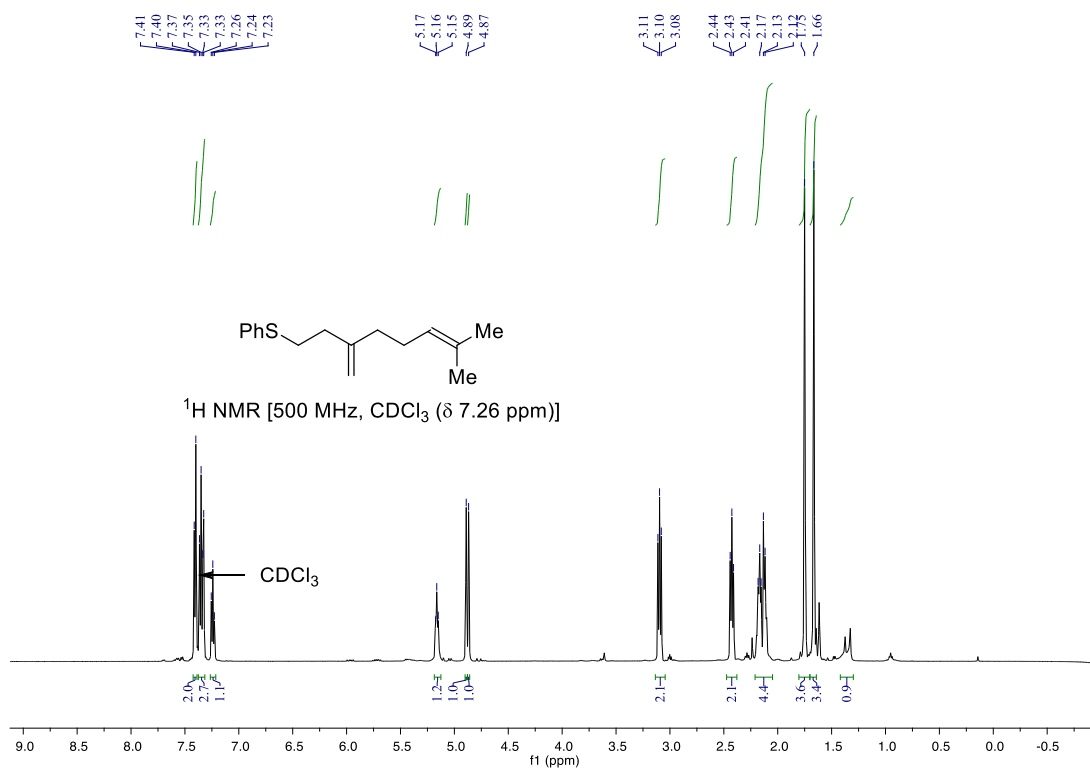
(3-(3-chlorophenyl)but-3-en-1-yl)(phenyl)sulfane (6ai)



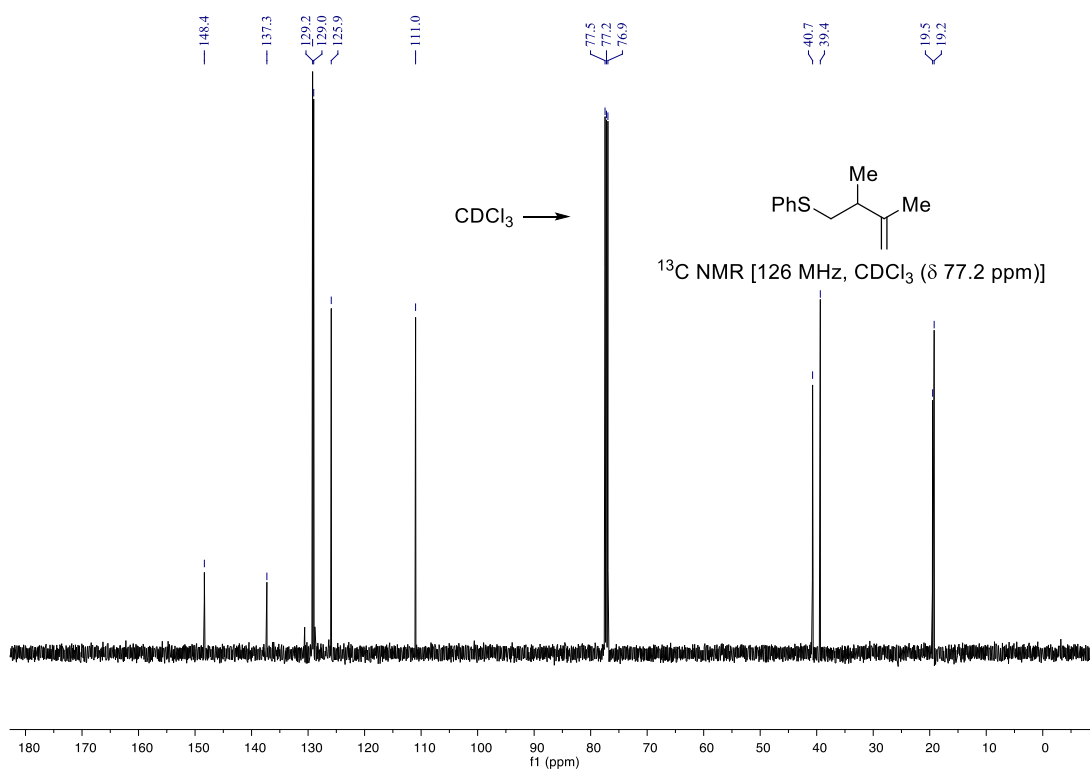
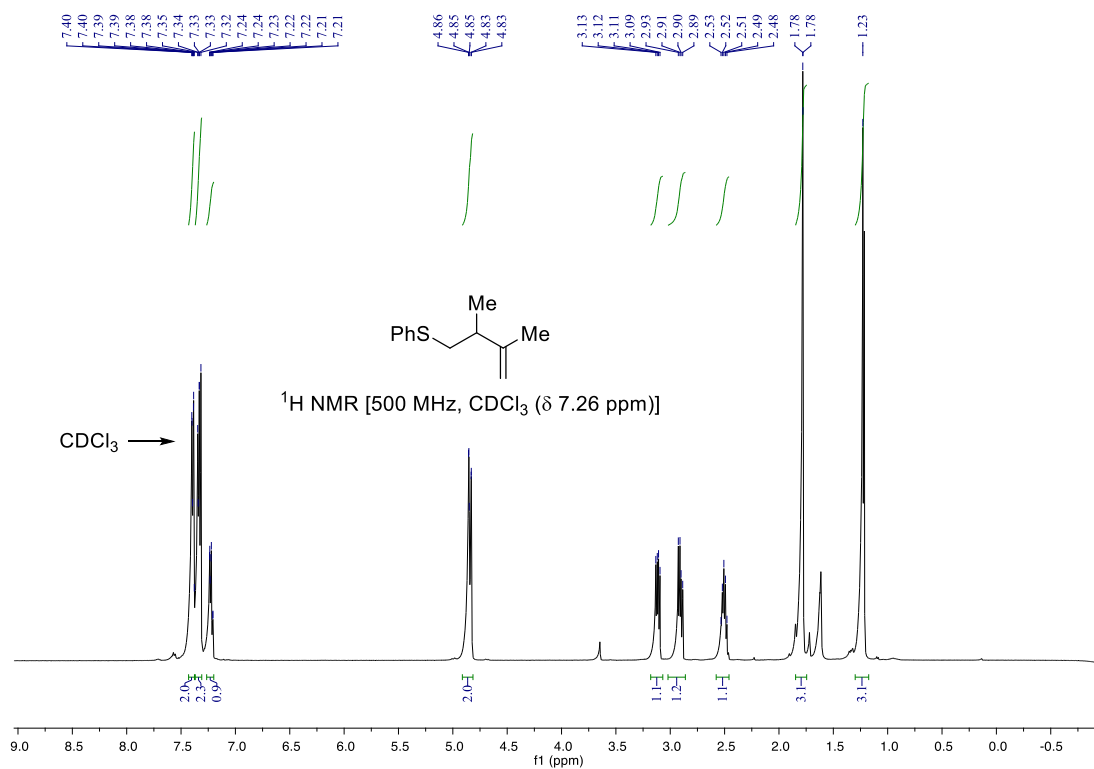
(4-cyclohexylbut-3-en-1-yl)(phenyl)sulfane (6aj)



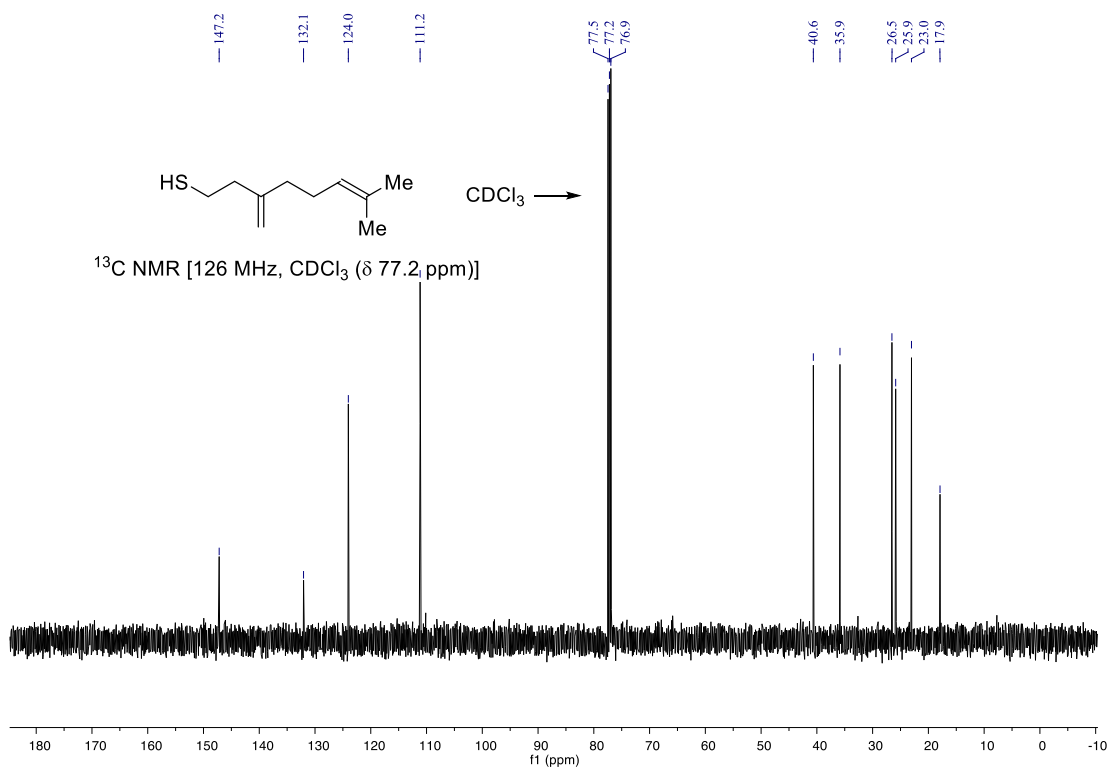
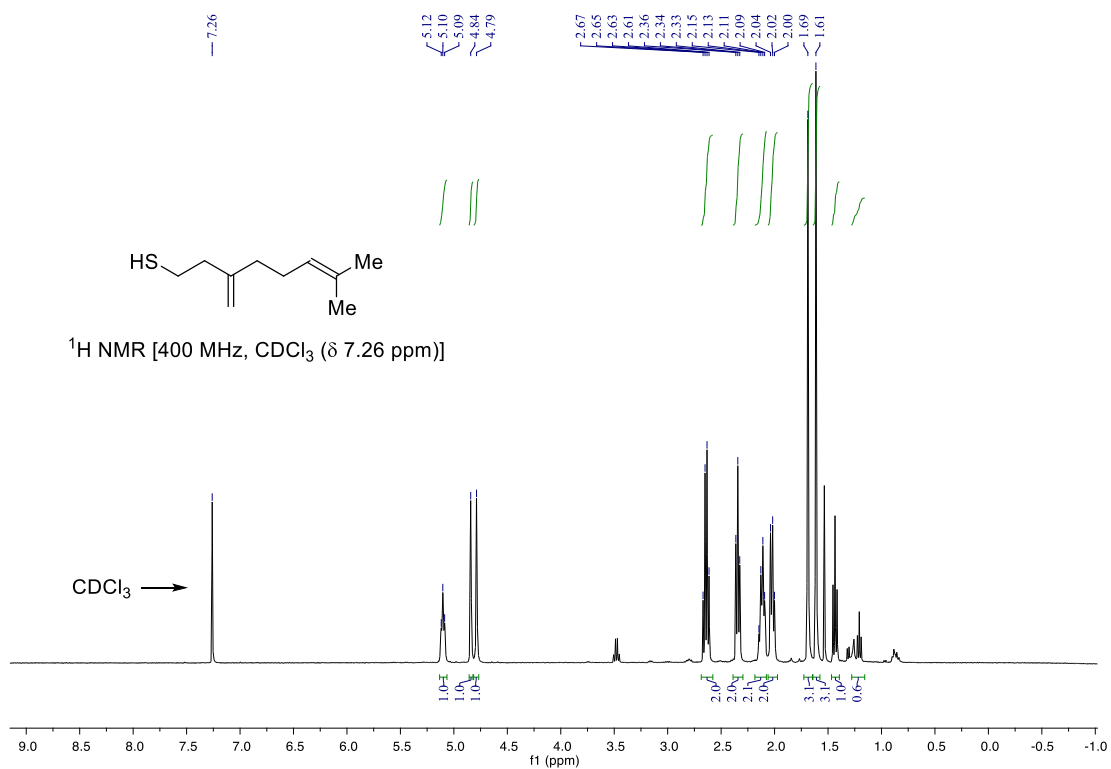
(5-methyl-3-methyleneoct-6-en-1-yl)(phenyl)sulfane (6aa)



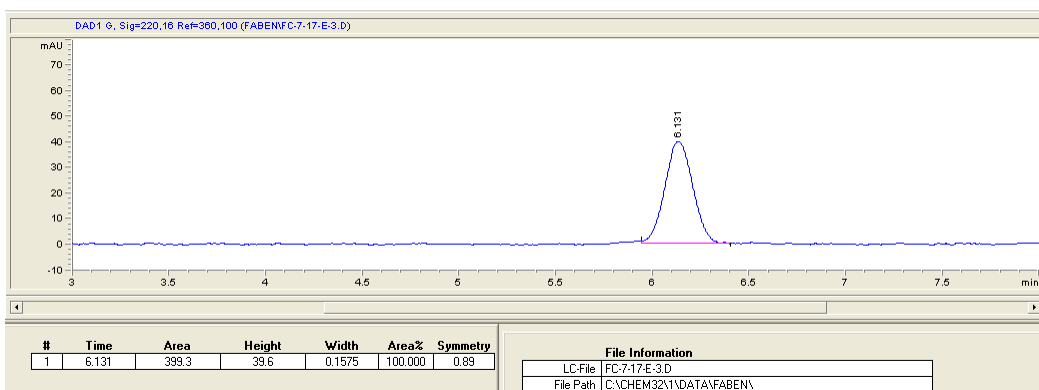
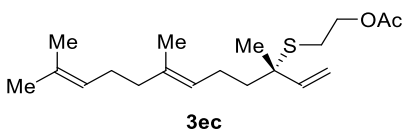
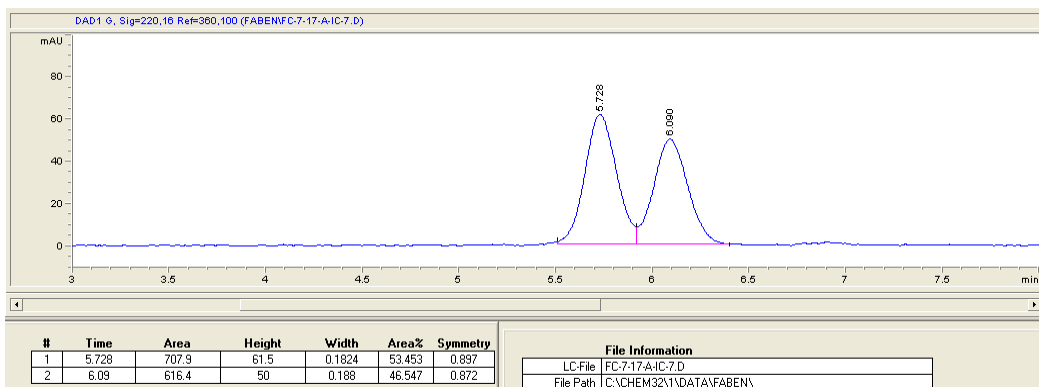
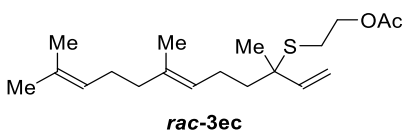
(2,3-dimethylbut-3-en-1-yl)(phenyl)sulfane (6a)



Compound 8



9. SFC spectra



Appendix 3 Supporting Information for Chapter 3

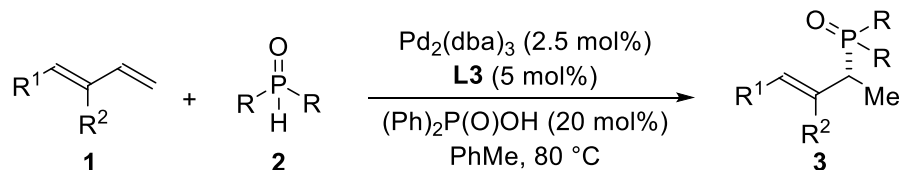
Enantioselective Coupling of Dienes and Phosphine Oxides¹

Table of Contents	Page
1. General	216
2. General procedures for the hydrophosphinylation of 1,3-dienes	217
3. Mechanism studies	228
4. NMR spectra of unknown compounds	237
5. X-ray crystallography data for 3an	293
6. SFC spectra	303
7. References	329

¹ For additional details, see: Nie, S.-Z.; Davison, R. T.; Dong, V. M. *J. Am. Chem. Soc.* **2018**, *140*, 16450–16454.

1. General: Commercial reagents were purchased from Sigma Aldrich, Strem, Alfa Aesar, Acros Organics or TCI and used without further purification. Toluene was purified using an Innovative Technologies Pure Solv system, degassed by three freeze-pump-thaw cycles, and stored over 3 Å MS within a N₂ filled glove box. All experiments were performed in oven-dried or flame-dried glassware. Reactions were monitored using either thin-layer chromatography (TLC) or gas chromatography using an Agilent Technologies 7890A GC system equipped with an Agilent Technologies 5975C inert XL EI/CI MSD. Visualization of the developed plates was performed under UV light (254 nm) or KMnO₄ stain. Organic solutions were concentrated under reduced pressure on a Büchi rotary evaporator. Purification and isolation of products were performed via silica gel chromatography (both column and preparative thin-layer chromatography). Column chromatography was performed with Silicycle Silia-P Flash Silica Gel using glass columns. Solvent was purchased from Fisher. ¹H, ²H, ¹³C, and ³¹P NMR spectra were recorded on Bruker CRYO500 or DRX400 spectrometer. ¹H NMR spectra were internally referenced to the residual solvent signal or TMS. ¹³C NMR spectra were internally referenced to the residual solvent signal. Data for ¹H NMR are reported as follows: chemical shift (δ ppm), multiplicity (s = singlet, d = doublet, t = triplet, q = quartet, m = multiplet), coupling constant (Hz), integration. Data for ²H, ¹³C, and ³¹P NMR are reported in terms of chemical shift (δ ppm). Infrared (IR) spectra were obtained on a Nicolet iS5 FT-IR spectrometer with an iD5 ATR and are reported in terms of frequency of absorption (cm⁻¹). High resolution mass spectra (HRMS) were obtained on a micromass 70S-250 spectrometer (EI) or an ABI/Sciex QStar Mass Spectrometer (ESI). Enantiomeric ratio for enantioselective reactions was determined by chiral SFC analysis using an Agilent Technologies HPLC (1200 series) system and Aurora A5 Fusion. 1,3-Dienes **1a-1l** used here were known compounds and synthesized according to reported methods.^{1,2} Phosphine oxides **2b-2n** used here were known compounds and synthesized according to reported methods.³⁻⁵

2. General procedure for the hydrophosphinylation of 1,3-dienes



In a N₂-filled glovebox, ligand (0.0050 mmol), acid (0.020 mmol) and toluene (0.40 mL) were added to a 1-dram vial containing Pd₂(dba)₃ (0.0025 mol). The resulting mixture was stirred for 10 min and then phosphine oxide (0.10 mmol) and 1,3-diene (0.12 mmol) were added. The mixture was held at 80 °C until no starting material was observed by TLC. The resulting mixture was then cooled to rt. The regioselectivity ratio was determined by ³¹P NMR analysis of the unpurified reaction mixture. Isolated yields (obtained by column chromatography on silica gel or preparative thin-layer chromatography) of the title compound are reported.

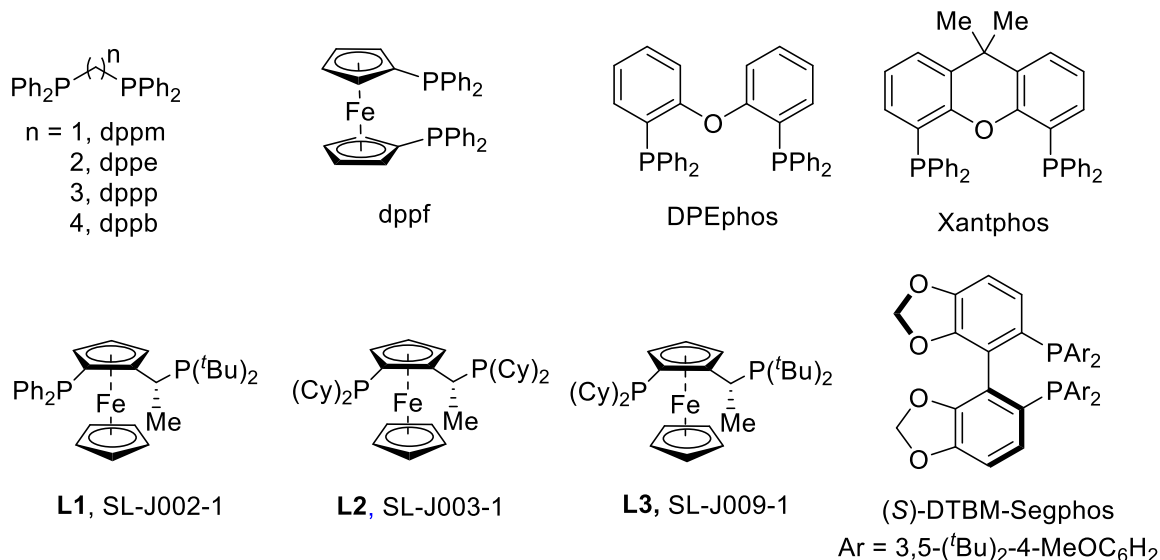
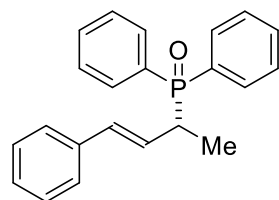


Figure S1. Ligands used for the hydrophosphinylation of 1,3-dienes

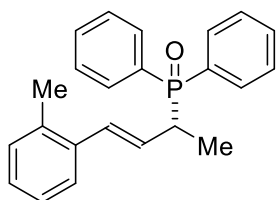
(*R,E*)-diphenyl(4-phenylbut-3-en-2-yl)phosphine oxide (3aa)



White solid, 91% yield, 95:5 *er*, >20:1 *rr*, [α]_D²⁴ = +90.0 (*c* 0.3, CHCl₃). ³¹P NMR (162 MHz, CDCl₃) δ 34.46. ¹H NMR (400 MHz, CDCl₃) δ 7.95 – 7.78 (m, 4H), 7.63 – 7.45 (m, 6H), 7.35 – 7.24 (m, 5H), 6.38 (dd, *J* = 16.0, 4.4 Hz, 1H), 6.29 – 6.18 (m, 1H), 3.46 – 3.30 (m, 1H), 1.46 (dd, *J* = 16.0, 6.8 Hz, 3H). ¹³C NMR (101 MHz, CDCl₃) δ 137.30 (d, *J* = 3.0 Hz), 133.59 (d, *J* = 12.1 Hz), 132.13 (dd, *J* = 9.1, 3.0 Hz), 131.83 (dd, *J* = 20.2, 9.1, Hz), 128.92 (dd, *J* = 27.3, 11.1 Hz), 128.91, 127.92, 126.64, 126.63, 126.38 (d, *J* = 8.1 Hz), 39.00 (d, *J* = 69.7 Hz), 13.84. IR (ATR): 3056, 1437, 1179, 1117, 965, 711, 692 cm⁻¹. HRMS

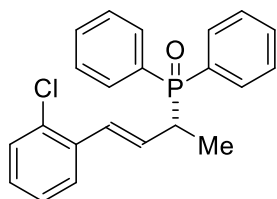
calculated for $C_{22}H_{21}OPNa$ $[M+Na]^+$ 355.1228, found 355.1237. **Chiral SFC:** 100 mm CHIRALCEL OJ-H, 2% *i*PrOH, 2.5 mL/min, 220 nm, 44 °C, nozzle pressure = 200 bar CO_2 , t_{R1} (major) = 10.2 min, t_{R2} (minor) = 13.6 min.

(*R,E*)-diphenyl(4-(*o*-tolyl)but-3-en-2-yl)phosphine oxide (3ba)



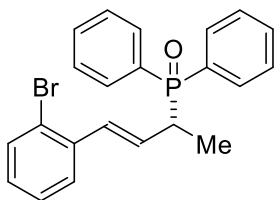
White solid, 86% yield, 95:5 *er*, >20:1 *rr*, $[\alpha]^{24}_D = +66.0$ (*c* 0.4, $CHCl_3$). ^{31}P NMR (162 MHz, $CDCl_3$) δ 35.09. 1H NMR (500 MHz, $CDCl_3$) δ 7.90 – 7.85 (m, 2H), 7.82 – 7.76 (m, 2H), 7.56 – 7.39 (m, 6H), 7.24 (d, $J = 3.5$ Hz, 1H), 7.13 – 7.02 (m, 3H), 6.52 (dd, $J = 16.0, 4.5$ Hz, 1H), 6.09 – 5.98 (m, 1H), 3.45 – 3.31 (m, 1H), 2.10 (s, 3H), 1.42 (dd, $J = 16.0, 7.0$ Hz, 3H). ^{13}C NMR (126 MHz, $CDCl_3$) δ 136.11 (d, $J = 2.5$ Hz), 135.20 (d, $J = 1.3$ Hz), 131.87 (dd, $J = 94.5, 63.0$ Hz), 131.74 (dd, $J = 11.3, 2.5$ Hz), 131.46 (dd, $J = 35.3, 7.6$ Hz), 131.44, 130.12, 128.56 (dd, $J = 35.3, 11.3$ Hz), 127.48, 127.43, 126.10, 125.78 (d, $J = 2.5$ Hz), 39.00 (d, $J = 69.3$ Hz), 19.60, 13.60 (d, $J = 3.8$ Hz). **IR** (ATR): 3055, 1559, 1484, 1437, 1179, 1117, 751 cm^{-1} . **HRMS** calculated for $C_{23}H_{23}OPNa$ $[M+Na]^+$ 369.1384, found 369.1389. **Chiral SFC:** 100 mm CHIRALCEL OJ-H, 2% *i*PrOH, 2.5 mL/min, 220 nm, 44 °C, nozzle pressure = 200 bar CO_2 , t_{R1} (major) = 10.7 min, t_{R2} (minor) = 15.2 min.

(*R,E*)-(4-(2-chlorophenyl)but-3-en-2-yl)diphenylphosphine oxide (3ca)



White solid, 81% yield, 94:6 *er*, >20:1 *rr*, $[\alpha]^{24}_D = +39.4$ (*c* 0.5, $CHCl_3$). ^{31}P NMR (162 MHz, $CDCl_3$) δ 35.04. 1H NMR (500 MHz, $CDCl_3$) δ 7.96 – 7.88 (m, 2H), 7.87 – 7.82 (m, 2H), 7.64 – 7.45 (m, 6H), 7.44 – 7.38 (m, 1H), 7.36 – 7.33 (m, 1H), 7.24 – 7.15 (m, 2H), 6.77 (dd, $J = 16.0, 4.5$ Hz, 1H), 6.28 – 6.17 (m, 1H), 3.52 – 3.41 (m, 1H), 1.49 (dd, $J = 16.0, 7.5$ Hz, 3H). ^{13}C NMR (126 MHz, $CDCl_3$) δ 135.03 (d, $J = 1.3$ Hz), 132.54 (d, $J = 66.8$ Hz), 131.81 (dd, $J = 8.8, 2.5$ Hz), 131.39 (dd, $J = 23.9, 8.8$ Hz), 131.11, 129.62 (d, $J = 11.3$ Hz), 129.54, 129.11 (d, $J = 7.6$ Hz), 128.74 (dd, $J = 30.2, 11.3$ Hz), 128.58, 126.96 (d, $J = 1.3$ Hz), 126.87, 39.04 (d, $J = 68.0$ Hz), 13.50 (d, $J = 3.8$ Hz). **IR** (ATR): 3056, 1699, 1591, 1437, 1178, 1118, 721 cm^{-1} . **HRMS** calculated for $C_{22}H_{20}ClOPNa$ $[M+Na]^+$ 389.0838, found 389.0820. **Chiral SFC:** 100 mm CHIRALCEL OJ-H, 3.0% *i*PrOH, 2.0 mL/min, 220 nm, 44 °C, nozzle pressure = 200 bar CO_2 , t_{R1} (major) = 8.5 min, t_{R2} (minor) = 10.5 min.

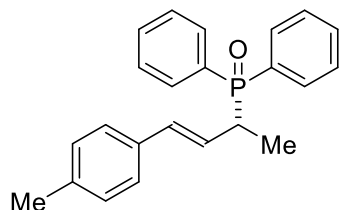
(*R,E*)-(4-(2-bromophenyl)but-3-en-2-yl)diphenylphosphine oxide (3da)



White solid, 36% yield, 96:4 *er*, >20:1 *rr*, $[\alpha]^{24}_D = +29.9$ (*c* 0.4, $CHCl_3$). ^{31}P NMR (162 MHz, $CDCl_3$) δ 35.07. 1H NMR (400 MHz, $CDCl_3$) δ 7.88 – 7.78 (m, 4H), 7.56 – 7.42 (m, 7H), 7.34 – 7.32 (m, 1H), 7.22 – 7.18 (m, 1H), 7.07 – 7.03 (m, 1H), 6.68 (dd, $J = 15.6, 4.0$ Hz, 1H), 6.20 – 6.10 (m, 1H), 3.49 – 3.35 (m, 1H), 1.44 (dd, $J = 16.8, 7.2$ Hz, 3H). ^{13}C NMR (126 MHz, $CDCl_3$) δ 136.79 (d, $J = 2.5$ Hz), 132.79, 132.25 (d, $J = 12.6$ Hz), 132.24, 131.86 (dd, $J = 8.8, 2.5$ Hz), 131.42 (dd, $J = 25.2, 8.8$ Hz), 129.29 (d, $J = 7.6$ Hz), 128.88, 128.66 (dd, $J = 27.7,$

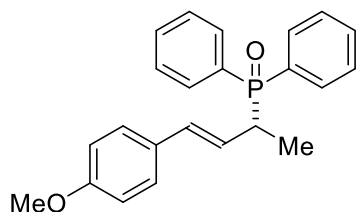
12.6 Hz), 127.54, 127.22 (d, $J = 1.3$ Hz), 123.37 (d, $J = 2.5$ Hz), 38.97 (d, $J = 69.3$ Hz), 13.52 (d, $J = 3.8$ Hz). **IR** (ATR): 2968, 1436, 1180, 1117, 1071, 1023, 965 cm^{-1} . **HRMS** calculated for $\text{C}_{22}\text{H}_{20}\text{BrOPNa}$ $[\text{M}+\text{Na}]^+$ 433.0333, found 433.0338. **Chiral SFC**: 100 mm CHIRALCEL OJ-H, 2.0% i PrOH, 2.0 mL/min, 254 nm, 44 $^{\circ}\text{C}$, nozzle pressure = 200 bar CO_2 , $t_{\text{R}1}$ (major) = 10.8 min, $t_{\text{R}2}$ (minor) = 13.8 min.

(*R,E*)-diphenyl(4-(*p*-tolyl)but-3-en-2-yl)phosphine oxide (3ea)



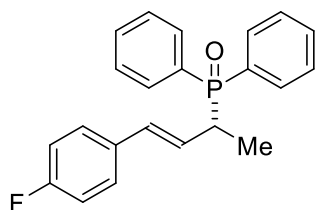
White solid, 82% yield, 92:8 *er*, >20:1 *rr*, $[\alpha]_{\text{D}}^{24} = +34.1$ (c 0.2, CHCl_3). ^{31}P NMR (162 MHz, CDCl_3) δ 34.66. ^1H NMR (400 MHz, CDCl_3) δ 7.94 – 7.78 (m, 4H), 7.63 – 7.45 (m, 6H), 7.20 – 7.08 (m, 4H), 6.34 (dd, $J = 16.0, 4.0$ Hz, 1H), 6.24 – 6.12 (m, 1H), 3.44 – 3.32 (m, 1H), 2.36 (s, 3H), 1.45 (dd, $J = 16.0, 7.2$ Hz, 3H). ^{13}C NMR (101 MHz, CDCl_3) δ 137.76 (d, $J = 1.0$ Hz), 134.55 (d, $J = 3.0$ Hz), 133.42 (d, $J = 2.0$ Hz), 132.70 (d, $J = 51.5$ Hz), 132.07 (dd, $J = 9.1, 3.0$ Hz), 131.85 (dd, $J = 24.2, 8.1$ Hz), 129.61 (d, $J = 1.0$ Hz), 128.88 (dd, $J = 29.3, 12.1$ Hz), 126.54 (d, $J = 2.0$ Hz), 125.31 (d, $J = 10.1$ Hz), 39.04 (d, $J = 69.7$ Hz), 21.57, 13.88. **IR** (ATR): 2968, 1511, 1435, 1175, 981, 803, 718 cm^{-1} . **HRMS** calculated for $\text{C}_{23}\text{H}_{23}\text{OPNa}$ $[\text{M}+\text{Na}]^+$ 369.1384, found 369.1399. **Chiral SFC**: 100 mm CHIRALPAK AD-H, 15% i PrOH, 2.5 mL/min, 220 nm, 44 $^{\circ}\text{C}$, nozzle pressure = 200 bar CO_2 , $t_{\text{R}1}$ (minor) = 15.3 min, $t_{\text{R}2}$ (major) = 17.0 min.

(*R,E*)-(4-(4-methoxyphenyl)but-3-en-2-yl)diphenylphosphine oxide (3fa)



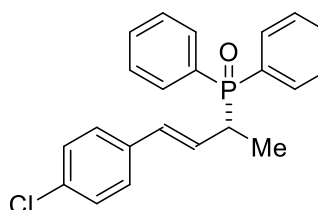
White solid, 80% yield, 88:12 *er*, >20:1 *rr*, $[\alpha]_{\text{D}}^{24} = +84.1$ (c 0.6, CHCl_3). ^{31}P NMR (162 MHz, CDCl_3) δ 35.20. ^1H NMR (500 MHz, CDCl_3) δ 7.84 (t, $J = 8.0$ Hz, 2H), 7.77 (t, $J = 8.0$ Hz, 2H), 7.57 – 7.45 (m, 4H), 7.43 – 7.38 (m, 2H), 7.15 (d, $J = 8.0$ Hz, 2H), 6.79 (d, $J = 8.0$ Hz, 2H), 6.26 (dd, $J = 15.5, 4.0$ Hz, 1H), 6.08 – 5.97 (m, 1H), 3.77 (s, 3H), 3.35 – 3.24 (m, 1H), 1.39 (dd, $J = 16.0, 7.0$ Hz, 3H). ^{13}C NMR (126 MHz, CDCl_3) δ 159.21, 132.62 (d, $J = 11.3$ Hz), 131.85 (dd, $J = 94.5, 56.7$ Hz), 131.71 (dd, $J = 7.6, 2.5$ Hz), 131.47 (d, $J = 29.0, 7.6$ Hz), 129.77 (d, $J = 3.8$ Hz), 128.52 (dd, $J = 35.3, 11.3$ Hz), 127.43 (d, $J = 1.3$ Hz), 123.62 (d, $J = 7.6$ Hz), 113.96, 55.31, 38.55 (d, $J = 69.3$ Hz), 13.55 (d, $J = 3.8$ Hz). **IR** (ATR): 2969, 2366, 1606, 1510, 1437, 1174, 1117 cm^{-1} . **HRMS** calculated for $\text{C}_{23}\text{H}_{23}\text{O}_2\text{PNa}$ $[\text{M}+\text{Na}]^+$ 385.1333, found 385.1345. **Chiral SFC**: 100 mm CHIRALPAK AD-H, 20% i PrOH, 3.0 mL/min, 220 nm, 44 $^{\circ}\text{C}$, nozzle pressure = 200 bar CO_2 , $t_{\text{R}1}$ (minor) = 7.6 min, $t_{\text{R}2}$ (major) = 9.9 min.

(*R,E*)-(4-(4-fluorophenyl)but-3-en-2-yl)diphenylphosphine oxide (3ga)



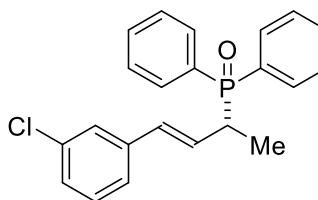
White solid, 87% yield, 91:9 *er*, >20:1 *rr*, $[\alpha]^{24}_D = +75.3$ (*c* 0.3, CHCl₃). ³¹P NMR (162 MHz, CDCl₃) δ 35.07. ¹H NMR (500 MHz, CDCl₃) δ 7.89 – 7.81 (m, 2H), 7.80 – 7.72 (m, 2H), 7.58 – 7.37 (m, 6H), 7.22 – 7.10 (m, 2H), 6.98 – 6.87 (m, 2H), 6.27 (dd, *J* = 15.5, 4.0 Hz, 1H), 6.16 – 6.05 (m, 1H), 3.38 – 3.26 (m, 1H), 1.40 (dd, *J* = 16.0, 7.0 Hz, 3H). ¹³C NMR (126 MHz, CDCl₃) δ 162.30 (d, *J* = 247.0 Hz), 133.08 (t, *J* = 2.5 Hz), 132.15 (d, *J* = 27.7 Hz), 132.03 (d, *J* = 11.3 Hz), 131.78 (dd, *J* = 12.6, 2.5 Hz), 131.40 (dd, *J* = 21.4, 8.8 Hz), 128.56 (dd, *J* = 35.3, 11.3 Hz), 127.75 (d, *J* = 7.6 Hz), 125.71 (dd, *J* = 7.6, 1.3 Hz), 115.44 (d, *J* = 21.4 Hz), 38.50 (d, *J* = 68.0 Hz), 13.45 (d, *J* = 3.8 Hz). IR (ATR): 3056, 2366, 1653, 1507, 1437, 1178, 717 cm⁻¹. HRMS calculated for C₂₂H₂₀FOPNa [M+Na]⁺ 373.1133, found 373.1141. Chiral SFC: 100 mm CHIRALPAK AD-H, 20% *i*PrOH, 2.5 mL/min, 220 nm, 44 °C, nozzle pressure = 200 bar CO₂, *t*_{R1} (minor) = 7.2 min, *t*_{R2} (major) = 8.6 min.

(*R,E*)-(4-(4-chlorophenyl)but-3-en-2-yl)diphenylphosphine oxide (3ha)



White solid, 71% yield, 93:7 *er*, >20:1 *rr*, $[\alpha]^{24}_D = +14.5$ (*c* = 0.2, CHCl₃). ³¹P NMR (162 MHz, CDCl₃) δ 35.14. ¹H NMR (500 MHz, CDCl₃) δ 7.90 (t, *J* = 7.5 Hz, 2H), 7.81 (t, *J* = 8.0 Hz, 2H), 7.64 – 7.52 (m, 4H), 7.51 – 7.44 (m, 2H), 7.30 – 7.24 (m, 2H), 7.22 – 7.14 (m, 2H), 6.32 (dd, *J* = 16.0, 4.0 Hz, 1H), 6.27 – 6.18 (m, 1H), 3.45 – 3.33 (m, 1H), 1.46 (dd, *J* = 16.0, 7.0 Hz, 3H). ¹³C NMR (126 MHz, CDCl₃) δ 135.38 (d, *J* = 3.8 Hz), 133.20, 132.02 (dd, *J* = 20.2, 8.8 Hz), 131.84 (dd, *J* = 13.9, 2.5 Hz), 131.39 (dd, *J* = 17.6, 8.8 Hz), 128.78, 128.70, 128.47 (d, *J* = 11.3 Hz), 127.45, 126.69 (d, *J* = 6.3 Hz), 38.57 (d, *J* = 68.0 Hz), 13.39 (d, *J* = 3.5 Hz). IR (ATR): 2970, 1738, 1435, 1175, 1119, 975, 809 cm⁻¹. HRMS calculated for C₂₂H₂₀ClOPNa [M+Na]⁺ 389.0838, found 389.0856. Chiral SFC: 100 mm CHIRALPAK AD-H, 20% *i*PrOH, 3.0 mL/min, 220 nm, 44 °C, nozzle pressure = 200 bar CO₂, *t*_{R1} (minor) = 10.2 min, *t*_{R2} (major) = 11.9 min.

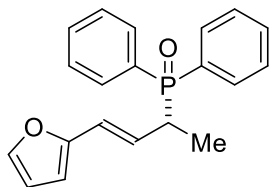
(*R,E*)-(4-(3-chlorophenyl)but-3-en-2-yl)diphenylphosphine oxide (3ia)



White solid, 88% yield, 90:10 *er*, >20:1 *rr*, $[\alpha]^{24}_D = +80.5$ (*c* 0.1, CHCl₃). ³¹P NMR (162 MHz, CDCl₃) δ 34.41. ¹H NMR (400 MHz, CDCl₃) δ 7.92 – 7.86 (m, 2H), 7.84 – 7.78 (m, 2H), 7.61 – 7.52 (m, 4H), 7.50 – 7.46 (m, 2H), 7.25 – 7.18 (m, 3H), 7.15 – 7.10 (m, 1H), 6.35 – 6.20 (m, 2H), 3.44 – 3.34 (m, 1H), 1.45 (dd, *J* = 16.0, 7.2 Hz, 3H). ¹³C NMR (101 MHz, CDCl₃) δ 139.11 (d, *J* = 3.0 Hz), 134.85, 132.50 (d, *J* = 26.5 Hz), 132.27 (d, *J* = 12.1 Hz), 132.23 (dd, *J* = 7.1, 2.0 Hz), 131.75 (dd, *J* = 14.1, 9.1 Hz), 131.54 (d, *J* = 24.2 Hz), 130.12, 128.98 (dd, *J* = 25.3, 11.1 Hz), 128.07 (d, *J* = 7.1 Hz), 127.85 (d, *J* = 1.0 Hz), 126.63 (d, *J* = 1.0 Hz), 124.75 (d, *J* = 1.0 Hz), 122.91, 39.98 (d, *J* = 68.7 Hz), 13.80 (d, *J* = 3.7 Hz). IR (ATR): 2931, 2360, 1592, 1437, 1176, 1117, 720 cm⁻¹. HRMS calculated for C₂₂H₂₀ClOPNa [M+Na]⁺ 389.0838, found 389.0822. Chiral SFC: 100 mm

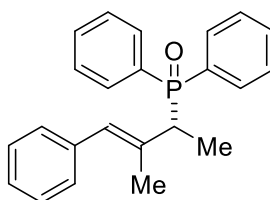
CHIRALCEL OJ-H, 4% *i*PrOH, 2.5 mL/min, 220 nm, 44 °C, nozzle pressure = 200 bar CO₂, *t*_{R1} (major) = 5.1 min, *t*_{R2} (minor) = 7.1 min.

(*R,E*)-(4-(furan-2-yl)but-3-en-2-yl)diphenylphosphine oxide (3ja)



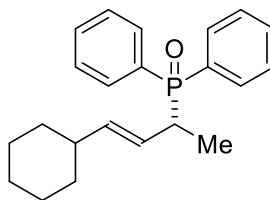
White solid, 88% yield, 92:8 *er*, >20:1 *rr*, $[\alpha]_D^{24} = +107.8$ (*c* 0.3, CHCl₃). ³¹P NMR (162 MHz, CDCl₃) δ 35.20. ¹H NMR (400 MHz, CDCl₃) δ 7.85 – 7.75 (m, 4H), 7.55 – 7.41 (m, 6H), 7.27 (m, 1H), 6.31 (dd, *J* = 3.3, 1.8 Hz, 1H), 6.20 – 6.09 (m, 3H), 3.37 – 3.27 (m, 1H), 1.38 (dd, *J* = 15.6, 6.8 Hz, 3H). ¹³C NMR (126 MHz, CDCl₃) δ 152.43, 141.96, 132.14 – 131.96 (m), 131.86 (dd, *J* = 5.0, 2.5 Hz), 131.46 (dd, *J* = 32.8, 8.8 Hz), 130.68, 128.60 (dd, *J* = 27.7, 11.3 Hz), 124.26 (d, *J* = 7.6 Hz), 121.57 (d, *J* = 11.3 Hz), 111.24, 107.68 (d, *J* = 2.5 Hz), 38.16 (d, *J* = 69.3 Hz), 13.18 (d, *J* = 3.8 Hz). IR (ATR): 2969, 1437, 1179, 1116, 1028, 745, 721 cm⁻¹. HRMS calculated for C₂₀H₁₉O₂PNa [M+Na]⁺ 345.1020, found 345.1005. Chiral SFC: 100 mm CHIRALCEL OJ-H, 2.0% *i*PrOH, 2.0 mL/min, 254 nm, 44 °C, nozzle pressure = 200 bar CO₂, *t*_{R1} (major) = 8.9 min, *t*_{R2} (minor) = 10.9 min.

(*R,E*)-(3-methyl-4-phenylbut-3-en-2-yl)diphenylphosphine oxide (3ka)



White solid, 78% yield, 97:3 *er*, >20:1 *rr*, $[\alpha]_D^{24} = +57.6$ (*c* 0.2, CHCl₃). ³¹P NMR (162 MHz, CDCl₃) δ 34.69. ¹H NMR (400 MHz, CDCl₃) δ 7.94 – 7.89 (m, 2H), 7.80 – 7.75 (m, 2H), 7.55 – 7.49 (m, 3H), 7.46 – 7.38 (m, 3H), 7.26 – 7.23 (m, 2H), 7.17 – 7.13 (m, 1H), 6.97 – 6.96 (m, 2H), 6.28 (d, *J* = 3.4 Hz, 1H), 3.20 (m, 1H), 1.86 (m, 3H), 1.45 (dd, *J* = 16.3, 7.3 Hz, 3H). ¹³C NMR (126 MHz, CDCl₃) δ 137.70 (d, *J* = 2.5 Hz), 135.49 (d, *J* = 6.3 Hz), 132.40 (dd, *J* = 98.3, 36.5 Hz), 131.59 (dd, *J* = 29.0, 2.5 Hz), 131.25 (d, *J* = 8.8 Hz), 129.81 (d, *J* = 10.1 Hz), 128.76 (d, *J* = 1.3 Hz), 128.75 (d, *J* = 11.3 Hz), 128.27 (d, *J* = 12.6 Hz), 128.00, 126.31, 44.25 (d, *J* = 68.0 Hz), 17.12 (d, *J* = 2.5 Hz), 13.18 (d, *J* = 3.8 Hz). IR (ATR): 3055, 1437, 1179, 998, 919, 745, 721 cm⁻¹. HRMS calculated for C₂₃H₂₃OPNa [M+Na]⁺ 369.1384, found 369.1391. Chiral SFC: 100 mm CHIRALCEL OJ-H, 2.0% *i*PrOH, 3.0 mL/min, 254 nm, 44 °C, nozzle pressure = 200 bar CO₂, *t*_{R1} (major) = 6.9 min, *t*_{R2} (minor) = 8.6 min.

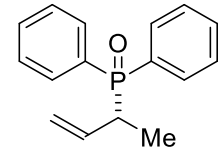
(*R,E*)-(4-cyclohexylbut-3-en-2-yl)diphenylphosphine oxide (3la)



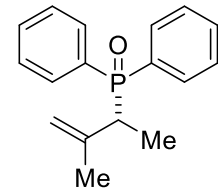
White solid, 35% yield, 86:14 *er*, 3:1 *rr*, $[\alpha]_D^{24} = +36.6$ (*c* 0.2, CHCl₃). ³¹P NMR (162 MHz, CDCl₃) δ 36.05. ¹H NMR (400 MHz, CDCl₃) δ 7.85 – 7.70 (m, 4H), 7.55 – 7.40 (m, 6H), 5.44 – 5.21 (m, 2H), 3.15 – 3.04 (m, 1H), 1.89 – 1.78 (m, 1H), 1.69 – 1.52 (m, 4H), 1.49 – 1.38 (m, 1H), 1.28 (dd, *J* = 16.4, 7.2 Hz, 3H), 1.23 – 1.01 (m, 3H), 0.95 – 0.78 (m, 2H). ¹³C NMR (126 MHz, CDCl₃) δ 140.71 (d, *J* = 11.3 Hz), 131.84 (dd, *J* = 94.5, 63.0 Hz), 131.59 (d, *J* = 8.8 Hz), 131.43 (d, *J* = 1.3 Hz), 131.24 (d, *J* = 8.8 Hz), 128.34 (dd, *J* = 46.4, 11.3 Hz), 123.12 (d, *J* = 7.6 Hz), 40.72, 38.07 (d, *J* = 69.3 Hz), 32.61 (d, *J* = 32.8 Hz), 25.92

(d, $J = 27.7$ Hz), 13.44. **IR** (ATR): 2922, 1437, 1180, 1117, 1028, 998, 719 cm^{-1} . **HRMS** calculated for $\text{C}_{22}\text{H}_{27}\text{OPNa}$ $[\text{M}+\text{Na}]^+$ 361.1697, found 361.1683. **Chiral SFC**: 250 mm CHIRALCEL IC-H, 20.0% *i*PrOH, 3.0 mL/min, 220 nm, 44 °C, nozzle pressure = 200 bar CO_2 , $t_{\text{R}1}$ (major) = 16.3 min, $t_{\text{R}2}$ (minor) = 21.0 min.

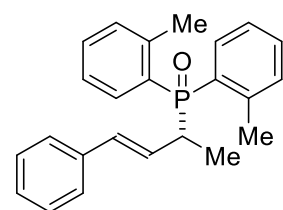
(*R*)-but-3-en-2-ylidiphenylphosphine oxide (3ma)

 White solid, 40% yield, 86:14 *er*, 4:1 *rr* $[\alpha]^{24}_{\text{D}} = +12.8$ (*c* 0.2, CHCl_3). **^{31}P NMR** (162 MHz, CDCl_3) δ 34.99. **^1H NMR** (400 MHz, CDCl_3) δ 7.91 – 7.70 (m, 4H), 7.60 – 7.32 (m, 6H), 5.92 – 5.73 (m, 1H), 5.21 – 4.95 (m, 2H), 3.28 – 3.12 (m, 1H), 1.31 (dd, $J = 16.0, 8.0$ Hz, 3H). **^{13}C NMR** (126 MHz, CDCl_3) δ 134.19 (d, $J = 6.3$ Hz), 131.69 (dd, $J = 97.2, 56.7$ Hz), 131.76 (d, $J = 6.3$ Hz), 131.40 (dd, $J = 32.8, 8.8$ Hz), 128.55 (dd, $J = 29.0, 11.3$ Hz), 118.41 (d, $J = 11.3$ Hz), 38.80 (d, $J = 69.3$ Hz), 12.68. **IR** (ATR): 2932, 1733, 1437, 1179, 1117, 997, 719 cm^{-1} . **HRMS** calculated for $\text{C}_{16}\text{H}_{18}\text{OP}$ $[\text{M}+\text{H}]^+$ 257.1095, found 257.1086. **Chiral SFC**: 250 mm CHIRALPAK AD-H, 15% *i*PrOH, 2.0 mL/min, 220 nm, 44 °C, nozzle pressure = 200 bar CO_2 , $t_{\text{R}1}$ (minor) = 11.3 min, $t_{\text{R}2}$ (major) = 12.6 min.

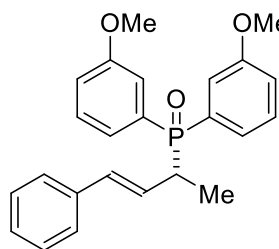
(*R*)-(3-methylbut-3-en-2-yl)diphenylphosphine oxide (3na)

 White solid, 25% yield, 72:28 *er*, 1:1 *rr*, $[\alpha]^{24}_{\text{D}} = +32.0$ (*c* 0.2, CHCl_3). **^{31}P NMR** (162 MHz, CDCl_3) δ 33.94. **^1H NMR** (400 MHz, CDCl_3) δ 7.90 – 7.81 (m, 2H), 7.80 – 7.72 (m, 2H), 7.55 – 7.34 (m, 6H), 4.90 – 4.78 (m, 2H), 3.20 – 3.05 (m, 1H), 1.73 (s, 3H), 1.35 (dd, $J = 16.4, 7.2$ Hz, 3H). **^{13}C NMR** (126 MHz, CDCl_3) δ 142.36 (d, $J = 6.3$ Hz), 132.48 (dd, $J = 97.0, 15.1$ Hz), 131.51 (dd, $J = 16.4, 2.5$ Hz), 131.20 (dd, $J = 8.8, 6.3$ Hz), 128.45 (dd, $J = 49.1, 11.3$ Hz), 115.31 (d, $J = 10.1$ Hz), 41.86 (d, $J = 68$ Hz), 22.14, 13.56 (d, $J = 2.5$ Hz). **IR** (ATR): 3056, 1739, 1641, 1436, 1178, 1116, 890 cm^{-1} . **HRMS** calculated for $\text{C}_{17}\text{H}_{20}\text{OP}$ $[\text{M}+\text{H}]^+$ 271.1252, found 271.1241. **Chiral SFC**: 250 mm CHIRALPAK AD-H, 15% *i*PrOH, 2.0 mL/min, 220 nm, 44 °C, nozzle pressure = 200 bar CO_2 , $t_{\text{R}1}$ (major) = 10.5 min, $t_{\text{R}2}$ (minor) = 11.1 min.

(*R,E*)-(4-phenylbut-3-en-2-yl)di-*o*-tolylphosphine oxide (3ab)

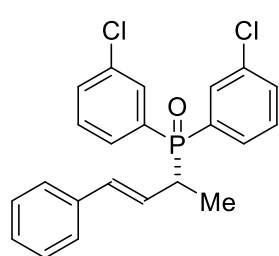
 White solid, 75% yield, 97.5:2.5 *er*, >20:1 *rr*, $[\alpha]^{24}_{\text{D}} = +69.0$ (*c* 0.2, CHCl_3). **^{31}P NMR** (162 MHz, CDCl_3) δ 38.39. **^1H NMR** (400 MHz, CDCl_3) δ 7.85 – 7.70 (m, 2H), 7.49 – 7.43 (m, 1H), 7.41 – 7.33 (m, 2H), 7.31 – 7.20 (m, 7H), 7.19 – 7.15 (m, 1H), 6.47 (dd, $J = 16.0, 4.0$ Hz, 1H), 6.40 – 6.31 (m, 1H), 3.63 – 3.55 (m, 1H), 2.44 (s, 3H), 2.40 (s, 3H), 1.56 (dd, $J = 15.2, 6.8$ Hz, 3H). **^{13}C NMR** (126 MHz, CDCl_3) δ 142.46 (dd, $J = 13.4, 7.7$ Hz), 137.07, 132.61 (d, $J = 11.8$ Hz), 132.01 (dd, $J = 36.5, 11.3$ Hz), 132.00 (d, $J = 5.0$ Hz), 131.56 (dd, $J = 16.4, 2.5$ Hz), 130.71, 128.49, 127.45, 126.98 (d, $J = 6.3$ Hz), 126.25, 125.35 (t, $J = 12.6$ Hz), 37.42 (d, $J = 55.6$ Hz), 21.38 (dd, $J = 7.9, 3.7$ Hz), 14.54 (d, $J = 3.5$ Hz). **IR** (ATR): 2929, 1594, 1450, 1160, 1137, 752, 693 cm^{-1} . **HRMS** calculated for $\text{C}_{24}\text{H}_{25}\text{OPNa}$ $[\text{M}+\text{Na}]^+$ 383.1541, found 383.1555. **Chiral SFC**: 250 mm CHIRALCEL OJ-H, 5% *i*PrOH, 2.0 mL/min, 220 nm, 44 °C, nozzle pressure = 200 bar CO_2 , $t_{\text{R}1}$ (major) = 9.9 min, $t_{\text{R}2}$ (minor) = 13.2 min.

(*R,E*)-bis(3-methoxyphenyl)(4-phenylbut-3-en-2-yl)phosphine oxide (3ac)



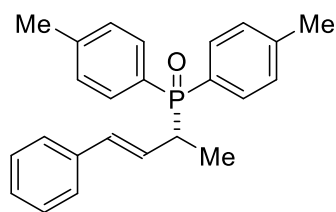
White solid, 86% yield, 93:7 *er*, >20:1 *rr*, $[\alpha]^{24}_D = +28.0$ (*c* 0.7, CHCl₃). ³¹P NMR (162 MHz, CDCl₃) δ 35.50. ¹H NMR (500 MHz, CDCl₃) δ 7.51 – 7.45 (m, 2H), 7.44 – 7.37 (m, 3H), 7.36 – 7.33 (m, 1H), 7.32 – 7.28 (m, 4H), 7.28 – 7.25 (m, 1H), 7.15 – 7.09 (m, 1H), 7.09 – 7.03 (m, 1H), 6.40 (dd, *J* = 16.0, 4.0 Hz, 1H), 6.32 – 6.21 (m, 1H), 3.89 (s, 3H), 3.79 (s, 3H), 3.40 – 3.31 (m, 1H), 1.48 (dd, *J* = 16.0, 7.1 Hz, 3H). ¹³C NMR (126 MHz, CDCl₃) δ 159.65 (dd, *J* = 35.3, 13.9 Hz), 136.92 (d, *J* = 3.8 Hz), 133.19 (d, *J* = 11.3 Hz), 133.14 (dd, *J* = 93.2, 32.8 Hz), 129.69 (dd, *J* = 36.5, 13.9 Hz), 128.55, 127.57, 126.27 (d, *J* = 2.5 Hz), 126.00 (d, *J* = 7.6 Hz), 123.33 (dd, *J* = 29.0, 8.8 Hz), 118.12 (dd, *J* = 20.2, 2.5 Hz), 116.35 (d, *J* = 8.8 Hz), 55.45 (d, *J* = 15.1 Hz), 39.72 (d, *J* = 69.3 Hz), 13.50 (d, *J* = 6.3 Hz). IR (ATR): 2936, 1576, 1419, 1286, 1237, 1161, 692 cm⁻¹. HRMS calculated for C₂₄H₂₅O₃PNa [M+Na]⁺ 415.1439, found 415.1436. Chiral SFC: 100 mm CHIRALCEL OJ-H, 5% ⁱPrOH, 2.0 mL/min, 220 nm, 44 °C, nozzle pressure = 200 bar CO₂, *t*_{R1} (major) = 13.0 min, *t*_{R2} (minor) = 16.4 min.

(*R,E*)-bis(3-chlorophenyl)(4-phenylbut-3-en-2-yl)phosphine oxide (3ad)



White solid, 80% yield, 90:10 *er*, >20:1 *rr*, $[\alpha]^{24}_D = +68.0$ (*c* 0.2, CHCl₃). ³¹P NMR (162 MHz, CDCl₃) δ 33.20. ¹H NMR (400 MHz, CDCl₃) δ 7.88 (d, *J* = 11.2 Hz, 1H), 7.80 (d, *J* = 10.9 Hz, 1H), 7.78 – 7.72 (m, 1H), 7.71 – 7.65 (m, 1H), 7.61 – 7.56 (m, 1H), 7.54 – 7.49 (m, 2H), 7.47 – 7.39 (m, 1H), 7.35 – 7.30 (m, 2H), 7.29 – 7.23 (m, 3H), 6.43 (dd, *J* = 16.0, 4.0 Hz, 1H), 6.25 – 6.10 (m, 1H), 3.43 – 3.30 (m, 1H), 1.47 (dd, *J* = 16.4, 7.2 Hz, 3H). ¹³C NMR (126 MHz, CDCl₃) δ 136.47 (d, *J* = 2.5 Hz), 135.23 (dd, *J* = 36.5, 15.1 Hz), 134.05 (dd, *J* = 26.5, 15.1 Hz), 133.31 (d, *J* = 46.6 Hz), 132.17 (dd, *J* = 13.9, 1.3 Hz), 131.19 (dd, *J* = 23.9, 8.8 Hz), 130.07 (dd, *J* = 37.8, 12.6 Hz), 129.20 (dd, *J* = 25.2, 7.6 Hz), 128.55, 127.78, 126.27, 124.82 (d, *J* = 7.6 Hz), 38.45 (d, *J* = 69.3 Hz), 13.41 (d, *J* = 3.8 Hz). IR (ATR): 2963, 1559, 1492, 1400, 1183, 1133, 752 cm⁻¹. HRMS calculated for C₂₂H₁₉Cl₂OPNa [M+Na]⁺ 423.0448, found 423.0461. Chiral SFC: 100 mm CHIRALCEL OJ-H, 2% ⁱPrOH, 2.0 mL/min, 220 nm, 44 °C, nozzle pressure = 200 bar CO₂, *t*_{R1} (major) = 13.4 min, *t*_{R2} (minor) = 17.9 min.

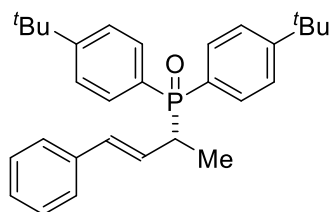
(*R,E*)-(4-phenylbut-3-en-2-yl)di-*p*-tolylphosphine oxide (3ae)



White solid, 83% yield, 96:4 *er*, >20:1 *rr*, $[\alpha]^{24}_D = +34.9$ (*c* 0.4, CHCl₃). ³¹P NMR (162 MHz, CDCl₃) δ 34.91. ¹H NMR (400 MHz, CDCl₃) δ 7.80 – 7.66 (m, 4H), 7.36 – 7.31 (m, 3H), 7.30 – 7.22 (m, 6H), 6.39 (dd, *J* = 15.6, 4.0 Hz, 1H), 6.28 – 6.19 (m, 1H), 3.44 – 3.28 (m, 1H), 2.45 (s, 3H), 2.41 (s, 3H), 1.44 (dd, *J* = 16.0, 7.2 Hz, 3H). ¹³C NMR (101 MHz, CDCl₃) δ 142.44 (dd, *J* = 10.0, 2.0 Hz), 137.44 (d, *J* = 2.0 Hz), 133.27 (d, *J* = 12.1 Hz), 131.84 (dd, *J* = 24.2, 9.1 Hz), 129.75, 129.63 (dd, *J* = 25.3, 12.1 Hz), 128.89, 127.84 (d, *J* = 1.0 Hz), 126.80 (d, *J* = 7.1 Hz), 126.64 (d, *J* = 1.0 Hz), 39.10

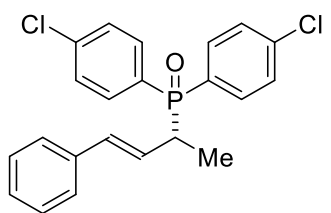
(d, $J = 68.7$ Hz), 21.95, 13.90. **IR** (ATR): 3025, 1601, 1448, 1115, 1098, 718, 697 cm^{-1} . **HRMS** calculated for $\text{C}_{24}\text{H}_{25}\text{OPNa}$ $[\text{M}+\text{Na}]^+$ 383.1541, found 383.1545. **Chiral SFC**: 100 mm CHIRALCEL OJ-H, 4% i PrOH, 2.5 mL/min, 220 nm, 44 $^{\circ}\text{C}$, nozzle pressure = 200 bar CO_2 , $t_{\text{R}1}$ (major) = 4.5 min, $t_{\text{R}2}$ (minor) = 5.9 min.

(*R,E*)-bis(4-(*tert*-butyl)phenyl)(4-phenylbut-3-en-2-yl)phosphine oxide (3af)



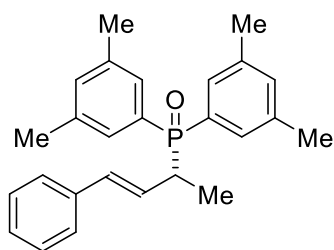
White solid, 88% yield, 96:4 *er*, >20:1 *rr*, $[\alpha]_{\text{D}}^{24} = +80.2$ (c 0.3, CHCl_3). **^{31}P NMR** (162 MHz, CDCl_3) δ 35.23. **^1H NMR** (400 MHz, CDCl_3) δ 7.80 – 7.65 (m, 4H), 7.54 – 7.40 (m, 4H), 7.27 – 7.24 (m, 2H), 7.23 – 7.16 (m, 3H), 6.31 (dd, $J = 16.4, 2.8$ Hz, 1H), 6.25 – 6.16 (m, 1H), 3.36 – 3.25 (m, 1H), 1.41 (dd, $J = 16.0, 7.2$ Hz, 3H), 1.34 (s, 9H), 1.30 (s, 9H). **^{13}C NMR** (126 MHz, CDCl_3) δ 155.04 (dd, $J = 14.4, 2.8$ Hz), 137.13 (d, $J = 2.5$ Hz), 132.89 (d, $J = 11.6$ Hz), 131.36 (dd, $J = 27.7, 8.8$ Hz), 128.64 (dd, $J = 97.0, 55.4$ Hz), 128.50, 127.42, 126.54 (d, $J = 6.3$ Hz), 126.26 (d, $J = 2.5$ Hz), 125.48 (dd, $J = 11.5, 32.8$ Hz), 38.87 (d, $J = 68.0$ Hz), 35.00 (d, $J = 5.0$ Hz), 31.15 (d, $J = 3.8$ Hz), 13.56 (d, $J = 3.8$ Hz). **IR** (ATR): 2963, 1601, 1393, 1181, 1092, 827, 748 cm^{-1} . **HRMS** calculated for $\text{C}_{30}\text{H}_{37}\text{OPNa}$ $[\text{M}+\text{Na}]^+$ 467.2480, found 467.2496. **Chiral SFC**: 100 mm CHIRALCEL OJ-H, 2% i PrOH, 2.0 mL/min, 220 nm, 44 $^{\circ}\text{C}$, nozzle pressure = 200 bar CO_2 , $t_{\text{R}1}$ (major) = 6.0 min, $t_{\text{R}2}$ (minor) = 8.8 min.

(*R,E*)-bis(4-chlorophenyl)(4-phenylbut-3-en-2-yl)phosphine oxide (3ag)



White solid, 80% yield, 95:5 *er*, >20:1 *rr*, $[\alpha]_{\text{D}}^{24} = +42.4$ (c 0.1, CHCl_3). **^{31}P NMR** (162 MHz, CDCl_3) δ 34.57. **^1H NMR** (400 MHz, CDCl_3) δ 7.80 – 7.72 (m, 2H), 7.71 – 7.65 (m, 2H), 7.53 – 7.46 (m, 2H), 7.45 – 7.39 (m, 2H), 7.32 – 7.26 (m, 2H), 7.24 – 7.18 (m, 3H), 6.35 (dd, $J = 16.0, 4.4$ Hz, 1H), 6.25 – 6.05 (m, 1H), 3.38 – 3.22 (m, 1H), 1.40 (dd, $J = 16.4, 7.2$ Hz, 3H). **^{13}C NMR** (126 MHz, CDCl_3) δ 138.66 (dd, $J = 12.6, 2.5$ Hz), 136.55 (d, $J = 2.5$ Hz), 133.81 (d, $J = 11.3$ Hz), 132.76 (dd, $J = 26.5, 8.8$ Hz), 129.94 (dd, $J = 97.8, 54.2$ Hz), 129.07 (dd, $J = 34.0, 11.3$ Hz), 128.66, 127.85, 126.29 (d, $J = 1.3$ Hz), 125.13 (d, $J = 6.3$ Hz), 38.65 (d, $J = 69.3$ Hz), 13.45 (d, $J = 3.8$ Hz). **IR** (ATR): 3025, 1581, 1481, 1172, 1086, 1013, 746 cm^{-1} . **HRMS** calculated for $\text{C}_{22}\text{H}_{19}\text{Cl}_2\text{OPNa}$ $[\text{M}+\text{Na}]^+$ 423.0448, found 423.0464. **Chiral SFC**: 100 mm CHIRALCEL OJ-H, 5% i PrOH, 3.0 mL/min, 220 nm, 44 $^{\circ}\text{C}$, nozzle pressure = 200 bar CO_2 , $t_{\text{R}1}$ (major) = 4.4 min, $t_{\text{R}2}$ (minor) = 5.1 min.

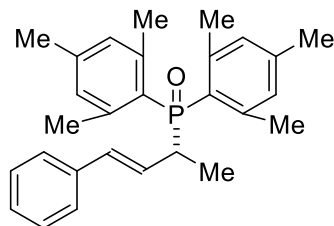
(*R,E*)-bis(3,5-dimethylphenyl)(4-phenylbut-3-en-2-yl)phosphine oxide (3ah)



White solid, 76% yield, 95.5:4.5 *er*, >20:1 *rr*, $[\alpha]_{\text{D}}^{24} = +57.6$ (c 0.5, CHCl_3). **^{31}P NMR** (162 MHz, CDCl_3) δ 35.61. **^1H NMR** (400 MHz, CDCl_3) δ 7.44 (d, $J = 10.8$ Hz, 2H), 7.37 (d, $J = 11.2$ Hz, 2H), 7.25 (s, 1H), 7.24 – 7.18 (m, 4H), 7.16 (s, 1H), 7.09 (s, 1H), 6.33 (dd, $J = 15.6, 4.0$ Hz, 1H), 6.24 – 6.14 (m, 1H), 3.38 – 3.26 (m, 1H), 2.36 (s, 6H), 2.29 (s, 6H), 1.40 (dd, $J = 15.6, 7.2$ Hz, 3H). **^{13}C NMR** (101 MHz, CDCl_3) δ 138.49 (dd, $J = 37.4, 12.1$ Hz), 133.79 (dd, $J = 11.1, 3.0$ Hz),

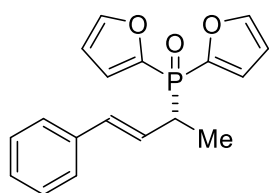
133.31 (d, $J = 12.1$ Hz), 132.02 (dd, $J = 93.9, 37.4$ Hz), 129.40 (dd, $J = 29.3, 8.1$ Hz), 128.84, 127.77, 126.88 (d, $J = 7.1$ Hz), 126.62 (d, $J = 1.0$ Hz), 122.93, 38.83 (d, $J = 68.7$ Hz), 21.74 (d, $J = 8.1$ Hz), 13.81. **IR** (ATR): 2917, 1600, 1447, 1273, 1177, 967, 851 cm^{-1} . **HRMS** calculated for $\text{C}_{26}\text{H}_{29}\text{OPNa}$ $[\text{M}+\text{Na}]^+$ 411.1854, found 411.1868. **Chiral SFC**: 100 mm CHIRALCEL OJ-H, 3% i PrOH, 2.0 mL/min, 220 nm, 44 $^{\circ}\text{C}$, nozzle pressure = 200 bar CO_2 , t_{R1} (major) = 4.0 min, t_{R2} (minor) = 5.4 min.

(*R,E*)-dimesityl(4-phenylbut-3-en-2-yl)phosphine oxide (3ai)



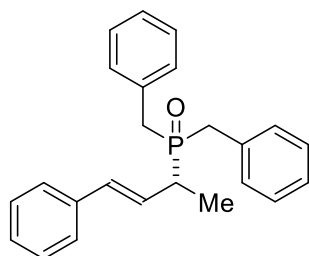
White solid, 62% yield, 98:2 *er*, >20:1 *rr*, $[\alpha]_{\text{D}}^{24} = +95.6$ (c 0.3, CHCl_3). ^{31}P NMR (162 MHz, CDCl_3) δ 44.95. ^1H NMR (400 MHz, CDCl_3) δ 7.33 – 7.26 (m, 2H), 7.24 – 7.16 (m, 3H), 6.88 (s, 2H), 6.80 (s, 2H), 6.49 – 6.45 (m, 1H), 6.40 – 6.29 (m, 1H), 3.70 – 3.58 (m, 1H), 2.53 (s, 6H), 2.45 (s, 6H), 2.31 (s, 3H), 2.25 (s, 3H), 1.60 (dd, $J = 14.4, 5.2$ Hz, 3H). ^{13}C NMR (101 MHz, CDCl_3) δ 141.32 (dd, $J = 14.1, 10.1$ Hz), 140.44, 137.29, 131.93 (d, $J = 12.1$ Hz), 130.97 (dd, $J = 26.3, 11.1$ Hz), 130.37 (d, $J = 12.1$ Hz), 128.45 (d, $J = 7.1$ Hz), 128.34, 127.18, 126.11, 41.36 (d, $J = 63.6$ Hz), 22.81 – 22.74 (m), 20.83, 16.10. **IR** (ATR): 2926, 1604, 1447, 1376, 1164, 849, 694 cm^{-1} . **HRMS** calculated for $\text{C}_{28}\text{H}_{33}\text{OPNa}$ $[\text{M}+\text{Na}]^+$ 439.2167, found 439.2160. **Chiral SFC**: 250 mm CHIRALCEL OJ-H, 5% i PrOH, 2.0 mL/min, 220 nm, 44 $^{\circ}\text{C}$, nozzle pressure = 200 bar CO_2 , t_{R1} (major) = 9.5 min, t_{R2} (minor) = 12.9 min.

(*R,E*)-di(furan-2-yl)(4-phenylbut-3-en-2-yl)phosphine oxide (3aj)



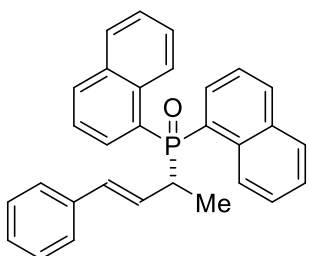
White solid, 51% yield, 74:26 *er*, >20:1 *rr*, $[\alpha]_{\text{D}}^{24} = +55.1$ (c 0.1, CHCl_3). ^{31}P NMR (162 MHz, CDCl_3) δ 17.09. ^1H NMR (400 MHz, CDCl_3) δ 7.81 – 7.69 (m, 2H), 7.34 – 7.29 (m, 4H), 7.28 – 7.25 (m, 1H), 7.22 – 7.16 (m, 2H), 6.61 – 6.50 (m, 2H), 6.43 (dd, $J = 15.6, 5.2$ Hz, 1H), 6.28 – 6.12 (m, 1H), 3.48 – 3.34 (m, 1H), 1.53 – 1.44 (m, 3H). ^{13}C NMR (126 MHz, CDCl_3) δ 148.09 (dd, $J = 7.6, 2.5$ Hz), 146.52 (dd, $J = 136.1, 41.6$ Hz), 136.89 (d, $J = 3.8$ Hz), 133.54 (d, $J = 12.6$ Hz), 128.54, 127.65, 126.38 (d, $J = 1.3$ Hz), 124.57 (d, $J = 8.8$ Hz), 123.01 (dd, $J = 31.5, 17.6$ Hz), 110.97 (dd, $J = 7.6, 1.3$ Hz), 39.58 (d, $J = 76.9$ Hz), 12.78 (d, $J = 2.5$ Hz). **IR** (ATR): 3421, 2360, 1554, 1457, 1211, 1132, 1008 cm^{-1} . **HRMS** calculated for $\text{C}_{18}\text{H}_{17}\text{O}_3\text{PNa}$ $[\text{M}+\text{Na}]^+$ 335.0813, found 335.0825. **Chiral SFC**: 100 mm CHIRALPAK AD-H, 15% i PrOH, 3.0 mL/min, 220 nm, 44 $^{\circ}\text{C}$, nozzle pressure = 200 bar CO_2 , t_{R1} (minor) = 3.9 min, t_{R2} (major) = 4.4 min.

(*R,E*)-dibenzyl(4-phenylbut-3-en-2-yl)phosphine oxide (3ak)



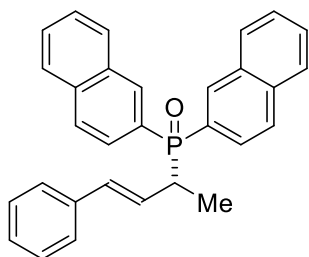
White solid, 67% yield, 95:5 *er*, >20:1 *rr*, $[\alpha]^{24}_{\text{D}} = +34.1$ (*c* 0.2, CHCl₃). ³¹P NMR (162 MHz, CDCl₃) δ 46.61. ¹H NMR (400 MHz, CDCl₃) δ 7.35 – 7.33 (m, 2H), 7.33 – 7.31 (m, 4H), 7.31 – 7.29 (m, 5H), 7.28 – 7.26 (m, 2H), 7.25 – 7.24 (m, 2H), 6.41 (dd, *J* = 16.0, 4.4 Hz, 1H), 6.22 – 6.06 (m, 1H), 3.24 – 3.14 (m, 1H), 3.13 – 3.08 (m, 2H), 3.06 – 3.00 (m, 1H), 2.86 – 2.70 (m, 1H), 1.33 (dd, *J* = 15.2, 7.2 Hz, 3H). ¹³C NMR (126 MHz, CDCl₃) δ 136.64, 132.96 (d, *J* = 11.3 Hz), 131.88 (t, *J* = 6.3 Hz), 130.00 (t, *J* = 6.3 Hz), 128.81, 128.72, 127.86, 126.98, 126.31, 126.12 (d, *J* = 6.3 Hz), 37.35 (t, *J* = 63.0 Hz), 33.91 (dd, *J* = 59.2, 17.6 Hz), 13.17. IR (ATR): 3028, 1600, 1495, 1165, 1120, 830, 752 cm⁻¹. HRMS calculated for C₂₄H₂₅OPNa [M+Na]⁺ 383.1541, found 383.1534. Chiral SFC: 250 mm CHIRALPAK AD-H, 15% *i*PrOH, 2.0 mL/min, 220 nm, 44 °C, nozzle pressure = 200 bar CO₂, *t*_{R1} (major) = 27.8 min, *t*_{R2} (minor) = 29.6 min.

(*R,E*)-di(naphthalen-1-yl)(4-phenylbut-3-en-2-yl)phosphine oxide (3al)



White solid, 69% yield, 95:5 *er*, >20:1 *rr*, $[\alpha]^{24}_{\text{D}} = +32.3$ (*c* 0.6, CHCl₃). ³¹P NMR (162 MHz, CDCl₃) δ 40.59. ¹H NMR (500 MHz, CDCl₃) δ 8.82 (d, *J* = 8.0 Hz, 2H), 8.05 – 7.90 (m, 4H), 7.83 (dd, *J* = 31.0, 7.5 Hz, 2H), 7.55 – 7.30 (m, 6H), 7.23 – 7.12 (m, 3H), 7.11 – 7.02 (m, 2H), 6.44 – 6.26 (m, 2H), 3.88 – 3.75 (m, 1H), 1.57 (dd, *J* = 16.0, 7.0 Hz, 3H). ¹³C NMR (126 MHz, CDCl₃) δ 136.95 (d, *J* = 1.3 Hz), 134.20 – 133.9 (m), 133.00 (dd, *J* = 12.6, 2.5 Hz), 132.58 (d, *J* = 11.3 Hz), 131.87 (dd, *J* = 10.1, 5.0 Hz), 129.55 (d, *J* = 6.3 Hz), 128.87 (d, *J* = 18.9 Hz), 128.38, 127.37 (d, *J* = 7.6 Hz), 127.25 – 127.00 (m), 126.45, 126.28, 126.23, 124.32 (dd, *J* = 12.6, 10.1 Hz), 39.28 (d, *J* = 69.3 Hz), 14.75 (d, *J* = 2.5 Hz). IR (ATR): 2928, 1591, 1505, 1158, 1025, 986, 773 cm⁻¹. HRMS calculated for C₃₀H₂₅OPNa [M+Na]⁺ 455.1541, found 455.1536. Chiral SFC: 100 mm CHIRALCEL OJ-H, 5% *i*PrOH, 3.0 mL/min, 220 nm, 44 °C, nozzle pressure = 200 bar CO₂, *t*_{R1} (major) = 14.6 min, *t*_{R2} (minor) = 17.2 min.

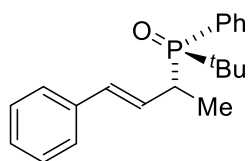
(*R,E*)-di(naphthalen-2-yl)(4-phenylbut-3-en-2-yl)phosphine oxide (3am)



White solid, 65% yield, 88:12 *er*, >20:1 *rr*, $[\alpha]^{24}_{\text{D}} = +81.9$ (*c* 0.1, CHCl₃). ³¹P NMR (162 MHz, CDCl₃) δ 34.74. ¹H NMR (500 MHz, CDCl₃) δ 8.56 (dd, *J* = 28.0, 13.0 Hz, 2H), 8.08 – 7.78 (m, 8H), 7.70 – 7.52 (m, 4H), 7.34 – 7.18 (m, 5H), 6.49 (dd, *J* = 16.0, 4.0 Hz, 1H), 6.40 – 6.31 (m, 1H), 3.70 – 3.61 (m, 1H), 1.55 (dd, *J* = 16.0, 7.0 Hz, 3H). ¹³C NMR (126 MHz, CDCl₃) δ 136.87 (d, *J* = 2.5 Hz), 134.67 (dd, *J* = 5.0, 2.5 Hz), 133.72 (dd, *J* = 35.3, 7.6 Hz), 133.38 (d, *J* = 11.3 Hz), 132.66 (dd, *J* = 16.4, 12.6 Hz), 129.00 (dd, *J* = 94.5, 55.4 Hz), 128.99, 128.53, 128.47, 128.19 (d, *J* = 10.1 Hz), 128.13 (d, *J* = 11.3 Hz), 127.84 (d, *J* = 7.6 Hz), 127.57, 126.96 (d, *J* = 18.9 Hz), 126.36,

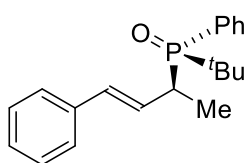
126.29, 126.01 (d, $J = 8.8$ Hz), 38.59 (d, $J = 69.3$ Hz), 13.60 (d, $J = 2.5$ Hz). **IR** (ATR): 3054, 1591, 1448, 1271, 1174, 1087, 744 cm^{-1} . **HRMS** calculated for $\text{C}_{30}\text{H}_{25}\text{OPNa}$ $[\text{M}+\text{Na}]^+$ 455.1541, found 455.1545. **Chiral SFC**: 100 mm CHIRALCEL OJ-H, 8% i PrOH, 3.0 mL/min, 220 nm, 44 $^{\circ}\text{C}$, nozzle pressure = 200 bar CO_2 , t_{R1} (major) = 9.9 min, t_{R2} (minor) = 12.0 min.

(*R*)-tert-butyl(phenyl)((*R,E*)-4-phenylbut-3-en-2-yl)phosphine oxide (3an)



White solid, 88% yield, 95:5 *dr*, >20:1 *rr*, $[\alpha]_{\text{D}}^{24} = +35.1$ (c 0.4, CHCl_3). ^{31}P NMR (162 MHz, CDCl_3) δ 51.36. ^1H NMR (400 MHz, CDCl_3) δ 7.83 (t, $J = 7.6$ Hz, 2H), 7.60 – 7.53 (m, 3H), 7.47 (d, $J = 7.6$ Hz, 2H), 7.43 – 7.35 (m, 2H), 7.35 – 7.27 (m, 1H), 6.70 – 6.55 (m, 2H), 3.37 – 3.24 (m, 1H), 1.29 – 1.23 (m, 3H), 1.22 – 1.15 (m, 9H). ^{13}C NMR (101 MHz, CDCl_3) δ 136.89, 131.76 (d, $J = 11.1$ Hz), 131.53 (d, $J = 7.1$ Hz), 131.28 (t, $J = 2.0$ Hz), 130.48, 128.67, 128.29 (d, $J = 10.1$ Hz), 128.08 (d, $J = 6.1$ Hz), 127.57, 126.25, 36.20 (d, $J = 61.6$ Hz), 33.90 (d, $J = 66.7$ Hz), 25.28, 15.84 (d, $J = 4.3$ Hz). **IR** (ATR): 2979, 1599, 1449, 1160, 1105, 818, 718 cm^{-1} . **HRMS** calculated for $\text{C}_{20}\text{H}_{25}\text{OPNa}$ $[\text{M}+\text{Na}]^+$ 335.1541, found 335.1544.

(*R*)-tert-butyl(phenyl)((*S,E*)-4-phenylbut-3-en-2-yl)phosphine oxide (3an')

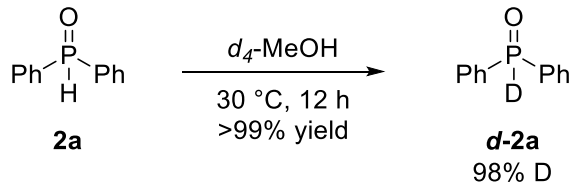


White solid, 85% yield, 91:9 *dr*, >20:1 *rr*, $[\alpha]_{\text{D}}^{24} = -14.5$ (c 0.2, CHCl_3). ^{31}P NMR (162 MHz, CDCl_3) δ 49.32. ^1H NMR (400 MHz, CDCl_3) δ 7.82 (t, $J = 9.6$ Hz, 2H), 7.56 – 7.43 (m, 3H), 7.34 – 7.25 (m, 4H), 7.24 (s, 1H), 6.43 (dd, $J = 16.0, 3.6$ Hz, 1H), 6.26 – 6.14 (m, 1H), 3.40 – 3.26 (m, 1H), 1.52 (dd, $J = 14.0, 7.2$ Hz, 3H), 1.29 (d, $J = 14.4$ Hz, 9H). ^{13}C NMR (126 MHz, CDCl_3) δ 136.81, 132.16 (d, $J = 7.6$ Hz), 132.03 (d, $J = 11.3$ Hz), 131.28, 129.84 (d, $J = 83.2$ Hz), 128.51, 127.98, 127.90, 127.44, 126.07, 36.47 (d, $J = 59.2$ Hz), 34.20 (d, $J = 64.3$ Hz), 25.56, 14.89. **IR** (ATR): 2970, 1738, 1448, 1356, 1152, 966, 751 cm^{-1} . **HRMS** calculated for $\text{C}_{20}\text{H}_{25}\text{OPNa}$ $[\text{M}+\text{Na}]^+$ 335.1541, found 335.1541.

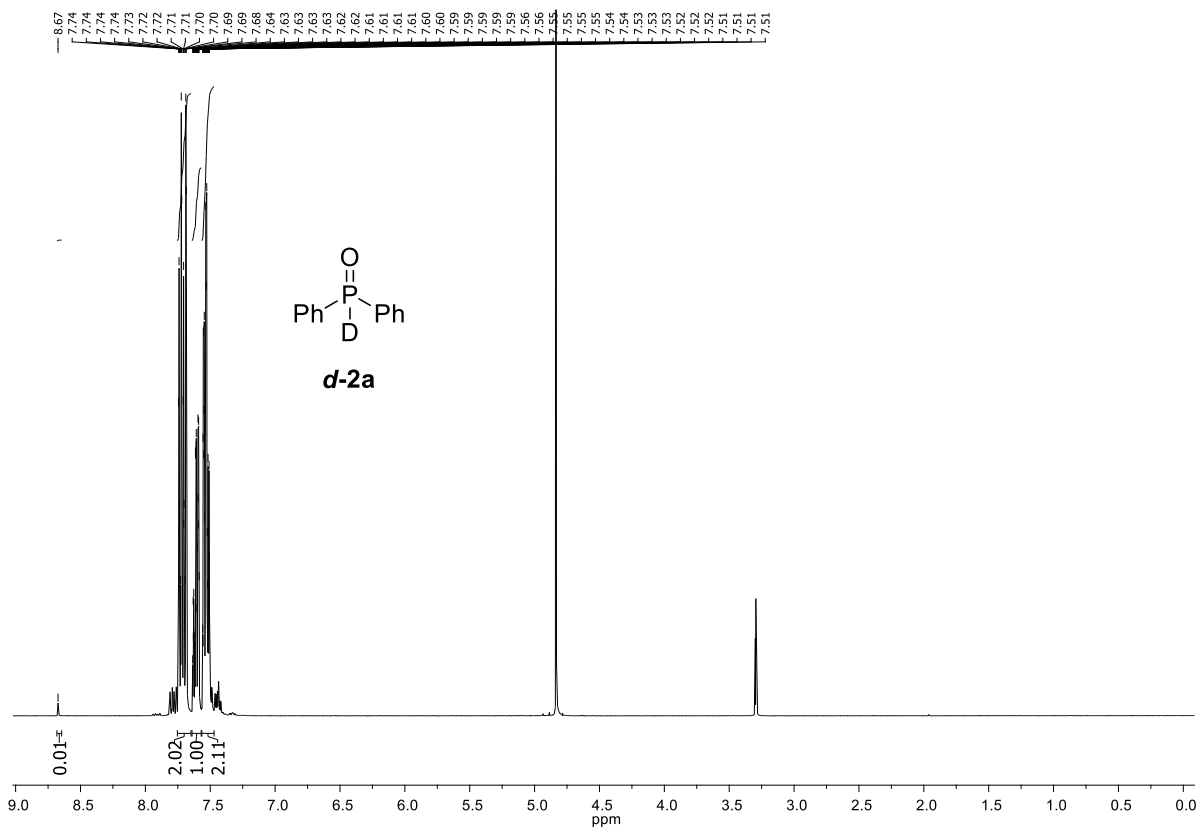
3. Mechanism studies

3A. Deuterium-Labeling Study

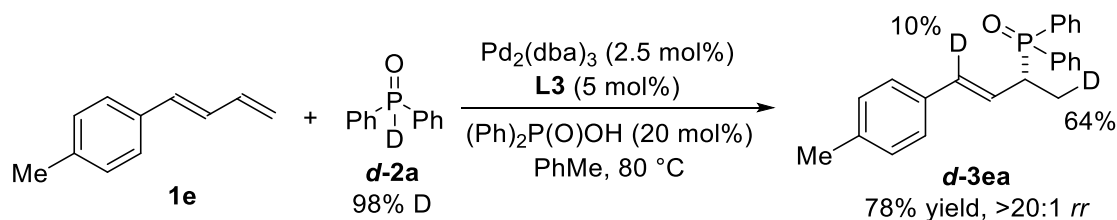
(1) Synthesis of *d*-2a:



To an oven dried 4-dram vial was added diphenylphosphine oxide (**2a**, 0.3 mmol) and a stir-bar. The solid was then dissolved in d_4 -MeOH (0.6 mL) to obtain a 0.5 M solution. The resulting solution was stirred at 30 °C for 12 hours. The clear solution was concentrated *in vacuo* and resulted in quantitative (>99%) yield of the title compound **d-2a**. ^1H NMR spectrum showed 98% D incorporation (note: the P–H resonance at 8.67 is a doublet where the other peak is underneath the aryl region due to P–H splitting). ^1H NMR (400 MHz, d_4 -MeOH) δ 8.67 (d, 0.02H), 7.75 – 7.65 (m, 2H), 7.64 – 7.57 (m, 1H), 7.56 – 7.47 (m, 2H).

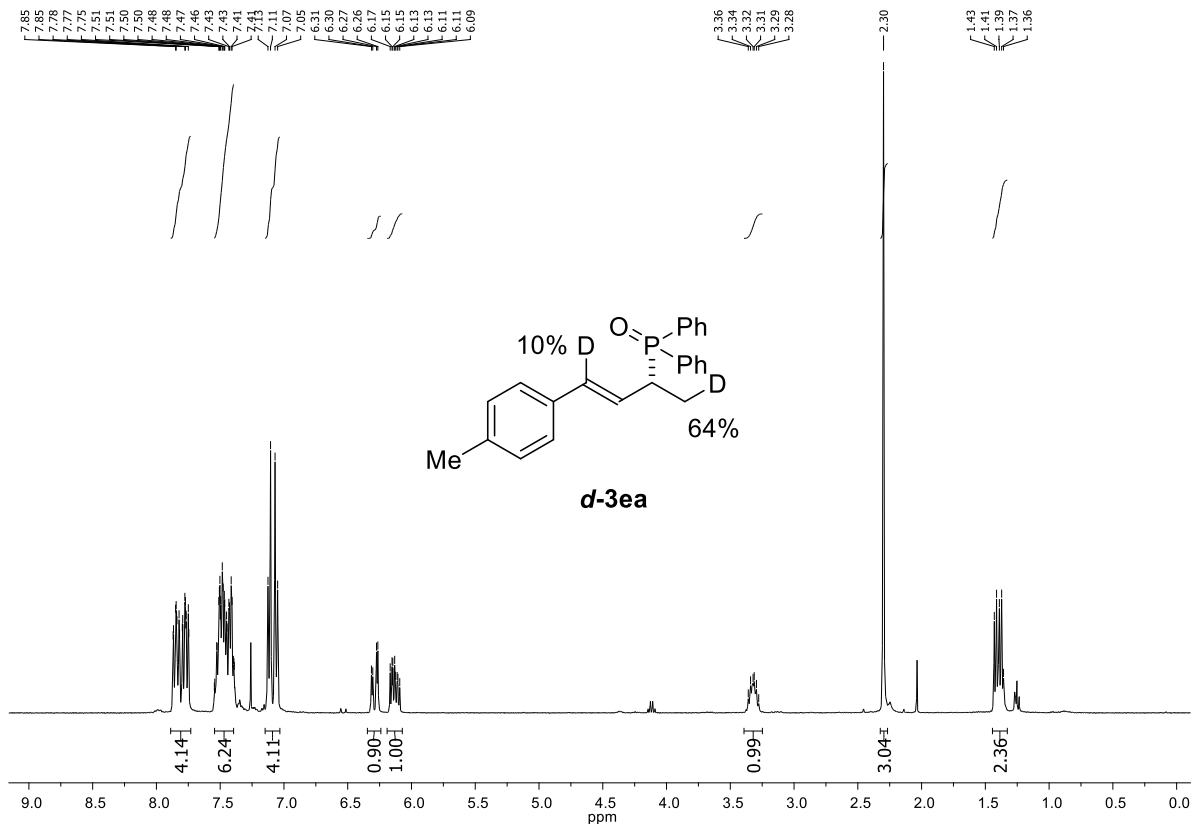


(2) Synthesis of *d*-3ea:

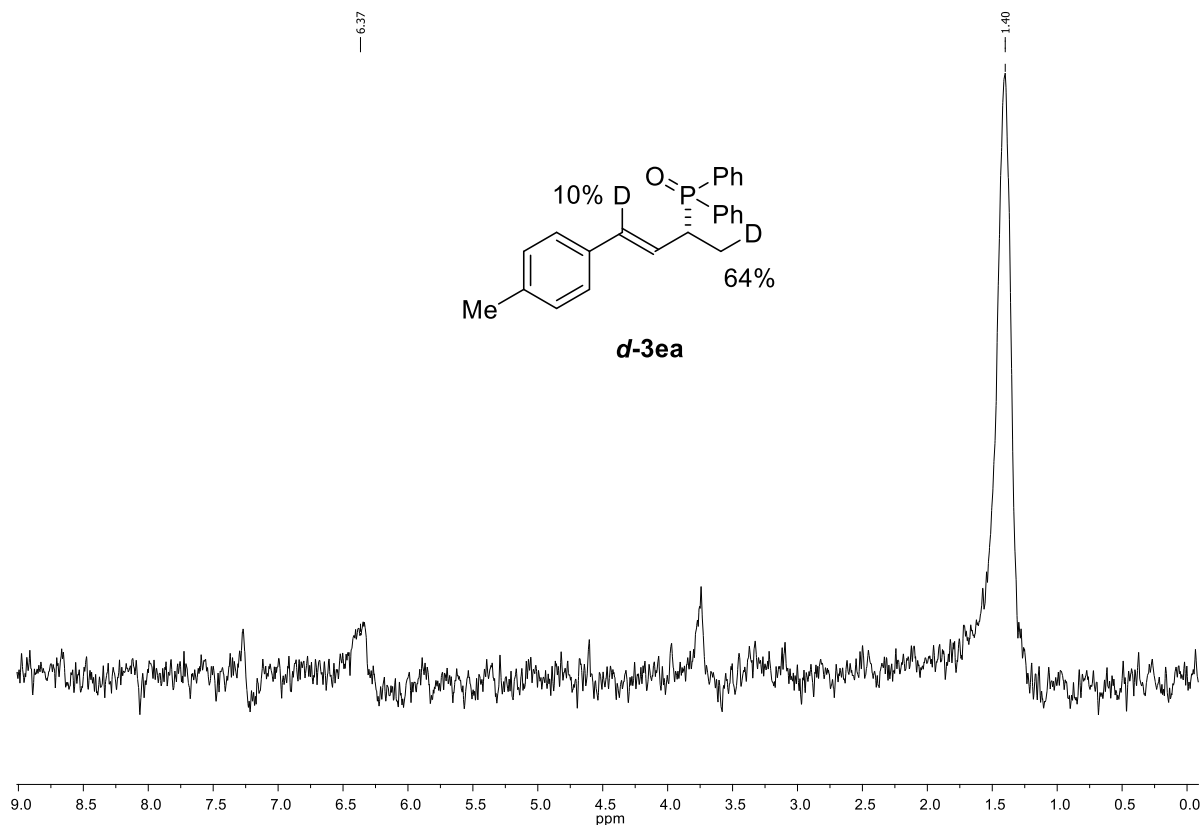


Following the **General procedure for the hydrophosphinylation of 1,3-dienes**, *d*-2a was used as the phosphine oxide partner. White solid, 78% yield, >20:1 *rr*. $^1\text{H NMR}$ (400 MHz, CDCl_3) δ 7.87 – 7.75 (m, 4H), 7.55 – 7.39 (m, 6H), 7.13 – 7.05 (m, 4H), 6.29 (dd, $J = 15.9, 4.2$ Hz, 0.90H), 6.17 – 6.09 (m, 1H), 3.32 (m, 1H), 2.30 (s, 3H), 1.39 (m, 2.36H). $^2\text{H NMR}$ (61 MHz, CHCl_3) δ 6.37, 1.40. Deuterium incorporation was determined by $^1\text{H NMR}$. Percent deuterium (% D) incorporation is depicted as the amount of deuterium in place of a single hydrogen atom at that site.

$^1\text{H NMR}$ of *d*-3ea:

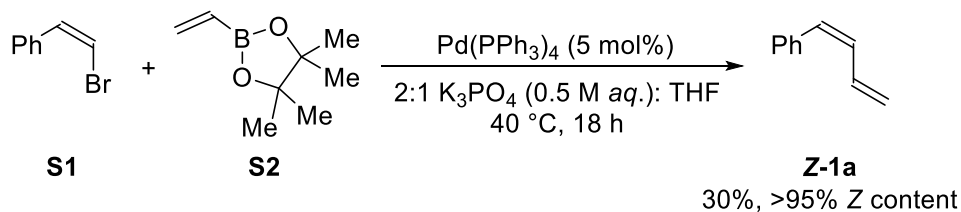


^2H NMR of *d*-3ea:



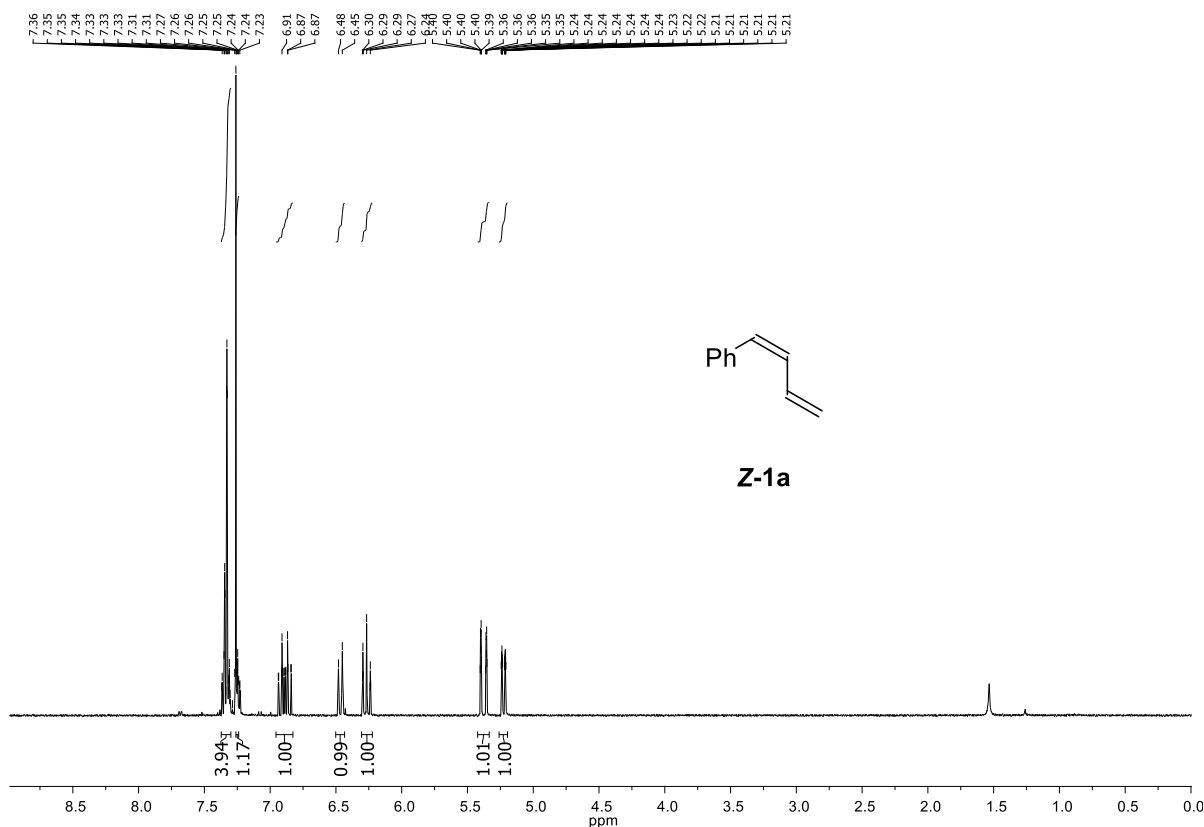
3B. Diene Geometry Study

(1) Synthesis of *Z*-1a:

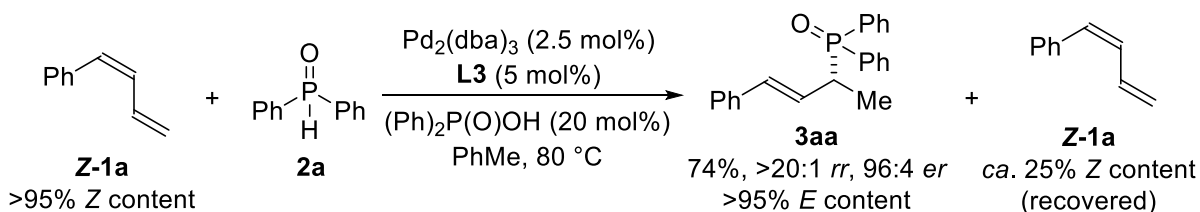


To a 50 mL round-bottom flask, in a N_2 -filled glovebox, was added a magnetic stir-bar, **S1** (183.1 mg, 1 mmol, 1 equiv),⁶ **S2** (184.8 mg, 1.2 mmol, 1.2 equiv), and $\text{Pd}(\text{PPh}_3)_4$ (57.8 mg, 0.05 mmol, 0.05 equiv). The flask was capped with a rubber septum and removed from the glovebox. THF (2 mL) and 0.5 M aq. K_3PO_4 (4 mL, degassed by sparging with N_2 for 30 min.) were added sequentially via syringe. The reaction mixture was then heated to 40 °C for 18 h with vigorous stirring. The flask was cooled to rt and the reaction mixture was diluted with 10 mL of H_2O and 10 mL of Et_2O . The mixture was extracted with Et_2O (2 x 15 mL) and the combined organic

fractions were washed with 20 mL of sat. *aq.* brine and then dried over MgSO₄ and filtered. The pale-yellow solution was concentrated *in vacuo* to produce a yellow oil, which was purified by flash silica gel chromatography (100% hexanes) to yield **Z-1a** as a clear oil (39 mg, 0.30 mmol, 30% yield) as a single *Z*-isomer. ¹H NMR (400 MHz, CDCl₃) δ 7.37 – 7.30 (m, 4H), 7.27 – 7.23 (m, 1H), 6.88 (dddd, *J* = 16.9, 11.2, 10.1, 1.1 Hz, 1H), 6.47 (d, *J* = 11.7 Hz, 1H), 6.30 – 6.24 (m, 1H), 5.40 – 5.35 (m, 1H), 5.24 – 5.21 (m, 1H). The spectral data match those previously reported.⁷



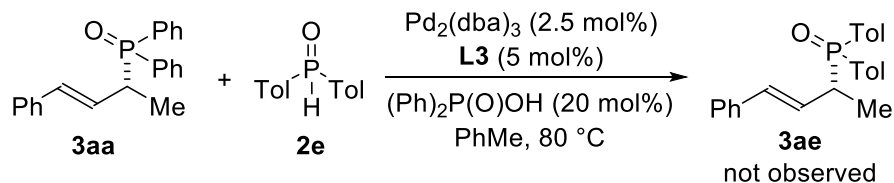
(2) Synthesis of **3aa** from **Z-1a**:



Following the **General procedure for the hydrophosphinylation of 1,3-dienes**, **Z-1a** was used as the 1,3-diene partner. Isolated **3aa**, which was consistent with spectral data from the general method preparation. White solid, 74% yield, 96:4 *er*, $>20:1$ *rr*. ¹H NMR (400 MHz, CDCl₃) δ 7.89 – 7.75 (m, 4H), 7.56 – 7.38 (m, 6H), 7.27 – 7.18 (m, 5H), 6.32 (dd, *J* = 16.0, 4.1 Hz, 1H), 6.22 – 6.14 (m, 1H), 3.40 – 3.28 (m, 1H), 1.46 – 1.35 (dd, *J* = 16.0, 7.1 Hz, 3H). **Z-1a** was recovered (ca.

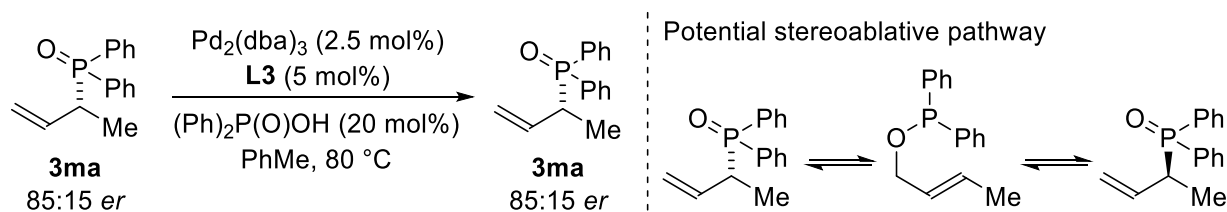
25% *Z* content, compared with **Z-1a** standard).

3C. Cross-Over Study



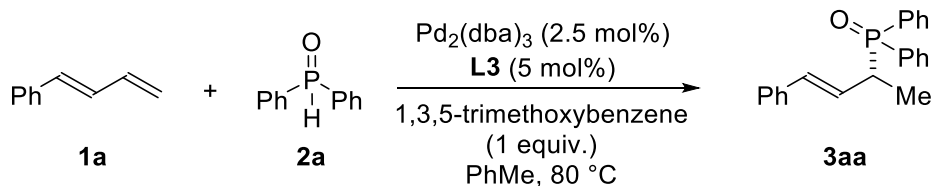
Following the **General procedure for the hydrophosphinylation of 1,3-dienes**, **3aa** and **2e** were used for a cross-over experiment (for 24 h instead of the standard 3 h reaction time). We observe no reactivity (i.e. incorporation of **2e** to form product **3ae**), but rather remaining starting materials after 24 h.

3D. Stereoablative Pathway Study



Following the **General procedure for the hydrophosphinylation of 1,3-dienes**, **3ma** was used to probe the potential of a stereoablative pathway being operable (right). We observe no change in enantioenrichment (i.e., **3ma** retains a 85:15 *er*) after 12 hours under the reaction conditions.

3E. Induction Period Study *Without Acid*



Following the **General procedure for the hydrophosphinylation of 1,3-dienes**, **1a** and **2a** were used for an induction period study with changes including the absence of acid (diphenylphosphinic acid) and the addition of an internal standard (1,3,5-trimethoxybenzene, 1 equiv.). The reaction was heated to 80°C and 10 μL aliquots were taken at the given time points (see below). The aliquots were immediately quenched in EtOAc (reaction does not proceed in this solvent) and the

relative product to internal standard ratio was obtained via GC-FID analysis. The raw and graphical data are reported immediately below. We observe a long induction period for the acid-omitted hydrophosphinylation of **1a** with **2a**.

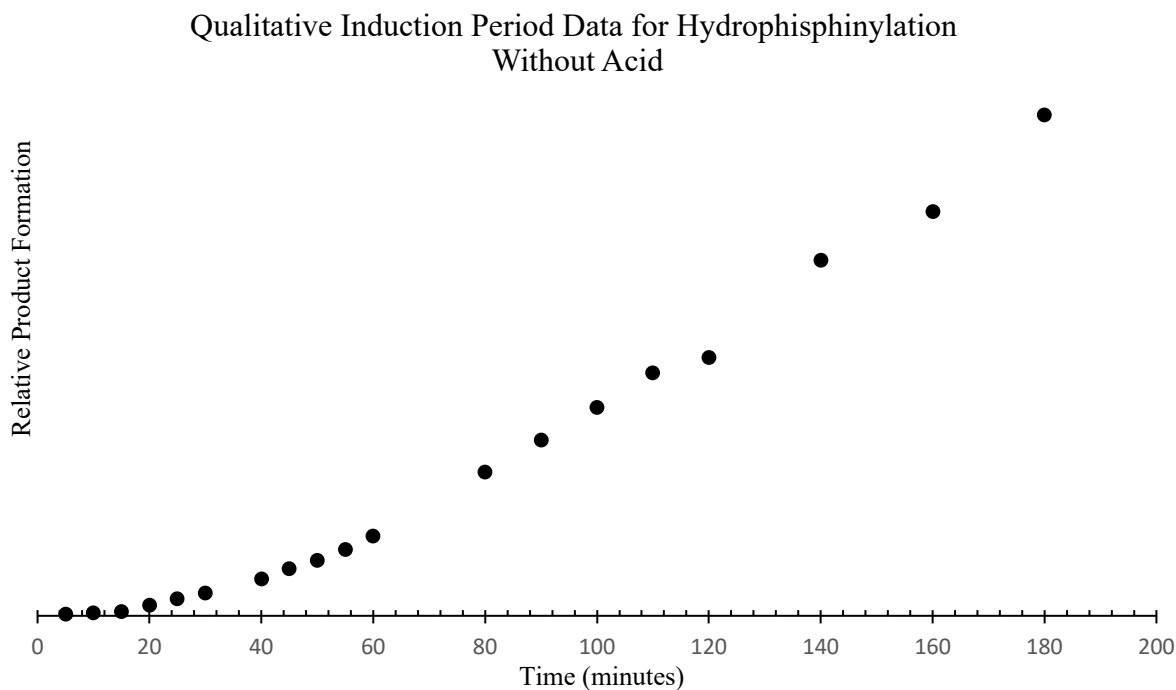


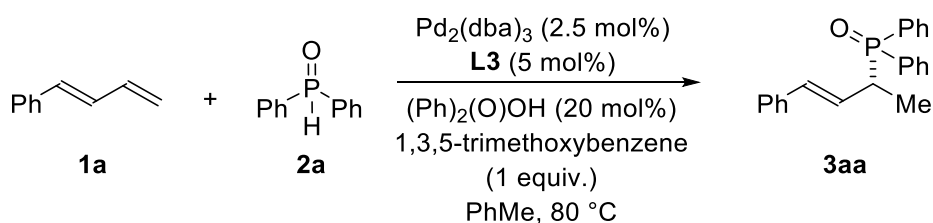
Figure S2. Qualitative graph of induction period study for acid-omitted hydrophosphinylation.

Raw Data:

Entry	Time (min)	Internal Standard		Product/Internal Standard	
		Area	Product Area	Area	Ratio
1	5	153.0	0.8	0.005	0.005
2	10	107.5	1.0	0.009	0.009
3	15	106.7	1.3	0.012	0.012
4	20	107.4	3.3	0.031	0.031
5	25	100.1	4.8	0.048	0.048
6	30	133.9	8.6	0.064	0.064
7	40	120.7	12.3	0.102	0.102
8	45	106.0	13.8	0.130	0.130
9	50	96.3	14.7	0.153	0.153
10	55	89.8	16.4	0.183	0.183
11	60	111.4	24.6	0.221	0.221
12	80	115.6	45.8	0.396	0.396

13	90	97.1	47.1	0.485
14	100	92.9	53.4	0.575
15	110	108.0	72.3	0.669
16	120	109.8	78.1	0.711
17	140	108.8	106.5	0.979
18	160	145.2	161.6	1.113
19	180	165.8	228.8	1.380

3F. Induction Period Study *With Acid*



Following the **General procedure for the hydrophosphinylation of 1,3-dienes**, **1a** and **2a** were used for an induction period study with changes including the addition of an internal standard (1,3,5-trimethoxybenzene, 1 equiv.). The reaction was heated to 80 °C and 10 μL aliquots were taken at the given time points (see below). The aliquots were immediately quenched in EtOAc (reaction does not proceed in this solvent) and the relative product to internal standard ratio was obtained via GC-FID analysis. The raw and graphical data are reported immediately below. We observe a short induction period for the acid-included hydrophosphinylation of **1a** with **2a**.

Qualitative Induction Period Data for Hydrophosphinylation
With Acid

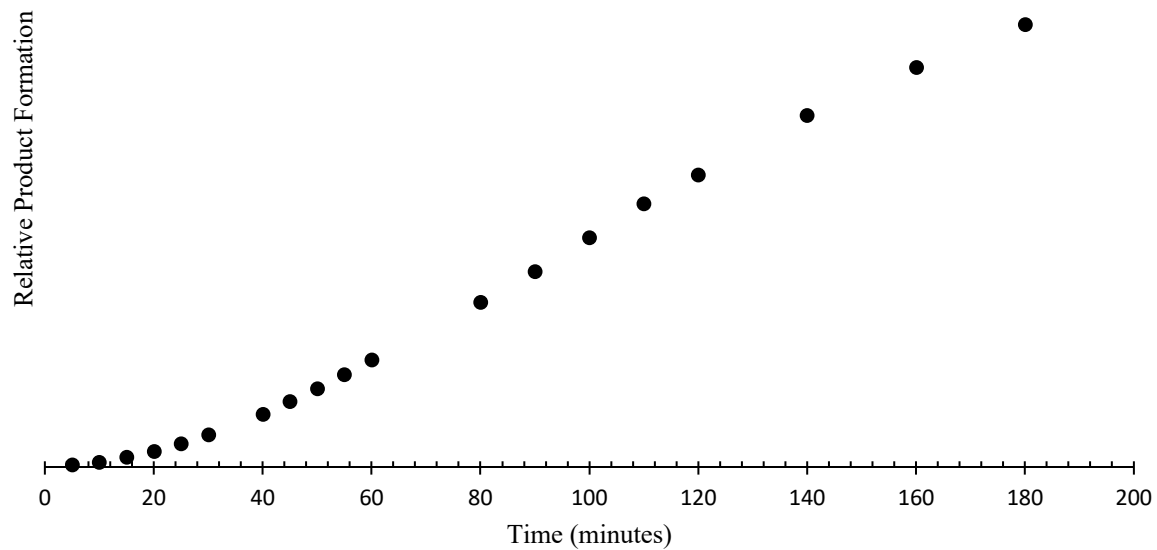


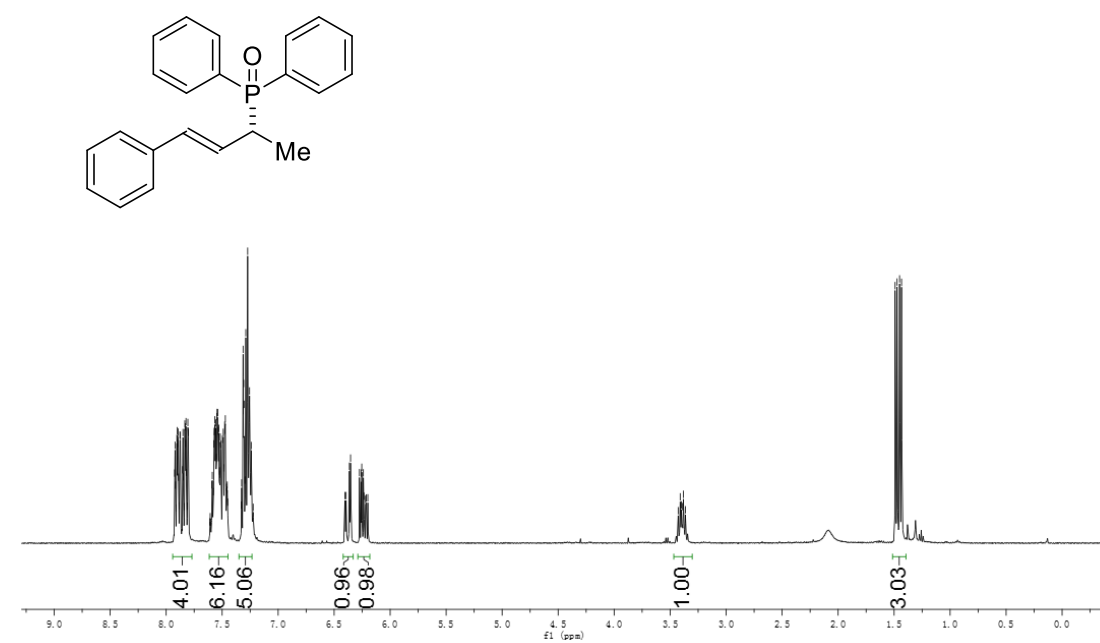
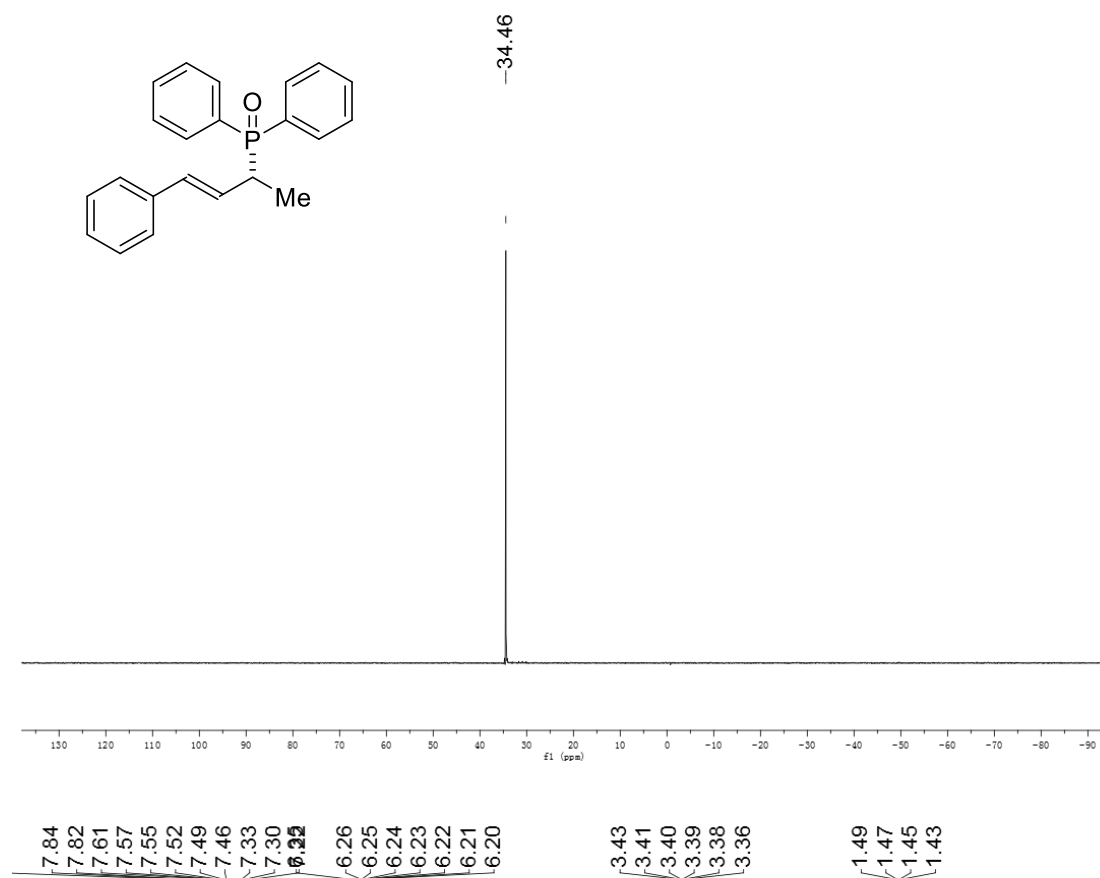
Figure S3. Qualitative graph of induction period study for acid-included hydrophosphinylation.

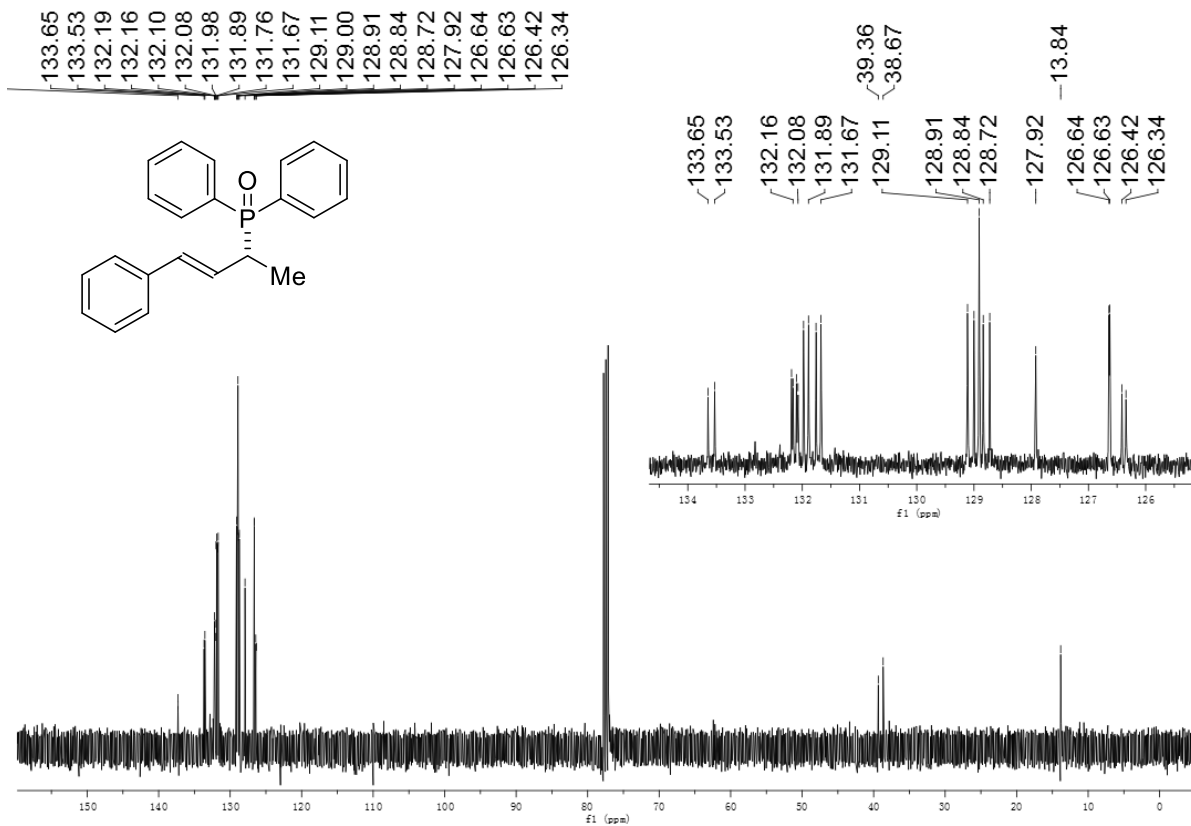
Raw Data

Entry	Time (min)	Internal Standard Area	Product Area	Product/Internal Standard Ratio
1	5	156.1	1.9	0.012
2	10	56.9	1.8	0.032
3	15	110.0	7.0	0.064
4	20	91.2	9.6	0.105
5	25	97.6	15.2	0.156
6	30	72.7	15.8	0.217
7	40	106.0	38.0	0.358
8	45	85.5	37.9	0.443
9	50	43.9	23.3	0.531
10	55	62.0	38.8	0.626
11	60	39.9	28.9	0.724
12	80	39.0	43.6	1.118
13	90	39.5	52.4	1.327
14	100	52.8	82.1	1.555
15	110	38.8	69.3	1.786
16	120	49.3	97.7	1.982
17	140	52.9	126.2	2.386
18	160	62.6	169.8	2.712
19	180	80.1	240.6	3.004

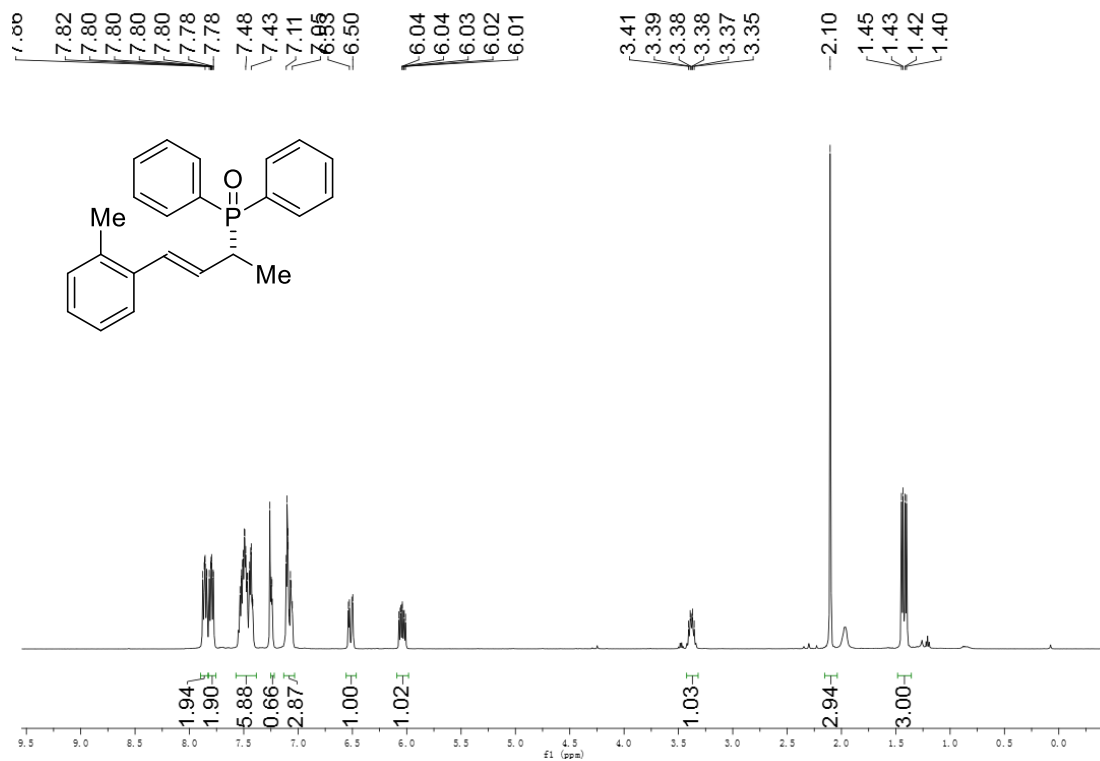
4. NMR spectra of unknown compounds

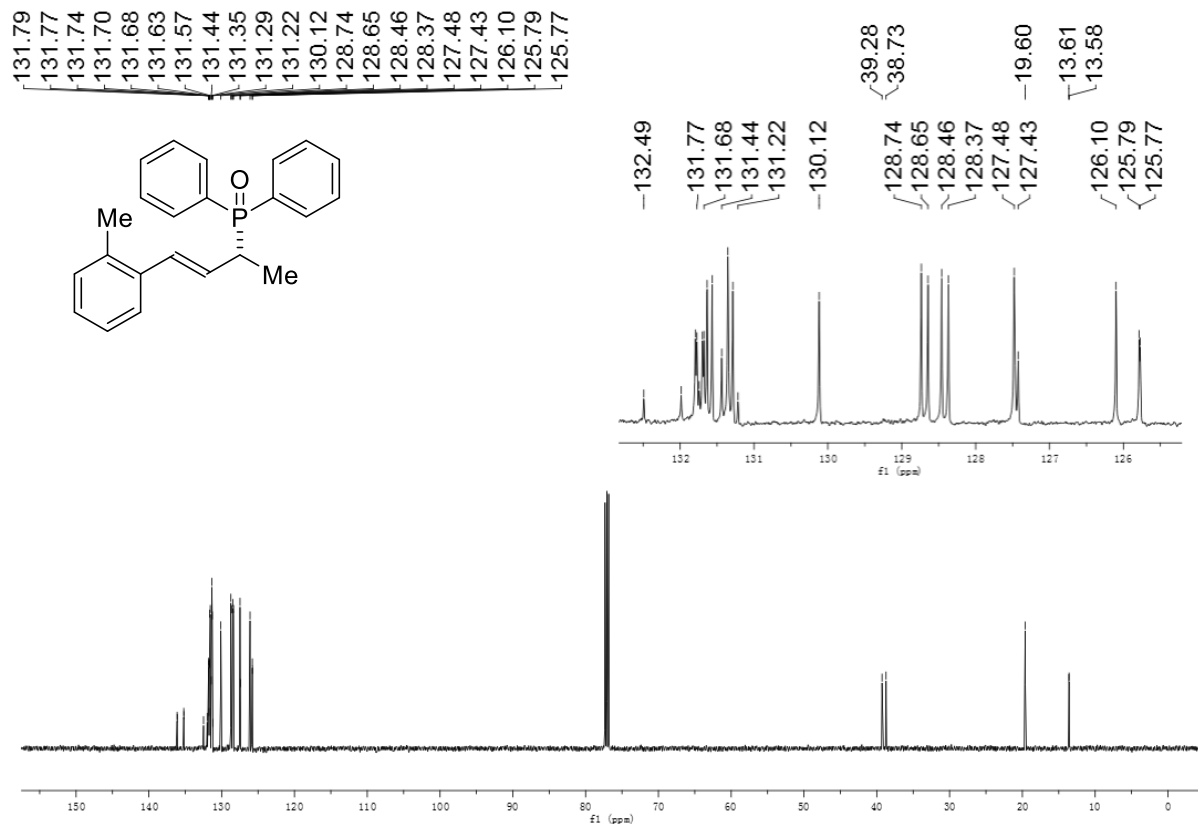
(*R,E*)-diphenyl(4-phenylbut-3-en-2-yl)phosphine oxide (3aa)



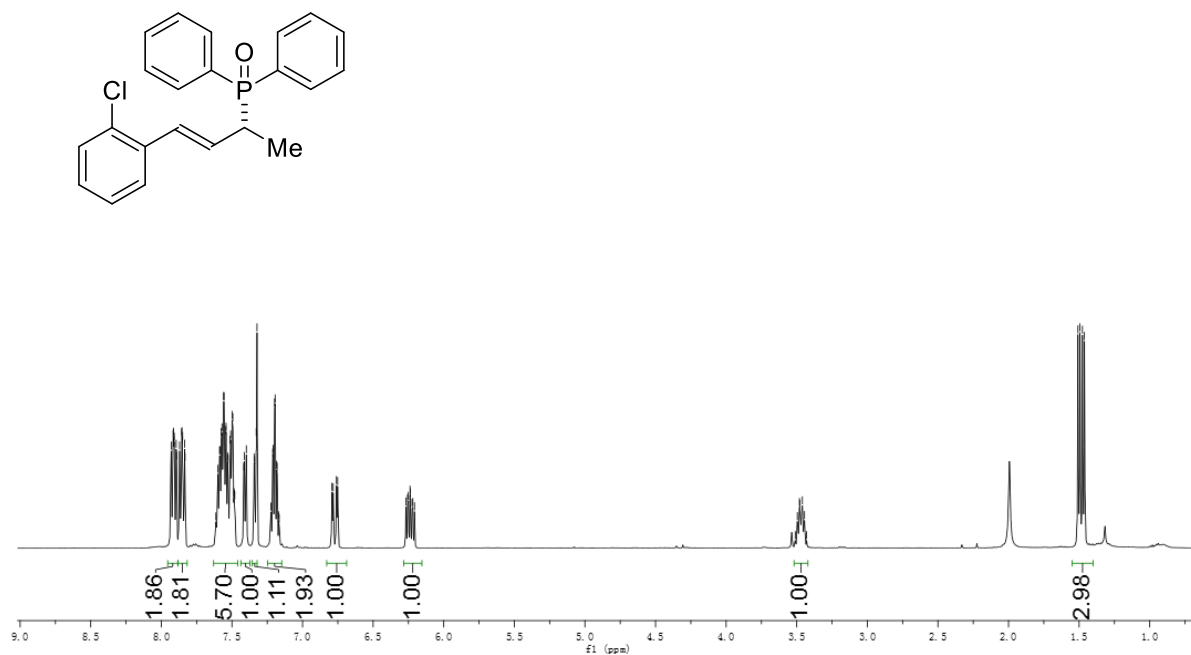
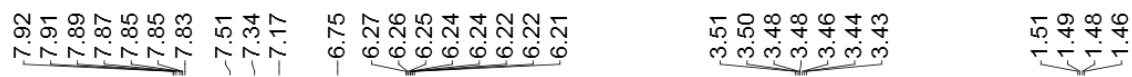


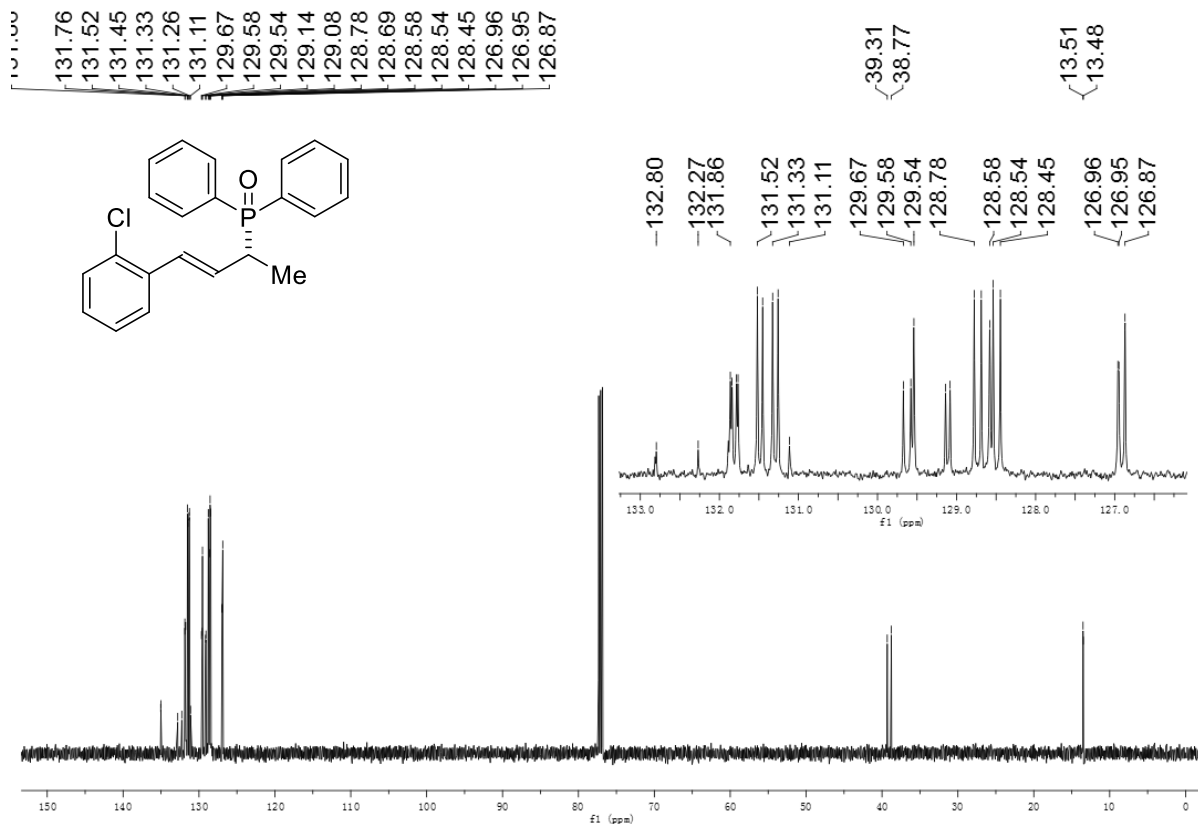
(*R,E*)-diphenyl(4-(*o*-tolyl)but-3-en-2-yl)phosphine oxide (3ba)



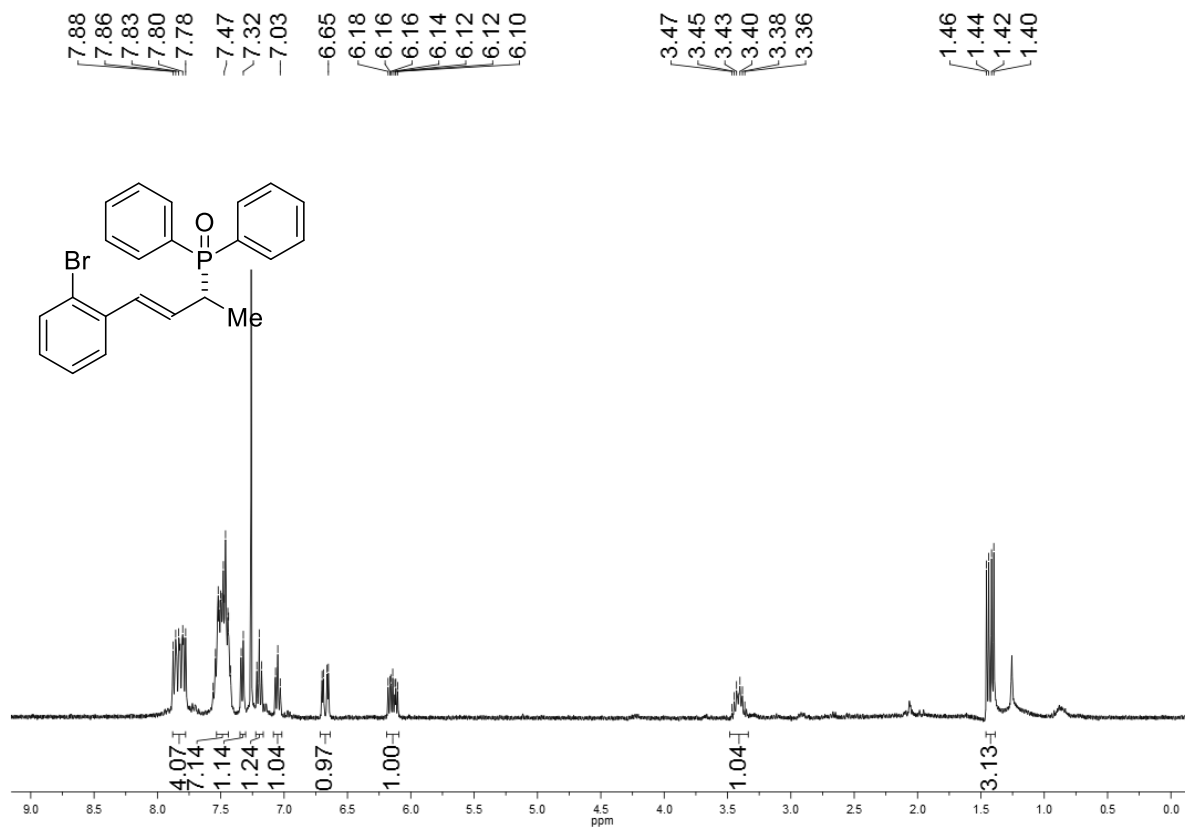
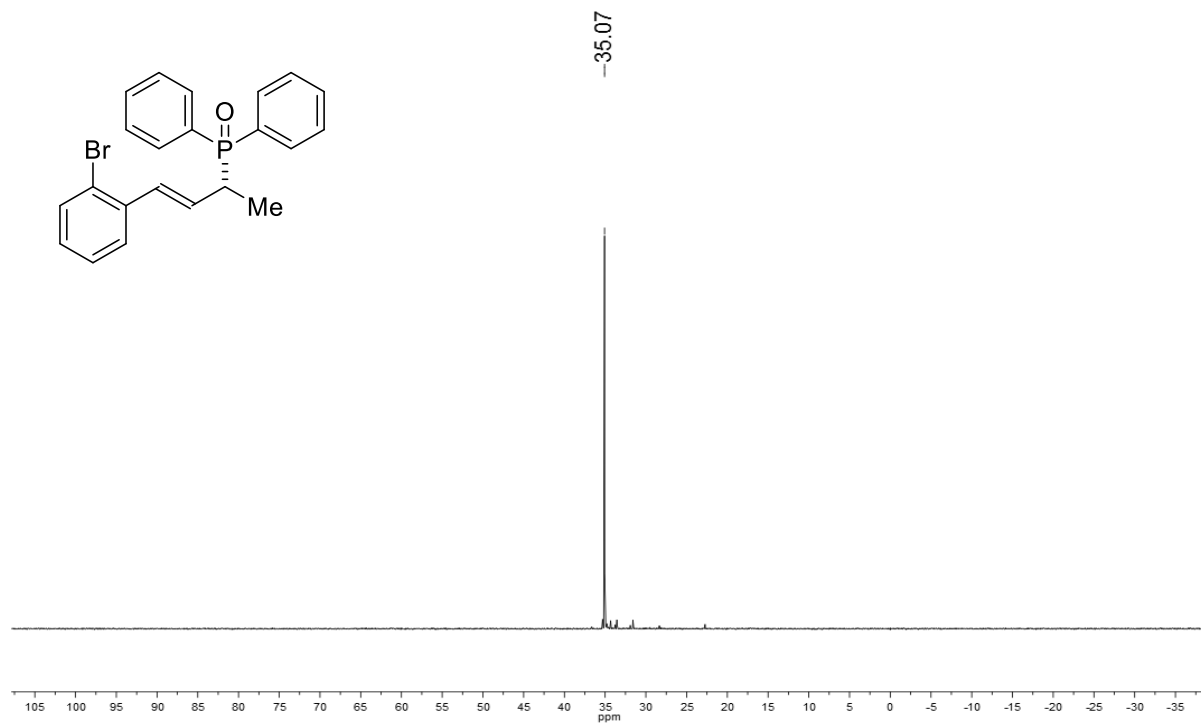


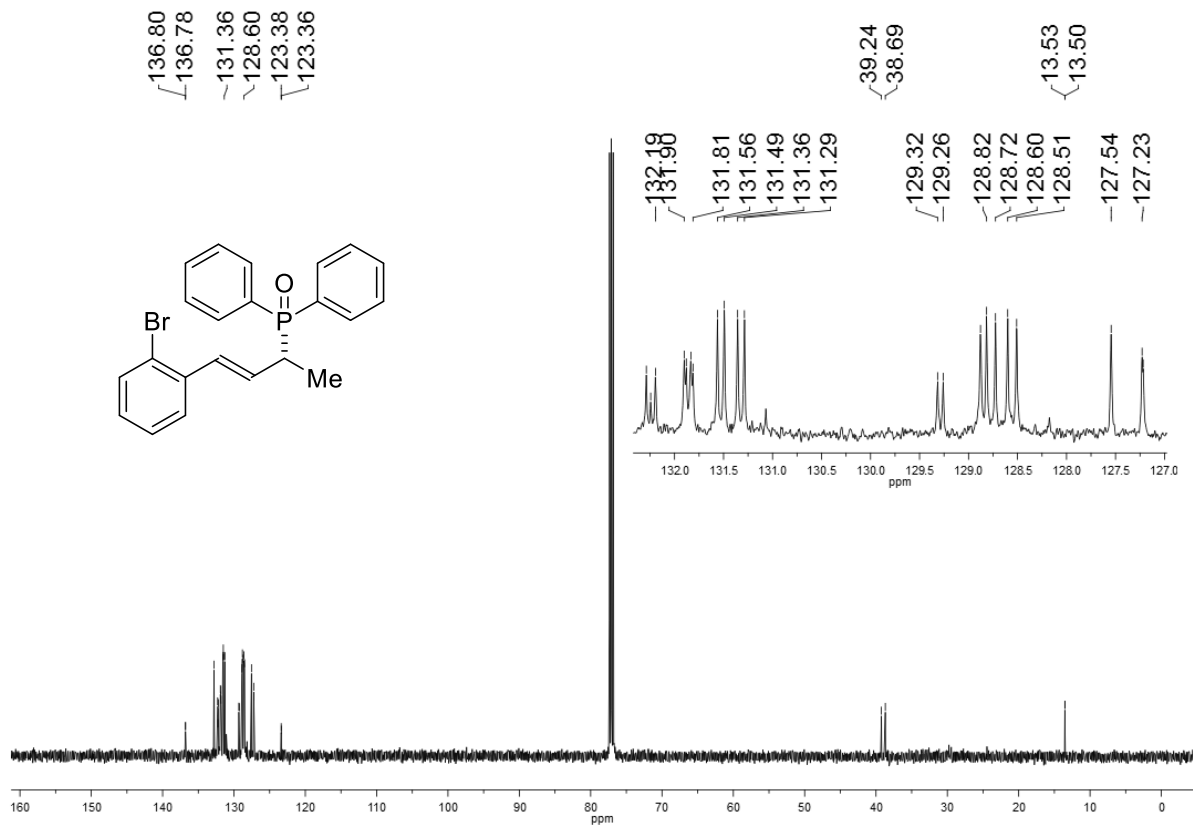
(*R,E*)-(4-(2-chlorophenyl)but-3-en-2-yl)diphenylphosphine oxide (3ca)



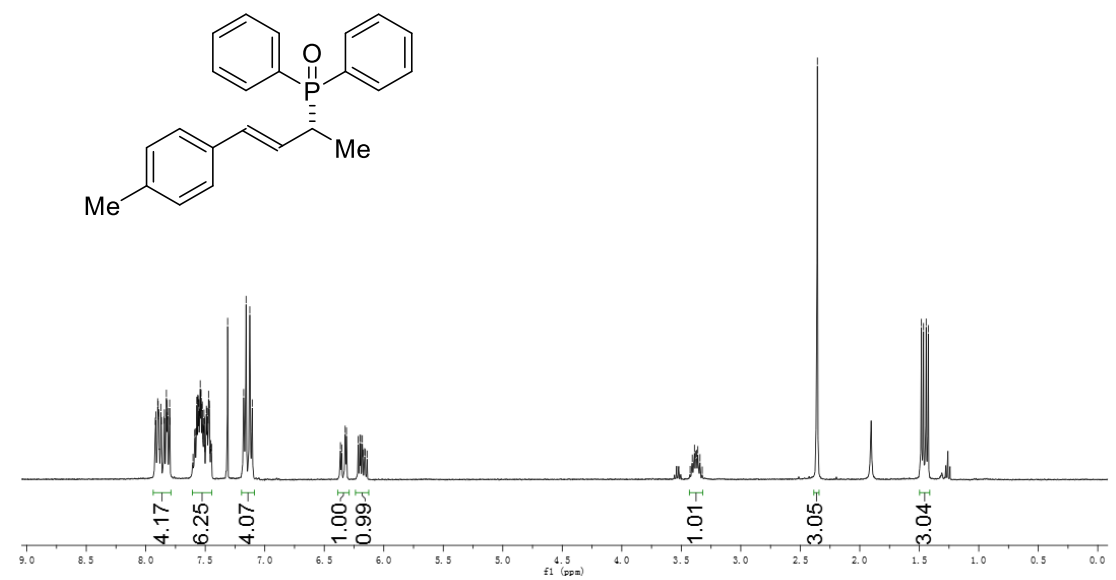
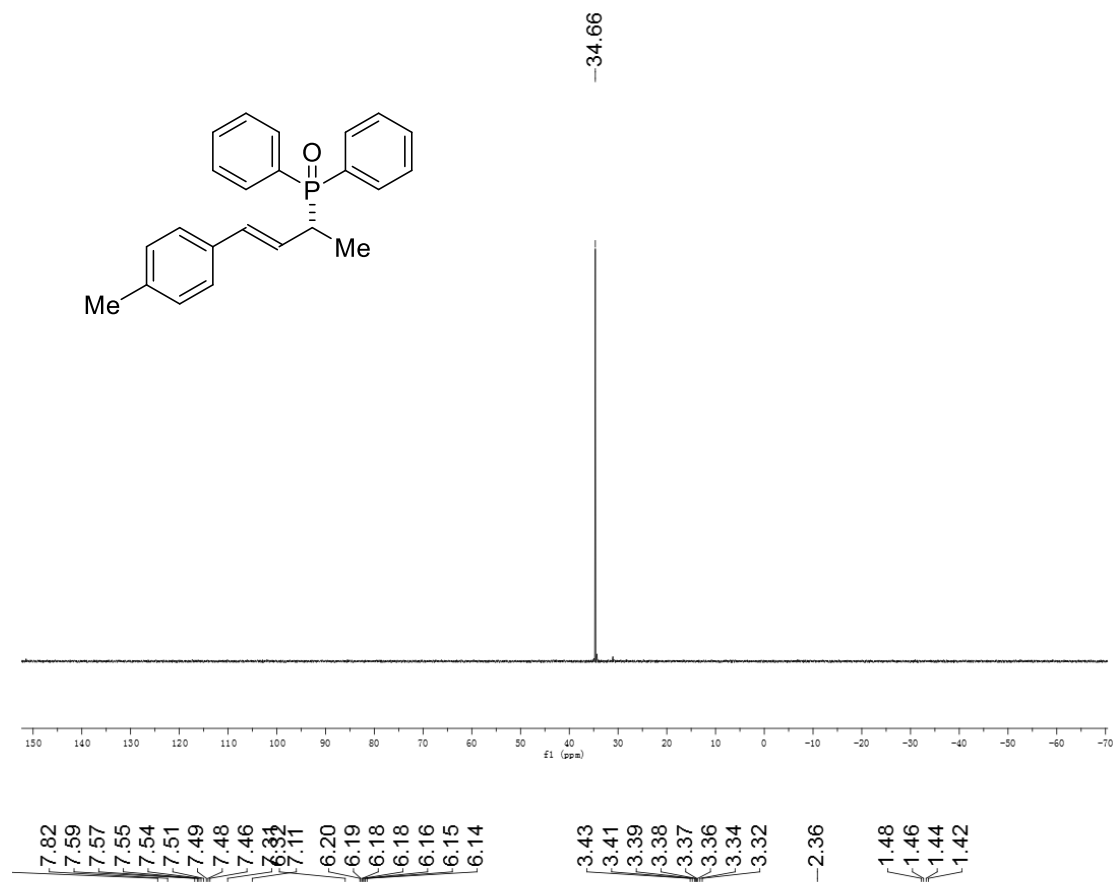


(*R,E*)-(4-(2-bromophenyl)but-3-en-2-yl)diphenylphosphine oxide (3da)

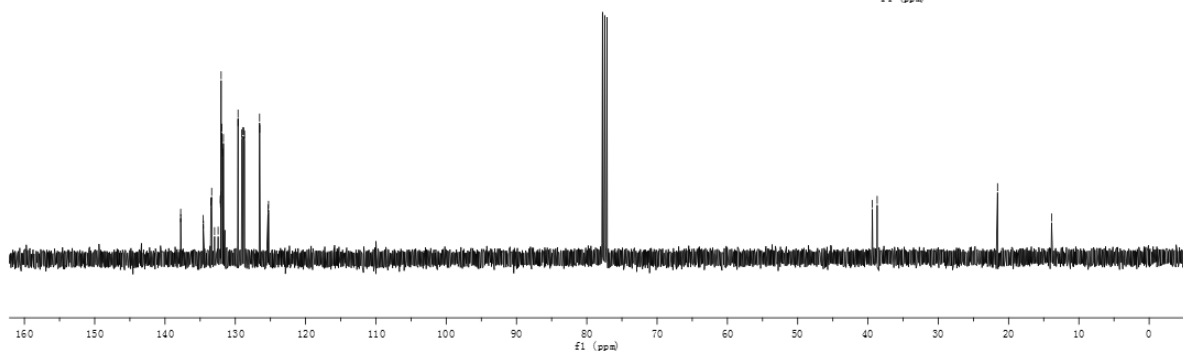
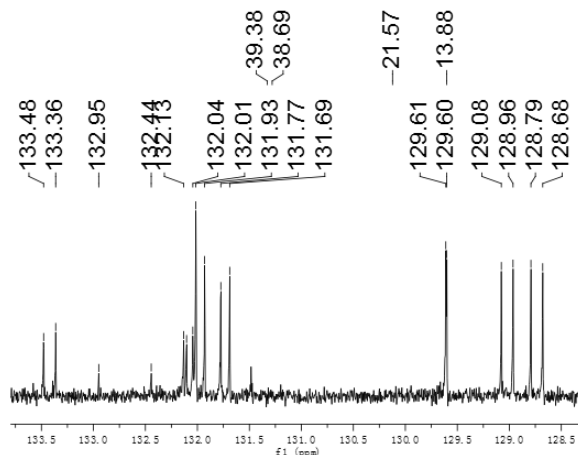
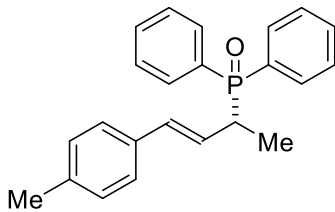




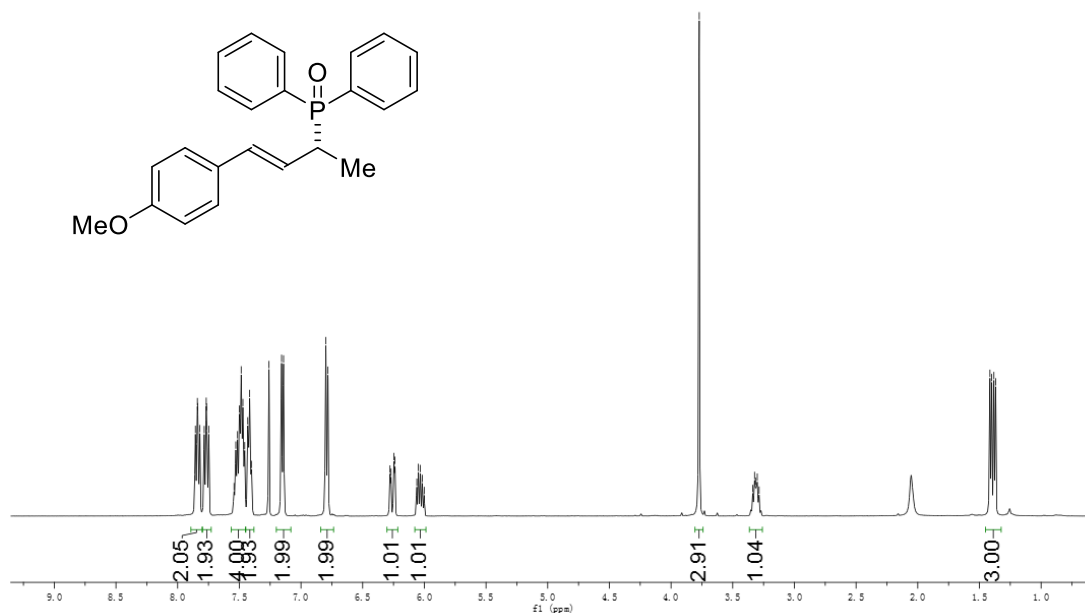
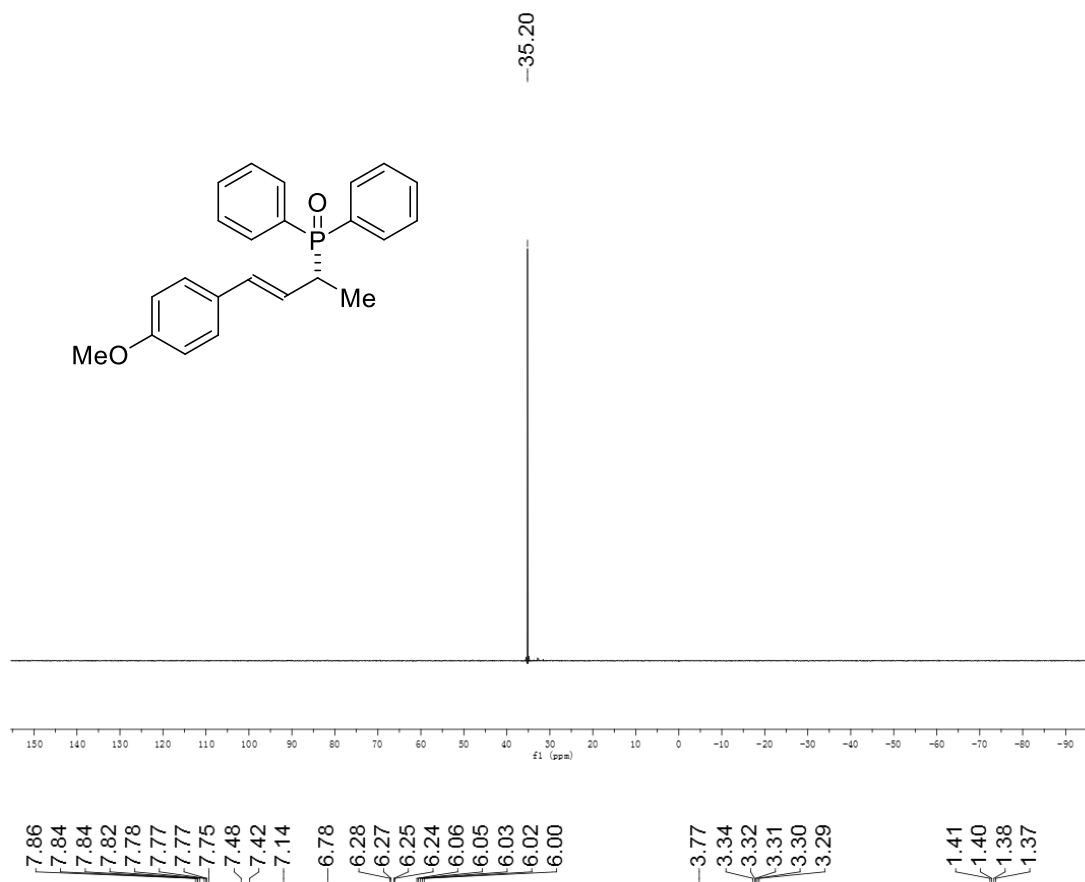
(*R,E*)-diphenyl(4-(*p*-tolyl)but-3-en-2-yl)phosphine oxide (3ea)

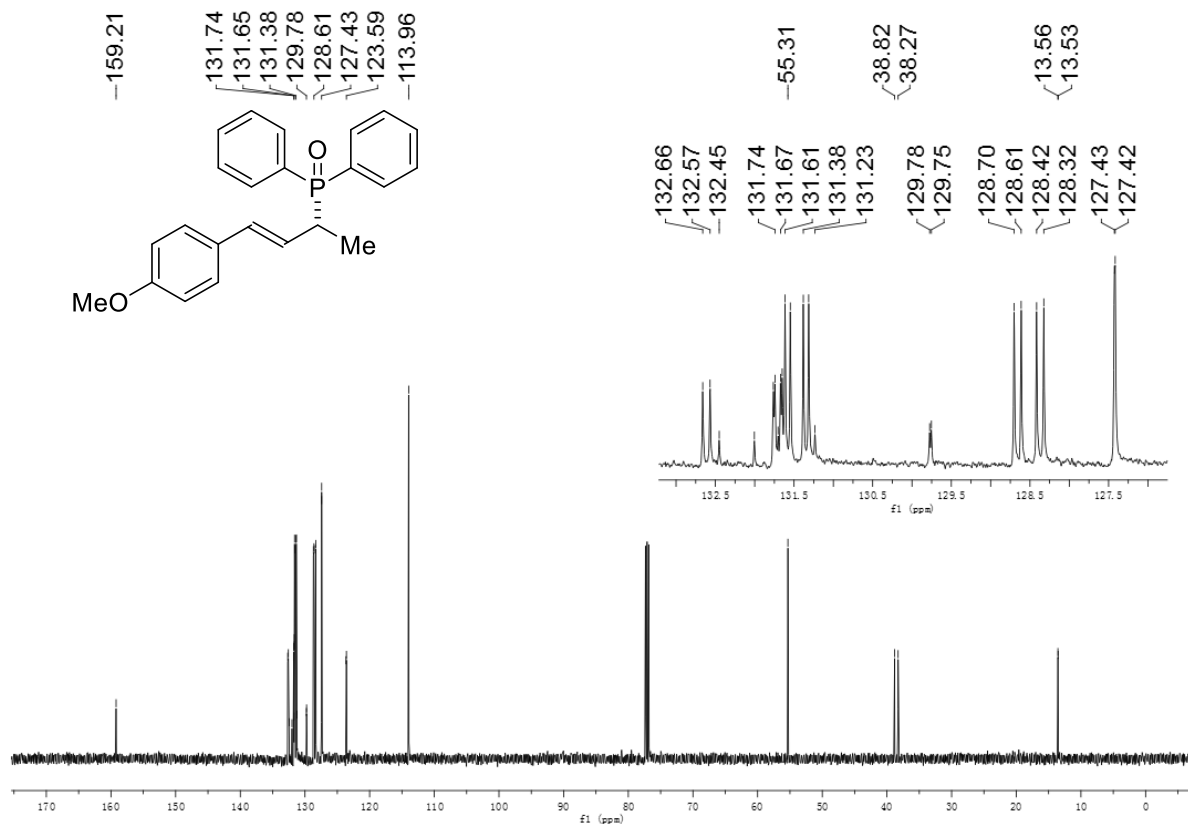


133.48
133.36
132.95
132.44
132.13
132.10
132.04
132.01
131.93
131.77
131.69
129.61
129.60
129.08
128.96
128.79
128.68
126.55
126.53
125.35
125.27

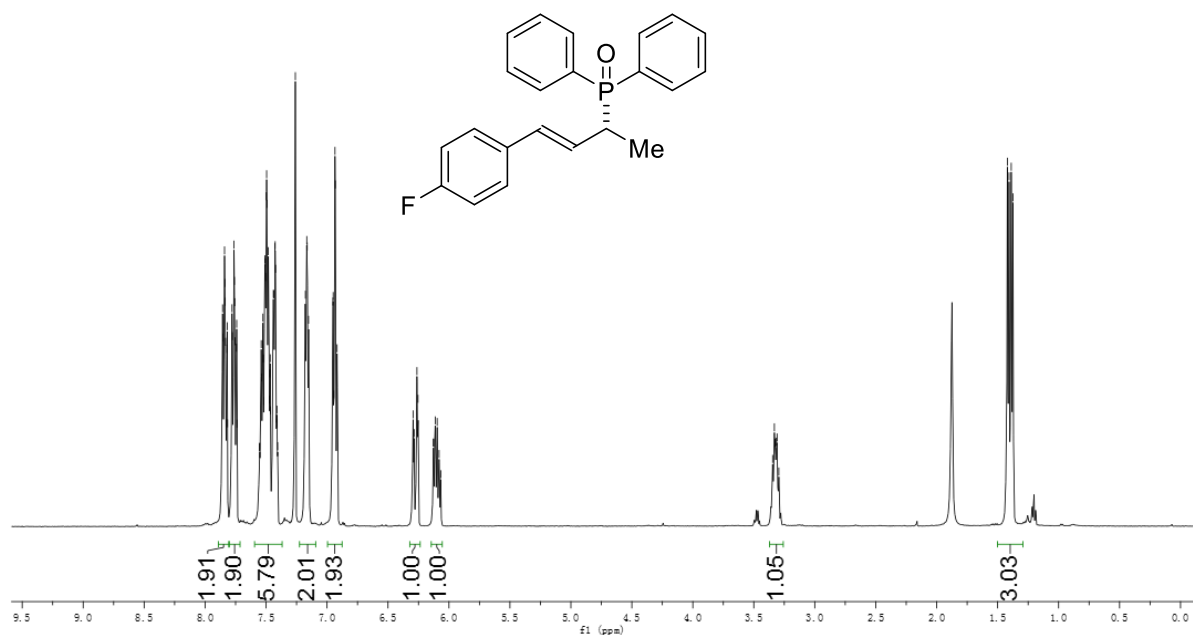
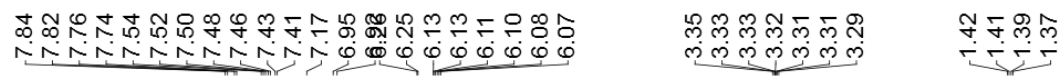
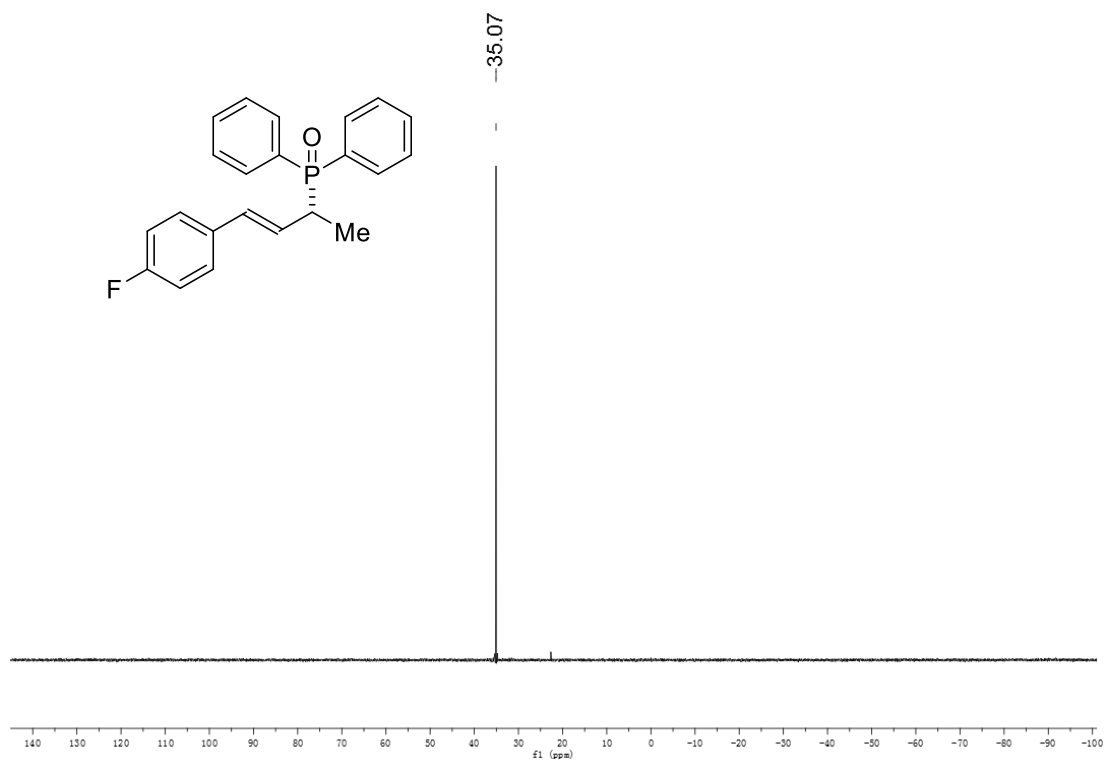


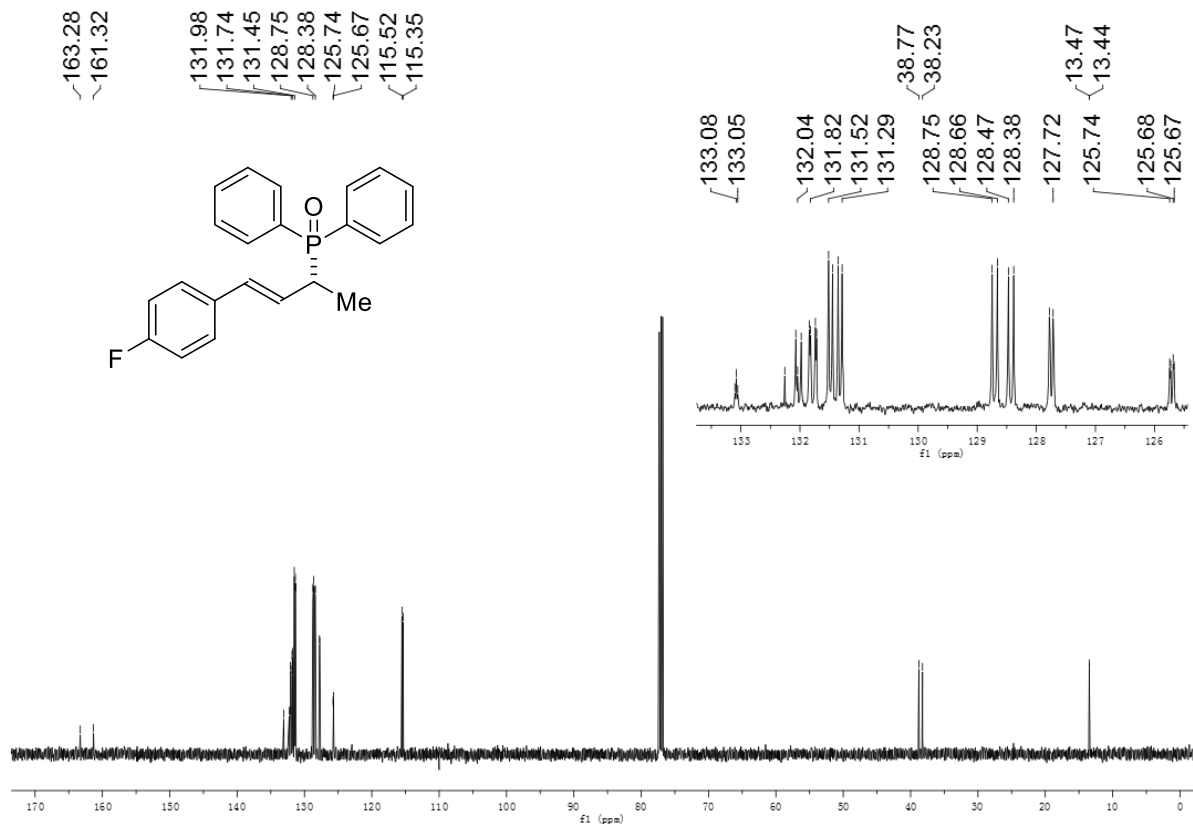
(*R,E*)-(4-(4-methoxyphenyl)but-3-en-2-yl)diphenylphosphine oxide (3fa)



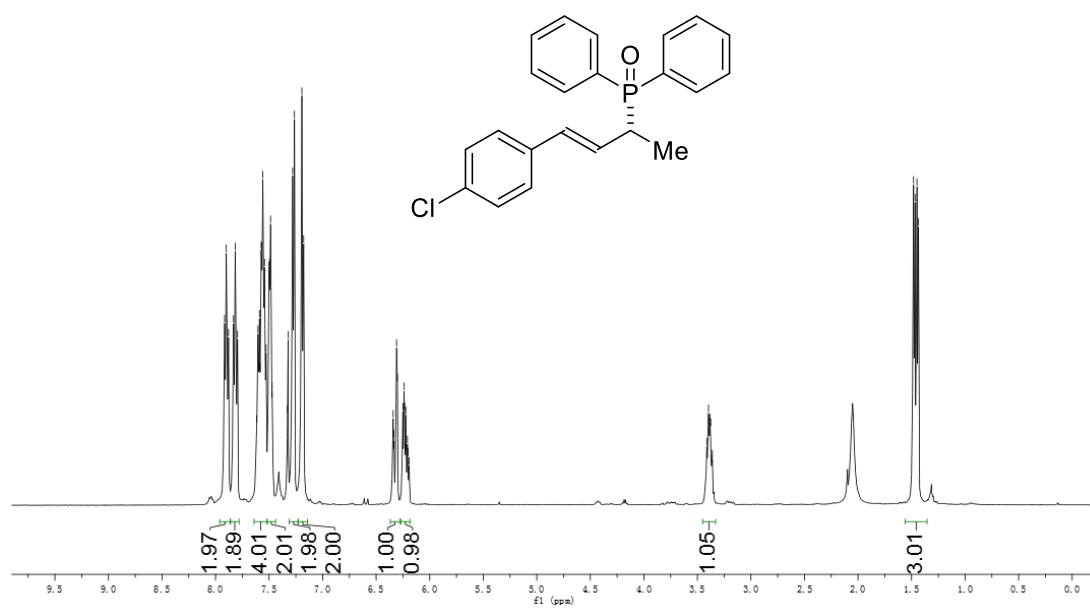
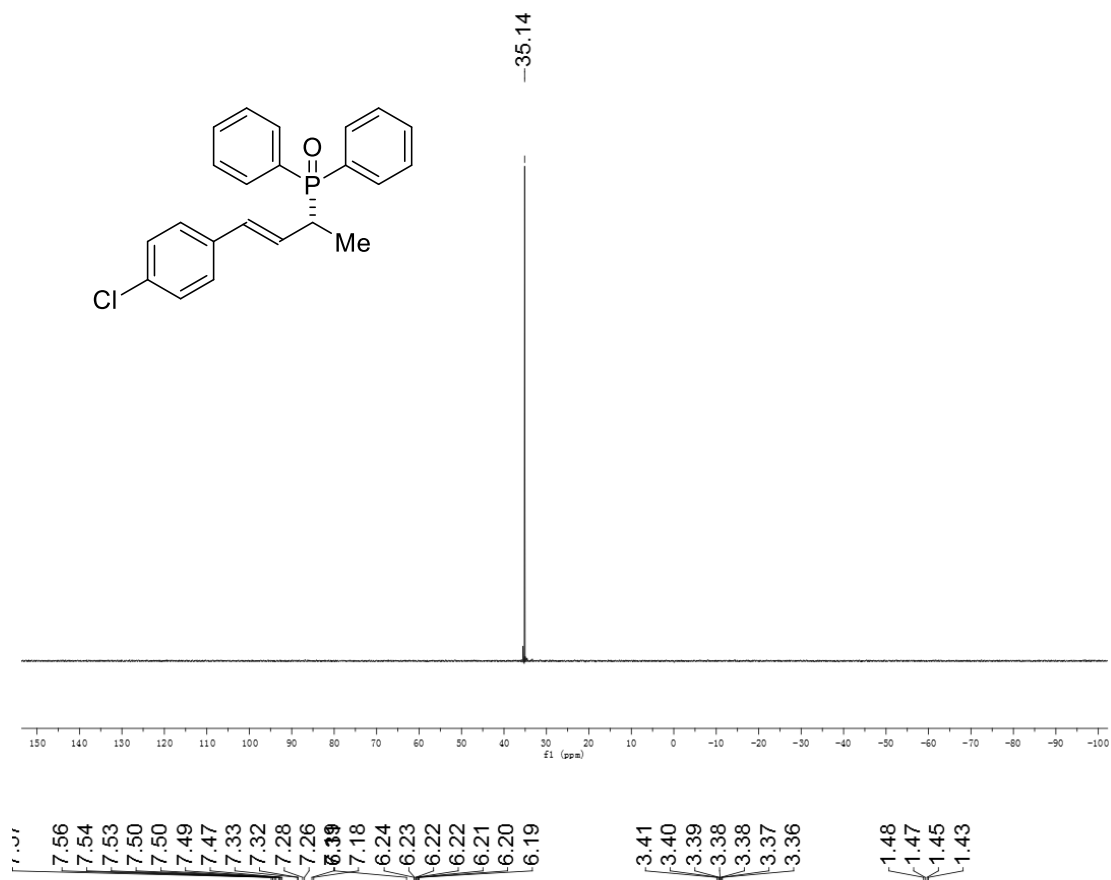


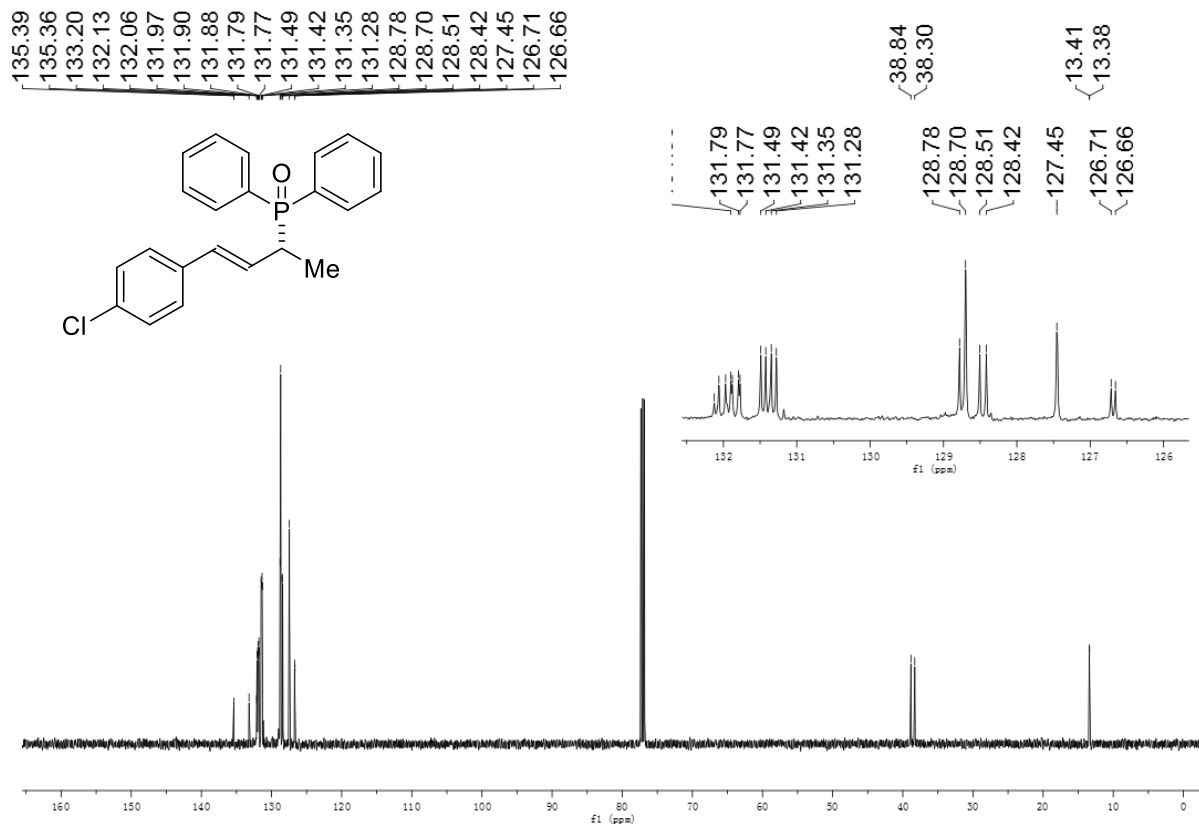
(*R,E*)-(4-(4-fluorophenyl)but-3-en-2-yl)diphenylphosphine oxide (3ga)



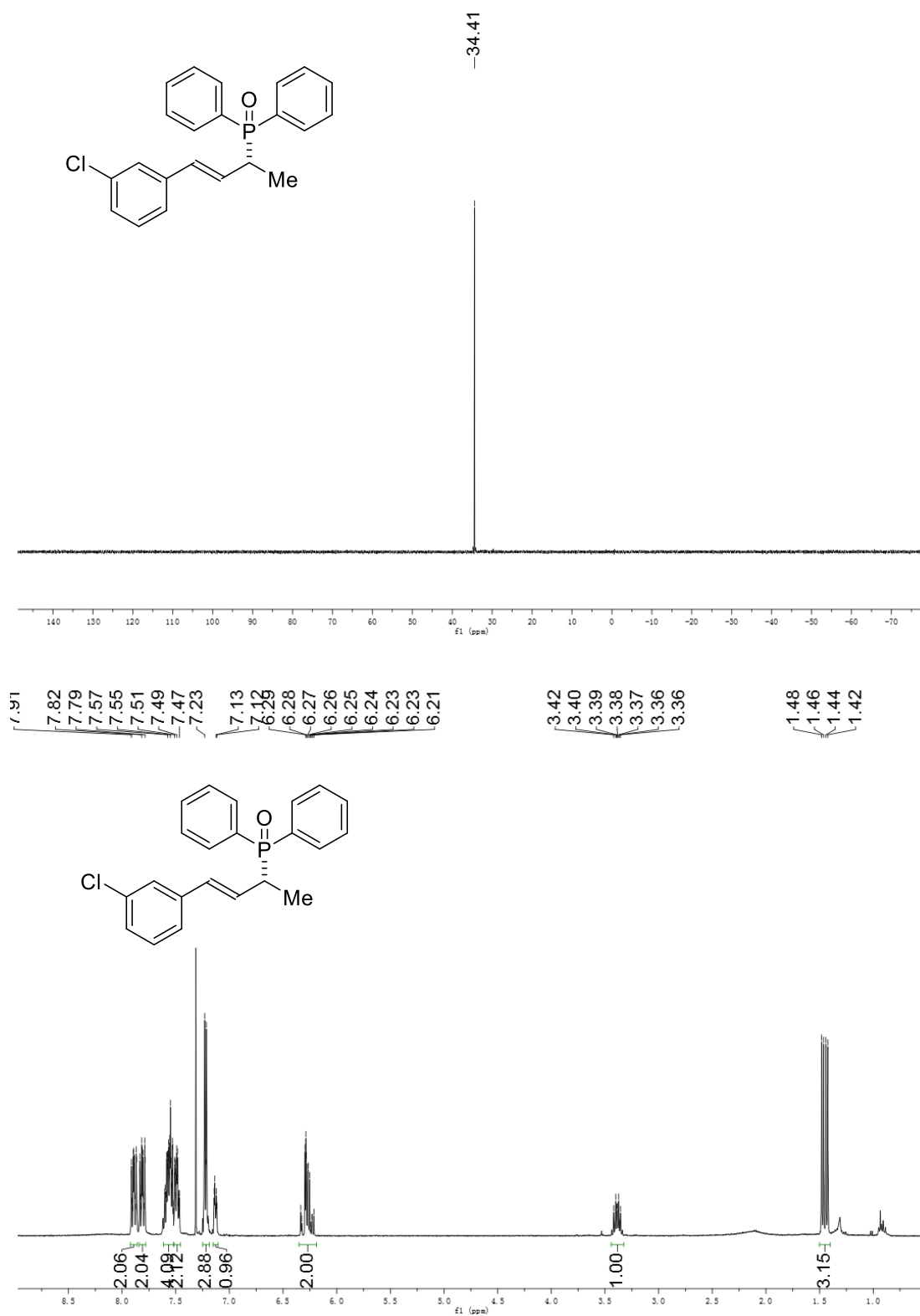


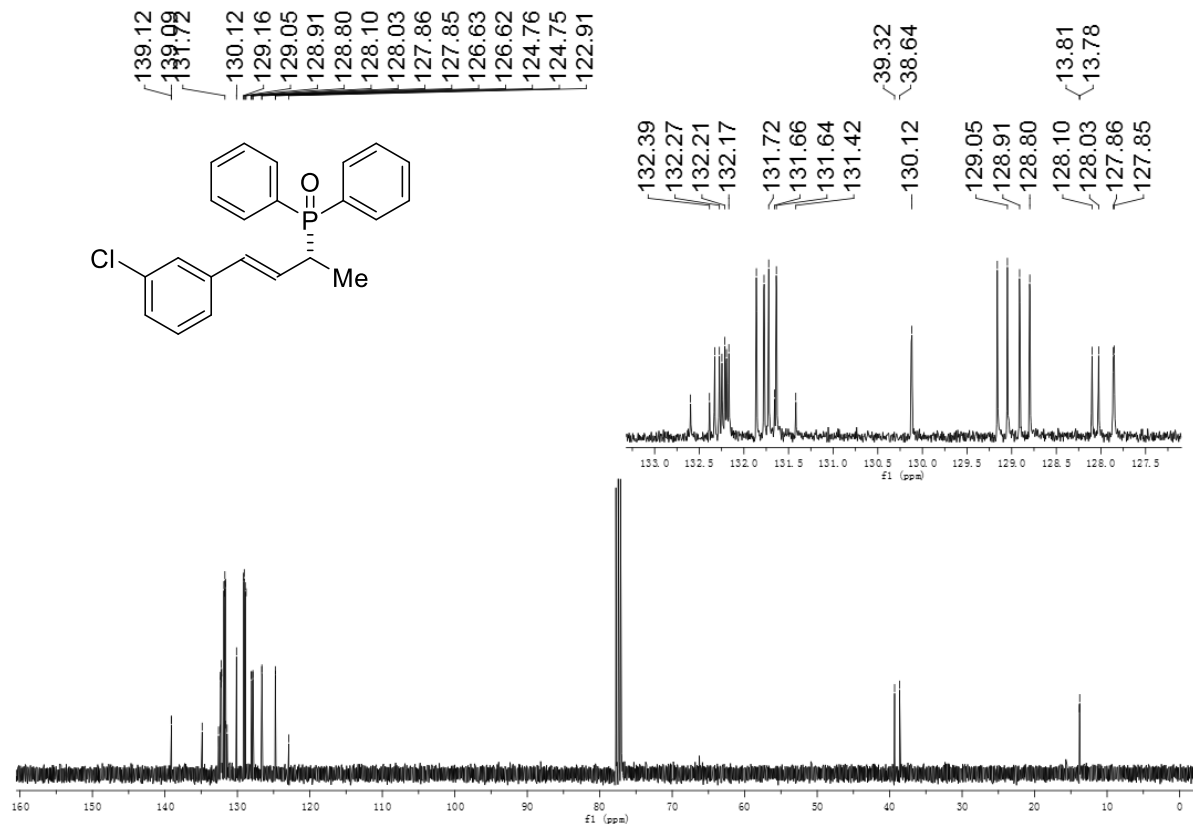
(*R,E*)-(4-(4-chlorophenyl)but-3-en-2-yl)diphenylphosphine oxide (3ha)



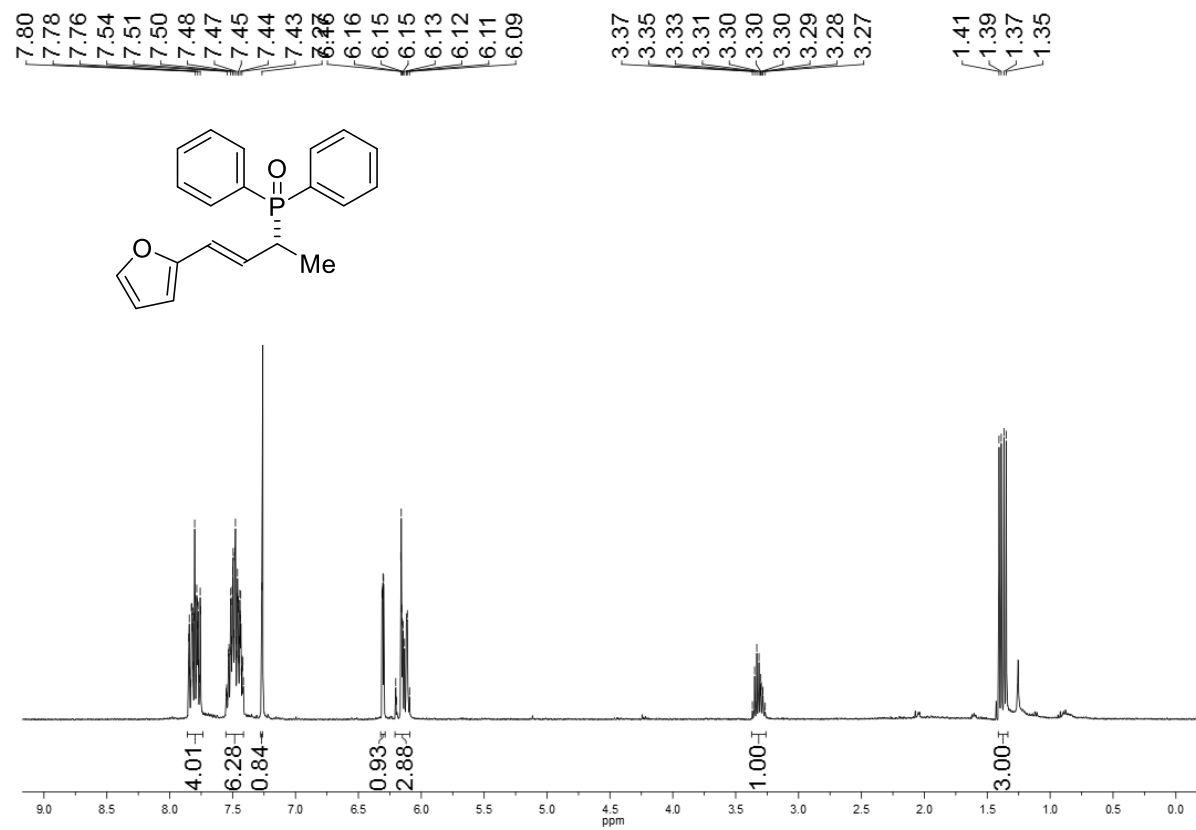
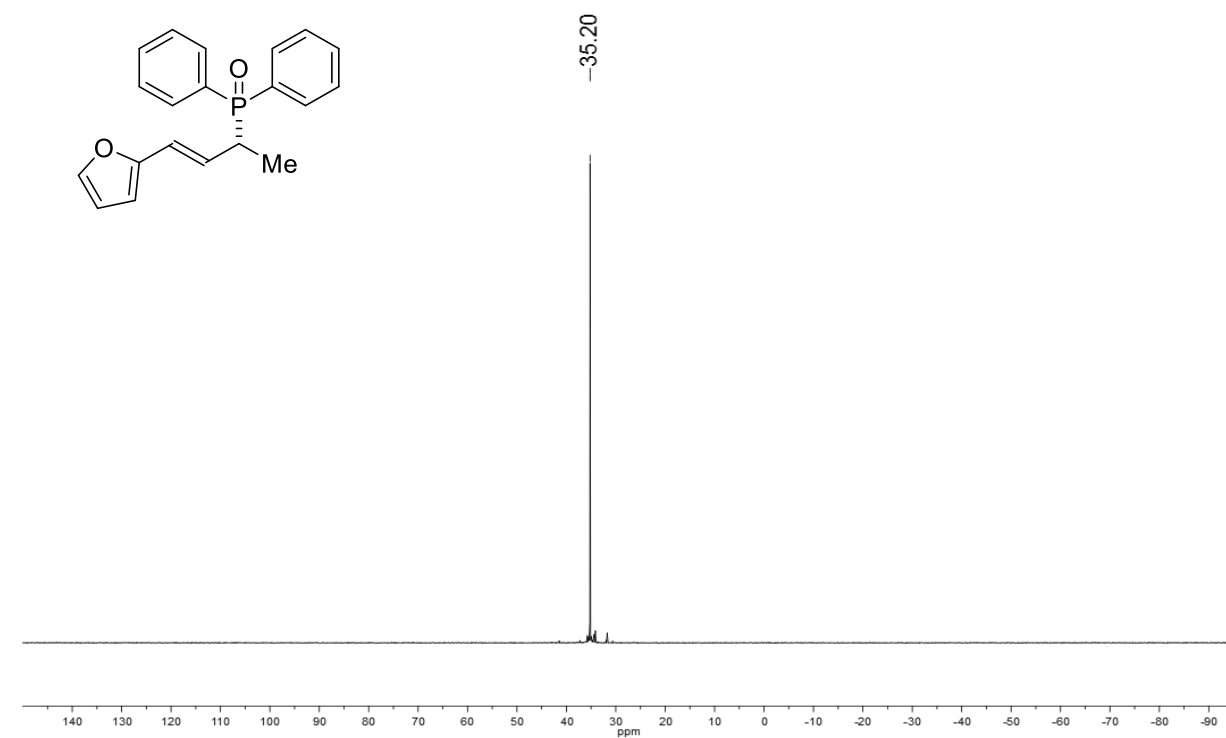


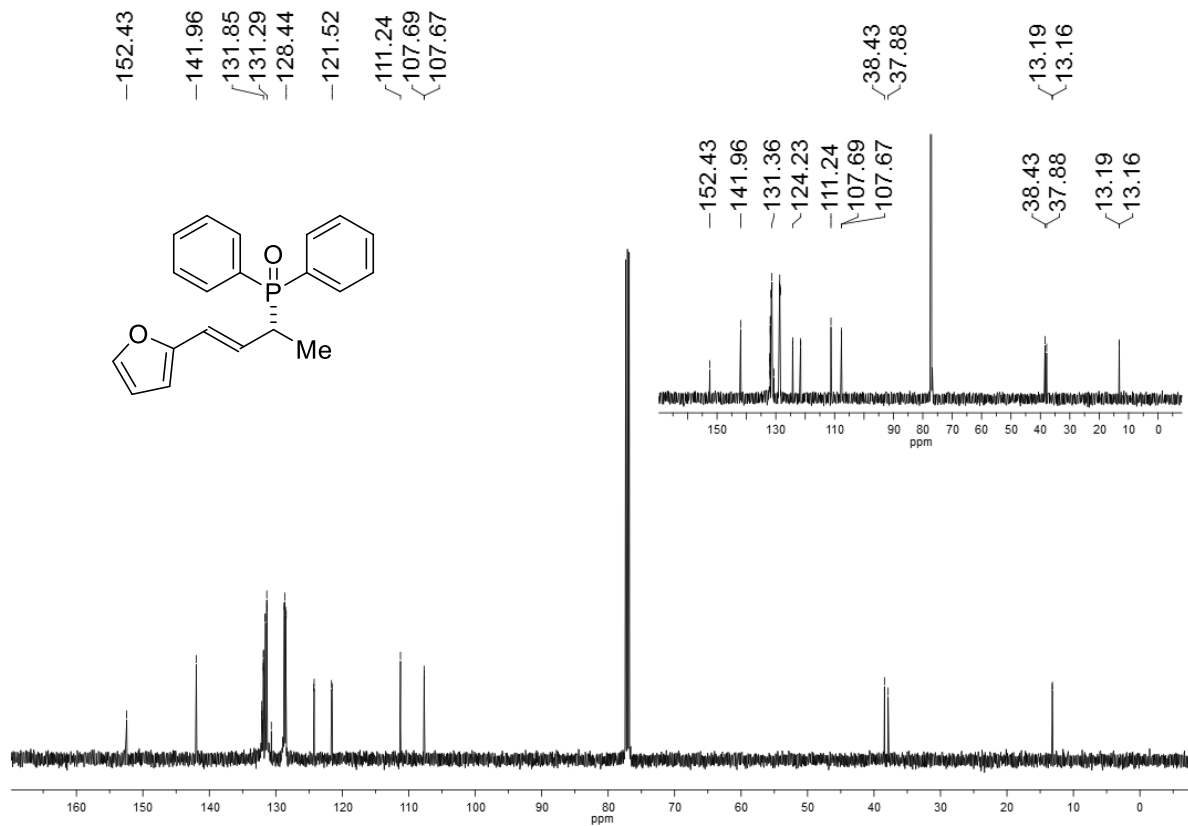
(*R,E*)-(4-(3-chlorophenyl)but-3-en-2-yl)diphenylphosphine oxide (3ia)



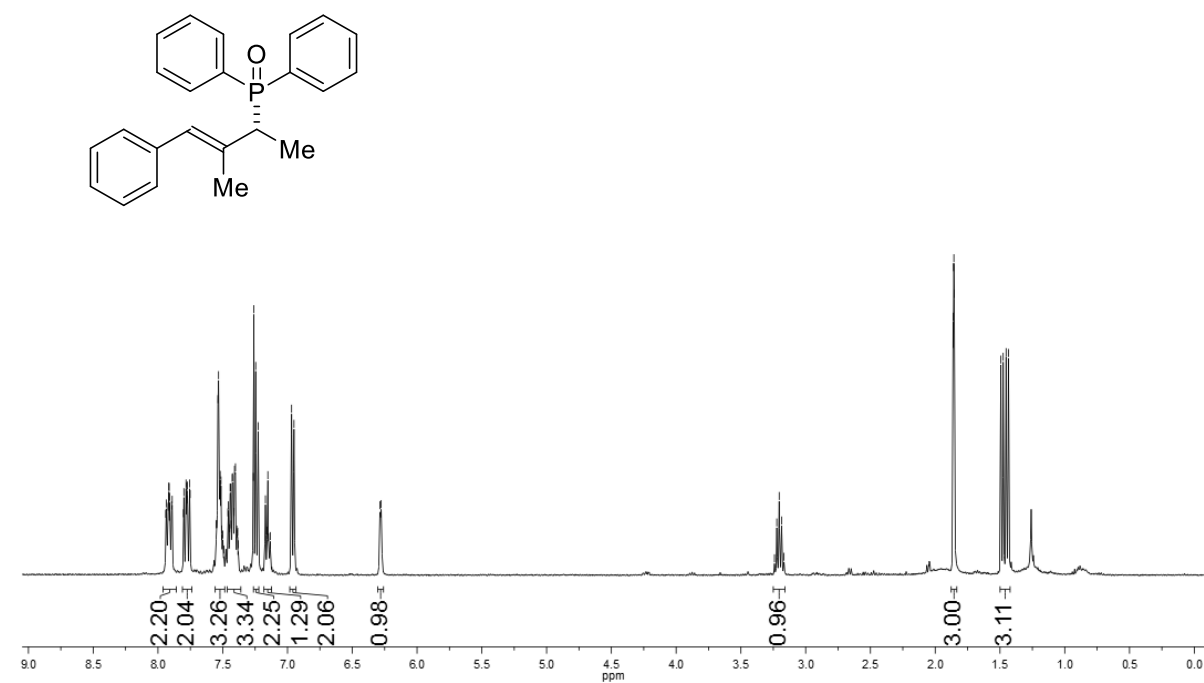
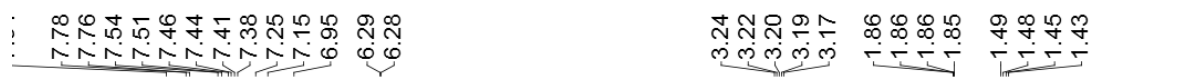
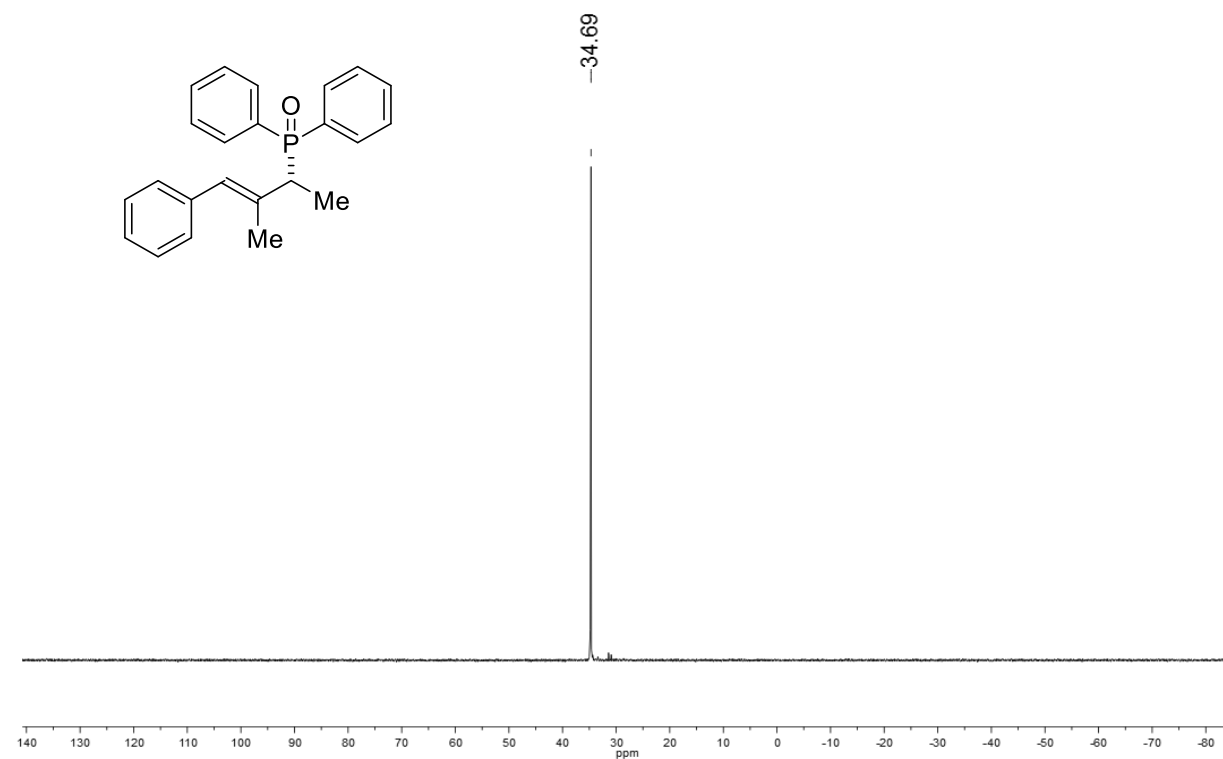


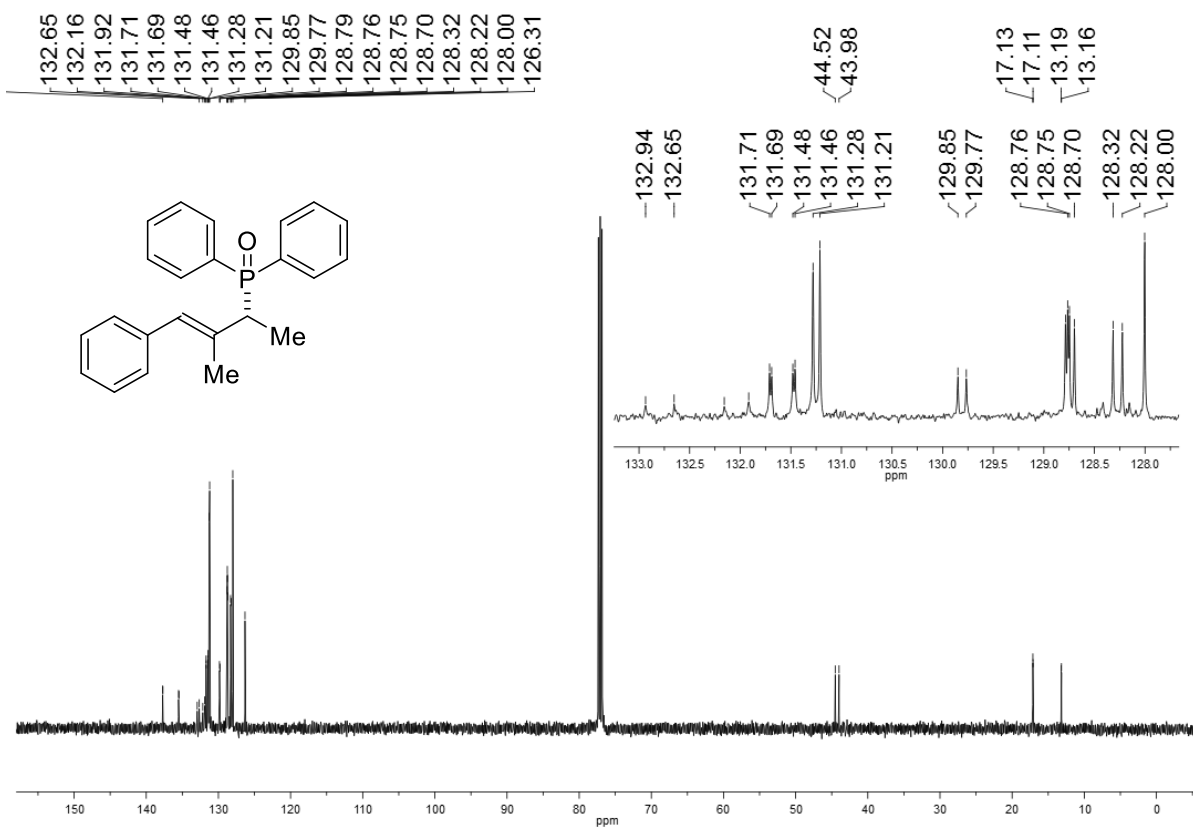
(*R,E*)-(4-(furan-2-yl)but-3-en-2-yl)diphenylphosphine oxide (3ja)



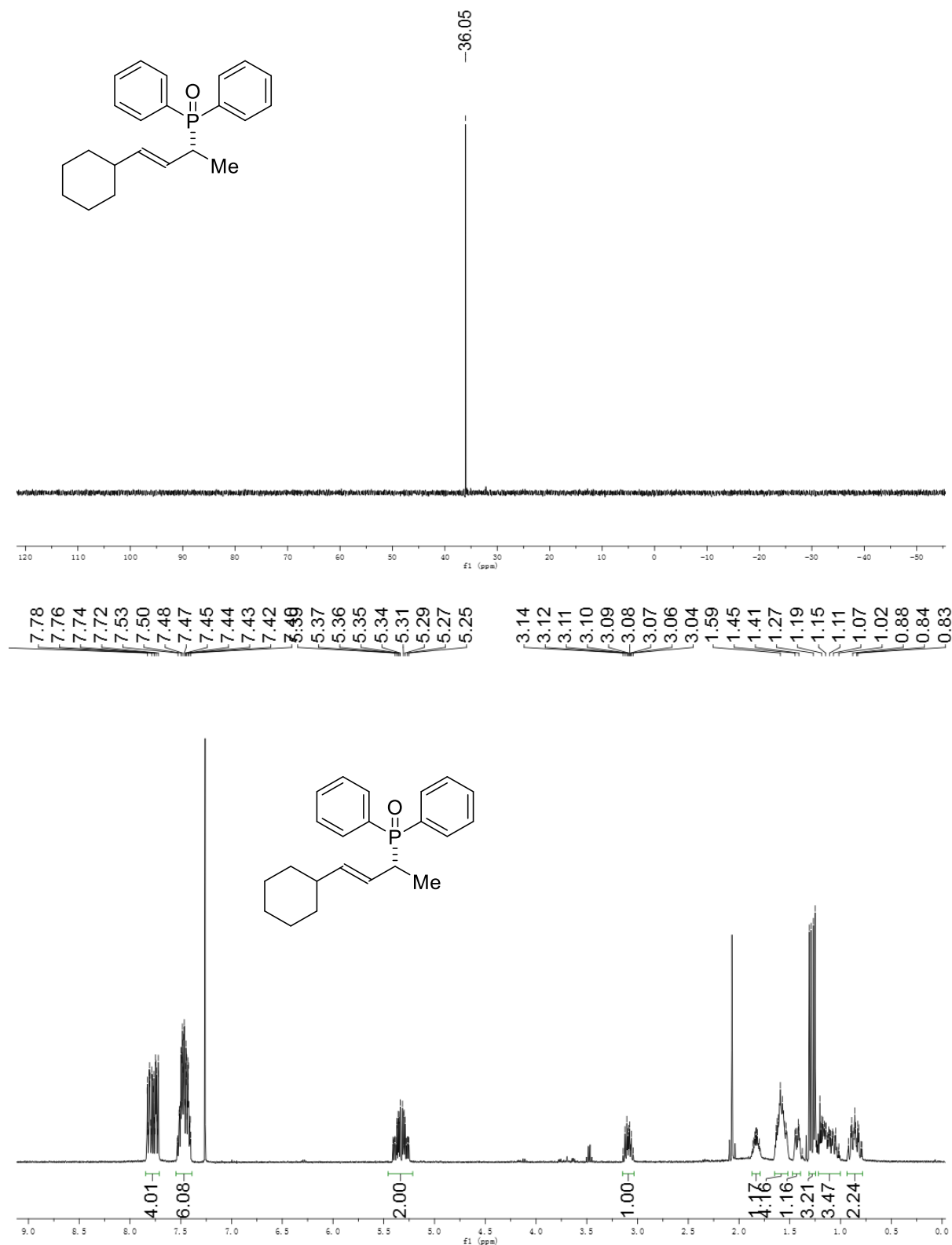


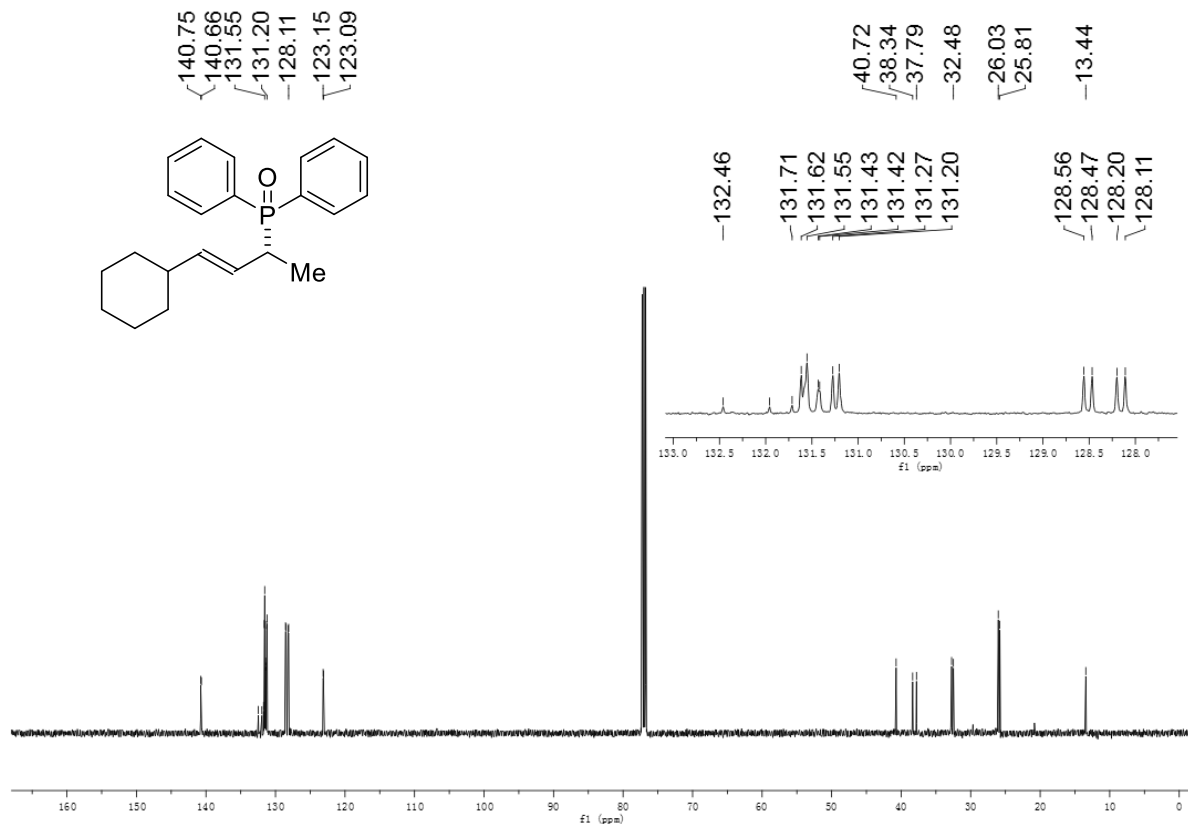
(*R,E*)-(3-methyl-4-phenylbut-3-en-2-yl)diphenylphosphine oxide (3ka)



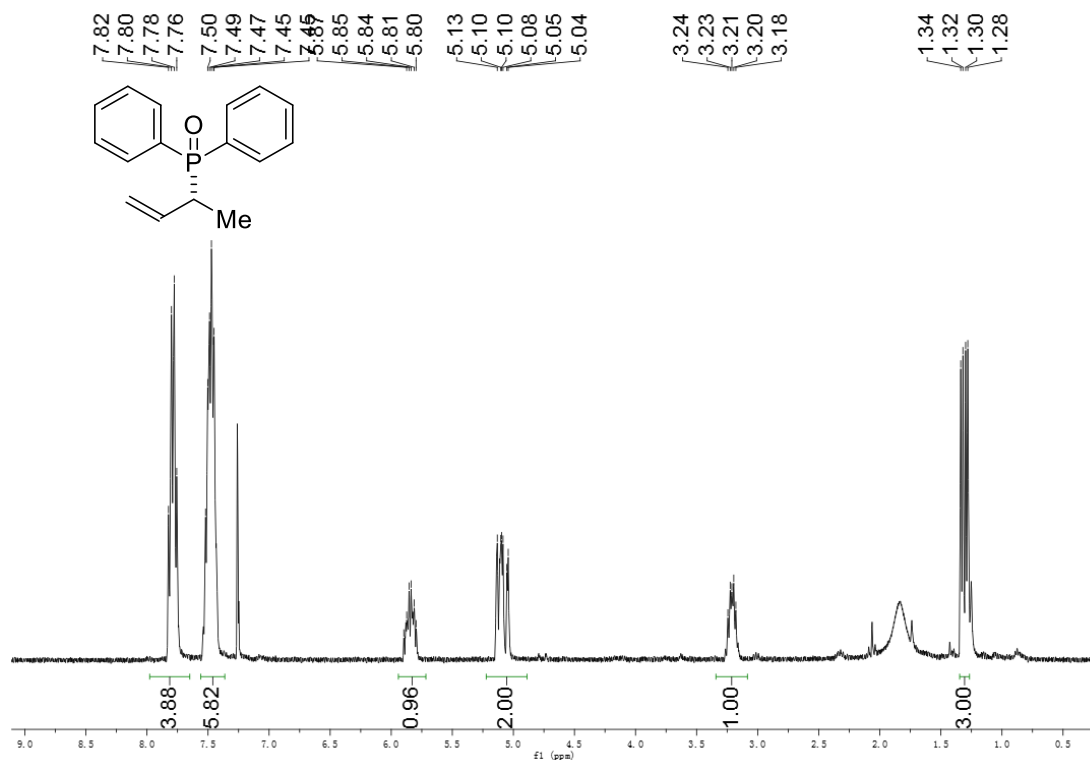
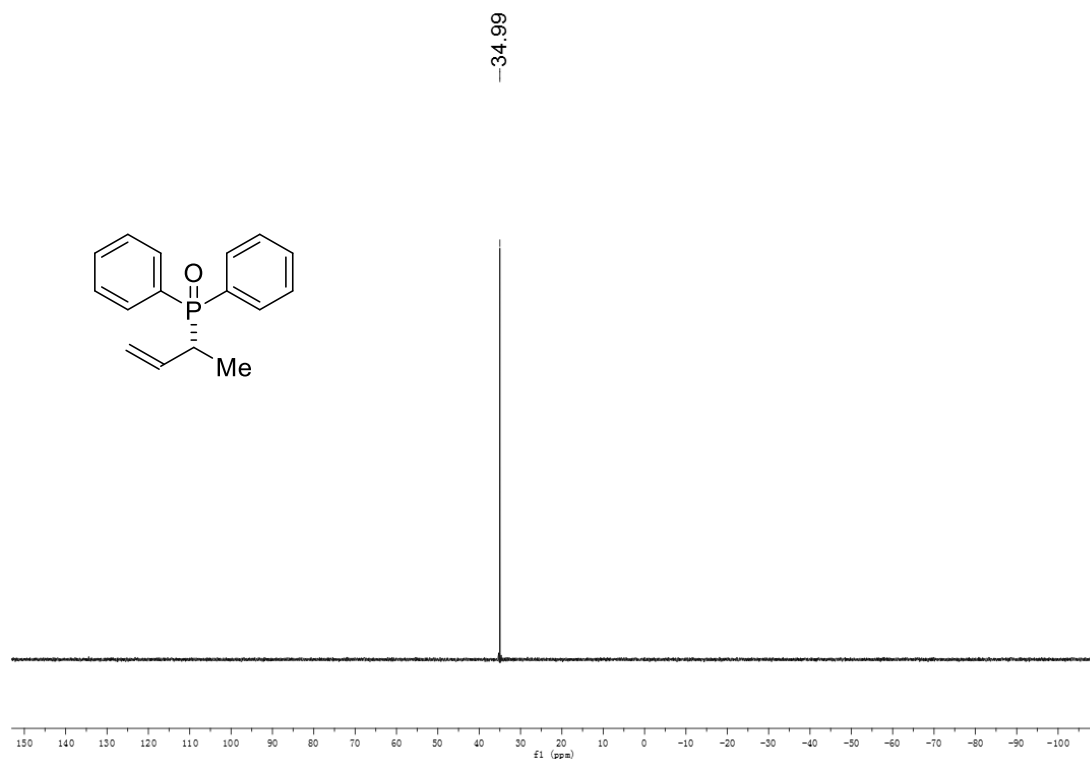


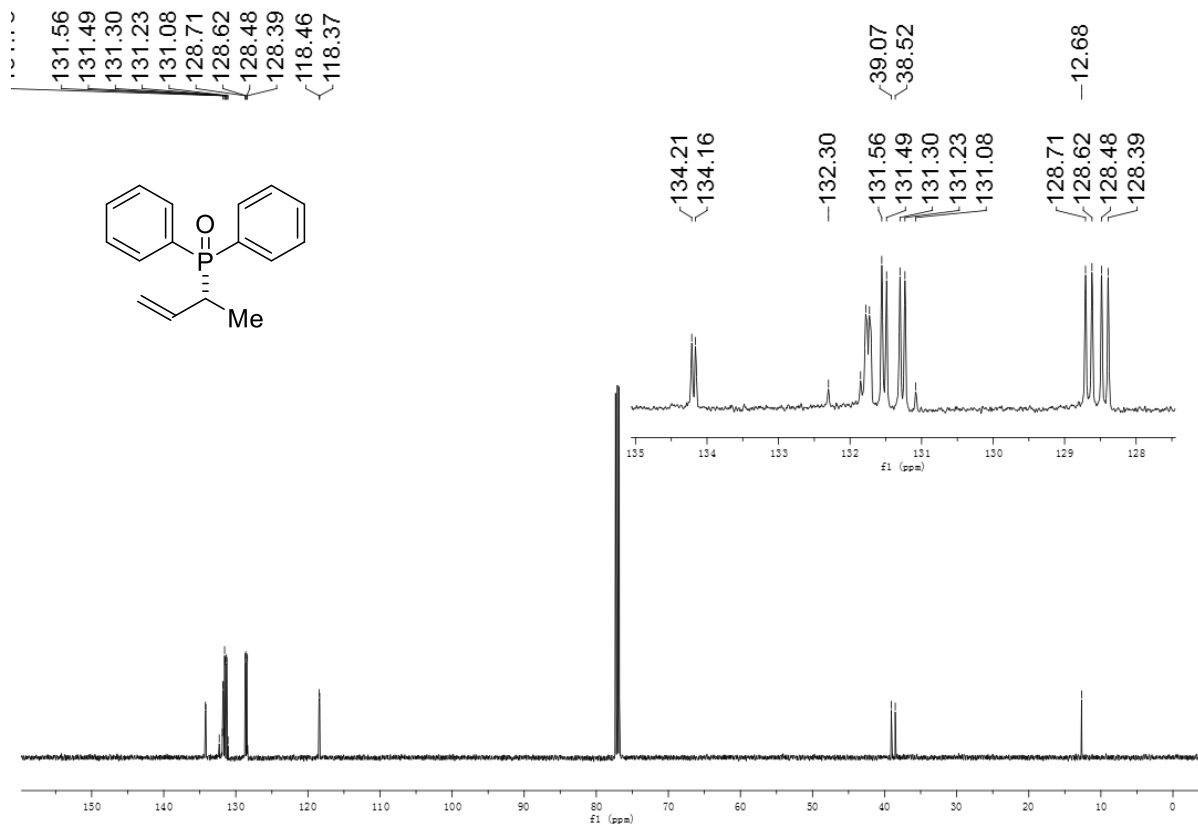
(*R,E*)-(4-cyclohexylbut-3-en-2-yl)diphenylphosphine oxide (31a)



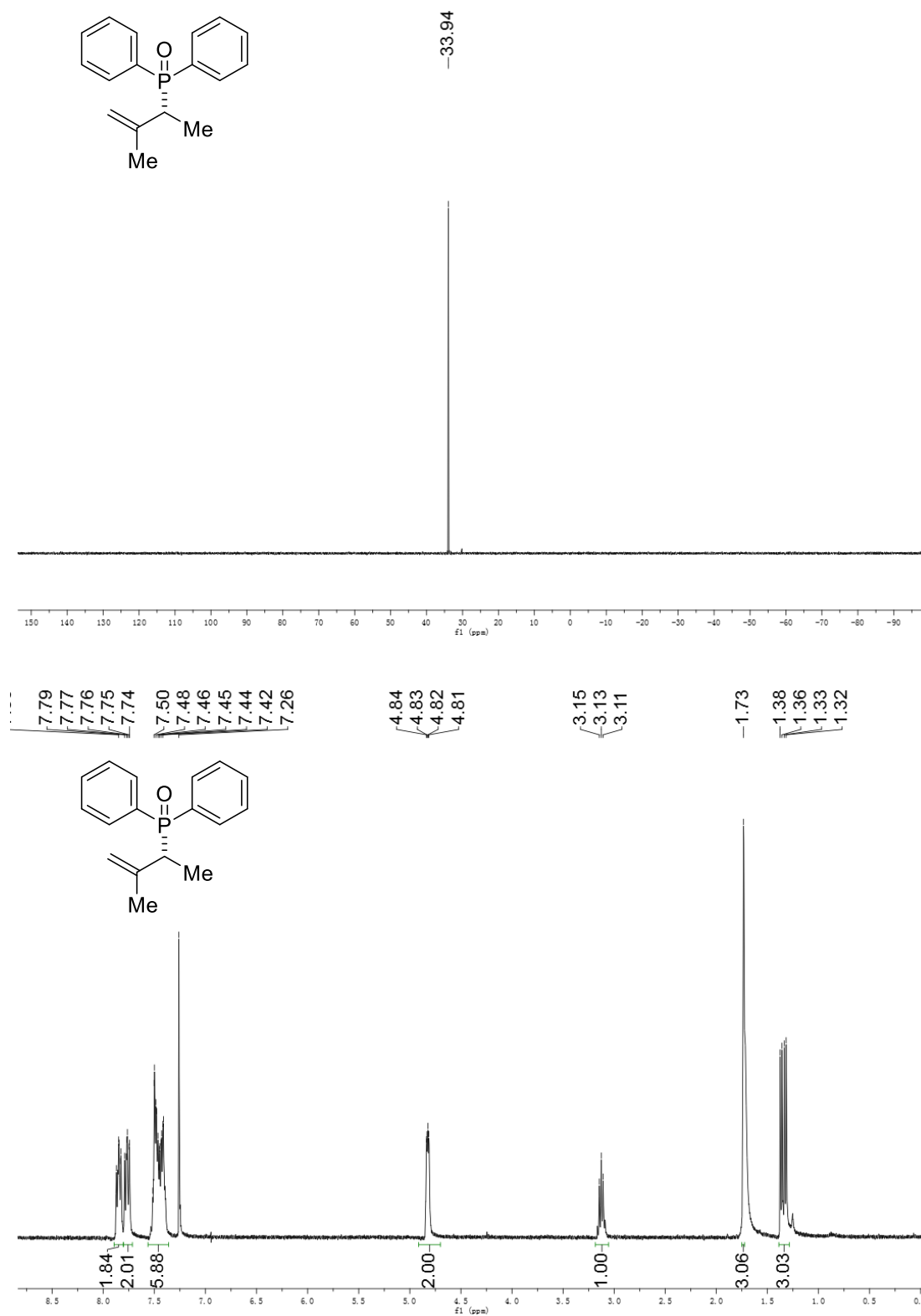


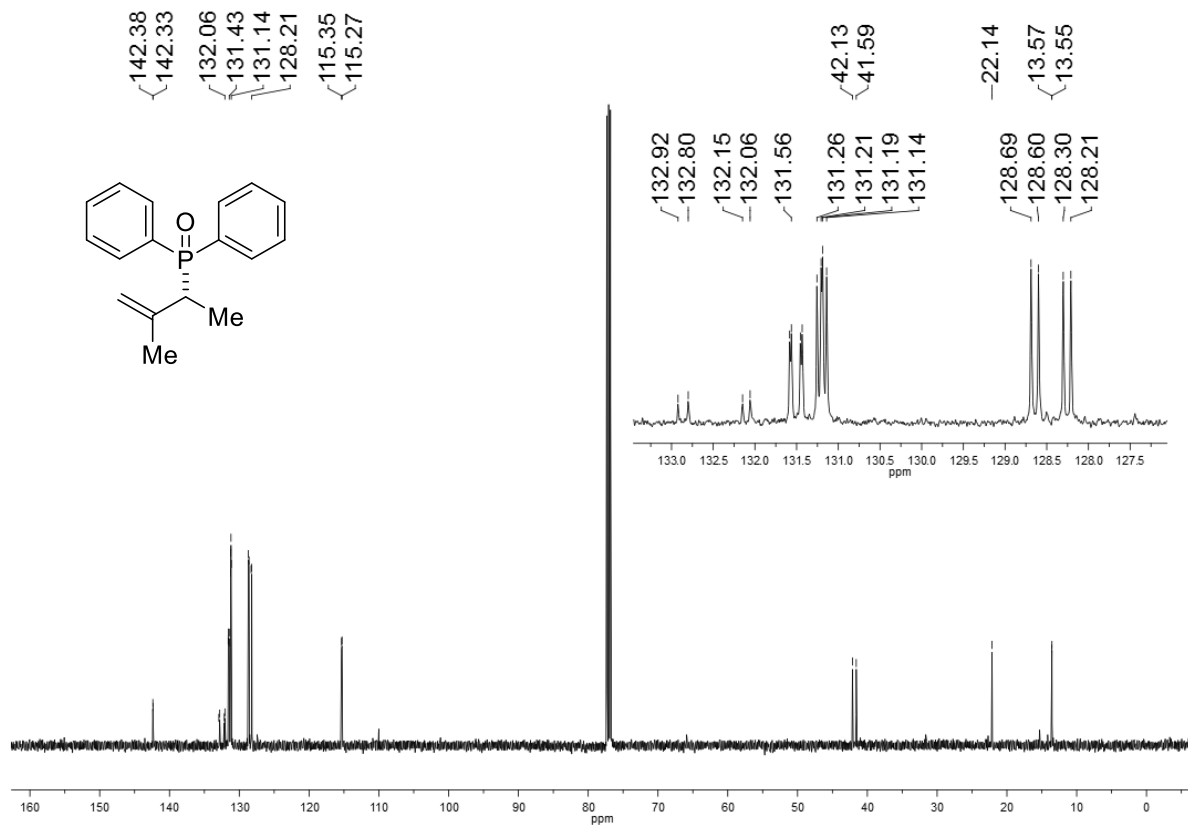
(R)-but-3-en-2-ylidiphenylphosphine oxide (3ma)



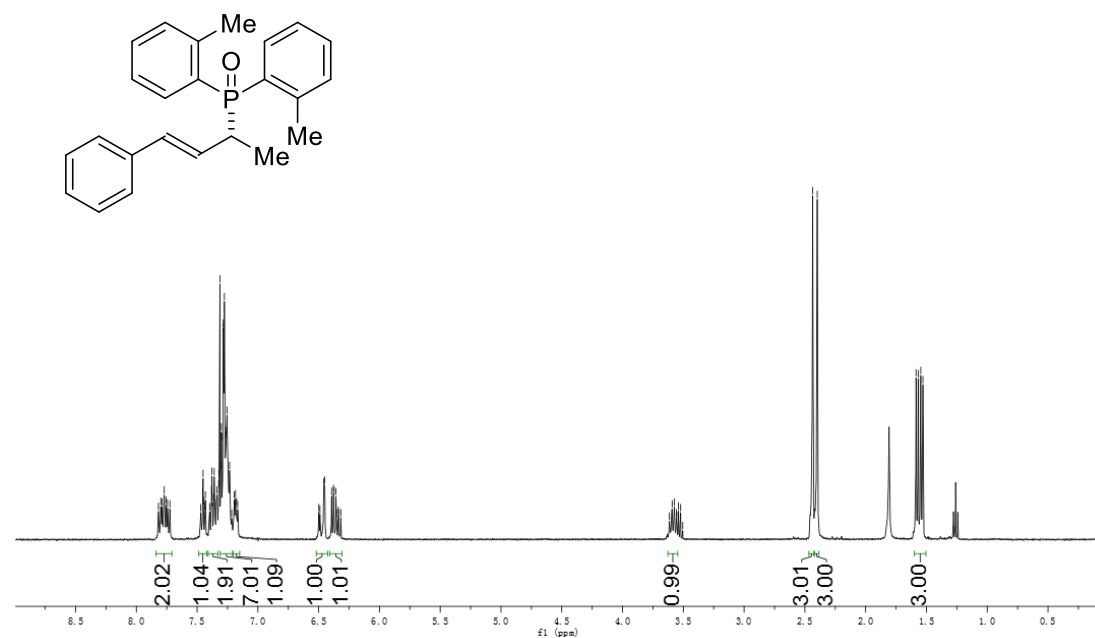
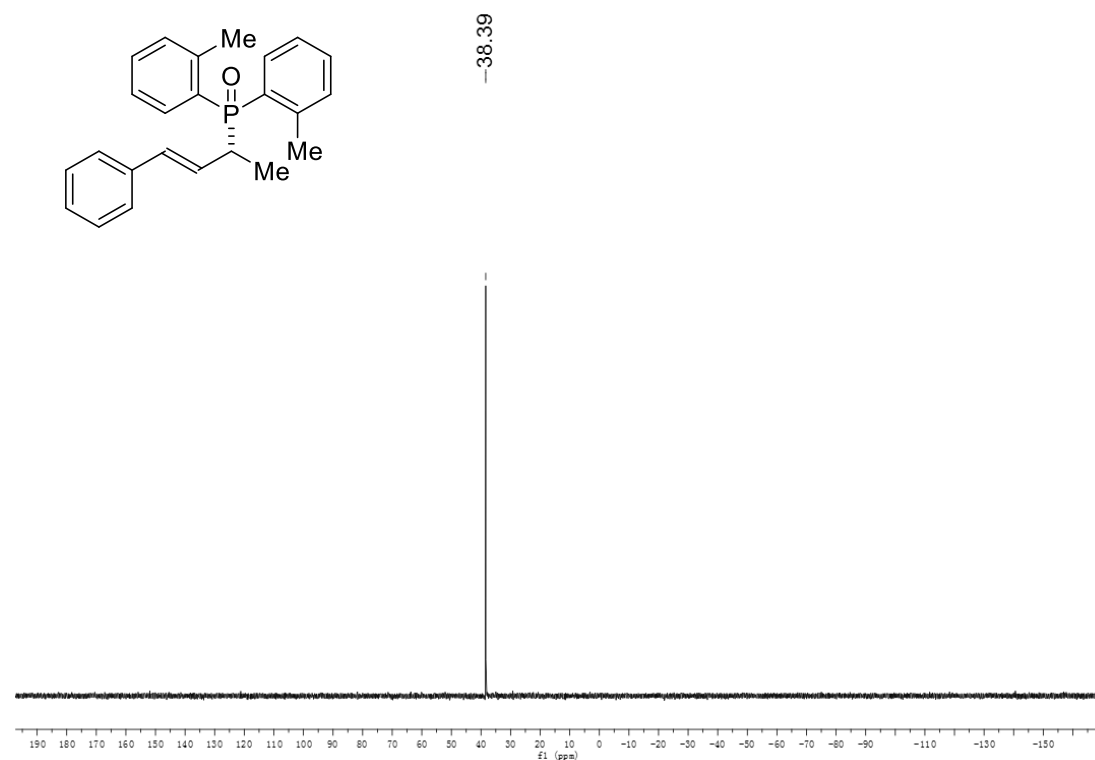


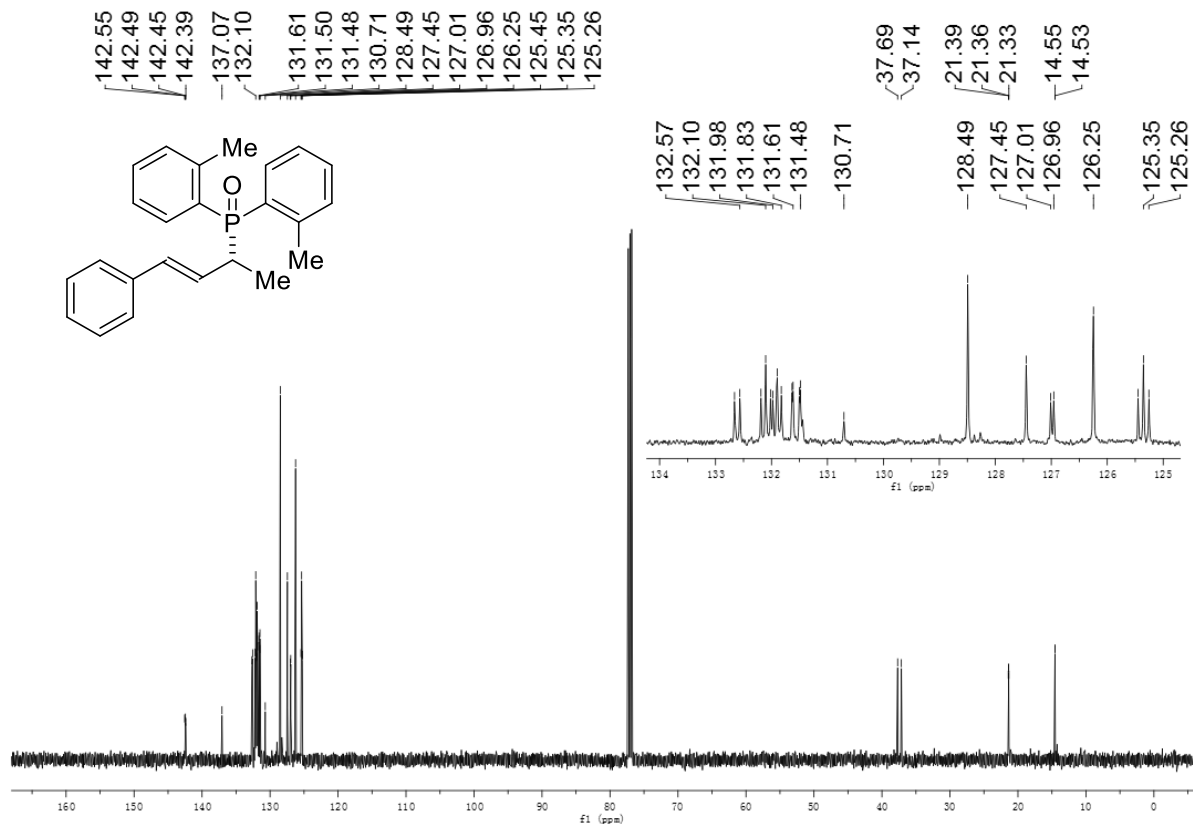
(R)-(3-methylbut-3-en-2-yl)diphenylphosphine oxide (3na)



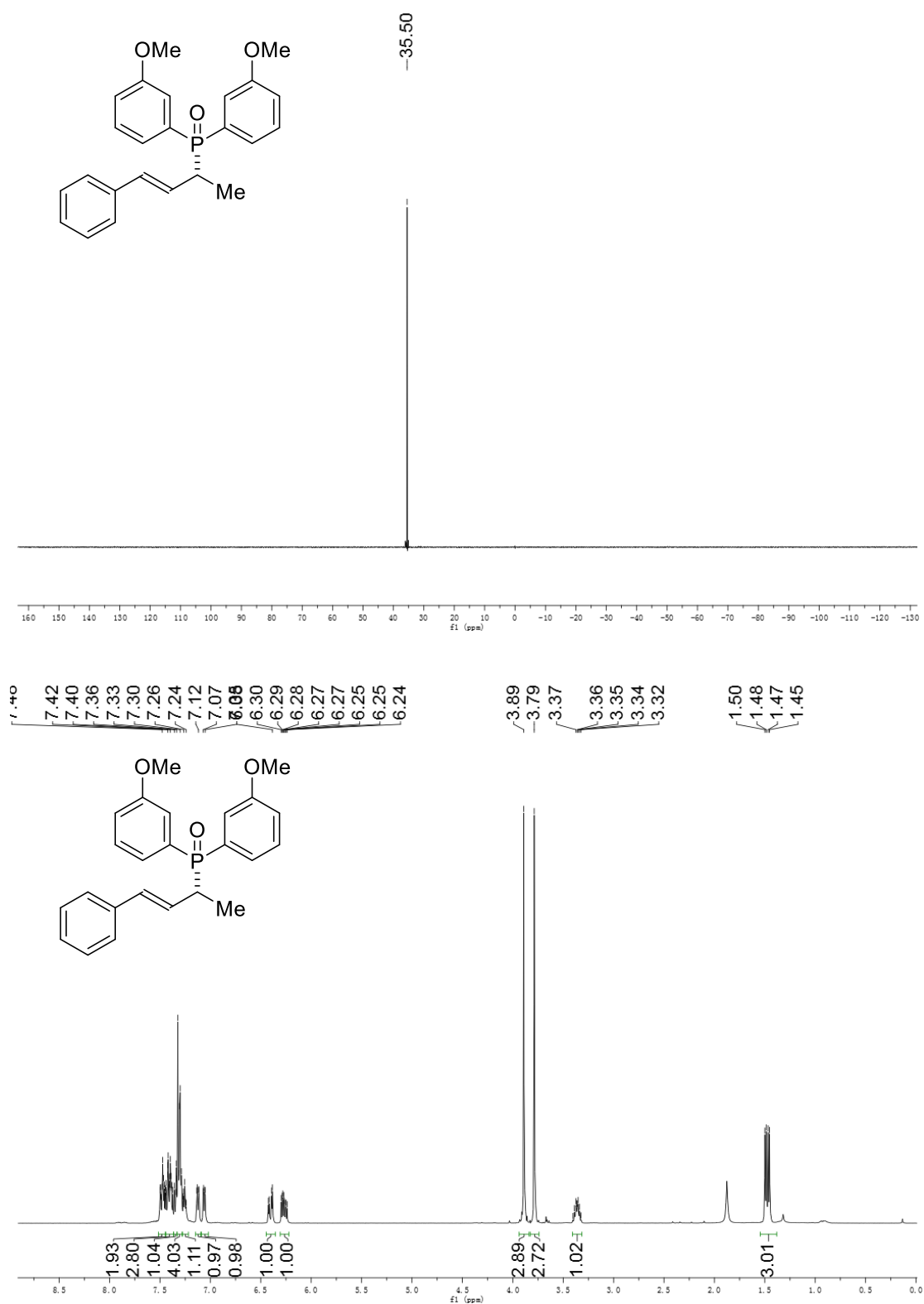


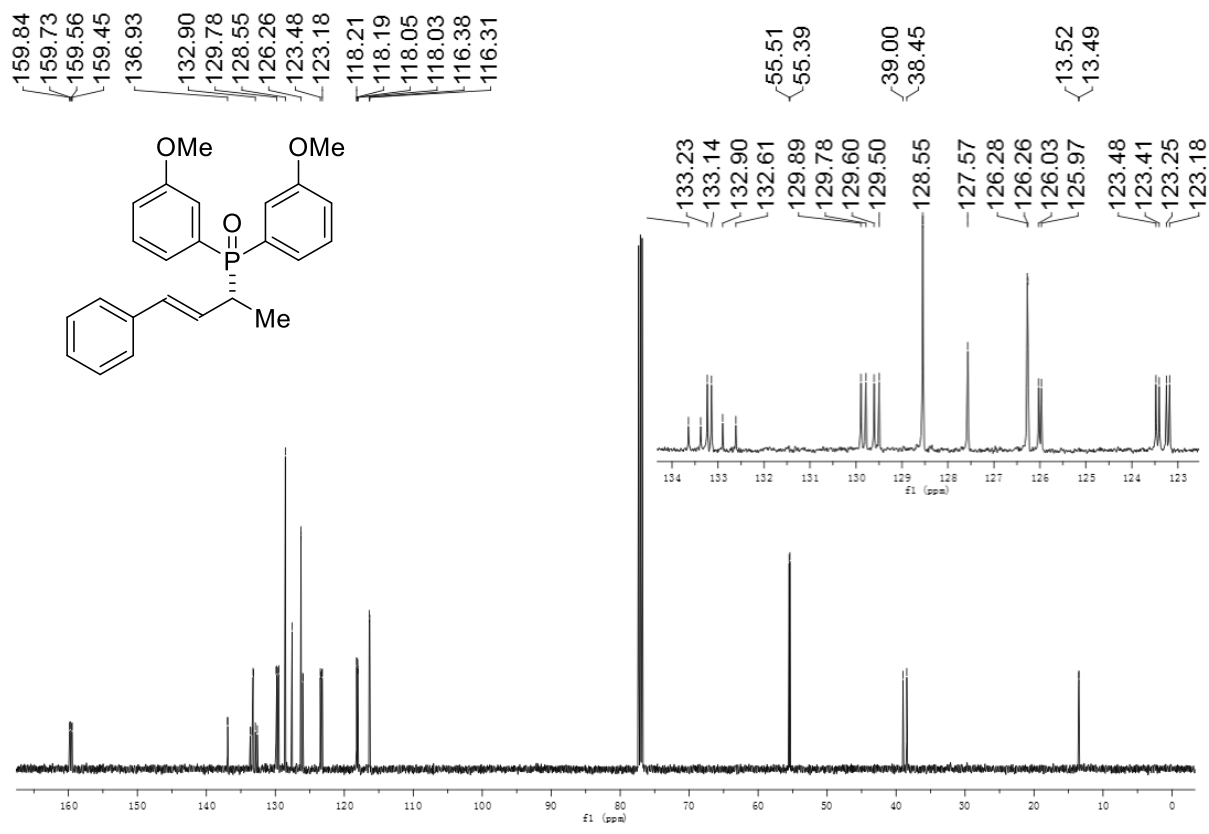
(*R,E*)-(4-phenylbut-3-en-2-yl)di-*o*-tolylphosphine oxide (3ab)



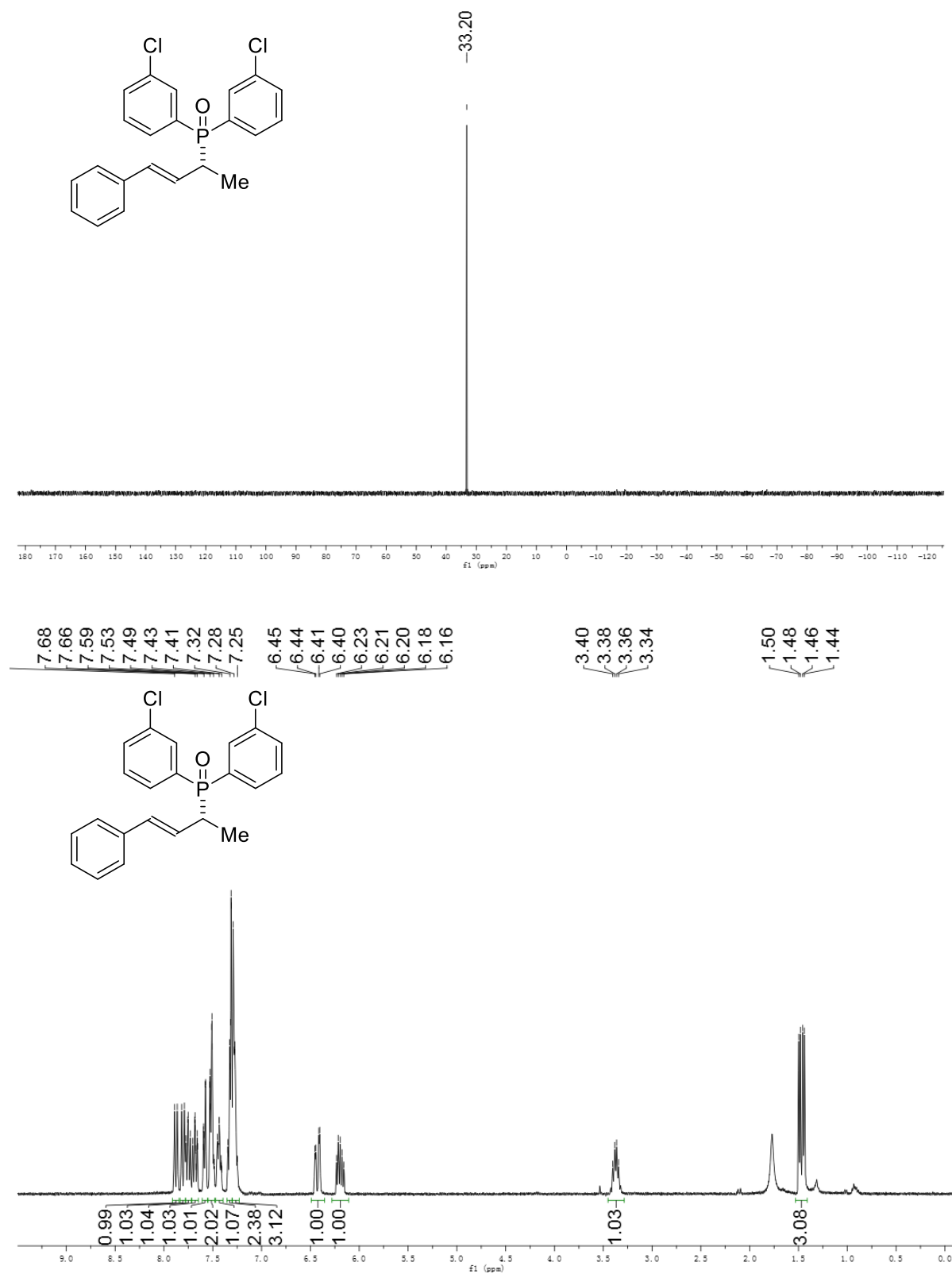


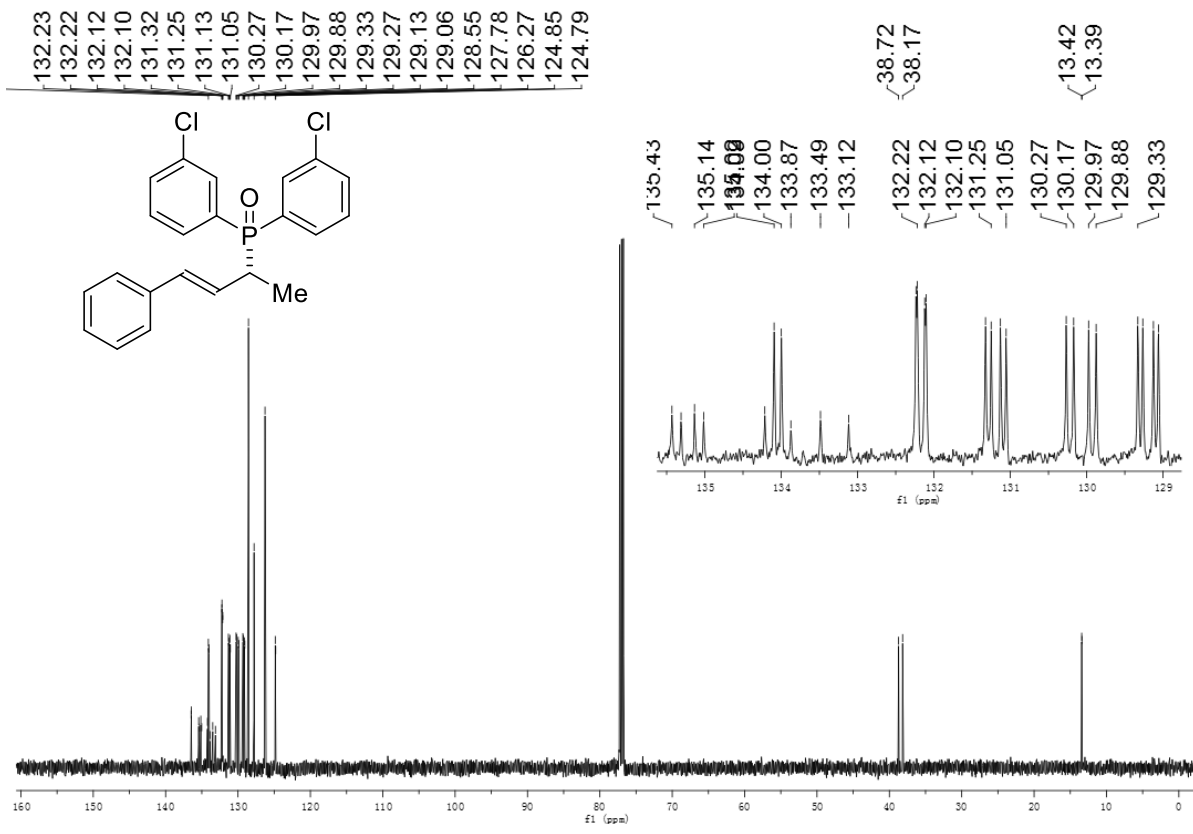
(*R,E*)-bis(3-methoxyphenyl)(4-phenylbut-3-en-2-yl)phosphine oxide (3ac)



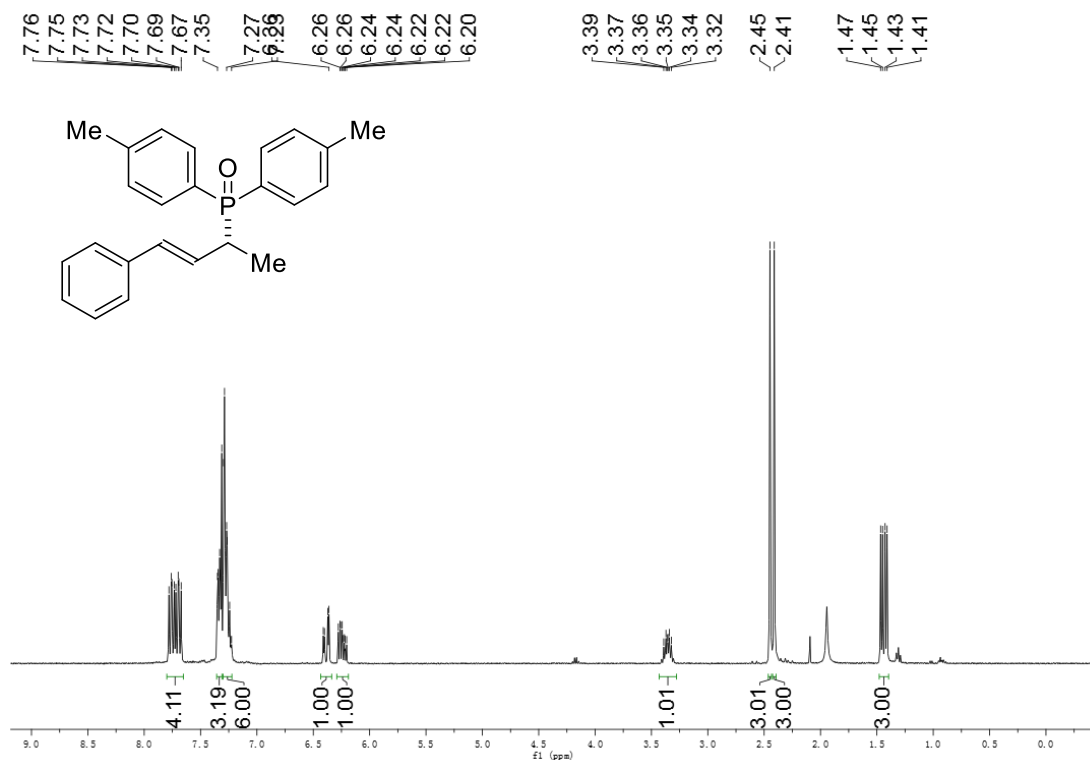


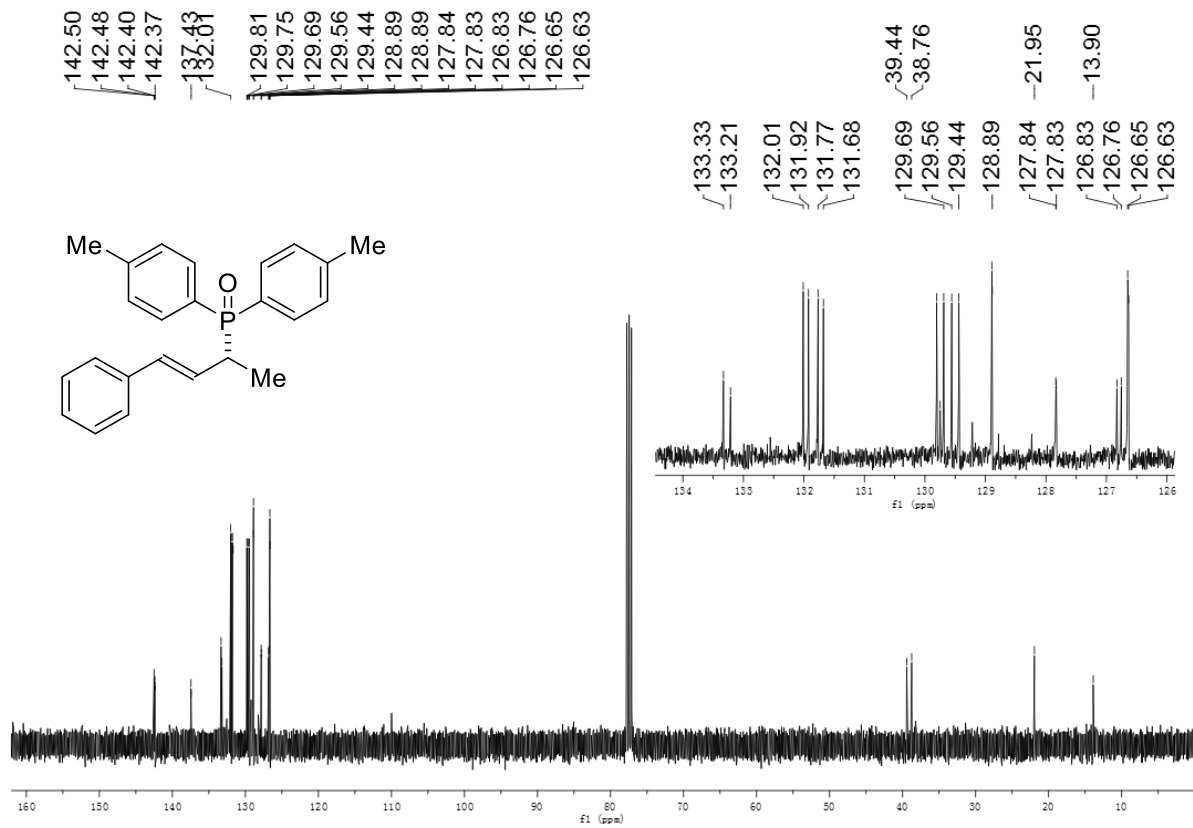
(*R,E*)-bis(3-chlorophenyl)(4-phenylbut-3-en-2-yl)phosphine oxide (3ad)



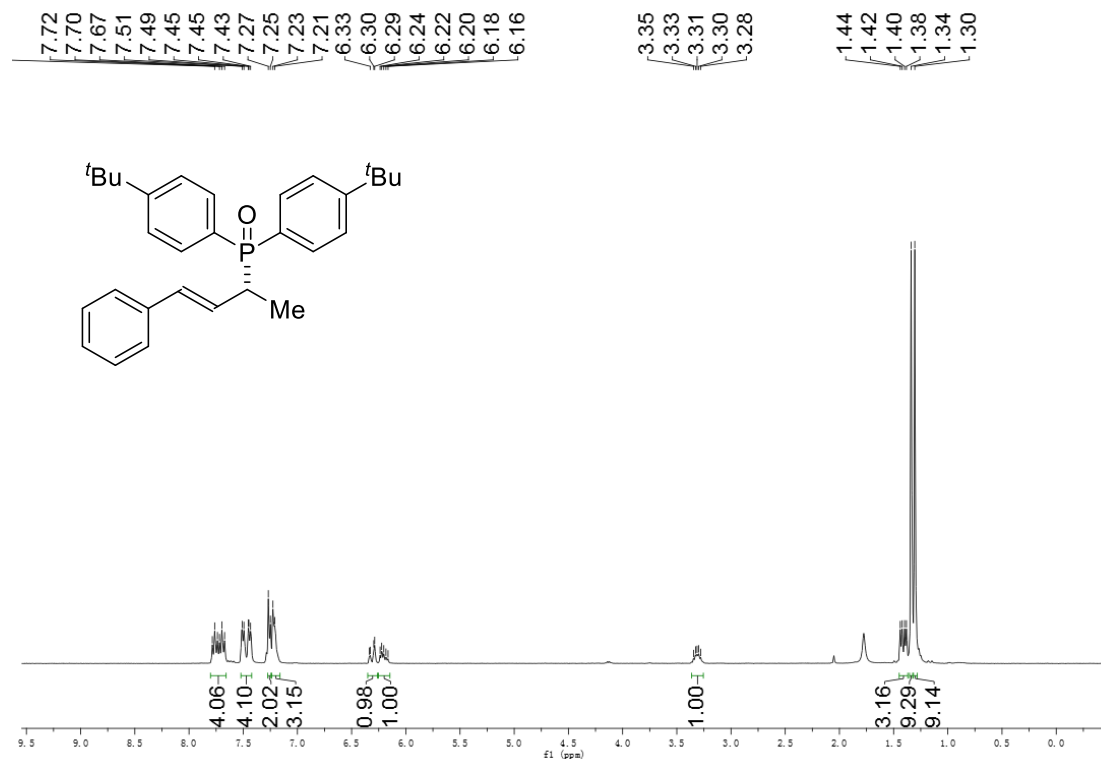
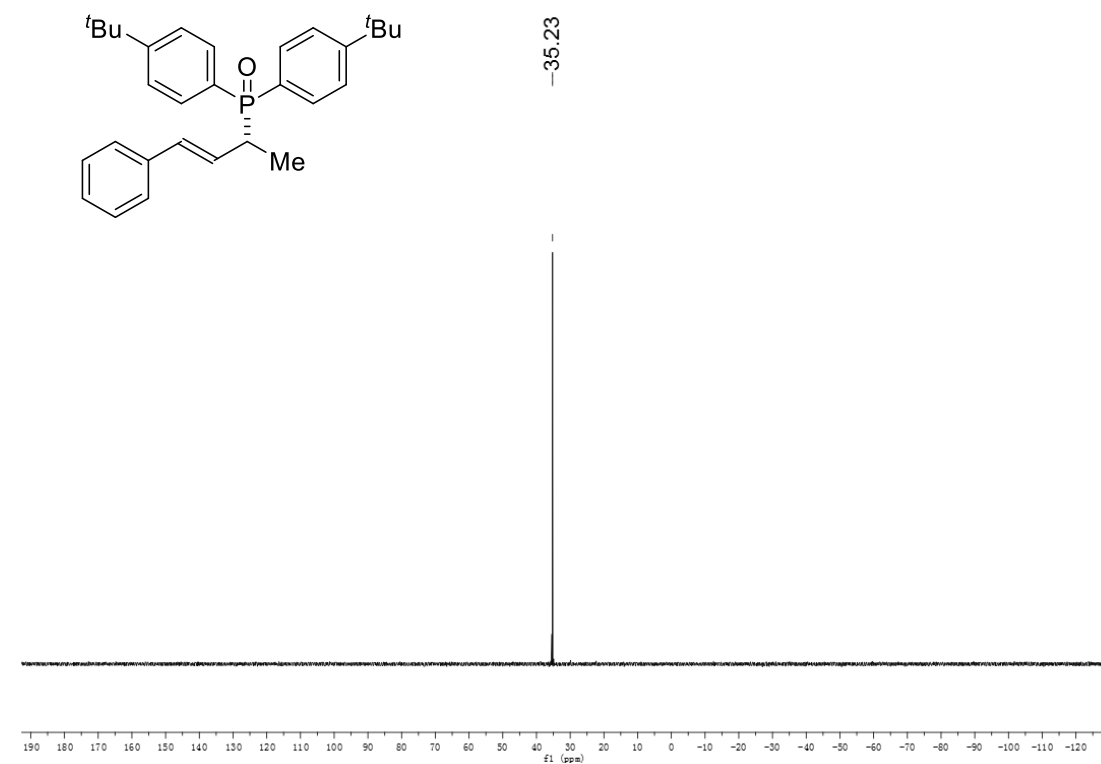


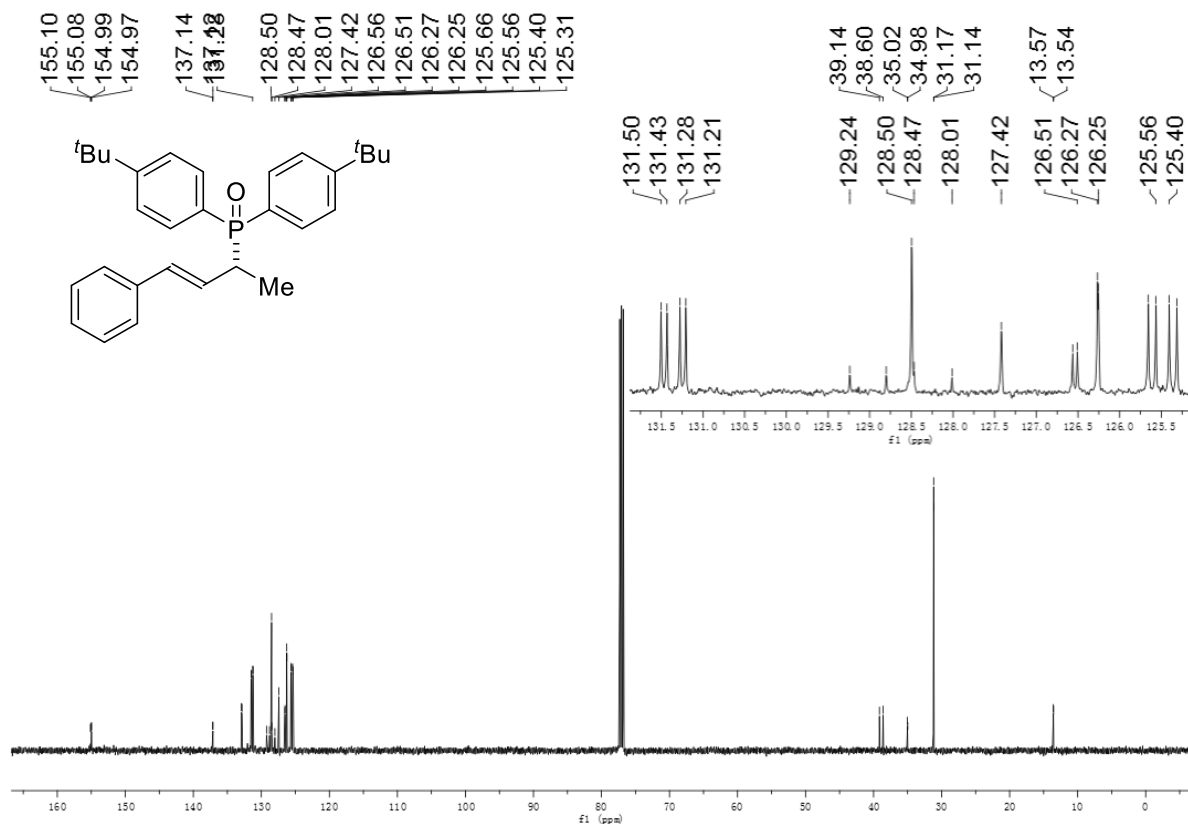
(*R,E*)-(4-phenylbut-3-en-2-yl)di-*p*-tolylphosphine oxide (3ae)



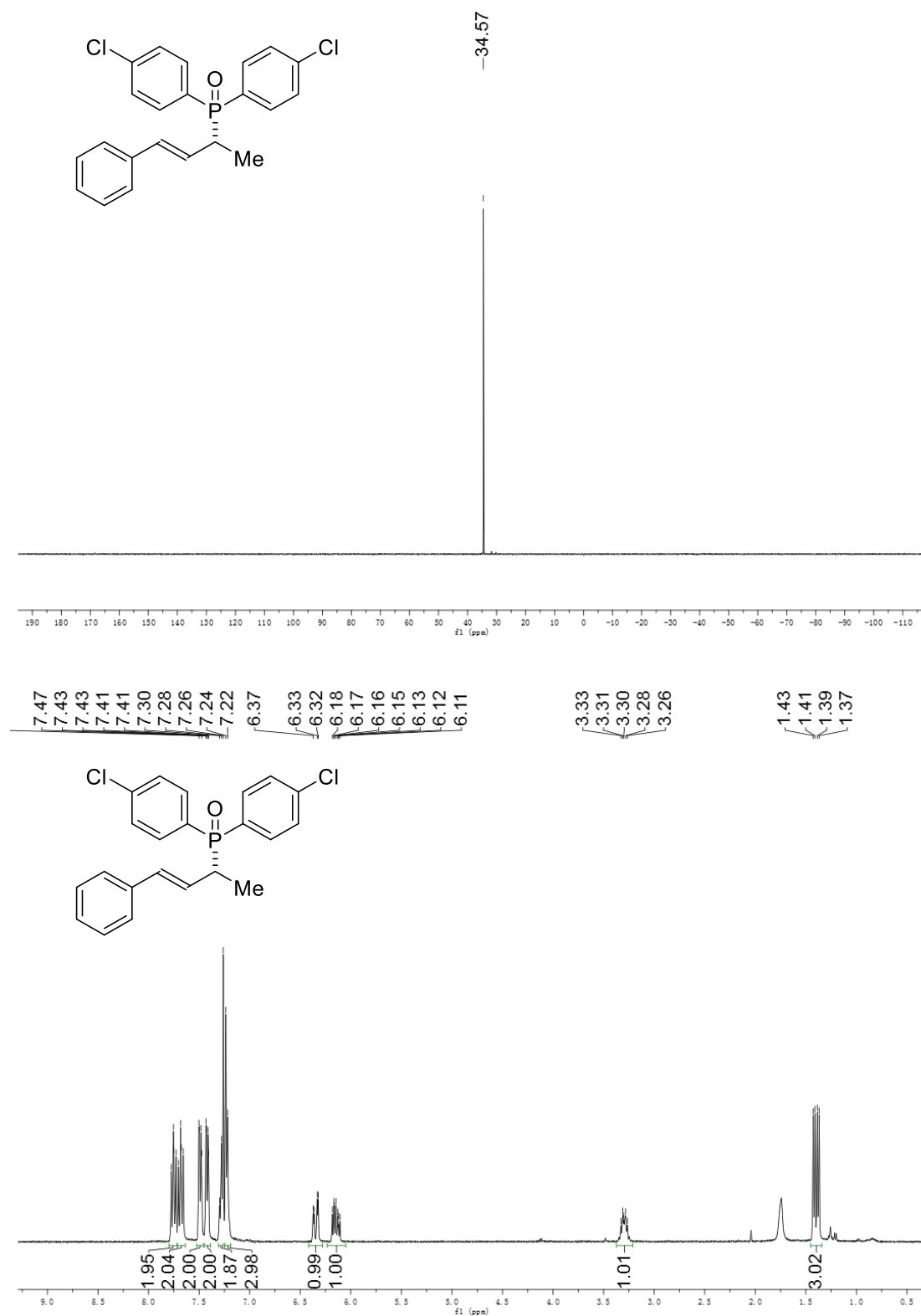


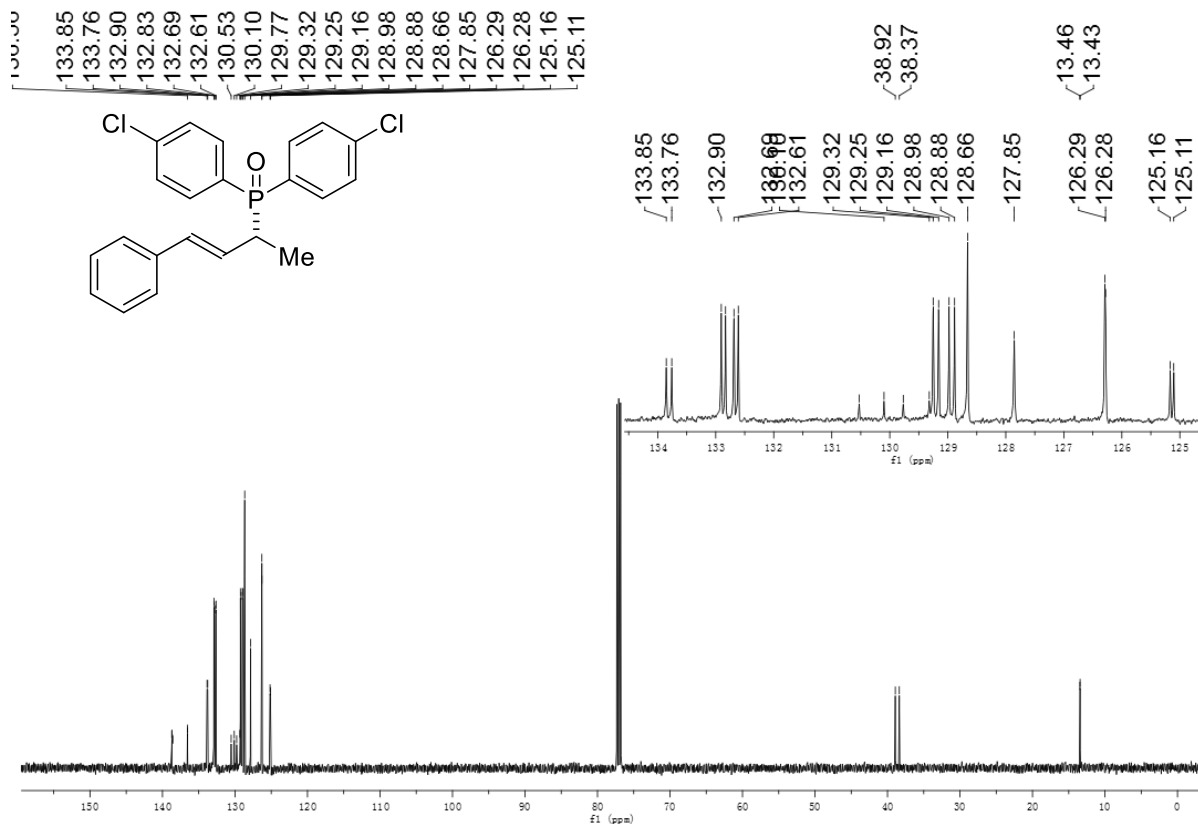
(*R,E*)-bis(4-(*tert*-butyl)phenyl)(4-phenylbut-3-en-2-yl)phosphine oxide (3af)



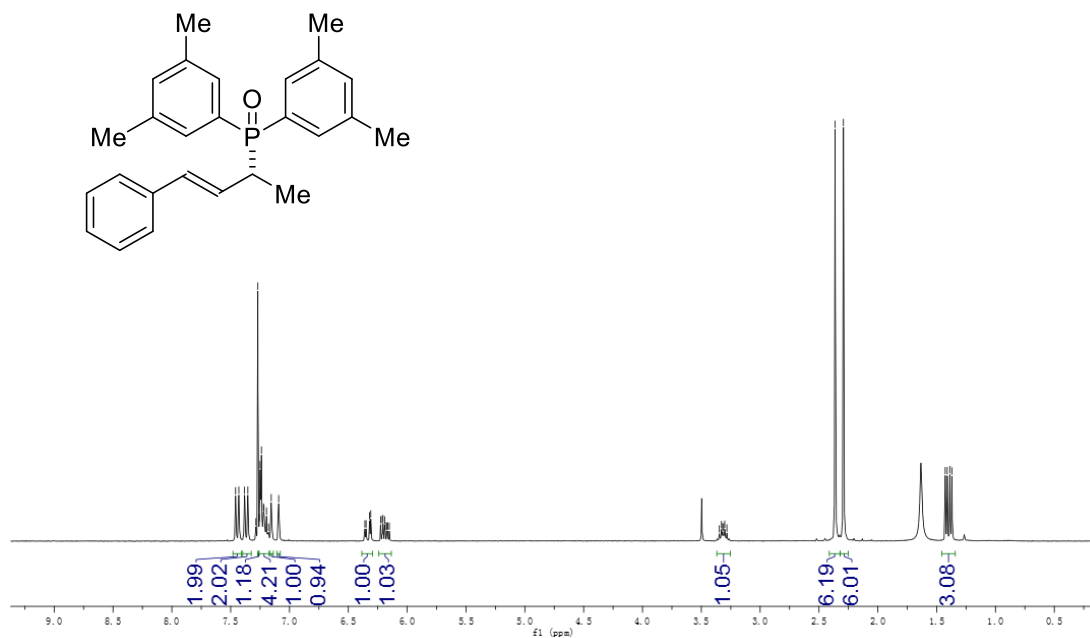
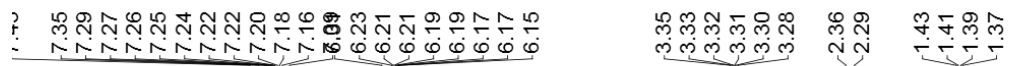
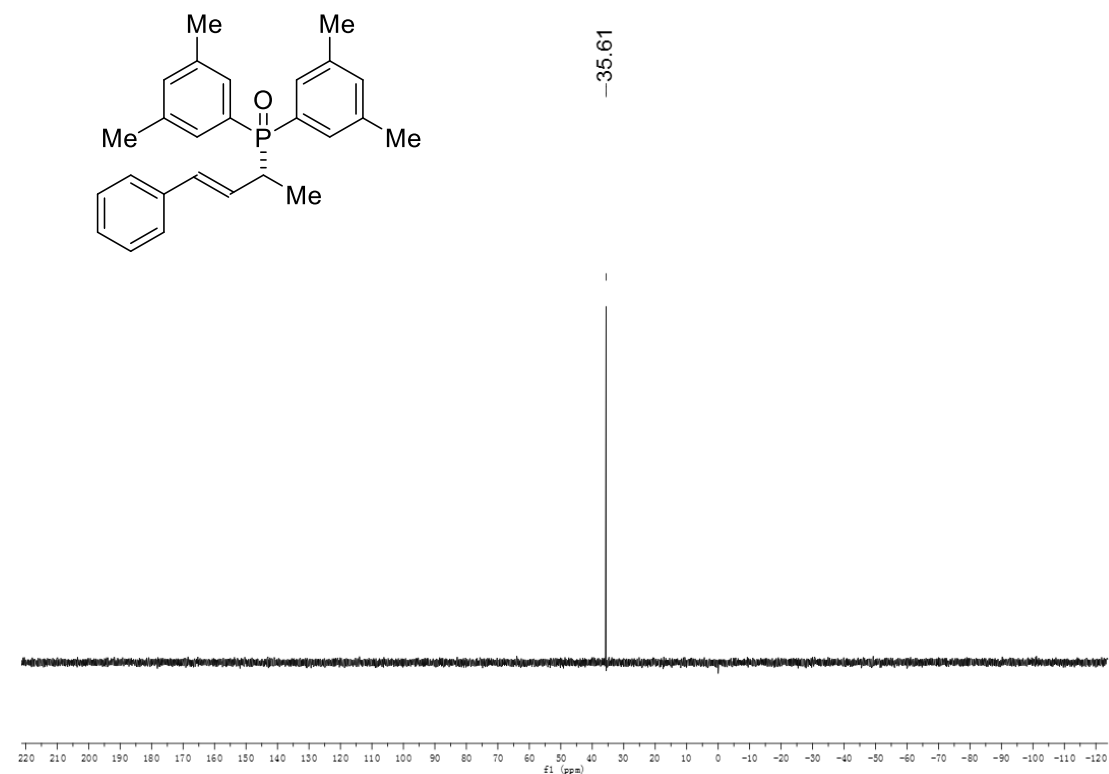


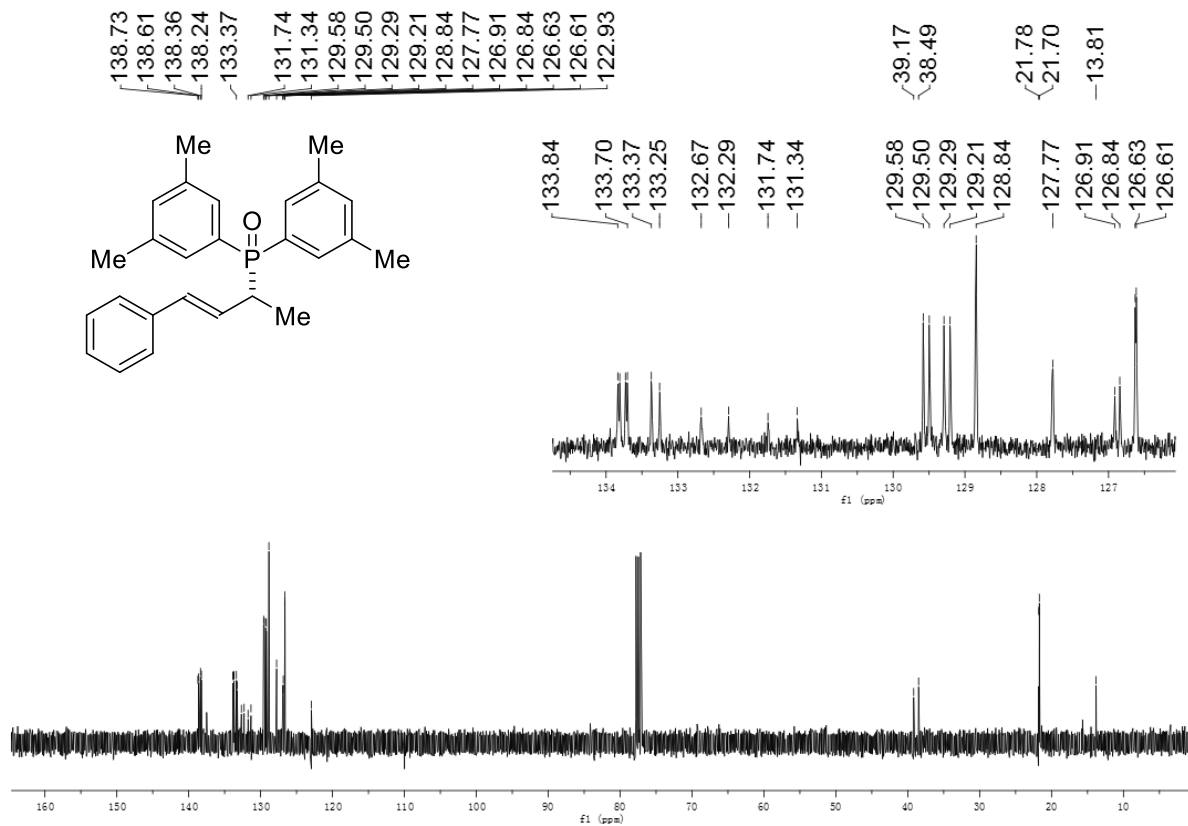
(*R,E*)-bis(4-chlorophenyl)(4-phenylbut-3-en-2-yl)phosphine oxide (3ag)



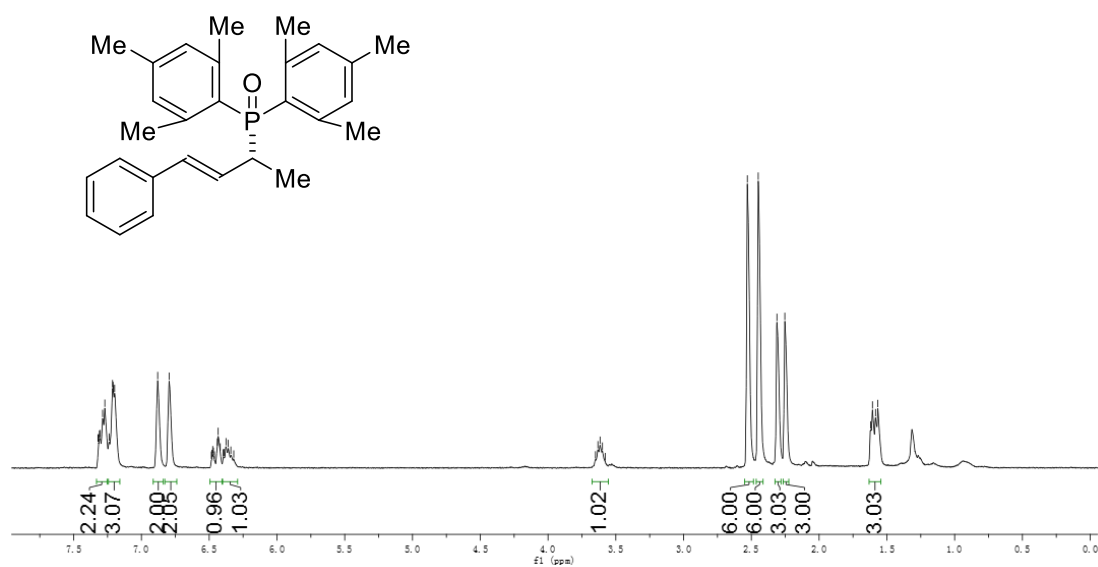
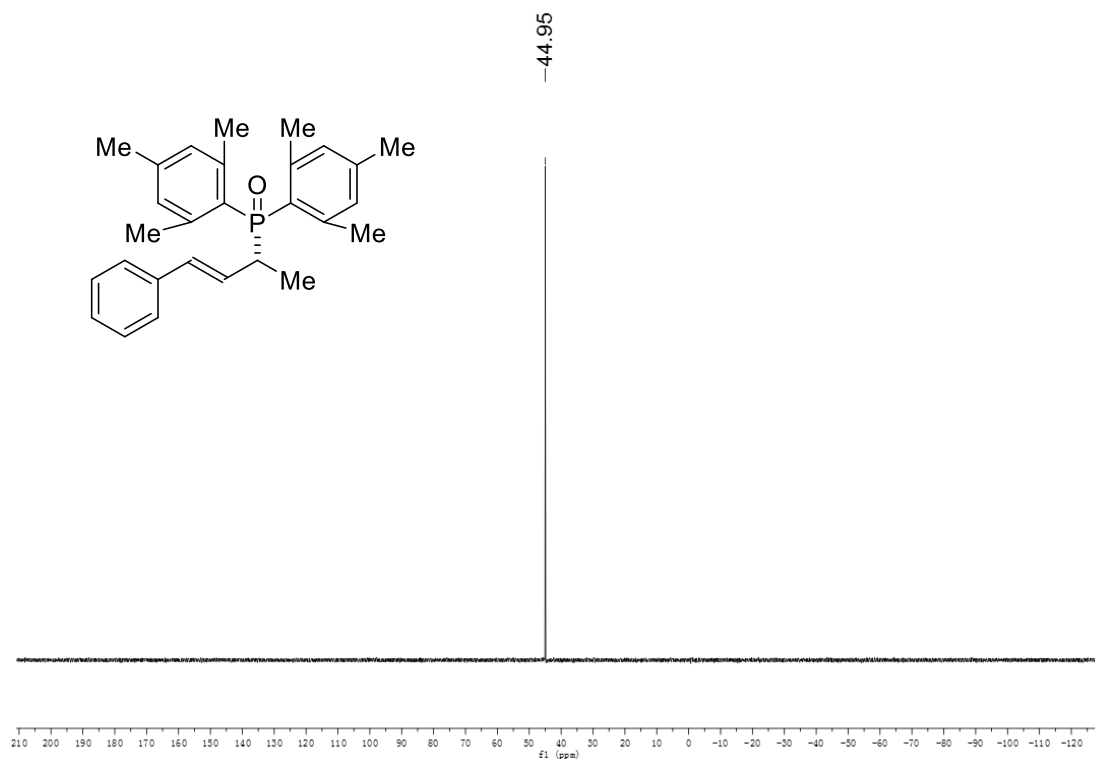


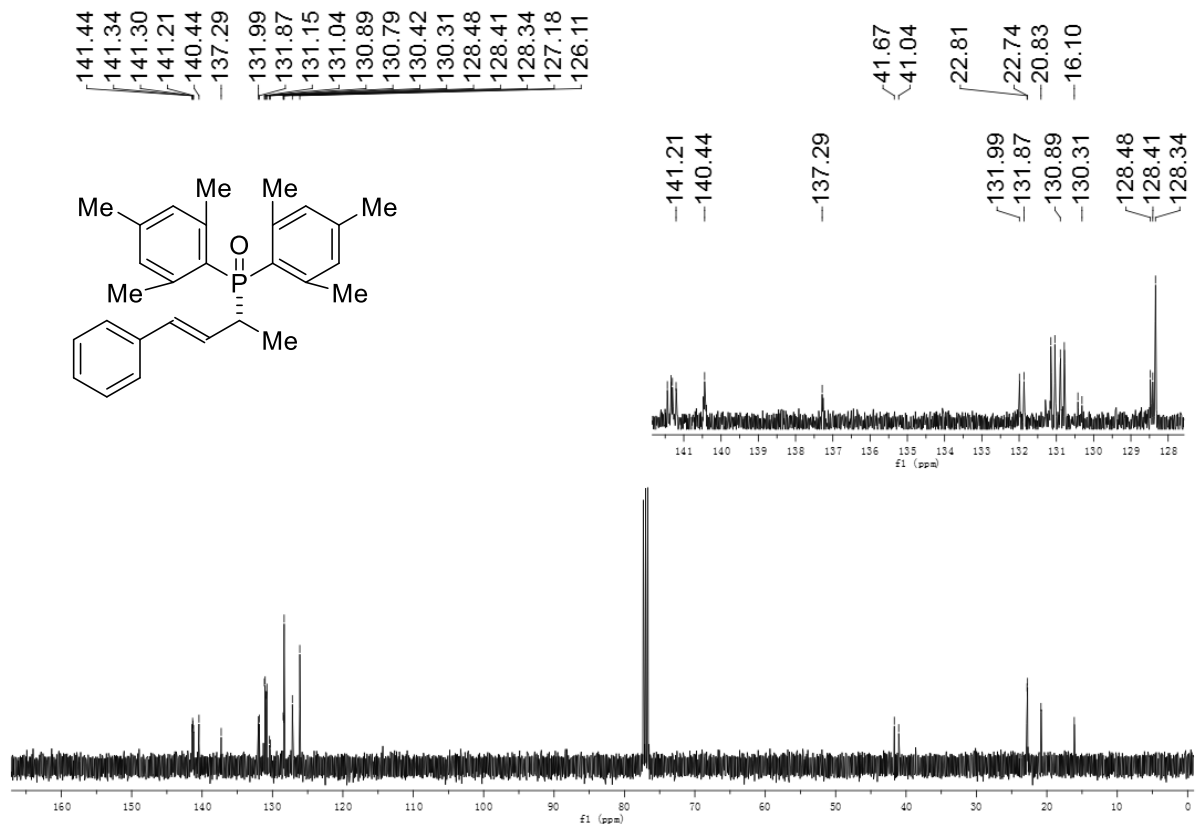
(*R,E*)-bis(3,5-dimethylphenyl)(4-phenylbut-3-en-2-yl)phosphine oxide (3ah)



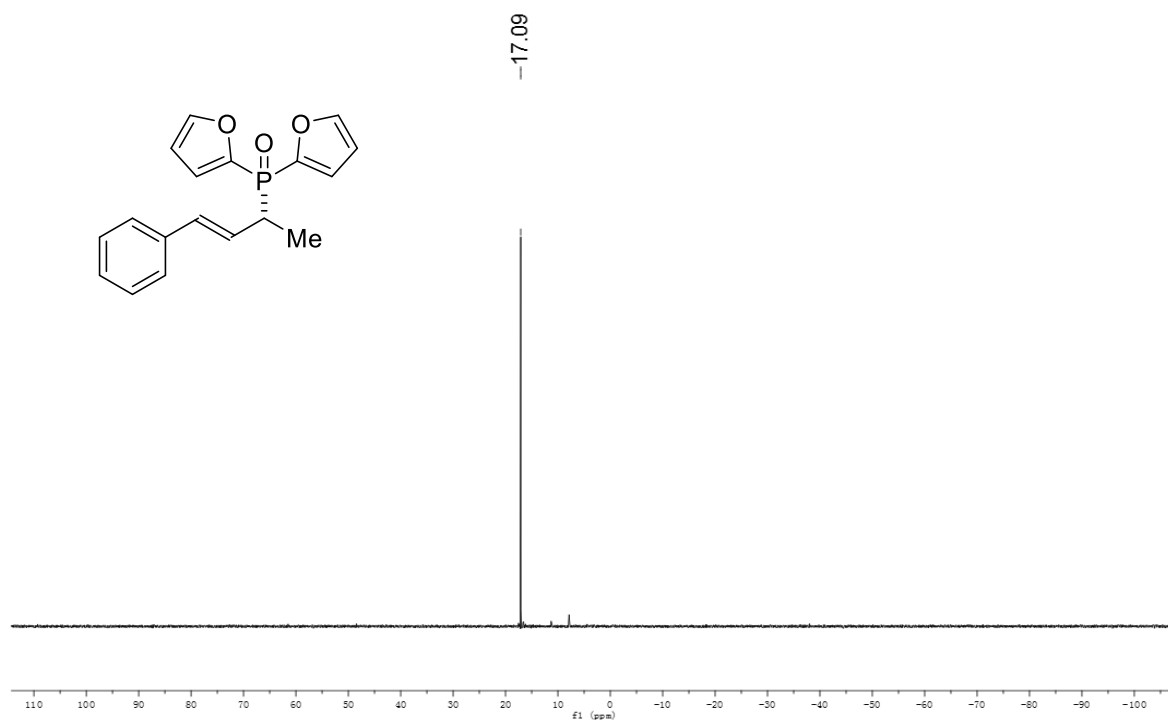


(*R,E*)-dimesityl(4-phenylbut-3-en-2-yl)phosphine oxide (3ai)





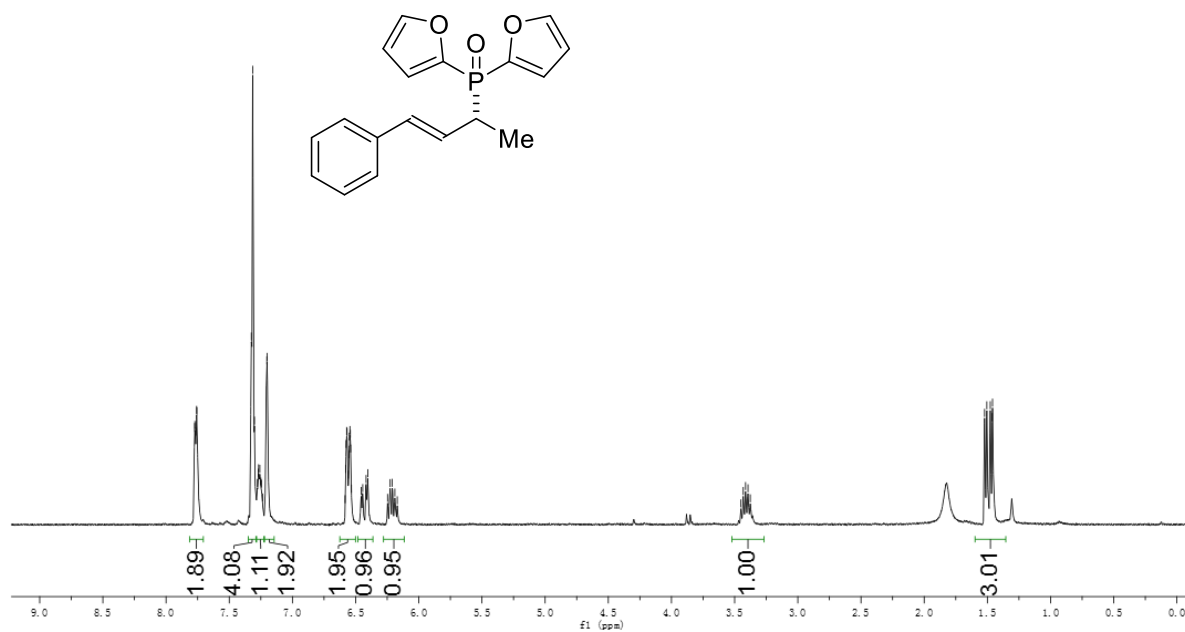
(*R,E*)-di(furan-2-yl)(4-phenylbut-3-en-2-yl)phosphine oxide (3aj)

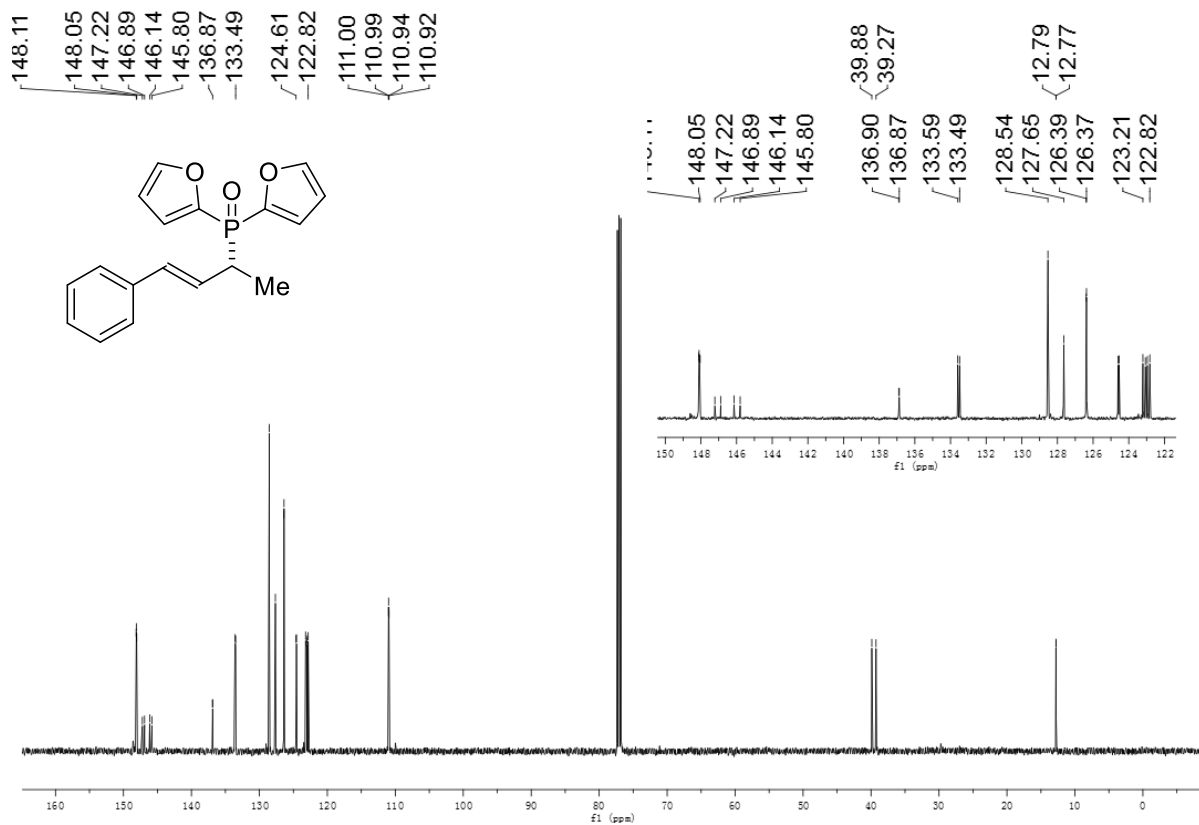


7.77
7.77
7.76
7.76
7.36
7.27
7.25
7.20
6.57
6.55
6.54
6.54
6.46
6.42
6.25
6.21
6.17

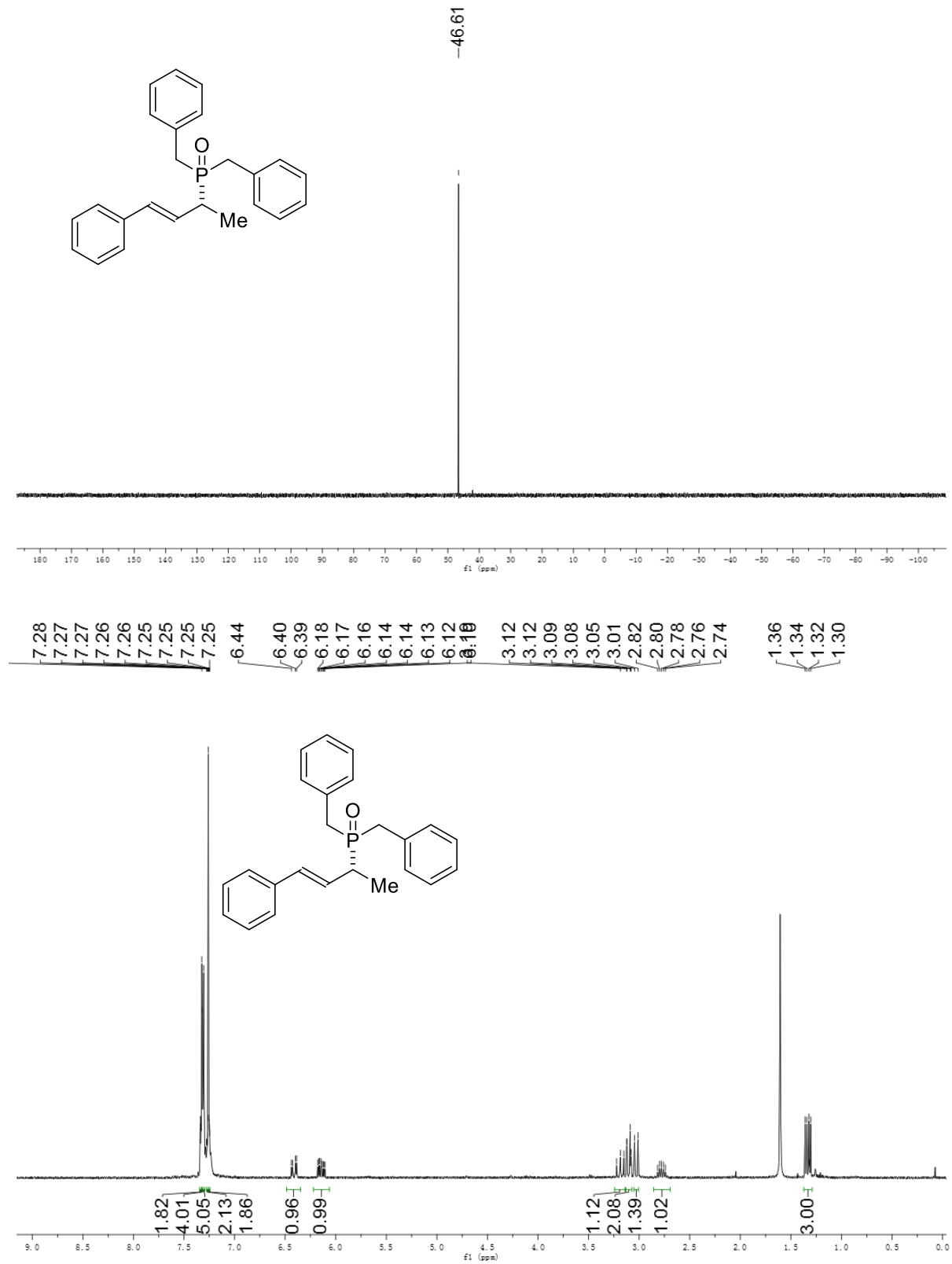
3.45
3.43
3.41
3.39
3.38

1.52
1.50
1.48
1.46
1.46

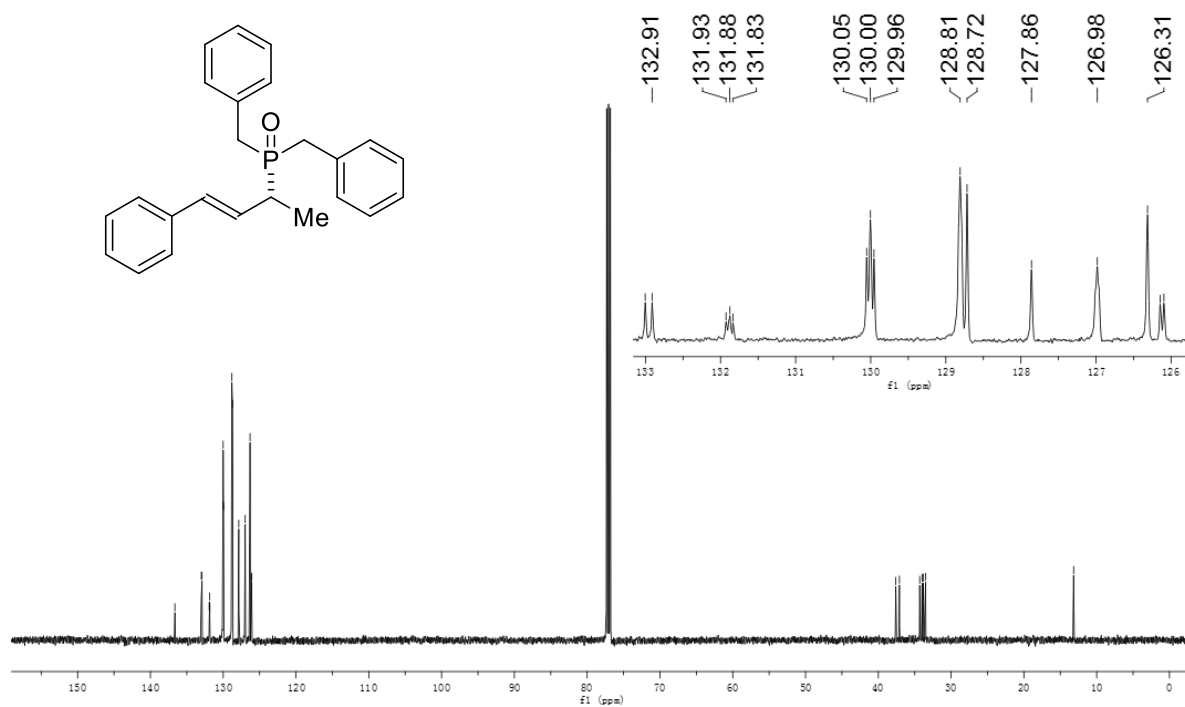
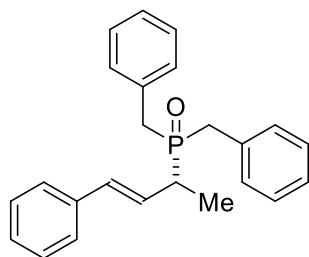




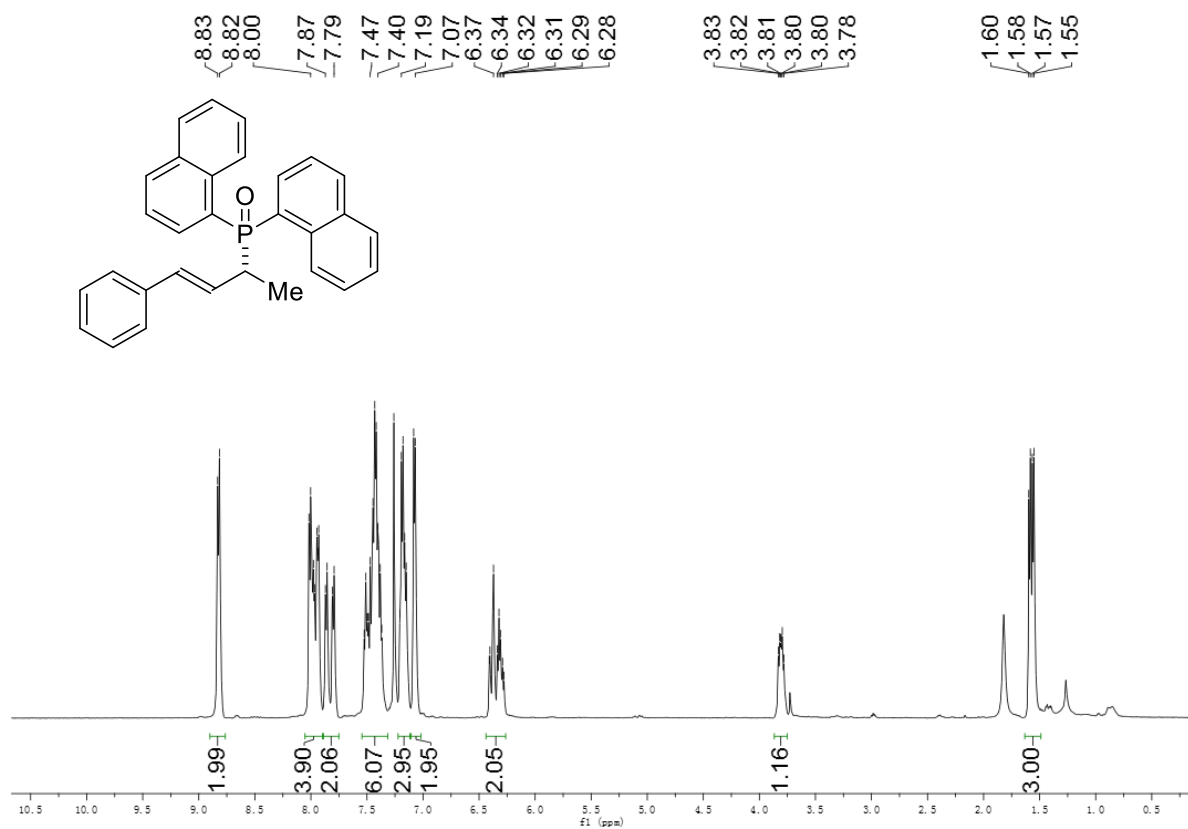
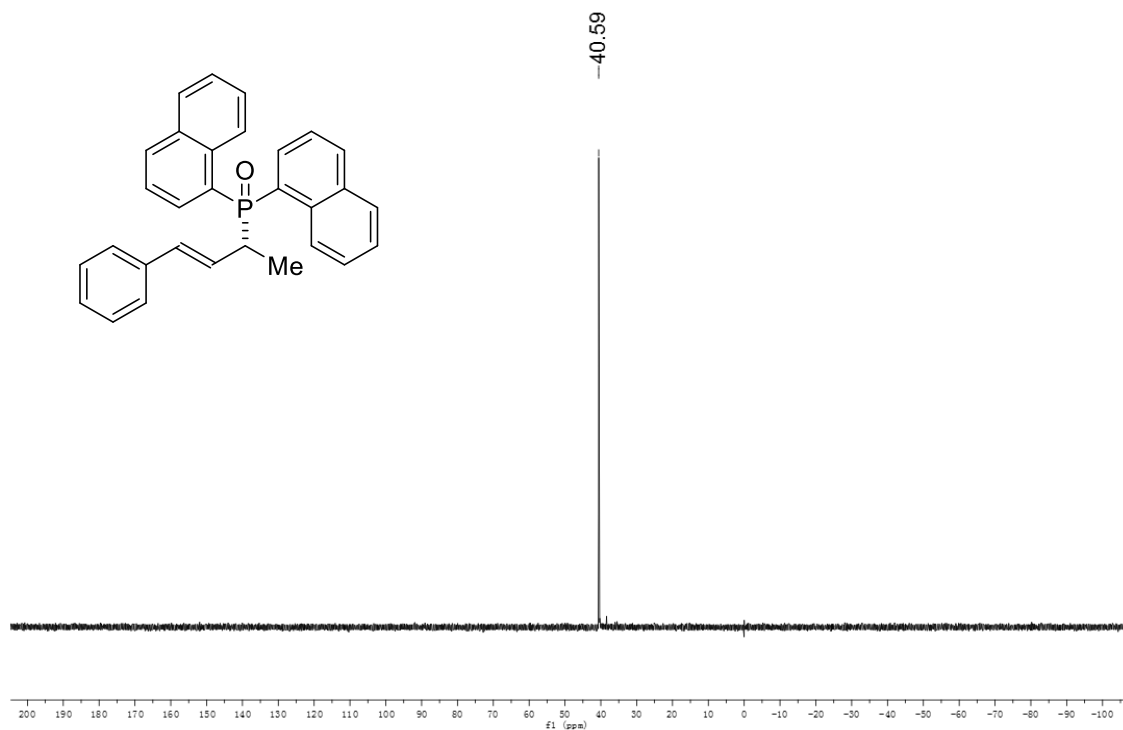
(*R,E*)-dibenzyl(4-phenylbut-3-en-2-yl)phosphine oxide (3ak)

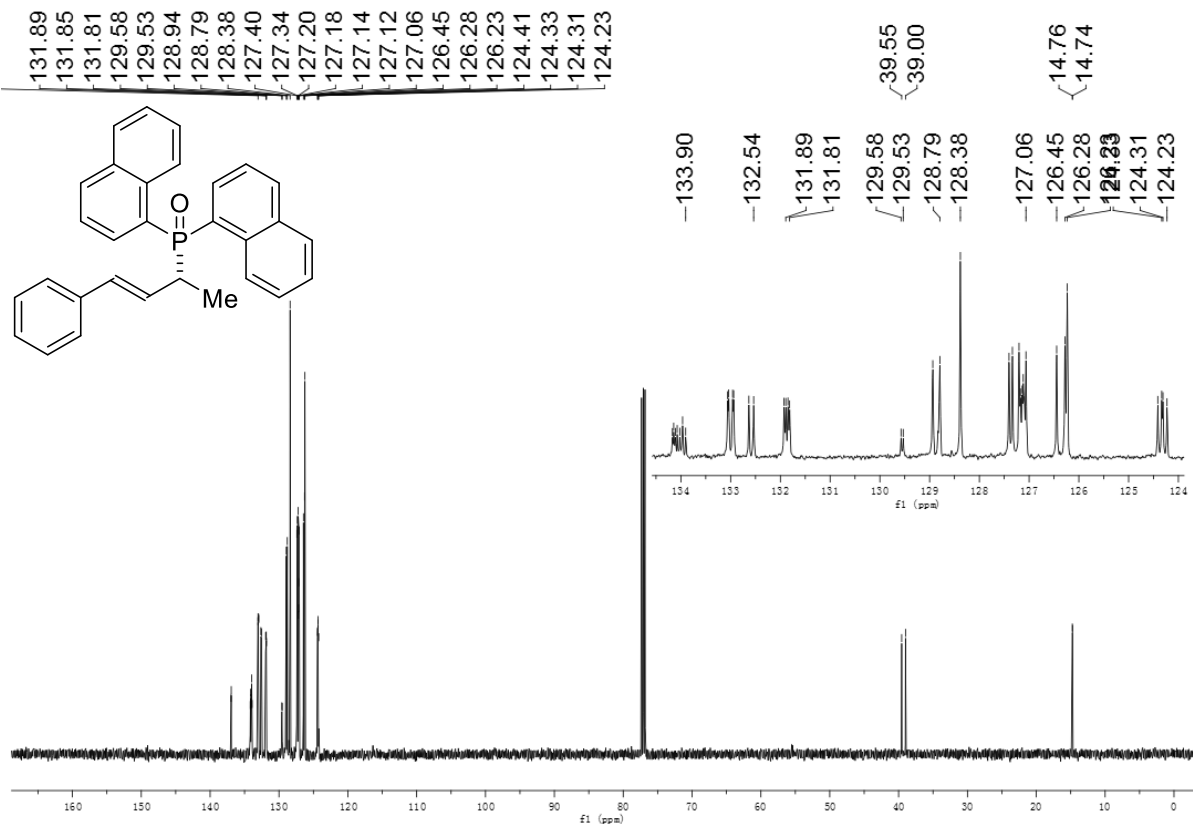


136.64
133.00
132.91
131.93
131.88
131.83
130.05
130.00
129.96
128.81
128.72
127.86
126.98
126.31
126.15
126.10

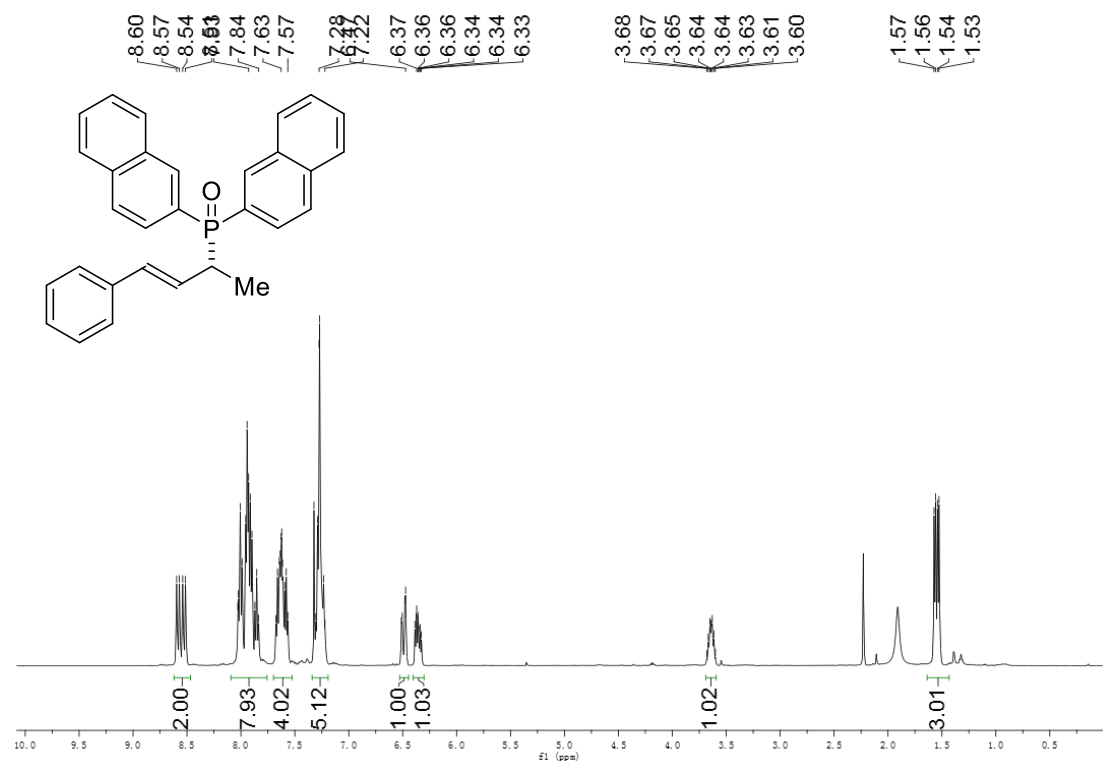
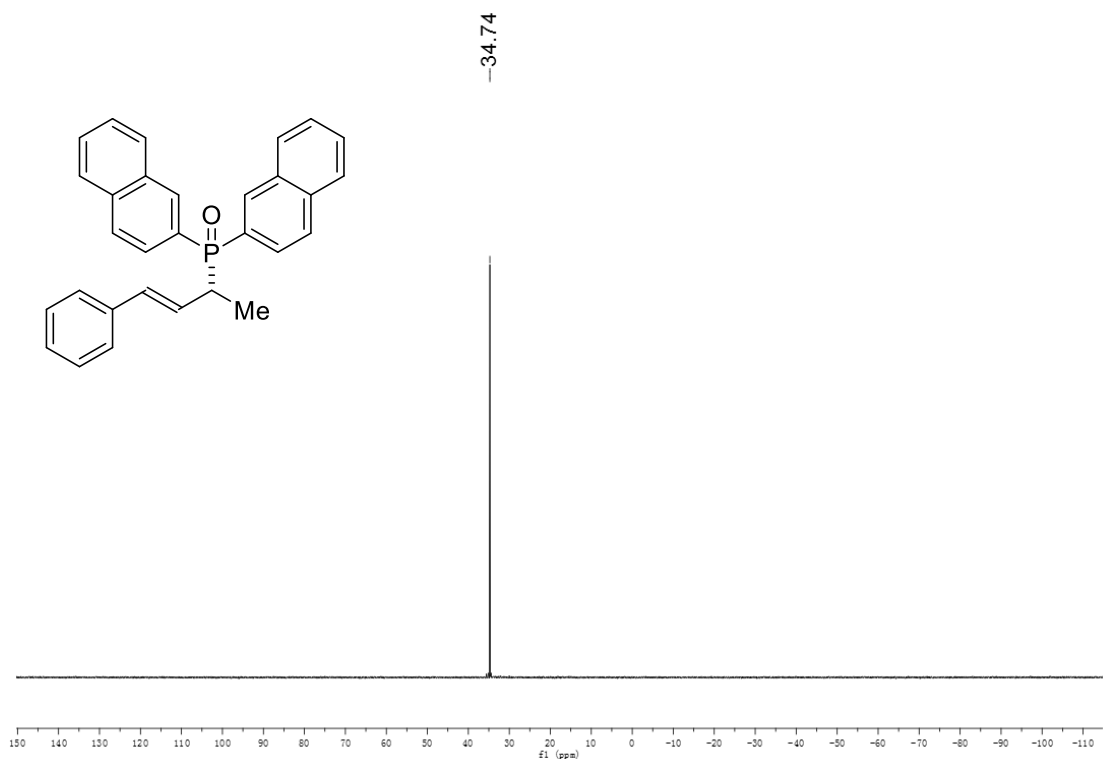


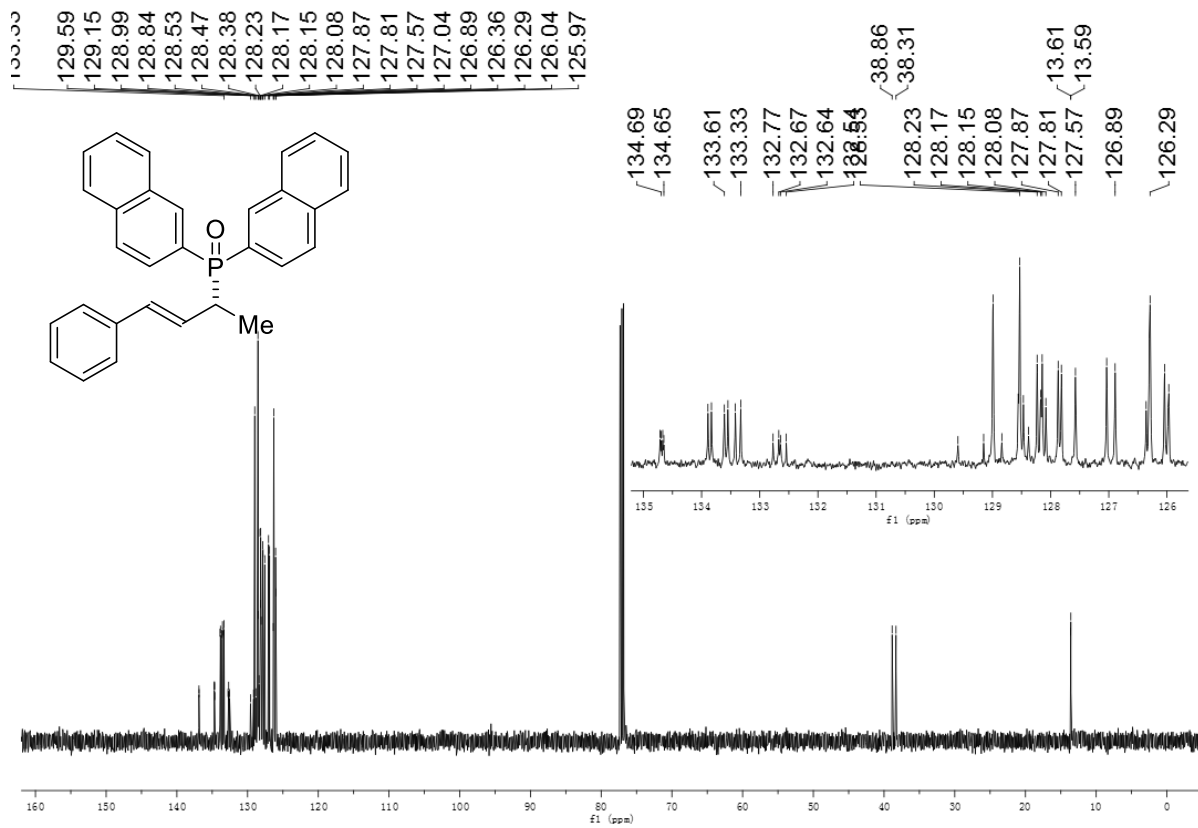
(*R,E*)-di(naphthalen-1-yl)(4-phenylbut-3-en-2-yl)phosphine oxide (3a)



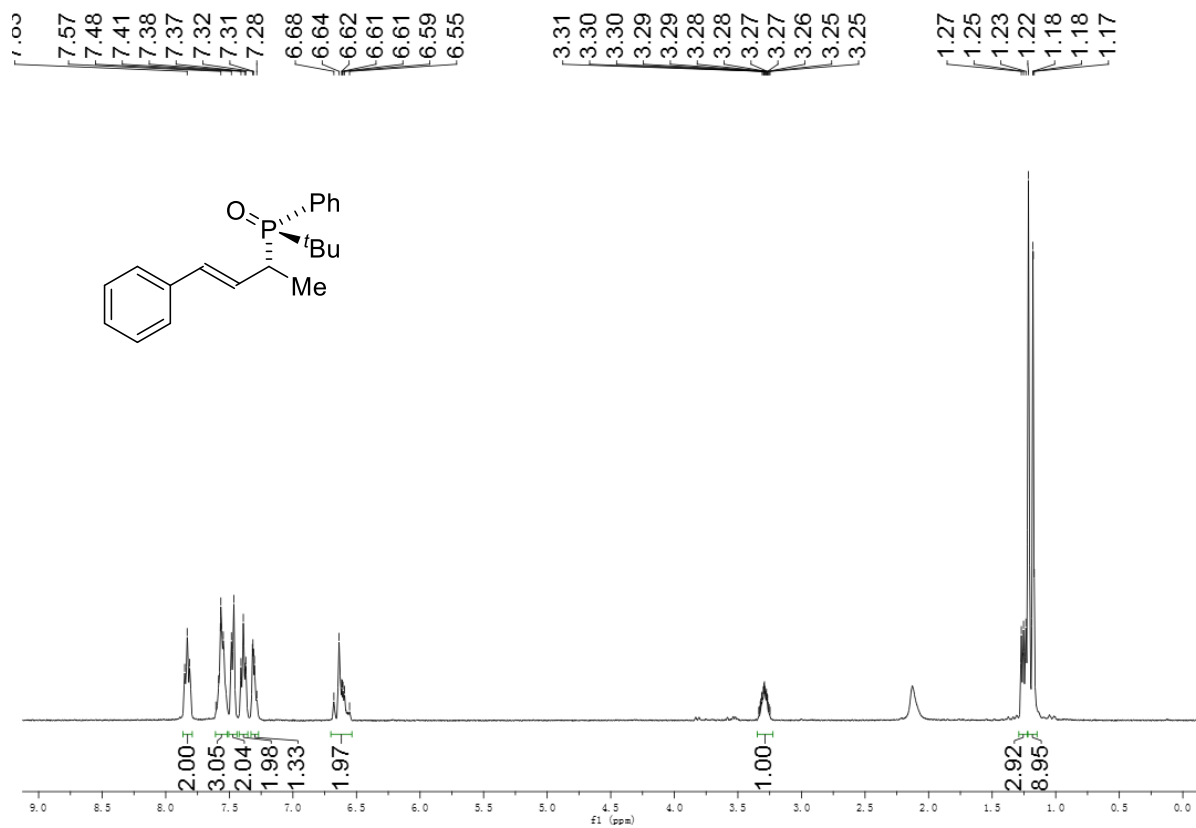
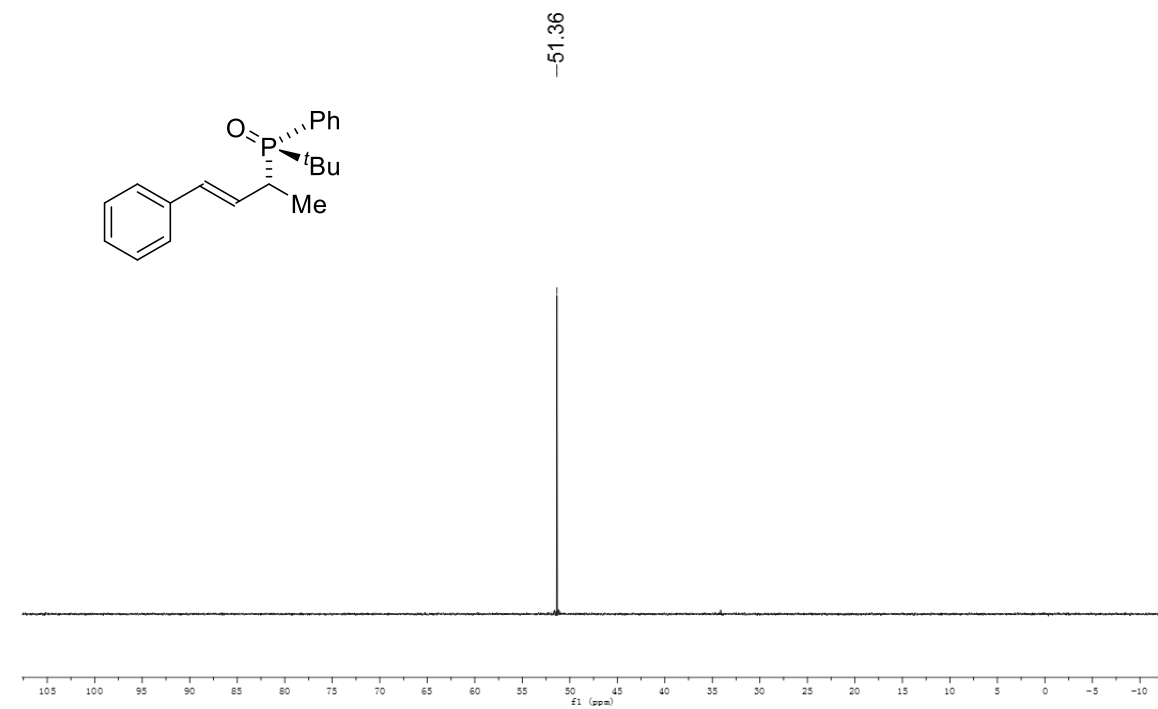


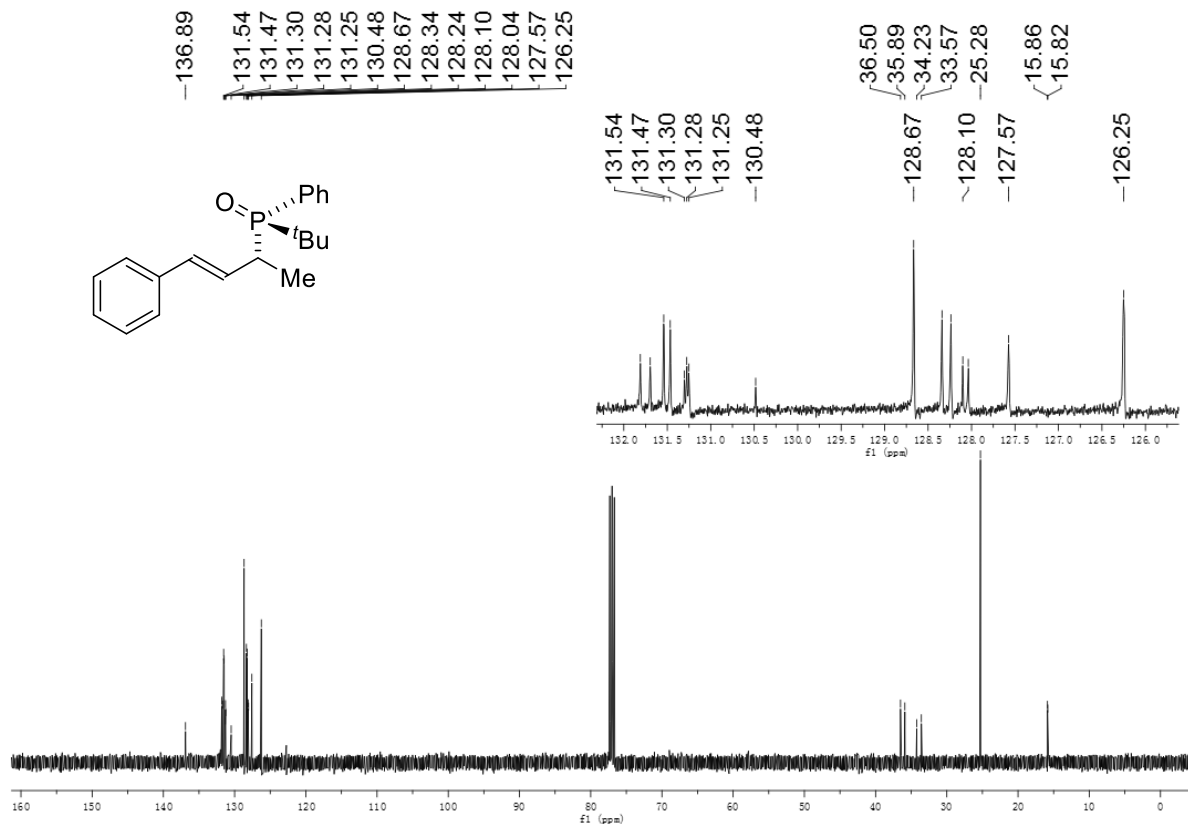
(*R,E*)-di(naphthalen-2-yl)(4-phenylbut-3-en-2-yl)phosphine oxide (3am)



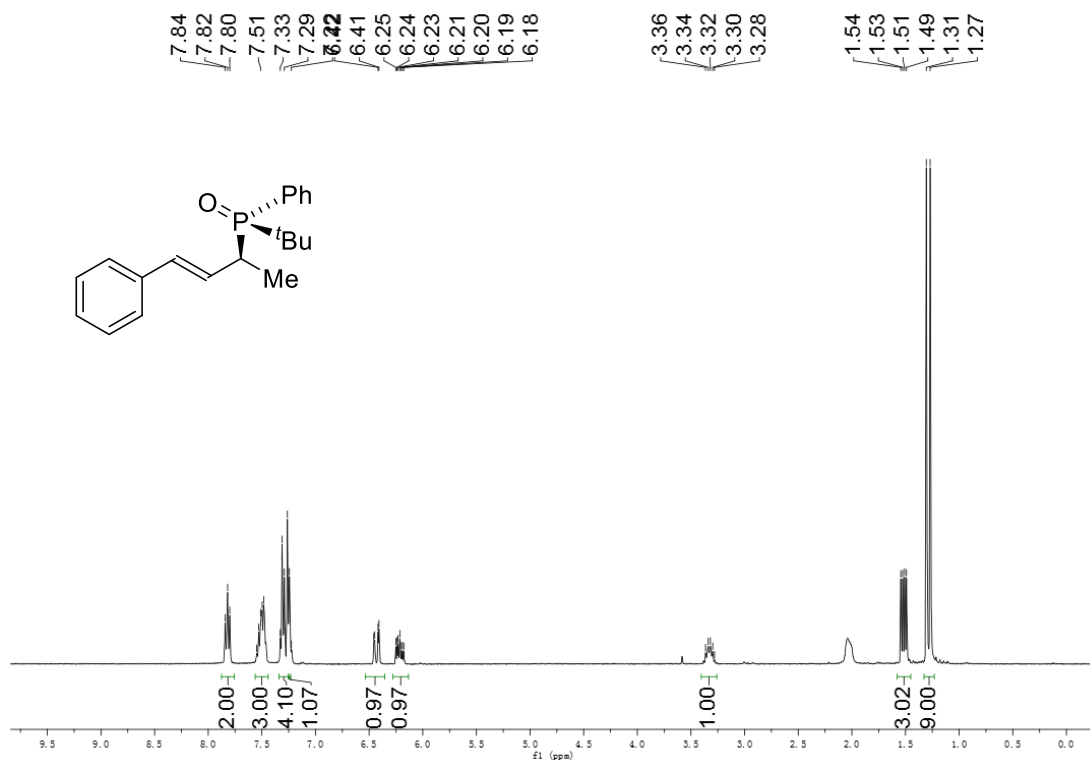
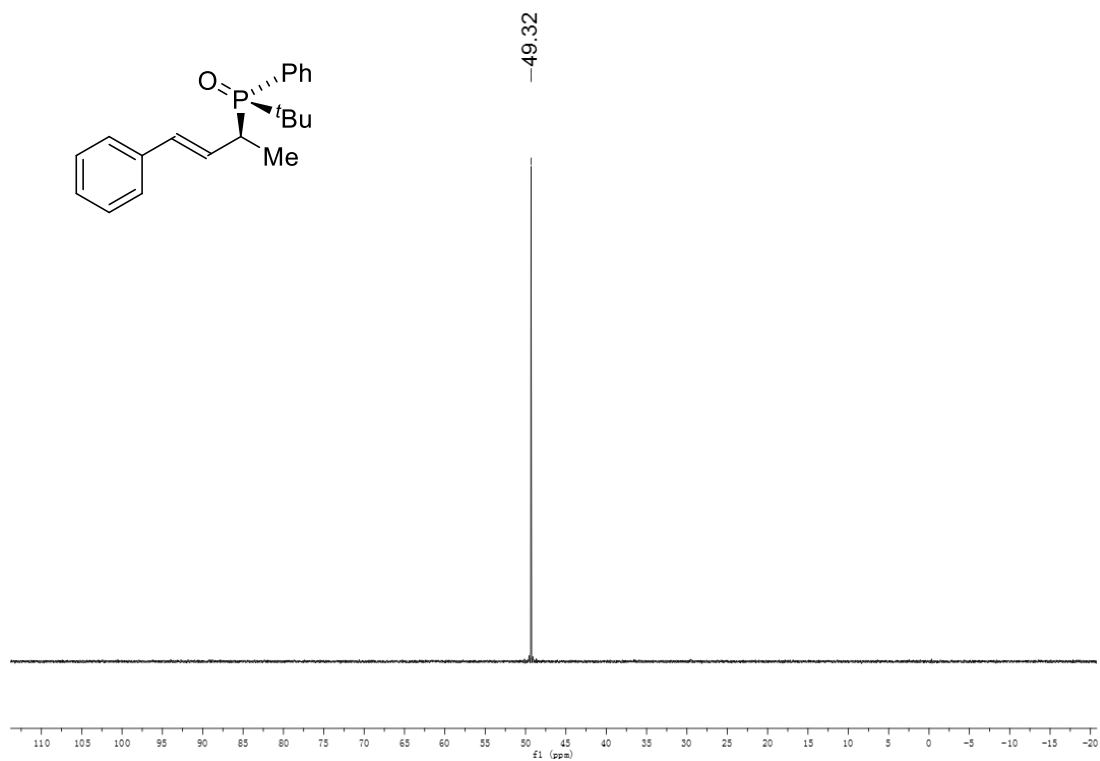


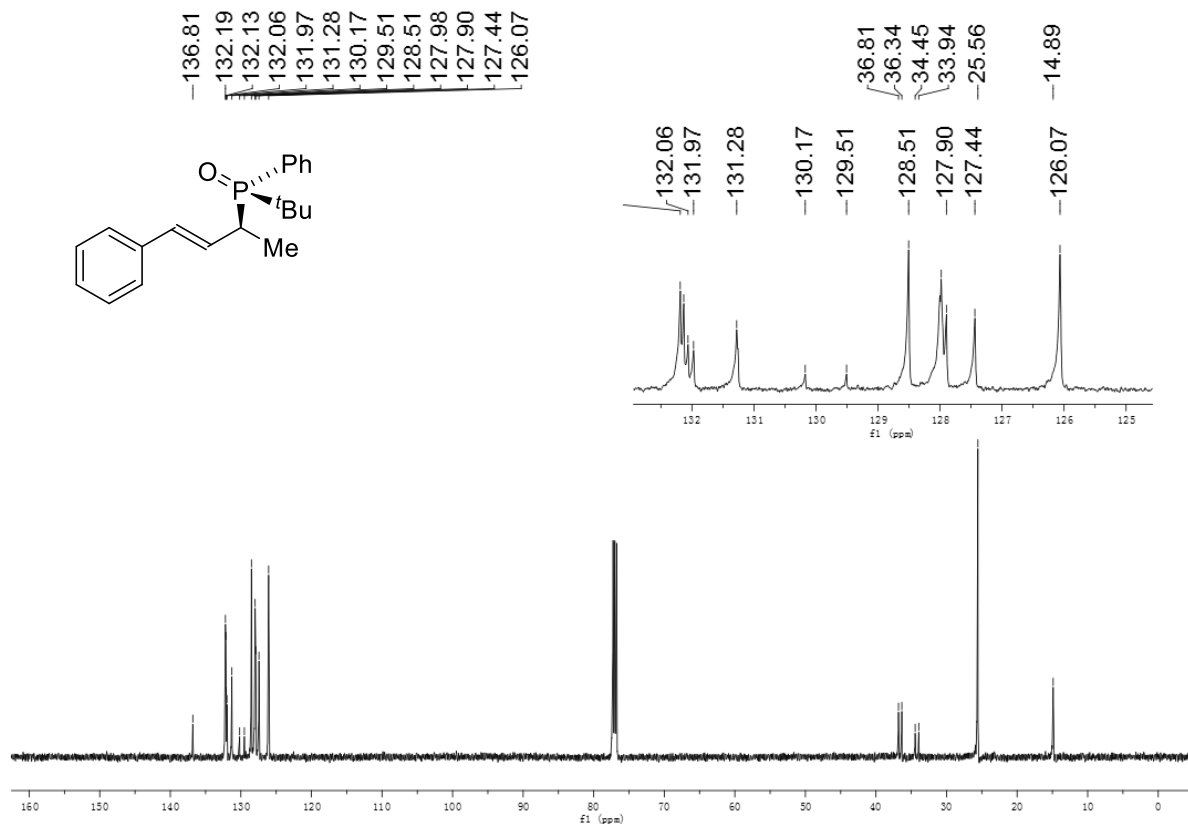
(R)-tert-butyl(phenyl)((R,E)-4-phenylbut-3-en-2-yl)phosphine oxide (3an)





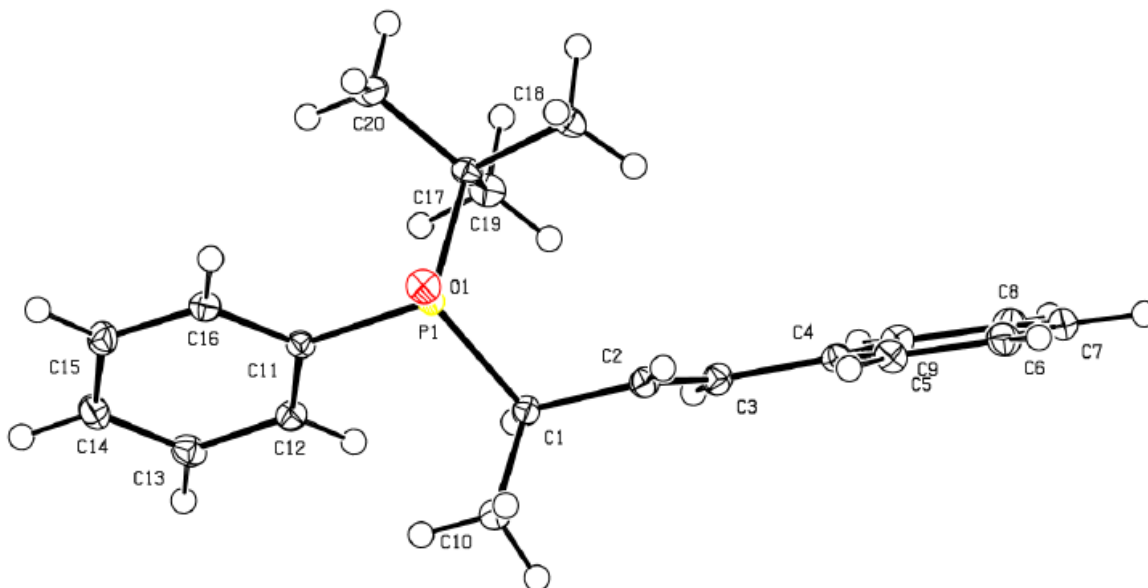
(R)-tert-butyl(phenyl)((S,E)-4-phenylbut-3-en-2-yl)phosphine oxide (3an')





5. X-ray Crystallography Data for 3an

X-ray crystallography data for (*R*)-*tert*-butyl(phenyl)((*R,E*)-4-phenylbut-3-en-2-yl)phosphine oxide (3an):



Experimental Summary

A colorless crystal of approximate dimensions 0.404 x 0.322 x 0.249 mm was mounted in a cryoloop and transferred to a Bruker SMART APEX II diffractometer. The APEX2 program package was used to determine the unit-cell parameters and for data collection (30 sec/frame scan time for a sphere of diffraction data). The raw frame data was processed using SAINT and SADABS to yield the reflection data file. Subsequent calculations were carried out using the SHELXTL program. The diffraction symmetry was *mmm* and the systematic absences were consistent with the orthorhombic space group $P2_12_12_1$ that was later determined to be correct.

The structure was solved by direct methods and refined on F by full-matrix least-squares techniques. The analytical scattering factors for neutral atoms were used throughout the analysis. Hydrogen atoms were located from a difference-Fourier map and refined (x, y, z and U_{iso}).

Least-squares analysis yielded $wR2 = 0.0678$ and $Goof = 1.034$ for 299 variables refined against 4398 data (0.73 Å), $R1 = 0.0246$ for those 4300 with $I > 2.0\sigma(I)$. The absolute structure was assigned based on refinement of the Flack parameter.

Definitions:

$$wR2 = [\Sigma[w(F_o^2 - F_c^2)^2] / \Sigma[w(F_o^2)^2]]^{1/2}$$

$$R1 = \Sigma||F_o| - |F_c|| / \Sigma|F_o|$$

Goof = S = $[\Sigma[w(F_o^2 - F_c^2)^2] / (n-p)]^{1/2}$ where n is the number of reflections and p is the total number of parameters refined.

The thermal ellipsoid plot is shown at the 50% probability level.

Table S1. Crystal data and structure refinement for 3an.

Identification code	3an	
Empirical formula	C ₂₀ H ₂₅ O P	
Formula weight	312.37	
Temperature	88(2) K	
Wavelength	0.71073 Å	
Crystal system	Orthorhombic	
Space group	P2 ₁ 2 ₁ 2 ₁	
Unit cell dimensions	a = 5.9083(9) Å	α = 90°.
	b = 13.523(2) Å	β = 90°.
	c = 21.616(3) Å	γ = 90°.
Volume	1727.0(5) Å ³	
Z	4	
Density (calculated)	1.201 Mg/m ³	
Absorption coefficient	0.159 mm ⁻¹	
F(000)	672	
Crystal color	colorless	
Crystal size	0.404 x 0.322 x 0.249 mm ³	
Theta range for data collection	1.776 to 29.095°	
Index ranges	-7 ≤ h ≤ 8, -18 ≤ k ≤ 18, -28 ≤ l ≤ 29	
Reflections collected	21305	
Independent reflections	4398 [R(int) = 0.0192]	
Completeness to theta = 25.500°	100.0 %	
Absorption correction	Semi-empirical from equivalents	
Max. and min. transmission	0.7458 and 0.7181	

Refinement method	Full-matrix least-squares on F^2
Data / restraints / parameters	4398 / 0 / 299
Goodness-of-fit on F^2	1.034
Final R indices [$I > 2\sigma(I) = 4300$ data]	R1 = 0.0246, wR2 = 0.0671
R indices (all data, 0.73 Å)	R1 = 0.0253, wR2 = 0.0678
Absolute structure parameter	-0.006(16)
Largest diff. peak and hole	0.302 and -0.178 e.Å ⁻³

Table S2. Atomic coordinates ($\times 10^4$) and equivalent isotropic displacement parameters ($\text{\AA}^2 \times 10^3$) for 3an. $U(\text{eq})$ is defined as one third of the trace of the orthogonalized U_{ij} tensor.

	x	y	z	U(eq)
P(1)	8120(1)	9042(1)	8455(1)	11(1)
O(1)	10553(2)	8816(1)	8321(1)	15(1)
C(1)	6155(2)	8175(1)	8081(1)	13(1)
C(2)	6022(2)	8294(1)	7389(1)	14(1)
C(3)	4089(2)	8519(1)	7100(1)	14(1)
C(4)	3743(2)	8609(1)	6426(1)	13(1)
C(5)	5353(3)	8296(1)	5991(1)	16(1)
C(6)	4905(3)	8363(1)	5360(1)	18(1)
C(7)	2850(3)	8741(1)	5154(1)	18(1)
C(8)	1239(2)	9056(1)	5577(1)	18(1)
C(9)	1692(2)	8992(1)	6209(1)	16(1)
C(10)	6945(3)	7116(1)	8244(1)	18(1)
C(11)	7488(2)	8911(1)	9275(1)	12(1)
C(12)	5402(2)	8573(1)	9502(1)	14(1)
C(13)	5094(3)	8436(1)	10136(1)	17(1)
C(14)	6821(3)	8667(1)	10548(1)	17(1)
C(15)	8870(2)	9035(1)	10329(1)	17(1)
C(16)	9217(2)	9138(1)	9694(1)	14(1)
C(17)	7385(2)	10328(1)	8248(1)	12(1)
C(18)	8168(3)	10540(1)	7581(1)	18(1)
C(19)	4837(2)	10514(1)	8317(1)	16(1)
C(20)	8690(3)	11020(1)	8687(1)	17(1)

Table S3. Bond lengths [\AA] and angles [$^\circ$] for 3an.

P(1)-O(1)	1.4981(10)
P(1)-C(11)	1.8195(13)
P(1)-C(1)	1.8371(15)
P(1)-C(17)	1.8469(14)
C(1)-C(2)	1.5066(18)
C(1)-C(10)	1.546(2)
C(2)-C(3)	1.337(2)
C(3)-C(4)	1.4751(18)
C(4)-C(9)	1.3994(19)
C(4)-C(5)	1.4039(19)
C(5)-C(6)	1.392(2)
C(6)-C(7)	1.391(2)
C(7)-C(8)	1.386(2)
C(8)-C(9)	1.3955(19)
C(11)-C(16)	1.4008(18)
C(11)-C(12)	1.4032(18)
C(12)-C(13)	1.3932(19)
C(13)-C(14)	1.391(2)
C(14)-C(15)	1.392(2)
C(15)-C(16)	1.3938(18)
C(17)-C(19)	1.5339(19)
C(17)-C(18)	1.5403(19)
C(17)-C(20)	1.5406(19)
O(1)-P(1)-C(11)	111.42(6)
O(1)-P(1)-C(1)	113.03(6)
C(11)-P(1)-C(1)	103.67(6)
O(1)-P(1)-C(17)	111.77(6)
C(11)-P(1)-C(17)	106.21(6)
C(1)-P(1)-C(17)	110.24(6)
C(2)-C(1)-C(10)	109.94(11)
C(2)-C(1)-P(1)	113.65(10)
C(10)-C(1)-P(1)	107.46(10)
C(3)-C(2)-C(1)	122.23(13)
C(2)-C(3)-C(4)	126.79(13)
C(9)-C(4)-C(5)	118.25(12)
C(9)-C(4)-C(3)	118.82(12)

C(5)-C(4)-C(3)	122.89(13)
C(6)-C(5)-C(4)	120.56(14)
C(7)-C(6)-C(5)	120.24(14)
C(8)-C(7)-C(6)	120.10(13)
C(7)-C(8)-C(9)	119.66(13)
C(8)-C(9)-C(4)	121.19(13)
C(16)-C(11)-C(12)	118.97(12)
C(16)-C(11)-P(1)	117.39(10)
C(12)-C(11)-P(1)	123.62(10)
C(13)-C(12)-C(11)	120.19(13)
C(14)-C(13)-C(12)	120.26(14)
C(13)-C(14)-C(15)	120.03(13)
C(14)-C(15)-C(16)	119.90(13)
C(15)-C(16)-C(11)	120.57(13)
C(19)-C(17)-C(18)	110.82(12)
C(19)-C(17)-C(20)	109.31(12)
C(18)-C(17)-C(20)	108.23(12)
C(19)-C(17)-P(1)	111.22(9)
C(18)-C(17)-P(1)	109.37(10)
C(20)-C(17)-P(1)	107.79(9)

Table S4. Anisotropic displacement parameters ($\text{\AA}^2 \times 10^3$) for 3an. The anisotropic displacement

factor exponent takes the form: $-2\pi^2 [h^2 a^{*2} U^{11} + \dots + 2 h k a^* b^* U^{12}]$

	U11	U22	U33	U23	U13	U12
P(1)	9(1)	12(1)	11(1)	0(1)	1(1)	0(1)
O(1)	10(1)	18(1)	18(1)	0(1)	2(1)	2(1)
C(1)	12(1)	15(1)	12(1)	-1(1)	0(1)	-1(1)
C(2)	14(1)	15(1)	13(1)	-1(1)	2(1)	-1(1)
C(3)	14(1)	16(1)	13(1)	-2(1)	2(1)	-1(1)
C(4)	14(1)	12(1)	14(1)	-1(1)	0(1)	-2(1)
C(5)	16(1)	16(1)	16(1)	1(1)	1(1)	1(1)
C(6)	21(1)	17(1)	16(1)	0(1)	4(1)	-1(1)
C(7)	23(1)	17(1)	14(1)	2(1)	-3(1)	-4(1)
C(8)	16(1)	18(1)	21(1)	2(1)	-4(1)	-1(1)
C(9)	15(1)	17(1)	18(1)	-1(1)	1(1)	0(1)
C(10)	24(1)	14(1)	16(1)	0(1)	-1(1)	-1(1)
C(11)	13(1)	11(1)	12(1)	0(1)	1(1)	1(1)
C(12)	12(1)	15(1)	15(1)	0(1)	0(1)	-1(1)
C(13)	17(1)	16(1)	17(1)	2(1)	4(1)	0(1)
C(14)	22(1)	17(1)	14(1)	2(1)	1(1)	3(1)
C(15)	18(1)	16(1)	15(1)	0(1)	-4(1)	2(1)
C(16)	12(1)	14(1)	17(1)	1(1)	-1(1)	0(1)
C(17)	11(1)	12(1)	14(1)	2(1)	1(1)	0(1)
C(18)	19(1)	18(1)	17(1)	4(1)	4(1)	0(1)
C(19)	11(1)	17(1)	21(1)	2(1)	1(1)	2(1)
C(20)	17(1)	13(1)	22(1)	-1(1)	-3(1)	-1(1)

Table S5. Hydrogen coordinates ($\times 10^4$) and isotropic displacement parameters ($\text{\AA}^2 \times 10^3$) for 3an.

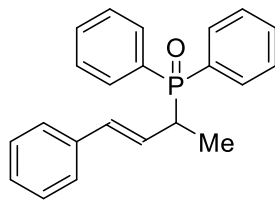
	x	y	z	U(eq)
H(1)	4740(30)	8302(15)	8257(9)	18(5)
H(2)	7400(30)	8191(14)	7179(8)	16(5)
H(3)	2800(40)	8625(14)	7337(9)	19(5)
H(5)	6780(40)	8019(15)	6139(9)	21(5)
H(6)	6090(40)	8151(15)	5071(10)	28(5)
H(7)	2530(40)	8773(15)	4700(10)	26(5)
H(8)	-150(40)	9303(16)	5442(10)	25(5)
H(9)	460(40)	9225(16)	6521(9)	26(5)
H(10A)	5980(40)	6608(16)	8094(9)	25(5)
H(10B)	7000(40)	7021(15)	8679(10)	25(5)
H(10C)	8360(40)	6968(16)	8079(10)	31(6)
H(12)	4210(40)	8422(15)	9233(10)	24(5)
H(13)	3710(40)	8184(14)	10283(9)	20(5)
H(14)	6640(40)	8564(16)	10996(9)	28(5)
H(15)	10100(40)	9208(15)	10610(10)	26(5)
H(16)	10570(30)	9374(13)	9549(8)	14(4)
H(18A)	8000(40)	11252(15)	7512(9)	24(5)
H(18B)	7340(30)	10149(14)	7278(9)	18(5)
H(18C)	9710(50)	10402(18)	7541(11)	34(6)
H(19A)	4500(40)	11234(16)	8230(10)	28(6)
H(19B)	4310(40)	10356(15)	8757(10)	25(5)
H(19C)	3920(40)	10110(16)	8040(10)	27(5)
H(20A)	8420(40)	11678(15)	8582(9)	22(5)
H(20B)	10260(40)	10894(17)	8669(10)	27(5)
H(20C)	8160(30)	10947(14)	9102(9)	18(4)

Table S6. Torsion angles [°] for 3an.

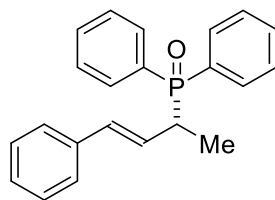
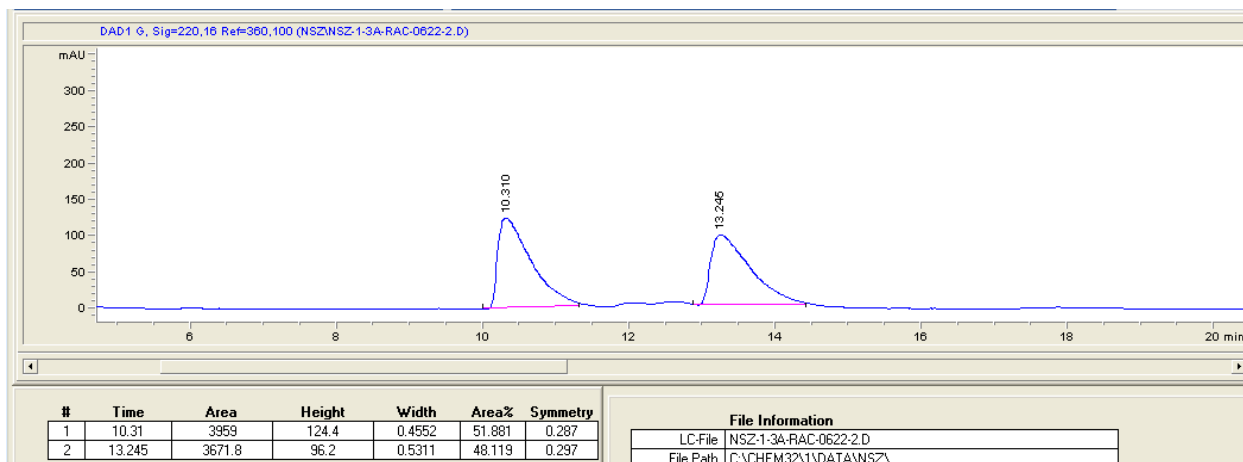
O(1)-P(1)-C(1)-C(2)	-70.84(12)
C(11)-P(1)-C(1)-C(2)	168.37(10)
C(17)-P(1)-C(1)-C(2)	55.05(12)
O(1)-P(1)-C(1)-C(10)	51.04(11)
C(11)-P(1)-C(1)-C(10)	-69.75(11)
C(17)-P(1)-C(1)-C(10)	176.93(9)
C(10)-C(1)-C(2)-C(3)	119.58(15)
P(1)-C(1)-C(2)-C(3)	-119.92(14)
C(1)-C(2)-C(3)-C(4)	-177.06(13)
C(2)-C(3)-C(4)-C(9)	-170.60(15)
C(2)-C(3)-C(4)-C(5)	11.6(2)
C(9)-C(4)-C(5)-C(6)	-0.3(2)
C(3)-C(4)-C(5)-C(6)	177.50(13)
C(4)-C(5)-C(6)-C(7)	0.0(2)
C(5)-C(6)-C(7)-C(8)	0.2(2)
C(6)-C(7)-C(8)-C(9)	0.1(2)
C(7)-C(8)-C(9)-C(4)	-0.4(2)
C(5)-C(4)-C(9)-C(8)	0.5(2)
C(3)-C(4)-C(9)-C(8)	-177.36(13)
O(1)-P(1)-C(11)-C(16)	32.39(13)
C(1)-P(1)-C(11)-C(16)	154.25(11)
C(17)-P(1)-C(11)-C(16)	-89.55(11)
O(1)-P(1)-C(11)-C(12)	-145.88(11)
C(1)-P(1)-C(11)-C(12)	-24.02(13)
C(17)-P(1)-C(11)-C(12)	92.18(12)
C(16)-C(11)-C(12)-C(13)	-2.2(2)
P(1)-C(11)-C(12)-C(13)	176.07(11)
C(11)-C(12)-C(13)-C(14)	2.4(2)
C(12)-C(13)-C(14)-C(15)	-0.2(2)
C(13)-C(14)-C(15)-C(16)	-2.2(2)
C(14)-C(15)-C(16)-C(11)	2.5(2)
C(12)-C(11)-C(16)-C(15)	-0.3(2)
P(1)-C(11)-C(16)-C(15)	-178.62(11)
O(1)-P(1)-C(17)-C(19)	173.54(10)
C(11)-P(1)-C(17)-C(19)	-64.74(11)
C(1)-P(1)-C(17)-C(19)	46.94(12)

O(1)-P(1)-C(17)-C(18)	50.80(11)
C(11)-P(1)-C(17)-C(18)	172.52(9)
C(1)-P(1)-C(17)-C(18)	-75.79(11)
O(1)-P(1)-C(17)-C(20)	-66.66(11)
C(11)-P(1)-C(17)-C(20)	55.06(11)
C(1)-P(1)-C(17)-C(20)	166.75(9)

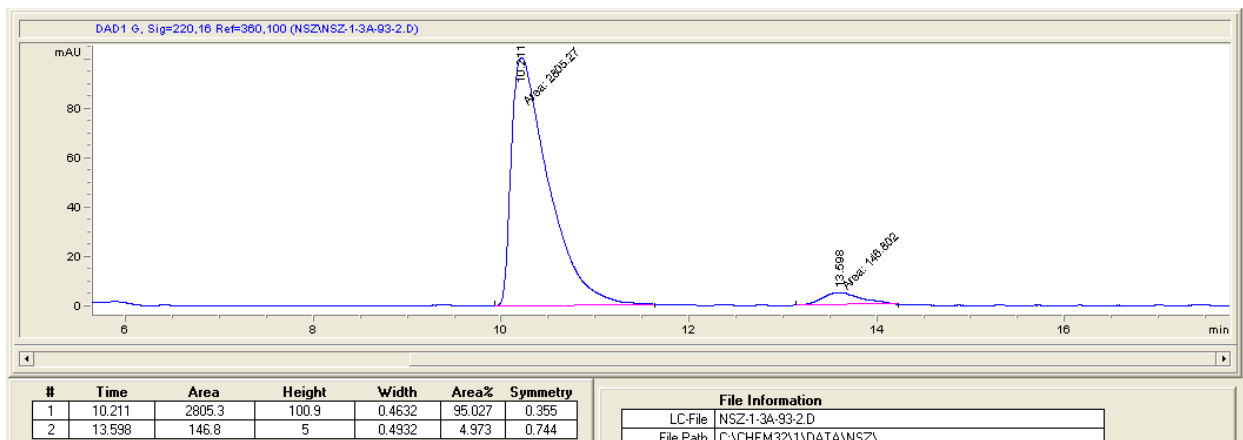
6. SFC Spectra

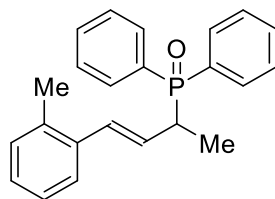


rac-3aa

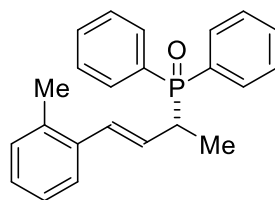
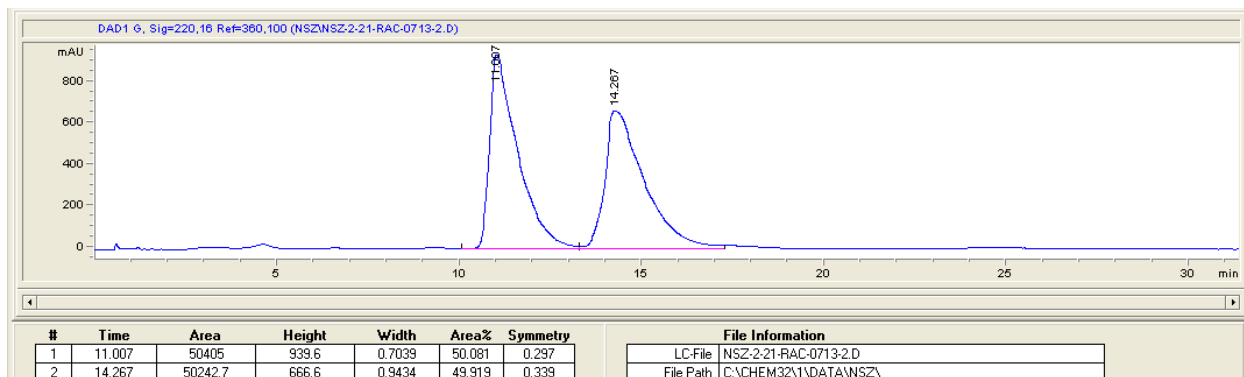


3aa

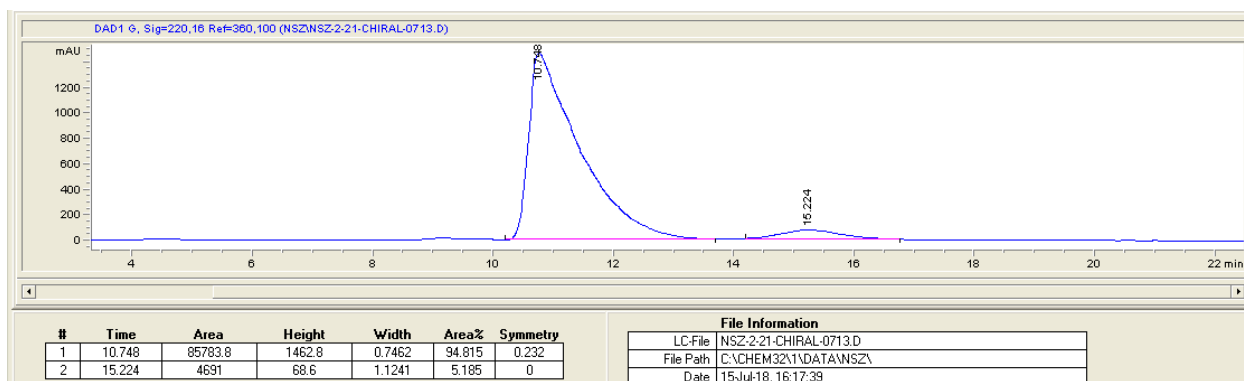


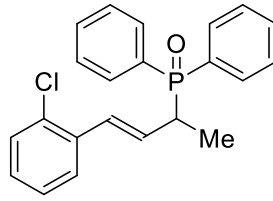


rac-3ba

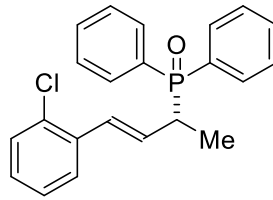
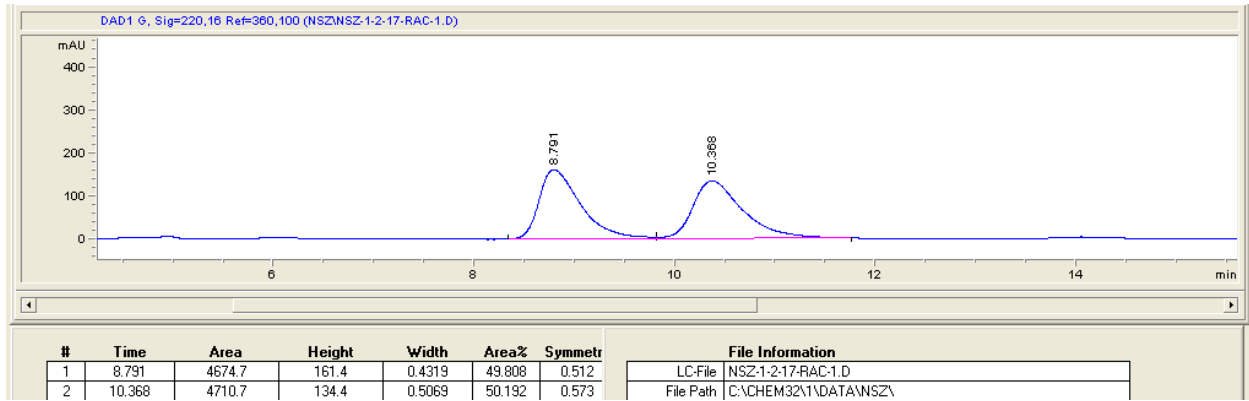


3ba

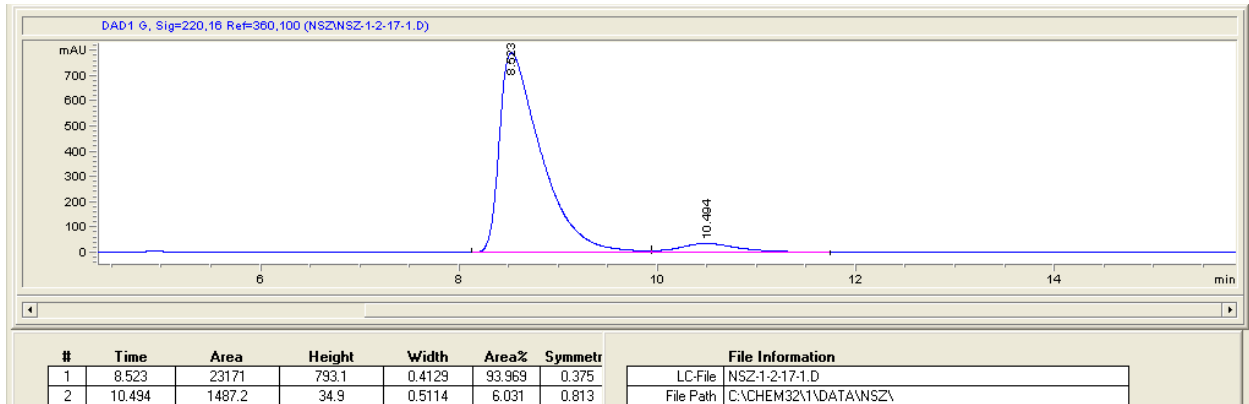


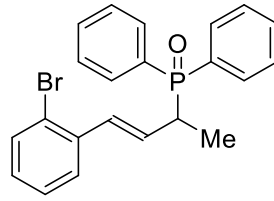


rac-3ca

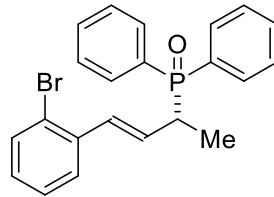
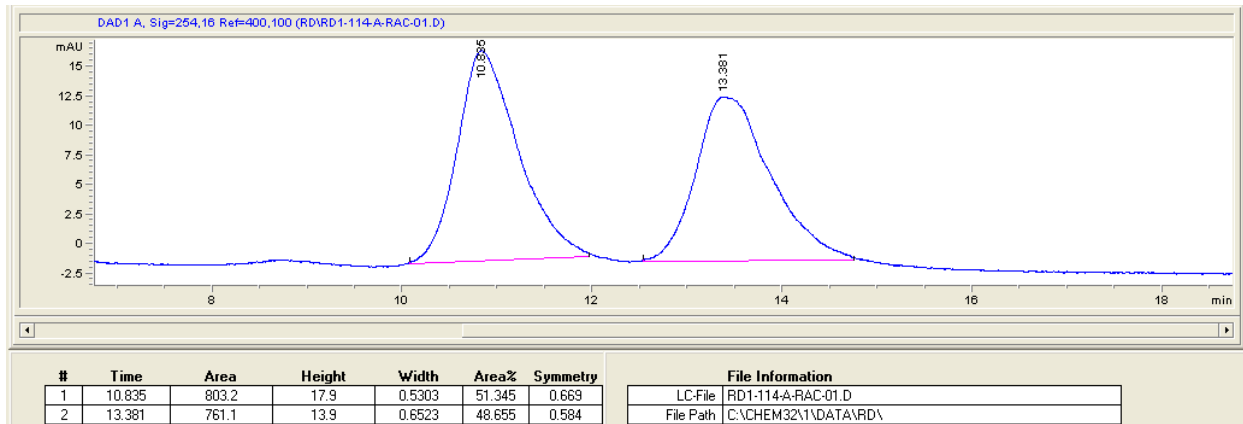


3ca

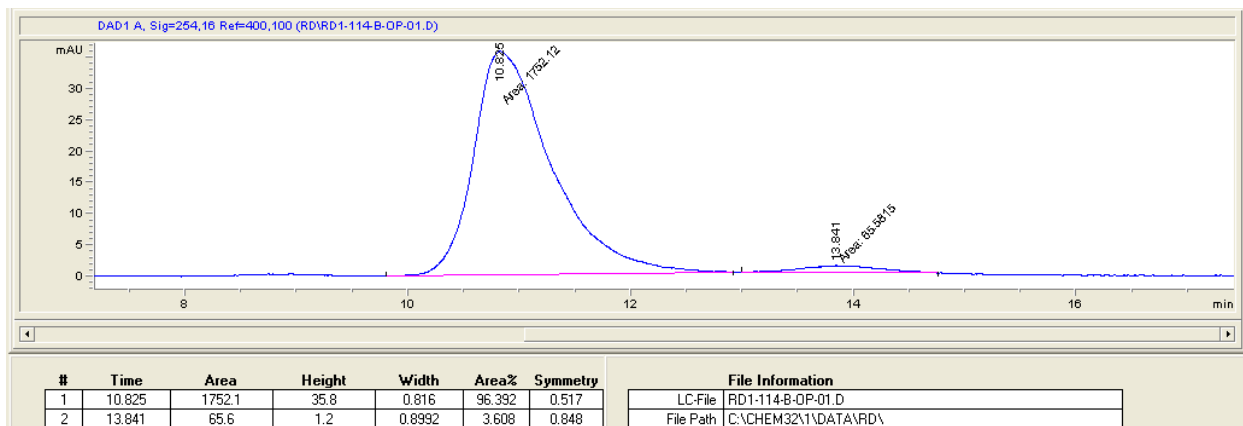


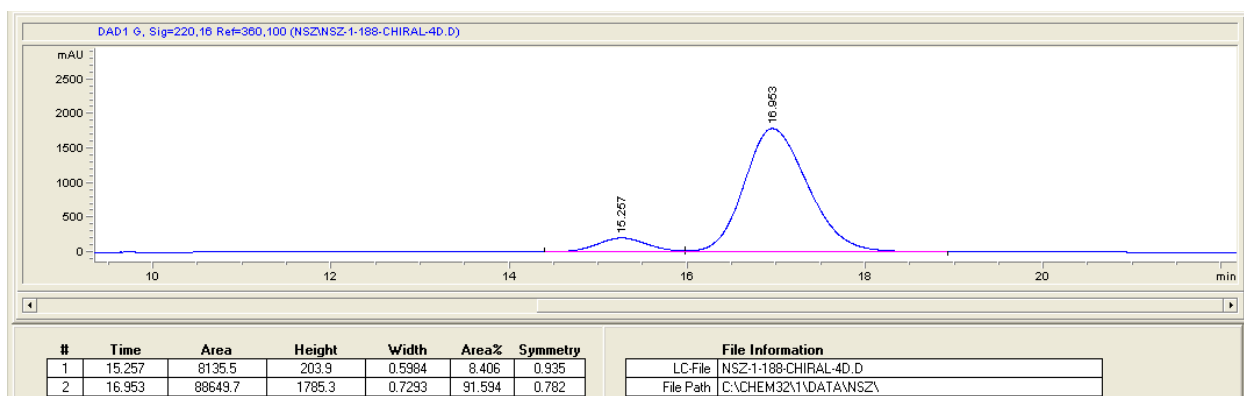
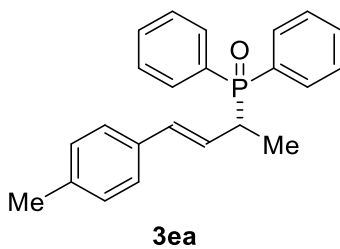
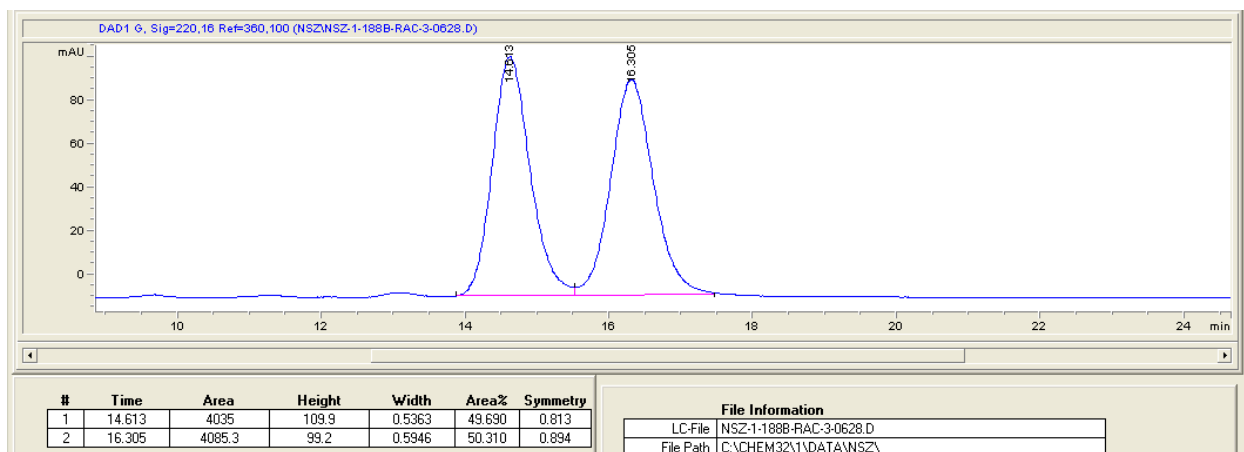
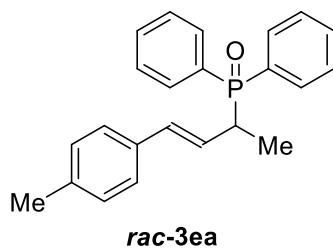


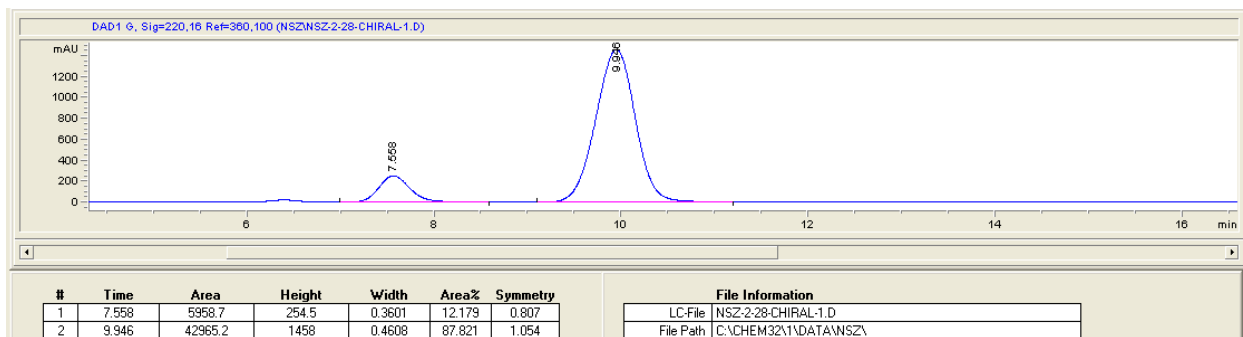
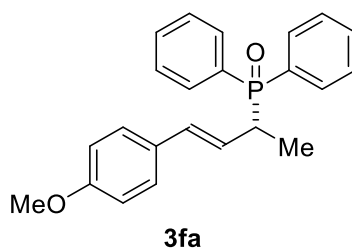
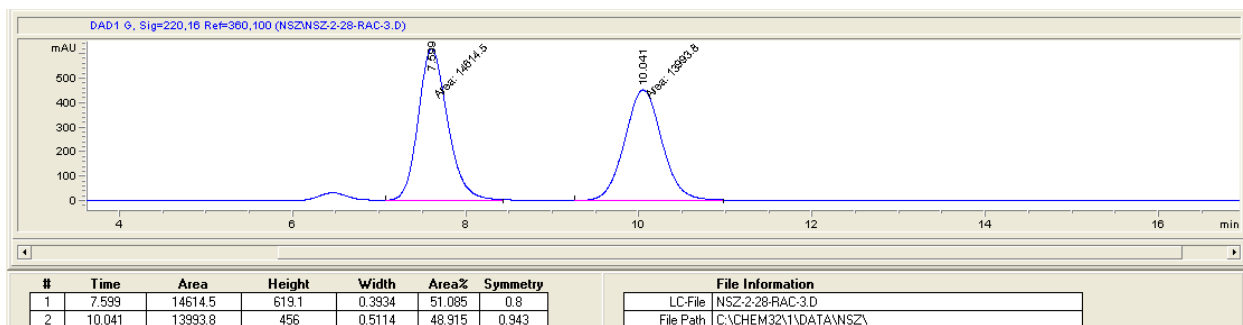
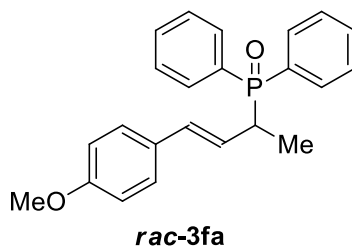
rac-3da

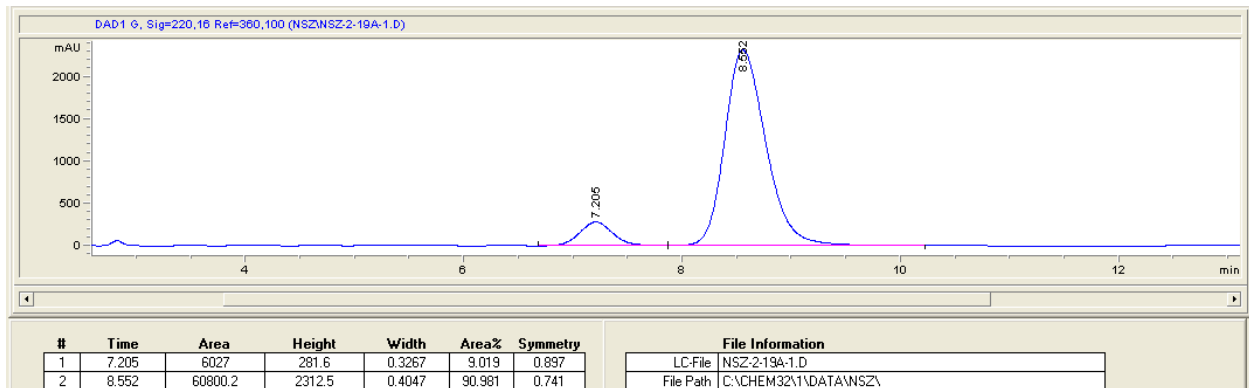
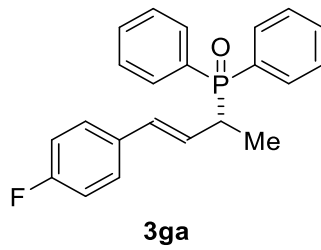
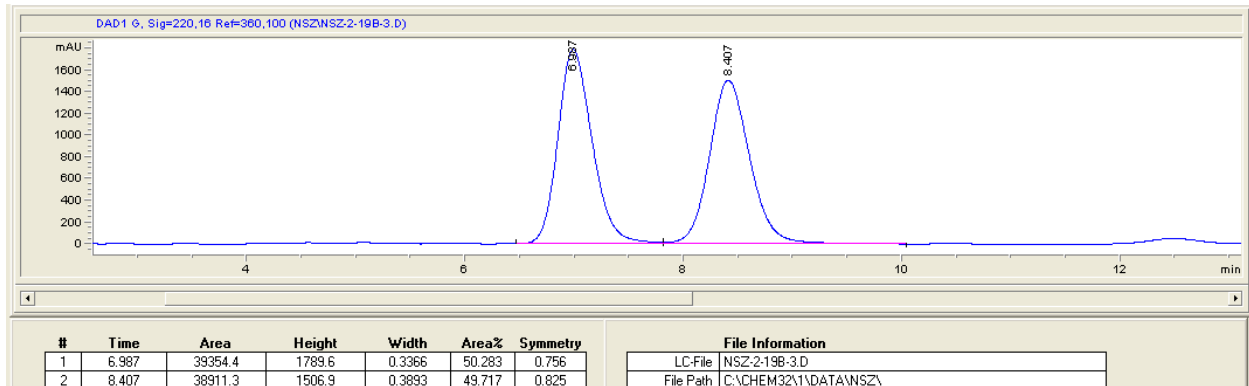
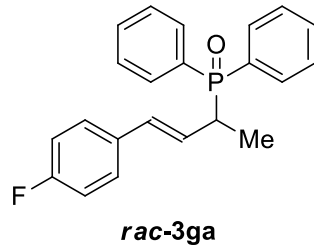


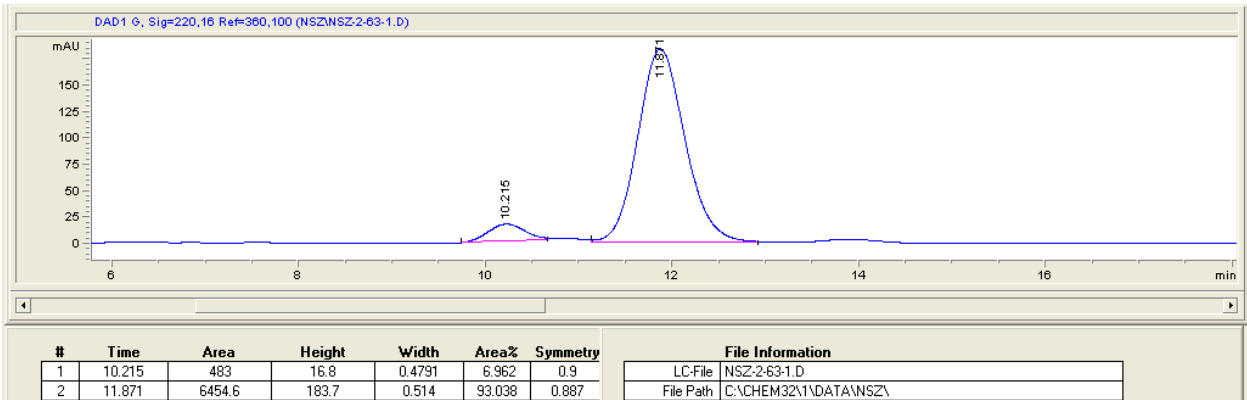
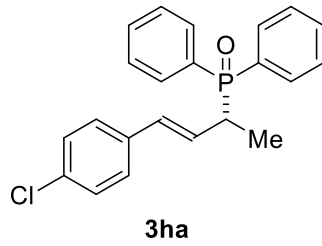
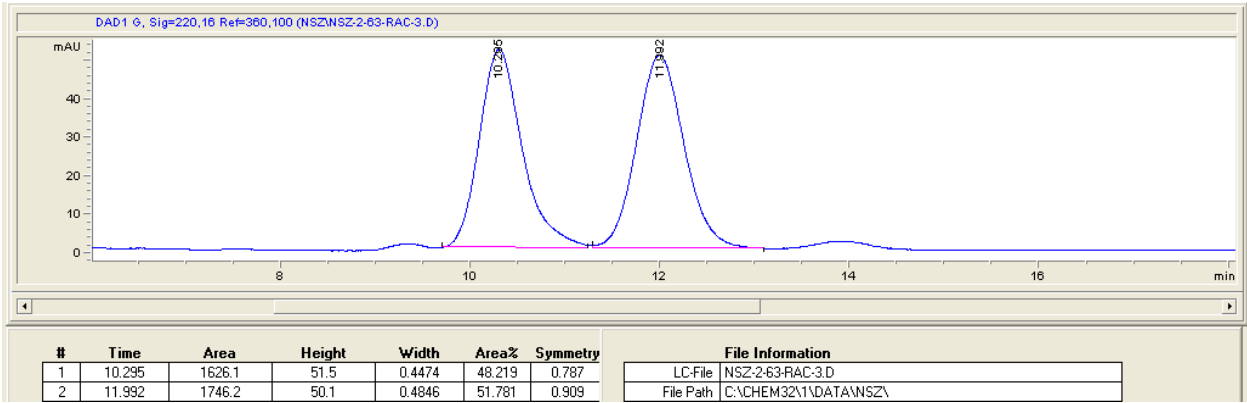
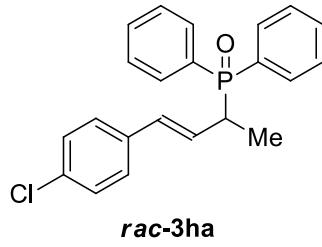
3da

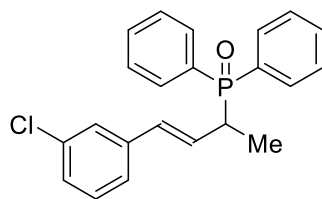




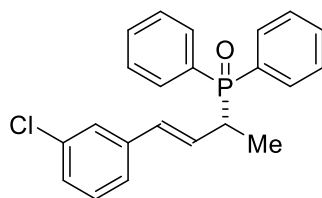
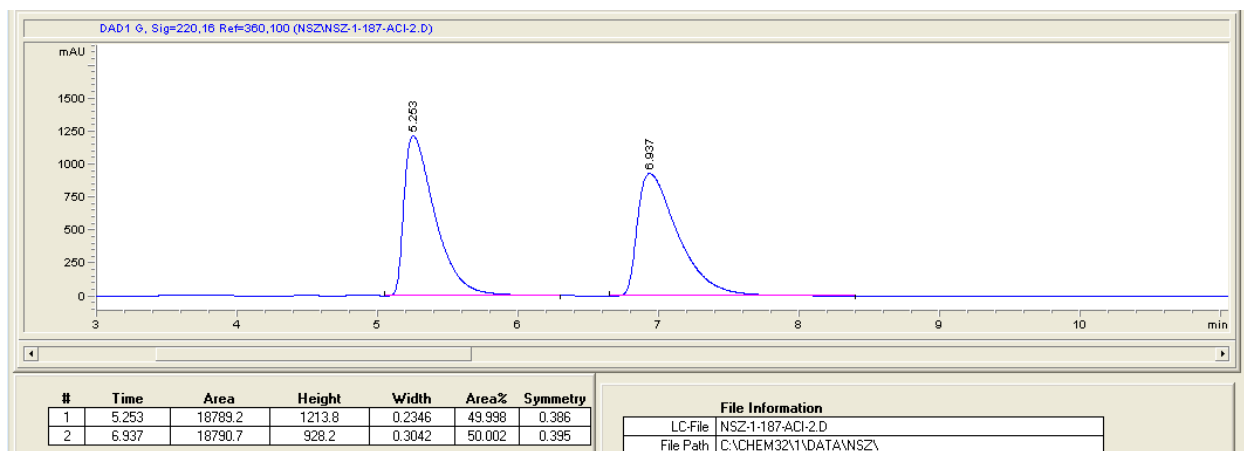




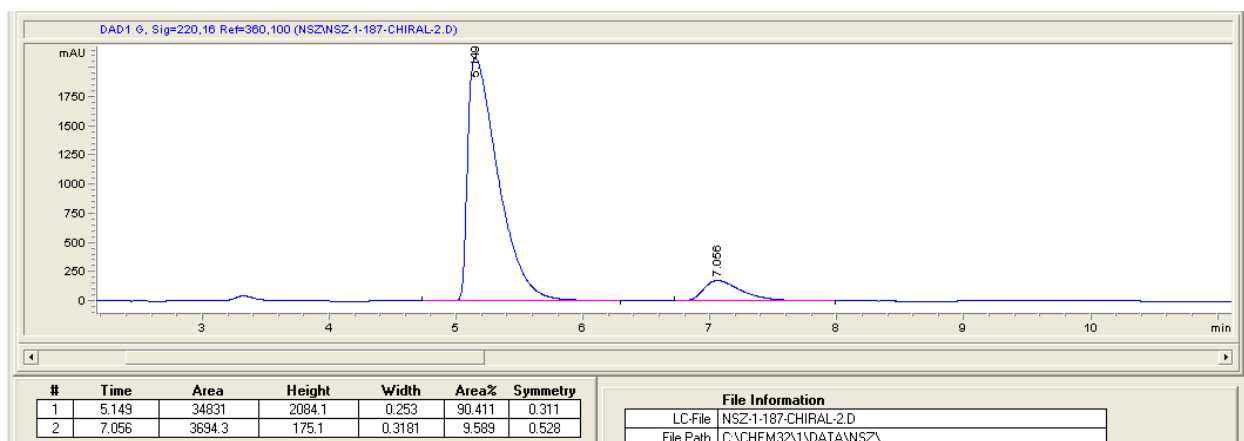


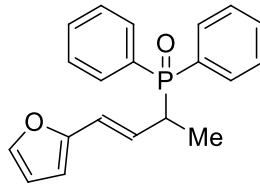


rac-3ia

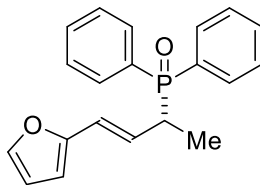
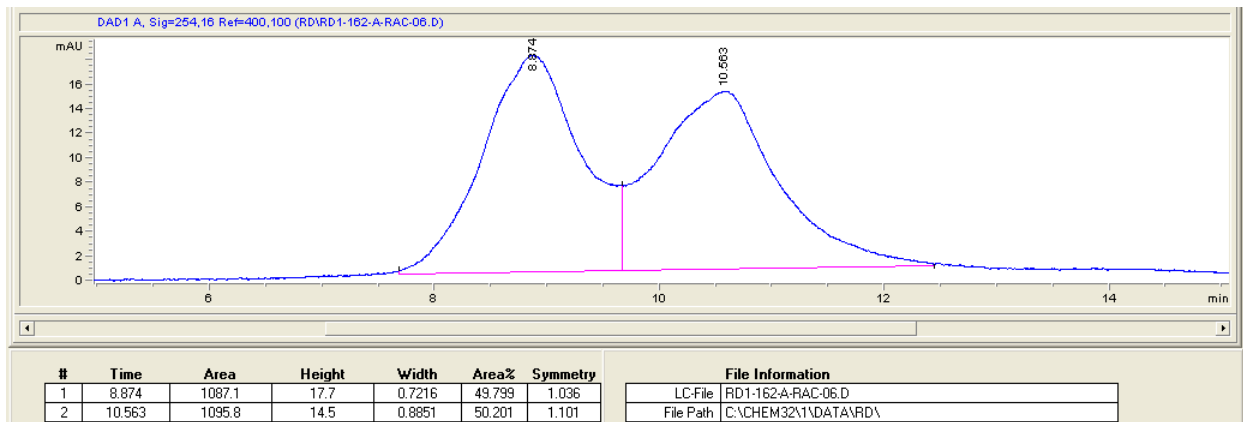


3ia

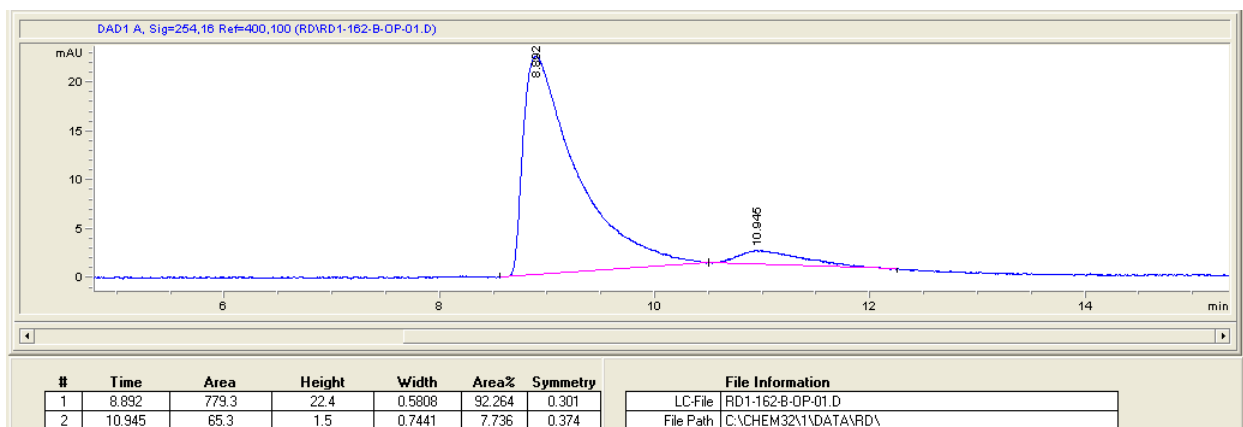


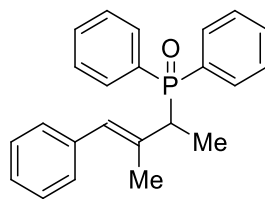


rac-3ja

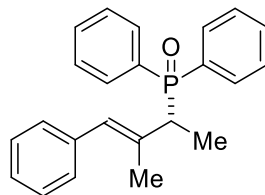
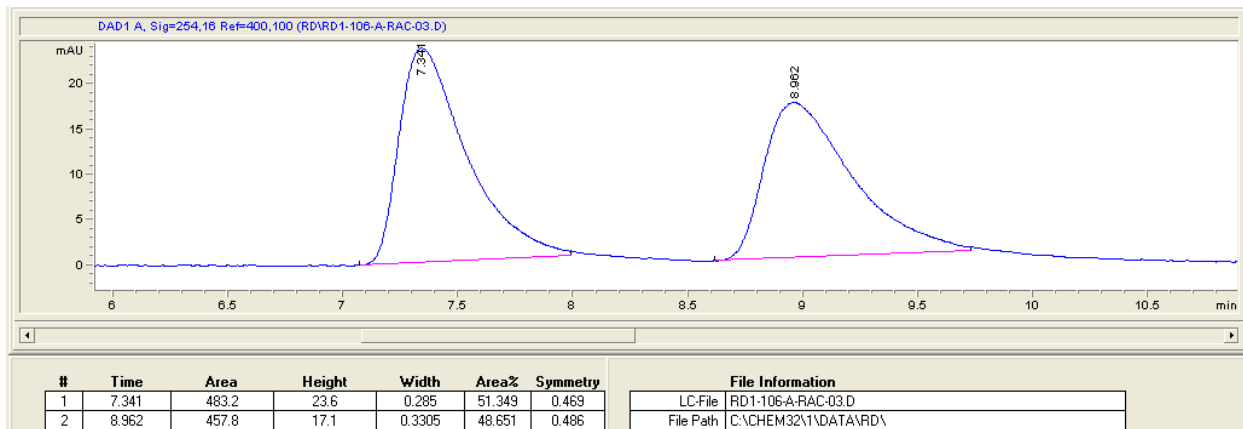


3ja

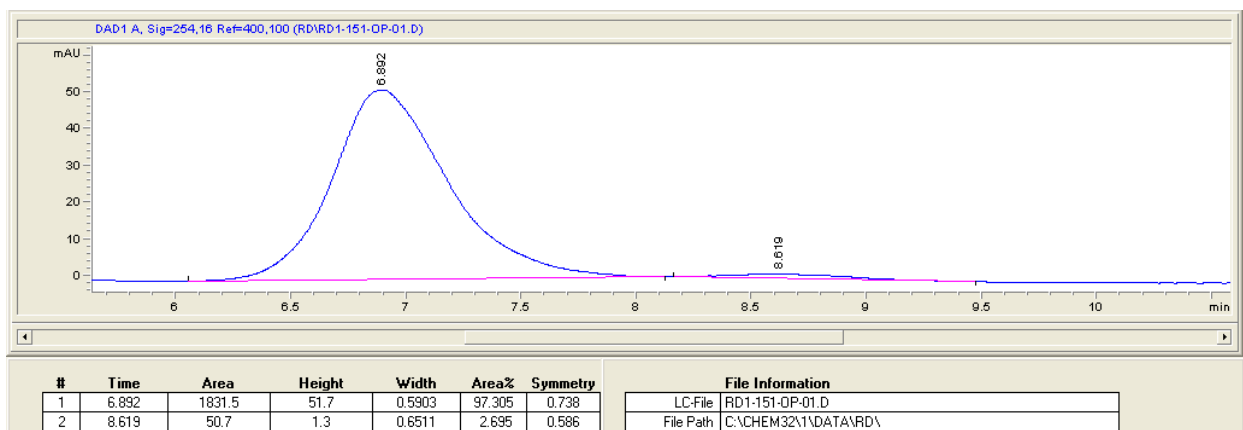


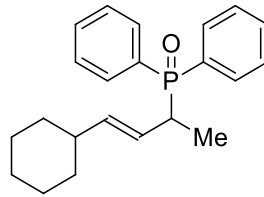


rac-3ka

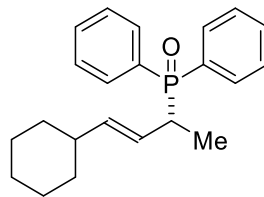
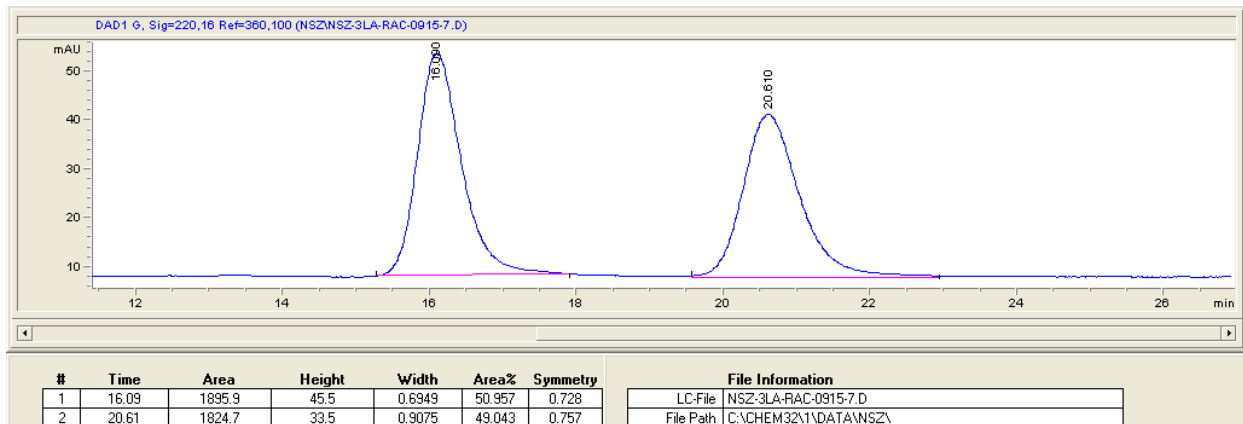


3ka

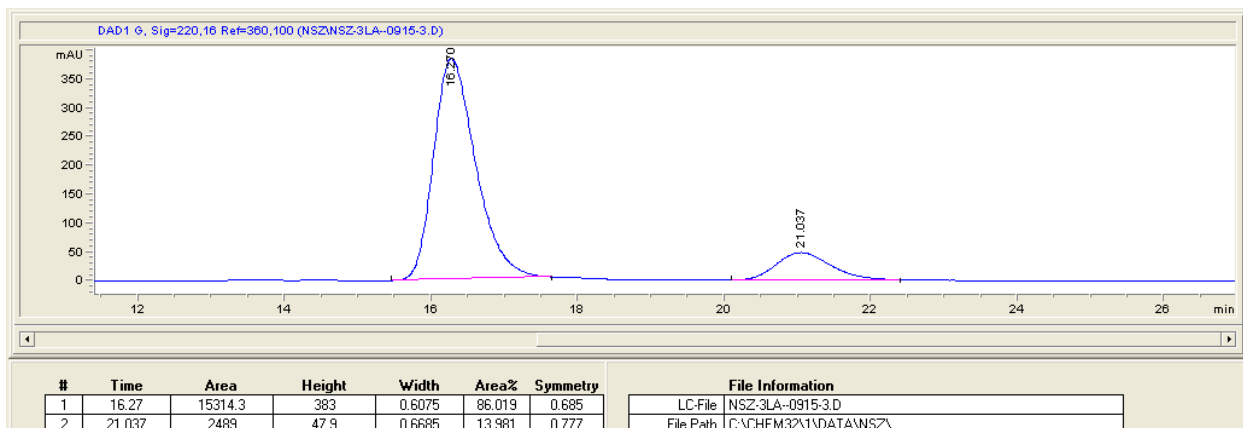


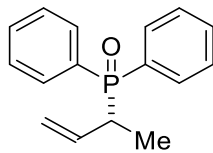


rac-3la

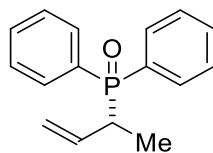
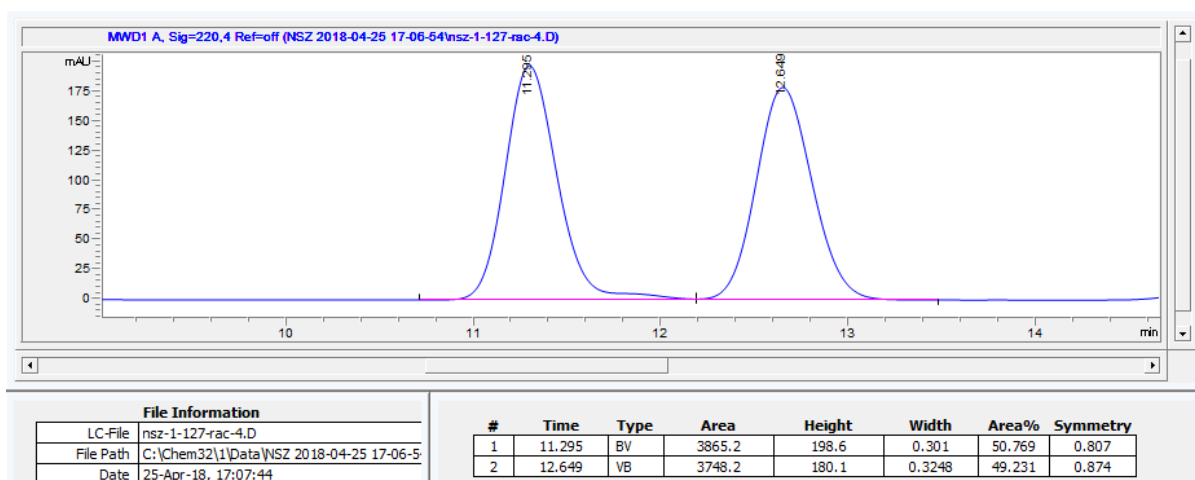


3la

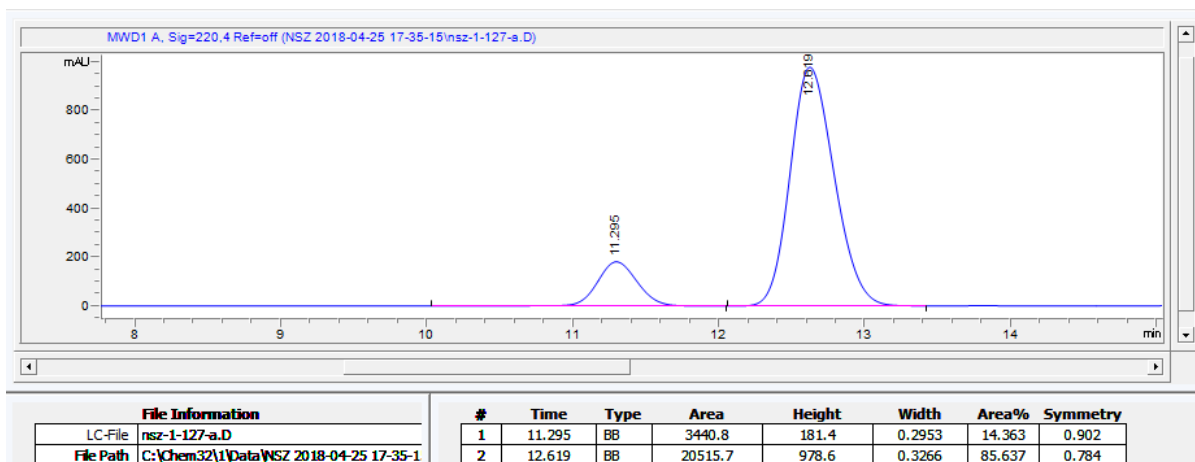


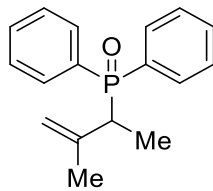


rac-3ma

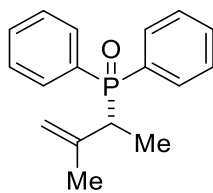
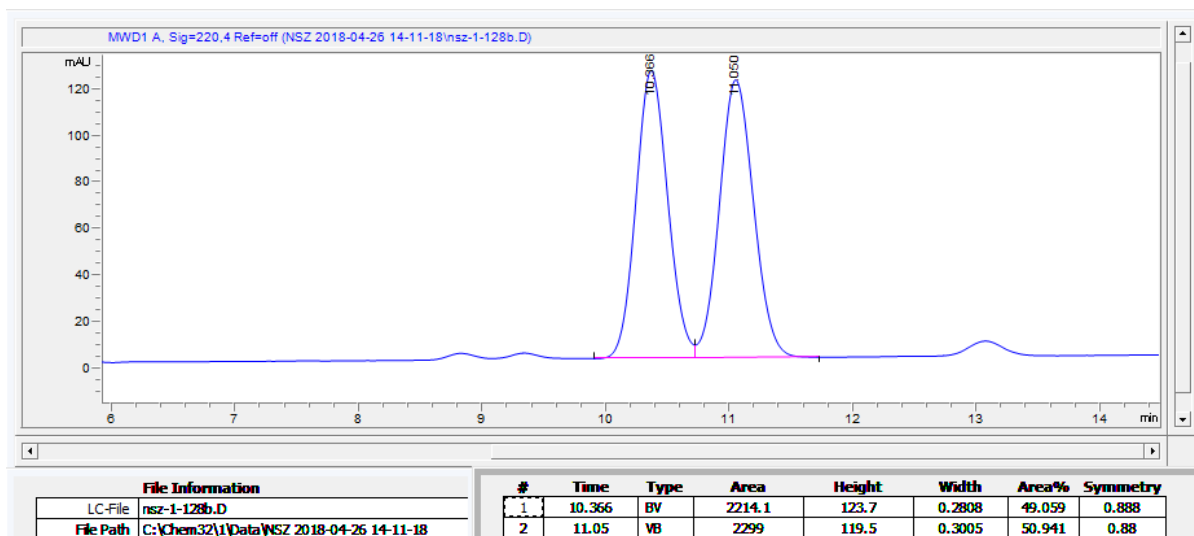


3ma

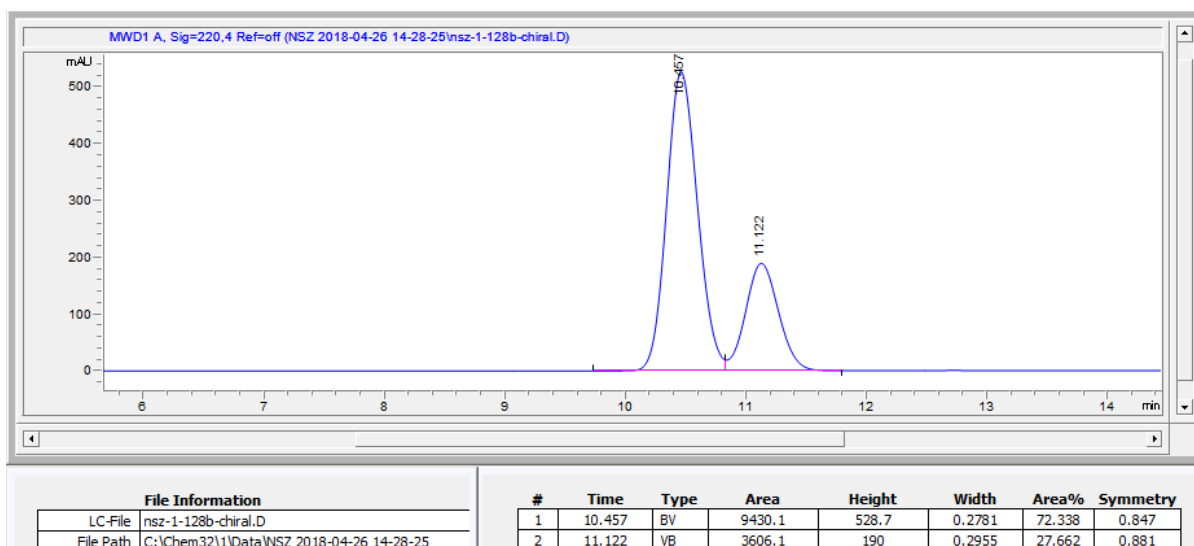


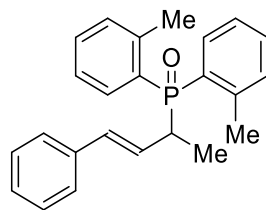


rac-3na

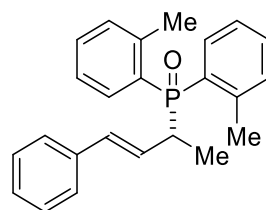
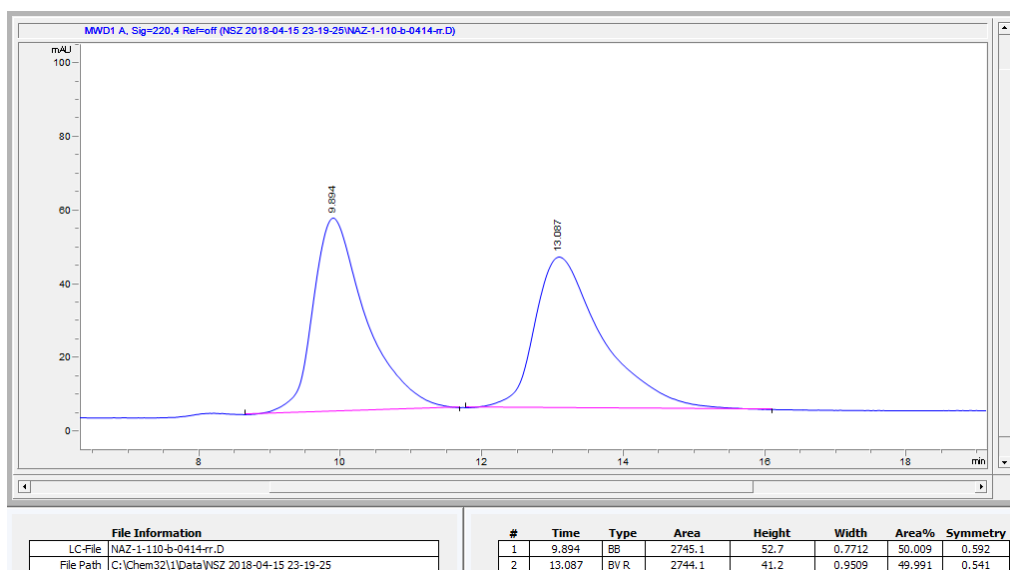


3na

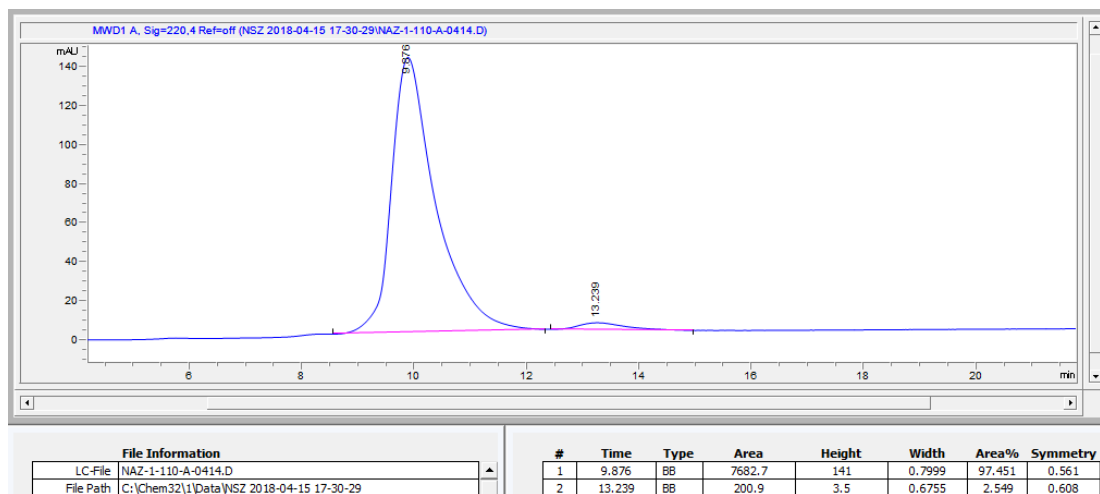


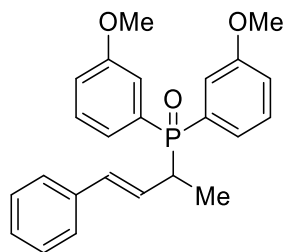


rac-3ab

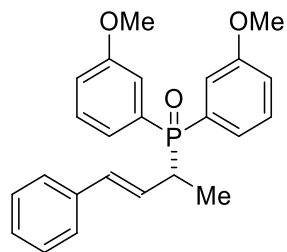
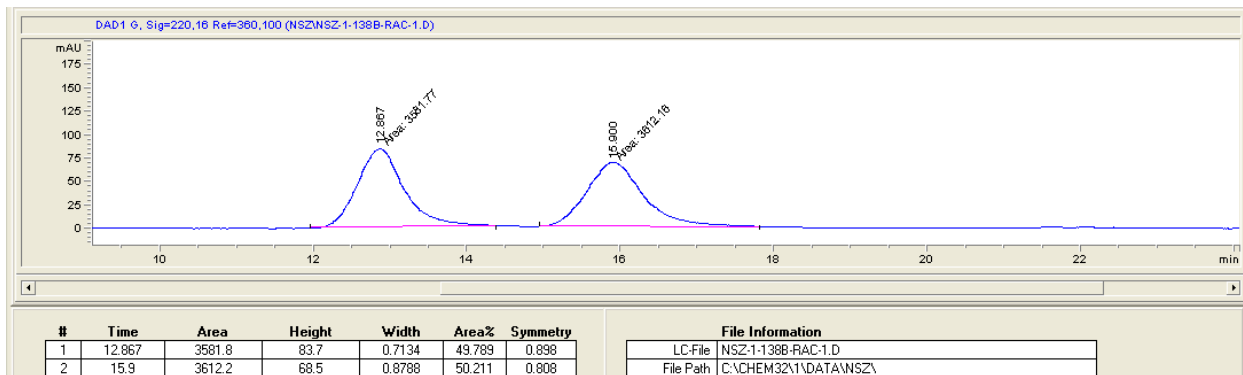


3ab

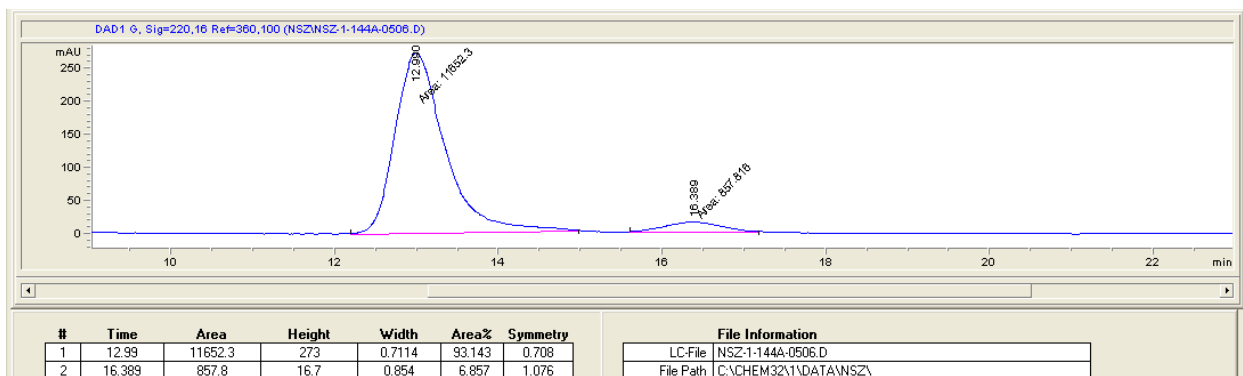


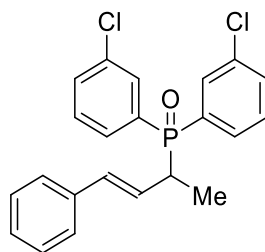


rac-3ac

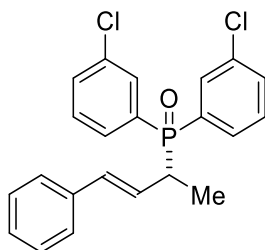
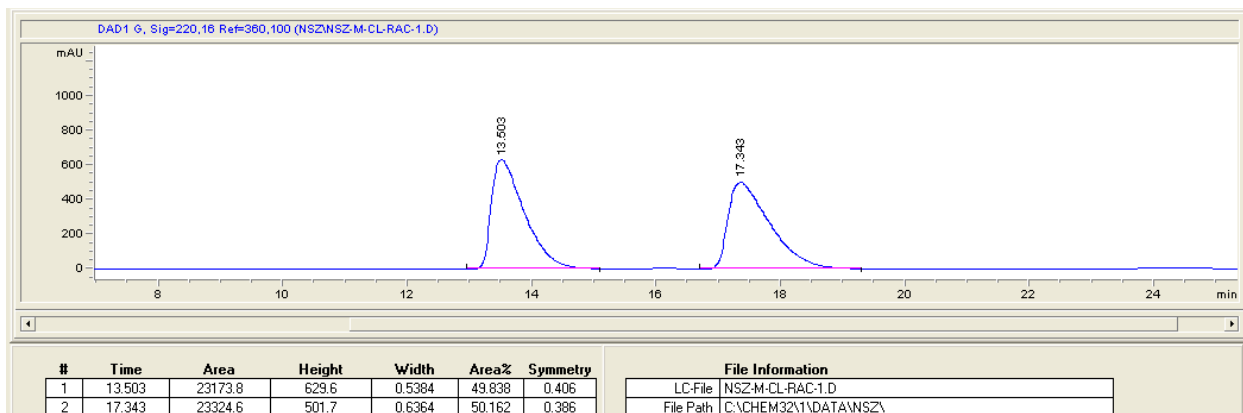


3ac

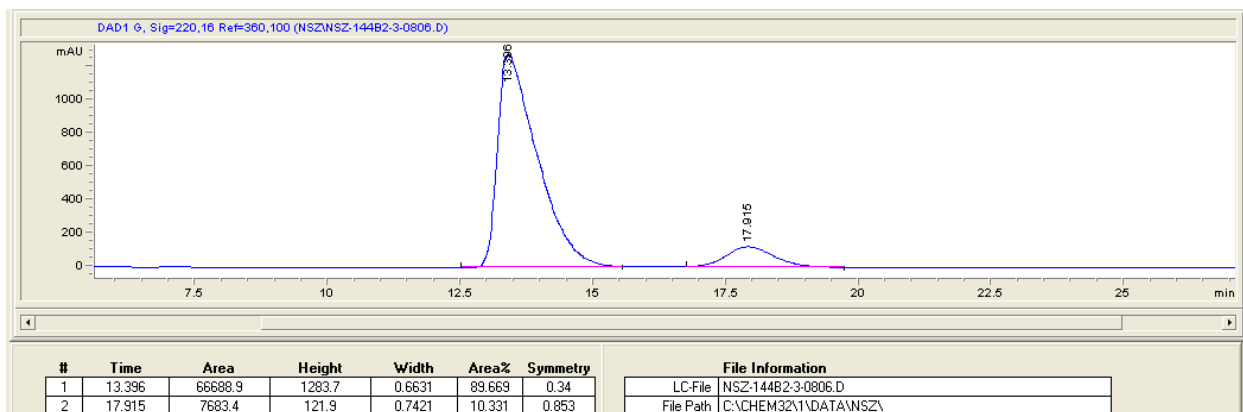


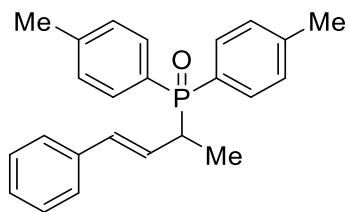


rac-3ad

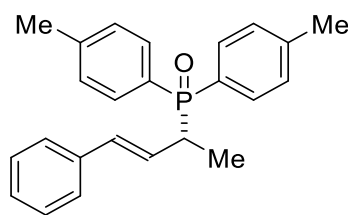
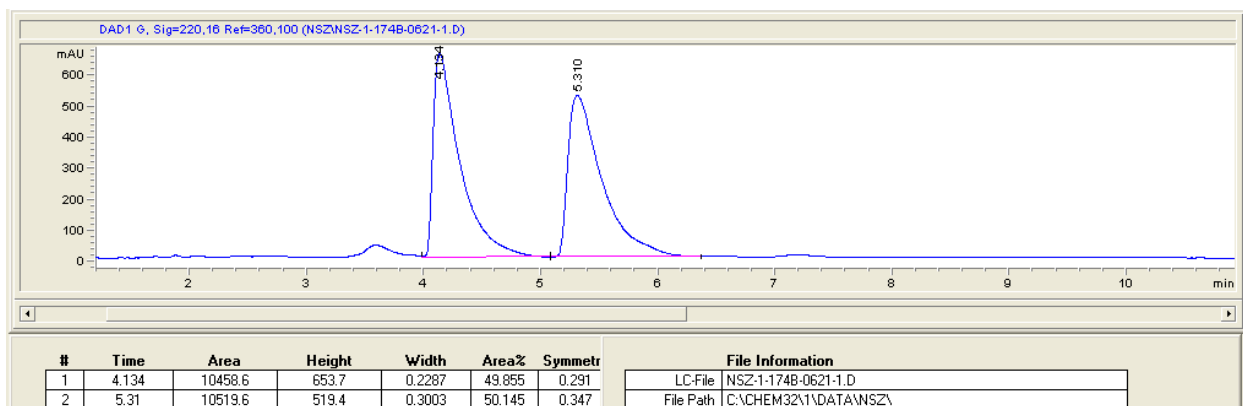


3ad

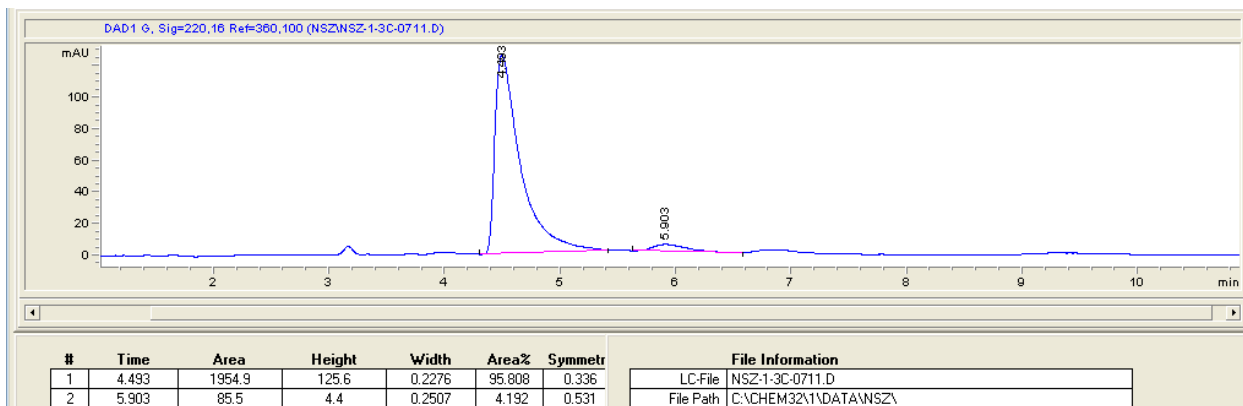


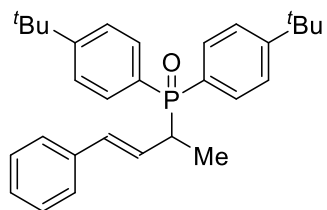


rac-3ae

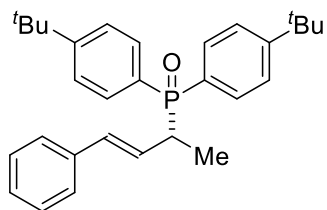
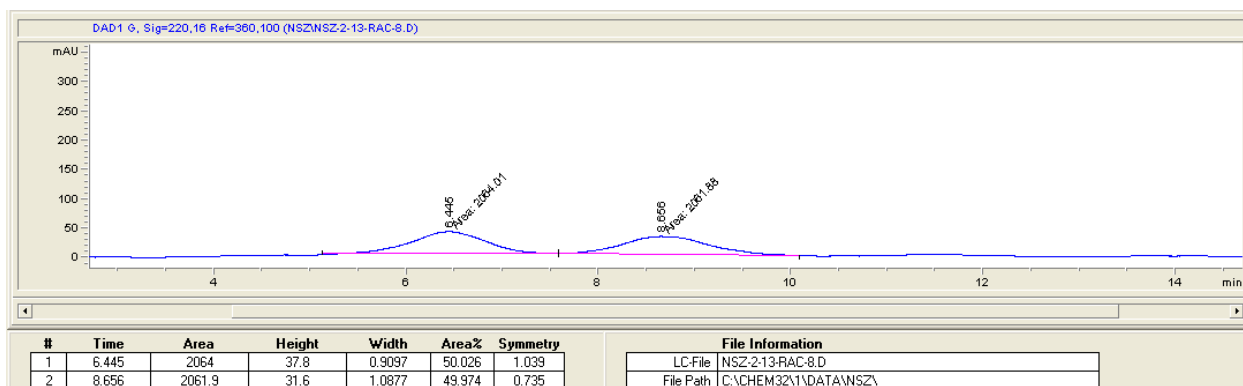


3ae

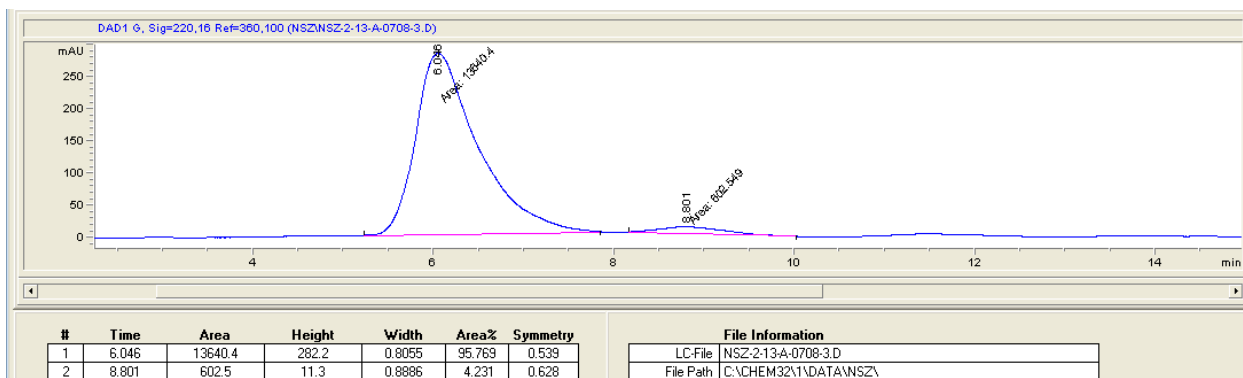


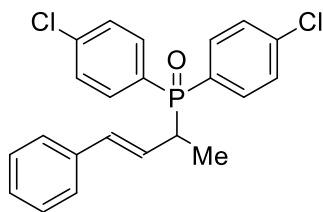


rac-3af

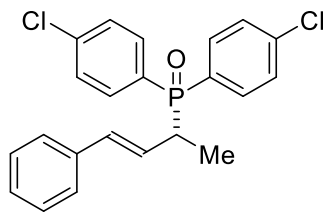
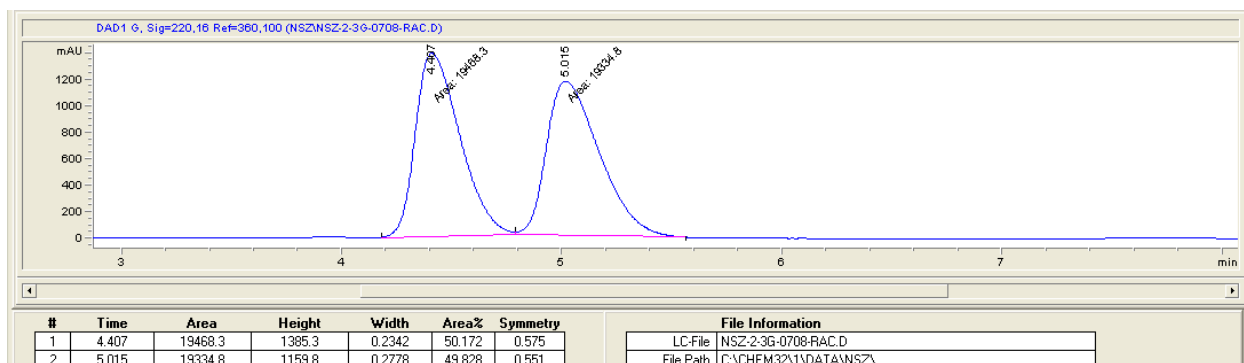


3af

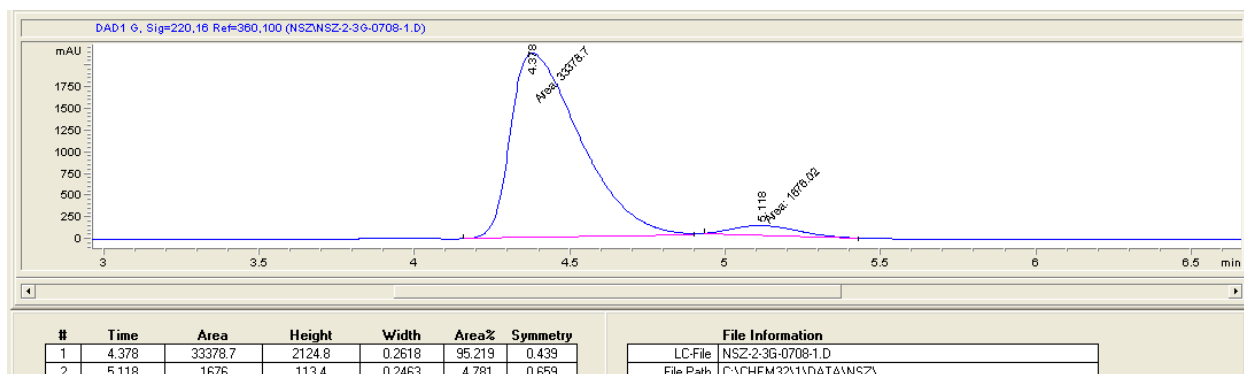


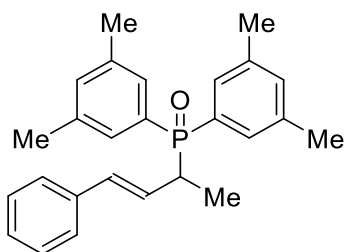


***rac*-3ag**

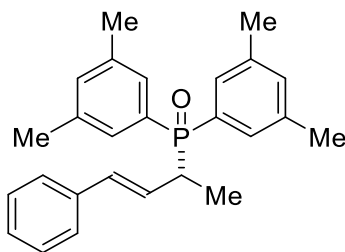
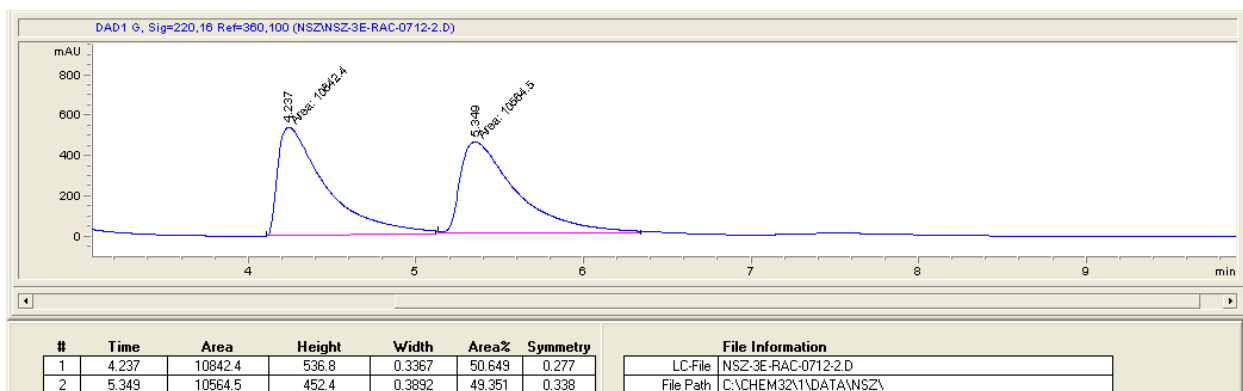


3ag

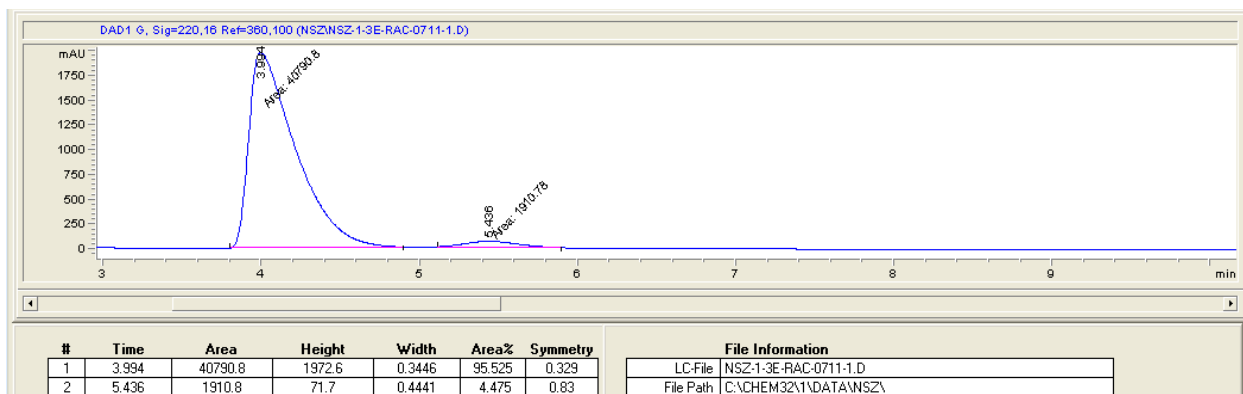


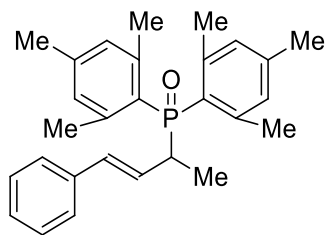


rac-3ah

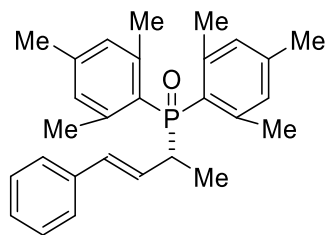
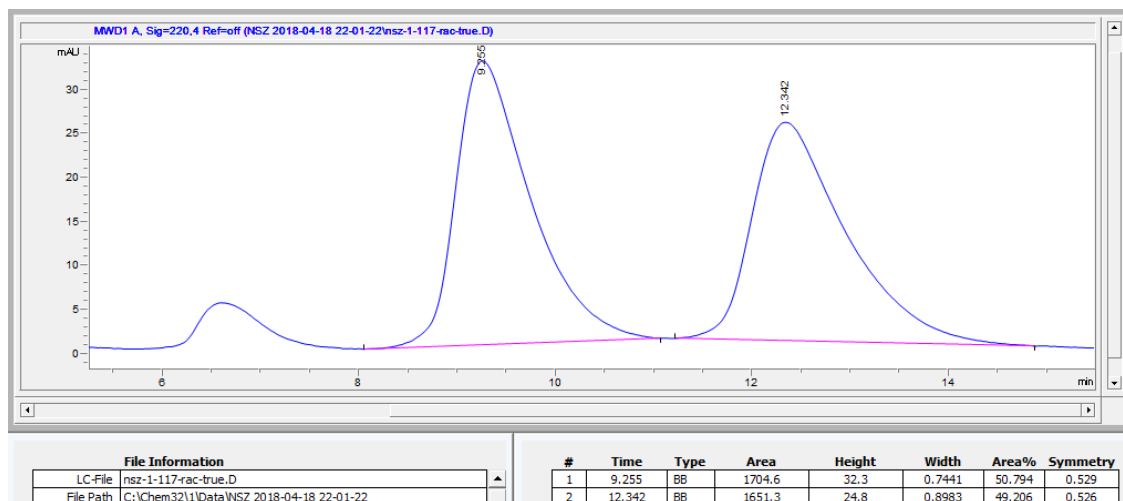


3ah

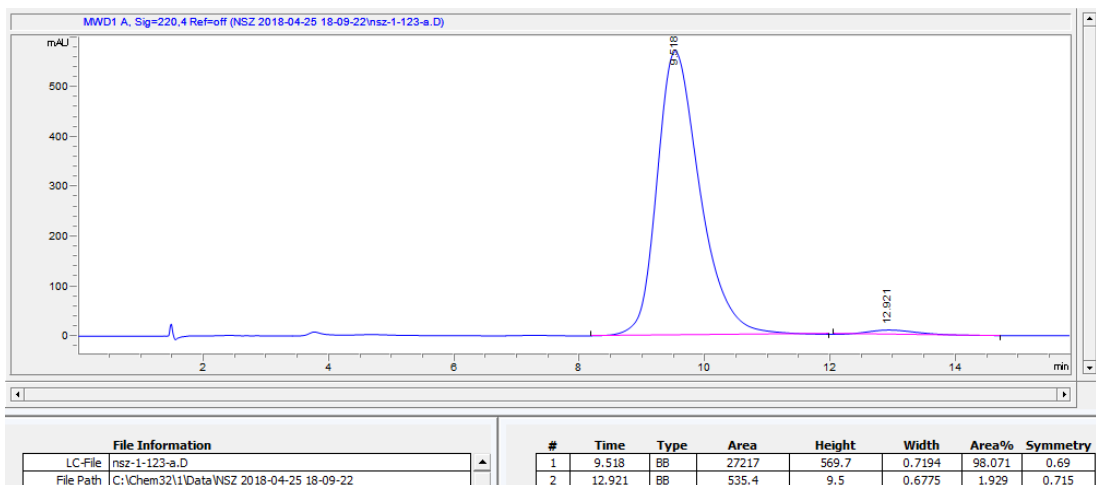


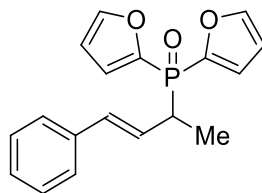


rac-3ai

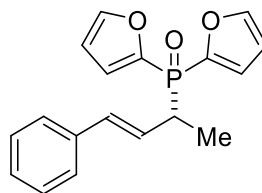
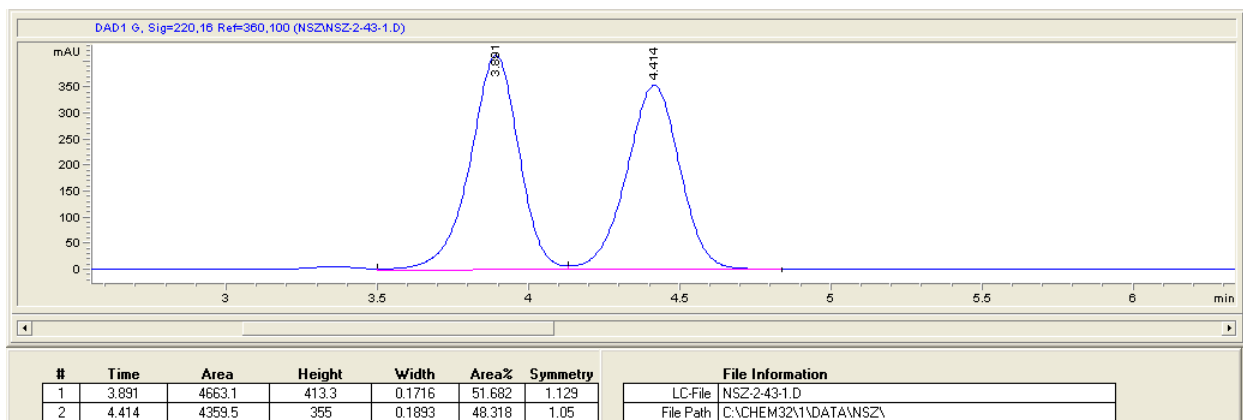


3ai

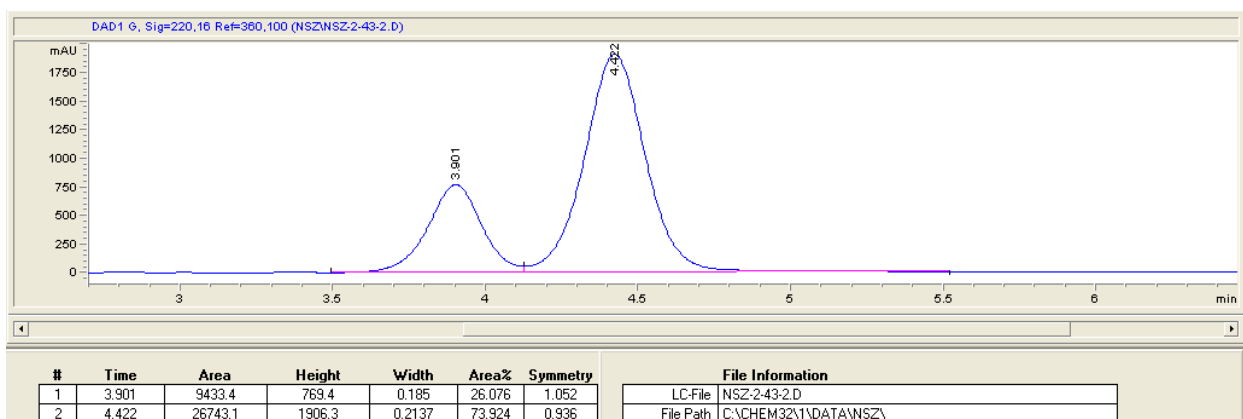


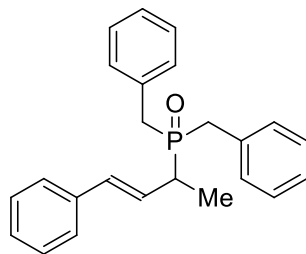


rac-3aj

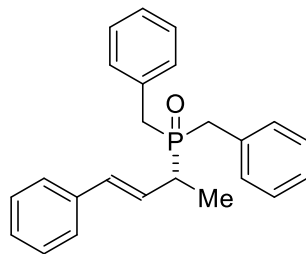
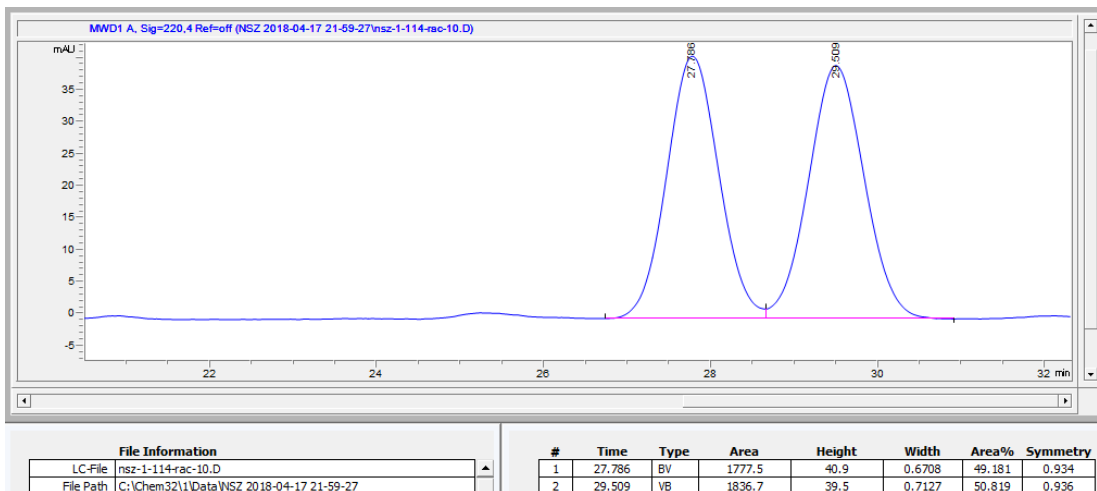


3aj

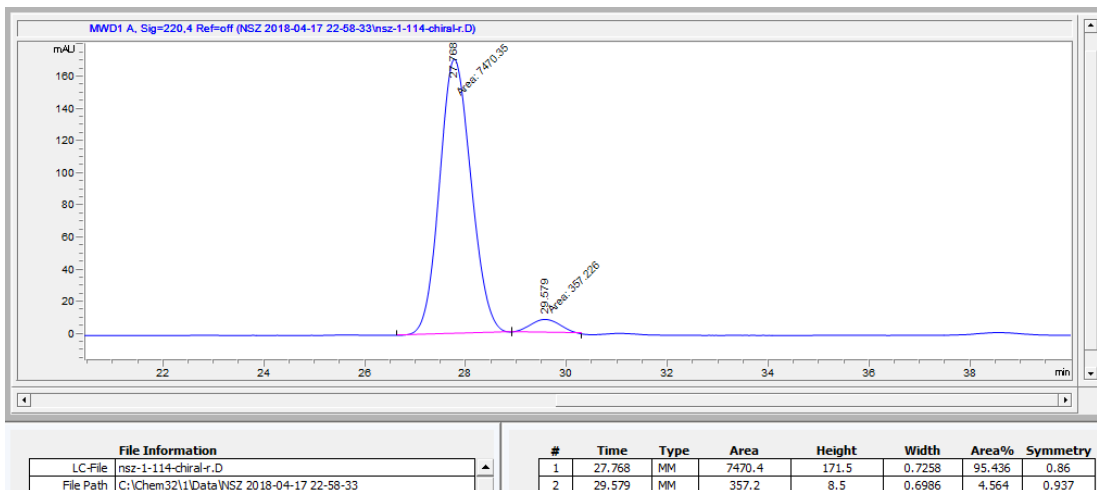


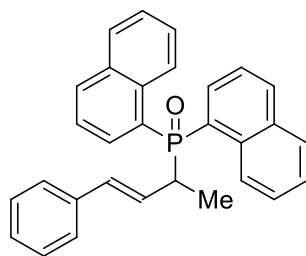


rac-3ak

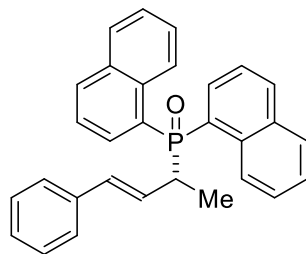
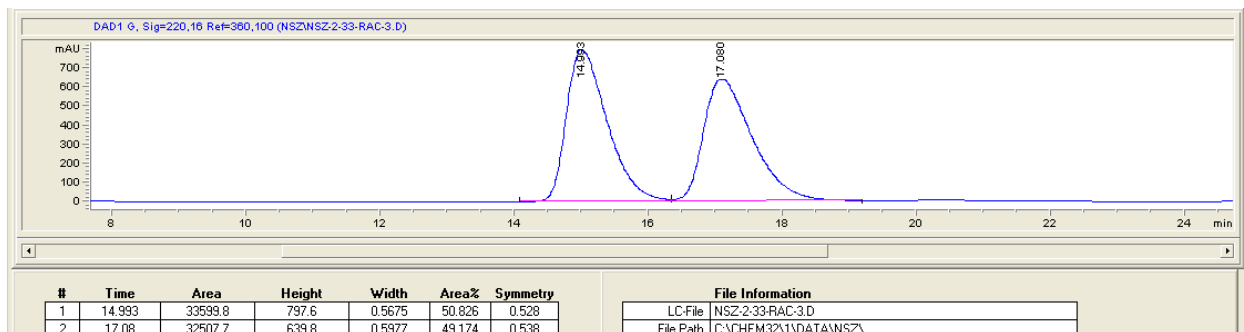


3ak

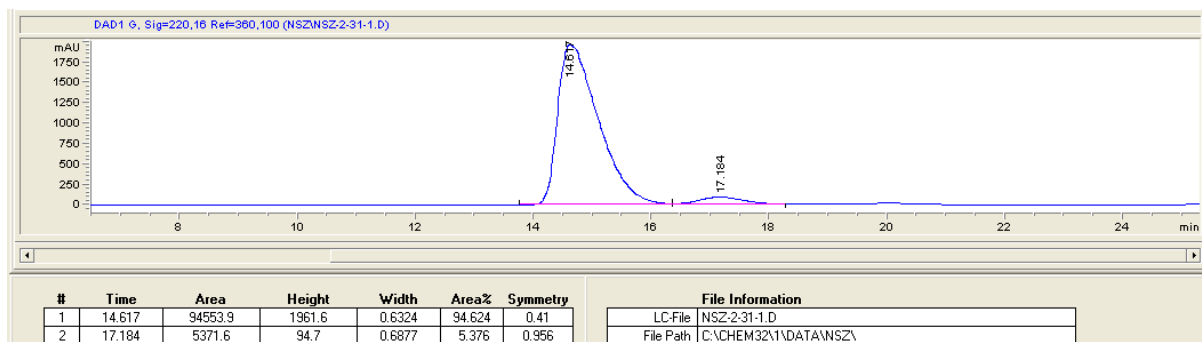


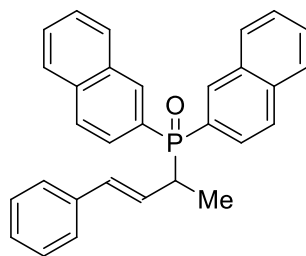


rac-3al

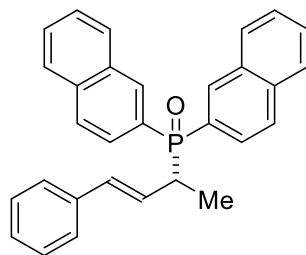
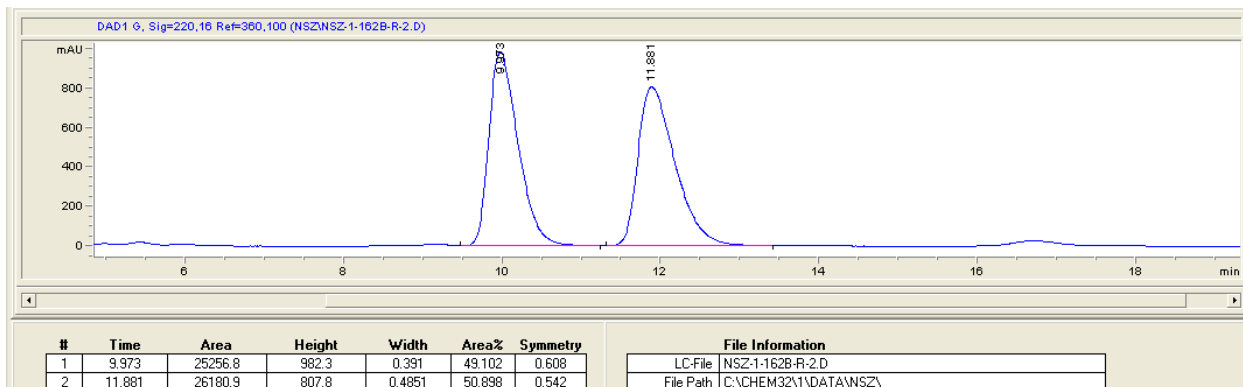


3al

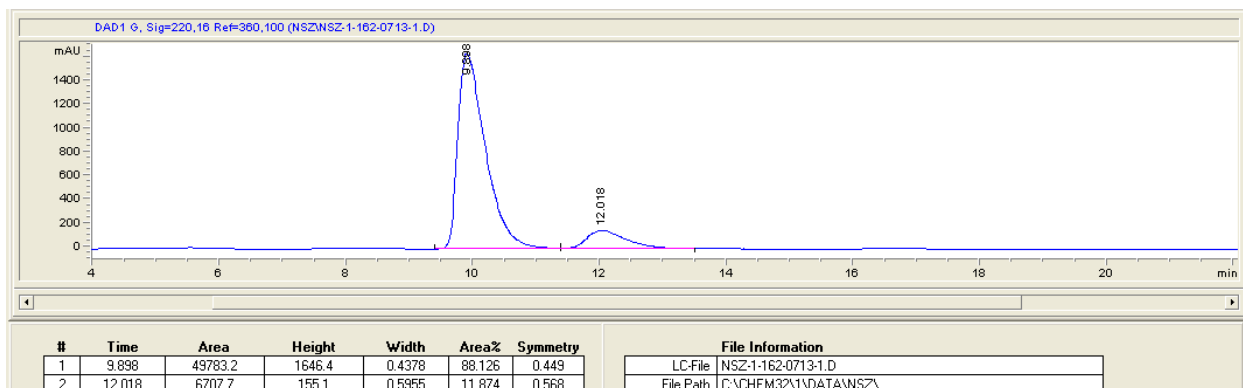




rac-3am



3am



7. References

- (1) Preuß, T.; Saak, W.; Doye, S. *Chem. Eur. J.* **2013**, *19*, 3833.
- (2) Adamson, N. J.; Hull, E.; Malcolmson, S. J. *J. Am. Chem. Soc.* **2017**, *139*, 7180.
- (3) Busacca, C. A.; Lorenz, J. C.; Grinberg, N.; Haddad, N.; Hrapchak, M.; Latli, B.; Lee, H.; Sablia, P.; Saha, A.; Sarvestani, M.; Shen, S.; Varsolona, R.; Wei, X.; Senanayake, C. H. *Org. Lett.* **2005**, *7*, 4277.
- (4) Bunlaksananusorn, T.; Knochel, P. *J. Org. Chem.* **2004**, *69*, 4595.
- (5) Kortmann, F. A.; Chang, M. C.; Otten, E.; Couzijn, E. P. A.; Lutz, M.; Minnaard, A. J. *Chem. Sci.* **2014**, *5*, 1322.
- (6) Compound **S1** was prepared following a known procedure, see: Mao, J.; Bao, W. *Org. Lett.* **2014**, *16*, 2646.
- (7) Wang, Q.; Wei, H.-X.; Schlosser, M. *Eur. J. Org. Chem.* **1999**, 3263.

Appendix 4 Supporting Information for Chapter 4
Enantioselective Addition of α -Nitroesters to Alkynes¹

Table of Contents	Page
1. Materials and Methods	331
2. Nitrocarbonyl and Alkyne Coupling	332
3. Nitrocarbonyl and Alkyne Coupling Optimization	342
4. Preparation of Starting Materials	347
5. Mechanistic Experiments	357
6. Reduction of Allylic Nitroester 3aa to Amino Ester 6	361
7. X-Ray Crystallographic Data	362
8. References	374
9. NMR Spectra	375
10. SFC Traces	425

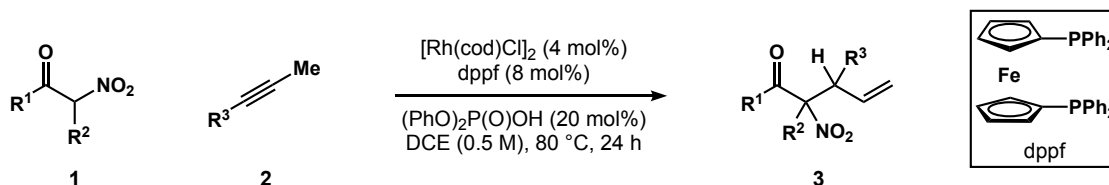
¹ For additional details, see: Davison, R. T.; Parker, P. D.; Hou, X.; Chung, C. P.; Augustine, S. A.; Dong, V. M. *Angew. Chem. Int. Ed.* **2021**, *60*, 4599–4603.

1. Materials and Methods

Commercial reagents were purchased from Sigma Aldrich, Strem, Alfa Aesar, Acros Organics or TCI and used without further purification. 1,2-Dichloroethane (DCE), toluene (PhMe), and tetrahydrofuran (THF) were purified using an Innovative Technologies Pure Solv system, degassed by three freeze-pump-thaw cycles, and stored over 3 Å MS within a N₂ filled glove box. Dimethylsulfoxide (DMSO), bromoform (CHBr₃) and dimethylformamide (DMF) were used without further purification (anhydrous >99.9% from Sigma Aldrich). All experiments were performed in oven-dried or flame-dried glassware under an atmosphere of N₂ or in a glove box with a N₂ atmosphere. Reactions were monitored using either thin-layer chromatography (TLC; EMD Silica Gel 60 F₂₅₄ plates) or gas chromatography using an Agilent Technologies 7890A GC system equipped with an Agilent Technologies 5975C inert XL EI/CI MSD. Visualization of the developed plates was performed under UV light (254 nm) or with a KMnO₄ stain. Organic solutions were concentrated under reduced pressure on a Büchi rotary evaporator. Purification and isolation of products was performed via silica gel chromatography (flash column chromatography or preparative thin-layer chromatography). Column chromatography was performed with Silicycle Silia-P Flash Silica Gel using glass columns. ¹H, ²H, ¹³C, and ¹⁹F NMR spectra were recorded on a Bruker CRYO-500 or DRX-400 spectrometer. ¹H NMR spectra were internally referenced to the residual solvent signal or TMS. ¹³C NMR spectra were internally referenced to the residual solvent signal. Data for ¹H NMR are reported as follows: chemical shift (δ ppm), multiplicity (s = singlet, d = doublet, t = triplet, q = quartet, m = multiplet, br = broad), coupling constant (Hz), integration. Data for ¹³C and ¹⁹F NMR are reported in terms of chemical shift (δ ppm). Infrared (IR) spectra were obtained on a Nicolet iS5 FT-IR spectrometer equipped with an iD5 ATR accessory, and are reported in terms of frequency of absorption (cm⁻¹). High resolution mass spectra (HRMS) were obtained by the University of California, Irvine Mass Spectrometry Center on a Micromass 70S-250 Spectrometer (EI) or an ABI/Sciex QStar Mass Spectrometer (ESI). Enantiomeric ratio (*er*) for enantioselective reactions was determined by chiral SFC analysis using an Agilent Technologies HPLC (1200 series) system and Aurora A5 Fusion. Starting materials **1a**, **2a**, **2n** and all other reagents used for the synthesis of non-commercial starting materials **1**, **2**, and **5** were used without further purification from commercial sources (Sigma Aldrich, Combi-Blocks, Solvias and Alfa Aesar).

2. Nitrocarbonyl and Alkyne Coupling

A. General Procedure for Racemic Allylic Nitrocarbonyls



In a N_2 -filled glovebox, to a 1 dram vial equipped with a magnetic stir bar was added $[\text{Rh}(\text{cod})\text{Cl}]_2$ (2.0 mg, 0.004 mmol, 4 mol%), dppf (4.4 mg, 0.008 mmol, 8 mol%), diphenyl phosphate (5.0 mg, 0.02 mmol, 20 mol%), nitrocarbonyl **1** (0.1 mmol, 1 equiv.), alkyne **2** (0.15 mmol, 1.5 equiv.) and DCE (200 μL , 0.5 M). The vial was then sealed with a Teflon-lined screw cap and heated to 80 °C for 24 hours. The resulting mixture was then cooled to room temperature, filtered through a pad of silica gel, and concentrated *in vacuo*. Diastereo- and regioselectivity ratios (*dr* and *rr*, respectively) were determined by ^1H NMR analysis of the crude reaction mixture. Allylic nitrocarbonyl **3** was isolated by flash column chromatography or preparatory TLC.

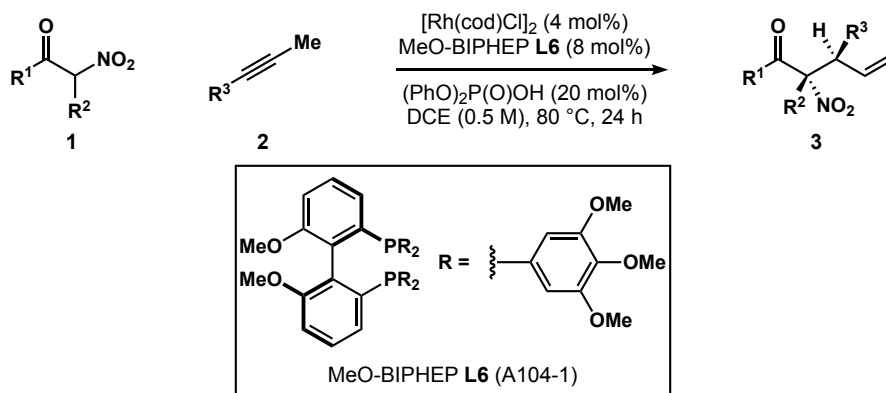
N-benzyl-2-methyl-2-nitro-3-phenylpent-4-enamide (Table 4.1, entry 3)

The title compound was synthesized according to general procedure A on 0.05 mmol scale and isolated by preparatory TLC (90:10 hexanes:EtOAc) as a yellow solid [85% yield (^1H NMR yield internally referenced to triphenylmethane), 10:1 *dr*, >20:1 *rr*]. ^1H NMR (400 MHz, CDCl_3) δ 7.36 – 7.31 (m, 3H), 7.28 – 7.26 (m, 3H), 7.21 – 7.19 (m, 2H), 7.14 – 7.12 (m, 2H), 6.93 (s, 1H), 6.23 (ddd, $J = 16.8, 10.1,$ and 8.9 Hz, 1H), 5.22 – 5.17 (m, 2H), 4.42 (dd, $J = 14.7$ and 6.0 Hz, 1H), 4.35 – 4.31 (m, 2H), 1.78 (s, 3H). ^{13}C NMR (126 MHz, CDCl_3) δ 165.0, 136.9, 136.3, 133.8, 129.1, 128.9, 128.8, 128.2, 128.1, 128.0, 120.2, 98.4, 57.3, 44.5, 18.9. IR (ATR): 3341, 2931, 1659, 1550, 1537, 1362, 934, 868 cm^{-1} . HRMS calculated for $\text{C}_{19}\text{H}_{20}\text{N}_2\text{O}_3\text{Na}$ $[\text{M}+\text{Na}]^+$ 347.1372, found 347.1364.

N-benzyl-2-methyl-2-nitro-*N*,3-diphenylpent-4-enamide (Table 4.1, entry 4)

The title compound was synthesized according to general procedure A on 0.05 mmol scale and isolated by preparatory TLC (90:10 hexanes:EtOAc) as a yellow solid [30% yield (^1H NMR yield internally referenced to triphenylmethane), 5:1 *dr*, >20:1 *rr*]. ^1H NMR (500 MHz, CDCl_3) δ 7.29 – 7.23 (m, 11H), 7.17 – 7.15 (m, 2H), 7.12 – 7.10 (m, 2H), 6.31 (ddd, $J = 17.1, 10.4,$ and 7.5 Hz, 1H), 5.18 (dt, $J = 10.5$ and 1.3 Hz, 1H), 5.05 (dt, $J = 16.9$ and 1.4 Hz, 1H), 4.93 (d, $J = 14.1$ Hz, 1H), 4.75 (d, $J = 14.2$ Hz, 1H), 4.59 (d, $J = 7.5$ Hz, 1H), 1.45 (s, 3H). ^{13}C NMR (126 MHz, CDCl_3) δ 165.8, 137.1, 136.3, 135.8, 130.2, 128.97, 128.95, 128.45, 128.44, 127.7, 127.7, 119.0, 96.5, 56.8, 56.6, 22.0. IR (ATR): 2962, 1653, 1542, 1494, 1394, 1260, 1078, 1023, 799 cm^{-1} . HRMS calculated for $\text{C}_{25}\text{H}_{24}\text{N}_2\text{O}_3\text{Na}$ $[\text{M}+\text{Na}]^+$ 423.1685, found 423.1689.

B. General Procedure for Enantioenriched Allylic Nitrocarbonyls



In a N_2 -filled glovebox, to a 1 dram vial equipped with a magnetic stir bar was added $[\text{Rh}(\text{cod})\text{Cl}]_2$ (2.0 mg, 0.004 mmol, 4 mol%), (*R*)-MeO-BIPHEP (Solvias Catalog #: A104-1, 7.5 mg, 0.008 mmol, 8 mol%), diphenyl phosphate (5.0 mg, 0.02 mmol, 20 mol%), nitrocarbonyl **1** (0.1 mmol, 1 equiv.), alkyne **2** (0.15 mmol, 1.5 equiv.) and DCE (200 μL , 0.5 M). The vial was then sealed with a Teflon-lined screw cap and heated to 80 $^\circ\text{C}$ for 24 hours. The resulting mixture was then cooled to room temperature and concentrated *in vacuo*. Diastereo- and regioselectivity ratios (*dr* and *rr*, respectively) were determined by ^1H NMR analysis of the crude reaction mixture. Allylic nitrocarbonyl **3** was isolated by flash column chromatography or preparatory TLC.

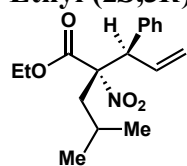
Ethyl (2*S*,3*R*)-2-methyl-2-nitro-3-phenylpent-4-enoate (**3aa**)

The title compound was synthesized according to general procedure B on 1 mmol scale and isolated by FCC (20:1 hexanes:EtOAc) as a yellow oil [237 mg, 90% yield, 97:3 *er*, >20:1 *dr*, >20:1 *rr*, $[\alpha]_D^{24} = -52.1^\circ$ (*c* 1.0, CHCl_3)]. ^1H NMR (400 MHz, CDCl_3) δ 7.34 – 7.28 (m, 3H), 7.25–7.22 (m, 2H), 6.31 (ddd, $J = 16.9, 10.3, 8.4$ Hz, 1H), 5.24 (d, $J = 8$ Hz, 1H), 5.18 (d, $J = 16$ Hz, 1H), 4.41 (d, $J = 8.4$ Hz, 1H), 4.21 – 4.09 (m, 2H), 1.78 (s, 3H), 1.20 (t, $J = 7.1$ Hz, 3H). ^{13}C NMR (101 MHz, CDCl_3) δ 166.7, 136.7, 134.6, 129.8, 128.9, 128.2, 120.0, 96.4, 63.1, 55.3, 20.2, 13.9. IR (ATR): 2985, 1746, 1637, 1549, 1454, 1243, 1144, 855, 702 cm^{-1} . HRMS calculated for $\text{C}_{14}\text{H}_{17}\text{NO}_4\text{Na}$ $[\text{M}+\text{Na}]^+$ 286.1055, found 286.1057. Chiral SFC: 150 mm CHIRALCEL OJ-H, 2% *i*PrOH, 2 mL/min, 220 nm, 44 $^\circ\text{C}$, nozzle pressure = 200 bar CO_2 , t_{R1} (minor) = 1.4 min, t_{R2} (major) = 1.6 min.

Methyl (2*S*,3*R*)-2-ethyl-2-nitro-3-phenylpent-4-enoate (**3ba**)

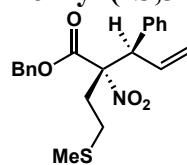
The title compound was synthesized according to general procedure B and isolated by preparatory TLC (10:1 hexanes:EtOAc) as a yellow oil [22.0 mg, 84% yield, 95:5 *er*, >20:1 *dr*, >20:1 *rr*, $[\alpha]_D^{24} = -66.6^\circ$ (*c* 0.7, CHCl_3)]. ^1H NMR (400 MHz, CDCl_3) δ 7.33 – 7.28 (m, 3H), 7.12 (dd, $J = 7.6$ and 2.0 Hz, 2H), 6.35 (ddd, $J = 17.0, 10.2,$ and 8.1 Hz, 1H), 5.21 (d, $J = 10.2$ Hz, 1H), 5.10 (d, $J = 11.9$ Hz, 1H), 4.23 (d, $J = 8.1$ Hz, 1H), 3.79 (s, 3H), 2.14 (dq, $J = 14.7$ and 7.4 Hz, 1H), 1.99 (dq, $J = 14.8$ and 7.4 Hz, 1H), 0.92 (t, $J = 7.4$ Hz, 3H). ^{13}C NMR (126 MHz, CDCl_3) δ 166.9, 136.5, 135.6, 129.2, 128.8, 128.2, 118.9, 99.8, 55.0, 53.2, 28.9, 8.8. IR (ATR): 2955, 1749, 1546, 1456, 1436, 1232, 1127, 992, 927 cm^{-1} . HRMS calculated for $\text{C}_{14}\text{H}_{17}\text{NO}_4\text{Na}$ $[\text{M}+\text{Na}]^+$ 281.1501, found 281.1514. Chiral SFC: 150 mm CHIRALCEL OJ-H, 2% *i*PrOH, 2 mL/min, 210 nm, 44 $^\circ\text{C}$, nozzle pressure = 200 bar CO_2 , t_{R1} (minor) = 1.7 min, t_{R2} (major) = 2.0 min.

Ethyl (2*S*,3*R*)-2-isobutyl-2-nitro-3-phenylpent-4-enoate (3da)



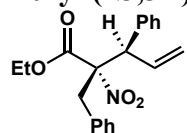
The title compound was synthesized according to general procedure B and isolated by preparatory TLC (98:2 hexanes:EtOAc) as a yellow oil [10.7 mg, 35% yield, 97:3 *er*, >20:1 *dr*, >20:1 *rr*, $[\alpha]^{24}_{\text{D}} = -13.7^\circ$ (*c* 0.6, CHCl₃)]. **¹H NMR** (400 MHz, CDCl₃) δ 7.33 – 7.28 (m, 3H), 7.10 – 7.09 (m, 2H), 6.34 (ddd, *J* = 17.5, 10.2, and 8.1 Hz, 1H), 5.20 (d, *J* = 10.3 Hz, 1H), 5.07 (d, *J* = 16.9 Hz, 1H), 4.31 – 4.21 (m, 3H), 2.01 (dd, *J* = 14.9 and 5.4 Hz, 1H), 1.83 (dd, *J* = 14.9 and 5.7 Hz, 1H), 1.77 – 1.70 (m, 1H), 1.29 (t, *J* = 7.2 Hz, 3H), 0.86 (d, *J* = 6.7 Hz, 3H), 0.83 (d, *J* = 6.6 Hz, 3H). **¹³C NMR** (126 MHz, CDCl₃) δ 166.7, 136.6, 135.7, 129.3, 128.8, 128.2, 119.0, 98.7, 62.7, 56.1, 43.9, 24.5, 23.8, 23.8, 14.0. **IR** (ATR): 2961, 2928, 2854, 1747, 1668, 1548, 1454, 1369, 1224, 1133, 1032, 925 cm⁻¹. **HRMS** calculated for C₁₇H₂₃NO₄Na [M+Na]⁺ 328.1525, found 328.1531. **Chiral SFC** (of the corresponding benzamide): 150 mm CHIRALCEL AD-H, 4% *i*PrOH, 2 mL/min, 210 nm, 44 °C, nozzle pressure = 200 bar CO₂, *t*_{R1} (major) = 4.2 min, *t*_{R2} (minor) = 7.2 min.

Benzyl (2*S*,3*R*)-2-(2-(methylthio)ethyl)-2-nitro-3-phenylpent-4-enoate (3ea)



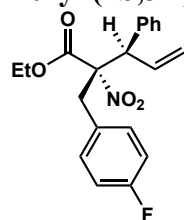
The title compound was synthesized according to general procedure B and isolated by preparatory TLC (10:1 hexanes:EtOAc) as a white solid [13.2 mg, 34% yield (76% brsm), 97:3 *er*, 6:1 *dr*, >20:1 *rr*, $[\alpha]^{24}_{\text{D}} = -14.5^\circ$ (*c* 0.7, CHCl₃)]. **¹H NMR** (500 MHz, CDCl₃) δ 7.40 – 7.36 (m, 3H), 7.34 – 7.28 (m, 5H), 7.13 – 7.10 (m, 2H), 6.34 (ddd, *J* = 16.9, 10.2, and 8.2 Hz, 1H), 5.23 (d, *J* = 12.0 Hz, 1H), 5.20 (d, *J* = 12.0 Hz, 1H), 5.19 (d, *J* = 10.3 Hz, 1H), 5.06 (dt, *J* = 16.9 and 1.1 Hz, 1H), 4.20 (d, *J* = 8.2 Hz, 1H), 2.46 – 2.32 (m, 2H), 2.24 – 2.17 (m, 2H), 1.92 (s, 3H). **¹³C NMR** (126 MHz, CDCl₃) δ 165.8, 136.0, 135.0, 134.3, 129.2, 129.1, 129.0, 129.0, 128.9, 128.4, 119.5, 98.6, 68.7, 55.9, 35.7, 28.4, 15.4. **IR** (ATR): 2913, 1738, 1545, 1453, 1263, 1227, 1166, 933 cm⁻¹. **HRMS** calculated for C₂₁H₂₃NO₄SNa [M+Na]⁺ 408.1245, found 408.1229. **Chiral SFC**: 150 mm CHIRALCEL AD-H, 1% *i*PrOH, 2 mL/min, 220 nm, 44 °C, nozzle pressure = 200 bar CO₂, *t*_{R1} (minor) = 9.8 min, *t*_{R2} (major) = 11.7 min.

Ethyl (2*S*,3*R*)-2-benzyl-2-nitro-3-phenylpent-4-enoate (3fa)



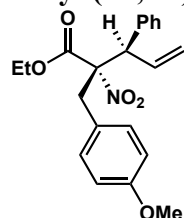
The title compound was synthesized according to general procedure B and isolated by preparatory TLC (10:1 hexanes:EtOAc) as a pale yellow solid [19.2 mg, 57% yield, 96:4 *er*, >20:1 *dr*, >20:1 *rr*, $[\alpha]^{24}_{\text{D}} = -4.8^\circ$ (*c* 0.5, CHCl₃)]. **¹H NMR** (500 MHz, CDCl₃) δ 7.39 – 7.30 (m, 3H), 7.24 – 7.23 (m, 3H), 7.19 – 7.13 (m, 4H), 6.35 (ddd, *J* = 17.5, 10.0, and 7.8 Hz, 1H), 5.23 (d, *J* = 10.3 Hz, 1H), 5.10 (d, *J* = 16.9 Hz, 1H), 4.34 (d, *J* = 7.8 Hz, 1H), 4.07 – 3.97 (m, 2H), 3.48 (d, *J* = 14.8 Hz, 1H), 3.18 (d, *J* = 14.8 Hz, 1H), 1.01 (t, *J* = 7.2 Hz, 3H). **¹³C NMR** (126 MHz, CDCl₃) δ 165.9, 136.4, 135.6, 134.0, 130.5, 129.5, 128.9, 128.4, 128.3, 127.8, 119.3, 100.2, 62.7, 56.3, 41.7, 13.6. **IR** (ATR): 2984, 1739, 1548, 1496, 1455, 1265, 1199, 1092, 928 cm⁻¹. **HRMS** calculated for C₂₀H₂₁NO₄Na [M+Na]⁺ 362.1368, found 362.1371. **Chiral SFC**: 150 mm CHIRALCEL OJ-H, 2% *i*PrOH, 2 mL/min, 210 nm, 44 °C, nozzle pressure = 200 bar CO₂, *t*_{R1} (minor) = 1.7 min, *t*_{R2} (major) = 2.4 min.

Ethyl (2*S*,3*R*)-2-(4-fluorobenzyl)-2-nitro-3-phenylpent-4-enoate (3ga)



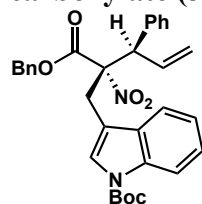
The title compound was synthesized according to general procedure B and isolated by preparatory TLC (10:1 hexanes:EtOAc) as a white solid [17.4 mg, 49% yield (96% brsm), 95:5 *er*, >20:1 *dr*, >20:1 *rr*, $[\alpha]_D^{24} = -2.1^\circ$ (*c* 0.4, CHCl₃)]. **¹H NMR** (400 MHz, CDCl₃) δ 7.38 – 7.31 (m, 3H), 7.18 – 7.12 (m, 4H), 6.94 – 6.90 (m, 2H), 6.34 (ddd, *J* = 16.9, 10.3, and 7.9 Hz, 1H), 5.24 (dd, *J* = 10.4 and 1.2 Hz, 1H), 5.10 (dt, *J* = 16.9 and 1.3 Hz, 1H), 4.32 (d, *J* = 7.9 Hz, 1H), 4.09 – 3.95 (m, 2H), 3.44 (d, *J* = 14.8 Hz, 1H), 3.16 (d, *J* = 14.8 Hz, 1H), 1.05 (t, *J* = 7.2 Hz, 3H). **¹³C NMR** (101 MHz, CDCl₃) δ 165.8, 162.5 (d, *J* = 246.7 Hz), 136.2, 135.5, 132.2 (d, *J* = 8.0 Hz), 129.8 (d, *J* = 3.4 Hz), 129.4, 129.0, 128.4, 119.4, 115.3 (d, *J* = 21.3 Hz), 100.2, 62.8, 56.5, 40.9, 13.7. **¹⁹F NMR** (376 MHz, CDCl₃) δ -114.9. **IR** (ATR): 2987, 1745, 1605, 1545, 1507, 1267, 1245, 1227, 1210, 1099, 1026, 995, 858 cm⁻¹. **HRMS** calculated for C₂₀H₂₀FNO₄Na [M+Na]⁺ 380.1274, found 380.1280. **Chiral SFC**: 150 mm CHIRALCEL OJ-H, 2% *i*PrOH, 2 mL/min, 220 nm, 44 °C, nozzle pressure = 200 bar CO₂, *t*_{R1} (minor) = 2.2 min, *t*_{R2} (major) = 5.2 min.

Ethyl (2*S*,3*R*)-2-(4-methoxybenzyl)-2-nitro-3-phenylpent-4-enoate (3ha)



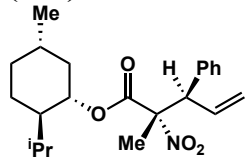
The title compound was synthesized according to general procedure B and isolated by preparatory TLC (10:1 hexanes:EtOAc) as a pale yellow solid [14.2 mg, 38% yield (65% brsm), 98:2 *er*, >20:1 *dr*, >20:1 *rr*, $[\alpha]_D^{24} = +9.5^\circ$ (*c* 0.7, CHCl₃)]. **¹H NMR** (500 MHz, CDCl₃) δ 7.36 – 7.30 (m, 3H), 7.17 – 7.16 (m, 2H), 7.07 (d, *J* = 8.7 Hz, 2H), 6.76 (d, *J* = 8.7 Hz, 2H), 6.34 (ddd, *J* = 17.0, 10.3, and 7.9 Hz, 1H), 5.23 (d, *J* = 10.3 Hz, 1H), 5.09 (d, *J* = 16.9 Hz, 1H), 4.32 (d, *J* = 7.9 Hz, 1H), 4.09 – 4.01 (m, 2H), 3.76 (s, 3H), 3.42 (d, *J* = 14.8 Hz, 1H), 3.14 (d, *J* = 14.8 Hz, 1H), 1.06 (t, *J* = 7.2 Hz, 3H). **¹³C NMR** (126 MHz, CDCl₃) δ 166.0, 159.2, 136.5, 135.7, 131.6, 129.5, 128.9, 128.3, 125.8, 119.2, 113.8, 100.3, 62.7, 56.2, 55.3, 40.9, 13.7. **IR** (ATR): 2962, 1738, 1612, 1548, 1513, 1455, 1250, 1180, 1114, 1032, 929 cm⁻¹. **HRMS** calculated for C₂₁H₂₃NO₅Na [M+Na]⁺ 392.1474, found 392.1457. **Chiral SFC**: 150 mm CHIRALCEL OJ-H, 2% *i*PrOH, 2 mL/min, 210 nm, 44 °C, nozzle pressure = 200 bar CO₂, *t*_{R1} (minor) = 3.0 min, *t*_{R2} (major) = 7.3 min.

Tert-butyl-3-((2*S*,3*R*)-2-((benzyloxy)carbonyl)-2-nitro-3-phenylpent-4-en-1-yl)-1*H*-indole-1-carboxylate (3ia)



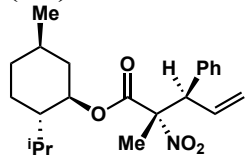
The title compound was synthesized according to general procedure B (modifications: 8.0 mol% Rh-precatalyst and 16 mol% **L6**) and isolated by preparatory TLC (9:1 hexanes:EtOAc) as a yellow solid [35.0 mg, 65% yield, 98:2 *er*, >20:1 *dr*, >20:1 *rr*, $[\alpha]_D^{24} = -11.6^\circ$ (*c* 0.4, CHCl₃)]. **¹H NMR** (500 MHz, CDCl₃) δ 8.16 (d, *J* = 7.2 Hz, 1H), 7.50-7.39 (m, 5H), 7.38-7.33 (m, 2H), 7.32-7.24 (m, 5H), 6.98 (d, *J* = 6.8 Hz, 2H), 6.44 (ddd, *J* = 17.0, 10.2, and 7.8 Hz, 1H), 5.27 (d, *J* = 10.3 Hz, 1H), 5.14 (d, *J* = 16.9 Hz, 1H), 4.86 (d, *J* = 12.1 Hz, 1H), 4.75 (d, *J* = 12.1 Hz, 1H), 4.50 (d, *J* = 7.9 Hz, 1H), 3.58 (d, *J* = 15.5 Hz, 1H), 3.41 (d, *J* = 15.5 Hz, 1H), 1.69 (s, 9H). **¹³C NMR** (101 MHz, CDCl₃) δ 166.2, 149.6, 136.2, 135.4, 135.2, 134.0, 130.6, 129.5, 129.2, 128.8, 128.64, 128.59, 128.5, 126.3, 124.7, 122.7, 119.6, 118.9, 115.5, 112.3, 99.3, 84.0, 68.8, 56.6, 31.4, 28.4. **IR** (ATR): 2978, 1732, 1548, 1452, 1367, 1256, 1211, 1152, 769, 747, 700 cm⁻¹. **HRMS** calculated for C₃₂H₃₂N₂O₆Na [M+Na]⁺ 563.2158, found 563.2151. **Chiral SFC**: 150 mm CHIRALCEL AD-H, 4% *i*PrOH, 2 mL/min, 210 nm, 44 °C, nozzle pressure = 200 bar CO₂, *t*_{R1} (major) = 3.9 min, *t*_{R2} (minor) = 4.8 min.

(1*S*,2*R*,5*S*)-2-Isopropyl-5-methylcyclohexyl (2*S*,3*R*)-2-methyl-2-nitro-3-phenylpent-4-enoate (3ka)



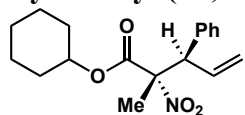
The title compound was synthesized according to general procedure B and isolated by preparatory TLC (10:1 hexanes:EtOAc) as a yellow oil [32.0 mg, 86% yield, >20:1 *dr*, >20:1 *rr*, $[\alpha]^{24}_D = +3.5^\circ$ (*c* 1.4, CHCl₃)]. **¹H NMR** (500 MHz, CDCl₃) δ 7.33 – 7.28 (m, 3H), 7.24 – 7.23 (m, 2H), 6.29 (ddd, *J* = 17.0, 9.9, and 8.1 Hz, 1H), 5.23 (d, *J* = 9.9 Hz, 1H), 5.15 (d, *J* = 16.9 Hz, 1H), 4.68 (td, *J* = 10.9 and 4.4 Hz, 1H), 4.41 (d, *J* = 8.0 Hz, 1H), 1.87 (d, *J* = 11.9 Hz, 1H), 1.77 (s, 3H), 1.67 – 1.59 (m, 3H), 1.46 – 1.36 (m, 2H), 1.04 – 0.92 (m, 2H), 0.89 (d, *J* = 6.6 Hz, 3H), 0.87 – 0.80 (m, 1H), 0.83 (d, *J* = 7.0 Hz, 3H), 0.66 (d, *J* = 7.0 Hz, 3H). **¹³C NMR** (126 MHz, CDCl₃) δ 166.2, 136.7, 134.8, 129.9, 128.7, 128.1, 119.7, 96.2, 77.8, 55.0, 46.8, 40.1, 34.1, 31.5, 26.0, 23.2, 22.0, 20.9, 20.4, 15.9. **IR** (ATR): 2956, 2928, 2870, 1741, 1551, 1454, 1386, 1343, 1245, 1143, 1037, 981 cm⁻¹. **HRMS** calculated for C₂₂H₃₁NO₄Na [M+Na]⁺ 396.2151, found 396.2148.

(1*R*,2*S*,5*R*)-2-Isopropyl-5-methylcyclohexyl (2*S*,3*R*)-2-methyl-2-nitro-3-phenylpent-4-enoate (3la)



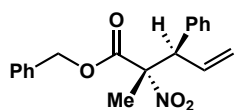
The title compound was synthesized according to general procedure B and isolated by preparatory TLC (10:1 hexanes:EtOAc) as a yellow oil [26.8 mg, 72% yield, >20:1 *dr*, >20:1 *rr*, $[\alpha]^{24}_D = -45.6^\circ$ (*c* 1.3, CHCl₃)]. **¹H NMR** (500 MHz, CDCl₃) δ 7.33 – 7.28 (m, 3H), 7.23 – 7.22 (m, 2H), 6.32 (ddd, *J* = 17.0, 10.2, and 8.3 Hz, 1H), 5.21 (d, *J* = 10.2 Hz, 1H), 5.14 (d, *J* = 16.9 Hz, 1H), 4.71 (td, *J* = 11.0 and 4.4 Hz, 1H), 4.34 (d, *J* = 8.3 Hz, 1H), 1.82 (d, *J* = 11.5 Hz, 1H), 1.79 – 1.75 (m, 1H), 1.73 (s, 3H), 1.69 – 1.65 (m, 2H), 1.49 – 1.41 (m, 1H), 1.39 – 1.33 (m, 1H), 1.05 – 1.00 (m, 1H), 0.88 (d, *J* = 1.7 Hz, 3H), 0.87 (d, *J* = 2.2 Hz, 3H), 0.84 – 0.81 (m, 2H), 0.72 (d, *J* = 6.9 Hz, 3H). **¹³C NMR** (126 MHz, CDCl₃) δ 166.6, 136.7, 134.9, 129.8, 128.8, 128.1, 119.6, 96.3, 77.6, 55.4, 46.9, 40.1, 34.1, 31.5, 25.9, 23.1, 22.0, 21.0, 20.8, 15.9. **IR** (ATR): 2956, 2870, 1738, 1551, 1454, 1387, 1245, 1143, 1037, 981 cm⁻¹. **HRMS** calculated for C₂₂H₃₅N₂O₄ [M+NH₄]⁺ 391.2597, found 391.2585.

Cyclohexyl (2*S*,3*R*)-2-methyl-2-nitro-3-phenylpent-4-enoate (3ma)



The title compound was synthesized according to general procedure B and isolated by preparatory TLC (10:1 hexanes:EtOAc) as a yellow oil [30.4 mg, 96% yield, 95:5 *er*, >20:1 *dr*, >20:1 *rr*, $[\alpha]^{24}_D = -35.8^\circ$ (*c* 1.3, CHCl₃)]. **¹H NMR** (400 MHz, CDCl₃) δ 7.33 – 7.27 (m, 3H), 7.25 – 7.22 (m, 2H), 6.31 (ddd, *J* = 16.9, 10.3, and 8.3 Hz, 1H), 5.23 (d, *J* = 10.2 Hz, 1H), 5.17 (d, *J* = 16.9 Hz, 1H), 4.81 – 4.75 (m, 1H), 4.39 (d, *J* = 8.3 Hz, 1H), 1.80 – 1.74 (m, 1H), 1.77 (s, 3H), 1.74 – 1.59 (m, 3H), 1.51 – 1.42 (m, 2H), 1.41 – 1.26 (m, 4H). **¹³C NMR** (126 MHz, CDCl₃) δ 166.1, 136.7, 134.7, 129.8, 128.7, 128.1, 119.8, 96.3, 75.7, 55.1, 31.1, 31.0, 25.3, 23.4, 23.4, 20.2. **IR** (ATR): 2939, 2861, 1742, 1551, 1453, 1387, 1345, 1265, 1146, 1117, 1008, 928 cm⁻¹. **HRMS** calculated for C₁₈H₂₇N₂O₄ [M+NH₄]⁺ 335.1971, found 335.1975. **Chiral SFC**: 150 mm CHIRALCEL OJ-H, 2% *i*PrOH, 2 mL/min, 210 nm, 44 °C, nozzle pressure = 200 bar CO₂, *t*_{R1} (minor) = 1.5 min, *t*_{R2} (major) = 1.8 min.

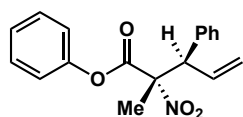
Benzyl (2*S*,3*R*)-2-methyl-2-nitro-3-phenylpent-4-enoate (3na)



The title compound was synthesized according to general procedure B and isolated by preparatory TLC (10:1 hexanes:EtOAc) as a yellow oil [29.0 mg, 89% yield, 95:5 *er*, >20:1 *dr*, >20:1 *rr*, $[\alpha]^{24}_{\text{D}} = -34.4^{\circ}$ (*c* 1.3, CHCl₃)]. ¹H

NMR (500 MHz, CDCl₃) δ 7.36 (dd, *J* = 5.0 and 1.8 Hz, 3H), 7.28 (dd, *J* = 5.1 and 1.8 Hz, 3H), 7.24 (dd, *J* = 6.6 and 2.5 Hz, 2H), 7.20 (dd, *J* = 7.0 and 2.3 Hz, 2H), 6.30 (ddd, *J* = 16.9, 10.2, and 8.5 Hz, 1H), 5.22 (d, *J* = 10.3 Hz, 1H), 5.16 (d, *J* = 16.9 Hz, 1H), 5.13 (d, *J* = 12.5 Hz, 1H), 5.09 (d, *J* = 12.2 Hz, 1H), 4.42 (d, *J* = 8.4 Hz, 1H), 1.79 (s, 3H). ¹³C **NMR** (126 MHz, CDCl₃) δ 166.5, 136.5, 134.4, 134.3, 129.7, 128.8, 128.8, 128.8, 128.5, 128.1, 120.0, 96.3, 68.5, 55.2, 20.0. **IR** (ATR): 1748, 1550, 1497, 1454, 1387, 1343, 1263, 1235, 1142, 1121, 1030, 992, 931 cm⁻¹. **HRMS** calculated for C₁₉H₂₃N₂O₄ [M+NH₄]⁺ 343.1658, found 343.1671. **Chiral SFC**: 150 mm CHIRALCEL AD-H, 3% *i*PrOH, 2 mL/min, 210 nm, 44 °C, nozzle pressure = 200 bar CO₂, *t*_{R1} (major) = 3.0 min, *t*_{R2} (minor) = 3.4 min.

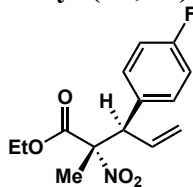
Phenyl (2*S*,3*R*)-2-methyl-2-nitro-3-phenylpent-4-enoate (3oa)



The title compound was synthesized according to general procedure B and isolated by preparatory TLC (10:1 hexanes:EtOAc) as a yellow oil [7.4 mg, 24% yield, 84:16 *er*, >20:1 *dr*, >20:1 *rr*, $[\alpha]^{24}_{\text{D}} = -20.3^{\circ}$ (*c* 0.4, CHCl₃)]. ¹H

NMR (500 MHz, CDCl₃) δ 7.37 – 7.31 (m, 6H), 7.24 – 7.23 (m, 2H), 6.92 (d, *J* = 8.5 Hz, 2H), 6.38 (ddd, *J* = 16.9, 10.1, and 8.5 Hz, 1H), 5.31 (d, *J* = 10.2 Hz, 1H), 5.26 (d, *J* = 16.9 Hz, 1H), 4.54 (d, *J* = 8.5 Hz, 1H), 1.97 (s, 3H). ¹³C **NMR** (126 MHz, CDCl₃) δ 165.2, 150.1, 136.4, 134.3, 129.9, 129.7, 128.9, 128.4, 126.8, 121.0, 120.4, 96.3, 55.2, 20.2. **IR** (ATR): 1767, 1555, 1492, 1454, 1387, 1265, 1231, 1188, 1161, 1106, 932 cm⁻¹. **HRMS** calculated for C₁₈H₂₁N₂O₄ [M+NH₄]⁺ 329.1501, found 329.1503. **Chiral SFC**: 150 mm CHIRALCEL OJ-H, 2% *i*PrOH, 2 mL/min, 210 nm, 44 °C, nozzle pressure = 200 bar CO₂, *t*_{R1} (minor) = 4.0 min, *t*_{R2} (major) = 5.4 min.

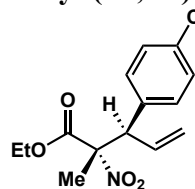
Ethyl (2*S*,3*R*)-3-(4-fluorophenyl)-2-methyl-2-nitropent-4-enoate (3ab)



The title compound was synthesized according to general procedure B and isolated by preparatory TLC (20:1 hexanes:EtOAc) as a yellow oil [25.5 mg, 88% yield, 97:3 *er*, >20:1 *dr*, >20:1 *rr*, $[\alpha]^{24}_{\text{D}} = -45.2^{\circ}$ (*c* 1.3, CHCl₃)]. ¹H

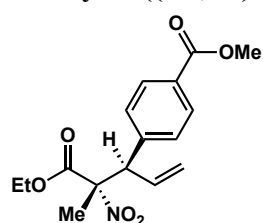
NMR (500 MHz, CDCl₃) δ 7.26 – 7.19 (m, 2H), 7.05 – 6.98 (m, 2H), 6.26 (ddd, *J* = 16.9, 10.2, 8.3 Hz, 1H), 5.28 – 5.21 (m, 1H), 5.16 (dt, *J* = 16.9, 1.2 Hz, 1H), 4.39 (d, *J* = 8.3 Hz, 1H), 4.22 – 4.11 (m, 2H), 1.76 (s, 3H), 1.21 (t, *J* = 7.2 Hz, 3H). ¹³C **NMR** (126 MHz, CDCl₃) 166.4, 162.4 (d, *J* = 247.4 Hz), 134.3, 132.3 (d, *J* = 3.4 Hz), 131.3 (d, *J* = 8.0 Hz), 120.0, 115.6 (d, *J* = 21.4 Hz), 96.0, 63.0, 54.4, 20.0, 13.8. ¹⁹F **NMR** (376 MHz, CDCl₃) δ -114.3. **IR** (ATR): 2985, 1746, 1550, 1509, 1241, 1227, 1163, 1015, 836, 733 cm⁻¹. **HRMS** calculated for C₁₄H₁₆FNO₄Na [M+Na]⁺ 304.0961, found 304.0970. **Chiral SFC** (of the corresponding benzamide): 150 mm CHIRALCEL AD-H, 6% *i*PrOH, 2 mL/min, 220 nm, 44 °C, nozzle pressure = 200 bar CO₂, *t*_{R1} (minor) = 4.6 min, *t*_{R2} (major) = 5.1 min.

Ethyl (2*S*,3*R*)-3-(4-chlorophenyl)-2-methyl-2-nitropent-4-enoate (3ac)



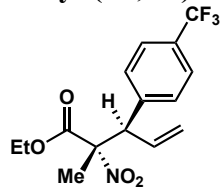
The title compound was synthesized according to general procedure B and isolated by preparatory TLC (20:1 hexanes:EtOAc) as a yellow oil [25.5 mg, 86% yield, 95.5:4.5 *er*, >20:1 *dr*, >20:1 *rr*, $[\alpha]_D^{24} = -61.1^\circ$ (*c* 1.1, CHCl₃)]. **¹H NMR** (400 MHz, CDCl₃) δ 7.31 – 7.27 (m, 2H), 7.21 – 7.16 (m, 2H), 6.25 (ddd, *J* = 16.9, 10.2, 8.4 Hz, 1H), 5.27 – 5.20 (m, 1H), 5.16 (dt, *J* = 16.9, 1.2 Hz, 1H), 4.37 (d, *J* = 8.4 Hz, 1H), 4.25 – 4.08 (m, 2H), 1.76 (s, 3H), 1.22 (t, *J* = 7.1 Hz, 3H). **¹³C NMR** (126 MHz, CDCl₃) δ 166.4, 135.1, 134.04, 134.00, 131.0, 128.9, 120.2, 95.9, 63.0, 54.5, 20.1, 13.8. **IR** (ATR): 2984, 1746, 1550, 1492, 1242, 1124, 1093, 1014, 930, 830 cm⁻¹. **HRMS** calculated for C₁₄H₁₆ClNO₄Na [M+Na]⁺ 320.0666, found 320.0664. **Chiral SFC** (of the corresponding benzamide): 150 mm CHIRALCEL AD-H, 6% ⁱPrOH, 2 mL/min, 220 nm, 44 °C, nozzle pressure = 200 bar CO₂, *t*_{R1} (minor) = 6.6 min, *t*_{R2} (major) = 8.1 min.

Methyl 4-((3*R*,4*S*)-5-ethoxy-4-methyl-4-nitro-5-oxopent-1-en-3-yl)benzoate (3ad)



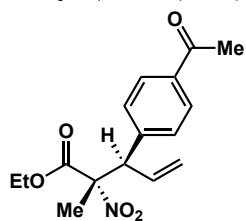
The title compound was synthesized according to general procedure B and isolated by preparatory TLC (5:1 hexanes:EtOAc) as a yellow oil [26.0 mg, 81% yield, 96:4 *er*, >20:1 *dr*, >20:1 *rr*, $[\alpha]_D^{24} = -48.8^\circ$ (*c* 1.1, CHCl₃)]. **¹H NMR** (400 MHz, CDCl₃) δ 8.03 – 7.95 (m, 2H), 7.37 – 7.30 (m, 2H), 6.28 (ddd, *J* = 16.9, 10.2, 8.5 Hz, 1H), 5.29 – 5.23 (m, 1H), 5.18 (dt, *J* = 16.9, 1.1 Hz, 1H), 4.46 (d, *J* = 8.4 Hz, 1H), 4.22 – 4.09 (m, 2H), 3.90 (s, 3H), 1.77 (s, 3H), 1.20 (t, *J* = 7.1 Hz, 3H). **¹³C NMR** (126 MHz, CDCl₃) δ 166.6, 166.3, 141.8, 133.7, 129.88, 129.86, 129.71, 120.5, 95.8, 63.1, 55.0, 52.2, 20.1, 13.8. **IR** (ATR): 2984, 1748, 1721, 1611, 1552, 1436, 1280, 1111, 858, 761 cm⁻¹. **HRMS** calculated for C₁₆H₁₉NO₆Na [M+Na]⁺ 344.1110, found 344.1110. **Chiral SFC**: 150 mm CHIRALCEL AD-H, 2% ⁱPrOH, 2 mL/min, 220 nm, 44 °C, nozzle pressure = 200 bar CO₂, *t*_{R1} (major) = 3.5 min, *t*_{R2} (minor) = 4.5 min.

Ethyl (2*S*,3*R*)-2-methyl-2-nitro-3-(4-(trifluoromethyl)phenyl)pent-4-enoate (3ae)



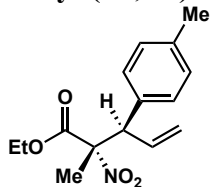
The title compound was synthesized according to general procedure B and isolated by preparatory TLC (10:1 hexanes:EtOAc) as a colorless oil [18.5 mg, 56% yield, 95:5 *er*, >20:1 *dr*, >20:1 *rr*, $[\alpha]_D^{24} = -47.7^\circ$ (*c* 0.6, CHCl₃)]. **¹H NMR** (400 MHz, CDCl₃) δ 7.58 (d, *J* = 8.1 Hz, 2H), 7.39 (d, *J* = 8.2 Hz, 2H), 6.28 (ddd, *J* = 16.9, 10.2, 8.5 Hz, 1H), 5.28 (dt, *J* = 10.2, 1.0 Hz, 1H), 5.19 (dt, *J* = 16.9, 1.1 Hz, 1H), 4.45 (d, *J* = 8.5 Hz, 1H), 4.22 – 4.13 (m, 2H), 1.78 (s, 3H), 1.21 (t, *J* = 7.1 Hz, 3H). **¹³C NMR** (101 MHz, CDCl₃) δ 166.4, 140.99, 140.98, 133.8, 130.3, 125.7 (q, *J* = 3.7 Hz), 123.4, 120.8, 95.9, 63.3, 55.1, 20.3, 13.9. **¹⁹F NMR** (376 MHz, CDCl₃) δ -63.0. **IR** (ATR): 2987, 1747, 1619, 1552, 1447, 1324, 1245, 1122, 1069, 1017, 846, 736 cm⁻¹. **HRMS** calculated for C₁₅H₁₆F₃NO₄Na [M+Na]⁺ 354.0929, found 354.0937. **Chiral SFC** (of the corresponding benzamide): 150 mm CHIRALCEL OD-H, 3% ⁱPrOH, 2 mL/min, 220 nm, 44 °C, nozzle pressure = 200 bar CO₂, *t*_{R1} (major) = 3.5 min, *t*_{R2} (minor) = 4.0 min.

Ethyl (2*S*,3*R*)-3-(4-acetylphenyl)-2-methyl-2-nitropent-4-enoate (**3af**)



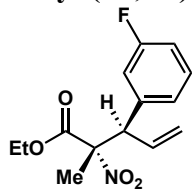
The title compound was synthesized according to general procedure B and isolated by preparatory TLC (5:1 hexanes:EtOAc) as a colorless oil [20.9 mg, 68% yield, 96:4 *er*, >20:1 *dr*, >20:1 *rr*, $[\alpha]_D^{24} = -82.5^\circ$ (*c* 0.8, CHCl₃)]. ¹H NMR (400 MHz, CDCl₃) δ 7.93 – 7.86 (m, 2H), 7.39 – 7.32 (m, 2H), 6.29 (ddd, *J* = 16.9, 10.2, 8.5 Hz, 1H), 5.33 – 5.22 (m, 1H), 5.19 (dt, *J* = 16.9, 1.1 Hz, 1H), 4.45 (d, *J* = 8.5 Hz, 1H), 4.23 – 4.10 (m, 2H), 2.58 (s, 3H), 1.78 (s, 3H), 1.21 (t, *J* = 7.1 Hz, 3H). ¹³C NMR (126 MHz, CDCl₃) δ 197.5, 166.3, 142.0, 136.7, 133.7, 129.9, 128.6, 120.5, 95.8, 63.1, 55.0, 26.6, 20.2, 13.8. IR (ATR): 2984, 1746, 1683, 1550, 1359, 1267, 1244, 1146, 1016, 854 cm⁻¹. HRMS calculated for C₁₆H₁₉NO₅Na [M+Na]⁺ 328.1161, found 328.1174. Chiral SFC: 150 mm CHIRALCEL AD-H, 3% ⁱPrOH, 2 mL/min, 254 nm, 44 °C, nozzle pressure = 200 bar CO₂, *t*_{R1} (major) = 2.9 min, *t*_{R2} (minor) = 4.0 min.

Ethyl (2*S*,3*R*)-2-methyl-2-nitro-3-(*p*-tolyl)pent-4-enoate (**3ag**)



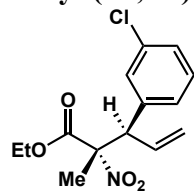
The title compound was synthesized according to general procedure B (modifications: 7.5 mol% Rh-precatalyst and 15 mol% **L6**) and isolated by preparatory TLC (20:1 hexanes:EtOAc) as a yellow oil [24.5 mg, 88% yield, 97:3 *er*, >20:1 *dr*, >20:1 *rr*, $[\alpha]_D^{24} = -57.4^\circ$ (*c* 1.2, CHCl₃)]. ¹H NMR (400 MHz, CDCl₃) δ 7.12 (s, 4H), 6.29 (ddd, *J* = 16.9, 10.3, 8.4 Hz, 1H), 5.21 (ddd, *J* = 10.3, 1.4, 0.9 Hz, 1H), 5.19 – 5.13 (m, 1H), 4.36 (d, *J* = 8.4 Hz, 1H), 4.20 – 4.12 (m, 2H), 2.32 (s, 3H), 1.76 (s, 3H), 1.21 (t, *J* = 7.1 Hz, 3H). ¹³C NMR (126 MHz, CDCl₃) δ 166.6, 137.8, 134.6, 133.4, 129.43, 129.38, 119.5, 96.2, 62.8, 54.8, 21.1, 20.0, 13.8. IR (ATR): 2984, 1746, 1550, 1384, 1242, 1144, 1017, 927, 856, 820 cm⁻¹. HRMS calculated for C₁₅H₁₉NO₄Na [M+Na]⁺ 300.1212, found 300.1215. Chiral SFC: 150 mm CHIRALCEL OJ-H, 2% ⁱPrOH, 2 mL/min, 220 nm, 44 °C, nozzle pressure = 200 bar CO₂, *t*_{R1} (minor) = 1.3 min, *t*_{R2} (major) = 1.5 min.

Ethyl (2*S*,3*R*)-3-(3-fluorophenyl)-2-methyl-2-nitropent-4-enoate (**3ah**)



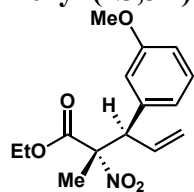
The title compound was synthesized according to general procedure B and isolated by preparatory TLC (20:1 hexanes:EtOAc) as a yellow oil [24.2 mg, 86% yield, 98:2 *er*, >20:1 *dr*, >20:1 *rr*, $[\alpha]_D^{24} = -52.7^\circ$ (*c* 1.0, CHCl₃)]. ¹H NMR (400 MHz, CDCl₃) δ 7.32 – 7.25 (m, 1H), 7.05 – 6.95 (m, 3H), 6.25 (ddd, *J* = 16.9, 10.2, 8.5 Hz, 1H), 5.28 – 5.23 (m, 1H), 5.19 (dt, *J* = 16.9, 1.2 Hz, 1H), 4.40 (d, *J* = 8.5 Hz, 1H), 4.23 – 4.12 (m, 2H), 1.78 (s, 3H), 1.21 (t, *J* = 7.1 Hz, 3H). ¹³C NMR (126 MHz, CDCl₃) δ 166.3, 162.7 (d, *J* = 246.6 Hz), 139.0 (d, *J* = 7.1 Hz), 133.8, 130.1 (d, *J* = 8.3 Hz), 125.3 (d, *J* = 3.0 Hz), 120.3, 116.7 (d, *J* = 22.2 Hz), 115.0 (d, *J* = 21.0 Hz), 95.9, 63.0, 54.7, 20.0, 13.8. ¹⁹F NMR (376 MHz, CDCl₃) δ -112.49. IR (ATR): 2986, 1746, 1551, 1244, 1154, 1135, 1014, 932, 876, 788 cm⁻¹. HRMS calculated for C₁₄H₁₆FNO₄Na [M+Na]⁺ 304.0961, found 304.0966. Chiral SFC (of the corresponding benzamide): 150 mm CHIRALCEL AD-H, 7% ⁱPrOH, 2 mL/min, 220 nm, 44 °C, nozzle pressure = 200 bar CO₂, *t*_{R1} (minor) = 3.9 min, *t*_{R2} (major) = 4.2 min.

Ethyl (2*S*,3*R*)-3-(3-chlorophenyl)-2-methyl-2-nitropent-4-enoate (3ai)



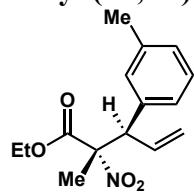
The title compound was synthesized according to general procedure B and isolated by preparatory TLC (20:1 hexanes:EtOAc) as a yellow oil [23.5 mg, 79% yield, 96:4 *er*, >20:1 *dr*, >20:1 *rr*, $[\alpha]^{24}_{\text{D}} = -47.9^\circ$ (*c* 1.0, CHCl₃)]. ¹H NMR (400 MHz, CDCl₃) δ 7.29 – 7.22 (m, 3H), 7.17 – 7.10 (m, 1H), 6.24 (ddd, *J* = 16.9, 10.2, 8.5 Hz, 1H), 5.28 – 5.23 (m, 1H), 5.19 (dt, *J* = 16.9, 1.2 Hz, 1H), 4.38 (d, *J* = 8.5 Hz, 1H), 4.23 – 4.11 (m, 2H), 1.78 (s, 3H), 1.22 (t, *J* = 7.1 Hz, 3H). ¹³C NMR (126 MHz, CDCl₃) δ 166.3, 138.7, 134.7, 133.7, 129.90, 129.89, 128.2, 127.7, 120.4, 95.9, 63.1, 54.7, 20.0, 13.8. IR (ATR): 2984, 1746, 1550, 1243, 1145, 1094, 932, 858, 774, 698 cm⁻¹. HRMS calculated for C₁₄H₁₆ClNO₄Na [M+Na]⁺ 320.0666, found 320.0665. Chiral SFC (of the corresponding benzamide): 150 mm CHIRALCEL OD-H, 2% ⁱPrOH, 2 mL/min, 220 nm, 44 °C, nozzle pressure = 200 bar CO₂, *t*_{R1} (minor) = 2.0 min, *t*_{R2} (major) = 2.2 min.

Ethyl (2*S*,3*R*)-3-(3-methoxyphenyl)-2-methyl-2-nitropent-4-enoate (3aj)



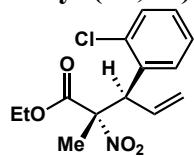
The title compound was synthesized according to general procedure B (modifications: 7.5 mol% Rh-precatalyst and 15 mol% L6) and isolated by preparatory TLC (10:1 hexanes:EtOAc) as a colorless oil [28.1 mg, 96% yield, 96:4 *er*, >20:1 *dr*, >20:1 *rr*, $[\alpha]^{24}_{\text{D}} = -48.4^\circ$ (*c* 1.2, CHCl₃)]. ¹H NMR (400 MHz, CDCl₃) δ 7.24 (t, *J* = 7.9 Hz, 1H), 6.85 – 6.77 (m, 3H), 6.29 (ddd, *J* = 16.9, 10.3, 8.4 Hz, 1H), 5.22 (ddd, *J* = 19.3, 14.1, 0.9 Hz, 2H), 4.38 (d, *J* = 8.4 Hz, 1H), 4.22 – 4.12 (m, 2H), 3.80 (s, 3H), 1.78 (s, 3H), 1.22 (d, *J* = 7.1 Hz, 3H). ¹³C NMR (126 MHz, CDCl₃) δ 166.6, 159.7, 138.0, 134.3, 129.6, 121.8, 119.8, 115.7, 113.1, 96.1, 62.9, 55.3, 55.1, 20.1, 13.8. IR (ATR): 2983, 1746, 1550, 1243, 1161, 1141, 1047, 1016, 858, 772 cm⁻¹. HRMS calculated for C₁₅H₁₉NO₅Na [M+Na]⁺ 316.1161, found 316.1148. Chiral SFC (of the corresponding benzamide): 150 mm CHIRALCEL AD-H, 6% ⁱPrOH, 2 mL/min, 220 nm, 44 °C, nozzle pressure = 200 bar CO₂, *t*_{R1} (minor) = 6.2 min, *t*_{R2} (major) = 9.3 min.

Ethyl (2*S*,3*R*)-2-methyl-2-nitro-3-(*m*-tolyl)pent-4-enoate (3ak)



The title compound was synthesized according to general procedure B and isolated by preparatory TLC (20:1 hexanes:EtOAc) as a yellow oil [16.0 mg, 58% yield, 98:2 *er*, >20:1 *dr*, >20:1 *rr*, $[\alpha]^{24}_{\text{D}} = -49.9^\circ$ (*c* 0.7, CHCl₃)]. ¹H NMR (500 MHz, CDCl₃) δ 7.20 (t, *J* = 7.6 Hz, 1H), 7.12 – 7.07 (m, 1H), 7.05 – 7.00 (m, 2H), 6.30 (ddd, *J* = 16.9, 10.2, 8.5 Hz, 1H), 5.23 (ddd, *J* = 10.2, 1.4, 0.9 Hz, 1H), 5.21 – 5.15 (m, 1H), 4.37 (d, *J* = 8.5 Hz, 1H), 4.21 – 4.10 (m, 2H), 2.33 (s, 3H), 1.77 (s, 3H), 1.21 (t, *J* = 7.2 Hz, 3H). ¹³C NMR (126 MHz, CDCl₃) δ 166.6, 138.3, 136.5, 134.6, 130.3, 128.8, 128.6, 126.5, 120.0, 96.2, 62.9, 55.1, 21.5, 20.0, 13.8. IR (ATR): 2983, 1746, 1550, 1246, 1141, 1016, 929, 858, 768, 706 cm⁻¹. HRMS calculated for C₁₅H₁₉NO₄Na [M+Na]⁺ 300.1212, found 300.1206. Chiral SFC: 150 mm CHIRALCEL OJ-H, 0.5% ⁱPrOH, 2 mL/min, 220 nm, 44 °C, nozzle pressure = 200 bar CO₂, *t*_{R1} (minor) = 1.3 min, *t*_{R2} (major) = 1.4 min.

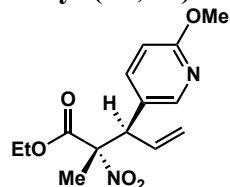
Ethyl (2*S*,3*R*)-3-(2-chlorophenyl)-2-methyl-2-nitropent-4-enoate (3al)



The title compound was synthesized according to general procedure B and isolated by preparatory TLC (20:1 hexanes:EtOAc) as a colorless oil [12.7 mg, 43% yield, 96:4 *er*, >20:1 *dr*, >20:1 *rr*, $[\alpha]^{24}_{\text{D}} = -41.9^\circ$ (*c* 0.7, CHCl₃)]. ¹H NMR (500 MHz, CDCl₃) δ 7.47 – 7.39 (m, 1H), 7.26 – 7.20 (m, 2H), 7.18 – 7.12 (m, 1H), 6.28 (ddd, *J* = 17.0, 10.2, 7.5 Hz, 1H), 5.23 (d, *J* = 10.3 Hz, 1H), 5.17 – 5.07

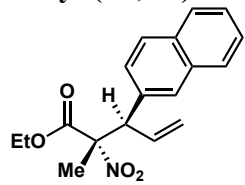
(m, 2H), 4.23 (q, $J = 7.1$ Hz, 2H), 1.74 (s, 3H), 1.25 (t, $J = 7.1$ Hz, 3H). ^{13}C NMR (126 MHz, CDCl_3) δ 166.9, 135.2, 134.5, 134.4, 130.0, 129.4, 129.1, 127.4, 119.6, 96.0, 63.1, 49.7, 20.9, 13.8. IR (ATR): 2984, 1747, 1549, 1242, 1132, 1107, 1036, 1015, 929, 755 cm^{-1} . HRMS calculated for $\text{C}_{14}\text{H}_{16}\text{ClNO}_4\text{Na}$ $[\text{M}+\text{Na}]^+$ 320.0666, found 320.0657. Chiral SFC: 150 mm CHIRALCEL OJ-H, 1% i PrOH, 2.5 mL/min, 220 nm, 44 °C, nozzle pressure = 200 bar CO_2 , $t_{\text{R}1}$ (minor) = 1.3 min, $t_{\text{R}2}$ (major) = 1.6 min.

Ethyl (2*S*,3*R*)-3-(6-methoxypyridin-3-yl)-2-methyl-2-nitropent-4-enoate (3am)



The title compound was synthesized according to general procedure B (modifications: 7.5 mol% Rh-precatalyst and 15 mol% **L6**) and isolated by preparatory TLC (5:1 hexanes:EtOAc) as a yellow oil [13.1 mg, 45% yield, 88:12 *er*, 15:1 *dr*, >20:1 *rr*, $[\alpha]^{24}_{\text{D}} = -58.9^\circ$ (c 0.7, CHCl_3)]. ^1H NMR (400 MHz, CDCl_3) δ 8.05 (dd, $J = 2.5, 0.5$ Hz, 1H), 7.49 – 7.44 (m, 1H), 6.73 – 6.66 (m, 1H), 6.24 (ddd, $J = 16.9, 10.2, 8.2$ Hz, 1H), 5.27 – 5.23 (m, 1H), 5.16 (dt, $J = 16.9, 1.2$ Hz, 1H), 4.34 (d, $J = 8.2$ Hz, 1H), 4.19 (qd, $J = 7.1, 0.7$ Hz, 2H), 3.92 (s, 3H), 1.78 (s, 3H), 1.23 (t, $J = 7.1$ Hz, 3H). ^{13}C NMR (126 MHz, CDCl_3) δ 166.3, 163.8, 148.0, 139.4, 133.9, 125.0, 120.2, 110.9, 95.8, 63.1, 53.6, 52.0, 20.0, 13.8. IR (ATR): 2983, 1747, 1550, 1493, 1393, 1295, 1244, 1132, 1015, 832 cm^{-1} . HRMS calculated for $\text{C}_{14}\text{H}_{18}\text{N}_2\text{O}_4\text{Na}$ $[\text{M}+\text{Na}]^+$ 317.1113, found 317.1115. Chiral SFC: 150 mm CHIRALCEL AD-H, 1% i PrOH, 2 mL/min, 220 nm, 44 °C, nozzle pressure = 200 bar CO_2 , $t_{\text{R}1}$ (major) = 2.4 min, $t_{\text{R}2}$ (minor) = 2.9 min.

Ethyl (2*S*,3*R*)-2-methyl-3-(naphthalen-2-yl)-2-nitropent-4-enoate (3ao)

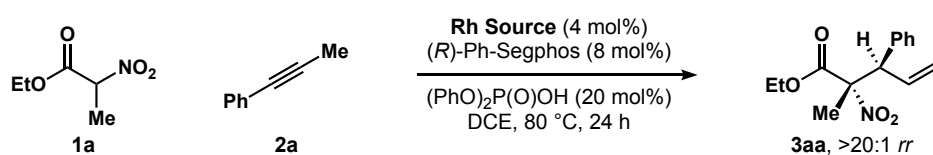


The title compound was synthesized according to general procedure B and isolated by preparatory TLC (20:1 hexanes:EtOAc) as a yellow solid [14.4 mg, 46% yield, 97:3 *er*, >20:1 *dr*, >20:1 *rr*, $[\alpha]^{24}_{\text{D}} = -64.5^\circ$ (c 0.4, CHCl_3)]. ^1H NMR (500 MHz, CDCl_3) δ 7.81 (td, $J = 7.8, 3.6$ Hz, 3H), 7.72 (d, $J = 1.5$ Hz, 1H), 7.52 – 7.45 (m, 2H), 7.35 (dd, $J = 8.6, 1.9$ Hz, 1H), 6.41 (ddd, $J = 16.9, 10.3, 8.3$ Hz, 1H), 5.31 – 5.25 (m, 1H), 5.22 (dt, $J = 16.9, 1.2$ Hz, 1H), 4.60 (d, $J = 8.3$ Hz, 1H), 4.21 – 4.10 (m, 2H), 1.83 (s, 3H), 1.18 (t, $J = 7.2$ Hz, 3H). ^{13}C NMR (126 MHz, CDCl_3) δ 166.6, 134.48, 134.45, 134.0, 133.3, 132.9, 129.1, 128.3, 128.0, 127.6, 127.0, 126.4, 120.0, 96.2, 62.9, 55.2, 20.2, 13.8. IR (ATR): 2987, 1741, 1548, 1246, 1122, 994, 862, 814, 745 cm^{-1} . HRMS calculated for $\text{C}_{18}\text{H}_{19}\text{NO}_4$ $[\text{M}+\text{Na}]^+$ 336.1212, found 336.1213. Chiral SFC: 150 mm CHIRALCEL OJ-H, 1% i PrOH, 2 mL/min, 220 nm, 44 °C, nozzle pressure = 200 bar CO_2 , $t_{\text{R}1}$ (minor) = 5.6 min, $t_{\text{R}2}$ (major) = 6.2 min.

3. Nitroester and Alkyne Coupling Optimization

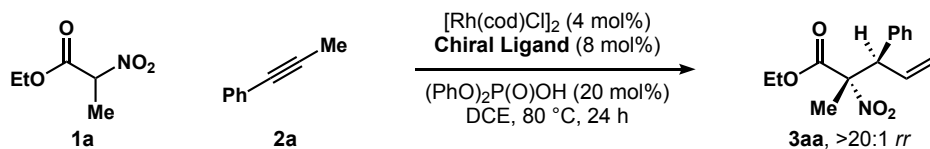
General Procedure for Figures S1-S7: To a 1 dram vial equipped with a magnetic stir bar was added Rh-precatalyst (0.004 mmol, 8 mol% Rh), chiral ligand (0.004 mmol, 8 mol%), acid co-catalyst (0.01 mmol, 20 mol%), nitrocarbonyl **1** (0.05 mmol, 1 equiv.), alkyne **2** (0.075 mmol, 1.5 equiv.) and DCE (100 μ L, 0.5 M). The vial was then sealed with a Teflon-lined screw cap and heated to 80 $^{\circ}$ C for 24 hours. The resulting mixture was then cooled to room temperature and concentrated *in vacuo*. Diastereo- and regioselectivity ratios (*dr* and *rr*, respectively) were determined by ^1H NMR analysis of the crude reaction mixture. ^1H NMR yields, which were referenced to an internal standard (triphenylmethane), are reported. Chiral SFC analysis for enantioselectivity ratios (*er*).

A. Rh Sources (Figure S1):



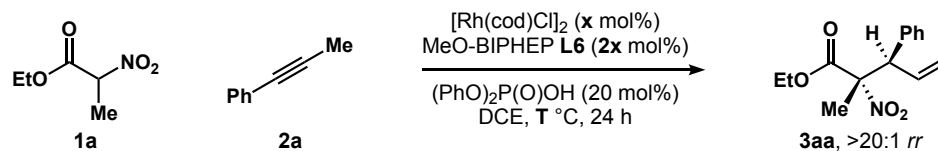
Entry	Rh Source	Result
1	[Rh(cod)Cl] ₂	53%, 90:10 <i>er</i> , 11:1 <i>dr</i>
2	[Rh(coe)Cl] ₂	45%, 88:12 <i>er</i> , 11:1 <i>dr</i>
3	[Rh(C ₂ H ₄) ₂ Cl] ₂	51%, 89:11 <i>er</i> , 8:1 <i>dr</i>
4	[Rh(cod)OMe] ₂	trace
5	[Rh(cod) ₂]SbF ₆	trace
6	[Rh(cod) ₂]BF ₄	trace

B. Chiral Ligands (Figure S2):



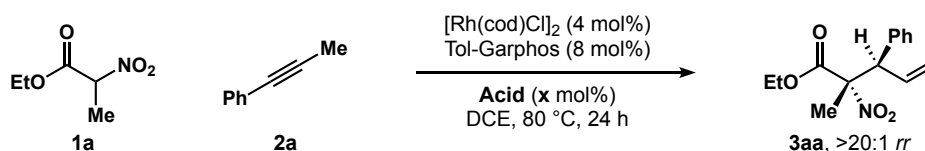
Entry	Chiral Ligand	Result
1	(<i>R</i>)-Ph-Segphos	53%, 90:10 <i>er</i> , 11:1 <i>dr</i>
2	(<i>R</i>)-DM-Segphos	55%, 65:35 <i>er</i> , 10:1 <i>dr</i>
3	(<i>R</i>)-DTBM-Segphos	24%, 77:23 <i>er</i> , n/a <i>dr</i>
4	(<i>R</i>)-Ph-BINAP	45%, 86:14 <i>er</i> , 16:1 <i>dr</i>
5	(<i>R</i>)-Tol-BINAP	39%, 85:15 <i>er</i> , 14:1 <i>dr</i>
6	(<i>R</i>)-Xyl-BINAP	24%, 92:8 <i>er</i> , 7:1 <i>dr</i>
7	(<i>R</i>)-DTBM-BINAP	25%, 68:32 <i>er</i> , 4:1 <i>dr</i>
8	(<i>R</i>)-MeO-BIPHEP (A101)	48%, 85:15 <i>er</i> , 13:1 <i>dr</i>
9	(<i>R</i>)-MeO-BIPHEP (A102)	38%, 89:11 <i>er</i> , >20:1 <i>dr</i>
10	(<i>R</i>)-MeO-BIPHEP (A104)	75%, 97:3 <i>er</i> , >20:1 <i>dr</i>
11	(<i>R</i>)-MeO-BIPHEP (A107)	43%, 68:32 <i>er</i> , 10:1 <i>dr</i>
12	(<i>R</i>)-MeO-BIPHEP (A108)	no reaction
13	(<i>R</i>)-MeO-BIPHEP (A109)	42%, 66:34 <i>er</i> , 16:1 <i>dr</i>
14	(<i>R</i>)-MeO-BIPHEP (A116)	trace
15	(<i>R</i>)-MeO-BIPHEP (A120)	21%, 88:12 <i>er</i> , 7:1 <i>dr</i>
16	(<i>R</i>)-MeO-BIPHEP (A121)	56%, 83:17 <i>er</i> , >20:1 <i>dr</i>
17	(<i>R</i>)-Ph-Garphos	66%, 85:15 <i>er</i> , 18:1 <i>dr</i>
18	(<i>R</i>)-Tol-Garphos	41%, 89:11 <i>er</i> , >20:1 <i>dr</i>
19	(<i>R</i>)-DMM-Garphos	45%, 90:10 <i>er</i> , 15:1 <i>dr</i>
20	(<i>R</i>)-BTFM-Garphos	no reaction
21	(<i>R</i>)-DTBM-Garphos	23%, 64:36 <i>er</i> , n/a <i>dr</i>
22	(<i>R</i>)-Ph-Synphos	63%, 82:18 <i>er</i> , 13:1 <i>dr</i>
23	(<i>R</i>)-Difluorphos	35%, 93:7 <i>er</i> , >20:1 <i>dr</i>

C. Catalyst Loadings and Temperature (Figure S3):



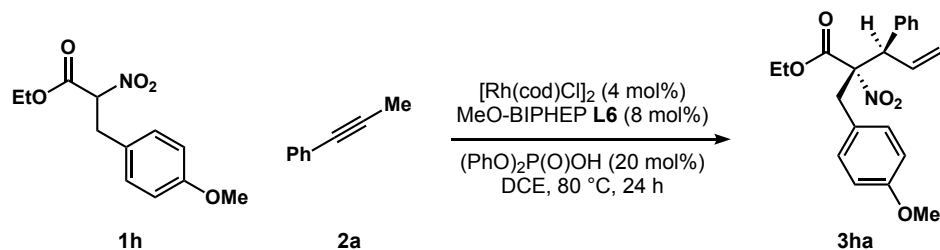
Entry	Catalyst Loading/Temperature	Result
1	$x = 2, T = 80$	47%, 98:2 <i>er</i> , >20:1 <i>dr</i>
2	$x = 1, T = 80$	23%, 98:2 <i>er</i> , >20:1 <i>dr</i>
3	$x = 4, T = 60$	47%, 98:2 <i>er</i> , >20:1 <i>dr</i>

D. Acid Co-Catalysts (Figure S4):



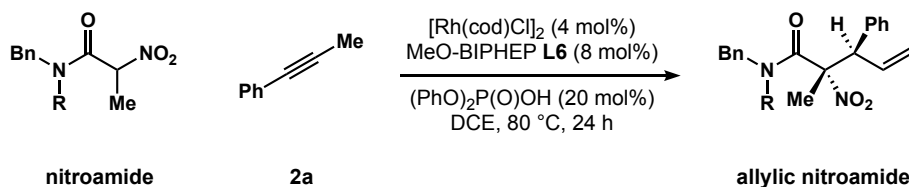
Entry	Catalyst Loading/Temperature	Result
1	$(\text{PhO})_2\text{P}(\text{O})\text{OH}, x = 0$	10%, 62:38 <i>er</i> , 15:1 <i>dr</i>
2	$(\text{PhO})_2\text{P}(\text{O})\text{OH}, x = 5$	58%, 85:15 <i>er</i> , 15:1 <i>dr</i>
3	$(\text{PhO})_2\text{P}(\text{O})\text{OH}, x = 10$	62%, 87:13 <i>er</i> , 15:1 <i>dr</i>
4	$(\text{PhO})_2\text{P}(\text{O})\text{OH}, x = 20$	41%, 89:11 <i>er</i> , >20:1 <i>dr</i>
5	$(\text{PhO})_2\text{P}(\text{O})\text{OH}, x = 50$	28%, 91:9 <i>er</i> , 15:1 <i>dr</i>
6	TsOH, $x = 20$	71%, 85:15 <i>er</i> , >20:1 <i>dr</i>
7	PPTS, $x = 20$	45%, 84:16 <i>er</i> , >20:1 <i>dr</i>
8	TFA, $x = 20$	41%, 90:10 <i>er</i> , 15:1 <i>dr</i>
9	BzOH, $x = 20$	13%, n/a <i>er</i> , 2:1 <i>dr</i>
10	PhOH, $x = 20$	10%, n/a <i>er</i> , 2:1 <i>dr</i>

E. Reaction Optimization for the Lower Yielding Substrate 3ha (Figure S5):



Entry	Changes from the Standard Conditions	Result (% yield)
1	[Rh(cod)Cl] ₂ (7.5 mol%), L6 (15 mol%)	43%
2	90 °C	37%
3	2a (3 equiv.)	46%
4	72 h	55%
5	1h (1.5 equiv.), 2a (1 equiv.)	27%

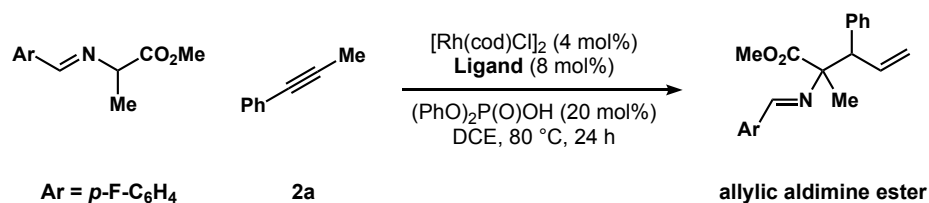
F. Initial Results for the Coupling of α -Nitroamides and Alkynes (Figure S6):



Entry	Nucleophile	Result
1	R = H	15%, 74:26 <i>er</i> , >20:1 <i>dr</i>
2	R = Ph	9%, 85:15 <i>er</i> , >20:1 <i>dr</i>

Note: Isolated yields are reported and the stereochemistry is assigned by analogy to **3** in the manuscript.

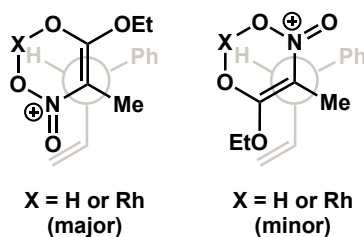
G. Aldimine Ester and Alkyne Coupling (Figure S7):



Entry	Ligand	Result (% yield)
1	dppm	n/r
2	dppe	n/r
3	dppp	n/r
4	dppb	n/r
5	dppf	n/r
6	Xantphos	n/r
7	<i>rac</i> -BINAP	n/r

Note: The aldimine ester examined in *Figure S7* was the model substrate in Zi's work on the Pd-catalyzed hydroalkylation of dienes (reference 7a in the manuscript). We prepared the aldimine ester following their reported procedure.

H. Diastereoselectivity Model (Figure S8):

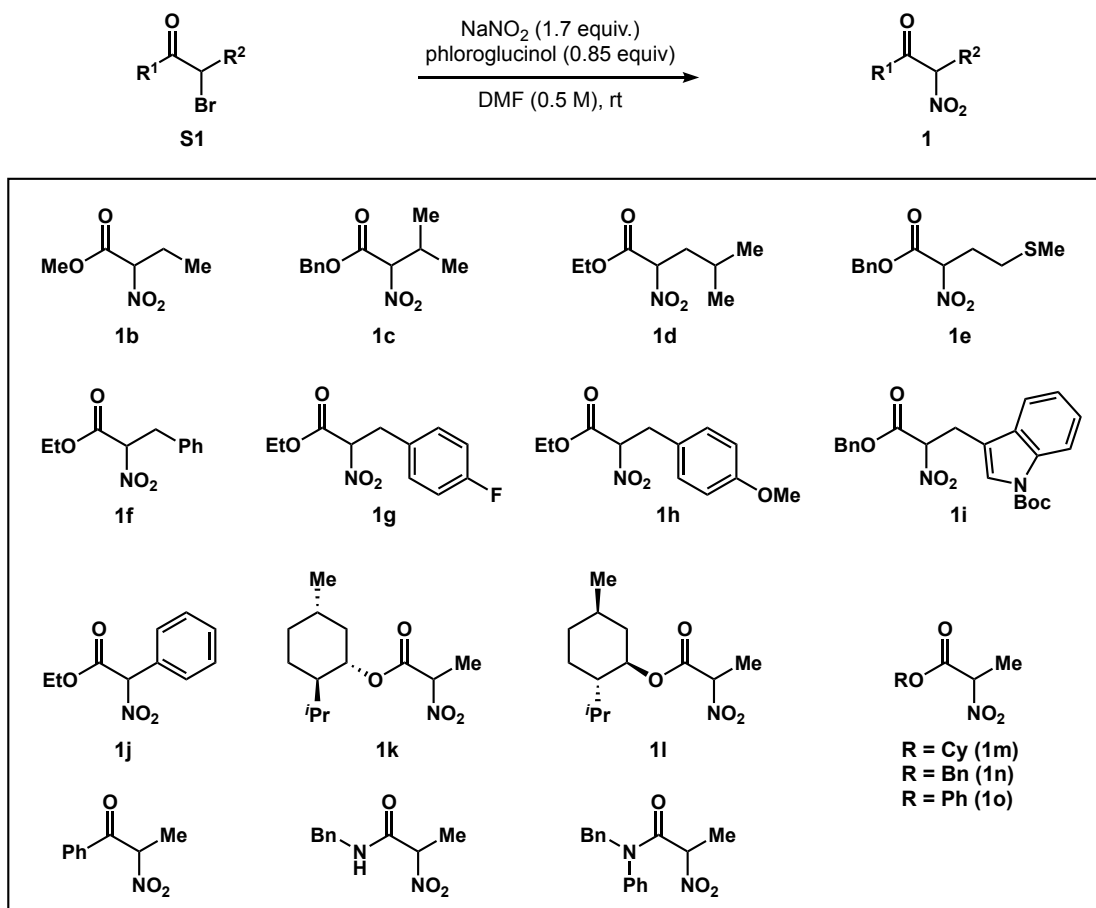


Note: This is a potential model for the high diastereoselectivity observed in the coupling of α -nitroesters and alkynes. We have represented the diastereoselective outcome in a similar fashion to a model published by Trost and coworkers on their study of asymmetric allylic alkylation of azlactones (reference 6b in the manuscript). Further mechanistic understanding is needed to support this proposal.

4. Preparation of Starting Materials

A. General Procedure for Nitration (α -Nitrocarbonyls)

The synthesis of α -bromo carbonyls were performed using standard literature-reported procedures.



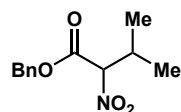
To a round bottom flask equipped with a stir bar was added sodium nitrite (1.7 equiv), phloroglucinol (0.85 equiv), and DMF (0.5 M). The heterogeneous solution was stirred at room temperature for 10 minutes to allow for maximum dissolution of the sodium nitrite. The α -bromocarbonyl **S1** (1.0 equiv) was added, and the reaction became yellow in color. Upon completion (as indicated by TLC and a homogeneous amber-brown color), the reaction was extracted with Et₂O ($\times 3$). The organic phase was washed with a saturated solution of NaHCO₃, H₂O ($\times 3$), and brine, dried with anhydrous MgSO₄, filtered, and concentrated *in vacuo*. The crude residue was purified by flash column chromatography to afford the desired α -nitrocarbonyl product (**1**).

Methyl 2-nitrobutanoate (**1b**)

Prepared according to the general procedure for nitration using NaNO₂ (1.8 g, 26 mmol), phloroglucinol (1.6 g, 13 mmol), and DMF (30 mL). To the resulting solution was added methyl 2-bromobutanoate (1.7 mL, 15 mmol). The reaction was complete after 4 hours at room temperature. Purification by flash column chromatography using 94:6 hexanes:EtOAc afforded the desired α -nitrocarbonyl as a colorless oil (1.2 g, 8.4 mmol, 56%). ¹H NMR (500 MHz, CDCl₃) δ 5.04 (dd, *J* = 5.5 and 9.3 Hz, 1H), 3.82 (s, 3H), 2.29 (ddq, *J*

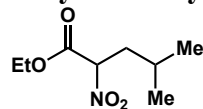
= 14.7, 9.2, and 7.4 Hz, 1H), 2.22 – 2.15 (m, 1H), 1.04 (t, $J = 7.5$ Hz, 3H). ^{13}C NMR (126 MHz, CDCl_3) δ 165.1, 89.4, 53.6, 24.0, 10.2. IR (ATR): 2961, 1750, 1557, 1507, 1438, 1373, 1289, 1209, 1093, 999 cm^{-1} . HRMS calculated for $\text{C}_5\text{H}_{13}\text{N}_2\text{O}_4$ $[\text{M}+\text{NH}_4]^+$ 165.0875, found 165.0879.

Benzyl 3-methyl-2-nitrobutanoate (1c)



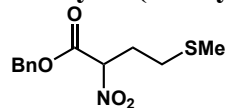
Prepared according to the general procedure for nitration using NaNO_2 (0.33 g, 4.8 mmol), phloroglucinol (0.30 g, 2.4 mmol), and DMF (5.6 mL). To the resulting solution was added benzyl 3-methyl-2-bromobutanoate (0.76 g, 2.8 mmol). The reaction was complete after 4 hours at room temperature. Purification by flash column chromatography using 99:1 hexanes:EtOAc afforded the desired α -nitrocarbonyl as a colorless oil (0.48 g, 2.0 mmol, 72%). ^1H NMR (400 MHz, CDCl_3) δ 7.41 – 7.33 (m, 5H), 5.26 (d, $J = 12.2$ Hz, 1H), 5.23 (d, $J = 12.2$ Hz, 1H), 4.92 (d, $J = 8.1$ Hz, 1H), 2.67 (dhept, $J = 8.0$ and 6.8 Hz, 1H), 1.07 (d, $J = 6.7$ Hz, 3H), 1.04 (d, $J = 6.8$ Hz, 3H). ^{13}C NMR (126 MHz, CDCl_3) δ 163.9, 134.5, 129.0, 128.9, 128.6, 93.7, 68.4, 30.4, 18.9, 18.5. IR (ATR): 2972, 1749, 1557, 1456, 1297, 1186, 1003, 907 cm^{-1} . HRMS calculated for $\text{C}_{12}\text{H}_{19}\text{N}_2\text{O}_4$ $[\text{M}+\text{NH}_4]^+$ 255.1345, found 255.1333.

Ethyl 4-methyl-2-nitropentanoate (1d)



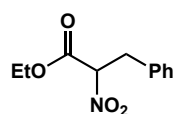
Prepared according to the general procedure for nitration using NaNO_2 (0.28 g, 4.0 mmol), phloroglucinol (0.25 g, 2.0 mmol), and DMF (4.8 mL). To the resulting solution was added ethyl 4-methyl-2-bromopentanoate (0.53 g, 2.4 mmol). The reaction was complete after 4 hours at room temperature. Purification by flash column chromatography using 96:4 hexanes:EtOAc afforded the desired α -nitrocarbonyl as a colorless oil (0.25 g, 1.3 mmol, 56%). ^1H NMR (400 MHz, CDCl_3) δ 5.18 (dd, $J = 9.9$ and 5.2 Hz, 1H), 4.28 (q, $J = 7.1$ Hz, 2H), 2.27 (ddd, $J = 15$, 9.9 and 5.7 Hz, 1H), 1.93 (ddd, $J = 14.1$, 8.5 and 5.2 Hz, 1H), 1.64 – 1.61 (m, 1H), 1.30 (t, $J = 7.2$ Hz, 3H), 0.97 (d, $J = 6.7$ Hz, 6H). ^{13}C NMR (126 MHz, CDCl_3) δ 165.0, 86.9, 63.1, 38.9, 25.2, 22.6, 21.5, 14.0. IR (ATR): 2964, 1749, 1559, 1372, 1268, 1193, 1018, 853 cm^{-1} . HRMS calculated for $\text{C}_8\text{H}_{19}\text{N}_2\text{O}_4$ $[\text{M}+\text{NH}_4]^+$ 207.1345, found 207.1337.

Benzyl 4-(methylthio)-2-nitrobutanoate (1e)



Prepared according to the general procedure for nitration using NaNO_2 (0.19 g, 2.8 mmol), phloroglucinol (0.18 g, 1.4 mmol), and DMF (3.3 mL). To the resulting solution was added benzyl 4-(methylthio)-2-bromobutanoate (0.50 g, 1.6 mmol). The reaction was complete after 4 hours at room temperature. Purification by flash column chromatography using 99:1 hexanes:EtOAc afforded the desired α -nitrocarbonyl as a colorless oil (0.21 g, 0.78 mmol, 47%). ^1H NMR (500 MHz, CDCl_3) δ 7.40 – 7.32 (m, 5H), 5.45 (dd, $J = 8.5$ and 5.2 Hz, 1H), 5.27 (d, $J = 12.1$ Hz, 1H), 5.24 (d, $J = 12.2$ Hz, 1H), 2.64 – 2.56 (m, 2H), 2.53 – 2.48 (m, 1H), 2.44 – 2.37 (m, 1H), 2.08 (s, 3H). ^{13}C NMR (126 MHz, CDCl_3) δ 164.4, 134.3, 129.0, 128.9, 128.5, 86.4, 68.8, 30.0, 29.6, 15.4. IR (ATR): 2919, 1748, 1557, 1456, 1435, 1291, 1267, 1192, 964 cm^{-1} . HRMS calculated for $\text{C}_{12}\text{H}_{15}\text{NO}_4\text{SNa}$ $[\text{M}+\text{Na}]^+$ 292.0620, found 292.0610.

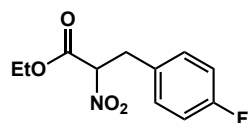
Ethyl 2-nitro-3-phenylpropanoate (1f)



Prepared according to the general procedure for nitration using NaNO_2 (0.29 g, 4.2 mmol), phloroglucinol (0.27 g, 2.1 mmol), and DMF (5.0 mL). To the resulting solution was added ethyl 2-bromo-3-phenylpropanoate (0.64 g, 2.5 mmol). The

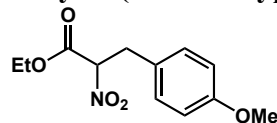
reaction was complete after 4 hours at room temperature. Purification by flash column chromatography using 99:1 hexanes:EtOAc afforded the desired α -nitrocarbonyl as a colorless oil (0.32 g, 1.4 mmol, 58%). $^1\text{H NMR}$ (500 MHz, CDCl_3) δ 7.33 – 7.28 (m, 3H), 7.21 (d, $J = 7.2$ Hz, 2H), 5.34 (dd, $J = 9.5$ and 5.8 Hz, 1H), 4.28 (q, $J = 6.6$ Hz, 2H), 3.56 (dd, $J = 14.6$ and 9.5 Hz, 1H), 3.48 (dd, $J = 14.6$ and 5.8 Hz, 1H), 1.28 (t, $J = 7.2$ Hz, 3H). $^{13}\text{C NMR}$ (126 MHz, CDCl_3) δ 164.2, 134.2, 129.1, 129.0, 127.9, 89.3, 63.3, 36.4, 14.0. **IR** (ATR): 2985, 1747, 1558, 1456, 1373, 1268, 1209, 1019, 859 cm^{-1} . **HRMS** calculated for $\text{C}_{11}\text{H}_{17}\text{N}_2\text{O}_4$ $[\text{M}+\text{NH}_4]^+$ 241.1188, found 241.1184.

Ethyl 2-nitro-3-(4-fluorophenyl)propanoate (**1g**)



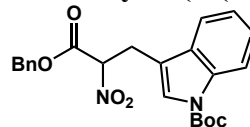
Prepared according to the general procedure for nitration using NaNO_2 (0.39 g, 5.6 mmol), phloroglucinol (0.36 g, 2.8 mmol), and DMF (6.6 mL). To the resulting solution was added ethyl 2-bromo-3-(4-fluorophenyl)propanoate (0.91 g, 3.3 mmol). The reaction was complete after 3 hours at room temperature. Purification by flash column chromatography using 99:1 hexanes:EtOAc afforded the desired α -nitrocarbonyl as a colorless oil (0.41 g, 1.7 mmol, 51%). $^1\text{H NMR}$ (500 MHz, CDCl_3) δ 7.20 – 7.17 (m, 2H), 7.03 – 6.98 (m, 2H), 5.29 (dd, $J = 9.5$ and 5.8 Hz, 1H), 4.28 (qd, $J = 7.2$ and 2.1 Hz, 2H), 3.53 (dd, $J = 14.7$ and 9.6 Hz, 1H), 3.45 (dd, $J = 14.7$ and 5.8 Hz, 1H), 1.28 (t, $J = 7.2$ Hz, 3H). $^{13}\text{C NMR}$ (126 MHz, CDCl_3) δ 164.0, 162.5 (d, $J = 246.5$ Hz), 130.7 (d, $J = 8.2$ Hz), 129.9 (d, $J = 3.3$ Hz), 116.1 (d, $J = 21.6$ Hz), 89.3, 63.4, 35.6, 14.0. $^{19}\text{F NMR}$ (376 MHz, CDCl_3) δ -114.6. **IR** (ATR): 2986, 1747, 1559, 1510, 1373, 1269, 1222, 1160, 1100, 1016, 861 cm^{-1} . **HRMS** calculated for $\text{C}_{11}\text{H}_{12}\text{FNO}_4\text{Na}$ $[\text{M}+\text{Na}]^+$ 264.0648, found 264.0649.

Ethyl 3-(4-methoxyphenyl)-2-nitropropanoate (**1h**)



Prepared according to the general procedure for nitration using NaNO_2 (0.21 g, 3.1 mmol), phloroglucinol (0.20 g, 1.5 mmol), and DMF (3.6 mL). To the resulting solution was added ethyl 3-(4-methoxyphenyl)-2-bromopropanoate (0.52 g, 1.8 mmol). The reaction was complete after 4 hours at room temperature. Purification by flash column chromatography using 99:1 hexanes:EtOAc afforded the desired α -nitrocarbonyl as a colorless oil (0.35 g, 1.4 mmol, 76%). $^1\text{H NMR}$ (500 MHz, CDCl_3) δ 7.12 (d, $J = 8.6$ Hz, 2H), 6.84 (d, $J = 8.6$ Hz, 2H), 5.28 (dd, $J = 9.5$ and 5.6 Hz, 1H), 4.28 (qd, $J = 7.1$ and 2.2 Hz, 2H), 3.78 (s, 3H), 3.50 (dd, $J = 14.6$ and 9.5 Hz, 1H), 3.42 (dd, $J = 14.7$ and 5.8 Hz, 1H), 1.28 (t, $J = 7.2$ Hz, 3H). $^{13}\text{C NMR}$ (126 MHz, CDCl_3) δ 164.2, 159.3, 130.1, 126.1, 114.5, 89.6, 63.3, 55.4, 35.7, 14.0. **IR** (ATR): 2938, 1747, 1559, 1514, 1465, 1373, 1302, 1179, 1029, 910, 861 cm^{-1} . **HRMS** calculated for $\text{C}_{12}\text{H}_{19}\text{N}_2\text{O}_5$ $[\text{M}+\text{NH}_4]^+$ 271.1294, found 271.1289.

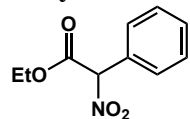
Tert-butyl 3-(3-(benzyloxy)-2-nitro-3-oxopropyl)-1*H*-indole-1-carboxylate (**1i**)



Prepared according to the general procedure for nitration using NaNO_2 (0.13 g, 1.9 mmol), phloroglucinol (0.12 g, 0.93 mmol), and DMF (2.2 mL). To the resulting solution was added *tert*-butyl 3-(3-(benzyloxy)-2-bromo-3-oxopropyl)-1*H*-indole-1-carboxylate (0.50 g, 1.1 mmol). The reaction was complete after 3 hours at room temperature. Purification by flash column chromatography using 90:10 hexanes:EtOAc afforded the desired α -nitrocarbonyl as a light yellow solid (0.15 g, 0.36 mmol, 33%). $^1\text{H NMR}$ (500 MHz, CDCl_3) δ 8.21 (bs, 1H), 7.57 (d, $J = 7.8$ Hz, 1H), 7.52 (s, 1H), 7.44-7.40 (m, 4H), 7.35-7.32 (m, 3H), 5.56 (dd, $J = 9.3$ and 5.7 Hz, 1H), 5.31 (s, 2H), 3.77 (dd, J

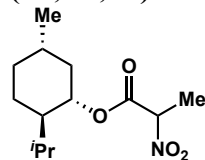
= 15.4 and 9.3 Hz, 1H), 3.67 (dd, $J = 15.3$ and 5.7 Hz, 1H), 1.73 (s, 9H). ^{13}C NMR (126 MHz, CDCl_3) δ 164.0, 149.4, 135.5, 134.1, 129.2, 129.0, 128.8, 128.4, 125.0, 124.8, 122.9, 118.3, 115.6, 112.8, 87.5, 84.1, 68.8, 28.2, 26.3. IR (ATR): 2979, 1722, 1562, 1450, 1390, 1360, 1332, 1255, 1153, 1092, 743, 697 cm^{-1} . HRMS calculated for $\text{C}_{23}\text{H}_{24}\text{N}_2\text{O}_6\text{Na}$ $[\text{M}+\text{Na}]^+$ 447.1515, found 447.1532.

Ethyl 2-nitro-2-phenylacetate (1j)



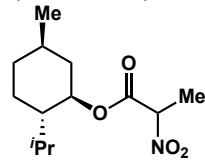
In a glove-box, to an oven-dried vial was added $\text{Pd}_2(\text{dba})_3$ (0.29 g, 32 μmol), $t\text{BuXPhos}$ (0.53 g, 0.13 mmol), and CsHCO_3 (0.29 g, 1.5 mmol). Next, toluene (6.3 mL), ethyl nitroacetate (0.28 mL, 2.5 mmol), and bromobenzene (0.13 mL, 1.3 mmol) were added to give a heterogeneous reaction mixture. The solution was then heated to 80°C and stirred vigorously for 6 h. After cooling, the reaction mixture was diluted with EtOAc and acidified with HCl (1 M). The aqueous layer was extracted with additional EtOAc ($\times 3$) and washed with brine. The combined organic layers were dried (MgSO_4) and concentrated in vacuo. The crude residue was purified by flash chromatography 97:3 hexanes:EtOAc to afford the desired α -nitrocarbonyl as a colorless oil (0.25 g, 1.2 mmol, 97%). The ^1H and ^{13}C NMRs are in accordance with the literature. ^1H NMR (500 MHz, CDCl_3) δ 7.51 – 7.41 (m, 5H), 6.16 (s, 1H), 4.39 – 4.28 (m, 2H), 1.30 (t, $J = 7.2$ Hz, 3H). ^{13}C NMR (126 MHz, CDCl_3) δ 164.1, 130.9, 130.0, 129.2, 91.0, 63.5, 14.0.

(1S,2R,5S)-2-Isopropyl-5-methylcyclohexyl 2-nitropropanoate (1k)



Prepared according to the general procedure for nitration using NaNO_2 (0.40 g, 5.8 mmol), phloroglucinol (0.37 g, 2.9 mmol), and DMF (6.9 mL). To the resulting solution was added (1S,2R,5S)-2-isopropyl-5-methylcyclohexyl 2-bromopropanoate (1.0 g, 3.4 mmol). The reaction was complete after 4 hours at room temperature. Purification by flash column chromatography using 97:3 hexanes:EtOAc afforded the desired α -nitrocarbonyl as a colorless oil (0.44 g, 1.7 mmol, 49%). ^1H NMR (500 MHz, CDCl_3) δ 5.17 (q, $J = 7.1$ Hz, 1H), 4.78 (td, $J = 10.9$ and 4.5 Hz, 1H), 2.02 – 2.01 (m, 1H), 1.82 – 1.78 (m, 1H), 1.78 (d, $J = 7.1$ Hz, 3H), 1.69 (d, $J = 12.5$ Hz, 2H), 1.54 – 1.46 (m, 1H), 1.42 (t, $J = 11$ Hz, 1H), 1.10 – 0.99 (m, 2H), 0.92 (d, $J = 6.6$ Hz, 3H), 0.89 (d, $J = 7.0$ Hz, 3H), 0.89 – 0.83 (m, 1H), 0.76 (d, $J = 7.0$ Hz, 3H). ^{13}C NMR (126 MHz, CDCl_3) δ 164.9, 164.8, 83.6, 83.5, 77.7, 47.0, 46.9, 40.4, 40.3, 34.2, 34.1, 31.5, 26.3, 26.3, 23.4, 22.0, 22.0, 20.8, 20.8, 16.2, 16.2, 15.9, 15.9. IR (ATR): 2956, 2871, 1745, 1560, 1452, 1389, 1203, 1024, 953 cm^{-1} . HRMS calculated for $\text{C}_{13}\text{H}_{27}\text{N}_2\text{O}_4$ $[\text{M}+\text{NH}_4]^+$ 275.1971, found 275.1958.

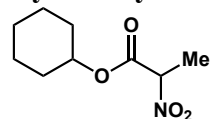
(1R,2S,5R)-2-Isopropyl-5-methylcyclohexyl 2-nitropropanoate (1l)



Prepared according to the general procedure for nitration using NaNO_2 (0.34 g, 4.9 mmol), phloroglucinol (0.31 g, 2.4 mmol), and DMF (5.7 mL). To the resulting solution was added (1S,2R,5S)-2-isopropyl-5-methylcyclohexyl 2-bromopropanoate (0.83 g, 2.9 mmol). The reaction was complete after 4 hours at room temperature. Purification by flash column chromatography using 97:3 hexanes:EtOAc afforded the desired α -nitrocarbonyl as a colorless oil (0.34 g, 1.3 mmol, 46%). ^1H NMR (500 MHz, CDCl_3) δ 5.17 (q, $J = 7.1$ Hz, 1H), 4.78 (td, $J = 10.9$ and 4.5 Hz, 1H), 2.02 – 2.01 (m, 1H), 1.82 – 1.78 (m, 1H), 1.78 (d, $J = 7.1$ Hz, 3H), 1.69 (d, $J = 12.5$ Hz, 2H), 1.54 – 1.46 (m, 1H), 1.42 (t, $J = 11$ Hz, 1H), 1.10 – 0.99 (m, 2H), 0.92 (d, $J = 6.6$ Hz, 3H), 0.89 (d, $J = 7.0$ Hz, 3H), 0.89 – 0.83 (m, 1H), 0.76 (d, $J = 7.0$ Hz, 3H). ^{13}C NMR (126 MHz, CDCl_3) δ 164.9, 164.8,

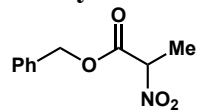
83.6, 83.5, 77.7, 47.0, 46.9, 40.4, 40.3, 34.2, 34.1, 31.5, 26.3, 26.3, 23.4, 22.0, 22.0, 20.8, 20.8, 16.2, 16.2, 15.9, 15.9. **IR** (ATR): 2956, 2871, 1745, 1560, 1452, 1389, 1203, 1024, 953 cm^{-1} . **HRMS** calculated for $\text{C}_{13}\text{H}_{27}\text{N}_2\text{O}_4$ $[\text{M}+\text{NH}_4]^+$ 275.1971, found 275.1980.

Cyclohexyl 2-nitropropanoate (1m)



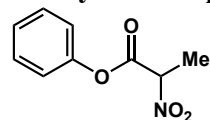
Prepared according to the general procedure for nitration using NaNO_2 (0.50 g, 7.3 mmol), phloroglucinol (0.46 g, 3.7 mmol), and DMF (8.6 mL). To the resulting solution was added cyclohexyl 2-bromopropanoate (1.0 g, 4.3 mmol). The reaction was complete after 4 hours at room temperature. Purification by flash column chromatography using 97:3 hexanes:EtOAc afforded the desired α -nitrocarbonyl as a colorless oil (0.52 g, 2.6 mmol, 60%). **$^1\text{H NMR}$** (400 MHz, CDCl_3) δ 5.17 (q, $J = 7.1$ Hz, 1H), 4.92 – 4.87 (m, 1H), 1.85 – 1.82 (m, 2H), 1.78 (d, $J = 7.2$ Hz, 3H), 1.72 – 1.68 (m, 2H), 1.53 – 1.46 (m, 3H), 1.42 – 1.35 (m, 2H), 1.32 – 1.32 (m, 1H). **$^{13}\text{C NMR}$** (126 MHz, CDCl_3) δ 164.7, 83.6, 75.9, 31.2, 31.1, 25.3, 23.4, 23.4, 15.9. **IR** (ATR): 2939, 2861, 1743, 1558, 1450, 1390, 1205, 1120, 1008, 901 cm^{-1} . **HRMS** calculated for $\text{C}_9\text{H}_{19}\text{N}_2\text{O}_4$ $[\text{M}+\text{NH}_4]^+$ 219.1336, found 219.1345.

Benzyl 2-nitropropanoate (1n)



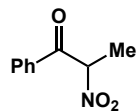
Prepared according to the general procedure for nitration using NaNO_2 (0.37 g, 5.4 mmol), phloroglucinol (0.34 g, 2.7 mmol), and DMF (6.4 mL). To the resulting solution was added benzyl 2-bromopropanoate (1.0 g, 3.2 mmol). The reaction was complete after 4 hours at room temperature. Purification by flash column chromatography using 96:4 hexanes:EtOAc afforded the desired α -nitrocarbonyl as a colorless oil (0.42 g, 2.0 mmol, 63%). **$^1\text{H NMR}$** (400 MHz, CDCl_3) δ 7.41 – 7.32 (m, 5H), 5.25 (s, 2H), 5.23 (q, $J = 7.1$ Hz, 1H), 1.80 (d, $J = 7.1$ Hz, 3H). **$^{13}\text{C NMR}$** (126 MHz, CDCl_3) δ 165.1, 134.4, 129.0, 128.9, 128.5, 83.3, 68.6, 15.8. **IR** (ATR): 1749, 1558, 1455, 1392, 1360, 1312, 1191, 1084, 1026, 873 cm^{-1} . **HRMS** calculated for $\text{C}_{10}\text{H}_{15}\text{N}_2\text{O}_4$ $[\text{M}+\text{NH}_4]^+$ 227.1032, found 227.1026.

Phenyl 2-nitropropanoate (1o)



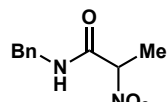
Prepared according to the general procedure for nitration using NaNO_2 (0.44 g, 6.3 mmol), phloroglucinol (0.40 g, 3.2 mmol), and DMF (3.7 mL). To the resulting solution was added phenyl 2-bromopropanoate (0.85 g, 3.7 mmol). The reaction was complete after 4 hours at room temperature. Purification by flash column chromatography using 97:3 hexanes:EtOAc afforded the desired α -nitrocarbonyl as a colorless oil (0.33 g, 4.8 mmol, 77%). **$^1\text{H NMR}$** (500 MHz, CDCl_3) δ 7.47 (dd, $J = 7.9$ and 7.9 Hz, 2H), 7.34 (dd, $J = 7.6$ and 7.6 Hz, 1H), 7.19 (d, $J = 8.5$ Hz, 2H), 5.48 (q, $J = 7.1$ Hz, 1H), 1.99 (d, $J = 7.2$ Hz, 3H). **$^{13}\text{C NMR}$** (126 MHz, CDCl_3) δ 163.7, 150.0, 129.8, 126.9, 121.0, 83.3, 15.9. **IR** (ATR): 1768, 1558, 1492, 1456, 1389, 1359, 1185, 1083, 1024, 923 cm^{-1} . **HRMS** calculated for $\text{C}_9\text{H}_{13}\text{N}_2\text{O}_4$ $[\text{M}+\text{NH}_4]^+$ 213.0875, found 213.0874.

2-Nitro-1-phenylpropan-1-one



Prepared according to the general procedure for nitration using NaNO_2 (0.55 g, 8.0 mmol), phloroglucinol (0.53 g, 4.2 mmol), and DMF (9.4 mL). To the resulting solution was added 2-bromopropiophenone (1.0 g, 4.7 mmol). The reaction was complete after 4 hours at room temperature. Purification by flash column chromatography using 90:10 hexanes:EtOAc afforded the desired α -nitrocarbonyl as a colorless oil (0.13 g, 0.72 mmol, 15%). The ^1H and ^{13}C NMRs are in accordance with the literature.² **$^1\text{H NMR}$** (500 MHz, CDCl_3)

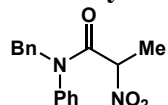
δ 7.90-7.87 (m, 2H), 7.55 (tt, $J = 6.8$ and 1.3 Hz, 1H), 7.47-7.42 (m, 2H), 5.12 (q, $J = 7.0$ Hz, 1H), 1.40 (d, $J = 7.0$ Hz, 3H). ^{13}C NMR (126 MHz, CDCl_3) δ 202.4, 134.0, 133.4, 128.9, 128.7, 69.4, 22.2.



***N*-benzyl-2-nitropropanamide**

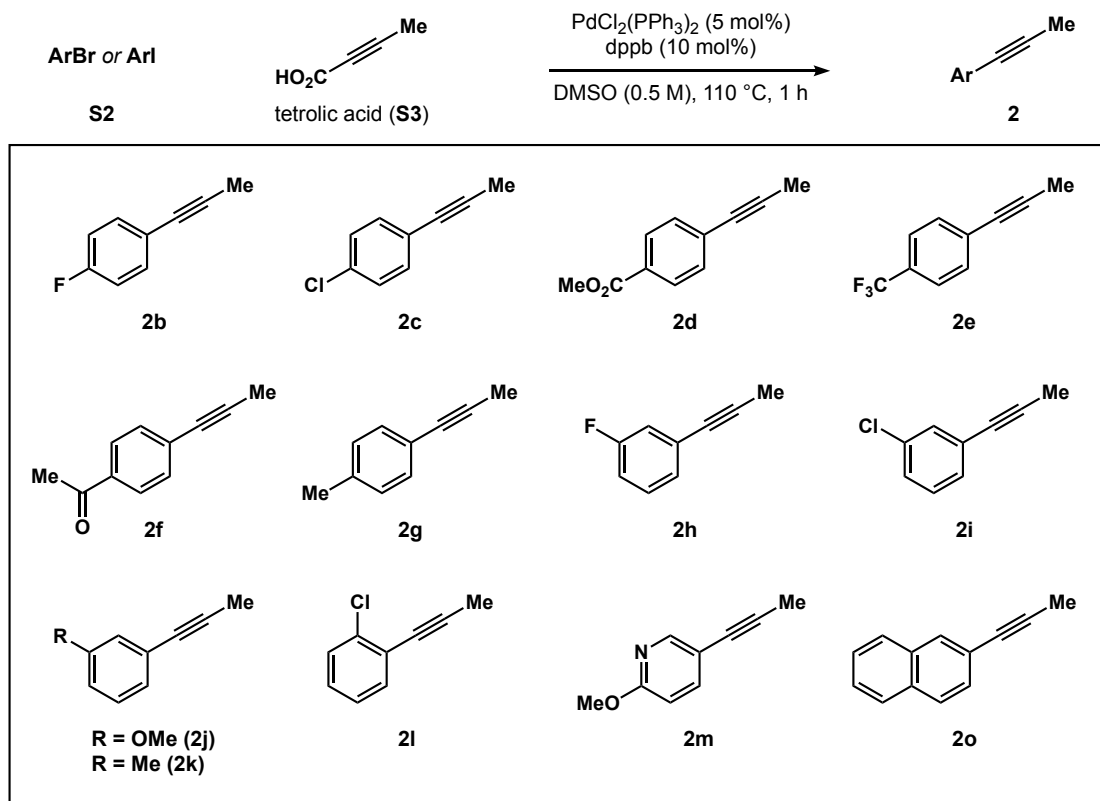
Prepared according to the general procedure for nitration using NaNO_2 (0.48 g, 7.0 mmol), phloroglucinol (0.44 g, 3.5 mmol), and DMF (8.3 mL). To the resulting solution was added *N*-benzyl-2-bromopropanamide (1.0 g, 4.1 mmol). The reaction was complete after 4 hours at room temperature. Purification by flash column chromatography using 97:3 hexanes:EtOAc afforded the desired α -nitrocarbonyl as a white solid (0.12 g, 0.58 mmol, 14%). ^1H NMR (500 MHz, CDCl_3) δ 7.36 – 7.28 (m, 3H), 7.26 – 7.23 (m, 2H), 6.71 (s, 1H), 5.12 (q, $J = 6.96$ Hz, 1H), 4.44 (dd, $J = 5.7$ and 1.5 Hz, 2H), 1.76 (d, $J = 7.0$ Hz, 3H). ^{13}C NMR (126 MHz, CDCl_3) δ 164.0, 136.9, 129.0, 128.0, 127.8, 84.6, 44.2, 16.2. IR (ATR): 3254, 3092, 2936, 1659, 1553, 1453, 1225, 1078 753 cm^{-1} . HRMS calculated for $\text{C}_{10}\text{H}_{12}\text{N}_2\text{O}_3$ $[\text{M}+\text{H}]^+$ 209.0926, found 209.0920.

***N*-benzyl-2-nitro-*N*-phenylpropanamide**



Prepared according to the general procedure for nitration using NaNO_2 (0.55 g, 8.0 mmol), phloroglucinol (0.51 g, 4.0 mmol), and DMF (9.5 mL). To the resulting solution was added *N*-benzyl-2-bromo-phenylpropanamide (1.5 g, 4.7 mmol). The reaction was complete after 4 hours at room temperature. Purification by flash column chromatography using 4:1 hexanes:EtOAc afforded the desired α -nitrocarbonyl as a white solid (1.0 g, 3.5 mmol, 74%). ^1H NMR (500 MHz, CDCl_3) δ 7.38 – 7.36 (m, 3H), 7.30 – 7.26 (m, 3H), 7.20 – 7.18 (m, 2H), 7.06 (s, 2H), 5.05 (d, $J = 6.8$ Hz, 1H), 5.02 (d, $J = 14.2$ Hz, 1H), 4.84 (d, $J = 14.2$ Hz, 1H), 1.65 (d, $J = 6.8$ Hz, 3H). ^{13}C NMR (126 MHz, CDCl_3) δ 165.1, 140.4, 136.2, 130.2, 129.2, 129.0, 128.7, 128.5, 127.9, 80.5, 53.8, 15.9. IR (ATR): 3058, 2936, 1659, 1553, 1497, 1453, 1417, 1245, 1202, 701 cm^{-1} . HRMS calculated for $\text{C}_{16}\text{H}_{20}\text{N}_3\text{O}_3$ $[\text{M}+\text{NH}_4]^+$ 302.1505, found 302.1515.

B. General Procedure for Decarboxylative Cross-Coupling (Alkynes)

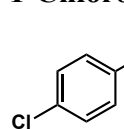


To a flame-dried Schlenk tube was added $\text{PdCl}_2(\text{PPh}_3)_2$ (5 mol%), 1,4-bis(diphenylphosphino)butane (10 mol%), and DMSO (0.5 M). To the resulting solution was added aryl halide **S2** (1 equiv.), tetrolic acid (**S3**, 1.2 equiv.), and DBU (3 equiv.). The reaction mixture was then heated to 110 °C. Upon reaction completion, the reaction mixture was cooled to room temperature, quenched with H_2O , and extracted with DCM (x3). The combined organic layers were washed with H_2O and brine, dried with anhydrous MgSO_4 , filtered, and concentrated *in vacuo*. The crude residue was purified by flash column chromatography to afford the desired alkyne product (**2**).

1-Fluoro-4-(prop-1-yn-1-yl)benzene (**2b**)

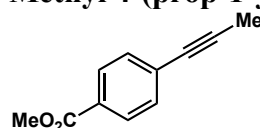
Prepared according to the general procedure for decarboxylative cross-coupling using $\text{PdCl}_2(\text{PPh}_3)_2$ (176 mg, 0.25 mmol, 5 mol%), 1,4-bis(diphenylphosphino)butane (213 mg, 0.50 mmol, 10 mol%), and DMSO (10 mL, 0.5 M). To the resulting solution was added 4-fluoroiodobenzene (1.11 g, 5 mmol, 1 equiv.), 2-butynoic acid (505 mg, 6 mmol, 1.2 equiv.), and DBU (2.2 mL, 15 mmol, 3 equiv.). The reaction was complete after 1 hour at 110 °C. Purification by flash column chromatography using hexanes afforded the desired alkyne as a colorless oil (209 mg, 1.56 mmol, 31%). The ^1H NMR was in accordance with the literature.³ ^1H NMR (400 MHz, CDCl_3): δ 7.39 – 7.32 (m, 2H), 7.00 – 6.93 (m, 2H), 2.03 (s, 3H).

1-Chloro-4-(prop-1-yn-1-yl)benzene (2c)



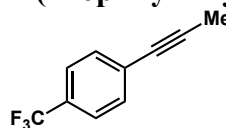
Prepared according to the general procedure for decarboxylative cross-coupling using $\text{PdCl}_2(\text{PPh}_3)_2$ (176 mg, 0.25 mmol, 5 mol%), 1,4-bis(diphenylphosphino)butane (213 mg, 0.50 mmol, 10 mol%), and DMSO (10 mL, 0.5 M). To the resulting solution was added 1-chloro-4-iodobenzene (1.19 g, 5 mmol, 1 equiv.), 2-butyric acid (505 mg, 6 mmol, 1.2 equiv.), and DBU (2.2 mL, 15 mmol, 3 equiv.). The reaction was complete after 1 hour at 110 °C. Purification by flash column chromatography using hexanes afforded the desired alkyne as a clear oil (590 mg, 3.92 mmol, 78%). The $^1\text{H NMR}$ was in accordance with the literature.³ $^1\text{H NMR}$ (400 MHz, CDCl_3): δ 7.34 – 7.28 (m, 2H), 7.27 – 7.22 (m, 2H), 2.04 (s, 3H).

Methyl 4-(prop-1-yn-1-yl)benzoate (2d)



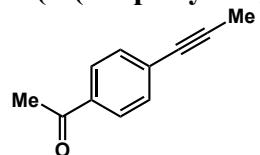
Prepared according to the general procedure for decarboxylative cross-coupling using $\text{PdCl}_2(\text{PPh}_3)_2$ (176 mg, 0.25 mmol, 5 mol%), 1,4-bis(diphenylphosphino)butane (213 mg, 0.50 mmol, 10 mol%), and DMSO (10 mL, 0.5 M). To the resulting solution was added methyl-4-bromobenzoate (1.08 g, 5 mmol, 1 equiv.), 2-butyric acid (505 mg, 6 mmol, 1.2 equiv.), and DBU (2.2 mL, 15 mmol, 3 equiv.). The reaction was complete after 1 hour at 110 °C. Purification by flash column chromatography using 20:1 hexanes:EtOAc afforded the desired alkyne as a white solid (298 mg, 1.71 mmol, 34%). The $^1\text{H NMR}$ was in accordance with the literature.³ $^1\text{H NMR}$ (400 MHz, CDCl_3): δ 7.98 – 7.91 (m, 2H), 7.48 – 7.40 (m, 2H), 3.91 (s, 3H), 2.08 (s, 3H).

1-(Prop-1-yn-1-yl)-4-(trifluoromethyl)benzene (2e)



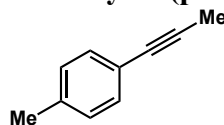
Prepared according to the general procedure for decarboxylative cross-coupling using $\text{PdCl}_2(\text{PPh}_3)_2$ (176 mg, 0.25 mmol, 5 mol%), 1,4-bis(diphenylphosphino)butane (213 mg, 0.50 mmol, 10 mol%), and DMSO (10 mL, 0.5 M). To the resulting solution was added 1-bromo-4-(trifluoromethyl)benzene (1.13 g, 5 mmol, 1 equiv.), 2-butyric acid (505 mg, 6 mmol, 1.2 equiv.), and DBU (2.2 mL, 15 mmol, 3 equiv.). The reaction was complete after 1 hour at 110 °C. Purification by flash column chromatography using 40:1 hexanes:EtOAc afforded the desired alkyne as a colorless oil (408 mg, 2.21 mmol, 44%). The $^1\text{H NMR}$ was in accordance with the literature.³ $^1\text{H NMR}$ (400 MHz, CDCl_3): δ 7.56 – 7.50 (m, 2H), 7.47 (d, J = 8.1 Hz, 2H), 2.07 (s, 3H).

1-(4-(Prop-1-yn-1-yl)phenyl)ethan-1-one (2f)



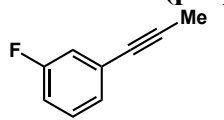
Prepared according to the general procedure for decarboxylative cross-coupling using $\text{PdCl}_2(\text{PPh}_3)_2$ (176 mg, 0.25 mmol, 5 mol%), 1,4-bis(diphenylphosphino)butane (213 mg, 0.50 mmol, 10 mol%), and DMSO (10 mL, 0.5 M). To the resulting solution was added 4'-bromoacetophenone (995 mg, 5 mmol, 1 equiv.), 2-butyric acid (505 mg, 6 mmol, 1.2 equiv.), and DBU (2.2 mL, 15 mmol, 3 equiv.). The reaction was complete after 1 hour at 110 °C. Purification by flash column chromatography using 10:1 hexanes:EtOAc afforded the desired alkyne as a white solid (201 mg, 1.27 mmol, 25%). The $^1\text{H NMR}$ was in accordance with the literature.³ $^1\text{H NMR}$ (400 MHz, CDCl_3): δ 7.90 – 7.84 (m, 2H), 7.49 – 7.42 (m, 2H), 2.58 (s, 3H), 2.08 (s, 3H).

1-Methyl-4-(prop-1-yn-1-yl)benzene (2g)



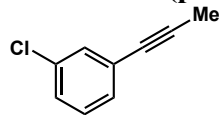
Prepared according to the general procedure for decarboxylative cross-coupling using $\text{PdCl}_2(\text{PPh}_3)_2$ (176 mg, 0.25 mmol, 5 mol%), 1,4-bis(diphenylphosphino)butane (213 mg, 0.50 mmol, 10 mol%), and DMSO (10 mL, 0.5 M). To the resulting solution was added 4-bromotoluene (855 mg, 5 mmol, 1 equiv.), 2-butynoic acid (505 mg, 6 mmol, 1.2 equiv.), and DBU (2.2 mL, 15 mmol, 3 equiv.). The reaction was complete after 1 hour at 110 °C. Purification by flash column chromatography using hexanes afforded the desired alkyne as a colorless oil (533 mg, 4.09 mmol, 82%). The $^1\text{H NMR}$ was in accordance with the literature.³ $^1\text{H NMR}$ (400 MHz, CDCl_3): δ 7.31 – 7.26 (m, 2H), 7.13 – 7.05 (m, 2H), 2.33 (s, 3H), 2.04 (s, 3H).

1-Fluoro-3-(prop-1-yn-1-yl)benzene (2h)



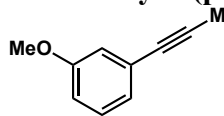
Prepared according to the general procedure for decarboxylative cross-coupling using $\text{PdCl}_2(\text{PPh}_3)_2$ (176 mg, 0.25 mmol, 5 mol%), 1,4-bis(diphenylphosphino)butane (213 mg, 0.50 mmol, 10 mol%), and DMSO (10 mL, 0.5 M). To the resulting solution was added 1-bromo-3-fluorobenzene (875 mg, 5 mmol, 1 equiv.), 2-butynoic acid (505 mg, 6 mmol, 1.2 equiv.), and DBU (2.2 mL, 15 mmol, 3 equiv.). The reaction was complete after 1 hour at 110 °C. Purification by flash column chromatography using hexanes afforded the desired alkyne as a colorless oil (342 mg, 2.55 mmol, 51%). The $^1\text{H NMR}$ was in accordance with the literature.⁴ $^1\text{H NMR}$ (400 MHz, CDCl_3): δ 7.25 – 7.19 (m, 1H), 7.16 (dt, $J = 7.7, 1.2$ Hz, 1H), 7.08 (ddd, $J = 9.6, 2.6, 1.4$ Hz, 1H), 6.97 (tdd, $J = 8.4, 2.6, 1.1$ Hz, 1H), 2.05 (s, 3H).

1-Chloro-3-(prop-1-yn-1-yl)benzene (2i)



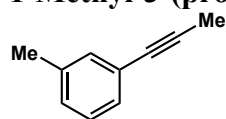
Prepared according to the general procedure for decarboxylative cross-coupling using $\text{PdCl}_2(\text{PPh}_3)_2$ (176 mg, 0.25 mmol, 5 mol%), 1,4-bis(diphenylphosphino)butane (213 mg, 0.50 mmol, 10 mol%), and DMSO (10 mL, 0.5 M). To the resulting solution was added 3-chloriodobenzene (1.19 g, 5 mmol, 1 equiv.), 2-butynoic acid (505 mg, 6 mmol, 1.2 equiv.), and DBU (2.2 mL, 15 mmol, 3 equiv.). The reaction was complete after 1 hour at 110 °C. Purification by flash column chromatography using hexanes afforded the desired alkyne as a yellow oil (250 mg, 1.66 mmol, 33%). The $^1\text{H NMR}$ was in accordance with the literature.⁵ $^1\text{H NMR}$ (400 MHz, CDCl_3): δ 7.37 (t, $J = 1.8$ Hz, 1H), 7.28 – 7.17 (m, 3H), 2.04 (s, 3H).

1-Methoxy-3-(prop-1-yn-1-yl)benzene (2j)



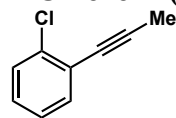
Prepared according to the general procedure for decarboxylative cross-coupling using $\text{PdCl}_2(\text{PPh}_3)_2$ (176 mg, 0.25 mmol, 5 mol%), 1,4-bis(diphenylphosphino)butane (213 mg, 0.50 mmol, 10 mol%), and DMSO (10 mL, 0.5 M). To the resulting solution was added 3-bromoanisole (935 mg, 5 mmol, 1 equiv.), 2-butynoic acid (505 mg, 6 mmol, 1.2 equiv.), and DBU (2.2 mL, 15 mmol, 3 equiv.). The reaction was complete after 1 hour at 110 °C. Purification by flash column chromatography using 20:1 hexanes:EtOAc afforded the desired alkyne as a colorless oil (582 mg, 3.98 mmol, 80%). The $^1\text{H NMR}$ was in accordance with the literature.³ $^1\text{H NMR}$ (400 MHz, CDCl_3): δ 7.21 – 7.16 (m, 1H), 6.98 (dt, $J = 7.6, 1.2$ Hz, 1H), 6.93 (dd, $J = 2.6, 1.4$ Hz, 1H), 6.83 (ddd, $J = 8.4, 2.7, 1.0$ Hz, 1H), 3.79 (s, 3H), 2.05 (s, 3H).

1-Methyl-3-(prop-1-yn-1-yl)benzene (2k)



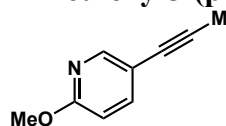
Prepared according to the general procedure for decarboxylative cross-coupling using $\text{PdCl}_2(\text{PPh}_3)_2$ (176 mg, 0.25 mmol, 5 mol%), 1,4-bis(diphenylphosphino)butane (213 mg, 0.50 mmol, 10 mol%), and DMSO (10 mL, 0.5 M). To the resulting solution was added 3-bromotoluene (855 mg, 5 mmol, 1 equiv.), 2-butynoic acid (505 mg, 6 mmol, 1.2 equiv.), and DBU (2.2 mL, 15 mmol, 3 equiv.). The reaction was complete after 1 hour at 110 °C. Purification by flash column chromatography using hexanes afforded the desired alkyne as a yellow oil (591 mg, 4.54 mmol, 91%). The $^1\text{H NMR}$ was in accordance with the literature.³ $^1\text{H NMR}$ (400 MHz, CDCl_3): δ 7.23 – 7.12 (m, 3H), 7.10 – 7.05 (m, 1H), 2.31 (s, 3H), 2.05 (s, 3H).

1-Chloro-2-(prop-1-yn-1-yl)benzene (2l)



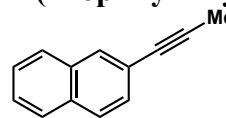
Prepared according to the general procedure for decarboxylative cross-coupling using $\text{PdCl}_2(\text{PPh}_3)_2$ (176 mg, 0.25 mmol, 5 mol%), 1,4-bis(diphenylphosphino)butane (213 mg, 0.50 mmol, 10 mol%), and DMSO (10 mL, 0.5 M). To the resulting solution was added 1-chloro-2-iodobenzene (1.19 g, 5 mmol, 1 equiv.), 2-butynoic acid (505 mg, 6 mmol, 1.2 equiv.), and DBU (2.2 mL, 15 mmol, 3 equiv.). The reaction was complete after 1 hour at 110 °C. Purification by flash column chromatography using hexanes afforded the desired alkyne as a colorless oil (541 mg, 3.59 mmol, 72%). The $^1\text{H NMR}$ was in accordance with the literature.⁶ $^1\text{H NMR}$ (400 MHz, CDCl_3): δ 7.42 (dt, $J = 7.6, 3.4$ Hz, 1H), 7.38 – 7.34 (m, 1H), 7.22 – 7.14 (m, 2H), 2.12 (s, 3H).

2-Methoxy-5-(prop-1-yn-1-yl)pyridine (2m)



Prepared according to the general procedure for decarboxylative cross-coupling using $\text{PdCl}_2(\text{PPh}_3)_2$ (176 mg, 0.25 mmol, 5 mol%), 1,4-bis(diphenylphosphino)butane (213 mg, 0.50 mmol, 10 mol%), and DMSO (10 mL, 0.5 M). To the resulting solution was added 5-bromo-2-methoxypyridine (940 mg, 5 mmol, 1 equiv.), 2-butynoic acid (505 mg, 6 mmol, 1.2 equiv.), and DBU (2.2 mL, 15 mmol, 3 equiv.). The reaction was complete after 1 hour at 110 °C. Purification by flash column chromatography using 20:1 hexanes:EtOAc afforded the desired alkyne as a yellow oil (632 mg, 4.30 mmol, 86%). The $^1\text{H NMR}$ was in accordance with the literature.⁵ $^1\text{H NMR}$ (400 MHz, CDCl_3): δ 8.21 (d, $J = 2.2$ Hz, 1H), 7.55 (dd, $J = 8.6, 2.3$ Hz, 1H), 6.66 (dd, $J = 8.6, 0.7$ Hz, 1H), 3.93 (s, 3H), 2.05 (s, 3H).

2-(Prop-1-yn-1-yl)naphthalene (2o)



Prepared according to the general procedure for decarboxylative cross-coupling using $\text{PdCl}_2(\text{PPh}_3)_2$ (176 mg, 0.25 mmol, 5 mol%), 1,4-bis(diphenylphosphino)butane (213 mg, 0.50 mmol, 10 mol%), and DMSO (10 mL, 0.5 M). To the resulting solution was added 2-bromonaphthalene (1.04 g, 5 mmol, 1 equiv.), 2-butynoic acid (505 mg, 6 mmol, 1.2 equiv.), and DBU (2.2 mL, 15 mmol, 3 equiv.). The reaction was complete after 1 hour at 110 °C. Purification by flash column chromatography using 40:1 hexanes:EtOAc afforded the desired alkyne as a colorless oil (584 mg, 3.51 mmol, 70%). The $^1\text{H NMR}$ was in accordance with the literature.⁶ $^1\text{H NMR}$ (400 MHz, CDCl_3): δ 7.93 – 7.89 (m, 1H), 7.83 – 7.72 (m, 3H), 7.51 – 7.42 (m, 3H), 2.11 (s, 3H).

5. Mechanistic Experiments

A. NMR Spectroscopy Experiments:

In a N₂-filled glovebox, (*R*)-MeO-BIPHEP **L6** (A104-1, 19.6 mg, 0.02 mmol, 8 mol%) and [Rh(cod)Cl]₂ (5.4 mg, 0.01 mmol, 4 mol%) were dissolved with DCE-*d*₄ (0.8 mL) in a 1-dram vial. The resulting solution was heated at 80 °C for 15 min and then diphenyl phosphate (13.8 mg, 0.06 mmol, 20 mol%) was added. The reaction mixture was then heated at 80 °C for an additional 30 min and transferred to a J. Young NMR tube to perform ¹H NMR spectroscopy. A resonance at -16.2 ppm was *observed* in less than ten minutes at rt in the ¹H NMR spectrum (Figure S9). Alkyne **2a** (48 mg, 0.41 mmol) was then added and the dark brown solution was heated at 80 °C for 30 min. The Rh-H resonance (at -16.2 ppm) was *not observed* in the ¹H NMR spectrum (Figure S10).

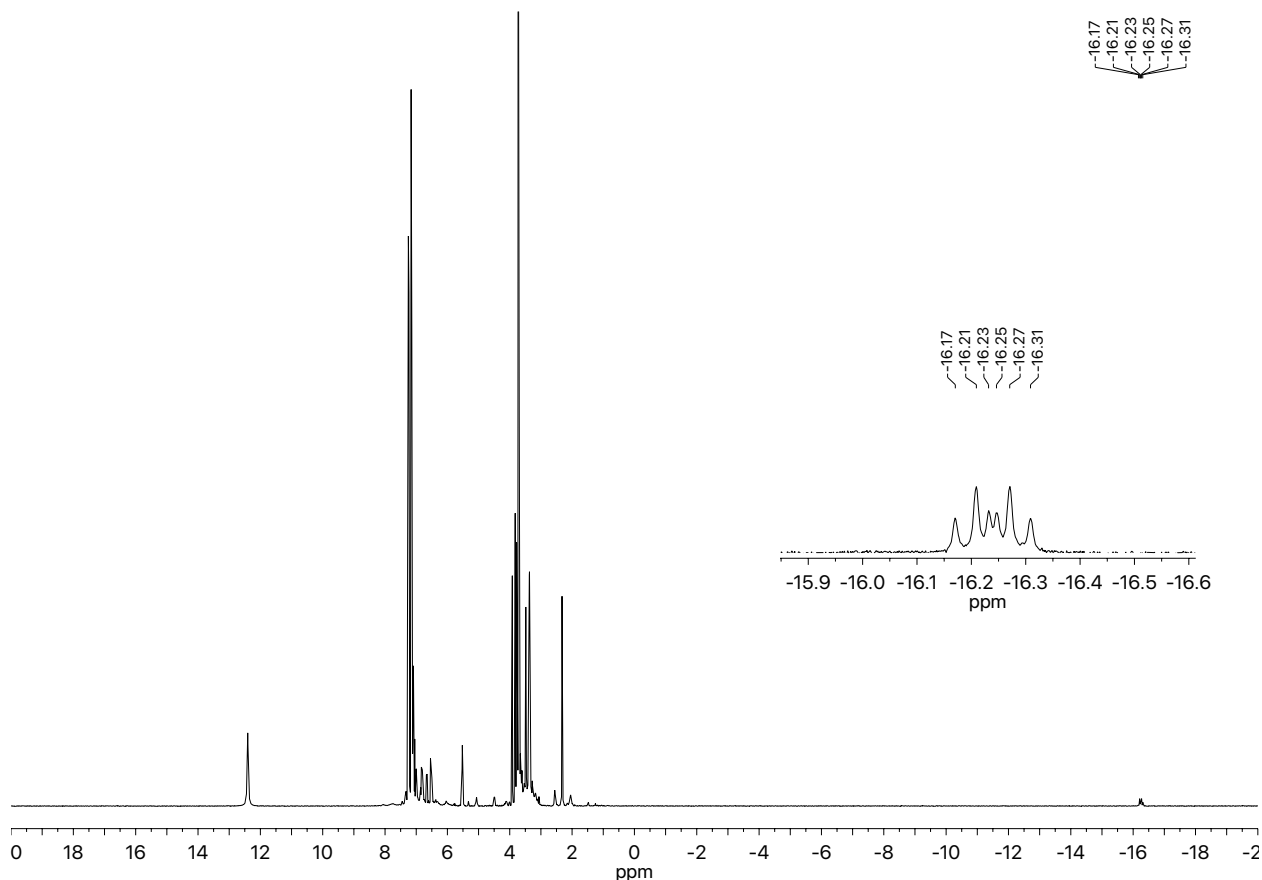


Figure S9. ¹H NMR (400 MHz) for a mixture of [Rh(cod)Cl]₂, (*R*)-MeO-BIPHEP **L6**, and diphenyl phosphate in DCE-*d*₄ (δ 3.79 ppm). Rh-H resonance is *observed* at -16.2 ppm.

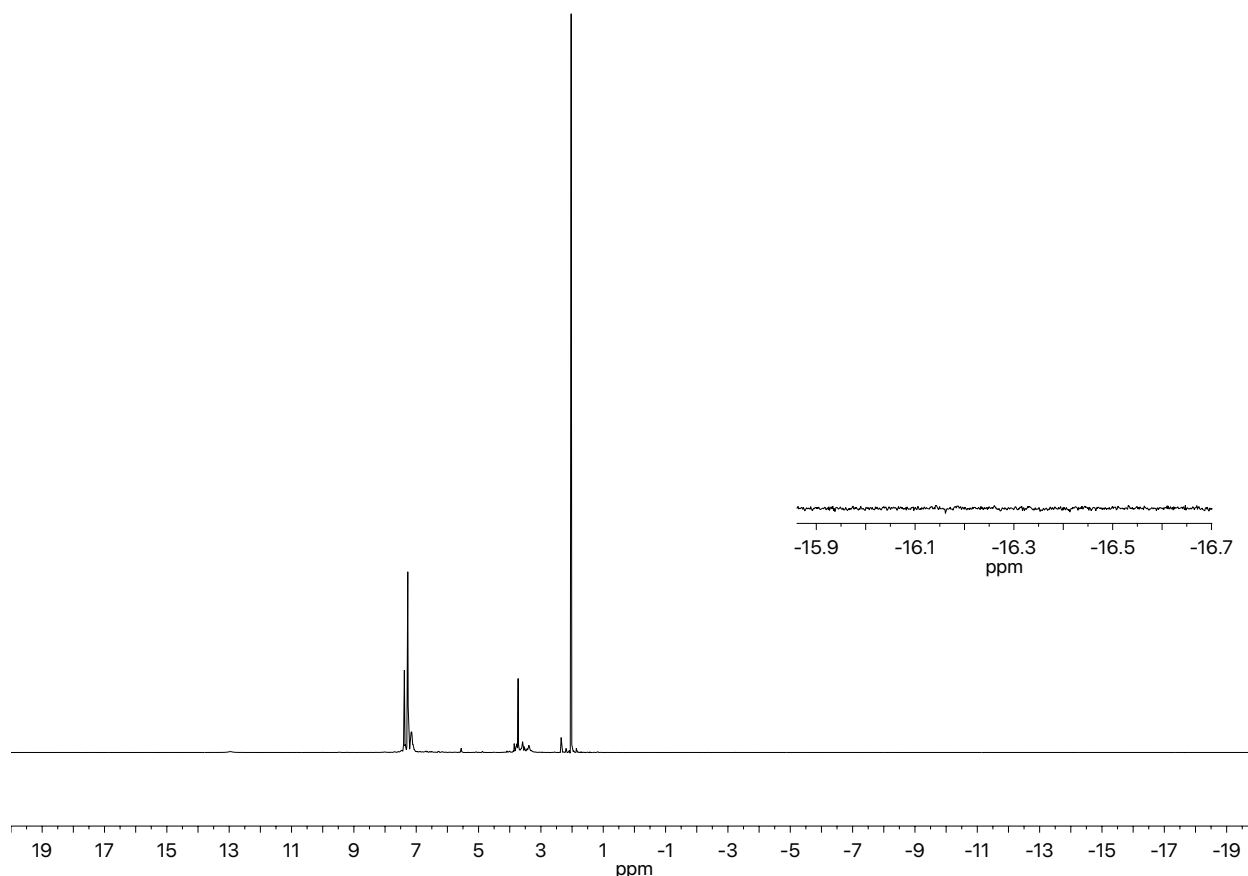
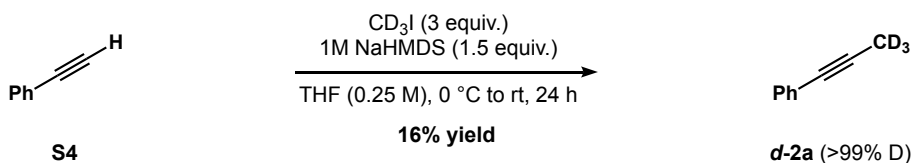
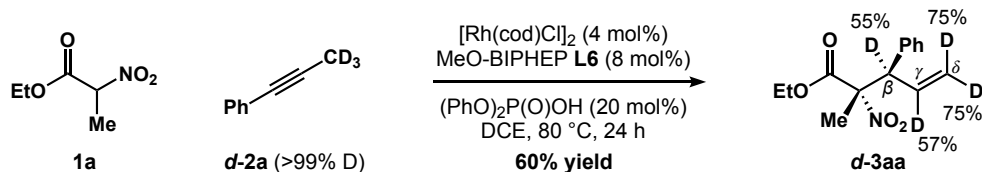


Figure S10. ^1H NMR (400 MHz) for a mixture of $[\text{Rh}(\text{cod})\text{Cl}]_2$, (*R*)-MeO-BIPHEP **L6**, diphenyl phosphate, and alkyne **2a** in $\text{DCE-}d_4$ (δ 3.79 ppm). Rh-H resonance is *not observed* at -16.2 ppm.

B. Deuterated Alkyne Synthesis and Experiment:

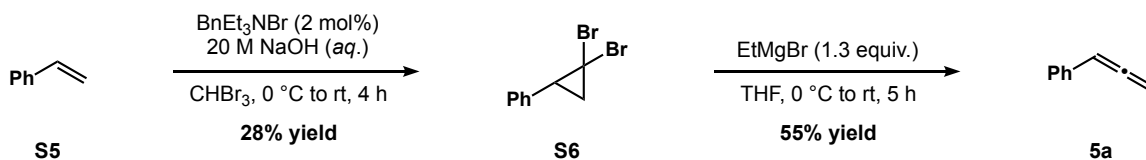


Preparation of (Prop-1-yn-1-yl- d_3)benzene-ethynylbenzene (*d*-2a): To a round bottom flask containing ethynylbenzene (**S4**, 204 mg, 2 mmol) in THF (8 mL) was slowly added 1M NaHMDS in THF (3 mL, 3 mmol, 1.5 equiv.) at 0 °C. To the resulting mixture was added iodomethane- d_3 (0.37 mL, 6 mmol, 3 equiv.). The reaction mixture was then stirred at rt for 24 h. Upon completion, the reaction mixture was quenched with H_2O and extracted with EtOAc (x3). The combined organic layers were washed with brine, dried with anhydrous MgSO_4 , filtered, and concentrated *in vacuo*. The crude residue was purified by flash column chromatography (hexanes) to afford alkyne **d-2a** as a clear, colorless oil [39 mg, 16% yield]. The ^1H NMR was in accordance with the literature.⁷ ^1H NMR (400 MHz, CDCl_3) δ 7.40 – 7.37 (m, 2H), 7.31 – 7.23 (m, 3H). ^2H NMR (61 MHz, CDCl_3) δ 2.03.

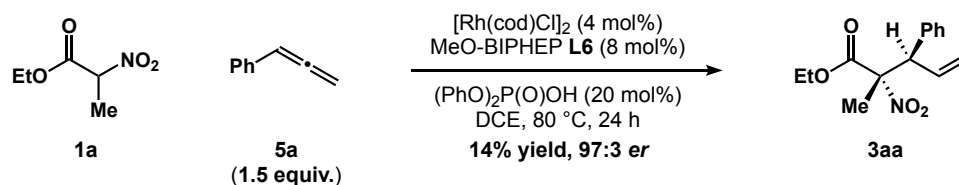


Deuterated Alkyne Mechanistic Experiment: According to *General Procedure for Enantioenriched Allylic Nitrocarbonyls* to a 1 dram vial equipped with a magnetic stir bar was added $[\text{Rh}(\text{cod})\text{Cl}]_2$ (2.0 mg, 0.004 mmol, 4 mol%), (*R*)-MeO-BIPHEP **L6** (A104-1, 7.5 mg, 0.008 mmol, 8 mol%), diphenyl phosphate (5.0 mg, 0.02 mmol, 20 mol%), ethyl-2-nitropropionate (14.7 mg, 0.1 mmol, 1 equiv.), alkyne **d-2a** (17.9 mg, 0.15 mmol, 1.5 equiv.) and DCE (200 μL , 0.5 M). The vial was then sealed with a Teflon-lined screw cap and heated to 80 $^\circ\text{C}$ for 24 hours. The resulting mixture was then cooled to room temperature and concentrated *in vacuo*. The crude residue was purified by preparatory TLC (20:1 hexanes:EtOAc) to afford allylic nitroester **d-3aa** as a clear, yellow oil [16.0 mg, 60% yield]. $^1\text{H NMR}$ (400 MHz, CDCl_3) δ 7.34 – 7.28 (m, 3H), 7.25 – 7.22 (m, 2H), 6.35 – 6.28 (m, 0.43H), 5.25 – 5.15 (m, 0.50 H), 4.42 – 4.40 (m, 0.45H), 4.18 – 4.12 (m, 2H), 1.78 (s, 3H), 1.20 (t, $J = 7.2$ Hz, 3H). $^2\text{H NMR}$ (61 MHz, CDCl_3) δ 6.33, 5.21, 4.40.

C. 1-Phenylallene Synthesis and Experiment:



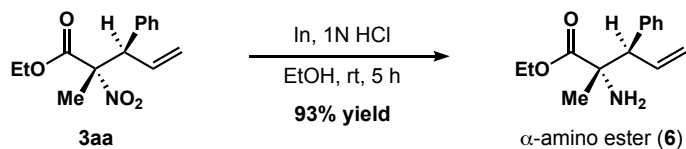
Preparation of 1-Phenylallene (5a): To a round bottom flask containing styrene (**S5**, 1.35 g, 13 mmol) in CHBr_3 (5 mL, 2.6 M) was added benzyltriethylammonium bromide (71 mg, 0.26 mmol, 0.02 equiv) in one portion. To the resulting mixture was added 20 M NaOH (*aq*, 5 mL) at 0 $^\circ\text{C}$. The reaction mixture was then stirred at 0 $^\circ\text{C}$ for 3 h and then at rt for 1 h. Upon completion, the reaction mixture was extracted with EtOAc (3 x 15 mL). The combined organic layers were washed with brine, dried with anhydrous MgSO_4 , filtered, and concentrated *in vacuo*. The crude residue was purified by flash column chromatography (hexanes) to afford **S6** as a clear, yellow oil [1 g, 28% yield]. The $^1\text{H NMR}$ was in accordance with the literature.⁸ $^1\text{H NMR}$ (400 MHz, CDCl_3) δ 7.39 – 7.29 (m, 3H), 7.26 (dd, $J = 5.4, 2.7$ Hz, 2H), 2.96 (dd, $J = 10.4, 8.4$ Hz, 1H), 2.14 (dd, $J = 10.5, 7.7$ Hz, 1H), 2.02 (t, $J = 8.0$ Hz, 1H). To a round bottom flask containing **S6** (994 mg, 3.6 mmol) in THF (7.2 mL, 0.5 M) was added 1M EtMgBr (4.68 mL, 4.68 mmol, 1.3 equiv) dropwise at 0 $^\circ\text{C}$. The reaction mixture was then gently warmed to rt and stirred for 3 h. Upon completion, the reaction mixture was quenched with water (10 mL) and extracted with EtOAc (3 x 15 mL). The combined organic layers were washed 1M HCl (10 mL), saturated NaHCO_3 (10 mL), and then brine. The combined organic layers were then dried with anhydrous MgSO_4 , filtered, and concentrated *in vacuo*. The crude residue was purified by flash column chromatography (hexanes) to afford allene **5a** as a clear, colorless oil [232 mg, 55% yield]. The $^1\text{H NMR}$ was in accordance with the literature.⁸ $^1\text{H NMR}$ (400 MHz, CDCl_3) δ 7.33 – 7.30 (m, 4H), 7.24 – 7.18 (m, 1H), 6.18 (t, $J = 6.8$ Hz, 1H), 5.16 (d, $J = 6.8$ Hz, 2H).



Allene Mechanistic Experiments: According to *General Procedure for Enantioenriched Allylic Nitrocarbonyls* a 1 dram vial equipped with a magnetic stir bar was added $[Rh(cod)Cl]_2$ (2.0 mg, 0.004 mmol, 4 mol%), (*R*)-MeO-BIPHEP (A104-1, 7.5 mg, 0.008 mmol, 8 mol%), diphenyl phosphate (5.0 mg, 0.02 mmol, 20 mol%), ethyl-2-nitropropanoate (14.7 mg, 0.1 mmol, 1 equiv.), 1-phenylallene (17.4 mg, 0.15 mmol, 1.5 equiv.) and DCE (200 μ L, 0.5 M). The vial was then sealed with a Teflon-lined screw cap and heated to 80 °C for 24 hours. The resulting mixture was then cooled to room temperature and concentrated *in vacuo*. Diastereo- and regioselectivity ratios (*dr* and *rr*, respectively) were determined by 1H NMR analysis of the crude reaction mixture. 1H NMR yield, which was referenced to an internal standard (triphenylmethane), is reported. Chiral SFC analysis for enantioselectivity ratios (*er*). Observed **3aa** (14% yield, 0.014 mmol, 97:3 *er*) in the crude 1H NMR spectrum.

***Note:** In the absence of nucleophile **1a**, 1-phenylallene (0.15 mmol) is completely consumed in the standard reaction conditions above. The 1-phenylallene mass appears to convert to a gel-like substance that is not soluble in the reaction medium.

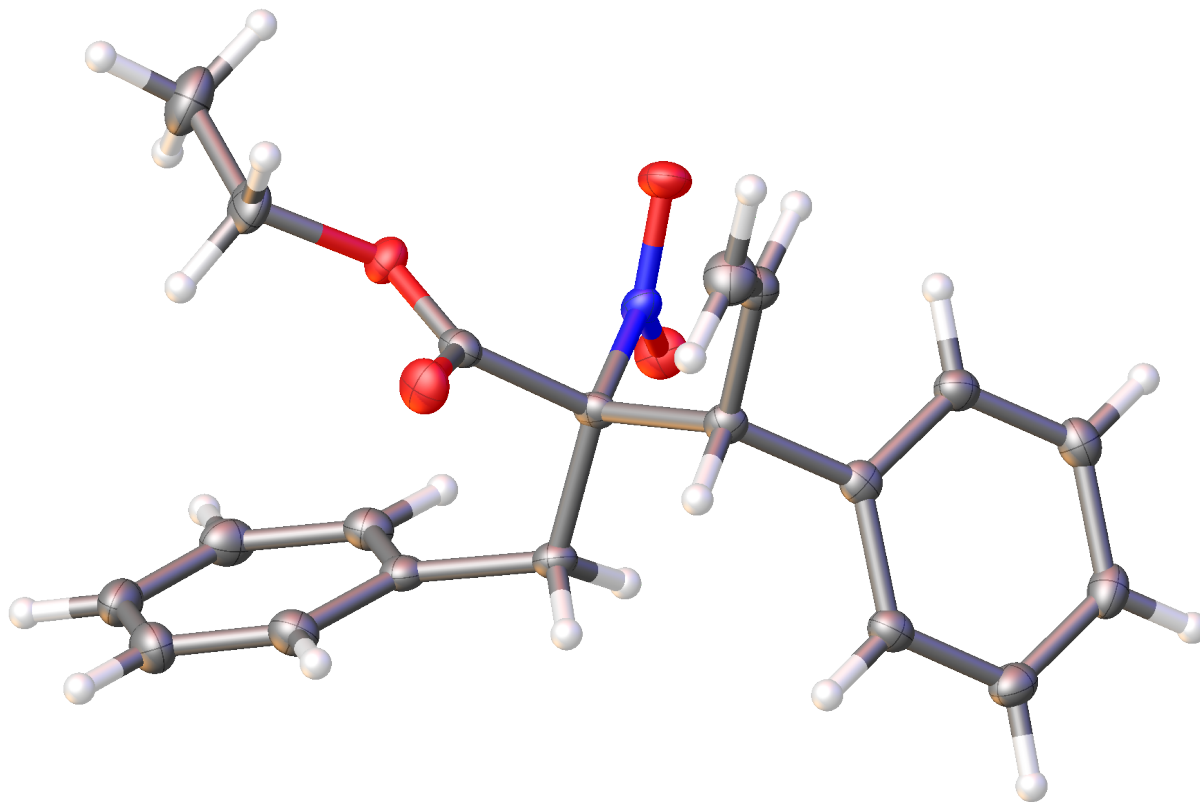
6. Reduction of Allylic Nitroester 3aa to Amino Ester 6



Preparation of Ethyl (2S,3R)-2-amino-2-methyl-3-phenylpent-4-enoate (6): To a round bottom flask containing nitroester (26 mg, 0.1 mmol) in EtOH (2 mL, 0.05 M) was added indium powder (115 mg, 1 mmol, 10 equiv, 325 mesh) in one portion. To the resulting suspension was added 1N HCl (aq, 1 mL, 1 mmol, 10 equiv.). The clear reaction mixture was then stirred at rt for 5 h. Upon completion (visible grey precipitate), the reaction mixture was cooled to 0 °C, quenched with saturated NaHCO₃ (aq) slowly, and extracted with EtOAc (3 x 5 mL). The combined organic layers were washed with brine, dried with anhydrous MgSO₄, filtered, and concentrated *in vacuo*. The crude residue was purified by preparatory TLC (2:1 hexanes:EtOAc) to afford the title compound as a clear, yellow oil [22 mg, 93% yield, >20:1 *dr*, 97:3 *er*, $[\alpha]^{24}_{\text{D}} = -29.9^\circ$ (*c* 1.0, CHCl₃)]. **¹H NMR** (400 MHz, CDCl₃) δ 7.33 – 7.20 (m, 5H), 6.25 (ddd, *J* = 17.0, 10.1, 9.3 Hz, 1H), 5.14 (dd, *J* = 10.2, 1.5 Hz, 1H), 5.09 (d, *J* = 17.0 Hz, 1H), 4.15 (q, *J* = 7.1 Hz, 2H), 3.62 (d, *J* = 9.2 Hz, 1H), 1.76 (br, 2H), 1.25 (t, *J* = 7.1 Hz, 3H), 1.19 (s, 3H). **¹³C NMR** (101 MHz, CDCl₃) δ 176.7, 139.6, 137.2, 129.7, 128.4, 127.2, 117.9, 61.5, 61.4, 58.8, 25.6, 14.4. **IR** (ATR): 3384, 3319, 2978, 2930, 1726, 1454, 1219, 1104, 1021, 916 cm⁻¹. **HRMS** calculated for C₁₄H₂₀NO₂ [M+H]⁺ 234.1494, found 234.1494. **Chiral SFC** (of the corresponding benzamide): 150 mm CHIRALCEL AD-H, 6% *i*PrOH, 2 mL/min, 220 nm, 44 °C, nozzle pressure = 200 bar CO₂, *t*_{R1} (minor) = 6.9 min, *t*_{R2} (major) = 9.9 min.

7. X-Ray Crystallographic Data

X-ray Crystallographic Data for 3fa (CCDC 2014416)



The single crystal X-ray diffraction studies were carried out on a Bruker SMART Platinum 135 CCD diffractometer equipped with Cu K_a radiation ($\lambda = 1.5478$). Crystals of the subject compound were used as received. (grown from acetonitrile/pentane by vapor diffusion.)

A 0.225 x 0.200 x 0.180 mm colorless block was mounted on a Cryoloop with Paratone oil. Data were collected in a nitrogen gas stream at 100(1) K using ϕ and ω scans. Crystal-to-detector distance was 45 mm using variable exposure time (1, 3 and 5s) depending on the detector θ position, with a scan width of 1.4°. Data collection was 100.0% complete to 67.679° in θ . A total of 14039 reflections were collected covering the indices, $-7 \leq h \leq 7$, $-17 \leq k \leq 16$, $-25 \leq l \leq 24$. 3399 reflections were found to be symmetry independent, with a R_{int} of 0.0368. Indexing and unit cell refinement indicated a **Primitive, Orthorhombic** lattice. The space group was found to be ***P2₁2₁2₁***. The data were integrated using the Bruker SAINT software program and scaled using the SADABS software program. Solution by direct methods (SHELXT) produced a complete phasing model consistent with the proposed structure.

All nonhydrogen atoms were refined anisotropically by full-matrix least-squares (SHELXL-2014). All hydrogen atoms were placed using a riding model. Their positions were constrained relative to their parent atom using the appropriate HFIX command in SHELXL-2014. Crystallographic data are summarized in Table S1.

Table S1. Crystal data and structure refinement for **3fa**.

Report date	2020-07-05
Identification code	pp01083

Empirical formula	C ₂₀ H ₂₁ N O ₄	
Molecular formula	C ₂₀ H ₂₁ N O ₄	
Formula weight	339.38	
Temperature	100.15 K	
Wavelength	1.54178 Å	
Crystal system	Orthorhombic	
Space group	P2 ₁ 2 ₁ 2 ₁	
Unit cell dimensions	a = 6.0404(3) Å	α = 90°.
	b = 14.3407(7) Å	β = 90°.
	c = 20.6337(10) Å	γ = 90°.
Volume	1787.36(15) Å ³	
Z	4	
Density (calculated)	1.261 Mg/m ³	
Absorption coefficient	0.716 mm ⁻¹	
F(000)	720	
Crystal size	0.225 x 0.2 x 0.18 mm ³	
Crystal color, habit	colorless block	
Theta range for data collection	3.753 to 70.261°.	
Index ranges	-7<=h<=7, -17<=k<=16, -25<=l<=24	
Reflections collected	14039	
Independent reflections	3399 [R(int) = 0.0368]	
Completeness to theta = 67.679°	100.0 %	
Absorption correction	Semi-empirical from equivalents	
Max. and min. transmission	0.7533 and 0.6729	
Refinement method	Full-matrix least-squares on F ²	
Data / restraints / parameters	3399 / 0 / 227	
Goodness-of-fit on F ²	1.077	
Final R indices [I>2sigma(I)]	R1 = 0.0268, wR2 = 0.0680	
R indices (all data)	R1 = 0.0270, wR2 = 0.0681	
Absolute structure parameter	-0.04(4)	
Largest diff. peak and hole	0.245 and -0.140 e.Å ⁻³	

Table S2. Atomic coordinates ($\times 10^4$) and equivalent isotropic displacement parameters ($\text{\AA}^2 \times 10^3$) for **3fa**. $U(\text{eq})$ is defined as one third of the trace of the orthogonalized U^{ij} tensor.

	x	y	z	U(eq)
O(1)	6640(2)	3553(1)	6535(1)	19(1)
O(2)	3256(2)	3277(1)	6112(1)	24(1)
O(3)	8826(2)	4308(1)	5486(1)	22(1)
O(4)	8318(2)	5657(1)	5926(1)	22(1)
N(1)	7644(2)	4894(1)	5746(1)	16(1)
C(1)	8607(4)	2601(1)	7286(1)	34(1)
C(2)	6443(3)	2716(1)	6935(1)	25(1)
C(3)	4919(2)	3733(1)	6152(1)	17(1)
C(4)	5180(2)	4668(1)	5798(1)	15(1)
C(5)	4240(2)	4617(1)	5089(1)	16(1)
C(6)	5050(3)	3791(1)	4700(1)	20(1)
C(7)	3769(3)	3081(1)	4543(1)	26(1)
C(8)	3971(2)	5428(1)	6198(1)	17(1)
C(9)	4117(3)	5328(1)	6931(1)	18(1)
C(10)	2376(3)	4900(1)	7260(1)	22(1)
C(11)	2435(3)	4801(1)	7934(1)	27(1)
C(12)	4237(3)	5127(1)	8278(1)	26(1)
C(13)	5986(3)	5549(1)	7957(1)	25(1)
C(14)	5916(3)	5660(1)	7286(1)	21(1)
C(15)	4555(3)	5543(1)	4735(1)	16(1)
C(16)	6520(3)	5745(1)	4405(1)	19(1)
C(17)	6794(3)	6585(1)	4082(1)	21(1)
C(18)	5114(3)	7245(1)	4085(1)	22(1)
C(19)	3159(3)	7060(1)	4415(1)	22(1)
C(20)	2878(3)	6211(1)	4734(1)	19(1)

Table S3. Bond lengths [Å] and angles [°] for **3fa**.

O(1)-C(2)	1.4613(18)	C(7)-C(6)-C(5)	123.01(15)
O(1)-C(3)	1.3312(19)	C(9)-C(8)-C(4)	115.86(12)
O(2)-C(3)	1.2013(19)	C(10)-C(9)-C(8)	118.80(14)
O(3)-N(1)	1.2261(17)	C(14)-C(9)-C(8)	122.37(14)
O(4)-N(1)	1.2259(17)	C(14)-C(9)-C(10)	118.82(14)
N(1)-C(4)	1.5271(19)	C(9)-C(10)-C(11)	120.71(16)
C(1)-C(2)	1.504(3)	C(12)-C(11)-C(10)	119.81(17)
C(3)-C(4)	1.535(2)	C(11)-C(12)-C(13)	120.12(15)
C(4)-C(5)	1.571(2)	C(12)-C(13)-C(14)	120.11(16)
C(4)-C(8)	1.550(2)	C(9)-C(14)-C(13)	120.40(16)
C(5)-C(6)	1.513(2)	C(16)-C(15)-C(5)	121.20(14)
C(5)-C(15)	1.528(2)	C(20)-C(15)-C(5)	120.49(13)
C(6)-C(7)	1.320(2)	C(20)-C(15)-C(16)	118.30(14)
C(8)-C(9)	1.522(2)	C(17)-C(16)-C(15)	120.96(15)
C(9)-C(10)	1.394(2)	C(16)-C(17)-C(18)	120.25(15)
C(9)-C(14)	1.394(2)	C(17)-C(18)-C(19)	119.56(14)
C(10)-C(11)	1.397(2)	C(18)-C(19)-C(20)	120.11(15)
C(11)-C(12)	1.382(3)	C(15)-C(20)-C(19)	120.81(15)
C(12)-C(13)	1.386(3)		
C(13)-C(14)	1.394(2)		
C(15)-C(16)	1.399(2)		
C(15)-C(20)	1.394(2)		
C(16)-C(17)	1.386(2)		
C(17)-C(18)	1.387(2)		
C(18)-C(19)	1.389(2)		
C(19)-C(20)	1.394(2)		
C(3)-O(1)-C(2)	115.50(13)		
O(3)-N(1)-C(4)	116.92(12)		
O(4)-N(1)-O(3)	123.48(13)		
O(4)-N(1)-C(4)	119.46(12)		
O(1)-C(2)-C(1)	106.97(14)		
O(1)-C(3)-C(4)	111.79(12)		
O(2)-C(3)-O(1)	126.10(14)		
O(2)-C(3)-C(4)	121.87(14)		
N(1)-C(4)-C(3)	108.63(12)		
N(1)-C(4)-C(5)	107.26(11)		
N(1)-C(4)-C(8)	110.34(12)		
C(3)-C(4)-C(5)	111.46(12)		
C(3)-C(4)-C(8)	108.18(12)		
C(8)-C(4)-C(5)	110.96(12)		
C(6)-C(5)-C(4)	114.42(12)		
C(6)-C(5)-C(15)	112.76(12)		
C(15)-C(5)-C(4)	111.08(12)		

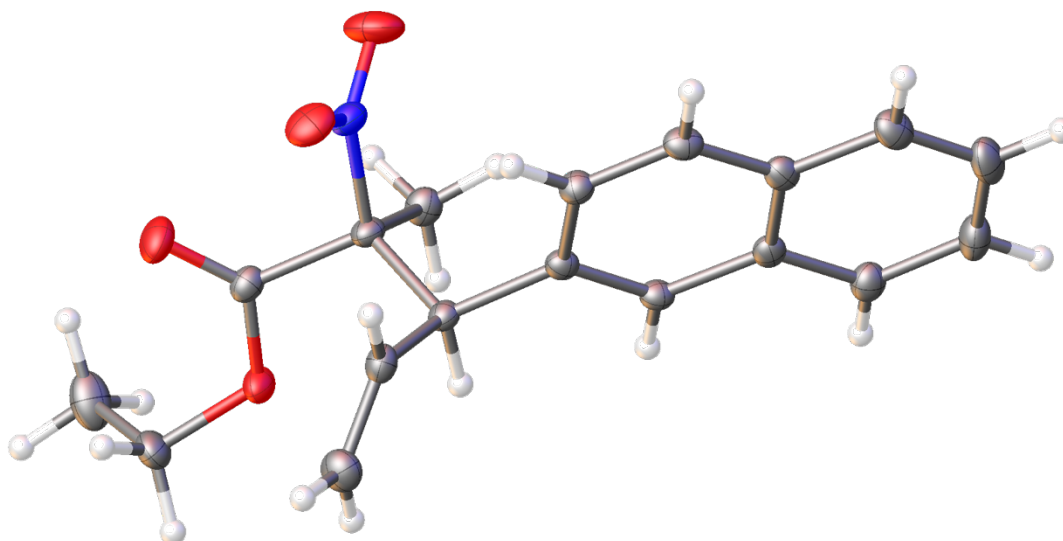
Table S4. Anisotropic displacement parameters ($\text{\AA}^2 \times 10^3$) for **3fa**. The anisotropic displacement factor exponent takes the form: $-2\pi^2 [h^2 a^2 U^{11} + \dots + 2 h k a^* b^* U^{12}]$

	U11	U22	U33	U23	U13	U12
O(1)	21(1)	15(1)	21(1)	4(1)	-1(1)	-1(1)
O(2)	21(1)	22(1)	28(1)	3(1)	1(1)	-7(1)
O(3)	16(1)	22(1)	29(1)	0(1)	4(1)	4(1)
O(4)	19(1)	19(1)	29(1)	0(1)	-1(1)	-6(1)
N(1)	13(1)	16(1)	19(1)	4(1)	0(1)	0(1)
C(1)	44(1)	28(1)	30(1)	11(1)	-8(1)	-2(1)
C(2)	32(1)	18(1)	26(1)	8(1)	1(1)	-1(1)
C(3)	17(1)	16(1)	18(1)	-1(1)	4(1)	0(1)
C(4)	11(1)	15(1)	19(1)	0(1)	2(1)	-1(1)
C(5)	13(1)	18(1)	18(1)	0(1)	-1(1)	-1(1)
C(6)	20(1)	19(1)	20(1)	0(1)	1(1)	1(1)
C(7)	33(1)	21(1)	25(1)	-3(1)	0(1)	-2(1)
C(8)	15(1)	16(1)	19(1)	0(1)	0(1)	2(1)
C(9)	18(1)	15(1)	20(1)	-1(1)	1(1)	4(1)
C(10)	20(1)	24(1)	24(1)	-1(1)	1(1)	1(1)
C(11)	27(1)	28(1)	25(1)	5(1)	6(1)	2(1)
C(12)	31(1)	29(1)	19(1)	3(1)	0(1)	9(1)
C(13)	24(1)	28(1)	24(1)	-4(1)	-4(1)	4(1)
C(14)	20(1)	21(1)	23(1)	-2(1)	2(1)	2(1)
C(15)	16(1)	18(1)	14(1)	-3(1)	-2(1)	-2(1)
C(16)	17(1)	21(1)	18(1)	-1(1)	0(1)	2(1)
C(17)	21(1)	24(1)	18(1)	0(1)	2(1)	-3(1)
C(18)	32(1)	17(1)	18(1)	2(1)	-2(1)	-2(1)
C(19)	26(1)	19(1)	21(1)	-1(1)	-2(1)	5(1)
C(20)	17(1)	22(1)	18(1)	-2(1)	1(1)	1(1)

Table S5. Hydrogen coordinates ($\times 10^4$) and isotropic displacement parameters ($\text{\AA}^2 \times 10^3$) for **3fa**.

	x	y	z	U(eq)
H(1A)	9819	2577	6971	51
H(1B)	8580	2021	7537	51
H(1C)	8833	3130	7580	51
H(2A)	6143	2165	6660	30
H(2B)	5215	2787	7249	30
H(5)	2604	4532	5135	20
H(6)	6551	3783	4562	23
H(7A)	2263	3073	4676	31
H(7B)	4353	2577	4298	31
H(8A)	4586	6043	6076	20
H(8B)	2388	5425	6073	20
H(10)	1137	4674	7024	27
H(11)	1239	4510	8154	32
H(12)	4277	5062	8736	31
H(13)	7234	5763	8194	30
H(14)	7103	5963	7069	25
H(16)	7685	5300	4402	23
H(17)	8137	6709	3859	26
H(18)	5299	7819	3862	27
H(19)	2011	7512	4424	26
H(20)	1528	6086	4954	23

X-ray Crystallographic Data for 3ao (CCDC 2014415)



The single crystal X-ray diffraction studies were carried out on a Bruker SMART APEX II CCD diffractometer equipped with Cu K α radiation ($\lambda = 1.5478$). Crystals of the subject compound were used as received. (Grown from ethyl acetate/hexane by vapor diffusion.)

A 0.225 x 0.200 x 0.180 mm colorless block was mounted on a Cryoloop with Paratone oil. Data were collected in a nitrogen gas stream at 100(1) K using ϕ and ω scans. Crystal-to-detector distance was 40 mm using variable exposure time (2, 4 and 8s) depending on the detector θ position, with a scan width of 1.4°. Data collection was 100.0% complete to 67.679° in θ . A total of 15586 reflections were collected covering the indices, $-7 \leq h \leq 7$, $-10 \leq k \leq 10$, $-37 \leq l \leq 31$. 3053 reflections were found to be symmetry independent, with a R_{int} of 0.0284. Indexing and unit cell refinement indicated a **Primitive, Orthorhombic** lattice. The space group was found to be ***P2₁2₁2₁***. The data were integrated using the Bruker SAINT software program and scaled using the SADABS software program. Solution by direct methods (SHELXT) produced a complete phasing model consistent with the proposed structure.

All nonhydrogen atoms were refined anisotropically by full-matrix least-squares (SHELXL-2014). All hydrogen atoms were placed using a riding model. Their positions were constrained relative to their parent atom using the appropriate HFIX command in SHELXL-2014. Crystallographic data are summarized in Table S1.

Table S6. Crystal data and structure refinement for **3ao**.

Report date	2020-07-05	
Identification code	rd3100	
Empirical formula	C ₁₈ H ₁₉ N O ₄	
Molecular formula	C ₁₈ H ₁₉ N O ₄	
Formula weight	313.34	
Temperature	100.0 K	
Wavelength	1.54178 Å	
Crystal system	Orthorhombic	
Space group	<i>P2₁2₁2₁</i>	
Unit cell dimensions	$a = 6.14300(10)$ Å	$\alpha = 90^\circ$.

	$b = 8.2993(2) \text{ \AA}$	$\beta = 90^\circ$.
	$c = 31.1195(7) \text{ \AA}$	$\gamma = 90^\circ$.
Volume	$1586.55(6) \text{ \AA}^3$	
Z	4	
Density (calculated)	1.312 Mg/m^3	
Absorption coefficient	0.761 mm^{-1}	
F(000)	664	
Crystal size	$0.34 \times 0.04 \times 0.03 \text{ mm}^3$	
Crystal color, habit	colorless needle	
Theta range for data collection	2.840 to 70.988° .	
Index ranges	$-7 \leq h \leq 7$, $-10 \leq k \leq 10$, $-37 \leq l \leq 31$	
Reflections collected	15586	
Independent reflections	3053 [R(int) = 0.0284]	
Completeness to theta = 67.679°	100.0 %	
Absorption correction	Semi-empirical from equivalents	
Max. and min. transmission	0.7534 and 0.6222	
Refinement method	Full-matrix least-squares on F^2	
Data / restraints / parameters	3053 / 0 / 211	
Goodness-of-fit on F^2	1.075	
Final R indices [$I > 2\sigma(I)$]	R1 = 0.0252, wR2 = 0.0632	
R indices (all data)	R1 = 0.0267, wR2 = 0.0638	
Absolute structure parameter	0.02(6)	
Extinction coefficient	0.0010(3)	
Largest diff. peak and hole	0.161 and $-0.123 \text{ e.\AA}^{-3}$	

Table S7. Atomic coordinates ($\times 10^4$) and equivalent isotropic displacement parameters ($\text{\AA}^2 \times 10^3$) for **3ao**. $U(\text{eq})$ is defined as one third of the trace of the orthogonalized U^{ij} tensor.

	x	y	z	$U(\text{eq})$
O(1)	7576(2)	6398(1)	7127(1)	21(1)
O(2)	4036(2)	6691(2)	7299(1)	28(1)
O(3)	1718(2)	6936(2)	6512(1)	29(1)
O(4)	1729(2)	4342(2)	6480(1)	38(1)
N(1)	2648(2)	5638(2)	6526(1)	21(1)
C(1)	5452(2)	6324(2)	7051(1)	18(1)
C(2)	5104(2)	5650(2)	6597(1)	17(1)
C(3)	6217(2)	6771(2)	6256(1)	15(1)
C(4)	5775(3)	8543(2)	6327(1)	18(1)
C(5)	7249(3)	9512(2)	6495(1)	25(1)
C(6)	5973(3)	3933(2)	6575(1)	20(1)
C(7)	8251(3)	7046(2)	7542(1)	24(1)
C(8)	7991(3)	5816(2)	7891(1)	33(1)
C(9)	5783(3)	6233(2)	5796(1)	16(1)
C(10)	7313(3)	5334(2)	5582(1)	16(1)
C(11)	6999(3)	4826(2)	5150(1)	16(1)
C(12)	8567(3)	3897(2)	4926(1)	21(1)
C(13)	8190(3)	3435(2)	4509(1)	25(1)
C(14)	6251(3)	3872(2)	4299(1)	27(1)
C(15)	4709(3)	4766(2)	4507(1)	23(1)
C(16)	5031(3)	5265(2)	4939(1)	18(1)
C(17)	3476(3)	6199(2)	5162(1)	19(1)
C(18)	3831(3)	6674(2)	5578(1)	18(1)

Table S8. Bond lengths [Å] and angles [°] for **3ao**.

O(1)-C(1)	1.3269(19)		
O(1)-C(7)	1.4601(19)	C(1)-O(1)-C(7)	116.92(12)
O(2)-C(1)	1.2020(19)	O(3)-N(1)-O(4)	123.81(14)
O(3)-N(1)	1.2201(18)	O(3)-N(1)-C(2)	117.53(13)
O(4)-N(1)	1.2228(19)	O(4)-N(1)-C(2)	118.65(14)
N(1)-C(2)	1.5253(19)	O(1)-C(1)-C(2)	108.45(12)
C(1)-C(2)	1.535(2)	O(2)-C(1)-O(1)	125.89(15)
C(2)-C(3)	1.568(2)	O(2)-C(1)-C(2)	125.65(14)
C(2)-C(6)	1.523(2)	N(1)-C(2)-C(1)	105.90(12)
C(3)-H(3)	1.0000	N(1)-C(2)-C(3)	109.71(12)
C(3)-C(4)	1.512(2)	C(1)-C(2)-C(3)	110.29(12)
C(3)-C(9)	1.524(2)	C(6)-C(2)-N(1)	109.48(13)
C(4)-H(4)	0.9500	C(6)-C(2)-C(1)	109.49(12)
C(4)-C(5)	1.318(2)	C(6)-C(2)-C(3)	111.80(13)
C(5)-H(5A)	0.9500	C(2)-C(3)-H(3)	105.5
C(5)-H(5B)	0.9500	C(4)-C(3)-C(2)	113.56(12)
C(6)-H(6A)	0.9800	C(4)-C(3)-H(3)	105.5
C(6)-H(6B)	0.9800	C(4)-C(3)-C(9)	113.00(12)
C(6)-H(6C)	0.9800	C(9)-C(3)-C(2)	112.74(12)
C(7)-H(7A)	0.9900	C(9)-C(3)-H(3)	105.5
C(7)-H(7B)	0.9900	C(3)-C(4)-H(4)	119.1
C(7)-C(8)	1.499(3)	C(5)-C(4)-C(3)	121.85(15)
C(8)-H(8A)	0.9800	C(5)-C(4)-H(4)	119.1
C(8)-H(8B)	0.9800	C(4)-C(5)-H(5A)	120.0
C(8)-H(8C)	0.9800	C(4)-C(5)-H(5B)	120.0
C(9)-C(10)	1.372(2)	H(5A)-C(5)-H(5B)	120.0
C(9)-C(18)	1.426(2)	C(2)-C(6)-H(6A)	109.5
C(10)-H(10)	0.9500	C(2)-C(6)-H(6B)	109.5
C(10)-C(11)	1.422(2)	C(2)-C(6)-H(6C)	109.5
C(11)-C(12)	1.417(2)	H(6A)-C(6)-H(6B)	109.5
C(11)-C(16)	1.423(2)	H(6A)-C(6)-H(6C)	109.5
C(12)-H(12)	0.9500	H(6B)-C(6)-H(6C)	109.5
C(12)-C(13)	1.373(2)	O(1)-C(7)-H(7A)	109.4
C(13)-H(13)	0.9500	O(1)-C(7)-H(7B)	109.4
C(13)-C(14)	1.406(3)	O(1)-C(7)-C(8)	111.11(14)
C(14)-H(14)	0.9500	H(7A)-C(7)-H(7B)	108.0
C(14)-C(15)	1.366(3)	C(8)-C(7)-H(7A)	109.4
C(15)-H(15)	0.9500	C(8)-C(7)-H(7B)	109.4
C(15)-C(16)	1.421(2)	C(7)-C(8)-H(8A)	109.5
C(16)-C(17)	1.413(2)	C(7)-C(8)-H(8B)	109.5
C(17)-H(17)	0.9500	C(7)-C(8)-H(8C)	109.5
C(17)-C(18)	1.369(2)	H(8A)-C(8)-H(8B)	109.5
C(18)-H(18)	0.9500	H(8A)-C(8)-H(8C)	109.5

H(8B)-C(8)-H(8C)	109.5	C(13)-C(14)-H(14)	119.7
C(10)-C(9)-C(3)	119.67(14)	C(15)-C(14)-C(13)	120.51(15)
C(10)-C(9)-C(18)	119.03(14)	C(15)-C(14)-H(14)	119.7
C(18)-C(9)-C(3)	121.28(14)	C(14)-C(15)-H(15)	119.7
C(9)-C(10)-H(10)	119.1	C(14)-C(15)-C(16)	120.68(16)
C(9)-C(10)-C(11)	121.77(15)	C(16)-C(15)-H(15)	119.7
C(11)-C(10)-H(10)	119.1	C(15)-C(16)-C(11)	118.67(15)
C(10)-C(11)-C(16)	118.36(14)	C(17)-C(16)-C(11)	119.25(14)
C(12)-C(11)-C(10)	122.34(14)	C(17)-C(16)-C(15)	122.07(15)
C(12)-C(11)-C(16)	119.30(14)	C(16)-C(17)-H(17)	119.5
C(11)-C(12)-H(12)	119.9	C(18)-C(17)-C(16)	120.97(15)
C(13)-C(12)-C(11)	120.19(16)	C(18)-C(17)-H(17)	119.5
C(13)-C(12)-H(12)	119.9	C(9)-C(18)-H(18)	119.7
C(12)-C(13)-H(13)	119.7	C(17)-C(18)-C(9)	120.61(14)
C(12)-C(13)-C(14)	120.64(16)	C(17)-C(18)-H(18)	119.1
C(14)-C(13)-H(13)	119.7		

Table S9. Anisotropic displacement parameters ($\text{\AA}^2 \times 10^3$) for **3ao**. The anisotropic displacement factor exponent takes the form: $-2\pi^2 [h^2 a^{*2} U^{11} + \dots + 2 h k a^* b^* U^{12}]$

	U11	U22	U33	U23	U13	U12
O(1)	17(1)	33(1)	14(1)	-2(1)	0(1)	-1(1)
O(2)	21(1)	41(1)	21(1)	-3(1)	5(1)	6(1)
O(3)	16(1)	34(1)	35(1)	5(1)	1(1)	7(1)
O(4)	22(1)	34(1)	57(1)	-2(1)	-2(1)	-11(1)
N(1)	14(1)	29(1)	19(1)	1(1)	2(1)	-2(1)
C(1)	17(1)	19(1)	17(1)	3(1)	2(1)	2(1)
C(2)	12(1)	21(1)	16(1)	1(1)	0(1)	-2(1)
C(3)	12(1)	18(1)	15(1)	0(1)	1(1)	0(1)
C(4)	20(1)	20(1)	16(1)	1(1)	2(1)	3(1)
C(5)	28(1)	20(1)	26(1)	-2(1)	0(1)	1(1)
C(6)	22(1)	18(1)	20(1)	2(1)	1(1)	1(1)
C(7)	23(1)	32(1)	18(1)	-6(1)	-3(1)	-3(1)
C(8)	45(1)	34(1)	21(1)	0(1)	-6(1)	12(1)
C(9)	16(1)	15(1)	16(1)	2(1)	-1(1)	-2(1)
C(10)	14(1)	17(1)	16(1)	2(1)	-2(1)	-1(1)
C(11)	19(1)	14(1)	16(1)	2(1)	2(1)	-3(1)
C(12)	23(1)	21(1)	18(1)	2(1)	2(1)	0(1)
C(13)	33(1)	23(1)	18(1)	-2(1)	7(1)	2(1)
C(14)	40(1)	26(1)	14(1)	0(1)	1(1)	-4(1)
C(15)	27(1)	23(1)	17(1)	3(1)	-5(1)	-2(1)
C(16)	21(1)	16(1)	16(1)	3(1)	-1(1)	-2(1)
C(17)	16(1)	20(1)	20(1)	4(1)	-4(1)	-1(1)

C(18) 15(1) 19(1) 19(1) 0(1) 0(1) 1(1)

Table S10. Hydrogen coordinates ($\times 10^4$) and isotropic displacement parameters ($\text{\AA}^2 \times 10^3$) for **3ao**.

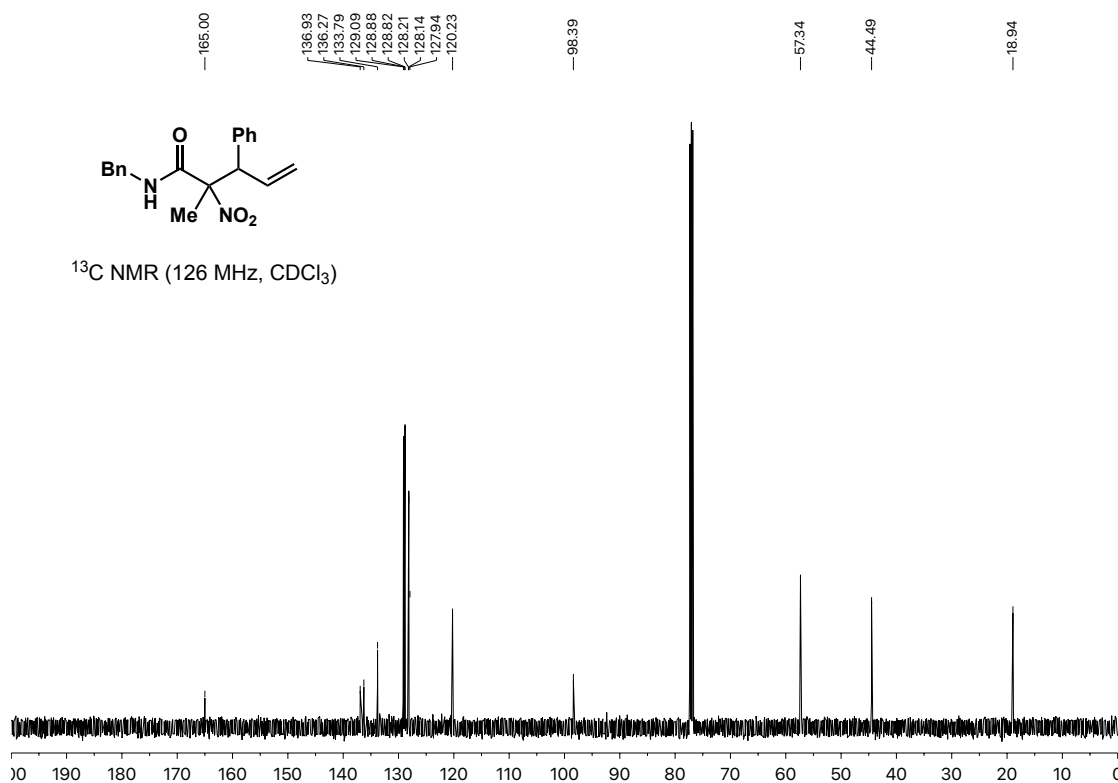
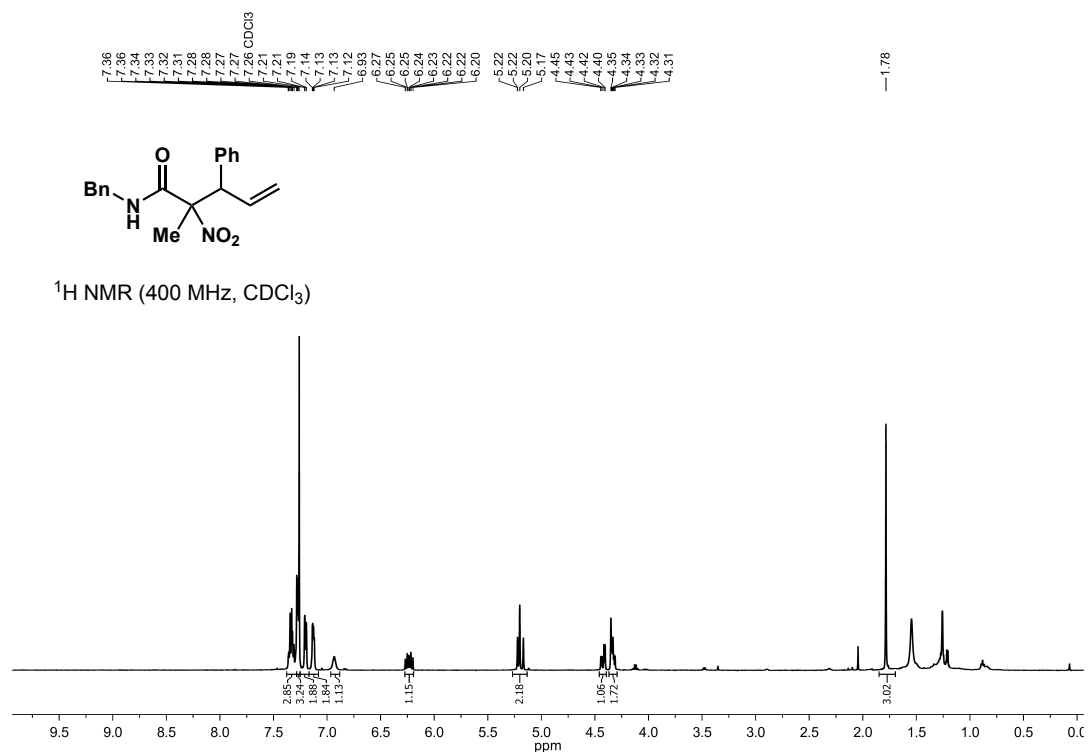
	x	y	z	U(eq)
H(3)	7819	6633	6300	18
H(4)	4397	8971	6248	22
H(5A)	8635	9101	6575	30
H(5B)	6926	10621	6535	30
H(6A)	5298	3285	6802	31
H(6B)	7555	3944	6615	31
H(6C)	5623	3467	6294	31
H(7A)	7362	8007	7611	29
H(7B)	9793	7386	7526	29
H(8A)	8853	4858	7821	50
H(8B)	6453	5517	7916	50
H(8C)	8497	6269	8164	50
H(10)	8617	5042	5727	19
H(12)	9883	3594	5064	25
H(13)	9249	2813	4361	30
H(14)	6011	3544	4011	32
H(15)	3409	5057	4361	27
H(17)	2165	6502	5022	22
H(18)	2766	7304	5722	21

8. References

- (1) A. E. Metz, S. Berritt, S. D. Dreher, M. C. Kozlowski, *Org. Lett.* **2012**, *14*, 760–763.
- (2) S. U. Dighe, S. Mukhopadhyay, K. Priyanka, S. Batra, *Org. Lett.* **2016**, *18*, 4190–4193.
- (3) J. H. Kim, T. Song, Y. K. Chung, *Org. Lett.* **2017**, *19*, 1248–1251.
- (4) R. Levene, J. Y. Becker, J. Klein, *J. Organomet. Chem.* **1974**, *67*, 467–471.
- (5) F. A. Cruz, V. M. Dong, *J. Am. Chem. Soc.* **2017**, *139*, 1029–1032.
- (6) W.-F. Wang, X.-F. Wu, *Catal. Commun.* **2020**, *133*, 105835–105837.
- (7) T. Jiang, X. Quan, C. Zhu, P. G. Andersson, J.-E. Bäckvall, *Angew. Chem. Int. Ed.* **2016**, *55*, 5824–5828.
- (8) T. Matsubara, K. Takahashi, J. Ishihara, S. Hatakeyama, *Angew. Chem. Int. Ed.* **2014**, *53*, 757–760.

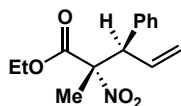
9. NMR Spectra

N-benzyl-2-methyl-2-nitro-3-phenylpent-4-enamide (Table 4.1, entry 3)



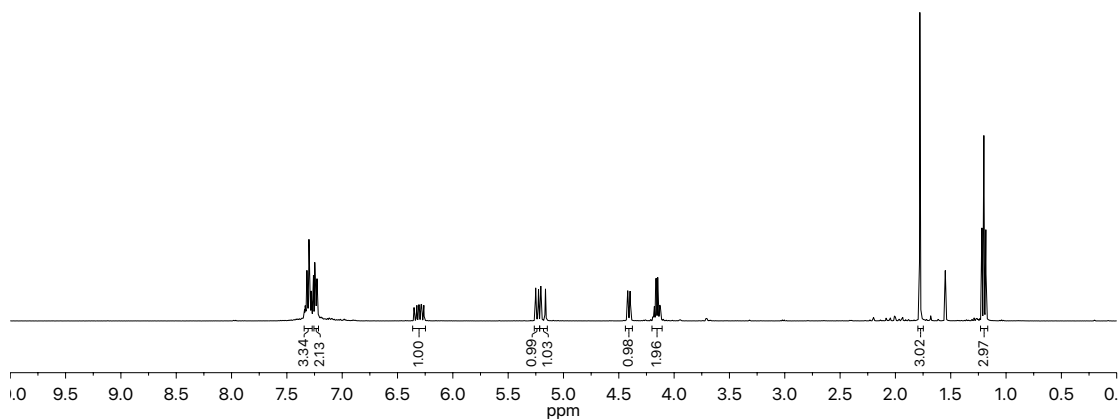
Ethyl (2*S*,3*R*)-2-methyl-2-nitro-3-phenylpent-4-enoate (3aa)

7.34, 7.33, 7.32, 7.31, 7.30, 7.29, 7.28, 7.27, 7.26, 7.25, 7.24, 7.23, 7.22, 6.95, 6.93, 6.91, 6.31, 6.30, 6.29, 6.28, 6.26, 5.95, 5.93, 5.90, 5.76, 5.74, 4.40, 4.21, 4.18, 4.18, 4.17, 4.16, 4.15, 4.14, 4.13, 4.12, 4.10, -1.78, -1.22, -1.20, -1.18

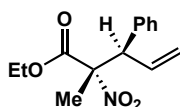


3aa

¹H NMR (400 MHz, CDCl₃)

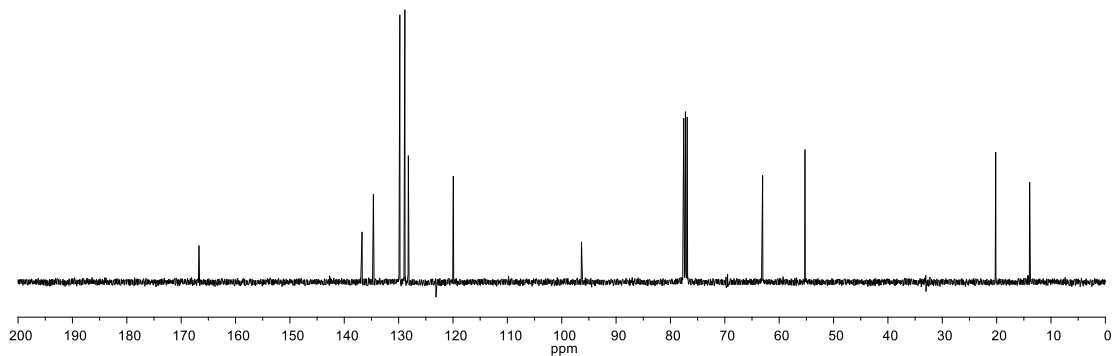


166.73, 136.73, 134.64, 128.78, 128.85, 128.21, 119.95, 96.37, 63.05, 55.26, 20.17, 13.93

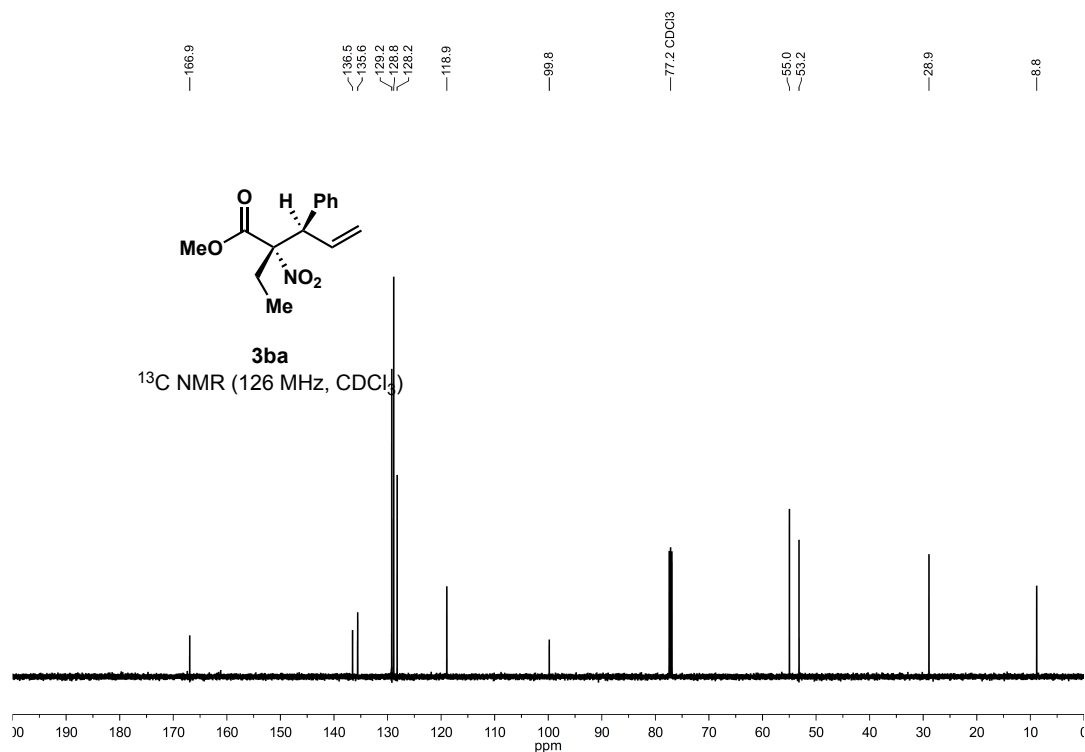
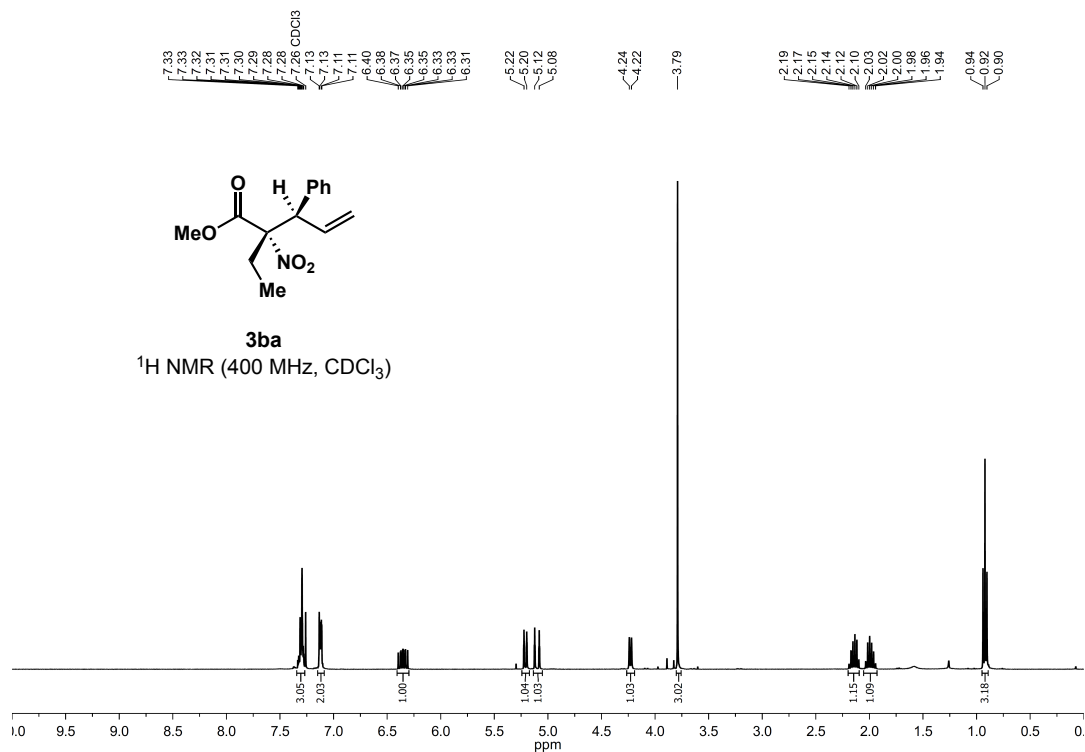


3aa

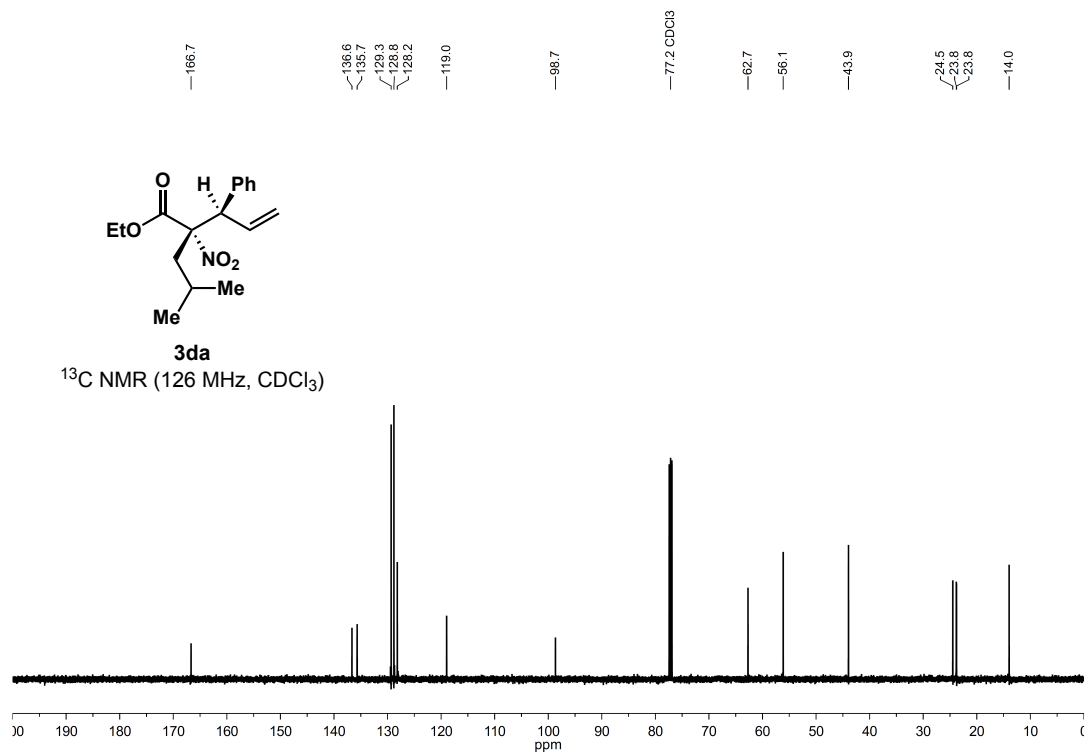
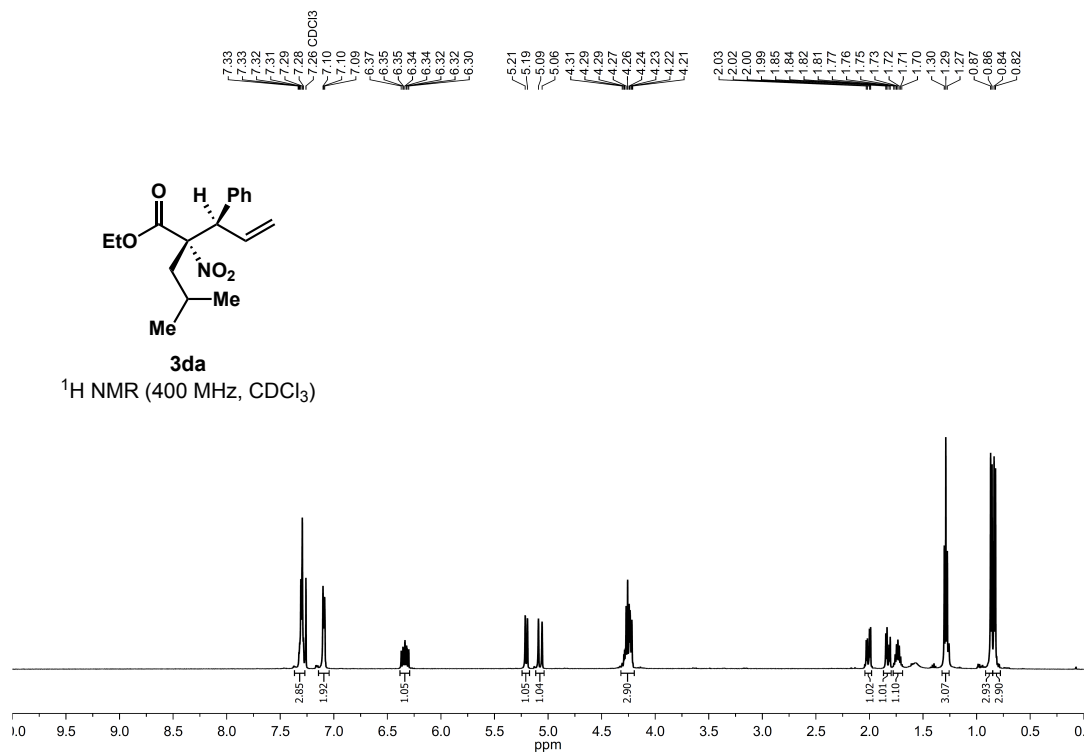
¹³C NMR (126 MHz, CDCl₃)



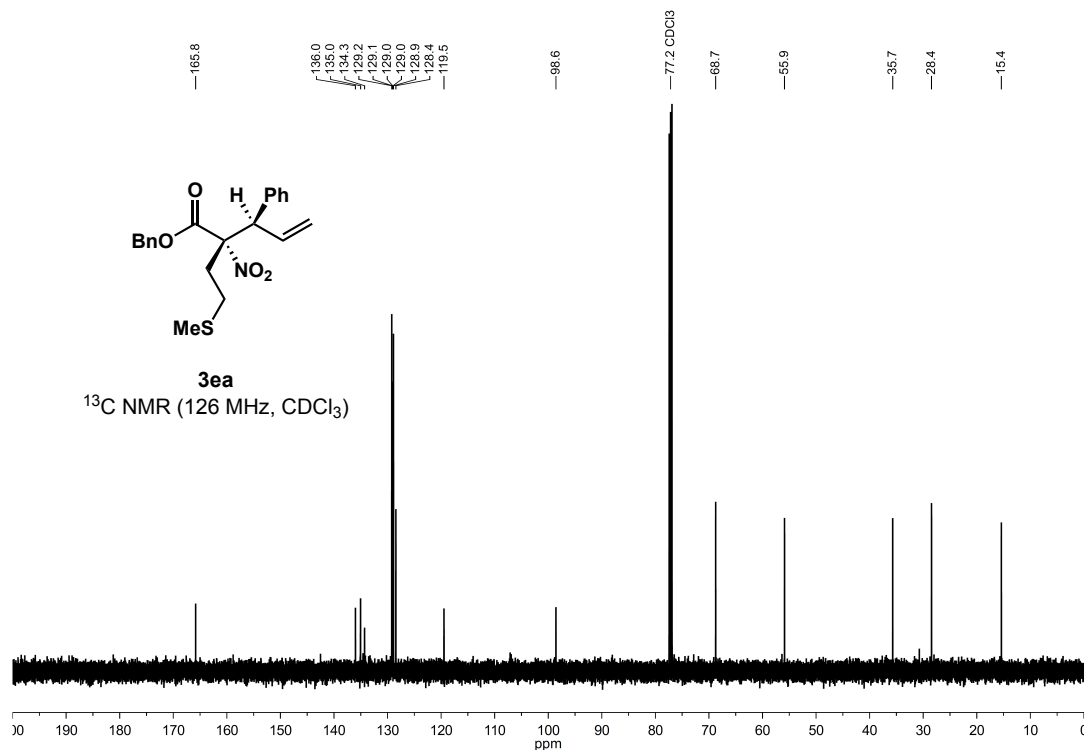
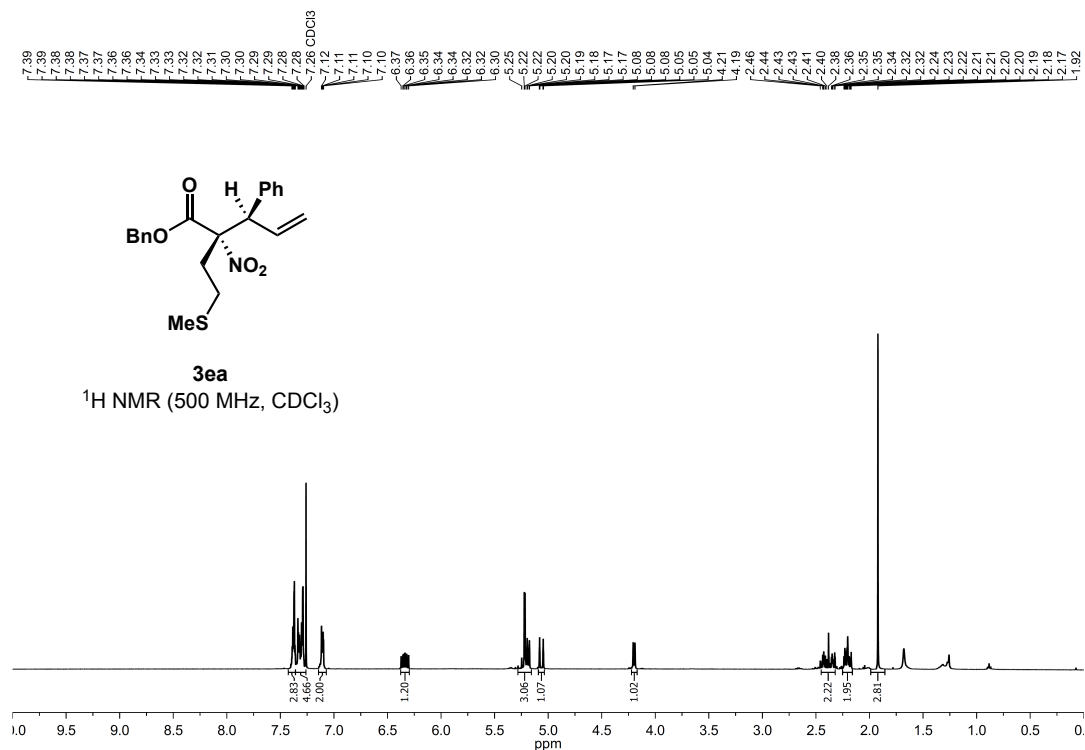
Methyl (2*S*,3*R*)-2-ethyl-2-nitro-3-phenylpent-4-enoate (3ba)



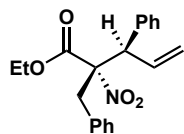
Ethyl (2*S*,3*R*)-2-isobutyl-2-nitro-3-phenylpent-4-enoate (3da)



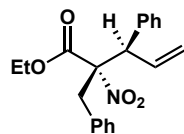
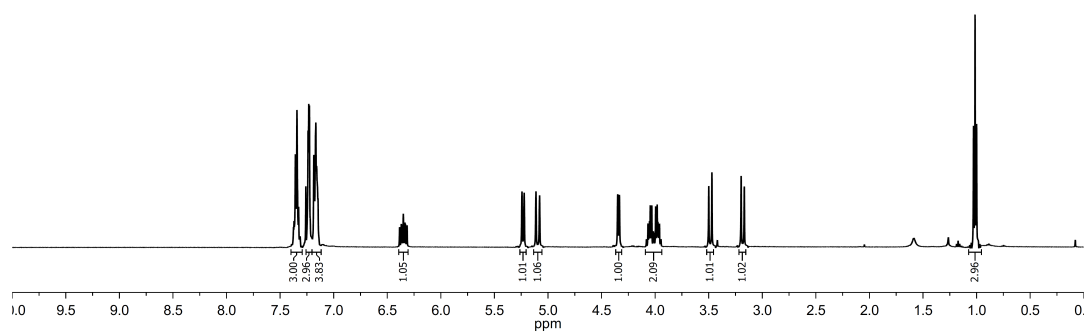
Benzyl (2*S*,3*R*)-2-(2-(methylthio)ethyl)-2-nitro-3-phenylpent-4-enoate (3ea)



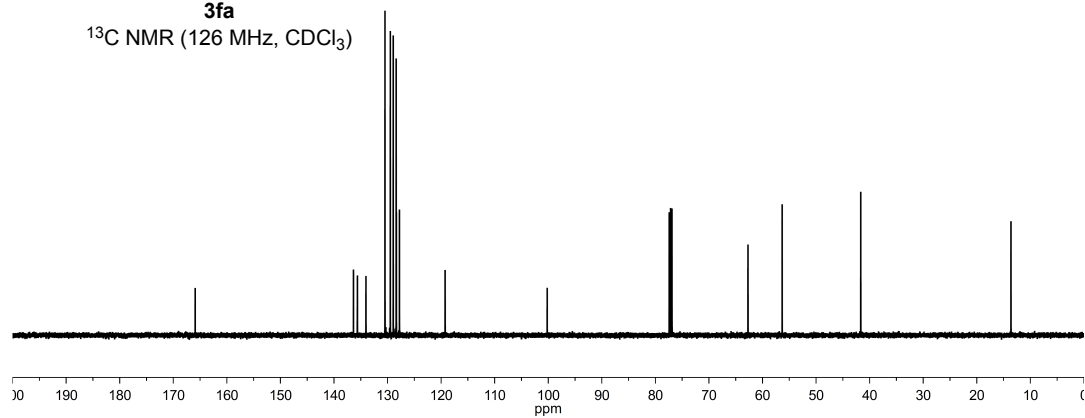
Ethyl (2*S*,3*R*)-2-benzyl-2-nitro-3-phenylpent-4-enoate (3fa)



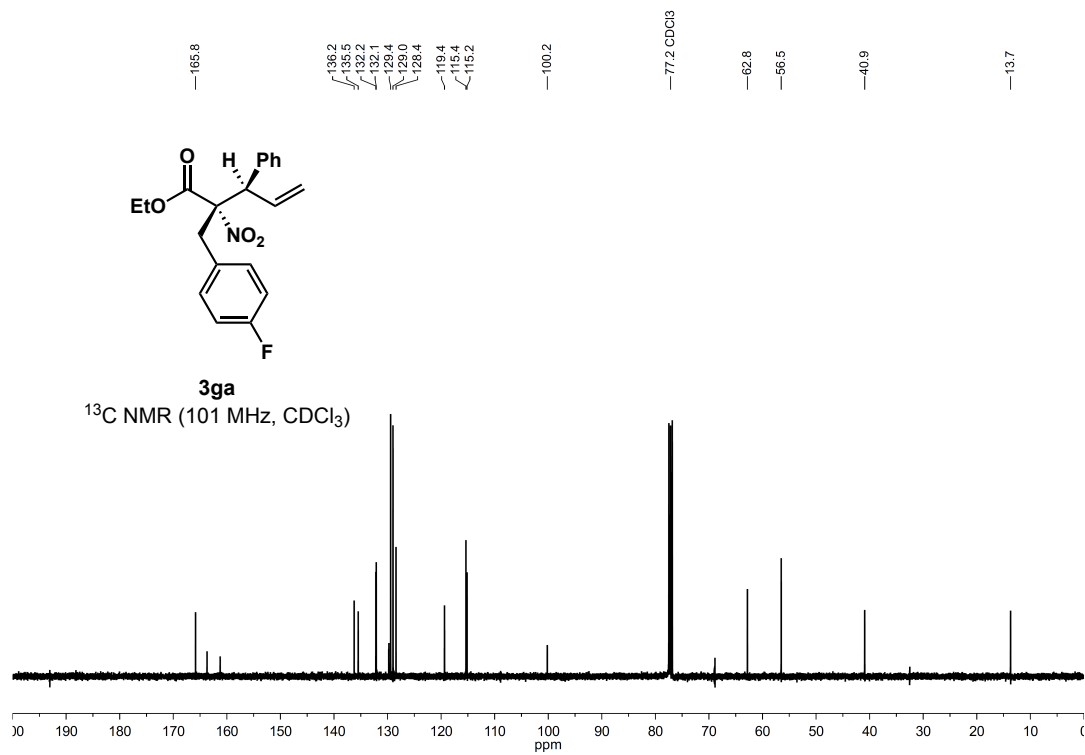
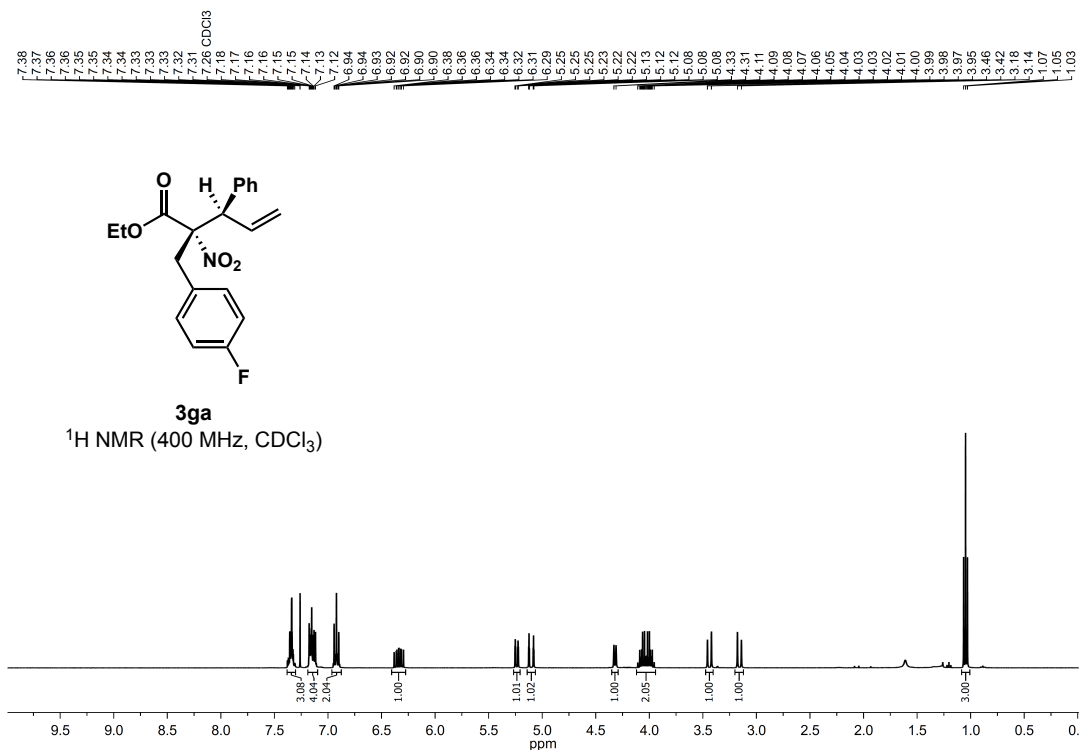
3fa
¹H NMR (500 MHz, CDCl₃)

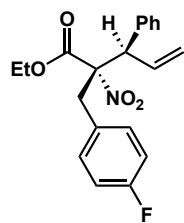


3fa
¹³C NMR (126 MHz, CDCl₃)



Ethyl (2*S*,3*R*)-2-(4-fluorobenzyl)-2-nitro-3-phenylpent-4-enoate (3ga)

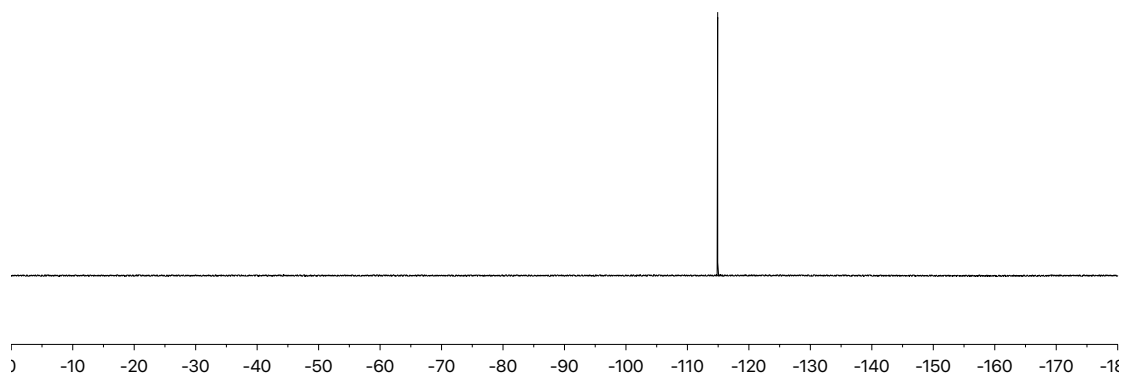




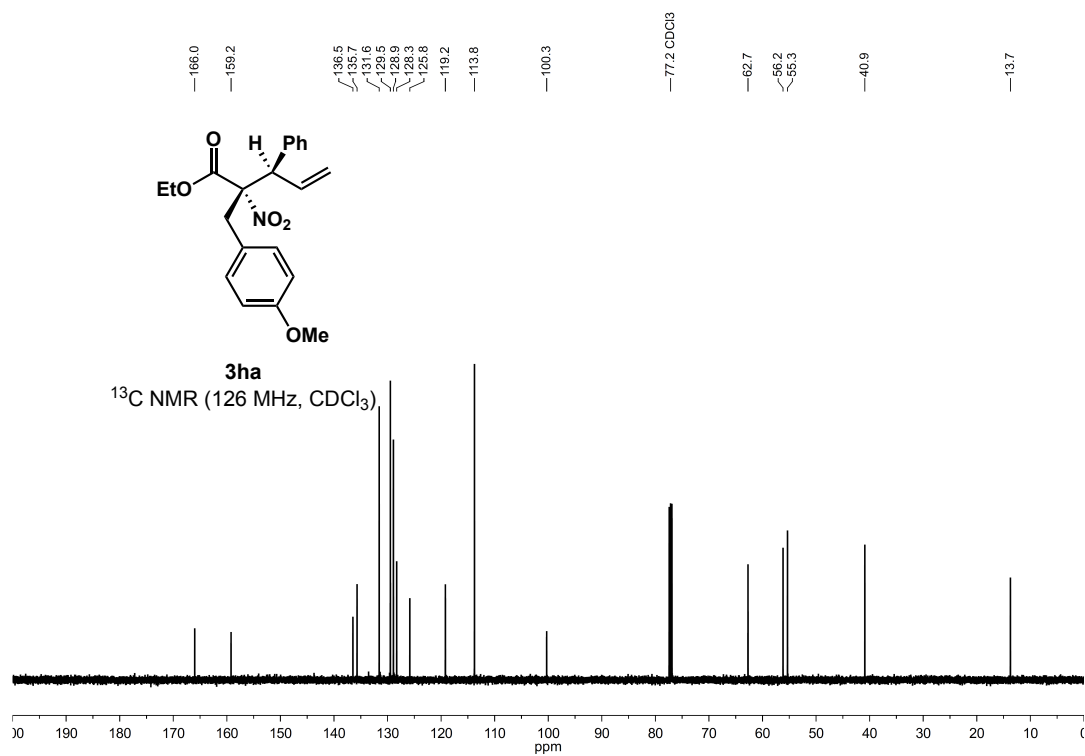
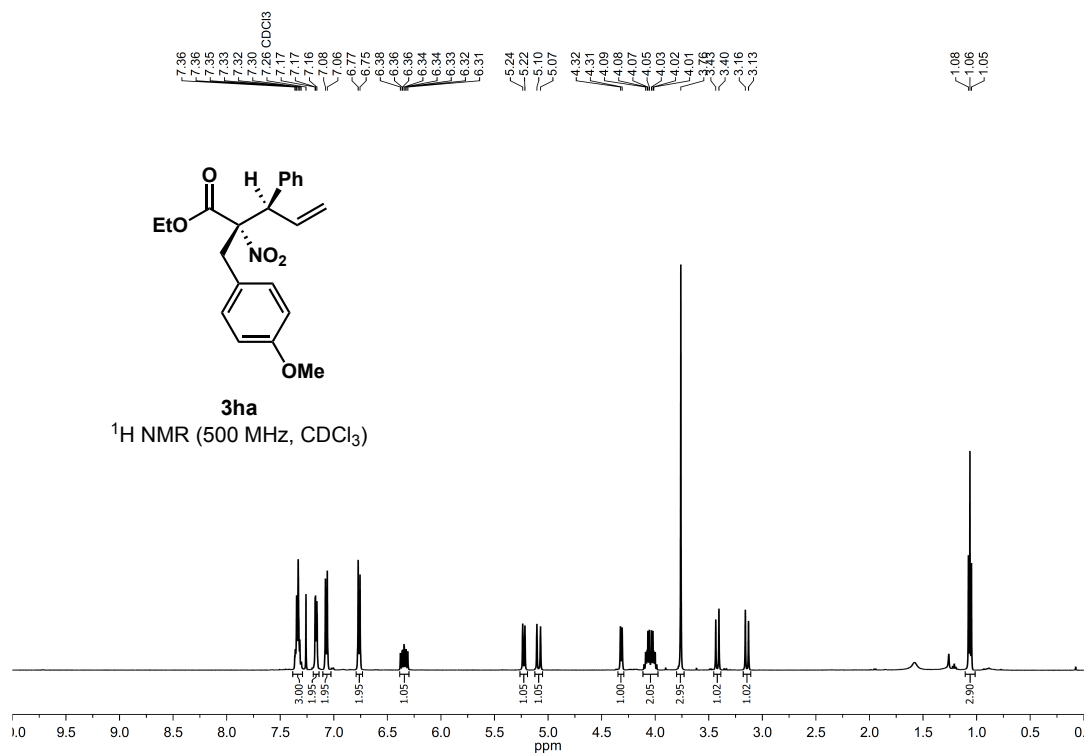
3ga

¹⁹F NMR (376 MHz, CDCl₃)

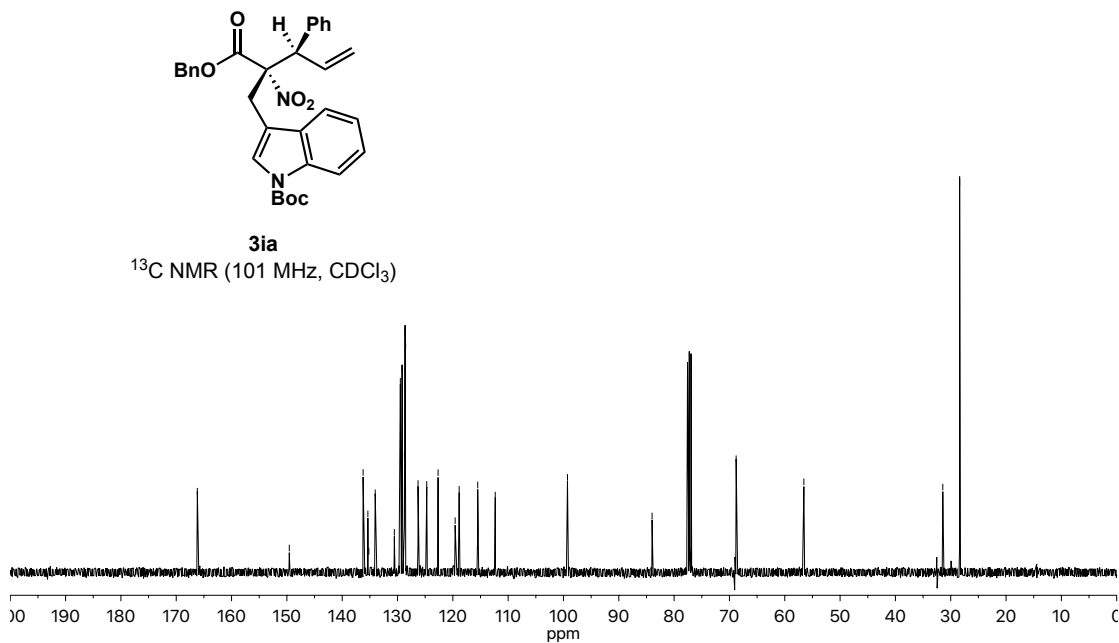
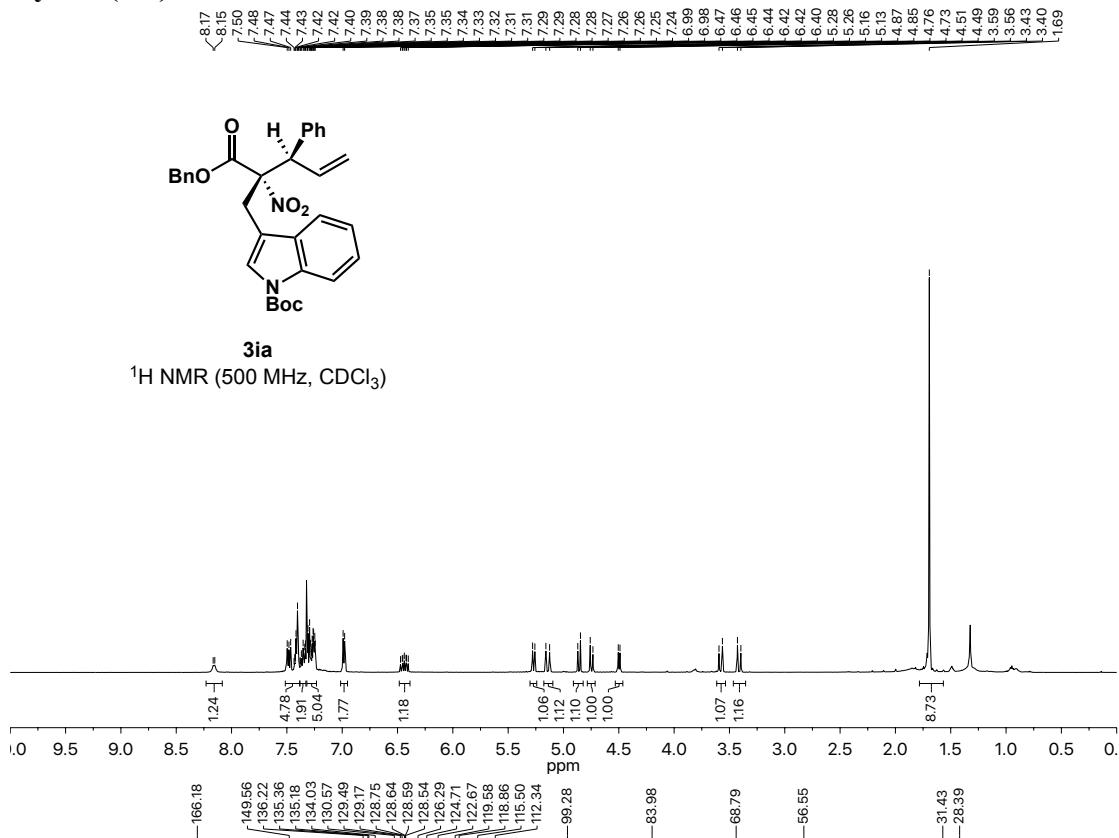
-114.92



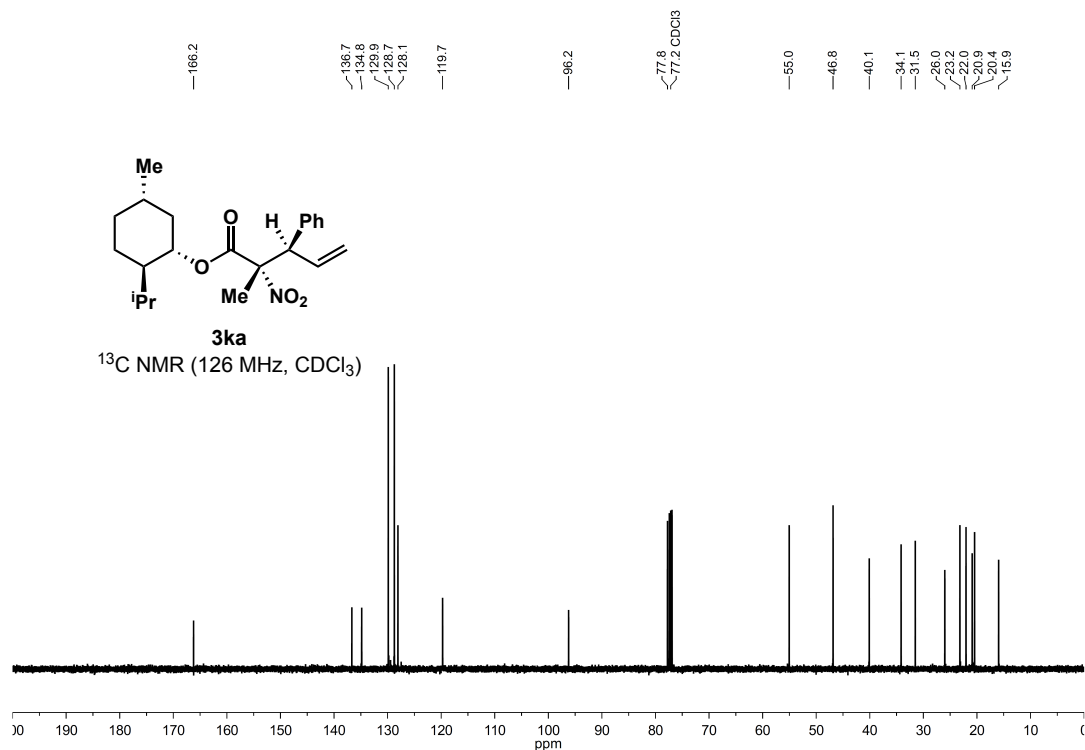
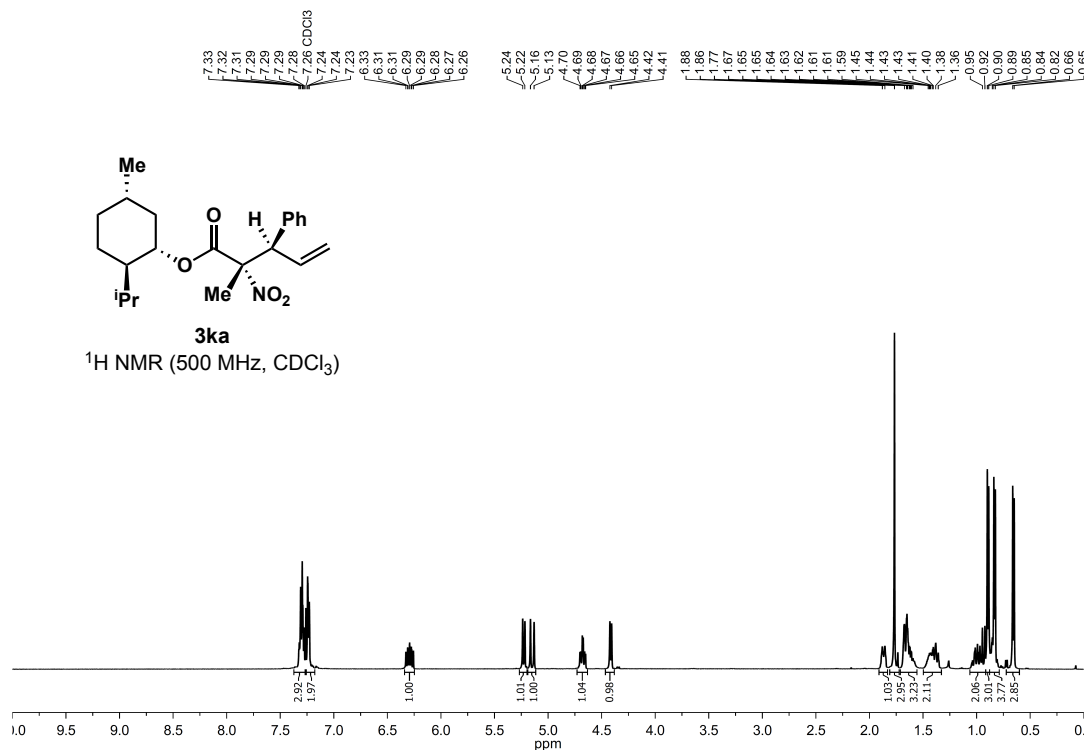
Ethyl (2*S*,3*R*)-2-(4-methoxybenzyl)-2-nitro-3-phenylpent-4-enoate (3ha)



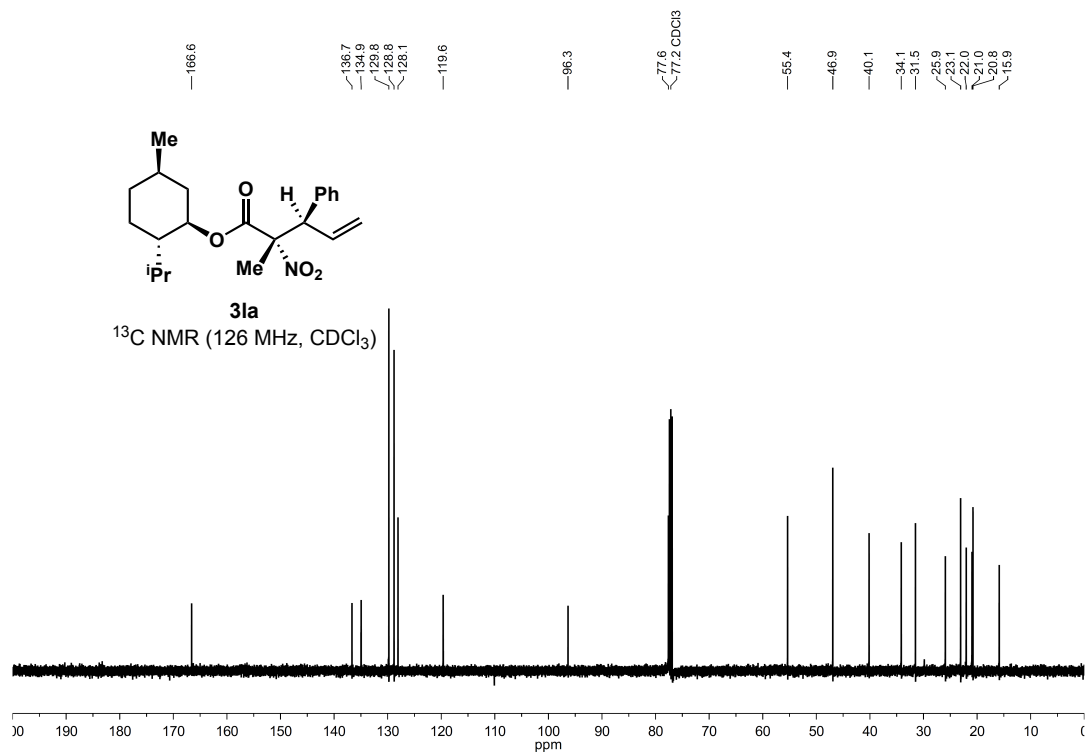
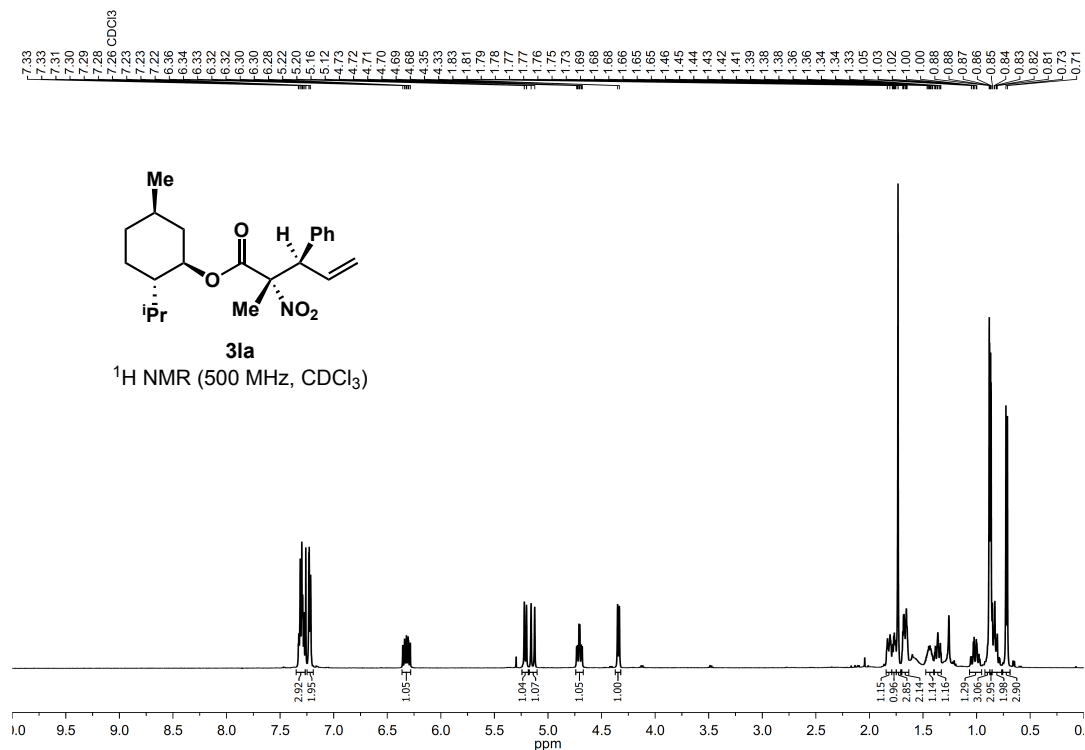
Tert-butyl-3-((2*S*,3*R*)-2-((benzyloxy)carbonyl)-2-nitro-3-phenylpent-4-en-1-yl)-1*H*-indole-1-carboxylate (3ia)



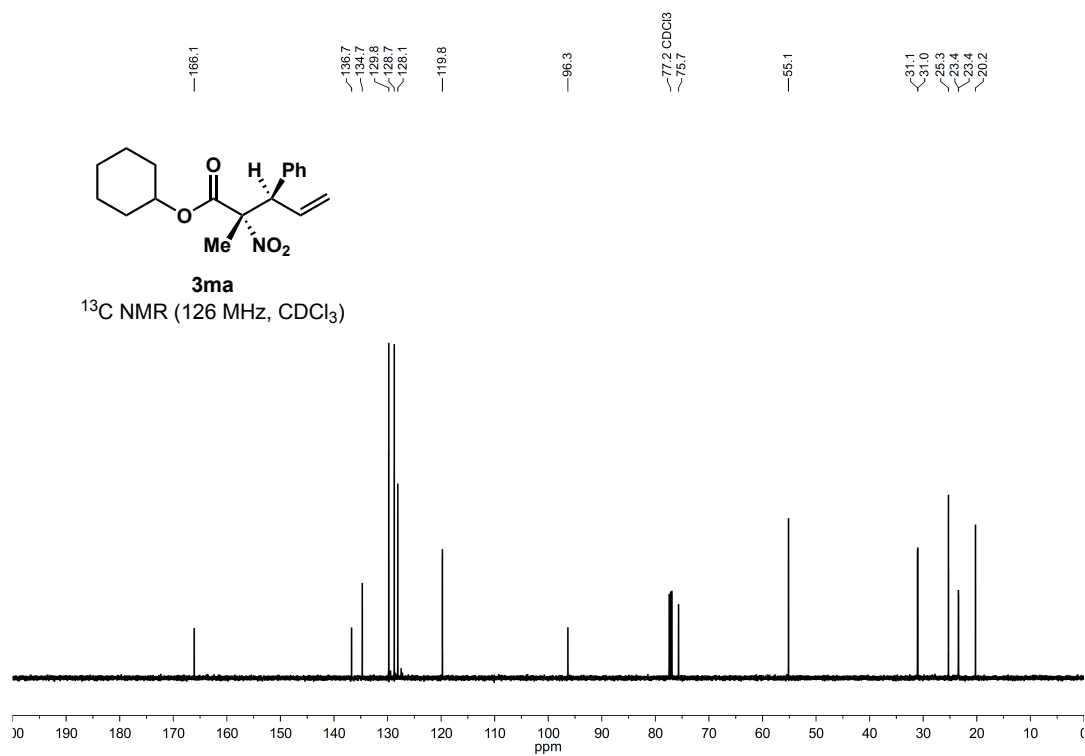
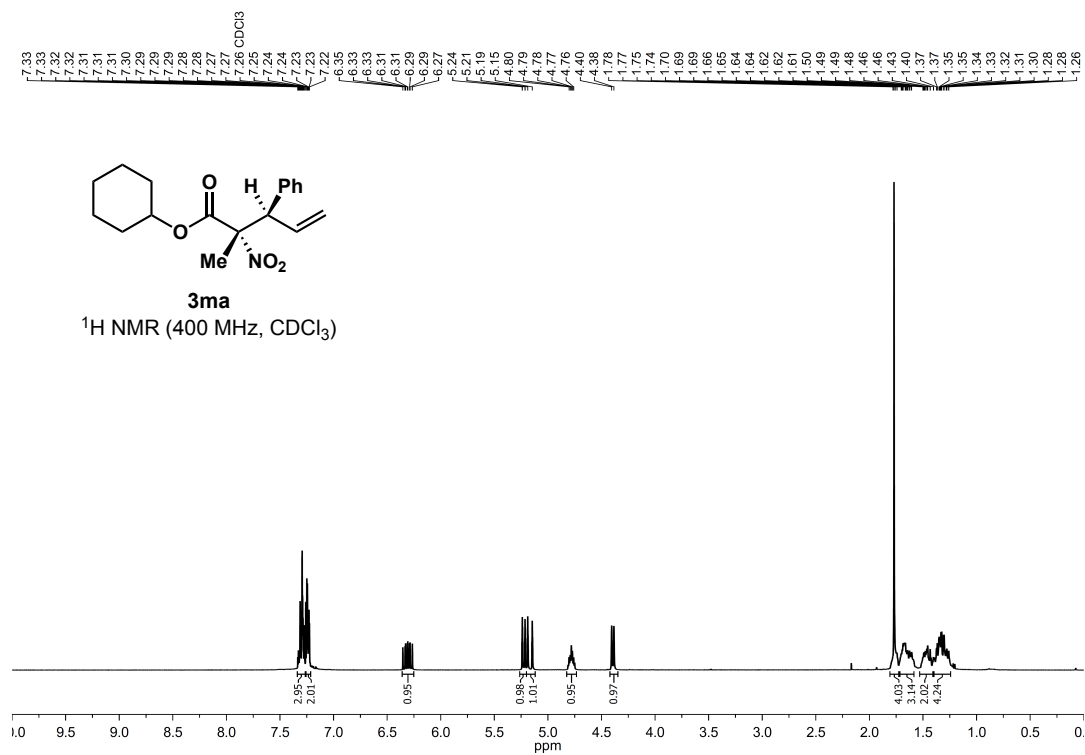
(1*S*,2*R*,5*S*)-2-Isopropyl-5-methylcyclohexyl (2*S*,3*R*)-2-methyl-2-nitro-3-phenylpent-4-enoate (3ka)



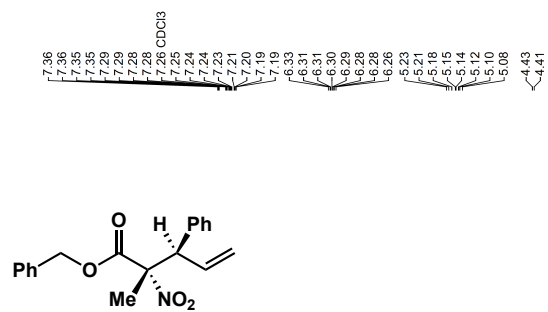
(1*R*,2*S*,5*R*)-2-Isopropyl-5-methylcyclohexyl (2*S*,3*R*)-2-methyl-2-nitro-3-phenylpent-4-enoate (3a)



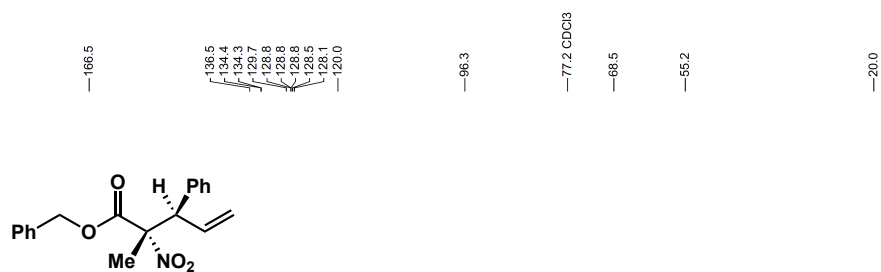
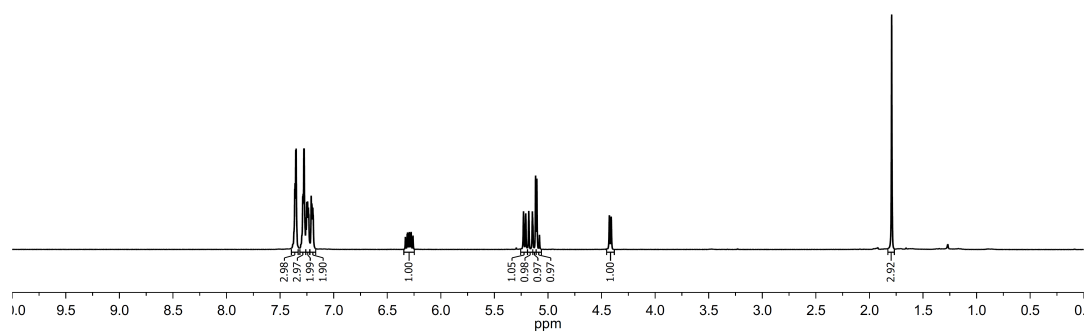
Cyclohexyl (2*S*,3*R*)-2-methyl-2-nitro-3-phenylpent-4-enoate (3ma)



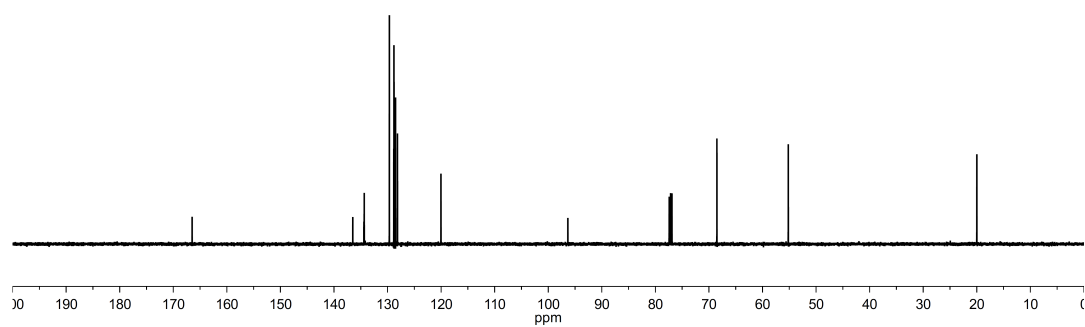
Benzyl (2*S*,3*R*)-2-methyl-2-nitro-3-phenylpent-4-enoate (**3na**)



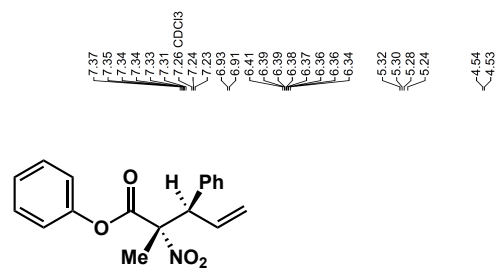
3na
 ^1H NMR (500 MHz, CDCl_3)



3na
 ^{13}C NMR (126 MHz, CDCl_3)

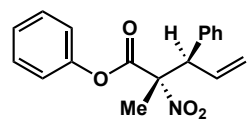
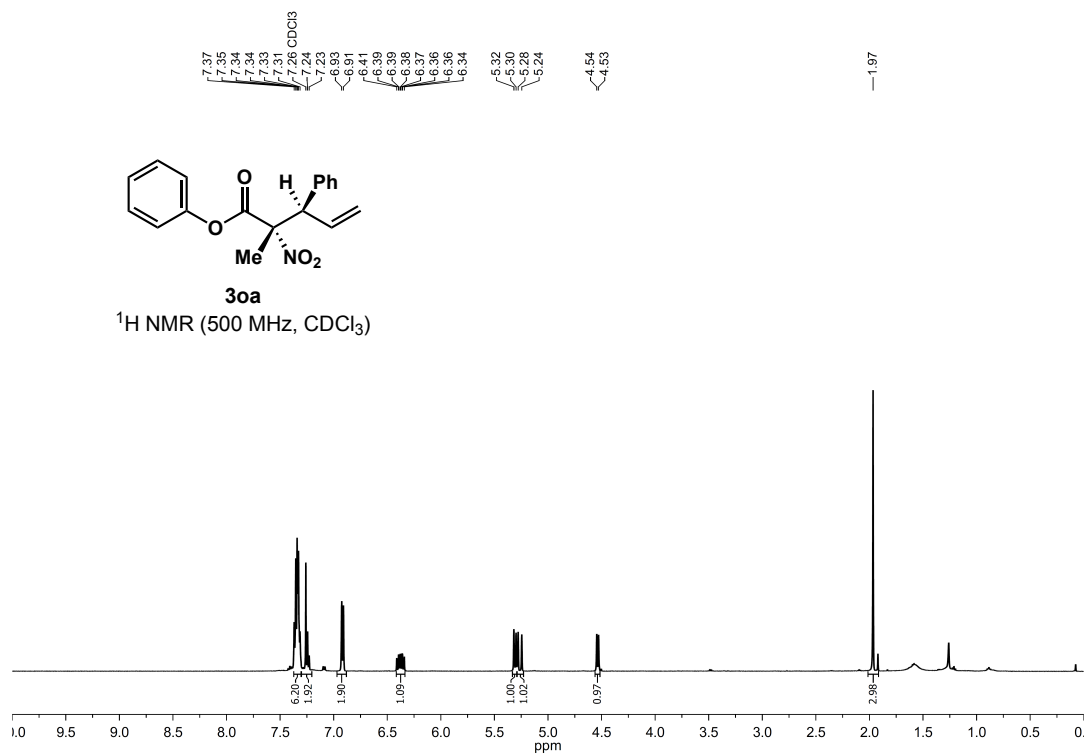


Phenyl (2*S*,3*R*)-2-methyl-2-nitro-3-phenylpent-4-enoate (3oa)



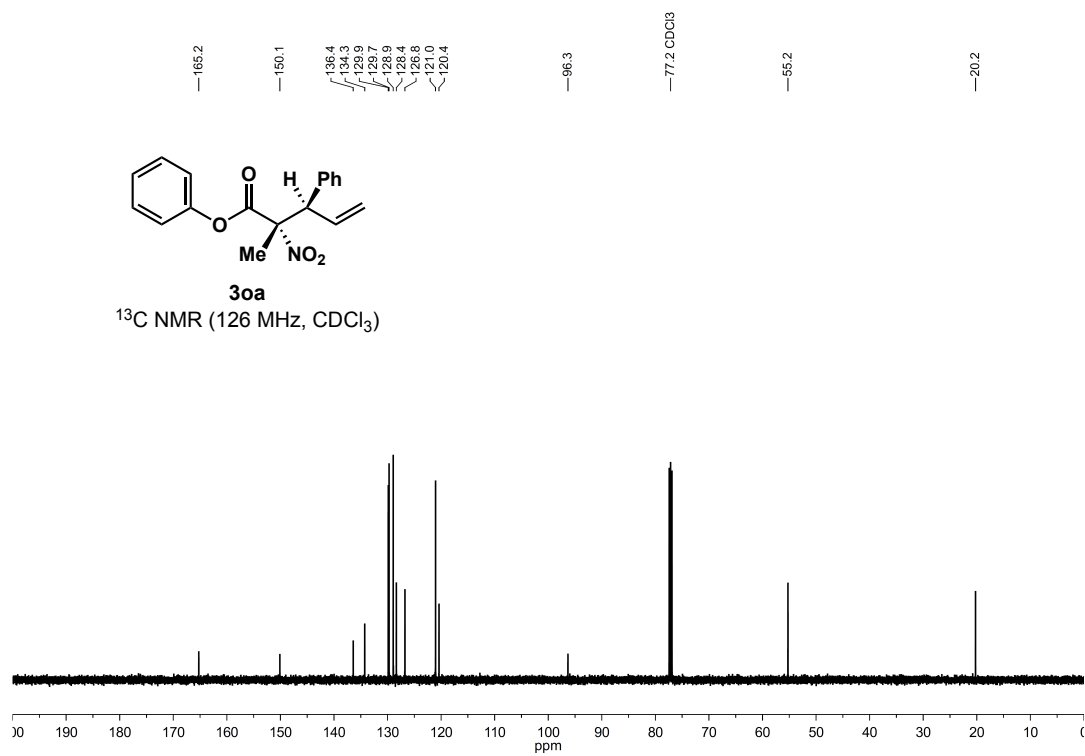
3oa

¹H NMR (500 MHz, CDCl₃)

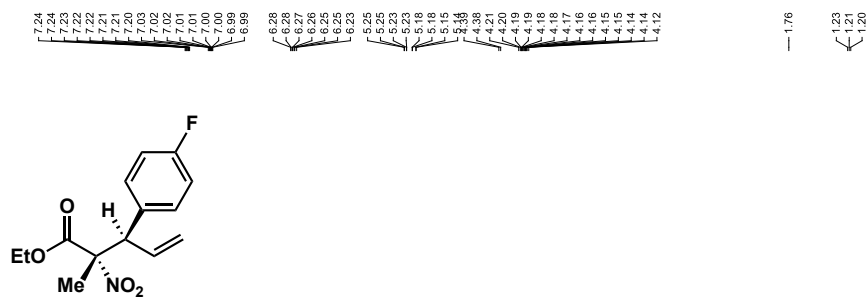


3oa

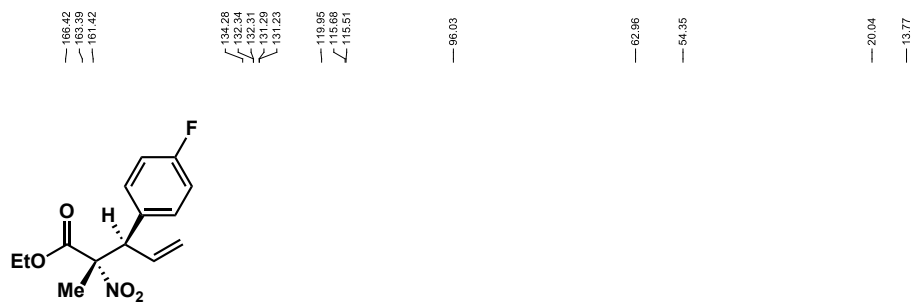
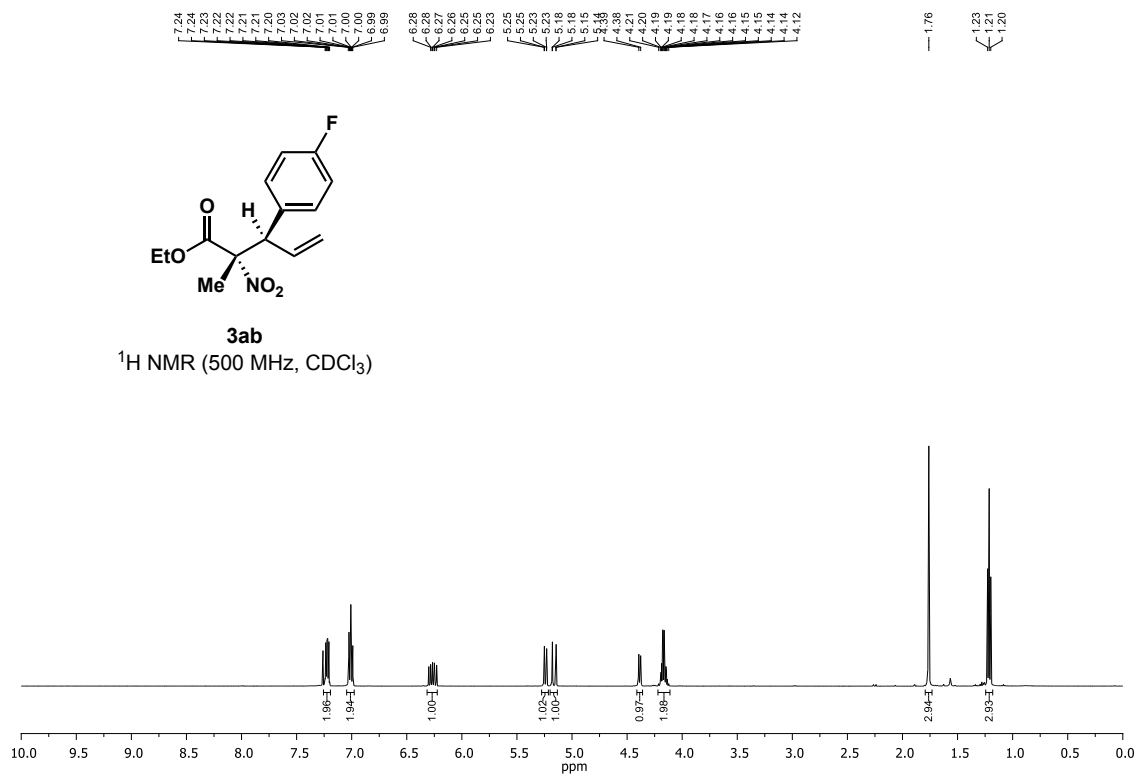
¹³C NMR (126 MHz, CDCl₃)



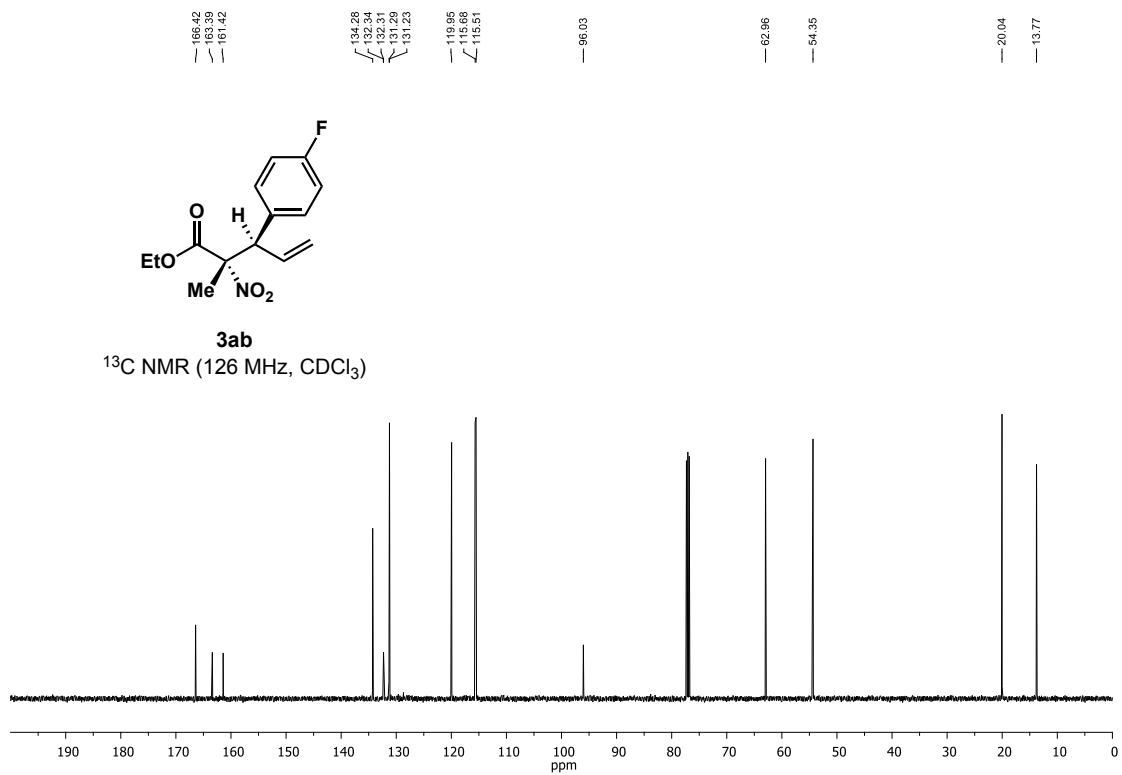
Ethyl (2*S*,3*R*)-3-(4-fluorophenyl)-2-methyl-2-nitropent-4-enoate (3ab)

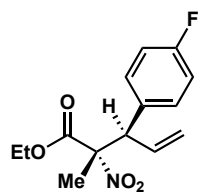


3ab
¹H NMR (500 MHz, CDCl₃)

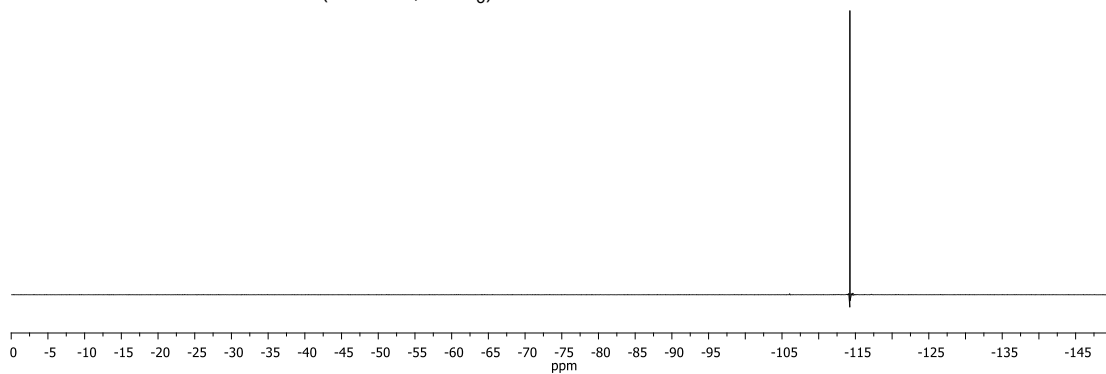


3ab
¹³C NMR (126 MHz, CDCl₃)

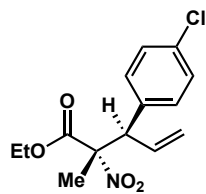




3ab
¹⁹F NMR (376 MHz, CDCl₃)

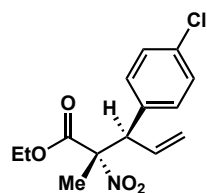
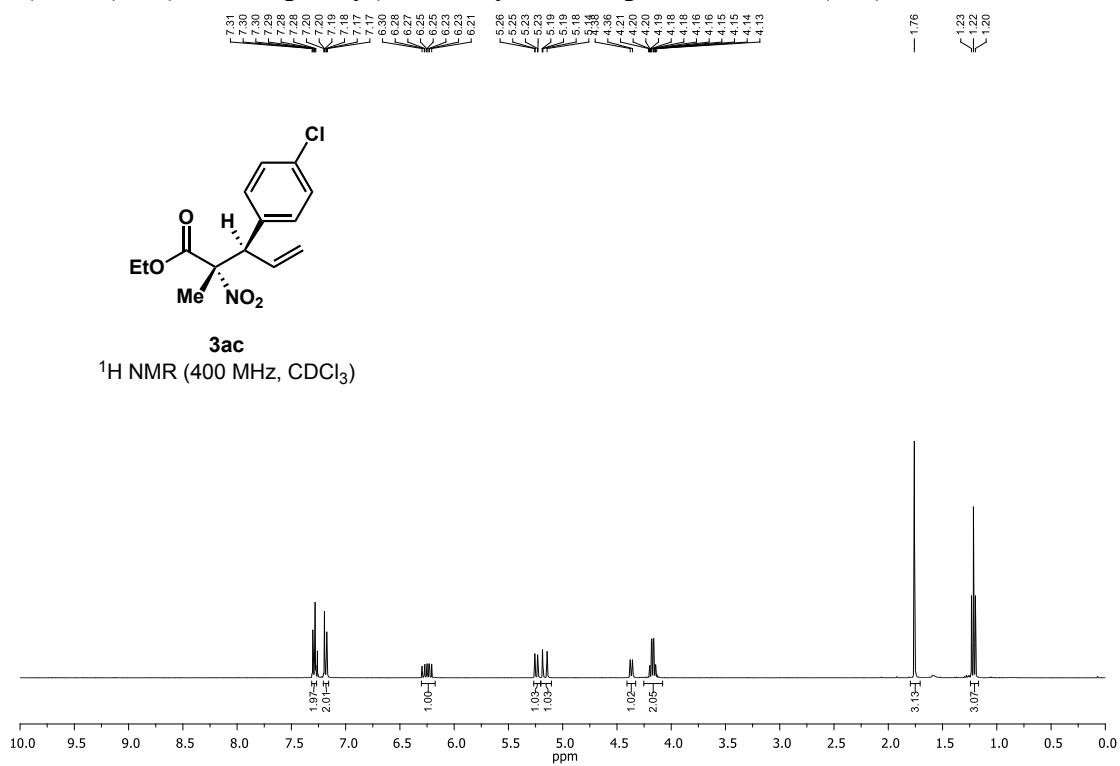


Ethyl (2*S*,3*R*)-3-(4-chlorophenyl)-2-methyl-2-nitropent-4-enoate (**3ac**)



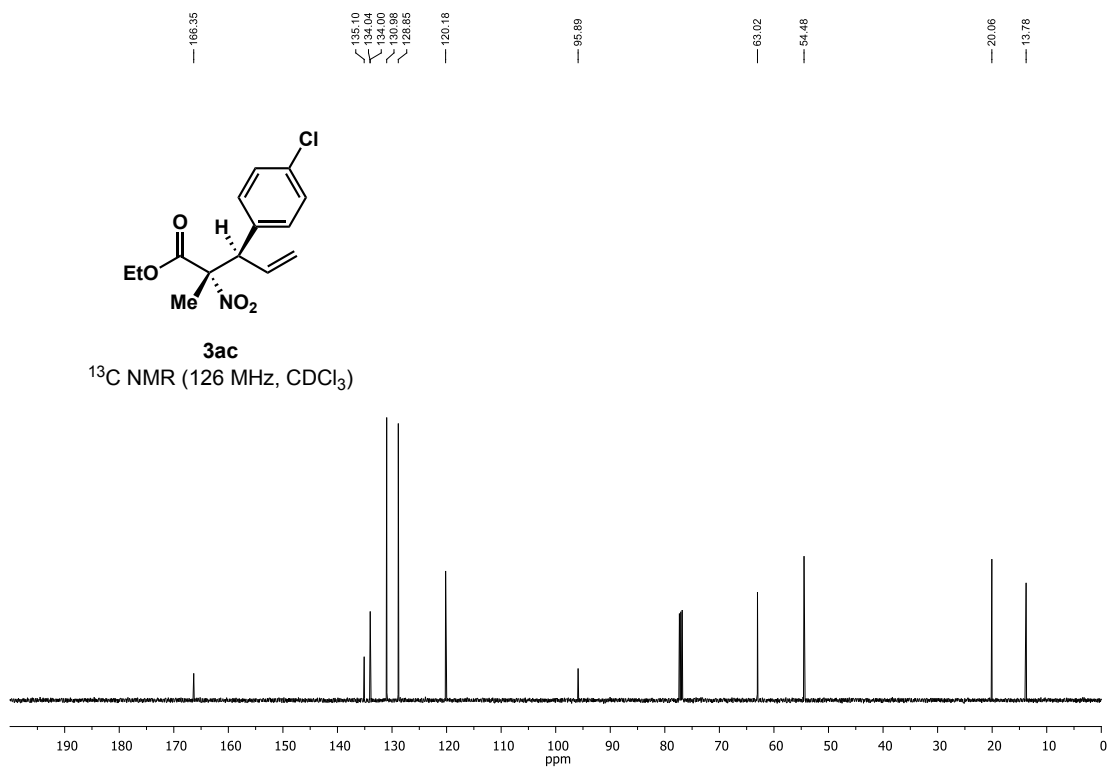
3ac

¹H NMR (400 MHz, CDCl₃)

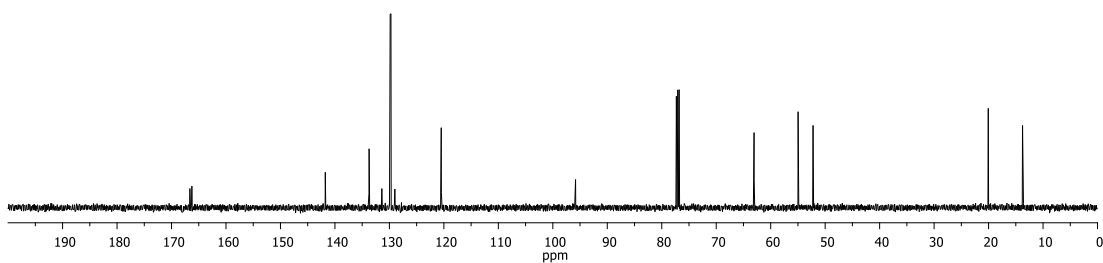
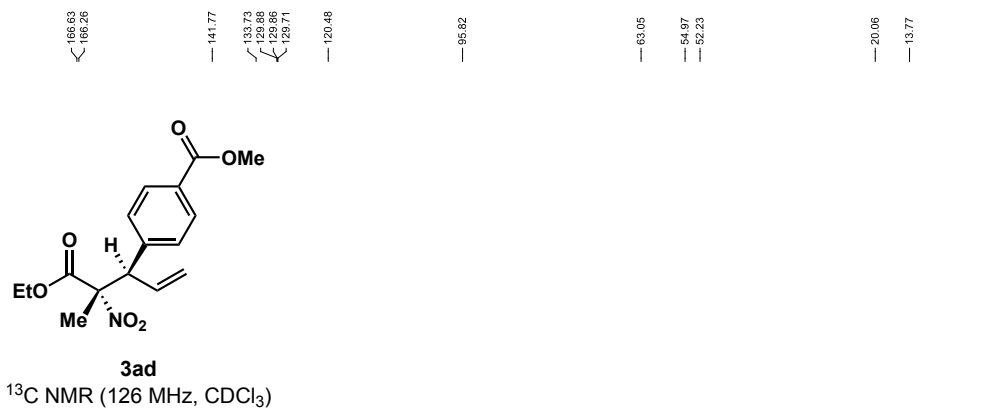
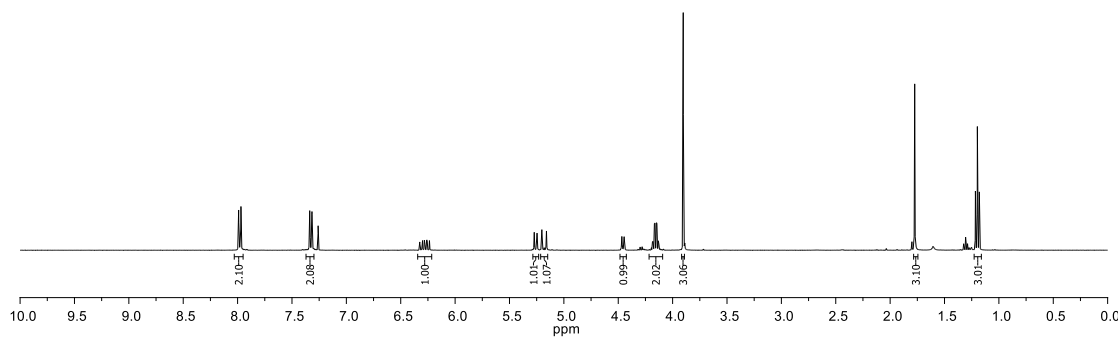
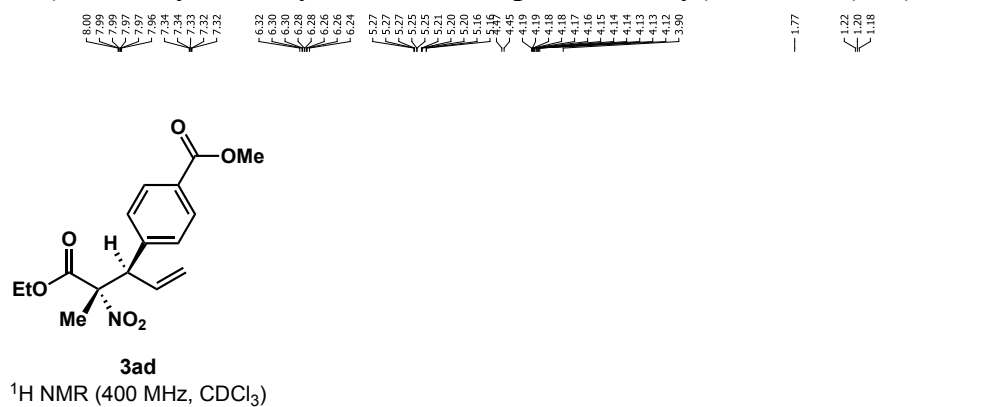


3ac

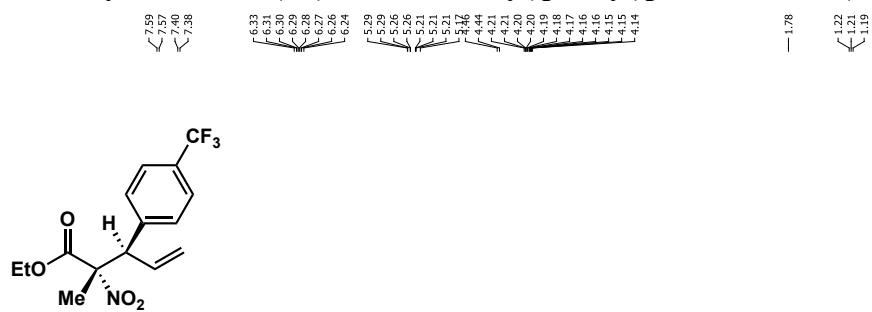
¹³C NMR (126 MHz, CDCl₃)



Methyl 4-((3*R*,4*S*)-5-ethoxy-4-methyl-4-nitro-5-oxopent-1-en-3-yl)benzoate (**3ad**)

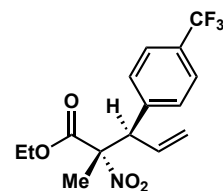
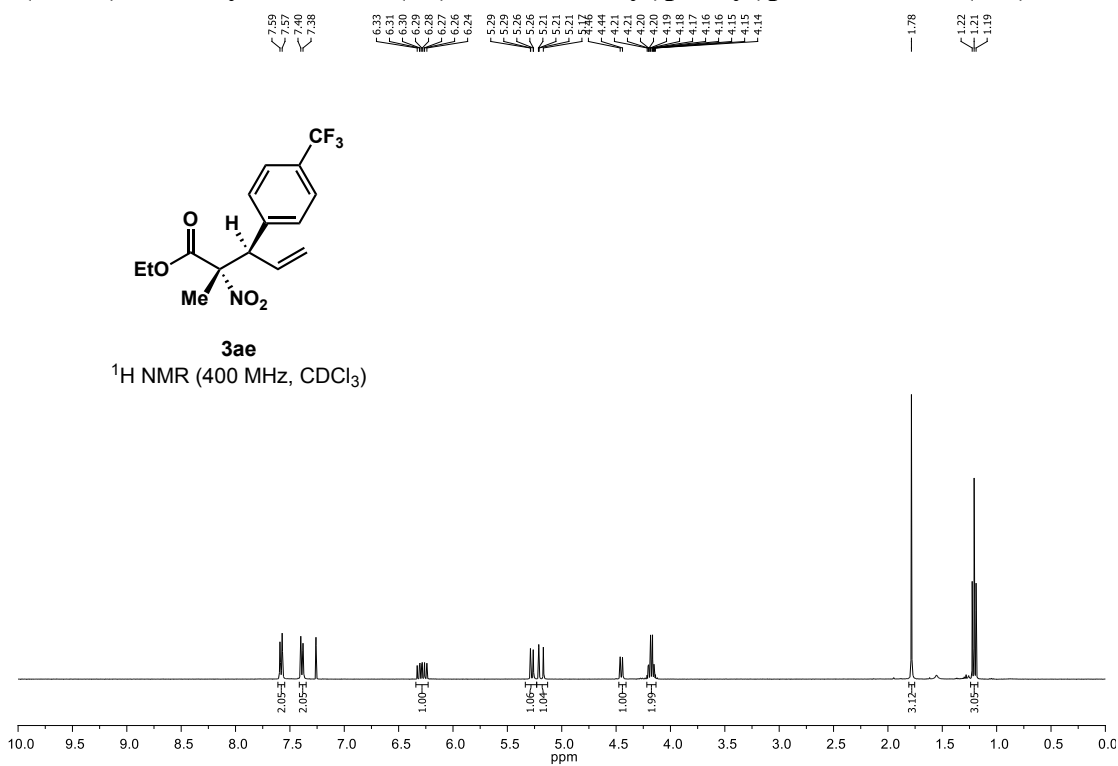


Ethyl (2*S*,3*R*)-2-methyl-2-nitro-3-(4-(trifluoromethyl)phenyl)pent-4-enoate (3ae)



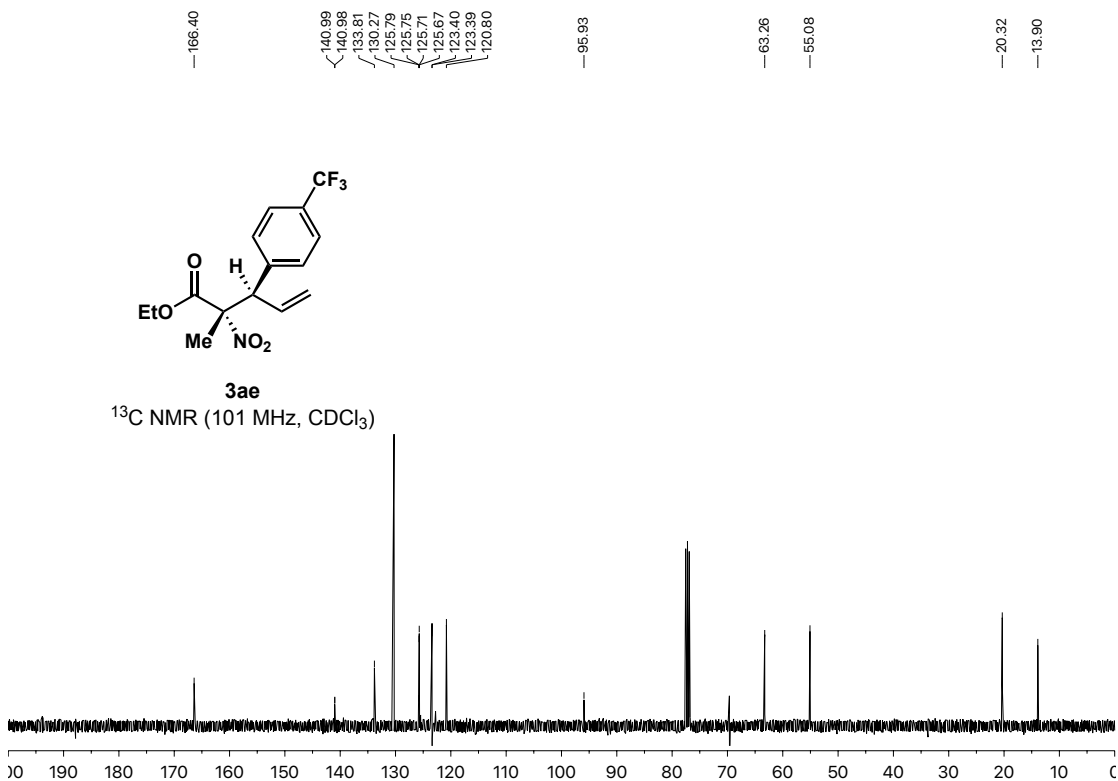
3ae

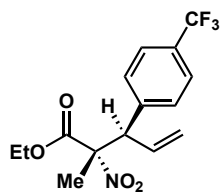
¹H NMR (400 MHz, CDCl₃)



3ae

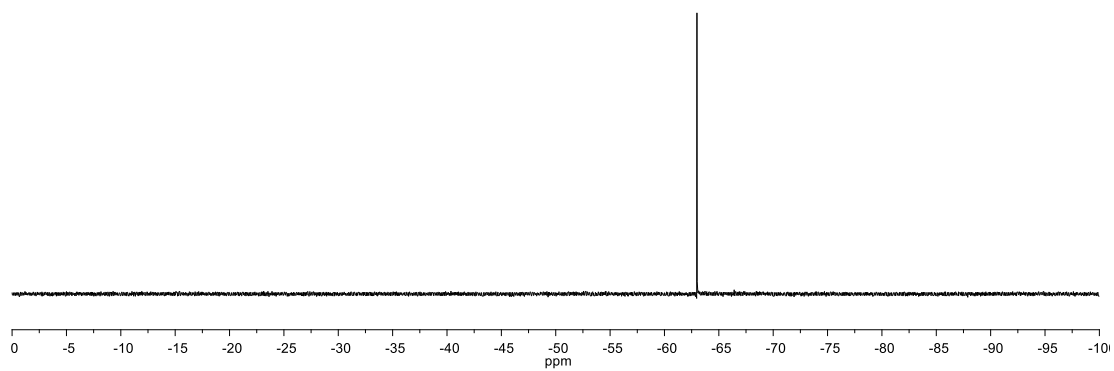
¹³C NMR (101 MHz, CDCl₃)



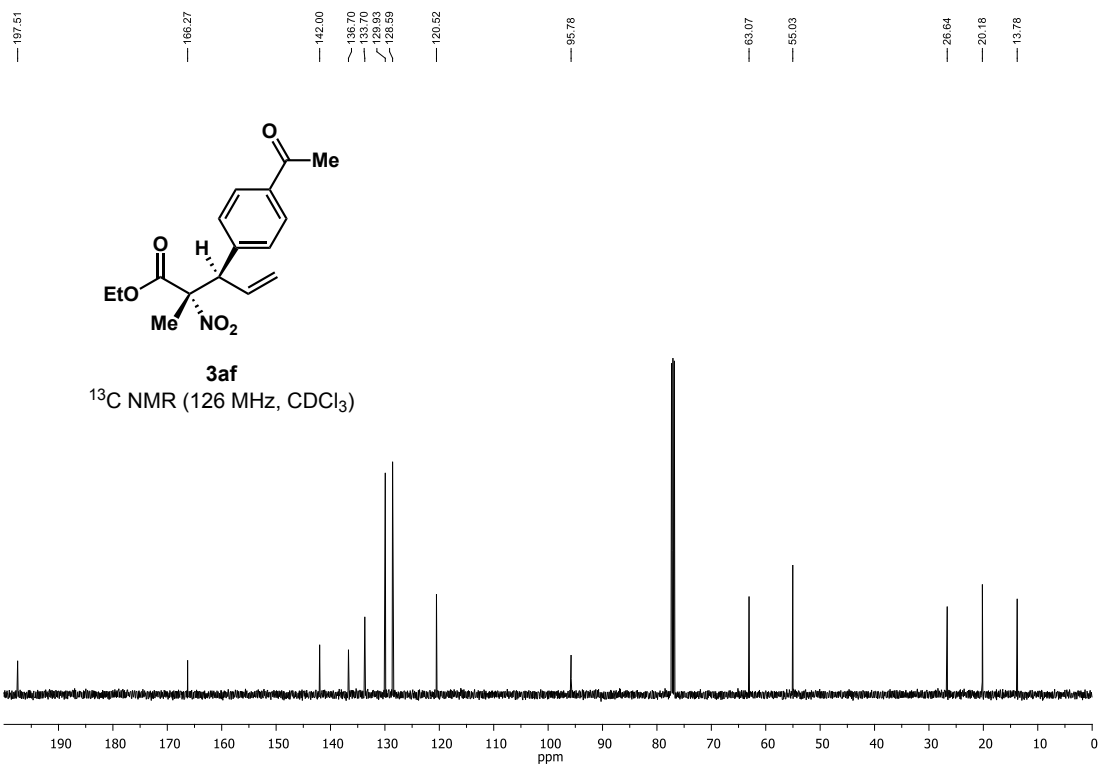
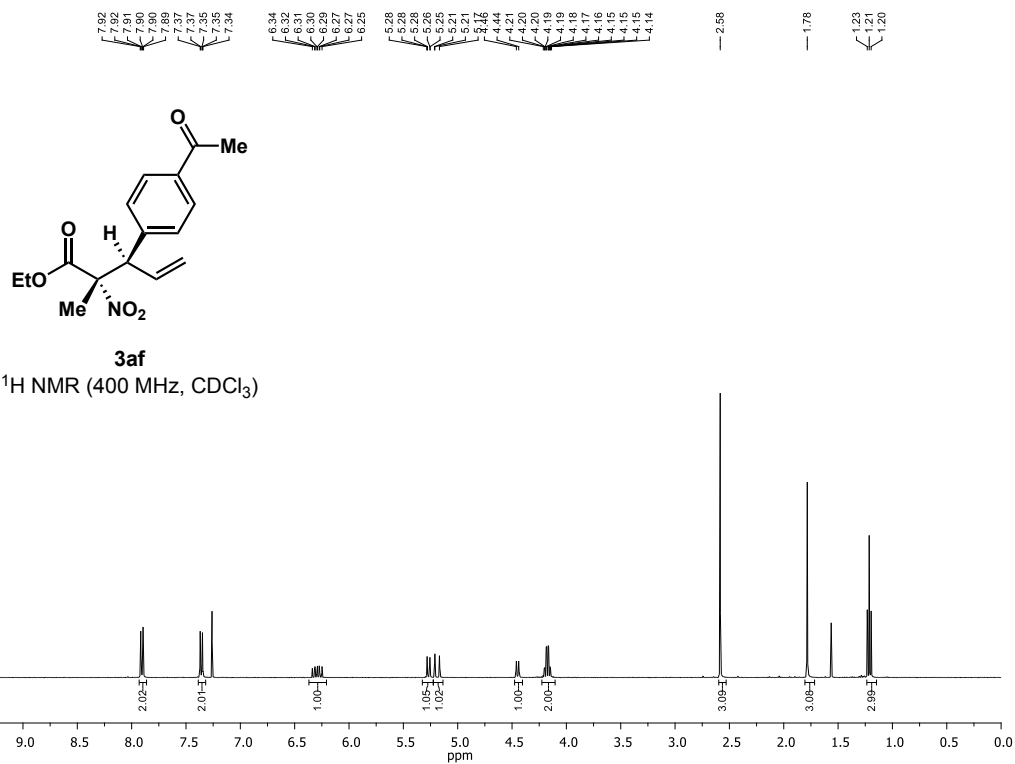


3ae

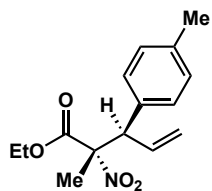
¹⁹F NMR (376 MHz, CDCl₃)



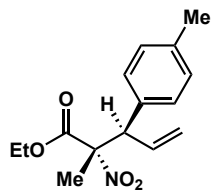
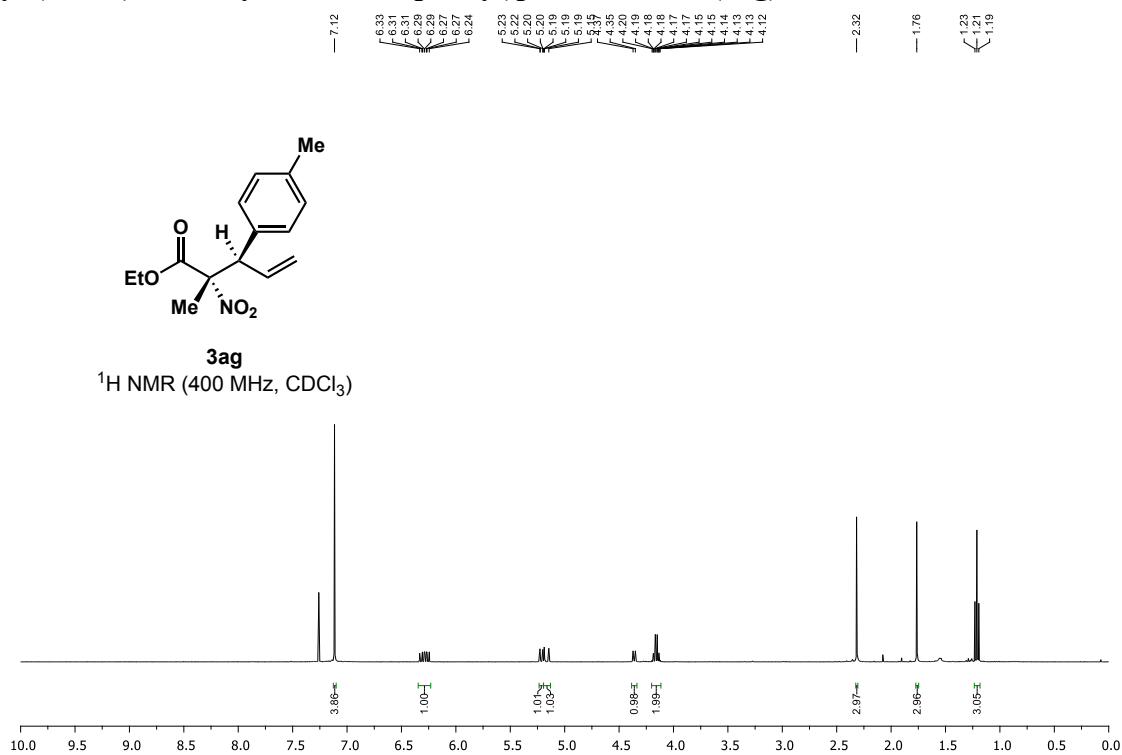
Ethyl (2*S*,3*R*)-3-(4-acetylphenyl)-2-methyl-2-nitropent-4-enoate (3af)



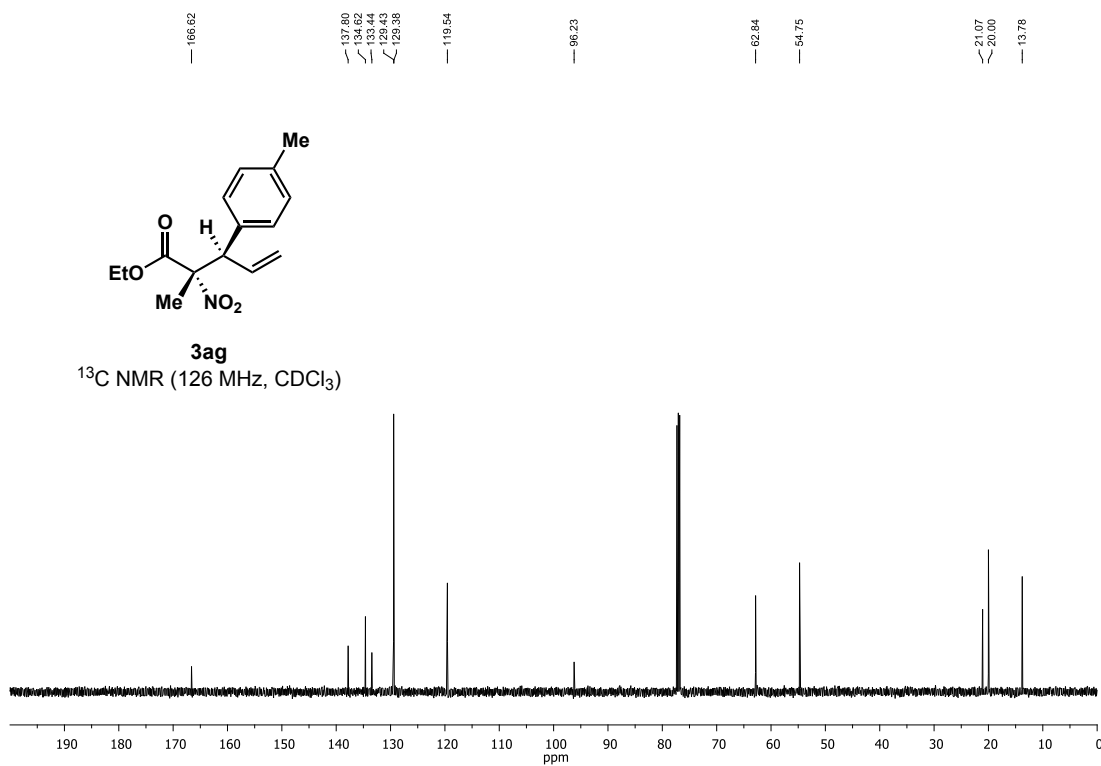
Ethyl (2*S*,3*R*)-2-methyl-2-nitro-3-(*p*-tolyl)pent-4-enoate (3ag**)**



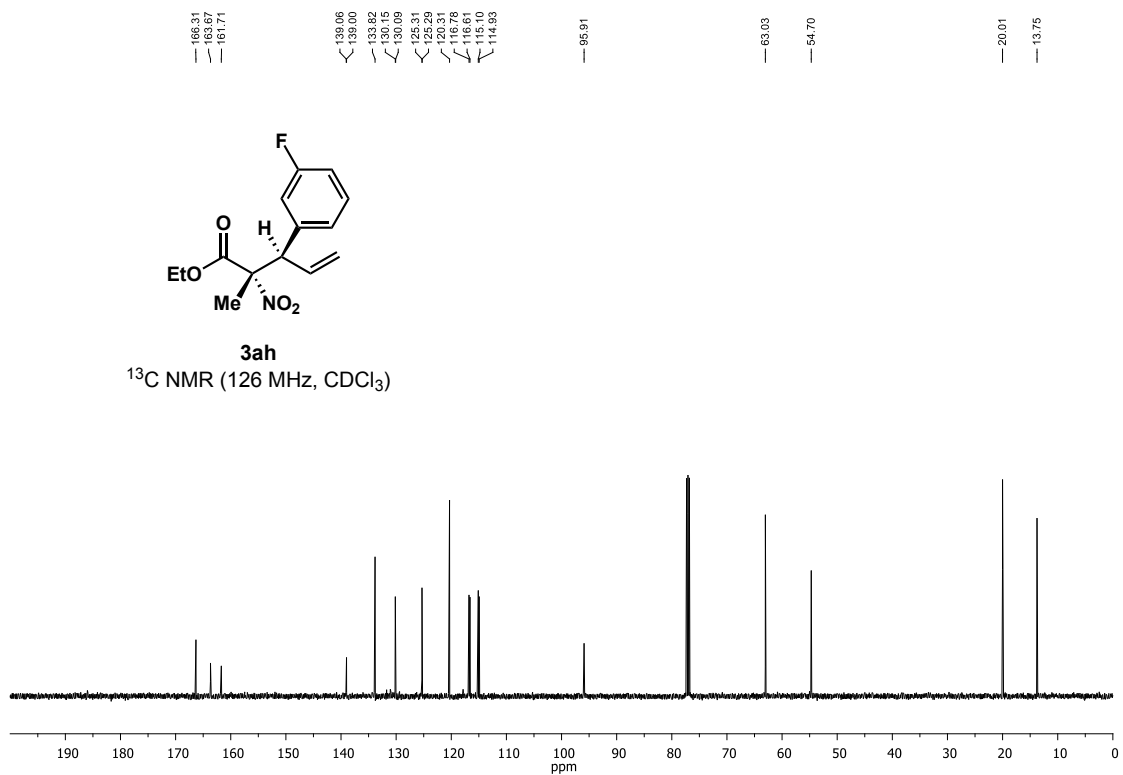
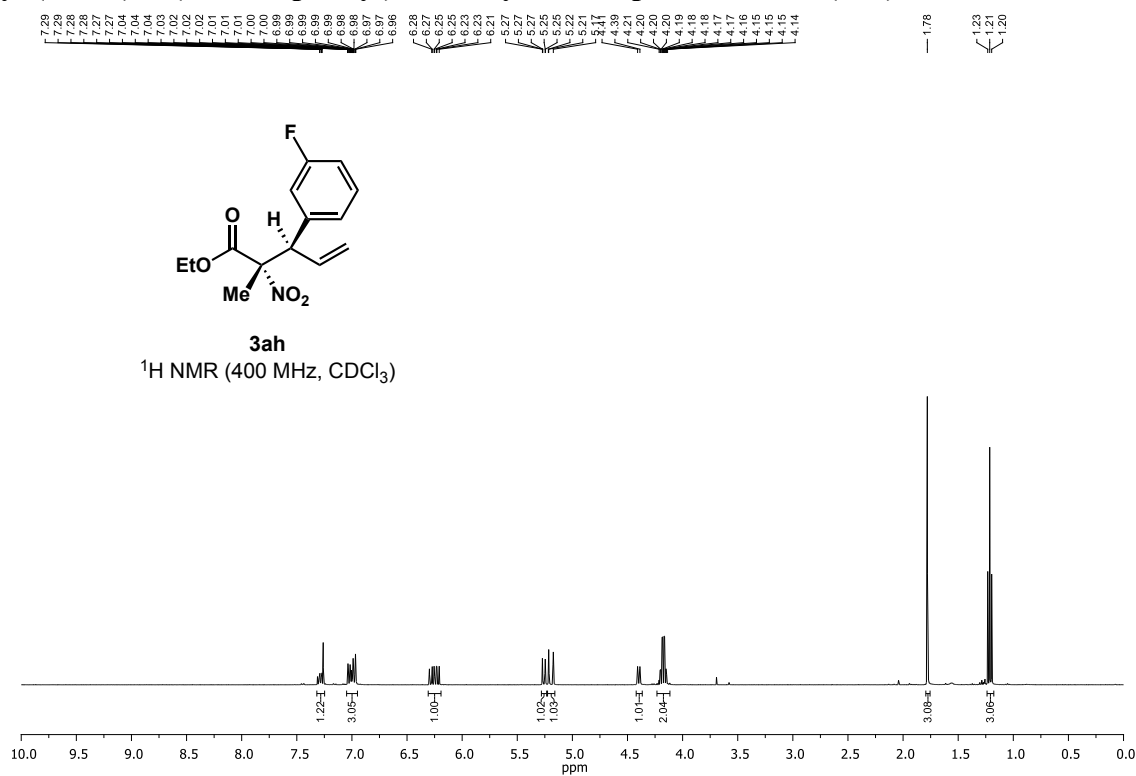
3ag
¹H NMR (400 MHz, CDCl₃)

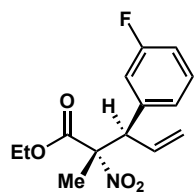


3ag
¹³C NMR (126 MHz, CDCl₃)



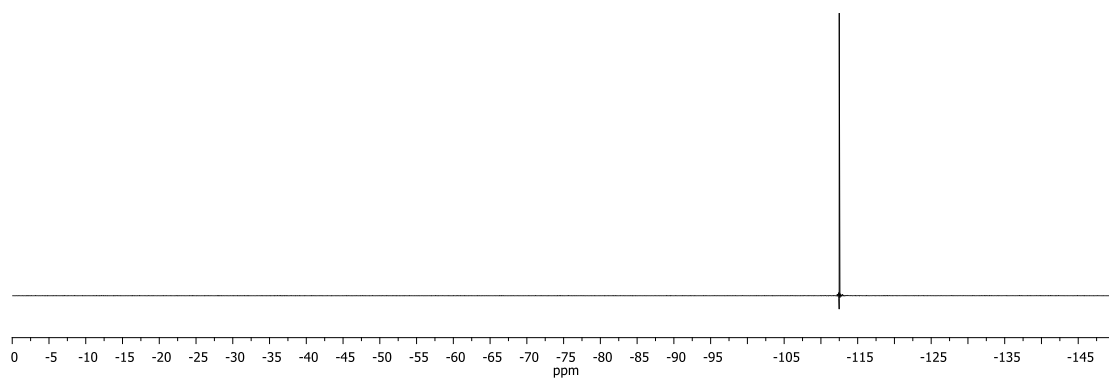
Ethyl (2*S*,3*R*)-3-(3-fluorophenyl)-2-methyl-2-nitropent-4-enoate (3ah)



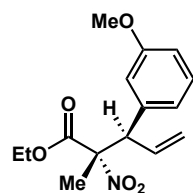


3ah

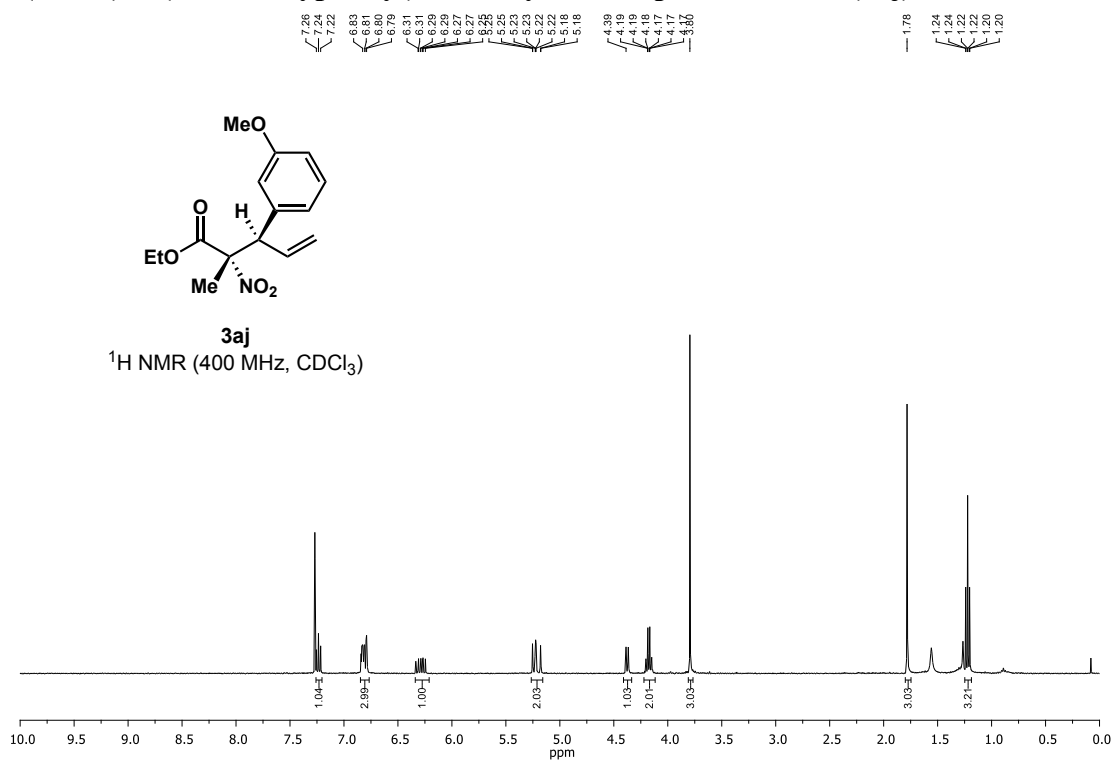
¹⁹F NMR (376 MHz, CDCl₃)



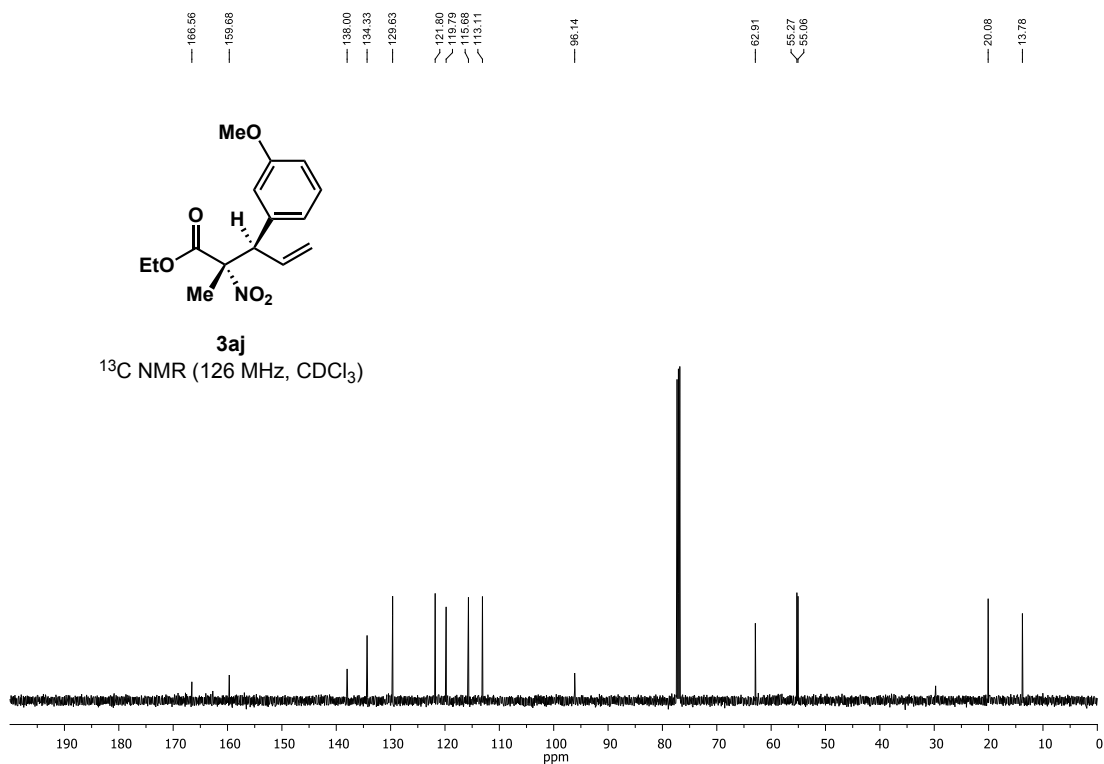
Ethyl (2*S*,3*R*)-3-(3-methoxyphenyl)-2-methyl-2-nitropent-4-enoate (**3aj**)



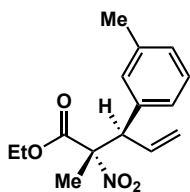
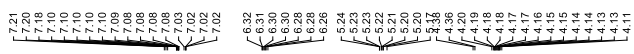
3aj
¹H NMR (400 MHz, CDCl₃)



3aj
¹³C NMR (126 MHz, CDCl₃)

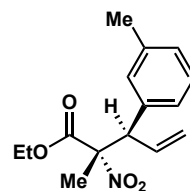
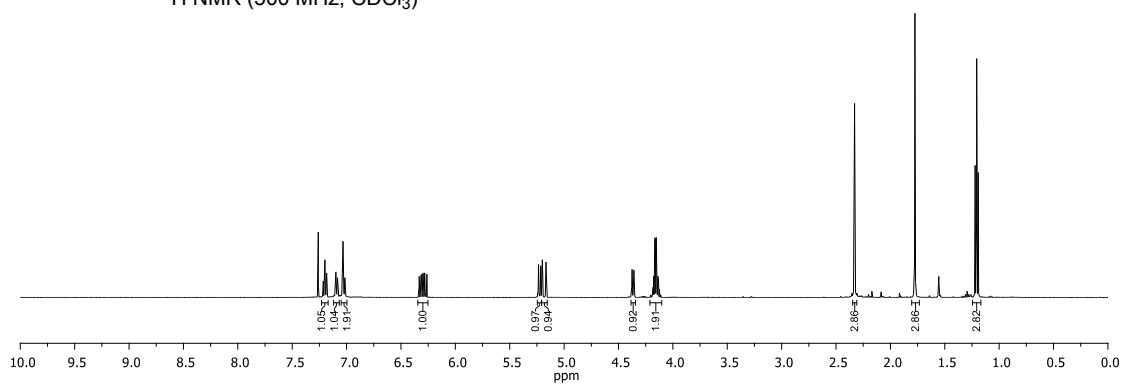


Ethyl (2*S*,3*R*)-2-methyl-2-nitro-3-(*m*-tolyl)pent-4-enoate (3ak)



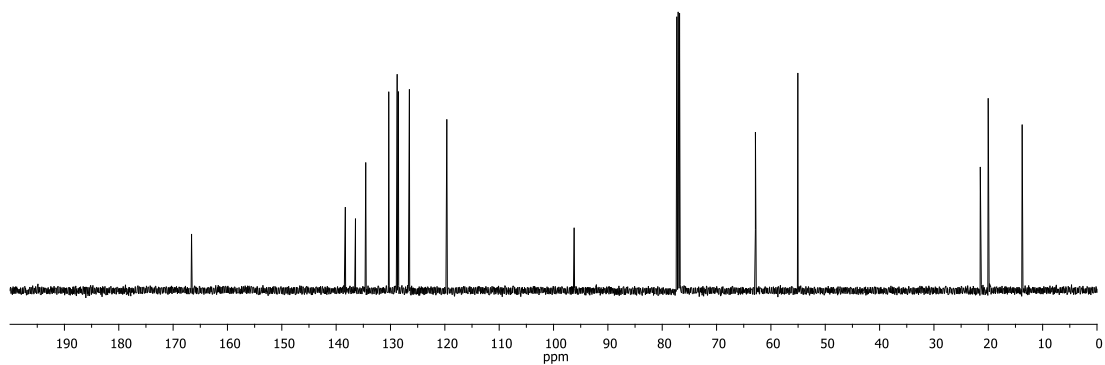
3ak

¹H NMR (500 MHz, CDCl₃)

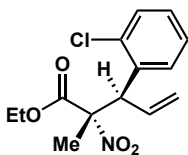
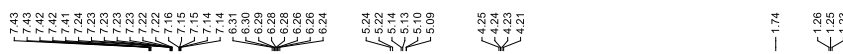


3ak

¹³C NMR (126 MHz, CDCl₃)

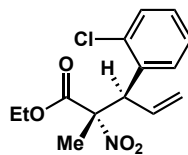
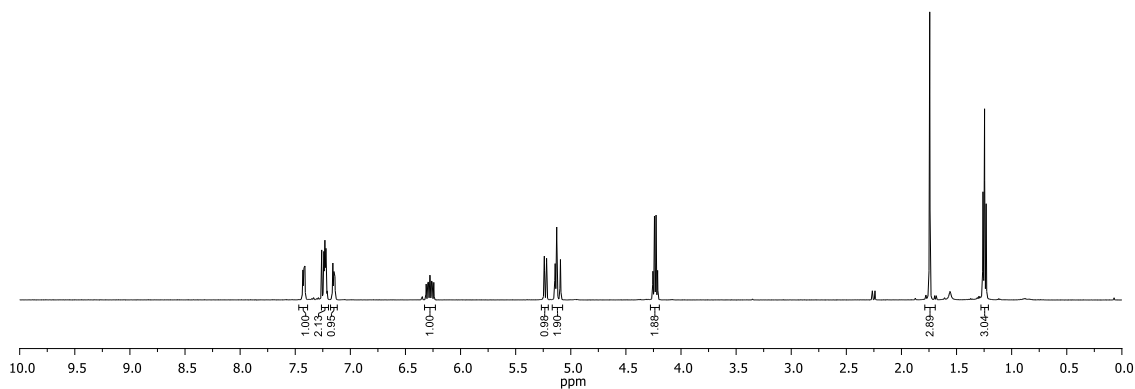


Ethyl (2*S*,3*R*)-3-(2-chlorophenyl)-2-methyl-2-nitropent-4-enoate (3a)



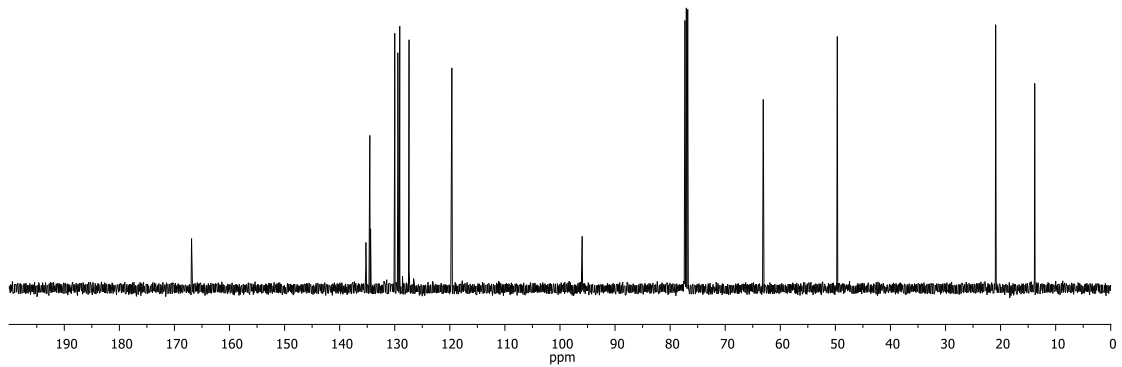
3a

¹H NMR (500 MHz, CDCl₃)

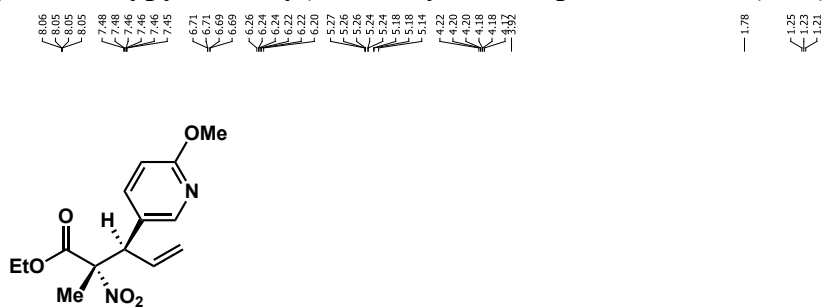


3a

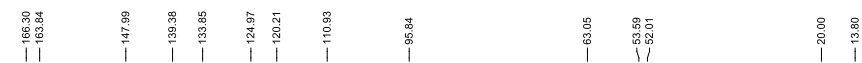
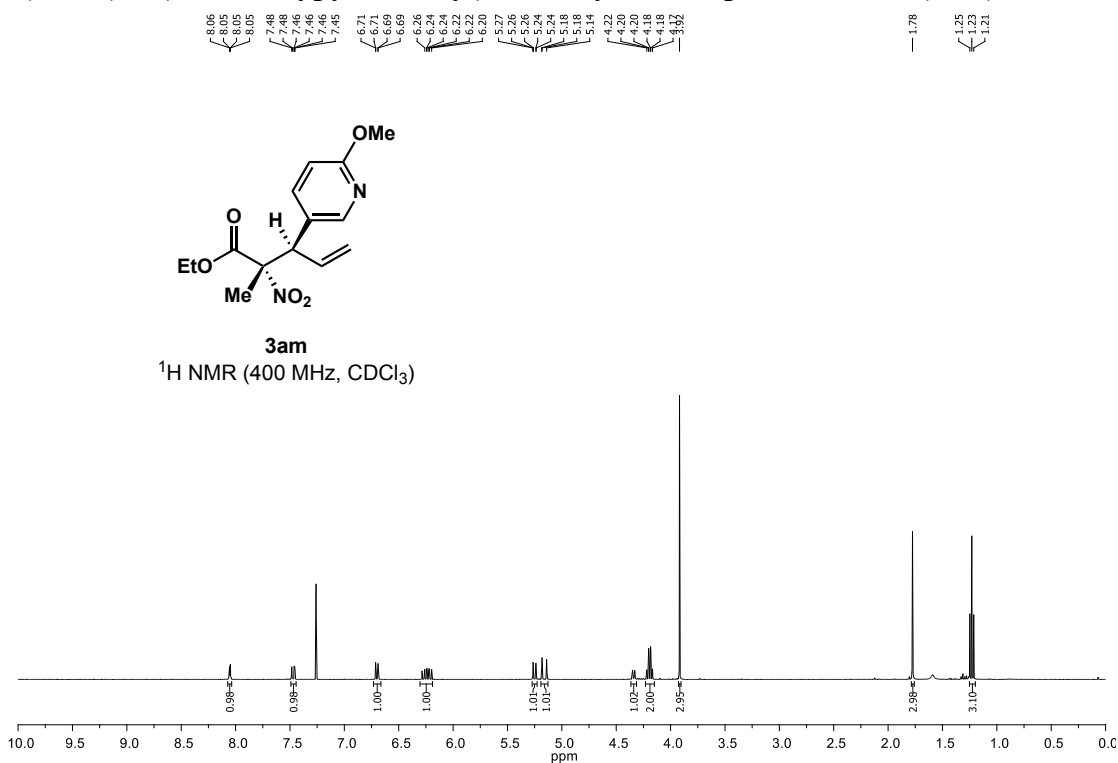
¹³C NMR (126 MHz, CDCl₃)



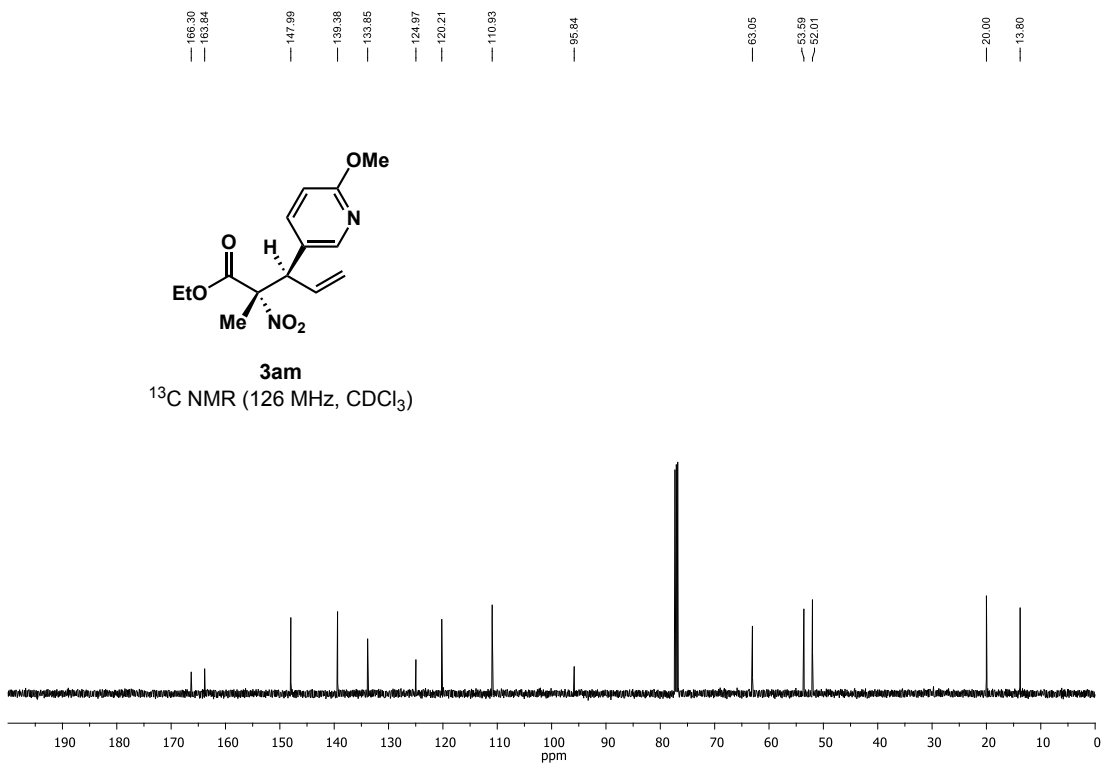
Ethyl (2*S*,3*R*)-3-(6-methoxypyridin-3-yl)-2-methyl-2-nitropent-4-enoate (**3am**)



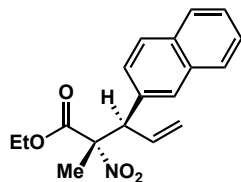
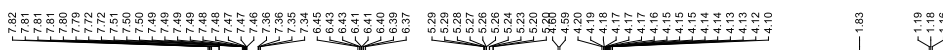
3am
¹H NMR (400 MHz, CDCl₃)



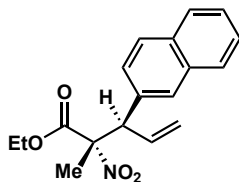
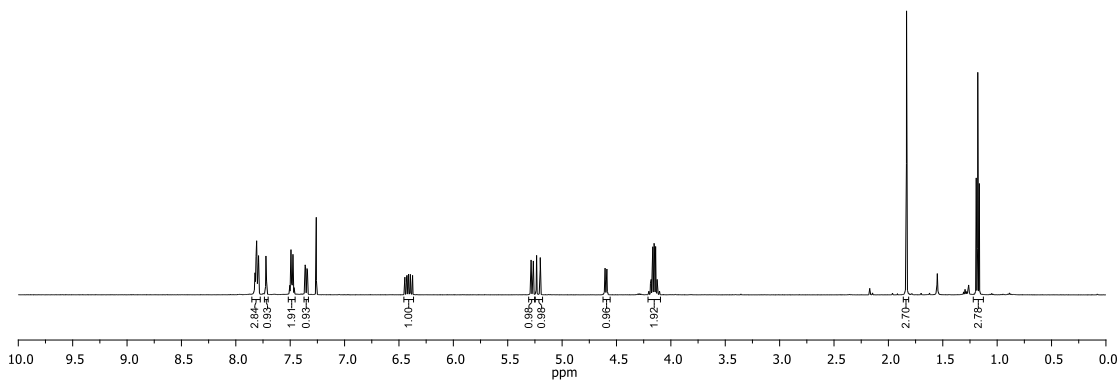
3am
¹³C NMR (126 MHz, CDCl₃)



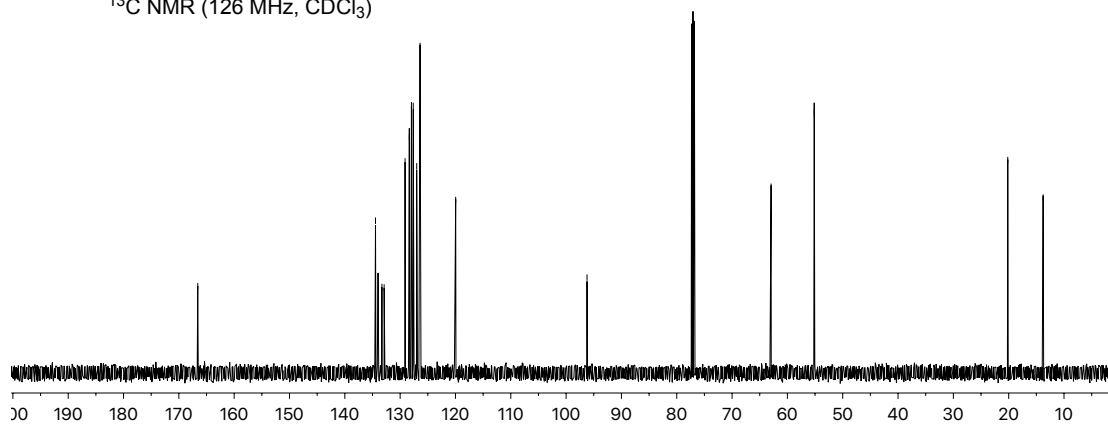
Ethyl (2*S*,3*R*)-2-methyl-3-(naphthalen-2-yl)-2-nitropent-4-enoate (3a0)



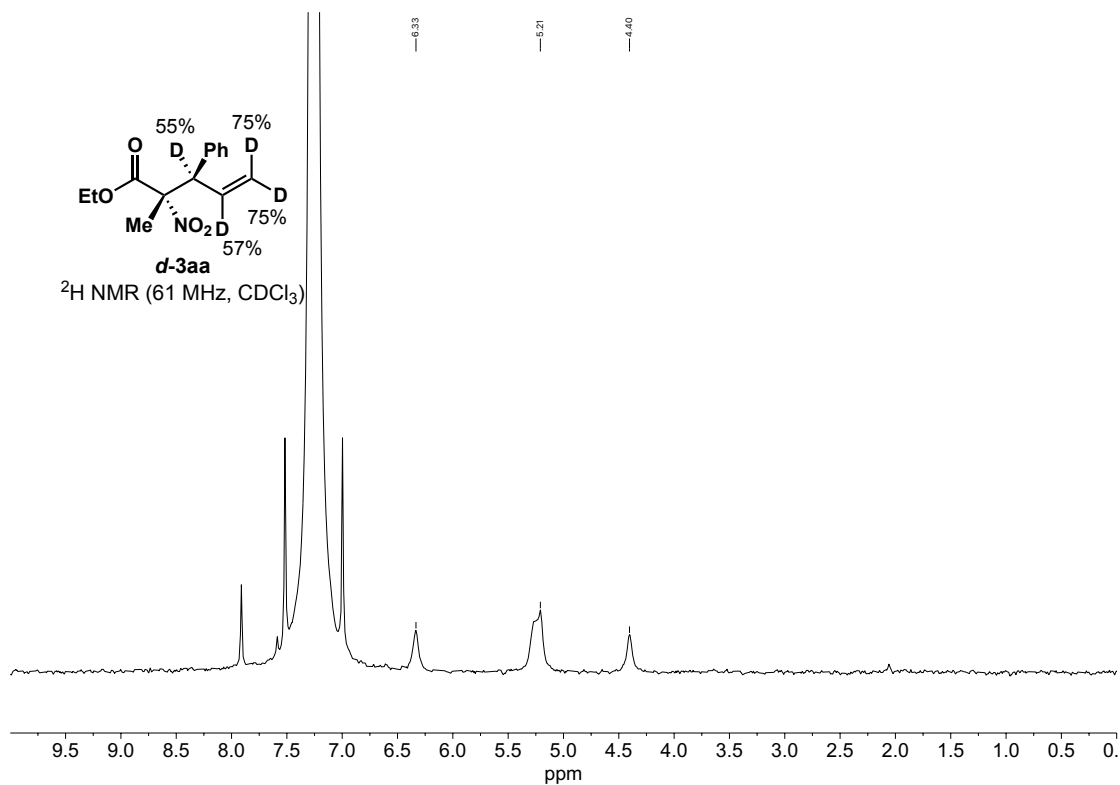
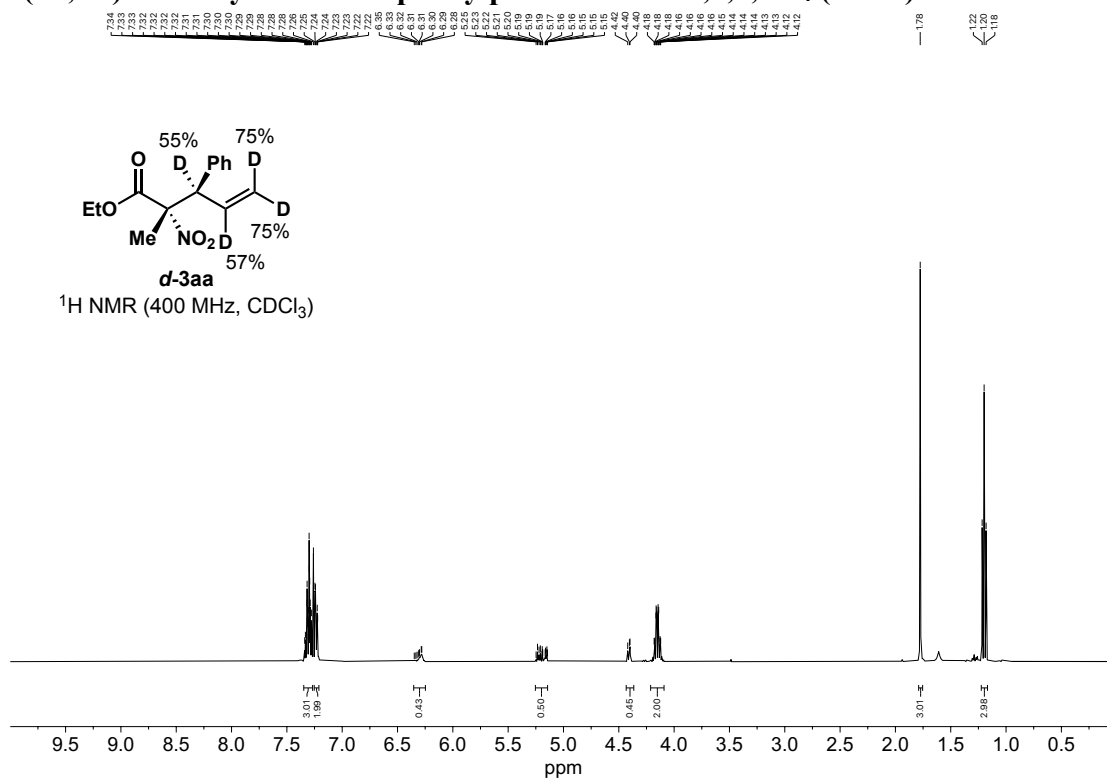
3a0
¹H NMR (500 MHz, CDCl₃)



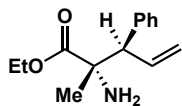
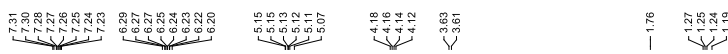
3a0
¹³C NMR (126 MHz, CDCl₃)



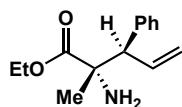
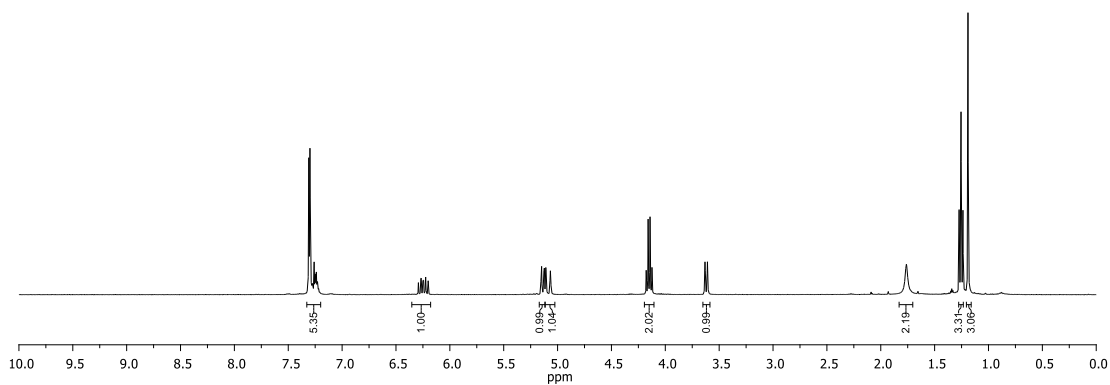
Ethyl (2*S*,3*R*)-2-methyl-2-nitro-3-phenylpent-4-enoate-3,4,5,5-*d*₄ (*d*-3aa)



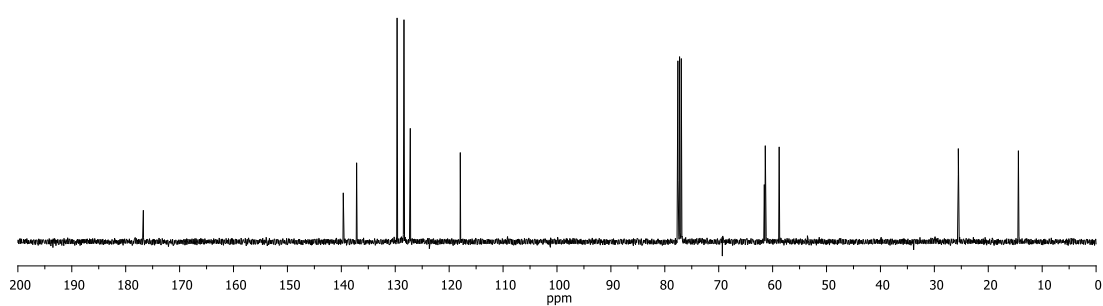
Ethyl (2*S*,3*R*)-2-amino-2-methyl-3-phenylpent-4-enoate (6)



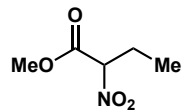
6
¹H NMR (400 MHz, CDCl₃)



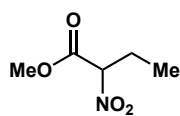
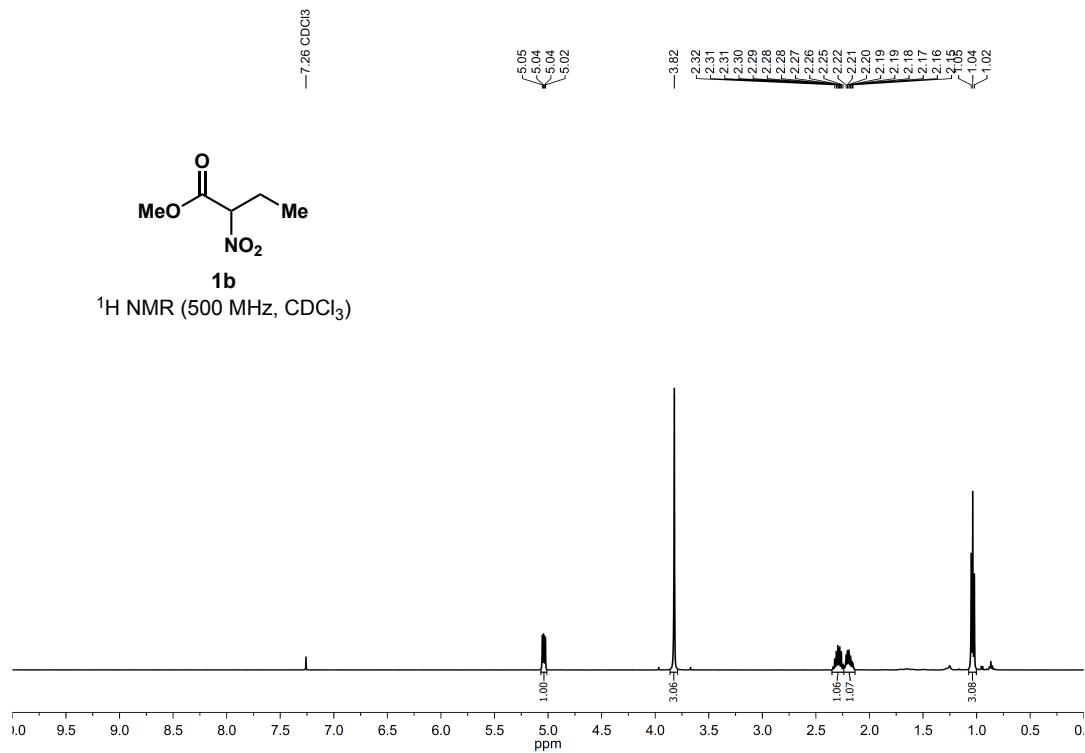
6
¹³C NMR (101 MHz, CDCl₃)



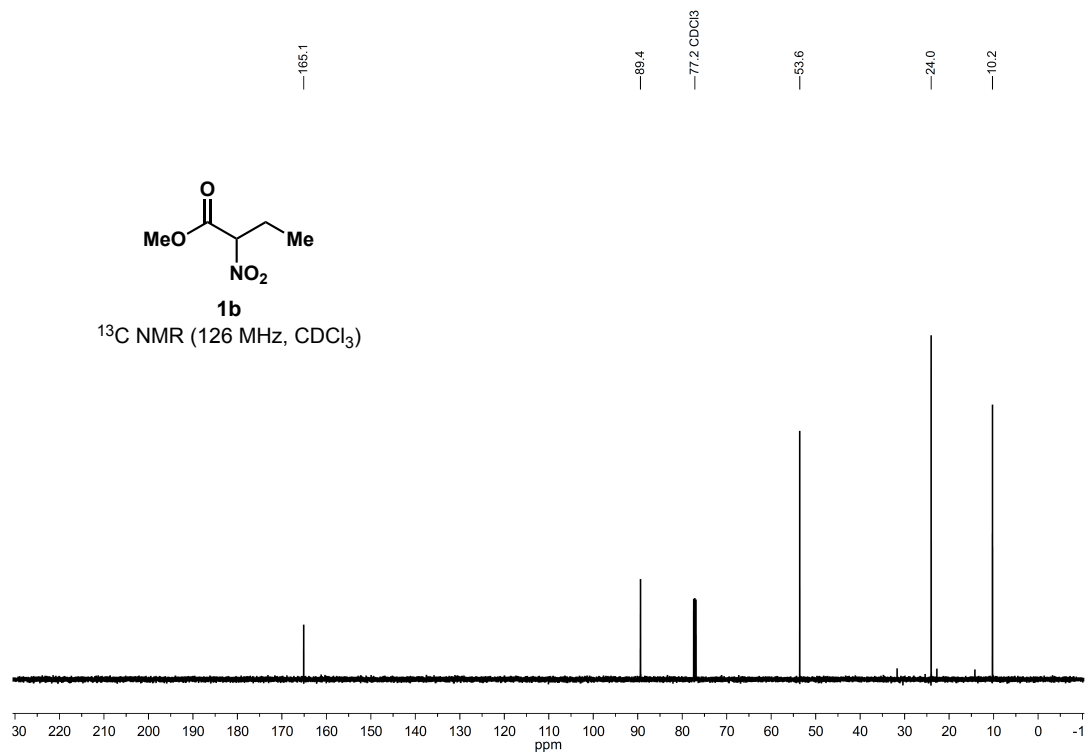
Methyl 2-nitrobutanoate (1b)



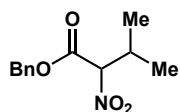
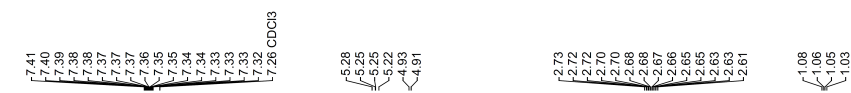
1b
¹H NMR (500 MHz, CDCl₃)



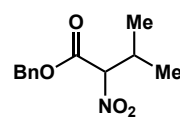
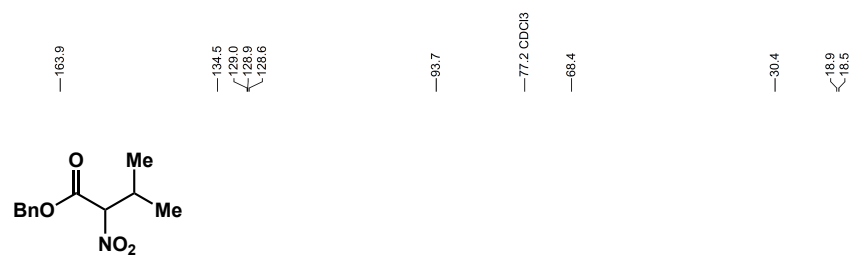
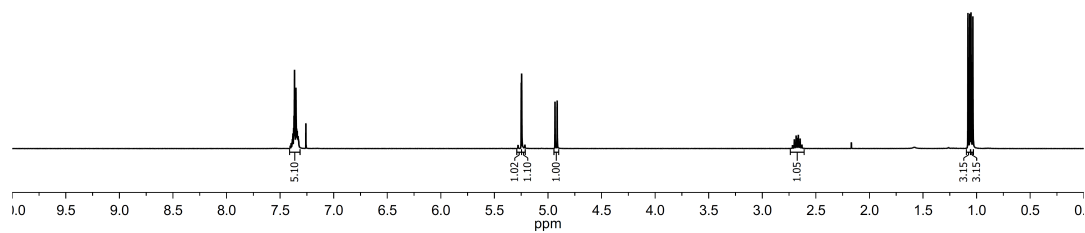
1b
¹³C NMR (126 MHz, CDCl₃)



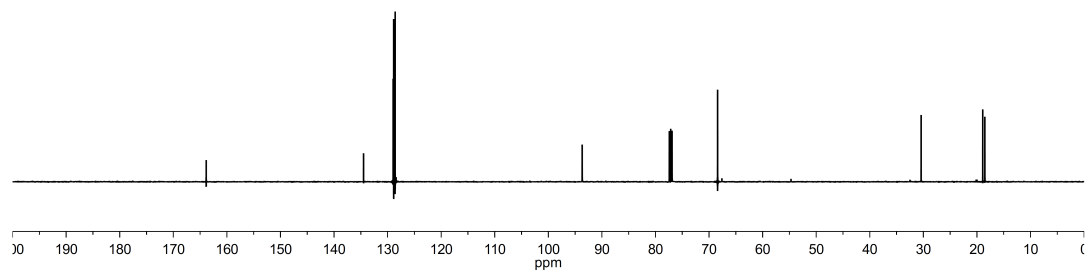
Benzyl 3-methyl-2-nitrobutanoate (1c)



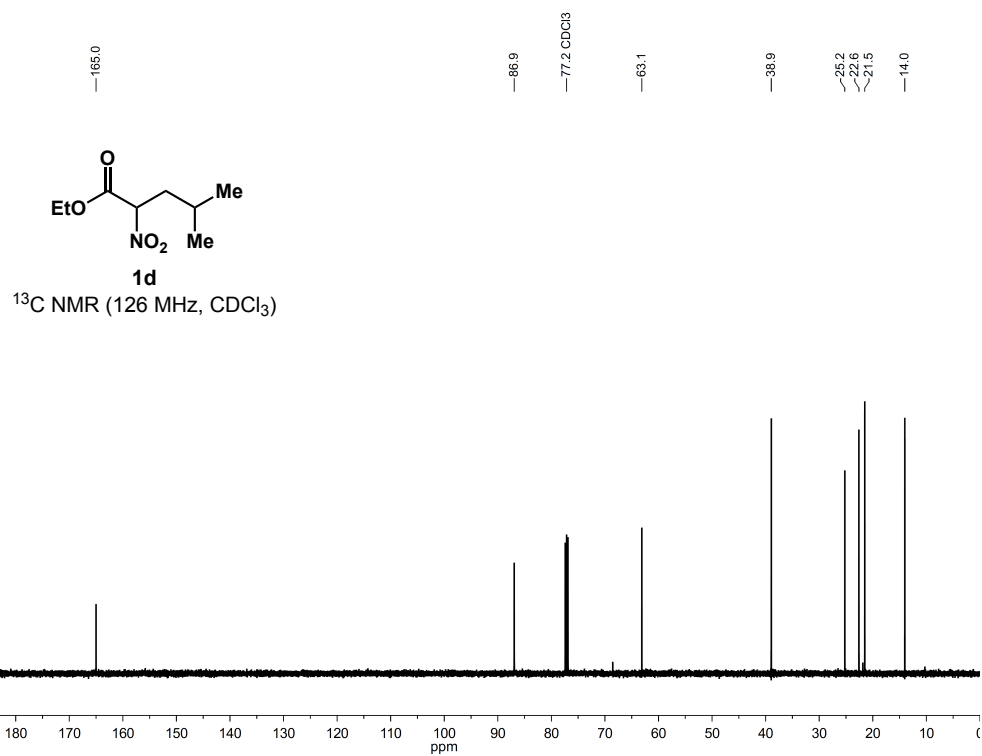
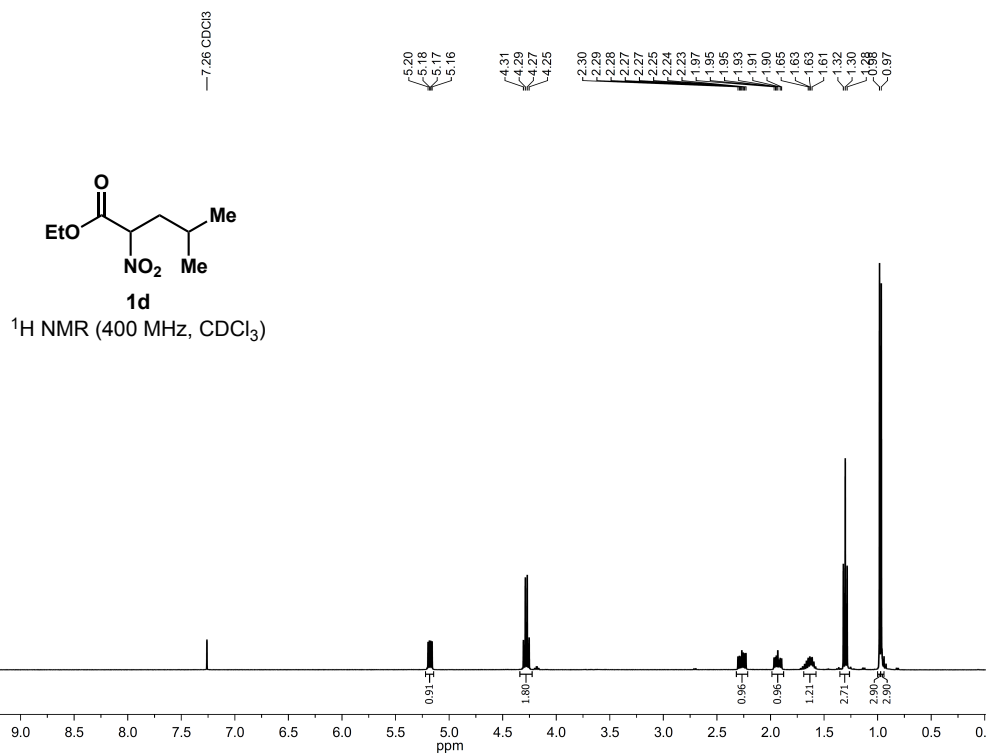
1c
¹H NMR (400 MHz, CDCl₃)



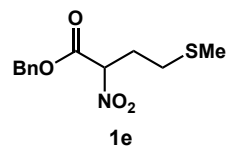
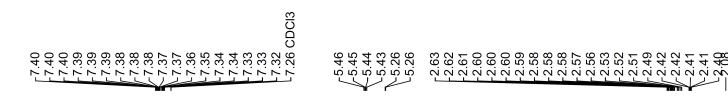
1c
¹³C NMR (126 MHz, CDCl₃)



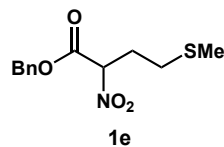
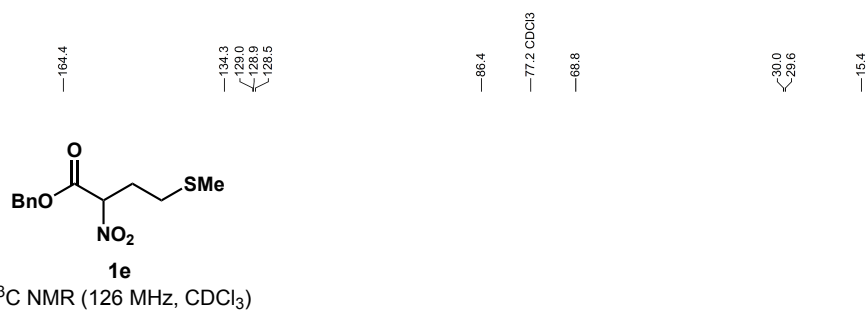
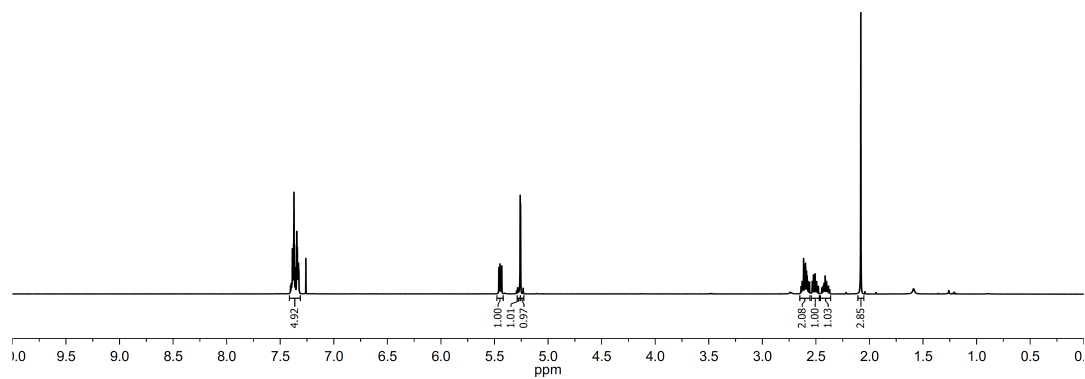
Ethyl 4-methyl-2-nitropentanoate (1d)



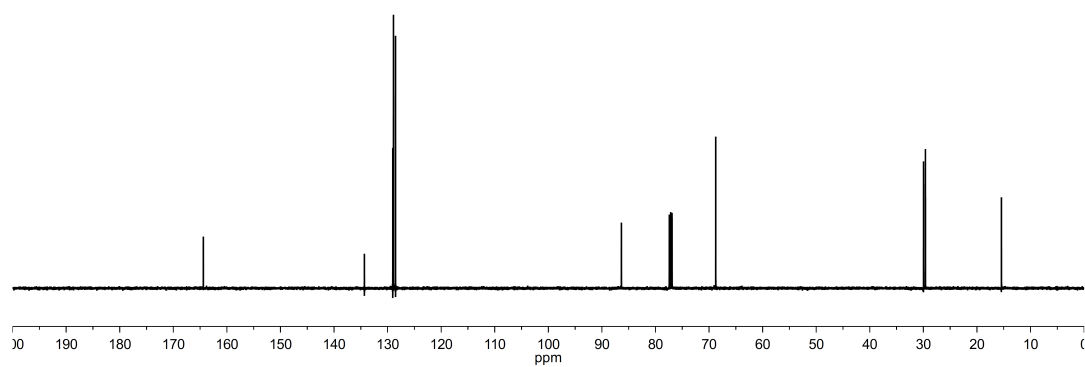
Benzyl 4-(methylthio)-2-nitrobutanoate (1e)



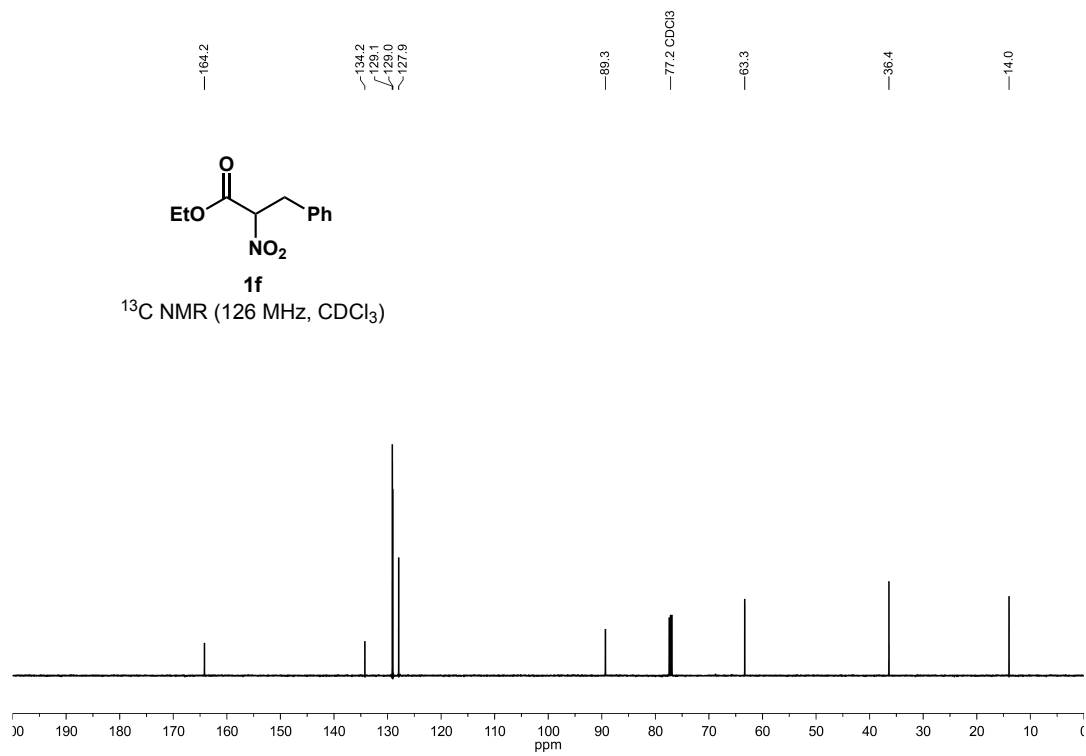
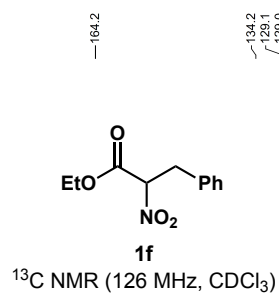
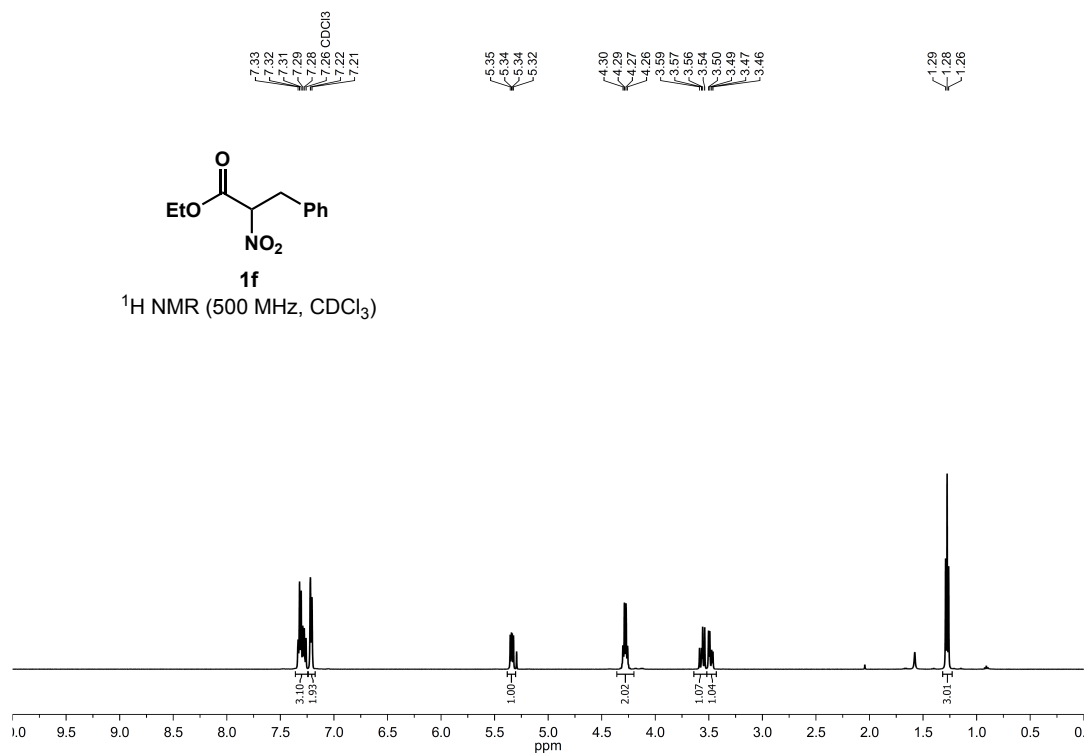
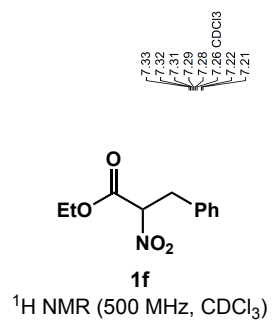
¹H NMR (500 MHz, CDCl₃)



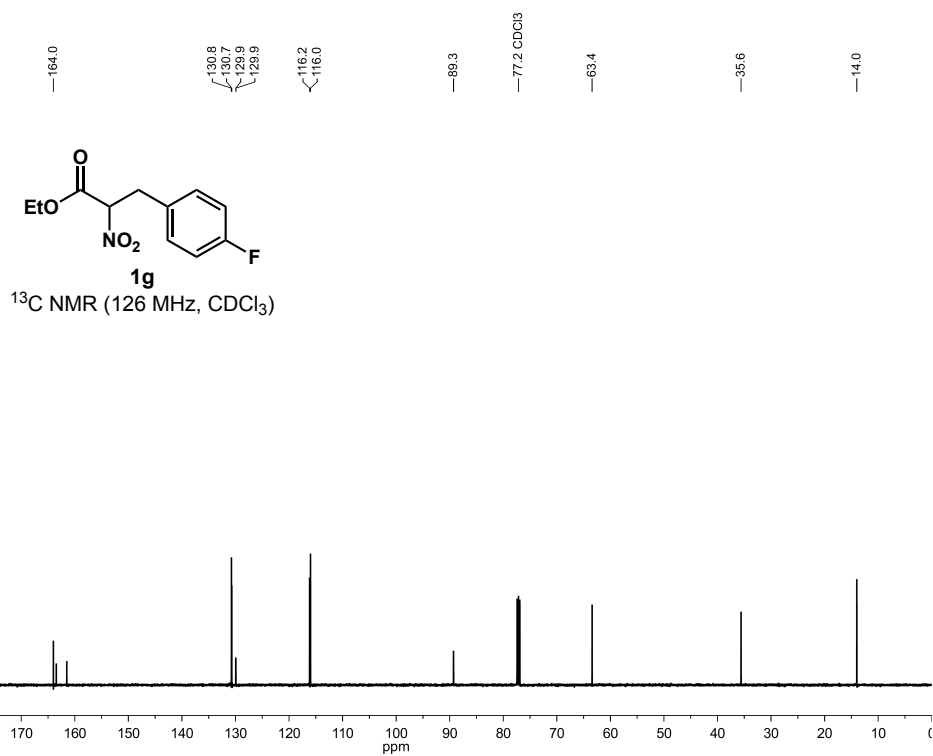
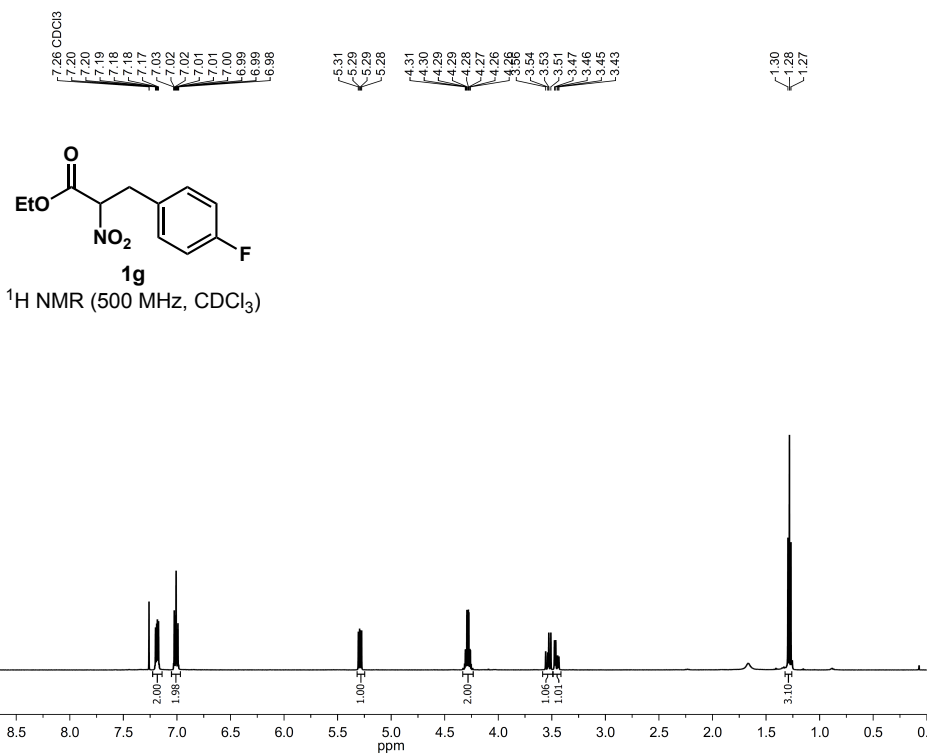
¹³C NMR (126 MHz, CDCl₃)

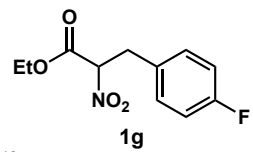


Ethyl 2-nitro-3-phenylpropanoate (1f)

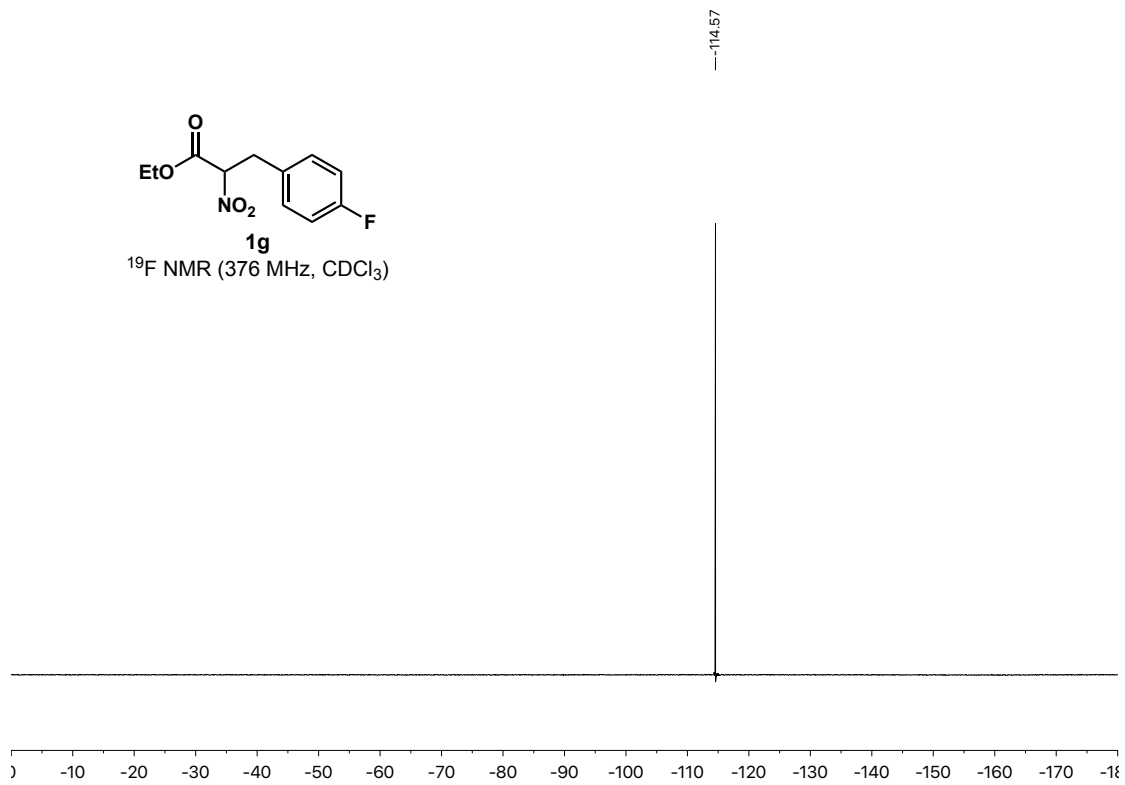


Ethyl 2-nitro-3-(4-fluorophenyl)propanoate (1g)

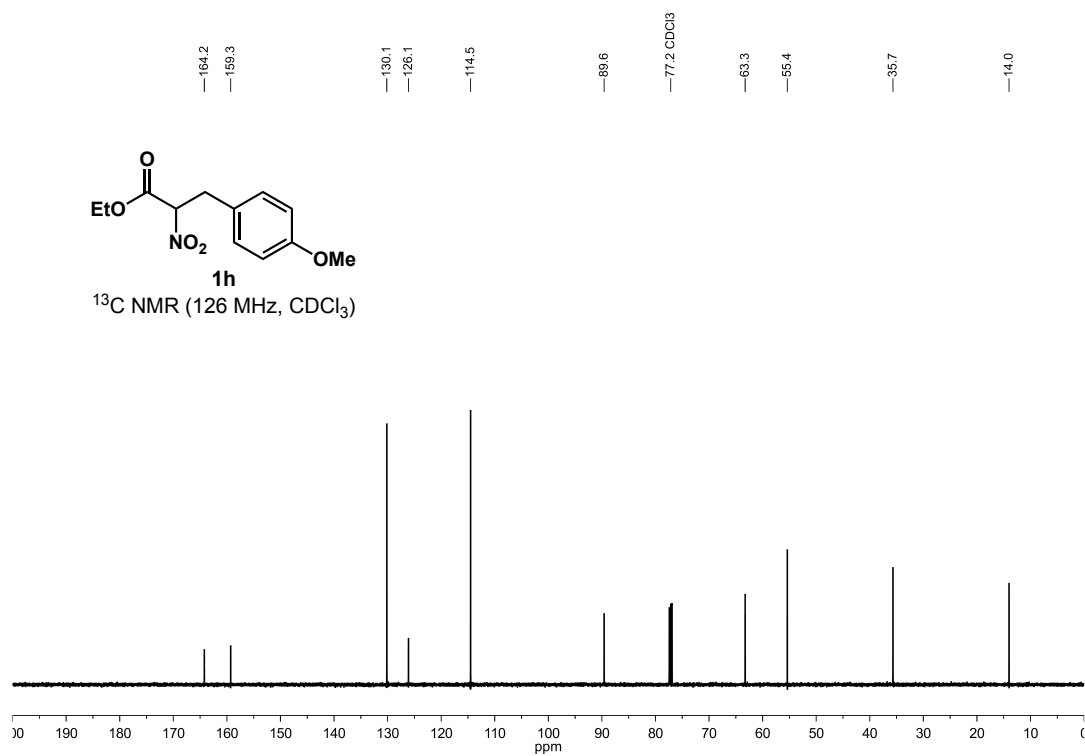
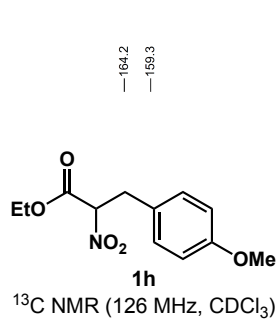
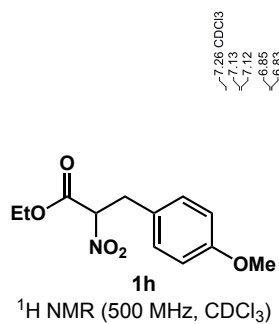




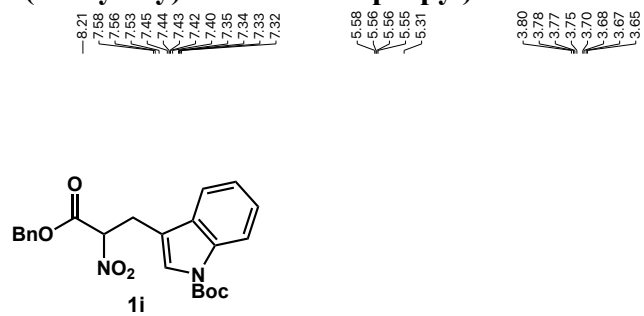
¹⁹F NMR (376 MHz, CDCl₃)



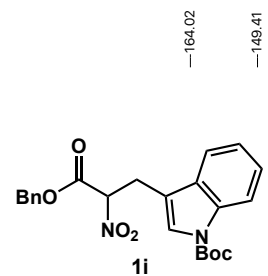
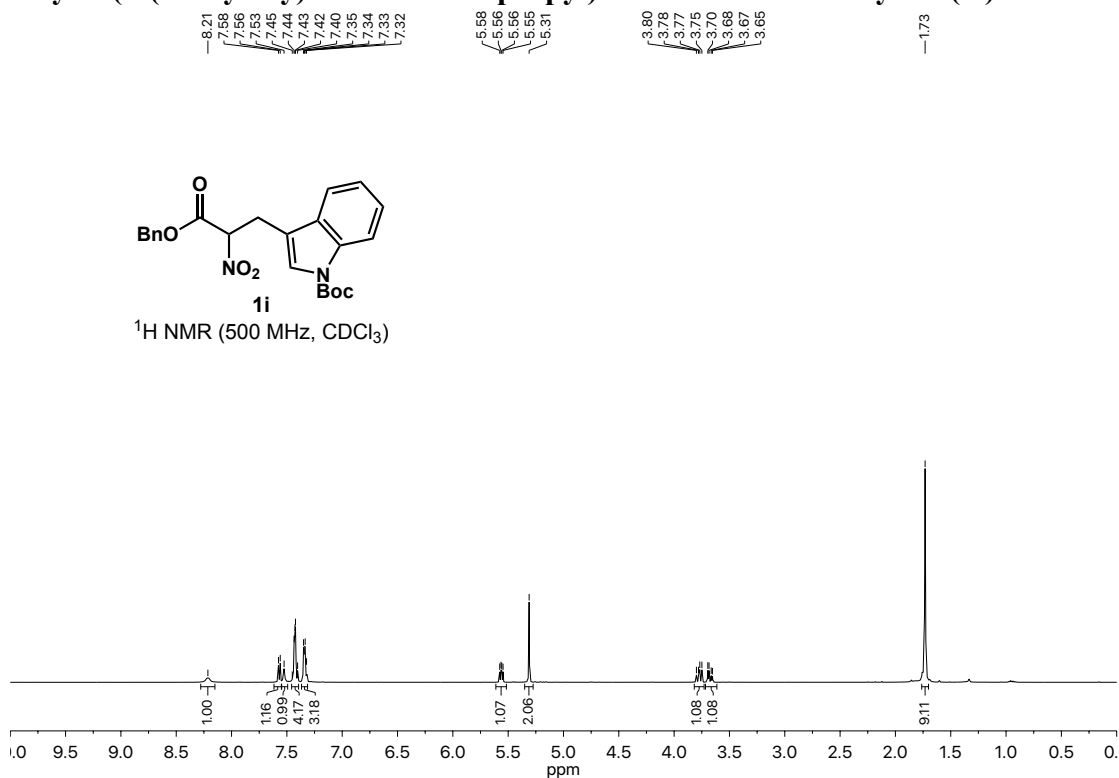
Ethyl 3-(4-methoxyphenyl)-2-nitropropanoate (1h)



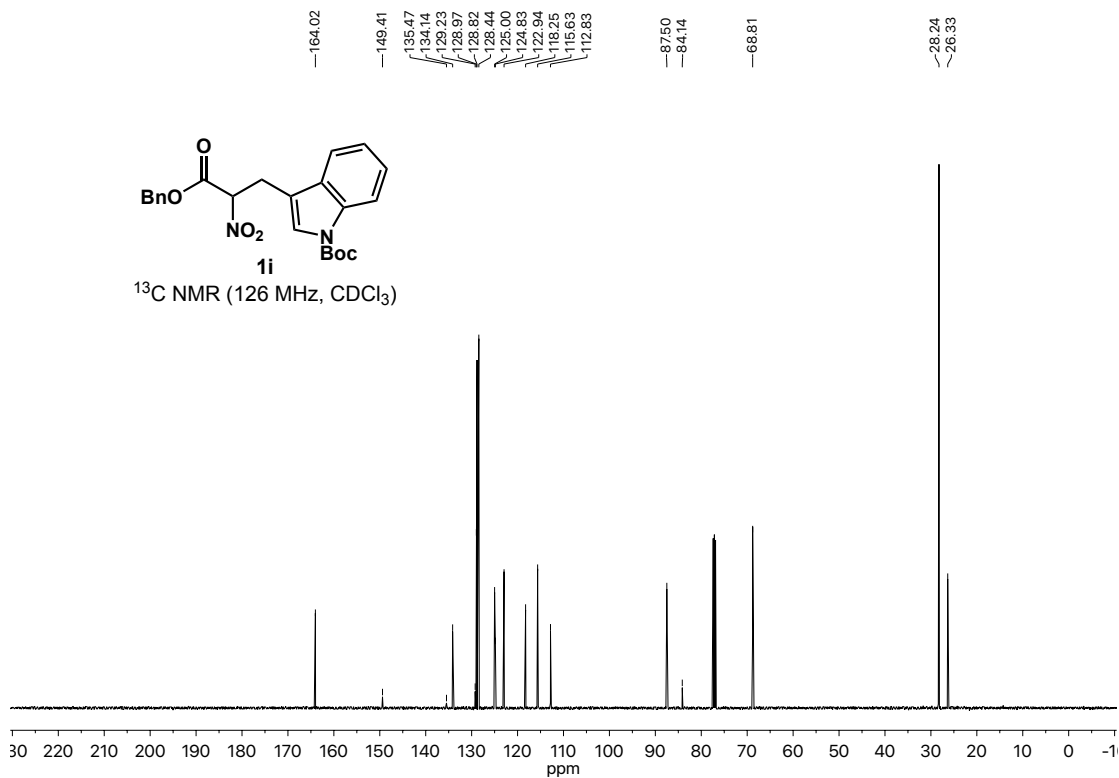
Tert-butyl 3-(3-(benzyloxy)-2-nitro-3-oxopropyl)-1H-indole-1-carboxylate (1i)



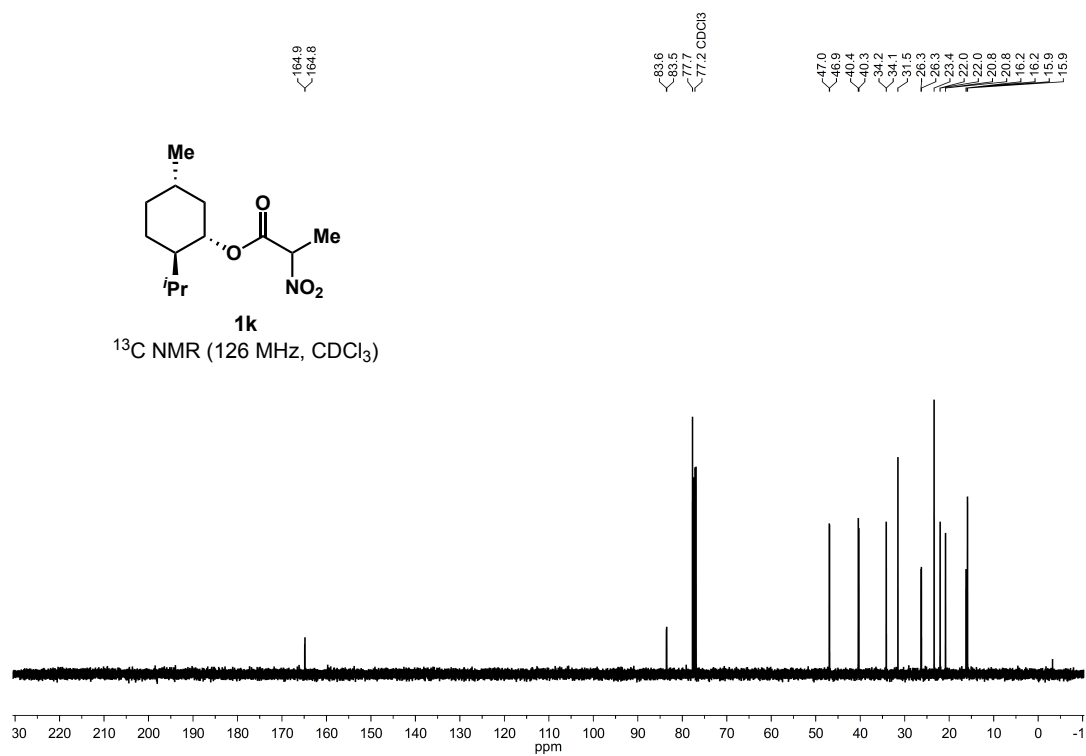
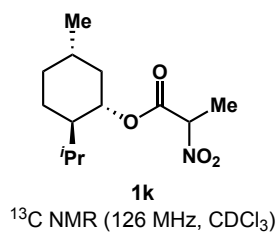
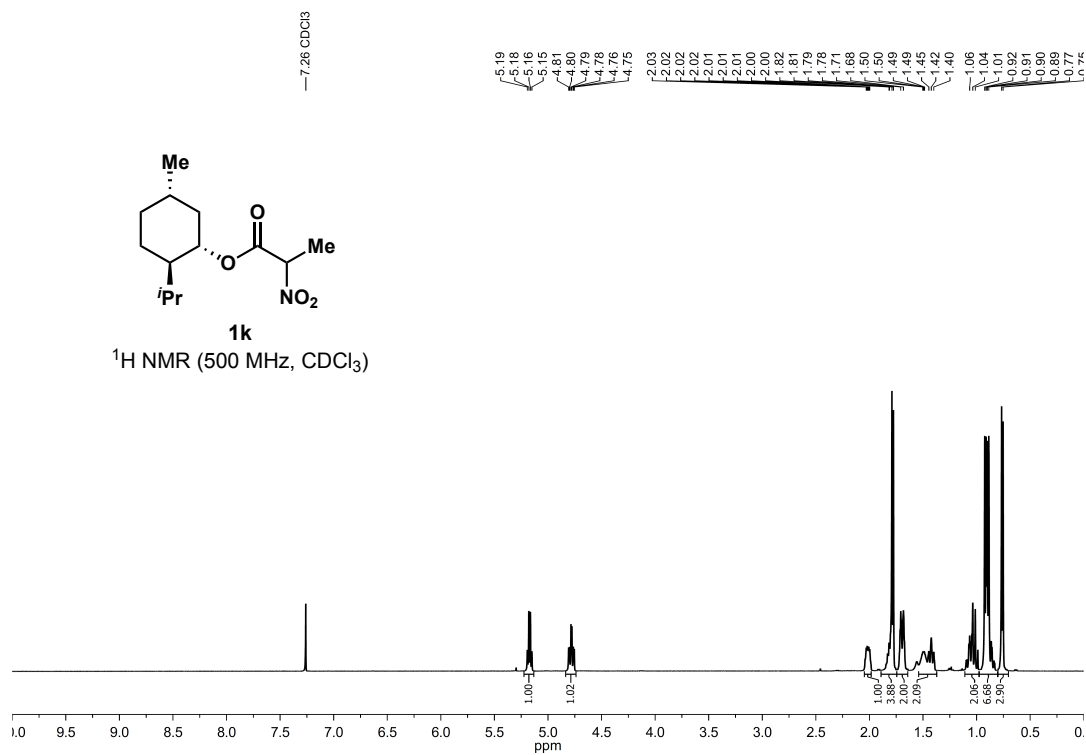
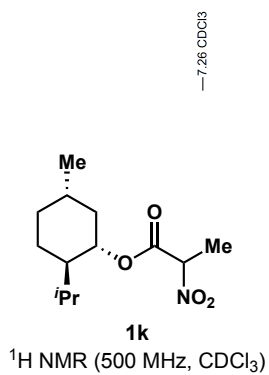
¹H NMR (500 MHz, CDCl₃)



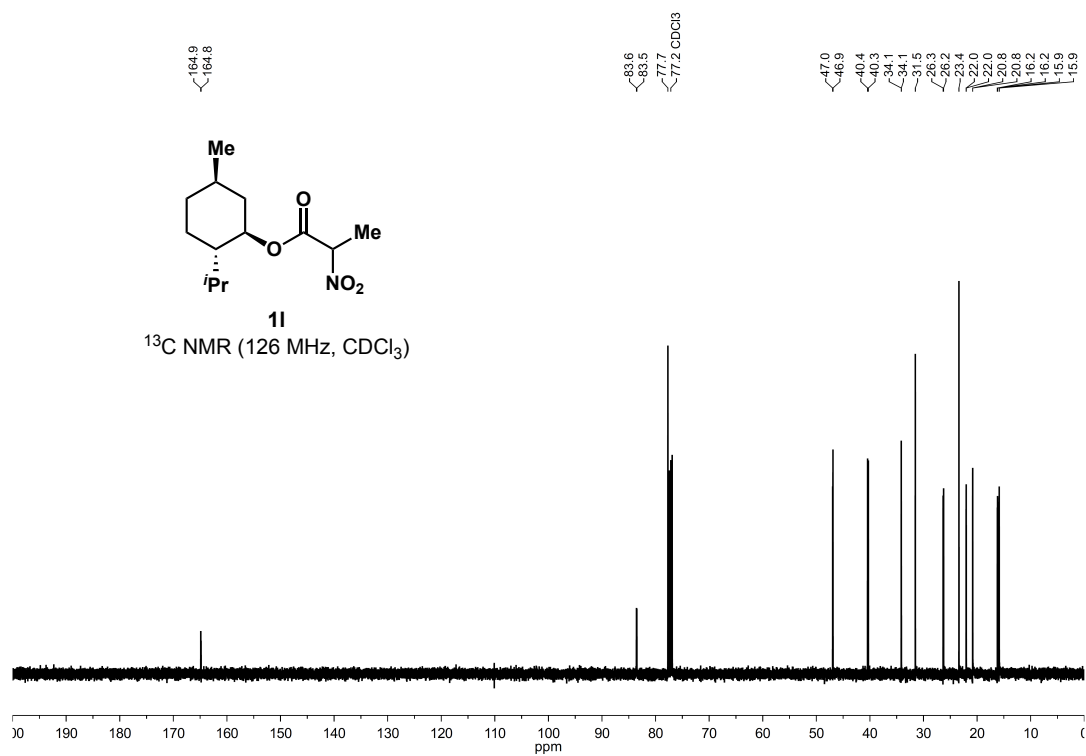
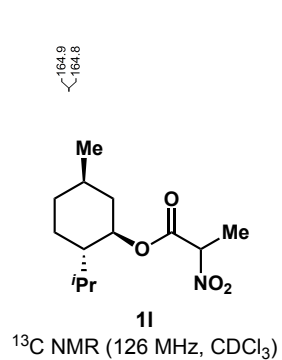
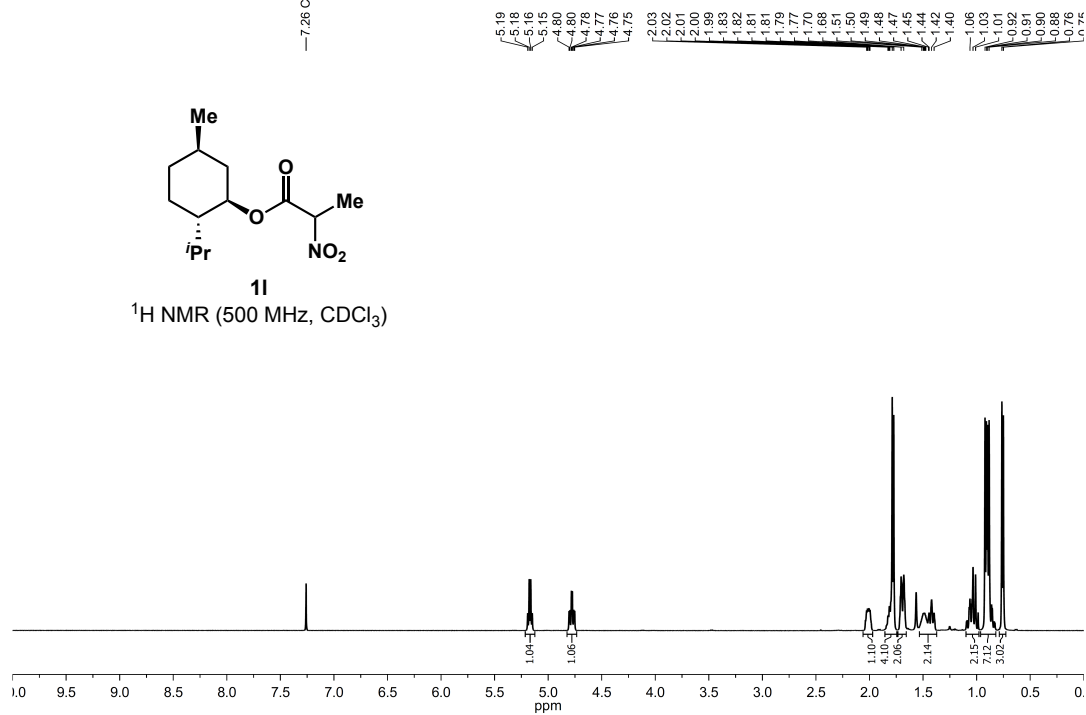
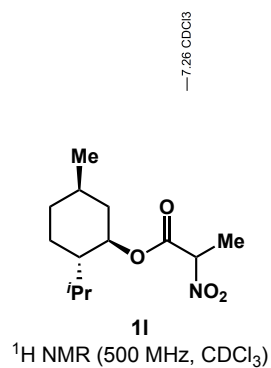
¹³C NMR (126 MHz, CDCl₃)



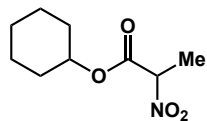
(1*S*,2*R*,5*S*)-2-Isopropyl-5-methylcyclohexyl 2-nitropropanoate (1k)



(1*R*,2*S*,5*R*)-2-Isopropyl-5-methylcyclohexyl 2-nitropropanoate (**1**)

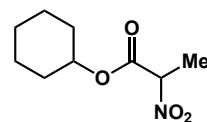
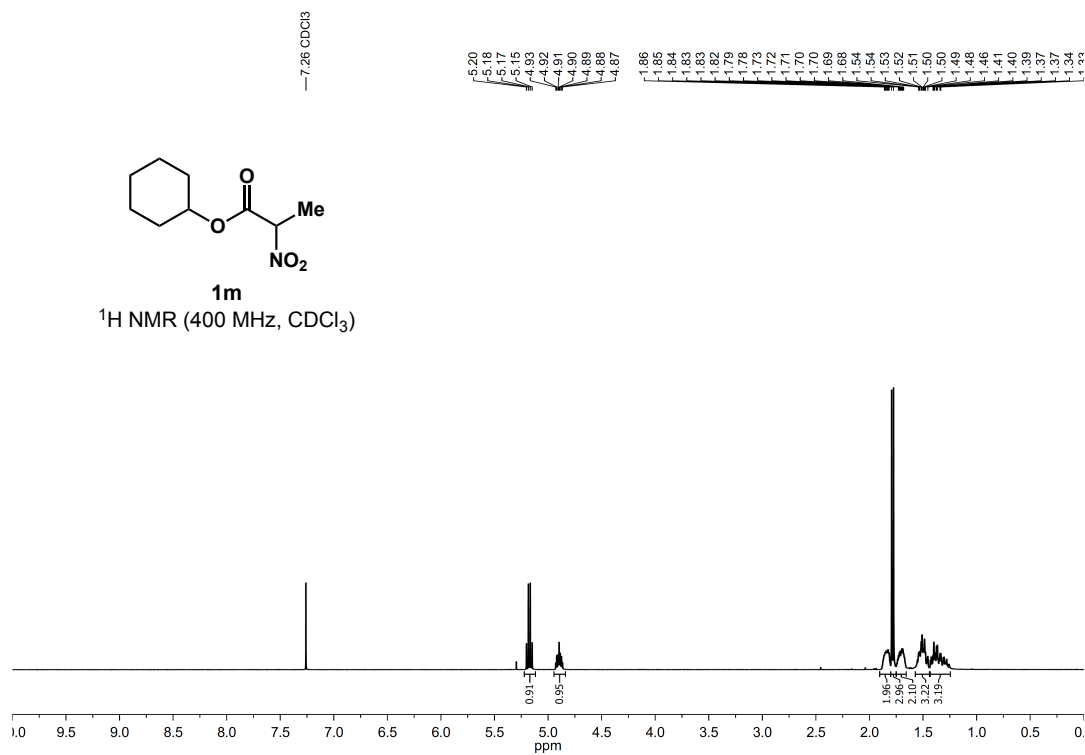


Cyclohexyl 2-nitropropanoate (1m)



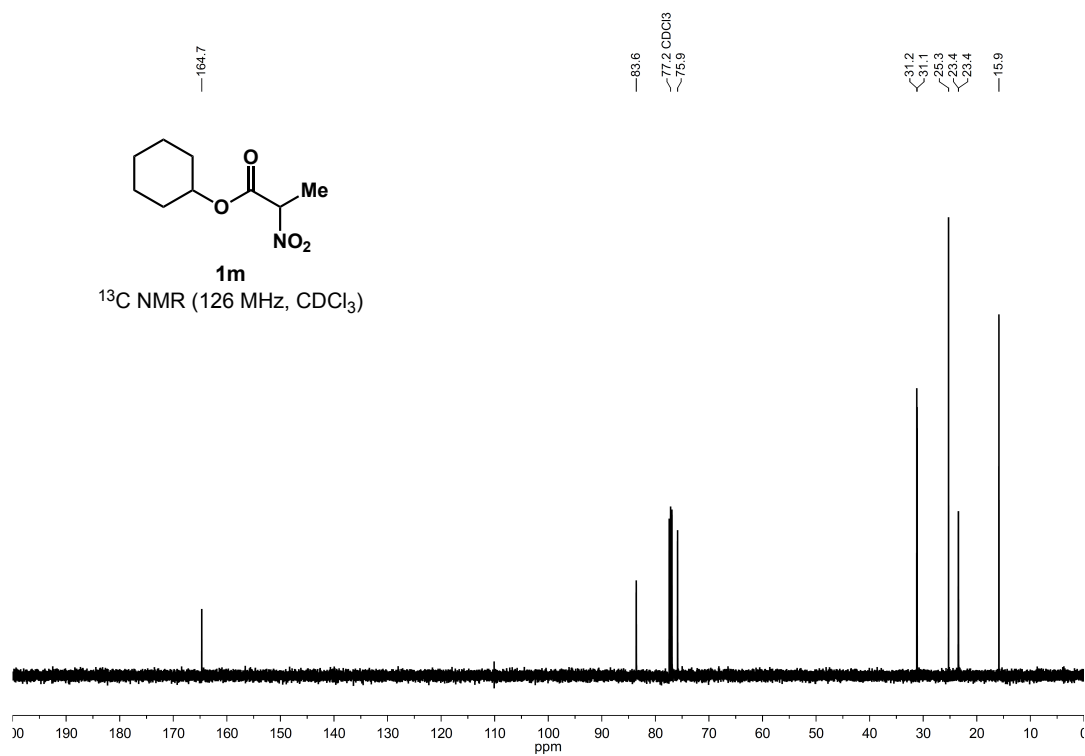
1m

¹H NMR (400 MHz, CDCl₃)

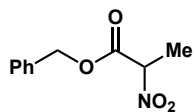
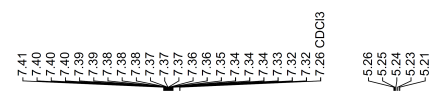


1m

¹³C NMR (126 MHz, CDCl₃)

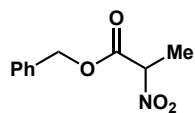
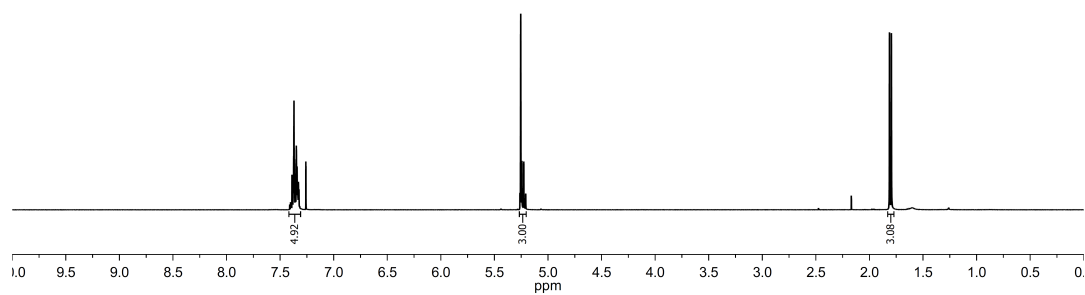


Benzyl 2-nitropropanoate (1n)



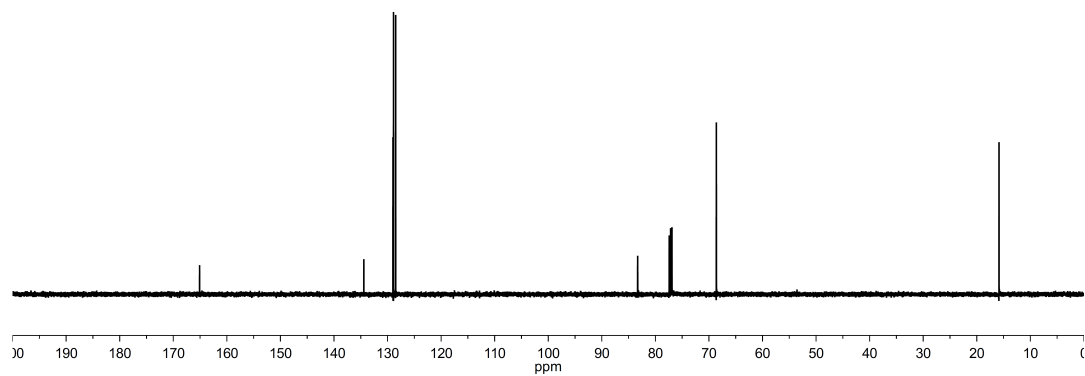
1n

¹H NMR (400 MHz, CDCl₃)

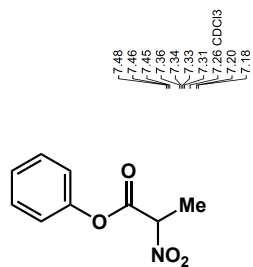


1n

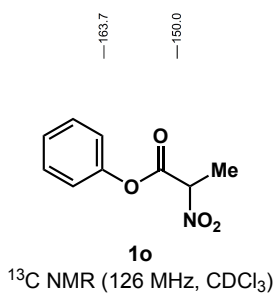
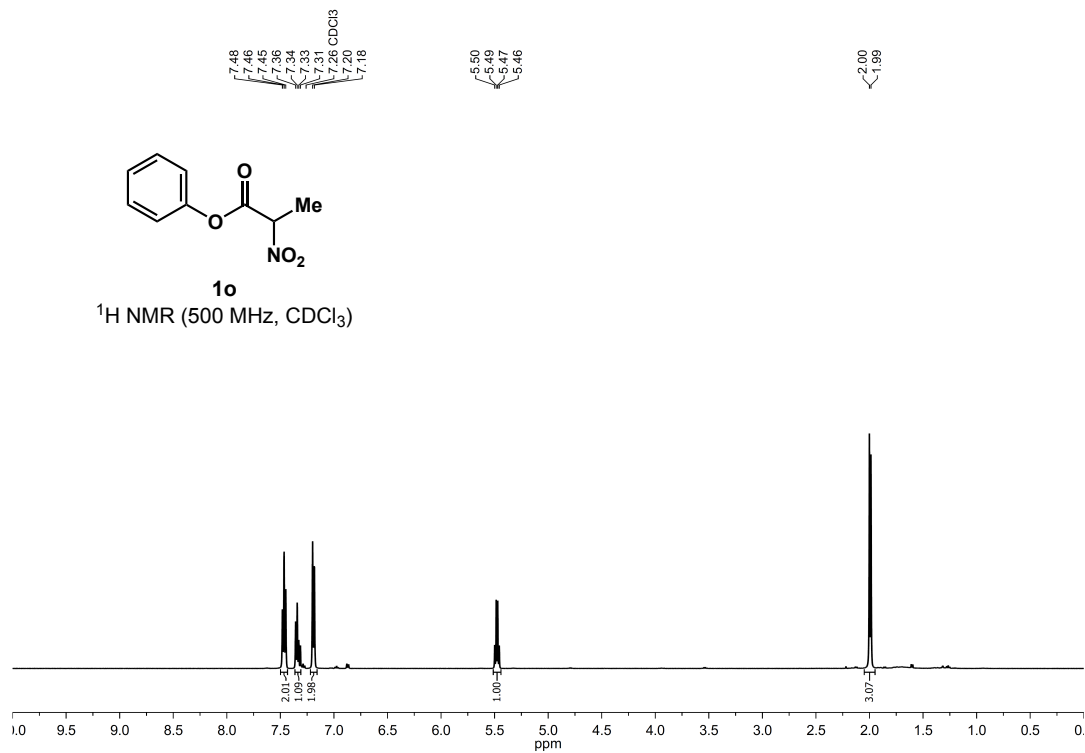
¹³C NMR (126 MHz, CDCl₃)



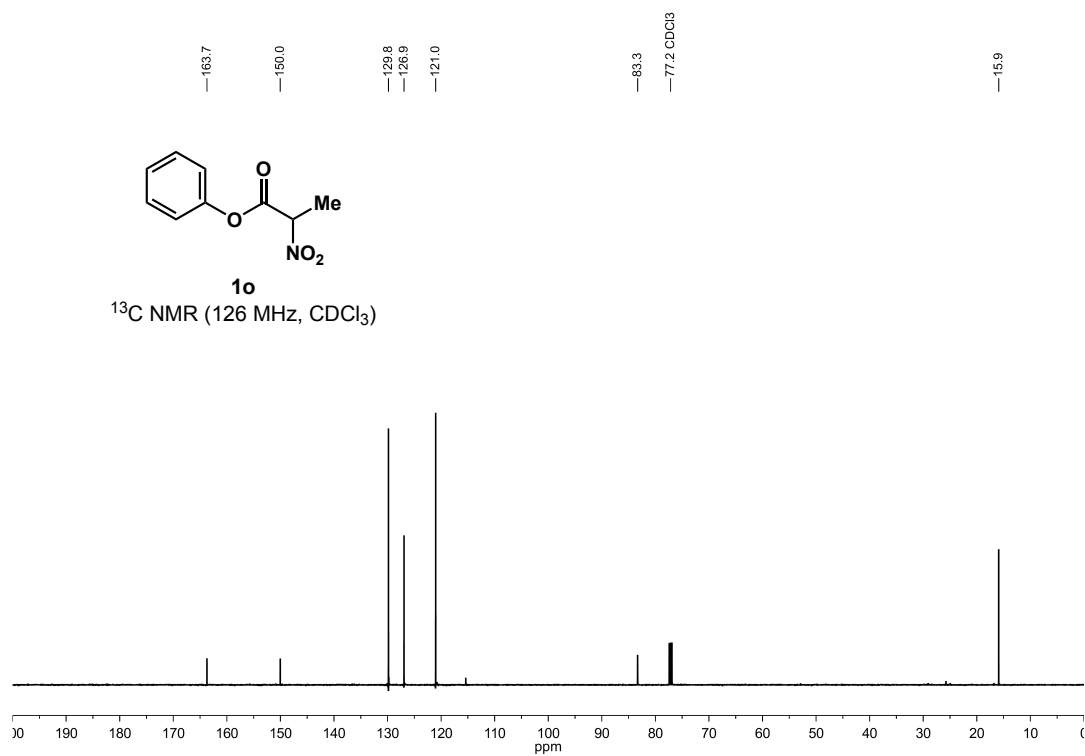
Phenyl 2-nitropropanoate (1o)



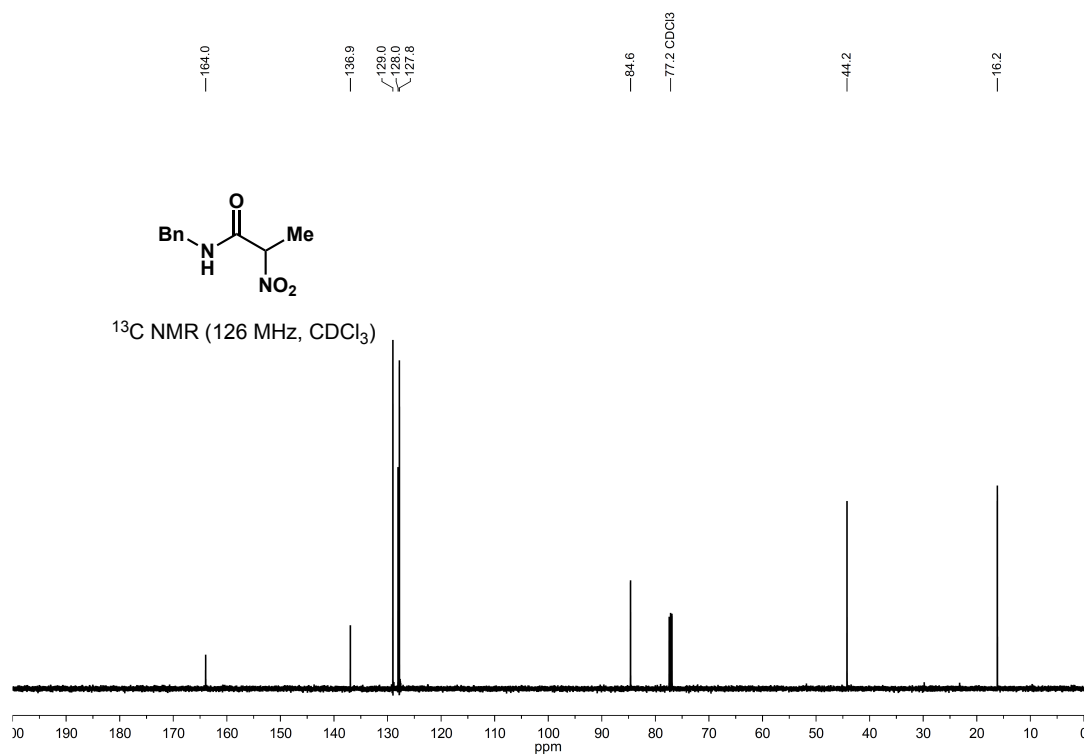
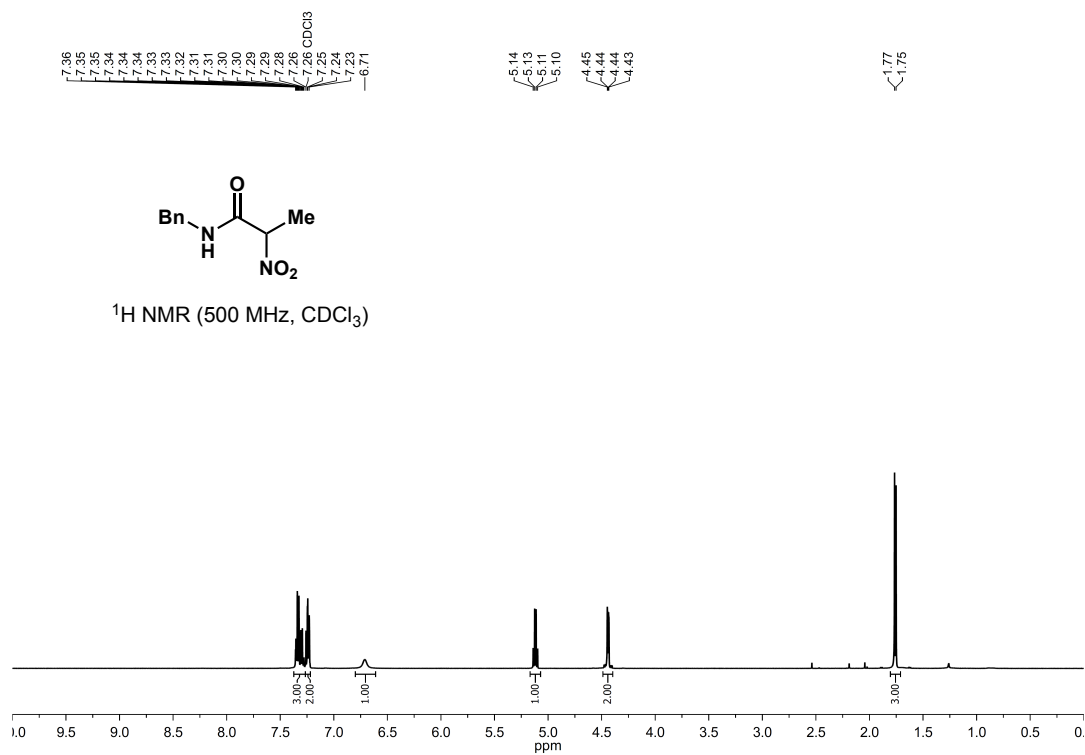
1o
¹H NMR (500 MHz, CDCl₃)



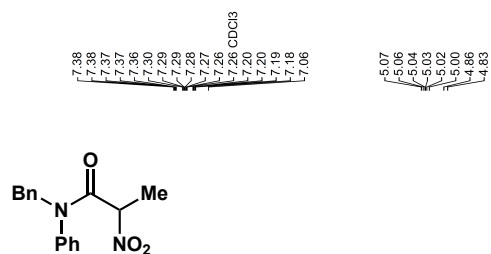
1o
¹³C NMR (126 MHz, CDCl₃)



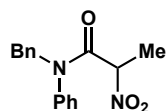
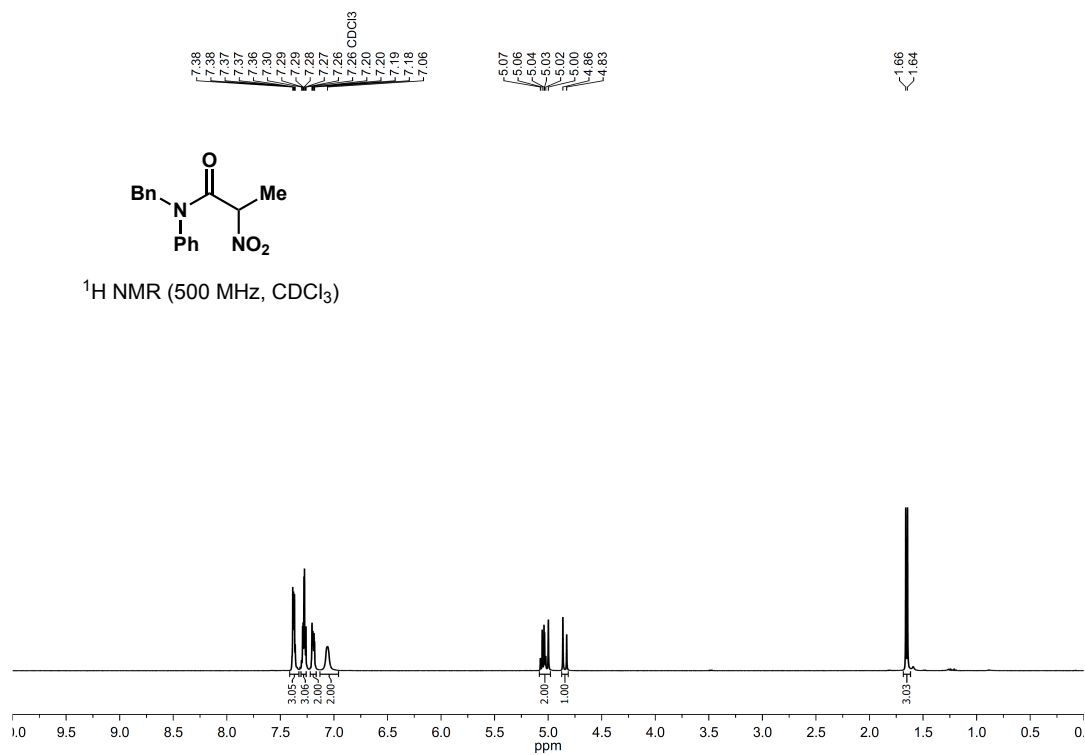
N-benzyl-2-nitropropanamide



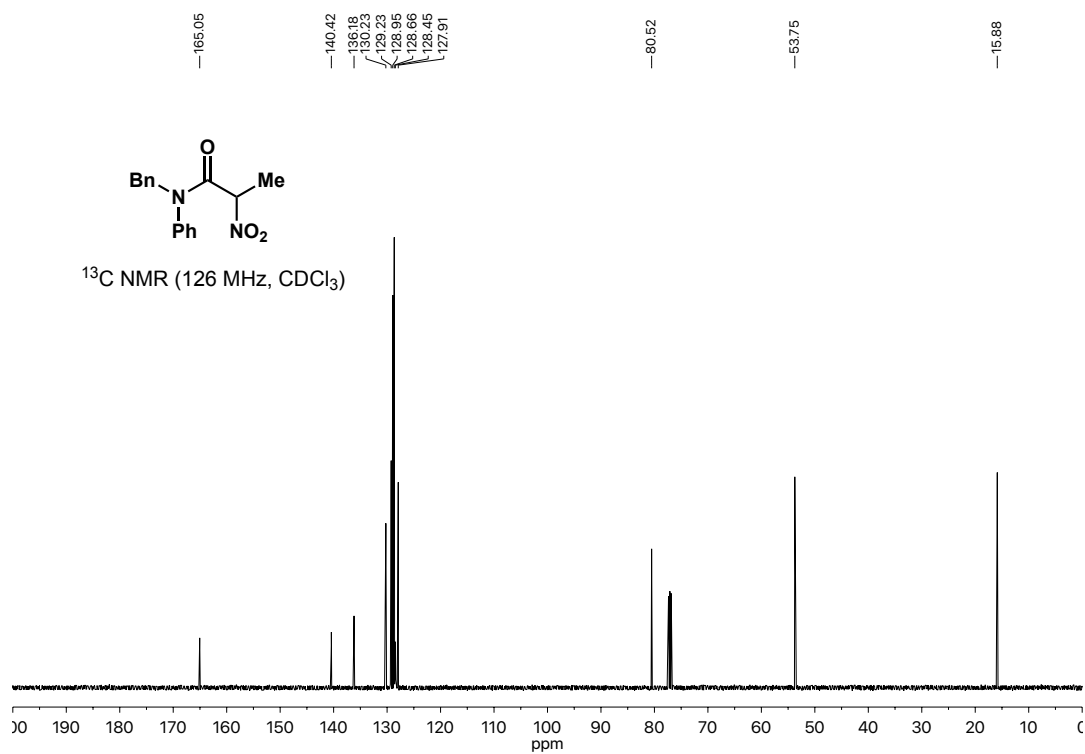
N-benzyl-2-nitro-N-phenylpropanamide



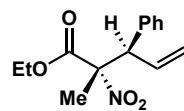
¹H NMR (500 MHz, CDCl₃)



¹³C NMR (126 MHz, CDCl₃)

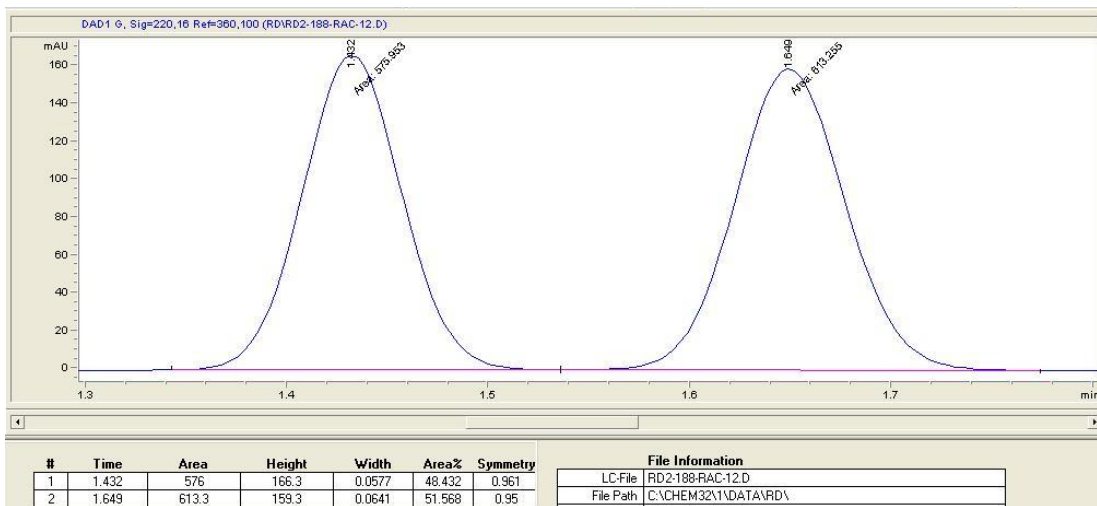


10. SFC Traces

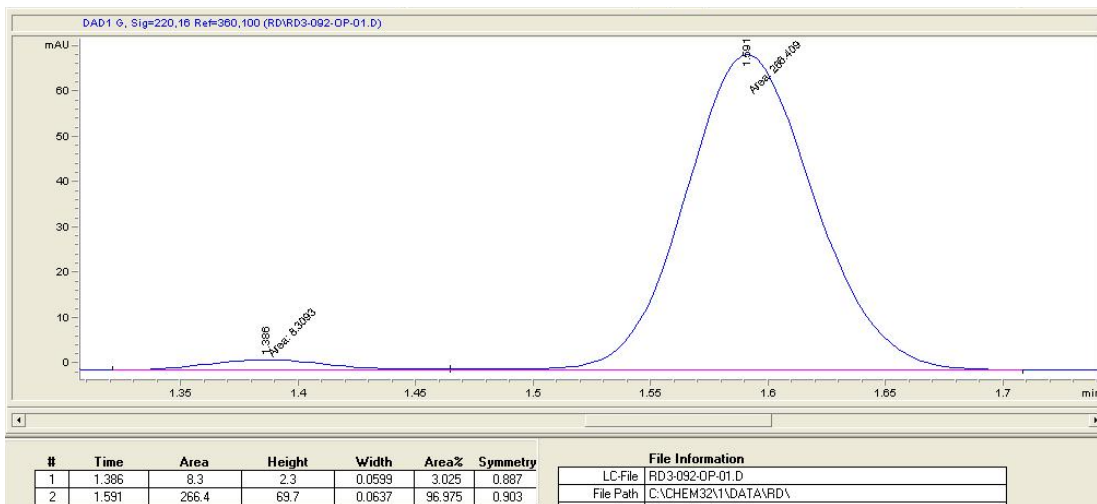


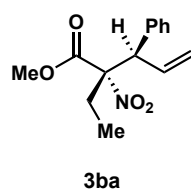
3aa

Racemic

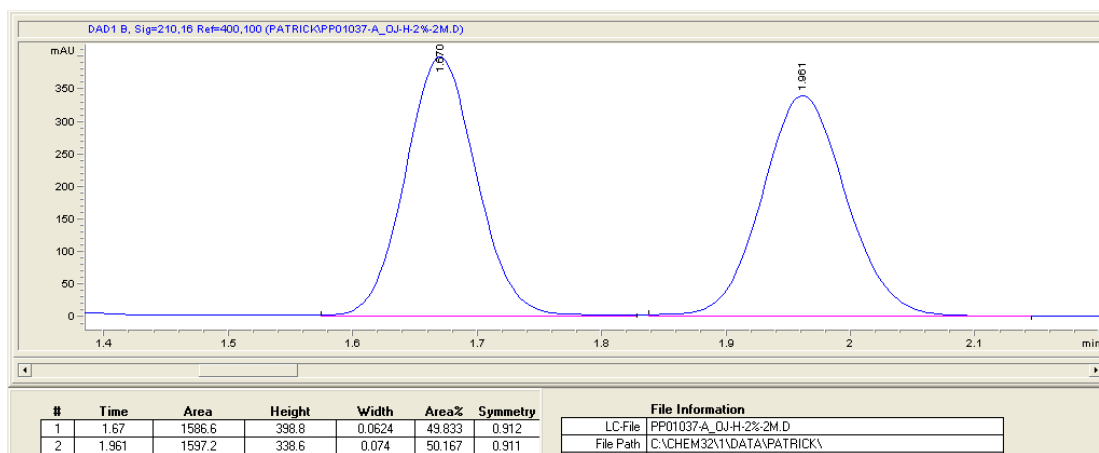


Enantiomerically Enriched

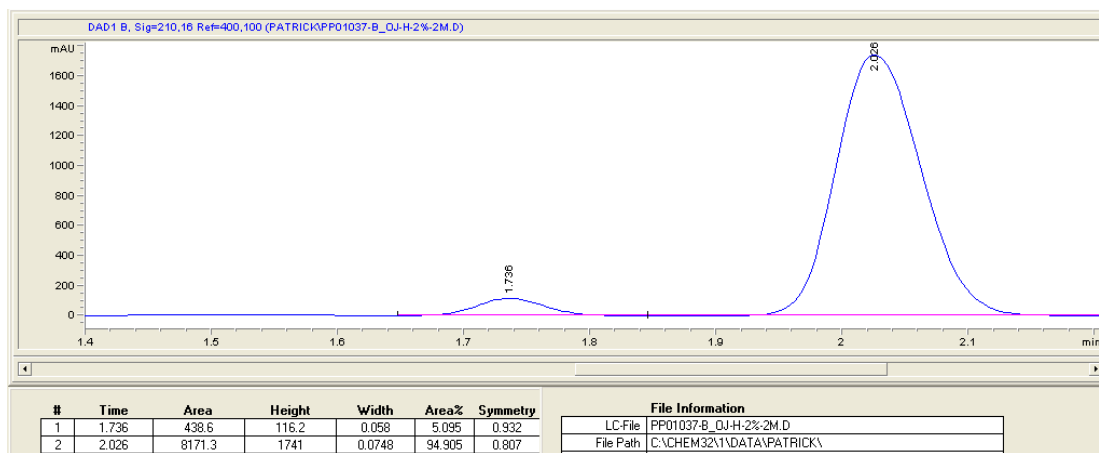


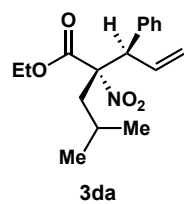


Racemic

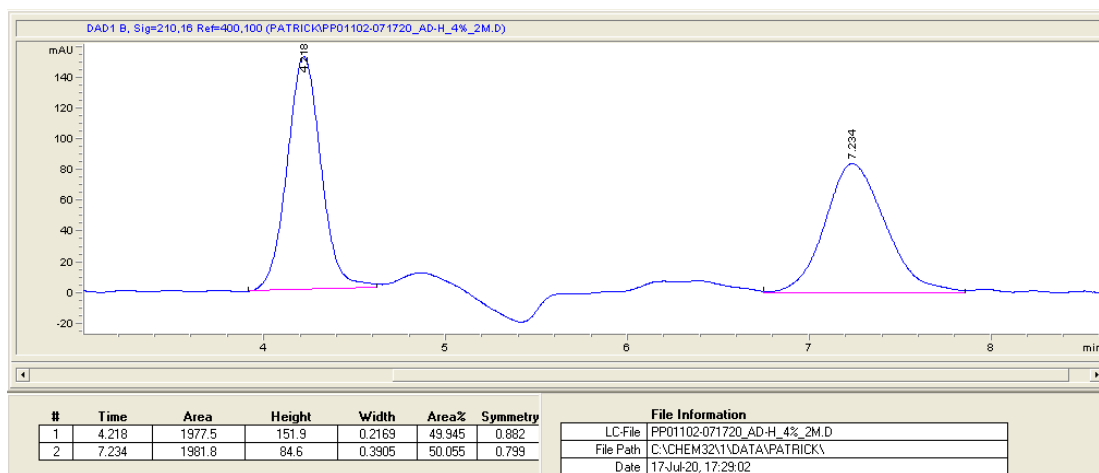


Enantiomerically Enriched

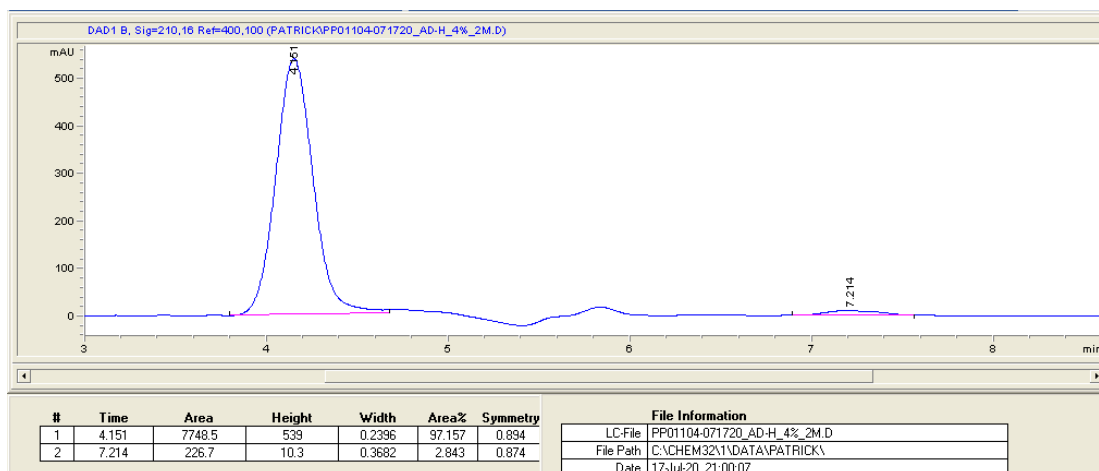


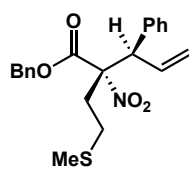


Racemic



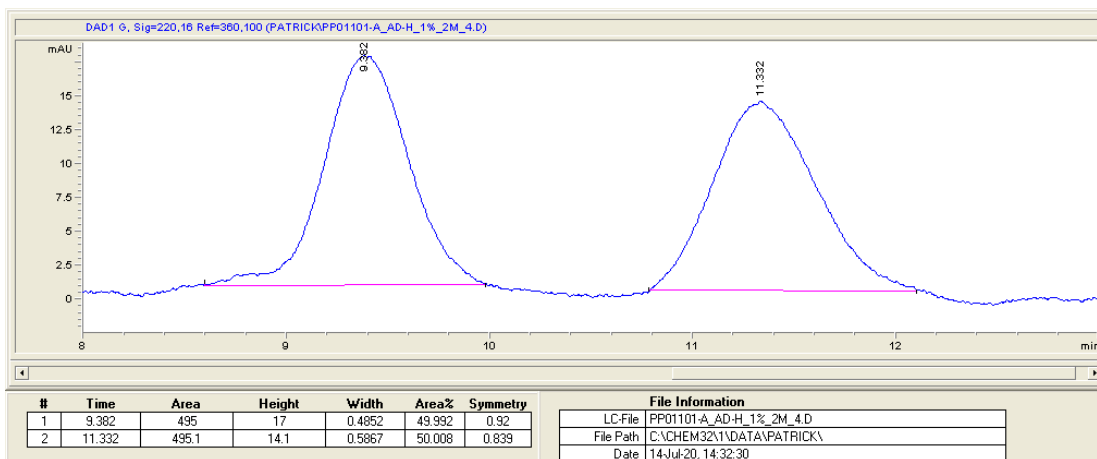
Enantiomerically Enriched



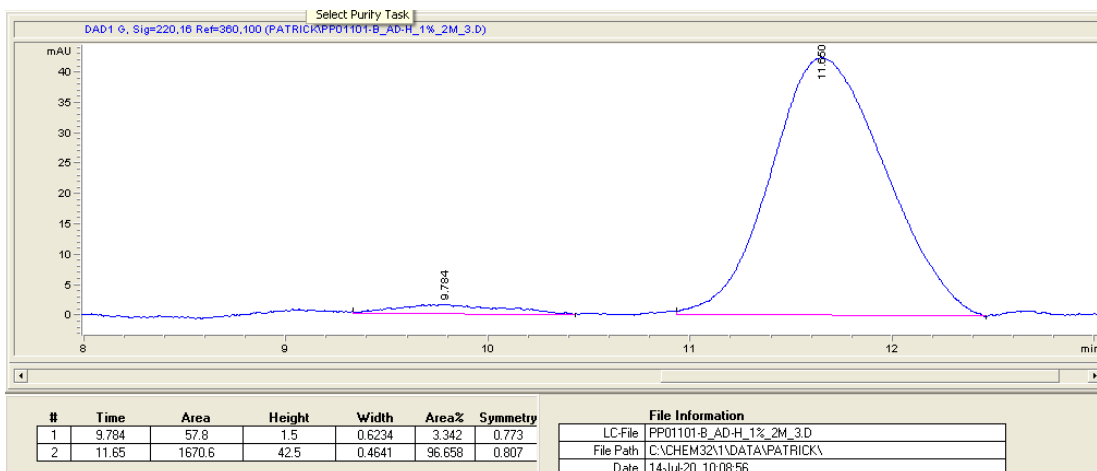


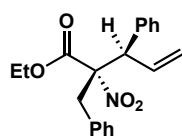
3ea

Racemic



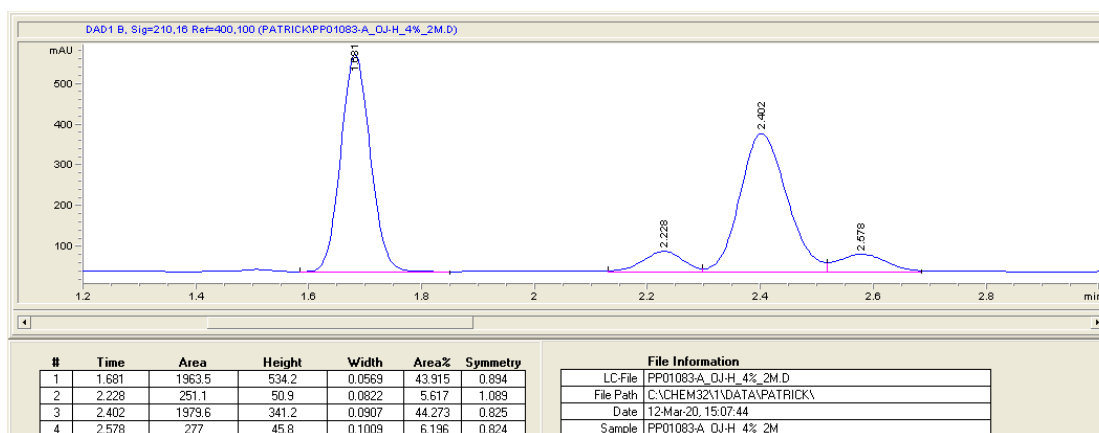
Enantiomerically Enriched



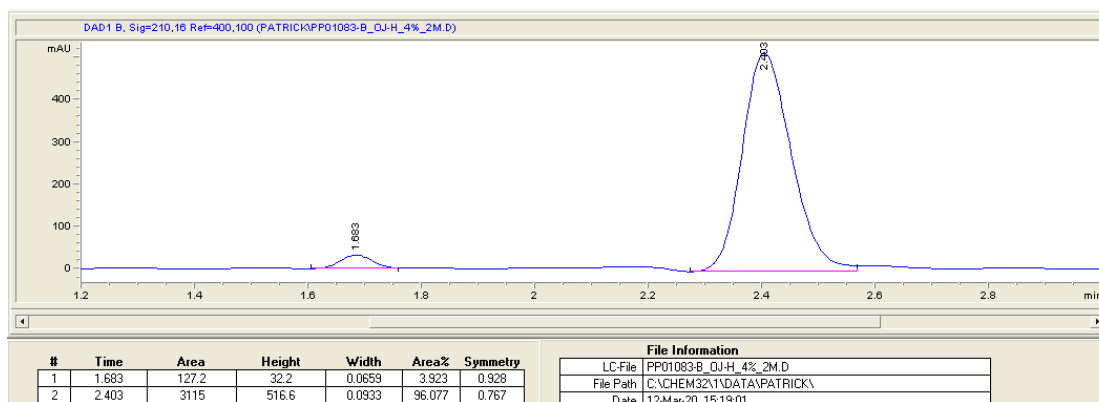


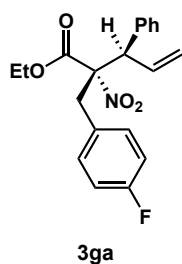
3fa

Racemic

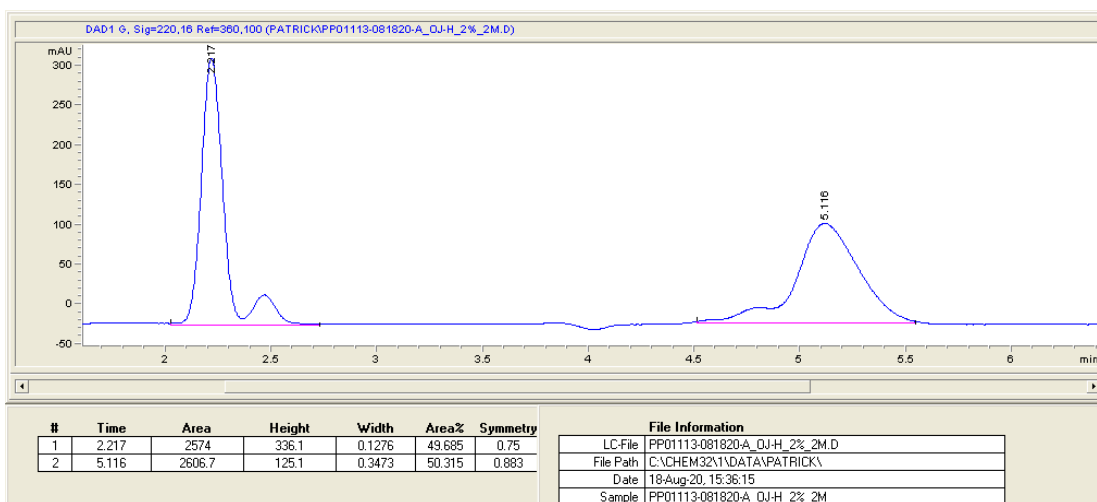


Enantiomerically Enriched

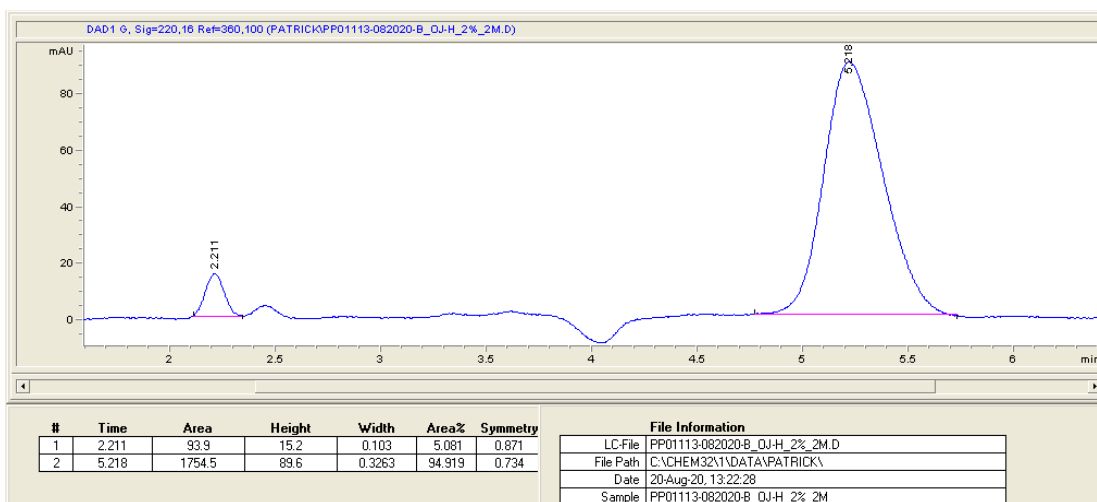


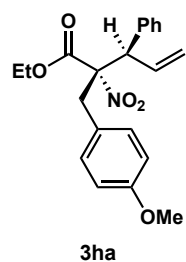


Racemic

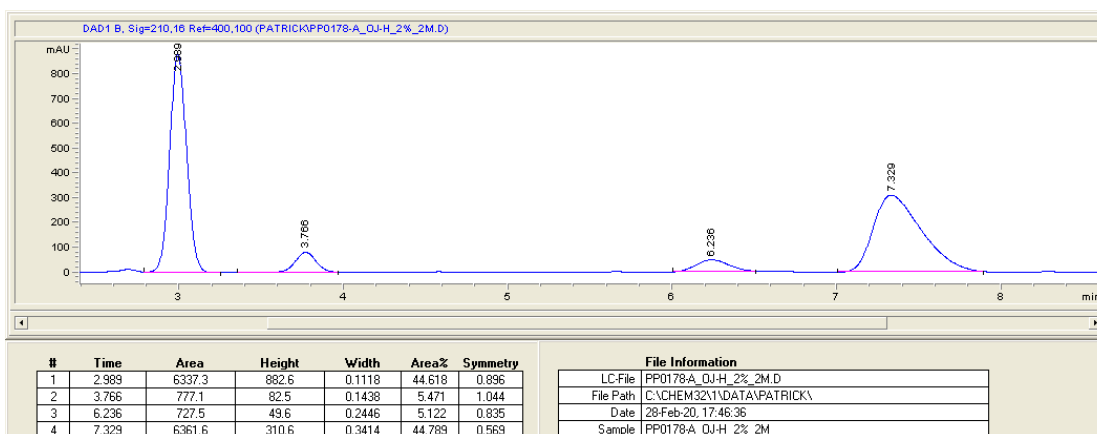


Enantiomerically Enriched

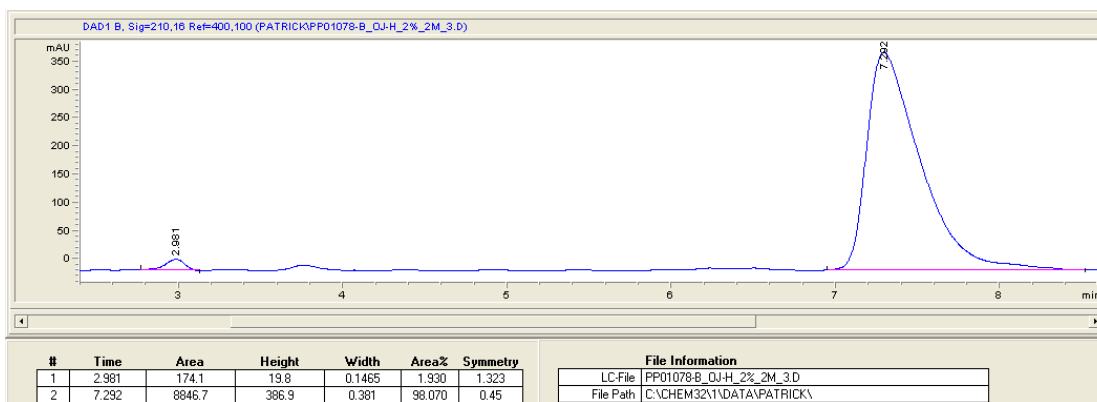


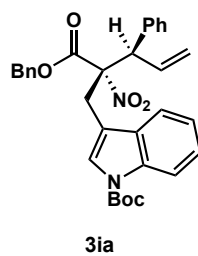


Racemic

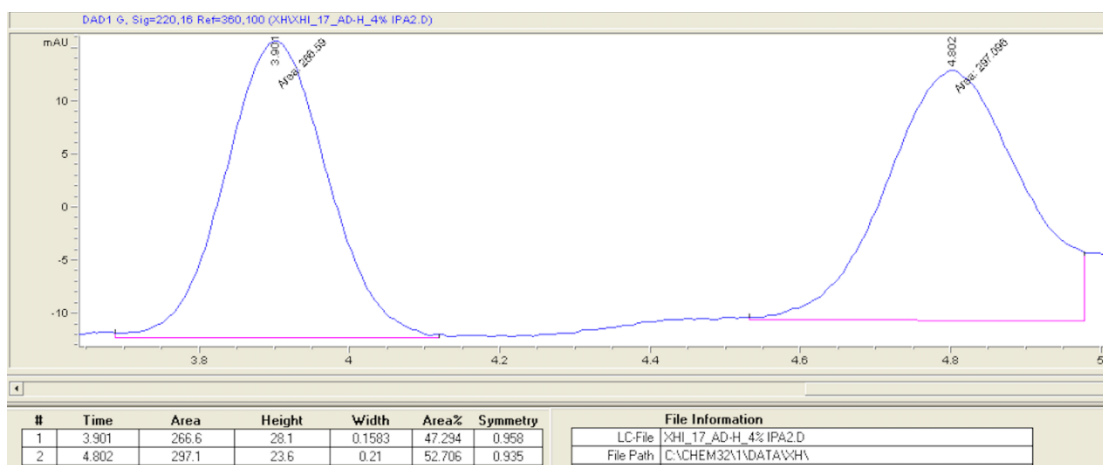


Enantiomerically Enriched

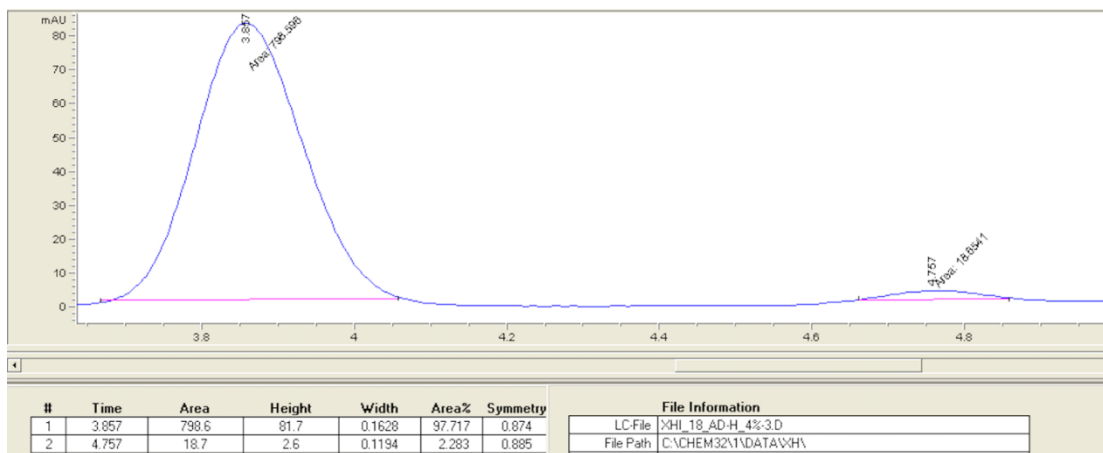


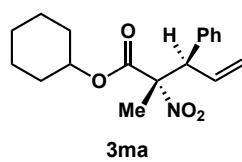


Racemic

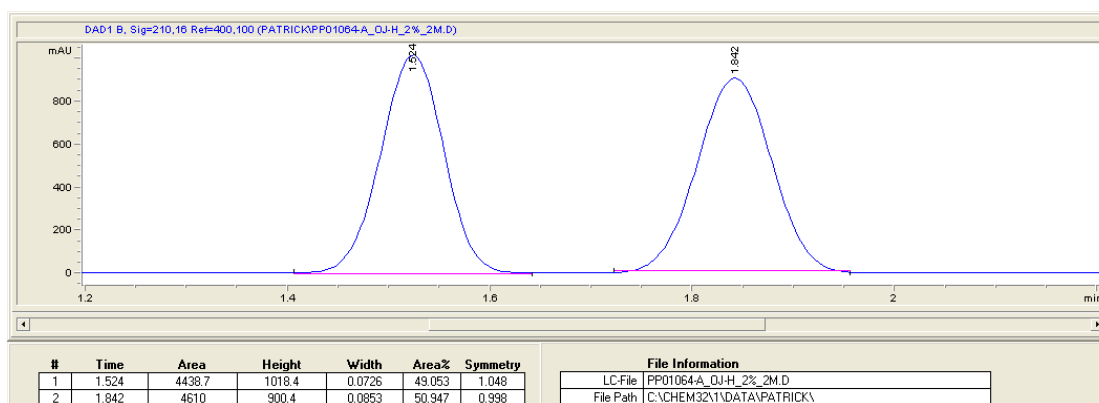


Enantiomerically Enriched

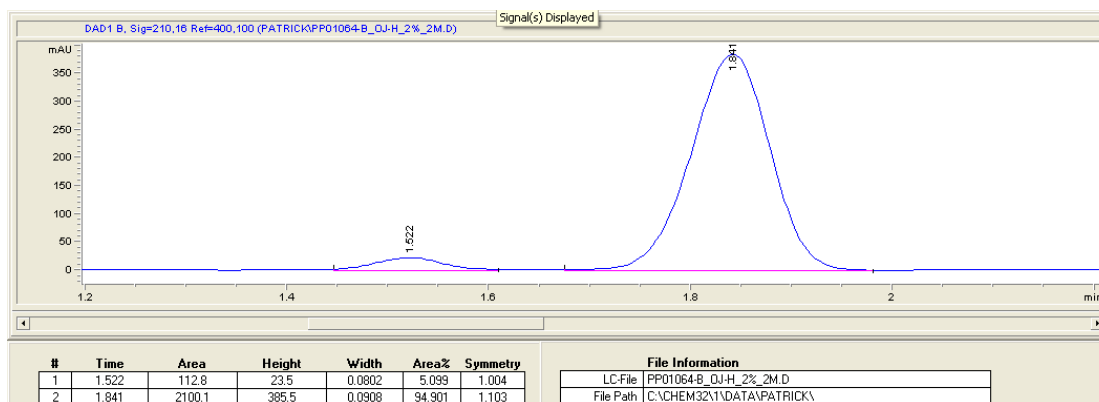


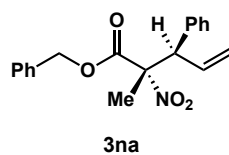


Racemic

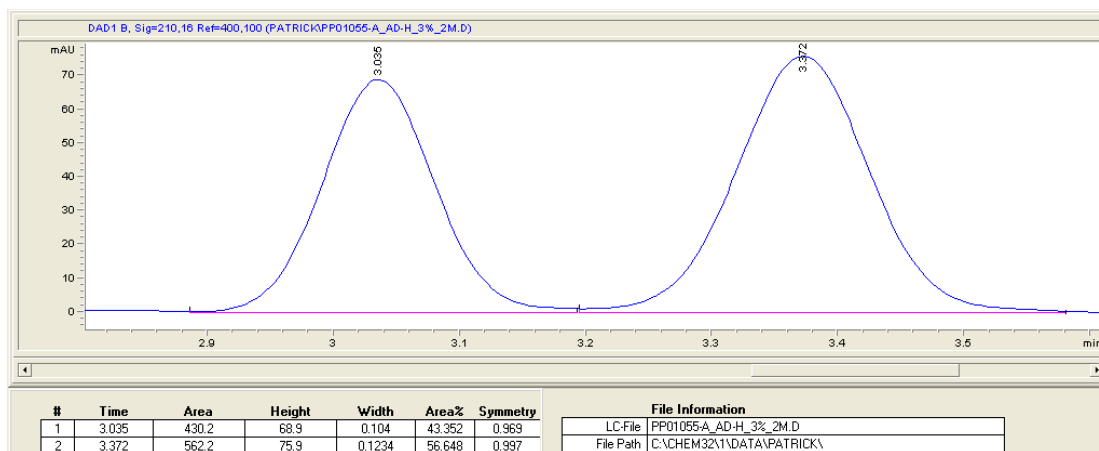


Enantiomerically Enriched

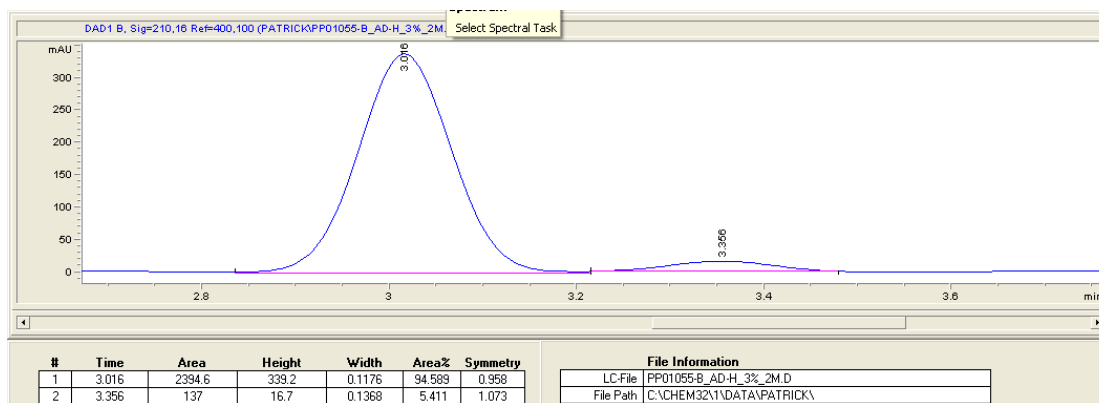


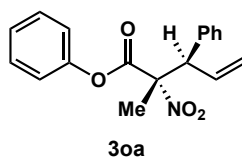


Racemic

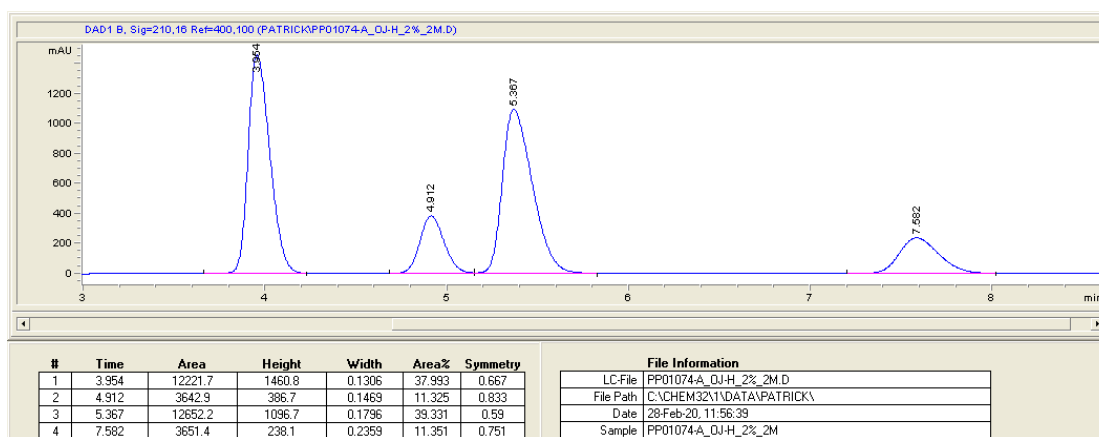


Enantiomerically Enriched

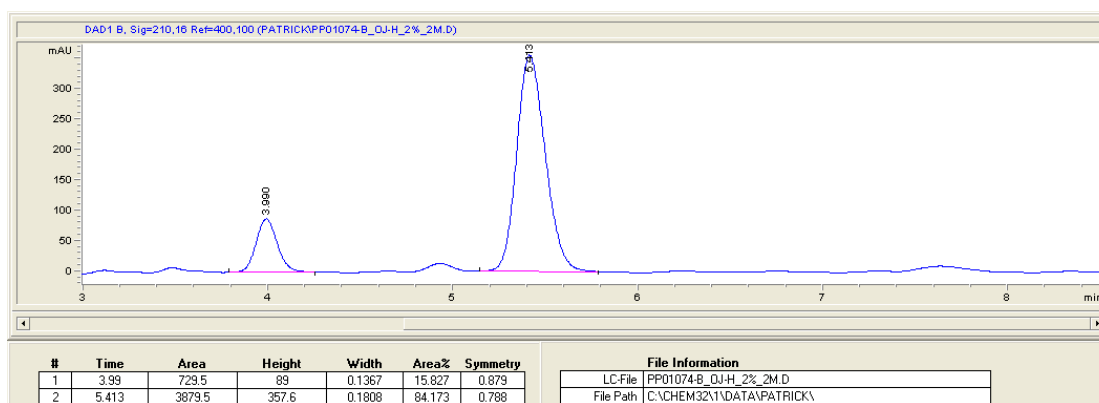


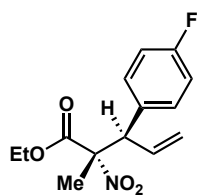


Racemic



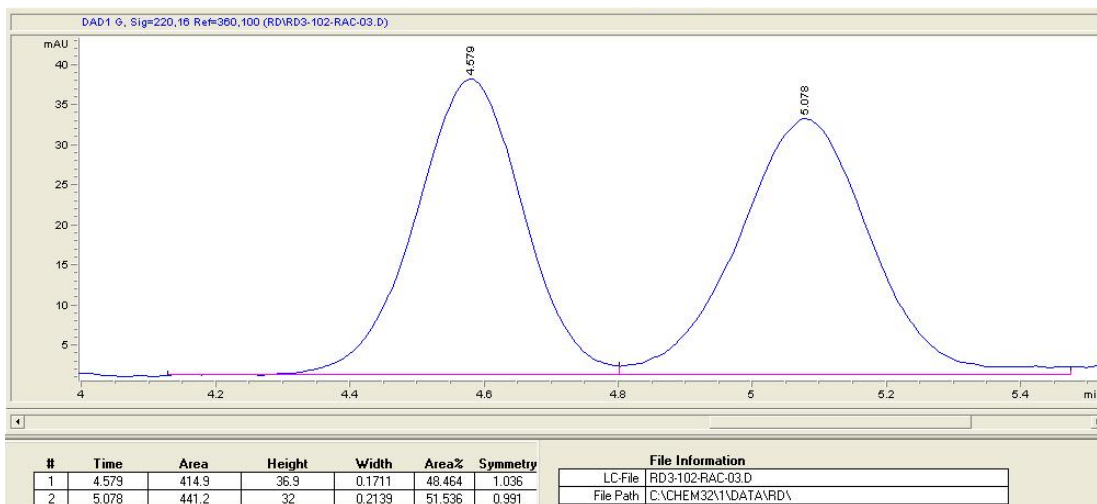
Enantiomerically Enriched



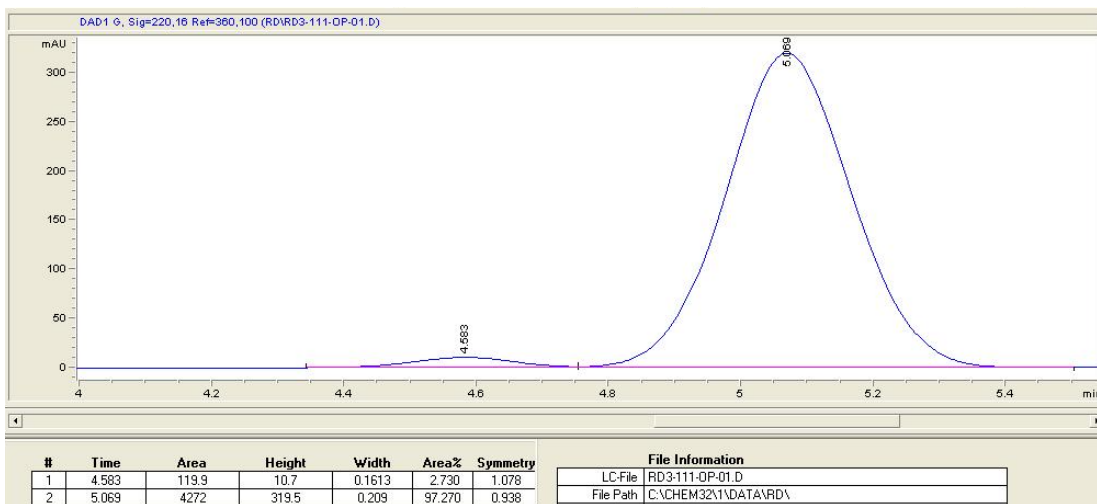


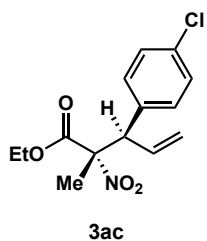
3ab

Racemic

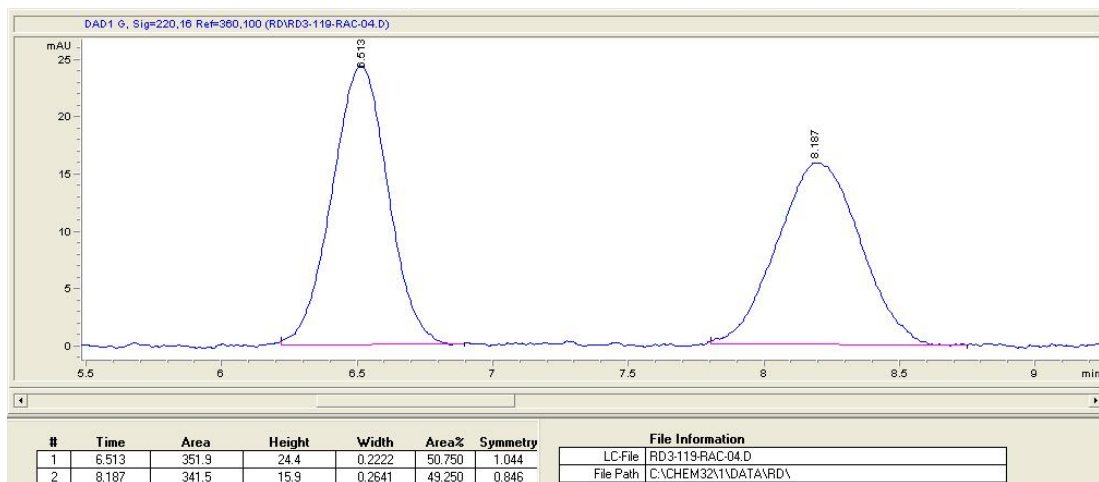


Enantiomerically Enriched

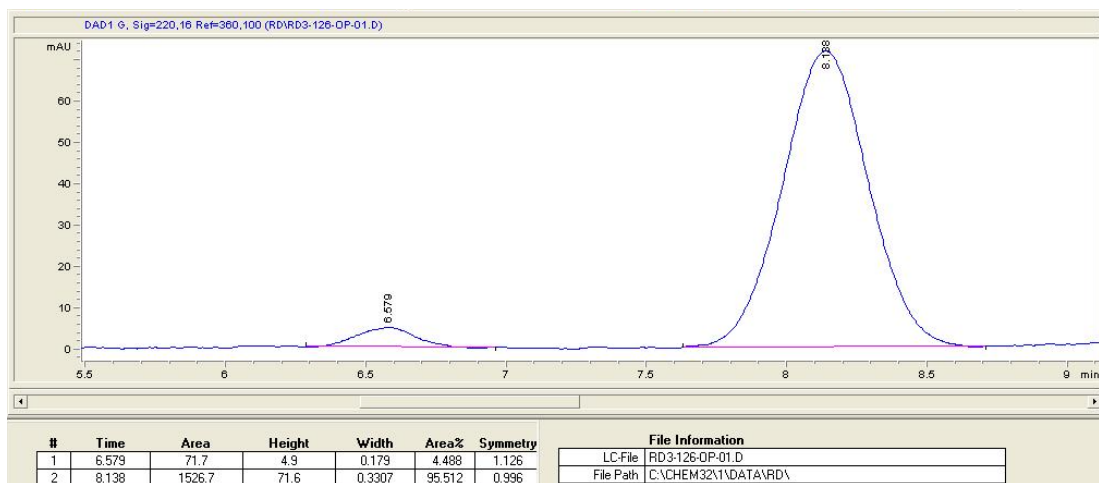


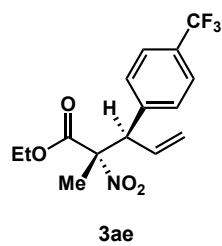


Racemic

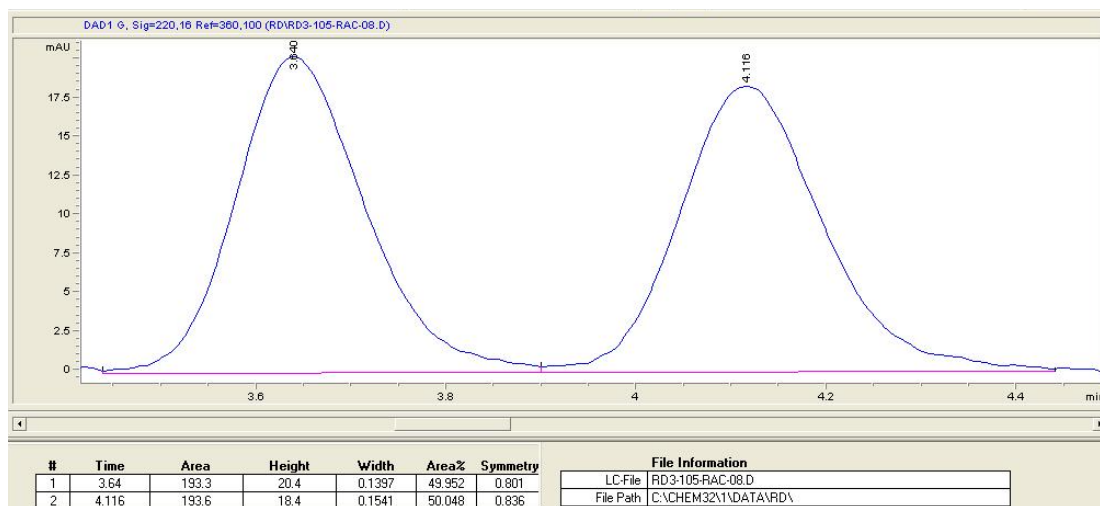


Enantiomerically Enriched

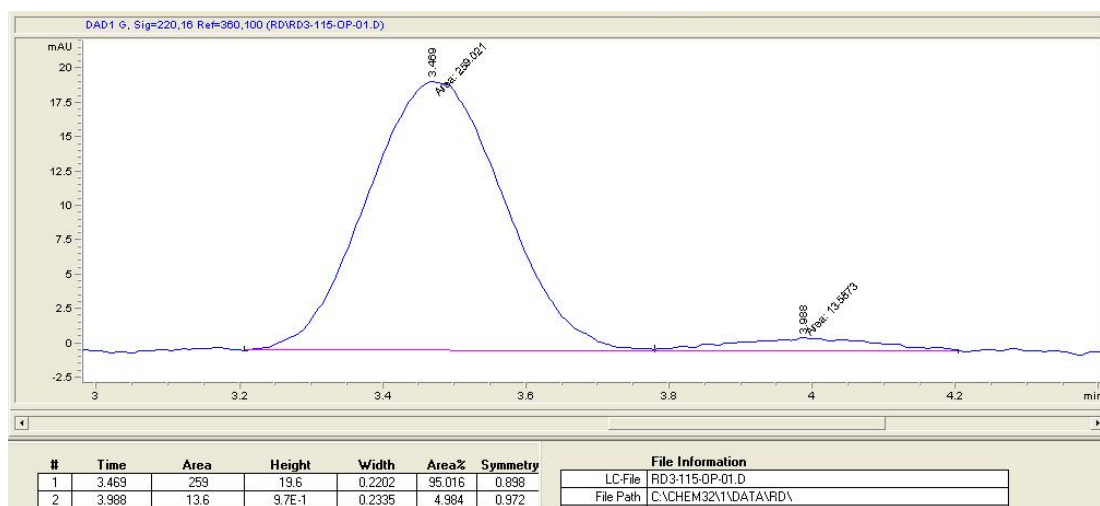


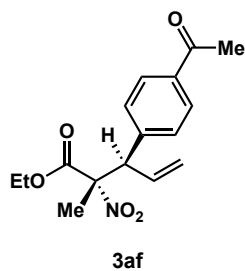


Racemic

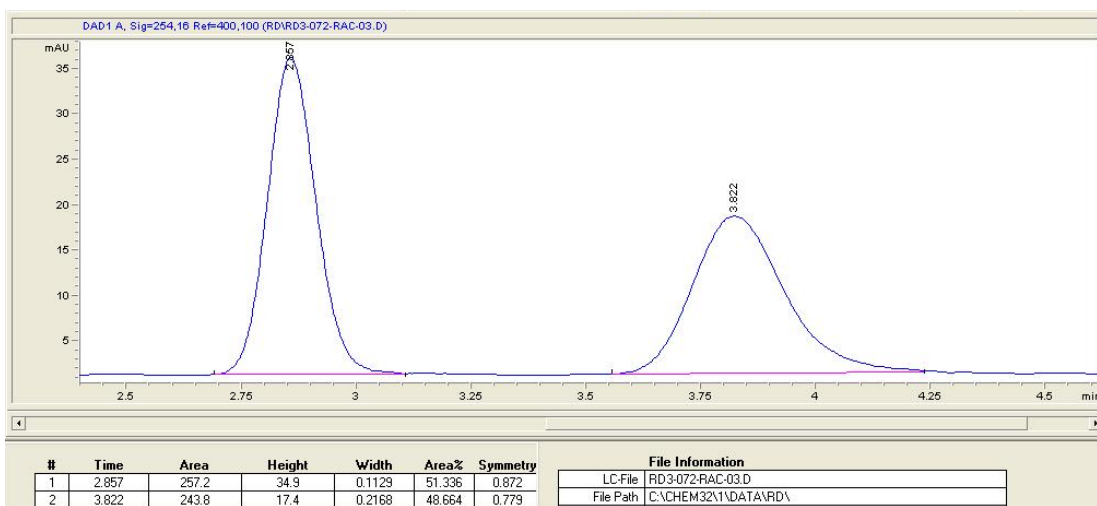


Enantiomerically Enriched

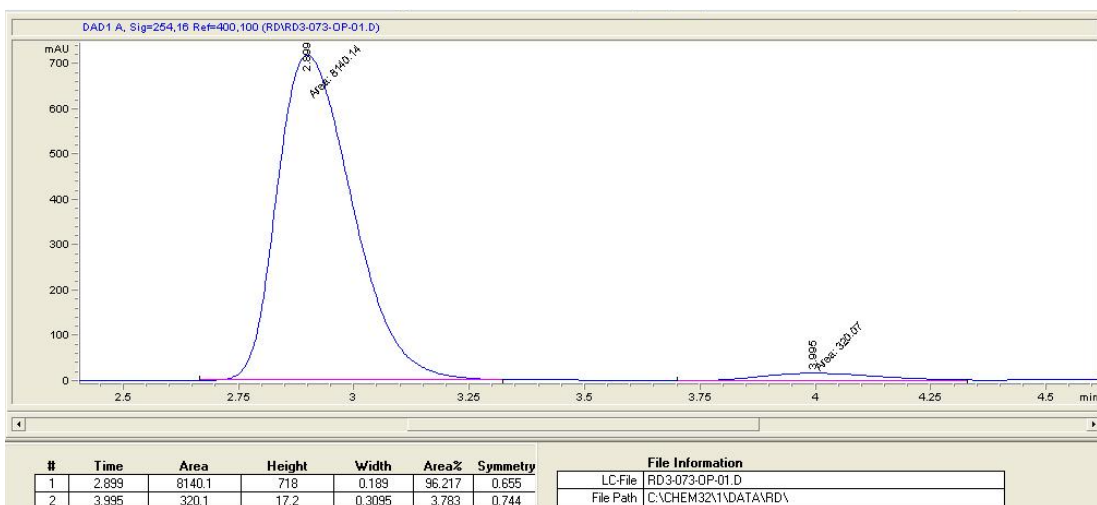


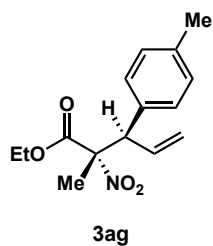


Racemic

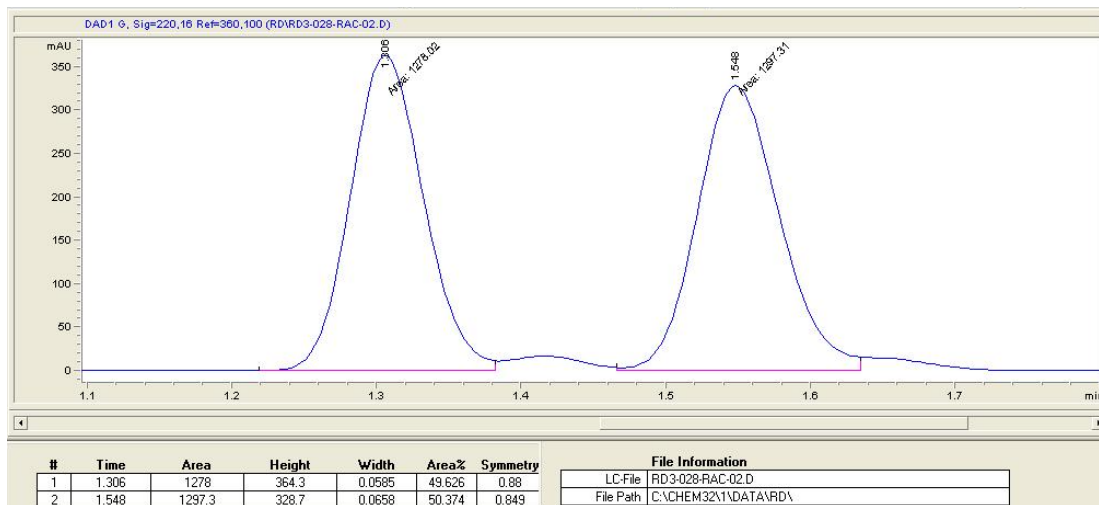


Enantiomerically Enriched

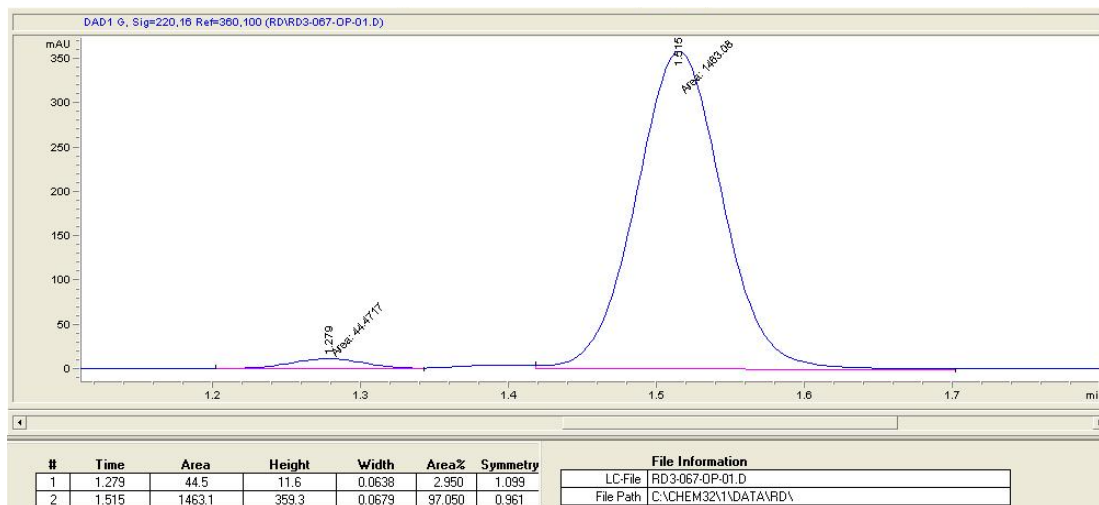


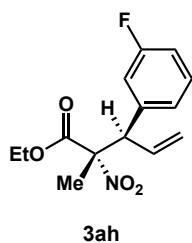


Racemic

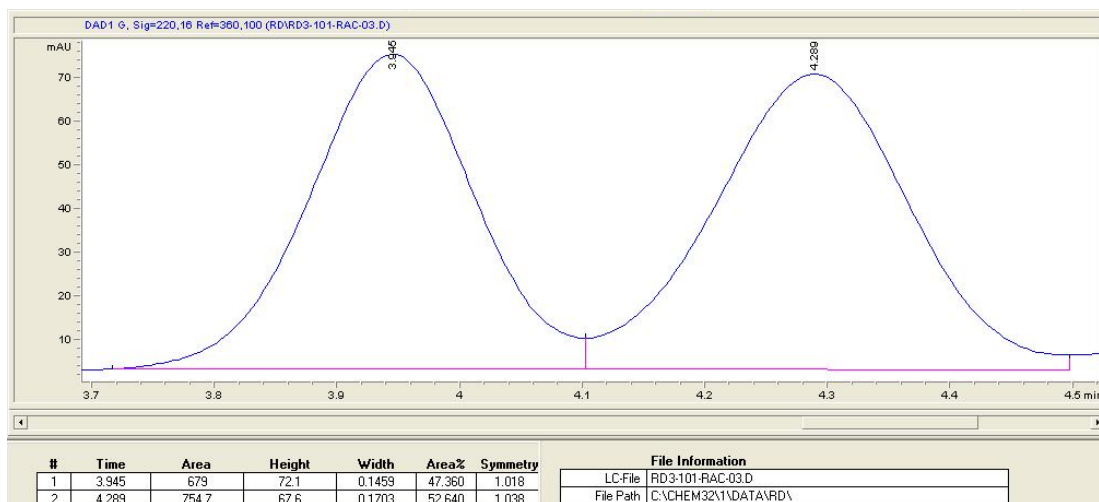


Enantiomerically Enriched

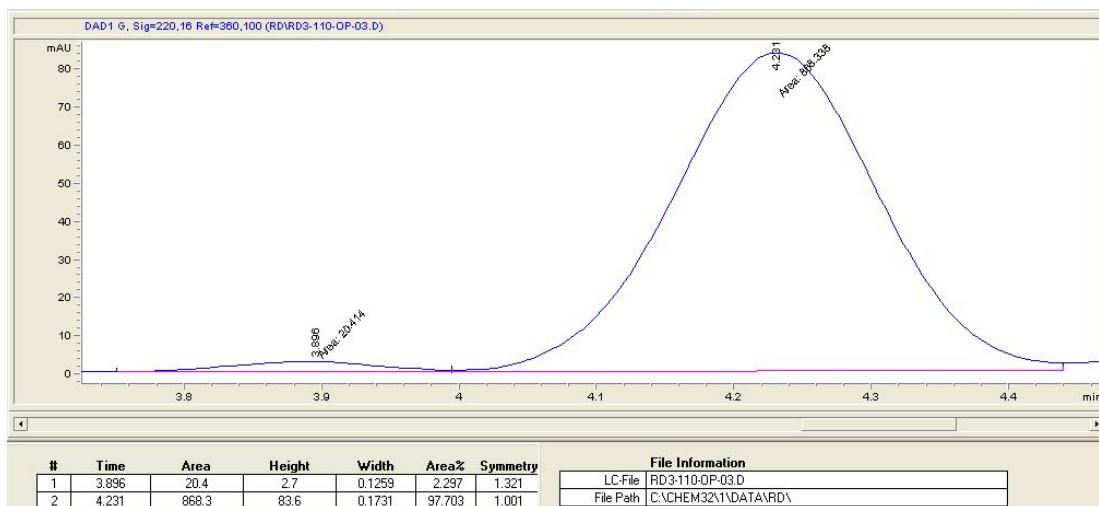


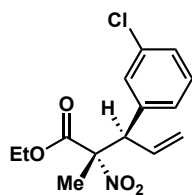


Racemic



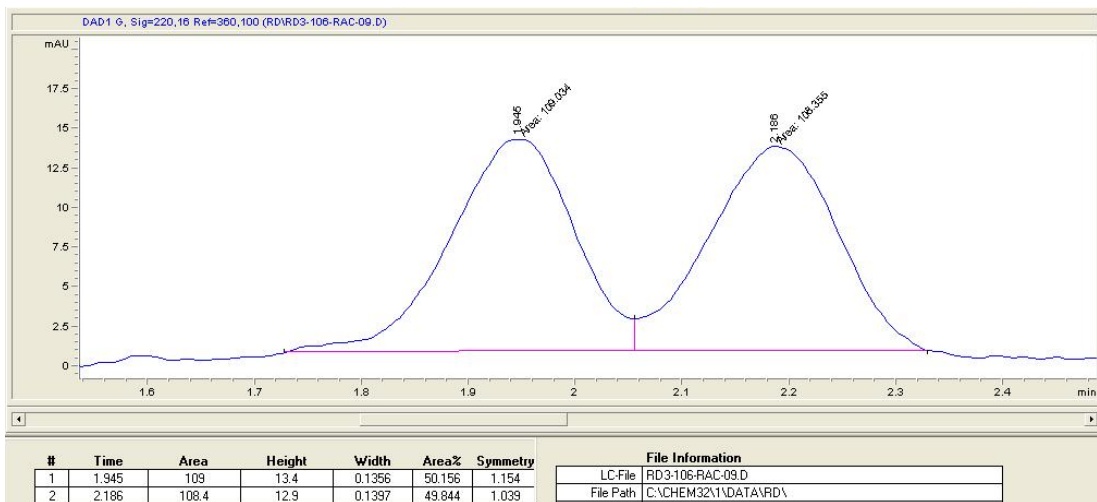
Enantiomerically Enriched



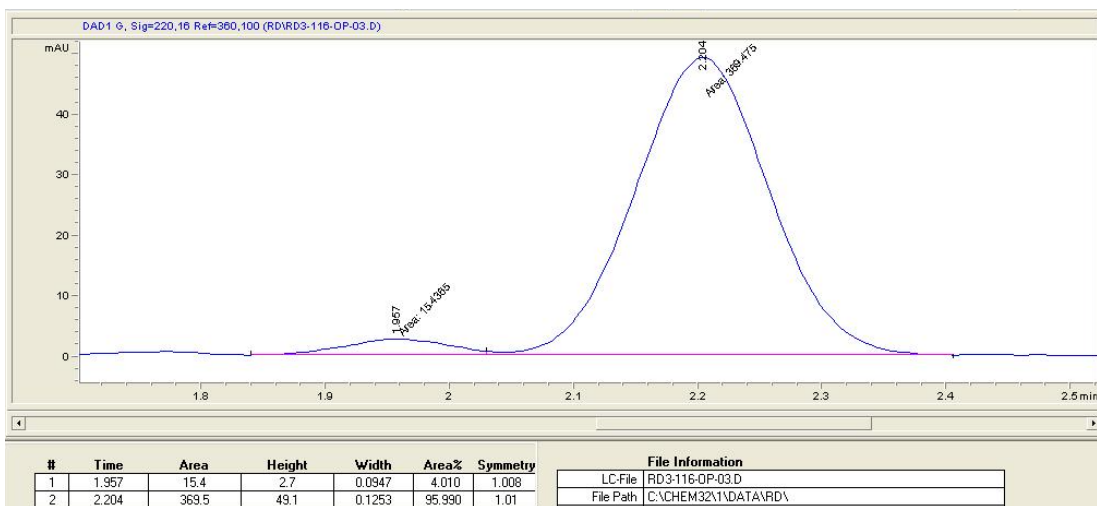


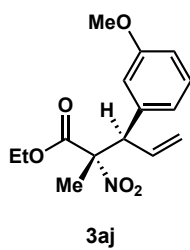
3ai

Racemic

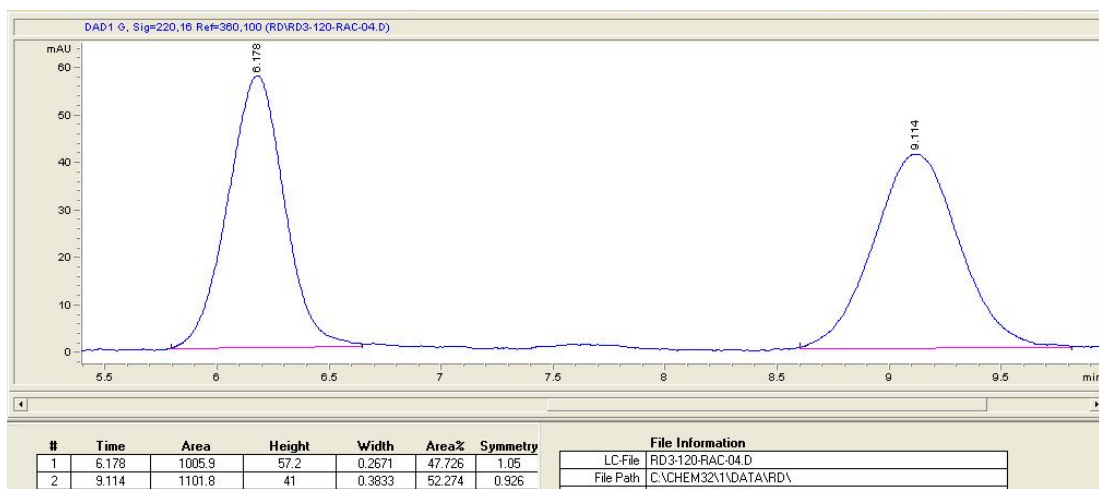


Enantiomerically Enriched

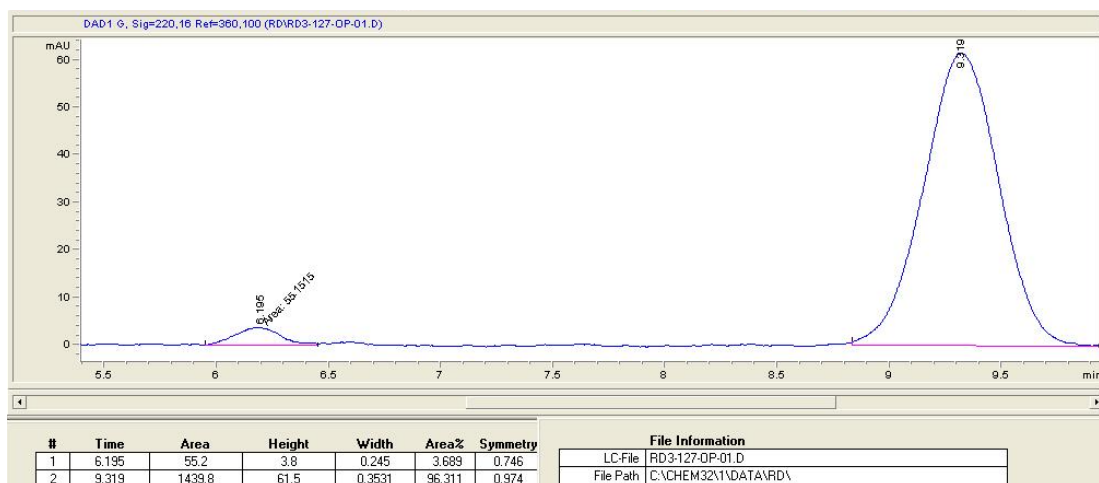


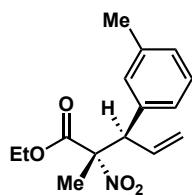


Racemic



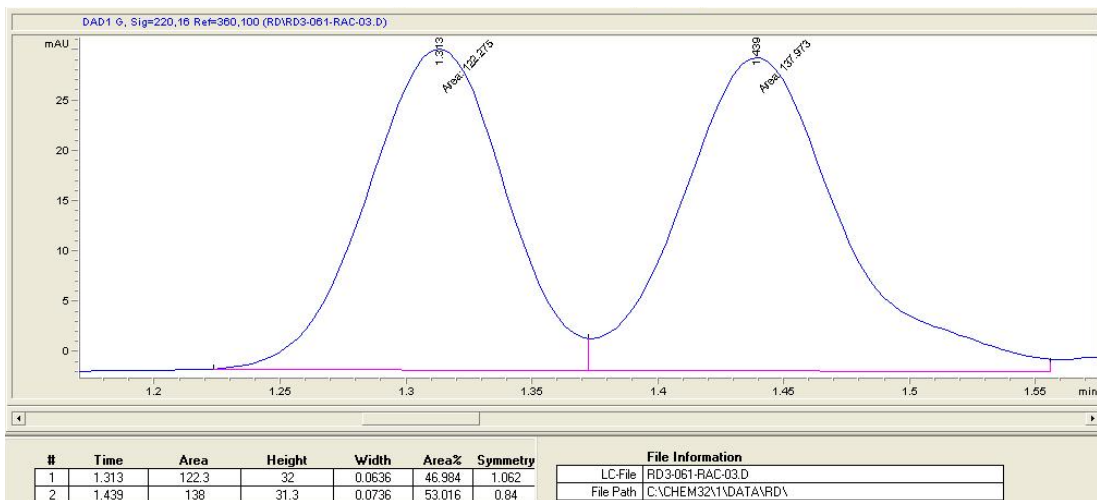
Enantiomerically Enriched



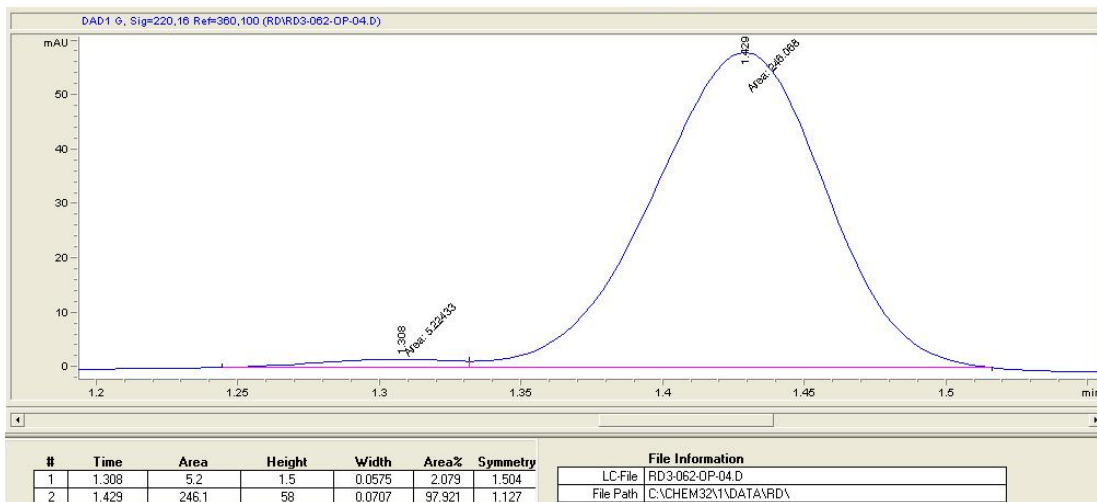


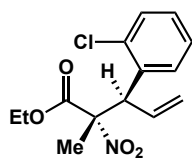
3ak

Racemic



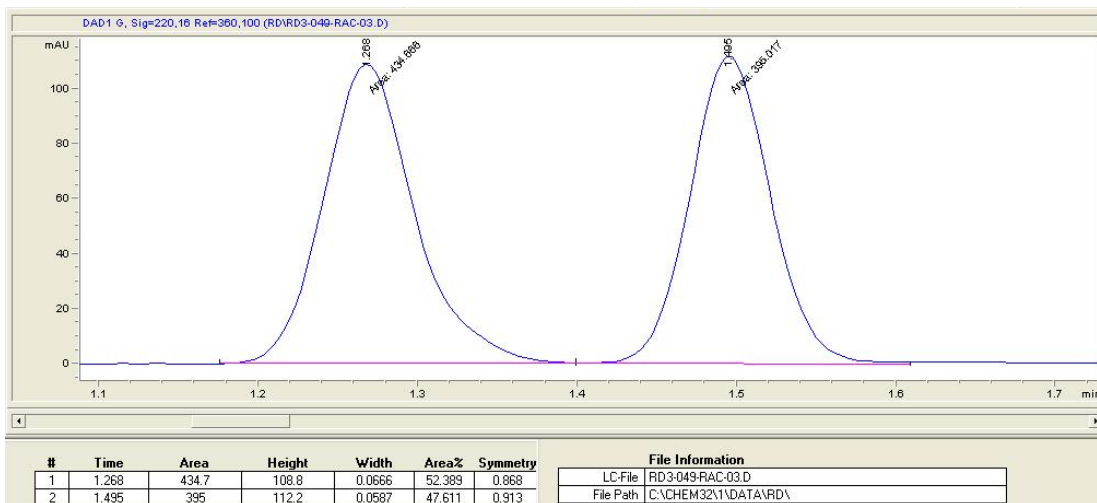
Enantiomerically Enriched



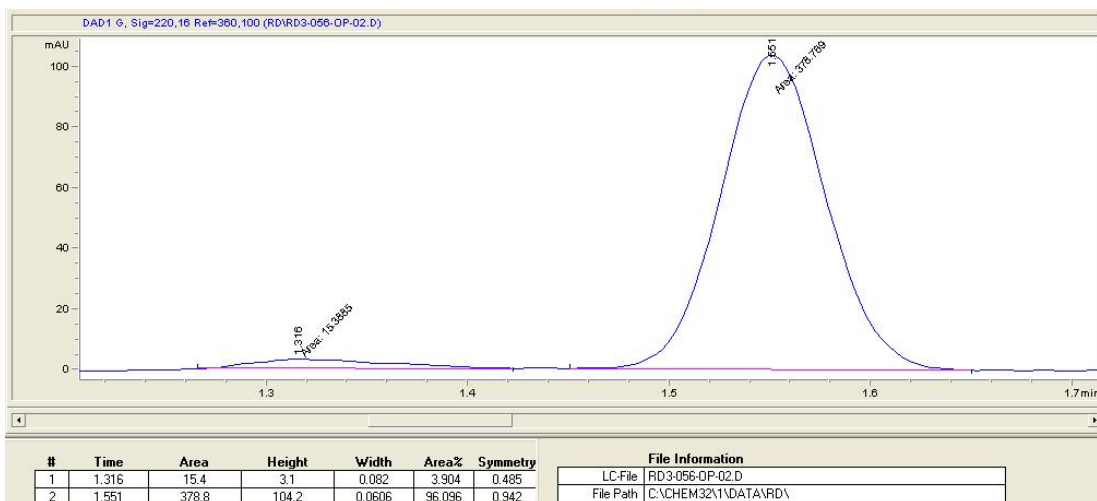


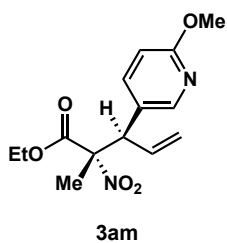
3aI

Racemic

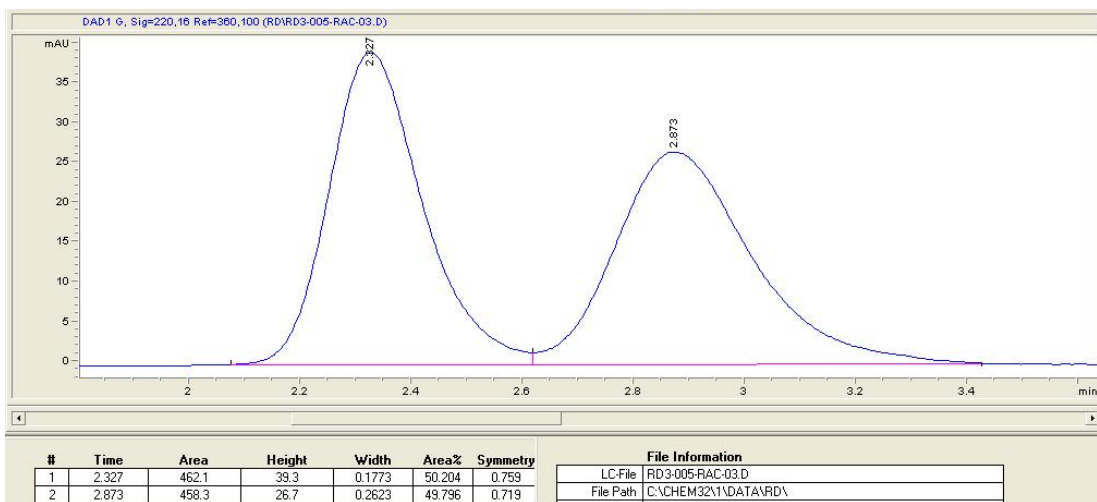


Enantiomerically Enriched

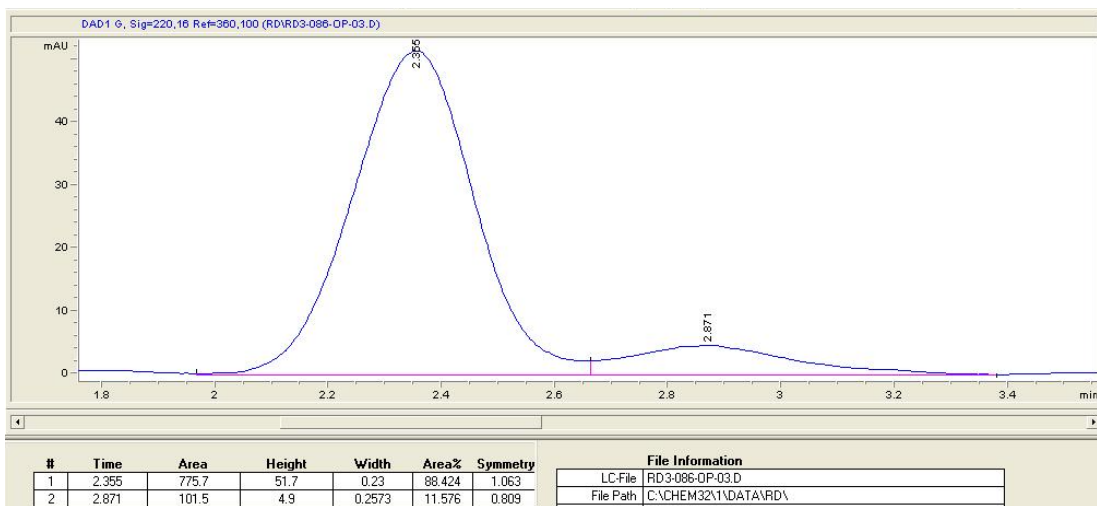


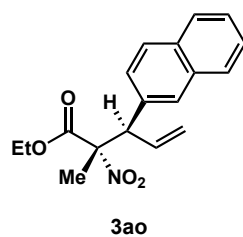


Racemic

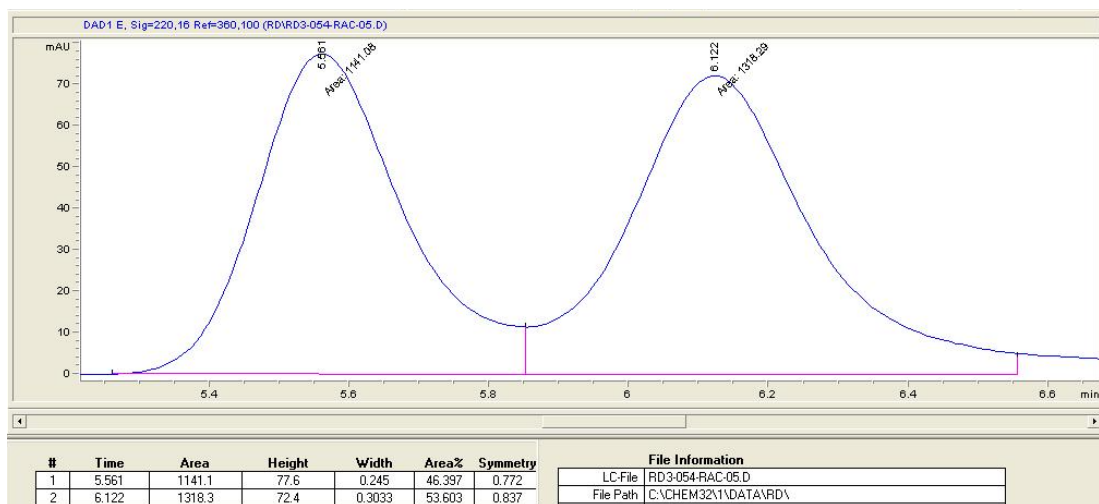


Enantiomerically Enriched

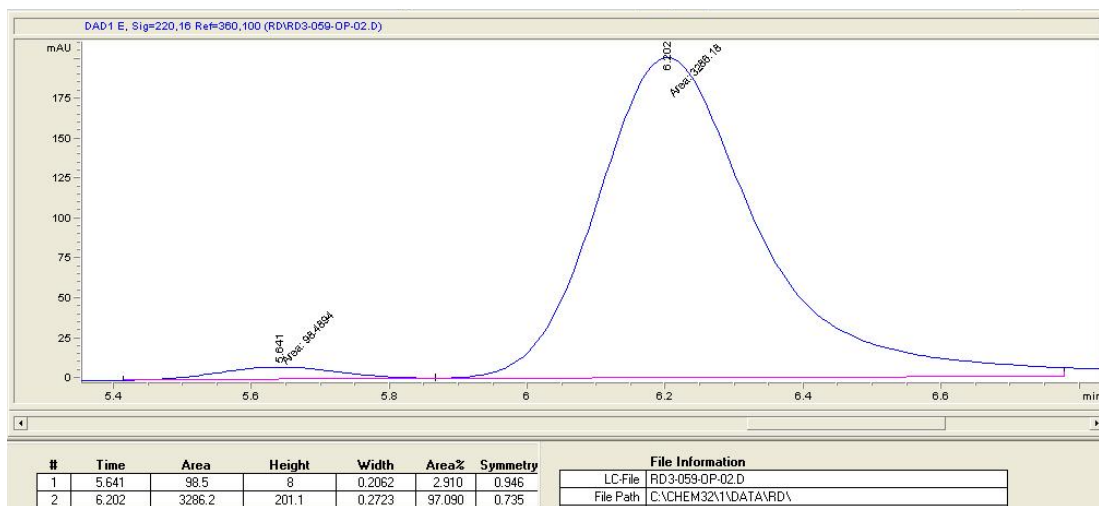


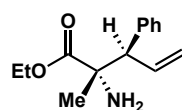


Racemic



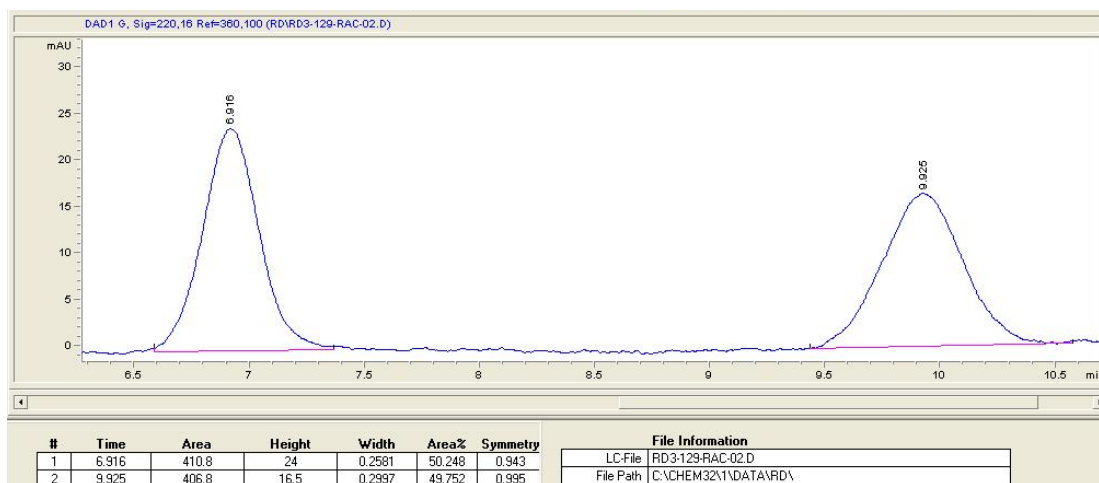
Enantiomerically Enriched



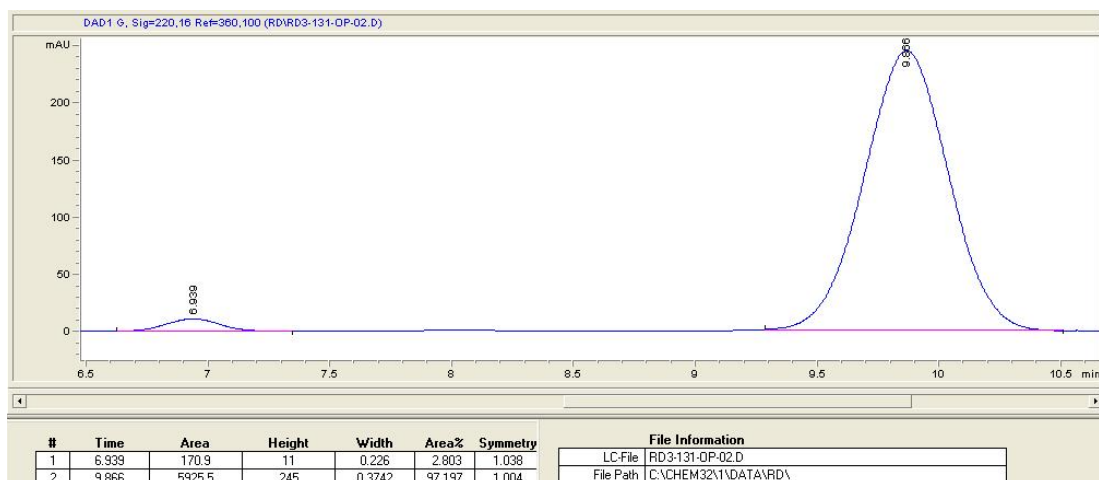


6

Racemic



Enantiomerically Enriched



Appendix 5 Supporting Information for Chapter 5

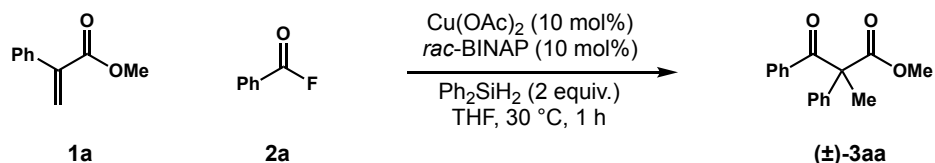
Cu-Catalyzed Olefin Hydroacylation

Table of Contents	Page
1. Materials and Methods	451
2. Racemic Cu-Catalyzed Hydroacylation	452
3. Asymmetric Cu-Catalyzed Hydroacylation Optimization	453
4. Preparation of Starting Materials	456
5. References	457
6. NMR Spectra	458
7. SFC Traces	459

1. Materials and Methods

Commercial reagents were purchased from Sigma Aldrich, Strem, Alfa Aesar, Acros Organics or TCI and used without further purification. Acetone, toluene (PhMe), and tetrahydrofuran (THF) were purified using an Innovative Technologies Pure Solv system, degassed by three freeze-pump-thaw cycles, and stored over 3 Å MS within a N₂ filled glove box. All experiments were performed in oven-dried or flame-dried glassware under an atmosphere of N₂ or in a glove box with a N₂ atmosphere. Reactions were monitored using either thin-layer chromatography (TLC; EMD Silica Gel 60 F₂₅₄ plates) or gas chromatography using an Agilent Technologies 7890A GC system equipped with an Agilent Technologies 5975C inert XL EI/CI MSD. Visualization of the developed plates was performed under UV light (254 nm) or with a KMnO₄ stain. Organic solutions were concentrated under reduced pressure on a Büchi rotary evaporator. Purification and isolation of products was performed via silica gel chromatography (flash column chromatography or preparative thin-layer chromatography). Column chromatography was performed with Silicycle Silia-P Flash Silica Gel using glass columns. ¹H and ¹³C NMR spectra were recorded on a Bruker CRYO-500 or DRX-400 spectrometer. ¹H NMR spectra were internally referenced to the residual solvent signal or TMS. ¹³C NMR spectra were internally referenced to the residual solvent signal. Data for ¹H NMR are reported as follows: chemical shift (δ ppm), multiplicity (s = singlet, d = doublet, t = triplet, q = quartet, m = multiplet, br = broad), coupling constant (Hz), integration. Data for ¹³C are reported in terms of chemical shift (δ ppm). Infrared (IR) spectra were obtained on a Nicolet iS5 FT-IR spectrometer equipped with an iD5 ATR accessory, and are reported in terms of frequency of absorption (cm⁻¹). High resolution mass spectra (HRMS) were obtained by the University of California, Irvine Mass Spectrometry Center on a Micromass 70S-250 Spectrometer (EI) or an ABI/Sciex QStar Mass Spectrometer (ESI). Enantiomeric ratio (*er*) for enantioselective reactions was determined by chiral SFC analysis using an Agilent Technologies HPLC (1200 series) system and Aurora A5 Fusion.

2. Racemic Cu-Catalyzed Hydroacylation



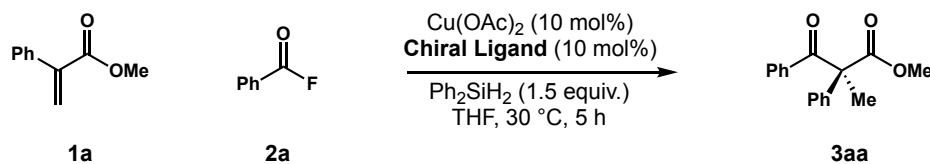
In a N_2 -filled glovebox, to a 1 dram vial (vial A) equipped with a magnetic stir bar was added $\text{Cu}(\text{OAc})_2$ (1.8 mg, 0.01 mmol, 10 mol%), *rac*-BINAP (6.2 mg, 0.01 mmol, 10 mol%), and half of the total reaction solvent (THF, 200 μL). The contents of vial A were then aged for 10 min at 30 °C. Diphenylsilane (36.9 mg, 0.2 mmol, 2 equiv.) was then added to vial A. The contents of vial A were then aged at 30 °C for 2 min or until a noticeable color change was observed (blue to green to orange). To a separate 1 dram vial (vial B) was added **1a** (16.2 mg, 0.1 mmol, 1 equiv.), **2a** (18.6 mg, 0.15 mmol, 1.5 equiv.), and the other half of the total reaction solvent (THF, 200 μL). The contents of vial B were then added to vial A in one portion. The reaction was aged at 30 °C for 1 h. The resulting mixture was removed from the glovebox, opened to atmosphere, and quenched with *sat.* NH_4F in MeOH (1 mL) at rt for 30 min (**caution: vigorous gas evolution**). The reaction mixture was then concentrated *in vacuo* to remove the volatiles, redissolved in EtOAc (2 mL), and passed through a pipet silica plug (1.5 inches). The crude mixture was then purified by preparatory TLC to afford **(±)-3aa**.

Methyl 2-methyl-3-oxo-2,3-diphenylpropanoate [(±)-3aa]

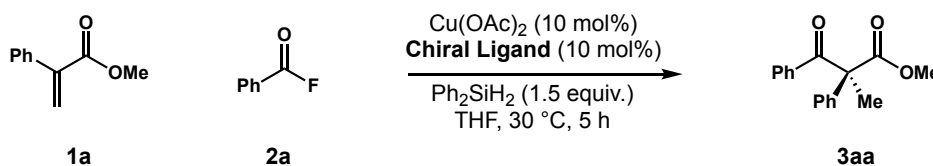
The title compound was isolated by preparatory TLC (20:1 hexanes:EtOAc) as a colorless oil (94% yield). $^1\text{H NMR}$ (400 MHz, CDCl_3) δ 7.67 – 7.64 (m, 2H), 7.46 – 7.41 (m, 3H), 7.35 – 7.26 (m, 5H), 3.67 (s, 3H), 1.93 (s, 3H). $^{13}\text{C NMR}$ (101 MHz, CDCl_3) δ 197.6, 173.1, 139.9, 135.8, 132.8, 129.9, 128.9, 128.5, 128.0, 127.8, 63.0, 53.0, 25.3. **IR** (ATR): 2922, 2851, 1738, 1686, 1446, 1250, 1001, 958, 697. **HRMS** calculated for $\text{C}_{17}\text{H}_{17}\text{O}_3$ $[\text{M}+\text{H}]^+$ 269.1178, found 269.1186.

3. Asymmetric Cu-Catalyzed Hydroacylation Optimization

A. General procedure for acid fluorides (Figures S1–S3)

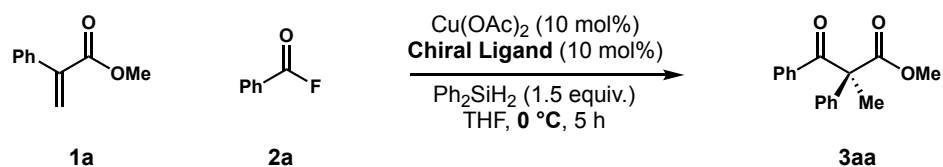


In a N_2 -filled glovebox, to a 1 dram vial (vial A) equipped with a magnetic stir bar was added $\text{Cu}(\text{OAc})_2$ (1.0 mg, 0.005 mmol, 10 mol%), chiral ligand (0.005 mmol, 10 mol%), and half of the total reaction solvent (THF, 100 μL). The contents of vial A were then aged for 10 min at 30 °C. Diphenylsilane (13.8 mg, 0.075 mmol, 1.5 equiv.) was then added to vial A. The contents of vial A were then aged at 30 °C for 2 min or until a noticeable color change was observed (blue to green to orange). To a separate 1 dram vial (vial B) was added **1a** (8.1 mg, 0.05 mmol, 1 equiv.), **2a** (9.3 mg, 0.075 mmol, 1.5 equiv.), and the other half of the total reaction solvent (THF, 100 μL). The contents of vial B were then added to vial A in one portion. The reaction was aged at 30 °C for 5 h. The resulting mixture was removed from the glovebox, opened to the atmosphere, and quenched with *sat.* NH_4F in MeOH (1 mL) at rt for 30 min (**caution: vigorous gas evolution occurs**). The reaction mixture was then concentrated *in vacuo* to remove the volatiles, redissolved in EtOAc (2 mL), and passed through a pipet silica plug (1.5 inches). ^1H NMR yields, which were referenced to an internal standard (1,3,5-trimethoxybenzene), are reported. **Chiral SFC**: 150 mm CHIRALCEL OJ-H, 1% i PrOH, 2 mL/min, 254 nm, 44 °C, nozzle pressure = 200 bar CO_2 , $t_{\text{R}1}$ (major) = 3.1 min, $t_{\text{R}2}$ (minor) = 3.3 min.



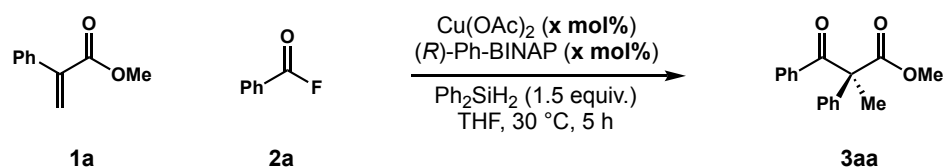
Entry	Chiral Ligand	Result
1	(<i>R</i>)-Ph-BINAP	84%, 60:40 <i>er</i>
2	(<i>R</i>)-Tol-BINAP	81%, 63.5:36.5 <i>er</i>
3	(<i>R</i>)-Xyl-BINAP	50%, 62:38 <i>er</i>
4	(<i>R</i>)-DTBM-BINAP	trace
5	Josiphos (J011-1)	31%, 60:40 <i>er</i>
6	Josiphos (J013-1)	67%, 53:47 <i>er</i>
7	Taniaphos (T001-1)	6%, 67:33 <i>er</i>
8	(<i>S,S</i>)-Ph-BPE	22%, 54:46 <i>er</i>
9	(<i>R</i>)-DTBM-Segphos	35%, 54:46 <i>er</i>

Figure S1. Select chiral ligands with acid fluorides.



Entry	Chiral Ligand	Result
1	Taniaphos (T001-1)	10%, 68:32 <i>er</i>
2	Josiphos (J011-1)	43%, 63:37 <i>er</i>
3	(<i>R</i>)-Ph-BINAP, -78 °C	19%, 62:38 <i>er</i>

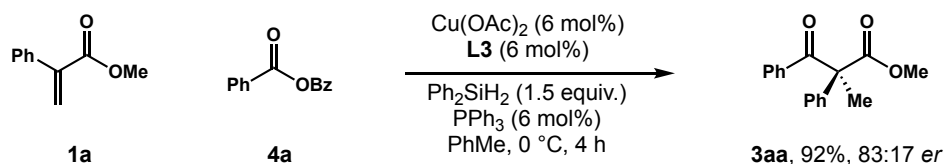
Figure S2. Reaction temperature with acid fluorides.



Entry	Chiral Ligand	Result
1	5 mol%	61%, 67:33 <i>er</i>
2	3 mol%	53%, 67:33 <i>er</i>
3	1 mol%	56%, 67:33 <i>er</i>

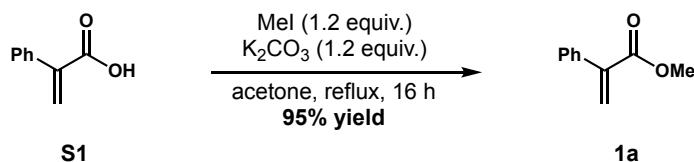
Figure S3. Copper/ligand loading with acid fluorides.

B. Procedure for carboxylic anhydrides



In a N₂-filled glovebox, to a 1 dram vial (vial A) equipped with a magnetic stir bar was added Cu(OAc)₂ (0.5 mg, 0.003 mmol, 6 mol%), **L3** (2.0 mg, 0.003 mmol, 6 mol%), and half of the total reaction solvent (PhMe, 100 μL). The contents of vial A were then aged for 10 min at 30 °C. Diphenylsilane (13.8 mg, 0.075 mmol, 1.5 equiv.) and triphenylphosphine (0.8 mg, 0.003 mmol, 6 mol%) were then added to vial A. The contents of vial A were then aged at 30 °C for 2 min or until a noticeable color change was observed (blue to green to orange). To a separate 1 dram vial (vial B) was added **1a** (8.1 mg, 0.05 mmol, 1 equiv.), **4a** (17 mg, 0.075 mmol, 1.5 equiv.) and the other half of the total reaction solvent (PhMe, 100 μL). Both vials were removed from the glovebox and placed under an N₂ atmosphere (balloon) at 0 °C (ice bath). The contents of vial B were then added to vial A in one portion. The reaction was aged at 0 °C for 4 h. The resulting mixture was warmed to rt, opened to the atmosphere, and quenched with *sat.* NH₄F in MeOH (1 mL) at rt for 30 min (**caution: vigorous gas evolution occurs**). The reaction mixture was then concentrated *in vacuo* to remove the volatiles, redissolved in EtOAc (2 mL), and passed through a pipet silica plug (1.5 inches). ¹H NMR yield, which was referenced to an internal standard (1,3,5-trimethoxybenzene), is reported (92% yield). **Chiral SFC**: 150 mm CHIRALCEL OJ-H, 1% *i*PrOH, 2 mL/min, 254 nm, 44 °C, nozzle pressure = 200 bar CO₂, t_{R1} (major) = 3.1 min, t_{R2} (minor) = 3.3 min.

4. Preparation of Starting Materials



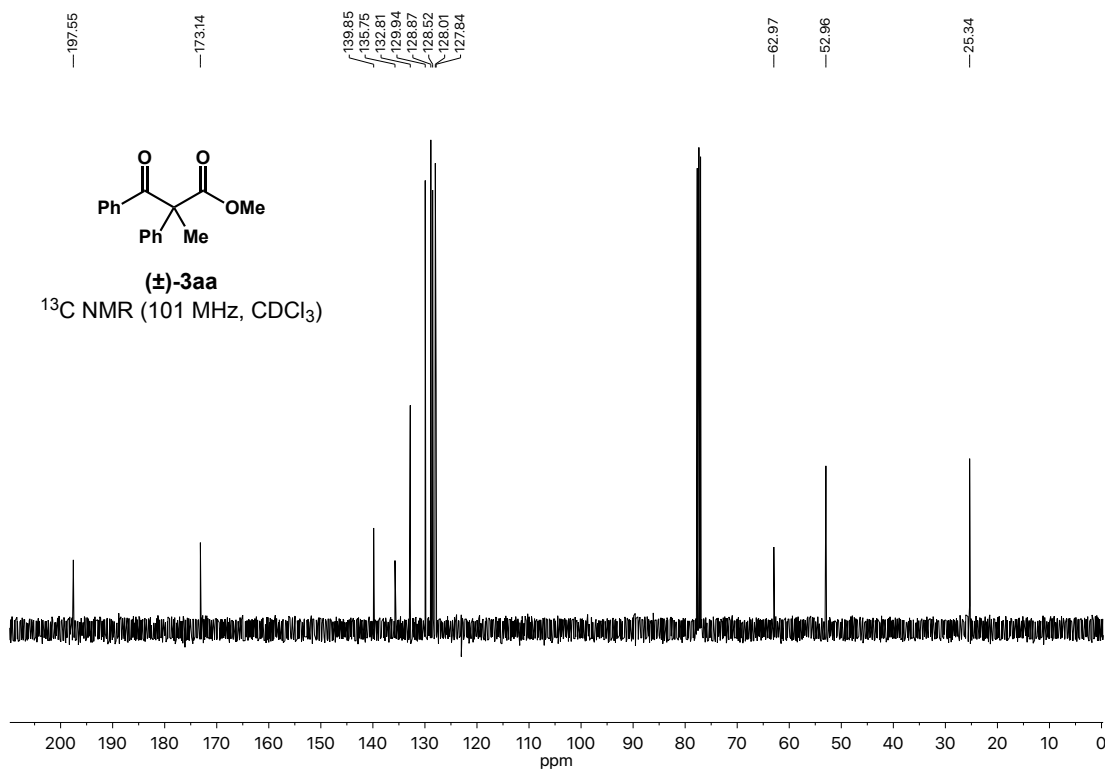
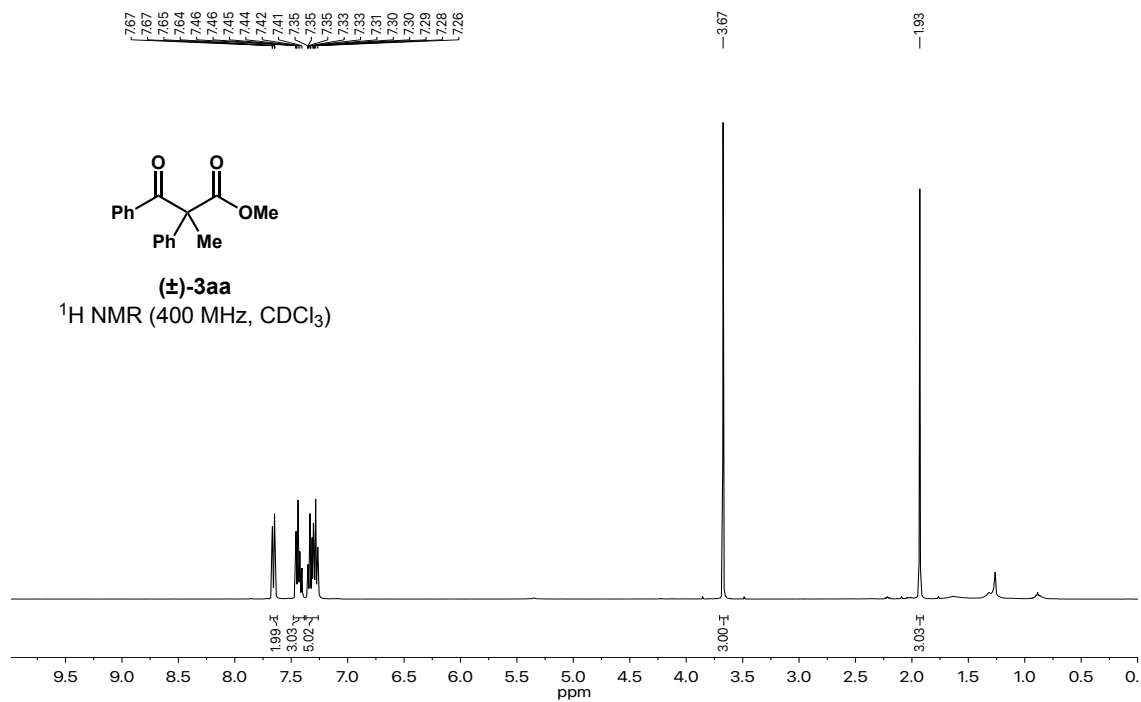
Preparation of methyl 2-phenylacrylate (1a): To a round bottom flask equipped with a magnetic stir bar was added 2-phenylacrylic acid (**S1**, 2.2 g, 15 mmol, 1 equiv.), acetone (60 mL, 0.25 M), potassium carbonate (2.5 g, 18 mmol, 1.2 equiv.), and then iodomethane (2.6 g, 18 mmol, 1.2 equiv.) at rt. The flask was then equipped with a reflux condenser and heated to reflux. The reaction was then aged at reflux for 16 h. Upon completion, the reaction mixture was concentrated *in vacuo* to remove the volatiles and then redissolved in EtOAc and H₂O (1:1, total of 50 mL). Extracted the mixture with EtOAc (3x10 mL), collected the organics, dried the organics with MgSO₄, filtered over filter paper, and then concentrated *in vacuo*. The crude material was then passed through a silica plug (4 in x 1 in) with 10:1 hexanes:EtOAc to afford **1a** as a clear, colorless liquid (95% yield). The ¹H NMR data is in accordance with the literature.¹ ¹H NMR (400 MHz, CDCl₃) δ 7.43 – 7.32 (m, 5H), 6.37 (d, *J* = 1.2 Hz, 1H), 5.90 (d, *J* = 1.2 Hz, 1H), 3.83 (s, 3H).

5. References

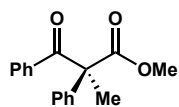
- (1) Tsukamoto, Y.; Itoh, S.; Kobayashi, M.; Obora, Y. *Org. Lett.* **2019**, *21*, 3299–3303.

6. NMR Spectra

Methyl 2-methyl-3-oxo-2,3-diphenylpropanoate [(±)-3aa]

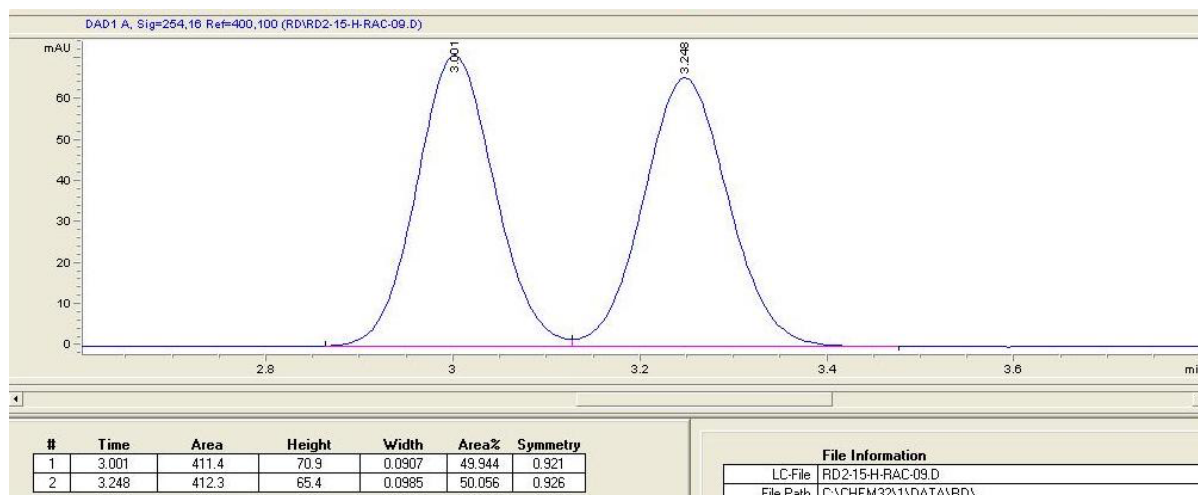


7. SFC Traces



3a

Racemic



Enantiomerically Enriched (Equation 5.2)

